1993

Effect of the El Nino/Southern Oscillation on Gulf of Mexico, Winter, Frontal-Wave Cyclones: 1960-1989. (Volumes I and II).

Rosemary Eileen Manty
Louisiana State University and Agricultural & Mechanical College

INFORMATION TO USERS

This manuscript has been reproduced from the microfilm master. UMI films the text directly from the original or copy submitted. Thus, some thesis and dissertation copies are in typewriter face, while others may be from any type of computer printer.

The quality of this reproduction is dependent upon the quality of the copy submitted. Broken or indistinct print, colored or poor quality illustrations and photographs, print bleedthrough, substandard margins, and improper alignment can adversely affect reproduction.

In the unlikely event that the author did not send UMI a complete manuscript and there are missing pages, these will be noted. Also, if unauthorized copyright material had to be removed, a note will indicate the deletion.

Oversize materials (e.g., maps, drawings, charts) are reproduced by sectioning the original, beginning at the upper left-hand corner and continuing from left to right in equal sections with small overlaps. Each original is also photographed in one exposure and is included in reduced form at the back of the book.

Photographs included in the original manuscript have been reproduced xerographically in this copy. Higher quality 6" x 9" black and white photographic prints are available for any photographs or illustrations appearing in this copy for an additional charge. Contact UMI directly to order.

U·M·I

University Microfilms International
A Bell & Howell Information Company
300 North Zeeb Road, Ann Arbor, MI 48106-1346 USA
313/761-4700 800/521-0600

Order Number 9401551

Effect of the El Niño/southern oscillation on Gulf of Mexico, winter, frontal-wave cyclones: 1960–1989. (Volumes I and II)

Manty, Rosemary Eileen, Ph.D.

The Louisiana State University and Agricultural and Mechanical Col., 1993

U·M·I
300 N. Zeeb Rd.
Ann Arbor, MI 48106

EFFECT OF THE EL NIÑO/SOUTHERN OSCILLATION ON GULF OF MEXICO, WINTER, FRONTAL-WAVE CYCLONES: 1960-89
VOLUME I

A Dissertation

Submitted to the Graduate Faculty of the
Louisiana State University and
Agricultural and Mechanical College
in partial fulfillment of the
requirements for the degree of
Doctor of Philosophy

in

The Department of Geology and Geophysics

by
Rosemary E. Manty
B.S., Wayne State University, 1977
M.S., Louisiana State University, 1981
May 1993

ACKNOWLEDGEMENTS

I wish to thank Dr. S. A. Hsu, advisory-committee chair, and committee members, Drs. O. K. Huh, M. Inoue, R. A. Muller, and D. Nummedal. Dr. R. A. Muller, Chief Climatologist, Southern Regional Climate Center, contributed the United States Climatological Division data on temperature and precipitation, and his own 30-year data set of gulf-region, synoptic weather-type occurrences. Dr. J. Grymes, Chief Climatologist, Louisiana Office of State Climatology, contributed state of Louisiana, Southeastern Division, temperature and precipitation records. Other, single-station temperature and precipitation records were obtained from the National Carbon Dioxide Information Analysis Center, Oak Ridge, Tennessee. Hurricane-frequency data was obtained from the National Climatic Data Center in Asheville, North Carolina. The gridded, upper-air data was taken from a CD-ROM prepared by the members of the Department of Meteorology at the University of Washington in Seattle, Washington. Dr. S. A. Hsu contributed the funds to purchase the CD-ROM. Land-suface elevation and ocean bathymetry were taken from the ETOPO5 data set, prepared by the National Geophysical Data Center, Boulder, Colorado. Jane Metcalf, formerly of the System Network Computer Center, Louisiana State University, provided use of a CD-ROM player. Mr. Roy Jenne and Mr. Dennis Joseph, National Center for Atmospheric Research, Boulder, Colorado, were of assistance in the mapping and unpacking of the University of Washington data.

CONTENTS

LIST OF TABLES

LIST OF FIGURES

ABSTRACT

Seasonal counts of frontal-wave cyclones forming over the Gulf of Mexico and its coastal plain show more storms in the five El Niño winters and fewer storms in the eight La Niña winters, from 1960 to 1989, significant at the .01 level by a rank sum test. This is corroborated by two results. First, during the same period, the frequency of frontal-overrunning weather conditions in the region, indicative of storms, was higher in El Niño winters and lower in La Niña winters, significant at the .05 level. Second, 100 years of precipitation and temperature records show wetter, cooler El Niño winters and drier, warmer La Niña winters at gulf-region land stations and climatic divisions. A threefold explanation, based on National Meteorological Center, upper-air data, is offered for the greater frequency of gulf-region cyclogenesis during El Niño winters between 1960 and 1989.

1. *Jet Stream* The winter, mean, 250-mb jet over the southern United States is intensified by 5 to 10 ms^{-1} and displaced southward between 110° and 75°W by an average of 200 to 285 km during the five El Niño winters between 1966 and 1989. This implies stronger and more-frequent episodes of jet-associated, upper-level troughing and divergence over the region, reinforcing surface, frontal-wave cyclones.

2. *Upper- and Intermediate-Level Troughs* In the five El Niño winters between 1963 and 1989, seasonal average heights and temperatures of the 850-, 700-, 500-, and 200-mb surfaces are lower over the region than they are in non-El Niño winters. This implies more-common presence of cold, low-pressure troughs at upper levels, reinforcing surface cyclones.

3. *850-mb Level Winds* A 10° eastward shift, at sea level, of the western edge of the Bermuda high during the eight El Niño winters between 1947 and 1989, changes normally due-easterly trades in the northwestern Caribbean Sea to slightly south of east, allowing greater advection of moisture and heat into the gulf from the tropics, preconditioning the area for development of surface cyclones.

Only winter season shows all three conditions and an icrease in cyclogenesis.

CHAPTER 1
INTRODUCTION

1.1 Background

Much storm-related research has focused on the nonfrontal, tropical and subtropical cyclones, hurricanes, typhoons, and their precursors originating in the easterlies of the tropics and subtropics, because of the threat these pose to coastal areas. Another type of major storm, the extratropical cyclone, has also received attention, due to its capacity to produce dangerous weather. Originating in the midlatitude westerlies, the well-developed cold and warm fronts associated with these extratropical cyclones can, on most days, be seen to nearly continuously encircle the midlatitude globe. Relatively fewer studies have examined the occurrence of smaller-scale, frontal-wave disturbances, here called frontal-wave cyclones, that form 'piggyback' along the fronts of the major extratropical storms, typically when those fronts become stationary. These storms are less severe, of smaller scale, and of shorter duration, one to three days, than the larger tropical and extratropical storms. In the Gulf of Mexico region of North and Central America and its surrounding coastal plain, however, they are an important element of fall, winter, and spring weather. Nearly all of the winter and spring precipitation in the region is associated with these secondary weather systems. The meteorological characteristics of these frontal-wave cyclones over the Gulf of Mexico have recently been discussed by Johnson et al. (1984), Hsu (1988, 1992), and by Lewis and Hsu (1992). Previously, Saucier (1949) has also reported on Gulf of Mexico region storms.

The present work is primarily concerned with these smaller-scale, frontal-wave cyclones. Before the objectives of the current study are presented, it will first be instructive to review the annual weather patterns in the Gulf of Mexico region.

From September to April, weather in the area is dominated by the passage of cold fronts, and the ensuing, so-called cold-air outbreaks. These are surges of relatively cool, dry, polar air behind the cold-front portions of major, synoptic-scale, extratropical cyclones as these track east across North America. Cold fronts in the southern United States have been studied by Mortimer et al. (1988) and Fernandez-Partegas and Mooers (1975). Recently, the entire August 1992 issue of the Journal of Applied Meteorology has been devoted to research on the modification of the cold-air mass while over the gulf and to the late-stage, landward or return flow associated with these cold-air outbreaks. The air-sea interactive characteristics of cold-air outbreaks have been studied by Walker et al. (1987), Schroeder et al. (1985), and Huh and Rouse (1984). The cold fronts become stationary near the coast or nearer to the shelf edge, depending on characteristics of the cool-air mass and on local factors, as discussed in Hsu (1988, 1992) and Lewis and Hsu (1992). The frontal-wave cyclones reported herein form along these stationary fronts, often over water. Once formed, they track to the northeast, some of them reaching the Atlantic Ocean where they may intensify into major storms. Few major synoptic-scale, extratropical storms, such as those generated in the lee of the North American Cordillera, ever track far enough south for the central low to directly cross the gulf or coastal plain. The greatest number of frontal-wave cyclones forming in the gulf region occurs in the winter months, December, January, and February, with secondary abundances in November and March. Nearly all of the remaining frontal-wave cyclones occur in September, October, and April. The rest of the year, May to August, the weather in the gulf region is not usually significantly affected by fronts, being dominated by local, mesoscale convective systems, by persistent high pressure which is an extension of the Bermuda high, and by the occasional hurricane, tropical storm, or tropical depression. These last also are an element of the fall, September to November, weather.

1.2 Brief Review of the El Niño/Southern Oscillation (ENSO)

The present work is focused on the occurrence, in the gulf region, of the frontal-wave cyclones introduced above, as affected by the quasi-periodic phenomenon known as the El Niño/Southern Oscillation (ENSO). Therefore, a brief review of the ENSO follows. Philander (1990) has produced a comprehensive work on the ENSO, with emphasis on its wave-like properties. A collection of papers on the extratropical effects of ENSO (Newton and Holopainen 1991) has recently been published. Rather than attempt to cite all the relevant ENSO literature, the interested reader is referred to these two works which contain extensive bibliographies.

The term, Southern Oscillation, refers to the see-sawing of mean sea-level pressure over the equatorial Pacific which occurs about every four to six years, but as often as only two years apart, and as rarely as once in ten years. Normally, mean sea-level pressure (MSLP) is lower in the west equatorial Pacific than in the east. Darwin, Australia is representative of the western equatorial Pacific; Tahiti is representative of the east. Normally, the quantity $MSLP_{Tahiti} - MSLP_{Darwin} > 0$. This quantity has been termed the Southern Oscillation index. Normally, easterly trade winds blow along the equatorial Pacific, down a pressure gradient from higher to lower pressure. Application of this steady force supports a higher sea level, by 40 cm (16 in), in the west than in the east. In the eastern equatorial Pacific, it also produces upwelling of cold water along the equator by the following mechanism. Easterly-trade-induced, Ekman transport in the surface layer produces poleward-flowing currents just off the equator. The resulting surface divergence, centered along the equator, causes the upwelling of cooler, deep water. Upwelling also occurs along the South American coast (in the Southern Hemisphere), because there, southeasterly trades, blowing parallel to the coast, produce offshore-directed,

surface, Ekman transport, resulting in surface divergence in coastal waters. It is also part of the normal situation that the easterly trades in the western Pacific are not as strong as those in the eastern Pacific. This allows the surface water in the west equatorial Pacific to be warmed by solar radiation to a deeper level than in the east. The net normal picture then, is higher sea level and a thicker (4X), warmer, surface layer in the western equatorial Pacific than in the eastern equatorial Pacific. Completing the atmospheric part of the normal picture is the presence of an east-west, vertical circulation cell, the Walker cell. The easterly trades are the surface leg of the Walker cell. As trades weaken from east to west across the Pacific, air warmed by passage over warm water rises over the west Pacific. A strong zone of atmospheric convection results over the west Pacific, accompanied by clouds and precipitation. This is the second leg of the Walker cell. Air in this zone can rise to jet-stream level and higher, up to 15 km (9 mi) (Philander 1989), before losing its moisture, finding its own density level, and joining the upper-level westerlies. Eventually, some of this air, having moved north, joins the descending branch of the meridional, vertical, Northern Hemisphere, Hadley circulation cell. This air descends to join the northeast trades again. The equatorial belts of convergence of surface trade winds and rising air are called, collectively, the Intertropical Convergence Zone (ITCZ). These occur preferentially over the warmest water, offset a bit from the equator, following the sun in a seasonal migration.

The term El Niño will be used here to describe the basin-wide oceanic circulation state that evolves when the normal state of affairs for some reason breaks down, and the pattern of warm water with atmospheric convection in the western equatorial Pacific and cooler water with dry zones in the eastern equatorial Pacific changes. The term La Niña will be used to refer to years during which an exaggeration occurs of the normal state described above. The terms El Niño and La Niña

are oceanographic terms, and the corresponding atmospheric states are referred to as the negative and positive phases of the Southern Oscillation. As a shorthand, when El Niño and La Niña are used in this work, these oceanographic terms will be understood to imply the accompanying negative and positive phases of the atmospheric, Southern Oscillation of surface pressure. Aceituno (1992) has recently compiled a history of all terms used in reference to the ENSO. Some workers now simply use 'warm event' for El Niño and 'cold event' for La Niña, emphasizing the fact that these are the two phases, negative and positive, of the tropical Pacific ocean-atmosphere system, for example, Deser and Wallace (1990) and van Loon and Madden (1981).

When the normal situation breaks down, and an El Niño event occurs, the pressure gradient from east to west decreases or even reverses. Surface pressure becomes either not much lower in the west Pacific than in the east, or it is even slightly higher in the west. The Southern Oscillation index, $MSLP_{Tahiti} - MSLP_{Darwin}$ is either smaller than normal or even negative in the negative phase of the Southern Oscillation. The cause of this surface-pressure reversal is not agreed upon. The result is that the normally strong, easterly trades in the east Pacific weaken, and so the warm, surface water piled up in the western Pacific, no longer supported by the wind stress, sloshes back eastward. The migration takes the form of an internal Kelvin wave, and requires two to three months the reach the Americas. This wave can be thought of as a pulse propagating along the thermocline. Afterward, there are one or more reflected waves, of lower speed, since the collision with the Americas is inelastic. The reflected waves are also like pulses propagating along the thermocline and take the form of Rossby waves, requiring 7 to 8 months to reach the west Pacific. Coastal Kelvin waves, propagating poleward, are also generated by the collision of both the original Kelvin wave and reflected Rossby waves with the

American and Asian coasts. The process of reflection continues like an echo until the vibration is totally damped. Another result of weaker easterly trades during an El Niño event is less divergence of surface water near the equator and, consequently, less upwelling of deep, cooler water. Less upwelling combined with imported, warm, surface water from the west produces the unusually warm water of the central and east Pacific basin which characterizes an El Niño event. The warm water near the South American coast, to which the term, El Niño, was originally applied, is caused by the weaker southeasterly trades, which cause less offshore-directed, surface, Ekman transport, from which less coastal upwelling results. Along with the warm water comes a warming of the air over the water and increased atmospheric convection and precipitation in the eastern equatorial Pacific. During an El Niño event, the zone of strongest atmospheric convection, which normally is located in the west Pacific, is displaced eastward, following the warmest water.

A major simplification was made in the preceding description of the onset of El Niño. It is not really thought that the surface pressure changes first and thus causes the change in surface winds. It is not agreed upon what happens first, or, what sets off an El Niño event. There is only agreement on what happens after the easterly trades in the east Pacific weaken. It is thought that perhaps sea-surface temperature (SST) changes come first, with warm, surface water in the east Pacific appearing first. This then would cause surface pressure in the east to fall, due to a warmer, moister atmosphere over warmer water (Trenberth 1991). After that, the El Niño event progresses as described. There is another school of thought that invokes surface winds in the west Pacific as the initial cause. These are thought to diminish greatly, or even reverse, becoming westerly, causing the warm, surface layer of the west Pacific to travel east as a Kelvin wave. Then this warm water, now in the east, causes surface pressure to fall, east trades to diminish

in the east Pacific, and the event continues as described (Trenberth 1991). The common ground between the two views is that the onset of El Niño is an initial-value problem. Different initial states can lead to somewhat different solutions, and this explains why El Niño events do not all develop in the same way. It seems likely that each hypothesis is correct some of the time, and that El Niño events have multiple trip mechanisms.

How can this have extratropical effects? The atmosphere must carry the signal since it travels so fast, almost concurrent with events in the equatorial Pacific. The extratropical signal seems to originate with the reversal in sea-level pressure in the equatorial Pacific. Like the analogy of the pulse traveling along the thermocline used to explain the El Niño-year changes in surface, oceanic currents and temperatures, reversing the surface pressure pattern in the equatorial Pacific may generate a traveling wave in the atmosphere, which manifests itself as a succession of high and low surface pressures traveling west to east (Trenberth 1991). An El Niño event's far-field effects are not confined to the surface layer of the atmosphere. Because of the involvement of the vertical circulation cells, the Walker and the Hadley cells (Bjerknes 1966, 1974a, 1974b), upper levels up to jet-stream level, are immediately involved in an El Niño event. Moving the main equatorial Pacific heat and moisture source two to three thousand kilometers eastward during an El Niño event has important effects on the vertical circulation cells, including their upper-level components. Once introduced to upper levels, high wind speeds transmit the signal rapidly around the globe. Extratropical effects of wide geographic distribution, particularly in the winter hemisphere, where circulation is strengthened, have been noted (Halpert and Ropelewski 1992a; White and Downton 1991; Tribbia 1991; Rasmussen 1991; Lindsay and Vogel 1990; Handler 1990; Held et al. 1989; Hamilton 1988; Yarnal and Leathers 1988; Ropelewski and Halpert 1987, 1986; Hamilton

and Garcia 1986; von Storch and Kruse 1985; Gray 1984a, 1984b; Rogers 1984: Quiroz 1983a, 1983b; Lau and Chan 1983a, 1983b; van Loon and Madden 1981; Horel and Wallace 1981; Bjerknes 1969, 1972).

1.3 Objectives and Previous Work

1.3.1 Objectives

There are two objectives to this work. First, how are frontal-wave cyclones originating over the Gulf of Mexico and its coastal plain affected by the El Niño/Southern Oscillation? (Chapters 2 and 5) Second, how can this be explained? (Chapters 3 and 4)

1.3.2 Previous Work

Based on the work of Johnson et al. (1984), it was suspected that more frontal-wave cyclones formed in the gulf area during El Niño winters than during non-El Niño winters. ('Storms' will be used interchangeably with frontal-wave cyclones from this point forward.) These workers counted storms in the gulf area between November and March of the 11-year period, November 1972 to March 1983, a time which included three El Niño events, 1972/73, 1976/77, and 1982/83. They noted that El Niño winters appear to have more, and stronger, storms than other winters although they did not test this statistically. Similarly, Gan and Rao (1991) observed an increase in the frequency of cyclogenesis over South America in El Niño years from 1979 to 1988, although no tests of significance were included in their paper.

A number of workers have examined tropical and extratropical precipitation in El Niño years. Those including the Gulf of Mexico region generally have found increased precipitation in El Niño winters, pointing to the possibility of more storms

in the gulf area in El Niño winters. Ropelewski and Halpert (1986, 1987), looking at historical, land-station data, cite above-normal precipitation and lower-than-normal temperatures in the southeastern United States from October to March of El Niño events in 18 of 22 El Niño events during the time studied, 1875 to 1980. Faiers (1988) looked at January precipitation at Lake Charles, Louisiana from 1951 to 1978 and found three of the six El Niño Januarys had a high frequency of precipitation events and frontal-overrunning conditions, indicative of storms. Douglas and Englehart (1981) examined winter precipitation in south-central Florida (one climatic division) from 1948 to 1975. They found a statistically significant, positive correlation between winter precipitation there and in the preceding autumn in the central equatorial Pacific, indicating wet winters in south-central Florida during El Niño years. These authors also presented some explanation, showing a 20 to 30 m (65 to 100 ft) negative height anomaly over the gulf region on a composite map of the 700-mb level for the six El Niño winters in the period. They suggested that southward displacement of the subtropical-jet stream over the southern United States in El Niño winters was responsible for increased cyclogenesis indicated by the increased precipitation, although no jet-level data was provided. Johnson et al. (1984) also proposed the same mechanism to explain the increased frequency of storms, and provided a schematic map of the jet for the 1982/83 El Niño winter, noting an apparent tendency for a split to develop in the jet in that winter. Quiroz (1983a, 1983b) presented data on the 1982/83, winter, 200-mb jet, showing south displacement and strengthening over the southern United States, compared to a five-year mean from 1976 to 1980. Horel and Wallace (1981) note a strengthening and south displacement of the subtropical jet over the tropical Pacific in the six El Niño winters from 1951 to 1978. Their work is based on composite maps of 200-mb height anomalies from 10 stations with 28 years of record and 22 stations with less than 28 years.

Based on the foregoing previous work, it was expected that a study of 30 years would show a statistically-testable increase, during El Niño winters, in the number of storms originating over the Gulf of Mexico and coastal plain. A 30-year storm count was made for the period, 1960 to 1989, along with a study of the frequency of occurrence of gulf-area, synoptic weather types, as a frontal-overrunning type was expected to be indicative of storms. A longer-term study of precipitation and temperature for the region is the third element of the surface-based study. This portion of the work is organized as a comparison, season by season, of El Niño and non-El Niño years, and likewise of La Niña and non-La Niña years. La Niña being the opposite of El Niño, it was expected that delineation of La Niña trends would substantiate and clarify El Niño trends. These results are presented in chapter 2.

Based on previous speculations that the jet stream is displaced southward over the gulf area in El Niño winters, and so is the cause for increased cyclogenesis, a study of 24 years of 250-mb level winds over the region, from 1966 to 1989, was undertaken to see if there actually is such displacement and if it is statistically significant. As supporting evidence, and recalling the 700-mb negative height anomaly reported by Douglas and Englehart (1981), 27 years of height and temperature data, from 1963 to 1989, from four constant pressure levels, were also examined to see if other levels showed a difference in height and temperature in El Niño years as opposed to other years. Analysis was again season by season, emphasizing comparison of El Niño and non-El Niño years. Other supporting data includes 850-mb level winds (23 years, 1967 to 1989) and sea-level pressure (43 years, 1947 to 1989). These results are presented in chapters 3 and 4. The area over which upper-level data was analysed is shown in Fig. 1.1.

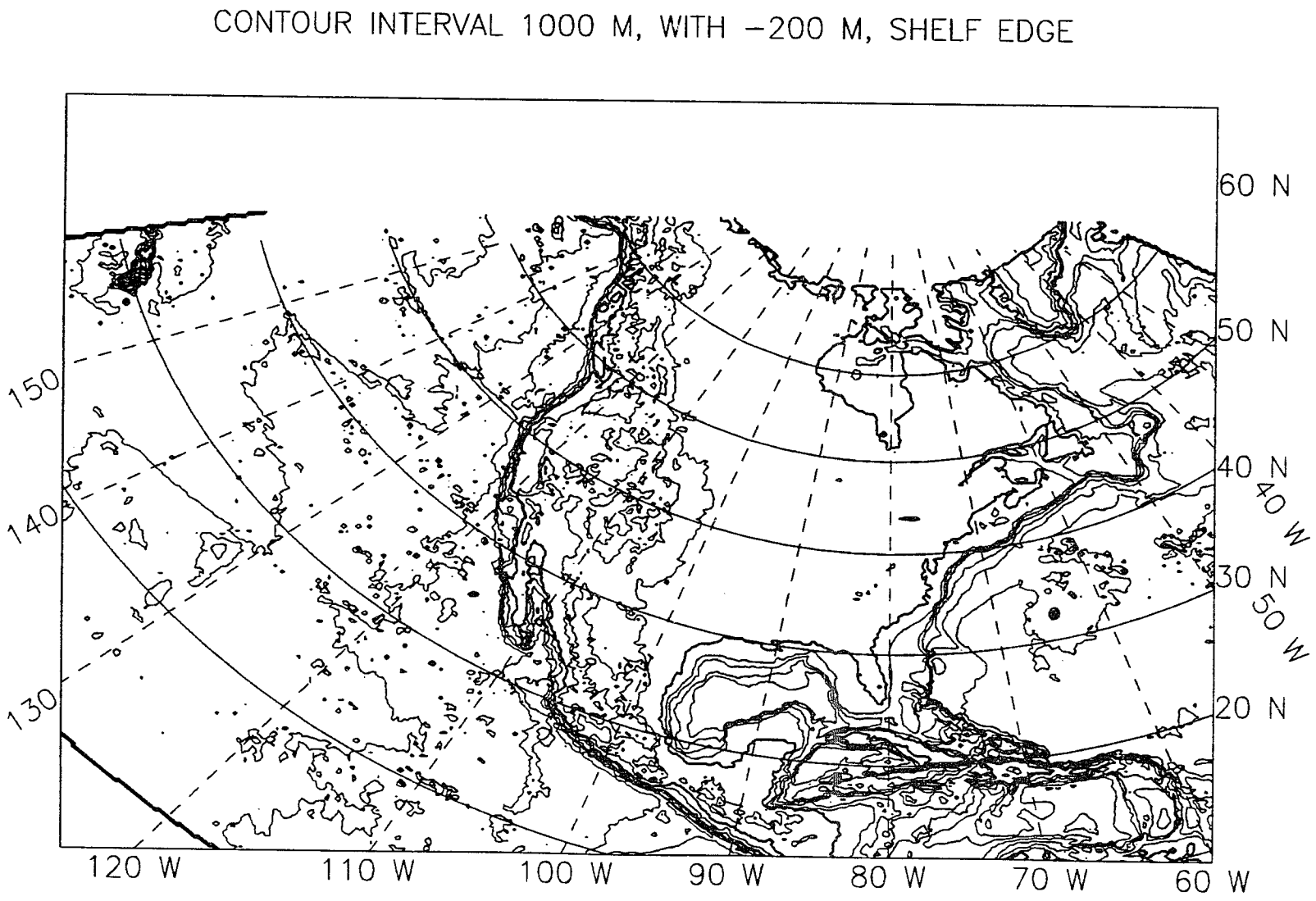

Figure 1.1: North America location map with elevation and bathymetry.

1.4 Units of Time

1.4.1 Winter Year and Seasons: Definitions and Naming Conventions

All analyses were done seasonally, using the four standard seasons. Winter is December-February; spring is March-May; summer is June-August; fall is September-November. Analyses were also done on an annual basis, which was not the calendar year. The 12-month period, from 1 September to 31 August, was chosen for annual calculations in an attempt to coincide with an average ENSO cycle, and to follow the cold-front season in the gulf region, since most cool-season storms in the region form in connection with the passage of a cold front. This 12-month period is here termed a 'winter year'. It resembles the 1 October to 30 September year recommended by Halpert and Ropelewski (1992) as well-suited to track ENSO cycles. The winter year is named according to the first four months. For example, winter year 1972 starts 1 September 1972, and ends 31 August 1973. The naming convention for standard winter seasons differs. Winter seasons take the year name of the included January and February. For example, winter 1973 consists of December 1972, January 1973, and February 1973. A third time unit was used, a six-month combination of winter and spring seasons, termed 'winter-plus-spring'. Named like a standard winter season, winter-plus-spring 1973, for example, runs from December 1972 to May 1973.

The correspondence is now described between the winter year and the method of counting ENSO time initiated by Rasmussen and Carpenter (1982), who studied ENSO events based on SST and surface winds in the Pacific, for the time period, 1854 to 1976. Rasmussen and Carpenter use three years per event. The year of the peak of the event is called 'year zero'. Months in year zero are denoted, for example, April(0). The year before the peak year is called year negative one. The year after

the peak year is called year one, and months are suffixed by (-1) and (1). September to December of the winter year are the last four months of their year negative one, which they call the Onset Phase. January to August of the winter year are in their year(0), which they call the Peak Phase. In the tropics, Rasmussen and Carpenter consider April(0) to be most representative of the Peak Phase, and December(-1) to best represent the Onset Phase. Winter season used in the present work thus includes December(-1), January(0), and February(0). Winter season, December to February, shows the most statistically significant, ENSO-related, weather effects in the gulf area. Therefore, the data and discussion presented in following chapters is focused on winter. Results from other seasons appear in the appendices.

1.5 Selection of El Niño and La Niña Years and Seasons

Since all analyses were done seasonally and annually (winter year), it was necessary to identify the seasons included in each El Niño and La Niña event. Tables 1.1 and 1.2 list the El Niño and La Niña seasons used in this work. Selection of particular seasons to include in the individual El Niño and La Niña events was done subjectively, by examination of seasonal plots of four indices of ENSO, and guided by published lists of El Niño and La Niña events. Events listed in the works of Quinn and Neal (1987) and Suppiah (1989) guided the selection of El Niño and La Niña seasons, respectively, from seasonal plots of published indices of ENSO made from data found in Parker (1983) and Wright (1989). Values of the Southern Oscillation index after 1983, not supplied in Parker's paper, were calculated directly from monthly average values of mean sea-level pressure at Tahiti and Darwin, Australia (National Climatic Data Center 1948-).

Table 1.1: El Niño seasons and winter years (1 September to 31 August) from 1851 to 1989, compiled from Wright's (1989) three indices of ENSO activity, the Southern Oscillation index (Parker, 1983), and the list of El Niño events published by Quinn and Neal (1987). Wright's indices are: the DT index, Darwin-Tahiti pressure; the SST index, central and eastern equatorial Pacific SST index; and the central equatorial Pacific islands rainfall index.

Int.*	Summer (Jun-Aug)	Fall (Sept-Nov)	Winter (Dec-Feb)	Spring (Mar-May)	Wnt+Spr (Dec-May)	Wyear (Sept-Aug)
W/M	1853	1853	1854	1854	1854	1853
M+	1857	1857	1858	1858	1858	1857
M	1860	1860	1860	1860	1860	1859
S	1864	1864	1865	1864	1865	1864
M	1866	1866	1866	1866	1866	1865
M	1868	1868	1868	1868	1868	1867
S+	1871	1871	1871	1871	1871	1870
M	1874	1873	1874	1874	1874	1873
VS	1877	1877	1877	1877	1877	1876
			1878	1878	1878	1877
M	1880	1880	1881	1881	1881	1880
S+	1884	1884	1885	1884	1885	1884
W/M		1887	1888	1888	1888	1887
	1888	1888	1889	1889	1889	1888
VS	1891	1891	1891	1891	1891	1890
M+	1896	1896	1897	1897	1897	1896
S	1899	1899	1900	1900	1900	1899
M+	1902	1902	1903	1902	1903	1902
W/M	1905	1905	1905	1905	1905	1904
M	1907	1907	1908	1907	1908	1907
S	1911	1911	1912	1911	1912	1911
				1912		
M+	1914	1914	1914	1914	1914	1913
S	1917	1917	1918	1918	1918	1917
W/M	1918	1918	1919	1919	1919	1918

Notes:

*: Intensity, from Quinn and Neal (1987). W - weak; M - moderate; S - strong; VS - very strong.

Table 1.1: continued.

Int.*	Summer (Jun-Aug)	Fall (Sept-Nov)	Winter (Dec-Feb)	Spring (Mar-May)	Wnt+Spr (Dec-May)	Wyear (Sept-Aug)
M	1923	1923	1924	1923	1924	1923
VS	1925	1925	1926	1926	1926	1925
W/M				1930		
	1930	1930	1931	1931	1931	1930
S	1932	1932	1932	1932	1932	1931
M+	1939	1939	1940	1940	1940	1939
S	1940	1940	1941	1941	1941	1940
	1941	1941				
M+	1943	1943	1944	1943	1944	1943
W/M	1951	1951	1952	1951	1952	1951
M+	1953	1953	1953	1953	1953	1952
S				1957		
	1957	1957	1958	1958	1958	1957
M+	1965	1965	1966	1966	1966	1965
S				1972		
	1972	1972	1973	1973	1973	1972
M	1976	1976	1977	1977	1977	1976
VS	1982	1982	1983	1983	1983	1982
M	1987	1987	1987	1987	1987	1986

Notes:

*: Intensity, from Quinn and Neal (1987). W - weak; M - moderate; S - strong; VS - very strong.

Table 1.2: La Niña seasons and winter years (1 September 1 to 31 August) from 1881 to 1989, compiled from Wright's (1989) three indices of ENSO activity, the Southern Oscillation index (Parker, 1983), and the list of La Niña events published by Suppiah (1989). Wright's indices are: the DT index, Darwin-Tahiti pressure index; the the SST index, central and eastern equatorial Pacific SST index; and the central equatorial Pacific islands rainfall index.

Summer (Jun-Aug)	Fall (Sept-Nov)	Winter (Dec-Feb)	Spring (Mar-May)	Wnt+Spr (Dec-May)	Wyear (Sept-Aug)
1882	1882	1882	1882	1882	1881
1886	1886	1887	1886	1887	1886
1889	1889	1890	1890	1890	1889
1893	1893	1894	1893	1894	1893
1898	1897	1898	1898	1898	1897
1903	1903	1904	1904	1904	1903
1909	1909	1910	1910	1910	1909
1916	1916	1917	1916	1917	1916
1921	1920	1921	1921	1921	1920
1924	1924	1925	1925	1925	1924
1933	1933	1934	1934	1934	1933
1938	1938	1939	1939	1939	1938
1959	1950	1950	1950	1950	1949
1955	1955	1956	1956	1956	1955
1961	1961	1962	1962	1962	1961
1962	1962	1963	1963	1963	1962
1964	1964	1965	1964	1965	1964
1968	1967	1968	1968	1968	1967
1971	1970	1971	1971	1971	1970
1973	1973	1974	1974	1974	1973
1975	1975	1976	1975	1976	1975
1988	1988	1989	1988	1989	1988
			1989		

1.5.1 ENSO Indices

The four indices of ENSO used are the Southern Oscillation index (Parker 1983) and three from Wright (1989): the DT index (also based on Darwin and Tahiti mean sea-level pressure), the SST index (based on central and eastern equatorial Pacific SST) and the rainfall index (based on central equatorial Pacific islands rainfall). All four indices agree well. Fig. 1.2 shows the Southern Oscillation index, plotted for the winter years 1936 to 1988. Winter years selected as El Niño years are marked by solid vertical lines; La Niña winter years are shown by dotted lines. Figs. 1.3, 1.4, 1.5, 1.6, 1.7, and 1.8 show Wright's DT index plotted seasonally from 1851 to 1984, with solid and dotted vertical lines marking El Niño and La Niña seasons, respectively. The two other indices, the SST and rainfall indices, appear in appendix R. A bold number next to a point in Figs. 1.3 to 1.8 indicates that season is part of an El Niño or La Niña event. The intensity of the El Niño events, after Quinn and Neal (1987), is listed at the bottom. The season is named at the top. Note that the DT index is calculated such that positive and negative (or high and low) values are opposite to the Southern Oscillation index. For example, El Niño events are characterized by very low or negative values of the Southern Oscillation index, but by very high or positive values of the DT index. This construction of the DT index, which postdates the Southern Oscillation index, facilitates visual comparison. The DT index has the longest record, about 40 years longer than Wright's other two indices, and about 85 years longer than the Southern Oscillation index. All three of Wright's indices stop in 1984. For reference, Figs. 1.3 to 1.8 list Quinn and Neal's (1987) events at the top. Quinn and Neal's events are in calendar years. This is the source of any apparent discrepancy between Quinn and Neal's events and the seasons selected for use here.

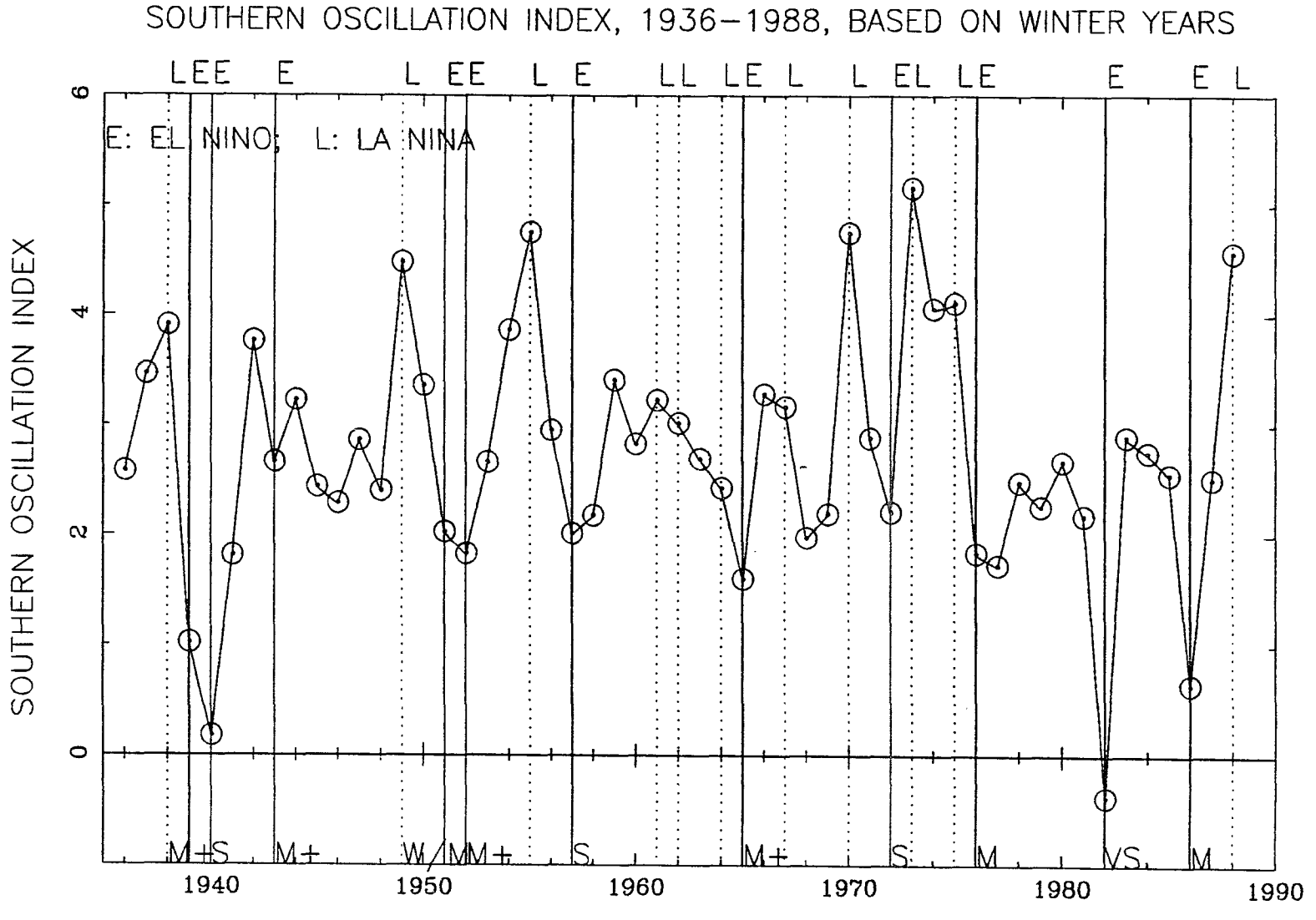

Figure 1.2: Southern Oscillation index by winter years, 1936–88.

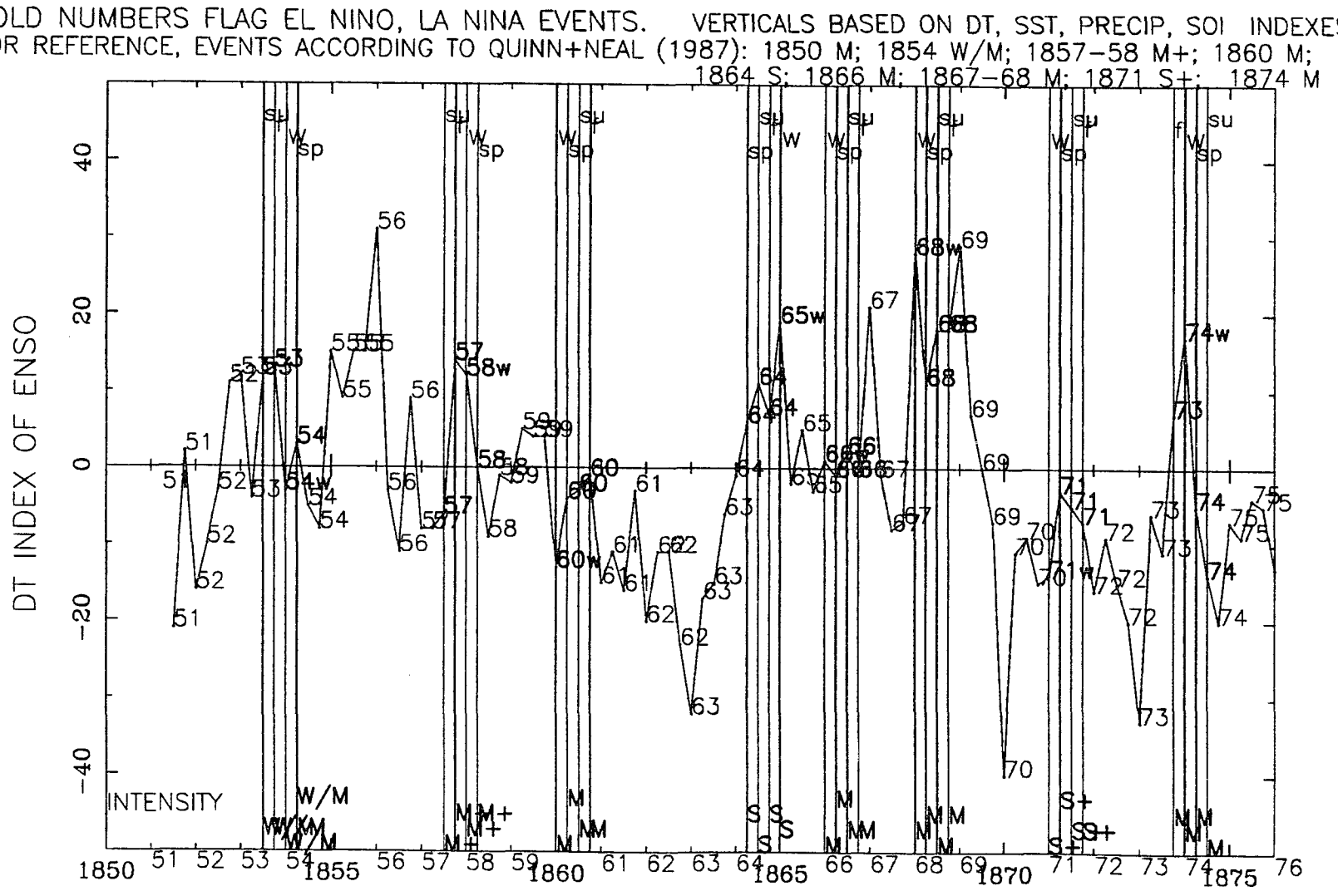

Figure 1.3: DT index (Wright 1989) of ENSO for consecutive seasons, 1851–75. Solid vertical lines mark El Niño seasons; dotted lines mark La Niña seasons.

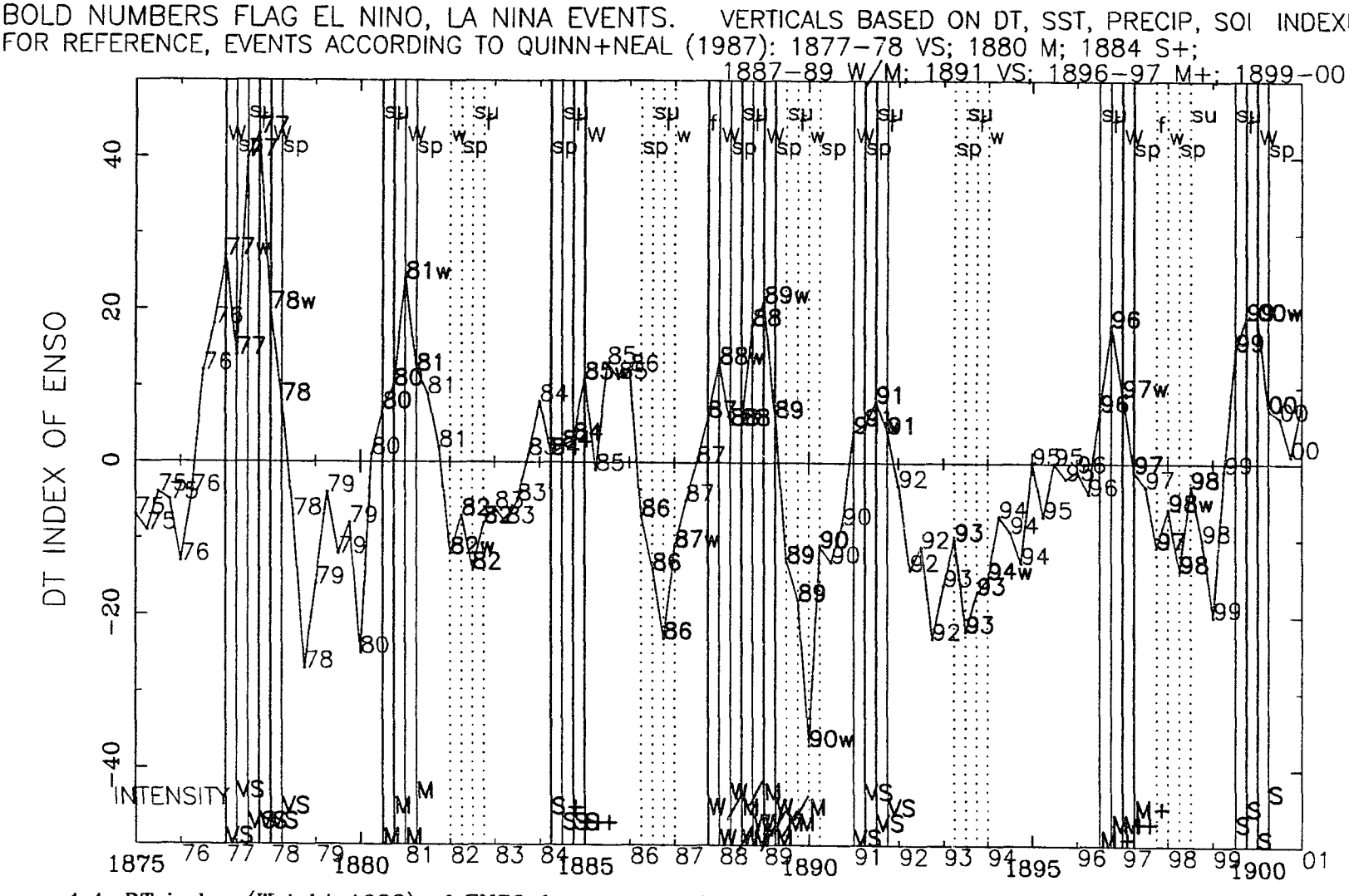

Figure 1.4: DT index (Wright 1989) of ENSO for consecutive seasons, 1875–1900. Solid vertical lines mark El Niño seasons; dotted lines mark La Niña seasons.

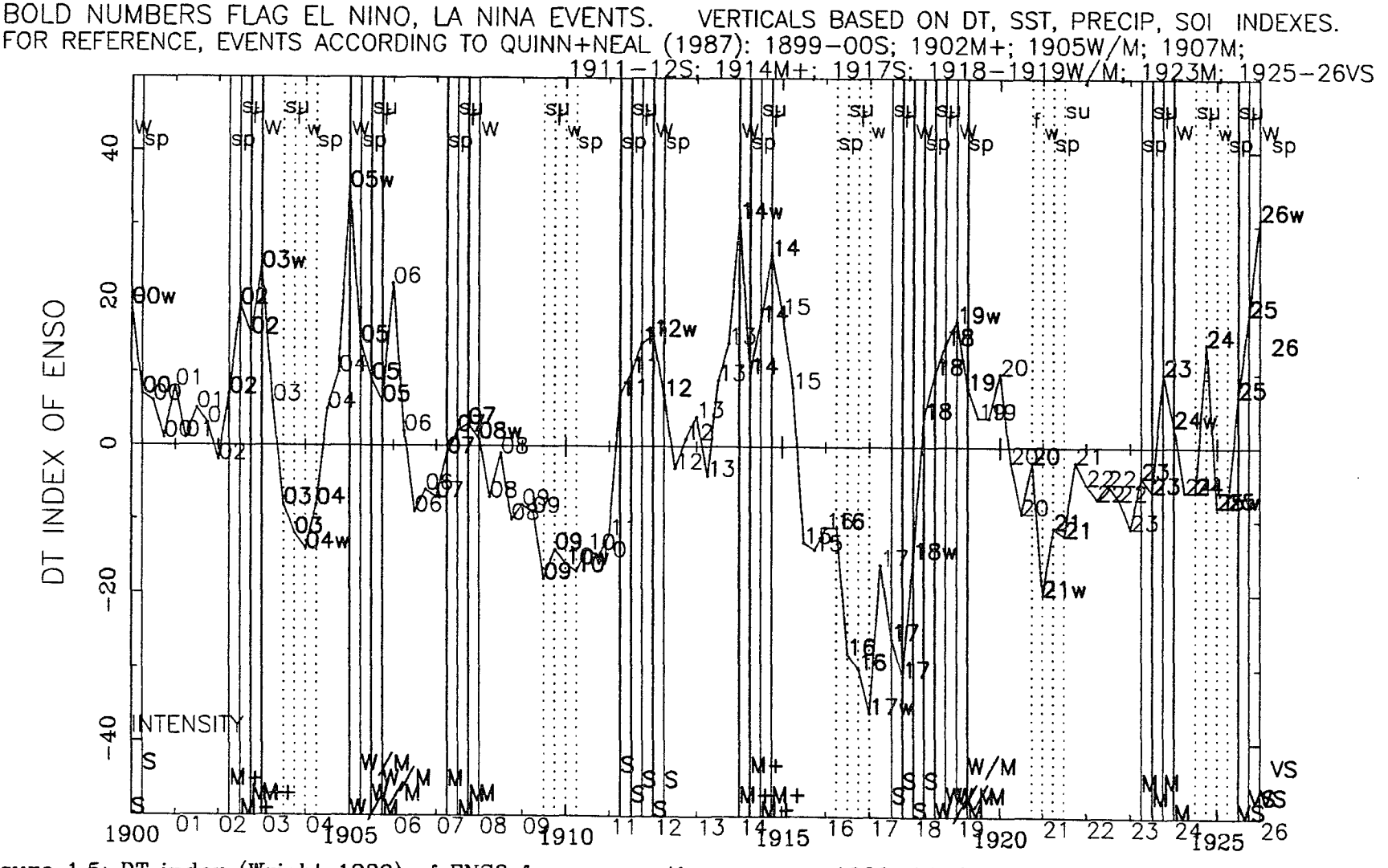

Figure 1.5: DT index (Wright 1989) of ENSO for consecutive seasons, 1900–25. Solid vertical lines mark El Niño seasons; dotted lines mark La Niña seasons.

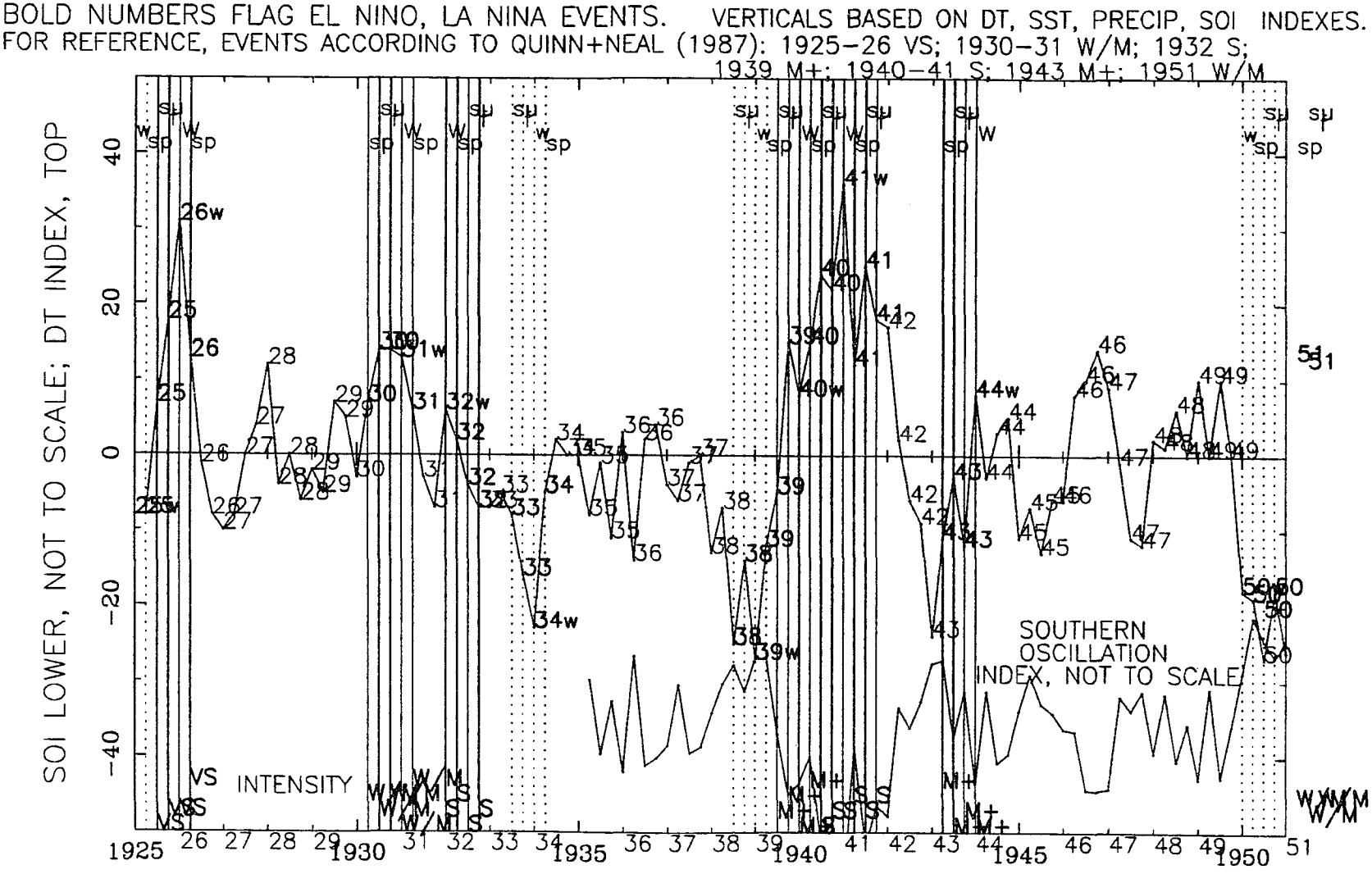

Figure 1.6: DT index (Wright 1989) of ENSO for consecutive seasons, 1925–50. Solid vertical lines mark El Niño seasons; dotted lines mark La Niña seasons.

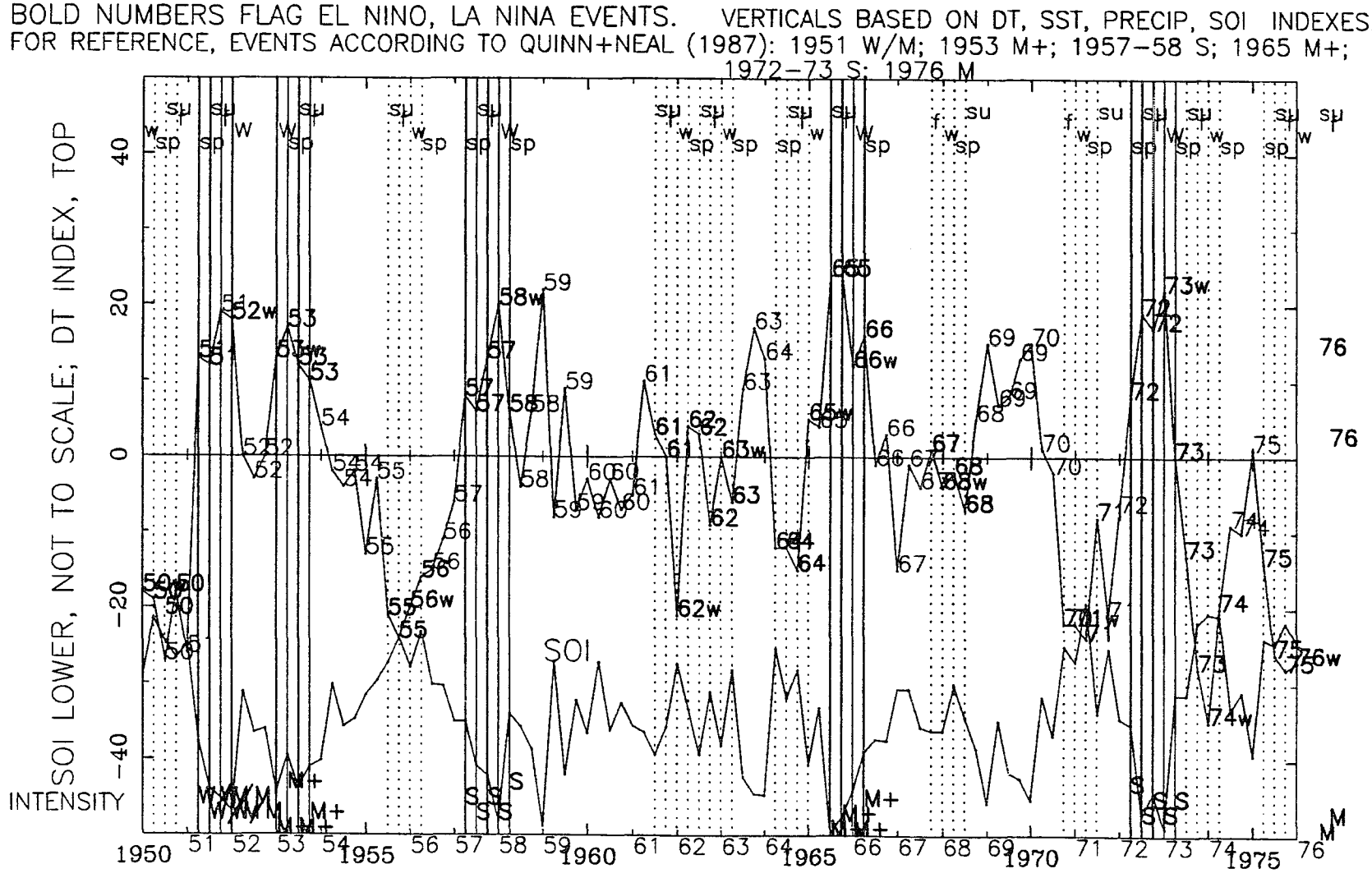

Figure 1.7: DT index (Wright 1989) of ENSO for consecutive seasons, 1950–75. Solid vertical lines mark El Niño seasons; dotted lines mark La Niña seasons.

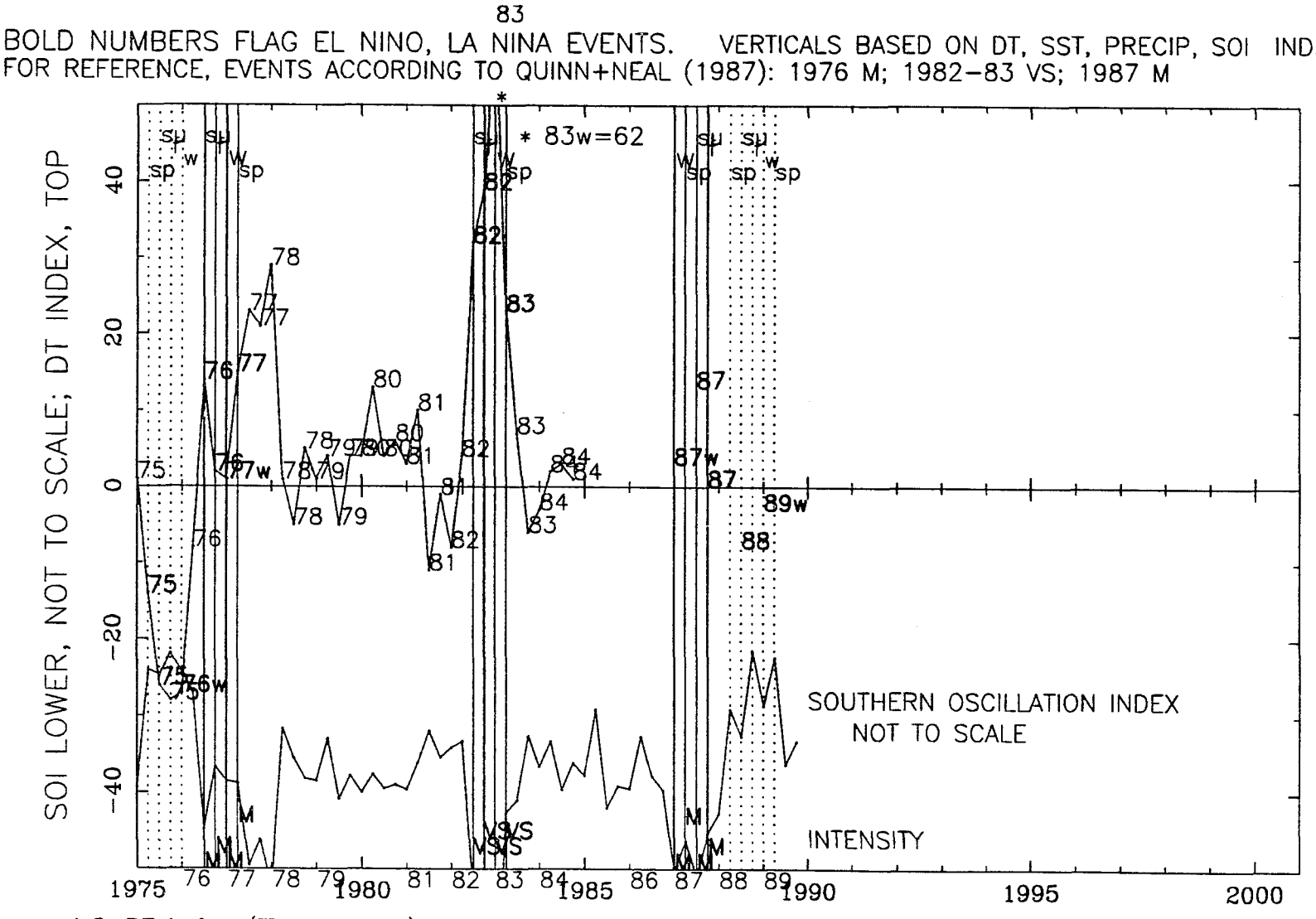

Figure 1.8: DT index (Wright 1989) of ENSO for consecutive seasons, 1975–84. Solid vertical lines mark El Niño seasons; dotted lines mark La Niña seasons.

1.5.2 Procedure for Selecting Seasons

The values of the indices and the published lists were the primary guides. Selected as El Niño and La Niña seasons are those having appropriate values of the indices that fell within or near to Quinn and Neal's events. Values of the index were honored over a literal interpretation of Quinn and Neal's listed events, which are in calendar years. Some of Quinn and Neal's events, as listed, were a season off from the low point on the Southern Oscillation Index. In these cases, the index was honored. The general model used for picking seasons as El Niño was that an event would probably start in spring or summer and be four to six seasons long. The technique was, generally, to select all seasons included in the spikes on the indices, between inflection points. This assumes that the indices are synchronous with the ENSO events. According to the indices, most La Niña events nearly coincided with calendar years, beginning in December. This picks a shorter, and more variable-length ENSO event than Rasmussen and Carpenter's method, (1982) which is to examine always three years, essentially, before, during, and after. This method, while computationally convenient, encounters a problem with artifactual overlap of back-to-back events, such as an El Niño followed by a La Niña. To avoid this, workers studying both types of events often confine their study to one or two seasons, such as winter and spring.

1.5.3 Winter-Plus-Spring: Combination Season

For the composite season, winter-plus-spring, the indices were replotted using the six-month averages and composite seasons were selected independently. In seven cases from 1851 to 1989, this caused a winter-plus-spring season to be selected as El Niño that included a 'trailing' spring which had not been included in the El Niño event on its own. These seven cases occurred before 1953, affecting the winter-plus-

spring combination of only the longest-term analyses. These are the precipitation and temperature data, and the mean sea-level pressure and 500-mb level height data; the last two start in 1946. Five La Niña winter-plus-springs, between 1881 and 1989, included such 'trailing' springs. Two of these fell within the time span of the upper-level data and of the surface data. No La Niña, winter-plus-spring results are presented for upper-level data.

CHAPTER 2
SURFACE ANALYSES

To test the hypothesis that more frontal-wave cyclones form over the Gulf of Mexico and surrounding coastal plain during El Niño years than during other years, three data sets will be examined. The first consists of frontal-wave cyclone and cold-front occurrences subjectively counted from Northern Hemisphere or North American daily, surface weather maps for the 30-year period, September 1960 to August 1990 (United States Department of Commerce September 1960; September 1970).

In chapter 5, storm and cold-front counts for the last 50 years are presented (United States Weather Bureau September 1940; Headquarters, Air Weather Service, October 1945). The results of only the last 30 years are emphasized in the remainder of this work because dynamic information used to explain the trends in the occurrence of storms, that is, upper-level winds, heights, and temperatures, is generally complete and of broad coverage for only the last 25 to 30 years. The results of only the last 30 years may still be significant. Justification for using 30 years as a standard climatological period is provided by Kunkel and Court (1990).

The second data set consists of twice-daily observations of gulf-region weather type (Muller 1961-, 1977) from January 1961 to August 1990. The third data set is composed of records of monthly average temperature and monthly total precipitation from 15 gulf-region, single, land stations and from eight gulf-area, climatic divisions. Periods of record vary; the average length is about 100 years. All single-station records used stop in 1980 but start at different times. Climatic-division records are all from 1895 to 1989. Each of the three data sets will now be described and results presented.

2.1 Storm and Cold-Front Counts: 1960-89

2.1.1 Frontal-Wave Cyclone Description

The storms referred to here as frontal-wave cyclones are the relatively small-scale, 75 to 175 km (45 to 110 mi) diameter, secondary or daughter cyclones that form 'piggyback' on cold fronts traversing the region from northwest to southeast during fall, winter, and spring. The cold fronts themselves are part of large, synoptic-scale, migratory, extratropical cyclones which track across North America from west to east in the prevailing westerlies. Collectively, the larger, 'parent' cyclones, together with the smaller, 'daughter' cyclones have been called a 'family of wave cyclones' (Petterssen 1958). Gulf-area storm formation and cold-air outbreak both peak in the winter months, December, January, and February, Figs. 2.1 and 2.2. The frontal-wave cyclones generated in the gulf region are an order of magnitude smaller than the parent cyclones, yet are important locally, forming the bulk of winter and spring precipitation. Hurricanes, tropical storms and depressions, and warm season, transient, localized, mesoscale, convective systems are not included in the study.

The storms typically form when a cold front from the north becomes stationary, frequently just as the front passes over the relatively warm water of the gulf. About half of the 524 storms counted during the 30 years formed over water, Fig. 2.3. The frontal-wave cyclones generally track to the northeast and have a one- to three-day duration. Some, however, such as the Presidents' Day cyclone of 18-19 February 1979, the *Scamp* storm of 23 February 1987, and the epic storm of 12-14 March 1993, may continue up the U.S. east coast, intensifying and attaining major storm status (Uccellini et al. 1984; Reed and Stoelinga 1992). Because of their close association with the storms, and because of their own potential impact on coastal

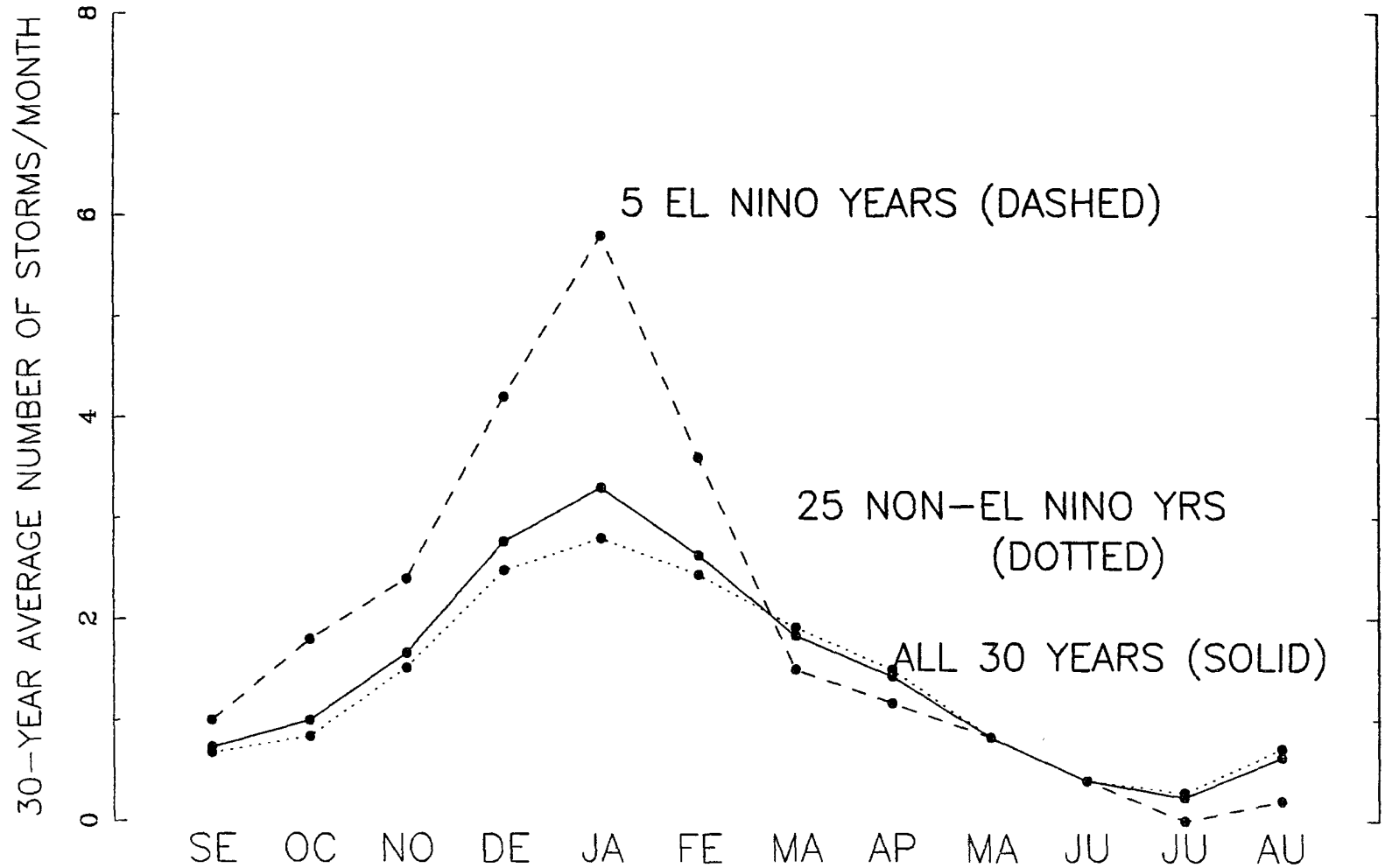

Figure 2.1: 30-year average number of storms/month, 1960-89, El Niño, non-El Niño, and all years.

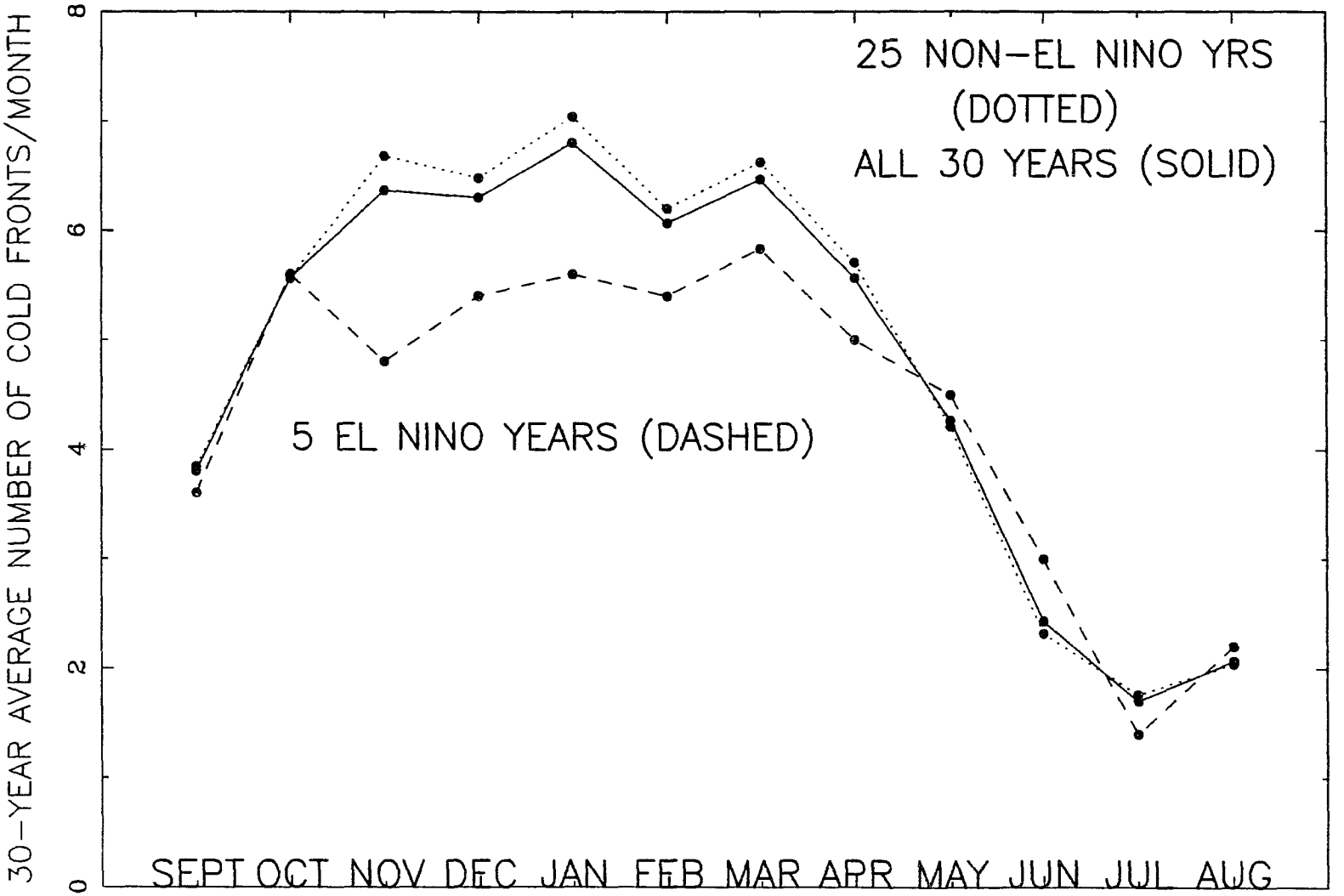

Figure 2.2: 30-year average number of cold fronts per month, 1960-89, El Niño, non-El Niño, and all years.

geomorphology (Roberts et al. 1987, 1989), a count was also made of the cold fronts reaching the region, and so, of the number of cold-air outbreaks occurring. Due to the diverse origins and histories of the cold-air masses coming to the area, and to the greater subjectivity of such a count, the cold-front data collected is inherently more heterogeneous and difficult to interpret than the storm data. Less emphasis is placed on these results because of the fairly wide margin of uncertainty associated with the cold-front counts.

2.1.2 Method of Counting Frontal-Wave Cyclones

A storm was counted if it originated over the gulf or the surrounding coastal plain. A storm was also counted if it originated elsewhere, if the center of low pressure subsequently came within the geographic region of study. The latter case is much less common. For example, given a window of 80° to 100°W and 17° to 33°N, only seven of the 524 storms counted from 1960 to 1989 originated outside of the window. The restriction that the central low had to come within the coastal plain or gulf ensures that extratropical storms originating elsewhere are nearly excluded from the data set. Some of these may influence the northern part of the area, but they were not counted. This was done because the desired emphasis is on the gulf region and cyclogenesis there in El Niño years.

To be accepted, a storm had to have the following characteristics.

1. A central trough of low pressure was required. Although some workers have more-stringently required a closed isobar (Whittaker and Horn 1982; Bell and Bosart 1989; Gan and Rao 1991), in this work, a closed isobar was not required for two reasons. First, regarding the the 24-hour map interval, it was assumed that if all other requirements were met, it was likely that a more-frequent map interval would show a closed isobar. A second reason for

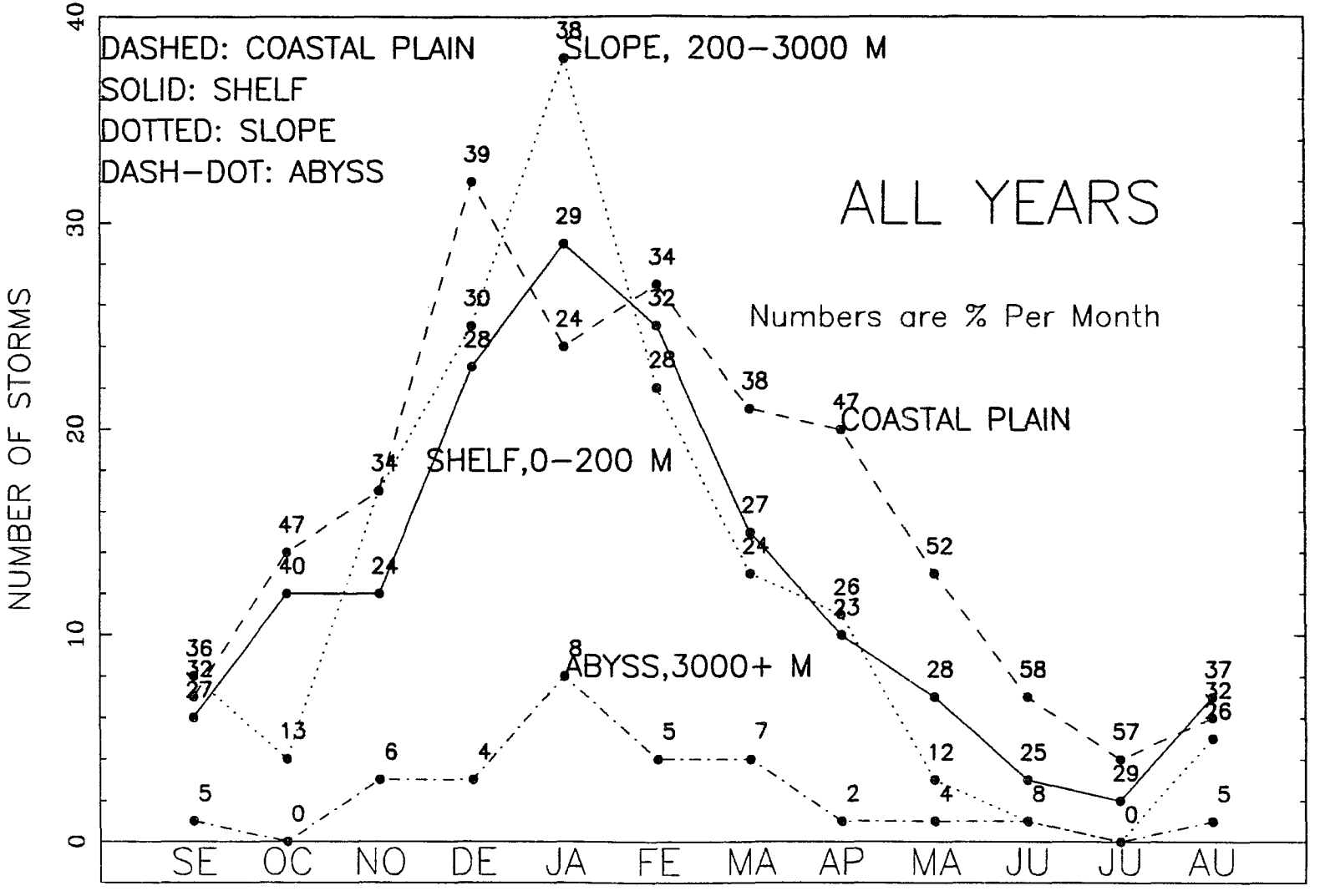

Figure 2.3: Storms/month, by water depth, Sept. 1960 – Aug. 1990, all years.

not requiring a closed isobar is that, in doing so, one accepts the map as completely correct. It was thought prudent to regard the analyses (maps) produced by the National Meteorological Center (NMC) analysts as a 'best guess', allowing perhaps a 10 to 20% margin of uncertainty, in view of the rather sparse data over water and south of the U.S. border.

2. Either a well developed warm front and cold front, or one of the preceeding with a stationary front in place of the other was required. The reasons for this rather loose requirement are the same as in number one above, with the added reason that much variability in storm structure exists, not all storms conforming to the ideal, Bjerknes model (Reed 1990).

Every attempt was made to determine the day and place of origin as closely as possible, recognizing the limitations of a 24-hour map. Origination of a storm was traced as far back in time as possible without ambiguity, to the first sign of disturbance. At times, this meant identifying a hook in a stationary front as the point of origin. When fast-moving lows were tracked by NMC analysts, and their position marked every six hours, the first mark was used. Locations were determined to a half degree, a precision judged appropriate considering other sources of error.

The lowest central pressure recorded at map time during the life of a storm was also noted. In most cases, this occurred on the first day the storm appeared on the map, degeneration occurring within one or two days. In cases where the storm did not decay quickly, but continued to deepen and traveled out of the region, the lowest pressure used was that attained while within the gulf area, again to emphasize gulf-region trends over those in other areas.

2.1.3 Method of Counting Cold Fronts

To determine the frequency of cold-air outbreak, each cold front reaching the gulf or coastal plain was counted, the cold fronts indicated on the daily weather maps being used as 'markers' of individual cold-air outbreaks. In counting the cold fronts, emphasis was again placed on the gulf region. Every cold front, identified on the daily weather map, that intersected the region was counted, regardless of its origin and previous history. This has the disadvantage of mixing cold-air influxes of diverse character. The advantage of such an indiscriminate count is that it yields maximum information about the gulf region. From the local perspective, one would like to know how many cold-air outbreaks occur per season or year, or, as these are referred to locally, how many cold fronts are there? Even fronts that did not cross the coast were counted because of their potential to generate storms, or at least to cause significant cloudiness and precipitation over the coastal plain. The date of crossing was taken as the date of the first map showing any part of the front intersecting or past the coastline.

2.1.4 Problems with the Daily Weather Map

The data set so compiled contains some subjectivity and some weaknesses inherent in relying on the daily weather map. One problem has already been indirectly mentioned. That is the use of a 24-hour map interval to study storm events of one- to three-day duration. Because of their greater persistence, the count of cold fronts was less affected by the map interval.

A more serious problem concerns the skill of the NMC analysis itself. Sparsity of data over water and south of the U.S. border must adversely affect the analyses. Regarding techniques, Janish and Lyons (1992) have examined NMC analyses and forecasts during several cold-air outbreaks over the Gulf of Mexico. They note

some low-level moisture errors, possibly resulting, they suggest, from inadequate boundary-layer physics in NMC models being used at the time. In the time following cold-air outbreaks, Janish and Lyons found that NMC forecasts over the gulf were too dry. Although they find several problems with various forecasts, Janish and Lyons find fewer problems with analyses. The daily weather maps used here are analyses, prepared after-the-fact, not forecasts. Further explanation of the difference between analyses and forecasts appears in 3.1. For the limited use made of analyses here, to obtain a simple count of events, it was judged that the advantages of using the daily weather map outweigh the disadvantages. First, the maps are widely available, free of charge, at U.S. Government Documents Depositories, and other investigators will have access to this data for review. Second, use of a 24-hour map allows coverage of a long time period fairly rapidly. Some precedent exists for using once-daily weather maps to count storms (Hanson and Long 1985; Saucier 1949).

2.1.5 Results of Frontal-Wave Cyclone and Cold-Front Counts

Figs. 2.4 and 2.5 show the number of frontal-wave cyclones occurring seasonally and per winter year for 1960 to 1989. Figs. 2.6 and 2.7 show the same for cold fronts. The rank sum test was used to determine if there was a statistically significant difference between the number of frontal-wave cyclones generated and cold fronts incident in El Niño years as opposed to all other years. The same was done for La Niña years. The results of the rank sum test are presented in Table 2.1, for El Niño years against all other years. Table 2.2 shows La Niña years versus all other years. A brief explanation of the rank sum test is in 2.1.6.

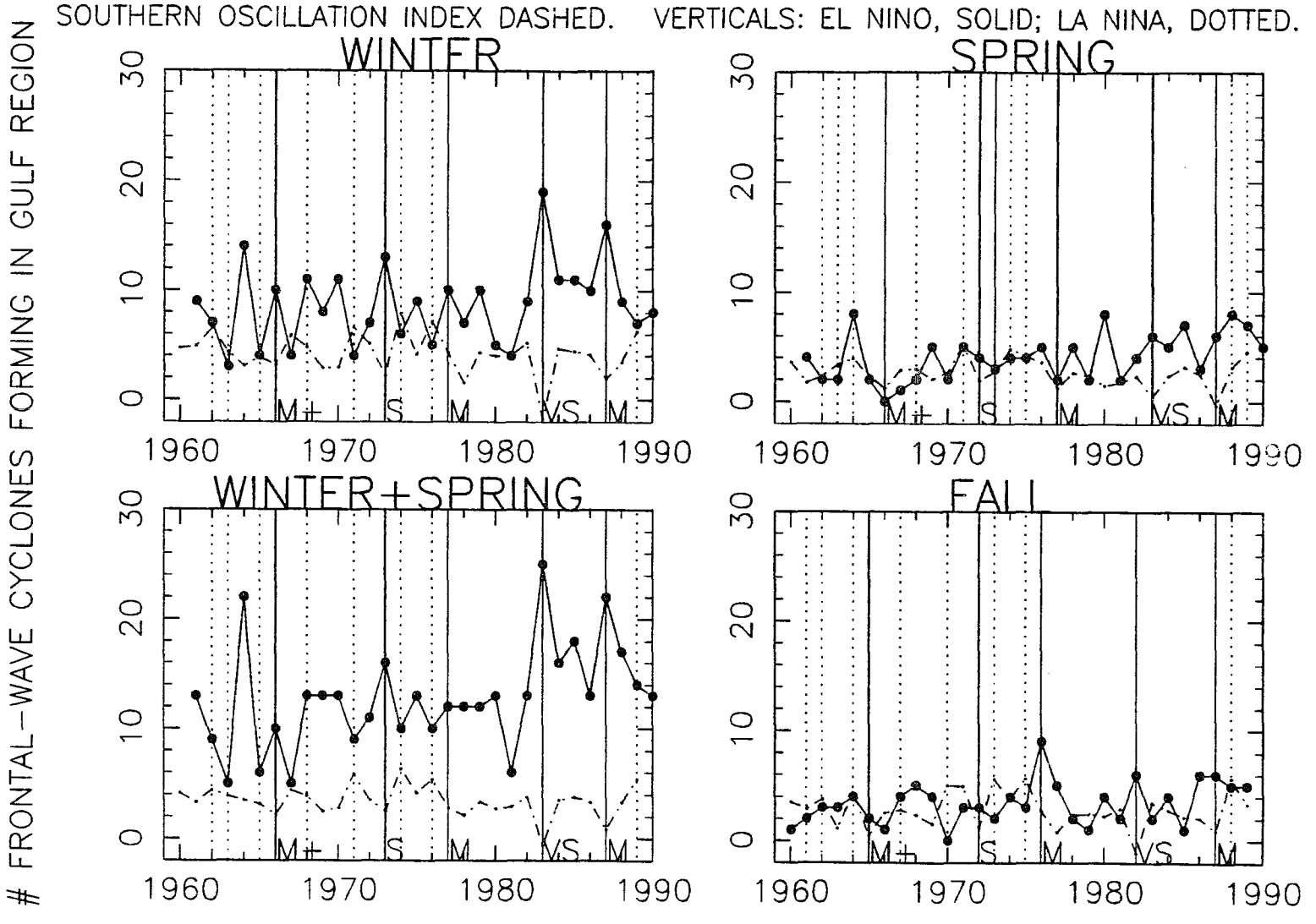

Figure 2.4: Number of frontal-wave cyclones by season, 1960-89.

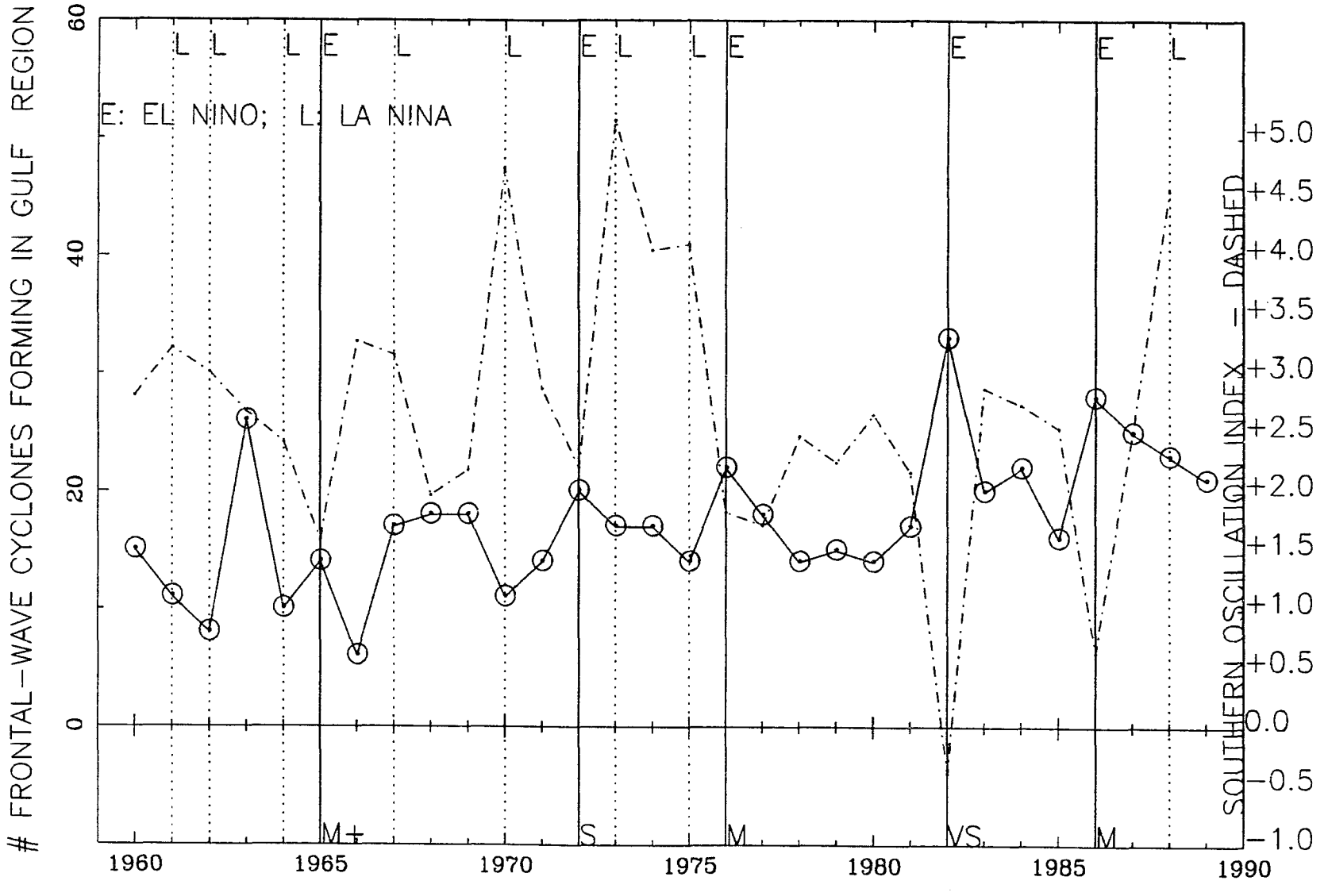

Figure 2.5: Number of frontal-wave cyclones per winter year, 1960-89.

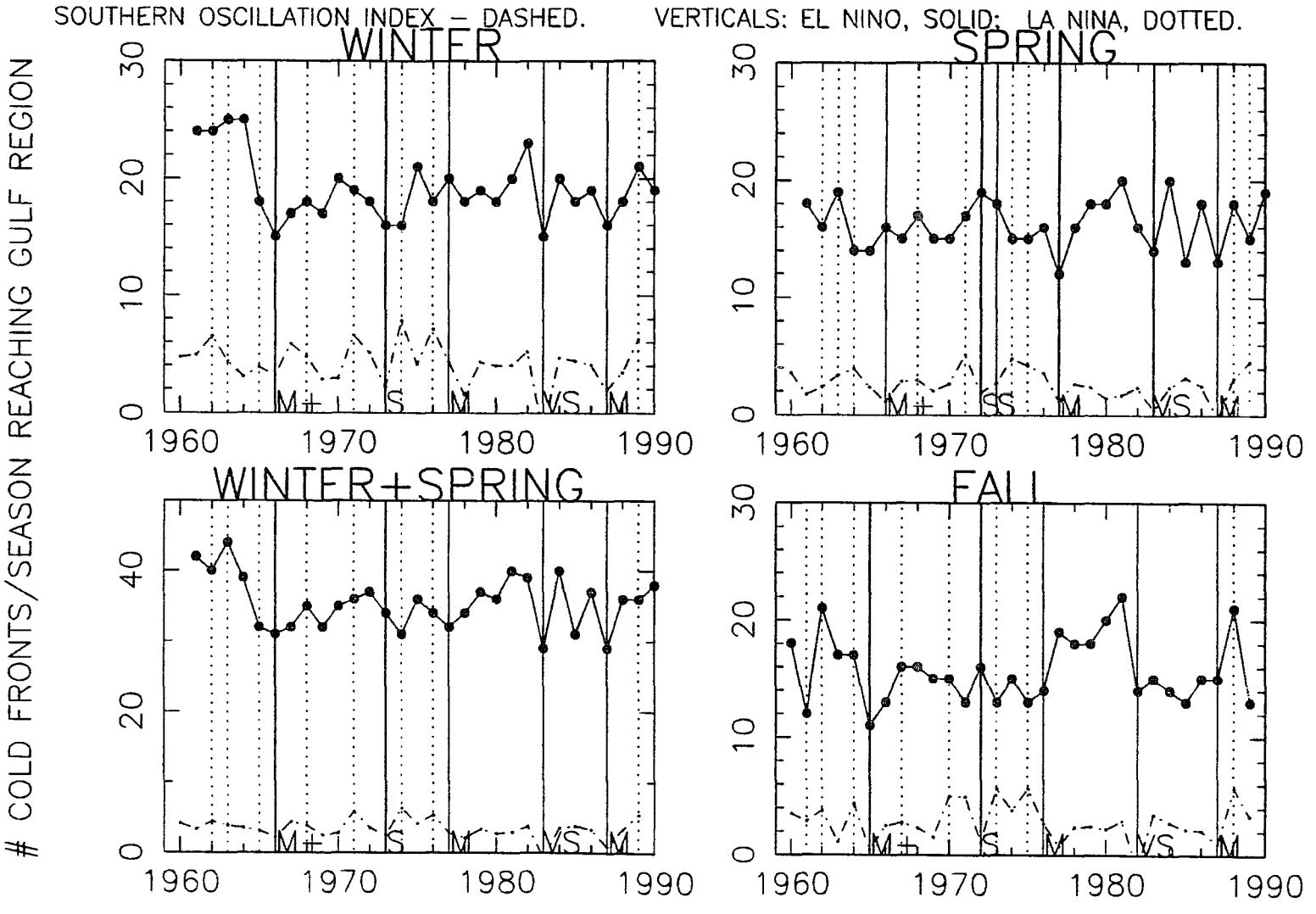

Figure 2.6: Number of cold fronts reaching gulf area, by season, 1960–89.

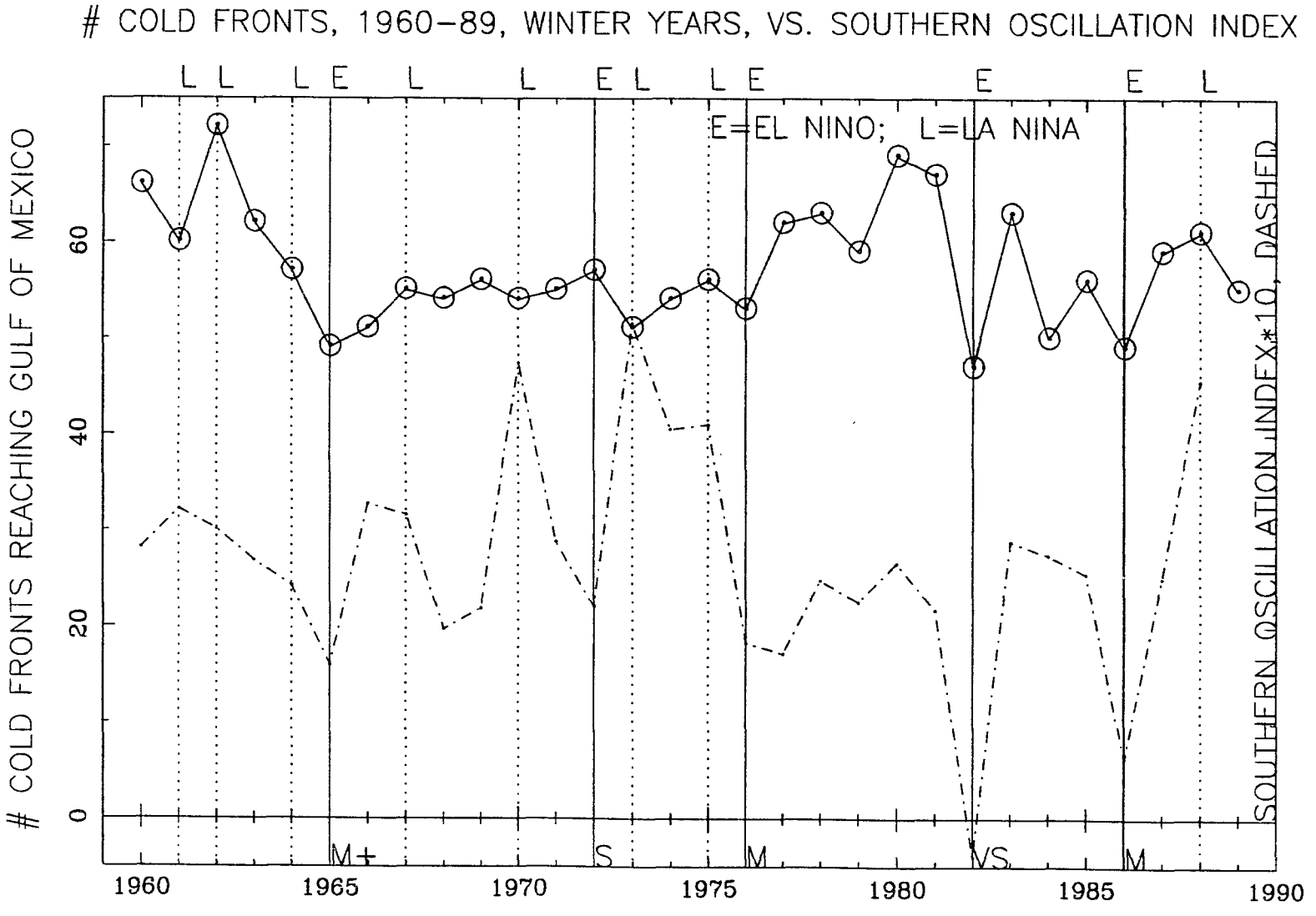

Figure 2.7: Number of cold fronts reaching gulf area per winter year, 1960–89.

Table 2.1: Frequency of frontal-wave cyclones, cold fronts, and hurricanes in El Niño years, 1960-1989. Results of the rank sum test, also known as the U-test, Wilcoxon test, or Mann-Whitney test, for differences between El Niño and all other years. z-Values, or T2-values if the number of observations is less than or equal to 30, are used in testing the hypothesis that values for the listed parameters vary between El Niño and other years. z-values are provided for inspection only when there are less than 31 observations. Two levels of significance are indicated by daggers: $\alpha = .01$, double dagger and $\alpha = .05$, single dagger. For the hurricane data, reject the null hypothesis at the .01 confidence level if $z > 2.575$ or $z < -2.575$, and reject it at the .05 level if $z > 1.960$ or $z < -1.960$.

Season	Time	z	T2 §	# Events El/Other	Means El Niño	Means Other
Frontal-Wave Cyclones						
winteryear †	1960-89	1.984	42	5/25	23	16
winter+spring	1961-90	1.441	52	5/25	17	12
winter ‡	1961-90	2.771	28	5/25	14	8
spring	1961-90	-0.527	83	6/24	4	4
summer	1961-90	-1.219	57	5/25	1	1
fall	1960-89	1.747	47	5/25	5	3
Cold Fronts						
winteryear ‡	1960-89	-2.621	31	5/25	51	59
winter+spring ‡	1961-90	-2.910	26	5/25	31	36
winter †	1961-90	-2.536	33	5/25	16	20
spring	1961-90	-1.049	73	6/24	15	17
summer	1961-90	0.423	70	5/25	7	6
fall	1960-89	-1.292	55	5/25	14	16
Hurricanes and Tropical Storms						
entering gulf/winteryr ‡	1886-1988	-3.894		27/76	3	4
originate gulf/winteryr	1886-1988	-1.052		27/76	1	1
entering gulf/calendryr	1886-1988	-1.637		28/76	3	4
originate gulf/calendryr	1886-1988	-0.211		28/76	1	1

Notes:

§: T2 = Number of X observations * (Number of X observations + Number of Y observations + 1) - Sum of the ranks of the X observations. The X observations are the smaller set, the El Niño or La Niña years.

‡ : indicates null hypothesis can be rejected at the .01 level of significance.

† : indicates null hypothesis can be rejected at the .05 level of significance.

Table 2.2: Frequency of frontal-wave cyclones, cold fronts, and hurricanes in La Niña years, 1960-89; results of the rank sum test, also known as the U-test, Wilcoxon test, or Mann-Whitney test, a test for differences between La Niña and other years; z-values, and T2-values when the number of observations is less than 30, are used in testing the hypothesis that values for the listed parameters vary between La Niña and other years. z-values are provided for inspection only when there are less than 31 observations. Two levels of significance are indicated by daggers: $\alpha = .01$, double dagger and $\alpha = .05$, single dagger. For the hurricane data, reject the null hypothesis at the .01 confidence level if $z > 2.575$ or $z < -2.575$, and reject it at the .05 level if $z > 1.960$ or $z < -1.960$.

				# Events	Means	
Season	Time	z	T2 §	La/Other	La Niña	Other
Frontal-Wave Cyclones						
winteryear †	1960-89	-2.119	79	8/22	14	19
winter+spring †	1961-90	-2.428	73	8/22	10	14
winter ‡	1961-90	-2.642	68	8/22	6	10
spring	1961-90	0.690	125	9/21	5	4
summer	1961-90	-0.660	111	8/22	1	1
fall	1960-89	-0.689	110	8/22	3	4
Cold Fronts						
winteryear	1960-89	0.376	116	8/22	58	57
winter+spring	1961-90	0.141	121	8/22	36	35
winter	1961-90	0.641	111	8/22	20	19
spring	1961-90	-0.206	135	9/21	16	16
summer	1961-90	-0.880	106	8/22	6	6
fall	1960-89	0.047	123	8/22	16	16
Hurricanes and Tropical Storms						
entering gulf/winteryr	1886-1988	0.355		21/82	4	4
originate gulf/winteryr	1886-1988	-0.416		21/82	1	1
entering gulf/calendryr	1886-1989	1.529		21/83	4	3
originate gulf/calendryr	1886-1989	-0.593		21/83	1	1

Notes:

§: T2 = Number of X observations * (Number of X observations + Number of Y observations + 1) - Sum of the ranks of the X observations. The X observations are the smaller set, the El Niño or La Niña years.

‡ : indicates null hypothesis can be rejected at the .01 level of significance.

† : indicates null hypothesis can be rejected at the .05 level of significance.

2.1.6 Rank Sum Test for Differences between Two Groups

The rank sum test, also called the U-test, Wilcoxon test, or Mann-Whitney test (Hoel 1962; Snedecor and Cochran 1980; Miller and Freund 1985) is basically a test of the hypothesis that the means of two groups differ significantly. In this case, it tests whether or not the mean of the number of frontal-wave cyclones per season in El Niño years differs from the mean number of frontal-wave cyclones per season in non-El Niño years. Parallel tests comparing La Niña years to non-La Niña years were also done. For a sample size greater than 30 (Snedecor and Cochran 1980) the result of the rank sum test is a z-value that can be referred to a table of the probability values of the normal distribution function. For a given level of significance, α , the null hypothesis can be rejected if the calculated z for a random variable exceeds a certain critical value. This is then the confidence level at which one's assertion, or the alternative hypothesis that the means actually differ, is correct. When sample size is less than or equal to 30, and the two groups being compared are of unequal size, as here, Snedecor and Cochran (1980) recommend calculating an additional statistic, T2, which also depends on sample size, and using it in place of z-values. The T2 statistic is defined as

$$T2 = \#X observations \times (\#X observations + \#Y observations + 1) \qquad (2.1)$$

$$- Sum\ of\ the\ ranks\ of\ the\ X\ observations.$$

The X observations are the smaller set, the El Niño or La Niña years. Tables for evaluation of the T2 statistic are available in Snedecor and Cochran (1980) for the .01 an .05 confidence levels. Additional tables for confidence levels up to .20 are available in Verdooren (1963). The International Library of Mathematics and Statistics (IMSL) subroutine, RNKSM, was used for the rank sum test, with enhancements as needed (IMSL 1987).

Inspection of the relative magnitude of parameter means for El Niño years as opposed to other years aids physical interpretation of rank sum test results. For example, from Table 2.1, the mean of the number of storms per winter year in El Niño years is 23 versus 16 in all other years. The T2 value, 42, passes as significant at the .05 confidence level, from reference to the tables. In this case of a sample size of 30, there are almost enough values to use the z statistic, and so the z-values look reasonable. Later, in the 50-year storm and cold-front counts in chapter 5, z-values will be used, so an example of their interpretation follows. The z-value for storms per winter year from Table 2.1 is positive 1.984, significant at the .05 level, according to z-tables. This says that in the 30 years analyzed, there are *more* frontal-wave cyclones in El Niño years than in non-El Niño years. If the z-value were negative, this would have indicated *fewer* storms in El Niño years than in non-El Niño years.

2.1.7 Summary of Frontal-Wave Cyclone and Cold-Front Results

Fig. 2.8 summarizes the storm and cold-front results for winter years. El Niño winters and winter years have more storms than their counterparts in other years, significant at the .01 and .05 confidence levels, respectively, by the rank sum test. El Niño winters, winter years, and winter-plus-springs have statistically significantly fewer cold fronts, at the .01 or .05 confidence levels, than their counterparts in other years. La Niña winters, winter-plus-springs, and winter years have fewer storms, significant at the .01 or .05 confidence levels, than their counterparts in other years. The number of cold fronts did not differ significantly, by the rank sum test, betwen La Niña and non-La Niña years in any season.

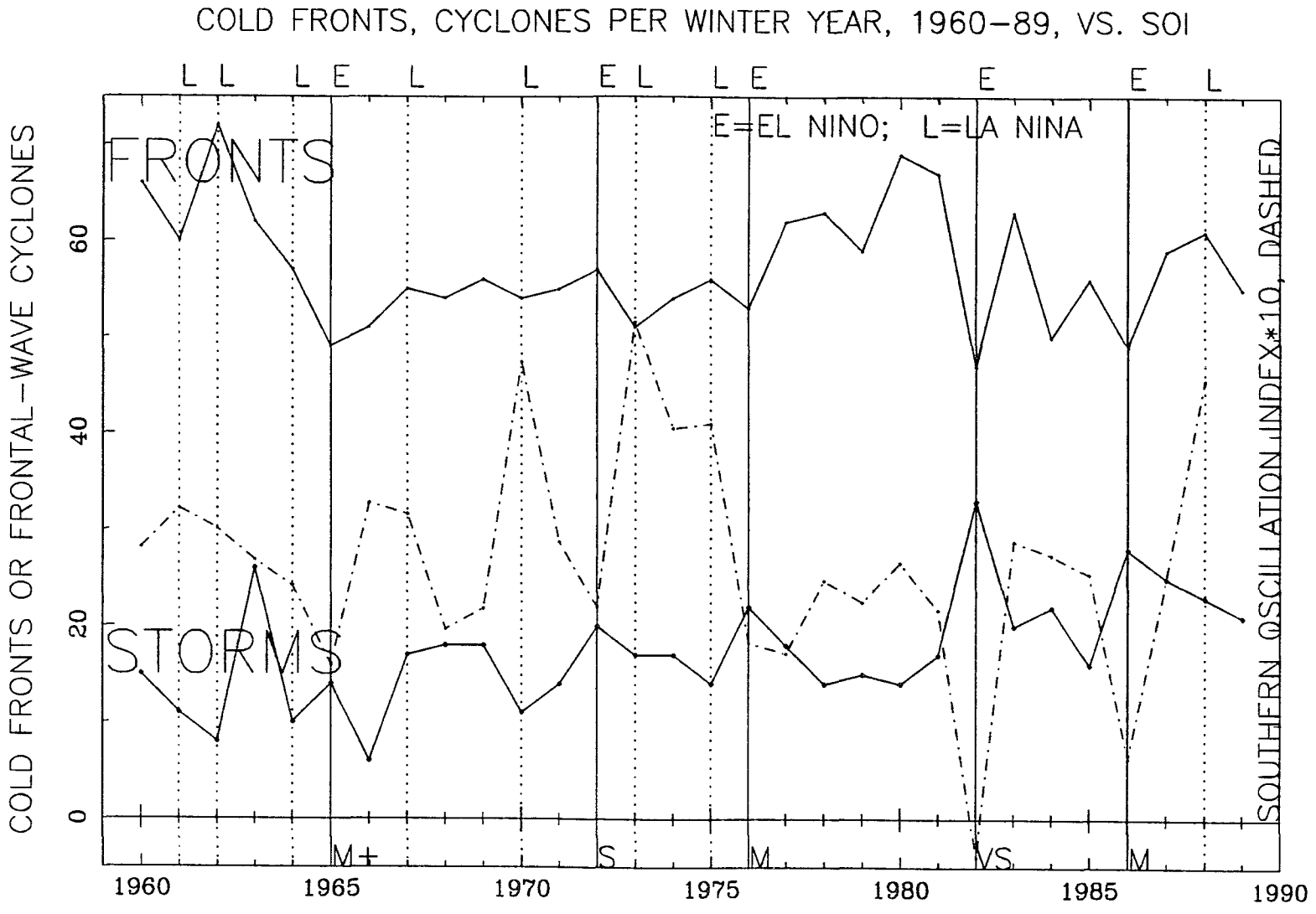

Figure 2.8: Frontal–wave cyclones and cold fronts, winter years, 1960–89.

2.2 Weather-Type Frequency: 1961-90

Twice-daily observations of synoptic weather type, judged with respect to a reference point at New Orleans, Louisiana, were also examined for the period, January 1961 to August 1990. This data was obtained from Dr. R. A. Muller, then of the Louisiana State Office of Climatology (Muller 1961-). Muller (1977) has identified eight synoptic weather patterns that, together with transition periods, encompass all the variability of gulf-region weather. These are described in the 1977 paper and summarized below.

2.2.1 Weather-Type Description

From November to April, gulf-region weather is markedly cyclic. A succession of four stages repeats with an average period of about seven days. (In early fall and late spring, the basic cycle holds, but it is less regular.) The typical sequence, starting just before a cold front from the north or northwest passes New Orleans follows.

1. Gulf Return and Frontal Gulf Return. The Gulf Return weather type occurs before a cold front crosses New Orleans. It is characterized by a flow of warm, moist air from the south or southeast. The Frontal Gulf Return weather type occurs when normal, southerly, Gulf Return flow is intensified ahead of an approaching cold front. Warm air rising along the approaching cold front can cause significant precipitation.

2. Frontal Overrunning. The Frontal Overrunning type often occurs after a frontal passage and when a cold front has crossed the coast and has, perhaps, become stationary, often along the coast or over the shelf. Frontal-wave cyclones frequently form along these stationary fronts (Faiers 1988). Frontal

Overrunning weather is typified by overcast conditions, north or northeast winds, cool temperatures, and rain.

3. Pacific High or Continental High. This is the clear, dry, cool, weather type in which high pressure - from the north in the case of Continental High type, or from the northwest, in the Pacific High type, spreads over the region. Winds are from the north or northwest, respectively.

4. Coastal Return. High pressure drifts eastward, and winds veer from northerly to easterly in this transition weather type. The basic cycle is complete, and a southerly flow is reestablished with the following onset of Gulf Return or Frontal Gulf Return weather.

Note that from stages one to three, winds veer from southerly to northerly, and then veer to easterly in the last stage, finally veering to southerly as the cycle starts over. Two last weather types occur dominantly in the warm season. These are: the Gulf Tropical Disturbance type, which includes tropical storms, tropical depressions, and hurricanes; and the Gulf High type, which occurs mainly in summer, as the Bermuda high extends westward over the gulf, producing hot, dry, summer weather.

2.2.2 Summary of Weather-Type Results

Three types show El Niño- and La Niña-year trends. These are first, the stormy, Frontal Overrunning type, and second, the two that occur before cold-front passage, the Gulf Return and Frontal Gulf Return types. The seasonal and winter-year occurrences of the three weather types appear as follow: Frontal Overrunning (Figs. 2.9, 2.10), Frontal Gulf Return (Figs. 2.11, 2.12), and Gulf Return (Figs. 2.13, 2.14). The sum of the last two types is also shown, Frontal Gulf Return plus Gulf Return (Figs. 2.15, 2.16), because it was expected to parallel the cold-front counts.

To see if the seasonal frequency of occurrence of any of these weather types was different during El Niño years or in La Niña years, the rank sum test was used on El Niño and all other years, and again on La Niña and all other years. Tables 2.3 and 2.4 show the rank sum test results for El Niño and La Niña tests, respectively. The results for the Frontal Overrunning weather type strongly parallel those for the previously-discussed frontal-wave cyclones in frequency of occurrence both in El Niño and La Niña years. This agrees with Faiers' (1988) finding of a positive correlation between January precipitation at Lake Charles, Louisiana from 1951 to 1988, and the occurrence of the Frontal Overrunning weather type. Results for the Frontal Gulf Return and Gulf Return weather types parallel those for cold-front frequencies, though less strongly. Statistically significant differences follow.

Table 2.3: Frequency of occurrence of the eight principal weather types at New Orleans, Louisiana, 1961-90, as defined by Muller (1977), in El Niño years versus other years; results of the rank sum test. There are two observations per day in Muller's data set and the number of observations per season or year is reported here on that basis. For example, the maximum number of observations per year is 730, or about 182 per season. Results of the rank sum test, also known as the U-test, Wilcoxon test, or Mann-Whitney test for differences between El Niño and other years. It is a test of the hypothesis that values for the listed parameters vary between El Niño and other years. T2-values are used in place of z-values since the number of observations is less than or equal to 30 and since the two groups are of unequal size. z-values are provided for inspection only. Two levels of significance are shown: $\alpha = .01$, double dagger, $\alpha = .05$, single dagger.

				# Events	Means	
Season	Time	z	T2 §	El Niño/Other	El Niño	Other
Frontal Overrunning (FOR) Parallels Number of Storms						
winteryear †	1961-89	2.050	40	5/24	157	124
winter+spring	1962-90	1.877	43	5/24	106	85
winter †	1962-90	2.140	38	5/24	73	56
spring	1961-90	-0.703	80	6/24	30	30
summer	1961-90	-0.530	68	5/25	9	10
fall	1961-89	0.404	68	5/24	34	31
Frontal Gulf Return (FGR) Parallels Number of Cold Fronts						
winteryear	1961-89	-0.521	66	5/24	85	90
winter+spring	1962-90	-0.924	59	5/24	49	56
winter	1962-90	-1.676	46	5/24	21	28
spring	1961-90	0.182	90	6/24	29	28
summer	1961-90	0.335	72	5/25	15	17
fall	1961-89	-0.550	66	5/24	16	18
Gulf Return (GR) Parallels Number of Cold Fronts						
winteryear	1961-89	-1.011	58	5/24	120	135
winter+spring †	1962-90	-2.485	32	5/24	54	74
winter †	1962-90	-2.083	39	5/24	13	22
spring	1961-90	-1.947	56	6/24	41	52
summer	1961-90	0.279	73	5/25	39	38
fall	1961-89	0.029	75	5/24	22	24
(Frontal Gulf Return+Gulf Return (FGR+GR)						
winteryear	1961-89	-0.924	59	5/24	205	225
winter+spring †	1962-90	-2.486	32	5/24	103	130
winter †	1962-90	-2.312	35	5/24	33	50
spring †	1961-90	-2.232	50	6/24	69	80
summer	1961-90	-0.028	77	5/25	54	55
fall	1961-89	-0.202	72	5/24	38	42

Table 2.3: continued.

Season	Time	z	T2 §	# Events El Niño/Other	Means El Niño	Means Other
Pacific High (PH)						
winteryear	1961-89	1.330	52	5/24	31	22
winter+spring	1962-90	1.272	53	5/24	27	17
winter	1962-90	1.187	55	5/24	13	8
spring	1961-90	1.899	57	6/24	15	8
summer	1961-90	****	78	5/25	0	0
fall	1961-89	0.350	69	5/24	5	5
Continental High (CH)						
winteryear	1961-89	-0.173	72	5/24	160	169
winter+spring	1962-90	-0.144	73	5/24	81	83
winter	1962-90	-0.520	66	5/24	42	45
spring	1961-90	0.856	77	6/24	42	37
summer	1961-90	0.390	71	5/25	26	22
fall	1961-89	0.867	60	5/24	68	61
Gulf High (GH)						
winteryear	1961-89	-0.780	62	5/24	66	75
winter+spring	1962-90	0.463	67	5/24	20	17
winter	1962-90	-0.174	72	5/24	8	9
spring	1961-90	0.441	85	6/24	10	9
summer	1961-90	-0.473	69	5/25	46	51
fall	1961-89	0.204	72	5/24	6	6
Gulf Tropical Disturbance (GTD)						
winteryear	1961-89	-0.405	68	5/24	25	25
winter+spring	1962-90	0.219	73	5/24	1	1
winter	1962-90	****	75	5/24	0	0
spring	1961-90	0.040	93	6/24	1	1
summer	1961-90	-1.282	55	5/25	10	17
fall	1961-89	0.262	71	5/24	9	9
Coastal Return (CR)						
winteryear	1961-89	-0.636	64	5/24	85	90
winter+spring	1962-90	-1.157	55	5/24	27	32
winter	1962-90	-0.842	61	5/24	10	13
spring	1961-90	-0.416	85	6/24	18	19
summer	1961-90	1.421	52	5/25	39	30
fall	1961-89	-1.214	54	5/24	21	29

Notes:

§: T2 = Number of X observations * (Number of X observations + Number of Y observations + 1) - Sum of the ranks of the X observations. The X observations are the smaller set, the El Niño or La Niña years.

‡ : indicates null hypothesis can be rejected at the .01 level of significance.

† : indicates null hypothesis can be rejected at the .05 level of significance.

In El Niño years, the frequency of Frontal Overrunning is significantly higher (.05 confidence level) in the winter season and in winter years, exactly as for storms, Figs. 2.9, 2.10. Taken alone, Frontal Gulf Return was less common in El Niño winters, winter-plus-springs, and winter years, but the reduction was not significant at either the .01 or .05 level, Figs. 2.11, 2.12. The Frontal Gulf Return, winter-season result was, however, significant at the .20 level, by reference to tables in Verdooren (1963). Taken alone, Gulf Return was significantly less common in El Niño winters and winter-plus-springs (.05 confidence level), Figs. 2.13, 2.14. When a sum of Frontal Gulf Return and Gulf Return weather-type occurrences is used, the sum occurs significantly less often (.05 confidence level) in winter, spring, and winter years, Figs. 2.15, 2.16. This is almost identical to the cold-front count results, fewer cold fronts in in El Niño winters, winter-plus-springs and winter years.

The La Niña results, Table 2.4, are almost equal and opposite to the El Niño results, Table 2.3. The Frontal Overrunning type is less common in La Niña winters and winter years than in non La Niña winters and winter years, significant at the .05 confidence level, echoing the low number of storms in La Niña winters and winter years (Figs. 2.9, 2.10). The parallelism to the direct cold-front counts in La Niña years is not as strong. Taken alone, the Frontal Gulf Return type was more common, but significant only at the .10 confidence level (Figs. 2.11, 2.12). Gulf Return, taken alone, was more common in winter-plus-spring, but only significant at the .20 level (Figs. 2.13, 2.14). In La Niña years, just the combination of Frontal Gulf Return plus Gulf Return types was significantly more common at the .05 confidence level, and only in winter-plus-spring. However, in La Niña winters, the sum of the two types was higher at the .10 confidence level (Figs. 2.15, 2.16). The hot, dry, summer weather type, Gulf High, is significantly more common in La Niña summers (.05 level).

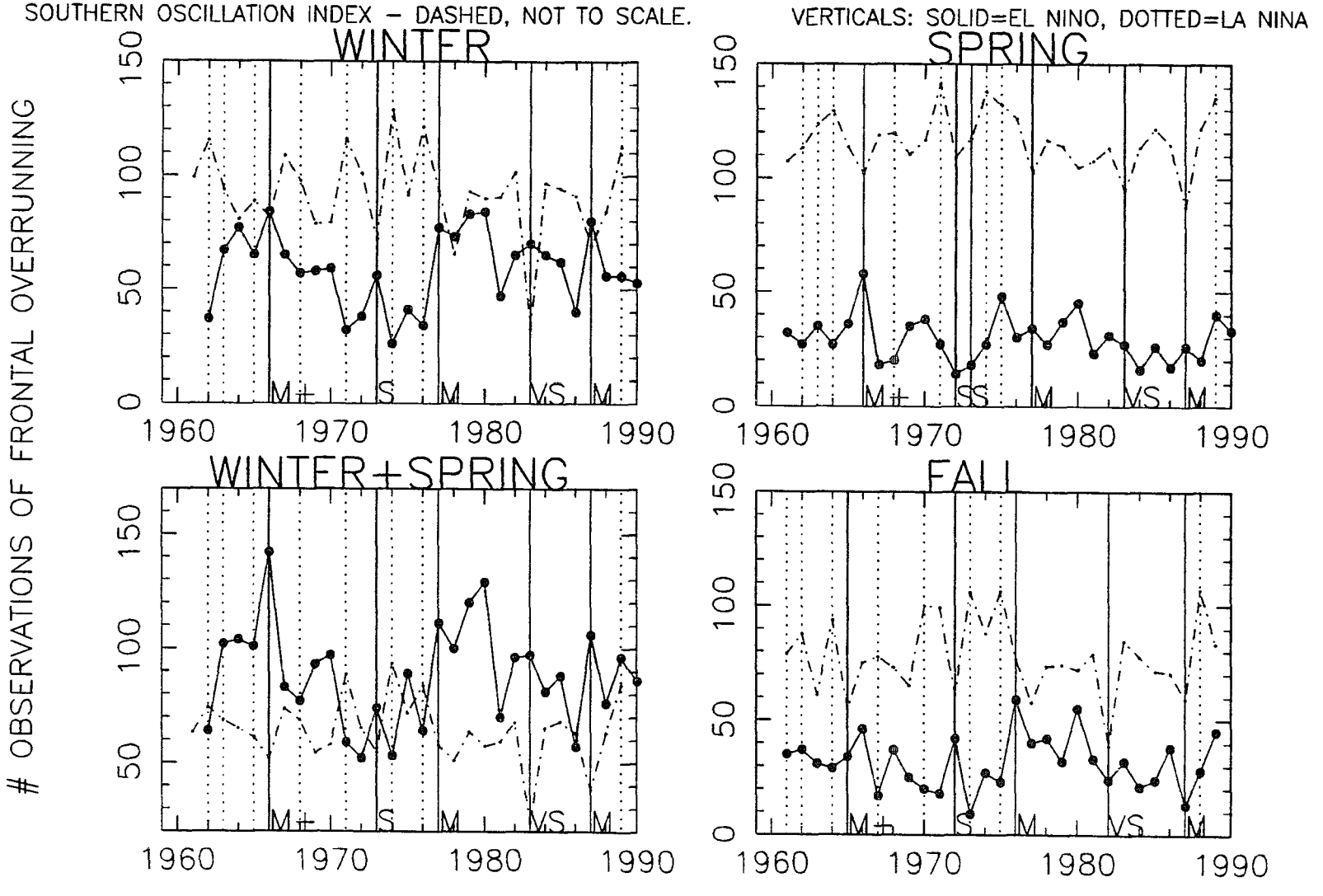

Figure 2.9: Number of occurrences of Frontal Overrunning, seasonally, 1961–90. Two observations/day. Parallels number of frontal–wave cyclones.

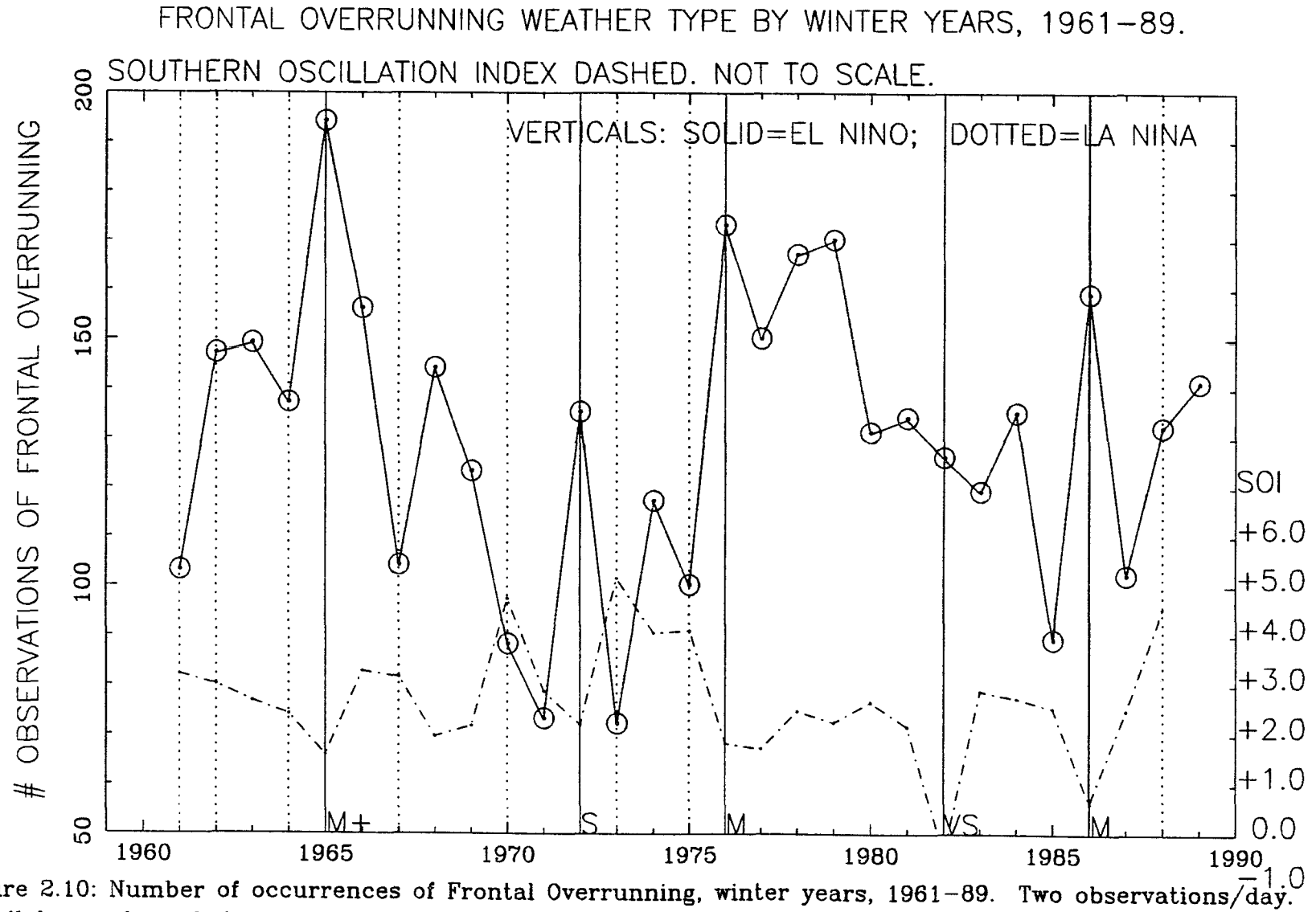

Figure 2.10: Number of occurrences of Frontal Overrunning, winter years, 1961-89. Two observations/day. Parallels number of storms.

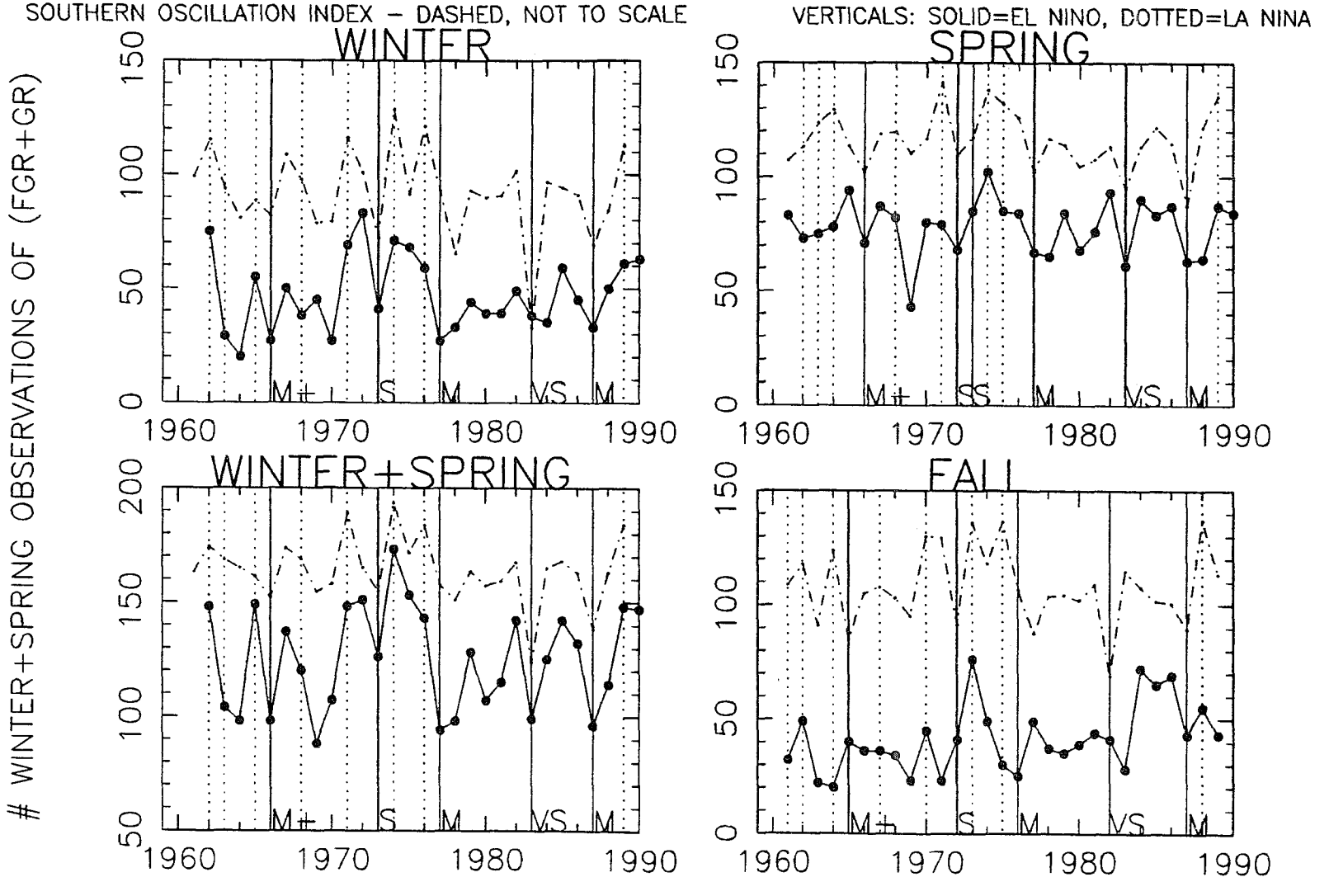

Figure 2.11: Number of occurrences of Frontal Gulf Return plus Gulf Return, seasonally, 1961–90. Two observations/day. Parallels number of cold fronts.

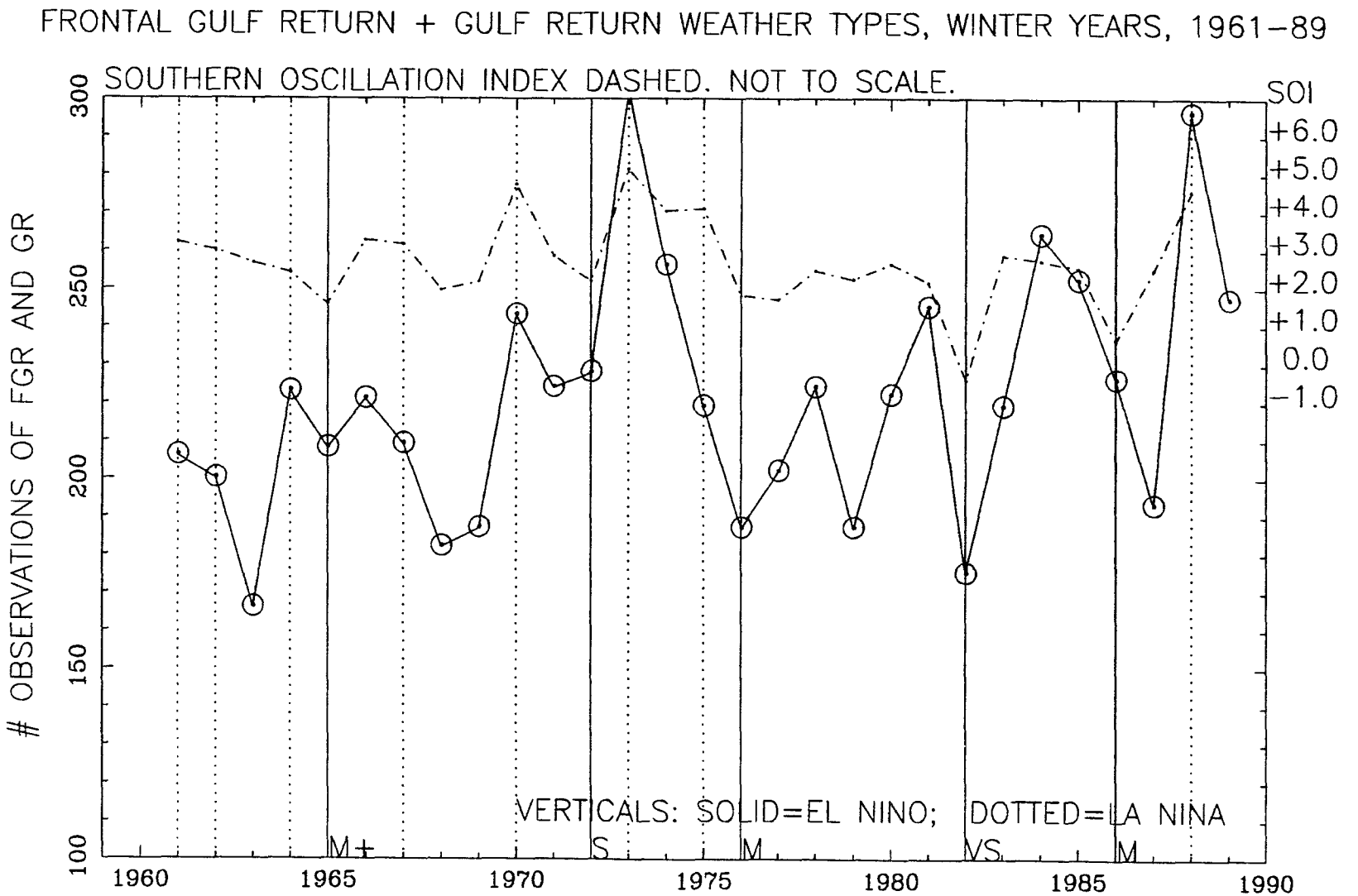

Figure 2.12: Number of occurrences of Frontal Gulf Return plus Gulf Return, winter years, 1961–89. Two observations/day. Parallels # of cold fronts.

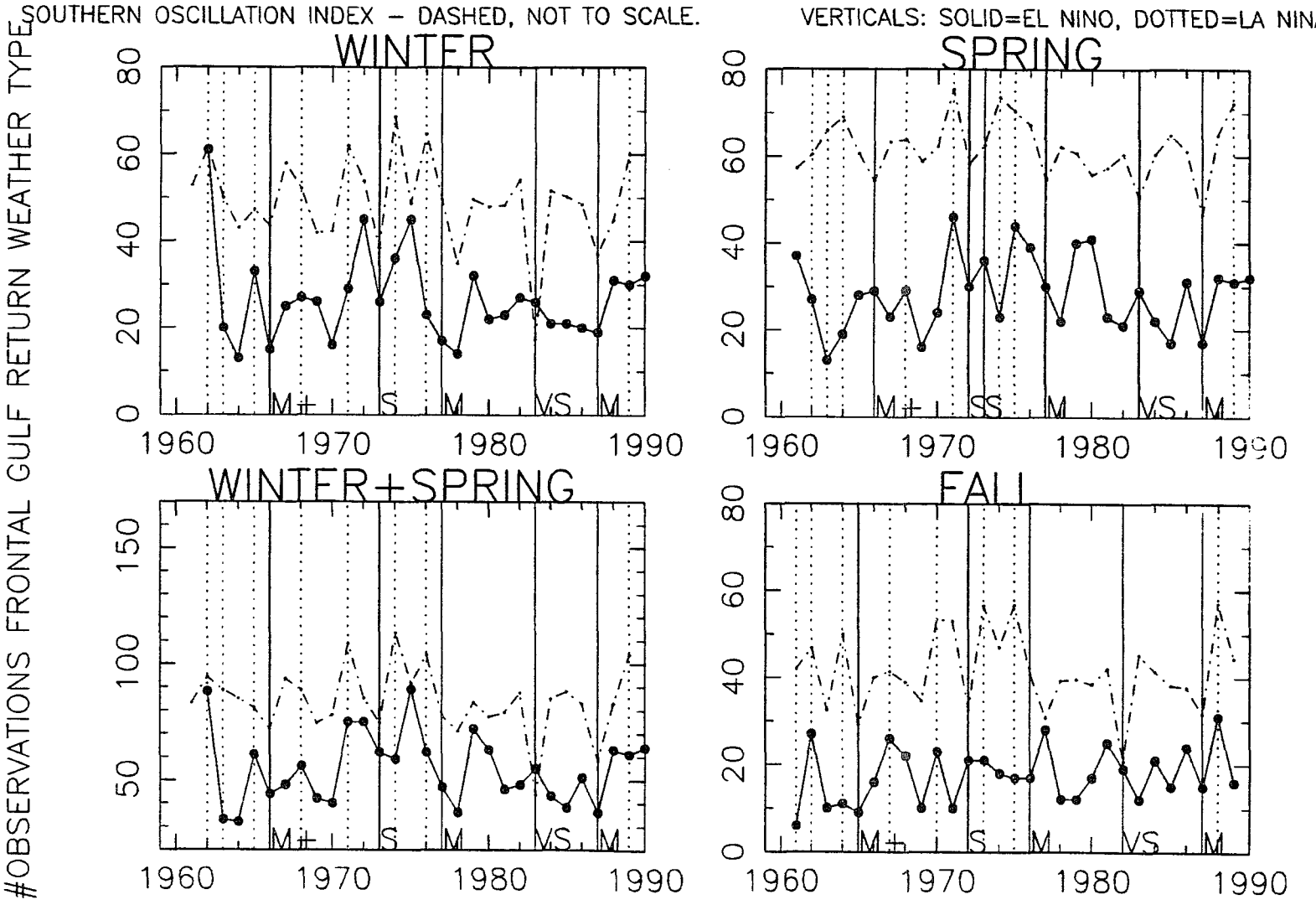

Figure 2.13: Number of occurrences of Frontal Gulf Return, seasonally, 1961–90. Two observations/day. Parallels number of cold fronts.

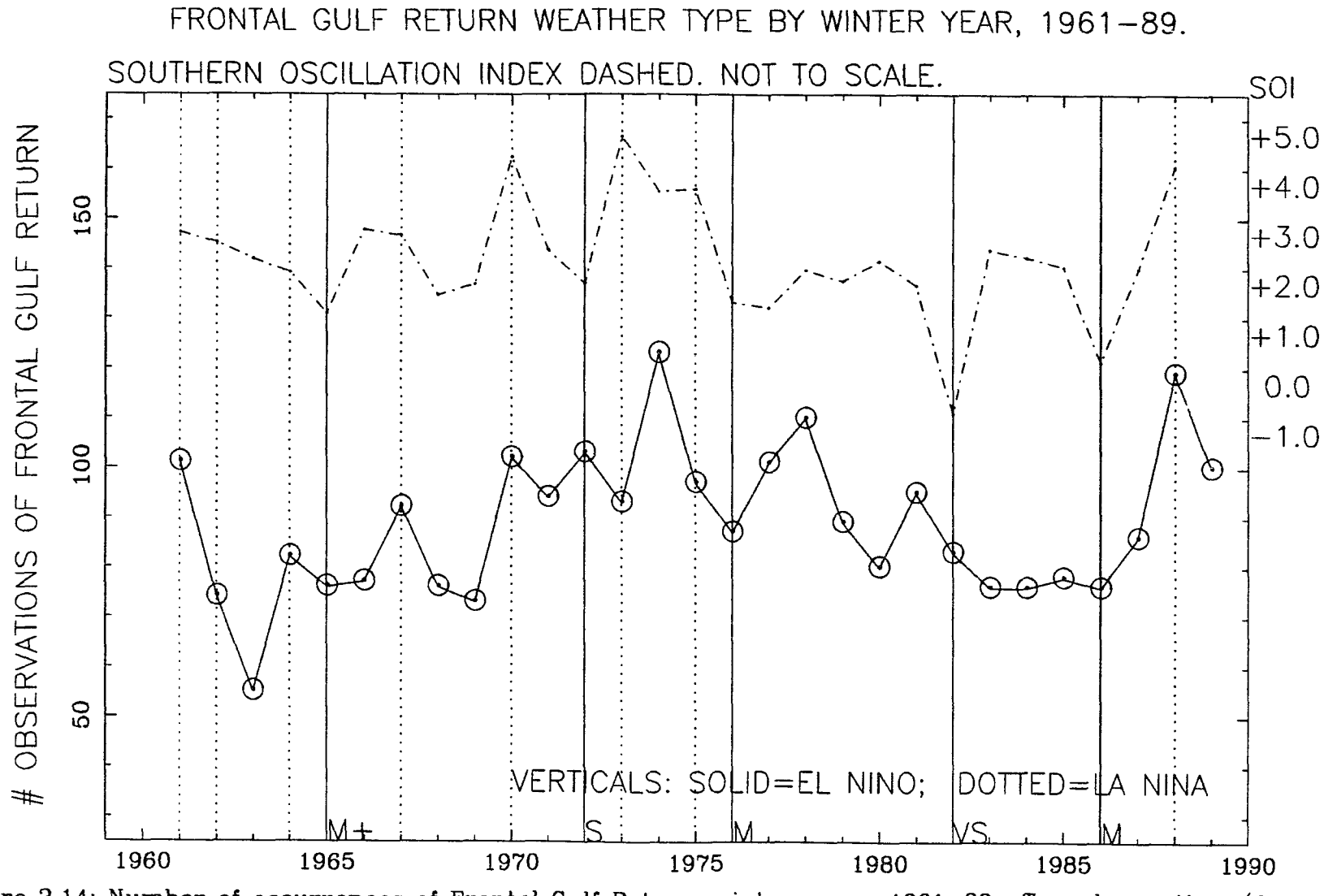

Figure 2.14: Number of occurrences of Frontal Gulf Return, winter years, 1961–89. Two observations/day. Parallels number of cold fronts.

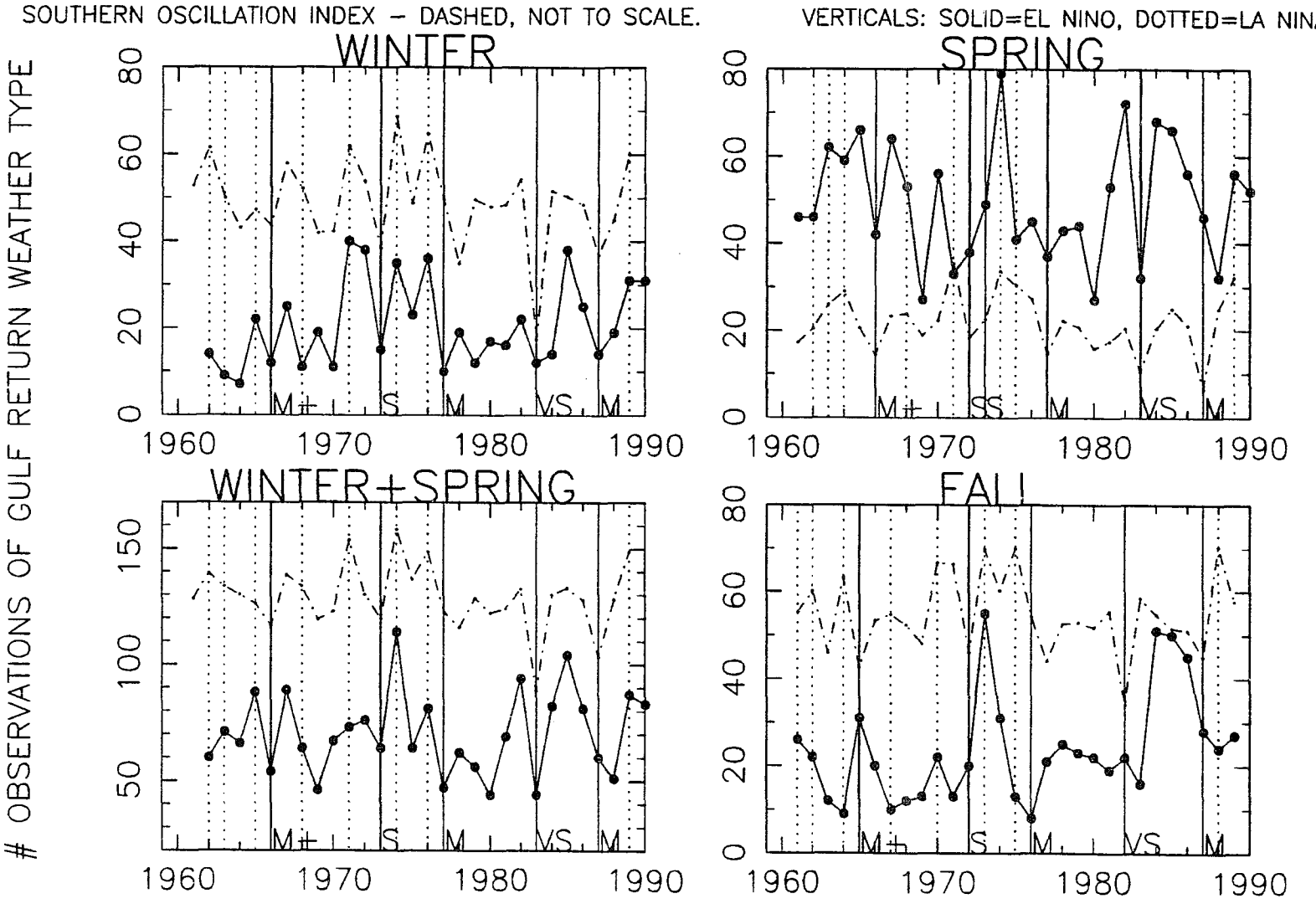

Figure 2.15: Number of occurrences of Gulf Return, seasonally, 1961–90. Two observations/day. Parallels number of cold fronts.

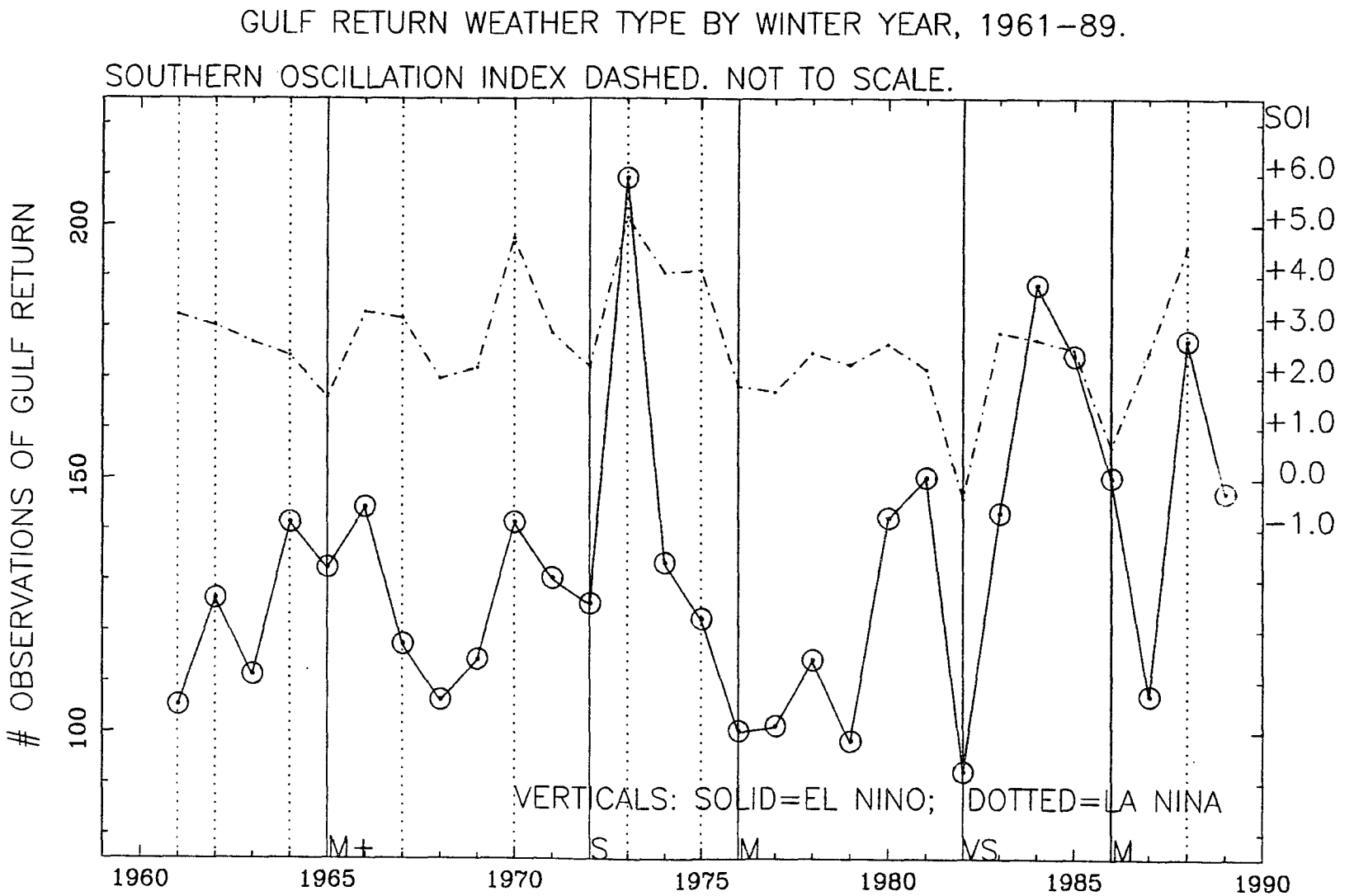

Figure 2.16: Number of occurrences of Gulf Return, winter years, 1961–89. Two observations/day. Parallels number of cold fronts.

Table 2.4: Frequency of the eight principal weather types at New Orleans, Louisiana, 1961-90, as defined by Muller (1977), in La Niña years versus other years. There are two observations per day in Muller's data set. The maximum number of observations per year is 730, or about 182 per season. Results of the rank sum test, also known as the U-test, Wilcoxon test, or Mann-Whitney test for differences between La Niña and other years. It is a test of the hypothesis that values for the listed parameters vary between La Niña and other years. T2-values are used in place of z-values since the number of observations is less than or equal to 30. z-values are provided for inspection. Two levels of significance are shown. α = .01, reject the null hypothesis if $z > 2.575$ or $z < -2.575$, double dagger. α = .05, reject the null hypothesis if $z > 1.960$ or $z < -1.960$, single dagger.

				# Events	Means	
Season	Time	z	T2 §	La Niña/Other	La Niña	Other
Frontal Overrunning (FOR) Parallels Number of Storms						
winteryear †	1961-89	-2.098	77	8/21	110	138
winter+spring	1962-90	-1.489	90	8/21	77	93
winter †	1962-90	-2.273	74	8/21	47	64
spring	1961-90	0.273	134	9/21	30	30
summer	1961-90	0.729	109	8/22	11	10
fall	1961-89	-1.928	81	8/21	25	34
Frontal Gulf Return (FGR) Parallels Number of Cold Fronts						
winteryear	1961-89	1.345	93	8/21	95	86
winter+spring	1962-90	1.318	93	8/21	62	52
winter	1962-90	1.930	81	8/21	32	25
spring	1961-90	0.340	132	9/21	29	28
summer †	1961-90	-2.279	76	8/22	12	18
fall	1961-89	1.320	93	8/21	20	17
Gulf Return (GR) Parallels Number of Cold Fronts						
winteryear	1961-89	0.732	105	8/21	142	129
winter+spring	1962-90	1.660	86	8/21	80	67
winter	1962-90	0.905	102	8/21	25	19
spring	1961-90	0.340	132	9/21	51	49
summer	1961-90	-0.611	111	8/22	36	39
fall	1961-89	-0.391	112	8/21	23	24
Frontal Gulf Return+Gulf Return (FGR+GR)						
winteryear	1961-89	0.952	101	8/21	237	215
winter+spring †	1962-90	2.394	71	8/21	142	119
winter	1962-90	1.954	80	8/21	57	44
spring	1961-90	0.272	134	9/21	81	77
summer	1961-90	-1.809	86	8/22	47	57
fall	1961-89	0.269	115	8/21	43	41

Table 2.4: continued.

Season	Time	z	T2 §	# Events La Niña/Other	Means La Niña	Means Other
Pacific High (PH)						
winteryear	1961-89	-1.246	95	8/21	20	25
winter+spring	1962-90	-1.051	99	8/21	17	19
winter	1962-90	-0.832	103	8/21	8	9
spring	1961-90	-0.341	132	9/21	8	10
summer	1961-90	****	124	8/22	0	0
fall	1961-89	-0.887	102	8/21	3	5
Continental High (CH)						
winteryear	1961-89	-0.781	104	8/21	162	169
winter+spring	1962-90	-0.977	100	8/21	77	85
winter	1962-90	0.220	116	8/21	45	45
spring	1961-90	-1.336	110	9/21	35	40
summer	1961-90	-1.314	96	8/22	18	24
fall	1961-89	-0.293	114	8/21	60	63
Gulf High (GH)						
winteryear	1961-89	1.734	85	8/21	89	68
winter+spring	1962-90	0.612	108	8/21	20	17
winter	1962-90	0.269	115	8/21	8	9
spring	1961-90	0.929	119	9/21	12	8
summer ‡	1961-90	2.534	70	8/22	62	46
fall	1961-89	0.665	107	8/21	7	6
Gulf Tropical Disturbance (GTD)						
winteryear	1961-89	0.024	120	8/21	24	26
winter+spring	1962-90	1.817	96	8/21	1	0
winter	1962-90	****	120	8/21	0	0
spring	1961-90	0.453	133	9/21	1	0
summer	1961-90	0.634	111	8/22	18	15
fall	1961-89	1.229	95	8/21	11	9
Coastal Return (CR)						
winteryear	1961-89	-0.317	114	8/21	87	90
winter+spring	1962-90	-0.196	116	8/21	31	32
winter	1962-90	1.804	83	8/21	15	11
spring	1961-90	-0.295	133	9/21	18	19
summer	1961-90	-0.775	108	8/22	27	33
fall	1961-89	1.636	87	8/21	34	25

Notes:

§: T2 = Number of X observations * (Number of X observations + Number of Y observations + 1) - Sum of the ranks of the X observations. The X observations are the smaller set, the El Niño or La Niña years.

‡ : indicates null hypothesis can be rejected at the .01 level of significance.

† : indicates null hypothesis can be rejected at the .05 level of significance.

2.3 Temperature and Precipitation Records

A third data set, temperature and precipitation records, was used in an attempt to support or refute the previous findings based on storm and cold-front counts and on weather-type frequencies. Based on more storms occurring in El Niño winters, one would expect more precipitation in El Niño winters and relatively less in La Niña winters. Also on the basis of more storms, lower average winter temperatures, resulting from frequent cloud cover associated with storms, may also be expected in El Niño winters, with the opposite expected in La Niña winters. Predictions based on the number of cold fronts are not considered, as insufficient information has been obtained about the fronts such as their speed of travel, or, more importantly, about the winds, pressure, temperature, and humidity of the air mass behind them, to allow adequate hypothesis testing, and because of the potential problems with the cold-front counts. (Solely on the basis of fewer cold fronts in El Niño winters, one might expect warmer average temperatures in the gulf region. Although this was the case in the 1991/92 El Niño, which is not included in this report, long-term temperature records show the opposite, cooler El Niño winters. See also 4.2.4.)

To test the above prediction based on storm frequency, that is, wetter, cooler El Niño winters and warmer, drier La Niña winters, average seasonal temperature and seasonal total precipitation records from 15 land stations in the gulf coastal plain were examined. Corresponding data from eight climatic divisions was also used, although the two types of data were analyzed separately because of their differing natures. Climatic-division data is produced by combining data from several stations within a small, ideally climatically homogeneous region, in an attempt to overcome possible single-station peculiarities. Station data was supplied by the National Carbon Dioxide Information Analysis Center (NCDIAC) (Bradley et al. 1985). The NCDIAC has compiled for distribution on magnetic tape or diskette global, histor-

ical, station data back as far as 1851, and up to 1980. Lengths of record vary. The original data comes from many sources, including The World Weather Records of the Smithsonian Institution. The data has been carefully reviewed by the NCDIAC for errors and consistency. The climatic-division data was supplied by The Southern Regional Climate Center, located in Baton Rouge, Louisiana (Southern Regional Climate Center). This data is also reviewed for quality. All division data used covers the period 1895 to 1989. Divisions were chosen to fill spatial gaps in station data, to achieve roughly even coverage over the gulf area. Stations used are, from east to west: Casa Blanca, Cuba; Key West, Miami, Tampa, Florida; Thomasville, Georgia.; Pensacola, Florida; Mobile, Alabama; New Orleans, Louisiana; Meridian, Vicksburg, Mississippi; Alexandria, Jennings, Louisiana; Galveston, Corpus Christi, Texas; and Merida, Mexico. Divisions used are, from east to west: Key West, St. Petersburg, Tallahassee, Fl.; New Orleans, Lake Charles, La.; Houston, Corpus Christi, Brownsville, Tx.

2.3.1 Temperature and Precipitation Results

The rank sum test was again used to determine El Niño- and La Niña-year differences. When using the rank sum test repeatedly on one field, as here, the probabilities of error are additive. To compensate, in the data from eight divisions, for example, the .05 confidence criterion used is not $z_{.05}$, but $z_{.05/8}$, or $z_{.00625}$, dividing by the number of places at which the test is used (Snedecor and Cochran 1980, p. 116, p. 166). Single-station data is not so compensated because of varying periods of record, although, because there is considerable overlap, unadjusted probabilities are likely to be optimistic and should be viewed as 'indices'.

Station and division locations and all seasons at each with statistically significant differences in total preciptation or average temperature between El Niño and

other years, and between La Niña and other years are contained in the following sequence of figures: El Niño and La Niña station temperature (Figs. 2.17, 2.18) and station precipitation (Figs. 2.19, 2.20); El Niño and La Niña division temperature (Figs. 2.21, 2.22) and division precipitation (Figs. 2.23, 2.24). Tables 2.5 and 2.6 summarize temperature and precipitation results from station data. Tables 2.7 and 2.8 summarize temperature and precipitation results from division data. Complete results, including those not significant at the .01 or .05 confidence level, are given in appendix Q. Briefly, these results appear to substantiate results from the storm and cold-front counts and from the weather-type frequencies by showing cooler, wetter El Niño winters and warmer, drier La Niña winters. In El Niño winters, nine of fifteen stations and six of eight divisions show statistically significantly greater winter precipitation. Eight stations and no divisions show significantly lower temperature (.01 or .05 confidence level). In La Niña winters, five of fifteen stations and two of eight divisions show statistically significantly lower winter precipitation. Nine stations and no divisions show significantly higher temperature (.01 or .05 confidence level). Although not all stations or divisions show significantly moister, cooler El Niño winters and drier, warmer La Niña winters, conflicting results of significance are absent, and nearly all stations and divisions follow the trends.

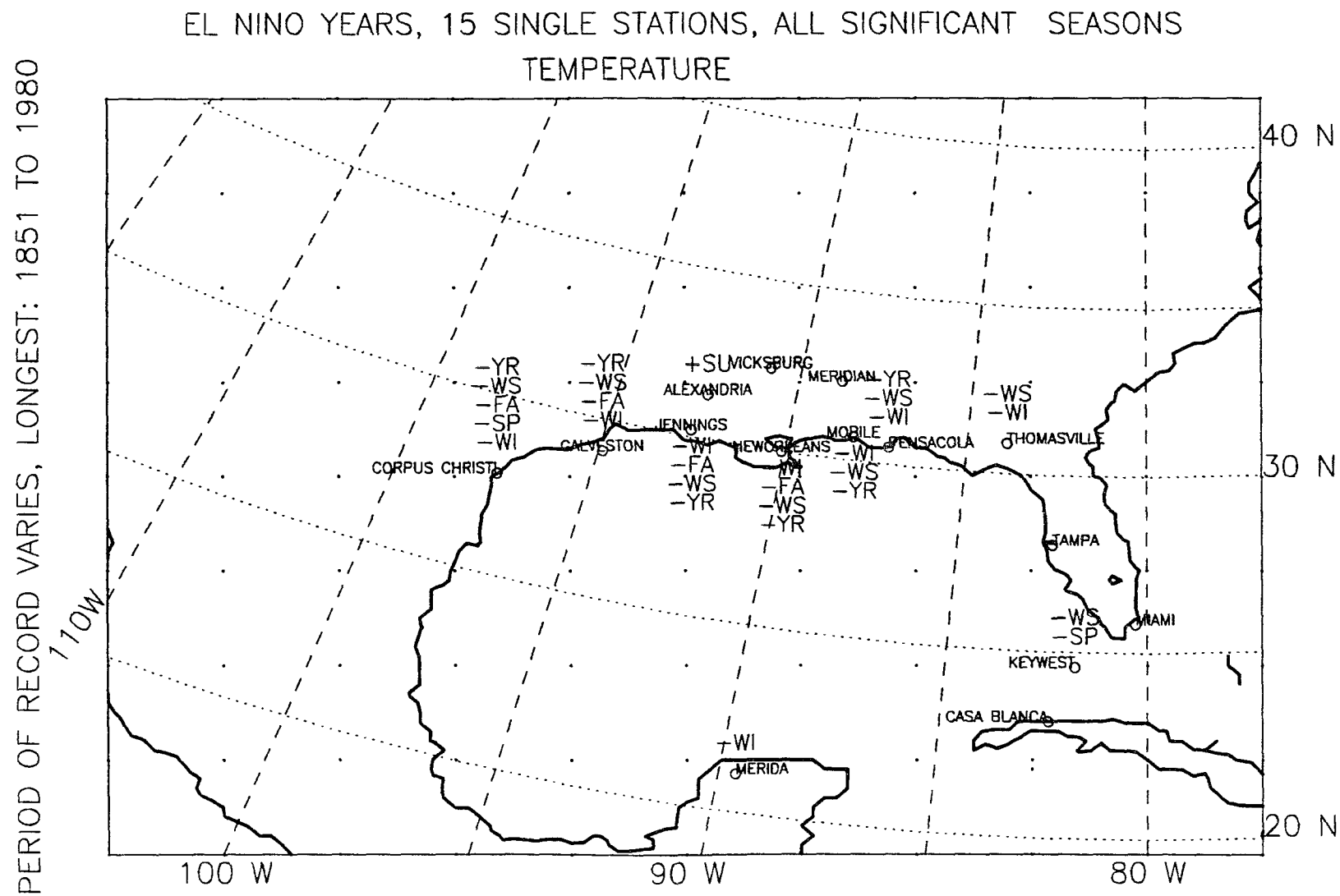

Figure 2.17: Single stations where seasonal average temperature differs significantly (at .01 or .05 level) in El Niño years. 15 Stations analyzed. Confidence criteria, z−values, unadjusted for multiple use of test.

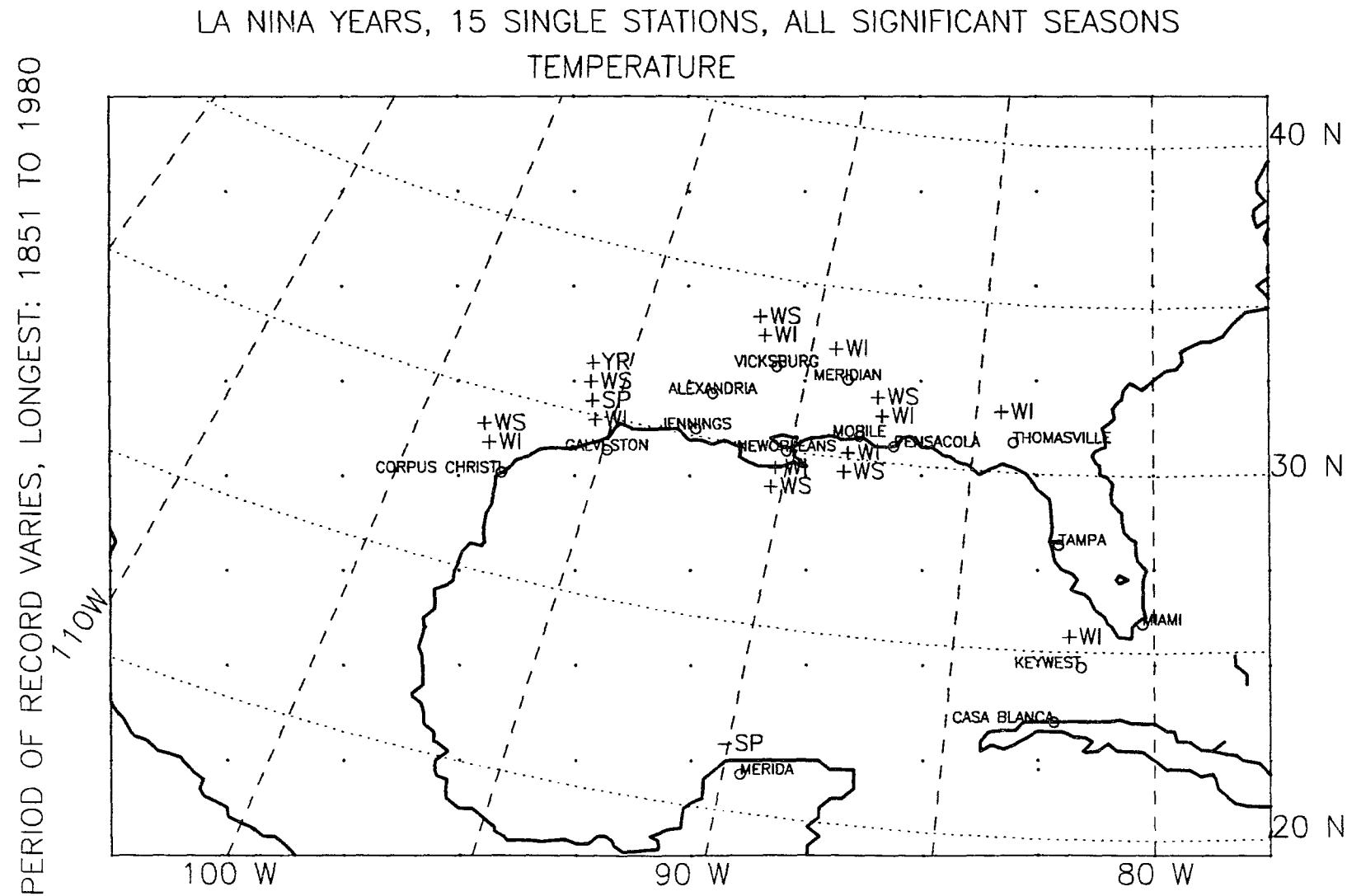

Figure 2.18: Single stations where seasonal average temperature differs significantly (at .01 or .05 level) in La Niña years. 15 Stations analyzed. Confidence criteria, z–values, unadjusted for multiple use of test.

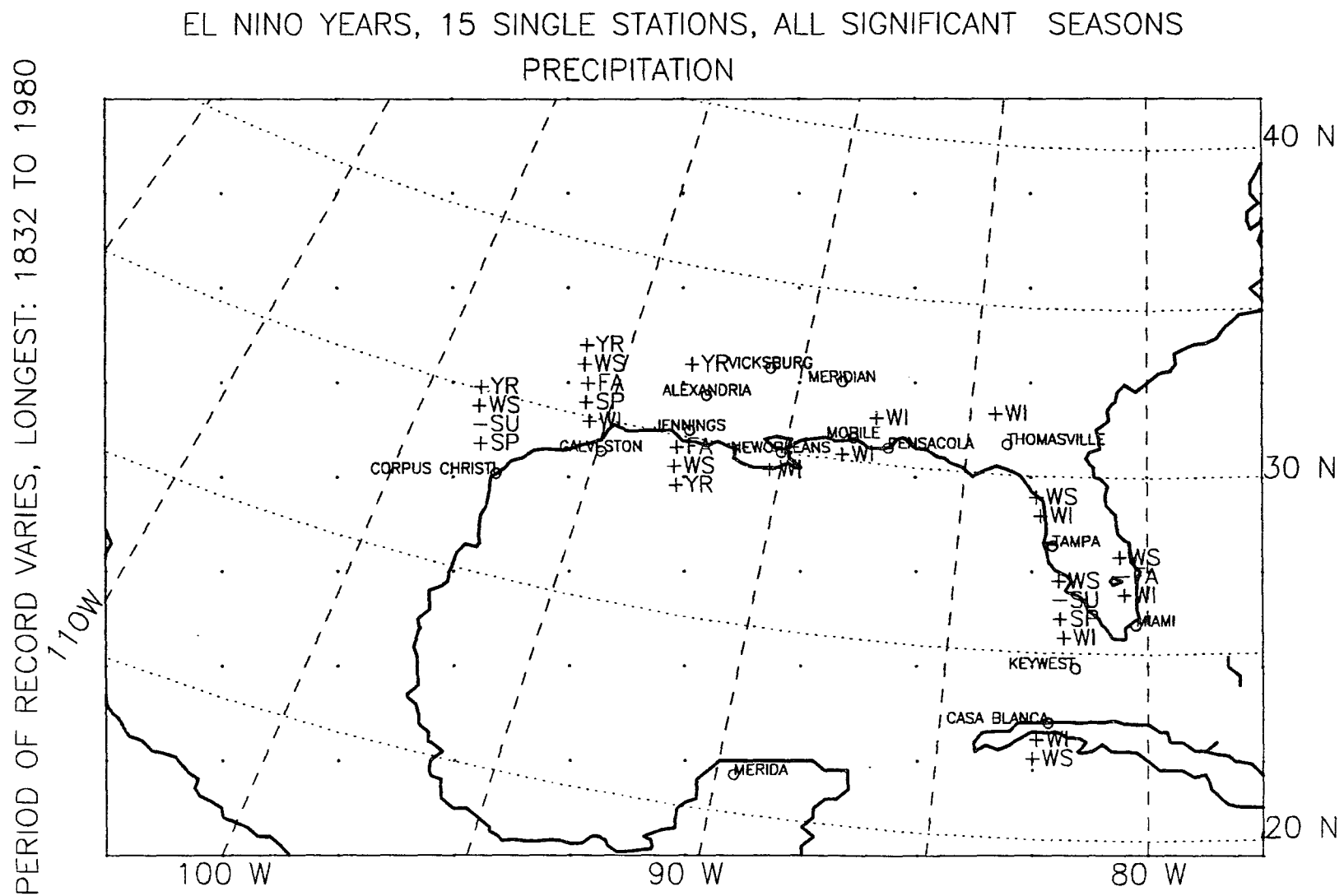

Figure 2.19: Single stations where seasonal average precipitation differs significantly (at .01 or .05 level) in El Niño years. 15 Stations analyzed. Confidence criteria, z–values, unadjusted for multiple use of test.

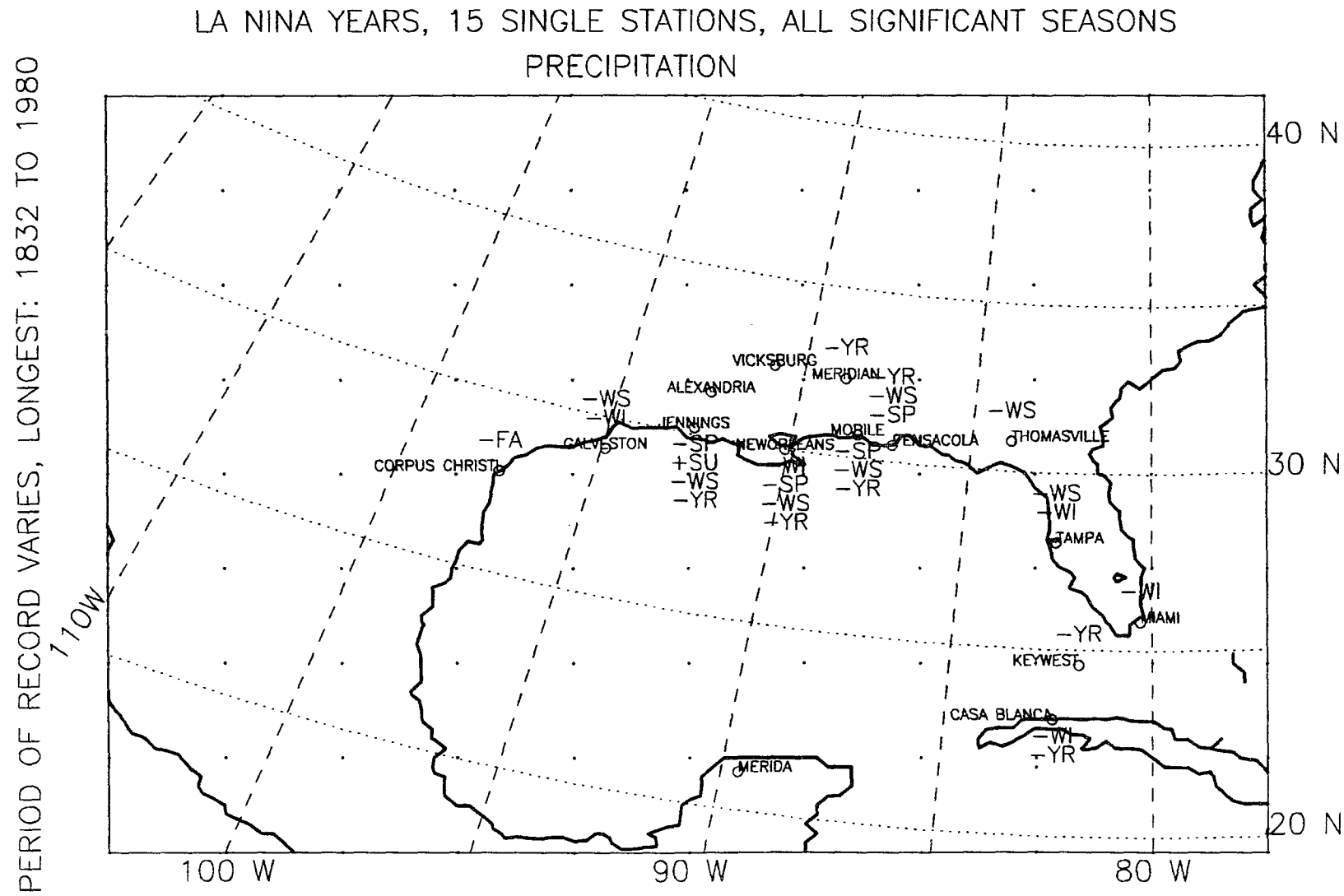

Figure 2.20: Single stations where seasonal average precipitation differs significantly (at .01 or .05 level) in La Niña years. 15 Stations analyzed. Confidence criteria, z-values, unadjusted for multiple use of test.

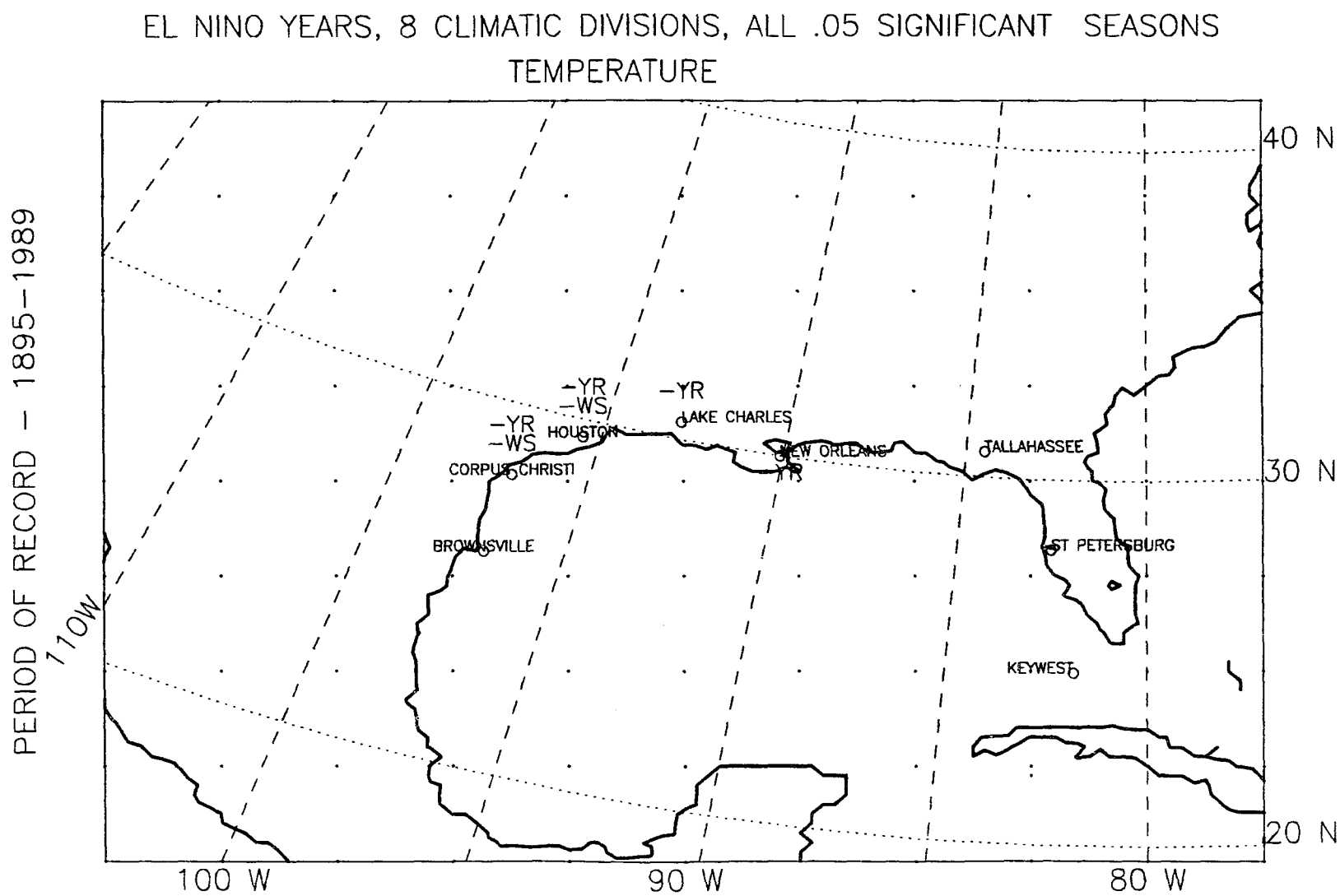

Figure 2.21: Climatic divisions where seasonal average temperature differs significantly (at .01 or .05 level) in El Niño years. Eight divisions analyzed. Confidence criteria, z-values, adjusted for multiple use of test.

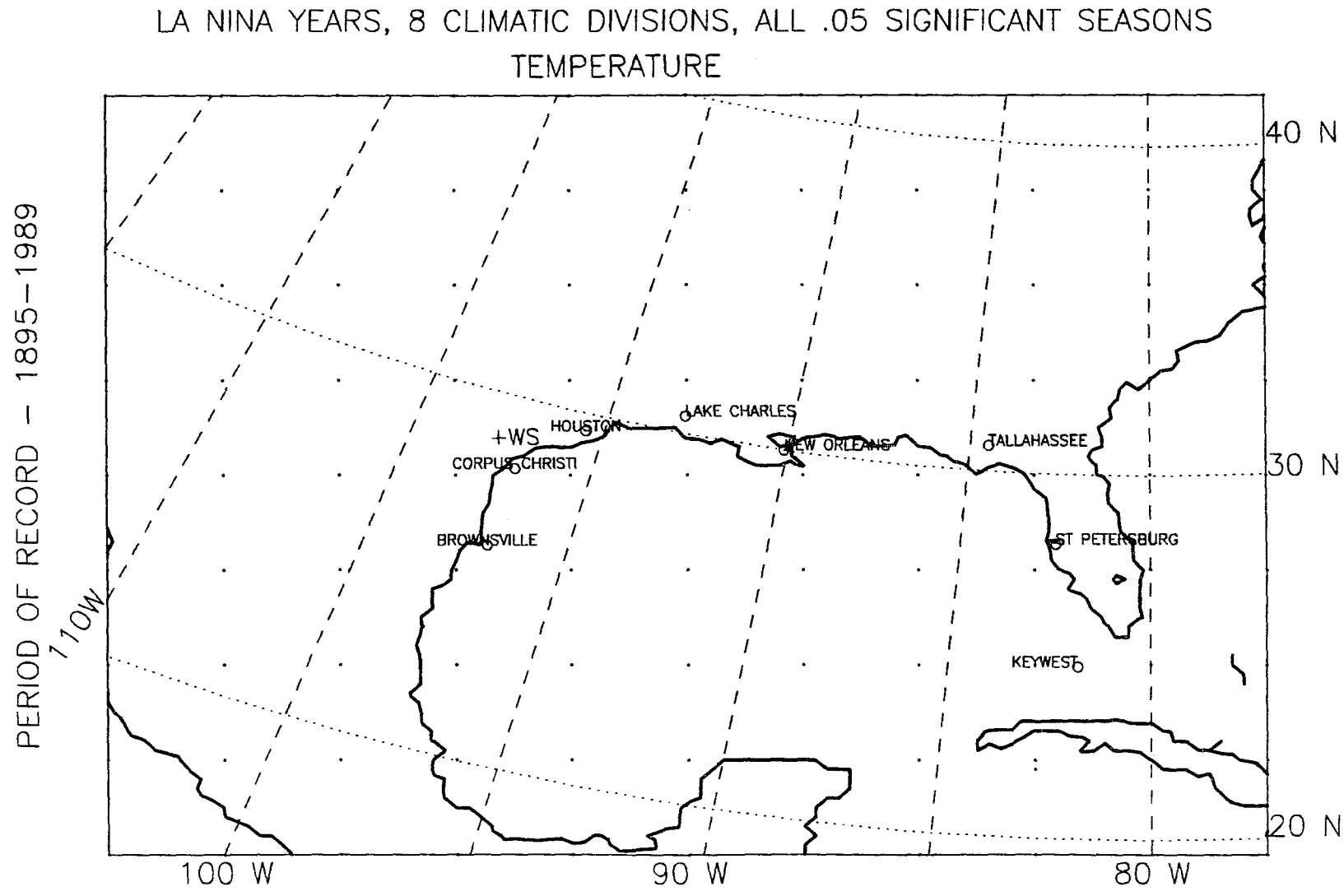

Figure 2.22: Climatic divisions where seasonal average temperature differs significantly (at .01 or .05 level) in La Niña years. Eight divisions analyzed. Confidence criteria, z-values, adjusted for multiple use of test.

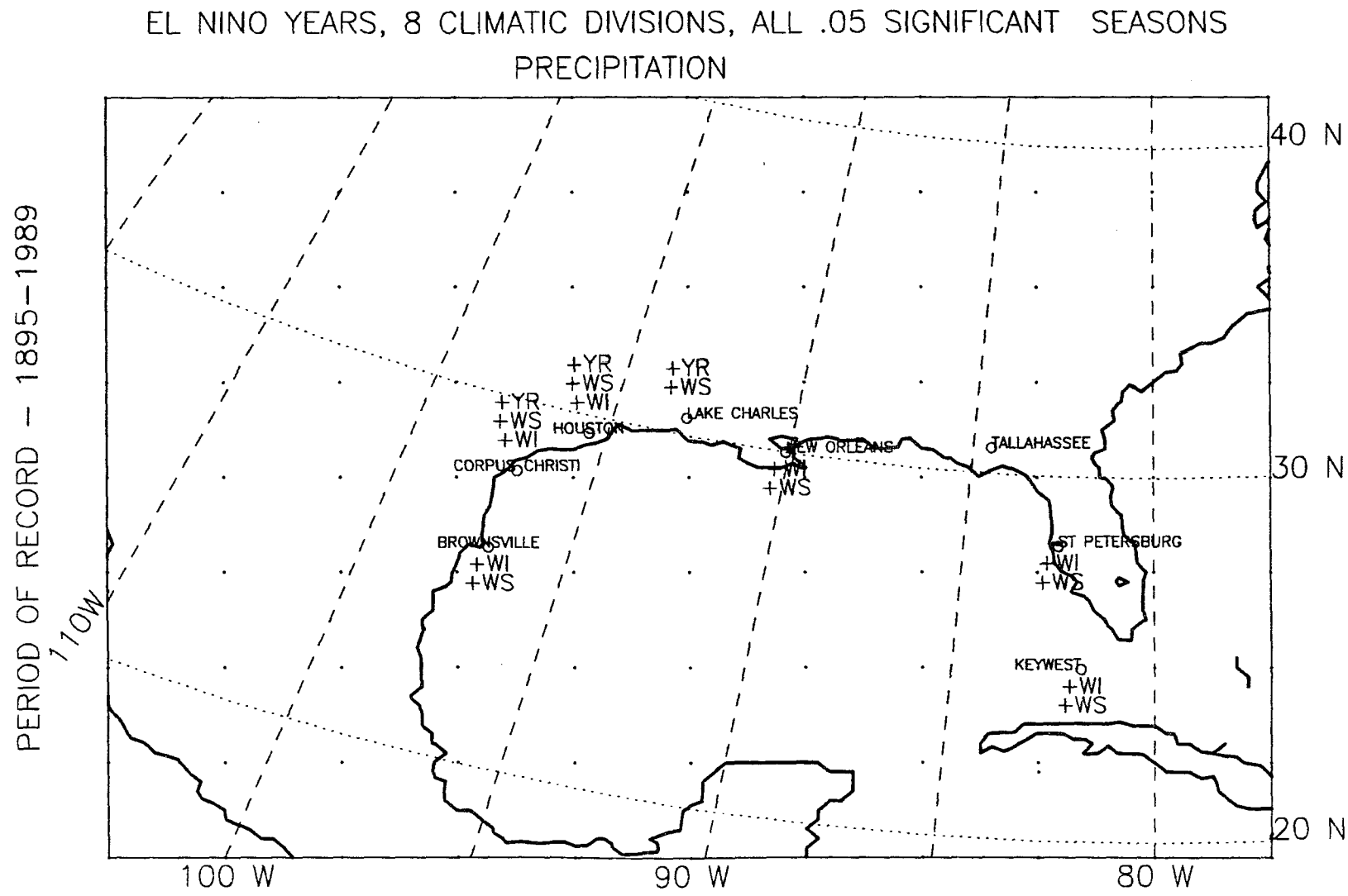

Figure 2.23: Climatic divisions where seasonal average precipitation differs significantly (at .01 or .05 level) in El Niño years. Eight divisions analyzed. Confidence criteria, z-values, adjusted for multiple use of test.

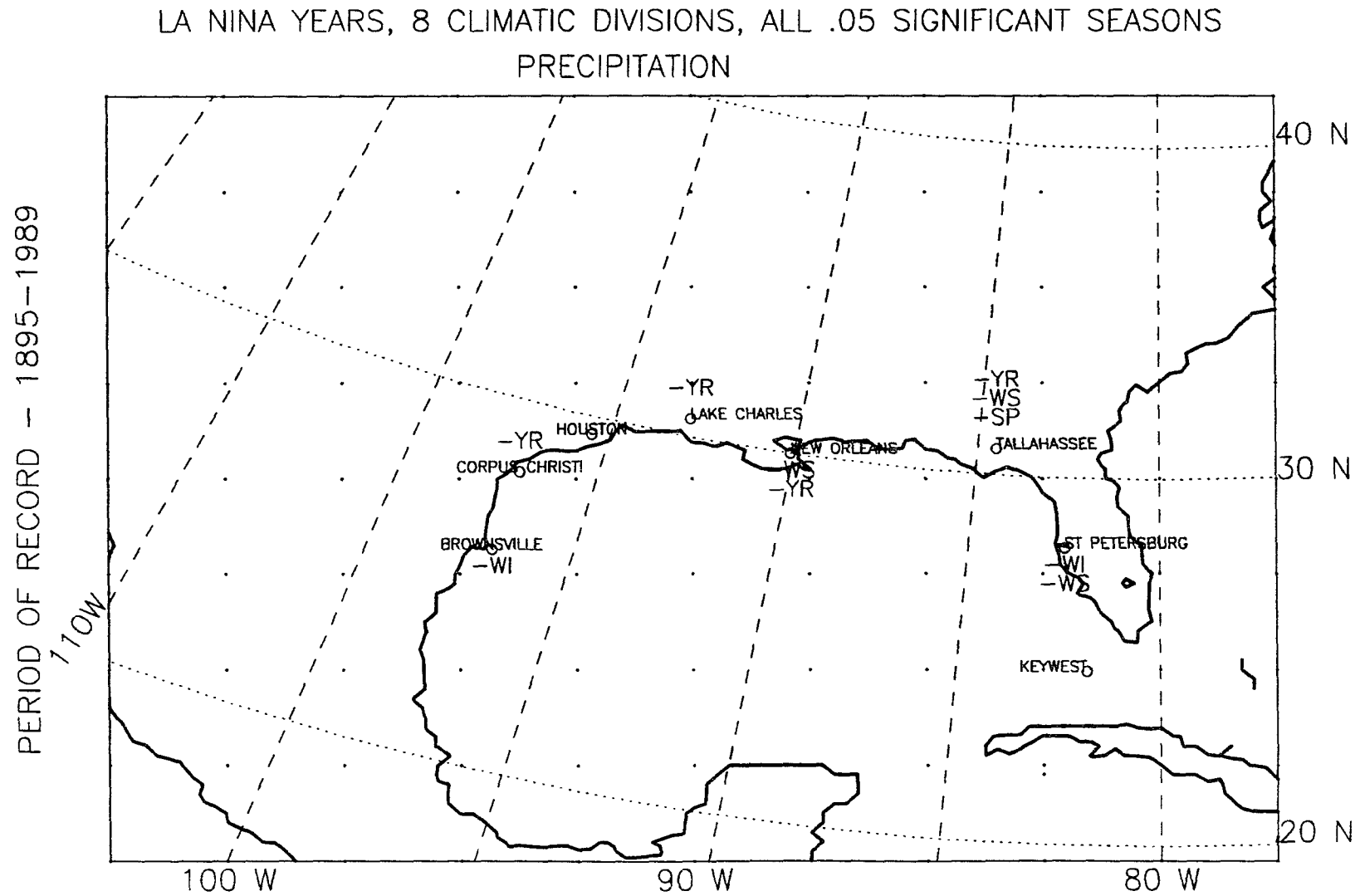

Figure 2.24: Climatic divisions where seasonal average precipitation differs significantly (at .01 or .05 level) in La Niña years. Eight divisions analyzed. Confidence criteria, z-values, adjusted for multiple use of test.

Table 2.5: Temperature at 15 gulf-region, single stations; all seasons with temperature differences significant at the .01 or .05 confidence level by the rank sum test. Confidence criteria on single-station data are not adjusted for multiple use of rank sum test because period of record varies from station to station. A blank indicates the parameter was not significant at either level. Stations used, from east to west: Casa Blanca, Cuba; Key West, Miami, Tampa, Fl.; Thomasville, Ga.; Pensacola, Fl.; Mobile, Al.; New Orleans, La.; Meridian, Vicksburg, Ms.; Alexandria, Jennings, La.; Galveston, Corpus Christi, Tx.; Merida, Mexico.

	Average Temperature °C			
Season	El Niño	Non-El Niño	La Niña	Non-La Niña
Key West, Fl, 1851-1970				
winter+spring	22.7	23.1		
winter			21.8	21.1
spring	24.4	24.8		
Thomasville, Ga, 1892-1980				
winter+spring	15.4	16.0		
winter	11.2	12.2	12.6	11.8
Pensacola, Fl, 1879-1980				
winteryear	19.6	20.0		
winter+spring	15.5	16.1	16.4	15.7
winter	11.7	12.4	13.0	12.0
Mobile, Al, 1873-1970				
winteryear	19.1	19.5		
winter+spring	14.9	15.5	15.9	15.2
winter	10.9	11.6	12.3	11.3
New Orleans, La, 1874-1980				
winteryear	20.6	20.9		
winter+spring	16.5	17.1	17.4	16.8
winter	12.6	13.4	14.0	13.0
spring	20.6	20.7		
fall	21.2	21.7		
Meridian, Ms, 1889-1980				
winter			9.8	8.9
Vicksburg, Ms, 1871-1980				
winter+spring			14.7	14.1
winter			10.7	9.6
Alexandria, La, 1894-1980				
summer	28.0	27.6		

Table 2.5. : continued.

Season	Average Temperature °C El Niño	Non-El Niño	La Niña	Non-La Niña
Jennings, La, 1897-1980				
winteryear	19.7	20.3		
winter+spring	15.6	16.3		
winter	11.4	12.4		
fall	20.3	21.0		
Galveston, Tx, 1873-1977				
winteryear	20.5	21.0	21.2	20.8
winter+spring	16.2	16.9	17.3	16.5
winter	12.4	13.4	13.9	12.9
spring			20.6	20.2
fall	21.7	22.4		
Corpus Christi, Tx, 1887-1950				
winteryear	21.3	21.9		
winter+spring	17.3	18.2	18.7	17.8
winter	13.8	14.8	15.7	14.2
spring	21.0	21.7		
fall	22.5	23.1		
Merida, Mexico, 1895-1980				
winter	23.0	23.3		
spring			26.6	27.1

Table 2.6: Precipitation at 15 gulf-region, single stations; all seasons with precipitation differences significant at the .01 or .05 confidence level by the rank sum test. Confidence criteria on single-station data are not adjusted for multiple use of rank sum test because period of record varies from station to station. A blank indicates the parameter was not significant at either level. Stations used, from east to west: Casa Blanca, Cuba; Key West, Miami, Tampa, Fl.; Thomasville, Ga.; Pensacola, Fl.; Mobile, Al.; New Orleans, La.; Meridian, Vicksburg, Ms.; Alexandria, Jennings, La.; Galveston, Corpus Christi, Tx.; Merida, Mexico.

	Average Total Precipitation (mm)			
Season	El Niño	Non-El Niño	La Niña	Non-La Niña
Key West, Fl, 1851-1970				
winteryear	1002	986	852	1019
winter+spring	337	279		
winter	159	130		
spring	185	143		
summer	287	347		
Miami, Fl, 1851-1970				
winter+spring	541	441		
winter	208	145	117	163
fall	435	529		
Tampa, Fl, 1851-1970				
winter+spring	445	372	304	411
winter	233	171	132	197
Thomasville, Ga, 1892-1980				
winter+spring			566	652
winter	376	295		
Pensacola, Fl, 1879-1980				
winteryear			1353	1570
winter+spring			527	721
winter	388	314		
spring			259	367
Mobile, Al, 1873-1970				
winteryear			1375	1638
winter+spring			628	823
winter	430	362		
spring			325	421
New Orleans, La, 1874-1980				
winteryear			1370	1591
winter+spring			592	791
winter	401	342	317	375
spring			309	407

Table 2.6. : continued.

Season	Average Total Precipitation (mm) El Niño	Non-El Niño	La Niña	Non-La Niña
Meridian, Ms, 1889-1980				
winteryear			1230	1401
Alexandria, La, 1894-1980				
winteryear	1546	1404		
Jennings, La, 1897-1980				
winteryear	1653	1436	1298	1541
winter+spring	828	728	633	784
spring			270	381
summer			472	410
fall	379	293		
Galveston, Tx, 1873-1977				
winteryear	1287	1065		
winter+spring	584	448	401	503
winter	305	234	215	263
spring	276	211		
fall	407	307		
Corpus Christi, Tx, 1887-1950				
winteryear	796	611		
winter+spring	362	257		
spring	212	150		
summer	122	183		
fall			135	229
Casa Blanca, Cuba, 1895-1980				
winteryear			1047	1201
winter+spring	432	356		
winter	213	151	107	179

Table 2.7: Temperature at 8 gulf-region, climatic divisions, 1895 to 1989; all seasons with temperature differences significant at the .01 or .05 confidence level by the rank sum test. Confidence criteria, z-values, are adjusted to compensate for the multiple use of the test on one field. A blank indicates the parameter was not significant at either level. Divisions used, from east to west: Key West, St. Petersburg, Tallahassee, Fl.; New Orleans, Lake Charles, La.; Houston, Corpus Christi, Brownsville, Tx.

	Average Temperature °C			
Season	El Niño	Non-El Niño	La Niña	Non-La Niña
New Orleans, La, 1889-1989				
winteryear	20.3	20.7		
Lake Charles, La, 1895-1989				
winteryear	19.5	19.9		
Houston, Tx, 1895-1989				
winteryear	20.4	20.8		
winter+spring	16.2	16.8		
Corpus Christi, Tx, 1895-1989				
winteryear	20.4	20.9		
winter+spring	15.9	16.7	17.0	16.3

Table 2.8: Precipitation at 8 gulf-region, climatic divisions, 1895 to 1989; all seasons with precipitation differences significant at the .01 or .05 confidence level by the rank sum test. Confidence criteria, z-values, are adjusted to compensate for the multiple use of the test on one field. A blank indicates the parameter was not significant at either level. Divisions used, from east to west: Key West, St. Petersburg, Tallahassee, Fl.; New Orleans, Lake Charles, La.; Houston, Corpus Christi, Brownsville, Tx.

	Average Total Precipitation (mm)			
Season	El Niño	Non-El Niño	La Niña	Non-La Niña
Key West, Fl, 1895-1989				
winter+spring	402	302		
winter	197	124		
St. Petersburg, Fl, 1895-1989				
winter+spring	475	394	322	437
winter	219	164	129	190
Tallahassee, Fl, 1895-1989				
winteryear			1331	1518
winter+spring			547	697
spring			264	351
New Orleans, La, 1895-1989				
winteryear			1338	1594
winter+spring	814	690	617	737
winter	424	345		
Lake Charles, La, 1895-1989				
winteryear	1680	1417	1326	1522
winter+spring	826	675		
Houston, Tx, 1895-1989				
winteryear	1363	1135		
winter+spring	632	505		
winter	319	254		
Corpus Christi, Tx, 1895-1989				
winteryear	1031	819	744	903
winter+spring	491	380		
winter	220	161		
Brownsville, Tx, 1895-1989				
winter+spring	303	224		
winter	145	94	71	115

2.4 Some Frontal-Wave Cyclone Characteristics: 1960-89

2.4.1 Frontal-Wave Cyclone Location of Origin

As stated earlier, the location of origin is a best estimate, being the location of first appearance of a disturbance on the daily map. Figs. 2.25 and 2.26 show the locations of origin for winter, frontal-wave cyclones in El Niño and in non-El Niño years, respectively. Other seasons appear in appendix P. Latitude, longitude, and water depth or land elevation at these points were subjected to the rank sum test to look for El Niño and La Niña year biases. (Here the rank sum test was used on all individual storms' latitude, longitude, and water depth or land elevation, rather than on seasonal means, giving greater sample size and more confidence in the results. T2-values were not needed as sample size was always greater than 30.) Tables 2.9 and 2.10 present results for latitude and longitude and for water depth or land elevation, respectively. A pairing of opposites is again evident. According to the rank sum test, in El Niño years, more winter storms form farther offshore, at lower latitudes and over deeper water than in all other years. In La Niña years, more winter storms form closer to shore, over shallower water. Fig. 2.27 and 2.28 show the breakdown by water depth (or land elevation) of origin for storms in El Niño years and La Niña years, respectively. In Table 2.10, the average water depth listed is an average of positive, land elevations for coastal plain storms, and of negative, water depths for marine storms. No longitude difference was found in El Niño or La Niña years. In all years, the highest concentration of winter storms is found over the northwestern gulf, Figs. 2.25 and 2.26. This is corroborated by Petterssen's (1956) finding of a local maximum in the frequency of winter cyclogenesis per 100 000 mi^2 (256 000 km^2 when examining nearly the entire Northern Hemisphere, for the period 1899 to 1939.

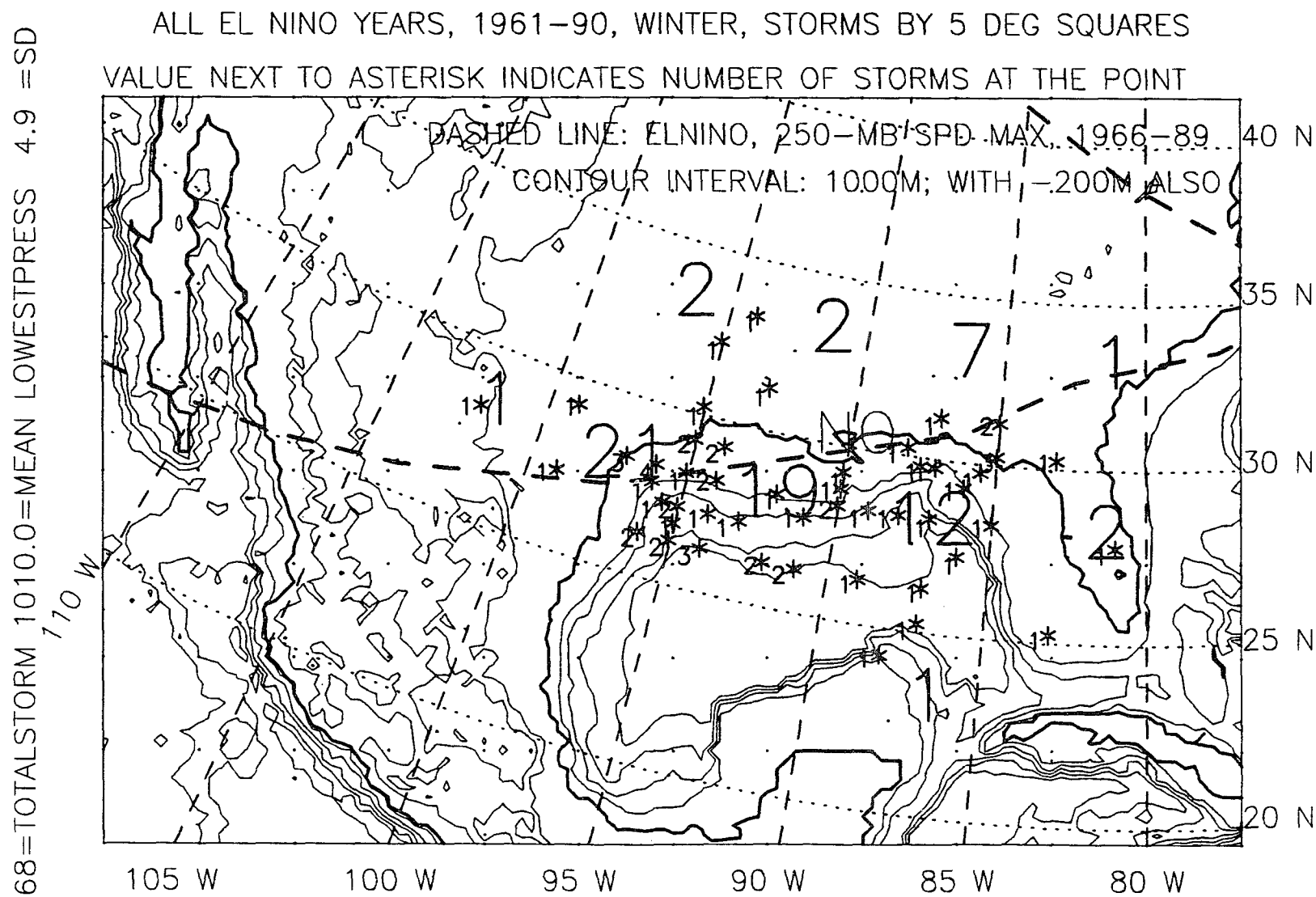

Figure 2.25: Storm locations, winter, 5 El Niño years, 1961–90.

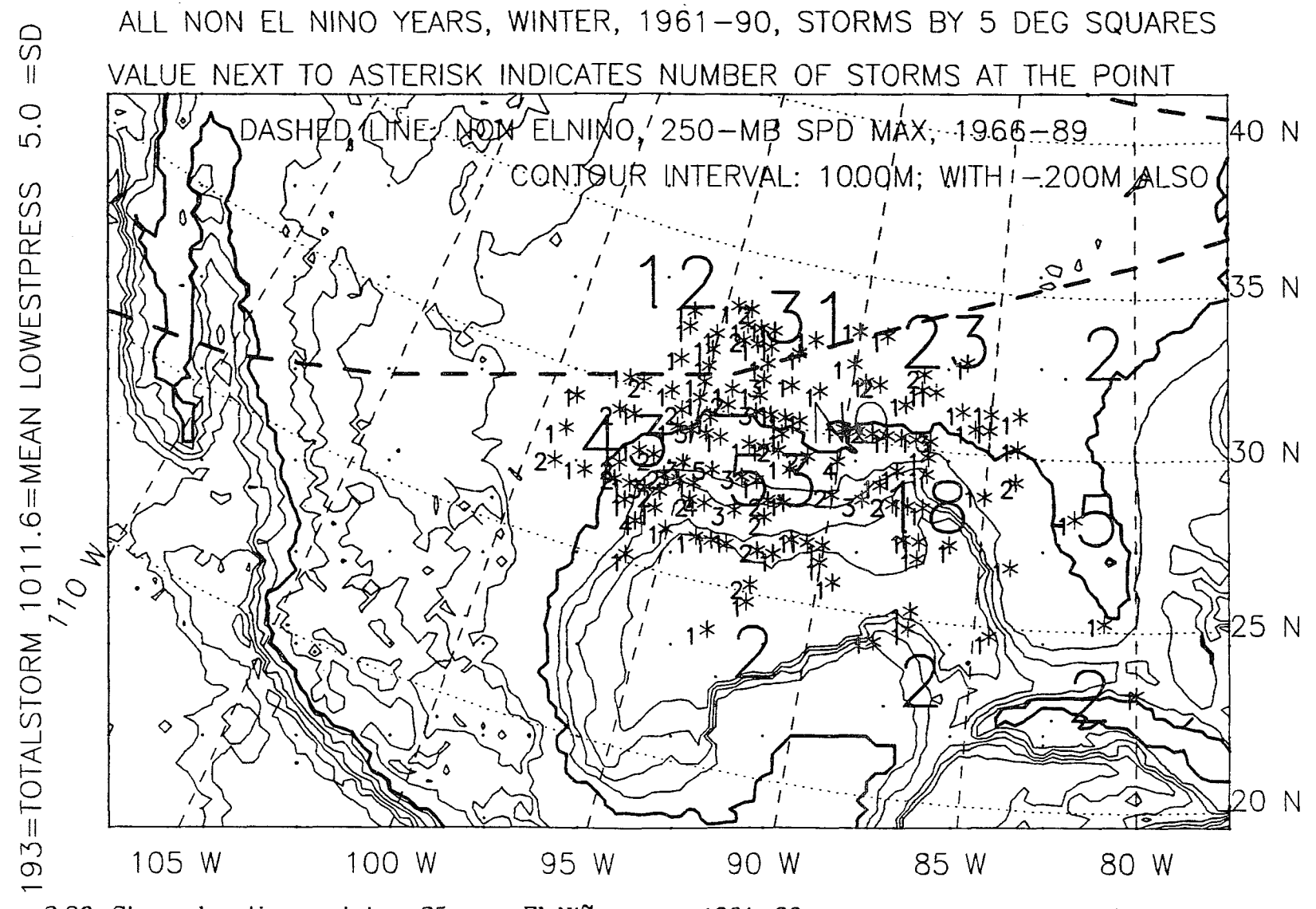

Figure 2.26: Storm locations, winter, 25 non-El Niño years, 1961-90.

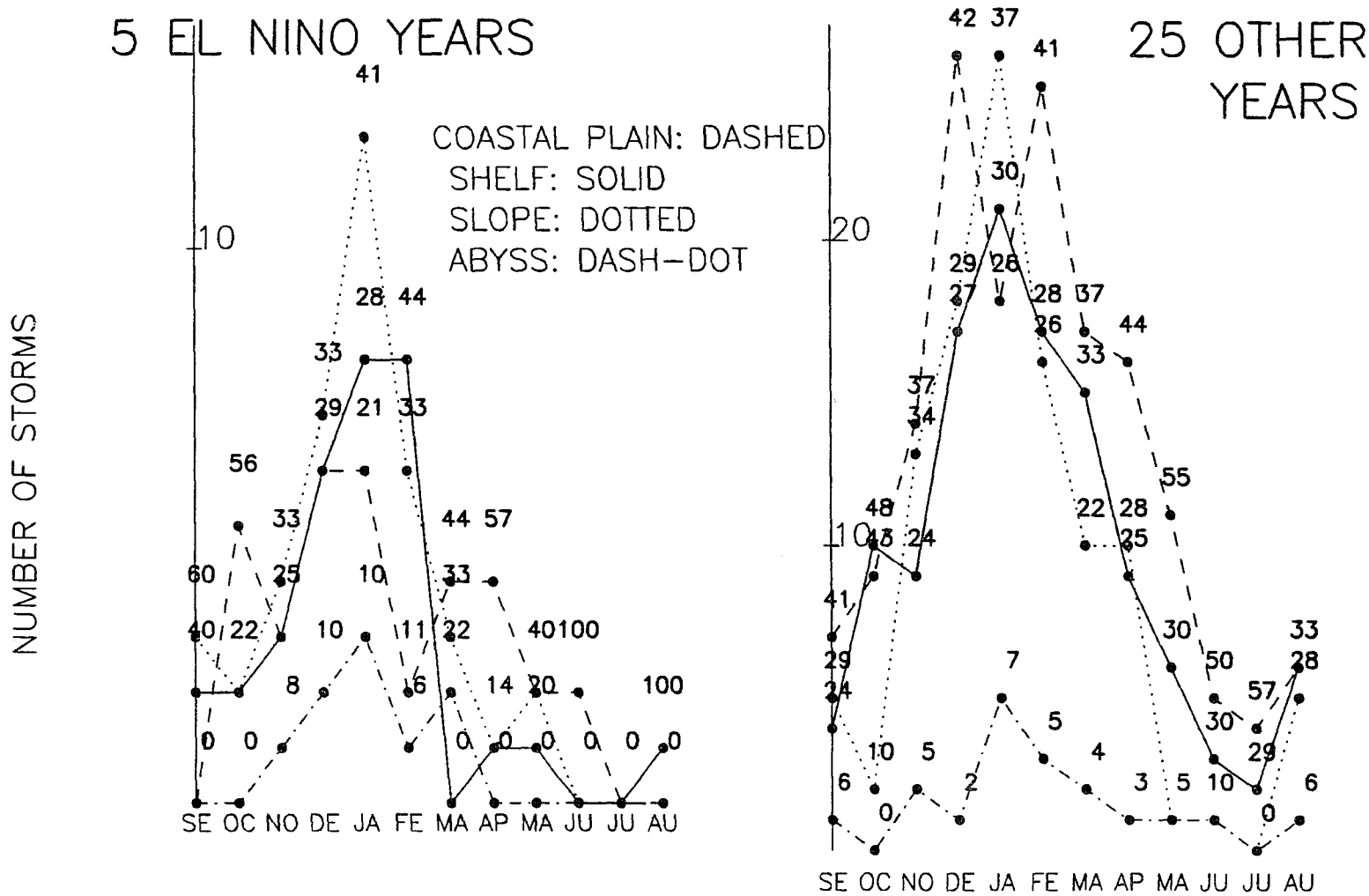

Figure 2.27: Storms/month, by water depth, 1960–89, El Niño vs other years. Bold numbers example: 41% of January storms occur on the slope in El Niño years.

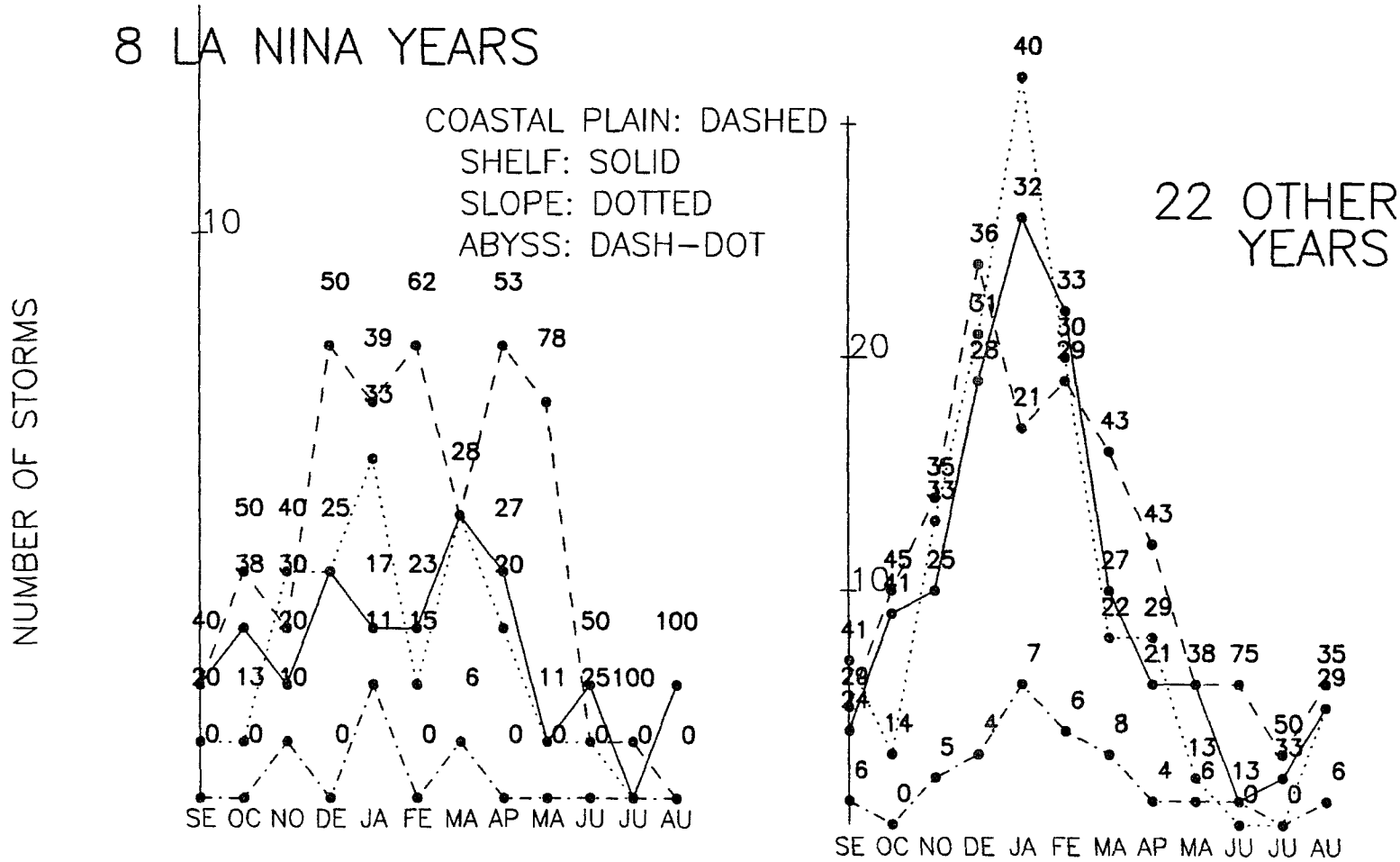

Figure 2.28: Storms/month, by water depth, 1960–89, La Niña vs other years. Bold numbers example: 39% of January storms occur on the coastal plain in La Niña years.

2.4.2 Frontal-Wave Cyclone Lowest Central Pressure

As with the three location parameters above, the lowest central pressures attained while in the gulf region, as available from the daily weather map, were subjected to the rank sum test. In El Niño years, winter storms had a significantly lower central pressure (.05 confidence level) than in all other years. In La Niña years, winter-storm central pressure was higher, also significant at the .05 level. Table 2.11 contains the pressure results. Figs. 2.29 and 2.30 show the distribution of lowest central pressure in El Niño and La Niña winters over the 30-year period. In El Niño winters there is a greater percent of storms in the category 1005 to 1010 mb than in non-El Niño winters. Similarly in La Niña winters there is a smaller percent of storms in the category 1005 to 1010 mb than in non-La Niña winters. A central pressure of 1010 mb is a fairly strong frontal-wave cyclone in the gulf area.

2.5 Summary of Surface Findings

Table 2.12 summarizes the findings presented in this chapter. The emerging picture is of relatively cool, wet, stormy, El Niño winters with fewer cold fronts than in other years. Opposite conditions prevail in La Niña years, that is, winters are warmer, drier, less-stormy, and the number of cold fronts is either greater or the same as in other years. This seems counter-intuitive. If most winter storms in the gulf area form along fronts, one would expect their frequencies to parallel each other, not to be indirectly proportional (or even unrelated) as indicted here. Speculating, perhaps this can be understood if storm formation is favored by a 'rest period' between frontal passages. During this time, a southerly flow of warm, moist air can be re-established, providing the necessary contrast in airmass characteristics when the next surge of cool, dry air arrives, so that storm formation is more likely, provided necessary, upper-level conditions are met, as discussed in chapter 4.

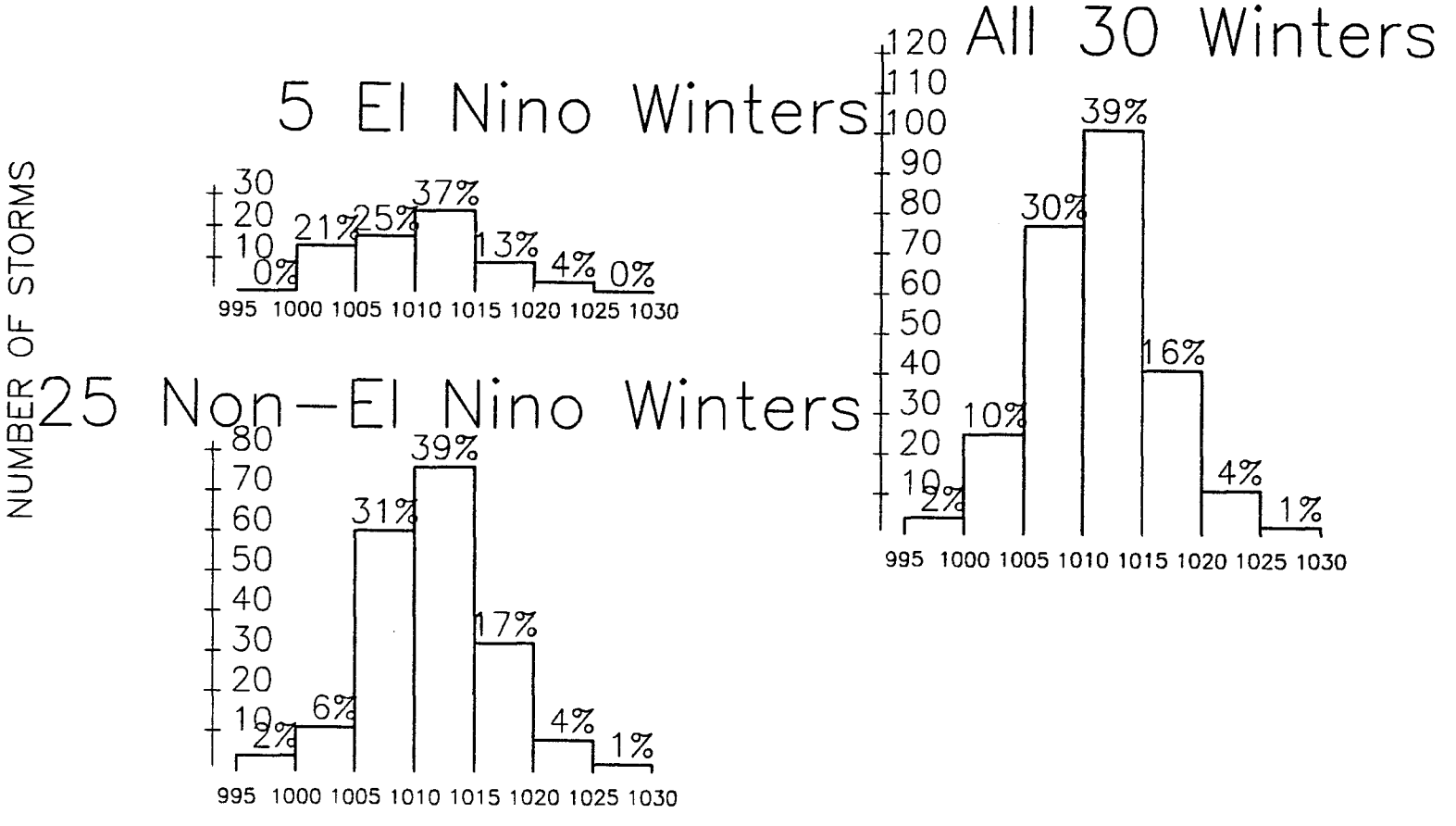

Figure 2.29: Histograms of lowest central pressure in frontal-wave cyclones, El Niño, other, and all winters, 1961-90.

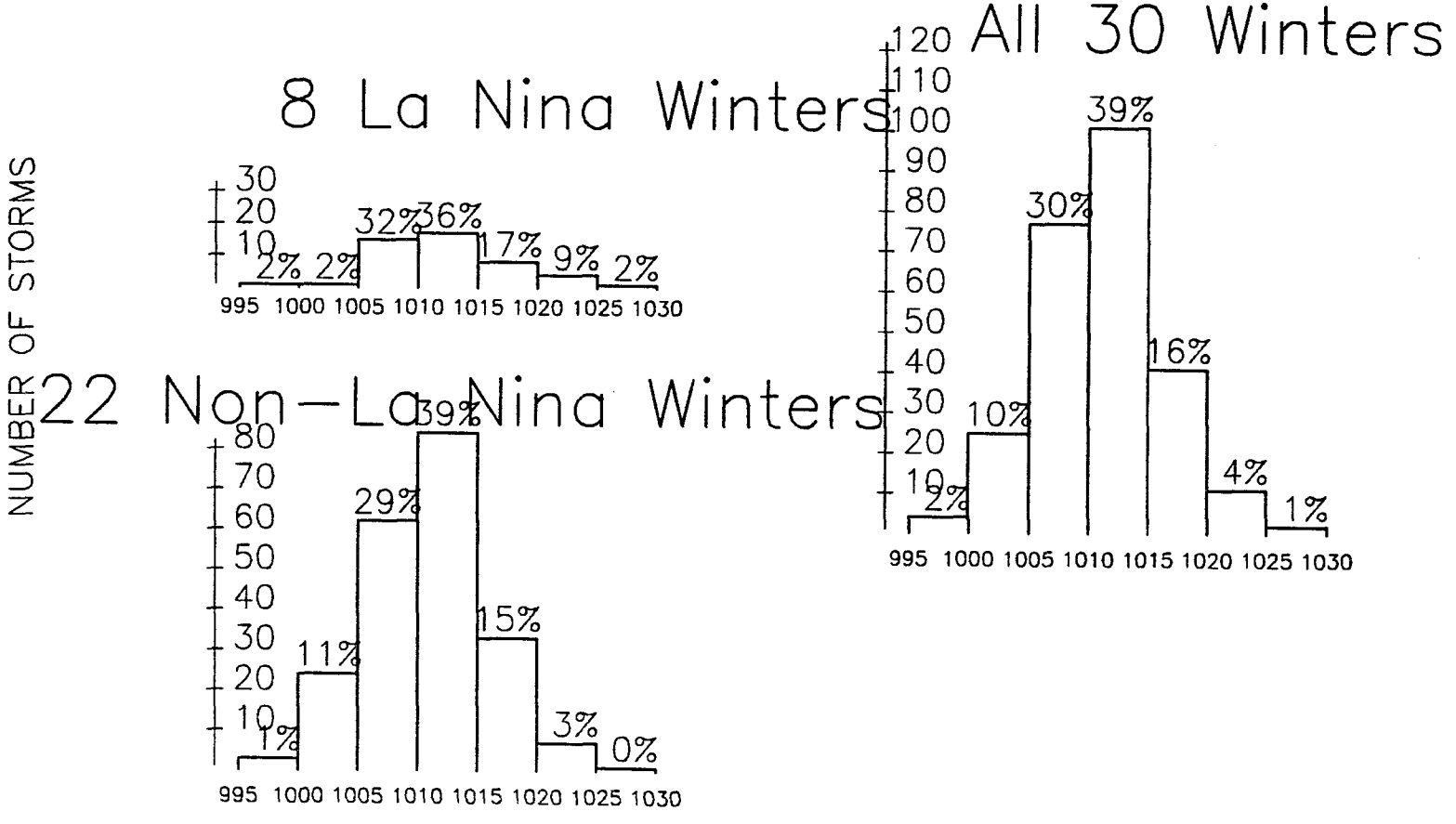

Figure 2.30: Histograms of lowest central pressure in frontal–wave cyclones, La Niña, other, and all winters, 1961–90.

Table 2.9: Average latitude and longitude of frontal-wave cyclones in El Niño and in La Niña years, 1960-89; results of the rank sum test, also known as the U-test, Wilcoxon test, or Mann-Whitney test, for differences between El Niño and non-El Niño years, and between La Niña and non-La Niña years. Latitudes and longitudes listed are those at the point where a storm was first observed on the weather map. Latitudes and longitudes were measured to the nearest half degree, therefore the averages listed are beyond the range of accuracy and are only for display. This is the closest point identifiable on 24-hour maps to the point of origin. The number of observations is the number of storms in each season, not the number of years analyzed. z-values are used to test significance since the number of observations is always greater than 30. Reject the null hypothesis at the $\alpha = .01$ level if $z > 2.575$ or $z < -2.575$. For $\alpha = .05$, reject the null hypothesis if $z > 1.960$ or $z < -1.960$. Levels of significance are indicated by daggers, $\alpha = .01$, double dagger; $\alpha = .05$, single dagger.

El Niño Versus Non-El Niño Years

		Average Latitude			Average Longitude			# of Storms
Season	Time	El	Non	z	El	Non	z	El/Non
winteryear	1960-89	28.4	28.9	-2.615 ‡	91.0	91.0	0.110	68/193
wntr+sprng	1961-90	28.2	28.9	-2.818 ‡	91.4	91.6	-0.256	85/299
winter	1961-90	28.0	28.7	-2.455 †	91.6	92.0	-0.438	68/193
spring	1961-90	29.1	29.2	-0.196	91.0	90.7	-0.013	21/102
summer	1961-90	27.0	29.5	-1.746	82.2	88.0	-2.739 ‡	3/35
fall	1960-89	28.4	29.0	-1.432	90.2	90.4	-0.058	26/76

La Niña Versus Non-La Niña Years

		Average Latitude			Average Longitude			# of Storms
Season	Time	La	Non	z	La	Non	z	La/Non
winteryear	1960-89	29.0	28.7	1.134	91.2	91.0	0.309	111/413
wntr+sprng	1961-90	29.0	28.6	1.254	92.1	91.4	1.068	76/308
winter	1961-90	29.2	28.4	2.379 †	92.8	91.7	1.345	47/214
spring	1961-90	29.0	29.2	-0.056	91.1	90.6	0.649	42/81
summer	1961-90	28.3	29.5	-1.309	88.3	87.4	0.170	7/31
fall	1960-89	29.1	28.7	0.844	90.7	90.2	0.573	23/79

‡ : indicates null hypothesis can be rejected at the .01 level of significance.
† : indicates null hypothesis can be rejected at the .05 level of significance.

Table 2.10: Water depth or land elevation (m) of frontal-wave cyclones in El Niño and in La Niña years, 1960-89; results of the rank sum test, also known as the U-test, Wilcoxon test, or Mann-Whitney test, for differences between El Niño and non-El Niño years, and between La Niña and non-La Niña years. Water depths or land elevations listed are those at the point where a storm was first observed on the weather map. It is the closest point identifiable to the point of origin. The average water depth listed is an average of positive, land elevations for coastal plain storms, and of negative, water depths for marine storms. The number of observations is the number of storms in each season, not the number of years analyzed. z-values are used to test significance since the number of observations is always greater than 30. Reject the null hypothesis at the $\alpha = .01$ level if $z > 2.575$ or $z < -2.575$. For $\alpha = .05$, reject the null hypothesis if $z > 1.960$ or $z < -1.960$. Levels of significance are indicated by daggers, $\alpha = .01$, double dagger; $\alpha = .05$, single dagger.

El Niño Versus Non-El Niño Years

		Average Water Depth or Land Elevation (m)			# of Storms	
Season	Time	El Niño	Other	z	ElNiño	Other
winteryear	1960-89	-701	-549	-1.370	84	440
winter+spring †	1961-90	-808	-549	-2.501	85	299
winter †	1961-90	-808	-589	-2.238	68	193
spring	1961-90	-845	-456	-0.316	21	102
summer	1961-90	17	-412	0.541	3	35
fall	1960-89	-680	-469	-1.333	26	76

La Niña Versus Non-La Niña Years

		Average Water Depth or Land Elevation (m)			# of Storms	
Season	Time	La Niña	Other	z	LaNiña	Other
winteryear	1960-89	-516	-594	1.002	137	387
winter+spring	1961-90	-572	-615	1.376	76	308
winter †	1961-90	-468	-685	2.417	47	214
spring	1961-90	-359	-607	1.150	42	81
summer	1961-90	-161	-427	-1.017	7	31
fall	1960-89	-395	-560	0.753	23	79

Notes:

‡ : indicates null hypothesis can be rejected at the .01 level of significance.

† : indicates null hypothesis can be rejected at the .05 level of significance.

Table 2.11: Lowest central pressure (mb) in frontal-wave cyclones in El Niño and in La Niña years, 1960-89; results of the rank sum test, also known as the U-test, Wilcoxon test, or Mann-Whitney test, for differences between El Niño and non-El Niño years, and between La Niña and non-La Niña years. Pressures listed are averages of the lowest central pressure observed on the weather map during a storm's duration, usually occurring on the first day. The number of observations is the number of storms in each season, not the number of years analyzed. z-values are used to test significance since the number of observations is always greater than 30. Reject the null hypothesis at the $\alpha = .01$ level if $z > 2.575$ or $z < -2.575$. For $\alpha = .05$, reject the null hypothesis if $z > 1.960$ or $z < -1.960$. Levels of significance are indicated by daggers, $\alpha = .01$, double dagger; $\alpha = .05$, single dagger.

El Niño Versus Non-El Niño Years

		Average Lowest Pressure(Std.Dev.)			# of Storms	
Season	Time	El Niño	Other	z	El	Non
winteryear	1960-89	1009.9(5.1)	1010.7(4.9)	-1.065	117	407
winter+spring	1961-90	1009.2(5.5)	1010.7(5.0)	-1.920	85	299
winter †	1961-90	1010.0(4.9)	1011.6(5.0)	-2.082	68	193
spring	1961-90	1006.6(6.2)	1009.1(4.6)	-1.694	21	102
summer†	1961-90	1004.3(2.2)	1012.4(3.6)	-2.573	3	35
fall	1960-89	1011.1(3.8)	1010.3(4.2)	0.952	26	76

La Niña Versus Non-La Niña Years

		Average Lowest Pressure(Std.Dev.)			# of Storms	
Season	Time	La Niña	Other	z	La	Non
winteryear †	1960-89	1011.4(5.0)	1010.3(4.9)	1.989	111	413
winter+spring	1961-90	1011.7(5.1)	1010.1(5.1)	2.217	76	308
winter †	1961-90	1012.8(5.4)	1010.9(4.9)	2.195	47	214
spring	1961-90	1009.5(4.5)	1008.2(5.1)	1.224	42	81
summer	1961-90	1011.1(3.8)	1011.9(4.3)	-0.697	7	31
fall	1960-89	1009.7(5.0)	1010.7(3.9)	-0.669	23	79

Notes:

‡ : indicates null hypothesis can be rejected at the .01 level of significance.

† : indicates null hypothesis can be rejected at the .05 level of significance.

Table 2.12: Number of storms, cold fronts, hurricanes, and weather-type frequency, 1960-89: summary of all parameters significant at the .01 or .05 confidence level. A blank indicates the parameter was not significant at either level.

	El Niño		La Niña		
	Value	Conf. Level	Value	Conf. Level	Time
Frontal-Wave Cyclone Frequency					
frontal-wave Cyclones/winteryear	High	.05	Low	.05	60-89
frontal-wave Cyclones/winter+spring			Low	.05	61-90
frontal-wave Cyclones/winter	High	.01	Low	.01	61-90
Frontal-Wave Cyclone Traits					
Water Depth of Origin/winter	Deep	.05	Less	.05	61-90
Water Depth of Origin/winter+spring	Deep	.05			61-90
Lowest Central Pressure/winter	Low	.05	High	.05	61-90
Lowest Central Pressure/winteryear			High	.05	60-89
Latitude of Origin/winter	South	.05	North	.05	61-90
Latitude of Origin/winter+spring	South	.01			61-90
Latitude of Origin/winteryear	South	.01			60-89
Longitude of Origin/summer	East	.01			61-90
Cold-Front Frequency					
Cold fronts/winteryear	Low	.01			60-89
Cold fronts/winter+spring	Low	.01			61-90
Cold fronts/winter	Low	.05			61-90
Weather-Type Frequency					
Frontal Overrunning/winteryear	High	.05	Low	.05	61-89
Frontal Overrunning/winter	High	.05	Low	.05	62-90
Frontal Gulf Return/summer			Low	.05	61-90
Gulf Return/winter+spring	Low	.05			62-90
Gulf Return/winter	Low	.05			62-90
FrontalGulfReturn+GulfReturn/wntr+sprg	Low	.05	High	.05	62-90
FrontalGulfReturn+GulfReturn/winter	Low	.05			62-90
FrontalGulfReturn+GulfReturn/spring	Low	.05			62-90
Gulf High/summer			High	.01	61-90
Hurricane Frequency					
Hurricanes entering gulf/winteryear	Low	.01			

CHAPTER 3
UPPER-AIR ANALYSES

3.1 Data and Analyses

This and the next chapter contain results from analyses of wind velocity at the 850- and 250-mb levels from 1967 or 1966 to 1989. The data comes from a compilation of NMC data, as archived at the National Center for Atmospheric Research in Boulder Colorado. The data compiled has been put on a CD-ROM by the Department of Atmospheric Sciences at the University of Washington, Seattle, and it covers most of the Northern Hemisphere (Department of Atmospheric Sciences 1990; Mass et al. 1987; Jenne and Spangler 1975). The bulk of the data comes from NMC final analyses with infill from operational analyses, Air Force and Navy sources, and from special projects. All data is gridded on a 1977-point, octagonal grid. This is superimposed on a north-polar stereographic projection of the Northern Hemisphere, true at 60°N. Most of the tropics are not covered; the grid stops at approximately 15°N. Grid spacing at 20°N is 274 km (170 mi) and at 60°N it is 381 km (240 mi). Grid-to-latitude and longitude coordinate transformations were done following Jenne (1970). For this work 621 grid points were used, covering most of North and Central America and flanking parts of the Atlantic and Pacific Oceans. A no-data zone appears in the lower left corner of all maps; this is outside of the grid. Topographic information is from the ETOPO5 data set of digital elevation and bathymetry, available from the National Geophysical Data Center (1988) in Boulder, Colorado. Elevation and bathymetry are given every five minutes of latitude and longitude to a precision of one meter.

NMC final analyses used are prepared twice daily, at 0000 UTC and 1200 UTC, or 6:00 PM Central Standard Time (CST) and 6:00 AM CST, local time in most of

the Gulf of Mexico area. A final analysis is now defined. A continuous chain of two products, analyses and forecasts is run. To make an analysis, the starting point is the last-made forecast. The forecast is updated and corrected through the addition of real observations of conditions at map time, and up to three and a half hours later. An objective-analysis scheme is used to blend the new observations and the forecast values. Objective-analysis schemes allow many different kinds of data from many different sources and places to be objectively evaluated, weighted, and meshed together coherently. These programs also interpolate irregularly-spaced data onto a regular grid. The updated and corrected map is called the final analysis for that map time. It is their best estimate of conditions at map time. After this, the forecast is made using the final analysis as the starting point. This forecast will be the starting point for the next analysis, and so on. For every separate parameter, there are separate final analyses and forecasts, although many parameters are used in making all analyses and forecasts. Since 1976, final analyses are actually done every six hours (Cooley 1976), although the University of Washington data uses only 0000 UTC and 1200 UTC analyses. Further, the methods of checking and correcting data, the objective-analysis programs and the forecast programs have evolved continuously throughout the time span covered by the data. A good description of these, as they stood in 1979, may be found in a National Weather Service forecasting handbook (National Weather Service 1979). The discussion is more relevant to the data used here than would be a discussion of the latest techniques. Ongoing changes can presently be found in a quarterly, performance summary (National Meteorological Center 1988-89).

Of the data used, only the 250-mb wind data is in twice-daily form. The remainder used is in the form of monthly averages constructed from twice-daily observations. Seasonal averages constructed by the author of 250-mb wind use both 0000

UTC and 1200 UTC times to match the monthly averages already constructed. All data sets are reasonably complete. The most missing data occurs in the 250-mb wind data, no doubt due to a difficult collection environment. Over an 8835.5-day span covering 17 671 sets of measurements (two per day), 887 sets of observations are missing, about 15 months. In many cases, however, there is at least one observation per day. The largest total gap is 66 days, 1 January to 7 March 1970, which is not part of an El Niño or La Niña event.

Quantities calculated from the wind data are horizontal divergence and relative vorticity. Horizontal divergence was calculated in order to test the hypothesis that the increase in the number of storms in El Niño winters is caused by stronger, or more frequent, upper-level divergence (due to the jet stream being over the area more often) and correspondingly increased, compensating, lower-level convergence. The upper-level divergence is posed as the cause, and the lower-level convergence and storms are posed as the effects.

Horizontal divergence is a measure of the tendency of a three-dimensional flow either to spread horizontally and contract vertically (positive divergence), or to shrink horizontally and stretch vertically (negative divergence, called convergence). Nonzero horizontal divergence implies vertical motion. It is the dot product of the wind vector and the del operator. At or near the surface of the earth, negative divergence (convergence) implies ascending air. In storms, air is lifted, cooled, and precipitation results; storms are areas of surface convergence. Areas of high pressure at or near the surface of the earth are beneath areas where air is descending. Regions of high pressure are areas of positive divergence. At upper and intermediate levels of the atmosphere, where there is no solid lower boundary, convergence and divergence may each result in air ascending or descending from a particular level. Saucier (1955) presents 12 possibilities. As a general rule, horizontal convergence

near the surface of the earth is accompanied by divergence aloft and vice versa (Saucier 1955). The compensating increase in lower-level convergence, in response to increased upper-level divergence, occurs to conserve mass. In the vertical, mass is conserved through the presence of alternating, compensating layers of convergence and divergence, so that the sum in the vertical is zero. This has been called Dines' compensation (Petterssen 1956).

Divergence and relative vorticity were calculated using the simplest method, the so-called kinematic method, in which each is calculated directly from the observed wind. More sophisticated forms such as the omega and vorticity equations (Holton 1979) would have required either more data or more assumptions. The following formulas are from Holton's book (1979) but can be found in all beginning, dynamic-meteorology texts.

$$Horizontal\ \ divergence = D = \frac{\partial u}{\partial x} + \frac{\partial v}{\partial y} \tag{3.1}$$

u and v are the components of the wind vector in the x and y directions. The finite-difference approximation is used to calculate divergence at each point, (x,y).

$$D_{x_0,y_0} \approx \frac{u(x_0 + d) - u(x_0 - d)}{2d} + \frac{v(y_0 + d) - v(y_0 - d)}{2d} \tag{3.2}$$

d is the distance between grid points.

By definition, the geostrophic wind is nondivergent. Following is a demonstration of this, starting from the equations of geostrophic equilibrium, adapted from Pond and Pickard (1978). Where

$$f = Coriolisparameter = 2\Omega \sin \phi, \quad \Omega = rateofEarth'srotation, \quad \phi = latitude$$

$$\alpha = \frac{1}{\rho}, \quad \rho = density$$

$p = pressure$

$x, y = Cartesian\ \ coordinates$

The equations of geostrophic equilibrium are

$$-fv = -\alpha\frac{\partial p}{\partial x} \tag{3.3}$$

$$fu = -\alpha\frac{\partial p}{\partial y}$$

. Differentiate both sides of each equation.

$$-f\frac{\partial v}{\partial y} = -\alpha\frac{\partial^2 p}{\partial x \partial y}$$

$$f\frac{\partial u}{\partial x} = -\alpha\frac{\partial^2 p}{\partial x \partial y}$$

Subtract the the second equation from the first.

$$-f(\frac{\partial v}{\partial y} - \frac{\partial u}{\partial x}) = -\alpha(\frac{\partial^2 p}{\partial x \partial y} - \frac{\partial^2 p}{\partial x \partial y})$$

$$f(\frac{\partial u}{\partial x} + \frac{\partial v}{\partial y}) = 0$$

Since f is not zero except at the equator, the divergence (the quantity in parentheses) is zero.

$$(\frac{\partial u}{\partial x} + \frac{\partial v}{\partial y}) = 0 \tag{3.4}$$

$$(\frac{\partial u}{\partial x} = -\frac{\partial v}{\partial y}) \tag{3.5}$$

At midlatitudes and on the synoptic scale, the horizontal wind is almost geostrophic. To the extent that it isn't, horizontal divergence is nonzero. A nonzero horizontal

divergence implies vertical motion, ascending or descending air, and so is a good indicator of weather conditions. Causes of ageostrophic motion include friction, advection, and convection. Accelerated flows are ageostrophic. For example, in places the high-speed core of a jet stream is accelerated. There the divergence is nonzero. There actually are regions of ascending and descending air associated with a strong jet (Sechrist and Whittaker 1979). This was confirmed by study of the rapid transport around the earth of radioactive debris at stratospheric levels (Reiter 1978).

As a parallel test, the relative vorticity at both levels was calculated. Anticyclonic motion is one way to achieve positive horizontal divergence and cyclonic motion is one way to achieve horizontal convergence. Divergence and convergence may be due to other or a combination of other factors. (Positive divergence can result from velocity increase or streamline spreading. Convergence, negative divergence, can result from velocity decrease or streamlines coming together.) Relative vorticity is the vertical component of the cross product of the wind vector and the del operator. It is a measure of the tendency of a force (the horizontal wind) to produce a rotation about an axis perpendicular to the plane of the force, in this case a vertical axis. According to the 'right-hand rule', with positive (cyclonic, or counterclockwise in the Northern Hemisphere) relative vorticity, the vertical component (the thumb) points upward, implying upward motion. In storms, cyclonic circulation is accompanied by ascending air at the center. With negative relative vorticity (anticyclonic, or clockwise motion in the Northern Hemisphere) the vertical component points downward, implying descending motion. Based on this, it was hypothesized that in El Niño winters the average 850-mb relative vorticity would be more cyclonic (positive) than in non-El Niño winters. Relative vorticity at the 250-mb level was expected to be more cyclonic, not anticyclonic, even

though the upper-level was expected to be more divergent. The cyclonic vorticity was expected to derive from the presence of upper-level troughs behind the 250-mb level jet stream, as explained in 3.8.

From Holton (1979), the relative vorticity is

$$Relative\ \ vorticity = \zeta = \frac{\partial v}{\partial x} - \frac{\partial u}{\partial y}. \tag{3.6}$$

In finite-difference form, relative vorticity at a point is

$$\zeta_{x_0,y_0} \approx \frac{v(x_0+d) - v(x_0-d)}{2d} + \frac{u(y_0+d) - u(y_0-d)}{2d}. \tag{3.7}$$

Seasonal average values of divergence calculated are of order of magnitude 10^{-6}sec^{-1}. Values of this magnitude are characteristic of planetary waves (Petterssen 1956). For comparison, tornadoes probably possess the highest values of divergence, of order of magnitude 10^{-4}sec^{-1}. The method of calculating horizontal divergence is sensitive to observational errors because the differences used are small. The small differences occur because the horizontal wind is almost in geostrophic balance, (3.5) $\frac{\partial u}{\partial x}$ and $\frac{\partial v}{\partial y}$ almost cancel. In constructing seasonal averages for four years, the fewest years in any composite, with 90 days per season and 2 observations per day, $4\times90\times2 = 720$ observations per point, random observational errors may reasonably be expected to cancel. Systematic observational errors, to the extent possible, have been eliminated in the NMC analyses. Nevertheless, both divergence and relative-vorticity maps should not be taken as exact, but should be allowed some margin of uncertainty.

3.2 Winter, 850-mb Wind Field: 1967-1989

3.2.1 General Circulation of the 850-mb Wind Field: El Niño Winters

The comments below and in the next section refer to Figs. 3.1 and 3.2, composites of the 850-mb wind field for the four El Niño winters and for the 19 non-El Niño winters, respectively, between 1967 and 1989. The 850-mb level, about 1500 m (5000 ft), is representative of surface winds, minus local effects. The plotting convention is such that arrows fly with the wind. The shafts have a dot at the base. The head is omitted. The major features of this circulation, in El Niño winters, are enumerated below. Following these are first, a discussion of the El Niño-winter, 850-mb circulation over the Gulf of Mexico, and second, a discussion of the differences between El Niño and non-El Niño winter circulations.

1. A large, anticyclonic cell is situated over the eastern Pacific Ocean centered at 25°N, 135°W, the Pacific subtropical high.

2. A belt of easterly trade winds south of 23.5°N extends from the western Atlantic Ocean across Central America and into the eastern Pacific, where these join the south limb of the anticyclone.

3. A belt of westerly winds extends from north of Hawaii in the Pacific toward the North American west coast. Maximum average wind speeds are 14 ms^{-1} (28 kt). Upon encountering the North American landmass, the westerlies are deflected to the north and south. Most of the flow is steered northward, deflected by the Rocky Mountains, crossing the northern Rockies, which are not as high as the southern Rockies. Wind speeds are diminished by the passage. Once past the mountains, the northwest winds curve south again, across the central plains, straightening out to due west over eastern North

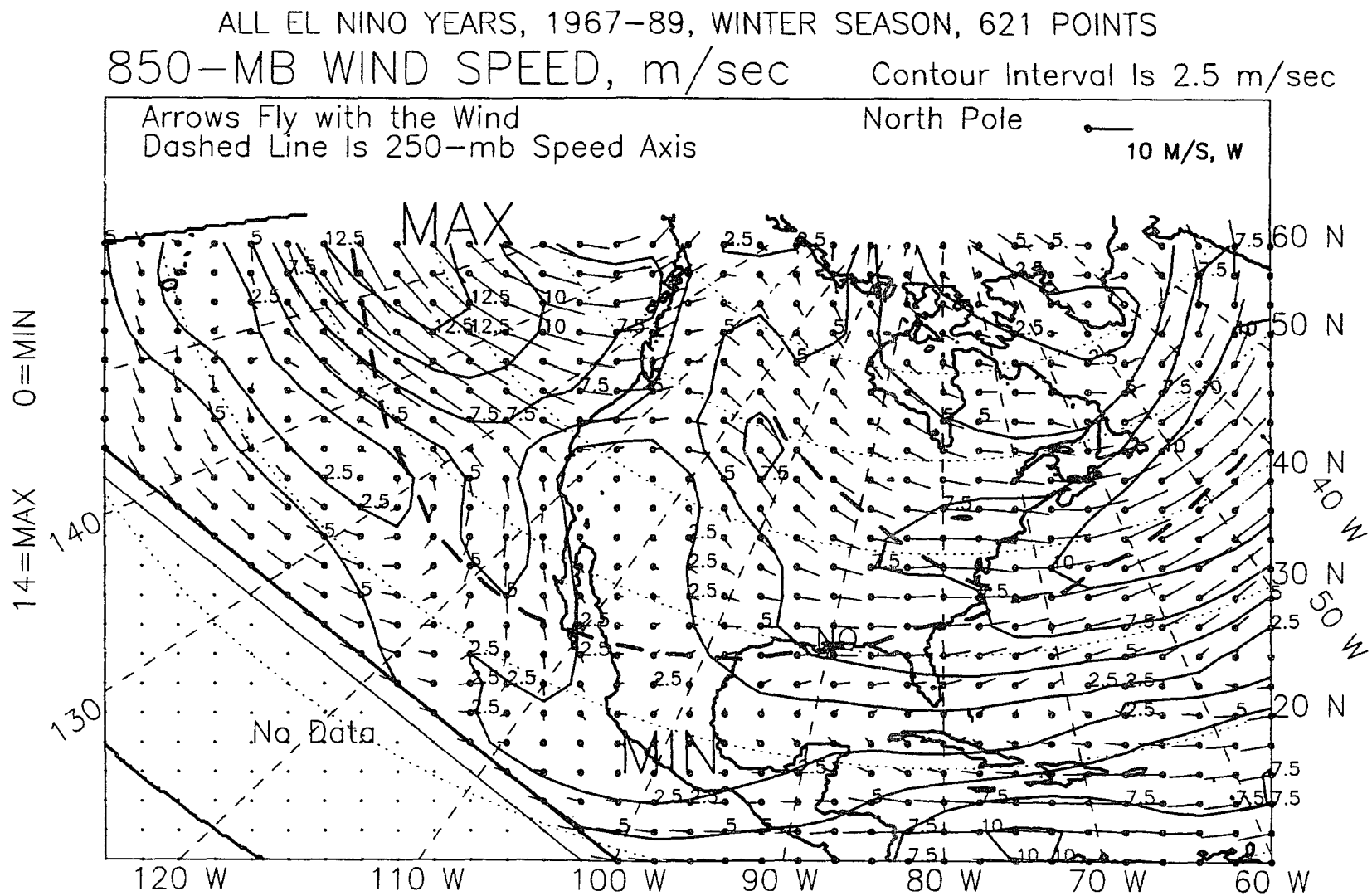

Figure 3.1: 850–mb wind vectors, winter, El Niño years, 1967–89.

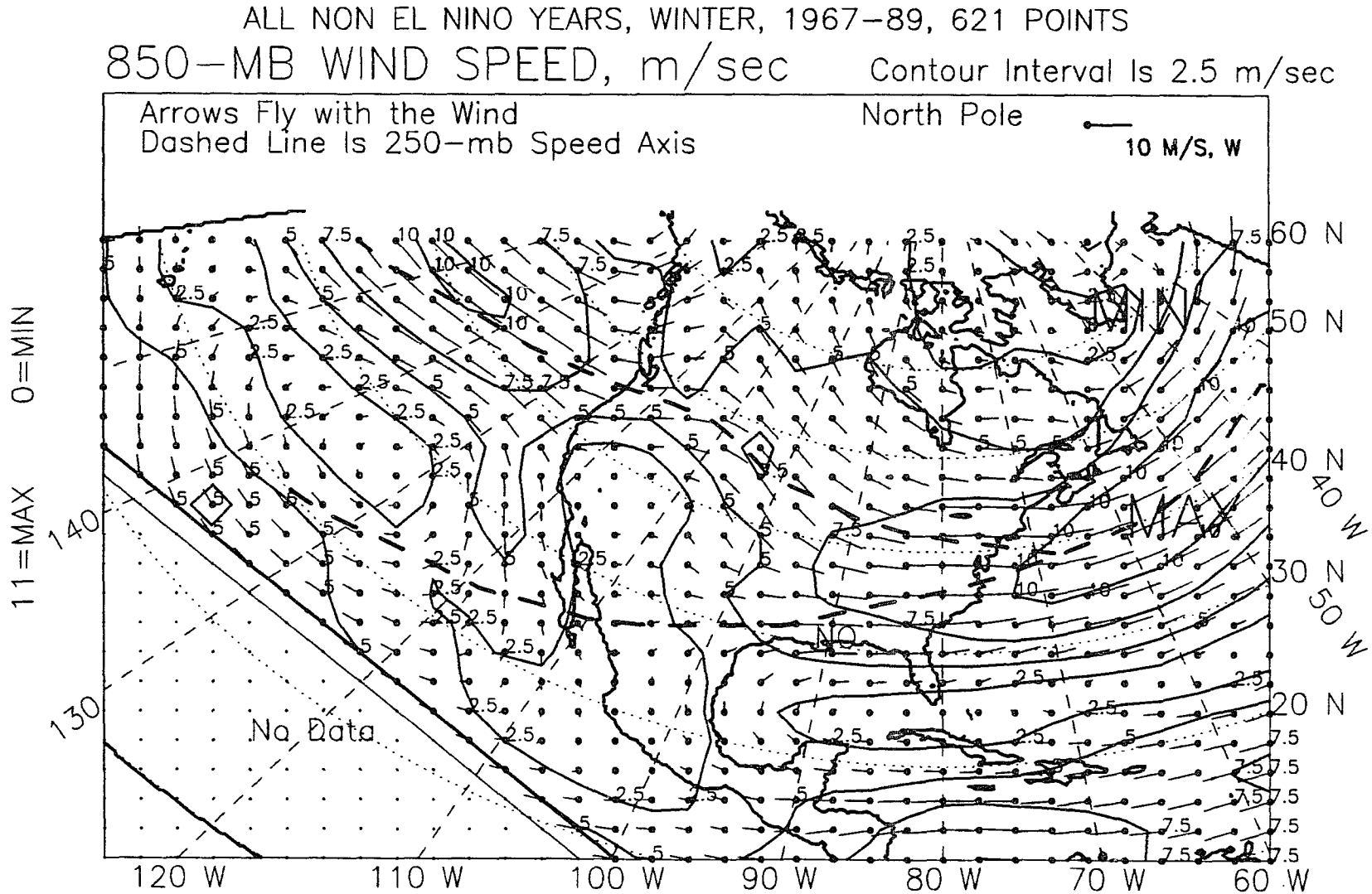

Figure 3.2: 850–mb wind vectors, winter, non–El Niño years, 1967–89.

America. The steep, south bend in the wind's trajectory is due to the conservation of potential vorticity. After crossing the Rockies, the flow depth increases and causes potential vorticity to decrease. The flow turns south, curving cyclonicly, conserving potential vorticity by adding positive relative vorticity. Once past the east coast of North America, wind speed increases again to 10 ms^{-1} (20 kt) and the direction is due west. Some of the west wind incident at the North American west coast is deflected southward, down the California and Mexico coasts, eventually joining the anticyclonic circulation around the Pacific subtropical high.

3.2.2 Gulf of Mexico: 850-mb Wind Field, El Niño Winters

1. The large-scale, average circulation over the Gulf of Mexico in winter is roughly anticyclonic, although it is not closed on the east end. The three limbs of the circulation that are present are first, the east trades south of 23.5°N, second, south winds along the western gulf coast, and last, southwesterlies along the north coast. The deep, central gulf has light, southwest winds. South winds along the western shelf of the gulf appear to be the result of northward deflection of the easterly trades by the Sierra Madre Orientals of the Mexican landmass. The mountains here are 1000 to 2000 m (3820 to 6560 ft) high, and the 850-mb level is about 1500 m (4920 ft) in elevation, so they are capable of acting as a barrier, at least at the 850-mb level and below.

2. Over the Gulf of Mexico, Caribbean Sea, and west Atlantic, the transition from the northernmost easterly trades to the southernmost westerlies occurs at about 23.5°N in winter, along an east-trending line dividing the southern

third of the Gulf, largely the Bay of Campeche and the Straits of Yucatan, from the northern two-thirds. Winds in the south are lighter than in the northern gulf, 2.5 ms^{-1} (5 kt) from the east and southeast. The northern two-thirds of the gulf and adjacent coastal plain has average winter winds from the southwest and west at 2.5 to 5 ms^{-1} (5 to 10 kt). The central-western gulf, from Brownsville, Texas to Tampico, Mexico, has light, south winds from the coast out to 3000 m (9850 ft) water depth.

3.2.3 Interpretation of Wind-Difference Maps

This section refers to a class of composite maps derived from other seasonal composites, such as Figs. 3.1 and 3.2 of the 850-mb wind field. They will be called 'difference maps', because they are produced by subtracting one map from another, point-by-point. For example, the wind-difference map, Fig. 3.3, is produced by subtracting, componentwise, the average non-El Niño-winter wind from the average El Niño-winter wind at each point. In this case, the magnitude of the wind-difference vectors is arbitrarily multiplied by four, relative to the source maps, for ease of reading. The speed contours, however, show true magnitude. Other workers (Held et al. 1989) have used a similar, simple difference of the composites of several El Niño seasons and several non-El Niño seasons.

It should be emphasized that the vector wind differences are the differences, at each point, between the seasonal average winds in El Niño winters and the seasonal average winds in non-El Niño winters. Because they are the differences of average winds, it is not generally possible to say with certainty exactly how the winds vary between winter type. For example, a west difference, or west residue, (the two words will be used interchangeably) may be the result of stronger, or more frequent westerlies in El Niño winters, and/or it may be the result of weaker or less

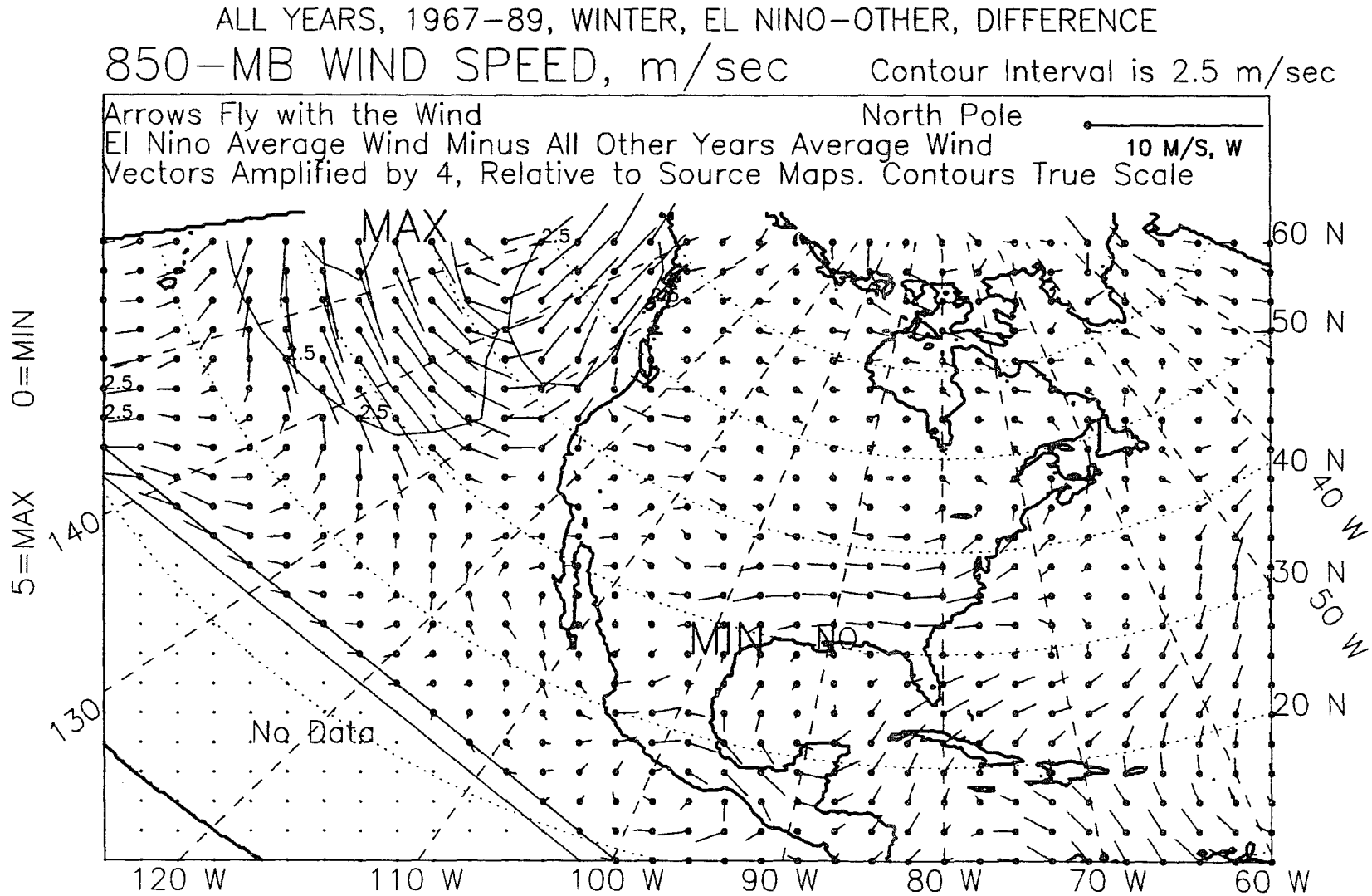

Figure 3.3: 850–mb wind vectors, winter, 1967–89, difference.

frequent easterlies in El Niño winters. Several possibilites exist unless a simplifying assumption can be made. If it is justified to assume that the all winds in both winter types are nearly always from the same direction, as in the case of the 250-mb, winter westerlies, or to a lesser extent, for the 850-mb westerlies and tropical easterlies, then the interpretation of the difference is more constrained. For example, in the 250-mb westerlies, a west-difference vector can safely be interpreted to result from stronger westerlies in El Niño winters. For west wind, (u>0, v=0) if $u_{ElNiño} = +6$ and $u_{Non-ElNiño} = +4$,

$$u_{difference} = u_{ElNiño} - u_{Non-ElNiño} \tag{3.8}$$

$$u_{difference} = +6 - +4 = +2,$$

a west difference. The order of subtraction was deliberately selected so that positive values indicate an excess in El Niño years, while negative values indicate a deficit.

In the more general case, where it is likely that the average wind is composed of several directions of varying frequency, the simplifying assumption is not justified and a physical reason is needed to select from the possibilities listed earlier. Table 3.1 shows a quick guide to wind-residue interpretation.

There is no frequency weighting in the source wind vectors. For example, one observation of 10 ms^{-1} north wind counts as much in the final average as two observations of 5 ms^{-1} south winds. Therefore, a few large events could greatly influence the final average. This is justifiable on the basis that major events should hold more sway in the final result because of their disproportionately large physical influence.

These simple differences, or residues, are not anomalies. Anomalies are constructed by subtracting, for example, a 30-year, winter mean from, for example, a

Table 3.1: Wind-difference (or wind-residue) interpretation chart. Order of subtraction is El Niño minus other.

Observe:	**SOUTH WIND DIFFERENCE**		
If Assume:	Always south wind	Always north wind	North and south wind
Difference	South wind excess	North wind deficit	More or stronger southerlies and/or Fewer or weaker northerlies
Due to:			
Observe:	**NORTH WIND DIFFERENCE**		
If Assume:	Always north wind	Always south wind	North and south wind
Difference	North wind excess	South wind deficit	More or stronger northerlies and/or Fewer or weaker southerlies
Due to:			
Observe:	**WEST WIND DIFFERENCE**		
If Assume:	Always west wind	Always east wind	West and east wind
Difference	West wind excess	East wind deficit	More or stronger westerlies and/or Fewer or weaker easterlies
Due to:			
Observe:	**EAST WIND DIFFERENCE**		
If Assume:	Always east wind	Always west wind	West and east wind
Difference	East wind excess	West wind deficit	More or stronger easterlies and/or Fewer or weaker westerlies
Due to:			
Observe:	**ANTICYCLONIC DIFFERENCE**		
If Assume:	Always anticyclonic	Always cyclonic	Combination
Difference	Anticyclonic excess	Cyclonic deficit	More or stronger anticyclonic circ. and/or Less or weaker cyclonic circulation
Due to:			
Observe:	**CYCLONIC DIFFERENCE**		
If Assume:	Always cyclonic	Always anticyclonic	Combination
Difference	Cyclonic excess	Anticyclonic deficit	More or stronger cyclonic circ. and/or Less or weaker anticyclonic circulation
Due to:			

mean of five El Niño winters, to obtain the El Niño-winter anomaly. The differences described above were used rather than standard anomalies in an attempt to amplify the differences between El Niño winters and all other winters. Using the anomaly technique, the four El Niño winters would be included in the 23-year average to be subtracted from the four-year, El Niño-winter average, diluting the results.

3.2.4 Differences in the 850-mb Wind Field between El Niño and Non-El Niño Winters

The following comments refer primarily to Fig. 3.3, a vector plot of the difference between the 850-mb wind field in the four El Niño and in the 19 non-El Niño winters from 1967 to 1989.

3.2.4.1 General-Circulation Differences in the 850-mb Wind Field between El Niño and Non-El Niño Winters

The largest difference in the area mapped (Fig. 3.3) is in the zone of strengthened westerlies over the northeast Pacific. In El Niño winters these westerlies are 2.5 to 5 ms^{-1} (5 to 10 kt) stronger than in non-El Niño winters. The strengthening is caused by an increased pressure gradient from south to north between the Pacific subtropical high and the Aleutian low. In the winter average, the Aleutian low is deepened by up to five millibars in El Niño winters, being 998.9 mb compared with an average 1004 mb in non-El Niño winters. Several workers have reported this intensification of the Aleutian low, including Bjerknes (1972) reporting on the 1964/65 Pacific equatorial warming, Horel and Wallace (1981), and Rasmussen (1991). Figs. 3.4 and 3.5 show the composite, mean sea-level pressure field in eight El Niño winters and in 35 non-El Niño winters from 1947 to 1989. Fig. 3.6 shows the difference between them. The pressure difference is constructed by subtracting

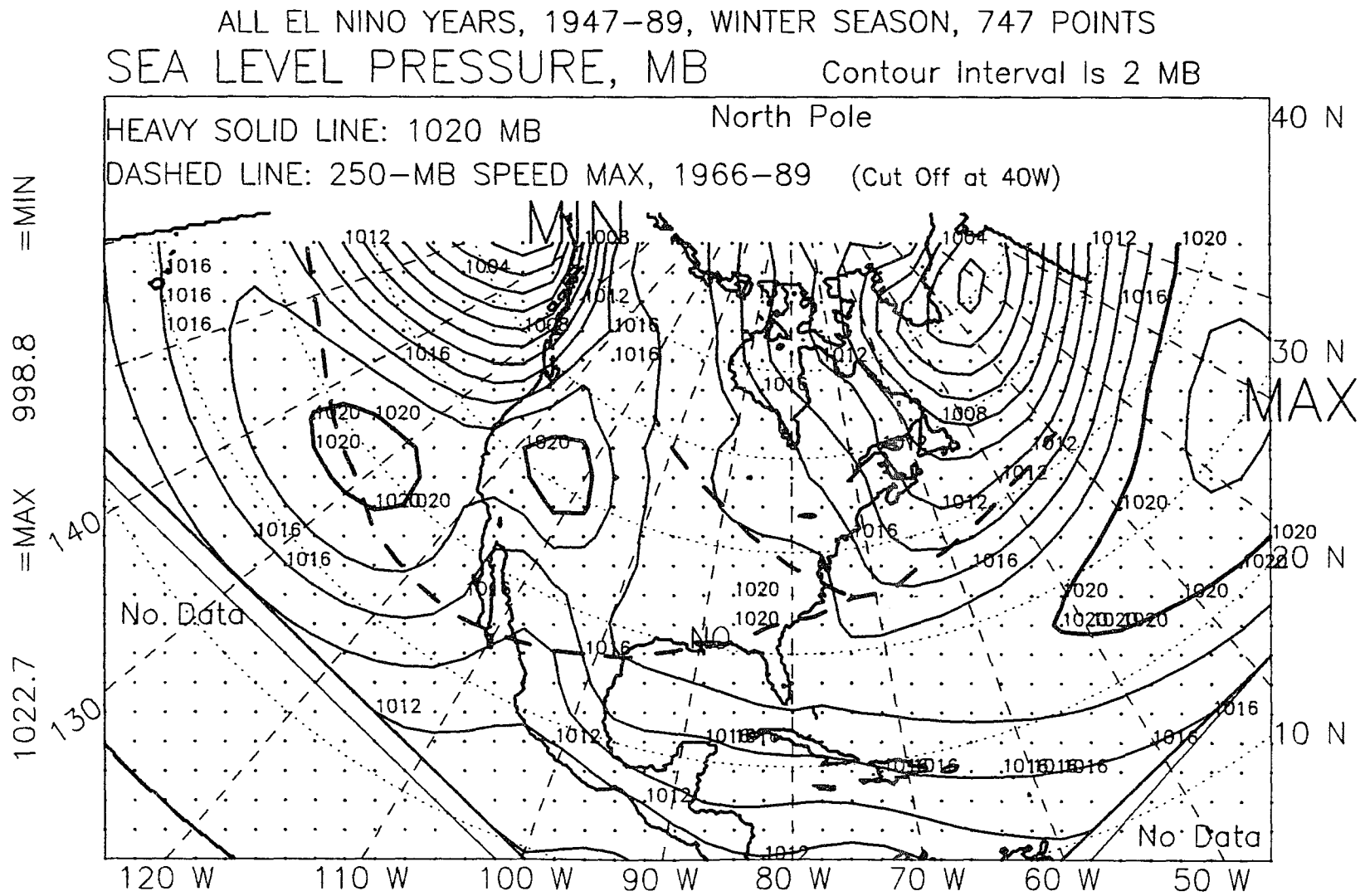

Figure 3.4: Mean sea–level pressure, winter, El Niño years, 1947–89.

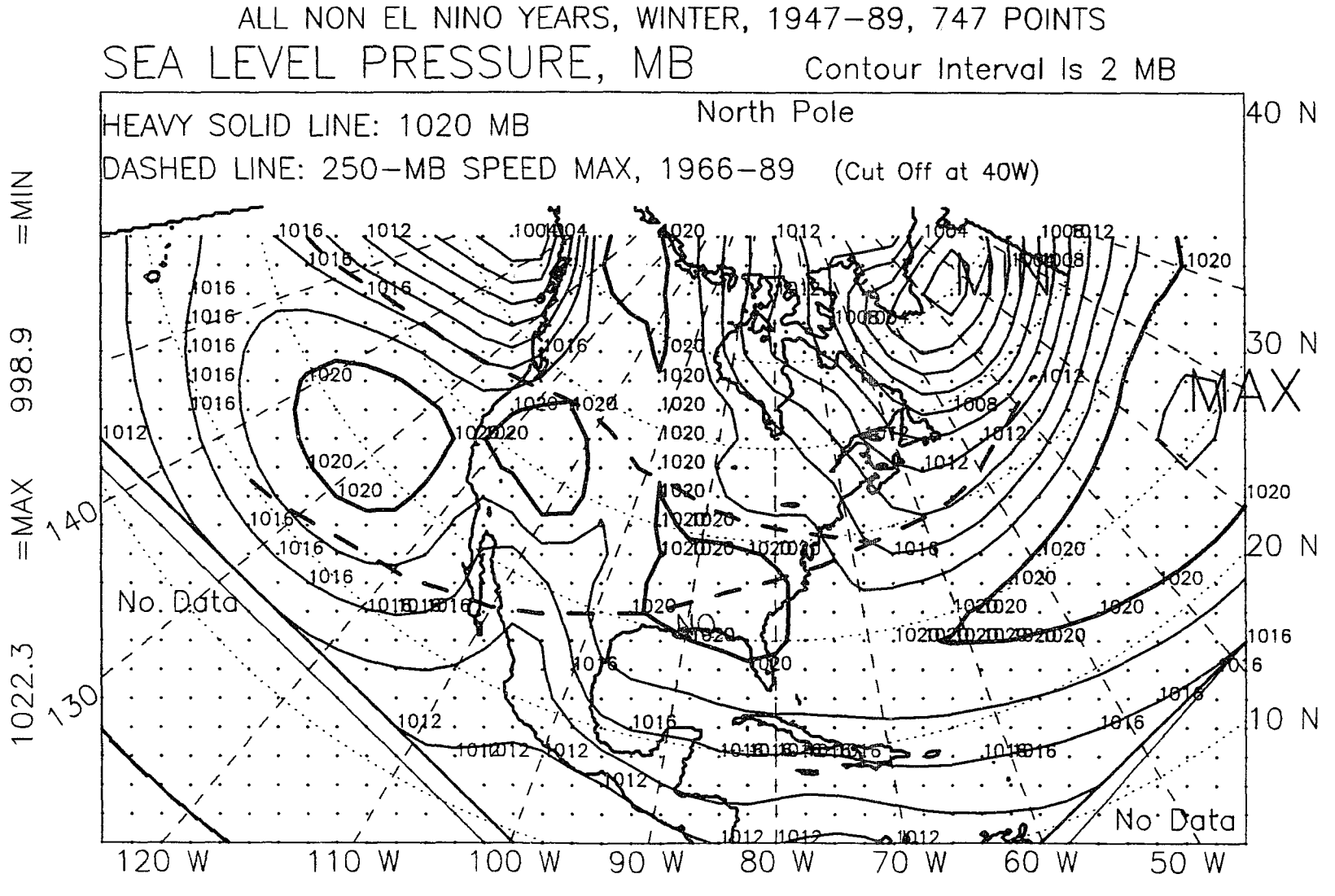

Figure 3.5: Mean sea–level pressure, winter, non–El Niño years, 1947–89.

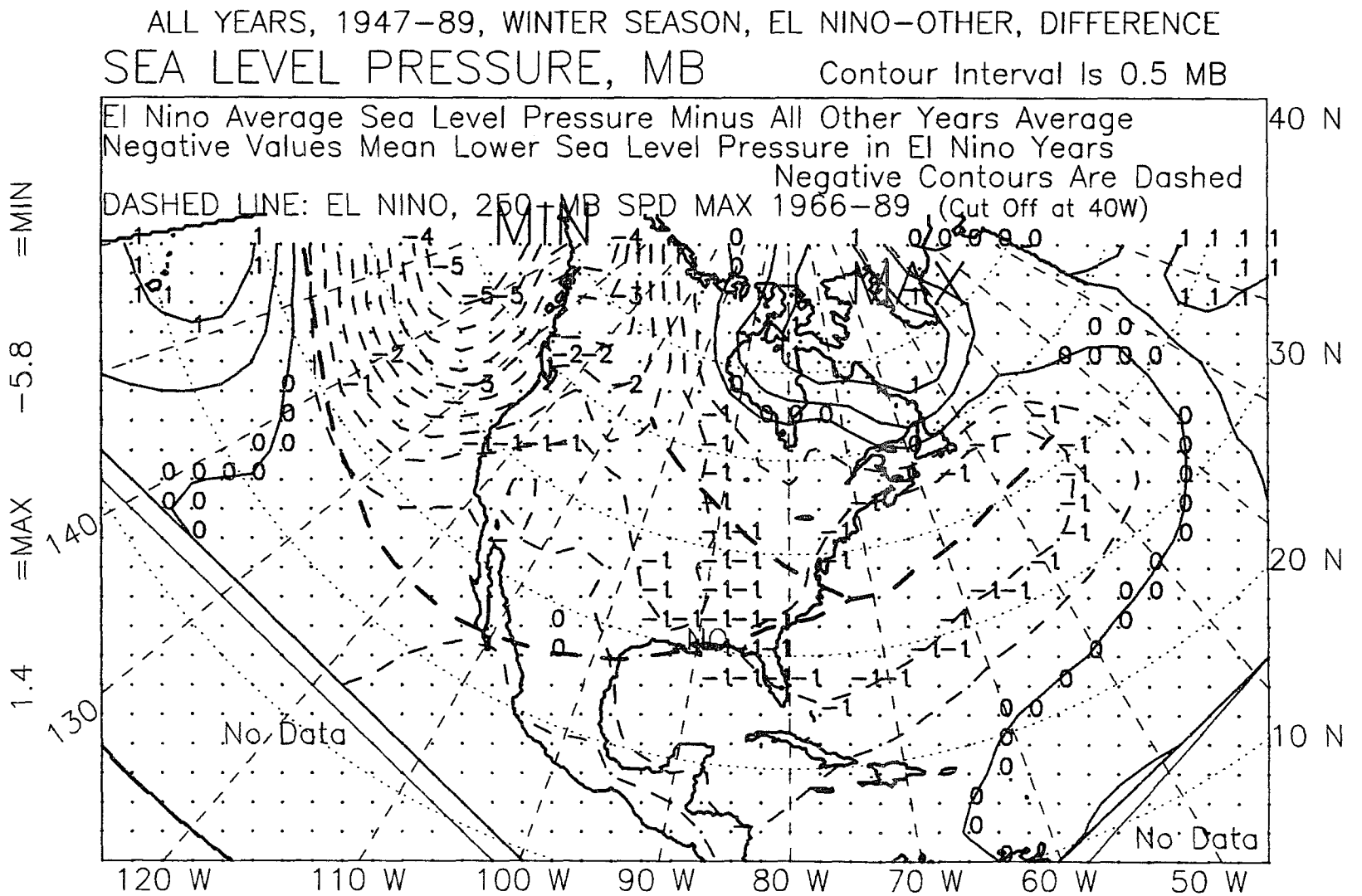

Figure 3.6: Mean sea–level pressure, winter, 1947–89, difference.

non-El Niño winters' average sea-level pressure from El Niño winters' average sea-level pressure. Done this way, a negative difference indicates lower average pressure in El Niño winters and a positive difference indicates higher average pressure in El Niño winters. The increased southerly component of the winds immediately east-adjacent to the stronger, northeast Pacific westerlies, those just off the Canadian Pacific coast, may be attributed to increased inward turning toward the center of the Aleutian low. Since the wind speed is greater, the Coriolis and the frictional accelerations must be proportionately greater, putting more curvature into the trajectory.

The remaining differences in the 850-mb wind are smaller, of magnitude less than 2.5 ms^{-1} (5 kt). Important circulation differences may exist, however, masked in the averages. A list of those differences follows.

1. There is anticyclonic residue in the Pacific, centered on 20°N and ranging from 120°W to the map edge at 160°W, indicating intensified circulation around the Pacific subtropical high during El Niño winters. A smaller, anticyclonic residue exists off the Pacific Central American coast in the easterly trades.

2. Winds over the southwest part of the Atlantic shown have an added, southerly component in El Niño winters. South of Cuba, in the northwest Caribbean, there is also an increased flow from the south, but also a slightly decreased easterly component, as indicated by the southwest residues. In the trade wind belt, east and south of Haiti and the Dominican Republic, El Niño-winter winds are from slightly south of east, while in other winters they are directly from the east. The increased southerly component in El Niño winters may be at least partially due to an eastward-shifted (or possibly west-side-truncated) Bermuda high in El Niño winters. Comparing Figs. 3.4 and 3.5, the 1020 mb contour reaches as far west as 63°W in non-El Niño winters, but only to 53°W

in El Niño winters. This apparent, east shift in El Niño winters places this region of the Atlantic under the far west limb of the high in El Niño winters, where outward-flowing winds curve around from the southeast, as opposed to a more central position in non-El Niño winters, where outward-flowing winds are coming from the east. The effect of this increased flow from the south in El Niño winters must be to transport more warm, moist air from the tropical Atlantic and Caribbean into the Gulf of Mexico area over the Florida Straits and the islands of Cuba and Haiti/Dominican Republic, thus conditioning the region for increased cyclogenesis in El Niño winters. It was stated above that the position of the Bermuda high is perhaps only a partial explanation for the increased south component of the wind in El Niño winters because the high is equally east-shifted in El Niño springs as opposed to non-El Niño springs, appendix A. However, the 850-mb wind differences in El Niño springs are sharply different from those in winter and show little south residue, Fig. 4.34.

3. Southernmost Mexico and the Yucatan show west and northwest residue, indicating a weakening of the easterlies here at their northernmost limit. Further south, in the Pacific west of southern Mexico, Guatemala, and El Salvador, the weakening is no longer present, being replaced by a slight strengthening of the easterlies.

4. A wide area of cyclonic residue is centered on the Pacific Baja coast. This may be a reflection, or cause, of the increased storminess in southern California in El Niño winters (Lau and Sheu 1991). Two other, smaller areas of cyclonic residue are found off the east coast of Florida and over the Grand Banks.

3.2.4.2 Gulf of Mexico: Differences in the 850-mb Wind Field between El Niño and Non-El Niño Winters

The following comments refer again to Fig. 3.3, the 850-mb wind-difference field for the four El Niño winters and 19 non-El Niño winters between 1967 and 1989.

1. From 30° to 40°N over the southeastern United States and over much of the eastern seaboard, there is a zone of weakened westerlies in El Niño winters. This is indicated by the east residue. The weakening of the westerlies in this area may be explained by a slightly decreased pressure gradient from south to north in this region in El Niño winters. Fig. 3.6 shows that average sea-level pressure is lower by 1 mb, over the southeastern United States during El Niño winters. Contributing to the decreased south to north pressure gradient in this region is the previously-mentioned, apparent, eastward shift in the Bermuda high in El Niño winters, lowering the highest pressures in the southeastern United States somewhat. The average strength of the center of the Icelandic low is the same in both types of winter, 1000 mb, although during El Niño winters, average sea-level pressure over the Labrador Sea and Davis Strait is higher by 1.4 mb. This contributes to the weakening of the south to north pressure gradient. One possible consequence for the Gulf of Mexico area of weakened westerlies across the southern states may be a decreased transport of relatively cold, dry air from the west, except during cold-air outbreaks. This would tend to preserve the heat and moisture content of gulf air between cold-front passages by virtue of less interim dilution. This would make for greater contrast in airmass characteristics when the next cold front arrives, increasing the likelihood of storm formation, all other things being equal.

2. The western half of the Gulf of Mexico and the Bay of Campeche area have a northerly residue in an average southerly flow. This is either due to less frequent or weaker southerlies, and/or to more frequent or stronger northerlies. If the latter is true, and stronger northerlies are seen in the El Niño winters, then the observation of fewer cold fronts in El Niño winters may now be accompanied by the hypothesis that, though they are fewer, some of the cold-air outbreaks are stronger in El Niño winters. This accomodates the other possibility, that of more frequent northerlies, because after a strong cold front, the wind will be out of the north longer. This postulated strengthening of some cold-air outbreaks is consistent with the observation of more winter storms in El Niño years if storm formation is more likely the greater the contrast between incoming cold, dry air and ambient, warm, moist air. During the El Niño winter of December 1982 to February 1983 the gulf region experienced several intense cold-air outbreaks. Data on cold fronts during the winter year, 1982 (1 September 1982 to 31 August 1983), appears in appendix T. Additionally, stronger cold fronts can be expected to advance farther south before becoming stationary and possibly returning as a warm front. Supporting this is the observation that there are more deep-water storms in El Niño winters, significant at the .05 level by the rank sum test, Table 2.10. Fig. 2.27 shows a higher percentage of slope, 200 to 3000 m (650 to 9850 ft), and abyssal, greater than 3000 m (9850 ft), storms in El Niño winters. 33% of December storms during the five El Niño winters from 1960 to 1989 occurred on the slope as opposed to 29% of December storms occurring on the slope in the other 25 winters of the same time period. The comparable percents for January and February are: 41% and 33% of storms originate on the slope in El Niño winters as opposed to 37% and 26% in non-El Niño Januarys and Februarys. Although the absolute number of storms over abyssal water depths is small,

the percents show the same trend. For December, January, and February, the percents of abyssal storms in El Niño winters are 10%, 10%, and 6%, as opposed to 2%, 7%, and 5% in non-El Niño winters.

3. It is intriguing that the northerly residue discussed above is confined to the area over the western gulf. This could imply the existence of a preferred channel for north winds behind a front. At the 850-mb level (and at the surface) the trajectory of the north wind is restricted by high topography from spreading westward. A physical eastern boundary, however, is not obvious. Simple, westward turning of the north wind, due to the Coriolis effect, may provide sufficient 'confinement' on the east. This concept is discussed further in 3.3.2, below.

4. There is weak cyclonic residue over the Gulf of Mexico in El Niño winters west of 85°W. This may either result from, or contribute to, more-frequent cyclogenesis in El Niño winters than in non-El Niño winters. Over the gulf, circulation is weakly anticyclonic in both winter types, but less so in El Niño winters, Figs. 3.1 and 3.2.

5. The southeast corner of the gulf region shows added, south wind and diminished easterlies, likely caused by the eastward shift of the Bermuda high, discussed above.

6. 850-mb circulation over the deep, central Gulf of Mexico is the same in both winter types. It is a calm zone of wind reversal along an east-west line following the Tropic of Cancer. Winds are from the southeast on the south side, and from the southwest on the north side.

3.3 Winter, 850-mb Divergence: 1967-1989

3.3.1 General Circulation: 850-mb Divergence, El Niño Winters

The following comments and those in the next section refer to Figs. 3.7 and 3.8, composites of the 850-mb divergence field for the four El Niño winters and for the 19 non-El Niño winters, respectively, between 1967 and 1989.

1. The North American continent in winter is largely divergent, indicating cold, descending air.

2. The strongly divergent zone over the Colorado Plateau corresponds to a sea-level pressure high, Fig. 3.4.

3. The divergent area of the Pacific Ocean is under the Pacific subtropical high pressure cell. Anticyclonic circulation is visible on the 850-mb, vector wind map, Fig. 3.1, although only the east half of the area of anticyclonic circulation is divergent. The divergent area of the Pacific may also be due to cool water, perhaps of upwelling origin. This area may be too far north for upwelling diminishment in El Niño winters.

4. The area of the Atlantic Ocean mapped is generally convergent, while the area of the Pacific flanking the southern United States and Mexico is generally divergent. In winter, the eastern portion of the Atlantic which is closest to the southeastern United States is generally a few degrees warmer than the Pacific off California and Mexico, as shown by maps of Equatorial Pacific Ocean Climate Studies (EPOCS) data (Sadler et al. 1987). The convergence over the Atlantic may be due to warm water and rising air.

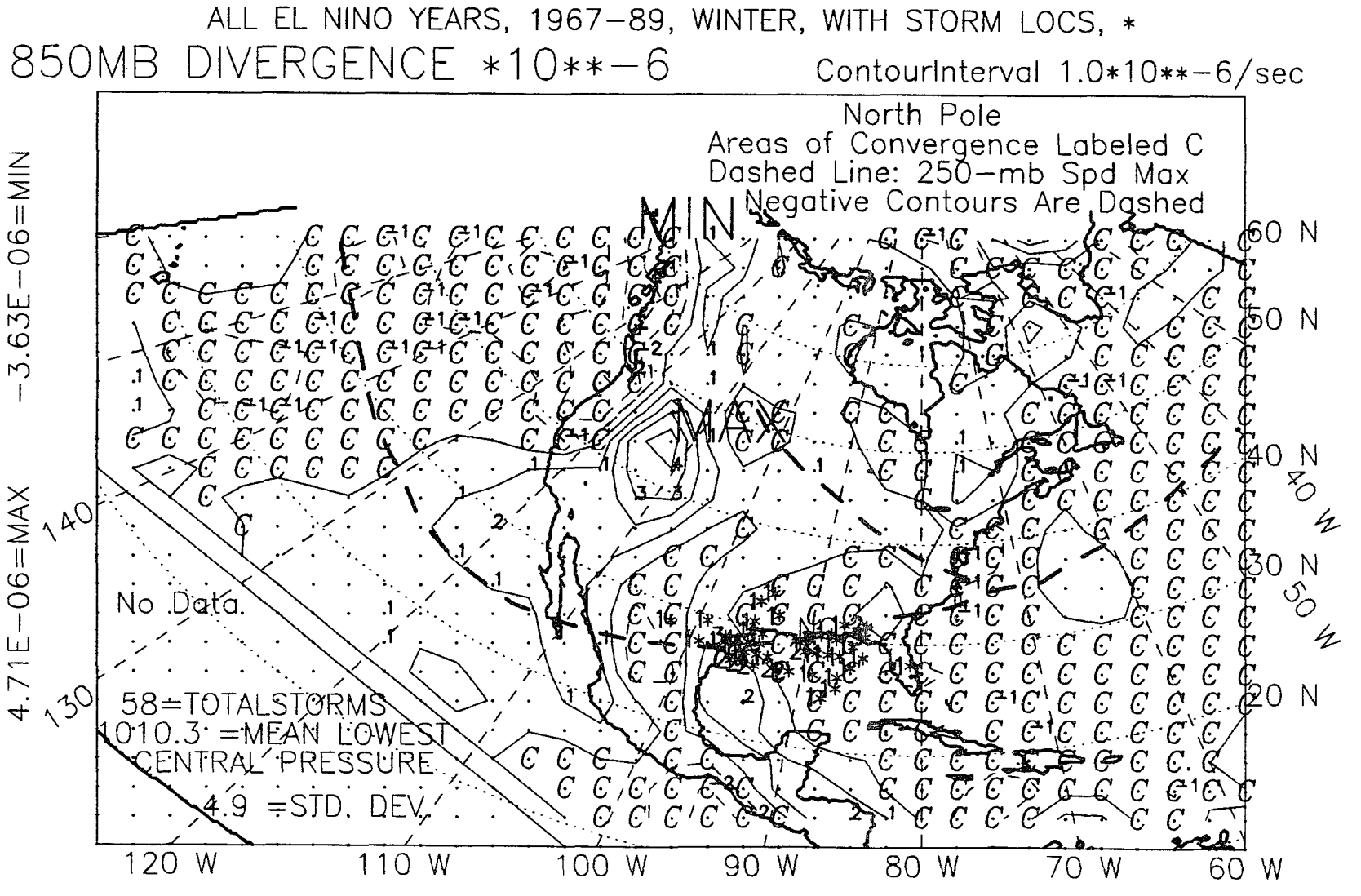

Figure 3.7: 850–mb divergence, winter, El Niño years, 1967–89.

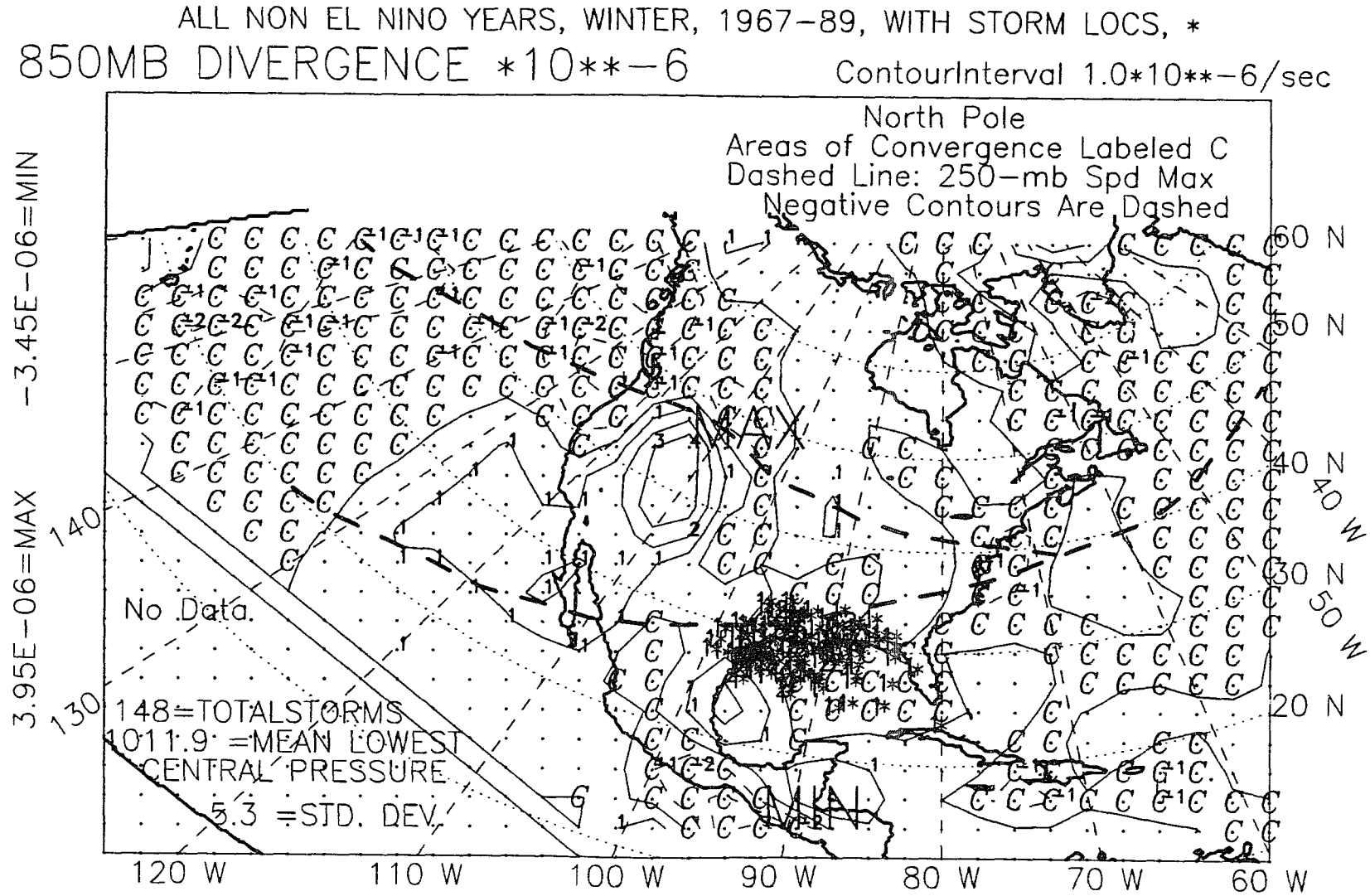

Figure 3.8: 850-mb divergence, winter, non-El Niño years, 1967-89.

5. The convergent area of the northern Pacific is partly under the Aleutian low. Another reason for the convergence here may be the decrease in the 850-mb, westerly wind speed from 12.5 to 5 ms^{-1} (25 to 10 kt) upon approaching the North American coast.

6. Except for the Pacific under the Pacific subtropical high, the atmosphere over the ocean areas south of about 20°N is convergent, roughly marking the equatorial convergence zone.

7. The Great Lakes region is a zone of convergence, owing to the relatively warm water of the lakes, compared to land temperatures.

8. The Bermuda Rise, water depth 0 to 5000 m (16 400 ft), is a divergent patch in a generally convergent Atlantic. This may be due to the shallower, and thus more rapidly chilled, water on the platform.

9. To the east of the Canadian Rockies, over Alberta, the 850-mb level is convergent. This fits well with the observation that storms (called Alberta clippers) traveling from west to east often reform in the lee of the Rockies, after having previously decayed in the west.

3.3.2 Gulf of Mexico: 850-mb Divergence, El Niño Winters

1. The eastern two-thirds of the Gulf of Mexico, the Mississippi Embayment, the upper gulf coast, and the southeastern and mid-Atlantic coastal plains of the United States are convergent at the 850-mb level. Nearly all of the coastal plain takes on the same low-level convergence as adjacent marine areas.

2. A continuous, curvilinear band of convergence exists over the mountains of Mexico, the Sierra Madre Orientals and the Sierra Madre Occidentals, and

extends northward up over the southern Rocky Mountains and the Great Plains. The outer edge of the convergence zone corresponds closely to the 1000 m (3280 ft) elevation contour. The maximum height of these mountains is at least 2000 m (6550 ft), but less than 3000 m (9850 ft), placing their crest above the 850-mb level, 1500 m (4900 ft), but well below the westward, 500-mb flow at 5500 m (18 000 ft). South of about 20°N, the convergence over the mountains may be due to rising air of the easterly trade winds orographically lifted from east to west. North of 20°N latitude, the convergence may be due to orographic lifting of the westerlies from west to east. The strongest area of convergence is located south of 30°N. Additionally, south of 30°N, these mountains are asymmetric, being steeper on the western flank. Strongest convergence is, however, seen on the gentler, east-facing slope, downhill from 2000 m (6550 ft) elevation.

3. The western third of the Gulf of Mexico is under a tongue of divergence stretching from the North American continent down south to the Yucatan Peninsula. The wind-vector map of El Niño winters, Fig. 3.1, shows weak anticyclonic circulation, less than 2.5 ms^{-1} (5 kt), over the western gulf. As previously noted, Fig. 3.3, the wind-difference map, shows a north residue over the western gulf. As noted above, during the cold-front season, November to April, this may represent a preferred channel for the southward flow of cold, continental air accompanying the passage of a cold front, with the mountains to the west may forming a barrier to westward spreading of the cold air. The easterly trades and westward, Coriolis turning of the north wind would tend to inhibit eastward spreading of cold air. The foregoing is in agreement with the cold-air damming idea discussed by Lewis and Hsu (1992) and mentioned briefly by Cotton (1990), both in reference to the Sierra Madre Orientals, and

is similar to the cold-air damming reported east of the Appalachian Mountains by Bell and Bosart (1988). This western Gulf of Mexico divergence cell is present in all seasons however, and in El Niño and other years, although its strength and position vary somewhat. (Seasonal divergence maps appear in appendix E.) At least a partial explanation for its presence in the warm season may involve the fetch available to the east trades. In crossing the Gulf of Mexico, the trades may pick up speed. An increase in speed, if not accompanied by confluence, is a way to achieve a pattern of mass divergence. Summer, 850-mb wind-vector maps do show a strengthening of southeasterly winds, traveling from east to west. These southeast winds appear to be due to deflection northward of the easterly trades as they approach the Mexican landmass. (Seasonal, 850-mb wind maps are in appendix C.)

3.3.3 Differences in the 850-mb Divergence Field between El Niño and Non-El Niño Winters

3.3.3.1 General Circulation: Differences in the 850-mb Divergence Field in Non-El Niño Winters

The comments in this and the next section refer primarily to Fig. 3.9, a difference map of the divergence field for the four El Niño and the 19 non-El Niño winters between 1967 and 1989. Secondary reference is made to Figs. 3.7 and 3.8, composites of the 850-mb divergence field for the four El Niño winters and the 19 non-El Niño winters. In Fig. 3.9, points that are more convergent (have a smaller or more negative value of divergence) in El Niño winters are labeled 'C'. These areas may still, in the average, be divergent in both types of winter. They are, however, less divergent (more convergent) in El Niño winters. A negative result, when subtracting divergence in non-El Niño winters from that in El Niño winters, means fewer

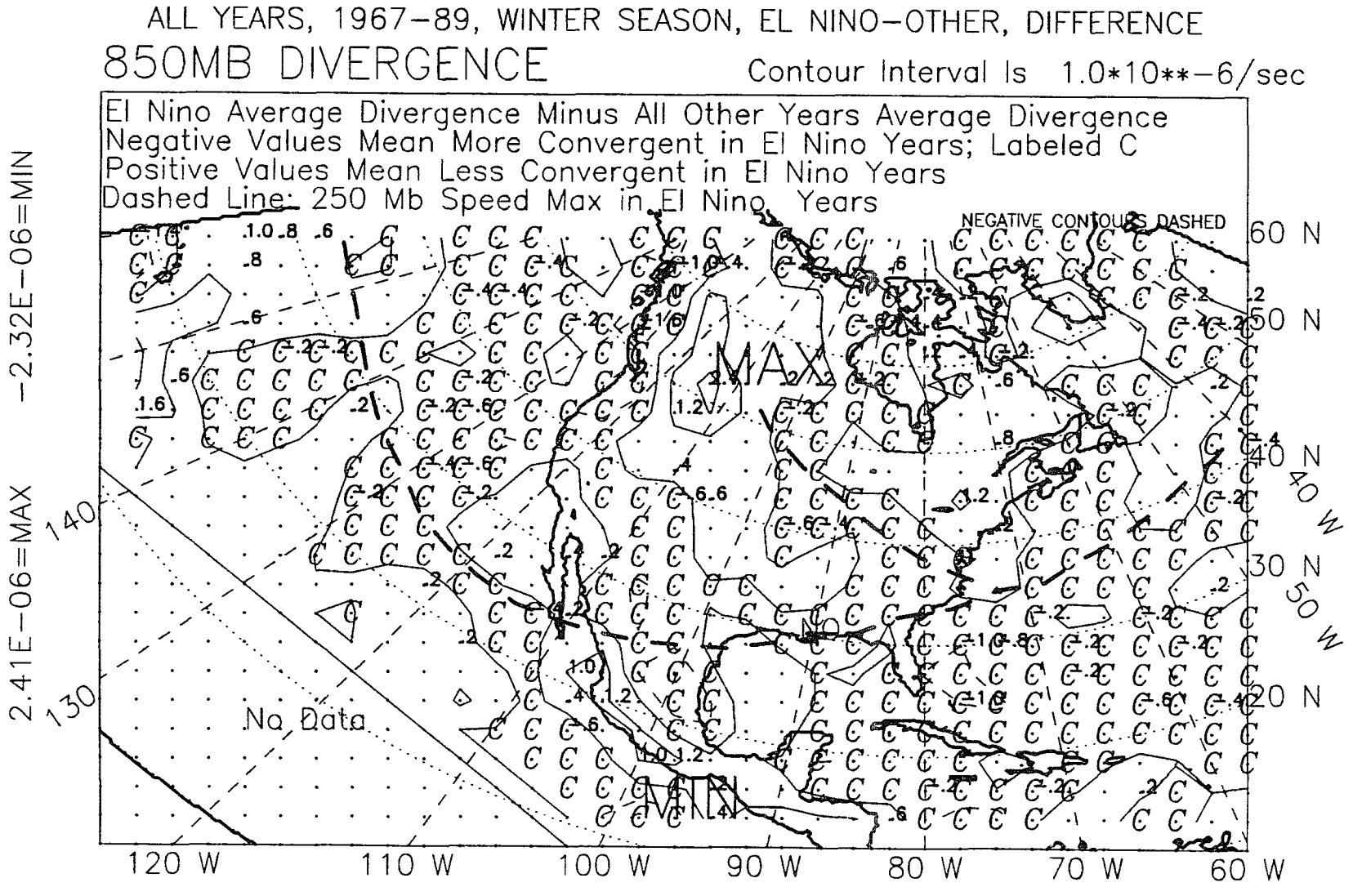

Figure 3.9: 850–mb divergence, winter, 1967–89, difference.

or weaker episodes of actually positive divergence in El Niño winters, and/or more or stronger episodes of convergence in El Niño winters.

1. In El Niño winters much of the North American continent is a little less divergent, as indicated by the wide areas of negative (convergent) residue. The Canadian and Northern Rockies and northern Appalachians are, however, somewhat more divergent.

2. The atmosphere over the western Atlantic Ocean is more convergent in El Niño winters, indicated by the negative (convergent) difference in Fig. 3.9. At the 850-mb level, south of 30°N, the temperature is .2 to .6°C warmer in El Niño winters, Fig. 4.19.

3. Over the portion of the northeastern Pacific mapped, the atmosphere is generally more convergent in El Niño winters. The patch of convergence in the Pacific Ocean off of Central America, south of 15°N, is larger in El Niño winters than in non-El Niño winters, Figs. 3.7 and 3.8. In El Niño winters, this patch may indicate the northernmost extent of the anomalously warm water known to occur in the eastern Pacific in El Niño winters (Deser and Wallace 1990).

3.3.3.2 Gulf of Mexico Differences in the 850-mb Divergence Field between El Niño and Non-El Niño Winters

1. The 850-mb level atmosphere over the eastern Gulf of Mexico and surrounding Atlantic and Caribbean is more convergent in El Niño winters. The atmosphere over the entire coastal plain is more convergent, except over Texas. Over much of the western gulf, however, the 850-mb level atmosphere is weakly more divergent in El Niño winters.

2. In El Niño winters the north-south curvilinear zone of convergence over the mountains of Mexico is more continuous than in non-El Niño winters, when there is a gap over Texas and the southwestern United States.

3. In El Niño winters there is more north-south linearity in the divergence field in the area south of 30°N over the Gulf of Mexico and Mexico. The pattern is one of alternating belts of convergence and divergence and is less pronounced in non-El Niño winters. Perhaps the meridional character in El Niño years is allowed to develop due to the weakened westerlies across the southern Unites States and the somewhat relaxed easterly trades over the southeastern gulf, the northwestern Caribbean south of Cuba, and over Yucatan and adjacent Central America.

4. In El Niño winters the core of the western Gulf of Mexico divergence zone is slightly weaker and the entire zone does not extend as far onshore as in non-El Niño winters. A wind map of El Niño winters, Fig. 3.1, shows that anticyclonic circulation over the western gulf is 2.5 ms^{-1} (5 kt), a little weaker than in non-El Niño winters, when it is 2.5 to 5 ms^{-1} (5 to 10 kt). Using the previous explanation offered for the winter, western-gulf divergence zone, since there are more cold fronts in non-El Niño winters, and if the western-gulf divergence zone is due to an average condition of entrapment of cold air against the mountains, then it is not unreasonable to find some strengthening and westward expansion of the divergence zone in non-El Niño winters.

3.4 Winter, 850-mb Relative Vorticity, 1967-1989

3.4.1 General Circulation: 850-mb Relative Vorticity, El Niño Winters

The comments below and in the next section refer to Figs. 3.10 and 3.11, composites of the 850-mb relative-vorticity field for the four El Niño winters and 19 non-El Niño winters, respectively, between 1967 and 1989.

1. In both winter types the general structure consists of three wide relative-vorticity bands that are positive at low latitudes, negative in midlatitudes, and positive at high latitudes.

2. Much of the North American continent has negative relative vorticity in both types of winter. This matches its generally divergent nature in both winter types, and allows the conclusion that the divergence over the continents is due to anticyclonic motion in cold, descending air.

3. The atmosphere over the eastern shelf and slope of North America has negative relative vorticity over these cold, inshore waters, and positive relative vorticity over the warmer waters of the Gulf Stream and abyssal plain. This matches the nearshore divergence and offshore convergence observed in El Niño winters, Fig. 3.7, which are now indicated to be due to relatively cool and warm surface waters, respectively, and the accompanying modification of overlying air.

4. Over the northeastern Pacific, the 850-mb level shows nearly uniform negative relative vorticity over the the area of the Pacific subtropical high. In the southeast part of the ocean mapped, the 850-mb level is divergent. These three observations are consistent. West of 130°W and south of 30°N, however,

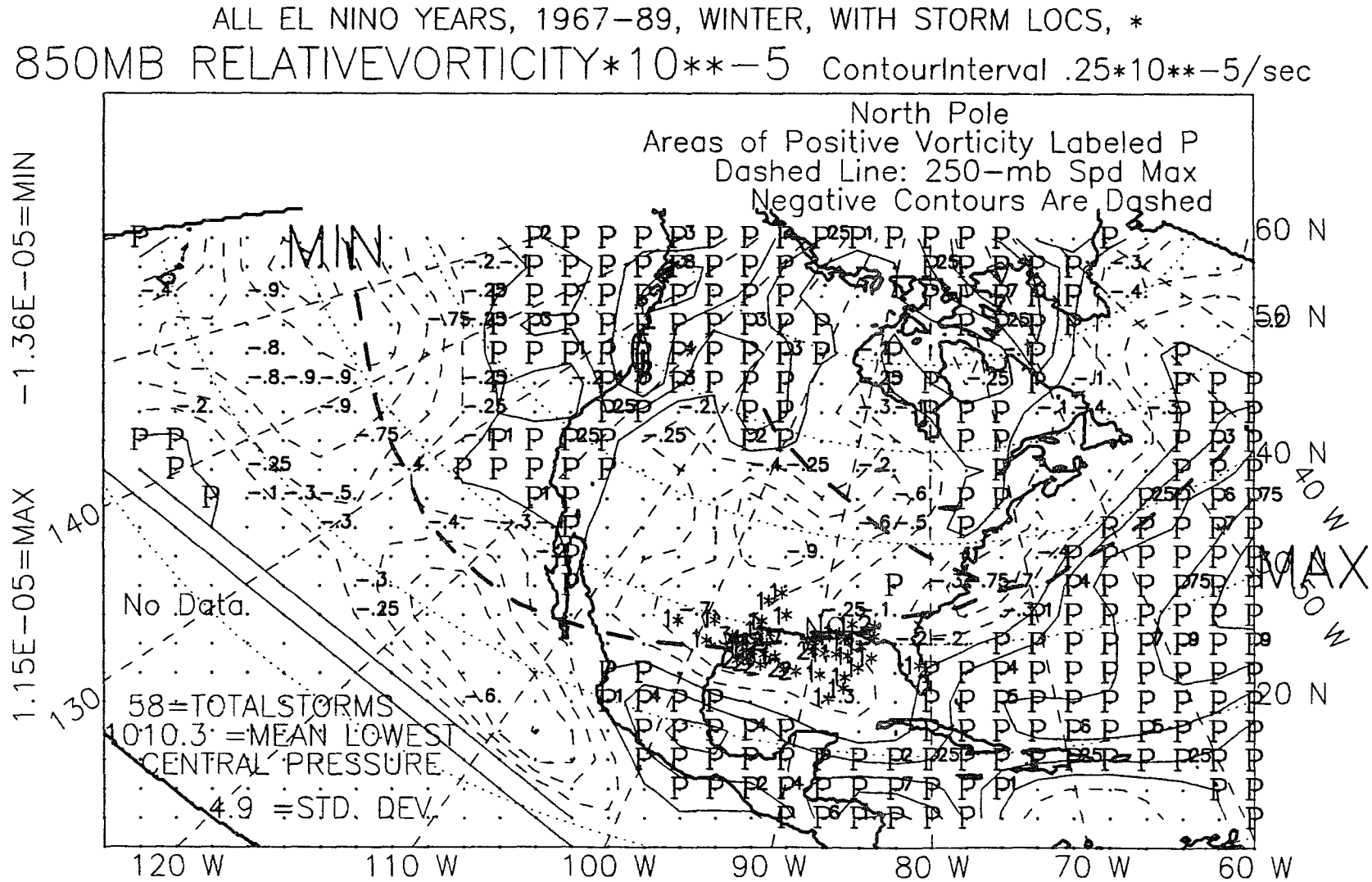

Figure 3.10: 850-mb relative vorticity, winter, El Niño years, 1967-89.

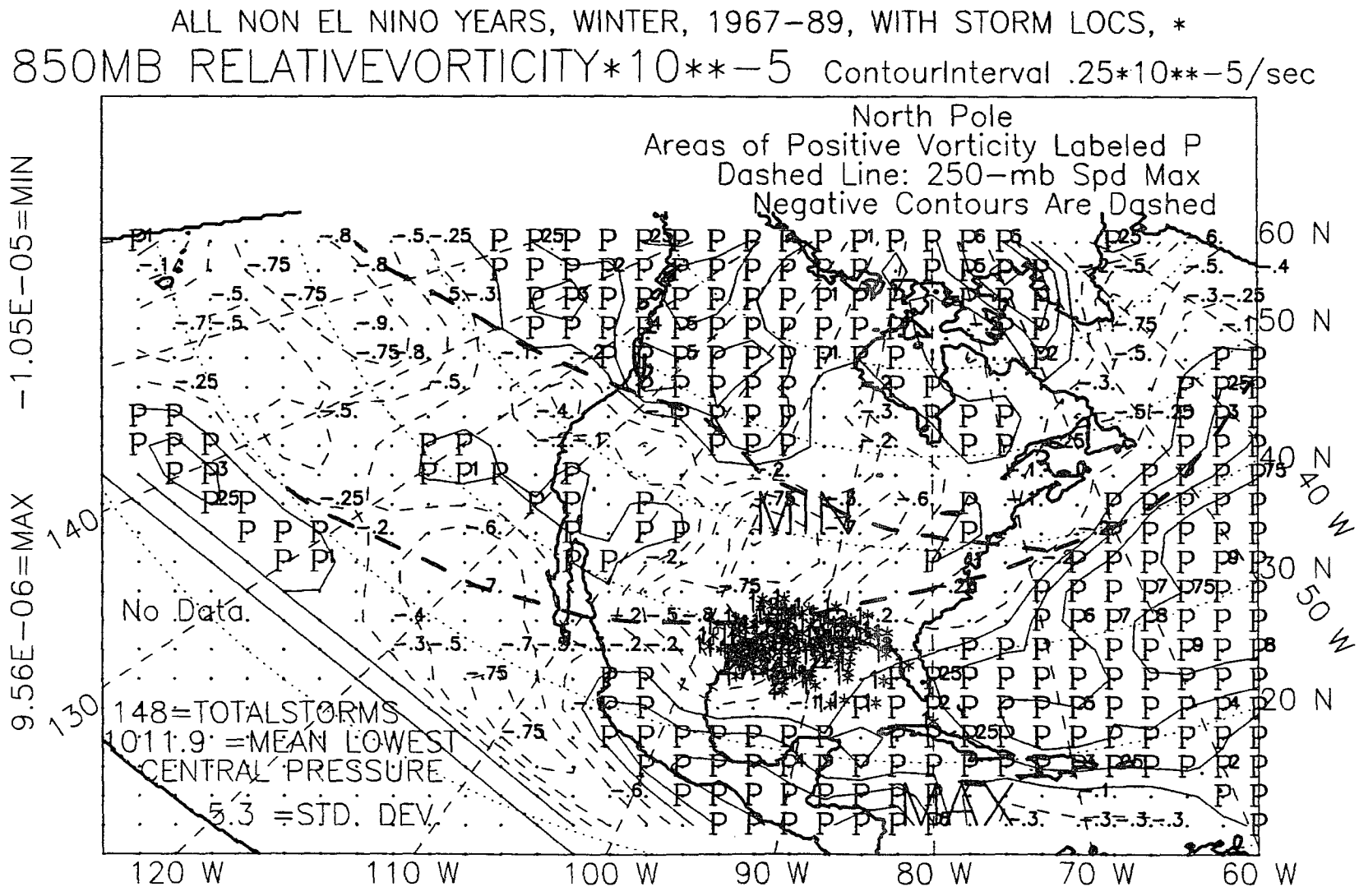

Figure 3.11: 850-mb relative vorticity, winter, non-El Niño years, 1967-89.

the 850-mb level is convergent. This does not fit with the negative relative vorticity or the anticyclonic wind field there.

5. The area of the Colorado Plateau previously noted to be strongly divergent has negative relative vorticity. These two facts are consistent with the high sea-level pressure there (Fig. 3.4) and indicate anticyclonic motion in descending air.

6. The convergent area in the lee of the Canadian Rockies has positive relative vorticity, consistent with the area's well known cyclogenetic potential.

7. The convergent zone along the Cascades and the Coast Ranges has positive relative vorticity.

3.4.2 Gulf of Mexico Circulation: 850-mb Relative Vorticity, El Niño Winters

1. The lobe of negative relative vorticity extending over the Gulf of Mexico from the North American continental interior may represent the average southward excursion of cold air during cold-air outbreaks. It appears to intrude into a wide band of positive relative vorticity covering the adjacent, warmer Atlantic and Carribean. Fig. 3.1 shows weak, less than 2.5 ms^{-1} (5 kt), anticyclonic motion over the gulf in El Niño winters, consistent with the area's negative relative vorticity.

2. The Bay of Campeche, the southwest corner of the Gulf of Mexico, is the only part of the gulf region to show positive relative vorticity in El Niño winters or non-El Niño winters. The bay is, however, in the divergent belt noted previously at this level. The divergence and positive relative vorticity can be reconciled if the divergence is not due to rotary motion, but is due

to speeding up of air in the earlier-postulated channel for transport of cold air southward during cold-air outbreak. This, however, requires a separate explanation for the positive vorticity. At the head of the channel, in Texas, cold air would move due south. It may then curve southeastward, to conserve absolute vorticity by adding positive relative vorticity to compensate for the decrease in the Coriolis parameter with southward transport. Carrying the idea further, the southeastward flow may eventually recurve northeast, north, or northwestward, again to conserve absolute vorticity. After this much transport, the air may be sufficiently warmed from below to constitute a return warm front. Note that this explanation for the positive relative vorticity over the southwestern gulf during El Niño winters only applies during cold-air outbreak, since average winter winds are from the south here.

3.4.3 Differences in the 850-mb Relative-Vorticity Field between El Niño and Non-El Niño Winters

The comments below refer primarily to Fig. 3.12, the difference field of 850-mb relative vorticity for the four El Niño winters and the 19 non-El Niño winters between 1967 and 1989. Secondary reference is made to Figs. 3.10 and 3.11, composites of the 850-mb relative vorticity field for the four El Niño winters and the 19 Non-El Niño winters. In Fig. 3.12, points that have more positive relative vorticity (have a larger or less negative value of relative vorticity) in El Niño winters are labeled 'P'. These areas may still, in the average, have negative relative vorticity in both types of winter, though less negative in El Niño winters. A positive result, when subtracting relative vorticity in non-El Niño winters from that in El Niño winters, means more or stronger episodes of positive relative vorticity in El Niño winters, and/or fewer or weaker episodes of negative relative vorticity in El Niño winters.

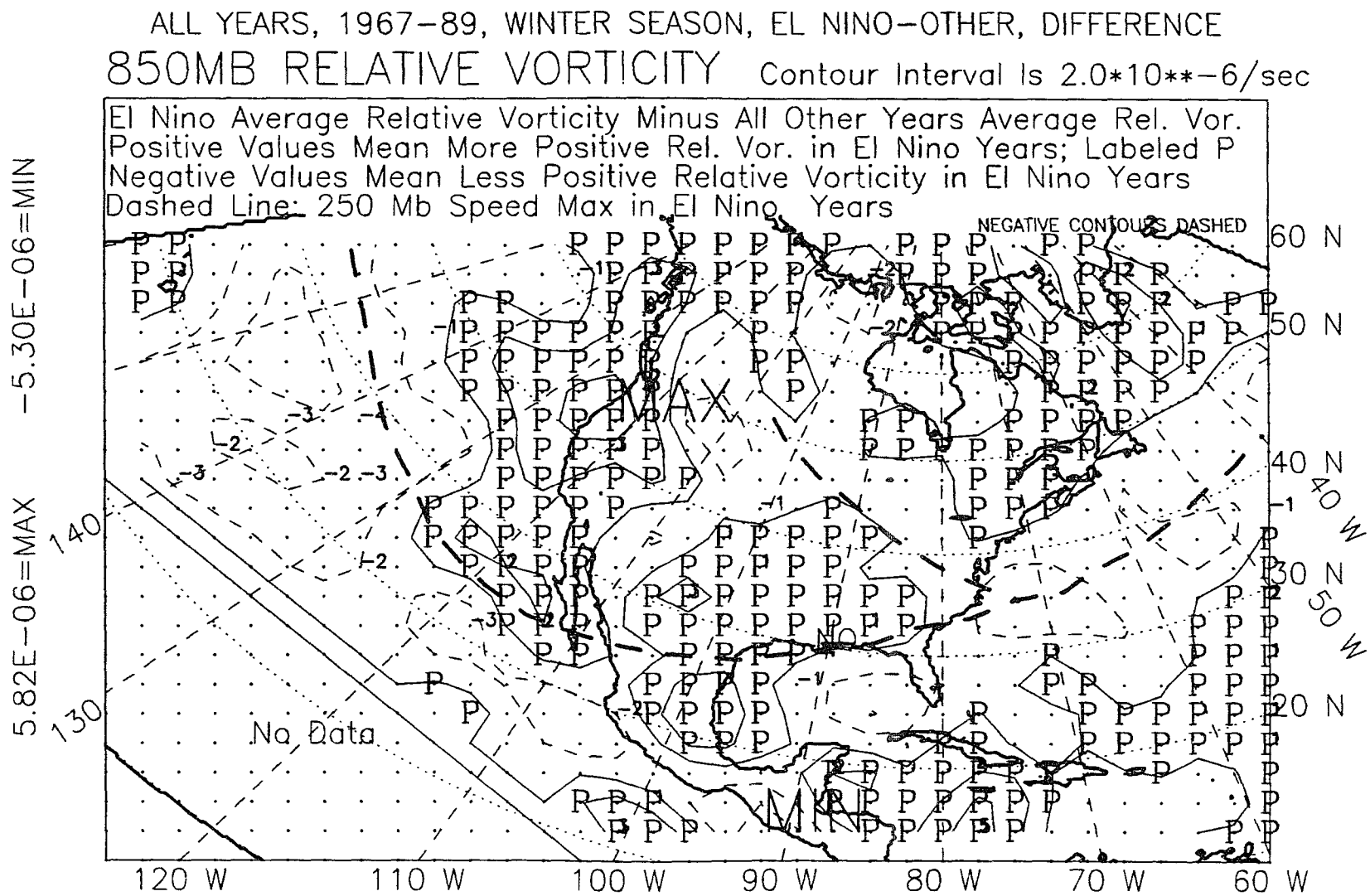

Figure 3.12: 850-mb relative vorticity, winter, 1967-89, difference.

1. The lobe of negative relative vorticity over the Gulf of Mexico extends farther south in El Niño winters, Fig. 3.10, than in non-El Niño winters, Fig. 3.11. In El Niño winters the lobe extends approximately 500 km (315 mi) farther to the southeast, presumably reflecting the southward shift of the seasonal mean jet stream and the accompanying southward shift of the average southern limit of cold air at the 850-mb level, indicating further-south advance of cold-air masses in El Niño winters. (This illustrates the type of information obtainable from maps of seasonal means of dynamic quantities. Study of dynamic parameters on a climatologic time scale has been called 'dynamic climatology' (Riehl 1954).)

2. The areas over the western third of the gulf and the north and west coastal plains, though areas of average, 850-mb level, negative relative vorticity in both winter types, is less negative (more positive) in El Niño winters. Over the eastern two-thirds of the gulf, though also an area of average negative relative vorticity in both winters, the opposite is seen, slightly more-negative relative vorticity in El Niño winters. The positive relative-vorticity difference over the far west gulf in El Niño winters may owe to the diminishment of the easterly trades to the southeast of there, as follows. If the average, winter flow along the western shelf (in any year) is the result of northward deflection of the trades by high topography on the Mexican landmass, then trade weakening in El Niño winters will produce less south wind along the western shelf. In any year, northward curving of easterly trades contributes anticyclonic (negative) relative vorticity. Weaker trades and weaker south winds in El Niño winters result in less negative relative-vorticity input over the southwest and west gulf. The positive relative-vorticity difference in El Niño winters may be generated this way, or it may simply reflect the greater number of winter storms.

3. Over the California and Baja coasts, the 850-mb level has a positive relative-vorticity difference. Even though Baja has a seasonal average negative relative vorticity in both winter types, it is less negative in El Niño winters. The excess positive relative vorticity is consistent with Lau and Sheu's (1991) observation of more storms during El Niño winters in California.

4. An area of positive relative vorticity at about 15°N and 140°W in the Pacific is much smaller in the mapped region in El Niño winters, Figs. 3.10 and 3.11. This far north, if equatorial convergence is seen at all, one would expect the opposite, anticipating that perhaps the northern edge of the convective region in the eastern Pacific would be visible in El Niño winters.

3.5 Winter, 250-mb Wind Field: 1966-1989

3.5.1 General Circulation of the 250-mb Wind Field, El Niño Winters

The following comments refer to Figs. 3.13 and 3.14, composites of the 250-mb, horizontal wind field for the five El Niño and 19 non-El Niño winters between 1966 and 1989. At this altitude and latitude the winds are all westerly. In Fig. 3.13, El Niño winters, a wide belt of maximum speed, 30 to 45 ms^{-1} (60 to 90 kt) curves cyclonicly across the entire southern United States and most of Mexico. Maximum average speed is attained just off the Carolinas over the Atlantic, a well-known, cyclogenetic province. A secondary 'ridge' of maximum speed is suggested to the north, trending northwest to southeast across the midcontinent, and possibly joining the southern branch near the latter's core speed maximum over the Atlantic. In nearly all seasonal means, the north and south jets appear to come together at the location of maximum speed for the North American sector, appendices O and J. This seems to be evidence of confluencing reported by Namias and Clapp (1949).

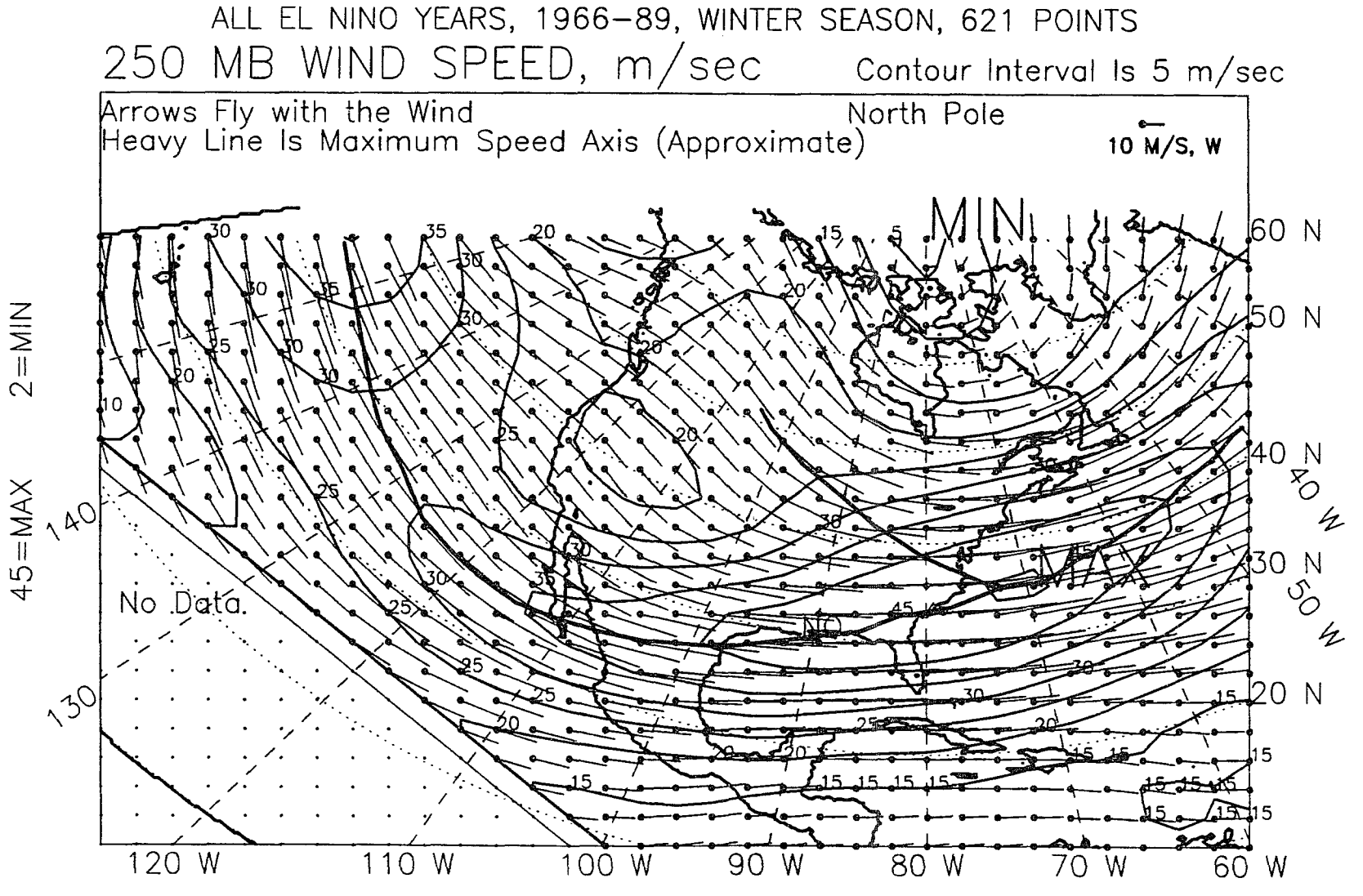

Figure 3.13: 250–mb wind vectors, winter, El Niño years, 1966–89.

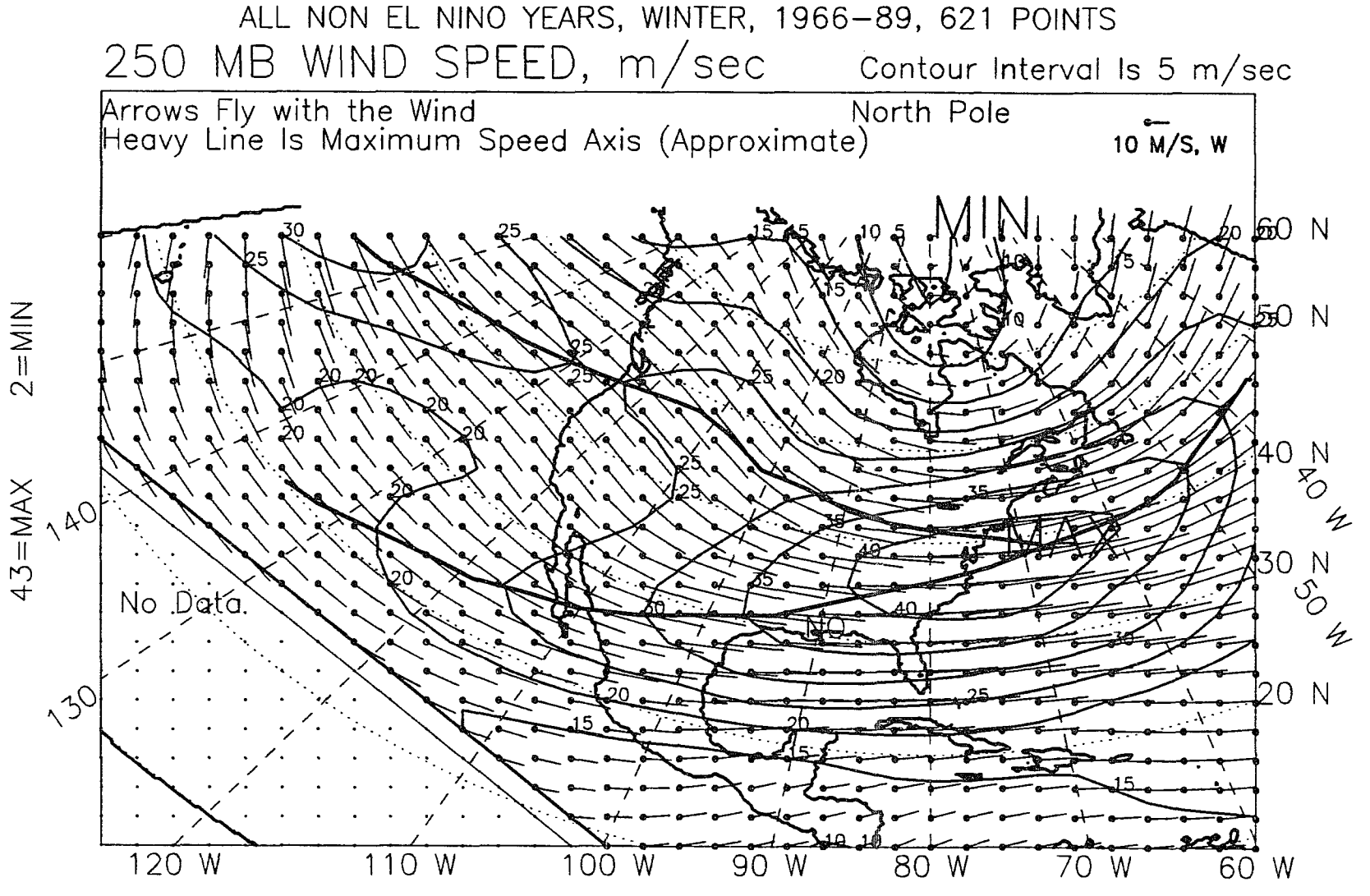

Figure 3.14: 250–mb wind vectors, winter, non–El Niño years, 1966–89.

All 250-mb speed analyses presented in this work deal exclusively with the southern speed maximum. The speed maxima are jet streams. Their dimensions agree with the definition of jet streams adopted by the World Meteorological Organization (WMO) (Reiter 1967b). In Resolution 25 (EC-IX), the WMO defines jet-stream dimensions as: 1000's of kilometers in length, (parallel to flow), 100's of kilometers in width (across flow), and a few kilometers in vertical depth. Resolution 25 also specifies that strong wind shears characterize a jet stream. Lateral wind shears are stated to be on the order of 5 ms^{-1} per 100 kilometers, or 5 ms^{-1} across a horizontal distance slightly less than 1 degree of latitude (10 kt per $\sim 1°lat.$). Vertical wind shears, though not discernible from any maps presented here, are stated to be on the order of 5 to 10 ms^{-1} per one kilometer (15 to 30 kt per mi).

At first glance, it seems that the northern 'branch' is the mean polar-front jet and the southern 'branch' is the mean subtropical jet (Krishnamurti 1961; Newton and Persson 1962). Broadly speaking, the core of the polar-front jet is found at the tropopause break at approximately the 300-mb level, at 40° to 45° N in winter, and the subtropical-jet core occurs south of there, at about 30° N in winter, at a second break, or 'step up' in the tropopause, at about the 200-mb level. In the middle, at 250 mb, the two names may still be appropriately applied to the north and south jets, however, the location of the jet axes drawn at 250 mb is probably not the exact core of either jet. These may be displaced somewhat, depending on the degree of asymmetry of the three-dimensional structure of the two jets. This is essentially a sampling bias, and though unfortunate, can safely be ignored for the application the present work makes of the role of jet streams. If jet-stream dynamics were being investigated, it could not be ignored, and in fact, vertical cross sections would be needed to better define the jets. A more serious problem in regarding the northern speed maximum as the polar-front jet and the southern one as the

subtropical jet, concerns the averaging process used to produce the composite maps shown here. Each jet migrates north and south (Phillips 1950) and streaks (local velocity maxima) in each jet migrate west to east, at the same time strengthening in the fore and weakening in the rear (Reiter 1963). Because of this, the mean picture is quite likely not the mean of either jet; they have probably become mixed. Even these means are probably biased to the south, as discussed by Reiter (1963). This error is systematic, and so for the purpose of finding the relative location of the jet stream over the southern United States and Gulf of Mexico during El Niño and other winters, it will be neglected. In view of the probable mixing of the polar-front jet and subtropical jet in the averaging, only the names north and south jet will be used.

The problem of polar-front jet versus subtropical jet is not merely one of semantics, the two being of somewhat different origin, having different associated surface features, and having some structural differences (Newton and Persson 1962). Reiter (1963) has shown that the subtropical jet exists in part to satisfy the hemispheric conservation of angular momentum. The subtropical jet is associated with the poleward boundary of the Hadley circulation cell (Palmén and Newton 1969). The polar-front jet is always associated with a surface front, while the subtropical jet is not, usually only being connected to a sometimes poorly-defined, upper-level front (Reiter 1963; Shapiro and Keyser 1990; Keyser and Shapiro 1986; Palmén and Newton 1969). Reiter (1963) has suggested that the subtropical jet is the decaying or mature phase of a polar-front jet that has become detached from its associated surface front, which may still exist as an upper-level front, as the jet migrates south. It has long been recognized that surface cyclogenesis is likely to occur when a tropospheric jet stream lies over a surface frontal zone (Riehl 1948). The lack of a surface front connected to the subtropical jet does not preclude a role

for it in surface cyclogenesis, because of the vertical motions, both thermally direct and indirect, associated with jet streams (Sechrist and Whittaker 1979). Uccellini et al. (1984, 1987) have shown that the subtropical jet played a role in cyclogenesis during the Presidents' Day storm over the eastern United States of 18-19 February 1979. Defant and Morth (1978), citing earlier work of Defant (1972), state that the subtropical jet was causal in the 14-17 February 1962, Hamburg, Germany storm that created a strong storm surge. Elsberry and Kirchoffer (1988) have noted the influence of the subtropical jet on storm development. Palmén and Newton (1969) present a map showing four wave cyclones developed under the subtropical jet. Both the polar-front jet and the subtropical jet can play a role in surface cyclogenesis, although the mechanisms may be different when dealing with the subtropical jet and an upper-level front as opposed to a surface front (Keyser and Shapiro 1986). The relative position of any tropopause jet is important because of the accompanying areas of divergence which contribute to surface cyclogenesis.

3.5.2 Differences in the 250-mb Wind Field between El Niño and Non-El Niño Winters

The following comments refer primarily to Fig. 3.15, a vector plot of the difference between the 250-mb wind field in the five El Niño and 19 non-El Niño winters from 1966 to 1989, and secondarily to Figs. 3.13 and 3.14, the individual wind fields. The magnitude of the 250-mb wind-difference vectors is arbitrarily multiplied by four, relative to the source maps, for ease of reading. The speed contours, however, are true magnitude. Following is a list of the differences between the two types of winters.

1. The south jet is stronger by 5 to 10 ms^{-1} (10 to 20 kt) in El Niño winters. The north jet is weaker by up to 5 ms^{-1} (10 kt) as evidenced by an east

residue in a westerly wind. Arkin (1982) noted a stronger subtropical jet over North America in the winters following a warming in the eastern and central tropical Pacific. Arkin's winters corresponds to those here called El Niño winters and correspond to December(-1), January(0), and February (0) in Rasmussen and Carpenter's notation (1982). Arkin made similar, 200-mb wind-speed composites, although monthly, of NMC final-analysis data for 1968 to 1979.

2. The south jet is displaced southward by an average 185 to 285 km (115 to 180 mi) between longitudes 100° and 70°W over the gulf region in El Niño winters, Table 4.1.

3. In El Niño winters the speed maximum over the northwest Pacific appears to be directly upstream of and connected to the south jet over Mexico and the southern United States, Fig. 3.13. In non-El Niño winters, the Pacific, speed maximum appears to be in line with the north jet, following a path across the Pacific northwest over Washington state and British Columbia, Fig. 3.14. The speed maximum mapped in the Pacific is the decelerating end of a jet maximum, or exit area (see 3.6.4). The exit region has been shown both theoretically and observationally to be a region favorable for surface cyclogenesis (Reiter 1963). It would appear that storms generated under this Pacific exit region in non-El Niño winters would cross over the North American continent in the northwestern United States and southwestern Canada. In El Niño winters these storms, and other, migratory cyclones, would be steered far southward by the upper-level current, crossing over land in the vicinity of the Baja peninsula. The mean south jet is located over Baja in both winter types, but in non-El Niño winters it is not downstream of a volatile exit region as it is in El Niño winters. Based on this and on the weakened north jet

in El Niño winters, it seems reasonable to expect, in El Niño winters, fewer extratropical storms tracking across the northern U.S. and more extratropical storms taking a route across the southern U.S. A similar, though theoretical, result was obtained by Held et al. (1989) using a general-circulation model and predicting its response to an El Niño forcing. In the model output, they note an equatorward movement of the storm track as evidenced by changes in the the eddy momentum flux at 200 mb.

A consequence of fewer north-tracking storms in El Niño winters may be fewer storms reforming in the lee of the northern and central Rockies, such as the storms of the Alberta and Colorado cyclogenetic areas identified by Whittaker and Horn (1982, 1984). Two further consequences of a southward-displaced extratropical-storm track would be first, increased storminess in southern California and second, a greater incidence of storms forming or reforming in the lee of the southern Rockies over Texas and the southwestern United States. Of the foregoing, only the increased storminess in southern California in El Niño winters has been well documented (Lau and Sheu 1991).

4. On the north, or cyclonic side of the south jet, so called because of the cyclonic sense of shear found there, the strengthening of the south jet in El Niño winters intensifies this cyclonic shear, as evidenced by the band of cyclonic residue lying across the southwest United States, Fig. 3.15. Conversely, the weakening of the north jet during these same winters diminishes the cyclonic shear on the north side of the north jet. This is shown by the anticyclonic residue over Canada, Fig. 3.15. On the south, or anticyclonic side of the south jet, the speed increase in El Niño winters leads to an intensification of anticyclonic shear there. This is represented by the anticyclonic residue in Fig. 3.15 over the Pacific between 135° and 155°W and from 10° to 20°N.

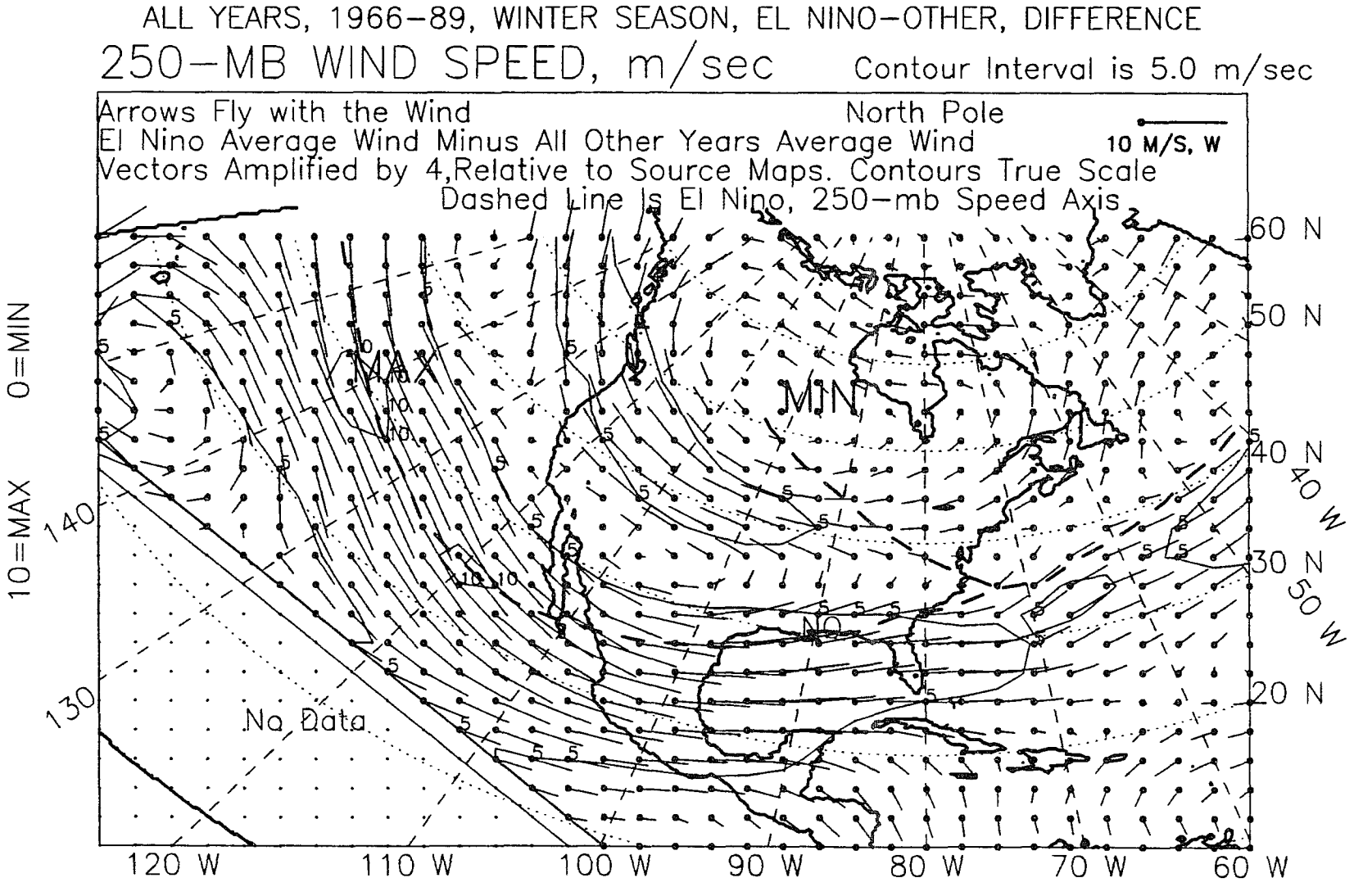

Figure 3.15: 250–mb wind vectors, winter, 1966–89, difference.

This region is on the southwest edge of the Pacific subtropical high in winter. The intensified anticyclonic shear on the south side of the south jet may contribute to a strengthening of the Pacific subtropical high pressure cell in El Niño winters. There is a one-millibar average increase in mean sea-level pressure under the high in El Niño winters, Fig. 3.6.

5. A north wind difference is visible over the Caribbean Sea and neighboring part of the Atlantic. In El Niño winters the 250-mb winds are due west here, while in non-El Niño winters the winds are somewhat south of west.

6. The westerlies over the north Atlantic and Labrador Sea are decreased slightly in El Niño winters, as shown by the wide area of east residue over the north Atlantic, Fig. 3.15. The decrease is slight, less than 5 ms^{-1} (10 kt).

3.6 Winter, 250-mb Divergence: 1966-1989

3.6.1 General Circulation: 250-mb Divergence, El Niño Winters

The following comments and those in the section below refer to Figs. 3.16 and 3.17, composites of the 250-mb divergence field for the five El Niño winters and for the 19 non-El Niño winters between 1966 and 1989.

1. In both winter types there is an east-west band, centered at about 30°N, in which the 250-mb level is largely convergent, reflecting the meeting of the first two meridional, vertical, circulation cells, the Hadley and Ferrel cells. North of this band, the 250-mb level is divergent, reflecting the meeting of the midlatitude Ferrel and the furthest-poleward vertical circulation cells.

2. In both winter types the south jet is located within the convergence zone between the Hadley and Ferrel cells, or at the break between the tropical and

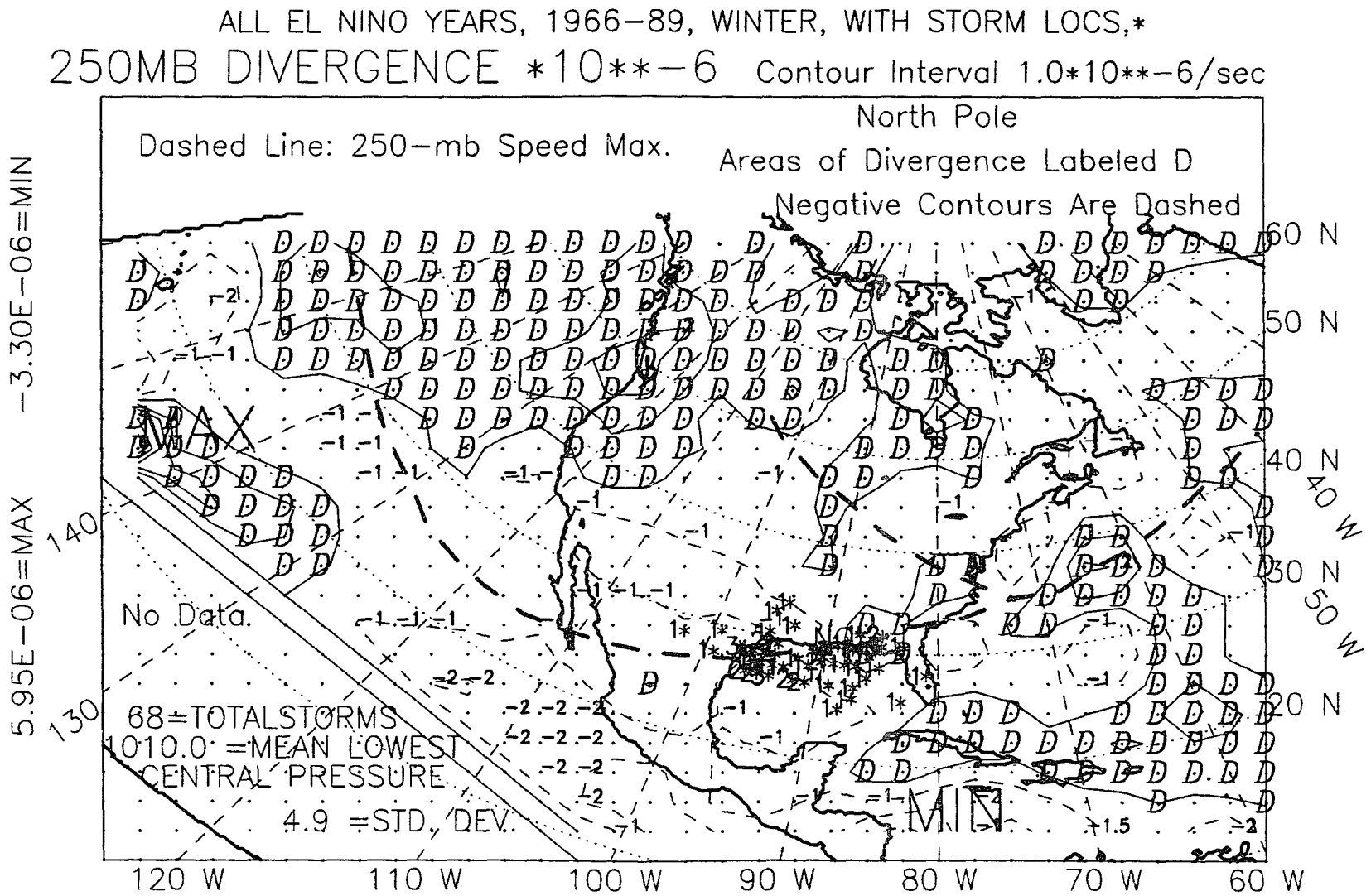

Figure 3.16: 250–mb divergence, winter, El Niño years, 1966–89.

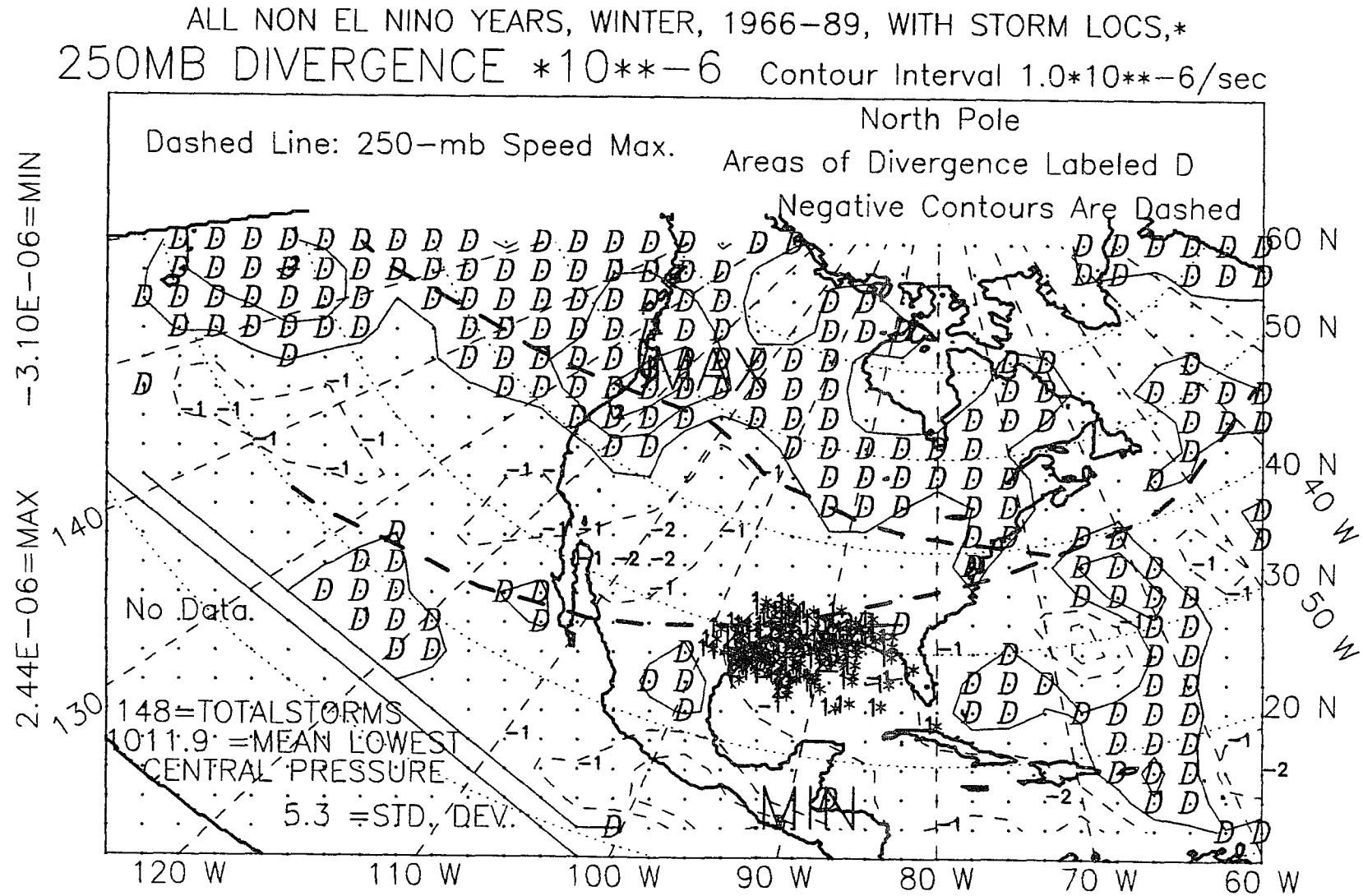

Figure 3.17: 250–mb divergence, winter, non–El Niño years, 1966–89.

subtropical tropopauses. 10° to 15° north of the south jet, the mean north jet tracks approximately along the south edge of the divergence zone seen over the northern third of the map. This seems to be at the junction of the Ferrel and most-poleward vertical circulation cells, or at the tropopause break between middle and higher latitudes.

3. The following is a list of pairings of opposite sign of divergence between the 850-mb level and the 250-mb level in El Niño and non-El Niño winters.

   (a) Over the western Atlanic Ocean the 250-mb level shows many regions of divergence over an area that is convergent at the 850-mb level.

   (b) Over the North American continent, there is much 250-mb level convergence situated over what is largely an area of divergence at the 850-mb level.

   (c) The area of the Pacific west of Mexico and Central America is convergent at the 250-mb level, while this is an area of 850-mb level divergence under the Pacific subtropical high.

   (d) The northeastern Pacific, west of the U.S. Pacific northwest and Canadian coasts, is divergent at the 250-mb level, while at the 850-mb level it is convergent.

   (e) The area over the northern and Canadian Rockies is divergent at the 250-mb level. This matches up with a zone of convergence on the 850-mb map. These mountains are much higher than the mountains in Mexico. That may be why there is coherent matching of the sign of the divergence field over the Rockies, but not over the Sierra Madre Orientals and Occidentals.

3.6.2 Gulf of Mexico: 250-mb Divergence, El Niño Winters

Matchings of opposite sign of 250-mb and 850-mb level divergence in the gulf area during both winter types follow.

1. In the winter-season averages, the area over the Gulf of Mexico is almost entirely convergent at the 250-mb level (although it is more divergent, or less convergent, during El Niño winters, 3.6.3). This 250-mb level convergence is difficult to reconcile with either the 850-mb level convergence seen over the eastern two-thirds of the Gulf of Mexico, or with the explanation previously offered for the western-gulf divergent zone, which was based on velocity increase in a cold-air channel. That is, not unless both of those features, the 850-mb level convergence and the supposed cold-air channel, are shallow and confined to low levels. This leaves the observed 250-mb level convergence over the gulf as the pair-mate of an inferred, lower-level divergence somewhere between 850- and 250-mb. Some mechanism is required to produce a midlevel divergence zone beneath the 250-mb level convergence zone centered at 30°N. The divergence could perhaps be related to the descent of air (below the 250-mb level) at the meeting of the first two vertical circulation cells north of the equator.

2. The band of surface convergence over the mountains of Mexico and the southwestern United States is not matched by a corresponding divergent zone at the 250-mb level. As in item 1 above, this is only reasonable if the surface convergent zone is shallow, due only to the local effect of the mountains, and does not extend much above the 850-mb level. Palmén and Newton (1969, p.347) discuss an example of this where the surface convergence over mountains is lost by the 700-mb level. If this is so, then the same explanation as

in item 1 above can be used. That is, this area is one of inherent divergence due to descending air below the meeting of the Hadley and Ferrel cells. Apparently, divergence is replaced by convergence only at the lowest levels, due to orographic lifting over the mountains.

3.6.3 Differences in the 250-mb Divergence Field between El Niño and Non-El Niño Winters

The following comments refer to Fig. 3.18, a difference of the composite fields of divergence at the 250-mb level in five El Niño winters and 19 non-El Niño winters between 1966 and 1989. Secondary reference is made to Figs. 3.16 and 3.17, the individual, El Niño and non-El Niño, 250-mb divergence fields. In Fig. 3.18, points that are more divergent (have a more positive value of divergence) in El Niño winters are labeled 'D'. These areas may still, in the average, be convergent in both types of winter. They are, however, less convergent (more divergent) in El Niño winters. A positive result when subtracting divergence in non-El Niño winters from that in El Niño winters means more or stronger episodes of actually positive divergence in El Niño winters, and/or fewer or weaker episodes of convergence in El Niño winters.

Although at the 250-mb level the atmosphere over the gulf region is, in the winter-season average, almost entirely convergent in both winter types, Figs. 3.16 and 3.17, all but the southwest corner is *more divergent* (less convergent) in El Niño winters, as indicated by the positive divergence difference, Fig. 3.18. Due to the intensification of the south jet in El Niño winters, it seems reasonable to interpret the positive divergence difference as owing to increased episodes of strong divergence at the 250-mb level. These episodes are likely to result from the more-frequent presence of short-lived (two to four days) jet streaks, as explained in the next section, 3.6.4.

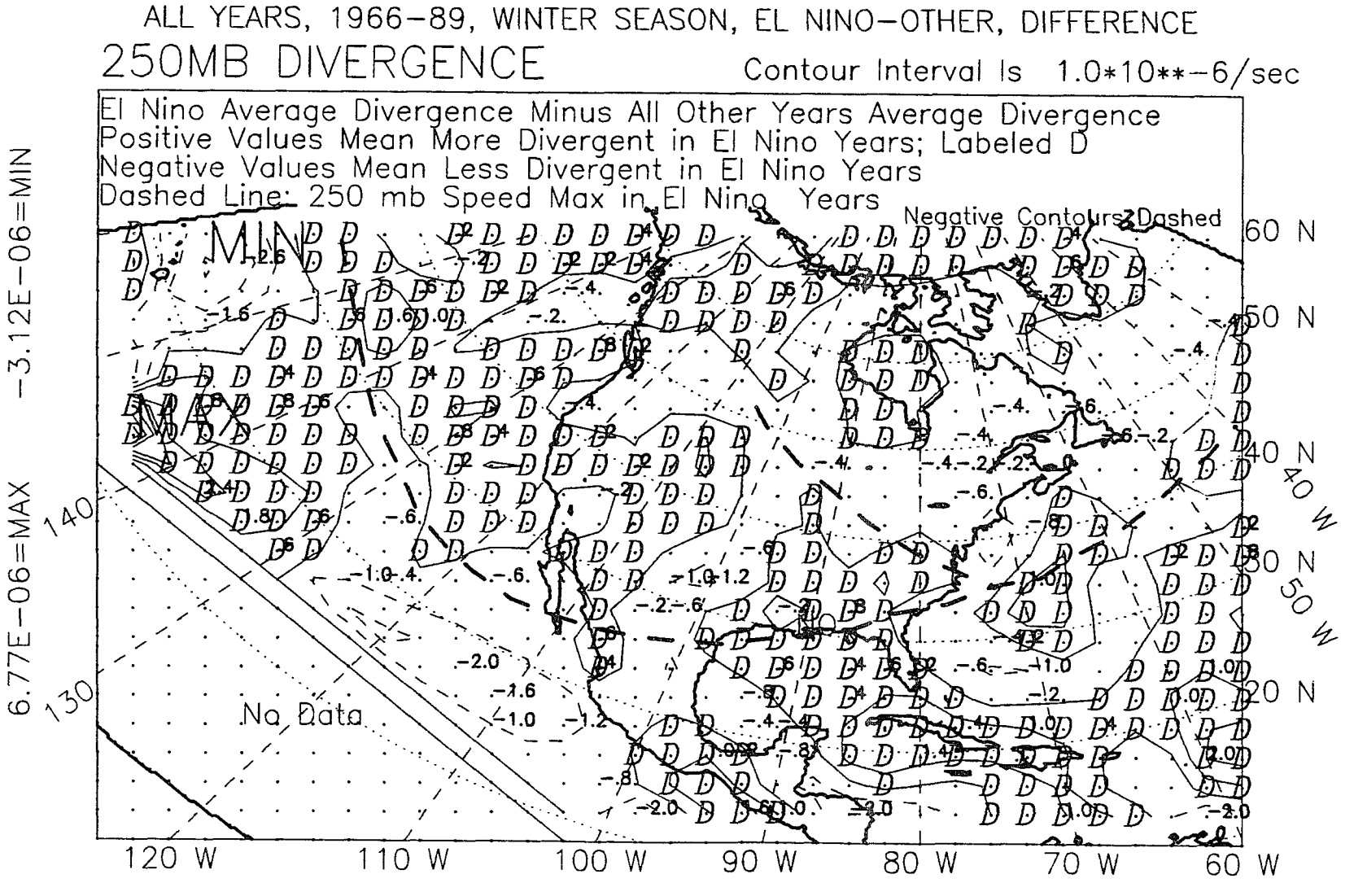

Figure 3.18: 250-mb divergence, winter, 1966-89, difference.

3.6.4 Jet Streaks, Exit, and Entrance Regions

Jet streaks, areas of highest wind speed defining the core of a jet, are neither permanent nor stationary. Streaks migrate west to east through the jet, through a process of decay in the west and strengthening in the east (Reiter 1963). An idealized pattern of divergence and convergence around a jet streak has been described by Riehl et al. (1954), Beebe and Bates (1955), Reiter (1963, 1967a) and summarized by Uccellini (1990). The basic model described below is still used, although as more-detailed observations accumulate, the simple picture is becoming more complicated and much variability in jet structure has been found, particularly in connection with the associated development of low-level jets. Strongest divergence is found in the left-front (exit) quadrant of the core, with weaker divergence found in the right-rear (entrance) quadrant. Strongest convergence is found in the right-front quadrant with weaker convergence in the left rear. This may be understood in terms of acceleration or deceleration and streamline spreading or confluencing. Air accelerates into the jet streak and decelerates on exiting. Based on this alone, one would expect divergence in the rear entrance region as air accelerates into the streak, and convergence in the fore exit region as air decelerates upon leaving the streak and piles up there. If the streak has any curvature, however, the effect of streamlines spreading out and coming together will be important. If the curvature is cyclonic, as is often case over the gulf region, on the north, inside of the curve, streamline effects will be more important than acceleration. On the inside of the curve, in the left rear, the effect of streamlines coming together greatly exceeds the effect of acceleration, and the area is strongly convergent. In the left-front quadrant, the effect of deceleration is overridden by streamline spreading and the region is strongly divergent. On the outside of the curve, streamline effects again oppose acceleration effects, but they do not generally overcome them. Convergences and

divergences on the outside of the curve are therefore generally weak. In the right-front quadrant, the tendency for convergence due to deceleration is opposed by streamline spreading, and the region is only weakly convergent. In the right-rear quadrant, divergence due to acceleration is opposed by streamline confluencing, and the region is only weakly divergent. In addition to these ageostrophic, horizontal motions, there are associated vertical circulations discussed by Reiter (1963, 1967a, 1978), Sechrist and Whittaker (1979), and Cammas and Ramond (1989). The two divergent areas of the jet streak cause warm, moist, tropospheric air from below to be pulled upward, creating areas of low pressure and convergence at the surface. These may grow into cyclones if the upper-level divergence is strong enough, persistent enough, and if surface conditions are favorable. Beneath the two convergent areas of the jet streak, cold, dry, stratospheric air descends, creating areas of high pressure and divergence at the surface. Superimposed on the vertical motion is horizontal, eastward transport in the upper-level westerlies. This ties together the entrance and exit regions of the jet streak. Some air that began rising under the right-rear divergence zone winds up rising into the left-front divergence zone. Some of the air that began to sink under the left-rear convergence zone winds up sinking to the surface beneath the right-front convergence zone.

The vertical circulations are of importance in the interaction of the jet with a surface cold front and with a developing cyclone. Browning (1990) and Cotton (1990) have used the vertical circulation to link surface fronts and an upper-level jet. These are their cold and warm 'conveyor belts'. Once a cyclone is formed under either of the divergent areas, the warm air being pulled upward from the surface is just the warm air rising ahead of the warm-front portion of the storm. The cold, dry air descending beneath the areas of convergence at jet level is just the cold-front part of the cyclone. A storm formed under the left-front exit region

will be stronger than one formed under the right-rear entrance region because the divergence is stronger in the exit region, and so, capable of causing greater surface pressure fall, and also because the exit area has air streams feeding into it from two places, from directly below and from the rear entrance region. The rear, rising current rises more slowly than the forward rising current, due to weaker upper-level divergence in the rear. So the rear rising current experiences more forward transport than does the air which rises below the exit region.

It is therefore the upper-level divergent areas associated with a jet streak that are most important in cyclogenesis. These are capable of creating surface low-pressure areas, and so causing or contributing to cyclogenesis. If the divergent areas are stronger, or more often present in El Niño winters, then a mechanism is suggested to explain the more-frequent occurrence of storms over the gulf region in El Niño winters, that is, through more-frequent provision of the necessary upper-level forcing. At the 250-mb level, the positive difference over the gulf area between divergence in El Niño winters and other winters would seem to indicate more of these divergent episodes in El Niño winters. In the average, due to the migratory nature of the jet and of jet streaks, the net divergence should be near zero, adjacent areas of convergence and divergence cancelling each other out with forward movement. That is, unless a certain area is consistently occupied by the jet. The average expected is small and not necessarily in proportion to the changes in the jet between the two types of winter. The averages observed over the gulf area are small, between 0 and $1\times10^{-6}s^{-1}$.

The areas of convergence and divergence around a jet streak suggest a connection between U.S. east-coast cyclogenesis and Gulf of Mexico-region cyclogenesis. Noting that the core of the south jet, Figs. 3.13 and 3.14, is just off the Carolinas, one might suppose that when a jet streak is present, there must be an exit

region somewhere off the southeastern coast of the United States, and an entrance region somewhere to the southwest of there. Taking 1000 to 2000 km (625 to 1250 miles) as a representative length of a jet streak, one may expect an entrance region perhaps in the vicinity of the Texas or Louisiana shelves in the northern Gulf of Mexico. Viewed as a single system, the gulf-region cyclones are lesser storms forming under the weaker, entrance-region divergent zone of a jet streak, and the U.S. east-coast storms are stronger storms formed under the more-strongly divergent zone of the exit region. This clarifies the relationship within a 'family' of wave cyclones (Petterssen 1958, referring to earlier work of Bjerknes and Solberg). Exactly this geometry is suggested by Uccellini et al. (1984, their Fig. 13) in their discussion of the Presidents' Day storm.

Does the averaging process leave any trace of these two postulated divergent zones? The El Niño-winter map, Fig. 3.16, shows a small, divergent area over the Florida panhandle, although it is only based on four points, and by itself, is of little significance. At the 250-mb level, the atmosphere over the western gulf shows not even a small patch of divergence in either winter type. This may be because of the weaker divergence expected in the entrance region. The 250-mb level, western-gulf atmosphere does, however, have a positive divergence difference. The other possible exit region shown on the 250-mb wind-speed map for El Niño winters, Fig. 3.13, in the Pacific at 140°W, 30°N, also shows an area of relatively strong, positive divergence in Fig. 3.16 in what may be the average left-front quadrant. The exit-region half of the ideal divergence pattern around a jet streak may be visible here, if the area of relatively strong convergence just south of 140°W, 30°N is the right-front quadrant. This area was discussed previously in connection with a possible more southerly track for winter storms approaching the North American continent from the northern Pacific in El Niño winters.

3.6.5 Other Differences in the 250-mb Divergence Field between El Niño and Non-El Niño Winters

Some other differences in the divergence fields for the two winter types are listed below.

1. At the 250-mb level, east of Hawaii, extending from 130° to 145°W, and from the map edge at 15° to 20°N, a strongly divergent area is seen in El Niño winters, Fig. 3.16, that is completely absent in non-El Niño winters, Fig. 3.17. It appears to be due to the increased anticyclonic shear on the south side of the south jet, as shown by the anticyclonic residue in Fig. 3.15. It may be instrumental in reinforcing central Pacific cloudiness and rainfall in El Niño winters.

2. There is some area of average divergence at the 250-mb level over the Caribean in El Niño winters, while in non-El Niño winters the entire region is convergent. The whole region has a strongly positive divergence difference, Fig. 3.18.

3. There is less area of divegence at the 250-mb level in northeastern Canada and the Great Lakes in El Niño winters. The divergence difference is negative (convergent).

4. In non-El Niño winters at the 250-mb level there appears to be a region of divergence, though only based on four points, above the 850-mb convergent region over the mountains of Mexico.

3.7 Winter, 250-mb Relative Vorticity: 1966-1989

3.7.1 General Circulation: 250-mb Relative Vorticity, El Niño Winters

These comments and those in the next section refer primarily to Figs. 3.19 and 3.20, composites of the 250-mb relative-vorticity field for the five El Niño winters and for the 19 non-El Niño winters between 1966 and 1989.

1. The most-pronounced feature of the relative-vorticity composite for El Niño winters, Fig. 3.19, is a strong band of positive relative vorticity at the 250-mb level, roughly centered on 30°N latitude, and present over the Atlantic Ocean from the Yucatan to the eastern map edge, at 40°W. In this location the 250-mb level is about half divergent and half convergent. (The 850-mb level was all convergent.) According to the general-circulation scheme, between about 30° and 60°N latitude, and shifted south in winter, the 250-mb level should be convergent. (This is the upper-level opposite pair-mate of the Bermuda High, though that is weakened in winter.) If the 250-mb level map is basically convergent, only modified by patches of divergence, this agrees with the model. The divergent patch off the Carolinas is close to the core of the maximum-speed axis, where the mean north jet appears to join the mean south jet. This area may owe its divergence to velocity increase due to confluencing (Namias and Clapp 1949).

2. In El Niño winters another area of positive relative vorticity is centered roughly on 50°N, over the northwest part of the Pacific mapped, California, the Canadian and U.S. Pacific northwest, and the Canadian arctic. This region is divergent at this level. This last is in agreement with the general-

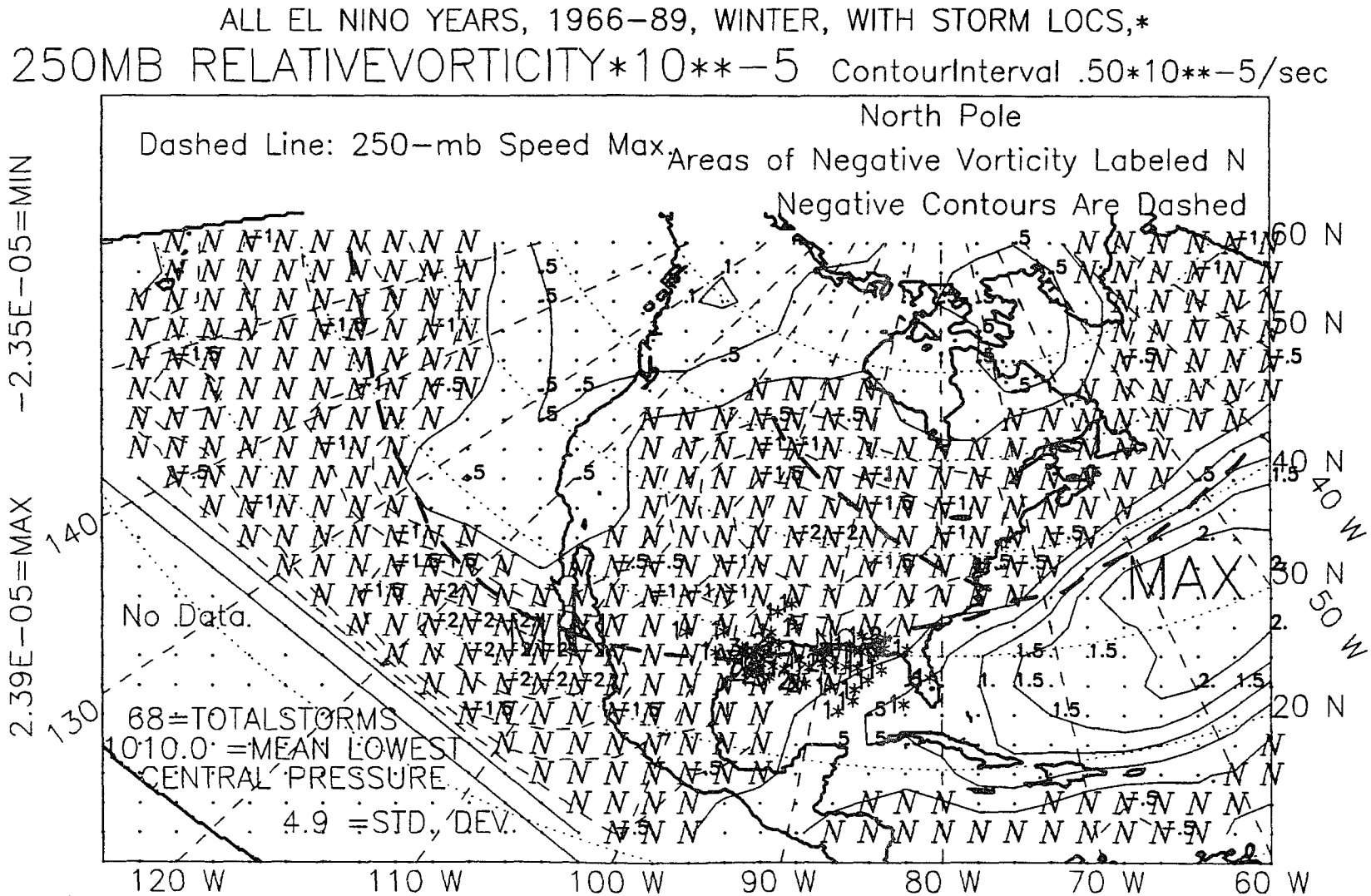

Figure 3.19: 250–mb relative vorticity, winter, El Niño years, 1966–89.

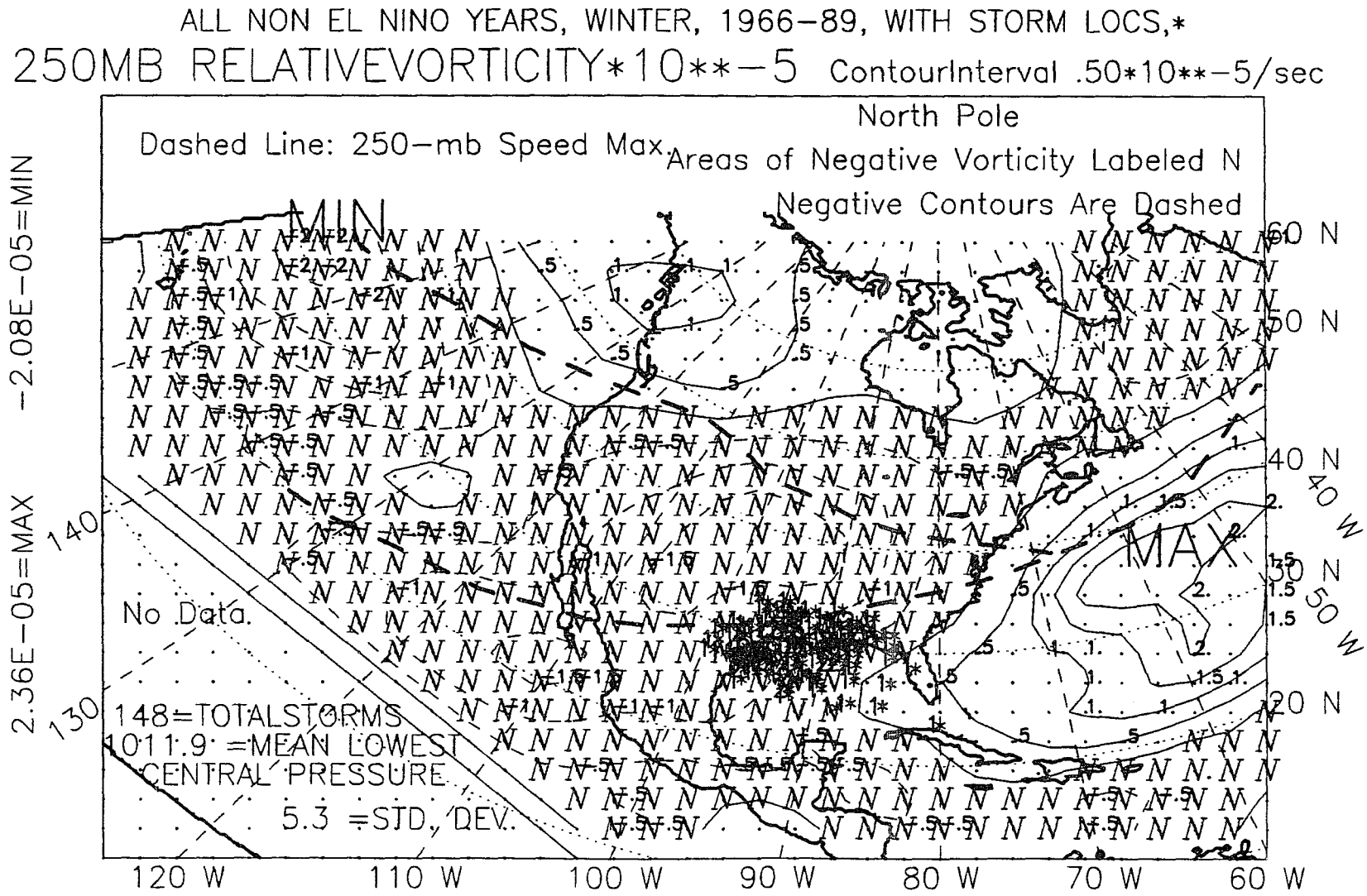

Figure 3.20: 250-mb relative vorticity, winter, non-El Niño years, 1966-89.

circulation model which calls for upper-level divergence between the middle and the most-poleward vertical circulation cells at about 60°N, shifted south in winter. This positive relative vorticity is, however, opposite to what would be expected based on the positive divergence seen here. This discrepancy is unresolved. Along the northwest coast of North America, this region of upper-level, positive relative vorticity extends about 10° farther south in El Niño winters, to cover the entire U.S. west coast, but not the continental interior.

3. Most of the North American continent and the remaining parts of the north Atlantic and Pacific show negative relative vorticity. Nearly all of these areas are convergent at the 250-mb level. Based on the general-circulation model, one would expect a band of convergence centered on 30°N or somewhat south of there, and a band of divergence north of that, at about 60°N. While the 250-mb convergence agrees with the model, the presence of all negative relative vorticity does not, and this is unresolved. Further, in the regions to the north of each of the two mean jets, one would expect positive relative vorticity based on the curvature and lateral velocity shear of the 250-mb jets. Almost the opposite is true, although a thin sliver, about three degrees wide, of positive relative vorticity does show up north of the south jet, over the Atlantic in El Niño winters. This is part of the same band of positive relative vorticity discussed in part 1 above.

3.7.2 Gulf of Mexico: 250-mb Relative Vorticity, El Niño Winters

1. In El Niño winters, the 250-mb atmosphere over all but the southeastern third of the Gulf of Mexico shows average negative relative vorticity, although the same area is, on average, convergent at this level.

2. Nearly all of the winter storms originating over the gulf region are under an area of average, 250-mb level, negative relative vorticity.

3.7.3 Differences in the 250-mb Relative-Vorticity Field between El Niño and Non-El Niño Winters

The following comments refer primarily to Fig. 3.21, the field of relative-vorticity difference for the five El Niño winters and the 19 non-El Niño winters between 1966 and 1989. Secondary reference is made to Figs. 3.19 and 3.20, the El Niño and non-El Niño composites. In Fig. 3.21, points that have more negative relative vorticity (have a smaller or more negative value of relative vorticity) in El Niño winters are labeled 'N'.

1. Fig. 3.21 shows a strong, continuous band of positive relative-vorticity difference reaching from the eastern Pacific, across the west coast of the United States, and dipping south over the southwestern states, the Gulf of Mexico, and Caribbean, and the western Atlantic. The maximum positive difference is centered between the mean north and south jets, located over California and the southwestern United States. In the western region the positive-difference band is neatly bounded on the south by the south jet, being on the cyclonic side of the jet. Presumably, the intensification of the south jet in El Niño winters is responsible for the increased cyclonic (positive) shear to its north, and creates the positive difference. This is supported by the cyclonic residue

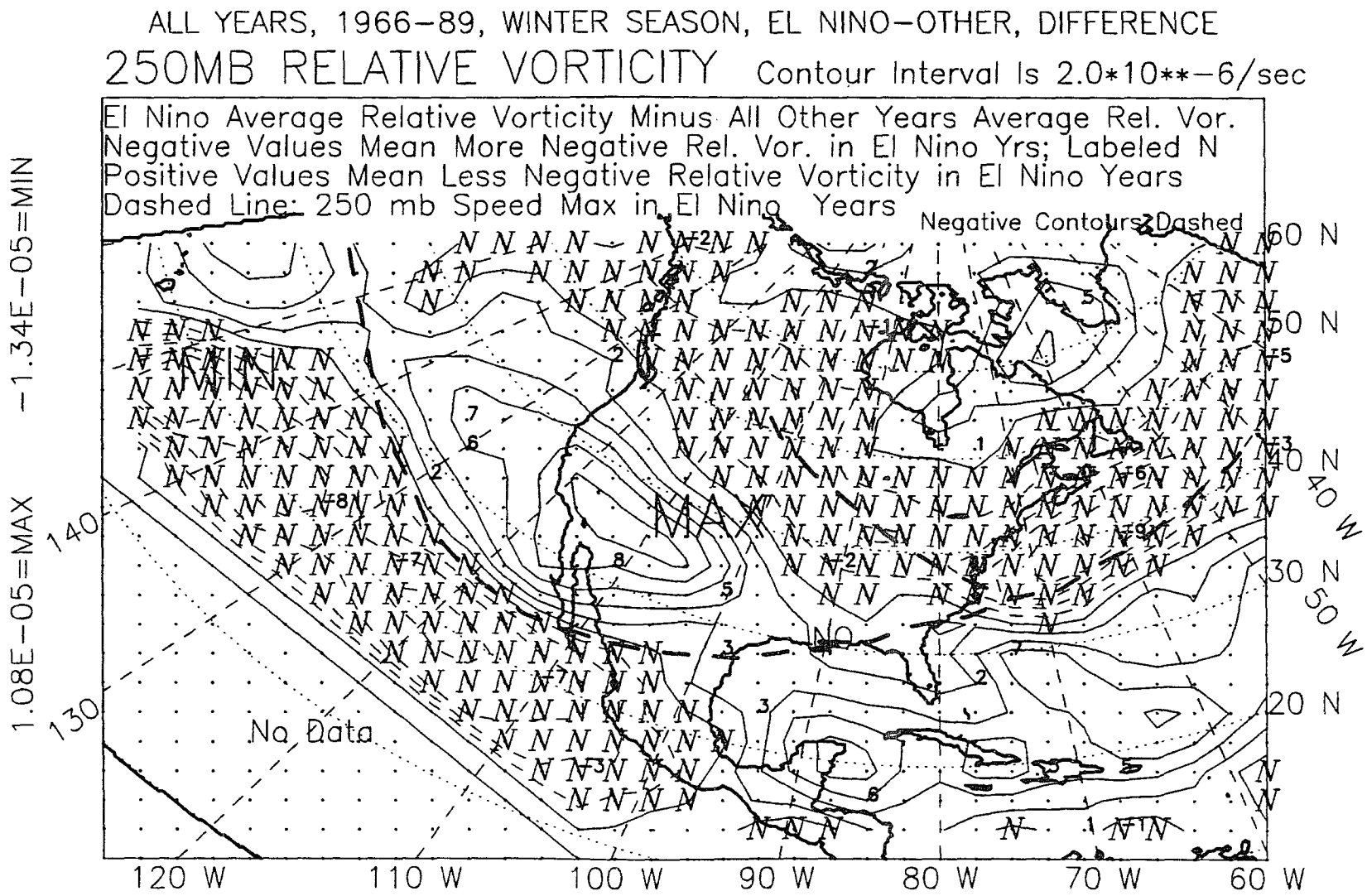

Figure 3.21: 250–mb relative vorticity, winter, 1966–89, difference.

in the region on the 250-mb, wind-difference map, Fig. 3.15. Fig. 3.16, the El Niño-winter, 250-mb divergence field, shows most of the positive-residue band is convergent, which is consistent. Likewise, the weakening of the north jet in El Niño winters results in less anticyclonic (negative) shear to its south and produces an apparent cyclonic (positive) residue south of it. This contributes to the band of positive relative-vorticity residue between the two branches. In the eastern region, over the Atlantic portion of the band of positive relative-vorticity difference, the mean south jet roughly divides a region of decreased wind speeds to the north from one of increased wind speeds to the south. This is just the opposite of the situation over the Pacific and western United States. This is reflected in a reversal in the sign of the relative-vorticity difference. North of the mean south jet, decreased velocities produce less cyclonic (positive) shear, resulting in a negative relative-vorticity difference. South of the mean south jet, increased velocities should produce more anticyclonic (negative) shear, resulting in a negative relative-vorticity difference. This is not observed. Instead, the difference is positive, and the explanation south of the mean jet axis must be more complex than simple lateral velocity shear as in the area to the north of the jet axis. The negative relative-vorticity difference due to increased lateral velocity shear must be outweighed by the advection of positive relative vorticity. This occurs when air moves from regions of higher relative vorticity to regions of lower relative vorticity, carrying, or advecting, its relative-vorticity 'signature' with it (Petterssen 1956). Since the winter, mean core of the south jet is located in this area, at approximately 70°W, the most likely source of positive relative vorticity is jet-level troughs that advance south during cold-air outbreaks (Namias and Clapp 1944).

Between the west and east ends of the band of positive relative-vorticity difference, over the gulf region, there is a zone of transition, and the mean south-jet axis cuts diagonally across the band of positive relative-vorticity difference. Over the gulf area, most of the band is actually to the south of the mean south jet. Only the positive relative-vorticity difference over the northernmost gulf and northern coastal plain can be explained by increased cyclonic shear north of the mean south jet. The remainder of the positive relative-vorticity difference over the gulf area may be due to the advection of positive relative vorticity, most likely within jet-level troughs during cold-air outbreaks. This amounts to claiming that the extra positive relative vorticity over the gulf area in El Niño winters results from more frequent excursions into the area of jet-level troughs, an idea supported by the south-displaced mean south jet (chapter 4), the region's positive divergence difference, and by negative height and temperature differences at near-surface, intermediate, and upper levels (chapter 4).

2. The area north of the weakened north jet shows a negative relative vorticity difference due to less cyclonic (positive) shear to its north, Fig. 3.21. Supporting this, the 250-mb, wind-difference map shows anticyclonic residue over the area, Fig. 3.15.

3. In El Niño winters a little more of the gulf is under positive relative vorticity than in non-El Niño winters, Figs. 3.19 and 3.20. This is because the region of positive relative vorticity over the Atlantic extends farther west in El Niño winters, encroaching more over the southeastern gulf.

4. The northeastern Pacific area of positive relative vorticity extends further south in El Niño winters, to Baja, Fig. 3.19. In non-El Niño winters it stops at British Columbia.

3.8 Idealized and Actual Fields of Divergence and Relative Vorticity

An idealized model to account for more storms in El Niño winters predicts more-frequent episodes of positive divergence and positive relative vorticity over the gulf region at the 250-mb level. These should be accompanied by convergence and positive relative vorticity at the 850-mb level during El Niño winters. The model predicts these based on the assumption that the probability of surface cyclogenesis will be enhanced first, by surface convergence due to cyclonic circulation (positive relative vorticity) and second, by upper-level divergence supplied by a deep, upper-level trough behind the jet stream (Petterssen 1956, p. 331) and the accompanying cyclonic circulation and cyclonic lateral velocity shear (positive relative vorticity) in the trough, north of the jet core. However, what is seen in the winter averages, or El Niño-winter composites, is: average 250-mb level convergence and negative relative vorticity over all but the southeast gulf. At the 850-mb level, the gulf region is, on average, convergent in the east, divergent in the west, and shows negative relative vorticity over all but the Bay of Campeche, the southwest corner of the gulf. *Only the difference maps show close-to-predicted conditions, the seasonal averages usually masking the ENSO effect.* Table 3.2 summarizes the predicted and actual findings. At the 850-mb level the divergence-difference map, Fig. 3.9, shows much of the gulf has the predicted excess of convergence, but only the west side of the western-gulf divergent zone is less divergent (more convergent). The map of 850-mb level, relative-vorticity differences, Fig. 3.12, shows the predicted positive difference over the western gulf, where many of the storms form, but a negative difference over the eastern gulf. At the 250-mb level, the divergence-difference map, Fig. 3.18, shows all but the southwest corner of the gulf has the predicted excess positive divergence. The map of 250-mb, relative-vorticity differences, Fig. 3.21, shows that

Table 3.2: El Niño-winter, 850-mb and 250-mb level divergence and relative vorticity: idealized and actual.

Level	Divergence	Relative Vorticity	Figures
Idealized Conditions (Model)			
850 mb	Convergent	Positive	
250 mb	Divergent	Positive	
Actual, Average Conditions			
850 mb	Convergent (East)	Negative	3.7, 3.10
	Divergent (West)	(Except southwest gulf)	
250 mb	Convergent	Negative	3.16, 3.19
		(Except southeast gulf)	
El Niño-Winter Differences			
850 mb	Convergent	Positive	3.9, 3.12
	(East and extreme west)	(Except east gulf)	
250 mb	Divergent	Positive	3.18, 3.21
	(Except southwest gulf)		

the entire area over the gulf has the predicted excess of positive relative vorticity. Summarizing, in El Niño winters, the lower level is more convergent (except most of the western-gulf divergence zone) and has more positive relative vorticity. The upper level is more divergent and has more positive relative vorticity in El Niño winters. The contrary result is the persistence of the western-gulf divergent zone at the 850-mb level. It should be more convergent in El Niño winters, yet is so only on its west, shore-side edge. Elsewhere the zone is slightly more divergent. Explanation of this follows.

First, the 850-mb divergence zone over the western gulf, since accompanied by an excess of positive relative vorticity and weaker anticyclonic circulation in El Niño winters, must not be solely due to anticyclonic circulation, but partly to velocity increase from north to south. The 850-mb wind-difference map, Fig. 3.3, shows a north residue over the western gulf, indicating either more north wind, or less south wind. If the north difference is due to more (or stronger) north winds over the western gulf during El Niño winters, then the portion of the divergence which

is not due to anticyclonic circulation, may be due to velocity increase in the above-postulated channel for transport of cold air during cold-air outbreaks. During cold-air outbreaks, wind speed may steadily increase from the coastal plain gulfward, heading south, since the frictional resistance over smooth grassland and water is less than over rougher upland terrain (Petterssen 1958). It may reach its maximum velocity in the Bay of Campeche, where transport over water has been sustained the longest. The few wind-difference vectors over the western gulf, Fig. 3.3, show the magnitude of the north wind difference increases from north to south. If the north difference is due to more north wind, and not to less south wind, then the north difference in El Niño winters must indicate that the proposed channelization of cold air during cold-air outbreaks (if it occurs) is more pronounced during El Niño winters. An 850-mb temperature-difference map, Fig. 4.19, shows a tongue of cooler temperatures in the western-gulf divergent zone, indicating cooler air in the west during El Niño winters than during non-El Niño winters. The western-gulf, onshore temperature records, Tables 2.5 and 2.7, and Figs. 2.17 and 2.21, show a statistically significant cooling in El Niño winters at Houston, Galveston, Corpus Christi, and Brownsville, Texas, and at Merida, Mexico. (The El Niño-winter, surface cooling noted in chapter 2 is, however, not confined to the western gulf.) Why this postulated cold-air channel should be more active in El Niño winters may relate to differences in the character of some cold-air outbreaks during El Niño winters, and/or to differences in the local atmosphere, over the gulf. Is the cold-air channel consistent with the observation of fewer cold fronts in El Niño winters? Possibly, if a sufficient number of cold-air outbreaks in El Niño winters are stronger. The work of Mortimer et al. (1988), characterizing severe cold-air outbreaks over Louisiana, may be of relevance here. Many strong cold fronts, in terms of temperature drop, reached the southern United States during the 1982/83 El Niño event, causing damage to crops and inadequately protected water lines.

Appendix T contains some details of the cold fronts and associated frontal-wave cyclones during winter year, 1982.

Finally, acceptance of the cold-air channel during cold-front passage as explanation for the winter, western-gulf divergent zone should be contingent upon the existence of a satisfactory explanation for the divergent zone's presence in the warm months (appendix E). For example, outside of the cold-front season, the sea-breeze system along the western gulf coast may set up the divergent zone. During the day, the onshore-directed sea breeze implies descending air offshore, supplying the necessary divergence. Wind data used to calculate divergence is from NMC final analyses at 6:00 AM and 6:00 PM local time (7:00 AM and 7:00 PM local daylight-savings time). Both times are used in the seasonal averages. Clearly, the sea breeze, and associated vertical motion, will be in opposite directions at these times. The explanation only works if the 6:00 PM sea-breeze system is stronger than the 6:00 AM system. Hsu (1988) has shown, for the Texas coast, that the 6:00 PM sea-breeze system is somewhat stronger than the 6:00 AM system, and more importantly, has greater vertical extent, extending farther into the 850-mb layer than in the early morning.

Another partial explanation for the divergence zone's presence in the warm season may involve the fetch available to the east trades, which increases to a maximum over the southwest gulf. There should be some increase in wind speed, heading west. Summer, 850-mb wind maps do show a strengthening of southeasterly winds, from east to west, which may contribute to the positive divergence.

Finally, the possibility of a mountain-wind system exists in any season. Downslope winds at night and upslope winds during the day, if present, and if close enough to the coast, would add constructively with the sea-breeze effect. A mountain-wind system would produce downslope, offshore-directed winds at 'night' (observations

at 6:00 AM local time) and upslope, onshore-directed winds during the 'day' (observations at 6:00 PM local time) (Petterssen 1958). Again, if the 6:00 PM wind is stronger than the 6:00 AM wind, the average will be divergence on the coastal plain and perhaps even some distance offshore, amplifying the offshore divergence from the sea breeze. Note that both of these mechanisms, mountain wind and sea breeze, are consistent with the zone of convergence over the mountains. In invoking the sea breeze and mountain wind to either generate or add to the west-gulf divergence zone, the obvious uncertainty is one of scale. Are the mountains close enough to the coast? How far inland would the sea breeze exist? Evidence at hand, though indirect, that the mountain-wind effect may be operating, is the similarity in size and shape of the mountain range, the divergence zone, and the convegence zone. One is encouraged to look for a sea-breeze system, on this scale, by reports elsewhere of a daytime convergence zone developing over peninsular Florida as a result of the coalescence of opposing sea breezes on each coast (Nicholls et al. 1991). There, the sea breeze can reach inland by about a degree of longitude.

CHAPTER 4
CYCLOGENESIS

Having established in chapter 2 that, between 1960 and 1989, more frontal-wave cyclones formed in the gulf area during El Niño winters than during non-El Niño winters, statistically significant at the .01 level, it remains to explain this. A number of workers have suggested that the subtropical-jet stream is the cause of the increased frequency of cyclogenesis, due to its south displacement and strengthening over the southern United States in El Niño winters (Johnson et al. 1984; Quiroz 1983a, 1983b; Douglas and Englehart 1981; Horel and Wallace 1981). Accordingly, the location of the 250-mb 'south' jet (see 3.5.1, approximately the subtropical jet, but likely to be a mix of that and the polar-front jet) over North America and flanking regions of the Pacific and Atlantic Oceans was examined seasonally from winter 1966 to spring 1989. Displacements of the south jet, in each season, were calculated from a 24-year mean position. Recalling the 700-mb, negative height anomaly over the southern United States reported by Douglas and Englehart (1981) and separately, by van Loon and Rogers (1981) from the latter's examination of 31 winters from 1948 to 1978, composite maps of height and of temperature were constructed for 27 years, 1963 to 1989. This was an attempt to duplicate the result, over a different time period and with somewhat different data. van Loon and Rogers used single stations. The gridded data used here is described in 3.1. 850-, 700-, 500-, and 200-mb levels were used, but no temperature maps were made for the 700- and 200-mb levels. 43 years, 1947 to 1989, were used for 500-mb level height.

4.1 Location of the Seasonal Mean Jet Stream (250-mb Speed Maximum) in El Niño and Non-El Niño Years, 1966 to 1989

The 250-mb wind-speed composites presented in 3.5 and in appendix J serve as the basis for the following discussion. Appendix K shows all seasonal jet axes for El Niño and other years. Appendix O shows the 24 individual, winter, 250-mb wind-speed maps from winter 1966 to 1989. All analyses were done on the south jet. As the first step in calculating displacement, axes of maximum wind speed were subjectively drawn for each individual season, including a winter-plus-spring season and a winter year, from winter 1966 (December 1965-February 1966) to spring 1989 (March 1989-May 1989). The individual seasonal axes for the five El Niño winters and 19 non-El Niño winters appear in Figs. 4.1 and 4.2. Figs. 4.3 and 4.4 show the six El Niño-spring axes and 18 non-El Niño-spring axes. Figs. 4.5 and 4.6 show the five El Niño, winter-plus-spring axes and 19 non-El Niño, winter-plus-spring axes. The next step in gauging jet displacement was to establish standard places at which to measure jet position. Ten longitudinal transects were arbitrarily chosen from 110° to 75°W, every five degrees of longitude, with two more, one at the west and one at the east edge of the gulf. The third step was to calculate the 24-season mean point at which the south jet intersected each transect, per season. Finally, for each year, the displacement of each seasonal mean's actual point of intersection from the 24-season, mean intersection point was calculated. The order of subtraction is such that north displacement is positive; south displacement is negative. Having thus generated for each season, a list of 24 positive and negative displacements in kilometers, each list was separated into El Niño and non-El Niño subsets and the rank sum test, described in 2.1.6, was used to determine if the displacements of the south jet from the 24-season mean differed in a statistically significant manner

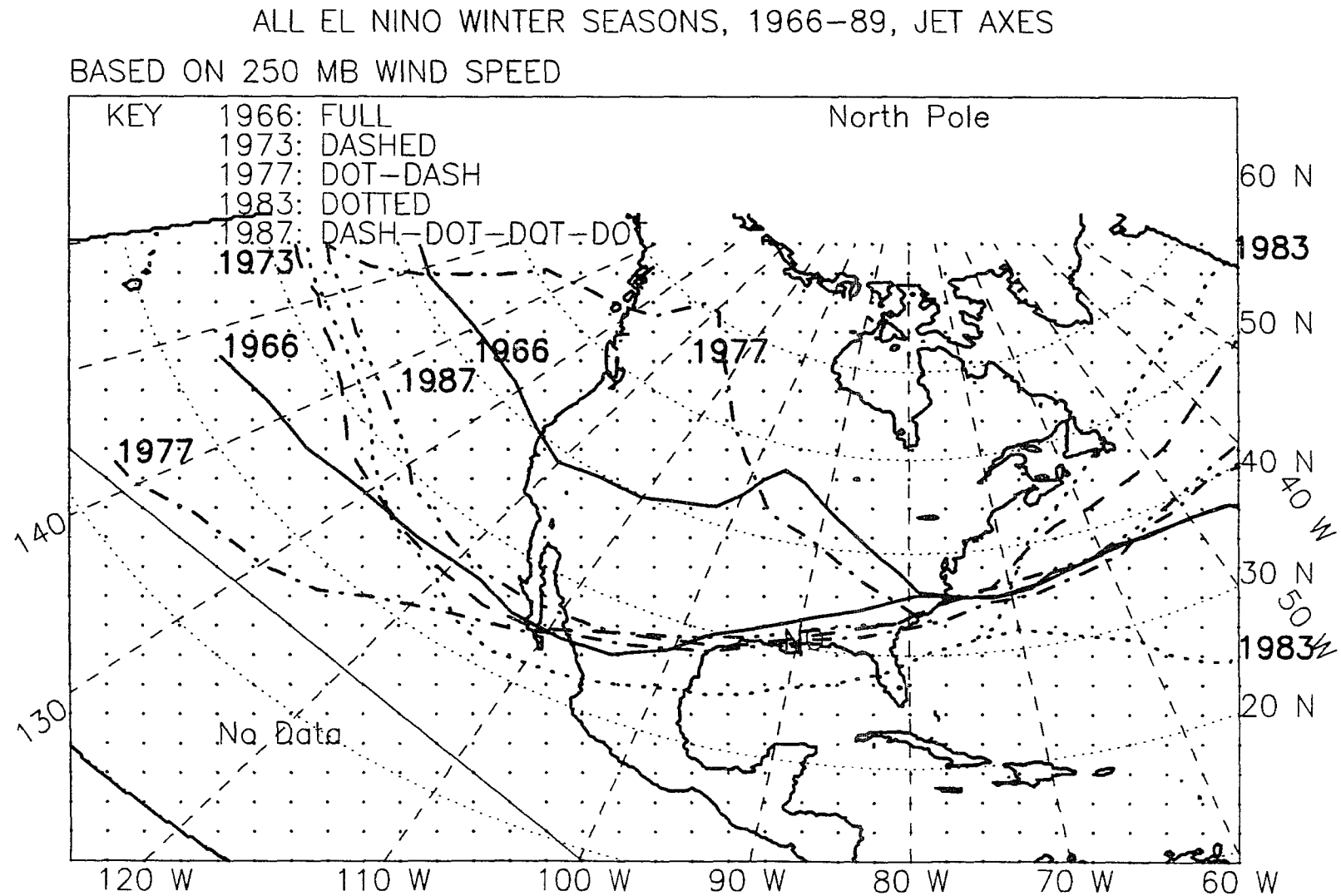

Figure 4.1: 250–mb jet axes, five El Niño winters from 1966–89.

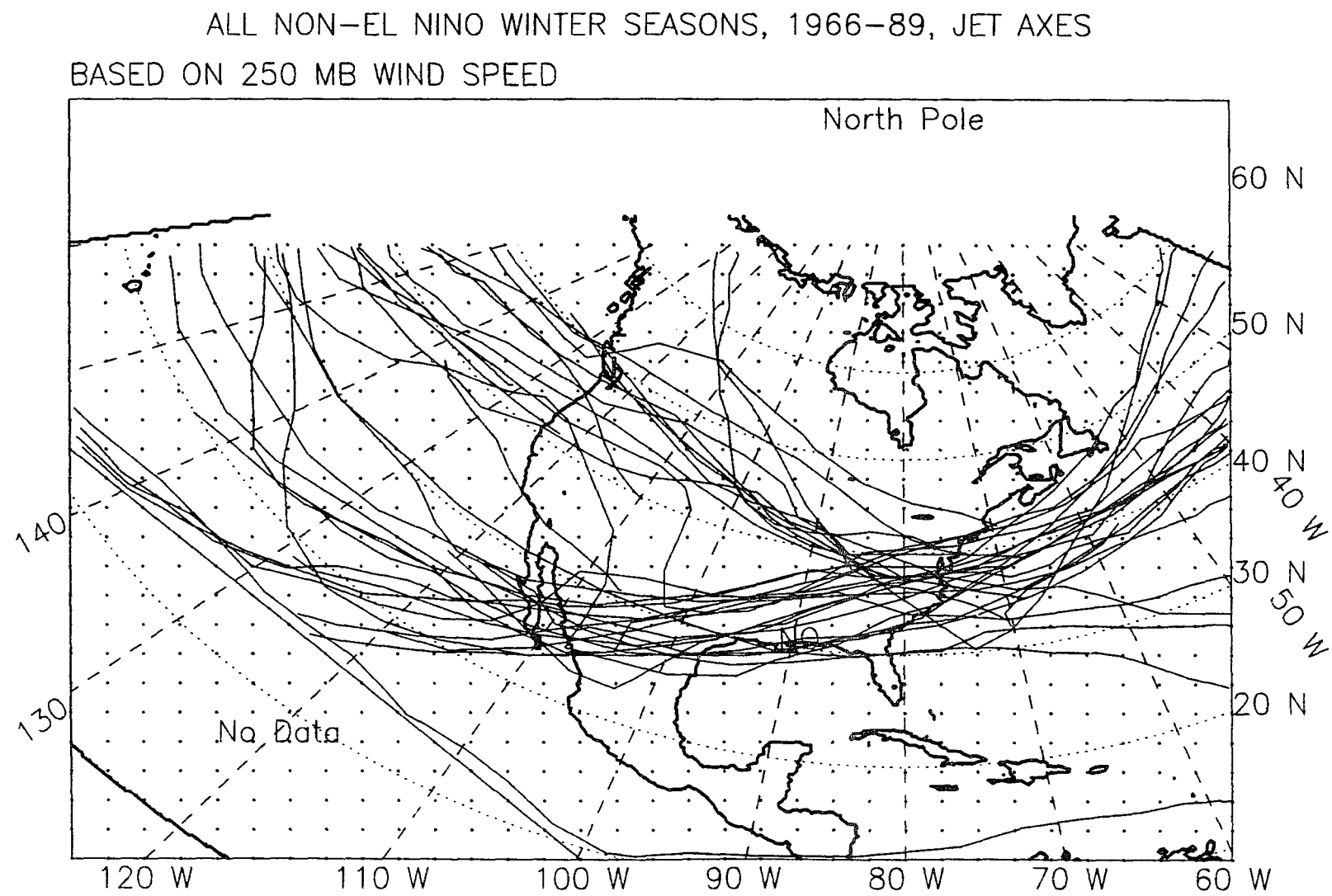

Figure 4.2: 250-mb jet axes, 19 non-El Niño winters from 1966-89.

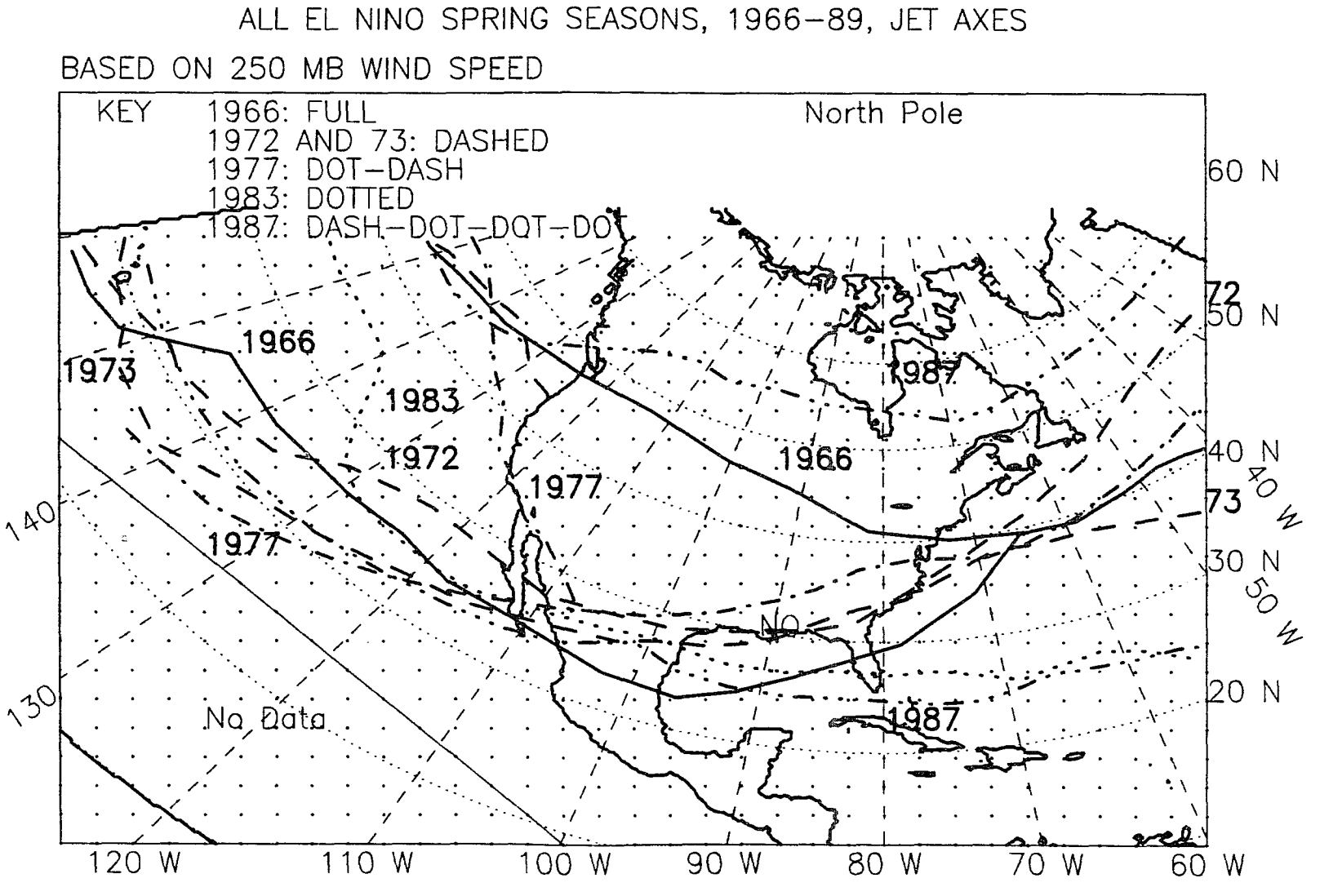

Figure 4.3: 250–mb jet axes, six El Niño springs from 1966–89.

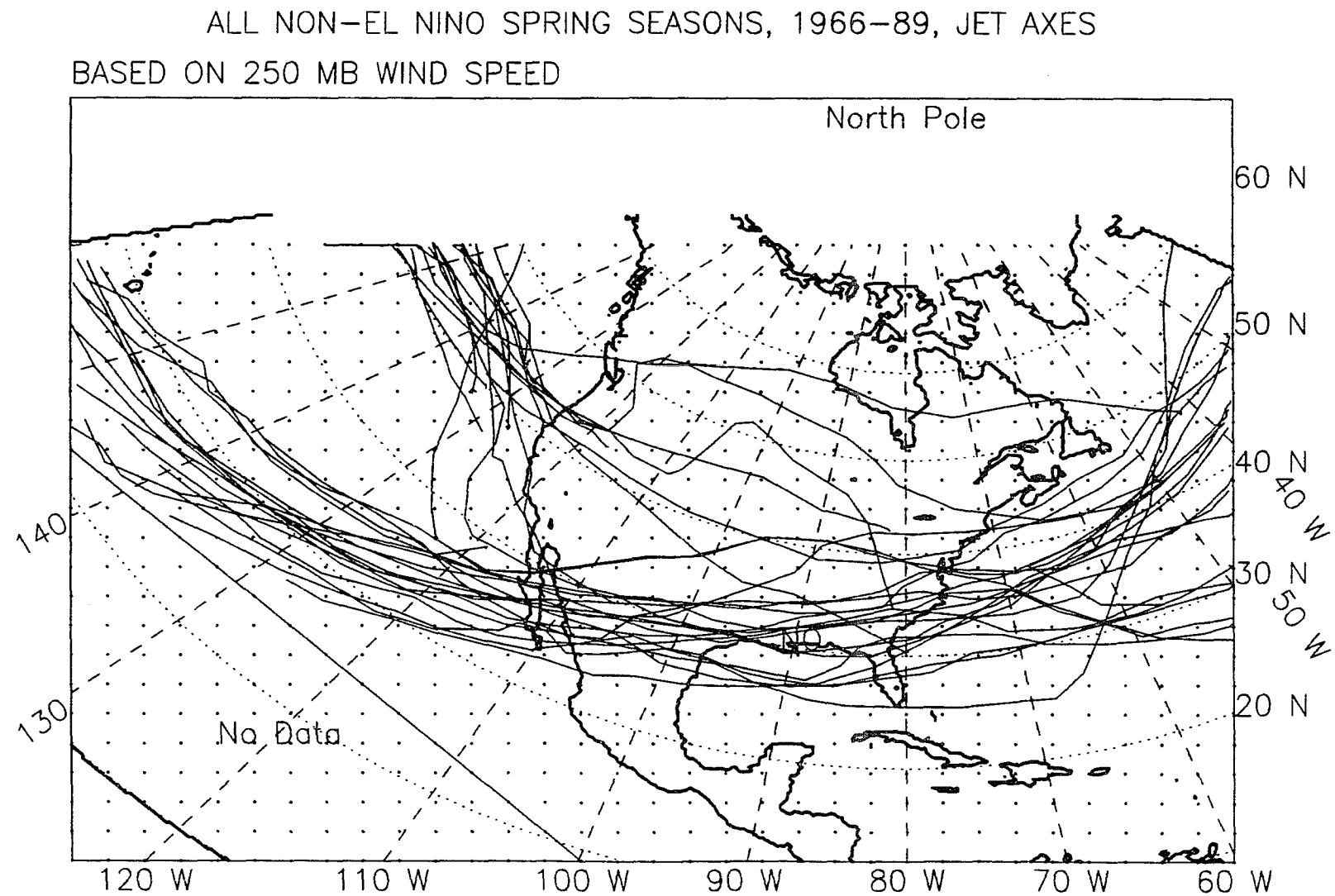

Figure 4.4: 250-mb jet axes, 18 non-El Niño springs from 1966-89.

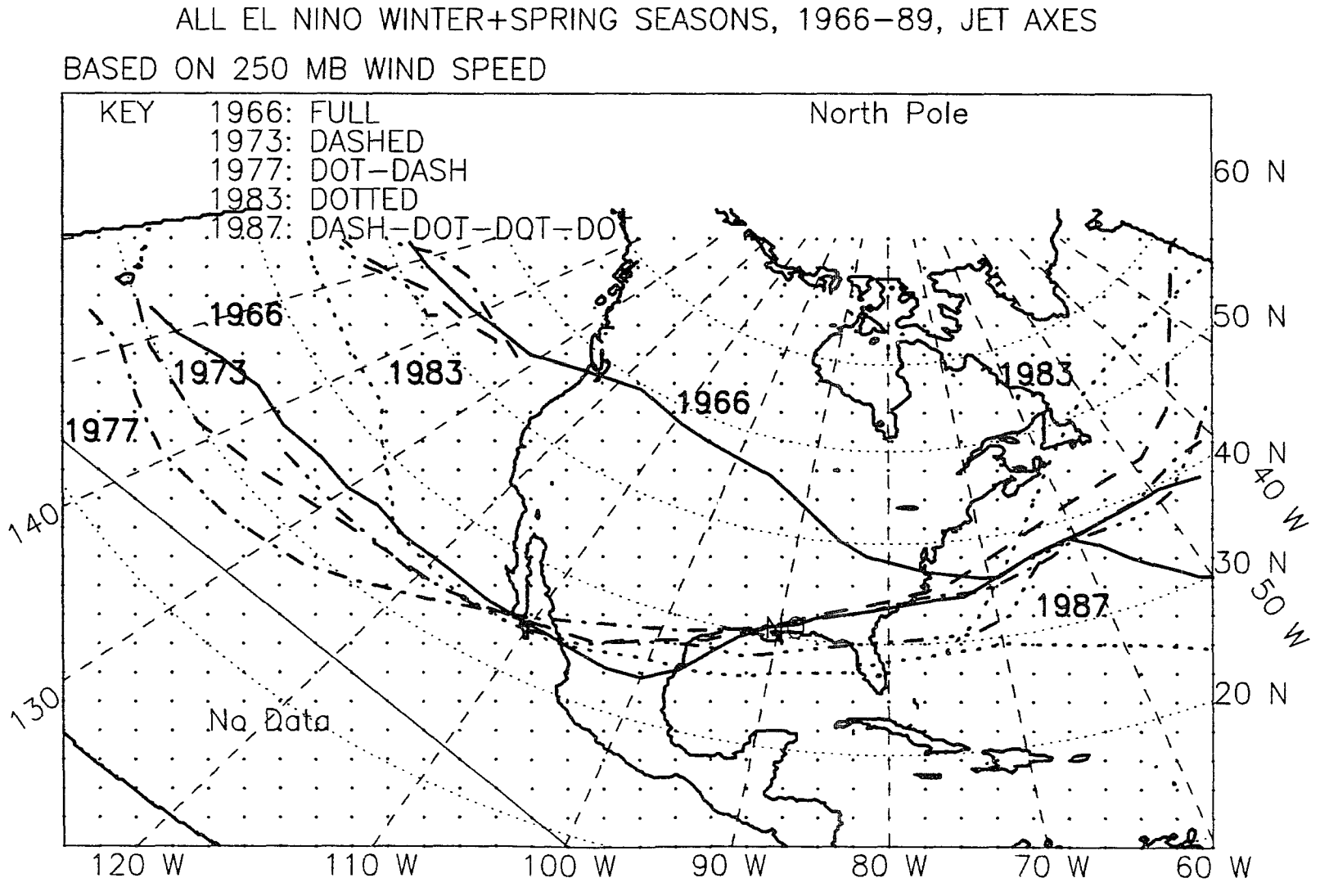

Figure 4.5: 250–mb jet axes, five El Niño winter–plus–springs from 1966–89.

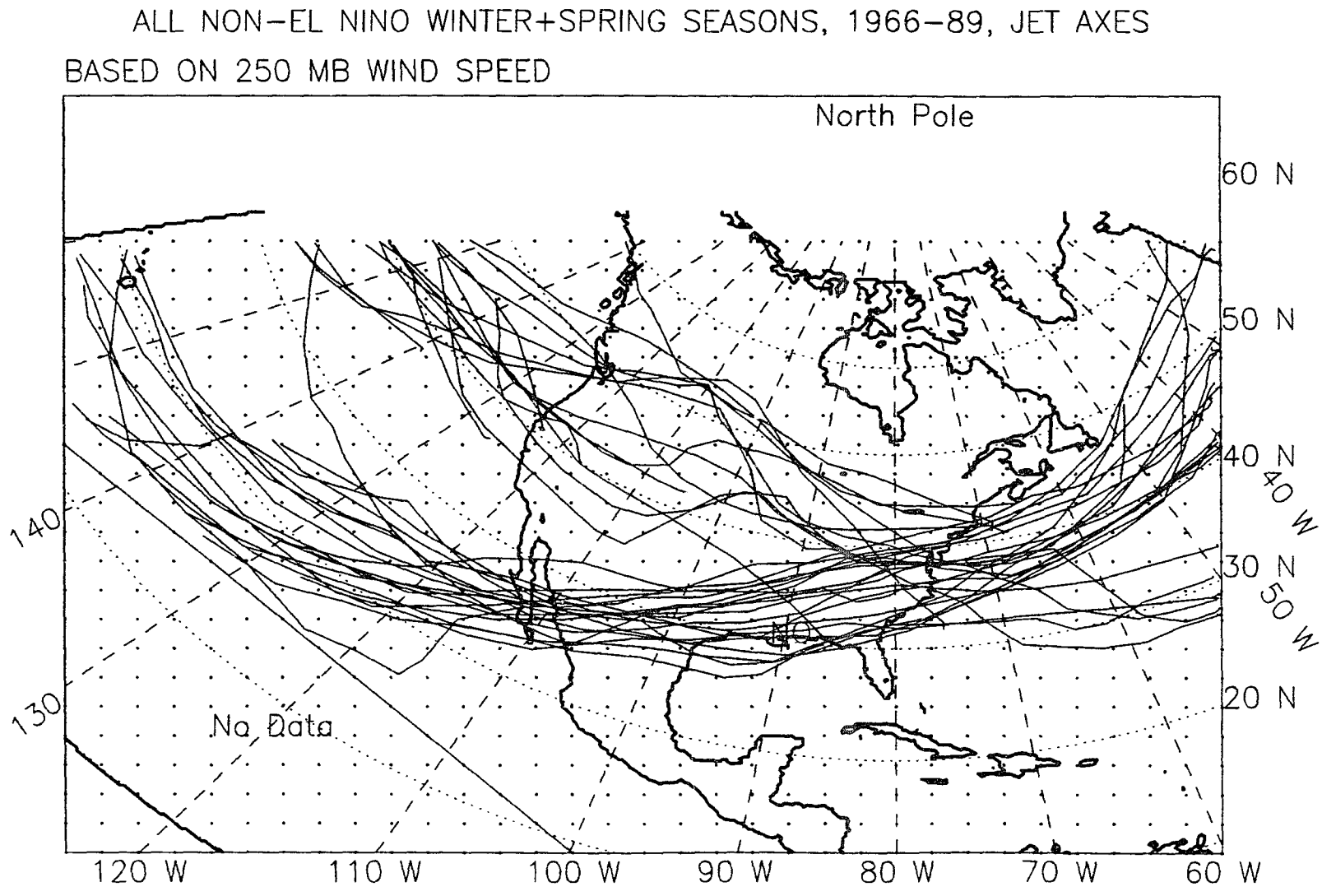

Figure 4.6: 250-mb jet axes, 19 non-El Niño winter-plus-springs from 1966-89.

between El Niño and non-El Niño years. The statistical significance of the El Niño-year displacements depends not only on their magnitude, but on the variability in the jet position over 24-year term. Where the position of the jet ranges widely, displacements must be quite large to be significant. As with the storm counts, there were less than 31 data points, and unequal numbers of years in each list, so the T2 statistic, 2.1.6, was evaluated, not z and not T. Significance was obtained from tables in Snedecor and Cochran (1980) and Verdooren (1963). Confidence criteria were adjusted, made more stringent, to account for additive probabilities of error, as in the division data. For example, to test for significance at the .02 level, one uses not $T_{.02}$, but $T_{.02/10}$, or $T_{.002}$, dividing by 10, the number of times the test is used, i.e., at 10 transects. La Niña and non-La Niña differences were sought in the same manner. Tables 4.1 and 4.2 contain rank sum test results for El Niño and La Niña tests, respectively. The statistically significant results of the rank sum tests, that is, those significant at the .20 confidence level or better, appear in Table 4.3 and again, graphically, in Figs. 4.7 and 4.8, for El Niño and La Niña tests, respectively.

Table 4.1: Location of the seasonal mean jet stream (250-mb speed maximum) in El Niño and non-El Niño years, 1966 to 1989: results of the rank sum test for differences between two groups on the north or south displacement of the seasonal mean jet stream in El Niño years versus all other years, 1966 to 1989. In each case, the displacement is taken from a base line that is the seasonal mean axis of the 250-mb jet in all 24 years. The displacement is measured at ten north-south transects, west longitudes 110° ,105°, 100°, 97°, 95°, 90°, 85°, 82°, 80°, and 75°. Displacement is listed in kilometers. North displacement is taken as positive; south displacement is taken as negative. The position of the jet was determined from contoured maps of the wind speed at 250 mb. The wind speeds are largely National Meteorological Center (NMC) data, and are all taken from a CD-ROM compiled by the University of Washington, Department of Atmospheric Sciences (Department of Atmospheric Sciences 1991). Significance is obtained from tabled values of T2 §, derived from the T (or W or U) statistic because the total number of observations is less than 31, there being five or six El Niño seasons and 18 or 19 other seasons in the data analyzed (Verdooren 1963). For sample size of 5 and 19, the null hypothesis can be rejected at the .02 confidence level for values of the T2 statistic less than or equal to 22, (double dagger) and it can be rejected at the .20 confidence level for values of the T2 statistic less than or equal to 30. Lower confidence levels, .10 and .20 are indicated by $^{\cdot 1}$ or $^{\cdot 2}$. Confidence criteria are adjusted for multiple use of the test on one field (Snedecor and Cochran 1980, p. 166).

			Displacement (km)		# of Events	
Longitude	Time	T2 §	El Niño	Other	El Niño	Other
110° West						
winteryear	1965-87	30	-392	109	5	18
winter+spring	1966-89	33	-161	43	5	19
winter	1966-89	48	-247	65	5	19
spring	1966-89	53	-187	63	6	18
summer	1965-88	50	-153	40	5	19
fall	1965-88	61	-149	40	5	19
105° West						
winteryear‡	1965-87	20	-424	118	5	18
winter+spring$^{\cdot 1}$	1966-89	24	-268	71	5	19
winter	1966-89	45	-217	57	5	19
spring	1966-89	43	-238	80	6	18
summer	1965-88	60	-36	10	5	19
fall	1965-88	61	-67	18	5	19
100° West						
winteryear‡	1965-87	18	-490	137	5	18
winter+spring$^{\cdot 1}$	1966-89	25	-319	84	5	19
winter	1966-89	43	-200	53	5	19
spring	1965-88	43	-275	92	6	18
summer	1965-88	56	6	-2	5	19
fall	1965-88	62	-41	11	5	19

Table 4.1: continued.

Longitude	Time	T2 §	Displacement (km) El Niño	Displacement (km) Other	# of Events El Niño	# of Events Other
97° West		Western Edge of the Gulf of Mexico				
winteryear‡	1965-87	21	-516	144	5	18
winter+spring[2]	1966-89	28	-308	81	5	19
winter	1966-89	40	-224	59	5	19
spring	1966-89	45	-306	102	6	18
summer	1965-88	47	51	-13	5	19
fall	1965-88	61	-67	18	5	19
95° West						
winteryear‡	1965-87	21	-522	145	5	18
winter+spring	1966-89	33	-290	76	5	19
winter	1966-89	41	-229	60	5	19
spring	1966-89	45	-323	108	6	18
summer	1965-88	41	98	-26	5	19
fall	1965-88	58	-109	29	5	19
90° West						
winteryear[1]	1965-87	24	-454	126	5	18
winter+spring	1966-89	32	-308	81	5	19
winter	1966-89	40	-249	66	5	19
spring	1966-89	49	-305	102	6	18
summer	1965-88	53	47	-12	5	19
fall	1965-88	53	-150	40	5	19
85° West						
winteryear[2]	1965-87	28	-386	107	5	18
winter+spring	1966-89	34	-347	92	5	19
winter	1966-89	39	-270	71	5	19
spring	1966-89	53	-254	85	6	18
summer	1965-88	61	31	-8	5	19
fall	1965-88	58	-142	37	5	19
82° West		Eastern Edge of the Gulf of Mexico				
winteryear[2]	1965-87	29	-333	93	5	18
winter+spring	1966-89	34	-356	94	5	19
winter	1966-89	36	-286	75	5	19
spring	1966-89	55	-242	81	6	18
summer	1965-88	58	4	-1	5	19
fall	1965-88	58	-143	38	5	19

Table 4.1: continued.

Longitude	Time	T2 §	Displacement (km) El Niño	Displacement (km) Other	# of Events El Niño	# of Events Other
80° West						
winteryear	1965-87	31	-296	82	5	18
winter+spring	1966-89	35	-354	93	5	19
winter	1966-89	36	-246	65	5	19
spring	1966-89	56	-254	85	6	18
summer	1965-88	62	-5	1	5	19
fall	1965-88	59	-125	33	5	19
75° West						
winteryear	1965-87	38	-212	59	5	18
winter+spring	1966-89	40	-340	90	5	19
winter	1966-89	38	-210	55	5	19
spring	1966-89	63	-196	65	6	18
summer	1965-88	56	-46	12	5	19
fall	1965-88	60	-69	18	5	19

Notes:

§: T2 Statistic = Number of X observations * (Number of X observations + Number of Y observations + 1) - Sum of the ranks of the X observations. The X observations are the smaller set, the El Niño or La Niña years.

‡ : indicates null hypothesis can be rejected at the .02 level of significance.

$^{.1}$: indicates null hypothesis can be rejected at the .10 level of significance.

$^{.2}$: indicates null hypothesis can be rejected at the .20 level of significance.

Table 4.2: Location of the seasonal mean jet stream (250-mb speed maximum) in La Niña and non-La Niña years, 1966 to 1989: results of the rank sum test for differences between two groups on the north or south displacement of the seasonal mean jet stream in La Niña years versus all other years. In each case, the displacement is taken from a base line that is the seasonal mean axis of the 250-mb jet in years. The displacement is measured at ten north-south transects, west longitudes 110° ,105°, 100°, 97°, 95°, 90°, 85°, 82°, 80°, and 75°. Displacement is listed in kilometers. North displacement is taken as positive; south displacement is taken as negative. The position of the jet was determined from contoured maps of the wind speed at 250 mb. The wind speeds are largely National Meteorological Center (NMC) data and are all taken from a CD-ROM compiled by the University of Washington, Department of Atmospheric Sciences (Department of Atmospheric Sciences 1991). Significance is obtained from tabled values of T2 §, derived from the T (or W or U) statistic because the number of observations in each set is less than 31, there being four to six La Niña seasons and 18 or 19 other seasons in the period analyzed (Verdooren 1963). For sample size of 5 and 19, the null hypothesis can be rejected at the .02 confidence level for values of the T2 statistic less than or equal to 22, and it can be rejected at the .20 confidence level for values of the T2 statistic less than or equal to 30. Lower confidence levels, .10 and .20 are indicated by $^{\cdot 1}$ or $^{\cdot 2}$. Confidence criteria are adjusted for multiple use of the test on one field (Snedecor and Cochran 1980, p. 166).

			Displacement (km)		# of Events	
Longitude	Time	T2 §	La Niña	Other	La Niña	Other
110° West						
winteryear	1965-87	32	326	-68	4	19
winter+spring	1966-89	48	118	-31	5	19
winter	1966-89	49	355	-93	5	19
spring	1966-89	53	275	-91	6	18
summer	1965-88	42	209	-55	5	19
fall	1965-88	62	219	-57	5	19
105° West						
winteryear	1965-87	28	338	-71	4	19
winter+spring	1966-89	41	182	-48	5	19
winter	1966-89	43	387	-102	5	19
spring	1966-89	47	265	-88	6	18
summer	1965-88	39	156	-41	5	19
fall	1965-88	60	124	-32	5	19
100° West						
winteryear	1965-87	33	305	-64	4	19
winter+spring$^{\cdot 1}$	1966-89	25	283	-74	5	19
winter$^{\cdot 2}$	1966-89	30	249	-65	5	19
spring$^{\cdot 2}$	1965-88	38	329	-109	6	18
summer	1965-88	37	159	-42	5	19
fall	1965-88	62	40	-10	5	19

Table 4.2: continued.

Longitude	Time	T2 §	Displacement (km) La Niña	Displacement (km) Other	# of Events La Niña	# of Events Other
97° West		Western Edge of the Gulf of Mexico				
winteryear	1965-87	34	258	-54	4	19
winter+spring^{-1}	1966-89	26	335	-88	5	19
winter	1966-89	31	277	-73	5	19
spring^{-1}	1966-89	37	349	-116	6	18
summer	1965-88	38	162	-42	5	19
fall	1965-88	57	31	-8	5	19
95° West						
winteryear	1965-87	32	259	-54	4	19
winter+spring^{-1}	1966-89	26	366	-96	5	19
winter^{-2}	1966-89	29	296	-78	5	19
spring	1966-89	41	350	-116	6	18
summer	1965-88	43	145	-38	5	19
fall	1965-88	62	-18	5	5	19
90° West						
winteryear	1965-87	30	234	-49	4	19
winter+spring^{-1}	1966-89	26	367	-96	5	19
winter^{-1}	1966-89	25	345	-92	5	19
spring	1966-89	47	344	-115	6	18
summer	1965-88	45	136	-36	5	19
fall	1965-88	60	-4	1	5	19
85° West						
winteryear	1965-87	30	228	-48	4	19
winter+spring^{-1}	1966-89	26	386	-101	5	19
winter^{-1}	1966-89	26	350	-92	5	19
spring	1966-89	47	342	-114	6	18
summer	1965-88	43	125	-33	5	19
fall	1965-88	60	-4	1	5	19
82° West		Eastern Edge of the Gulf of Mexico				
winteryear	1965-87	28	234	-49	4	19
winter+spring^{-1}	1966-89	27	380	-100	5	19
winter^{-1}	1966-89	24	380	-100	5	19
spring	1966-89	50	324	-108	6	18
summer	1965-88	45	139	-37	5	19
fall	1965-88	61	8	-2	5	19

Table 4.2: continued.

Longitude	Time	T2 §	Displacement (km) La Niña	Displacement (km) Other	# of Events La Niña	# of Events Other
80° West						
winteryear	1965-87	29	205	-43	4	19
winter+spring$^{\cdot 1}$	1966-89	25	381	-100	5	19
winter ‡	1966-89	22	374	-98	5	19
spring	1966-89	52	311	-103	6	18
summer	1965-88	40	141	-37	5	19
fall	1965-88	62	16	-4	5	19
75° West						
winteryear	1965-87	35	133	-28	4	19
winter+spring$^{\cdot 1}$	1966-89	26	384	-101	5	19
winter$^{\cdot 1}$	1966-89	25	360	-95	5	19
spring	1966-89	56	244	-81	6	18
summer	1965-88	42	110	-29	5	19
fall	1965-88	62	5	-1	5	19

Notes:

§: T2 Statistic = Number of X observations * (Number of X observations + Number of Y observations + 1) - Sum of the ranks of the X observations. The X observations are the smaller set, the El Niño or La Niña years.

‡ : indicates null hypothesis can be rejected at the .02 level of significance.

$^{\cdot 1}$: indicates null hypothesis can be rejected at the .10 level of significance.

$^{\cdot 2}$: indicates null hypothesis can be rejected at the .20 level of significance.

Table 4.3: Displacement of the seasonal mean jet stream at gulf-region transects, 1966-89: summary of all displacements significant at the .20 or better confidence level. Confidence criteria adjusted for multiple use of the test (Snedecor and Cochran 1980, p. 166). A blank indicates the parameter was not significant at the .20 level or better.

	El Niño		La Niña		
Season	Displacement km	Conf. Level	Displacement km	Conf. Level	Time
105° West					
Winter year	-424	.02			1966-89
Winter+spring	-268	.10			1966-89
100° West					
Winter year	-490	.02			1966-89
Winter+spring	-319	.10	283	.10	1966-89
Winter			249	.20	1966-89
Spring			329	.20	1966-89
97° West,	Western edge of Gulf of Mexico				
Winter year	-516	.02			1966-89
Winter+spring	-308	.20	335	.10	1966-89
Spring			349	.10	1966-89
95° West					
Winter year	-522	.02			1966-89
Winter+spring			366	.10	1966-89
Winter			296	.20	1966-89
90° West					
Winter year	-454	.10			1966-89
Winter+spring	-308	.05	367	.10	1966-89
Winter			351	.10	1966-89
85° West					
Winter year	-386	.20			1966-89
Winter+spring			386	.10	1966-89
Winter			350	.10	1966-89
82° West,	Eastern edge of Gulf of Mexico				
Winter year	-333	.20			1966-89
Winter+spring		380	.10	1966-89	
Winter			380	.10	1966-89
80° West					
Winter+spring			381	.10	1966-89
Winter			374	.02	1966-89
75° West					
Winter+spring			384	.10	1966-89
Winter			360	.10	1966-89

The 250-mb level, mean speed maximum over the southern United States, the 'south jet', is shifted south in El Niño winters between 110° and 75°W, by amounts of 200 to 285 km (125 to 180 mi) from the mean position of the south jet in all 24 winters, Fig. 4.9 and Table 4.1. These south displacements are not significant, even at the .20 confidence level. In El Niño winter years, however, the displacement is significant at the .20 level or better between 105° and 82°W, being .02 significant over the western half of this span, from 105° to 95°W. In winter-plus-spring, south displacement is significant at the .20 level or .10 level between 105° and 97°W. Averaging on a winter-year basis, however, mixes the polar-front jet and the subtropical jet more than just averaging on a winter-season basis. The fact that .02-significant displacements occur only on a winter-year basis, implies that the polar-front jet is more affected by El Niño events than the subtropical jet. This is consistent with Krishnamurti's (1961) report that the position of the subtropical jet varies little. The south jet is displaced even further south in El Niño springs, compared to non-El Niño-springs, by as much as 325 km (205 mi) at 95°W, but the displacement is not significant, even at the .20 level. Largest displacements are clustered near the location of the seasonal core, or speed maximum, of the south jet. In El Niño winters, when the jet core is centered on 70°W, Fig. 3.13, large south displacements are observed on the east side of the gulf area. In El Niño springs, when the core is far to the west, centered on 98°W, up against the east flank of the southern Rocky Mountains, large displacements are observed on the west end of the area, Fig. 4.10.

In La Niña winters, the average south jet is located north of the 24-winter mean, between 100° and 75°W, by 250 to 385 km (155 to 240 mi); displacement is significant at the .20 level or better, Fig. 4.8 and Table 4.2. At 80°W, north displacement is .02-significant during La Niña winters. La Niña-spring displacements are significant at the .10 or .20 levels only over the western gulf, between 100° and 97°W,

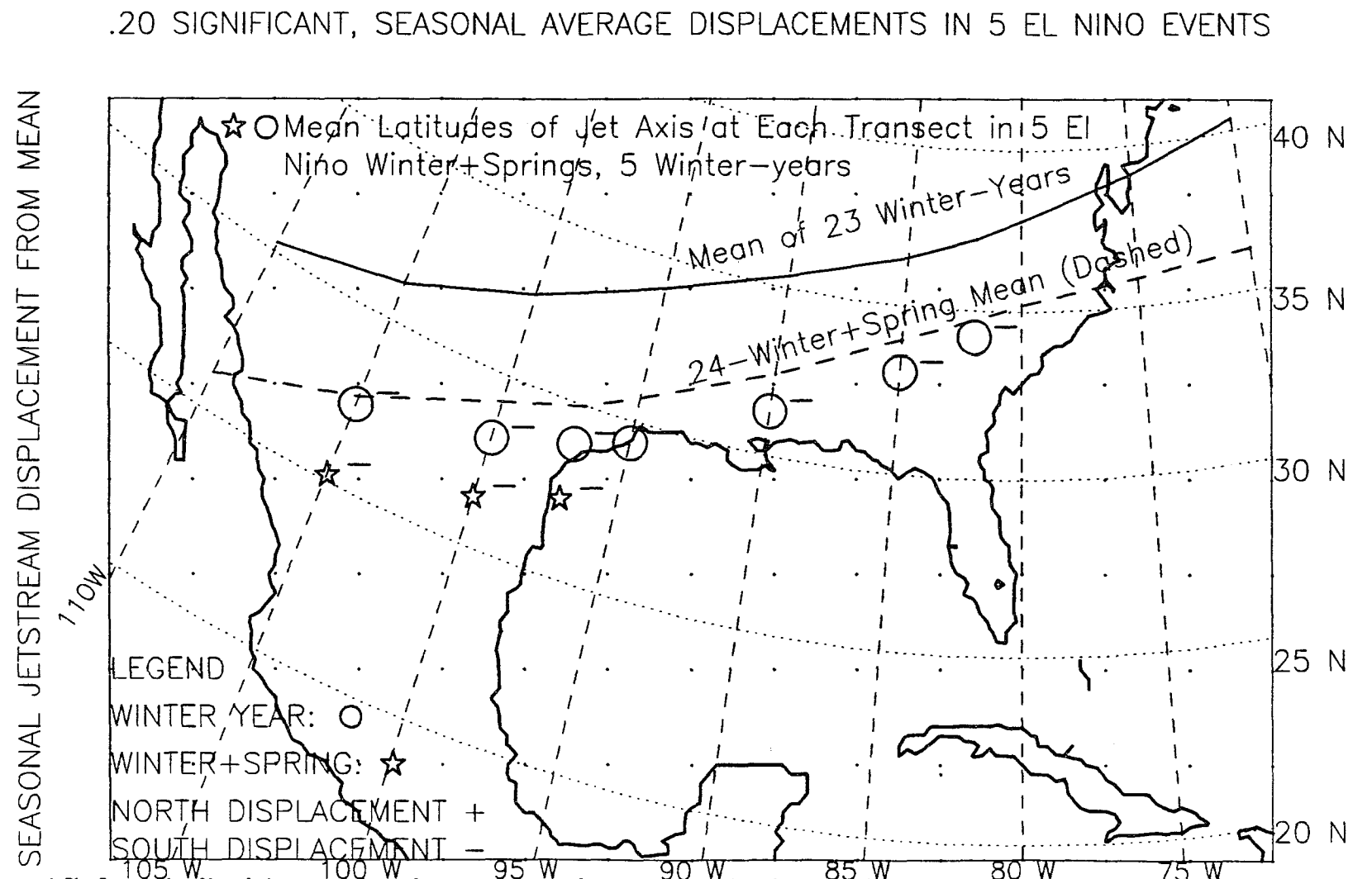

Figure 4.7: Longitudinal transects where seasonal average jet-stream displacement from 24-season mean differs significantly, .20 level or better, in El Niño years. Confidence criteria adjusted for multiple use of test. Western four winter-year points (circles) significant at .02 level.

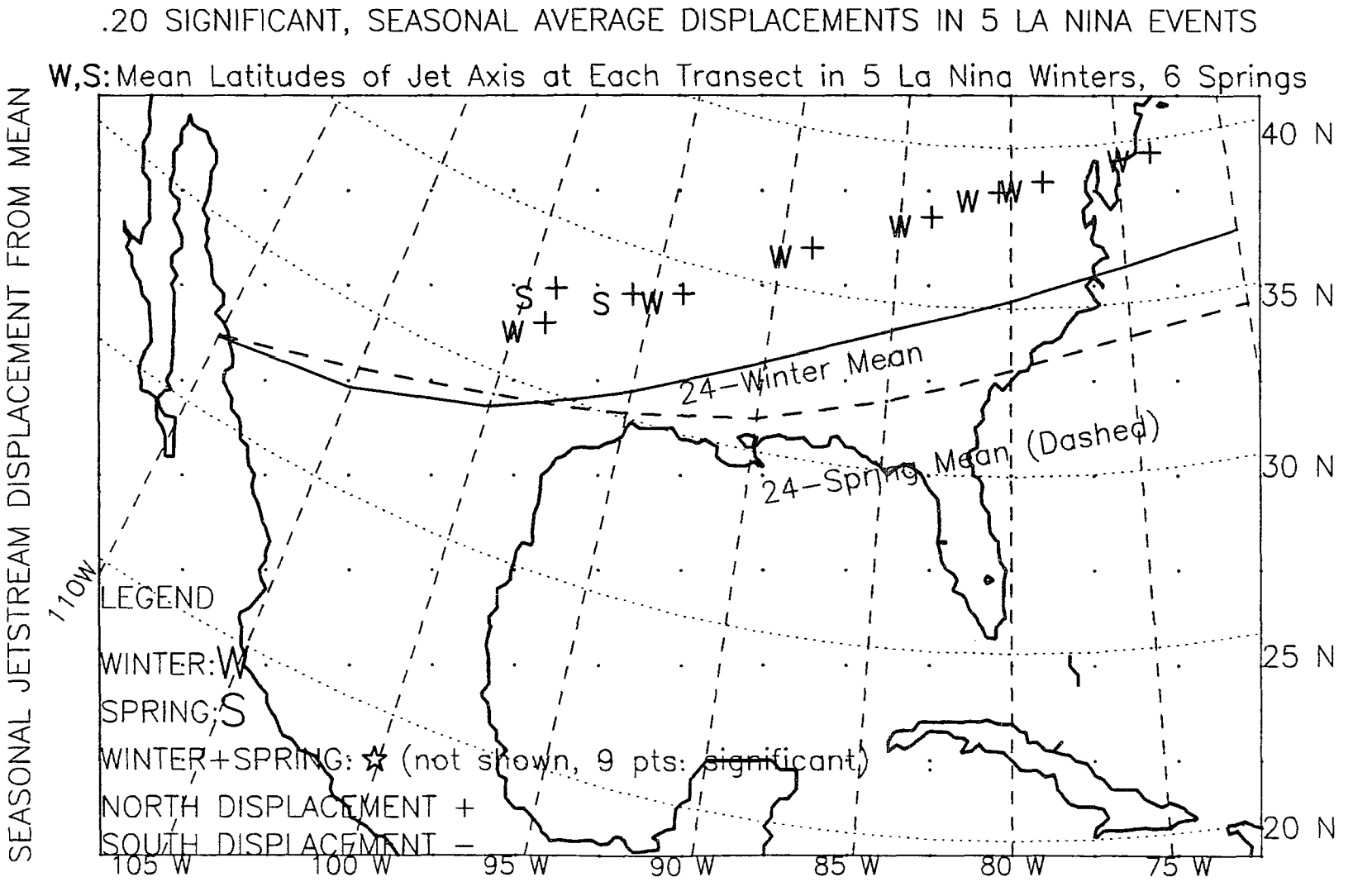

Figure 4.8: Longitudinal transects where seasonal average jet-stream displacement from 24-season mean differs significantly, .20 level or better, in La Niña years. Confidence criteria adjusted for multiple use of test.

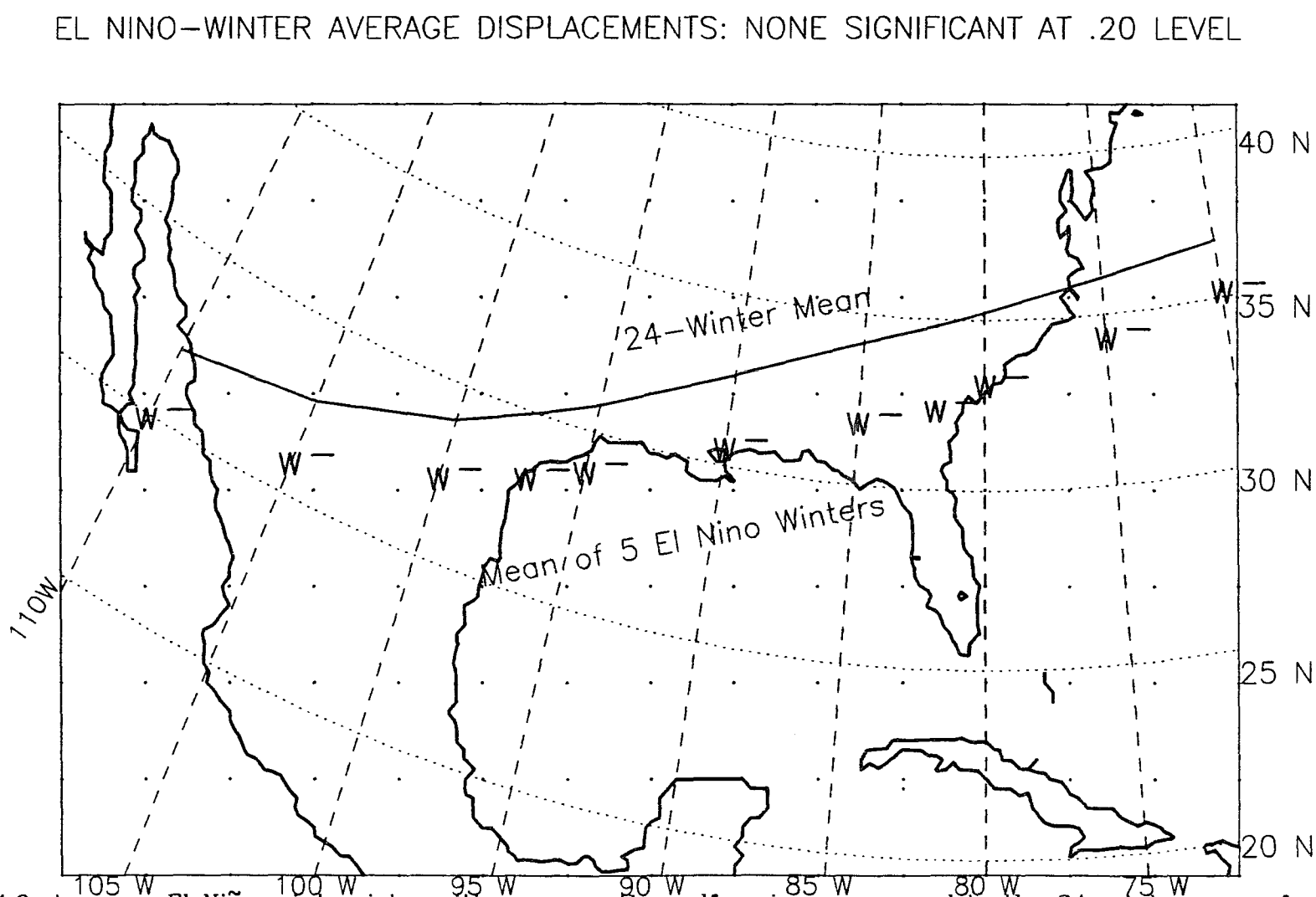

Figure 4.9: Average, El Niño–winter jet position across the gulf region, compared to the 24–winter mean for 1966–89. "W" indicates the mean of 5 El Niño winters at 10 longitudinal transects. South displacements are not significant at .20 level when confidence criteria are adjusted for multiple use of rank sum test.

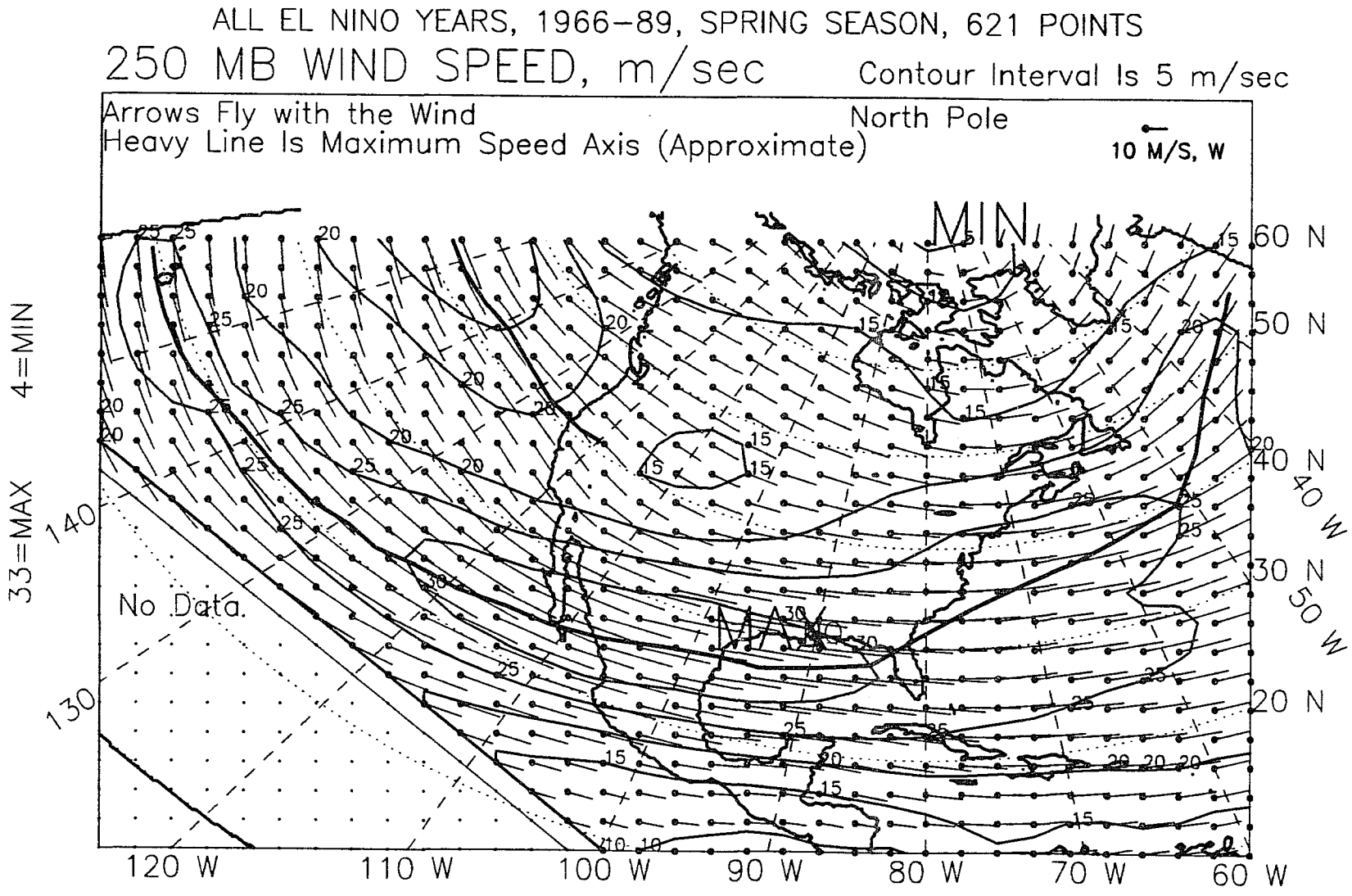

Figure 4.10: 250–mb wind vectors, spring, El Niño years, 1966–89.

Fig. 4.8. Winter-plus-spring results are left off Fig. 4.8, for clarity, however, north displacements are significant at the .10 or .20 level between 100° and 75°W. Many seasonal average displacements in La Niña years are actually larger than in El Niño years.

It should be emphasized that the increase in the number of frontal-wave cyclones originating in the gulf area in El Niño years was significant at either the .01 or .05 level in winter years and in the winter season, and at the .20 level in winter-plus-spring. On a winter-year basis, the south jet is significantly farther south, at the .02, .10, or .20 confidence level, which matches well with the winter-year storm increase. The south shift over the west gulf, during the combined season, winter-plus-spring, significant at the .10 or .20 level, matches the storm increase then, which is significant at the .20 level. Table 4.4 tabulates these correspondences for El Niño and La Niña years. In the winter season the south displacement is not significant even at the .10 or .20 confidence level. This does not match the increased winter-storm frequency in El Niño years, which is significant at the .01 level. The El Niño-winter jet displacement is only significant in the .30 confidence-level range, which generally is not 'good enough'. The forcing provided by the jet, however, depends on intensity, and so, only indirectly on position. The El Niño-winter, average, south jet is intensified by 5 to 10 ms^{-1} over the gulf region, Fig. 3.15, although no tests of significance were performed on intensification.

Accepting as important the lack of even .20-significant results for the winter jet displacement, requires an explanation for the lack of an increase in storms in El Niño springs, when the south jet is similarly farther south, although not .20-significant either. What is the difference between El Niño winters and El Niño springs, such that winter, but not spring, storms are more common in El Niño years, given that both seasons have an equally significantly south-displaced jet? In fact, there are

Table 4.4: Correspondence between seasonal jet displacement between 1966 and 1989, and frontal-wave cyclone increase or decrease in winter, spring, winter year, and winter-plus-spring between 1961 and 1990.

Season	Storm Increase Level of Significance	Jet Southward Level of Significance	Fit
El Niño vs Non-El Niño			
Winter	.01	Not Signif.	Bad
Spring	Decreased, Not Signif.	Not Signif.	Ok
Winter+Spring	.20	.10 or .20, West only	Ok
Winter year	.05	.02 West; .10 or .20 East	Good

La Niña vs Non-La Niña			
Season	Storm Decrease Level of Significance	Jet Northward Level of Significance	Fit
Winter	.01	.10 or .20	Good
Spring	Increased, Not Signif.	.10 or .20, West only	Ok
Winter+Spring	.05	.10 or .20	Good
Winter year	.05	Not Signif.	Bad

fewer storms in El Niño springs than in non-El Niño springs, Table 2.1, but the decrease is not significant at any reasonable level.

First, over the gulf area, the south jet is not as much intensified in El Niño springs relative to non-El Niño springs, Fig. 4.11, as it is in El Niño versus non-El Niño winters, Fig. 3.15. The El Niño-spring intensification over the gulf is less than 5 ms^{-1} while the El Niño-winter intensification is 5 to 10 ms^{-1}. Even in absolute terms, the mean, 250-mb south jet is not as strong in El Niño springs as in El Niño winters, 33 ms^{-1} compared to 45 ms^{-1}, respectively, Figs. 4.10 and 3.13. The zone of maximum intensification in El Niño springs is farther south than in El Niño winters, being over Central America and the adjacent Pacific instead of over the southern United States and the Gulf of Mexico; compare Figs. 4.11 and 3.15. In El Niño springs there is not the pattern of intensification of the south jet and weakening of the north jet that is present in winter, so there is less added cyclonic residue to the north of the south jet in El Niño springs.

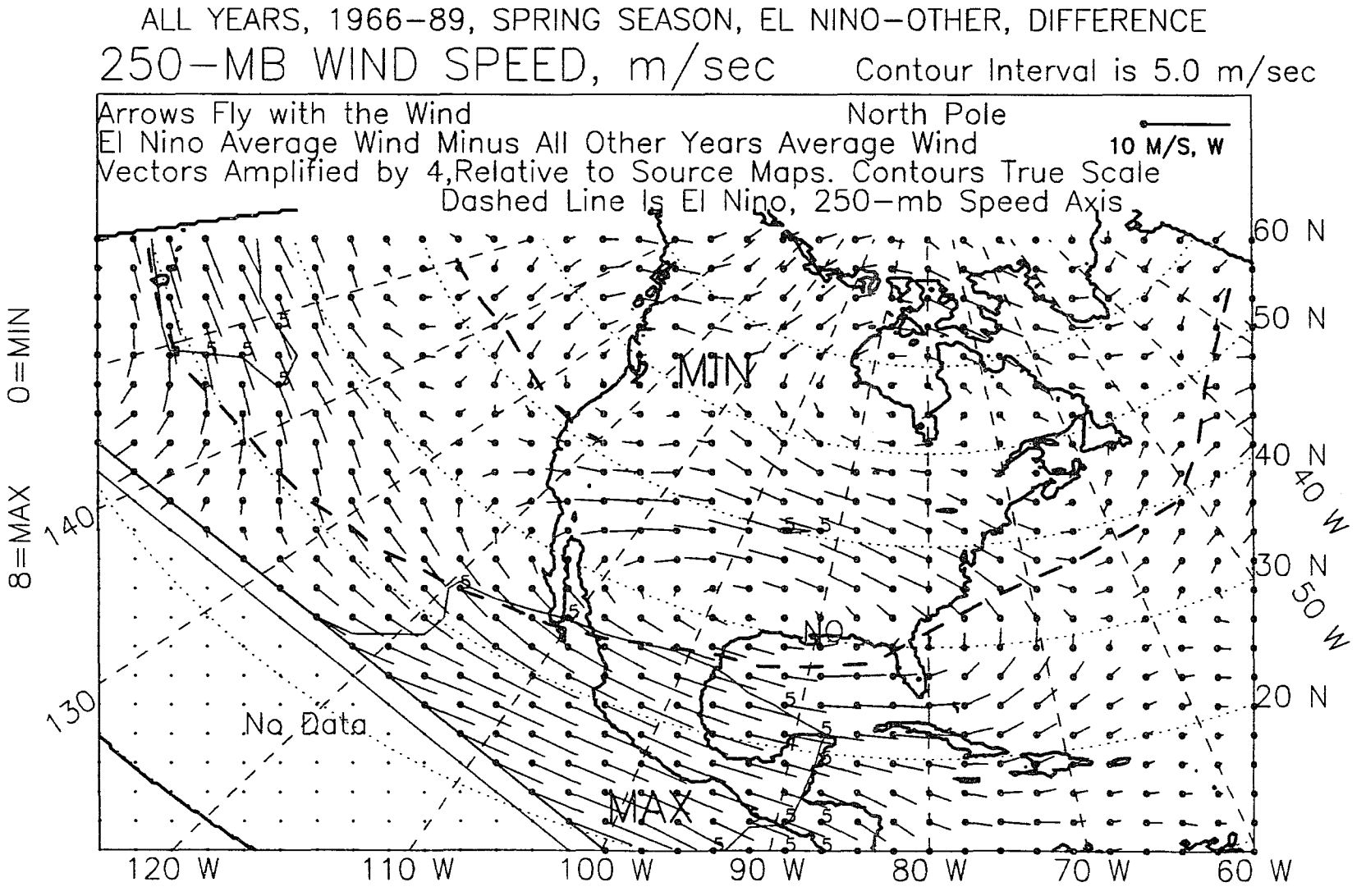

Figure 4.11: 250–mb wind vectors, spring, 1966–89, difference.

Further explanation for the lack of an increase in cyclogenesis during El Niño-springs compared to non-El Niño springs can be found from an inspection of a composite map of the El Niño-spring, divergence field at 250 mb, Fig. 4.12. There is a strong zone of convergence situated over the western Gulf of Mexico during El Niño springs that is three to four times stronger than the weak convergence found there during El Niño winters, $-3.77\times10^{-6}s^{-1}$ in spring compared to $-1.0\times10^{-6}s^{-1}$ in winter, Fig. 3.16. This upper-level convergent zone in spring evidently suppresses storm formation in the western gulf, where the greatest concentration of cool-season storms form in any year, Figs. 2.25 and 2.26 and appendix P. Comparing the El Niño-spring, 250-mb divergence-difference map, Fig. 4.13, with the same for winter, Fig. 3.18, shows that while the upper-level divergence difference is more positive over all but the Bay of Campeche in El Niño winters, in El Niño springs the critical area over the northwest gulf is not more divergent, being rather strongly more convergent, by a difference of $-1.0\times10^{-6}s^{-1}$ in El Niño springs.

Another possible factor in explaining the lack of an increase in spring storms in El Niño years, even though the jet is farther south, may involve the longitude spanned by the core of the south jet in El Niño winters as opposed to El Niño springs. Comparison of the 250-mb, El Niño-winter, wind-speed map, Fig. 3.13, with the same for El Niño springs, Fig. 4.10, shows the core of the jet in El Niño springs is shifted well to the west, at 98°W, against the east flank of the southern Rocky Mountains, relative to its mean position in El Niño winters at 70°W. It appears the gulf is likely to be under an exit region (part 3.6.3) of any jet streak that may develop during El Niño springs, while in El Niño winters, the gulf is more likely to be under an entrance region. Based on this alone, one would expect more, not fewer, storms in El Niño springs than in El Niño winters, due to the stronger divergence in the jet exit region than entrance region. Speculating,

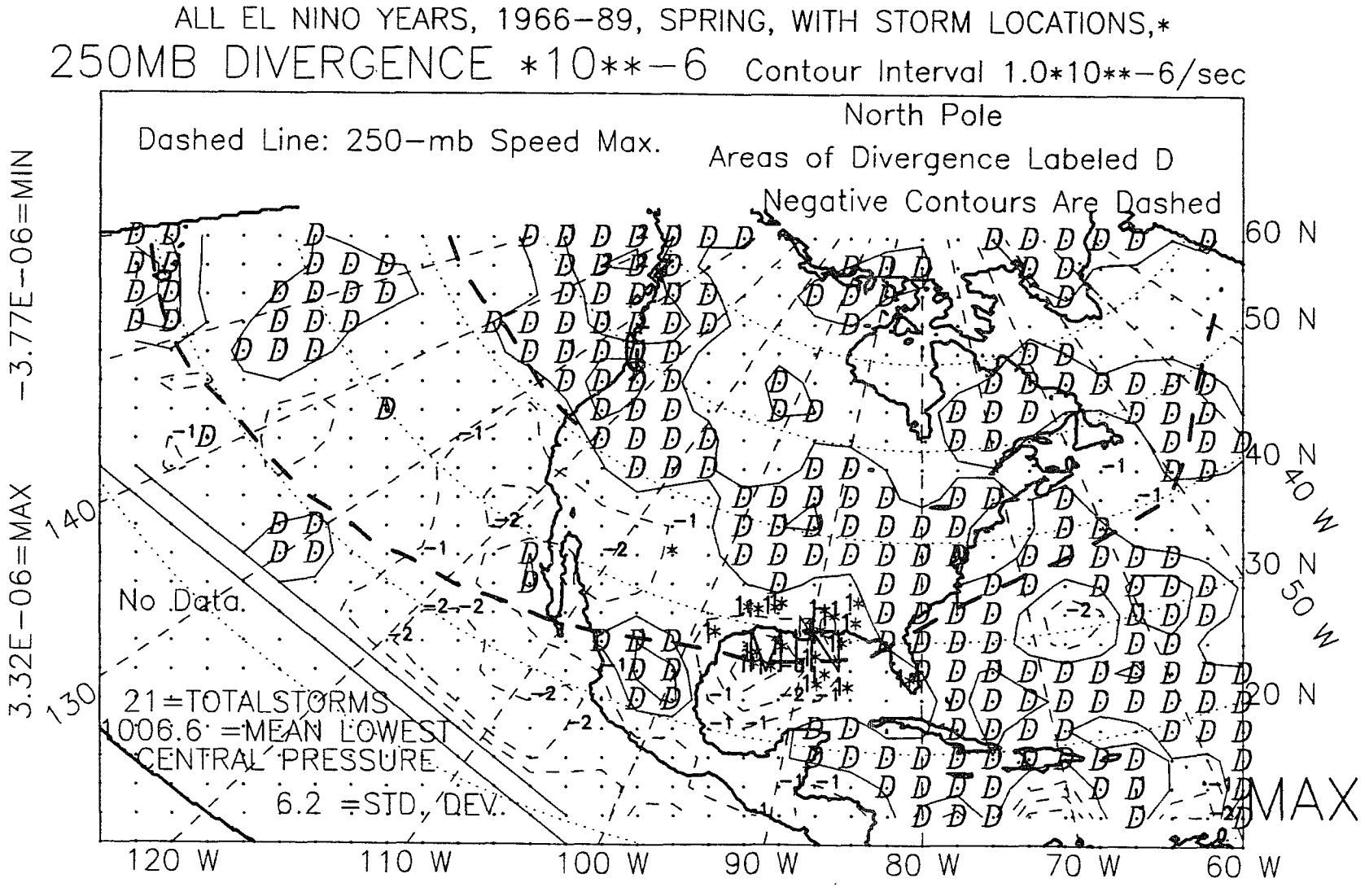

Figure 4.12: 250–mb divergence, spring, El Niño years, 1966–89.

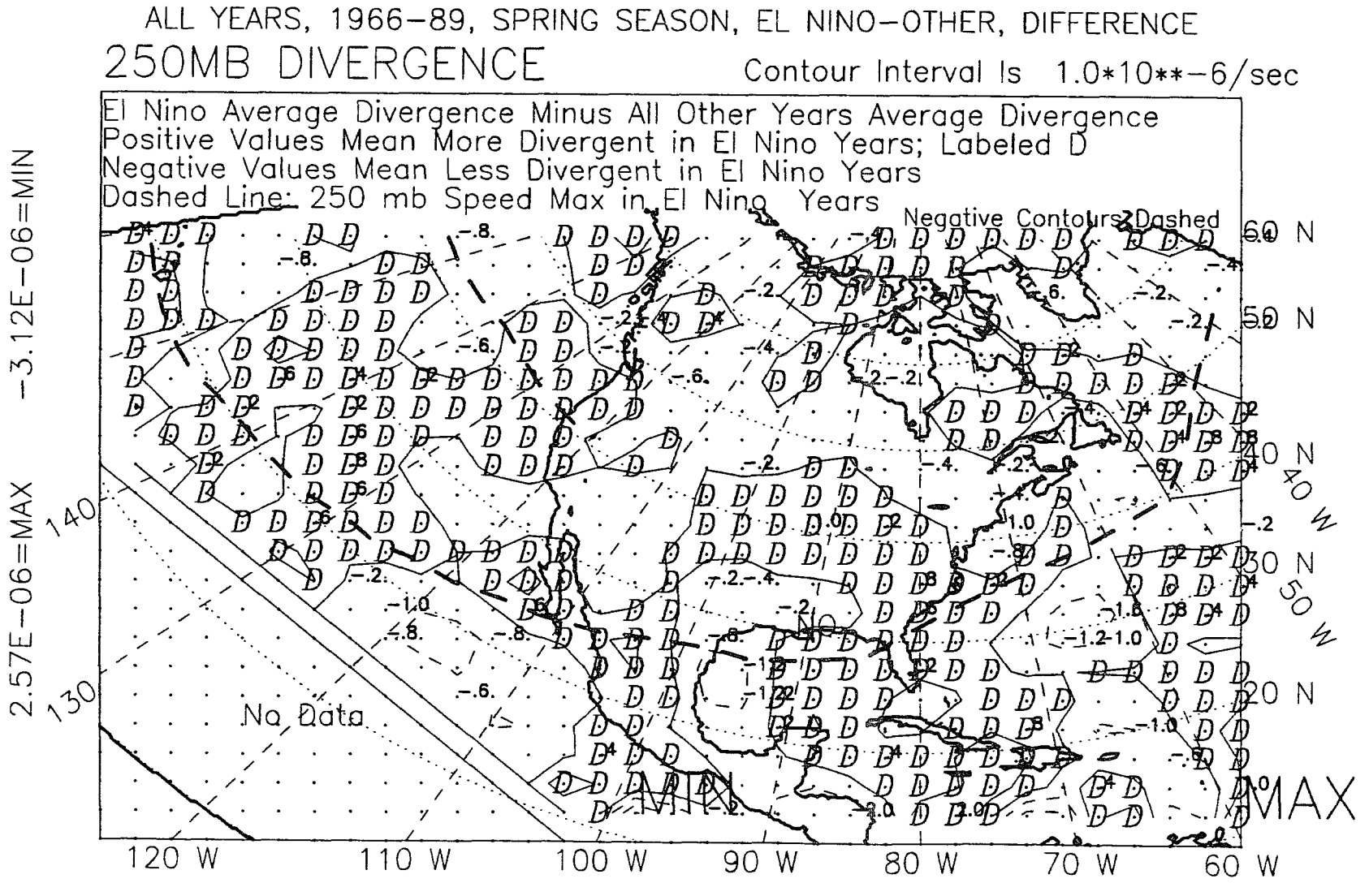

Figure 4.13: 250–mb divergence, spring, 1966–89, difference.

perhaps the longitudinal position of the jet core in El Niño winters is such that the pairing (the vertical motions from rear to fore) between the entrance region over the Gulf of Mexico and exit region over the U.S. southeast coast actively promotes the development of a family of wave cyclones behind the exit region. But in El Niño springs, the territory spanned by the jet core may be such that the pairing is somehow disconnected or weakened, perhaps by the strong, 250-mb level convergence zone over the west gulf in El Niño springs, or by passage of the jet over the southern Rocky Mountains, with the net effect of starving the exit-region, divergence zone. This is purely speculative.

For the La Niña years, the correspondence between a north-displaced jet and gulf-area storm suppression is good in winter and in the combination season, winter-plus-spring. That is, in winter and in winter-plus-spring of La Niña years, there are statistically fewer storms than in non-La Niña years, significant at the .01 or .05 confidence level. In these seasons, the south jet is displaced northward, statistically significant at the .10 or .20 confidence level. As in El Niño years versus non-El Niño years, there is an unexpected situation in spring. In La Niña springs, while the jet is farther north, there are not fewer storms than in non-La Niña springs, Table 4.4. In fact, counter to the trend, there are actually a few more storms in La Niña springs than in non-La Niña springs, Table 2.2, although the increase is not significant by any reasonable criterion. Compare Fig. 4.14, a composite map of La Niña-spring, 250-mb divergence to Fig. 4.15, the 250-mb divergence field for non-La Niña springs. The La Niña-spring map shows some convergence at the 250-mb level over the west gulf, $-2.0\times10^{-6}s^{-1}$, Fig. 4.14, but in non-La Niña springs, the area is much more strongly convergent, $-3.25\times10^{-6}s^{-1}$, Fig. 4.15. This explains why there are not fewer storms in La Niña springs than in non-La Niña springs. The upper-level convergence over the 'storm machine' of the western gulf is actually

somewhat diminished in La Niña springs as compared to non-La Niña springs, allowing more cyclogenesis in La Niña springs than in non-La Niña springs. (Note that the strong convergence zone in the western gulf just cited in non-La Niña springs, $-3.25\times10^{-6}s^{-1}$, is essentially the same as the one mentioned previously in El Niño springs, $-3.75\times10^{-6}s^{-1}$, in as much as the El Niño springs are a subset of the non-La Niña springs.)

4.2 Height and Temperature at Constant-Pressure Levels, 1963-89

Up to this point, it seems fairly certain that in El Niño winters between 1961 and 1990 there are more storms in the gulf area and that a south-displaced and strengthened south jet is at least part of the cause, through provision of upper-level divergence associated with an upper-level trough behind the jet. It was stated in part 3.6.3 that the upper-level divergence can reinforce nascent cyclones at the surface or initiate them in the presence of a surface front or baroclinic zone. The upper-level divergence does this by causing compensating surface convergence and pressure drop as air is drawn upward to replace air diverging outward at the jet level. That this is actually occurring will be supported if it can be shown that the troughing at the surface is continuous in the vertical through intermediate levels and up to jet level. Finally, it will need to be shown that the foregoing is more pronounced or common in El Niño winters than in non-El Niño winters, if a causal role for the jet is to be supported in increased, El Niño-winter, gulf-region cyclogenesis. To this end, composite maps of height and temperature for El Niño and non-El Niño winters are presented for the 850-, 700-, 500-, and 200-mb levels. There are no temperature maps for the 700- and 200-mb levels.

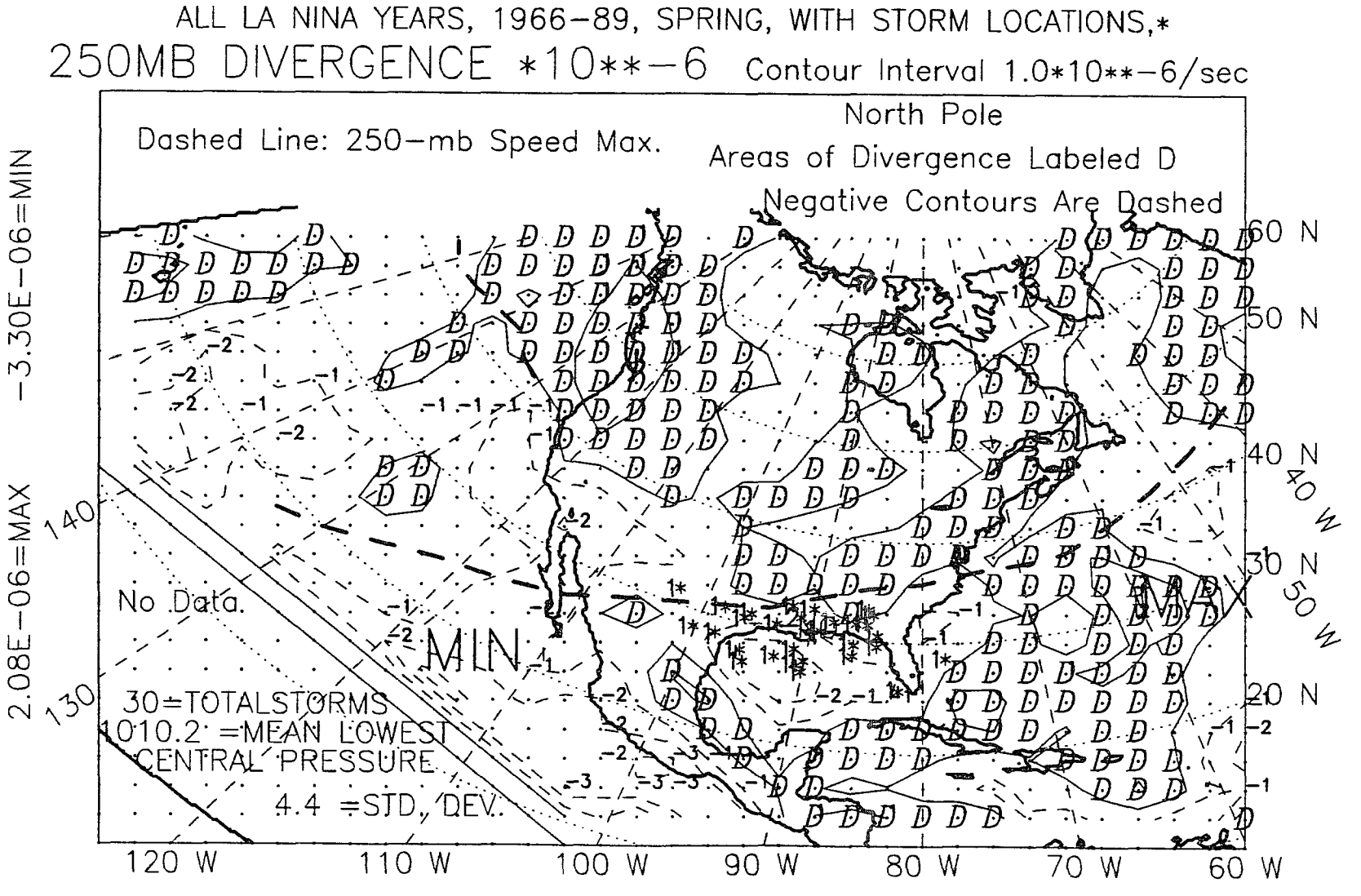

Figure 4.14: 250–mb divergence, spring, La Niña years, 1966–89.

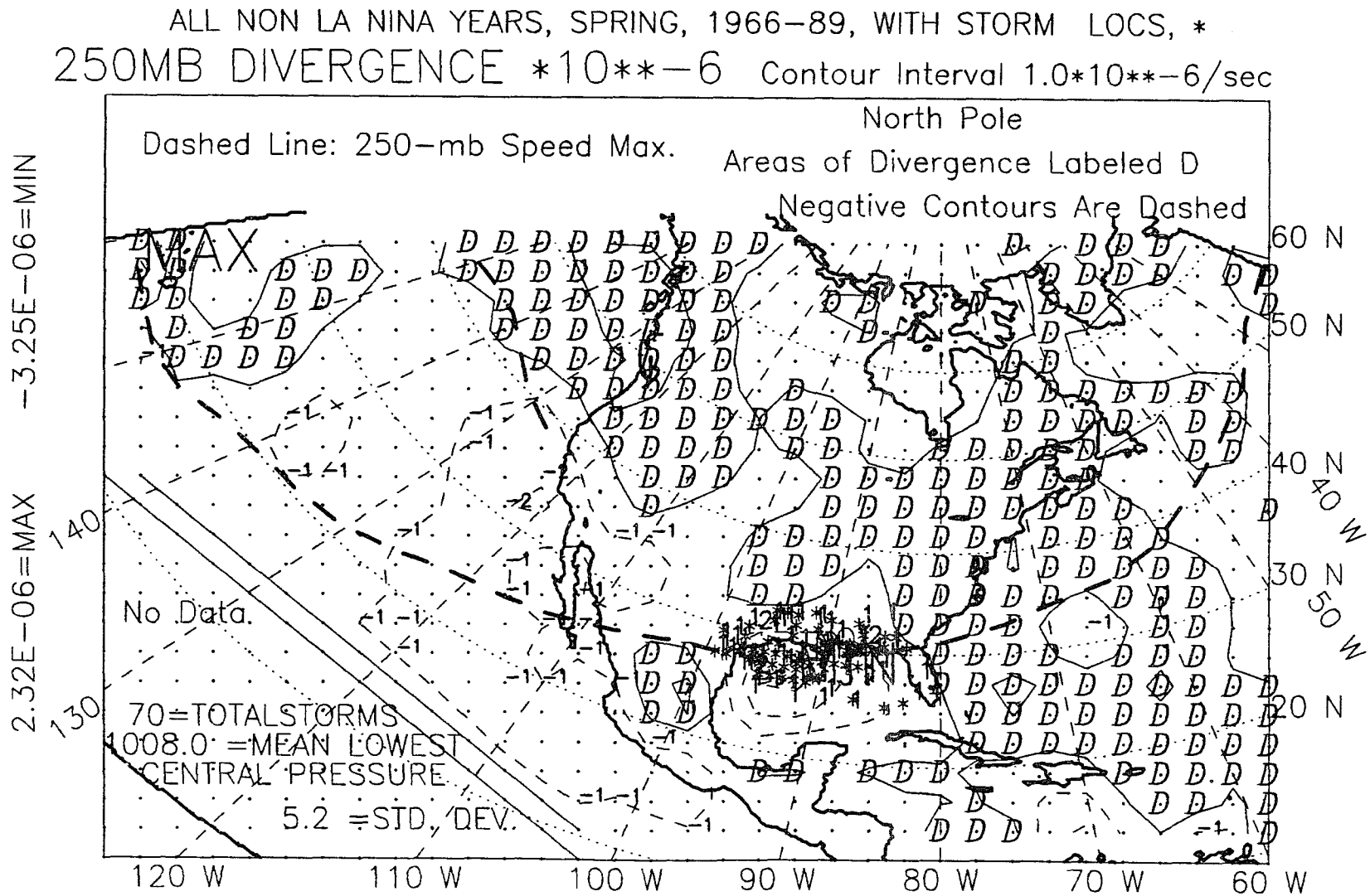

Figure 4.15: 250–mb divergence, spring, non–La Niña years, 1966–89.

Table 4.5: Average, gulf-region, winter differences in mean sea-level and in the height and temperature of four constant-pressure levels between El Niño and non-El Niño winters, 1963-89.

Level mb	Range of Differences over Gulf, in El Niño Winters mb, m or ^oC	Range of Real Values over Gulf in El Niño Winters mb, m or ^oC	Range of Differences over Gulf as Percent of Actual Values over Gulf
MSL Press.†	-1.0 to -0.5 mb	1014.0 to 1020.0mb Δ=6.0mb	-17 to -8%
850 Height	-10m (constant)	1500 to 1550m Δ=50m	-20%
850 Temp	-1.0 to 0.0°	6.0 to 16.0° Δ=10.0°	-10 to 0%
700 Height	-10m (constant)	3075 to 3150m Δ=75m	-13%
500 Height	-20 to 0m	5700 to 5850m Δ=150m	-13 to 0%
500 Temp	-0.8 to +1.0°	-16.0 to -7.0° Δ=9.0°	-9 to +11%
200 Height	-15 to +50m	12 000 to 12 350m Δ=350m	-4 to +14%

†: MSL pressure and 500-mb height data are from 1947 to 1989.

Some of the most relevant information presented in the following 18 maps is extracted in Tables 4.5 and 4.6. Table 4.5 shows the height and temperature differences over the gulf region in El Niño winters as a percentage of the range of actual values of height and temperature over the gulf area in El Niño winters. For height fields, this expresses the difference as a percent of the local relief of the surface in El Niño winters. The same is done for the temperature fields. Table 4.6 shows the same information for the Aleutian low, as a yardstick, in as much as it is the region of maximum change on the map. Changes in the Aleutian low are also relevant, because as the following maps demonstrate, the negative height and temperature differences over the gulf area in El Niño winters are the periphery of larger negative differences over the Aleutian low.

Table 4.6: Average, Aleutian low, winter differences in mean sea-level and in the height and temperature of four constant-pressure levels between El Niño and non-El Niño winters, 1963-89.

Level	Range of Differences over Aleutian Low, El Niño Winters mb, m or ^oC	Range of Real Values over Aleutian Low, El Niño Winters mb, m or ^oC	Range of Differences over Aleutian Low as % of Actual Values over Aleutian Low
MSL Press.†	-5.8 to -1.0 mb	998.8 to 1018.0mb Δ=19.2mb	-30 to -5%
850 Height	-47 to -10m	1300 to 1500m Δ=200m	-24 to -5%
850 Temp	-1.8 to -0.4^o	-6.0 to +2.0^o Δ=8.0^o	-23 to -5%
700 Height	-56 to -20m	2800 to 3050m Δ=250m	-22 to -8%
500 Height	-71 to -20m	5300 to 5650m Δ=350m	-20 to -6%
500 Temp	-1.7 to -0.8^o	-30.0 to -20.0^o Δ=10.0^o	-17 to -8%
200 Height	-90 to -30m	11 400 to 11 800m Δ=400m	-23 to -8%

†: MSL pressure and 500-mb height data are from 1947 to 1989.

4.2.1 Interpretation of Height and Temperature Maps

In the following height fields mapped for constant-pressure levels, a lower height indicates troughing and implies convergence. This can be understood by considering the intersection of the pressure surface with a horizontal plane, and imagining the pressure surface projected onto it, making a topographic map on the horizontal plane. On the horizontal plane, or map, pressure is lowest in the middle of a topographic low in the constant-pressure surface. Air will spiral in toward the center. If air from all levels below, such as from the ground up to the plane, was also spiraling inward, and in this example, necessarily rising, then at the plane under study, the converging air must also rise. Colder temperatures should accompany the lows, because temperature decreases with height, between the planetary boundary layer and the tropopause.

In the following height- and temperature-difference maps, the order of subtraction is the same as used in part 3.2.3, El Niño minus non-El Niño, (3.8). The order is chosen such that a negative difference indicates a lower average height or a cooler average temperature in El Niño winters than in non-El Niño winters. Positive or negative height differences (or temperature differences) are with respect to conditions at a particular area between El Niño and non-El Niño years, and not to neighboring areas on the same map. For example, places with negative temperature differences are not necessarily cooler than places with positive temperature differences.

4.2.1.1 Why Work on Constant-Pressure Surfaces?

The height and temperature maps, as nearly all the preceeding maps, are on isobaric, or constant-pressure surfaces. Most meteorological analysis is done on iso-

baric surfaces rather than on surfaces of constant height because of computational advantage. For example, calculation of the geostrophic wind on isobaric surfaces can be done without a density term, an advantage since density varies with height and pressure (Hess 1959). Working at a constant height, z, the geostrophic wind equations are

$$v_g = \frac{1}{\rho f}\frac{\partial P}{\partial x}|_z \tag{4.1}$$

$$u_g = -\frac{1}{\rho f}\frac{\partial P}{\partial y}|_z$$

where the subscript, g, denotes the geostrophic part of the u or v component of the wind; the notation, $|_z$, means holding z, height, constant; ρ is density; f is the Coriolis parameter; $2\Omega \sin \phi$; P is pressure. Using the hydrostatic equation

$$P = \rho g z \tag{4.2}$$

to express the horizontal pressure gradient (change in pressure per unit horizontal distance, x or y)

$$\frac{\partial P}{\partial x} = \rho g \frac{\partial z}{\partial x} \tag{4.3}$$

$$\frac{\partial P}{\partial y} = \rho g \frac{\partial z}{\partial y}$$

and substituting the new expression for the horizontal pressure gradient into the geostrophic wind equation, (4.1) becomes, on a constant-pressure surface,

$$v_g = \frac{g}{f}\frac{\partial z}{\partial x}|_p \tag{4.4}$$

$$u_g = -\frac{g}{f}\frac{\partial z}{\partial y}|_p$$

where the notation, $|_p$, means holding pressure constant.

4.2.2 Mean Sea-Level Pressure: El Niño and Non-El Niño Winters, 1947-1989.

Fig. 3.7 showed that mean sea-level pressure in the gulf area is -1.0 to -0.5 mb lower in El Niño winters than in non-El Niño winters, or -17 to -8% of the 6.0 mb range of values over the gulf region in El Niño winters, 1014.0 to 1020.0 mb. For comparison, the difference between El Niño and non-El Niño winters in mean sea-level pressure at the Aleutian low ranges from -5.8 to -1 mb, or -30 to -5% of the 19.2 mb range over the core of the low. The greatest negative differences in the mapped area occur at the Aleutian low, while the maximum positive differences occur at the Davis Strait. The drop in mean sea-level pressure in El Niño winters appears to be part of a larger drop at the Aleutian low. This pattern will be repeated in all the following maps.

4.2.3 850-mb Height: El Niño and Non-El Niño Winters, 1963-1989.

Fig. 4.16 shows the difference in heights of the 850-mb surface between El Niño winters and non-El Niño winters. Figs. 4.17 and 4.18 show the actual, winter, average heights for El Niño and non-El Niño winters, respectively. Total relief over the entire map is only 300 m (985 ft). Northern North America has a positive height difference, while the adjacent parts of the Atlantic and Pacific Oceans and the Gulf of Mexico have a negative height difference, or drop, in El Niño winters.

A height drop of -10 m (-33 ft) is fairly uniform over the gulf area, Fig. 4.16. It appears to be an outlier of a greater height drop, maximally -47 m (-155 ft), over the Aleutian low. The region of lower heights over the gulf connects the drop over the Aleutian low to a smaller drop over the Icelandic low. The height field is flat over the gulf, lying between 1500 and 1550 m (4920 and 5080 ft). In the context

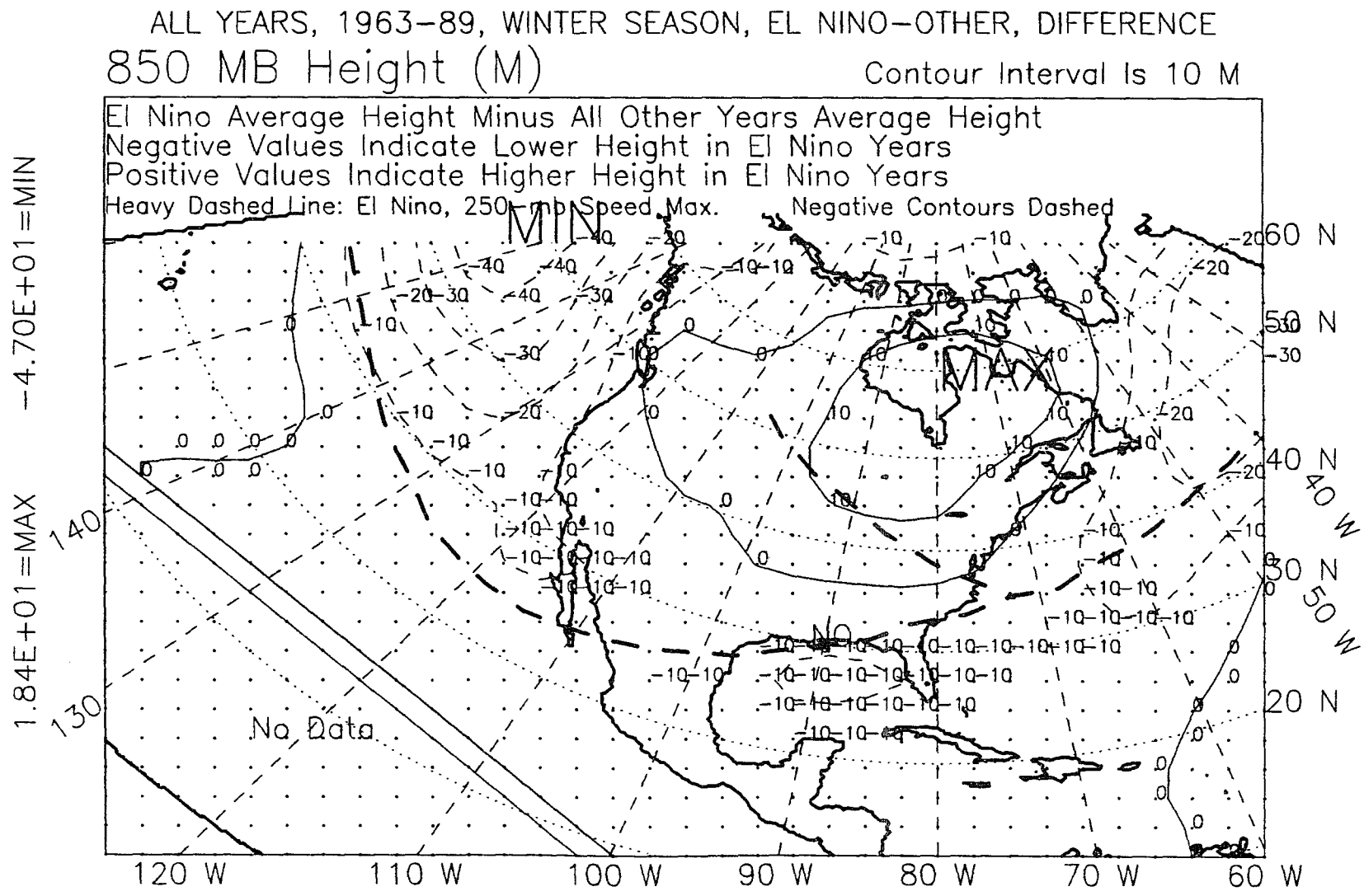

Figure 4.16: 850–mb height, winter, 1963–89, difference.

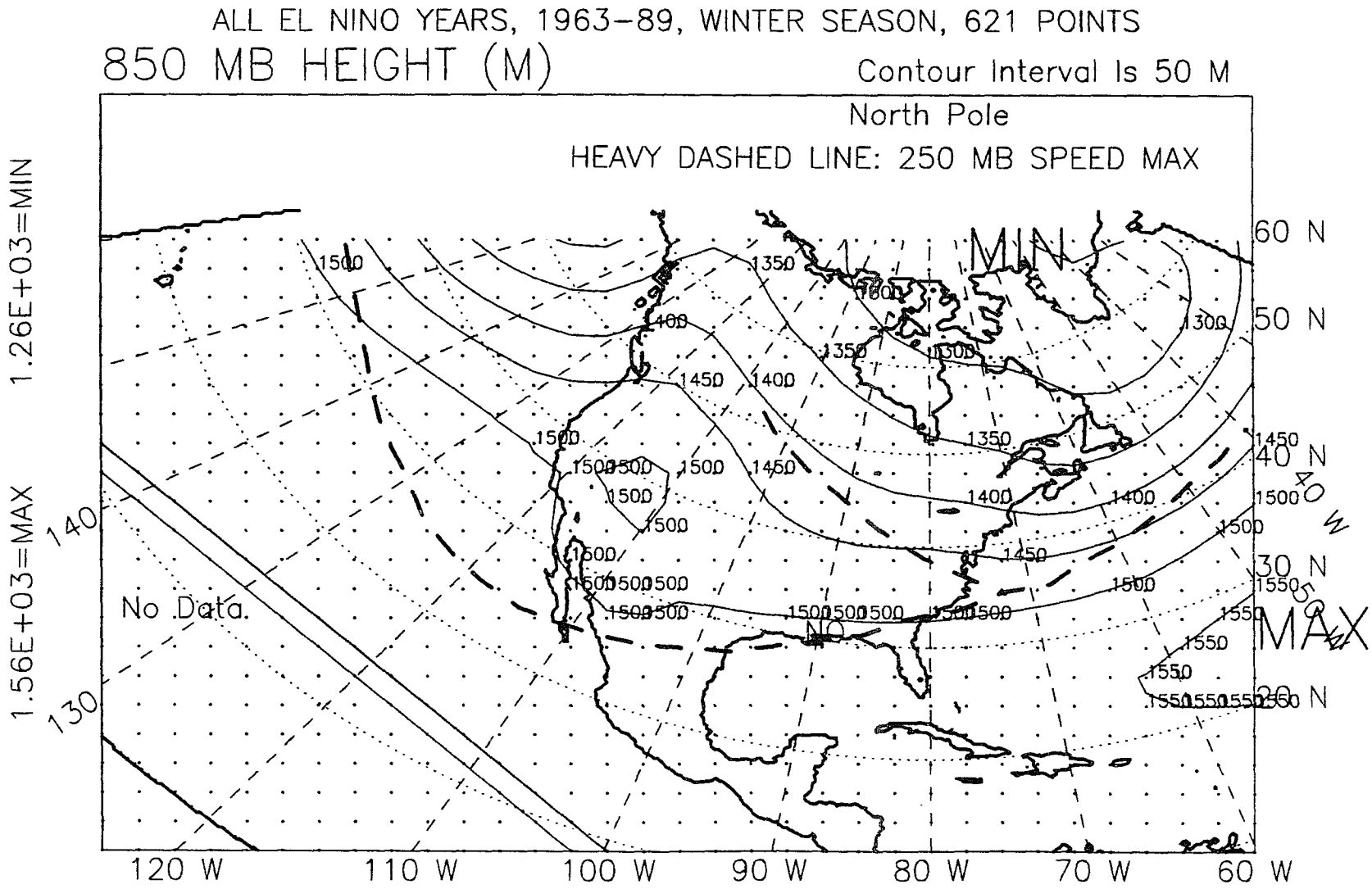

Figure 4.17: 850–mb height, winter, El Niño years, 1963–89.

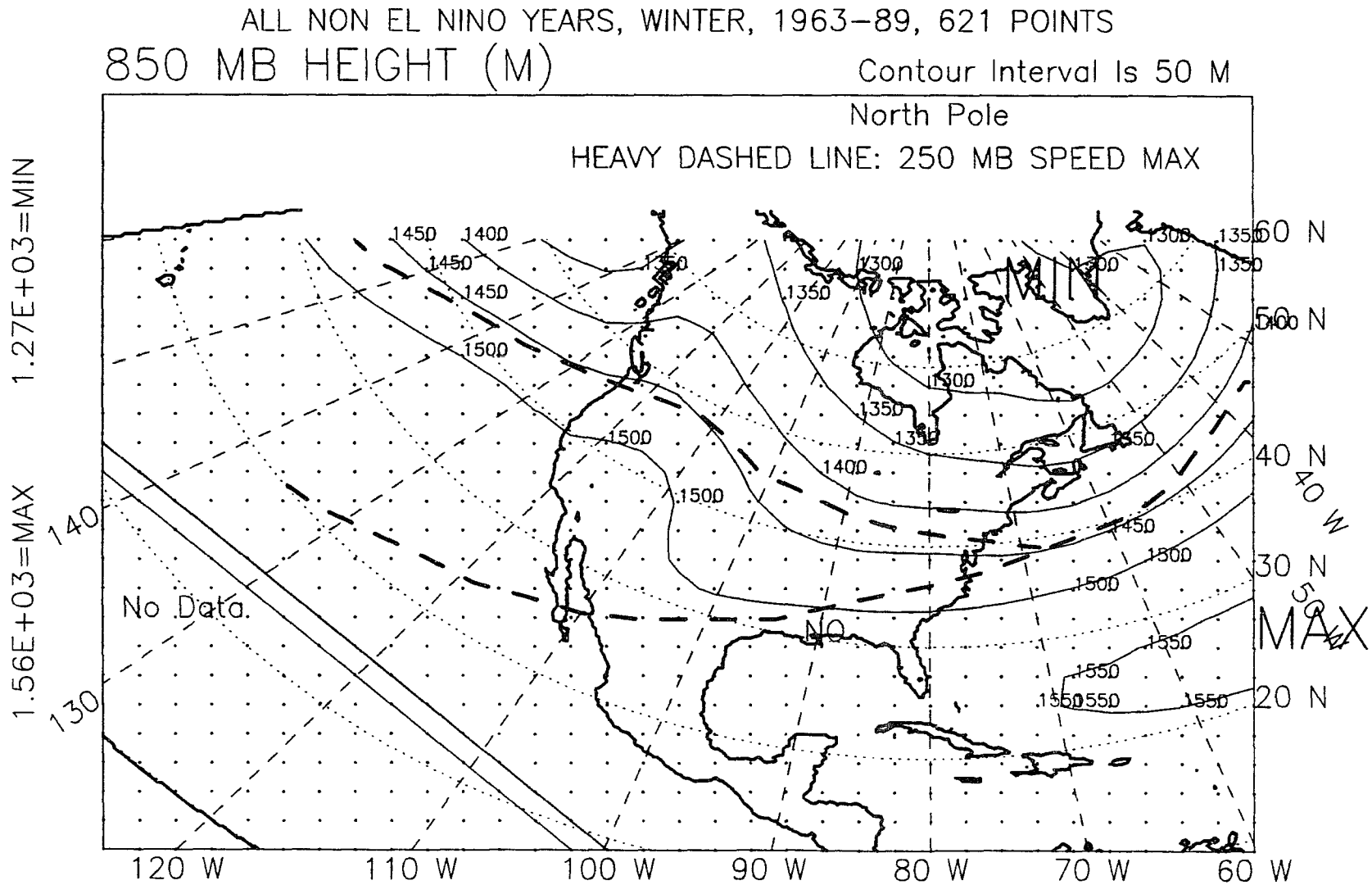

Figure 4.18: 850–mb height, winter, non–El Niño years, 1963–89.

of the 50 m (165 ft) range of actual average values over the gulf region, or 50 m local relief, the -10 m height difference is -20% of the local relief. For comparison, the average height differences over the Aleutian low, -47 to -10 m, are -24 to -5% of the range of actual values there, 200 m, this range being subjectively determined over the core, sharpest-gradient portion of the low. Expressed as a percent of local relief, the drop over the gulf is substantial, on the same order of magnitude as the drop over the most-affected area of the map, the Aleutian low.

4.2.4 850-mb Temperature: El Niño and Non-El Niño Winters, 1963-1989.

Fig. 4.19 shows the difference in temperature between El Niño and non-El Niño winters, and Figs. 4.20 and 4.21 show the actual temperature fields. Canada and the eastern United States show a warming in El Niño winters. Maximum warming, over Hudson Bay, is +3.7°C, Fig. 4.19. The eastern north Pacific, western United States, and Mexico show a cooling, -2°C. Maximum cooling is at the Icelandic low, -2.7°C. The range of average, El Niño-winter temperatures over the entire map is 19.7 to -25.0°C. Over the Gulf of Mexico, temperatures range from 8 to 16°C. In El Niño winters the average 850-mb temperature is -1.0 to 0°C cooler over the gulf area. This is -10 to 0% of the range over the gulf area in El Niño winters. For comparison, the air over the Aleutian low is on average, -0.4 to -1.8 °C cooler in El Niño winters than in non-El Niño winters. This is -23 to -5% of the 8 C° range of temperatures found in that area in El Niño winters.

Temperature contours over the gulf in both winter types are nearly zonal, but there is a barely-perceptible (at this scale) west-northwest tilt in non-El Niño winters, Fig. 4.21, indicating slightly warmer air, not more than +0.5°C, over the western gulf than over the eastern gulf in non-El Niño winters, compare Figs. 4.21

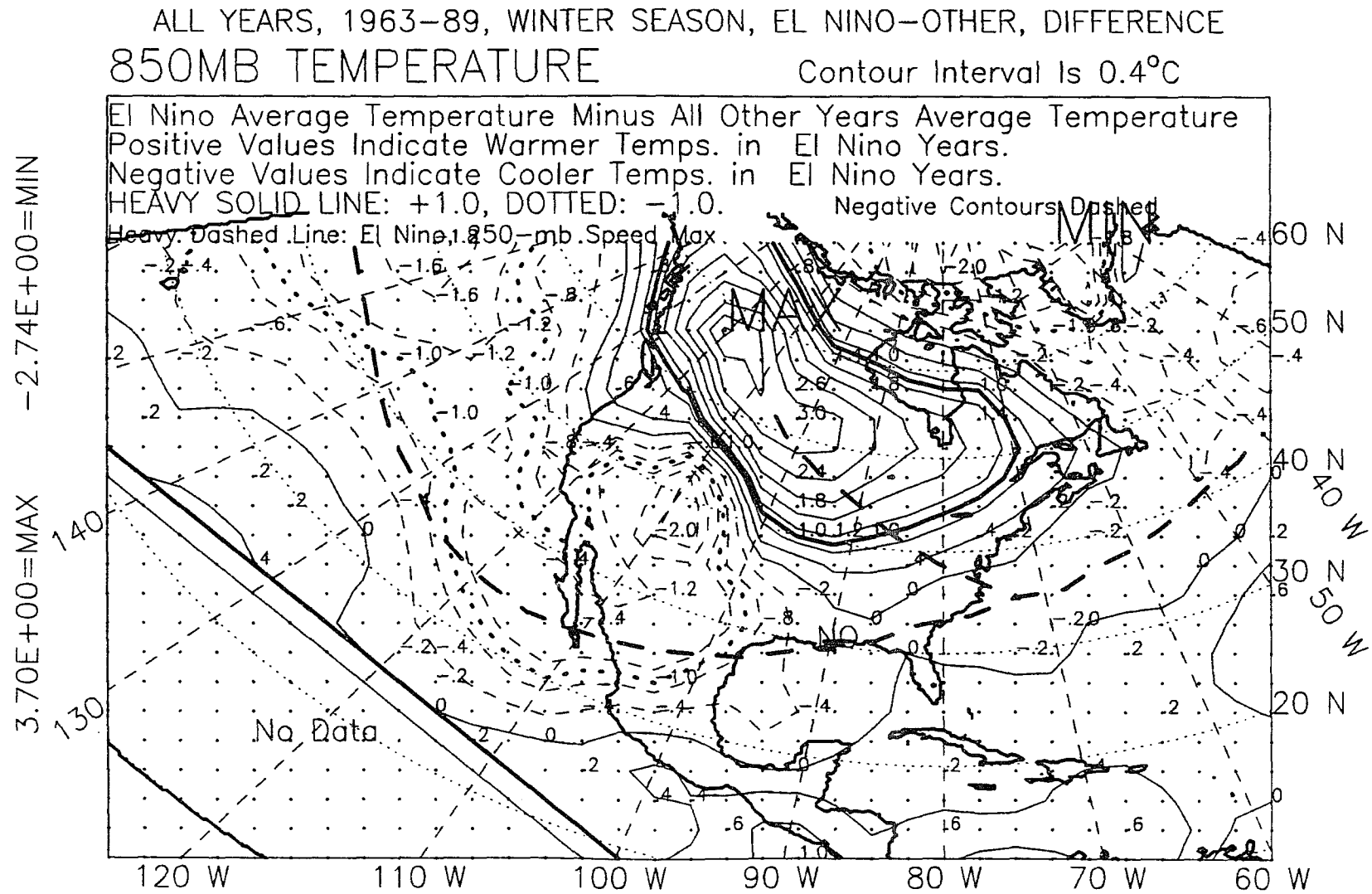

Figure 4.19: 850–mb temperature, winter, 1963–89, difference.

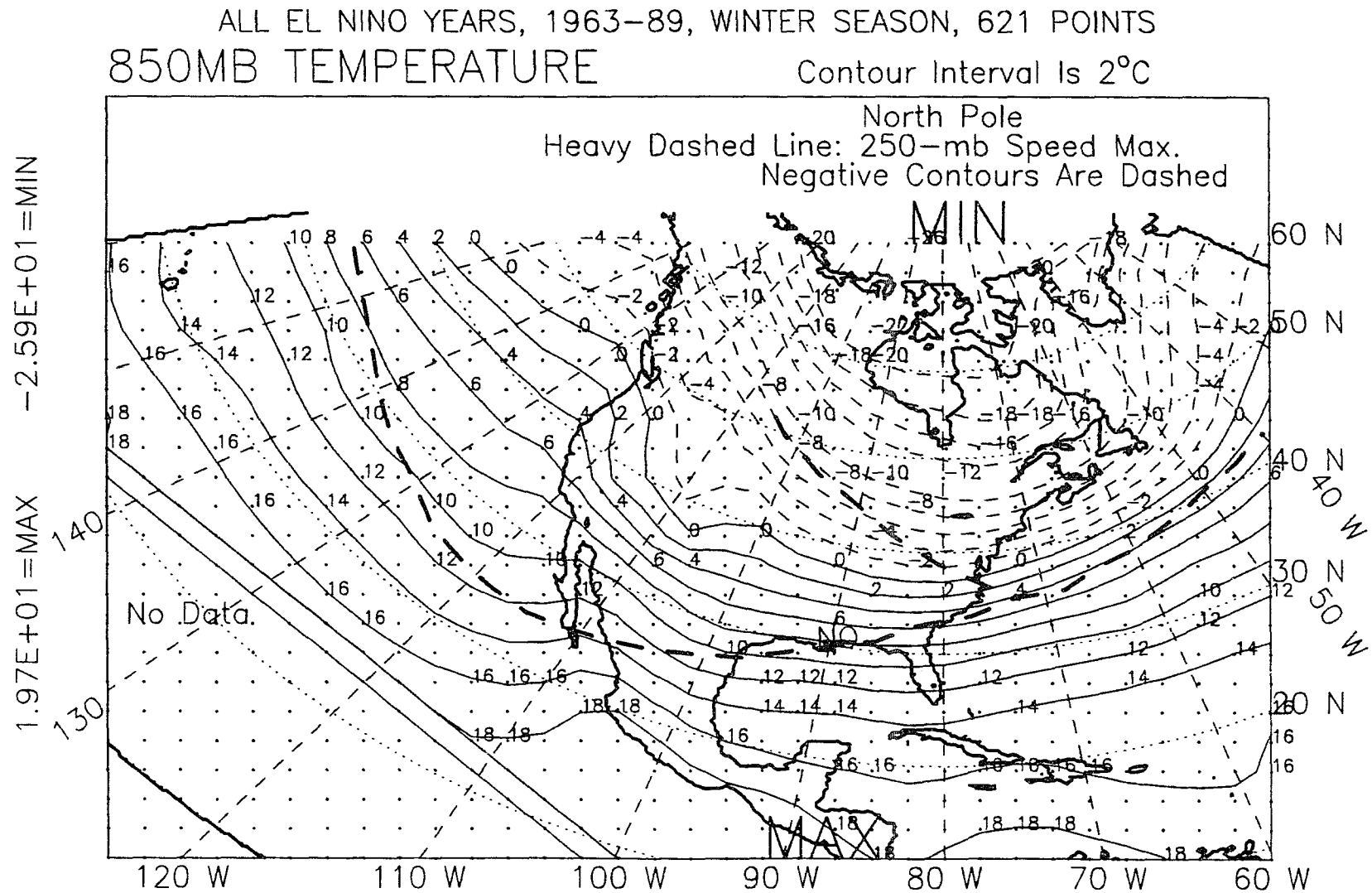

Figure 4.20: 850–mb temperature, winter, El Niño years, 1963–89.

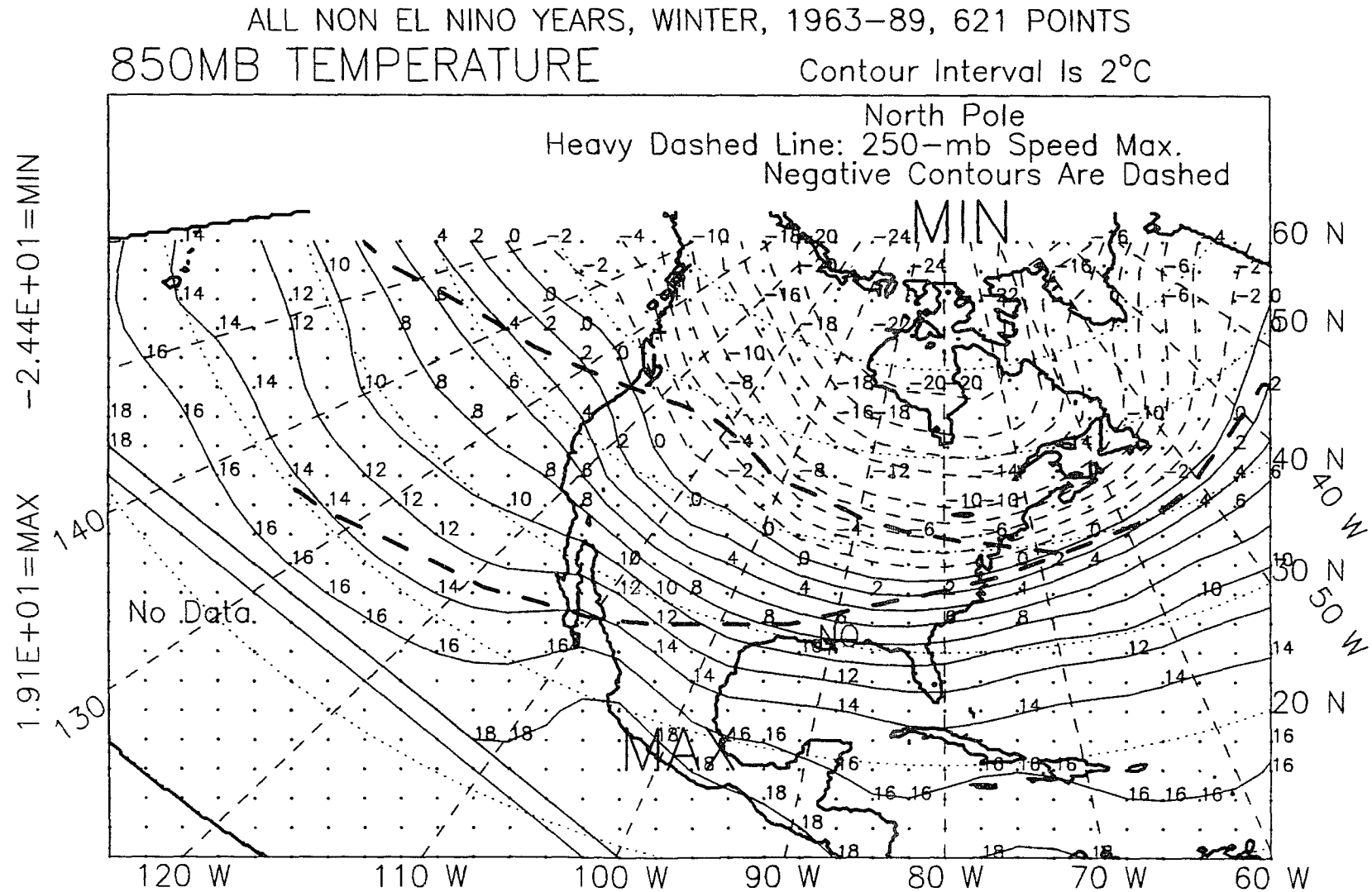

Figure 4.21: 850–mb temperature, winter, non–El Niño years, 1963–89.

and 4.20. At the 850-mb level, air over the western gulf region is -1.0 to 0.0°C cooler in El Niño winters than in non-El Niño winters, Fig. 4.19. This does not mean that air at the 850-mb level is cooler over the western gulf than over the eastern gulf in El Niño winters. Because of the small magnitude of the cooling in the air over the west gulf, -0.4°C in El Niño winters, the drop likely means that the slight west to east temperature decrease of normal years is eroded or erased in El Niño winters.

At the 850-mb level, the gulf region is located within the zone of average El Niño-winter cooling, but it is near the edge. Areas of average warming are not too far away. Individual variations on this average pattern can explain why the December 1991 to February 1992 El Niño winter was not cooler (based on the author's subjective observations) than a typical non-El Niño winter in the gulf area, as the temperature results presented in 2.3.1 would lead one to expect.

Similarly, the Denver, Colorado area, 40°N, 105°W, is located under a sharp gradient of 850-mb temperature differences. On the average, El Niño-winter, warming occurs from the Montana-Wyoming border northward; cooling is observed south of there, including in the Denver area, Fig. 4.19. Allowing for variations on this average pattern, that is, variations in where the line between average cooling and warming in a particular El Niño winter will fall, Fig. 4.19 is consistent with anecdotal evidence (D. Nummedal, 1992, personal communication), that during the El Niño winter of December 1991 to February 1992 northern Colorado experienced warm temperatures and fewer snow storms than did southern Colorado.

4.2.5 700-mb Height: El Niño and Non-El Niño Winters, 1963-1989.

Fig. 4.22 shows the 700-mb level height differences between El Niño and other winters. Figs. 4.23 and 4.24 show the actual height fields in El Niño and non-El

Niño winters. The same pattern as shown by the 850-mb level height maps is evident. That is, there is a strong negative difference centered over the Aleutian low, extending southeastward covering the gulf area, and a second, weaker, negative difference over the Icelandic low, Fig. 4.22. Much of northeastern North America has a higher 700-mb level in El Niño winters than in non-El Niño winters. The maximum increase is +27 m (+90 ft) over Hudson Bay, just as for the 850-mb level. The height field is almost flat over the gulf area, with 50 m (165 ft) relief, lying between 3100 and 3150 m (10 170 to 10 330 ft), Fig. 4.23. The height drop over the gulf area is a fairly uniform -10 m (-33 ft), or -13% of the relief, Fig. 4.22. For comparison, the average height drop over the Aleutian low ranges from -56 to -20 m (-185 to -65 ft), and this is -22 to -8% of the relief.

4.2.6 500-mb Height: El Niño and Non-El Niño Winters, 1947-1989.

Fig. 4.25 shows the difference in the height of the 500-mb surface between El Niño and other winters. Figs. 4.26 and 4.27 show the actual heights in El Niño and non-El Niño winters. The pattern observed at lower levels is almost repeated. Lower average height over the Aleutian low and higher height over northeastern North America. At this level, however, the smaller negative differences seen at lower levels over the Icelandic low are not replicated. Heights in El Niño winters are somewhat higher over the Icelandic low at the 500-mb level, Fig. 4.25. Height

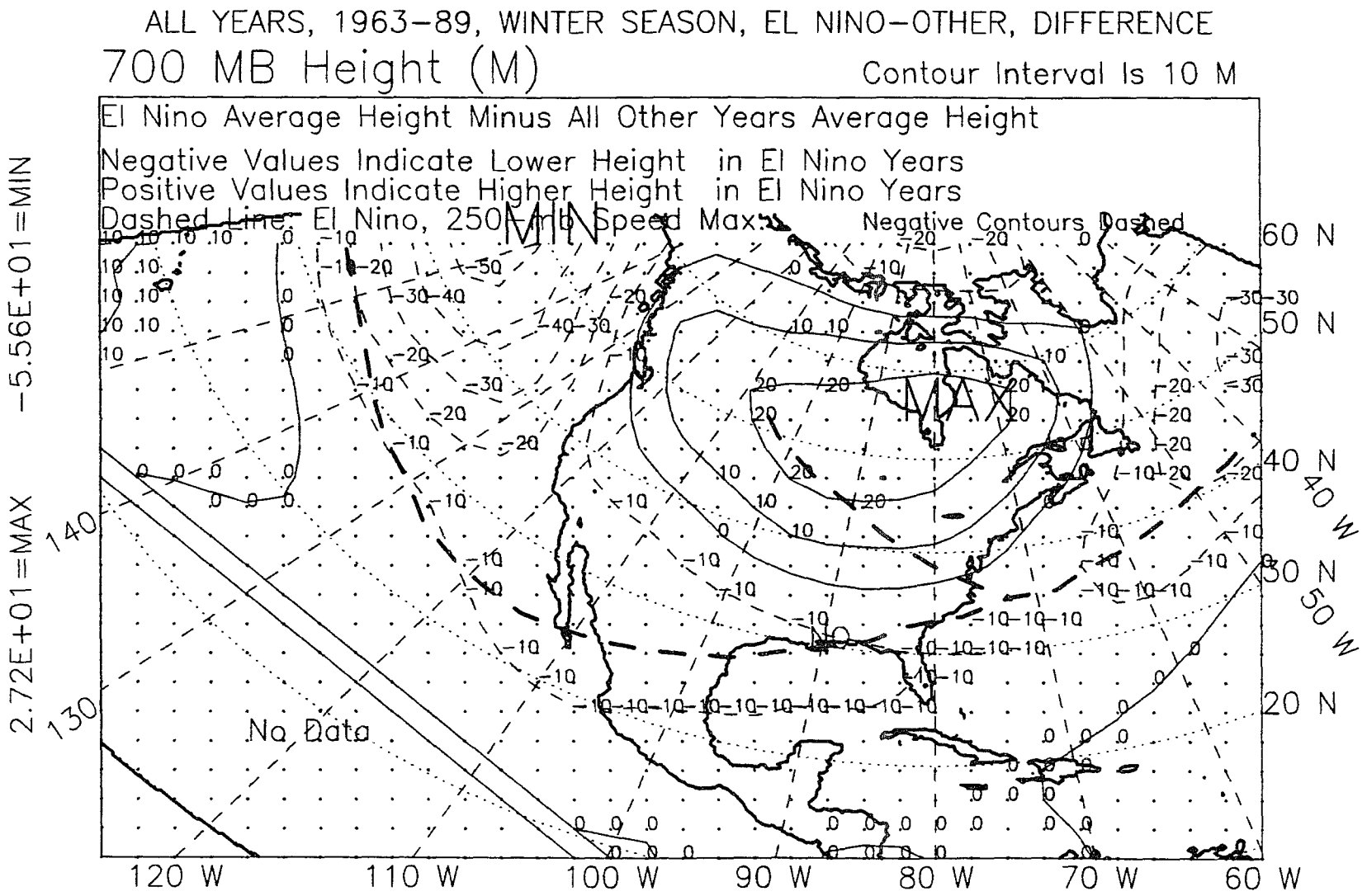

Figure 4.22: 700–mb height, winter, 1963–89, difference.

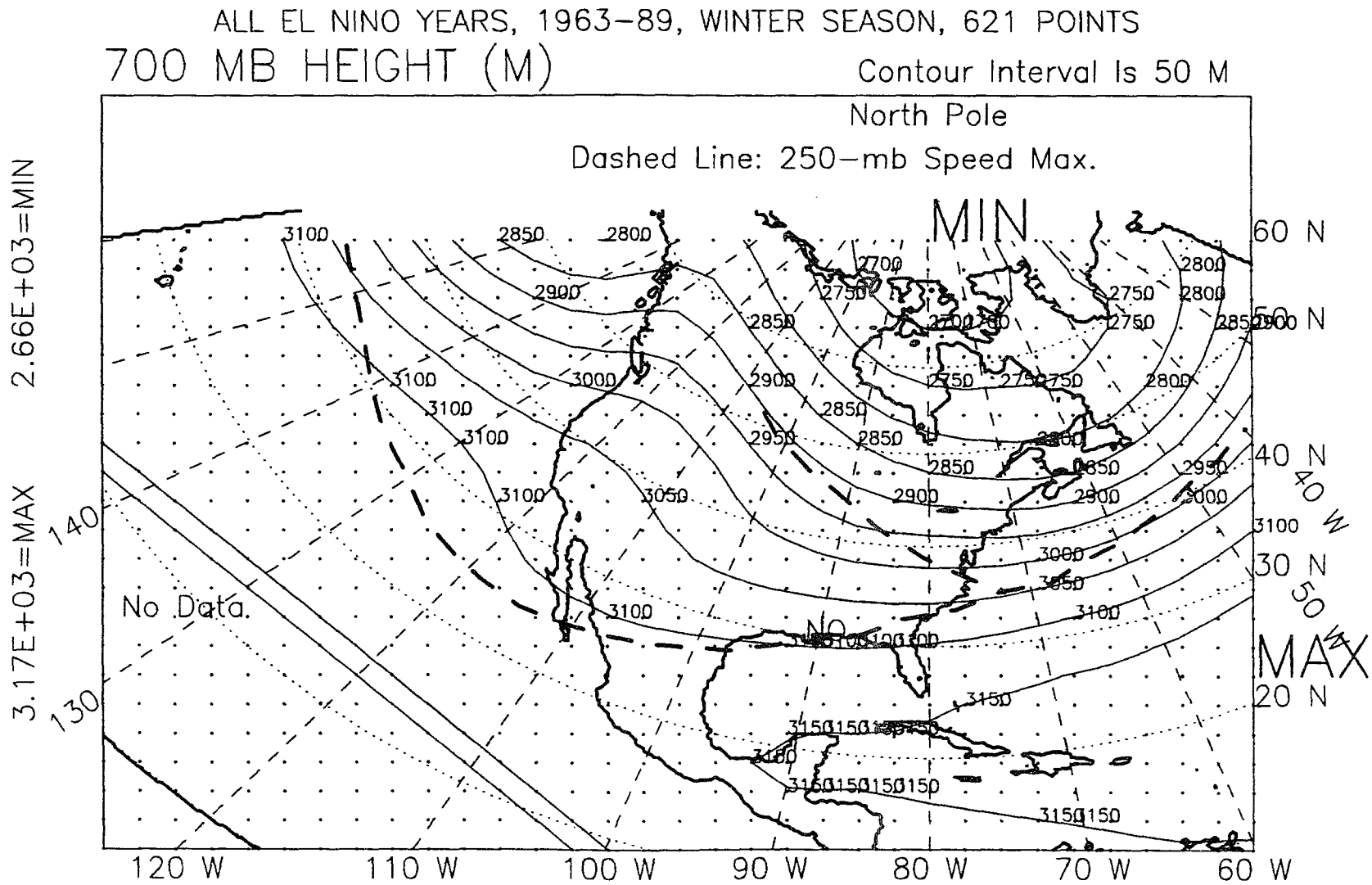

Figure 4.23: 700–mb height, winter, El Niño years, 1963–89.

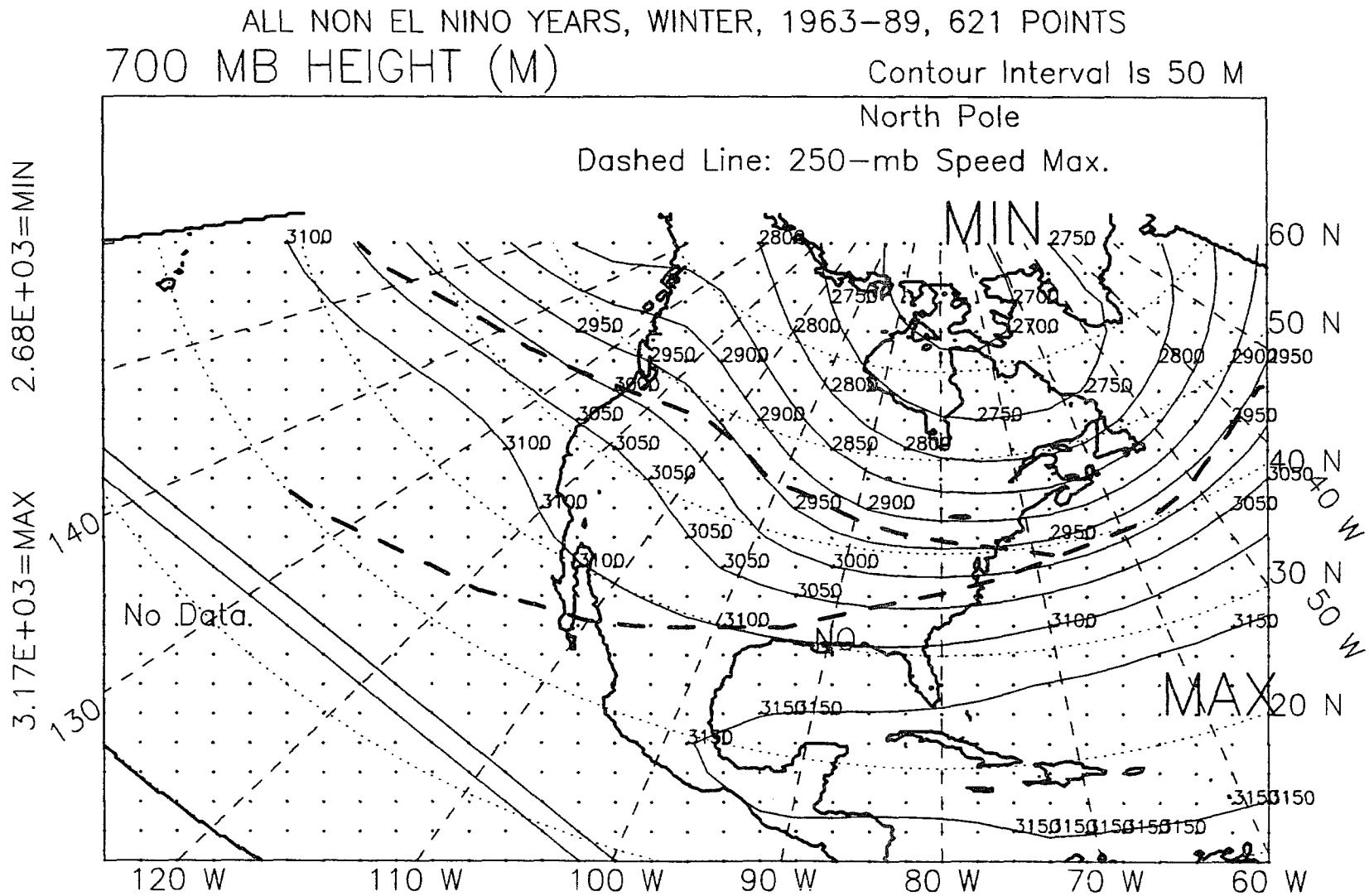

Figure 4.24: 700–mb height, winter, non–El Niño years, 1963–89.

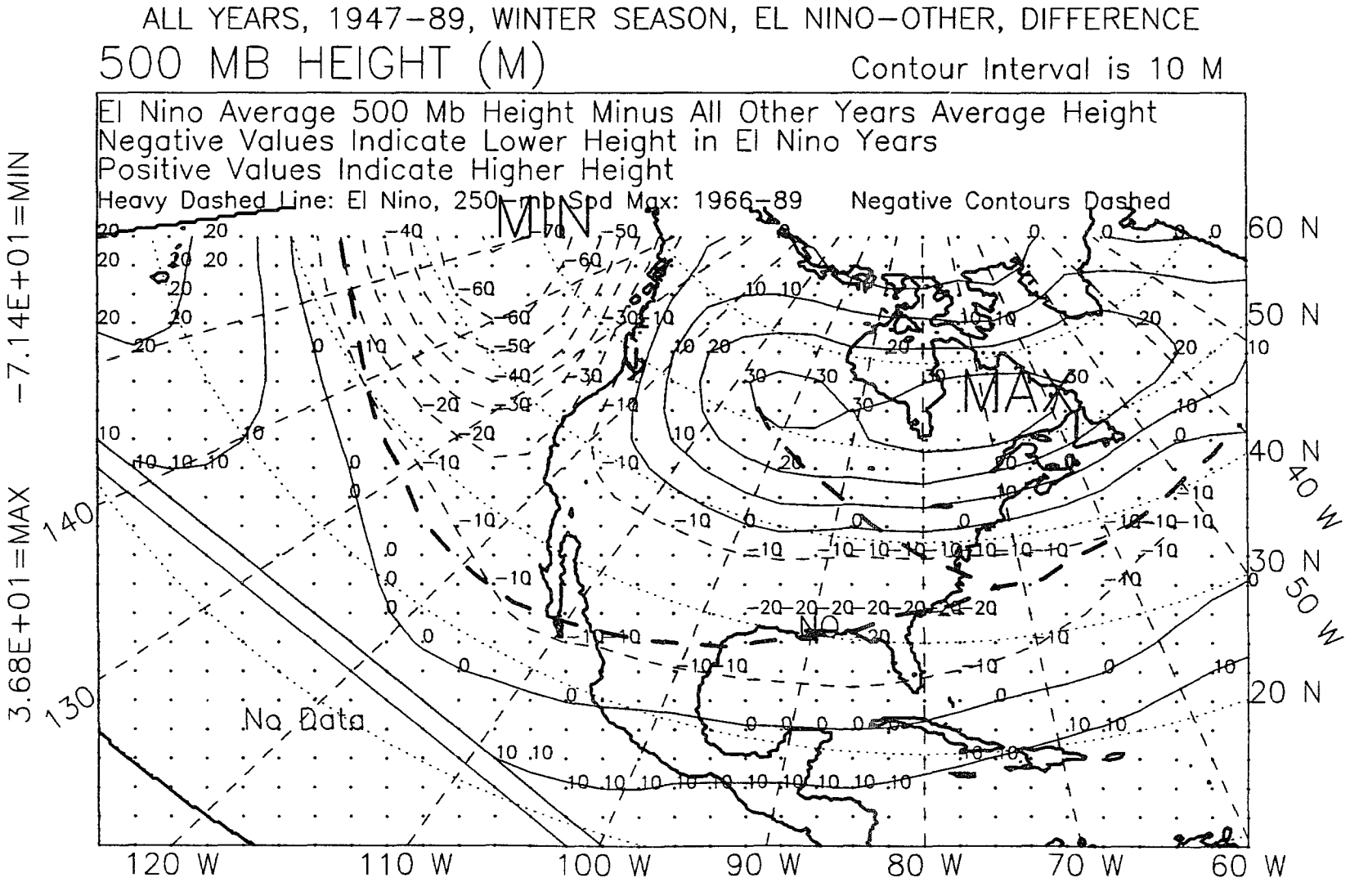

Figure 4.25: 500–mb height, winter, 1947–89, difference.

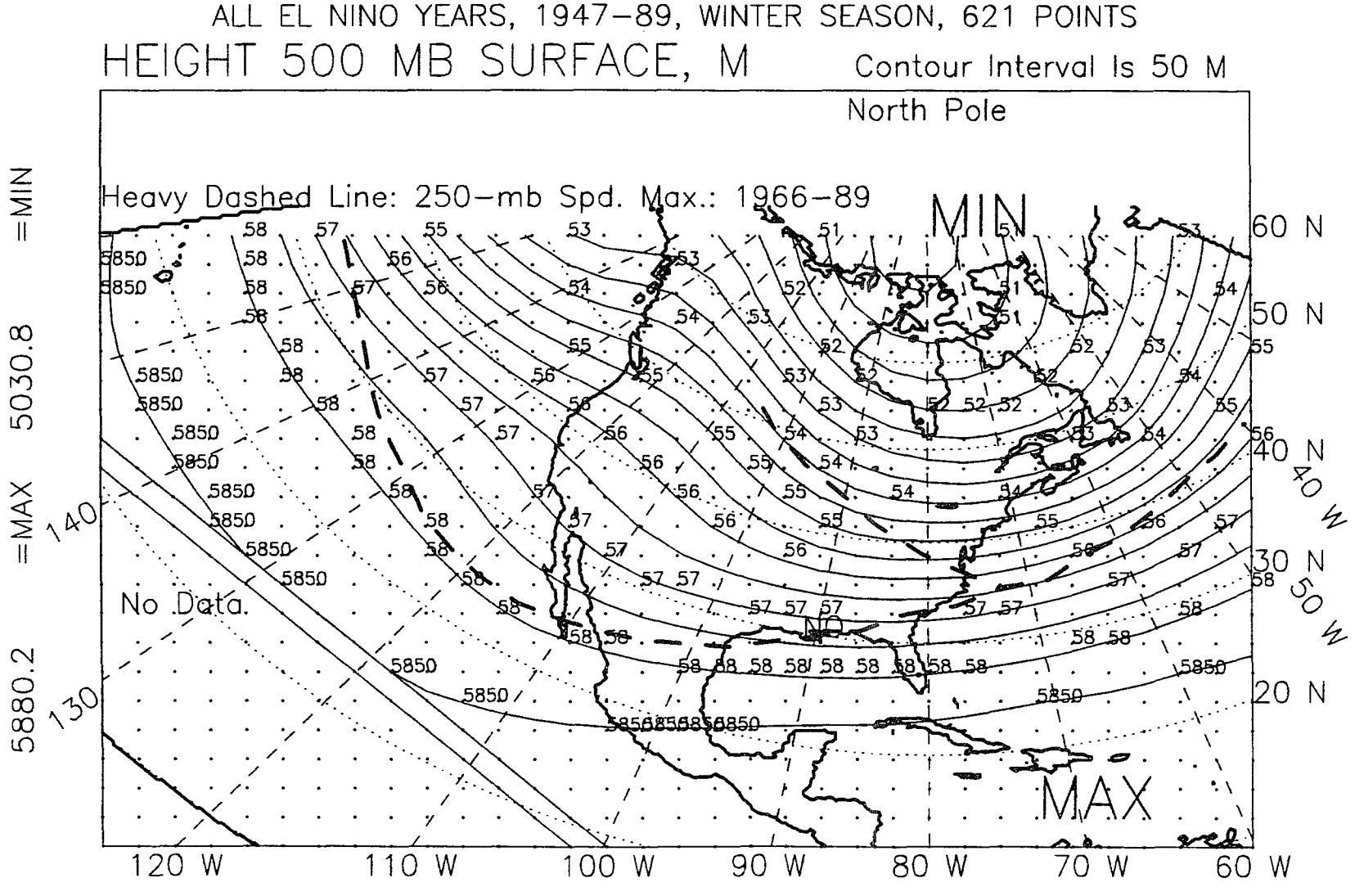

Figure 4.26: 500–mb height, winter, El Niño years, 1947–89.

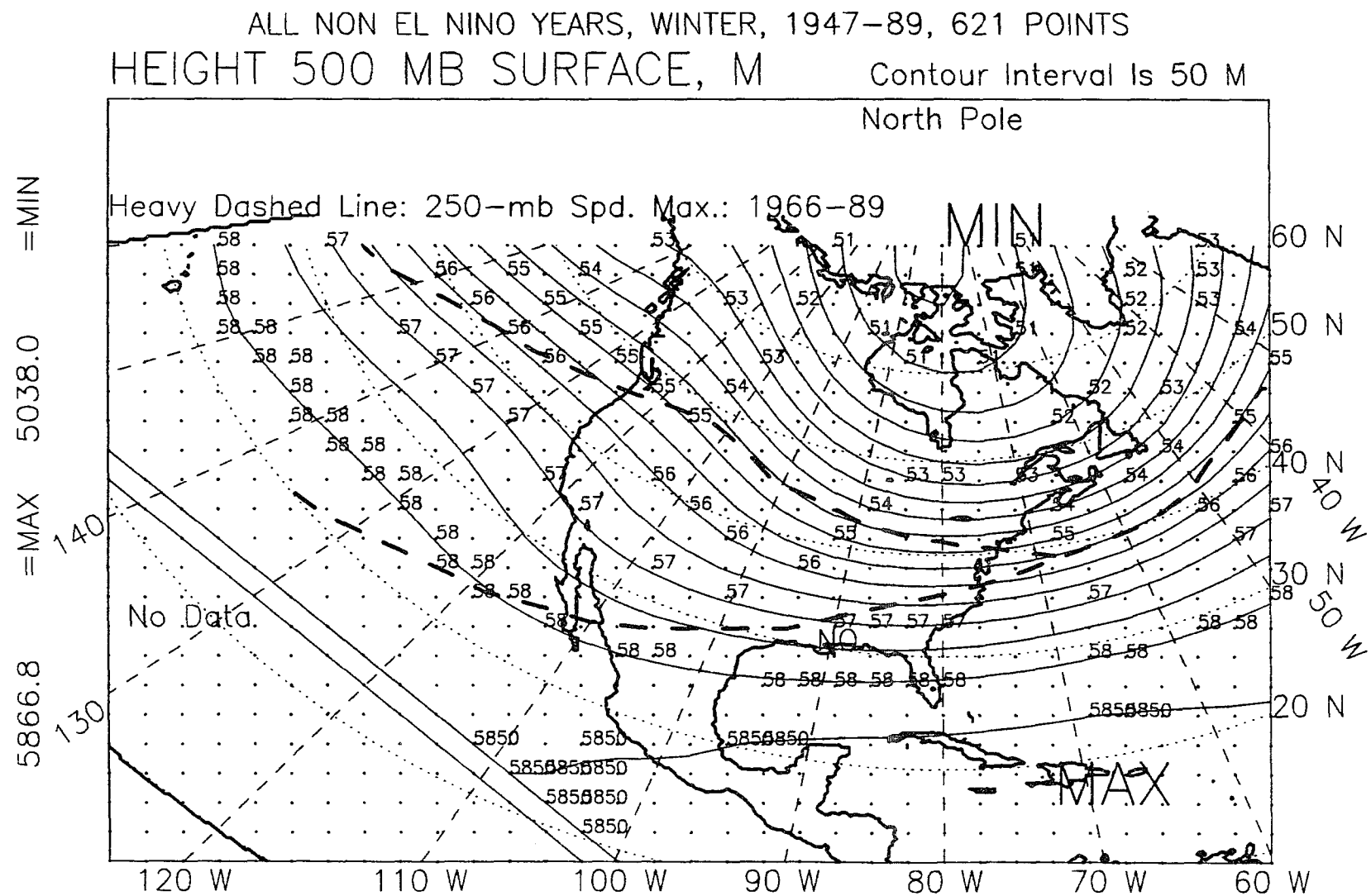

Figure 4.27: 500–mb height, winter, non–El Niño years, 1947–89.

differences over the gulf area range from -20 to 0 m (-65 to 0 ft), Fig. 4.25. This is -13 to 0% of the local relief of 150 m (500 ft) on the 500-mb surface. The 500-mb height lies between 5700 and 5850 m (18 700 to 19 200 ft) locally, in El Niño winters, Fig. 4.26. For reference, the average height drop in El Niño winters over the Aleutian low ranges from -71 to -20 m (-230 to -65 ft), which is -20 to -6% of the relief on the 500-mb surface over the low.

4.2.7 500-mb Temperature: El Niño and Non-El Niño Winters, 1963-1989.

Fig. 4.28 shows the difference in temperature at the 500-mb level between El Niño and non-El Niño winters. Figs. 4.29 and 4.30 show the actual temperature fields in El Niño and non-El Niño winters, respectively, between 1963 and 1989. Note that the area of the gulf most critical to gulf cyclogenesis, the northwest-gulf 'storm machine' is under an area of 500-mb temperature drop. It would seem that in order to influence gulf cyclogenesis, the El Niño-deepened, upper-level extension of the Aleutian low need only extend far enough southeastward to reach the northwest gulf. The average, 500-mb temperature difference over the gulf area, Fig. 4.28, ranges from -0.8 to +1.0°C. This is -9 to +11% of the 9°C range of gulf-region, average, 500-mb temperatures. (For reference, the Aleutian low area, has the maximum temperature drop on the map, -1.7 to -0.8°C, or -17 to -8% of the local 36°C range.) The difference is negative in the northwest and northern gulf and coastal plain, but positive southeast of there. The negative temperature differences to the northwest and the positive temperature differences over the remainder of the gulf area are an indication of the westward tilt of the upper-level extension of a surface trough. The three-dimensional core of depressed isobaric surfaces and cooler temperatures tilts westward, back from a surface cyclone (Palmén and Newton 1969; Bjerknes and Holmboe 1944). In fact, the northwestward position of locally most-

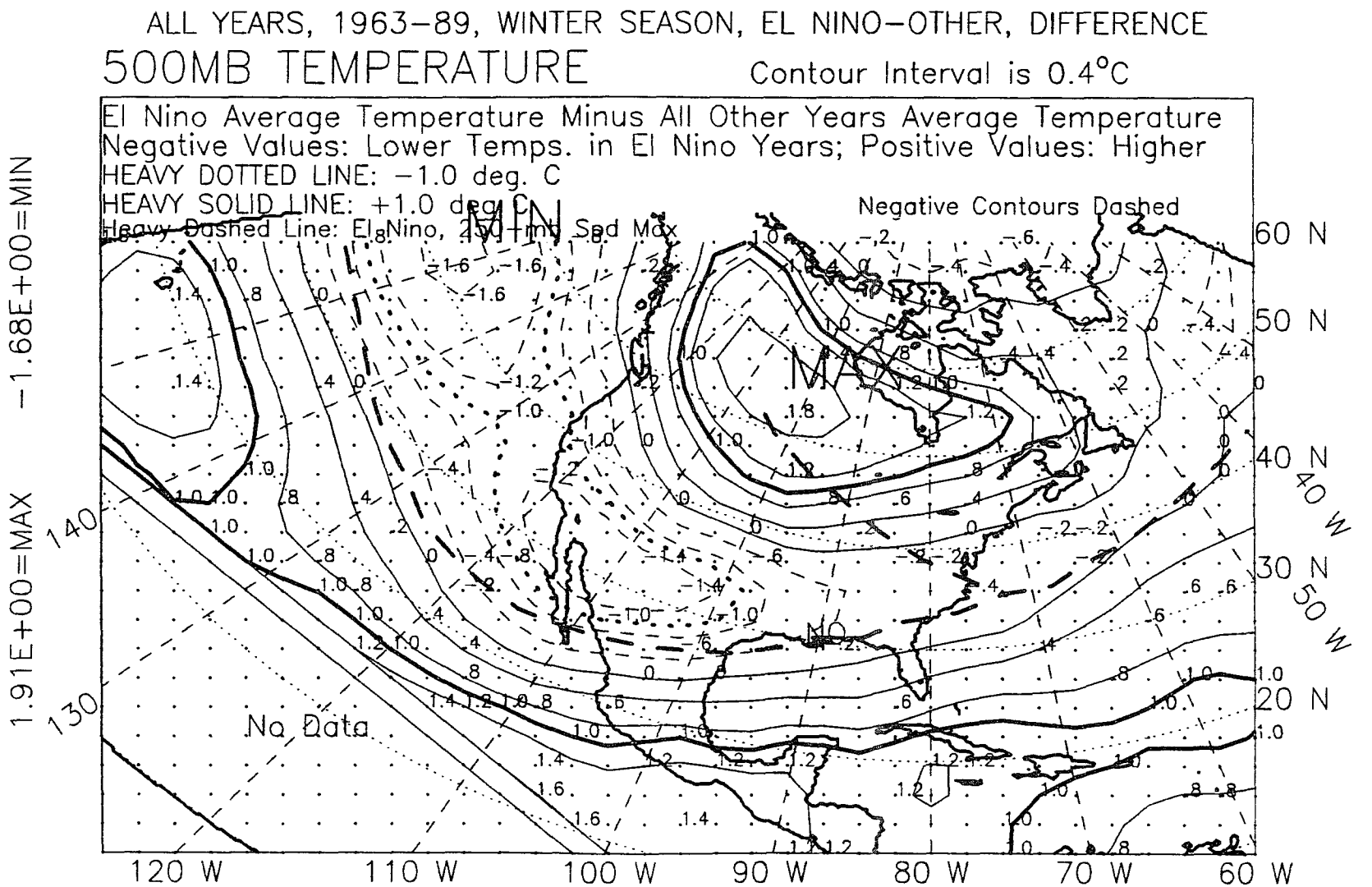

Figure 4.28: 500–mb temperature, winter, 1963–89, difference.

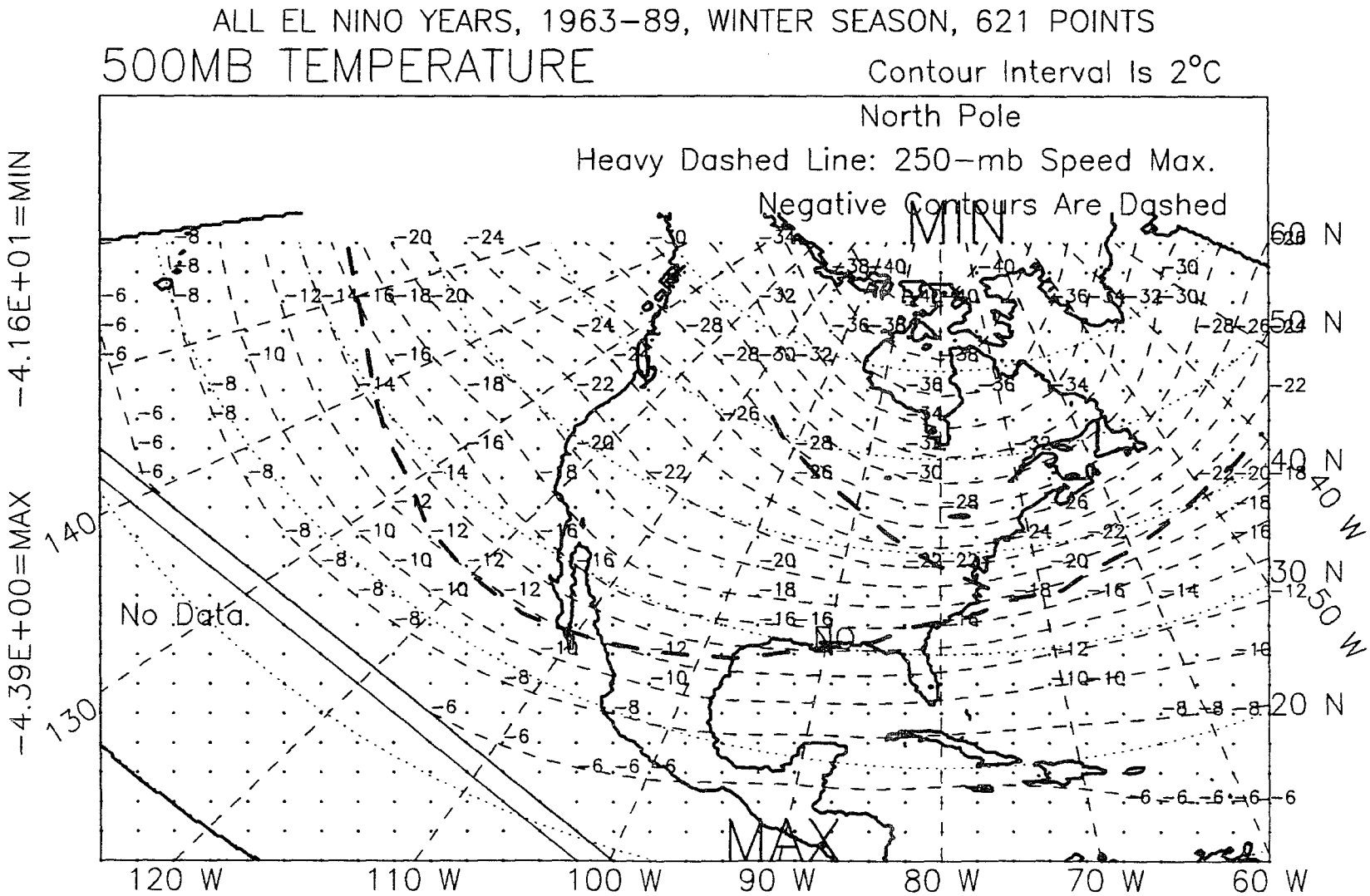

Figure 4.29: 500–mb temperature, winter, El Niño years, 1963–89.

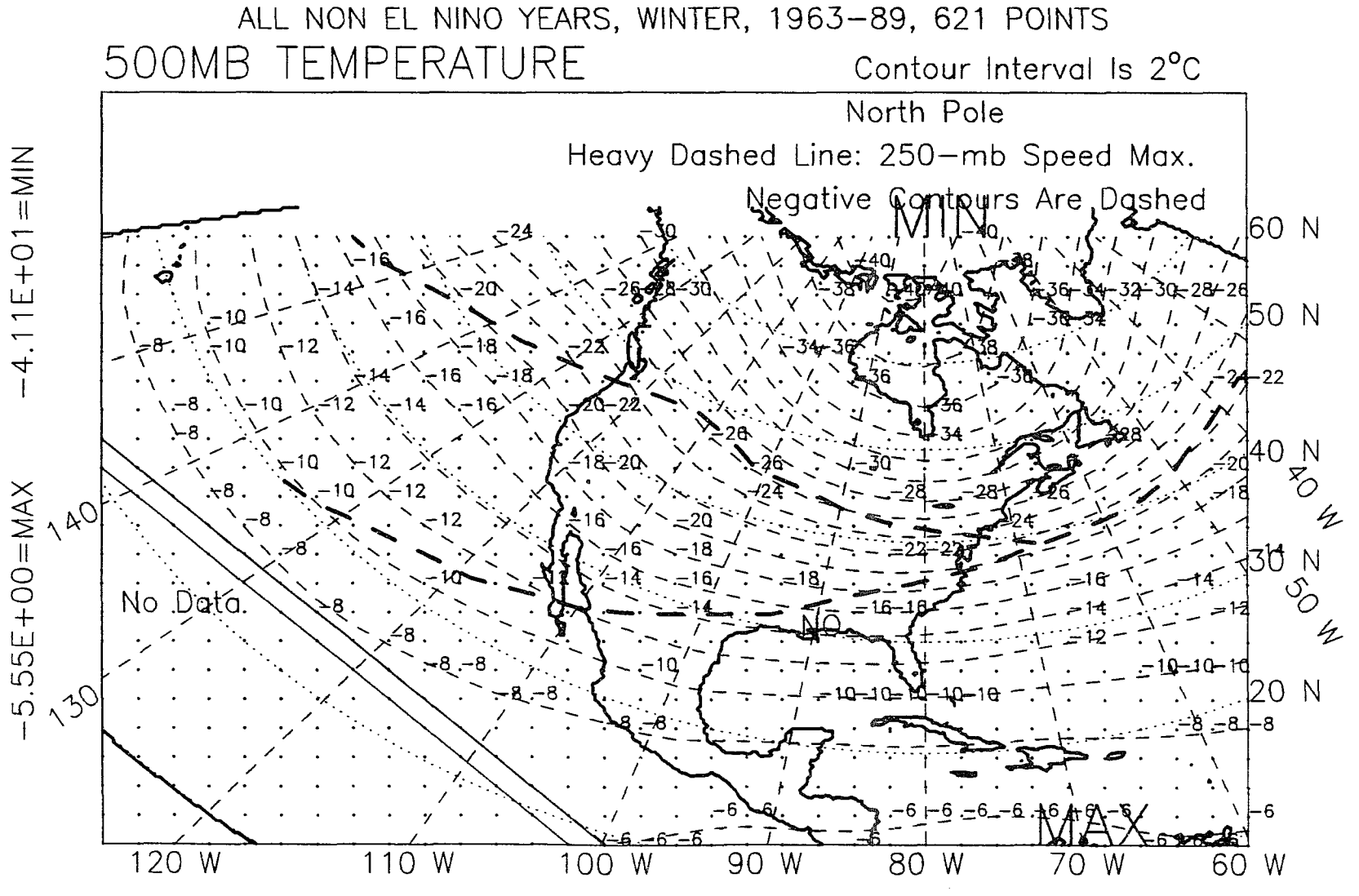

Figure 4.30: 500-mb temperature, winter, non-El Niño years, 1963-89.

depressed temperatures and heights on all height- and temperature-difference maps is a manifestation of this tilt with height. Why the 500-mb height differences do not parallel the 500-mb temperature differences, being instead, everywhere negative over the gulf region, is unresolved. It may indicate a rise of warm surface air up the tropical side of the trough. Alternatively, the 500-mb level is near the level of nondivergence, which may be important.

4.2.8 200-mb Height: El Niño and Non-El Niño Winters, 1963-1989.

Fig. 4.31 shows the difference in height of the 200-mb surface between El Niño and non-El Niño winters. Figs. 4.32 and 4.33 show the actual height fields for El Niño and non-El Niño winters. The 200-mb level is generally at or above jet level. The El Niño-winter, mean south jet (dashed line in Fig. 4.31) almost exactly tracks the edge of the region of height drop over the Aleutian low, and follows the zero-difference line over Mexico, the Gulf of Mexico, the east edge of the Gulf Stream, and the Icelandic low, which again displays a negative difference at this level, after showing positive differences at the 500-mb level. The subtropical jet stream is generally located at a vertical step in the tropopause, the tropopause stepping down poleward of the jet. The negative height differences to the north of the El Niño-winter, mean south jet, indicate an exaggeration of the normal step down-to-the-north in El Niño winters. This is intuitively consistent with the strengthening of the jet in El Niño winters, which in fact may cause the increased vertical step.

As seen in the 500-mb temperature difference, the 200-mb negative height difference centered over the Aleutian low extends toward the Gulf of Mexico, but only includes the northern coastal plain, Fig. 4.31. The 200-mb height difference over the gulf area, from northwest to southeast, is -15 to +50 m (-50 to +165 ft) or

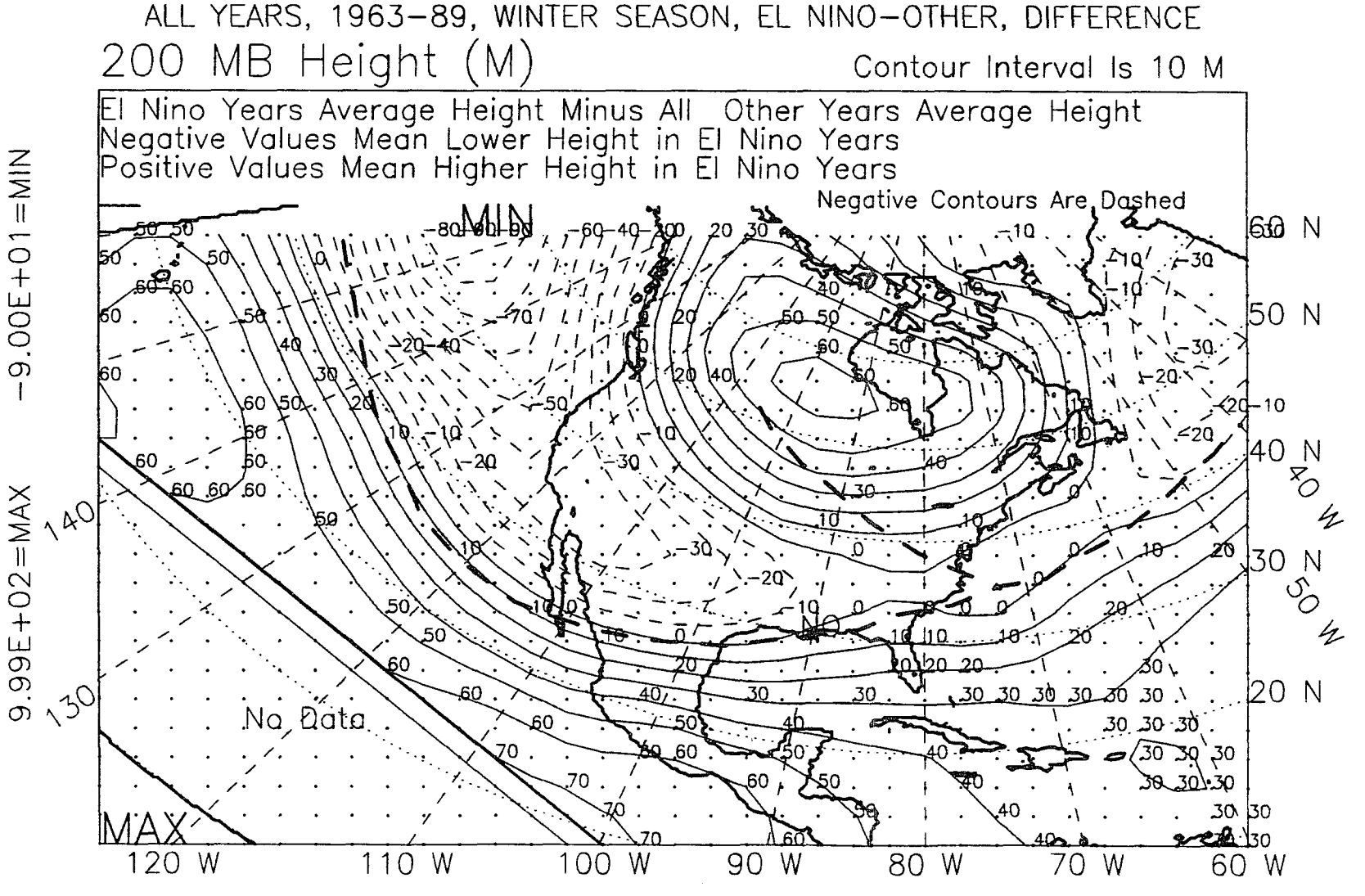

Figure 4.31: 200–mb height, winter, 1963–89, difference.

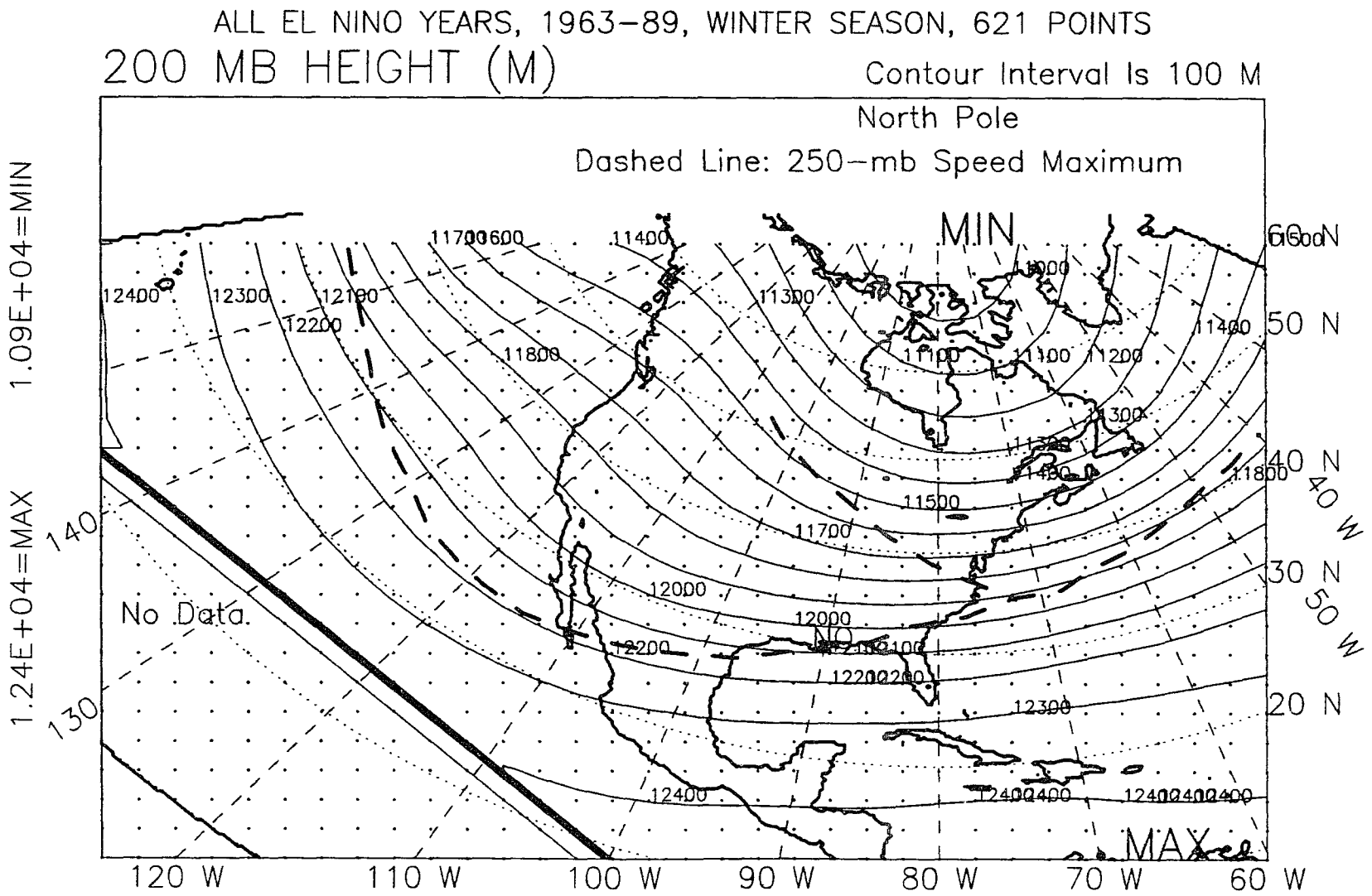

Figure 4.32: 200–mb height, winter, El Niño years, 1963–89.

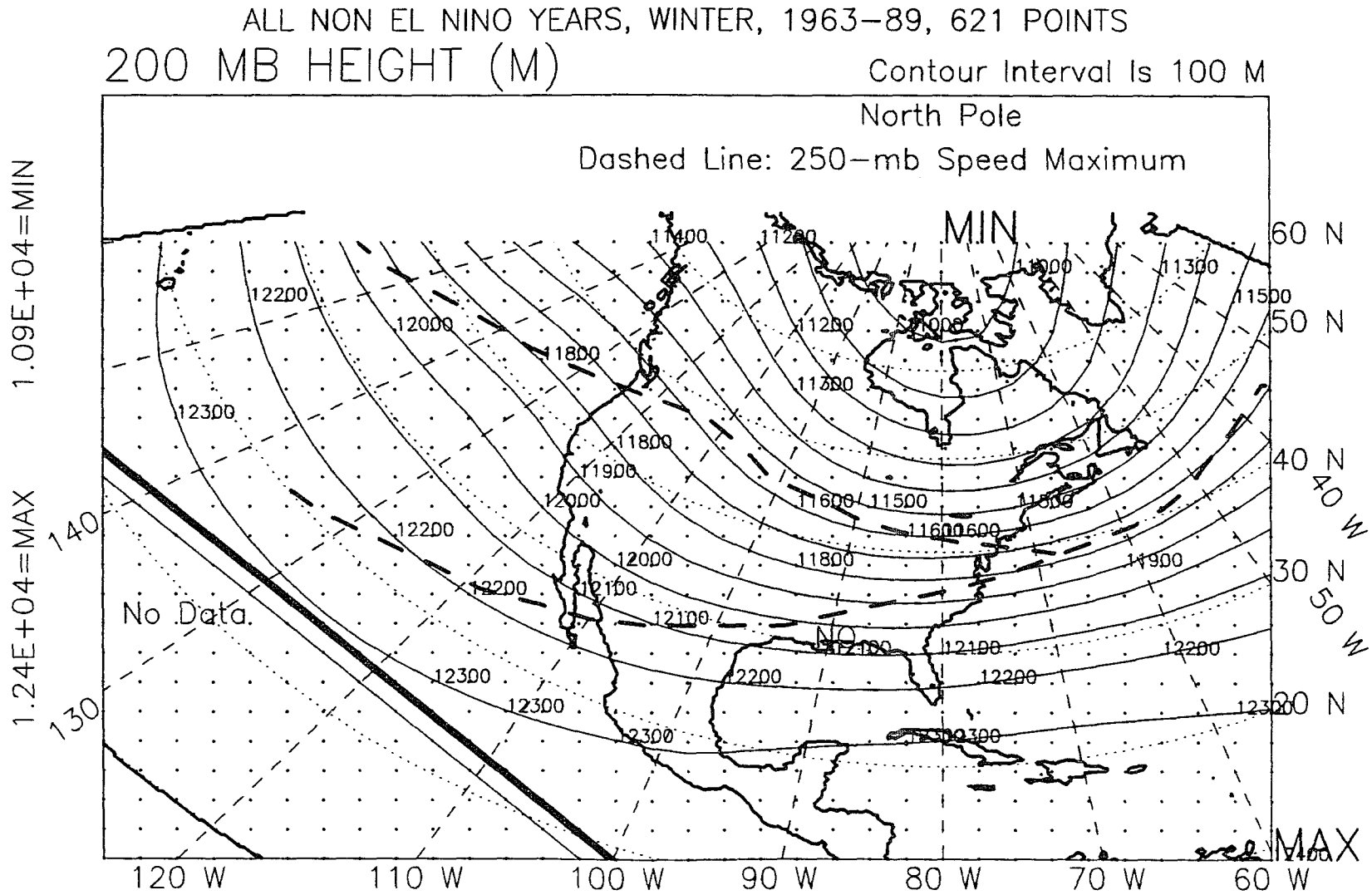

Figure 4.33: 200–mb height, winter, non–El Niño years, 1963–89.

-4 to +14% of the local relief of 350 m (1050 ft). (For comparison, the average height drops over the Aleutian low range from -90 to -30 m (-300 to -100 ft), or -23 to -8% of the 350 m (1150 ft) local relief.) Again, this is evidence of westward tilting with height of the core of maximum, negative height difference. Wallace and Hobbs (1977) provide an example of this at the 200-mb level. Petterssen (1956 p. 350) shows a map of successive, 12-hourly, sea-level positions of the center of a Gulf of Mexico frontal-wave cyclone and associated surface fronts, along with the corresponding location of a 300-mb level trough axis. The upper-level trough always lags behind, is to the west of, the surface low-pressure center.

4.3 Near-Surface Conditions, 850-mb

The three ingredients for increased cyclogenesis in El Niño winters are: a south-displaced, 250-mb level jet, a continuity of low-level troughing up through intermediate and upper levels, and surface conditions predisposed for storm formation. The 850-mb level will be taken as proxy information for surface conditions. The 850-mb level is more convergent in El Niño winters than in non-El Niño winters, as shown in 3.3.3.2, Fig. 3.9. It was also shown in 3.2.4.1 that the winter, mean, 850-mb level winds are such that a small southerly component exists over the Caribbean, southwest of Cuba, in El Niño winters. This is absent (in the seasonal mean) in non-El Niño winters, when winds in that area are nearly due east, Figs. 3.1-3.3. The adjacent region of the Atlantic has a reinforcing southerly wind difference during El Niño winters. It was suggested that the added, southerly component, though small, allows advection of more heat and moisture into the Gulf of Mexico in El Niño winters than in non-El Niño winters, preconditioning the region for increased frequency of cyclogenesis. Crisp and Lewis (1992), citing Rasmussen (1967), state that the moisture flux into the southern United States is at a maximum in Febru-

ary and March. The moisture comes from the Caribbean. Occurring at the time of maximum moisture import, the slight, added, southerly wind component in El Niño winters may make enough difference in surface moisture and heat to explain increased surface cyclogenesis. The 10° eastward shift of the west edge of the Bermuda high in El Niño winters, compared non-El Niño winters, was postulated as at least part of the cause for the change from normally due-east trades over the Caribbean, Fig. 3.2, to slightly south of east, Figs. 3.1 and 3.3. With an eastward shift in the Bermuda high in El Niño winters, the Caribbean is be more distally located, with respect to the center of the high, and so, subject to winds that are not simply flowing outward (due east), but have become deflected toward the north somewhat, producing a slightly south-of-east wind. In locations both near and distal, relative to the center of the high, winds are north-deflected, but theoretically at least, the further from the center of the high, the greater the deflection. The shift of the high must be only part of the reason for the south residue because the high is similarly shifted in spring, with much less added south wind.

All three ingredients must be present concurrently to produce an increase in cyclogenesis in the gulf area. For example, in El Niño springs there is not an increase in storm formation, even though the mean south jet is farther south, Figs. 4.3 and 4.4, and the negative height and temperature differences at intermediate levels are even greater and extend farther southeast than in El Niño winters, appendices B, D, G, H, I, and N. Proper surface conditions are lacking in spring. The 850-mb wind-residue pattern in El Niño springs, Fig. 4.34, is very different from that in El Niño winters, Fig. 3.3. The southerly component of the wind difference, directed gulfward in El Niño winters, is much diminished in El Niño springs. As an aside, the negative height and temperature differences at the 850-, 700-, 500-, and 200-mb levels in El Niño winters are now shown to be not just an effect of increased

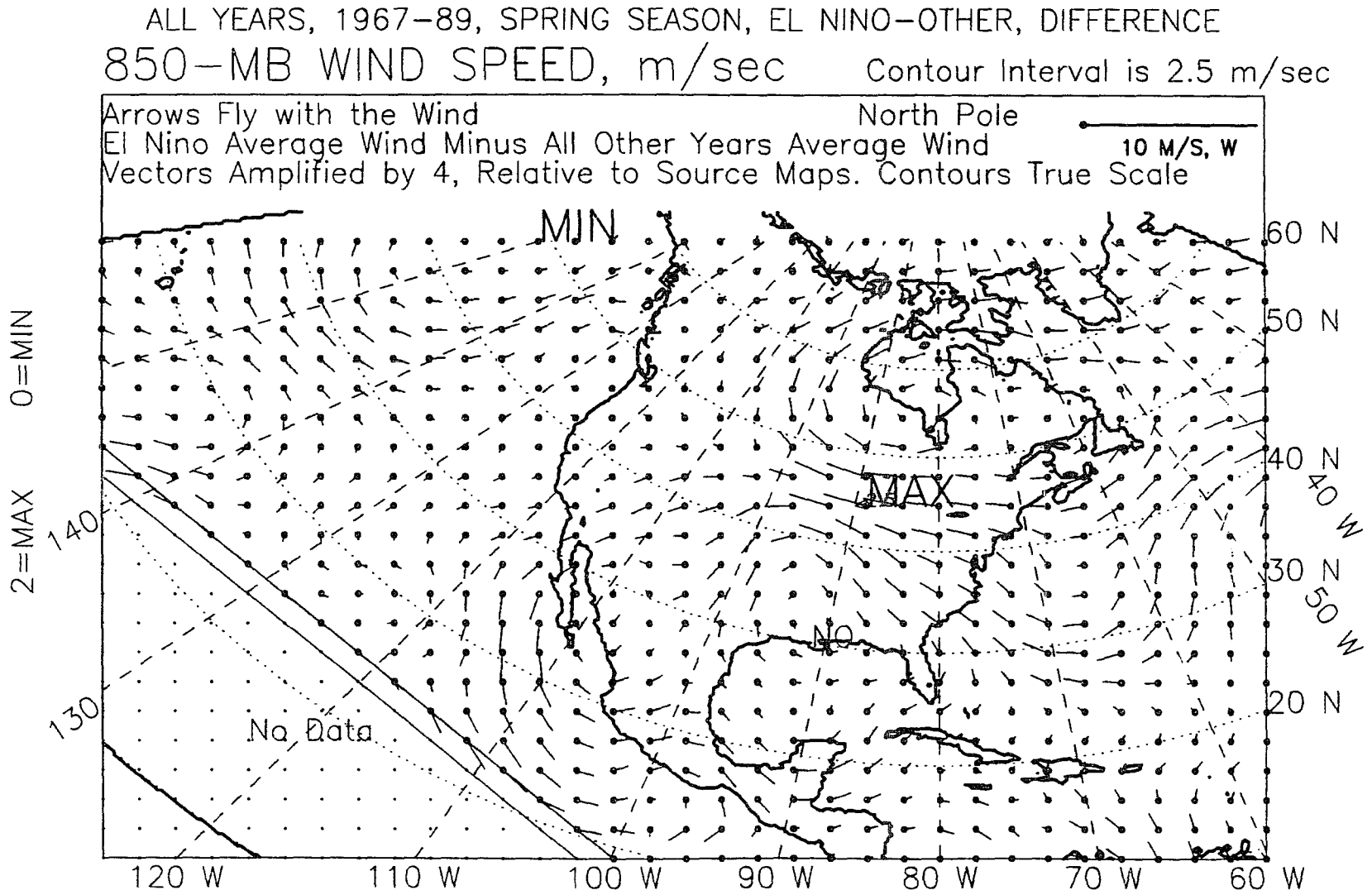

Figure 4.34: 850–mb wind vectors, spring, 1967–89, difference.

cyclogenesis. That they are present when cyclogenesis is not increased, means they are not an effect. It also means that they are not the only cause of increased of storm formation.

In El Niño springs, jet-level conditions are not right either, even though the south jet is farther south in El Niño springs, with respect to both the El Niño-winter position, and to the non-El Niño spring position. The south jet is not as strong in El Niño springs compared to El Niño winters, 33 ms^{-1} (66 kt) compared to 45 ms^{-1} (90 kt). The intensification of the south jet in El Niño springs over non-El Niño springs is less than in winter, 5 ms^{-1} (10 kt) compared to 5 to 10 ms^{-1} (10 to 20 kt), respectively. The area of maximum intensification is south of that in El Niño winters, being over Mexico and the adjacent Pacific, not over the southern United States and the Gulf of Mexico.

CHAPTER 5
FRONTAL-WAVE CYCLONES AND COLD FRONTS: 1940-89

5.1 Frontal-Wave Cyclones and Cold Fronts, 1940-89: El Niño and La Niña Trends

This chapter presents results for a 50-year period, 1940 to 1989, that correspond to those presented in 2.1.5, for the frontal-wave cyclone and cold-front counts. Results corresponding to those in 2.4 for frontal-wave cyclone characteristics, are also presented for the last 50 years. Some trends over time are considered last.

Although 30 years is a standard climatological period (Kunkel and Court 1990), the longer-term study was done for two reasons. First, it is recognized that the last decade, 1981 to 1990, was unusually warm (Halpert and Ropelewski 1992b). According to these authors, most Northern Hemisphere land areas had above-normal temperatures, with respect to the 1951 to 1980 base period. Many of the above-normal temperatures occurred in winter and spring, December to May. The southeastern United States was drier than average during spring, March to May, of the 1980's. Perhaps this unusual decade influenced the frontal-wave cyclone- and cold-front totals during the 1980's. Second, adding more years allowed the inclusion of ten El Niño events and ten La Niña events, double the number of El Niño events in the 1960 to 1989 segment, and adding two more La Niña events, Tables 1.1 and 1.2. 915 frontal-wave cyclones were counted between 1940 and 1989; 524 occurred from 1960 to 1989. 2991 cold fronts were counted between 1940 and 1989; 1722 of them occurred between 1960 and 1989.

During the last 50 years, winter was again the season with most frontal-wave cyclones originating over the gulf area, Fig. 5.1. Their distribution by water depth was again equally divided between coastal plain, shelf, and slope, Fig. 5.2. Compare to Figs. 2.1 and 2.3. The locations of origin of the 915 storms over the last 50 years appear in appendix S.

Tables 5.1 to 5.4 present for 1940 to 1989: frontal-wave cyclone and cold-front frequencies, water depth or land elevation of estimated point of origin of frontal-wave cyclones, latitude and longitude of origin of frontal-wave cyclones, and lowest central pressure of frontal-wave cyclones, attained while over the gulf area. Table 5.5 is a summary of just the statistically significant (.01 or .05 confidence level) quantities out of the preceding four tables. The results of the long and short time periods agree well; winter results are the most stable.

5.1.1 Frequency of Frontal-Wave Cyclones: El Niño and La Niña Trends, 1940-89 vs 1960-89

From 1940 to 1989, significantly more frontal-wave cyclones occurred in winter and in fall of El Niño years than in non-El Niño years, significant at the .05 confidence level, Table 5.1. From Table 2.1, between 1960 and 1989, there were more frontal-wave cyclones in winter of El Niño years (.01 level) and in El Niño winter years (.05 level) than in non-El Niño years. From 1960 to 1989, the fall increase is almost significant at the .05 level, and the winter-year increase is 'just barely' significant at the .05 level. The winter-season increase in the frequency of frontal-wave cyclones in El Niño years is common to both time periods.

From 1940 to 1989, significantly fewer frontal-wave cyclones occurred in La Niña winter years, in the combined season, winter-plus-spring, and in winter than in non-La Niña years, Table 5.1. All are significant at the .01 level. This is the same as

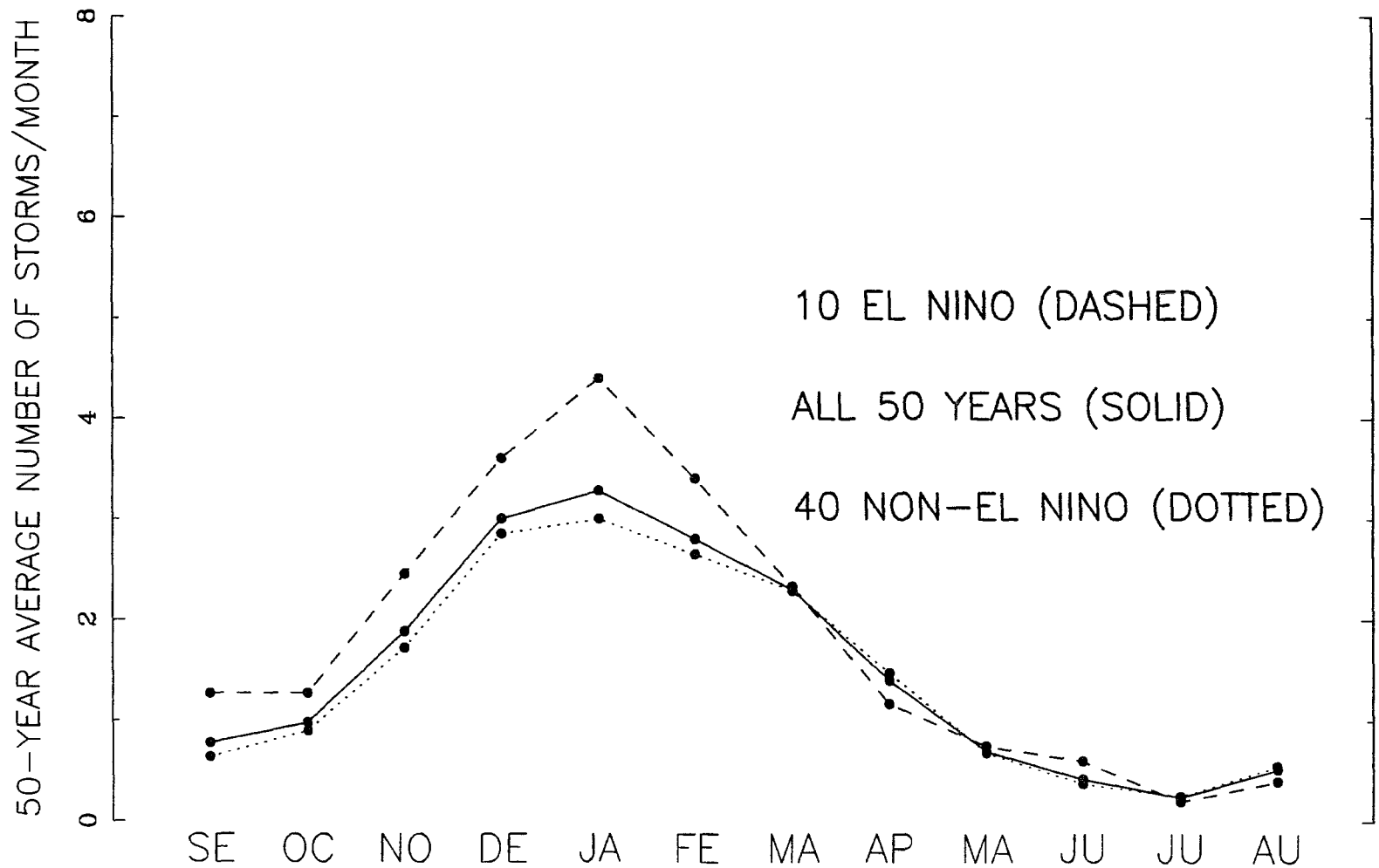

Figure 5.1: 50-year average number of storms/month, 1940-89, El Niño, non-El Niño, and all years.

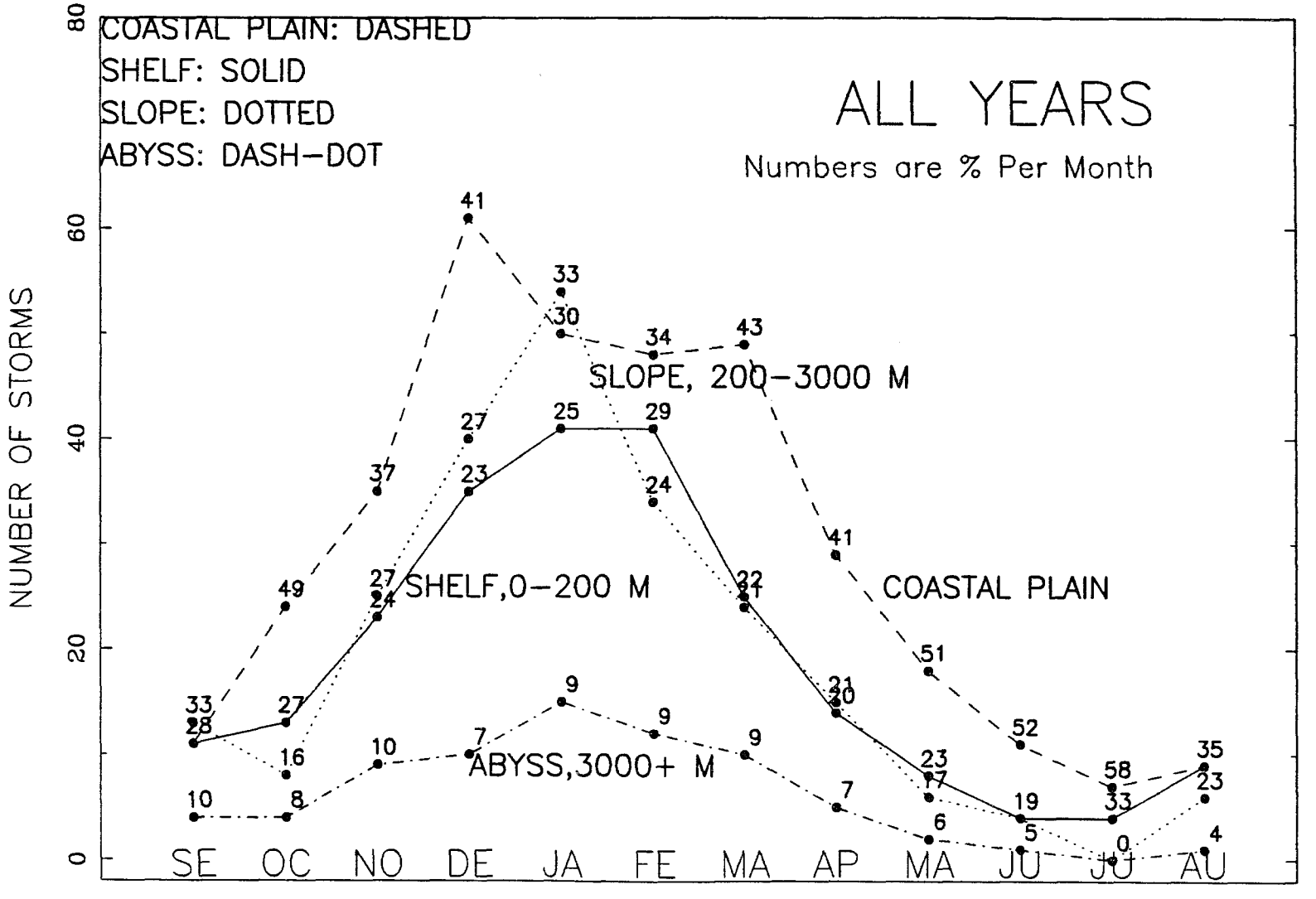

Figure 5.2: Storms/month, by water depth, Sept. 1940 – Aug. 1990, all years.

Table 5.1: Frequency of frontal-wave cyclones and cold fronts in El Niño and La Niña years, 1940-1989. Results of the rank sum test, also known as the U-test, Wilcoxon test, or Mann-Whitney test, for differences between El Niño and normal years. z-values are listed for test of the hypothesis that values for the listed parameters vary between El Niño and other years or La Niña years and other years. Two levels of significance are indicated by daggers, $\alpha = .01$, reject the null hypothesis if $z > 2.575$ or $z < -2.575$. $\alpha = .05$, reject the null hypothesis if $z > 1.960$ or $z < -1.960$.

El Niño

			Number of Events		Means	
Season	Time	z	El Niño	Other	El Niño	Other
Frontal-Wave Cyclones						
winteryear	1940-89	1.862	10	40	22	17
winter+spring	1941-90	1.235	10	40	16	13
winter †	1941-90	2.053	10	40	11	9
spring	1941-90	-0.035	12	38	4	4
summer	1941-90	-0.152	10	40	1	1
fall †	1940-89	2.149	11	39	5	3
Cold Fronts						
winteryear	1940-89	-1.749	10	40	57	61
winter+spring †	1941-90	-2.009	10	40	35	38
winter	1941-90	-1.459	10	40	19	20
spring	1941-90	-0.172	12	38	17	17
summer	1941-90	-0.110	10	40	7	7
fall	1940-89	-1.227	11	39	15	16

La Niña

			Number of Events		Means	
Season	Time	z	La Niña	Other	La Niña	Other
Frontal-Wave Cyclones						
winteryear ‡	1940-89	-3.030	10	40	13.3	19.5
winter+spring ‡	1941-90	-3.314	10	40	9.4	14.5
winter ‡	1941-90	-3.495	10	40	5.8	9.9
spring	1941-90	-0.213	11	39	4.5	4.4
summer	1941-90	-0.507	10	40	0.9	1.3
fall	1940-89	-1.562	10	40	2.7	3.9
Cold Fronts						
winteryear	1940-89	-0.328	10	40	60	60
winter+spring	1941-90	-0.645	10	40	36	37
winter	1941-90	-0.331	10	40	20	20
spring	1941-90	-0.567	11	39	17	17
summer	1941-90	-1.261	10	40	6	7
fall	1940-89	-0.354	10	40	16	16

Notes:

‡ : indicates null hypothesis can be rejected at the .01 level of significance.

† : indicates null hypothesis can be rejected at the .05 level of significance.

the 1960 to 1989 result, Table 2.2, except the significance level is just .05 for the 30-year data set in winter years and in winter-plus-spring.

5.1.2 Frequency of Cold Fronts: El Niño and La Niña Trends, 1940-89 vs 1960-89

From 1940 to 1989 there were fewer cold fronts in the combined, winter-plus-spring season in El Niño years than in non-El Niño years, significant at the .05 level, Table 5.1. This is down from the 1960 to 1989 results, in which there are fewer cold fronts, not only in winter-plus-spring (.01 level) of El Niño years as opposed to non-El Niño years, but also in winter year (.01) and in winter season (.05).

The La Niña results are the same for the 1940 to 1989 period as for 1960 to 1989. No La Niña season shows a significantly different number of cold fronts compared to non-La Niña seasons, Tables 5.1 and 2.2.

5.1.3 Frontal-Wave Cyclone Characteristics: El Niño and La Niña Trends, 1940-89 vs 1960-89

5.1.3.1 Latitude and Longitude of Origin of Frontal-Wave Cyclones, 1940-89 vs 1960-89

From 1940 to 1989, in El Niño years, the locations of origin of frontal-wave cyclones were significantly farther south in winter and in winter-plus-spring (.05 level), Table 5.2. The result was the same between 1960 and 1989, with the addition that the locations of storm origin were farther south in El Niño winter years, significant at the .01 level, Table 2.11.

For La Niña years, the 50-year results are the same as the 30-year results. The latitude of origin is significantly farther north in winter of La Niña years than in winter of non-La Niña years, Tables 5.2 and 2.11. In neither time period was there

Table 5.2: Average latitude and longitude of frontal-wave cyclones in El Niño and in La Niña years, 1940-89; results of the rank sum test, also known as the U-test, Wilcoxon test, or Mann-Whitney test, for differences between El Niño and non-El Niño years, and between La Niña and non-La Niña years. Latitudes and longitudes listed are those at the point where a storm was first observed on the weather map. This is the closest point identifiable on 24-hour maps to the point of origin. Latitudes and longitudes were measured to the nearest half degree, therefore the averages listed are beyond the range of accuracy and are only for display. The number of observations is the number of storms in each season, not the number of years analyzed. z-values are used to test significance since the number of observations is always greater than 30. Reject the null hypothesis at the $\alpha = .01$ level if $z > 2.575$ or $z < -2.575$. For $\alpha = .05$, reject the null hypothesis if $z > 1.960$ or $z < -1.960$. Levels of significance are indicated by daggers, $\alpha = .01$, double dagger; $\alpha = .05$, single dagger.

El Niño Versus Non-El Niño Years

		Average Latitude			Average Longitude			# of Storms
Season	Time	El	Non	z	El	Non	z	El/Non
winteryear	1940-89	28.4	28.7	-1.884	91.5	91.1	1.248	218/697
wntr+sprng	1941-90	28.2	28.7	-2.362 †	92.0	91.7	0.893	155/519
winter	1941-90	27.9	28.6	-2.432 †	91.8	91.9	0.007	114/340
spring	1941-90	29.2	29.0	0.743	91.9	91.4	0.452	51/169
summer	1941-90	29.5	29.7	-0.228	87.2	87.9	-0.538	12/47
fall	1940-89	28.2	28.6	-1.330	90.3	90.4	-0.049	55/127

La Niña Versus Non-La Niña Years

		Average Latitude			Average Longitude			# of Storms
Season	Time	La	Non	z	La	Non	z	La/Non
winteryear	1940-89	29.0	28.6	1.288	91.2	91.2	-0.181	133/782
wntr+sprng	1941-90	29.1	28.6	1.392	92.1	91.7	0.563	94/580
winter	1941-90	29.2	28.3	2.279 †	92.4	91.8	0.807	58/396
spring	1941-90	29.1	29.1	0.098	91.5	91.5	0.040	49/171
summer	1941-90	28.8	29.8	-1.381	87.6	87.8	-0.496	9/50
fall	1940-89	29.1	28.4	1.237	90.7	90.3	0.501	27/155

‡ : indicates null hypothesis can be rejected at the .01 level of significance.
† : indicates null hypothesis can be rejected at the .05 level of significance.

a bias in the longitude of location of origin between El Niño and non-El Niño years, or between La Niña and non-La Niña years, in any season, Tables 5.2 and 2.11.

5.1.3.2 Water Depth or Land Elevation of Origin of Frontal-Wave Cyclones, 1940-89 vs 1960-89

In El Niño years, frontal-wave cyclones originate over significantly deeper water (lower land elevation) in winter (.01 level of significance) and in winter-plus-spring (.05 level) than in non-El Niño years, Table 5.3. The 1960 to 1989 result is the same, Table 2.10, except the 30-winter result is only significant at the .05 level.

In La Niña winters from 1940 to 1989, the water depth of origin is significantly shallower (.05 level) in winter than in non-La Niña winters, Table 5.3. The 1960 to 1989 results are the same, Table 2.10.

5.1.3.3 Lowest Central Pressure of Frontal-Wave Cyclones, 1940-89 vs 1960-89

Between 1940 and 1989, the lowest central pressure attained by frontal-wave cyclones while over the gulf, was significantly lower in winter, spring, and in winter-plus-spring of El Niño years, as compared to non-El Niño years, Table 5.4. This is better than from 1960 to 1989. From 1960 to 1989, only winter storms of El Niño years had lower central pressure than non-El Niño years, although winter-plus-spring and spring were close, Table 2.9.

For La Niña years between 1940 and 1989, no season had significantly different lowest central pressure than in non-La Niña years. Although in winter and in winter years during 1960 to 1989, La Niña-year frontal-wave cyclones had significantly higher lowest central pressure than in non-La Nña years.

Table 5.3: Water depth or land elevation (m) of frontal-wave cyclones in El Niño and in La Niña years, 1940-89; results of the rank sum test, also known as the U-test, Wilcoxon test, or Mann-Whitney test, for differences between El Niño and non-El Niño years, and between La Niña and non-La Niña years. Water depths(elevations) listed are those at the point where a storm was first observed on the weather map. It is the closest point identifiable to the point of origin. The number of observations is the number of storms in each season, not the number of years analyzed. z-values are used to test significance since the number of observations is always greater than 30. Reject the null hypothesis at the $\alpha = .01$ level if $z > 2.575$ or $z < -2.575$. For $\alpha = .05$, reject the null hypothesis if $z > 1.960$ or $z < -1.960$. Levels of significance are indicated by daggers, $\alpha = .01$, double dagger; $\alpha = .05$, single dagger.

El Niño Versus Non-El Niño Years

		Average Water Depth or Land Elevation (m)			# of Storms	
Season	Time	El Niño	Other	z	ElNiño	Other
winteryear	1940-89	-694	-612	-0.715	168	747
winter+spring †	1941-90	-835	-579	-2.471	155	519
winter ‡	1941-90	-869	-627	-2.600	114	340
spring	1941-90	-571	-523	0.936	51	169
summer	1941-90	-169	-339	0.725	12	47
fall	1940-89	-781	-654	-1.183	55	127

La Niña Versus Non-La Niña Years

		Average Water Depth or Land Elevation (m)			# of Storms	
Season	Time	La Niña	Other	z	LaNiña	Other
winteryear	1940-89	-504	-656	1.115	173	742
winter+spring	1941-90	-548	-652	1.327	94	580
winter †	1941-90	-454	-722	2.357	58	396
spring	1941-90	-382	-578	0.744	49	171
summer	1941-90	-125	-337	-1.949	9	50
fall	1940-89	-451	-734	0.622	27	155

Notes:

‡ : indicates null hypothesis can be rejected at the .01 level of significance.

† : indicates null hypothesis can be rejected at the .05 level of significance.

Table 5.4: Lowest central pressure (mb) in frontal-wave cyclones in El Niño and in La Niña years, 1940-89; results of the rank sum test, also known as the U-test, Wilcoxon test, or Mann-Whitney test, for differences between El Niño and non-El Niño years, and between La Niña and non-La Niña years. Pressures listed are averages of the lowest central pressure observed on the weather map during a storm's duration, usually occurring on the first day. The number of observations is the number of storms in each season, not the number of years analyzed. z-values are used to test significance since the number of observations is always greater than 30. Reject the null hypothesis at the $\alpha = .01$ level if $z > 2.575$ or $z < -2.575$. For $\alpha = .05$, reject the null hypothesis if $z > 1.960$ or $z < -1.960$. Levels of significance are indicated by daggers, $\alpha = .01$, double dagger; $\alpha = .05$, single dagger.

El Niño Versus Non-El Niño Years

		Average Lowest Pressure(Std.Dev.)			# of Storms	
Season	Time	El Niño	Other	z	El	Non
winteryear	1940-89	1010.3(5.5)	1011.1(5.0)	-1.215	218	697
winter+spring †	1941-90	1009.6(6.0)	1011.1(5.1)	-2.225	155	519
winter †	1941-90	1010.5(5.9)	1012.1(5.1)	-2.170	114	340
spring dag	1941-90	1007.4(4.7)	1009.2(4.5)	-2.336	51	169
summer	1941-90	1011.0(4.3)	1012.2(3.5)	-0.801	12	47
fall	1940-89	1011.6(4.2)	1010.9(4.4)	0.976	55	127

La Niña Versus Non-La Niña Years

		Average Lowest Pressure(Std.Dev.)			# of Storms	
Season	Time	La Niña	Other	z	La	Non
winteryear	1940-89	1011.4(5.0)	1010.8(5.1)	0.879	133	782
winter+spring	1941-90	1011.6(4.9)	1010.6(5.4)	1.335	94	580
winter	1941-90	1012.7(5.0)	1011.6(5.4)	1.115	58	396
spring	1941-90	1009.5(4.5)	1008.6(4.8)	1.067	49	171
summer	1941-90	1010.7(3.4)	1012.2(3.7)	-1.360	9	50
fall	1940-89	1010.2(5.9)	1011.3(4.0)	-0.873	27	155

Notes:

‡ : indicates null hypothesis can be rejected at the .01 level of significance.

† : indicates null hypothesis can be rejected at the .05 level of significance.

Table 5.5: Storms and cold fronts, 1940-89: summary of all parameters significant at the .01 or .05 confidence level. A blank indicates the parameter was not significant at either level.

	El Niño		La Niña		
	Value	Conf. Level	Value	Conf. Level	Time
Frontal-Wave Cyclone Frequency					
Frontal-Wave Cyclones/winteryear			Low	.01	40-89
Frontal-Wave Cyclones/winter+spring			Low	.01	41-90
Frontal-Wave Cyclones/winter	High	.05	Low	.01	41-90
Frontal-Wave Cyclones/fall	High	.05			41-90
Frontal-Wave Cyclone Traits					
Water Depth of Origin/winter	Deep	.01	Less	.05	41-90
Water Depth of Origin/winter+spring	Deep	.05			41-90
Lowest Central Pressure/winter	Low	.05			41-90
Lowest Central Pressure/spring	Low	.05			40-89
Lowest Central Pressure/winter+spring	Low	.05			41-90
Latitude of Origin/winter	South	.05	North	.05	41-90
Latitude of Origin/winter+spring	South	.05			41-90
Cold-Front Frequency					
Cold fronts/winter+spring	Low	.05			41-90

A summary of just the statistically significant (.01 or .05 confidence level) quantities out of the preceding four tables is presented in Table 5.5. Compare it to Table 2.12 for 1960 to 1989.

5.2 Trends over Time

5.2.1 Numbers of Frontal-Wave Cyclones Originating over the Gulf Area: 1960-89 Compared to 1940-89

5.2.1.1 Increase in the Number of Storms, 1960-89

The number of frontal-wave cyclones per winter year from 1960 to 1989 appears in Fig. 5.3, divided into 5 El Niño years, all 30 years, and 25 non-El Niño years. To test the significance of the apparent increase from 1960 to 1989 in the number of storms per winter year, three best-fit, linear regression lines were prepared. The 25 non-El Niño years in the period, *all* 30 years and just the five El Nino years were analyzed

as three separate groups, with resulting correlation coefficients, r, (Anderson and Sclove 1974) of 0.53, 0.56 and 0.91 respectively. The statistical significance of the slopes of the regression lines was obtained by the Student's t-test (Hoel 1962). For the 25 non-El Niño years, the t-value of 3.018, with 23 degrees of freedom, leads to the acceptance at the .01 confidence level of the hypothesis that the number of frontal-wave cyclones occurring over the gulf region per winter year is increasing during the 25 years used from the period of 1960 to 1989. For all 30 years, from 1960 to 1989, the t-value of 3.620 leads to the same conclusion, at the .01 confidence level. The five El Niño years also show an increase, significant at the .05 confidence level, the t-value being 3.810. The three separate analyses were done in an attempt to remove the effect of El Niño from the long-term trend. As noted in an early review of the work, there are more El Niño events in the second half of the time series than in the first. This might be suspected as the cause of the increase in the number of storms over the period because of the increase in the frequency of winter storms during El Niño years, 2.1.5. Based on the similarity of the correlation coefficients and t-values for just the 25 non-El Niño winter years and all 30 years, the increase over the period seems to be independent of the effect of El Niño, and genuine, subject to the limitations of the data already noted in 2.1.4. What is surprising, is that the number of storms per winter year in the five El Niño years is increasing at a greater rate than the other winter years. Table 5.6 shows, for each season, results of the same test for increase or decrease over the last 30 years. Most of the seasons show the same pattern as the winter year, with stronger increases in El Niño years than in other years. However, the only increases significant at the .01 or .05 levels, occur in spring and summer. Therefore, the increase in storms during El Niño winter years is not likely due to an intensification, over the period, of the El Niño winter-storm effect, but to an increase in spring and summer cyclogenesis. Spring and summer increases must be independent of El Niño since there there is

no tendency for more storms to occur in spring or summer of El Niño years over the gulf area, Table 2.1.

It might be argued that the increase in the number of storms shown by this data is the effect of an expanding control network over the period of record. It is certainly true that more and better synoptic data have become available over the period 1960-89, notably with the introduction of satellite observations. It is equally likely, however, that an explanation for the increase in storm frequency over the period will be found in changing synoptic weather patterns, forced by broader scale climate change, such as global warming. For example, the unusually warm temperatures of the 1980's (Ropelewski and Halpert 1992) may be forcing the increase in some way.

Whittaker and Horn (1982) using NMC extratropical cyclone-track maps for 1958 to 1977, reported annual cyclogenesis counts for the entire North American sector, 150° to 50°W and 20° to 80°N. Over the whole area, they found a statistically significant decrease, $r = -0.73$, in the annual, calendar year, frequency of cyclogenesis, with January and July showing the greatest drops. They reported that most of the decrease was north of 40°N. They examined three cyclogenetically-active areas individually, Alberta, Colorado and the east coast of the United States. A decrease was found in Alberta and east coast storms, but no trend was found in the Colorado data. Citing previous studies, (Klein 1957; Pettersen 1956) Whittaker and Horn note that if the entire Northern Hemisphere is examined, no decrease is found, and conclude that decrease in cyclogenesis in some areas is compensated for by an increase in other areas. From the present results, it would seem that the Gulf of Mexico region is one such area of compensating increase, at least between 1960 and 1989.

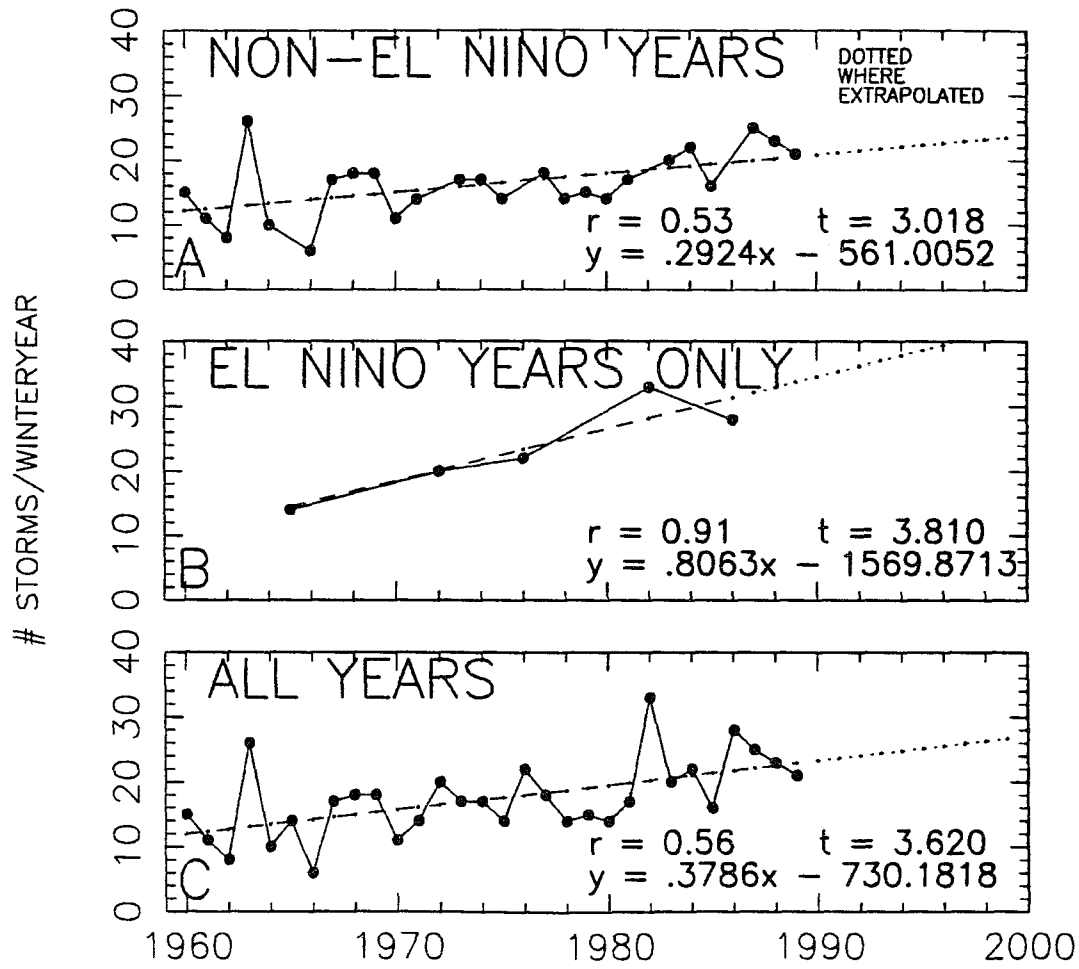

Figure 5.3: Number of frontal-wave cyclones per winter year, increasing from 1960 to 1989; (A) 25 non-El Niño, (B) 5 El Niño, (C) all 30 years. El Niño r significant at the .05 level, others, .01.

Table 5.6: Tests for trends over time: frontal-wave cyclones, 1960 to 1989 and 1940 to 1989. Correlation coefficient, r, and t-values and probabilities to test the null hypothesis that the slope of the linear regression line is zero. Two levels of significance, .01 and .05, are shown by the double and single daggers.

Season		Group	r	Student's t	Probability §
Frontal-Wave Cyclones, 1960-89					
Winteryear	†	El Niño	.91	3.810	.0317
	‡	Other	.53	3.018	.0061
	‡	All years	.56	3.620	.0012
Winter+spring		El Niño	.85	2.749	.0707
		Other	.35	1.782	.0879
	†	All years	.43	2.535	.0171
Winter		El Niño	.76	2.035	.1347
		Other	.16	0.775	.4460
		All years	.26	1.426	.1648
Spring	†	El Niño	.87	3.455	.0259
	†	Other	.44	2.313	.0305
	‡	All years	.50	3.031	.0052
Summer		El Niño	.35	0.653	.5606
	†	Other	.47	2.532	.0186
	†	All years	.43	2.528	.0174
Fall		El Niño	.61	1.320	.2785
		Other	.29	1.459	.1582
		All years	.36	2.016	.0535
Frontal-Wave Cyclones, 1940-89					
Winteryear		El Niño	.49	1.592	.1501
		Other	-.04	-0.247	.8060
		All years	.05	0.369	.7137
Winter+spring		El Niño	.52	1.701	.1273
		Other	-.13	-0.834	.4097
		All years	.01	0.046	.9638
Winter	‡	El Niño	.77	3.412	.0092
		Other	-.24	-1.511	.1391
		All years	-.03	-0.231	.7324
Spring		El Niño	-.04	-0.111	.9138
		Other	.11	0.668	.5085
		All years	.07	0.473	.6384
Summer		El Niño	-.39	-1.190	.2681
	†	Other	.38	2.520	.0161
		All years	.22	1.579	.1208
Fall		El Niño	.35	1.111	.2955
		Other	-.05	-0.286	.7765
		All years	.01	0.061	.9514

§: The significance level, α. Probability that you will be wrong if you reject the null hypothesis and conclude that there is a trend of increase(decrease) over time.

5.2.1.2 No Increase in the Number of Storms, 1940-89

The number of frontal-wave cyclones per winter year from 1940 to 1989 appears in Fig. 5.4, divided into ten El Niño years, all 50 years, and 40 non-El Niño years. Over the whole 50-year period, there is no statistically significant increase or decrease in the number of frontal-wave cyclones originating over the gulf area per winter year, as was seen for only the last 30 years. The breakdown by seasons appears in the lower half of Table 5.6 and follows the pattern of the winter years with the exception of El Niño-year, winter-season storms. From 1940 to 1989, El Niño-year, winter-season storms increased, significant at the .01 confidence level. During only the last 30 years, gulf-area, winter-storm increases in El Niño years are only significant at the .13 level, although the two correlation coefficients are almost the same, 0.76 and 0.77. Perhaps over the 50-year period, there has been intensification in the El Niño-year, winter-storm effect, but if so, it must have been strongest before 1960.

Comparing these results to other long-term cyclogenesis counts, Reitan (1979) found a decrease in cyclone activity over North America from 1949 to 1976. Hosler and Gamage (1956) found no trend over the 50 years from 1905 to 1954 in the frequency of cyclogenesis over just the contiguous United States. To the extent that they are comparable, both of these are consistent with the present results. Reitan's decrease from 1949 to 1976 may be indicative of the decrease prior to 1960 inferred from the present data, which has flattened out the storm counts over the 50-year term.

5.2.2 Numbers of Cold Fronts Reaching the Gulf Area: 1960-89 Compared to 1940-89

The number of cold fronts reaching the gulf region during the 30- and 50-year periods was analysed in the same way as the frontal-wave cyclones, Figs. 5.5 and 5.6

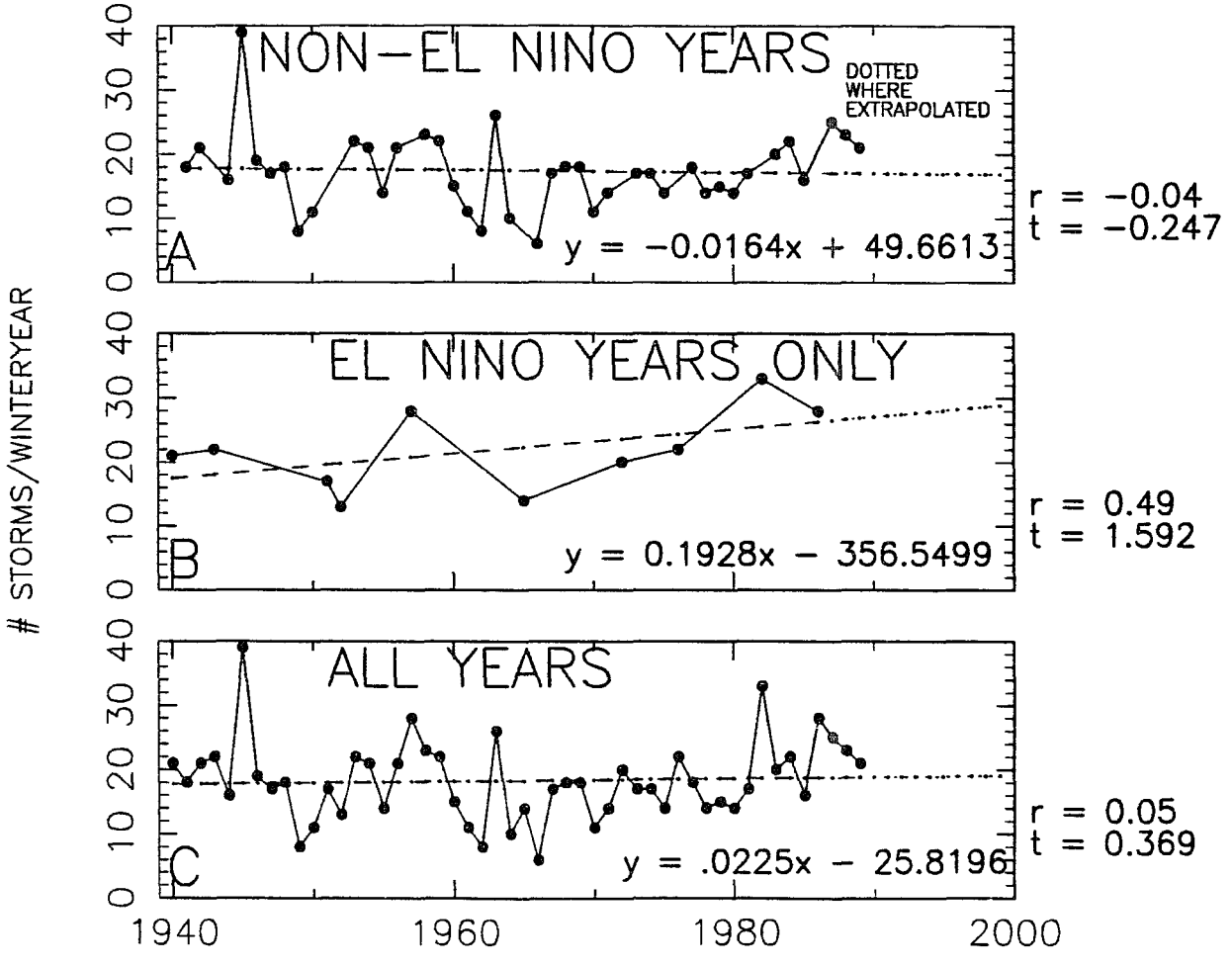

Figure 5.4: Number of frontal–wave cyclones per winter year, 1940–89; (A) 40 non–El Niño, (B) 10 El Niño, (C) all 50 years. El Niño r significant at .15 level.

and Table 5.7. The results were almost the opposite of the storm results. Over the last 30 years, the number of cold fronts reaching the area has remained flat, but over the last 50 years, a significant decrease (.01 or .05 level) has occurred annually and in all seasons but fall. The 1960 to 1989 increase in the number of storms originating over the gulf region has not been accompanied by a significant change in the number of cold fronts reaching the area. And the long-term drop in the incidence of cold fronts has not been accompanied by concurrent change in the number of storms originating here.

This is not the first instance in which the present data has shown apparent independence in the winter occurrence of frontal-wave cyclones and cold fronts in the gulf area. The same trend was seen in regard to the occurrence of each in El Niño and La Niña years between 1960 and 1989, and between 1940 and 1989. The increase in storms in El Niño winters is accompanied by a decrease in the number of cold fronts coming to the gulf area, Tables 2.1 and 5.1. The decrease in the number of storms in La Niña winters is accompanied by no significant difference, at any reasonable level, in the number of cold fronts, from the direct cold-front counts, Tables 2.2 and 5.1. The weather-type data, from 1961 to 1990, however, seems to indicate a winter-season increase in the frequency of cold front-associated weather types, yielding not an independent relationship between storms and cold fronts, but one that is indirectly proportional, Table 2.4. At least the seasonal abundances of storms and cold fronts parallel each other; both peak in the winter months, Figs. 2.1 and 2.2.

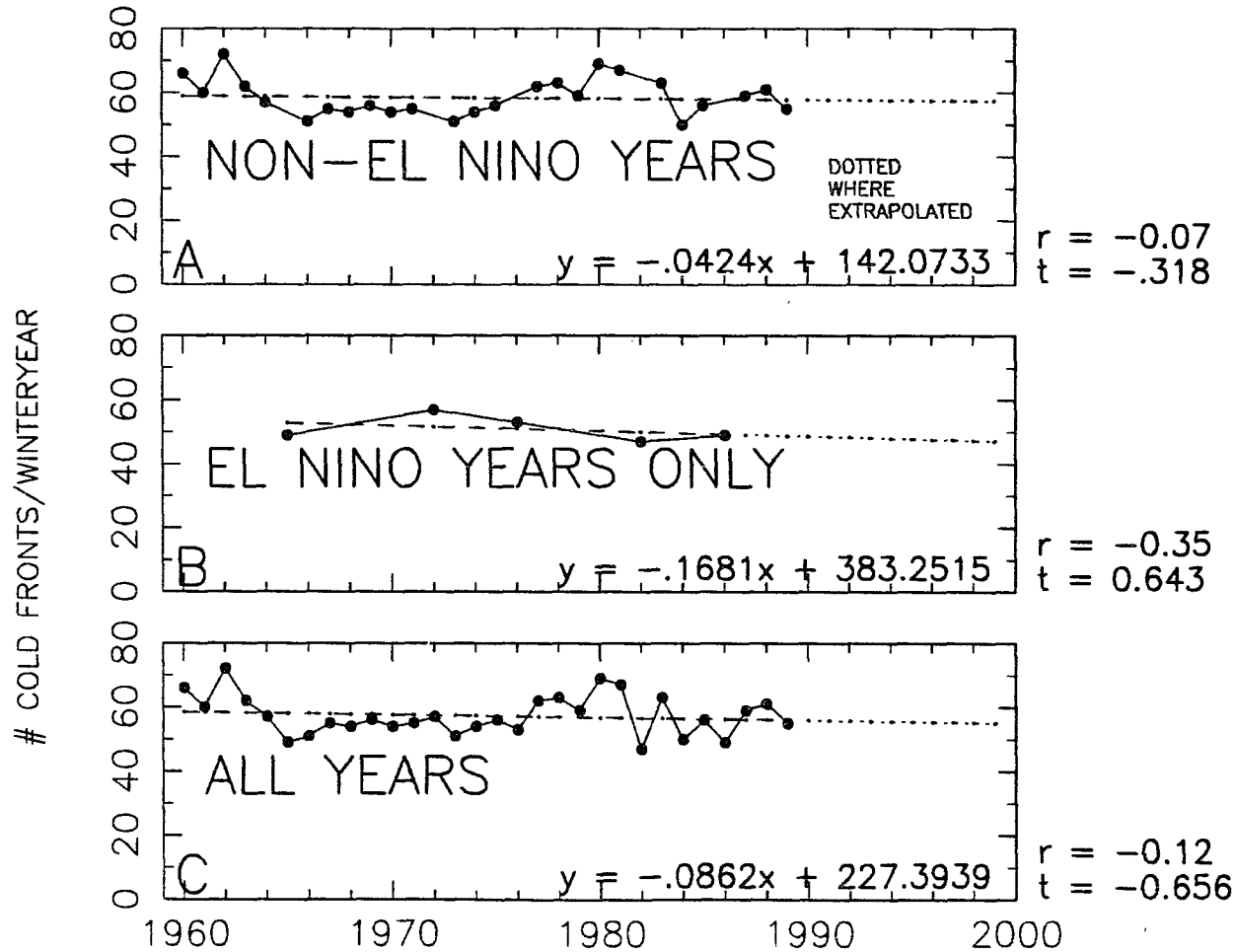

Figure 5.5: Number of cold fronts per winter year, from 1960 to 1989; (A) 25 non-El Niño, (B) 5 El Niño, (C) all 30 years.

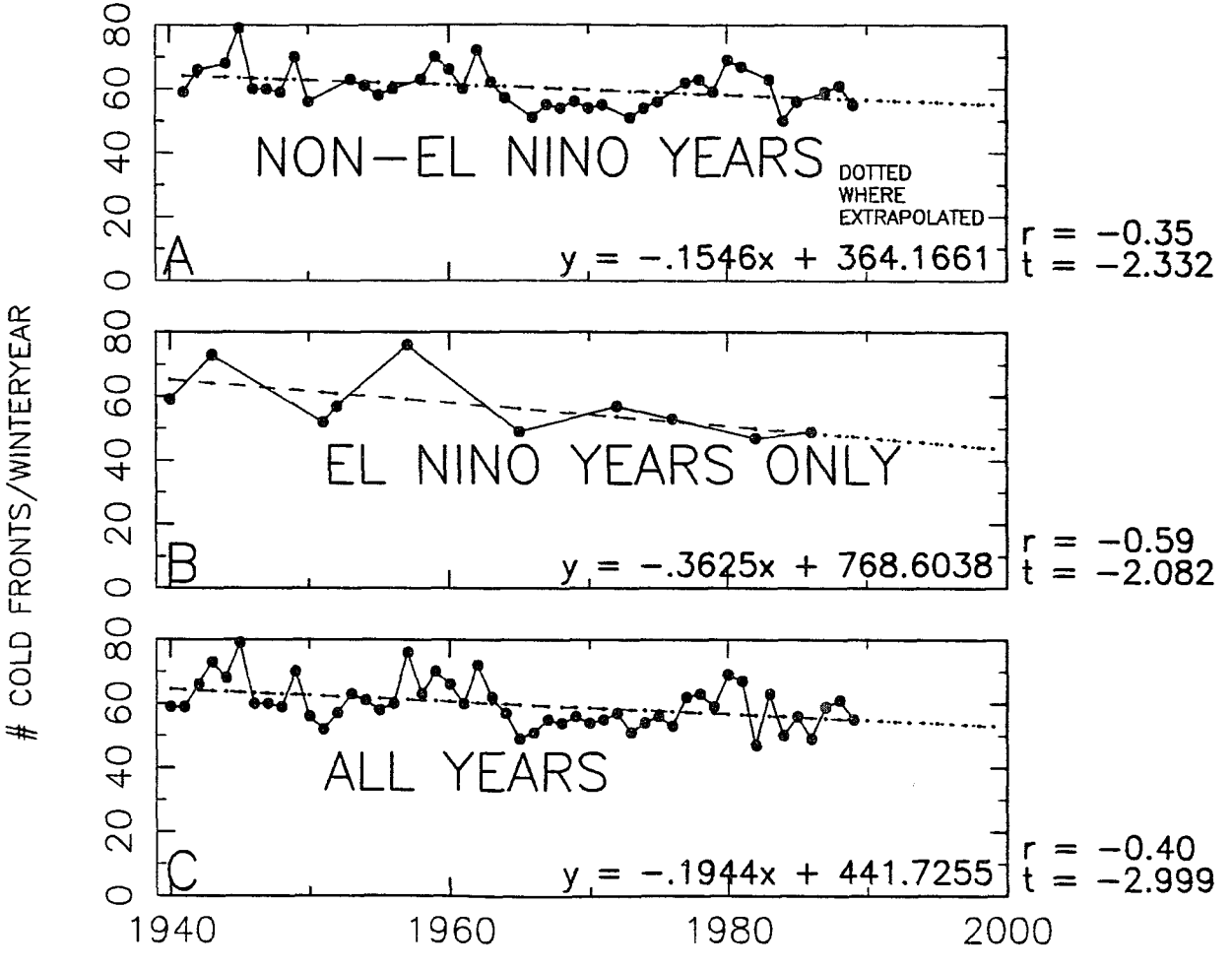

Figure 5.6: Number of cold fronts per winter year, 1940–89; (A) 40 non–El Niño, (B) 10 El Niño, (C) all 50 years. El Niño r significant at .07 level, others at the .01 and .05 levels.

Table 5.7: Tests for trends over time: cold fronts, 1960 to 1989 and 1940 to 1989. Correlation coefficient, r, and t-values and probabilities to test the null hypothesis that the slope of the linear regression line is zero. Two levels of significance, .01 and .05, are shown by the double and single daggers.

Season		Group	r	Student's t	Probability §
Cold Fronts, 1960-89					
Winteryear		El Niño	-.35	-0.643	.5659
		Other	-.07	-0.318	.7532
		All years	-.12	-0.656	.5174
Winter+spring		El Niño	-.63	-1.397	.2567
		Other	-.12	-0.579	.5679
		All years	-.18	-0.991	.3298
Winter		El Niño	.07	0.117	.9146
		Other	-.34	-1.734	.0963
		All years	-.30	-1.677	.1046
Spring		El Niño	-.63	-1.613	.1820
		Other	.27	1.296	.2084
		All years	.07	0.352	.7272
Summer		El Niño	-.49	-0.962	.4071
		Other	-.09	-0.416	.6813
		All years	-.14	-0.729	.4718
Fall		El Niño	.56	1.176	.3242
		Other	.05	0.220	.8278
		All years	.06	0.328	.7456
Cold Fronts, 1940-89					
Winteryear		El Niño	-.59	-2.082	.0709
	†	Other	-.35	-2.332	.0251
	‡	All years	-.40	-2.999	.0043
Winter+spring	†	El Niño	-.65	-2.419	.0419
	‡	Other	-.40	-2.729	.0096
	‡	All years	-.44	-3.421	.0013
Winter		El Niño	-.53	-1.754	.1175
	†	Other	-.35	-2.277	.0285
	‡	All years	-.37	-2.780	.0077
Spring	†	El Niño	-.66	-2.746	.0206
		Other	-.18	-1.122	.2691
	†	All years	-.31	-2.231	.0304
Summer		El Niño	-.35	-1.043	.3274
	‡	Other	-.52	-3.759	.0006
	‡	All years	-.48	-3.827	.0004
Fall		El Niño	.00	0.007	.9945
		Other	.11	0.706	.4846
		All years	.12	0.807	.4234

§: The significance level, α. Probability that you will be wrong if you reject the null hypothesis and conclude that there is a trend of increase(decrease) over time.

5.2.3 Frequency of Occurrence of the Eight Principal Weather Types: 1961-90

The same tests for trends over time that were described in the previous section were used on the principal weather type data (Muller 1961-), Table 5.8. No increase over the last 30 years was found in the frequency of occurrence of the Frontal Overrunning weather type. If found, such an increase would have substantiated the increase in the frequency of frontal-wave cyclones during the same period, at least to the extent that the Frontal Overrunning weather type is proxy information for the frontal-wave cyclone frequency. The sum of the two weather types, Frontal Gulf Return and Gulf Return, assumed here to be proprotional to the direct cold-front counts, shows no trend over time between 1961 and 1990, Table 5.8.

Table 5.8: Tests for trends over time in the frequency of occurrence of the eight principal weather types, as defined by Muller (1977). Shown are correlation coefficient, r, and t-values and probabilities to test the null hypothesis that the slope of the linear regression line is zero. Two levels of significance, $\alpha = .01$ and .05, are shown by the double and single daggers.

Season	Group	r	Student's t	Probability§	ν	Time
Frontal Overrunning (FOR)						
Winteryear	El Niño	-.53	-1.083	.3581	3	1961-89
	Other	.01	0.028	.9776	22	1961-89
	All	-.04	-0.183	.8561	27	1961-89
Winter+spring	El Niño	-.40	-0.746	.5095	3	1962-90
	Other	.00	0.012	.9908	22	1962-90
	All	-.03	-0.181	.8576	27	1962-90
Winter	El Niño	-.00	-0.007	.9951	3	1962-90
	Other	.02	0.112	.9119	22	1962-90
	All	.05	0.238	.8137	27	1962-90
Spring	El Niño	-.40	-0.871	.4329	4	1961-90
	Other	-.09	-0.413	.6838	22	1961-90
	All	-.16	-0.839	.4087	28	1961-90
Summer	El Niño	.51	1.002	.3900	3	1961-90
	Other	-.16	-0.772	.4482	23	1961-90
	All	-.09	-0.490	.6277	28	1961-90
Fall	El Niño	-.54	-1.109	.3482	3	1961-89
	Other	.13	-0.634	.5328	22	1961-89
	All	-.01	-0.032	.9751	27	1961-89
Frontal Gulf Return+Gulf Return (FGR+GR)						
Winteryear	El Niño	-.71	-1.760	.1759	3	1961-89
	Other	.16	0.753	.4590	22	1961-89
	All	.08	0.400	.6919	27	1961-89
Winter+spring	El Niño	-.64	-1.456	.2415	3	1962-90
	Other	.01	0.035	.9722	22	1962-90
	All	-.06	-0.293	.7719	27	1962-90
Winter	El Niño	.24	0.422	.7015	3	1962-90
	Other	-.10	0.487	.6313	22	1962-90
	All	-.05	-0.283	.7797	27	1962-90
Spring	El Niño	-.63	-1.636	.1772	4	1961-90
	Other	.04	0.174	.8637	22	1961-90
	All	-.08	-0.404	.6891	28	1961-90
Summer	El Niño	.75	1.937	.1481	3	1961-90
	Other	.09	0.409	.6863	23	1961-90
	All	.16	0.854	.4001	28	1961-90
Fall	El Niño	-.40	-0.762	.5017	3	1961-89
	Other	-.27	1.296	.2083	22	1961-89
	All	.13	0.670	.5085	27	1961-89

Table 5.8: continued.

Season	Group	r	Student's t	Probability§	ν	Time
Frontal Gulf Return (FGR)						
Winteryear	El Niño	-.20	-0.361	.7417	3	1961-89
	Other	.29	1.410	.1724	22	1961-89
	All	.23	1.207	.2379	27	1961-89
Winter+spring	El Niño	-.27	-0.493	.6557	3	1962-90
	Other	.01	0.034	.9736	22	1962-90
	All	-.03	-0.157	.8766	27	1962-90
Winter	El Niño	.33	0.611	.5841	3	1962-90
	Other	-.17	-0.811	.4258	22	1962-90
	All	-.14	-0.759	.4547	27	1962-90
Spring	El Niño	-.65	-1.702	.1637	4	1961-90
	Other	.14	0.664	.5134	22	1961-90
	All	.05	0.285	.7776	28	1961-90
Summer	El Niño	.70	1.716	.1847	3	1961-90
	Other	.26	1.278	.2141	23	1961-90
	All	.30	1.654	.1093	28	1961-90
Fall	El Niño	.40	0.763	.5007	3	1961-89
	Other	.27	1.325	.1986	22	1961-89
	All	.27	1.478	.1510	27	1961-89
Gulf Return (GR)						
Winteryear	El Niño	-.03	-0.044	.9678	3	1961-89
	Other	.37	1.867	.0752	22	1961-89
	All	.30	1.643	.1119	27	1961-89
Winter+spring	El Niño	-.14	-0.250	.8188	3	1962-90
	Other	.17	0.827	.4170	22	1962-90
	All	.10	0.548	.5882	27	1962-90
Winter	El Niño	.11	0.200	.8540	3	1962-90
	Other	.33	1.623	.1188	22	1962-90
	All	.26	1.393	.1749	27	1962-90
Spring	El Niño	-.14	-0.280	.7932	4	1961-90
	Other	-.01	-0.031	.9758	22	1961-90
	All	-.03	-0.167	.8687	28	1961-90
Summer	El Niño	-.04	-0.066	.9515	3	1961-90
	Other	.17	0.812	.4252	23	1961-90
	All	.15	0.791	.4355	28	1961-90
Fall	El Niño	-.08	-0.140	.8973	3	1961-89
†	Other	.47	2.527	.0192	22	1961-89
	All †	.41	2.309	.0288	27	1961-89

§: The significance level, α. Probability that you will be wrong if you reject the null hypothesis and conclude that there is a trend of increase(decrease) over time.
‡, † : indicates null hypothesis can be rejected at the .01 or .05 level of significance.

Table 5.8: continued.

Season		Group	r	Student's t	Probability§	ν	Time
Coastal Return (CR)							
Winteryear	†	El Niño	.91	3.726	.0336	3	1961-89
		Other	-.08	-0.383	.7055	22	1961-89
		All	.06	0.288	.7757	27	1961-89
Winter+spring		El Niño	.30	0.543	.6249	3	1962-90
		Other	-.28	-1.346	.1921	22	1962-90
		All	-.24	-1.259	.2189	27	1962-90
Winter		El Niño	-.44	-0.852	.4568	3	1962-90
		Other	-.39	-1.997	.0584	22	1962-90
		All †	-.40	-2.284	.0305	27	1962-90
Spring		El Niño	.34	0.731	.5054	4	1961-90
		Other	.04	0.180	.8589	22	1961-90
		All	.07	0.391	.6987	28	1961-90
Summer		El Niño	.69	1.657	.1961	3	1961-90
		Other	.22	1.105	.2808	23	1961-90
		All	.28	1.524	.1386	28	1961-90
Fall		El Niño	.00	0.006	.9913	3	1961-89
		Other	-.15	-0.729	.4737	22	1961-89
		All	-.15	-0.782	.4409	27	1961-89
Gulf High (GH)							
Winteryear		El Niño	-.19	-0.335	.7596	3	1961-89
		Other	-.40	-2.054	.0521	22	1961-89
		All †	-.38	-2.146	.0410	27	1961-89
Winter+spring		El Niño	.24	0.423	.7011	3	1962-90
		Other	-.06	-0.284	.7790	22	1962-90
		All	-.01	-0.075	.9406	27	1962-90
Winter		El Niño	-.21	-0.372	.7345	3	1962-90
		Other	.13	0.616	.5440	22	1962-90
		All	.09	0.456	.6519	27	1962-90
Spring		El Niño	.58	1.420	.2286	4	1961-90
		Other	-.24	-1.152	.2619	22	1961-90
		All	-.12	-0.617	.5425	28	1961-90
Summer	†	El Niño	-.91	-3.907	.0298	3	1961-90
	†	Other	-.49	-2.682	.0133	23	1961-90
		All ‡	-.52	-3.221	.0032	28	1961-90
Fall		El Niño	-.80	-2.321	.1030	3	1961-89
		Other	.10	0.490	.6289	22	1961-89
		All	-.01	-0.067	.9469	27	1961-89

§: The significance level, α. Probability that you will be wrong if you reject the null hypothesis and conclude that there is a trend of increase(decrease) over time. ‡, † : indicates null hypothesis can be rejected at the .01 or .05 level of significance.

Table 5.8: continued.

Season	Group	r	Student's t	Probability§	ν	Time
Pacific High (PH)						
Winteryear	El Niño	.19	0.332	.7616	3	1961-89
	Other	.11	0.512	.6137	22	1961-89
	All	.14	0.709	.4845	27	1961-89
Winter+spring	El Niño	-.41	0.768	.4984	3	1962-90
	Other	.05	0.232	.8184	22	1962-90
	All	.13	0.696	.4922	27	1962-90
Winter	El Niño	.16	0.278	.7994	3	1962-90
	Other	.16	0.751	.4608	22	1962-90
	All	.17	0.875	.3893	27	1962-90
Spring	El Niño	.33	0.690	.5283	4	1961-90
	Other	.06	0.275	.7862	22	1961-90
	All	.12	0.651	.5202	28	1961-90
Summer	El Niño	No PH			3	1961-90
	Other	No PH			23	1961-90
	All	No PH			28	1961-90
Fall	El Niño	-.43	-0.821	.4719	3	1961-89
	Other	.15	0.719	.4799	22	1961-89
	All	.07	0.360	.7218	27	1961-89
Continental High (CH)						
Winteryear	El Niño	-.48	-0.950	.4123	3	1961-89
	Other	-.29	-1.431	.1661	22	1961-89
	All	-.31	-1.717	.0974	27	1961-89
Winter+spring	El Niño	.65	1.500	.2307	3	1962-90
	Other	-.04	-0.174	.8637	22	1962-90
	All	-.00	-0.002	.9988	27	1962-90
Winter	El Niño	-.11	-0.188	.8625	3	1962-90
	Other	-.20	-0.975	.3399	22	1962-90
	All	-.20	-1.059	.2989	27	1962-90
Spring	El Niño	.15	0.312	.7702	4	1961-90
	Other	.05	0.253	.8027	22	1961-90
	All	.08	0.410	.6853	28	1961-90
Summer	El Niño	-.37	-0.683	.5435	3	1961-90
	Other	-.19	-0.905	.3749	23	1961-90
	All	-.21	-1.128	.2689	28	1961-90
Fall	El Niño	.77	2.062	.1313	3	1961-89
‡	Other	-.52	-2.858	.0091	22	1961-89
	All	-.32	-1.729	.0953	27	1961-89

§: The significance level, α. Probability that you will be wrong if you reject the null hypothesis and conclude that there is a trend of increase(decrease) over time. ‡, † : indicates null hypothesis can be rejected at the .01 or .05 level of significance.

Table 5.8: continued.

Season	Group	r	Student's t	Probability§	ν	Time
Gulf Tropical Disturbance(GTD)						
Winteryear	El Niño	.41	0.770	.4975	3	1961-89
	Other	.39	1.992	.0589	22	1961-89
	All†	.38	2.137	.0418	27	1961-89
Winter+spring	El Niño	.39	0.739	.5133	3	1962-90
	Other	-.03	-0.154	.8791	22	1962-90
	All	.04	0.214	.8323	27	1962-90
Winter	El Niño	No GTD			3	1962-90
	Other	No GTD			22	1962-90
	All	No GTD			27	1962-90
Spring	El Niño	.43	0.939	.4009	4	1961-90
	Other	-.01	-0.044	.9650	22	1961-90
	All	.06	0.338	.7379	28	1961-90
Summer	El Niño	-.47	0.921	.4249	3	1961-90
†	Other	.45	2.402	.0248	23	1961-90
	All†	.41	2.396	.0235	28	1961-90
Fall	El Niño	-.10	-0.169	.8768	3	1961-89
	Other	.10	0.480	.6361	22	1961-89
	All	.08	0.442	.6621	27	1961-89

Notes:

§: The significance level, α. Probability that you will be wrong if you reject the null hypothesis and conclude that there is a trend of increase(decrease) over time.

‡, † : indicates null hypothesis can be rejected at the .01 or .05 level of significance.

This agrees with the cold-front counts discussed above, Table 5.7, for which no trend was found between 1960 and 1989. The single type, Gulf Return, does show a statistically significant fall-season increase over the last 30 years. At the .01 or .05 level of significance, these other trends were found:

1. The frequency of Gulf Tropical Disturbance weather type increased from 1961 to 1990 on a winter-year basis and on a summer basis. This agrees with the increase over the last 103 years in hurricanes and tropical storms originating over the gulf, on both a winter-year and a calendar-year basis, Table 5.9.

2. The frequency of the summertime weather type, Gulf High, decreased from 1961 to 1990, on a winter-year and on a summer basis.

3. The Coastal Return weather type decreased for winter seasons between 1961 and 1990.

Table 5.9: Tests for trends over time: hurricanes and tropical storms, 1886 to 1988. Correlation coefficient, r, and t-values to test the null hypothesis that the slope of the linear regression line is zero. Two levels of significance, .01 and .05, are shown by the double and single daggers. For the hurricane data there are 101 and 102 degrees of freedom. For $\alpha = .01$, reject the null hypothesis if $|t| > 2.625$; for $\alpha = .05$, reject the null hypothesis if $|t| > 1.982$.

Season	Group	r	Student's t	Probability §
Hurricanes and Tropical Storms, 1886-1988				
Entering gulf/calendar year		-.08	-0.860	.3920
Originating in gulf/calendar year	‡	.25	2.632	.0098
Entering gulf/winteryear		-.07	-0.654	.5143
Originating in gulf/winter year	†	.24	2.448	.0161

Notes:

§: The significance level, α, or two-tail probability, the probability of finding a larger —t—. Probability (goes from 0 to 1) that you will be wrong if you reject the null hypothesis and conclude that there is a trend of increase(decrease) over time. Multiply by 100 for the percent of the time you will be wrong if you reject the null hypothesis.

‡, † :reject null hypothesis at .01, .05 levels of significance.

CHAPTER 6
DISCUSSION

6.1 Discussion

A summary of El Niño and La Niña contrasts in surface-based observations appears in Table 6.1. Surface findings have previously been summarized in Table 2.12. A summary of upper-level findings in El Niño winters appears in Table 6.2.

6.1.1 Gulf of Mexico-Region, Winter Storms: 1960-89

1. More frontal-wave cyclones formed in winter over the gulf area during the five El Niño years than during the 25 non-El Niño years between 1960 and 1989, Table 2.1 and Fig. 2.4. This is significant at the .01 level by the rank sum test. Conversely, fewer frontal-wave cyclones formed in winter during the eight La Niña years than during the 22 non-La Niña years in the same time period, significant at the .01 level, Table 2.2 and Fig. 2.4.

2. Considering the subjective nature of the storm counts and the weaknesses of the daily weather maps used as a data source, other evidence was sought to support item one above. First, over the same time period, the frequency of the Frontal Overrunning weather type (Muller 1977), indicative of storms, is greater in El Niño winters than in non-El Niño winters, significant at the .05 confidence level by the rank sum test, Table 2.3 and Fig. 2.9. Second, long-term (100 years, approximately) precipitation and temperature records at 9 of 15 land stations and 6 of 8 climatic divisions in the gulf area show increased precipitation at the .01 or .05 level in El Niño winters. 8 of 15 stations and no climatic divisions show cooler temperatures in El Niño winters, significant

Table 6.1: El Niño and La Niña contrasts, 1960-89: storms, cold fronts, hurricanes, weather types, temperature, and precipitation. A blank indicates the parameter did not differ between the two ENSO phases at the .01 or .05 confidence level. In temperature and precipitation results, number in parentheses indicates total stations or divisions displaying the trend at the .01 or .05 level. Station results not adjusted for multiple use of rank sum test due to varying periods of record; division results are so compensated.

Parameter	El Niño	Season	La Niña	Season
Frontal-Wave	High	winteryear	Low	winteryear
Cyclones	High	Winter	Low	Winter
			Low	Winter+spring
Cold Fronts	Low	Winteryear		
	Low	Winter+spring		
	Low	Winter		
FrontalOverrunning	High	Winteryear	Low	Winteryear
(parallels # storms)	High	Winter	Low	Winter
Frontal Gulf+	Low	Winter+spring	High	Winter+spring
Gulf Return	Low	Winter		
(parallels #cold fronts)	Low	Spring		
Gulf High			High	Summer
Hurricanes	Low	Winteryear		
Entering Gulf				
AverageTemperature	Low	Winteryear (6)	High	Winteryear (1)
at 15 Stations	Low	Winter+spring (8)	High	Winter+Spring (6)
	Low	Winter (8)	High	Winter (9)
	Low	Spring (2)	High	Spring (1)
	High	Summer (1)		
	Low	Fall (4)		
TotalPrecipitation	High	Winteryear (4)	Low	Winteryear (7)
at 15 Stations	High	Winter+spring (7)	Low	Winter+spring (7)
	High	Winter (9)	Low	Winter (5)
	High	Spring (3)	Low	Spring (4)
	Low	Summer (2)	Low	Summer (1)
	High	Fall (2)	Low	Fall (1)
Average Temperature	Low	Winteryear (4)		
at 8 Climatic	Low	Winter+spring (2)	High	Winter+spring (1)
Divisions				
Total Precipitation	High	Winteryear (3)	Low	Winteryear (4)
at 8 Climatic	High	Winter+spring (6)	Low	Winter+spring (3)
Divisions	High	Winter (6)	Low	Winter (2)
			Low	Spring (1)

Table 6.2: El Niño-winter, Gulf of Mexico-region, upper-level summary. A blank indicates parameter was not evaluated for that level. Fields of height and temperature all have lowest values in the northwest, increasing to the southeast.

	El Niño-Winter Differences				
Level (mb)	Height (m)	Temp °C	Wind	Divergence	Relative Vorticity
200	-15 to 50				
250			South jet farther south, intensified; North jet weaker;	More divergent (Except SW gulf)	More positive
500	-20 to 0	-0.8 to +1.0			
700	-10				
850	-10	-1.0 to 0	Weaker westerlies over southern U.S.; South residue and weaker easterlies over Caribbean; Cyclonic residue over gulf	More convergent (East and far west)	More positive (West)
MSL	-1 mb pressure				

at the .01 or .05 level, Figs. 2.17, 2.19, 2.21, 2.23, and Tables 2.5-2.8. The increased precipitation and cooler temperatures are believed to result from the rain and cloudiness associated with more frontal-wave cyclones in winters of El Niño years. The opposite is seen in La Niña winters. The frequency of the Frontal Overrunning weather type is lower in La Niña winters, significant at the .05 level, Table 2.4. and Fig. 2.9. 5 of 15 stations and 2 of 8 climatic divisions show drier La Niña winters; 9 of 15 stations and no climatic divisions show warmer La Niña winters, significant at the .01 or .05 level, Figs. 2.18, 2.20, 2.22, and 2.24 and Tables 2.5-2.8. The decreased precipitation and warmer temperatures are likely the result of fewer frontal-wave cyclones in La Niña winters. The areal and temporal coverages are not uniform, and not all stations and divisions show significant results, but nearly all follow the trends.

3. Frontal-wave cyclones forming during El Niño winters form over greater water depths, at lower latitudes, and have lower central pressure while over the gulf area than those in non-El Niño winters; all three are significant at the .05 level, Tables 2.10, 2.11, 2.9, and Fig. 2.29. During La Niña winters gulf-area frontal-wave cyclones form over shallower water depths, at higher latitudes, and have a higher central pressure while over the gulf area than in non-La Niña winters; all three are significant at the .05 level, Tables 2.10, 2.11, 2.9, and Fig. 2.30. No longitude difference in point of origin is observed between El Niño and non-El Niño years or between La Niña and non-La Niña years, in any season.

4. The greatest concentration of winter storms originates over the northwest Gulf of Mexico, Figs. 2.25 and 2.26 and appendices P and S. (This is true in any year and in any season except summer.) Speculating, contributing to this northwestern bias may be the fact that this is often the first place where northeast-trending cold fronts cross over water and encounter the warm, moist atmosphere over the gulf. In winter, when inshore waters are cooled, this explanation may still hold, due to a possible shoreward intrusion of relatively warm, deep water in the northwest corner of the gulf, the result of a re-entrant there in the bathymetric contours. Topography, bathymetry (through its effects on SST distribution), and the shape of the coastline may play a role in northwestern-gulf storm formation. Speculating again, perhaps these act together to focus instability in this area, by inducing a center of cyclonic circulation in the northwest gulf through offshore-directed flow originating along the coast, having a focal point in the northwest gulf. Some work along these lines has been done by Atlas and Chou (1983) concerning a sharp re-entrant in a coastline and its effects on the surface boundary layer during

cold-air outbreaks. In the Long Island Bight, they note the tendency for surface isobars to parallel the coastline, with low pressure offshore, induced by the SST distribution and the shape of the coastline.

Even though the average, winter flow in the western gulf is not perpendicular to the mountains, being southerly, Figs. 3.1 and 3.2, western gulf cyclogenesis may still have elements of lee-side cyclogenesis, at least during cold-air outbreaks. If winds are from the northwest, there is some flow perpendicular to the mountains, and a lee-type disturbance may form. Tibaldi et al. (1990) have discussed Alpine, orographic cyclogenesis during cold-air outbreaks, when surface, north winds are perpendicular to the Alps. They develop a theoretical case for lee cyclogenesis even in the presence of surface flow parallel to the mountains.

5. Genesis of frontal-wave cyclones over the gulf area peaks in the winter months: December, January, and February, in any year, Fig. 2.1.

6. During all 30 years, winter frontal-wave cyclones are about evenly distributed over the coastal plain, shelf, and slope, Fig. 2.3. (Over the Gulf of Mexico, storms rarely form over abyssal water depths ($\geq$3000 m, or 9840 ft). In non-El Niño years the greatest percent of all December storms originates over the coastal plain; the greatest percent of all January storms originates out over the slope; the greatest percent of all February storms originates back over the coastal plain, Fig. 2.27. In spring and summer the greatest percent of storms forms over the coastal plain. In fall the greatest percent of storms moves farther offshore every month. From September to November, the greatest percent of storms forms, in sequence, over the coastal plain, the shelf, and last, in November, nearly equal numbers of storms form over the slope and coastal plain. The offshore migration in the main locus of cyclogenesis during

autumn presumably follows the warmest water, as proposed by Lewis and Hsu (1992). The switch back to the coastal plain in December (and starting November) may represent an overriding factor then.

In the five El Niño winters, the main location of cyclogenesis is different, Fig. 2.27. The greatest percent of December and January storms forms over the slope, farther offshore than in Decembers of non-El Niño winters. The greatest percent of February storms forms over the shelf, also farther offshore than in non-El Niño Februarys. Spring and summer of El Niño years follow the same pattern as other years, with the greatest number of storms forming over the coastal plain. Fall storms in El Niño years do not display the offshore progression from September to November seen in other years, but form, in sequence, over the slope, the coastal plain, and then back over the slope. To explain the seaward shift in the location of cyclogenesis during El Niño winters, compared to non-El Niño winters, a further-southward advance of cold-air masses during cold-air outbreaks is hypothesized. This would also push the location of the warmest water southward during El Niño winters as compared to non-El Niño winters, based on evaporative cooling of surface waters under a cold, dry, air mass. Since there is a tendency for cooler winters in the gulf area in El Niño years, one may expect that only off the continental shelf, in water depths greater than 200 m (656 ft), will warm surface water be encountered in El Niño winters.

7. The origin points of winter frontal-wave cyclones are clustered under and south of the 250-mb level, mean speed maximum over the southern United States, or 'south jet', probably a mix of the subtropical jet and the polar-front jet, an artifact of the averaging in preparing seasonal composite maps. This clustering exists in El Niño and in other winters, Figs. 2.25 and 2.26. In El

Niño springs storms are clustered under and north of the mean south jet, Fig. 4.12; in non-El Niño springs storms are again clustered under and south of the mean jet, appendix P. Summer and fall storms do not cluster under the 250-mb, mean south jet, it being farther north then.

8. It is suggested that the concept of a 'family of wave cyclones' (Petterssen 1958) can be used to link gulf-area, winter storms with those forming off the east coast of the United States. This is done through the idealized pattern of divergence and convergence around a jet streak (Uccellini 1990). Considering the dimensions of a jet streak, one to two thousand kilometers (625 to 1250 mi) in length and a few hundred kilometers (125 to 250 mi) in width, the geometry fits a model in which most winter jet streaks would be positioned with the exit region off the Carolinas and the entrance region over the northwest Gulf of Mexico or coastal plain. The stronger divergence in the exit region can, in general, be related to stronger, east-coast storms. The weaker, gulf-region storms can be related to the weaker divergence of the entrance region. When gulf-region storms do not dissipate locally, but travel northeastward up the eastern seaboard of the United States and intensify, they are part of the succession in a family of wave cyclones, that is, decay in the front of the wave train and growth and eastward migration from rear to front.

6.1.2 Gulf of Mexico-Region, Winter Cold Fronts: 1960-89

1. From 1960 to 1989 fewer cold fronts were experienced in the gulf region during El Niño winters than in non-El Niño winters, significant at the .05 level, Table 2.1 and Fig. 2.6. No trend was observed for La Niña winters in the direct cold-front counts. The El Niño-winter results are supported by the weather-

type data which shows a lower frequency of occurrence of the sum of the two weather types, Frontal Gulf Return and Gulf Return, during El Niño winters than during non-El Niño winters, significant at the .05 level, Table 2.3 and Fig. 2.11. This support is only to the extent that the frequency of the sum of the two weather types, Frontal Gulf Return and Gulf Return, is representative of the number of cold fronts reaching the gulf and coastal plain. Taken alone, the Gulf Return weather type is less common in El Niño winters, significant at the .05 level, Table 2.3 and Fig. 2.15. The Frontal Gulf Return type is also less common during El Niño winters, but the drop is not significant at either the .01 or .05 level, Table 2.3 and Fig. 2.13. In La Niña winters, the frequency of occurrence of the sum of the two weather types indicative of cold front passage was greater, but only significant at the .10 level, Table 2.4 and Fig. 2.11, while the direct cold-front count showed no trend at all.

2. The observation of fewer cold fronts reaching the gulf area in El Niño winters between 1961 and 1990 implies that the above-mentioned cooler, El Niño-winter temperatures at gulf-area stations must result from either stronger cold-air outbreaks, or clouds and precipitation associated with more-frequent storms, or both. About an equal number of land stations show both significantly cooler temperatures and increased precipitation, but only two of eight climatic divisions show significantly cooler El Niño winters. This is less than the eight of eight divisions which show significantly increased precipitation. This, and the greater subjectivity of the cold-front counts, indicate a need for further work in this area. The suggestion that cold-air outbreaks may be 'stronger' over the gulf region during El Niño winters needs to be pursued, starting with a definition of 'strength' or 'intensity' of a cold-air outbreak, and development of indicators of this. Possible measures of intensity

include north-wind speed and duration, surface-temperature and dew-point drops, surface-pressure rise after frontal passage, and the extent of south advance before becoming stationary. During the 1982/83 El Niño event, many strong cold-air outbreaks were experienced in the gulf region, if the strength of cold-air outbreaks is measured by surface-temperature and dew-point falls, appendix T.

The notion, implicit throughout this work, that the best measure of the strength or intensity of a cold-air outbreak is its temperature and humidity content, (as these control pressure and so, wind speed) specifically, as they contrast with ambient gulf air, needs to be examined, as does another notion used here implicitly. That is the idea that stronger the contrast in airmass charactersitics between cold-surge air and gulf air, the more likely is the genesis of frontal-wave cyclones. Putting these last two together, conceptually, it would be quite neat if, all other things being equal, stronger cold-air outbreaks were more likely to generate frontal-wave cyclones, as an additional, (hypothesized) explanation for the increase in the number of frontal-wave cyclones in El Niño winters. In winter at least, this may be so. Strong fronts do not usually become stationary until far offshore, and in winter, warm, surface waters are likely to be first encountered there, shelf water being chilled by preceeding cold-air outbreaks (Lewis and Hsu 1992). Early and late in the cold-front season, where a front becomes stationary may not be as critical, the coastal plain and shelf waters both being relatively warm.

3. Since most winter storms originating over the gulf area form along cold fronts, one would expect the El Niño-winter increase in frontal-wave cyclones to be accompanied by an increase in the number of cold fronts reaching the area. Likewise, one might expect fewer cold fronts in La Niña winters. Instead they

are indirectly proportional in El Niño winters and in La Niña winters, either not related at all, or again weakly indirectly proportional. Either many of the cold-air surges in El Niño years differ in some way, such as in airmass characteristics, from those in other years, or gulf-area cyclogenesis is more likely when there is a longer time between frontal passages. Perhaps a longer recurrence interval allows recovery of the southerly flow of warm, moist air, enhancing the likelihood of cyclogenesis upon arrival of the next cold-air mass. The same state could also be effected simply by stronger cold-air outbreaks (higher pressure, cooler temperature, and drier air in the south-moving air mass), in as much as, the stronger the high pressure behind the front, the stronger the south winds preceding frontal passage, and presumably, the greater the transport northward of gulf-maritime air.

The lack of parallelism between the numbers of storms and cold fronts also shows up in the 1940 to 1989 data. Over the 50-year term, the number of cold fronts arriving in the region per winter year (1 September to 31 August, to coincide with the cold-front season in the gulf and with El Niño events) decreased, significant at the .01 level, while the number of frontal-wave cyclones remained flat, Figs. 5.4 and 5.6, Tables 5.6 and 5.7. If only the last 30 years are examined, the opposite is true. While the number of cold fronts per winter year has been flat over the last 30 years, the number of frontal-wave cyclones has increased, significant at the .01 level, Figs. 5.3 and 5.5, Tables 5.6 and 5.7.

6.1.3 850-mb Level Winds: Winter, Gulf of Mexico Region, 1967-89

1. A belt of weakened westerlies across the southern United States is present in the mean, winter, 850-mb wind field for the four El Niño winters between

1967 and 1989. The zone of weaker westerlies lies between 30° and 40°N between 70° and 110°W, Fig. 3.3. The amount of the weakening is less than 2.5 ms^{-1} (5 kt). It may be attributable to a decreased pressure gradient from south to north during El Niño winters. The decreased pressure gradient is indicated by slightly higher mean sea-level pressure (+1.4 mb) in the region of the Icelandic low, and by slightly lower high pressure (-1 mb) over the southern United States, the Gulf of Mexico region, and the western Atlantic, Fig. 3.6. The lowered high pressure over these last three areas is the result of a 10° eastward shift in (at least the western edge of) the Bermuda high in El Niño winters, compared to non-El Niño winters, Figs. 3.4 and 3.5. A consequence of the weakened westerlies over the southern United States during El Niño winters may be decreased advection of cold, dry air from the west, except during cold-air outbreaks, allowing a greater accumulation of heat and moisture between cold-air outbreaks. This is likely to favor cyclogenesis upon arrival of the next cold-air mass.

2. In any winter, the average, 850-mb level circulation over the gulf and coastal plain is weakly anticyclonic, 2.5 to 5 ms^{-1}, though not closed on the eastern end, Figs. 3.1 and 3.2. This anticyclonic circulation is the result of easterly trades in the southern gulf and westerlies across the northern gulf. (The switch between these two occurs at the Tropic of Cancer, over the deep, central gulf.) Southerly winds in the western gulf, connecting the trades and westerlies, appear to result from northward deflection of the trades by the Sierra Madre Orientals on the Mexican landmass. In El Niño winters this anticyclonic circulation is weakened, due partly to the above-mentioned weaker westerlies, and partly to some weakening of the easterly trades across the southern gulf, central Mexico, the Yucatan, and the northwestern Caribbean,

Fig. 3.3. Since the southerly mean flow along the western side of the gulf appears to be due to northward deflection of the easterly trades, diminishment of the trades in El Niño winters must lead to diminishment of the southerly flow. Average, south-wind speeds along the western shelf in El Niño winters are about half what they are in non-El Niño winters.

The weakened anticyclonic circulation over the gulf during El Niño winters is inferred from the presence of a cyclonic residue on the 850-mb wind-difference map, Fig. 3.3. Its cause could be as just outlined, or there could actually be more, basin-scale, cyclonic events in El Niño winters, events other than frontal-wave cyclones. For example, north wind difference seen in the western gulf may result from stronger or more-frequent north winds, rather than simply less south wind. Between Brownsville, Texas and the Bay of Campeche, at the 850-mb level (about 1500 m or 4920 ft) north winds may be prevented from spreading westward by high topography to the west. The Sierra Madre Orientals here are 1-2000 m (3280 to 6560 ft) elevation. Once past the Bay of Campeche and the Yucatan Peninsula, high topography in Central America prevents southward and westward advance, and north winds are forced to curve cyclonically to the east, thus constituting a basin-scale, cyclonic event. This also conserves potential vorticity. Since the Coriolis parameter decreases with south transport, potential vorticity can be conserved by adding positive (cyclonic) vorticity, assuming no change in flow depth while over the gulf and the coastal plain. Invoking more frequent north winds seems to contradict the finding of fewer cold fronts during El Niño winters. Therefore, this 'north wind' explanation, to be of any merit, must imply a greater number of strong cold-air outbreaks during El Niño winters, compared to non-El Niño winters. As discussed above, the strength of cold-air outbreaks in El Niño

winters compared to non-El Niño winters needs to be investigated. Evidence at hand, though indirect, for stronger cold-air outbreaks in El Niño winters is the observation that El Niño-winter storms form over deeper water than in non-El Niño winters, significant at the .05 level. This implies that cold-air masses advance farther south during El Niño winters before becoming stationary and spawning frontal-wave cyclones. Greater southward advance of cold-air masses also increases the likelihood of cyclogenesis in as much as, when a cold front becomes stationary and is likely to spawn frontal-wave cyclones, it will be positioned over the warmer surface waters of the deep gulf.

3. In El Niño winters, normally due-east trades in the northern Caribbean switch to slightly south of east, in addition to weakening somewhat, Figs. 3.1 and 3.2. This component of the wind effectively 'trains' a stream of heat and moisture from the tropics on the Gulf of Mexico during El Niño winters that bypasses the gulf during non-El Niño winters. Warm surface waters may also enter the gulf through the Straits of Yucatan, in response to the east-southeast winds. Both raise the likelihood of gulf cyclogenesis. Crisp and Lewis (1992), citing Rasmussen (1967), state that February and March are the months of maximum moisture import (from the Caribbean) into the gulf. The added, southerly component of the wind in El Niño winters is advantageously timed to have maximum impact on moisture advection. (Average spring winds over the northwest Caribbean are from the southeast in El Niño and non-El Niño years, appendix C.)

   At least a partial explanation for the added, southerly component of the 850-mb level winds over the northwest Caribbean during El Niño winters (Fig. 3.3) may involve the 10° eastward shift in (at least the west edge of)

the Bermuda high. During El Niño winters, this places the Caribbean in a more distal location relative to the center of the high than in non-El Niño winters. On the west side of the high, theoretically at least, at points farther from the center, outward-flowing winds will have undergone greater northward turning due to the Coriolis acceleration compared to more central locations, where winds should be nearer due east. This must be qualified as only a partial explanation for the south wind residue in the northwest Caribbean because the high is similarly shifted east in El Niño springs, compared to non-El Niño springs. The wind-difference pattern between El Niño and non-El Niño springs shows much less south residue in the area south and east of the gulf, the Caribbean and adjacent Atlantic, Fig. 4.34. If the 'Bermuda high' explanation is sufficient for winter, another feature of the 850-mb circulation must oppose the addition of south wind by this same mechanism in El Niño springs compared to non-El Niño springs.

4. At the 850-mb level, all but the west gulf is more convergent in El Niño winters than in non-El Niño winters, Fig. 3.9, this being compensation for increased upper-level divergence. However, the western gulf (but not the eastern gulf) shows more positive relative vorticity in El Niño winters, Fig. 3.12. The positive relative vorticity difference in the western gulf is the result of reduced anticyclonic circulation in El Niño winters. In both El Niño and non-El Niño winters, the average relative vorticity is negative over all but the extreme southeast and southwest corners of the gulf, Figs. 3.10 and 3.11. The lobe of negative average relative vorticity, visible in both winter types, quite likely indicates the average advance of cold-air masses during cold-air outbreaks. This is based on assuming high pressure and anticyclonic motion in these cold-air masses, implying negative relative vorticity. In El Niño years

this lobe extends farther southeast, reaching to western Cuba, while in non-El Niño winters, it stops about 500 km (315 mi) northwest of there. This implies quite strongly a strengthening of cold-air outbreaks (or more very strong ones) in El Niño winters, in as much as cold-air masses are able to maintain their integrity longer, and advance farther south before warming from below causes them to become stationary. The territories most affected by the longer reach of cold air in El Niño winters are the Straits of Yucatan and the Florida Straits, the gulf's oceanographic entrance and exit, respectively. There is thus a potential for episodic imprinting of surface waters entering (and leaving) the gulf by transient cold-air masses (a tracer-like concept).

5. The average, El Niño-winter, 850-mb divergence field over the gulf region shows an unexpected result. While much of the gulf and coastal plain is convergent on average, much of the western gulf is under a zone of divergence at the 850-mb level, Fig. 3.9. Much of the area of greatest concentration of cyclogenesis is beneath an area which is divergent on average. Further, this western-gulf divergent zone is present in every season and in any year, although its core is smaller and pushed farther offshore during El Niño winters compared to non-El Niño winters, Figs. 3.7 and 3.8 and appendix E. The zone is also present on monthly plots, not shown. The western-gulf divergent zone is a curvilinear band, elongate in the north-south direction. It parallels the mountains in Mexico and the southern Rockies and mirrors a zone of convergence above them of roughly equal dimensions. It is important to explain the origin of the western-gulf, 850-mb level divergence zone in a manner that is consistent with the observation that many frontal-wave cyclones form under that area. Initially, one would expect storms to form in regions of near-surface convergence. Three possible explanations for the western-gulf di-

vergent zone are now described: the 'topographic', the 'cyclone-induced', and the 'cold-air damming' explanations. Data is not at hand to prove or refute what follows. They are simply suggested ways to account for the western-gulf divergent zone. They raise as many questions as they answer and are intended as stimulus for future work.

(a) Topographic Explanation: Considering the close relationship to topography (parallel, and roughly the same length and width as the mountains to its west), and its persistence over the year, the divergence zone must, at least partially, be set up by the mountains. Along the northern extent of the divergent zone, in the latitude of the westerlies, divergence could result from streamline spreading and vertical lengthening as air columns expand vertically after crossing the mountains. In winter, the widest part of the zone, however, lies south of the westerlies, in an area of weak, average southerly wind blowing along the western shelf. This is so in both types of winter, although the southerlies are even weaker in El Niño winters. South of the westerlies, it is difficult to conceive of an orographic mechanism to create the divergence zone when the average flow is parallel to the mountains. To be sure, events will vary, but the average divergence field should represent the average flow.

Two other topographic effects may be important. These are diurnal, the sea breeze and the mountain wind, both due to differential heating. Divergence observed in the western gulf could in part be due to a daytime, onshore-directed, sea breeze, with descending motion offshore supplying the divergence there. Similarly, daytime, upslope, mountain winds, implying descending motion along the foot of the mountains, over the coastal plain, could contribute to the onshore portion of the diver-

gence zone. These effects add constructively. In each, to account for the divergence zone, the daytime effects must predominate in the averages. The obvious problems with each are: first, the average, winter winds in the divergence zone are south, not east; second, sea and mountain breezes may not be supported at this scale, although the sea breeze in peninsular Florida is capable of penetrating about a degree of longitude inland (Nicholls et al. 1991).

(b) Cyclone-Induced Explanation: Bjerknes and Holmboe (1944) first described a theoretical distribution of divergence and convergence around a surface cyclone that is still widely accepted, though recognized as general. Surface convergence is expected ahead of a surface low-pressure center and surface divergence is expected behind the cyclone. This represents pressure fall ahead of a cyclone and pressure rise behind it. In a broad sense, the average, El Niño-winter, 850-mb level convergence over the eastern gulf may be Bjerknes and Holmboe's convergence ahead of cyclones, and the western-gulf divergence may be their divergent region behind cyclones. This explanation for the western-gulf divergent zone will not work in summer, when few frontal-wave cyclones form over the gulf region.

(c) Cold-Air Damming Explanation: The western-gulf divergent zone, in winter, may result from cold-air damming along the east side of the southern Rockies and Sierra Madre Orientals. Just as the easterly trades appear to be deflected northward by the mountains in Mexico, perhaps north winds accompanying cold-air outbreak are prevented from spreading westward by topography, being forced, at least at the 850-mb level and below, into a cold-air 'channel'. During north-wind events, the diver-

gence may be due to velocity increase heading south, as air is constricted into the channel by a coastal plain that narrows to the south, and as the trajectory over water lengthens (a fetch-like concept). The increase in magnitude of the north wind residue from north to south in El Niño winters in the western gulf supports this velocity-increase, Fig. 3.3.

Further support is lent by the 850-mb level temperature differences between El Niño and non-El Niño winters, Fig. 4.19. At the 850-mb level the western gulf is 1.0 to 0.4°C cooler in El Niño winters than in non-El Niño winters. This means that if cold-air damming or channelization does occur, it is more active in El Niño winters than in non-El Niño winters. (It does not mean that the western gulf is cooler than the eastern gulf in El Niño winters. The slightly warmer 850-mb temperatures over the western gulf compared to the eastern gulf in normal winters are either eroded or erased in El Niño winters, Figs. 4.20 and 4.21.) Note that the tongue shape of the cooler temperatures over the western gulf in El Niño winters is not consistent with simply weaker south winds warming the region less in El Niño winters. If the cooler temperatures resulted only from weaker southerlies, the tongue should be pointing from south to north, since the north wind residue is greatest in the south and decreases northward.

As a cautionary note, the north wind residue in Fig. 3.3 implies either more north wind or less south wind, and a physical reason can be posed for each. These are: less south wind caused by a reduction in the easterly trades, and consequently, less northward deflection; alternatively, more north wind due to stronger cold-air outbreaks. In view of the decreased number of cold-air surges in El Niño winters, the obvious physical choice

is simply less south wind. Unfortunately, this provides no explanation for the western-gulf divergence zone and is inconsistent with the geometry of the 850-mb level temperature difference. An explanation which accounts for the divergence zone, the weaker south winds along the western shelf, the negative temperature difference in the western gulf, and which uses topography, is the the cold-air channel, or cold-air damming explanation. Unfortunately, this requires the additional postulate of stronger cold-air outbreaks in El Nino winters, leaving the matter unsettled.

It is suggested that all three proposed mechanisms may, at some time, account for the western-gulf divergent zone, though all do not operate in all seasons, nor contribute equally. The mountain-wind part of the topographic explanation works in all seasons, but the sea-breeze portion works best in the warm season. The 'cyclone-induced' explanation and the cold-air damming explanation work in winter, and to a lesser extent, in spring and fall.

6.1.4 250-mb Level Winds: Winter, Gulf of Mexico Region, 1966-89

1. The 250-mb level, mean speed maximum over the southern United States, the 'south jet', (approximately the subtropical jet, but quite likely a mix of that and the polar-front jet) is shifted south in El Niño winters between 110° and 75°W by amounts of 200 to 285 km (125 to 180 mi), Fig. 4.9 and Table 4.1. Compared to the mean position of the south jet in all 24 years, these south displacements are not significant, even at the .20 confidence level. Over the western gulf, the south jet is displaced even further south in El Niño springs compared to non-El Niño springs, by as much as 325 km (205 mi) at 95°W; the shift is not significant, even at the .20 level. The south displacement in

El Niño years is, however, significant at the .10 or .20 level in the combined season, winter-plus-spring, between 105° and 97°W. In El Niño winter years, displacement is significant at the .02 level between 105° and 95°W, and at the .10 or .20 level east of there, to 80°W, Table 4.1 and Fig. 4.7. In La Niña winters, the south jet is displaced north of the 24-year mean between 100° and 75°W by 250 to 385 km (155 to 240 mi), Fig. 4.8 and Table 4.2; this is significant at the .10 or .20 level. Similar results were obtained for winter-plus-spring. Over the western gulf, between 100° and 97°W, spring, north displacement is significant at the .10 or .20 level.

2. In winter and spring of El Niño years, there is a tendency for south displacements to occur nearset the longitude of the core of the south jet, to the east in winter, and to the west in spring.

3. Over the entire North American sector, the winter, 250-mb, mean velocity maximum is located off the Carolinas of the United States, over abyssal water depths ($\geq$3000 m or 9840 ft) in both El Niño and non-El Niño winters, Figs. 3.13 and 3.14.

4. The mean south jet is intensified over the southern United States by 5 to 10 ms^{-1} (10 to 20 kt) in El Niño winters compared to non-El Niño winters, Fig. 3.15. The mean north jet is weakened during El Niño winters by about 5 ms^{-1} (10 kt).

5. In the five El Niño winters between 1966 and 1989, there is an apparent consolidation in the 250-mb, mean velocity field. In the El Niño-winter, mean configuration, the north jet is less pronounced than in other winters. This is consistent with the strengthening of the south jet and weakening of the north jet in El Niño winters.

6. In El Niño winters, mean 250-mb level winds over the Caribbean are nearly due west, Fig. 3.13, while in non-El Niño winters they are from the southwest, Fig. 3.14.

7. In the northeastern Pacific, the mean jet in El Niño winters does not cross over the North American continent in the Pacific northwest around Vancouver, British Columbia, as it does in non-El Niño winters. Instead, it takes a track farther south, crossing over land at the southern tip of the Baja Peninsula. In the northeastern Pacific, the mean, 250-mb level jet decelerates off of a velocity maximum located still further west. The area is thus a potential exit region for any jet streak that may develop there. Owing to strong divergence on the left side of a jet-streak exit region, the area is a likely spot for cyclogenesis. Storms formed under this exit region would travel farther south and east before crossing over land in El Niño winters than in non-El Niño winters. This represents a southward shift in the eastern-Pacific, extratropical-storm track in El Niño winters compared to non-El Niño winters. It may account for the increased storminess in southern California during El Niño winters. Migratory cyclones passing over the northeastern Pacific, but formed elsewhere, would be similarly steered further south in El Niño winters by the south-turned, upper-level current.

8. The 250-mb level is more divergent in El Niño winters than in non-El Niño winters over all but the southwestern gulf, Fig. 3.18, although, in the El Niño-winter average, the whole area is convergent, Fig. 3.16. The area of increased divergence in El Niño winters covers all areas of winter, gulf-region cyclogenesis. The increased divergence in El Niño winters is the result of a stronger and south-displaced, 250-mb, south jet, and of the accompanying upper-level, cold trough behind it, as explained next. Bjerknes and Holmboe (1944) also

predicted the general, upper-level pattern of divergence and convergence over surface cyclones. This is based on the regions of divergence and convergence found in a jet-level trough, or long wave in the westerlies (Charney 1947). It also presumes a location of the center of the upper trough that is just behind, or to the west of, the surface cyclone, putting the center of the surface cyclone just below the forward half of the trough. This geometry favors cyclogenesis (Petterssen 1956). As streamlines will converge and air will pile up on entering the rear leg of the trough, this is an area of convergence. Once past the bottom of the trough, streamlines spread out, and air fans out, making the forward leg of the trough a zone of divergence. Therefore, above the surface cyclone, there is upper-level divergence. Behind the surface cyclone, under the rear leg of the upper-level trough, there is upper-level convergence. The roughly south-southwest location of convergent residue in the southwest gulf, situated behind the divergent residue of the rest of the gulf, may be the convergence predicted in the rear leg of the upper-level trough.

9. The increased positive divergence of El Niño winters is not accompanied by an increase in negative relative vorticity at the 250-mb level, Fig. 3.22. (The area over the gulf and coastal plain does show average negative relative vorticity in the winter mean in both types of year, Figs. 3.19 and 3.20.) Since the positive divergence difference results from upper-level troughing and jet-streak dynamics, rather than simple anticyclonic motion, extra positive divergence need not necessarily be accompanied by extra negative relative vorticity. In fact, the region has a strong positive relative-vorticity difference, Fig. 3.22. A wide band of positive relative-vorticity difference extends from the northeast Pacific, crossing much of the western United States and the entire gulf region, and extends into the Atlantic. Over the eastern Pacific, the band of positive

relative-vorticity difference is bounded on the south by the 250-mb south jet. This implies that the positive relative-vorticity difference over the Pacific in El Niño winters is due to the strengthening of the south jet and of the resulting added, cyclonic shear to its north. Over the gulf region, this pattern breaks down, with the mean, south-jet track cutting diagonally across the band of positive residue. Finally, over the Atlantic, the pattern is completely reversed. There, the mean, south-jet track roughly divides a region of negative relative-vorticity difference to the north from one of positive difference to the south. At this eastern end, again imperfectly, the mean south jet divides a region of decreased speeds to its north from one of increased speeds to its south, a reversal of the pattern over the western United States. Decreased speeds to the north of the jet result in less cyclonic (positive) shear north of the jet, producing the negative relative-vorticity difference to the north of the jet axis. South of the mean jet axis, where winds are generally stronger in El Niño winters, the explanation is not as simple. Increased speeds should result in more anticyclonic shear to the south of the jet axis, and this should show up as a negative relative-vorticity residue. Instead, it is positive.

The Gulf of Mexico region, midway between these two regimes on the west and east, is a zone of transition. The most obvious way to bring extra positive relative vorticity to the gulf area is within jet-level troughs, the circulation within them being cyclonic, or positive. The positive relative-vorticity difference over the gulf and adjacent Atlantic, during El Niño winters, may owe to more frequent advection of positive relative vorticity within upper-level troughs. Vorticity advection may also explain the imperfect fit of the pattern of negative relative-vorticity difference to the velocity decreases north of the jet over the Atlantic off the southeastern United States. (Note that the mean,

250-mb wind speed axes are drawn subjectively, and this too may account for the apparently imperfect fit.)

6.1.5 Intermediate- and Upper-Level Troughing: Winter, Gulf of Mexico Region, 1963-89

Intermediate- and upper-level troughing, indicated by lower heights and cooler temperatures of constant-pressure surfaces, is present in El Niño winters. Troughing is centered on the Aleutian low, reaches from sea level to the 200-mb level, and extends southeastward toward the Gulf of Mexico at all levels checked, that is, the 850-, 700-, 500-, and 200-mb levels, Figs. 4.16, 4.19, 4.22, 4.25, 4.28, and 4.31. Average height and temperature drops over the gulf area in El Niño winters are the southeastern periphery of those centered over the Aleutian low, making the Gulf of Mexico an 'outpost' of the low in El Niño winters. Enhanced troughing also reaches to the gulf during El Niño springs. The magnitude of the average negative height differences in El Niño winters is -10 to -20 m (-33 to -66 ft) which is 4 to 20% of the local, gulf-region, El Niño-winter relief of the constant pressure surfaces used. Average negative temperature differences are up to -1.0°C, which is about 10% of the range over the gulf region in El Niño winters. Sea-level pressure is one millibar lower, on average, over the area, Fig. 3.6. Expressed as percentages of the local range of values, these differences are about half the size of those over the central area of the Aleutian low.

In general, the region of negative height and temperature difference reaches over more of the gulf region at lower levels, the zero-difference line migrating to the northwest with height. In winter the average 850- and 700-mb levels are -10 m lower (-33 ft), Figs. 4.16 and 4.22, and the 850-mb temperature is -1.0 to 0°C cooler, Fig. 4.19. The 500-mb level is -20 to 0 m lower, Fig. 4.25; the -20 m difference is

located over the northwest coastal plain. 500-mb temperature differences are not negative over the whole area of negative height differences, reaching only as far as the western gulf, Fig. 4.28. The remainder of the gulf is up to 1.0°C warmer in El Niño winters. (The meaning of the lack of correspondence between the average height and temperature differences at the 500-mb level is not apparent. The 500-mb level is near the average level of nondivergence, and this may be a factor.) 200-mb level negative height differences retreat further northwest, only reaching to the northwest coastal plain (-15 m or 50 ft), while the rest of the gulf region has a positive 200-mb height difference, up to 50 m (165 ft) over the Bay of Campeche, Fig. 4.31. The northwest migration with height of the location of negative average height and temperature differences is evidence of the westward tilt with height of the upper-level continuation of surface troughs. That evidence of troughing is seen from the surface to the 200-mb level, is good indication of more frequent upper-level support for nascent surface disturbances in El Niño winters, as compared to non-El Niño winters.

Extensions of the Aleutian low are positioned to have maximum impact on the gulf region by their proximity to the critical, northwestern-gulf, cyclogenetic area. The extensions, and so, the upper-level support, need only reach the northwest gulf to increase the frequency of cyclogenesis, provided that other necessary conditions are met, such as the existence of a surface front or baroclinic zone and the presence of adequate heat and moisture for cyclone growth. As mentioned above, upper-level troughing exists in El Niño springs, but there is no increase in the number of storms formed in El Niño springs over non-El Niño springs. Presumably, in El Niño springs, necessary conditions near the surface or at the jet level are not met.

6.1.6 Spring Cyclogenesis

The three elements for gulf-area cyclogenesis, an upper-level jet, continuous troughing from the surface to the jet level, and adequate surface heat and moisture, in the presence of a front or baroclinic zone, must more often be present concurrently to produce an increase in cyclogenesis over the gulf area. For example, in El Niño springs there is not an increase in storm formation, even though the mean south jet is farther south, Figs. 4.3 and 4.4, and negative height and temperature differences at intermediate and upper levels are present, appendices B, D, G, H, I, and N. Proper surface conditions are lacking in El Niño springs. The 850-mb wind-residue pattern in El Niño springs, Fig. 4.34, is very different from that in El Niño winters, Fig. 3.3. The southerly component of the wind difference, directed gulfward in El Niño winters, is much diminished in El Niño springs, reducing the El Niño-spring, excess import of heat and moisture to the gulf from the Caribbean. Although the south jet is farther south in El Niño springs, with respect to both the El Niño-winter position, and to the non-El Niño spring position, Table 4.1, the intensification of the south jet in El Niño springs compared to non-El Niño springs is less than in winter, 5 ms^{-1} (10 kt) or less in spring, compared to 5 to 10 ms^{-1} (10 to 20 kt) in winter, Figs. 4.11 and 3.15. In absolute terms, the south jet is not as strong in El Niño springs compared to El Niño winters, 33 ms^{-1} (66 kt) compared to 45 ms^{-1} (90 kt) maximum speed, Figs. 3.13 and 4.10. In El Niño springs the area of maximum intensification is south of that in El Niño winters, being over Mexico and the adjacent Pacific, instead of over the Gulf of Mexico. Other factors acting to suppress gulf-region cyclogenesis in El Niño springs follow. First, there is a strong zone of convergence at the 250-mb level over the west gulf in El Niño springs, Fig. 4.12. The 250-mb divergence difference over the west gulf is negative in El Niño springs, indicating increased convergence instead of divergence, Fig. 4.13. Second,

the core of the south jet in El Niño springs, at 98°W, up aginst the east side of the southern Rockies, is shifted almost 30° west of its location in El Niño winters at 70°W, Figs. 4.10 and 3.13. Although this shift would appear to more often place the gulf area under the exit region of a jet streak in El Niño springs, storm formation is not increased. Speculating, perhaps the terrain most often spanned by a jet streak in El Niño springs is unfavorable for jet-to-surface or entrance-to-exit region pairing. Finally, although not an El Niño-non-El Niño difference, there are fewer cold fronts in any spring, which must decrease the likelihood of cyclogenesis in any spring.

CHAPTER 7
CONCLUSIONS

1. More frontal-wave cyclones were generated over the Gulf of Mexico and coastal plain in the five El Niño winters than in the 25 non-El Niño winters between 1960 and 1989. The three conditions accounting for the increase are satisfied concurrently only in winter, the only season that shows significantly increased cyclogenesis over the gulf in the five El Niño years. The three conditions follow.

   (a) Near-Surface Conditions: Near the surface, between 1967 and 1989, the 850-mb level is predisposed to cyclogenesis during El Niño winters by increased import of heat and moisture from the Caribbean by southeasterly winds over the northwest Caribbean, directed gulfward. In non-El Niño winters winds here are due east, bypassing the gulf. At the 850-mb level, the gulf region is more convergent and has more positive relative vorticity in El Niño winters than in non-El Niño winters. This is true over all but a portion of the western gulf, which is, on average, divergent in all seasons and all years. In winter the divergence may be surface-cyclone induced, being the divergent area predicted by Bjerknes and Holmboe (1944) behind a surface cyclone. During cold-air outbreaks, it may be produced by velocity increase from north to south in a cold-air channel, produced by cold-air damming of north winds against the Sierra Madre Orientals and southern Rocky Mountains. In the warm season, the divergence zone may owe to a large-scale sea-breeze system. In any season, the onshore portion may owe to a mountain-wind system. The last two would reinforce each other, and both depend on the daytime effect being stronger than the nightime effect.

(b) Intermediate- and Upper-Level Troughing: There is stronger upper-level support for surface disturbances in El Niño winters than in non-El Niño winters. Evidence for this is the presence of intensified troughing from the 850-mb level to the 200-mb level in El Niño winters between 1963 and 1989. Deeper troughing is inferred from negative height and temperature differences between El Niño and other winters at the 850-, 700-, 500-, and 200-mb levels. These indicate stronger upper-level extensions of surface troughs, continuous with height, and stronger troughs at jet level in El Niño winters than in non-El Niño winters.

(c) Jet Stream: The mean, 250-mb level winter jet over the gulf area is intensified, relative to non-El Niño winters, and displaced to the south, relative to all winters between 1966 and 1989. This is corroborated by a positive divergence difference and a positive relative-vorticity difference over the region between El Niño and non-El Niño winters.

2. During the five El Niño winters from 1966 to 1989, the 250-mb level, winter-season, average speed maximum, or jet stream, off the Pacific North American coast follows a more southerly track than in the 19 non-El Niño winters during the time. The El Niño-winter, average jet coming off the northeastern Pacific crosses over the North American continent from the Pacific Ocean in the vicinity of the Baja Peninsula, rather than over British Columbia and Washington state, as does the non-El Niño-winter average jet. This is likely to be the reason for the increase in the number of storms over southern California during El Niño winters.

3. Over approximately the last 100 years, in the Gulf of Mexico region, El Niño winters have been wetter and cooler than non-El Niño winters, and La Niña winters have been drier and warmer than non-La Niña winters, based on land-based precipitation and temperature records.

4. During extreme phases of the ENSO, that is, during Northern Hemisphere winters of El Niño and La Niña events, the number of cold fronts reaching the Gulf of Mexico or its coastal plain is inversely related to the number of frontal-wave cyclones forming there. This relationship is best documented between 1960 and 1989, a time which includes five El Niño and eight La Niña winters, by three independent lines of evidence, that is, direct storm and cold-front counts, synoptic weather-type frequencies, and land-based temperature and precipitation records. The relationship also appears to hold for the ten El Niño winters between 1940 and 1989, but not for the ten La Niña winters, on the basis of direct, storm and cold-front counts only.

5. Examining trends over time, from 1960 to 1989, the number of winter, frontal-wave cyclones forming over the Gulf of Mexico or its coastal plain increased, but the number of winter cold fronts reaching the area remained constant. From 1940 to 1989, number of cold fronts reaching the area in winter decreased, but the number of winter, frontal-wave cyclones forming over the Gulf of Mexico or its coastal plain neither increased nor decreased. The increase in the number of frontal-wave cyclones forming over the gulf area between 1960 and 1989 appears to compensate for a decrease observed by Whittaker and Horn (1982) over the North American sector, north of 40°N.

6. The greatest concentration of gulf-area frontal-wave cyclones forms over the northwest Gulf of Mexico in any year, and in any season but summer, when frontal-wave cyclone formation is rare. Therefore, the propensity for cycloge-

nesis there must be independent of ENSO state and of season. This points to a topographic/bathymetric explanation based on the Sierra Madre Orientals and southern Rocky Mountains and on the geometry of the continental shelf and its effect on SST distribution. The northwest gulf is the place where northeast-southwest trending cold fronts first encounter the warm, moist atmosphere over the gulf, probably a factor in the northwest gulf's predisposition to cyclogenesis.

7. Between 1960 and 1989, El Niño- and La Niña-winter effects on the Gulf of Mexico region are of equal magnitude and opposite sign regarding the formation of frontal-wave cyclones, total rainfall, average temperature, and possibly, cold-front incidence. From 1966 to 1989, El Niño- and La Niña-winter effects on the average position of the 250-mb level jet, over the southern United States, are equal and opposite.

8. Seasonal averages of dynamic quantities appear to be of some use for delineation of large-scale, long-term, ENSO-related, meteorological phenomena. Simple difference fields of these seasonal averages are even more useful for discerning regional differences between El Niño and non-El Niño seasons, as these may be masked in the seasonal averages. The rank sum test appears to be capable of discrimating differences between El Niño and non-El Niño years, and between La Niña and non-La Niña years.

REFERENCES

Aceituno, P., 1992: El Niño, the Southern Oscillation, and ENSO: confusing names for a complex ocean-atmosphere interaction. *Bull. Amer. Meteor. Soc.*, **73**, 483-485.

Anderson, T. W., and S. L. Sclove, 1974: *Introductory Statistical Analysis.* Houghton Mifflin, 499 pp.

Arkin, P. A., 1982: The relationship between interannual variability in the 200-mb tropical wind field and the Southern Oscillation. *Mon. Wea. Rev.*, **110**, 1393-1404.

Atlas, D., and S. -H. Chou, 1983: The influence of coastal shape on winter mesoscale air-sea interaction. *Mon. Wea. Rev.*, **111**, 245-252.

Beebe, R. G., and F. C. Bates, 1955: A mechanism for assisting in the release of convective instability. *Mon. Wea. Rev.*, **83**, 1-10.

Bell, G. D., and L. F. Bosart, 1988: Appalachian cold-air damming. *Mon. Wea. Rev.*, **116**, 137-161.

Bell, G. D., and L. F. Bosart, 1989: A 15-year climatology of Northern Hemisphere 500 mb closed cyclone and anticyclone centers. *Mon. Wea. Rev.*, **117**, 2142-2163.

Bjerknes, J., 1966: A possible response of the atmospheric Hadley circulation to equatorial anomalies of ocean temperature. *Tellus*, **4**, 820-828.

Bjerknes, J., 1969: Atmospheric teleconnections from the equatorial Pacific. *Mon. Wea. Rev.*, **97**, 163-172.

Bjerknes, J., 1972: Large-scale atmospheric response to the 1964-65 Pacific equatorial warming. *J. Phys. Oceanogr.*, **2**, 212-217.

Bjerknes, J., 1974a: *Preliminary study of the atmospheric circulation during the period preceding the 1972-73 El Niño*, A NORPAX contribution. Department of Meteorology, University of California at Los Angeles, Los Angeles CA, NTIS No. A006985, 24 pp.

Bjerknes, J., 1974b: *Analysis of the rhythmic variations of the Hadley Circulation over the Pacific during 1963-67.* Office of Naval Research Technical Report under contract N00014-69-A-0200-4044 NR 083-287, NTIS No. AD 770-599/96I 74-09 12B, 34 pp.

Bjerknes, J., and J. Holmboe, 1944: On the theory of cyclones. *J. Meteor.*, **1**, 1-22.

Bradley, R. S., P. M. Kelly, P. D. Jones, C. M. Goodess and H. F. Diaz: 1985, *Climatic Data for Northern Hemisphere Land Areas 1851-1980.* Carbon Dioxide Information Center, Information Resources Organization, now, Carbon Dioxide Information Analysis Center, Oak Ridge National Laboratory, P. O. Box 2008, Oak Ridge, TN, 37831-6335, 335 pp.

Browning, K. A., 1990: Organization of clouds and precipitation in extratropical cyclones. In *Extratropical Cyclones, The Erik Palmén Memorial Volume*, C. W. Newton, and E. O. Holopainen, Eds., Amer. Meteor. Soc., 129-154.

Cammas, J. P., and D. Ramond, 1989: Analysis and diagnosis of the composition of ageostrophic circulations in jet-front systems. *Mon. Wea. Rev.*, **117**, 2447-2462.

Charney, J. G., 1947: the dynamics of long waves in a baroclinic westerly current. *J. Meteor.*, 4, 135-163.

Climate Analysis Center: *Climate Diagnostics Bulletin, Near Real-Time Analyses Ocean/Atmosphere.* National Weather Service, National Meteorological Center, National Oceanic and Atmospheric Administration, U.S. Department of Commerce, U.S. Govt. Printing Office, Washington, DC.

Cotton, W. R., 1990: *Storms.* Aster Press, 158 pp.

Cooley, D. S., 1976: *Six-Hour Cycle in Final, Technical Procedures Bulletin No. 179.* National Weather Service, National Oceanographic and Atmospheric Administration, U.S. Department of Commerce, U.S. Govt. Printing Office, Washington, DC. 14 pp.

Crisp, C. A., and J. M. Lewis, 1992: Return flow in the Gulf of Mexico. Part I: A Classificatory approach with a global historical perspective. *J. Appl. Meteor.*, **31**, 868-881.

Defant, F., H. Fechner, and P. Speth, 1972: *Synoptic Meteorology and Atmospheric Energetics of the Hamburg Storm Tide Weather Situation of February 1962.* Deutscher Wetterdienst, Berichte, 17(127), 85 pp. (English and German summaries.)

Defant, F., and H. T. Morth, 1978: *Compendium of Meteorology Volume 1, Part 3 - Synoptic Meteorology.* World Meteorological Organization, Publication No. 364, 276 pp.

Department of Atmospheric Sciences, University of Washington, 1990: *Compact Disc of the National Meteorological Center Grid Point Data Set: Version II.* 9 pp. (Available from Department of Atmospheric Sciences AK-40, University of Washington, Seattle, WA 98195.)

Deser, C., and J. M. Wallace, 1990: Large-scale atmospheric circulation features of warm and cold episodes in the tropical Pacific. *J. Climate*, **3**, 1254-1281.

Douglas, A. V., and P. J. Englehart, 1981: On a statistical relationship between autumn rainfall in the central equatorial Pacific and subsequent winter precipitation in Florida. *Mon. Wea. Rev.*, **109**, 2377-2382.

Elsberry, R. L., and P. J. Kirchoffer, 1988: Upper-level forcing of explosive cyclogenesis over the ocean based on operationally analyzed fields, Pacific equatorial warming. *Wea. Forecasting*, **3**, 205-216.

Faiers, G. E., 1988: A synoptic weather type analysis of January hourly precipitation at Lake Charles, LA. *Phys. Geog.*, **9**, 223-231.

Fernandez-Partegas, J., and C. N. K. Mooers, 1975: A subsynoptic study of winter cold fronts in Florida. *Mon. Wea. Rev.*, **103**, 742-744.

Gan, M. A., and V. B. Rao, 1991: Surface cyclogenesis over South America. *Mon. Wea. Rev.*, **119**, 1293-1302.

Gray, W. M., 1984a: Atlantic seasonal hurricane frequency. Part I: El Niño and 30 mb Quasi-Biennial Oscillation influences. *Mon. Wea. Rev.*, **112**, 1649-1668.

Gray, W. M., 1984b: Atlantic seasonal hurricane frequency. Part II: forecasting its variability. *Mon. Wea. Rev.*, **112**, 1669-1683.

Halpert, M. S., and C. F. Ropelewski, 1992a: Surface temperature patterns associated with the Southern Oscillation. *J. Climate*, **5**, 577-593.

Halpert, M. S., and C. F. Ropelewski, 1992b: Climate variability during the decade of the 1980's and its influence on the 1961-1990 base period means. *12th Conference on Probability and Statistics in the Atmospheric Sciences*, Amer. Meteor. Soc., J22-J27.

Handler, P., 1990: USA corn yields, the El Niño and agricultural drought: 1867-1988. *J. Climatol.*, **10**, 819-828.

Hamilton, K., 1988: A detailed examination of the extratropical response to tropical El Niño/Southern Oscillation events. *J. Climatol.*, **8**, 67-86.

Hanson, H. P., and B. Long, 1985: Climatology of cyclogenesis over the East China Sea. *Mon. Wea. Rev.*, **113**, 697-707.

Headquarters, Air Weather Service, Army Air Force: October 1945 to December 1948: *Northern Hemisphere Historical Weather Maps, Sea Level and 500 Millibar Charts.* U.S. Govt. Printing Office, Washington, D.C.

Held, I. M., S. W. Lyons and S. Nigam, 1989: Transients and the extratropical response to El Niño. *J. Atmos. Sci.*, **46**, 163-174.

Hess, S. L., 1959: *Introduction to Theoretical Meteorology.* Krieger Publishing Company, 362 pp.

Hoel, P. G., 1962: *Introduction to Mathematical Statistics.* 3rd. ed., John Wiley and Sons, 427 pp.

Holton, J. R., 1979: *An Introduction to Dynamic Meteorology.* International Geophysics Series, Vol. 23, 2nd. ed., Academic Press, 391 pp.

Horel, J. D., and J. M. Wallace, 1981: Planetary-scale atmospheric phenomena associated with the Southern Oscillation. *Mon. Wea. Rev.*, **109**, 813-829.

Hosler, C. L., and L. A.Gamage, 1956: Cyclone frequencies in the United States for the period 1905 to 1954. *Mon. Wea. Rev.*, **84**, 388-390.

Hsu, S. A., 1988: *Coastal Meteorology.* Academic Press, 260 pp.

Hsu, S. A., 1992: Effects of surface baroclinicity on frontal overrunning along the central Gulf coast. *J. Appl. Meteor.*, **31**, 900-907.

Huh, O. K., and L. J. Rouse, Jr., 1984: Cold air outbreaks over the northwest Florida continental shelf: heat flux processes and hydrographic changes. *J. Geophys. Res. Oceans*, **89(C1)**, 717-726.

International Library of Mathematics and Statistics (IMSL), 1987: IMSL User's Manual, Stat/Library, FORTRAN Subroutines for Statistical Analysis, Version 1.0. 1231 pp. (Available from IMSL Inc., P.O. Box 4605, Houston, TX, 77210-4605.)

Janish, P. R., and S. W. Lyons, 1992: NGM performance during cold-air outbreaks and periods of return flow over the Gulf of Mexico with emphasis on moisture-field evolution. *J. Appl. Meteor.*, **31**, 995-1017.

Jenne, R. L., 1970: *The NMC Ocatgonal Grid.* Internal Memorandum of the Data Support Section, National Center for Atmospheric Research, 22 pp. (Available from: Data Support Section, National Center for Atmospheric Research, P.O. Box 3000, Boulder, CO, 80303.)

Jenne, R. L., and W. Spangler, 1975: *NCAR Tape Format for Northern Hemisphere Octagonal Grid Data.* Internal memorandum of the Data Support Section, National Center for Atmospheric Research, 7 pp. (Available from: Data Support Section, National Center for Atmospheric Research, P.O. Box 3000, Boulder, CO, 80303.)

Johnson, G. A., E. A. Meindl and E. B. Mortimer, 1984: Features associated with repeated strong cyclogenesis in the western Gulf of Mexico during the winter of 1982-1983. In *Third Conference, Meteorology of the Coastal Zone*, Amer. Meteor. Soc., 110-117.

Keyser, D., and M. A. Shapiro, 1986: A review of the structure and dynamics of upper-level frontal zones. *Mon. Wea. Rev.*, **114**, 452-499.

Klein, W. H., 1957: *Principal Tracks and Mean Frequencies of Cyclones and Anticyclones in the Northern Hemisphere.* Research Paper No.40, U.S. Weather Bureau, U.S. Govt. Printing Office, Washington D.C.

Krishnamurti, T. N., 1961: The subtropical jetstream of winter. *J. Meteor.*, **18**, 172-191.

Kunkel, K. E., and A. Court, 1990: Climatic means and normals - a statement of the American Association of State Climatologists. *Bull. Amer. Meteor. Soc.*, **71**, 201-204.

Lau, K. -M., and P. H. Chan, 1983a: Short-term climate variability and atmospheric teleconnections from satellite-observed outgoing longwave radiation. Part I: simultaneous relationships. *J. Atmos. Sci.*, **40**, 2735-2750.

Lau, K. -M., and P. H. Chan, 1983b: Short-term climate variability and atmospheric teleconnections from satellite-observed outgoing longwave radiation. Part II: lagged correlations. *J. Atmos. Sci.*, **40**, 2751-2767.

Lau, K. -M., and P. J. Sheu, 1991: Teleconnections in global rainfall anomalies: seasonal to interdecadal time scales. In *Teleconnections Linking Worldwide Climate Anomalies*, Eds. M. H. Glantz, R. W. Katz and N. Nicholls, Cambridge University Press, 227-256.

Lewis, J. K., and S. A. Hsu, 1992: Mesoscale air-sea interactions related to tropical and extra-tropical storms in the Gulf of Mexico. *J. Geophys. Res. Oceans*, **97(C2)**, 2215-2228.

Lindsay, J. A., and C. H. Vogel, 1990: Historical evidence for Southern Oscillation-southern African rainfall relationships. *J. Climatol.*, **10**, 679-689.

Mass, C. F., H. J. Edmon, H. J. Friedman, N. R. Cheney and E. E. Recker, 1987: The use of compact discs for the storage of large meteorological and oceanographic data sets. *Bull. Amer. Meteor. Soc.*, **68**, 1556-1558.

Miller, I., and J. E. Freund, 1985: *Probability and Statistics for Engineers.* Prentice Hall, 530 pp.

Mortimer, E. B., G. A. Johnson and H. N. W. Lau, 1988: Major arctic outbreaks affecting Louisiana. *Natl. Wea. Dig.*, **13**, 5-14.

Muller, R. A., 1977: A synoptic climatology for environmental baseline analysis: New Orleans. *J. Appl. Meteor.*, **16**, 20-33.

Muller, R. A., 1961-present: Weather type frequency database for the Gulf of Mexico, 1961-present. Archives of the Louisiana State Office of Climatology, Louisiana State University, Baton Rouge, LA. (Available from The Louisiana State Office of Climatology, Room 262, Howe-Russell Geoscience Complex, Louisiana State University, Baton Rouge, LA, 70803).

Namias, J., and P. F. Clapp, 1944: Studies of the motion and development of long waves in the westerlies. *J. Meteor.*, **1**, 57-77.

Namias, J., and P. F. Clapp, 1949: Confluence theory of the high tropospheric jet stream. *J. Meteor.*, **6**, 330-336..

National Climatic Data Center, 1948-present: *Monthly Climatic Data for the World*, National Climatic Data Center, Federal Building, Asheville, NC, 28801.

National Climatic Data Center, 1988: Summary of constant pressure data (WBAN-33). In *Selective Guide to Climatic Data Sources, Key to Meteorological Records Documentation No. 4.11*, National Climatic Data Center; National Environmental Satellite, Data, and Information Service; National Oceanographic and Atmospheric Administration; U.S. Department of Commerce, p. IV-11. (Available from: National Climatic Data Center, Federal Building, Asheville, NC, 28801.)

National Geophysical Data Center, 1988: ETOPO5, Digital Relief of the Surface of the Earth, National Geophysical Data Center, National Oceanographic and Atmospheric Administration, Code E/GC3, 325 Broadway, Boulder, CO, 80303-3328, Product No. 931A07002.

National Meteorological Center, 1988-89, *NMC Seasonal Performance Summary.* **2**, National Weather Service, National Oceanic and Atmospheric Administration, U.S. Department of Commerce, U.S. Govt. Printing Office, Washington, D.C., 88 pp.

National Weather Service, 1979: *Facsimile Products, National Weather Service Forecasting Handbook No. 1.* National Oceanic and Atmospheric Administration, U.S. Department of Commerce, U.S. Govt. Printing Office, Washington, D.C.

Newton, C. W., and A. V. Persson, 1962: Structural characteristics of the subtropical jet stream and certain lower-stratospheric wind systems. *Tellus*, **14**, 221-241.

Nicholls, M. E., R. A. Pielke, and W. R. Cotton, 1991: A two-dimensional numerical investigation of the interaction between sea breezes and deep convection over the Florida peninsula. *Mon. Wea. Rev.*, **119**, 298-323.

Newton, C. W., and E. O. Holopainen, Eds., 1990: *Extratropical cyclones, The Erik Palmén Memorial Volume.* Amer. Meteor. Soc., 262 pp.

Palmén, E., and C. W. Newton, 1969: *Atmospheric Circulation Systems.* International Geophysics Series, v. 13, Academic Press, 603 pp.

Parker, D. E., 1983: Documentation of a Southern Oscillation index. *Meteor. Mag.*, **112**, 184-188.

Petterssen, S., 1958: *Introduction to Meteorology.* McGraw-Hill, 327 pp.

Petterssen, S., 1956: *Weather Analysis and Forecasting, Vol. 1.* 2nd ed., McGraw-Hill, 428 pp.

Philander, S. G., 1989: El Niño and La Niña. *American Scientist*, **77**, 451-459.

Philander, S. G., 1990: *El Niño, La Niña and the Southern Oscillation.* Academic Press, 293 pp.

Phillips, N. A., 1950: The behavior of jet streams over eastern North America during January and February 1948. *Tellus*, **2**, 116-124.

Pond, S., and G. L. Pickard, 1978: *Introductory Dynamic Oceanography.* Pergamon Press, 241 pp.

Quinn, W. H., and V. T. Neal, 1987: El Niño occurrences over the past four and a half centuries. *J. Geophys. Res. Oceans* **92(C13)**, 14,449-14,461.

Quiroz, R. S., 1983a: Relationships among the stratospheric and tropospheric zonal flows and the Southern Oscillation. *Mon. Wea. Rev.*, **111**, 143-154.

Quiroz, R. S., 1983b: The climate of the "El Niño" winter of 1982/83 - a season of extraordinary climatic anomalies. *Mon. Wea. Rev.*, **111**, 1685-1706.

Rasmussen, E. M., 1967: Atmospheric water vapor transport and the water balance of North America: Part I. Characteristics of the water vapor flux field. *Mon. Wea. Rev.*, **95**, 403-426.

Rasmussen, E. M., 1991: Observational aspects of ENSO cycle teleconnections. In *Teleconnections Linking Worldwide Climate Anomalies*, Eds. M. H. Glantz, R. W. Katz and N. Nicholls, Cambridge University Press, 309-344.

Rasmussen, E. M., and T. H. Carpenter, 1982: Variations in tropical sea surface temperature and surface wind fields associated with the Southern Oscillation/El Niño. *Mon. Wea. Rev.*, **110**, 354-384.

Reed, R. J., 1990: Advances in knowledge and understanding of extratropical cyclones during the past quarter century: an overview. In *Extratropical Cyclones, The Erik Palmén Memorial Volume*, C. W. Newton, and E. O. Holopainen, Eds., Amer. Meteor. Soc., 27-45.

Reed, R. J., and M. T. Stoelinga, 1992: A model-aided study of the origin and evolution of the anomalously high potential vorticity in the inner region of a rapidly deepening marine cyclone. *Mon. Wea. Rev.*, **120**, 893-913.

Reitan, C. H., 1974: Frequencies of cyclones and cyclogenesis for North America, 1951-1970. *Mon. Wea. Rev.*, **102**, 861-868.

Reiter, E. R., 1963: *Jet Stream Meteorology*. The University of Chicago Press, 515 pp.

Reiter, E. R., 1967a: *Jet Streams*. Doubleday and Co., 189 pp.

Reiter, E. R., 1967b: Jet streams. *The Encyclopedia of Atmospheric Sciences and Astrogeology*, Ed. R. W. Fairbridge, Rheinhold Publishing Corporation, 510-514.

Reiter, E. R., 1978: *Atmospheric Transport Processes Part 4: Radioactive Tracers*. Technical Information Center, U.S. Department of Energy, U.S. Government Printing Office, Washington, D.C., 495 pp.

Riehl, H., 1948: Jet stream in upper troposphere and cyclone formation. *Trans. Am. Geophys. Union*, **29**, 175-186.

Riehl, H., 1954: *Tropical Meteorology.* McGraw-Hill, 392 pp.

Riehl, H., M. A. Alaka, C. L. Jordan and R. J. Renard, 1954: *The Jet Stream.* Meteorological Monographs Vol. 2, No.7, Amer. Meteor. Soc., 100 pp.

Roberts, H. H., O. K. Huh, S. A. Hsu, L. J. Rouse, Jr. and D. A. Rickman, 1987: Impact of cold front passages on geomorphic evolution and sediment dynamics of the complex Louisiana coast. Coastal Sediments '87: Proceedings of a Specialty Conference on Advances in Understanding of Coastal Sediment Processes , American Society of Civil Engineers, Waterways Division, 1950-1963.

Roberts, H. H., O. K. Huh, L. J. Rouse, Jr. and D. A. Rickman, 1989: Winter storm impacts on the chenier plain coast of southwestern Louisiana. *Trans. Gulf Coast Assoc. of Geol. Socs.*, **39**, 515-522.

Rogers, J. C., 1984: The association between the North Atlantic Oscillation and the Southern Oscillation in the Northern Hemisphere. *Bull. Amer. Meteor. Soc.*, **112**, 1999-2015.

Ropelewski, C. F., and M. S. Halpert, 1986: North American precipitation and temperature patterns associated with the El Niño/Southern Oscillation. *Mon. Wea. Rev.*, **114**, 2352-2361.

Ropelewski, C. F., and M. S. Halpert, 1987: Global and regional scale precipitation patterns associated with the El Niño/Southern Oscillation. *Mon. Wea. Rev.*, **115**, 1606-1626.

Sadler, J. C., M. A. Lander, A. M. Hori and L. K. Oda, 1987: *Tropical Marine Climate Atlas.* Vols. 1 and 2, University of Hawaii, Department of Meteorology, UHMET 87-01.

Saucier, W. J., 1949: Texas-west Gulf cyclones. *Mon. Wea. Rev.*, **77**, 219-231.

Saucier, W. J., 1955: *Principles of Meteorological Analysis.* Dover Publications Inc., 438 pp.

Sechrist, F. S., and T. M. Whittaker, 1979: Evidence of jet streak vertical circulations. *Mon. Wea. Rev.*, **107**, 1015-1021.

Schroeder, W. W., O. K. Huh, L. J. Rouse, Jr. and W. J. Wiseman, Jr., 1985: Satellite observations of the circulation east of the Mississippi River delta: cold-air outbreak conditions. *Remote Sens. Environ.*, **18**, 49-58.

Shapiro, M. A., and D. A. Keyser, 1990: Fronts, jet streams, and the tropopause. In *Extratropical Cyclones, The Erik Palmén Memorial Volume*, Eds. C. W. Newton, and E. O. Holopainen, Amer. Meteor. Soc., 167-193.

Snedecor, G. W., and W. G. Cochran, 1980: *Statistical Methods.* 7th ed., The Iowa State University Press, 507 pp.

Snedecor, G. W., and W. G. Cochran, 1989: *Statistical Methods.* 8th ed., The Iowa State University Press, 503 pp.

Southern Regional Climate Center: *Climatic Division Data, 1895 to 1989.* Southern Regional Climate Center, Room 262, Howe-Russell Geoscience Complex, Louisiana State University, Baton Rouge, LA, 70803.

Suppiah, R., 1989: Relationships between the Southern Oscillation and the rainfall of Sri Lanka. *J. Climatol.*, **9**, 601-618.

Tibaldi, S., A. Buzzi, and A. Speranza, 1990: Orographic cyclogenesis. In *Extratropical Cyclones, The Erik Palmén Memorial Volume*, C. W. Newton, and E. O. Holopainen, Eds., Amer. Meteor. Soc., 107-127.

Trenberth, K. E., 1991: General characteristics of El Niño-Southern Oscillation. In *Teleconnections Linking Worldwide Climate Anomalies*, Eds. M. H. Glantz, R. W. Katz and N. Nicholls, Cambridge University Press, 13-42.

Uccellini, L. W., P. J. Kocin, R. A. Petersen, C. H. Wash and K. F. Brill, 1984: The Presidents' Day cyclone of 18-19 February 1979: Synoptic overview and analysis of the subtropical jet streak influencing the pre-cyclogenetic period. *Mon. Wea. Rev.*, **112**, 31-55.

Uccellini, L. W., R. A. Petersen, K. F. Brill, P. J. Kocin and J. J. Tuccillo, 1987: Synergistic interactions between an upper-level jet streak and diabatic processes that influence the development of a low-level jet and a secondary coastal cyclone. *Mon. Wea. Rev.*, **115**, 2227-2261.

Uccellini, L. W., 1990: Processes contributing to the rapid development of extratropical cyclones. In *Extratropical Cyclones, The Erik Palmén Memorial Volume*, C. W. Newton, and E. O. Holopainen, Eds., Amer. Meteor. Soc., 81-105.

United States Weather Bureau, Sept. 1940 to Sept. 1944 and Jan. 1949 to Aug. 1970: *Daily Series Synoptic Weather Maps, Part I, Northern Hemisphere Sea Level and 500 Millibar Charts.* National Oceanic and Atmospheric Administration, Environmental Data Service, U.S. Govt. Printing Office, Washington, D.C.

United States Department of Commerce, Sept. 1960 to Aug. 1970: *Daily Series Synoptic Weather Maps, Part I, Northern Hemisphere Sea Level and 500 Millibar Charts.* National Oceanic and Atmospheric Administration, Environmental Data Service, U.S. Govt. Printing Office, Washington, D.C.

United States Department of Commerce, Sept. 1970 to Aug. 1990: *Daily Weather Maps, Weekly Series.* National Oceanic and Atmospheric Administration, Environmental Data Service, U.S. Govt. Printing Office, Washington, D.C.

van Loon, H., and J. C. Rogers, 1981: The Southern Oscillation, Part II: Association with changes in the middle troposphere in the northern winter. *Mon. Wea. Rev.*, **109**, 1163-1168.

Verdooren, L. R., 1963: Extended tables of critical values for Wilcoxon's test statistic. *Biometrika*, **50**, 177-186.

von Storch, H., and H. A. Kruse 1985: The significant tropospheric midlatitudinal El Niño response patterns observed in January 1983 and simulated by a GCM. *Coupled Ocean-Atmosphere Models*, Ed. J. C. J. Nihoul, Elsevier, Amsterdam, 275-287.

Walker, N. D., L. J. Rouse, Jr. and O. K. Huh, 1987: Response of subtropical shallow-water environments to cold-air outbreak events: satellite radiometry and heat flux modeling. *Cont. Shelf Res.*, **7**, 735-757.

White, M. E., and M. W. Downton, 1991: The shrimp fishery in the Gulf of Mexico: Relation to climatic variability and global atmospheric patterns. In *Teleconnections Linking Worldwide Climate Anomalies*, Eds. M. H. Glantz, R. W. Katz and N. Nicholls, Cambridge University Press, 459-492.

Whittaker, L. M., and L. H. Horn, 1982: Geographical and seasonal distribution of North American cyclogenesis, 1958-1977. *Mon. Wea. Rev.*, **109**, 2312-2322.

Wright, P. B., 1989: Homogenized long-period Southern Oscillation indices. *J. Climatol.*, **9**, 33-54.

Wright, P. B., 1984: Relationships between indices of the Southern Oscillation. *Mon. Wea. Rev.*, **112**, 1913-1919.

Yarnal, B., and D. J. Leather, 1988: Relationships between interdecadal and interannual climatic variations and their effect on Pennsylvania climate. *Ann. Assoc. Amer. Geog.*, **78**, 624-641

APPENDIX A
MEAN SEA-LEVEL PRESSURE FIELD

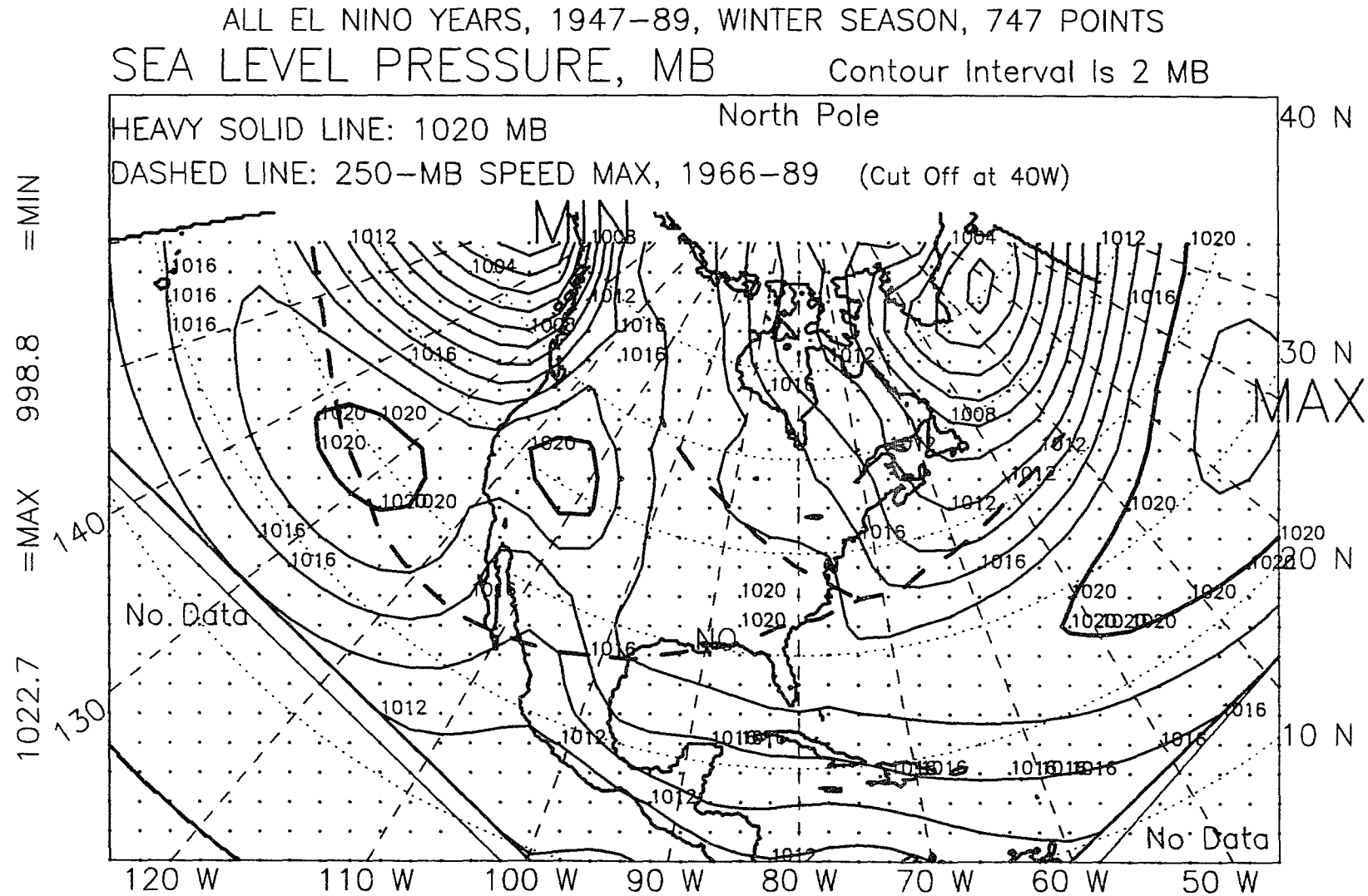

Figure A.1: Mean sea–level pressure, winter, El Niño years, 1947–89.

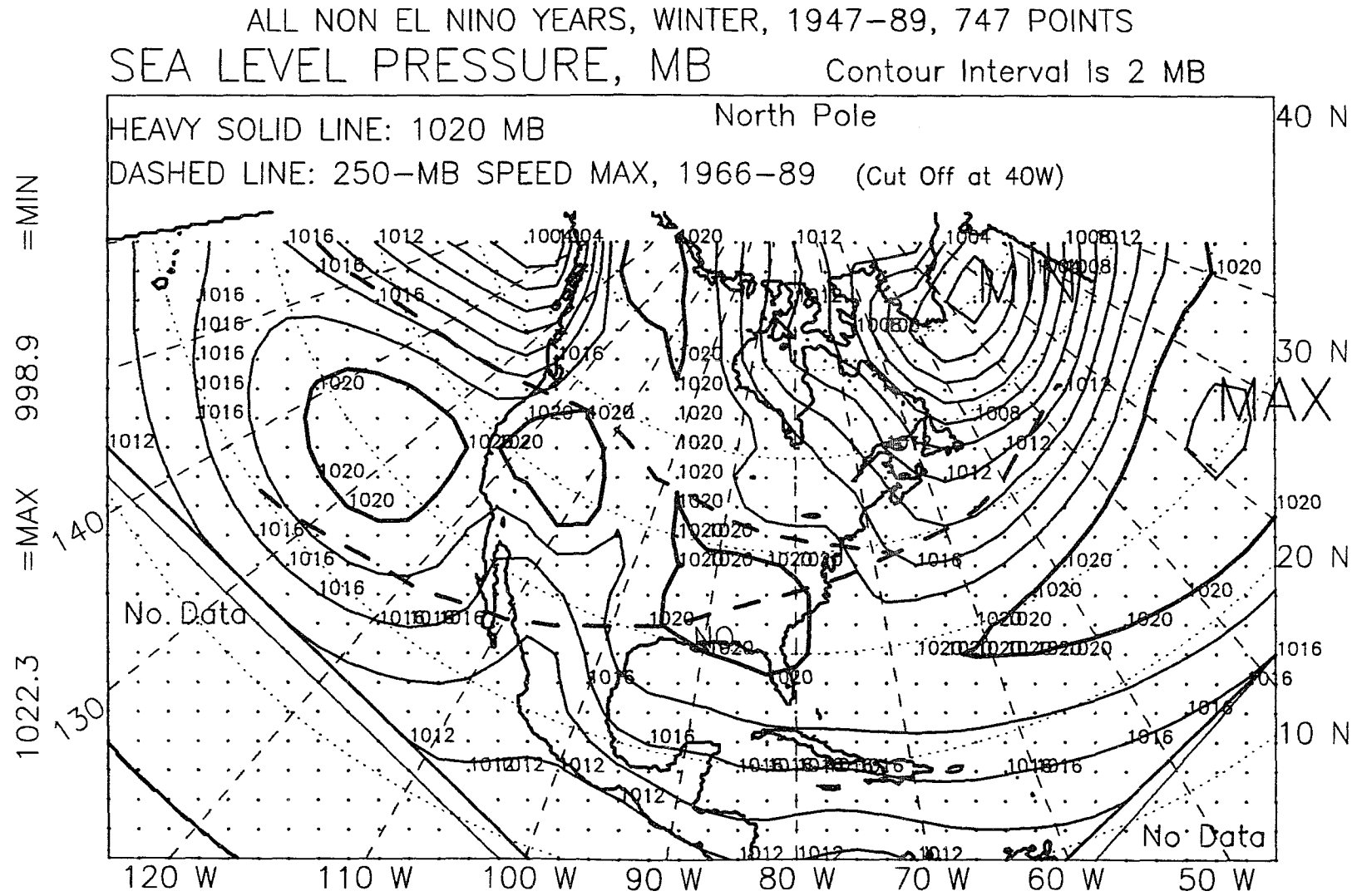

Figure A.2: Mean sea–level pressure, winter, non–El Niño years, 1947–89.

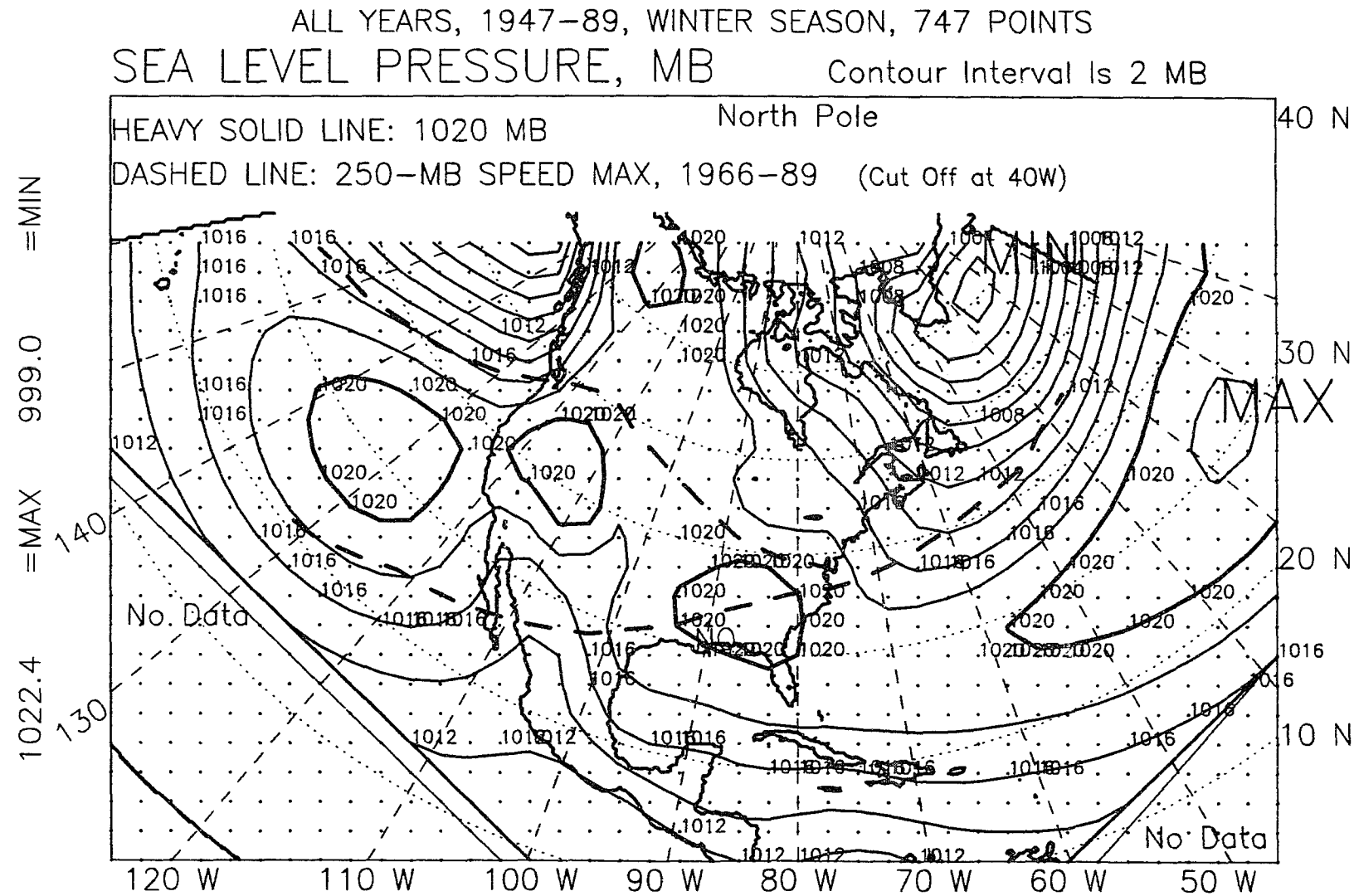

Figure A.3: Mean sea–level pressure, winter, all years, 1947–89.

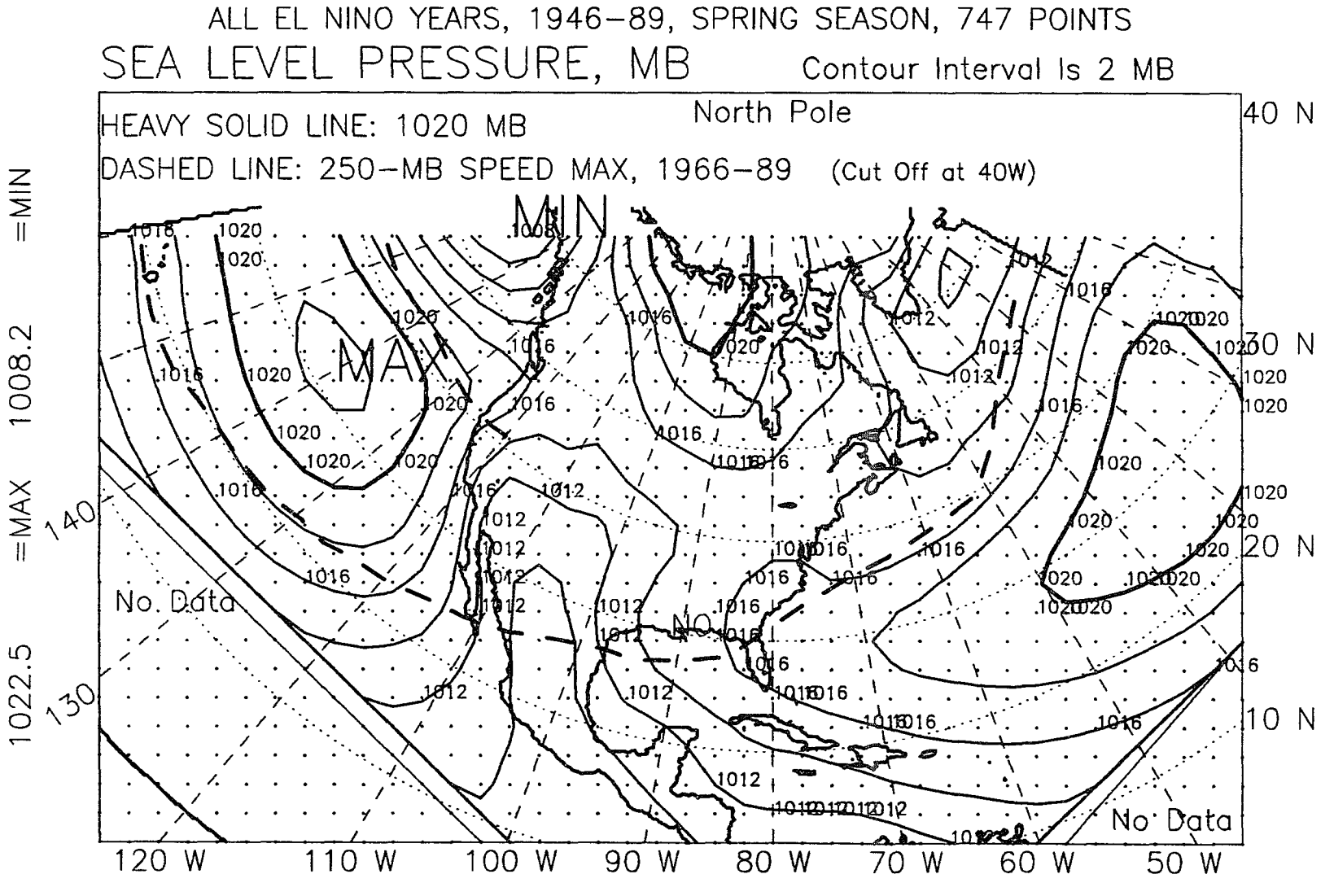

Figure A.4: Mean sea–level pressure, spring. El Niño years, 1947–89.

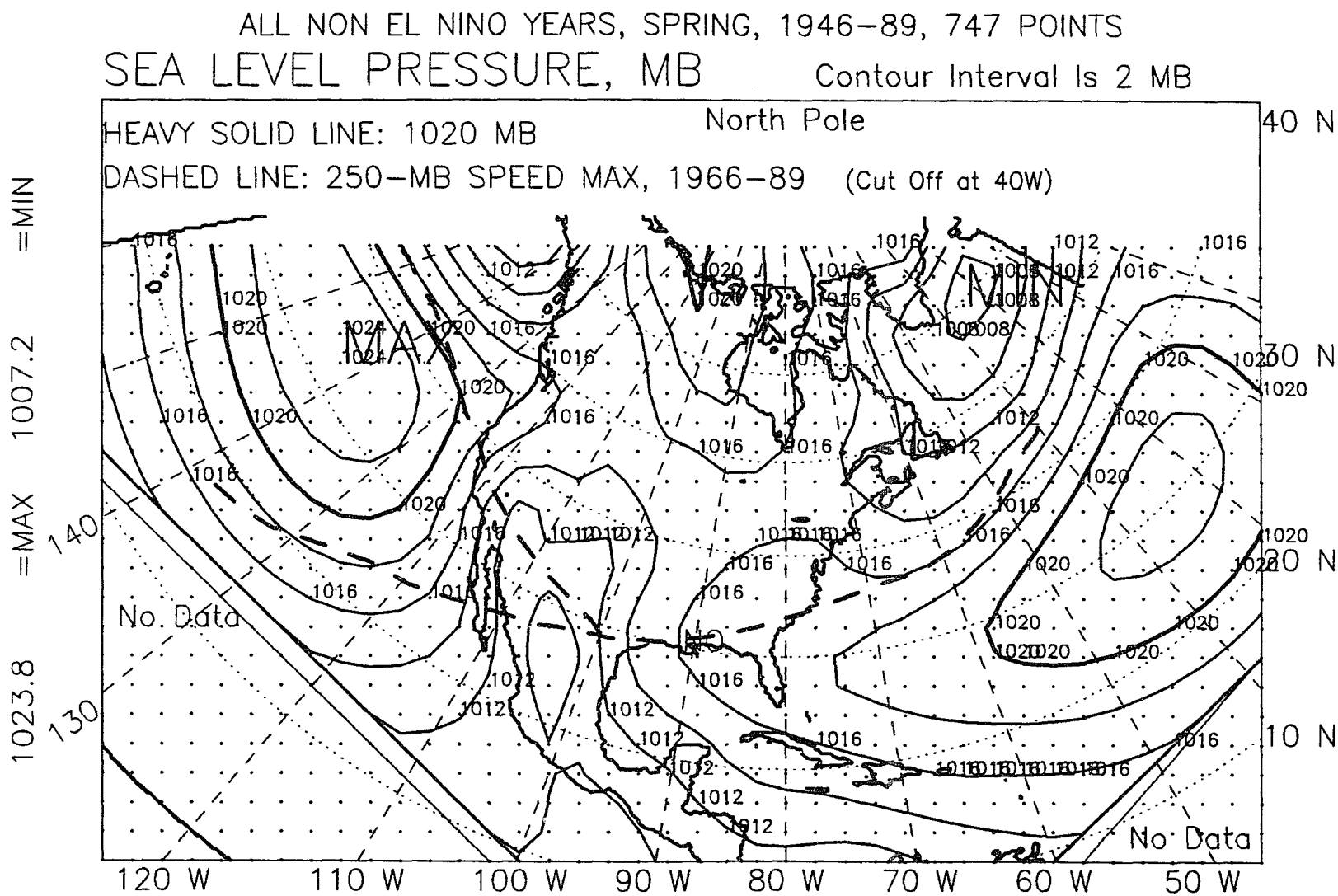

Figure A.5: Mean sea–level pressure, spring, non–El Niño years, 1947–89.

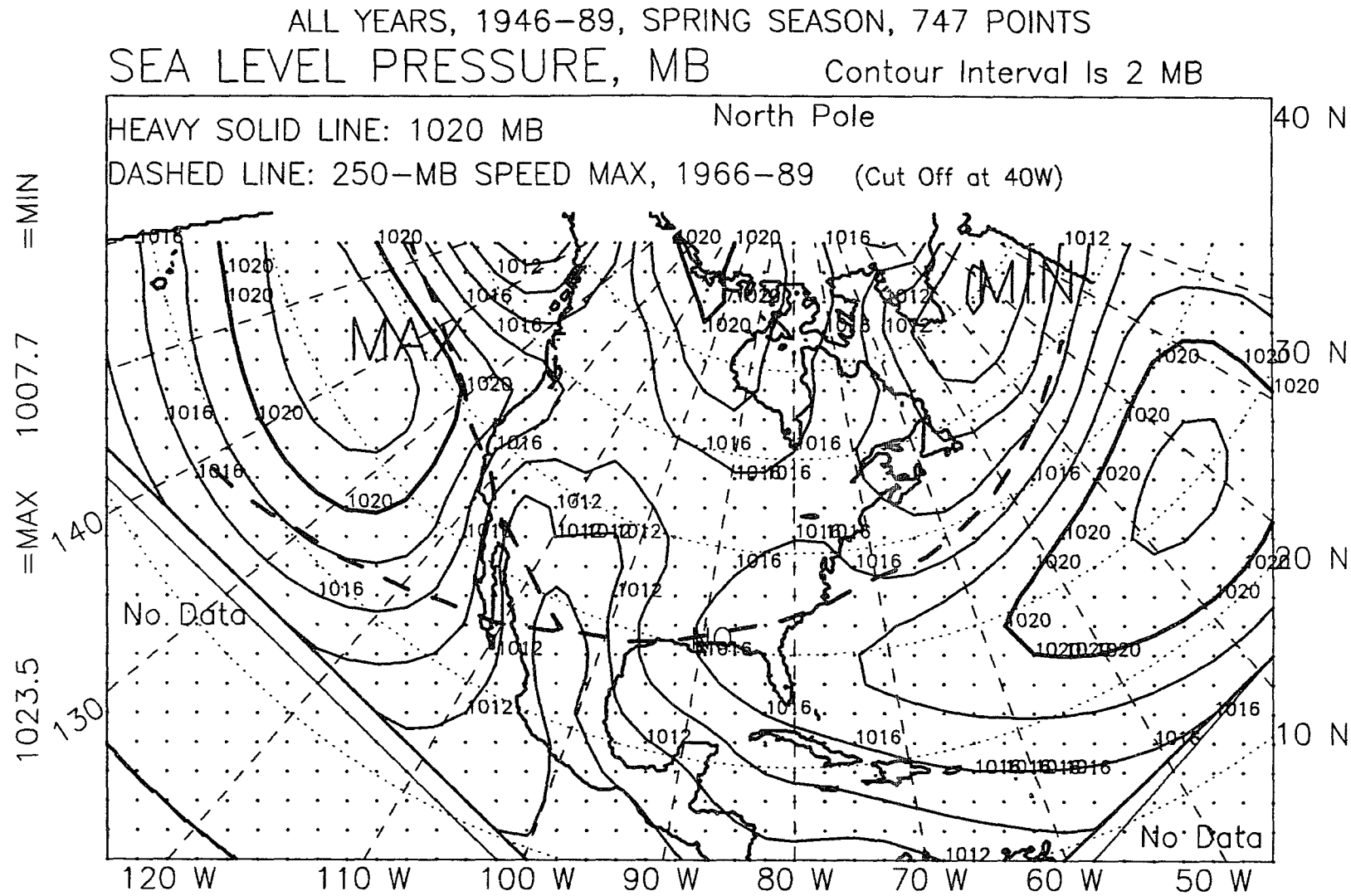

Figure A.6: Mean sea–level pressure, spring, all years, 1947–89.

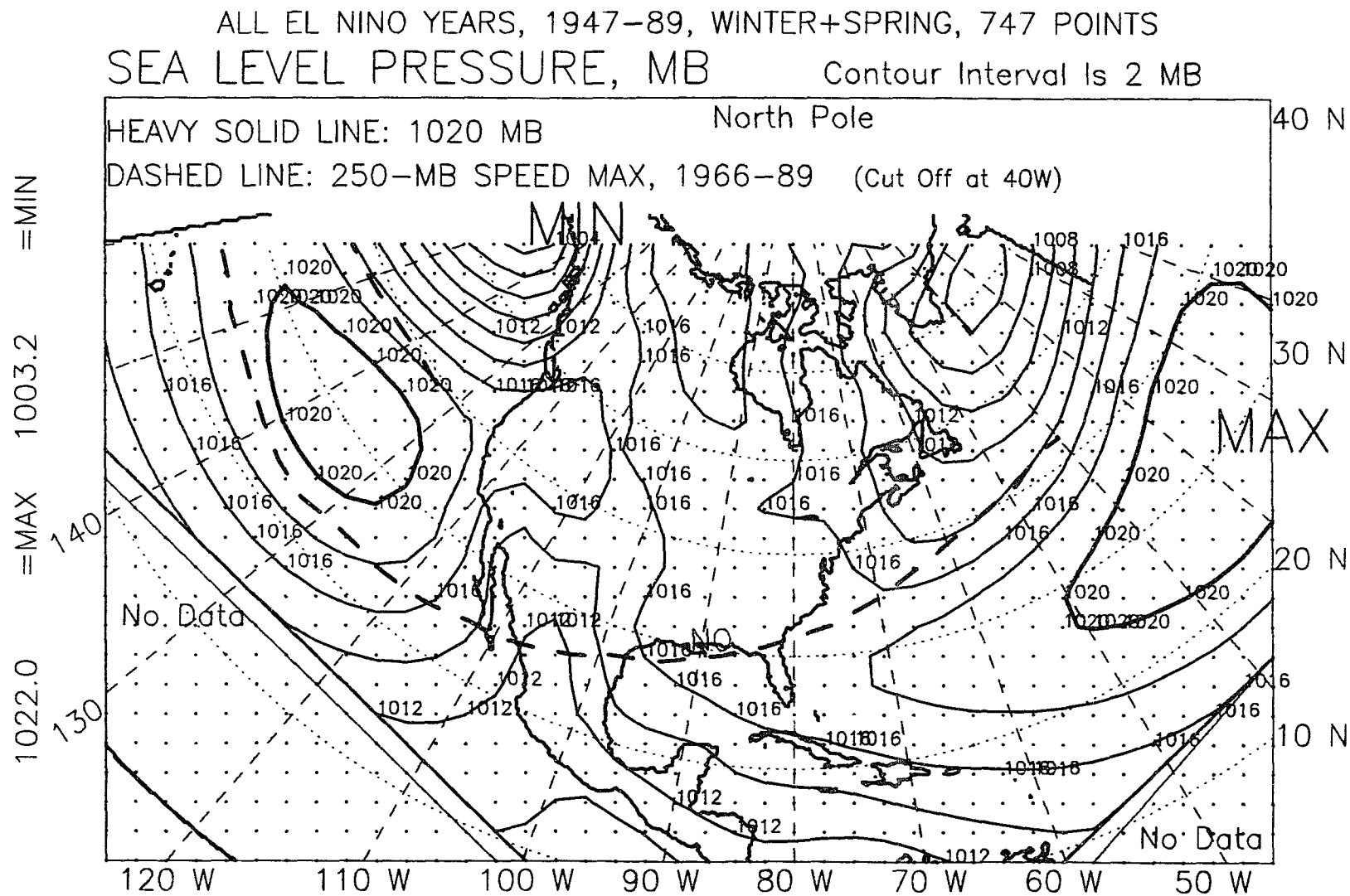

Figure A.7: Mean sea–level pressure, winter–plus–spring, El Niño years, 1947–89.

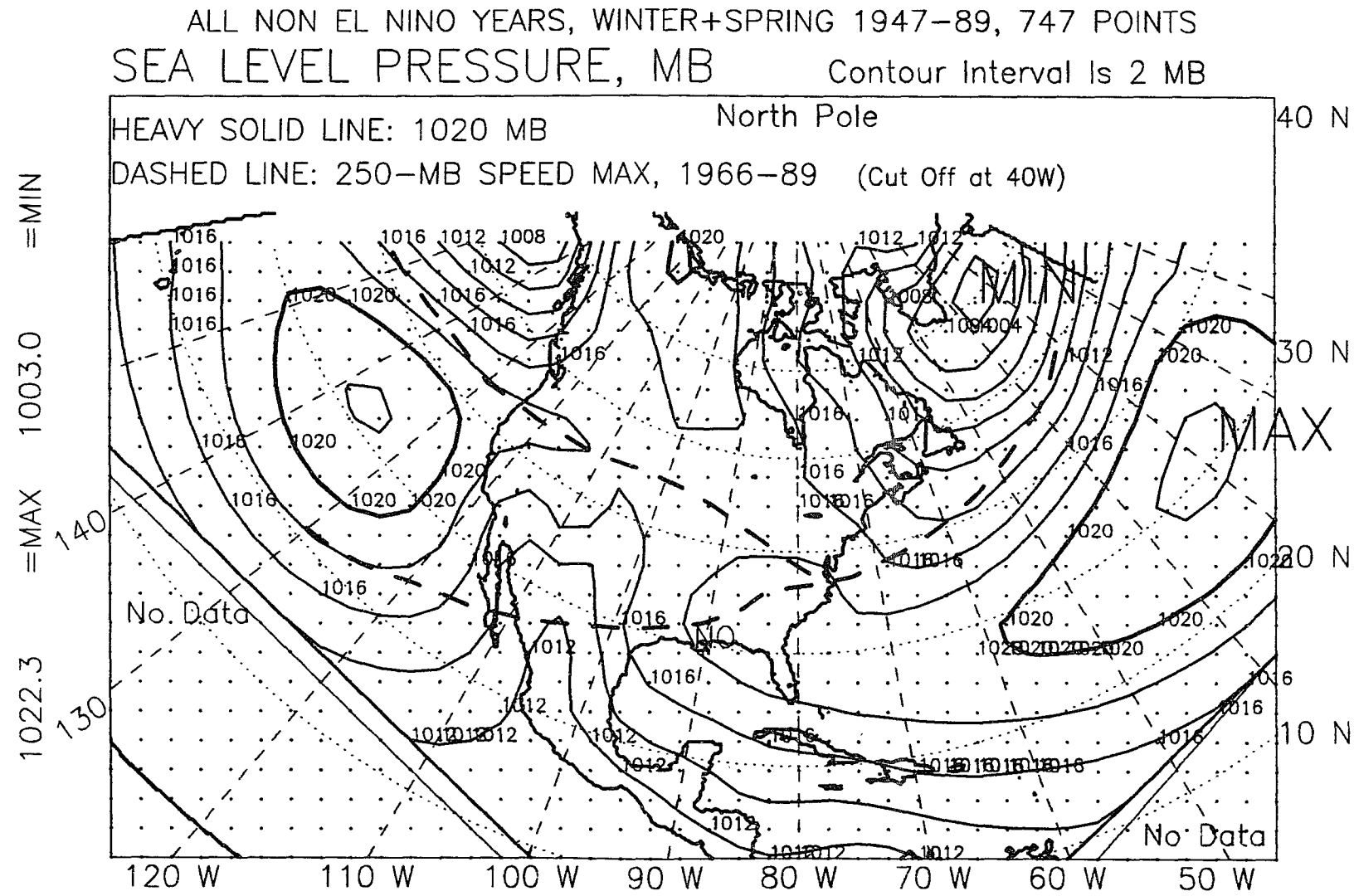

Figure A.8: Mean sea–level pressure, winter–plus–spring, non–El Niño years, 1947–89.

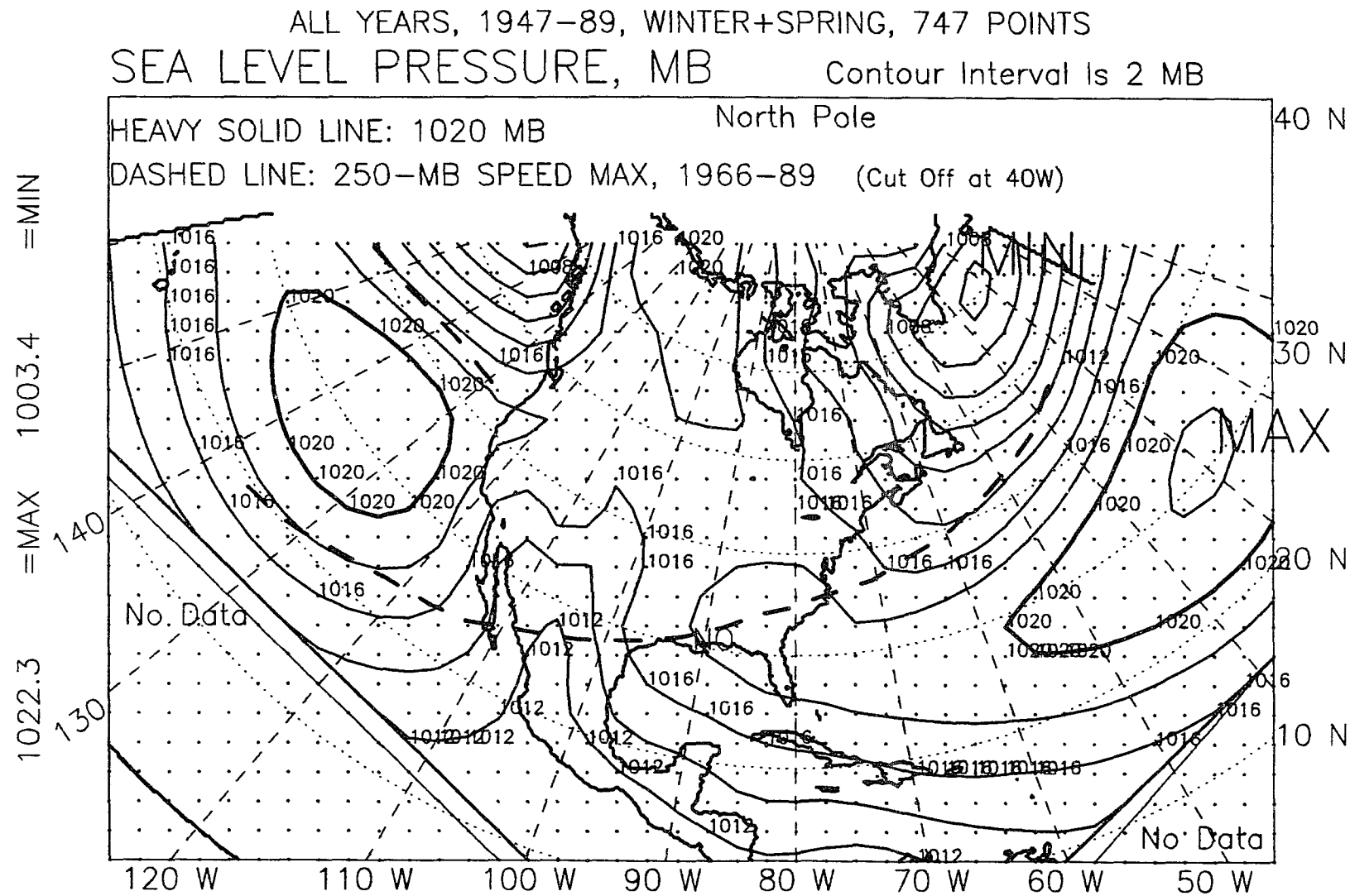

Figure A.9: Mean sea–level pressure, winter–plus–spring, all years, 1947–89.

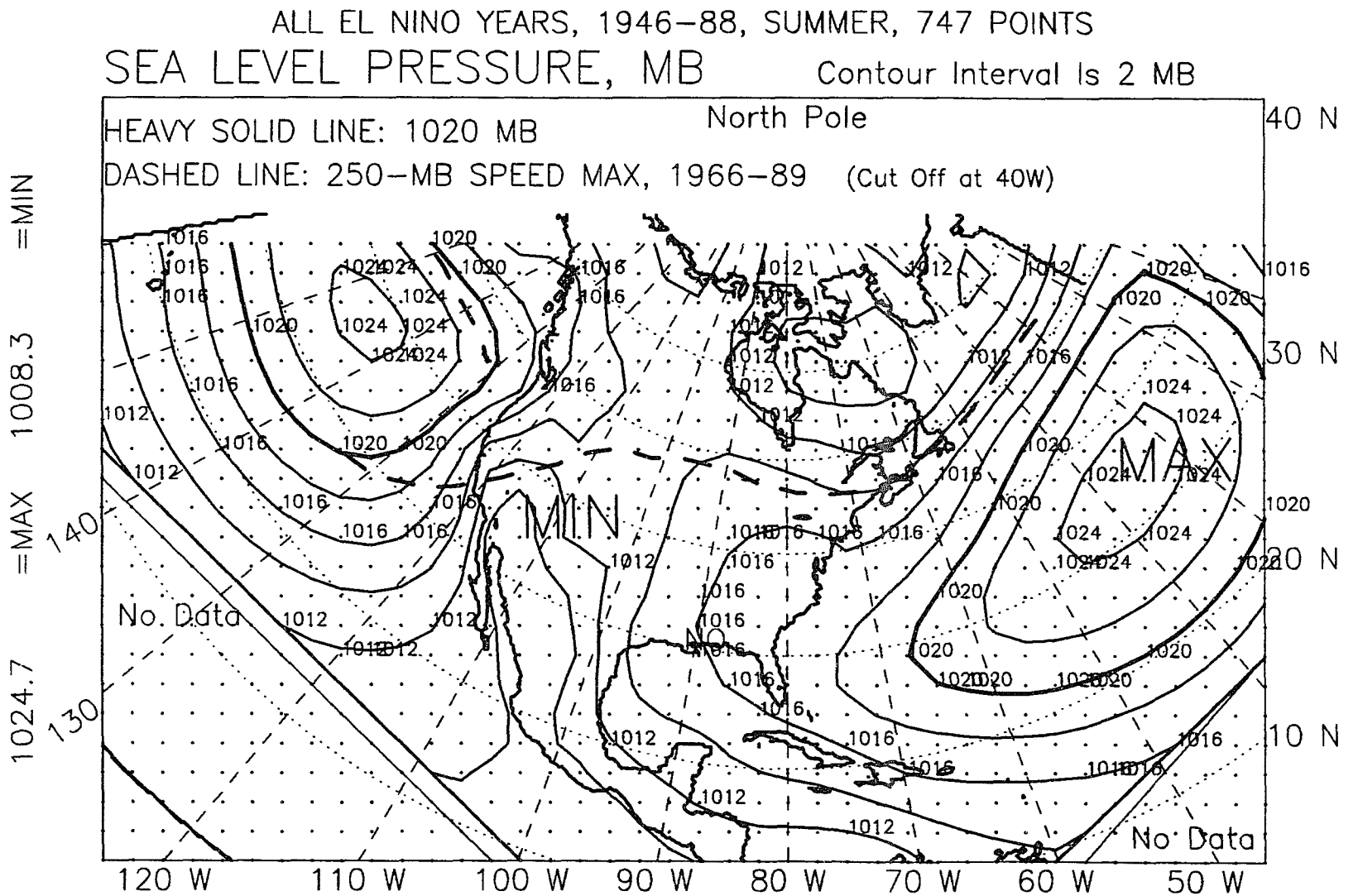

Figure A.10: Mean sea–level pressure, summer, El Niño years, 1946–88.

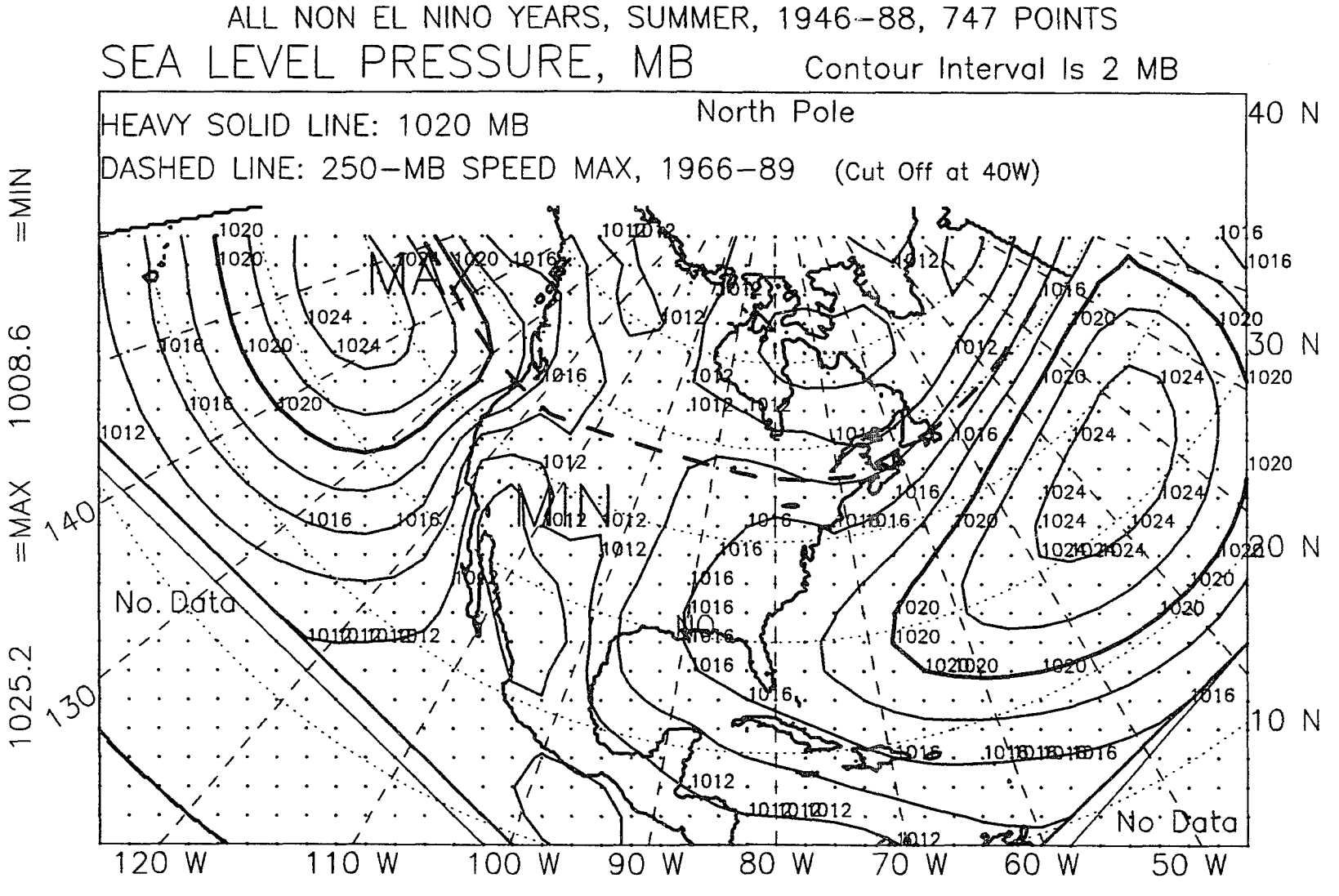

Figure A.11: Mean sea–level pressure, summer, non–El Niño years, 1946–88.

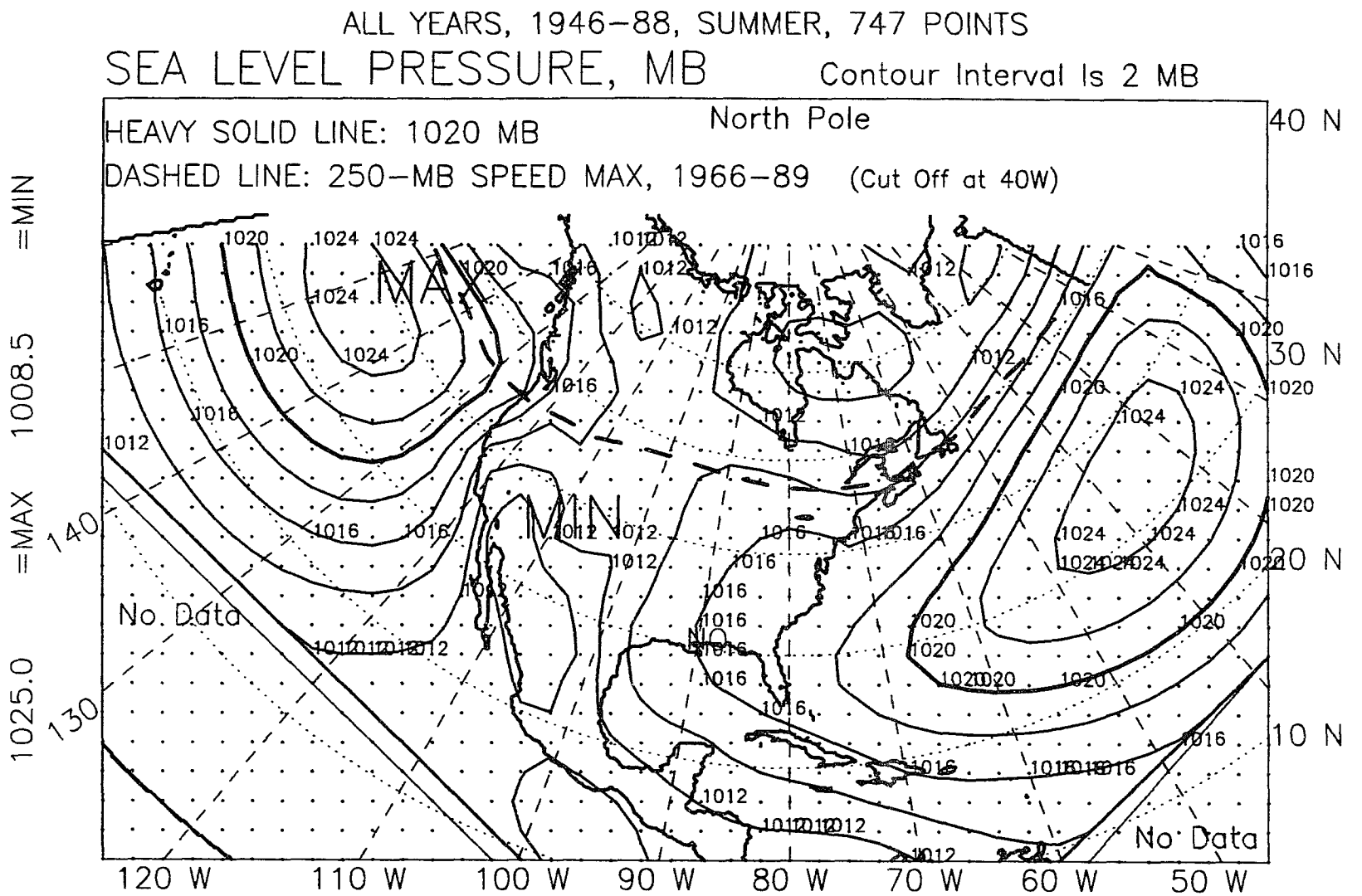

Figure A.12: Mean sea–level pressure, summer, all years, 1946–88.

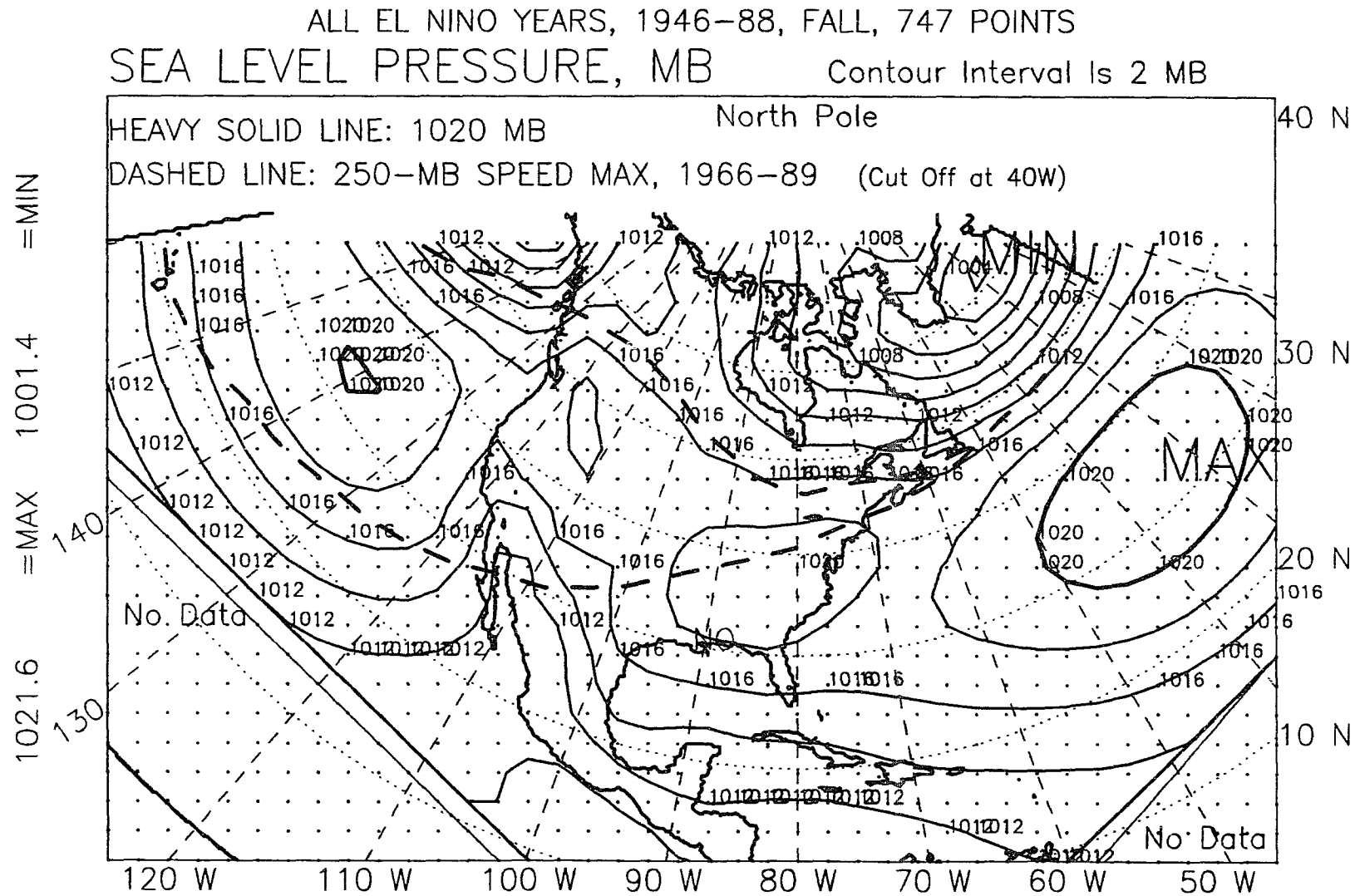

Figure A.13: Mean sea–level pressure, fall, El Niño years, 1946–88.

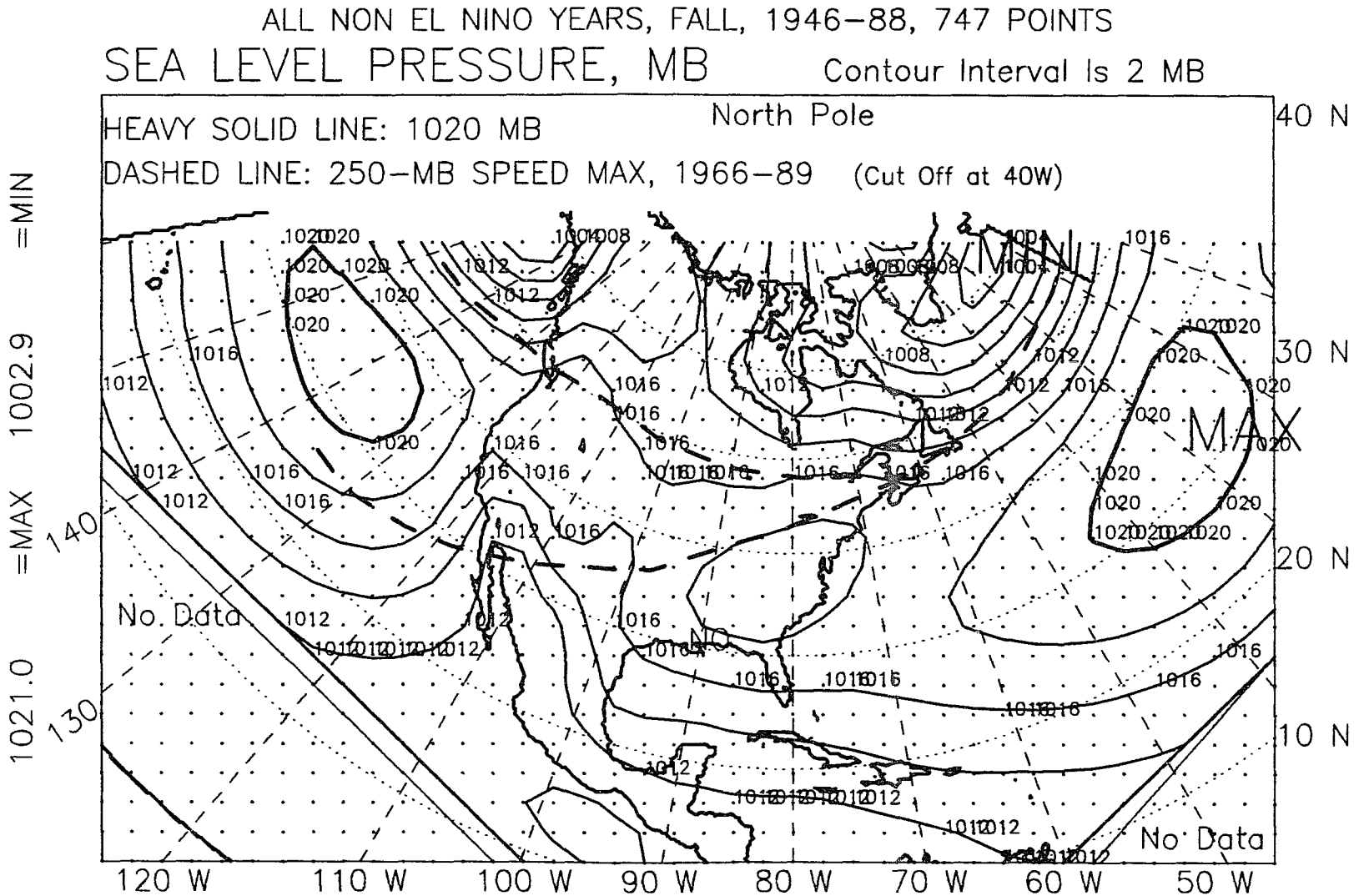

Figure A.14: Mean sea–level pressure, fall, non–El Niño years, 1946–88.

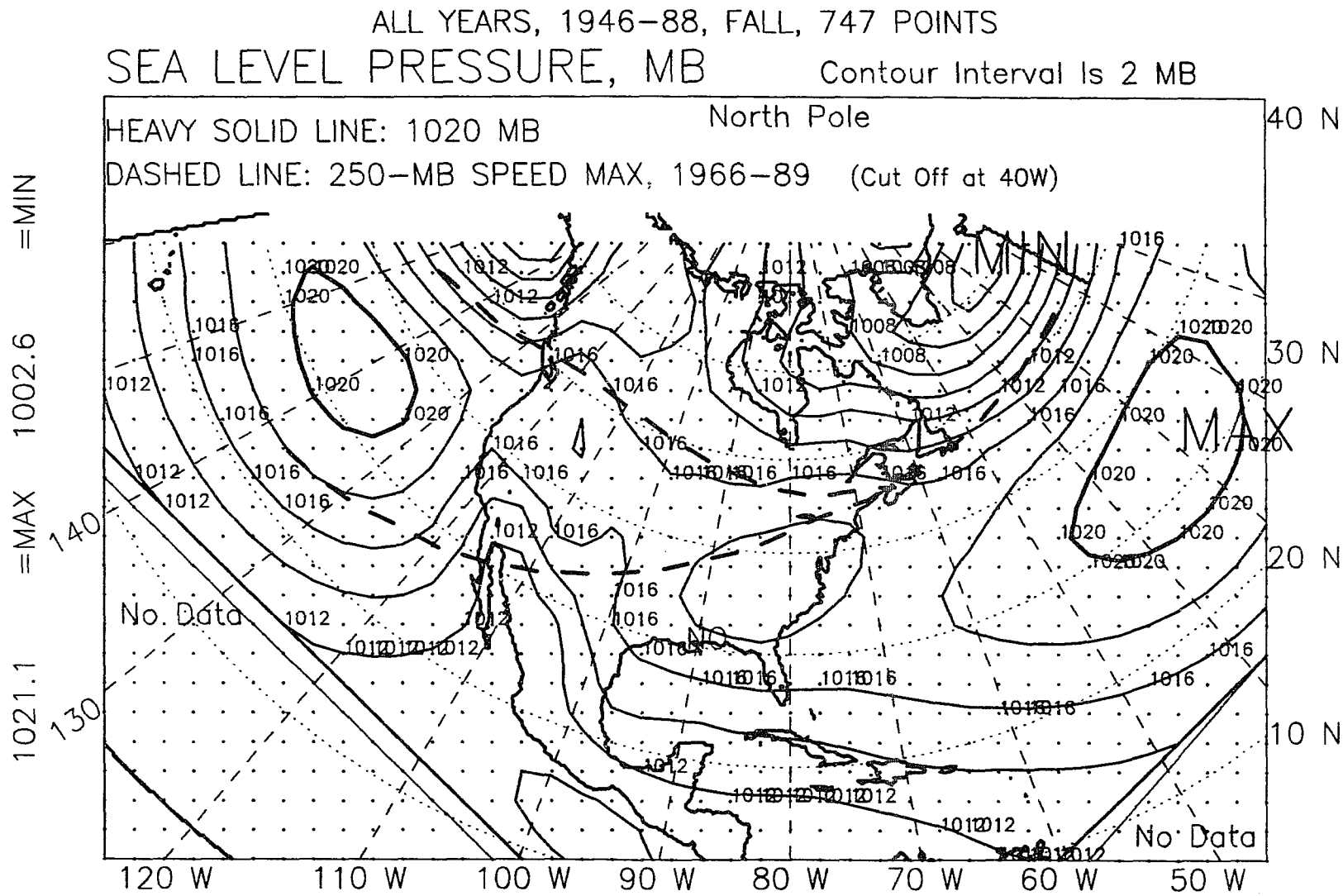

Figure A.15: Mean sea–level pressure, fall, all years, 1946–88.

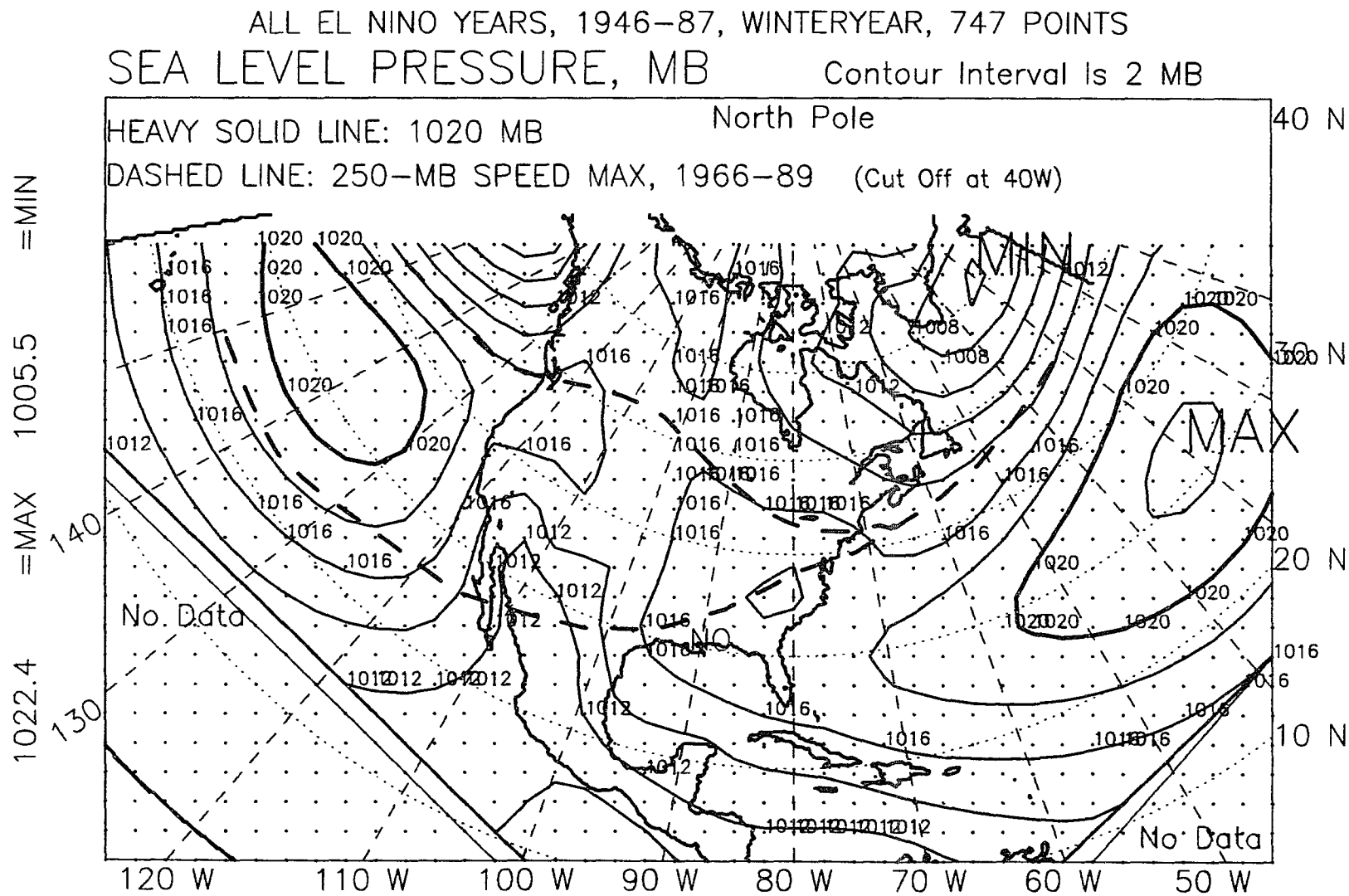

Figure A.16: Mean sea–level pressure, winter year, El Niño years, 1946–87.

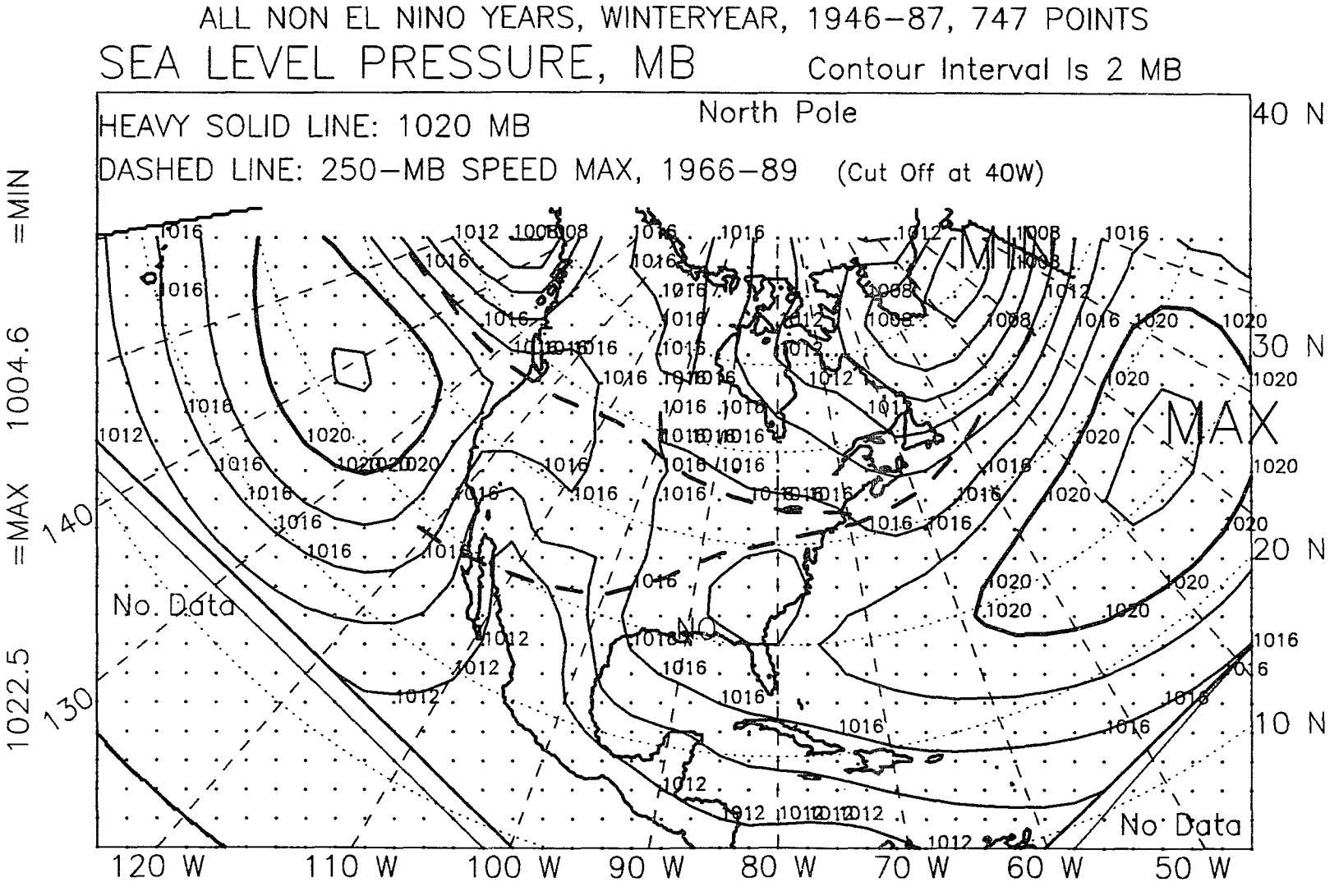

Figure A.17: Mean sea–level pressure, winter year, non–El Niño years, 1946–87.

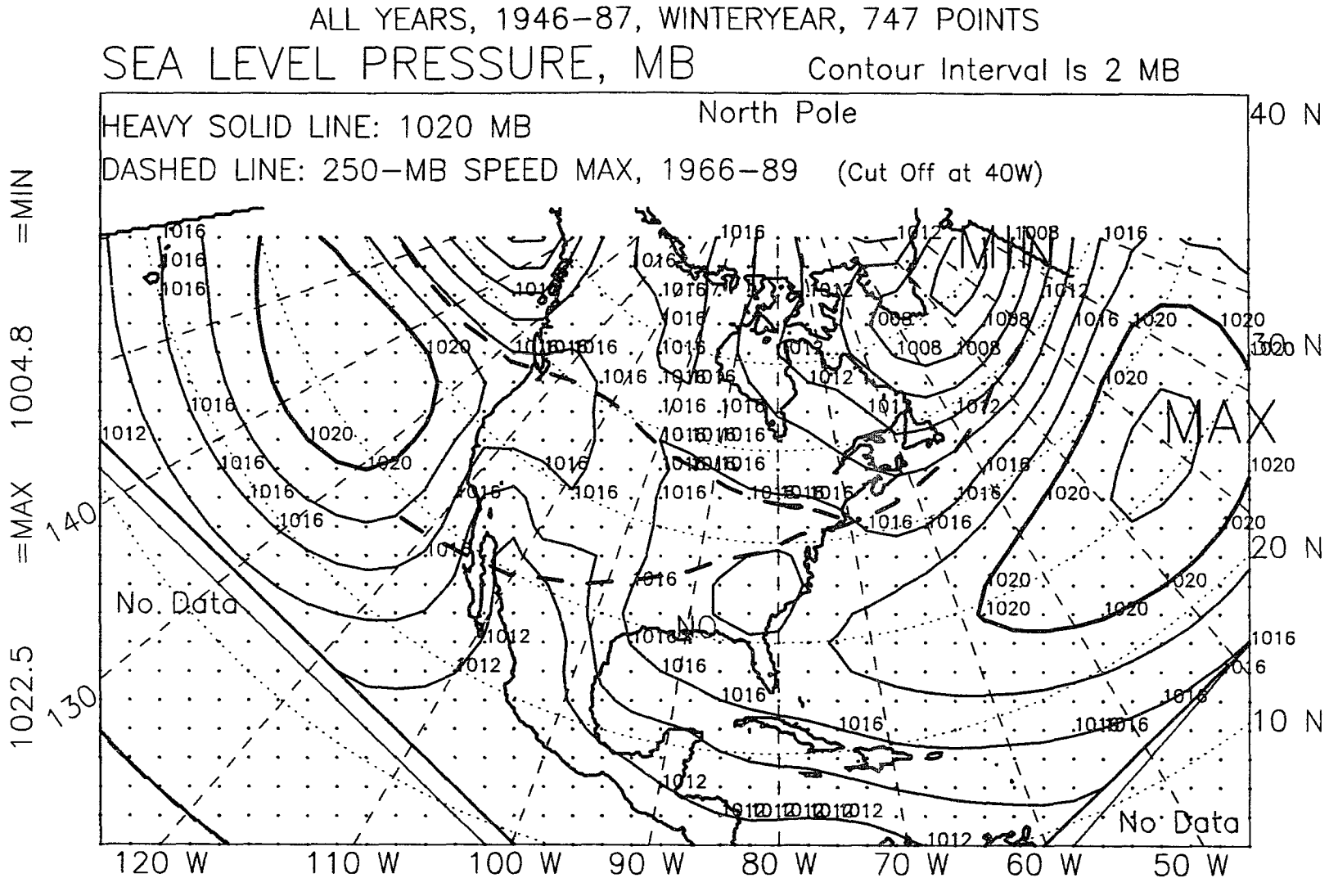

Figure A.18: Mean sea–level pressure, winter year, all years, 1946–87.

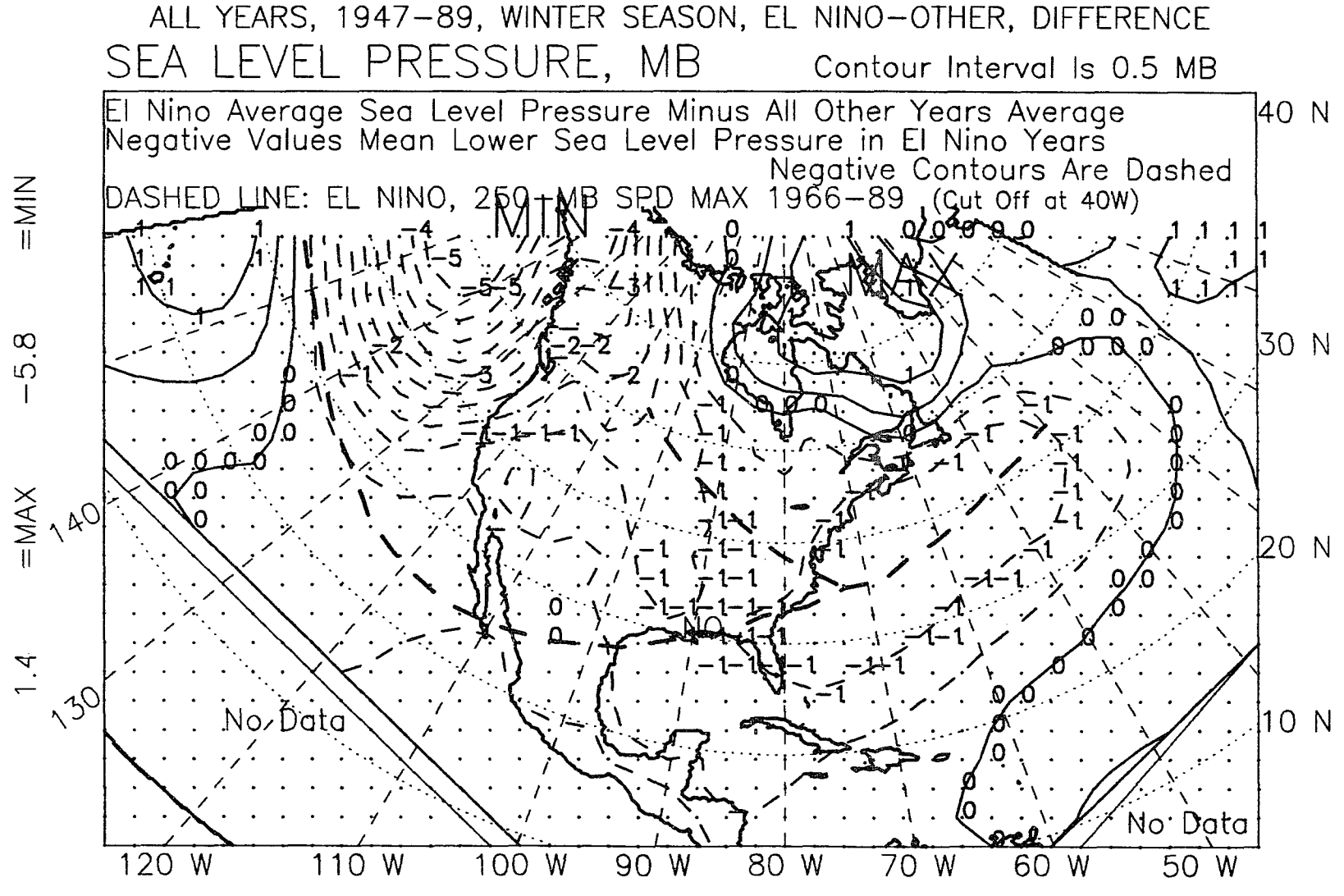

Figure A.19: Mean sea–level pressure, winter, 1947–89, difference.

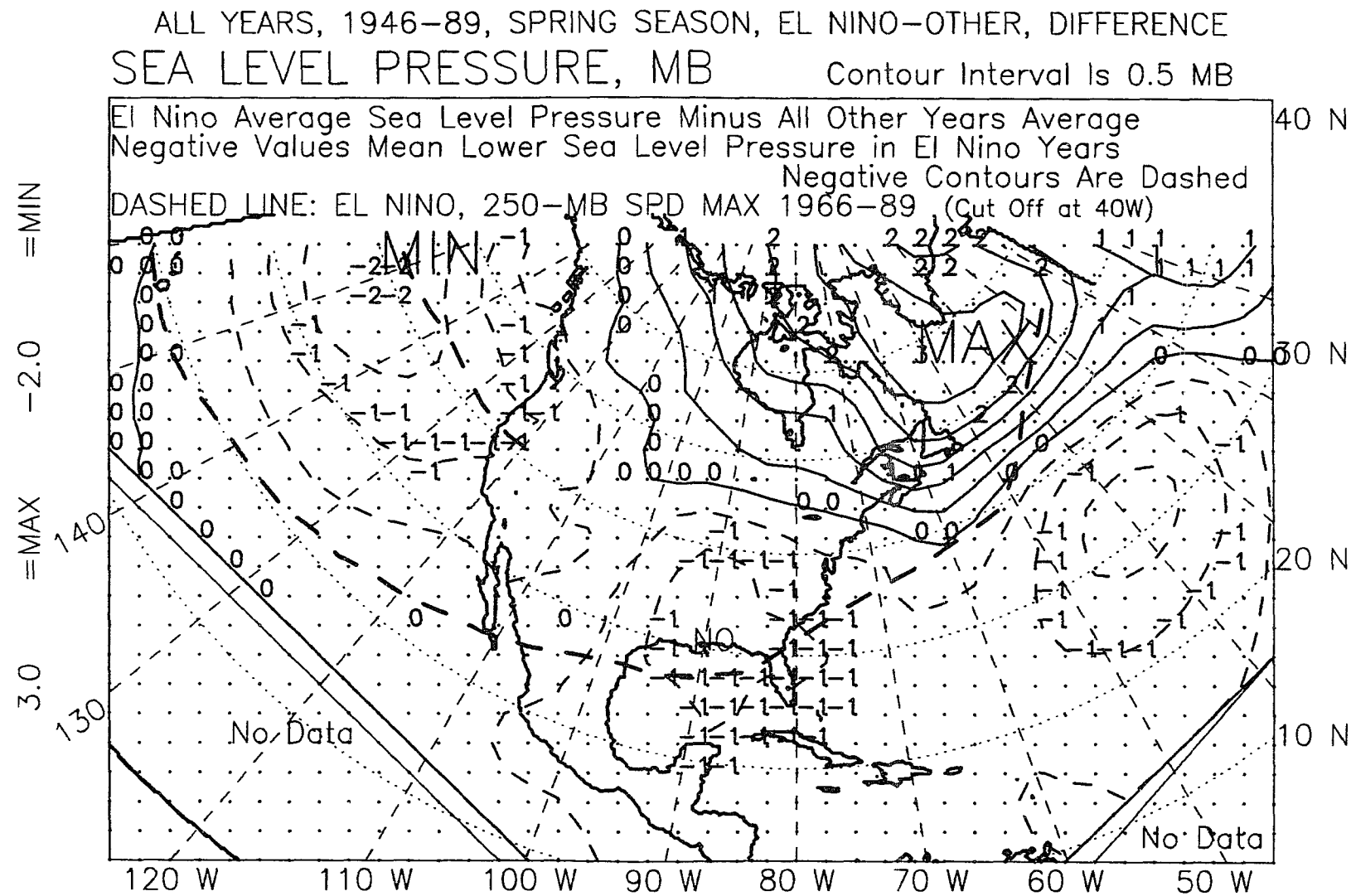

Figure A.20: Mean sea–level pressure, spring, 1947–89, difference.

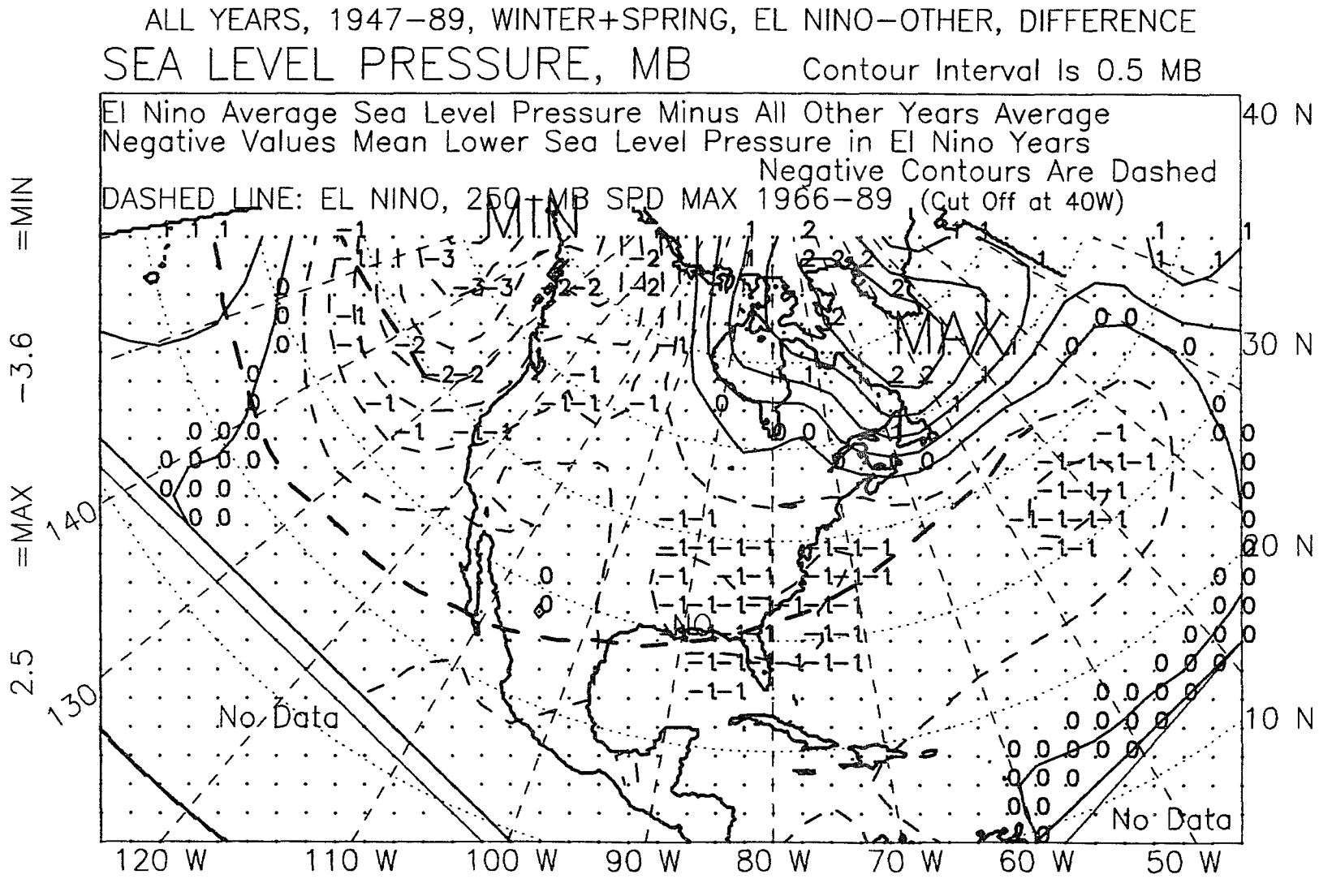

Figure A.21: Mean sea–level pressure, winter–plus–spring, 1947–89, difference.

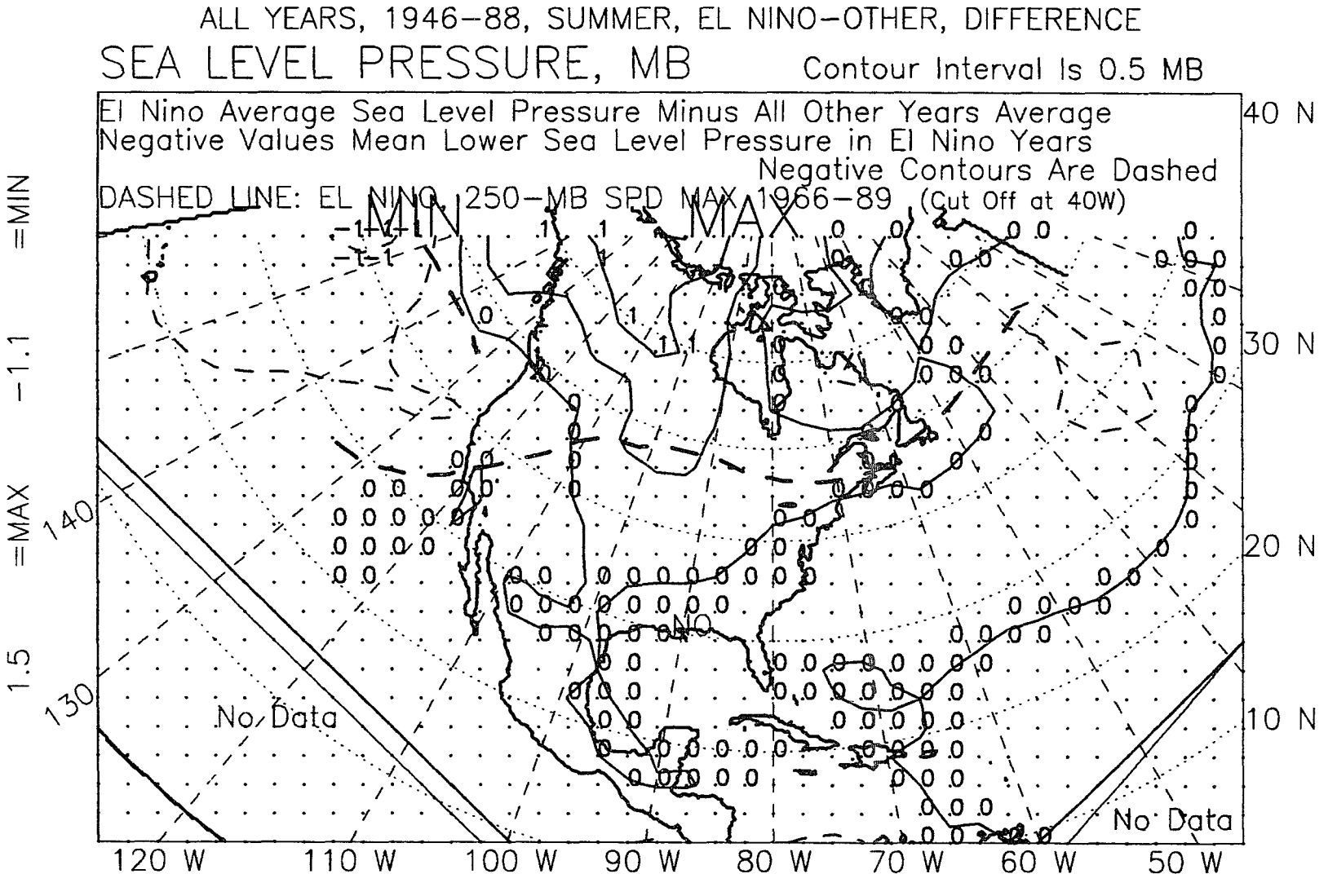

Figure A.22: Mean sea–level pressure, summer, 1946–88, difference.

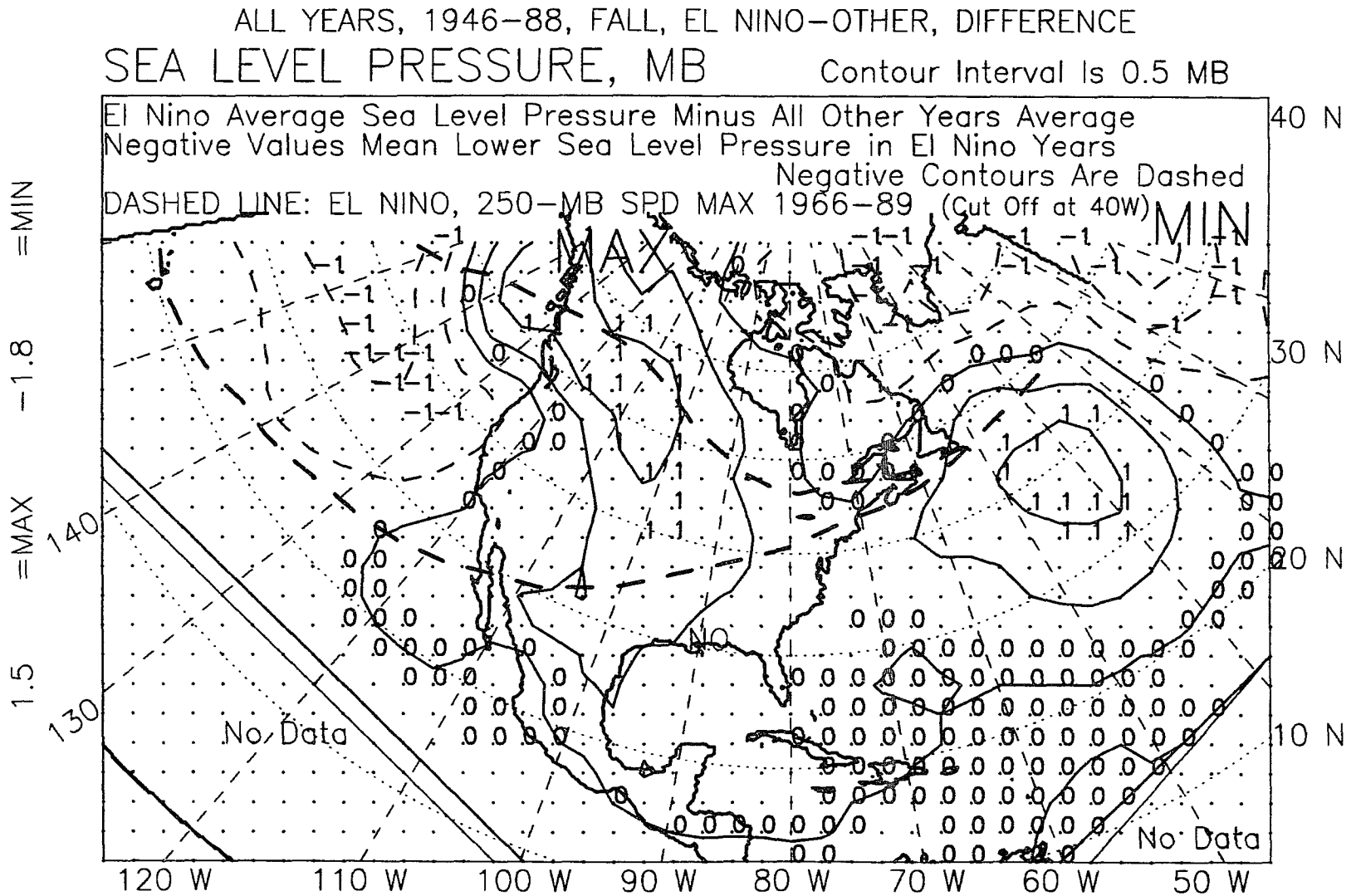

Figure A.23: Mean sea–level pressure, fall, 1946–88, difference.

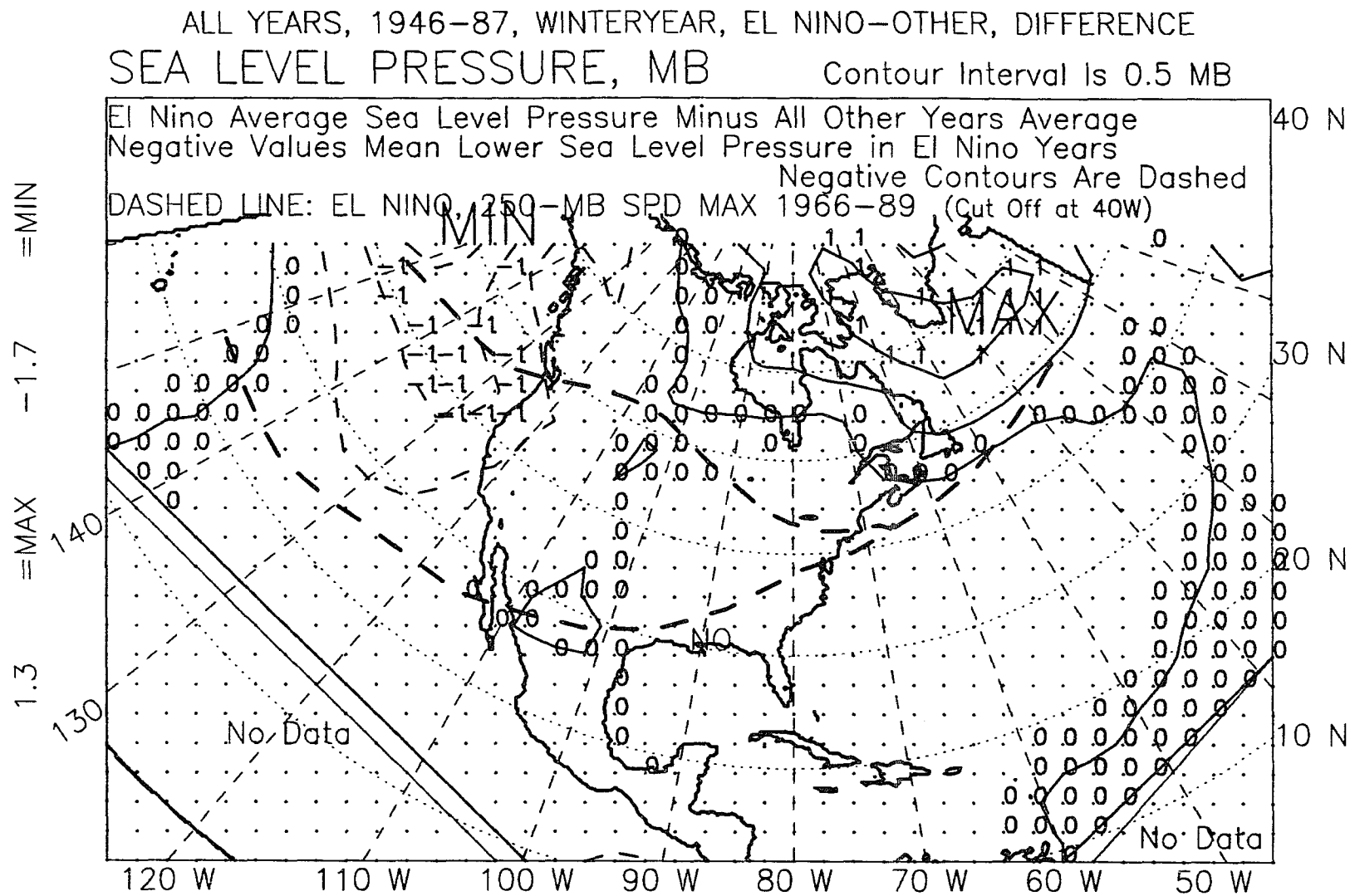

Figure A.24: Mean sea–level pressure, winter year, 1946–87, difference.

APPENDIX B
850-MB HEIGHT FIELD

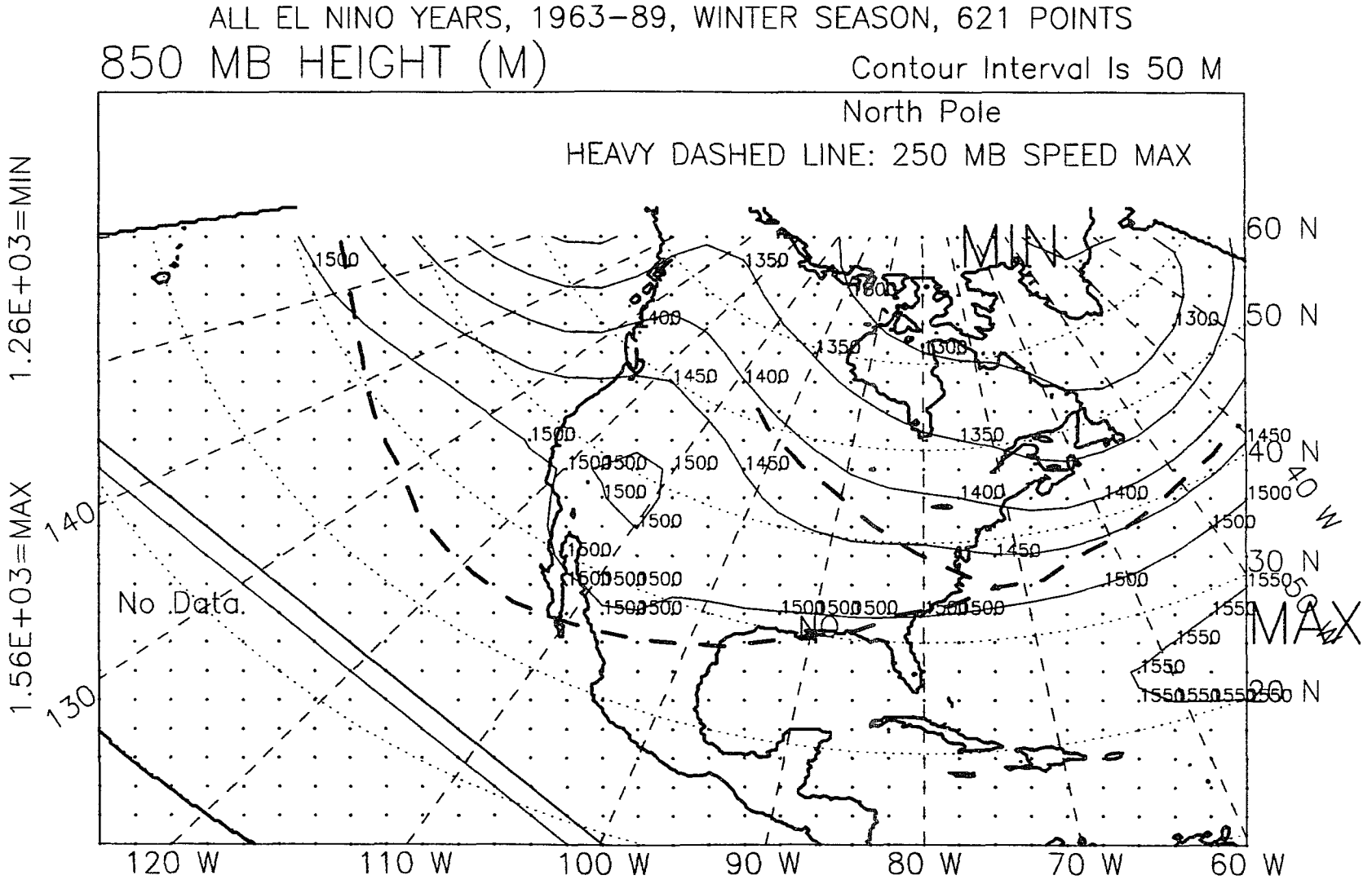

Figure B.1: 850–mb height, winter, El Niño years, 1963–89.

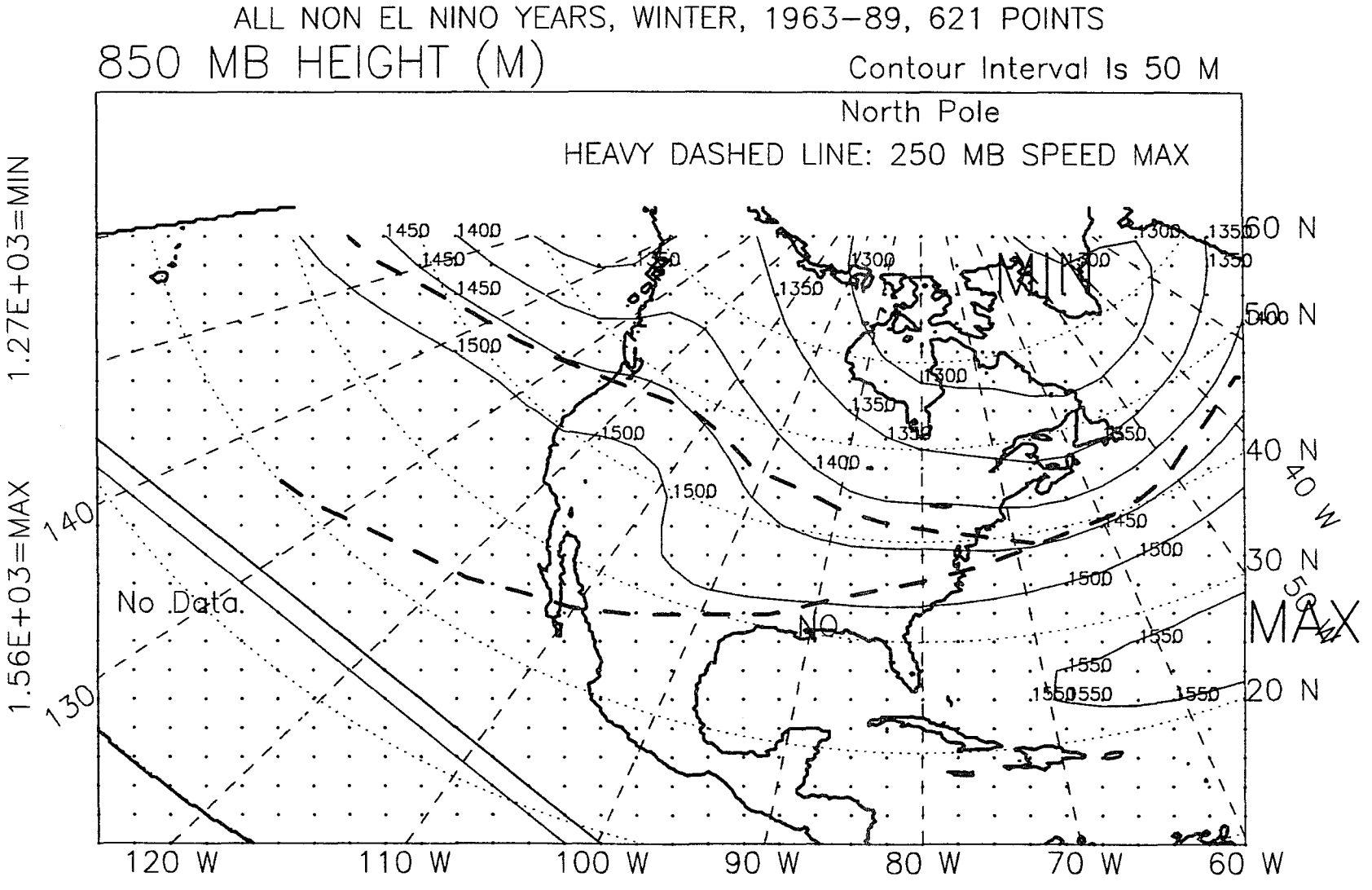

Figure B.2: 850–mb height, winter, non–El Niño years, 1963–89.

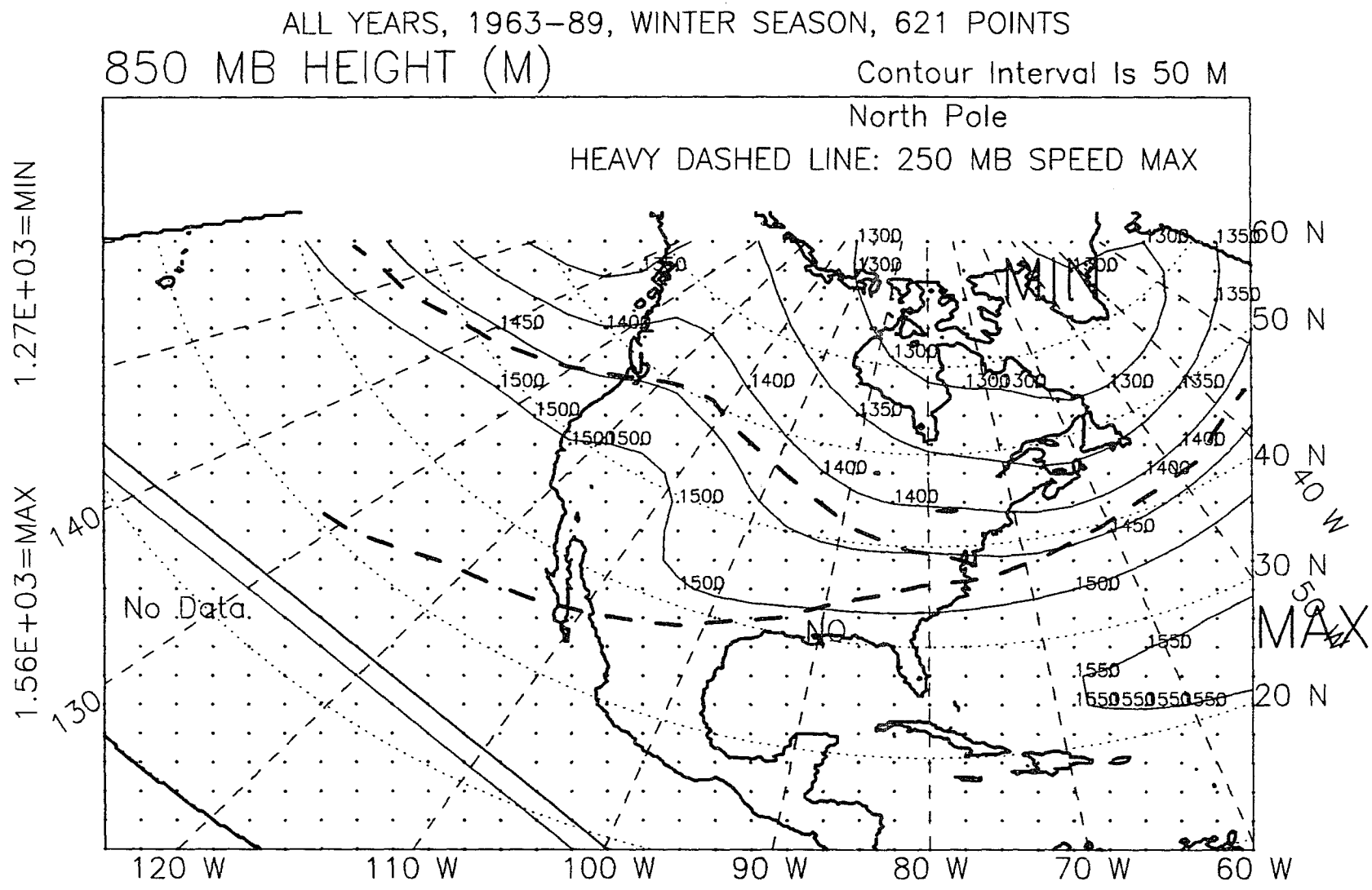

Figure B.3: 850–mb height, winter, all years, 1963–89.

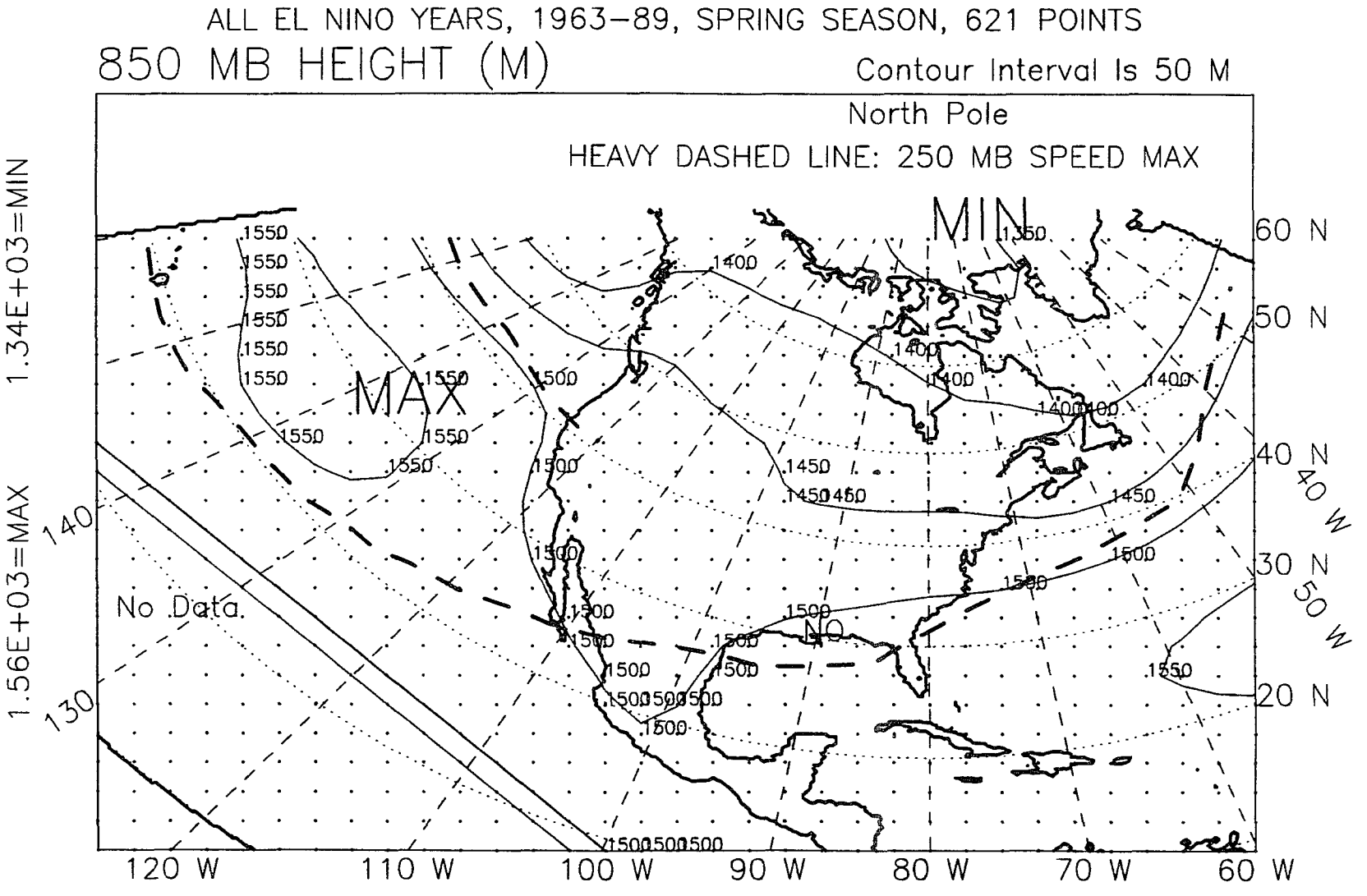

Figure B.4: 850–mb height, spring, El Niño years, 1963–89.

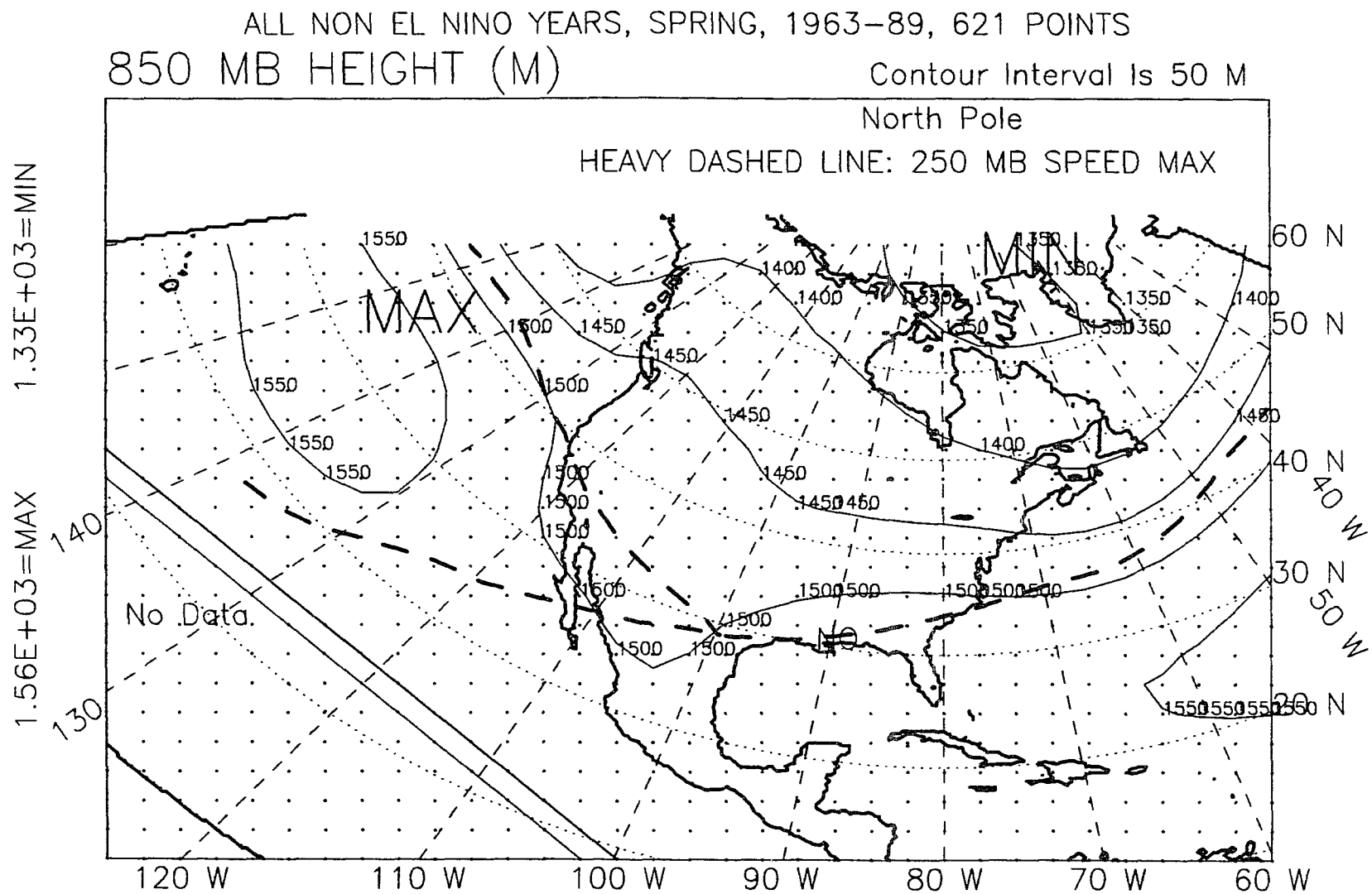

Figure B.5: 850–mb height, spring, non–El Niño years, 1963–89.

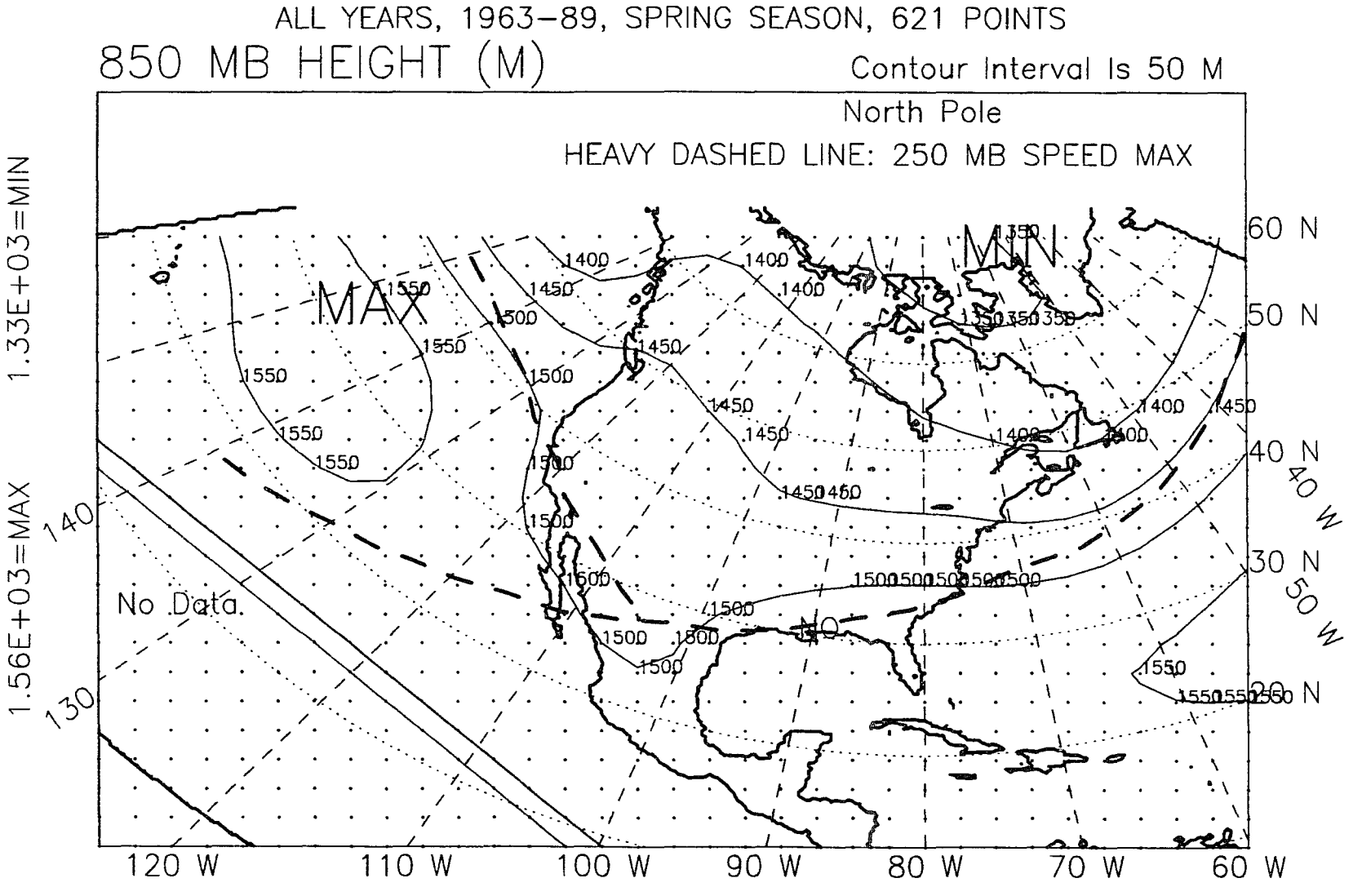

Figure B.6: 850–mb height, spring, all years, 1963–89.

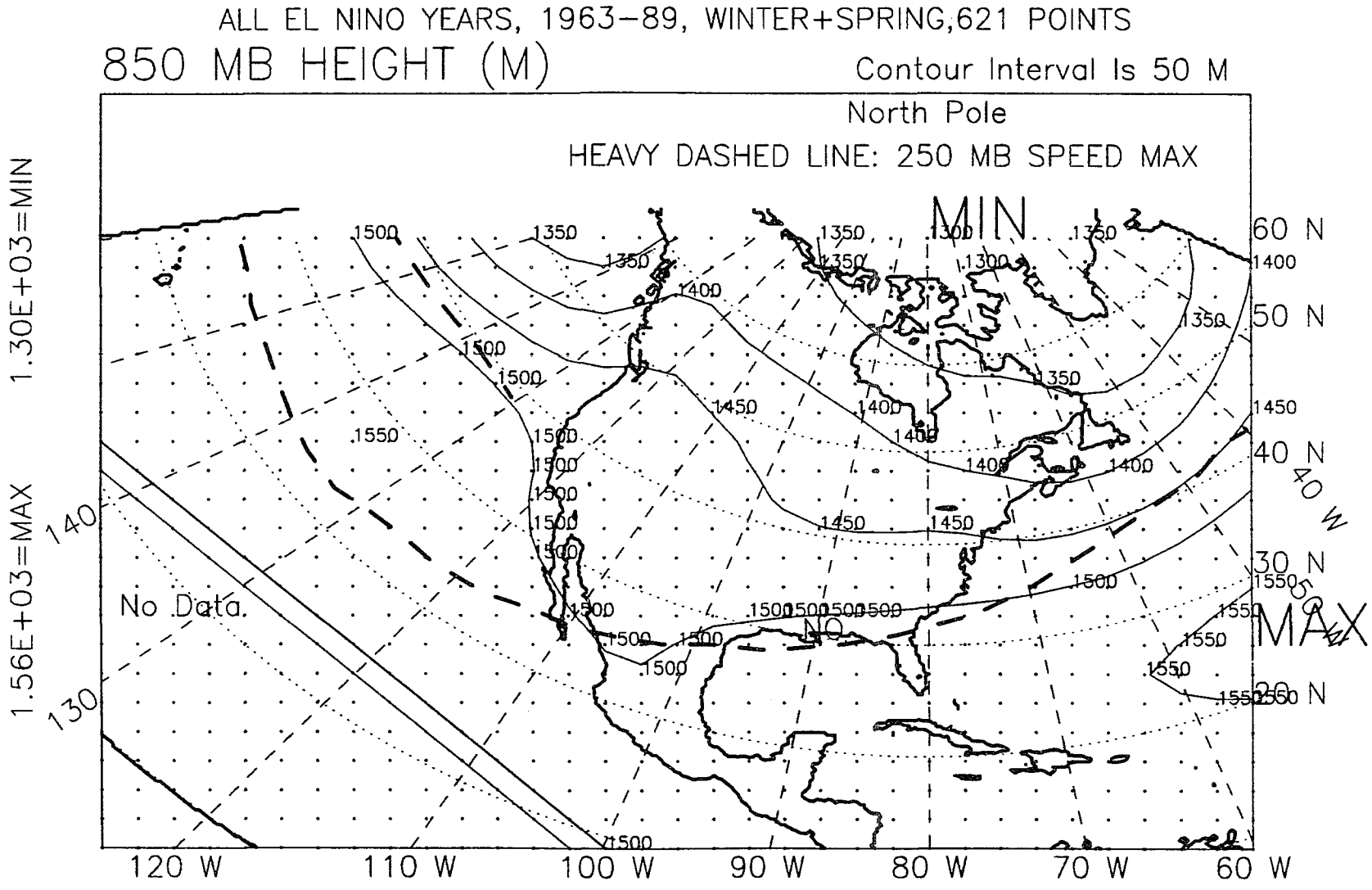

Figure B.7: 850–mb height, winter–plus–spring, El Niño years, 1963–89.

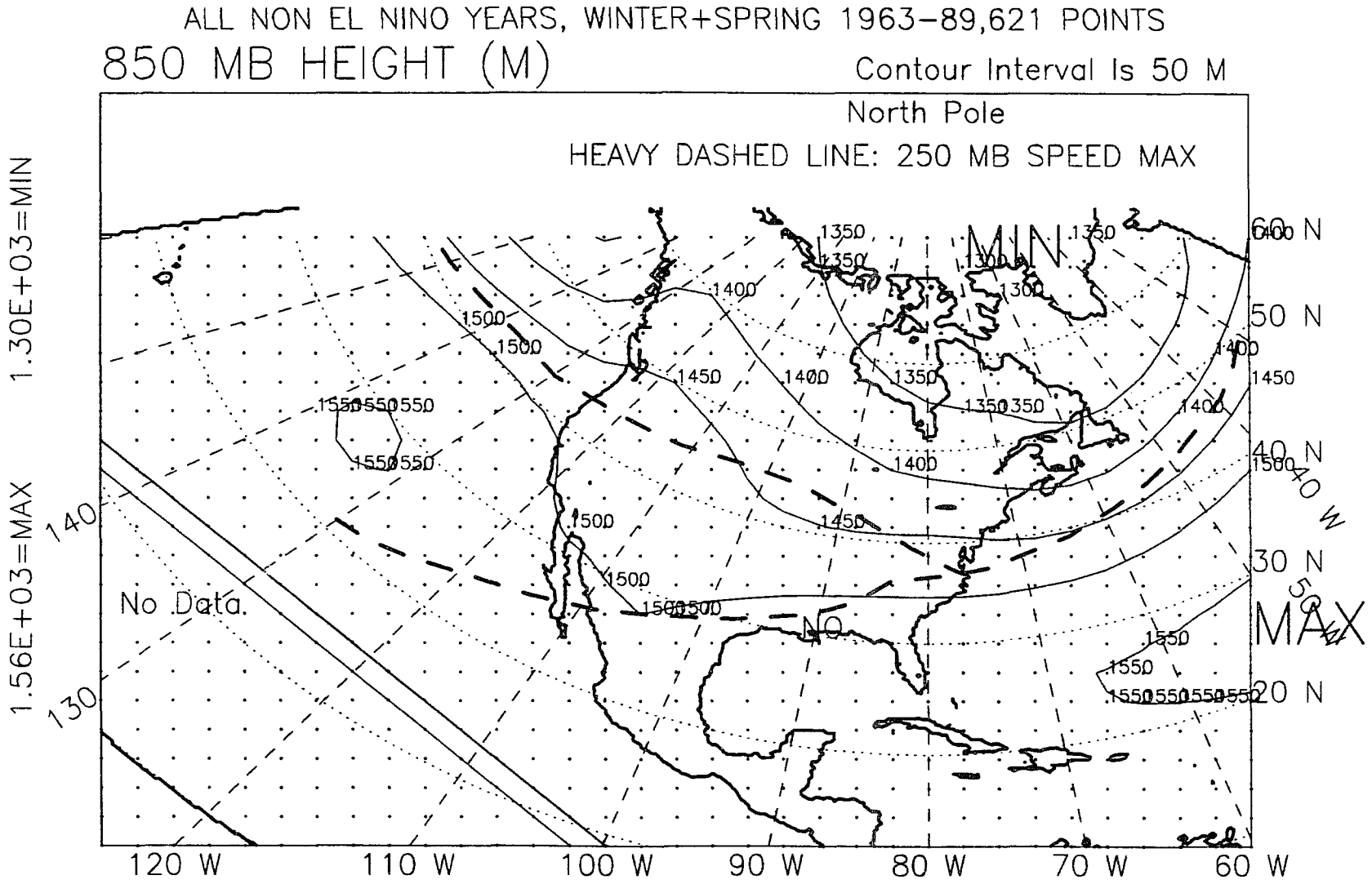

Figure B.8: 850-mb height, winter-plus-spring, non-El Niño years, 1963-89.

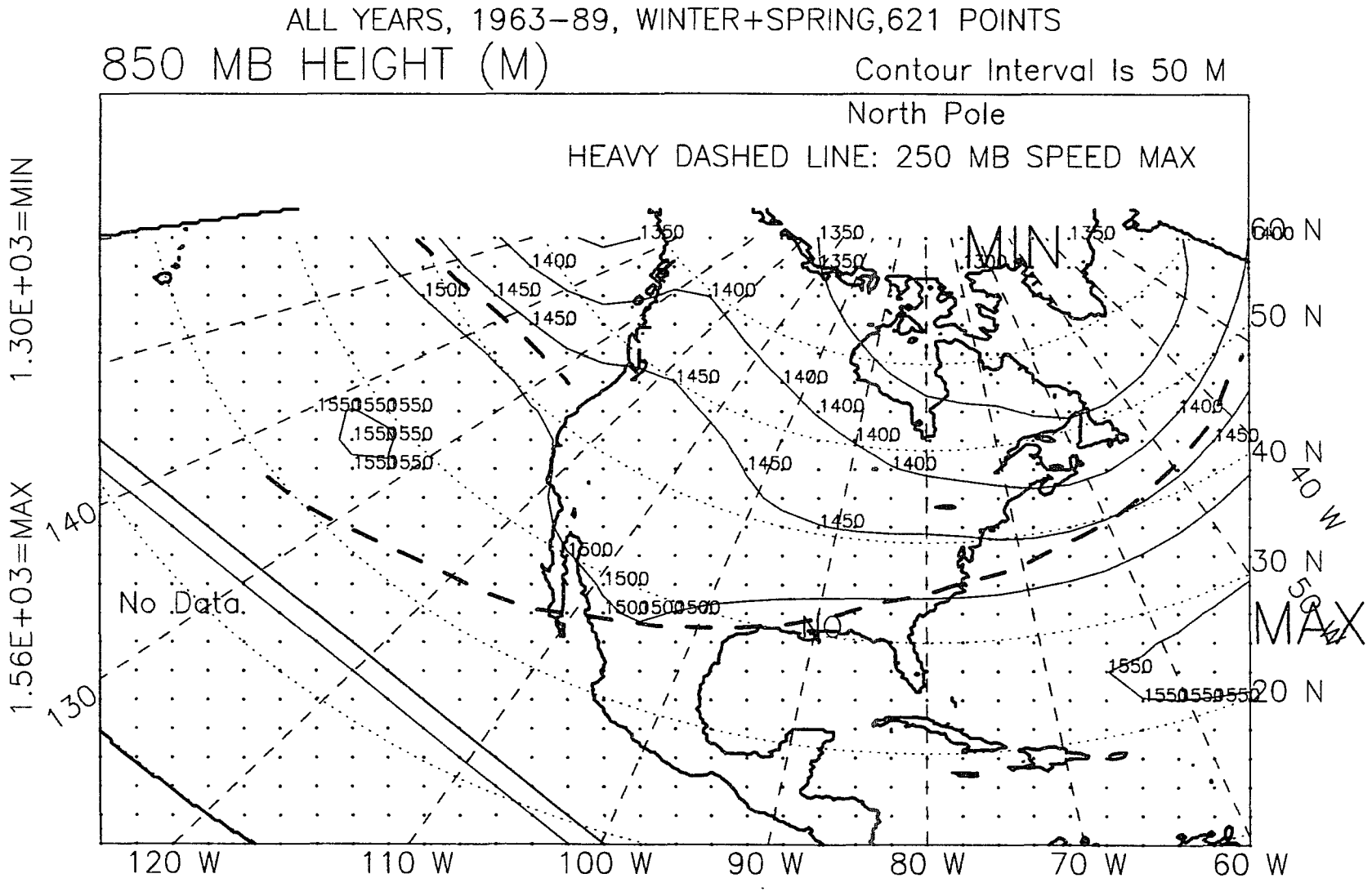

Figure B.9: 850–mb height, winter–plus–spring, all years, 1963–89.

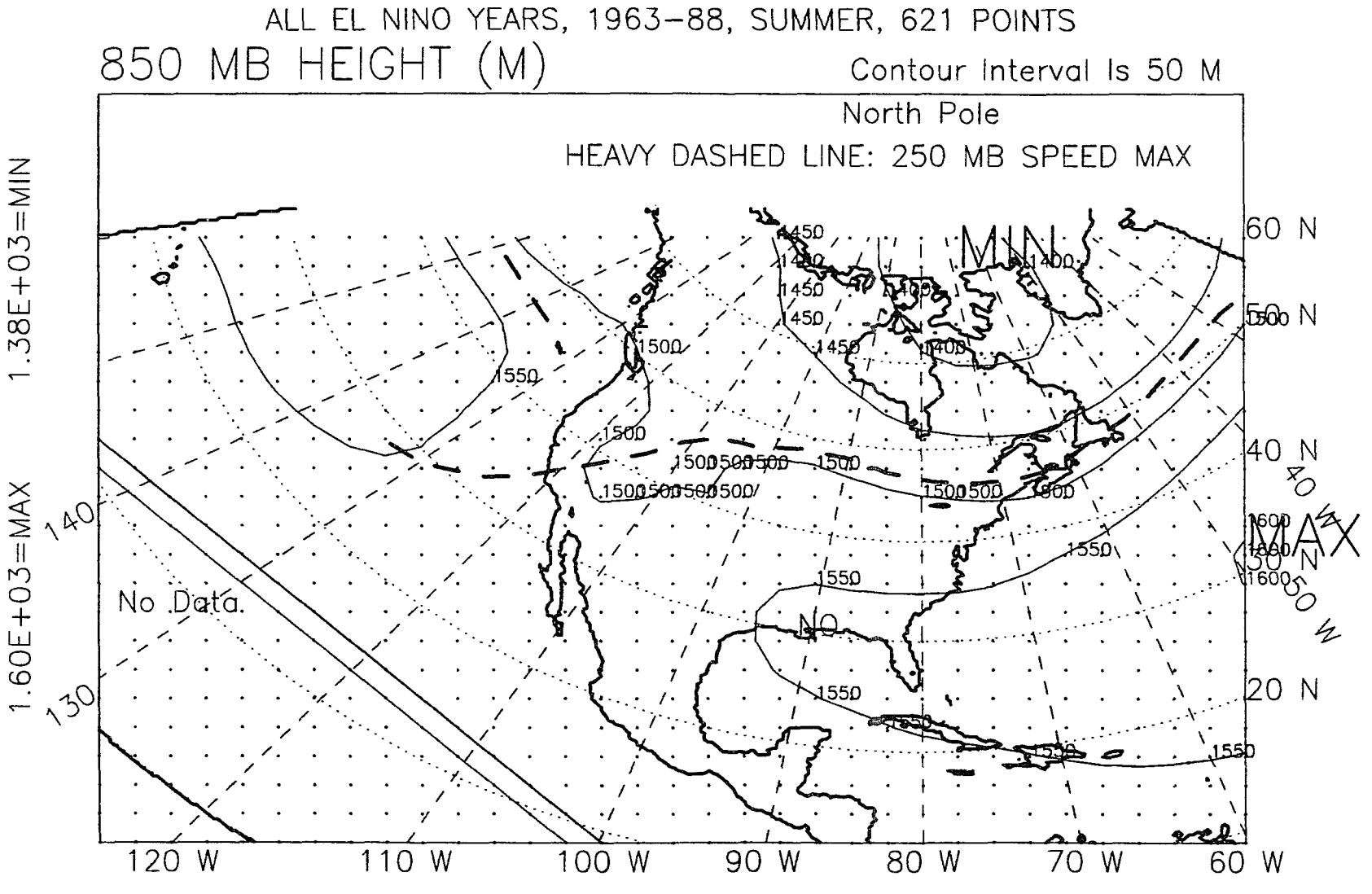

Figure B.10: 850–mb height, summer, El Niño years, 1963–88.

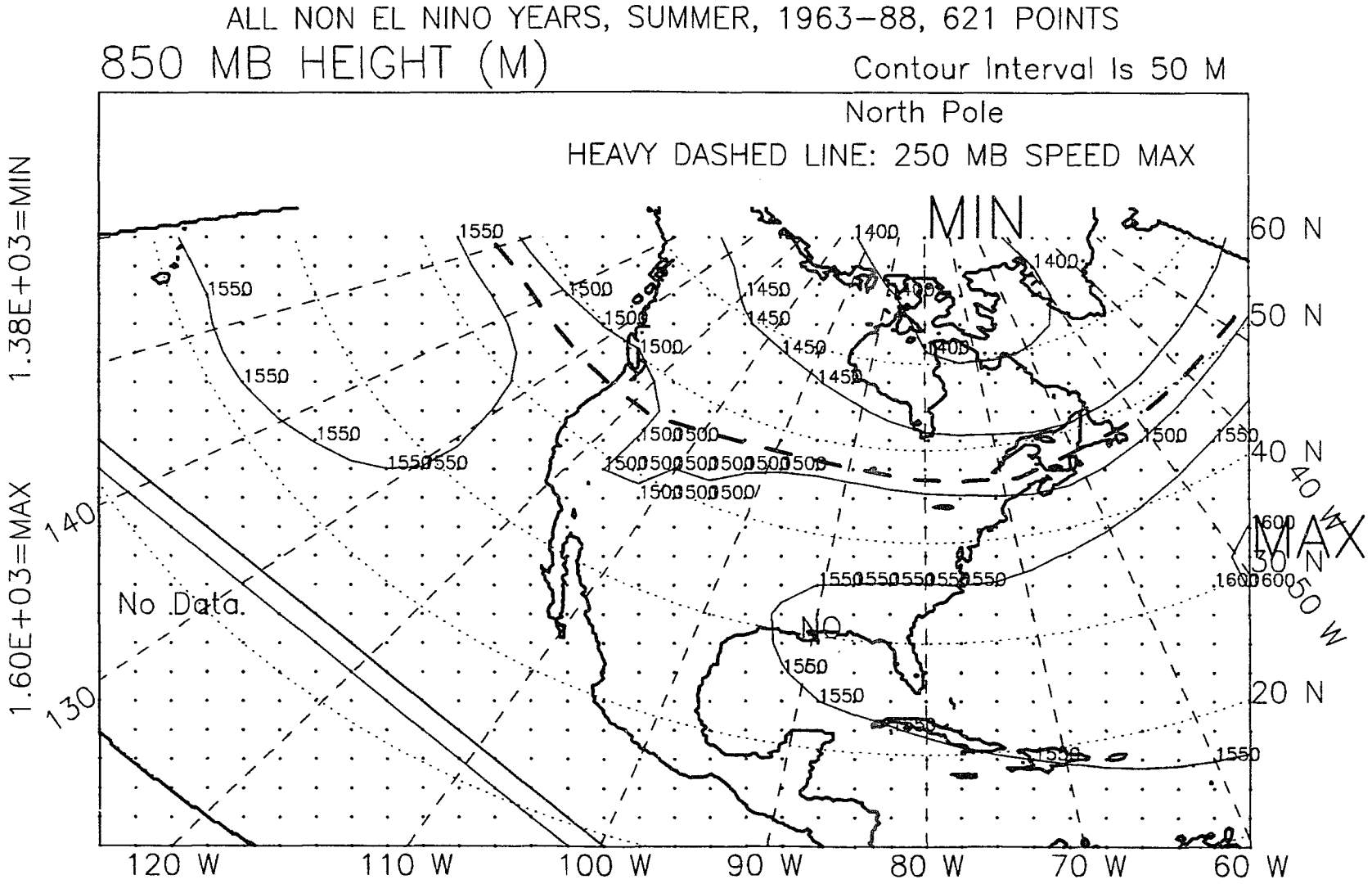

Figure B.11: 850–mb height, summer, non–El Niño years, 1963–88.

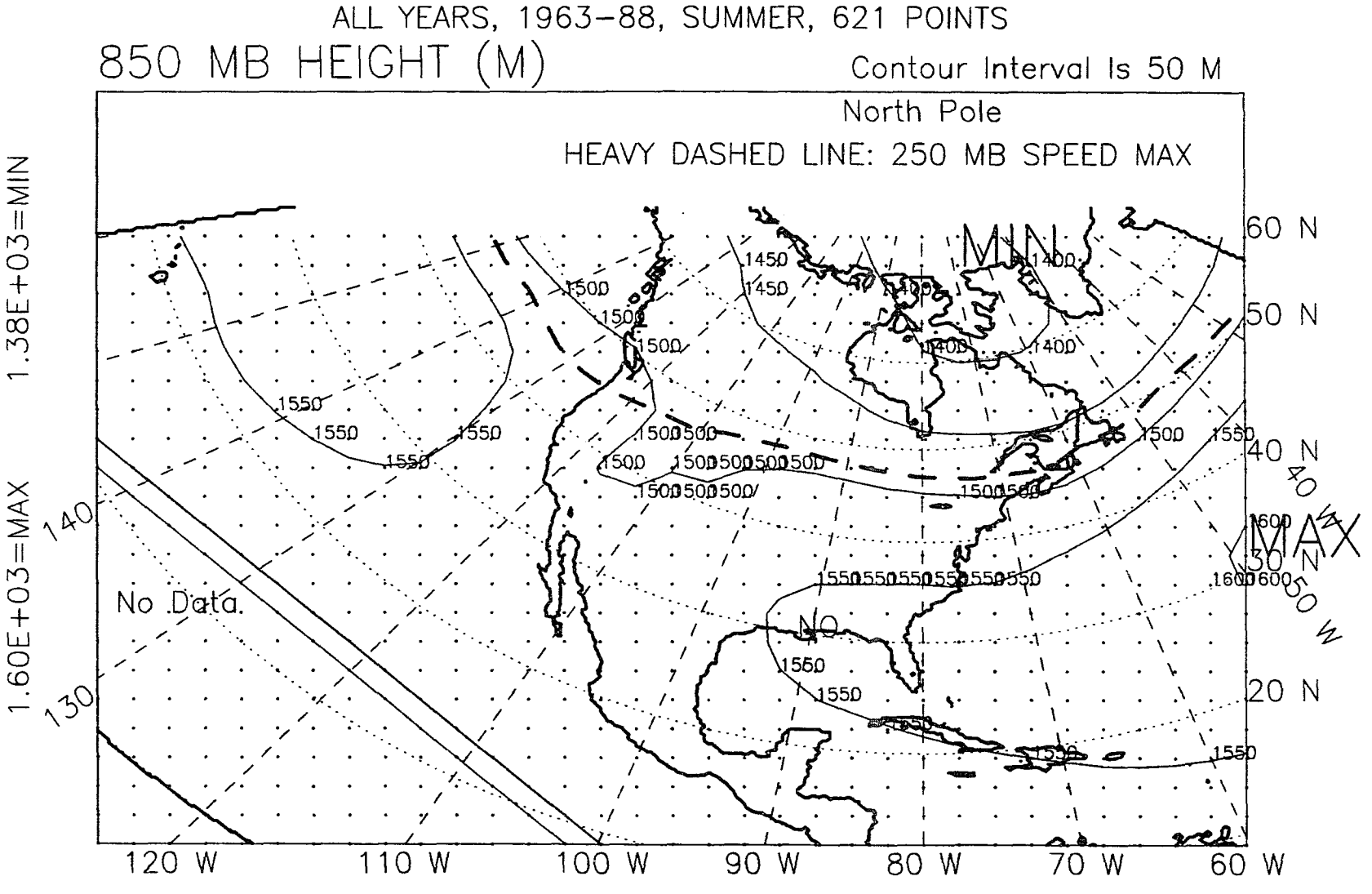

Figure B.12: 850–mb height, summer, all years, 1963–88.

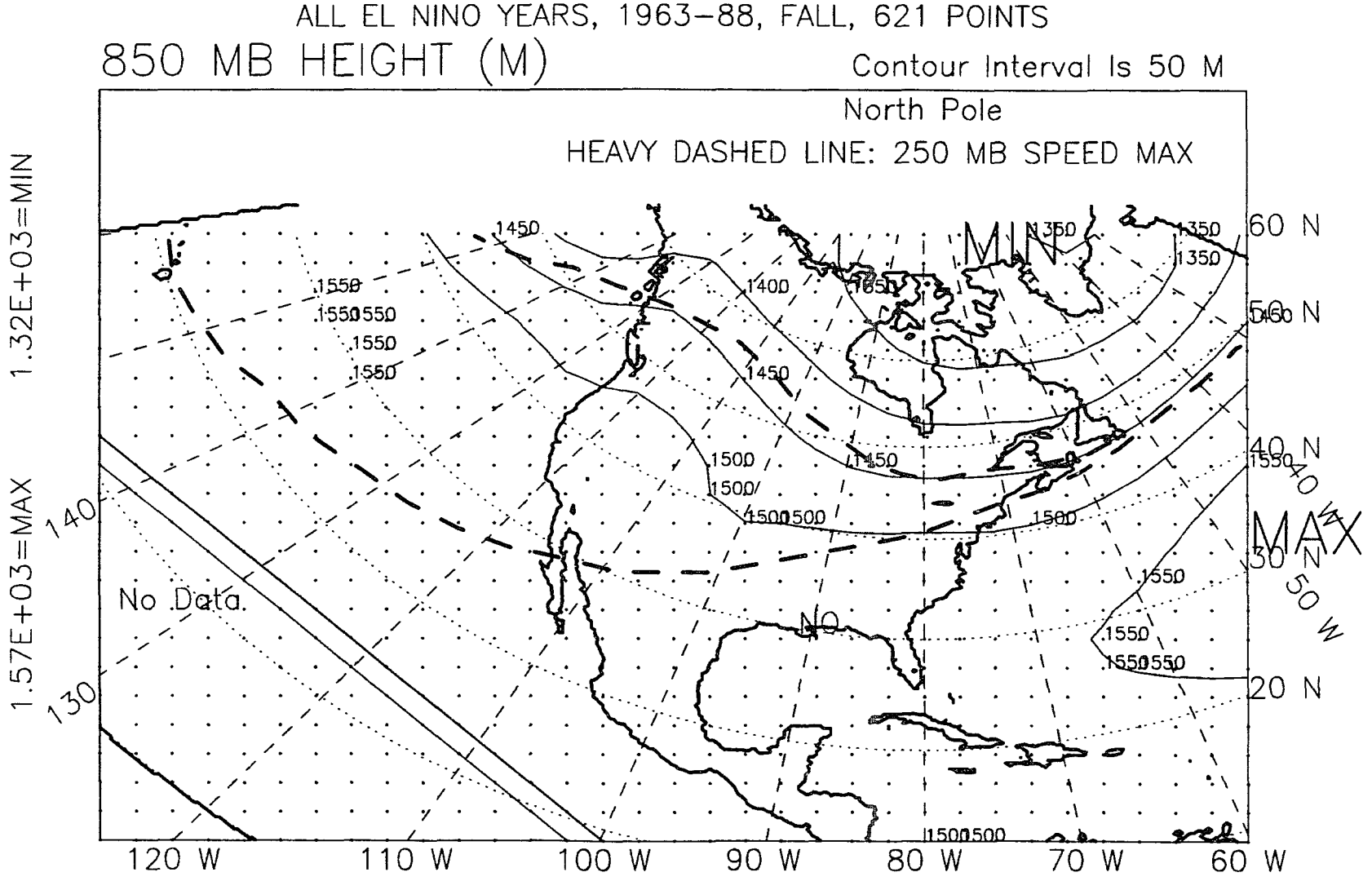

Figure B.13: 850–mb height, fall, El Niño years, 1963–88.

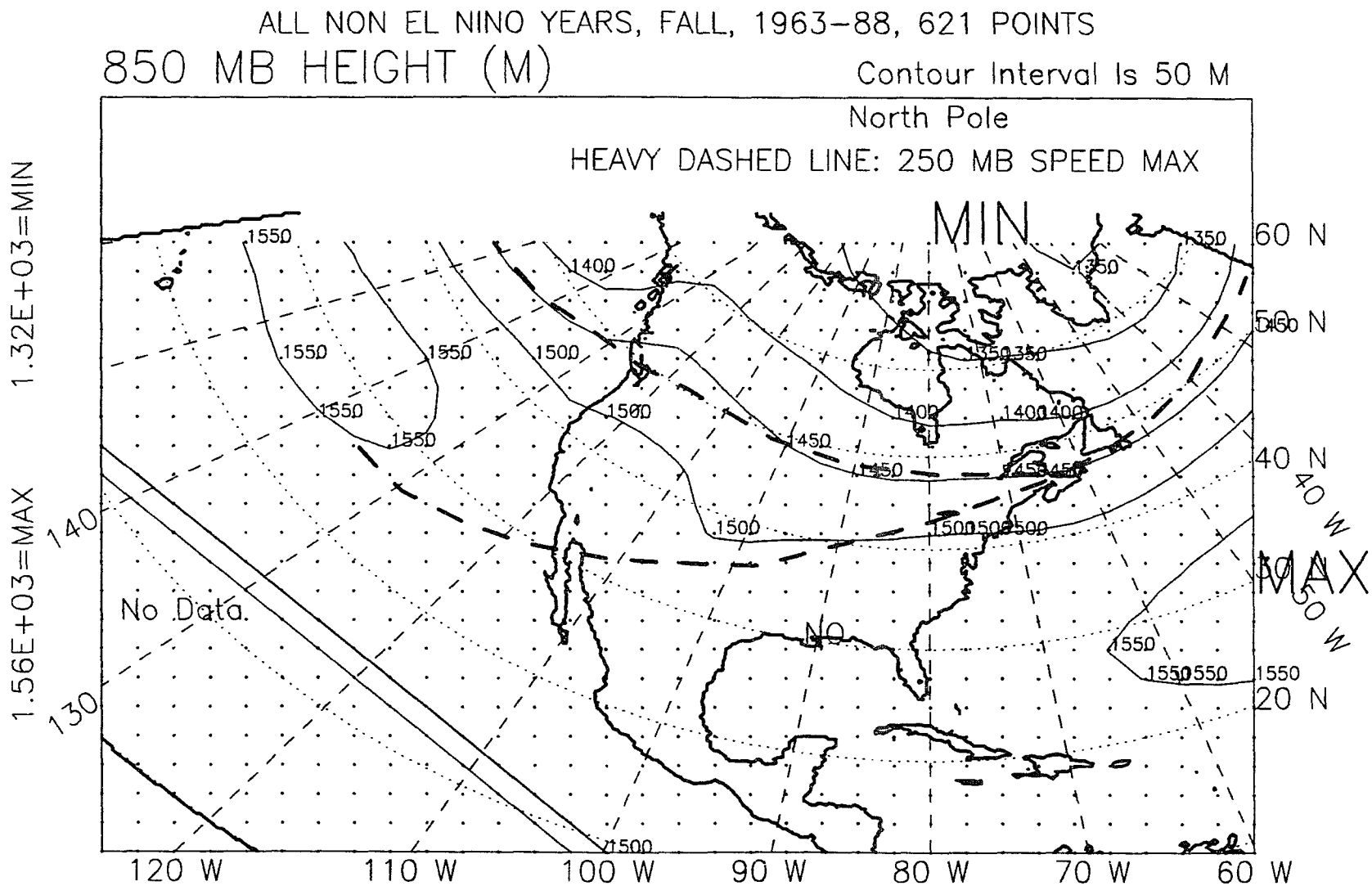

Figure B.14: 850-mb height, fall, non-El Niño years, 1963-88.

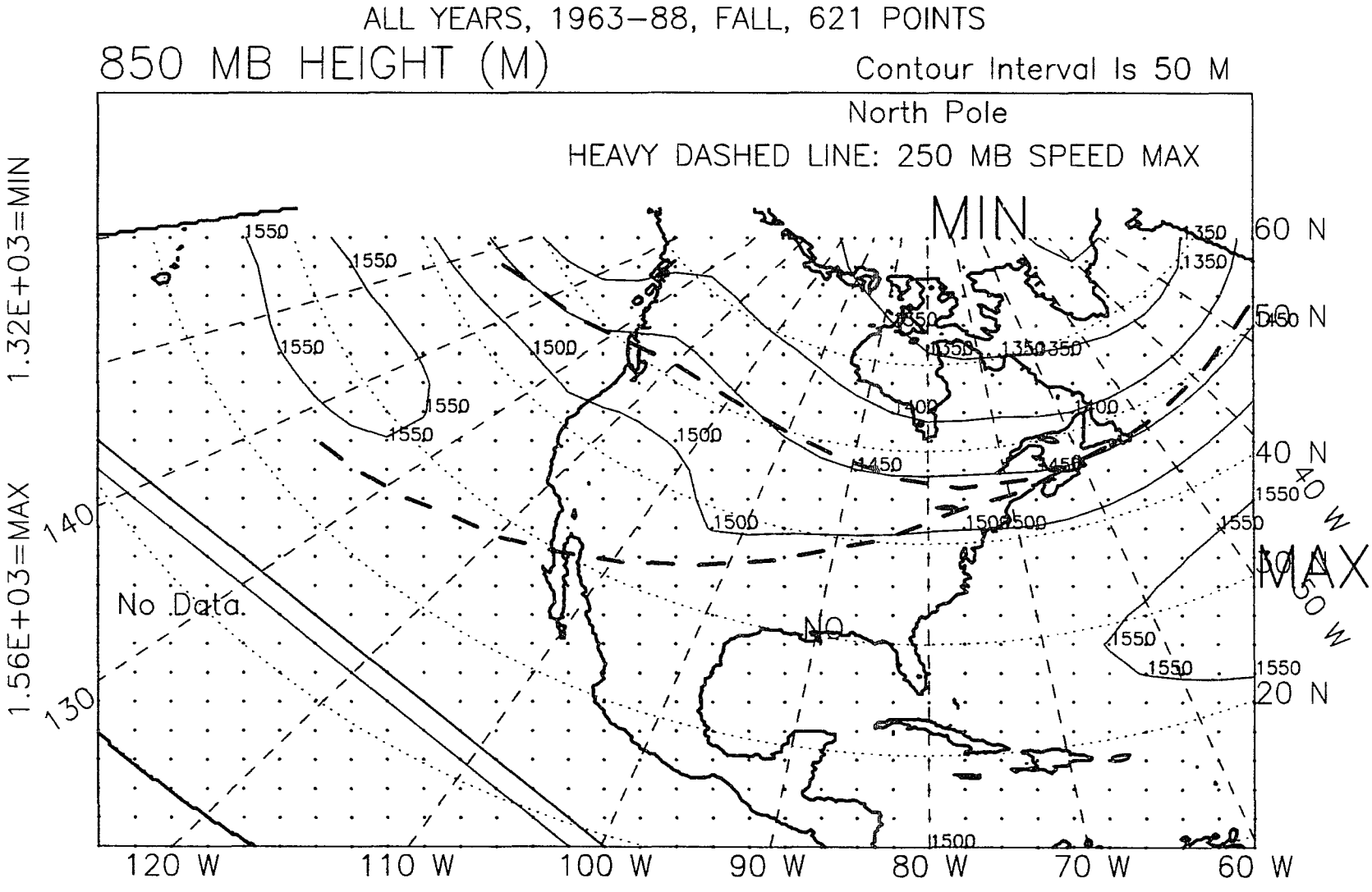

Figure B.15: 850–mb height, fall, all years, 1963–88.

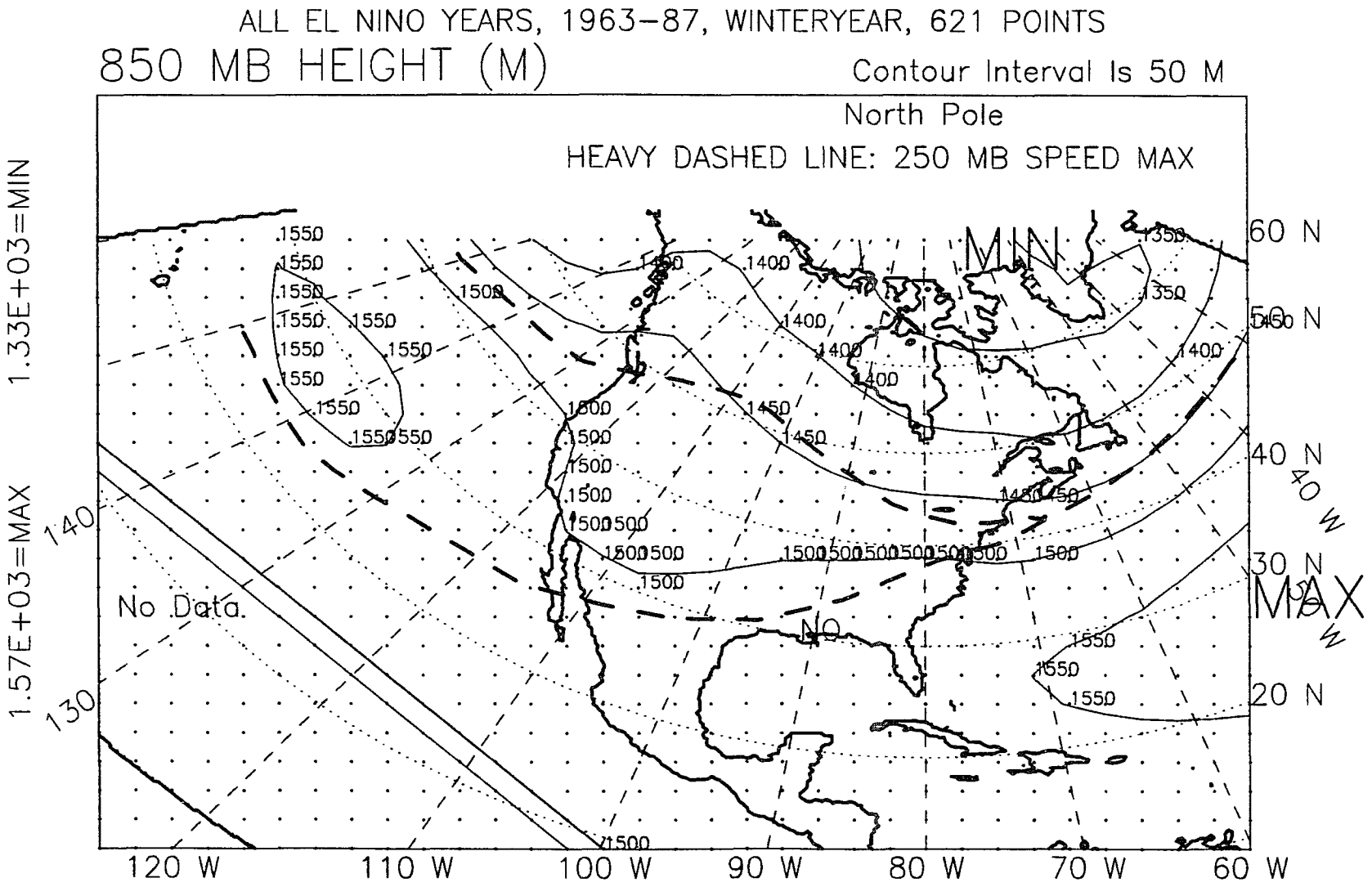

Figure B.16: 850–mb height, winter year, El Niño years, 1963–87.

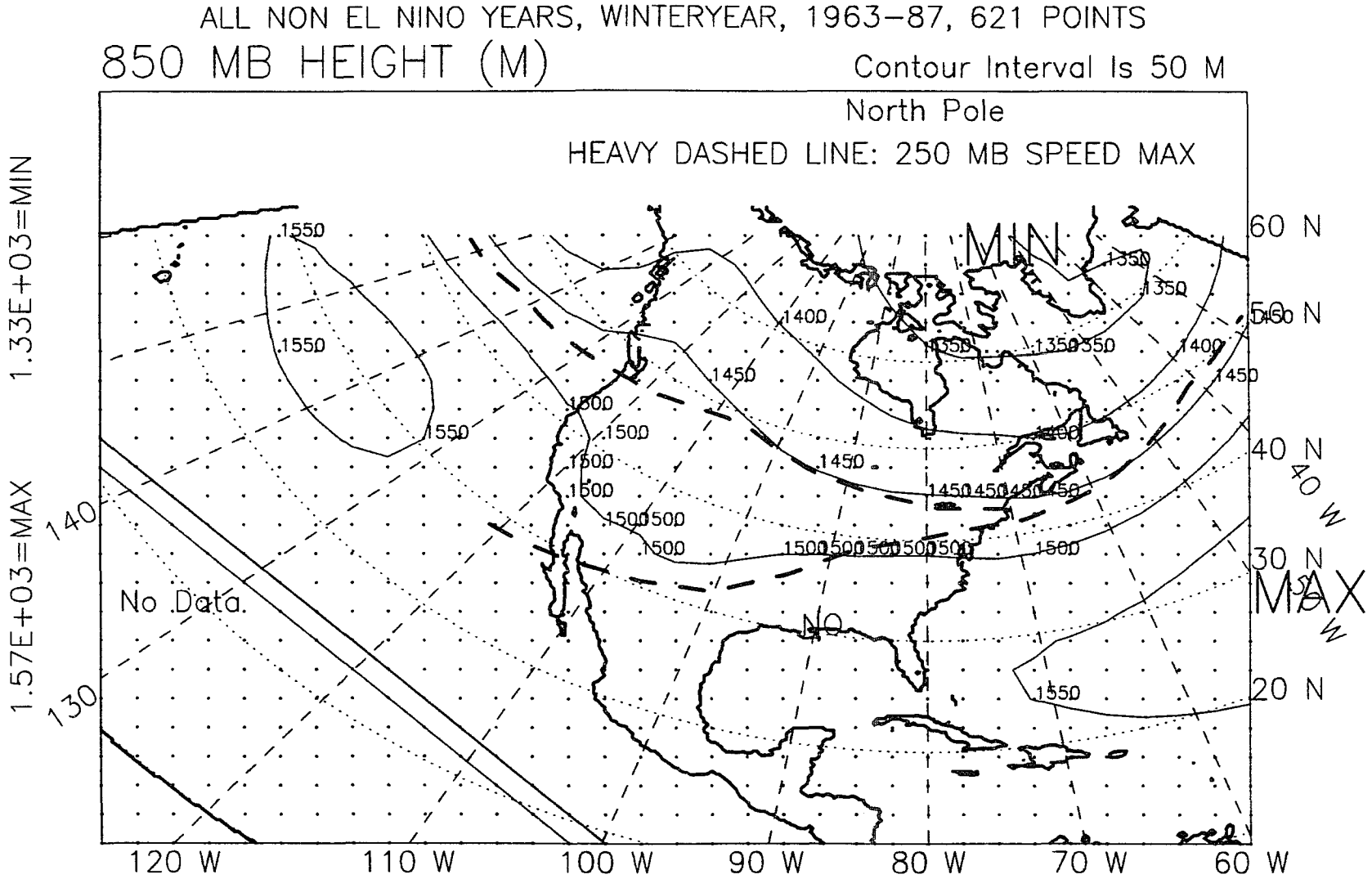

Figure B.17: 850-mb height, winter year, non-El Niño years, 1963-87.

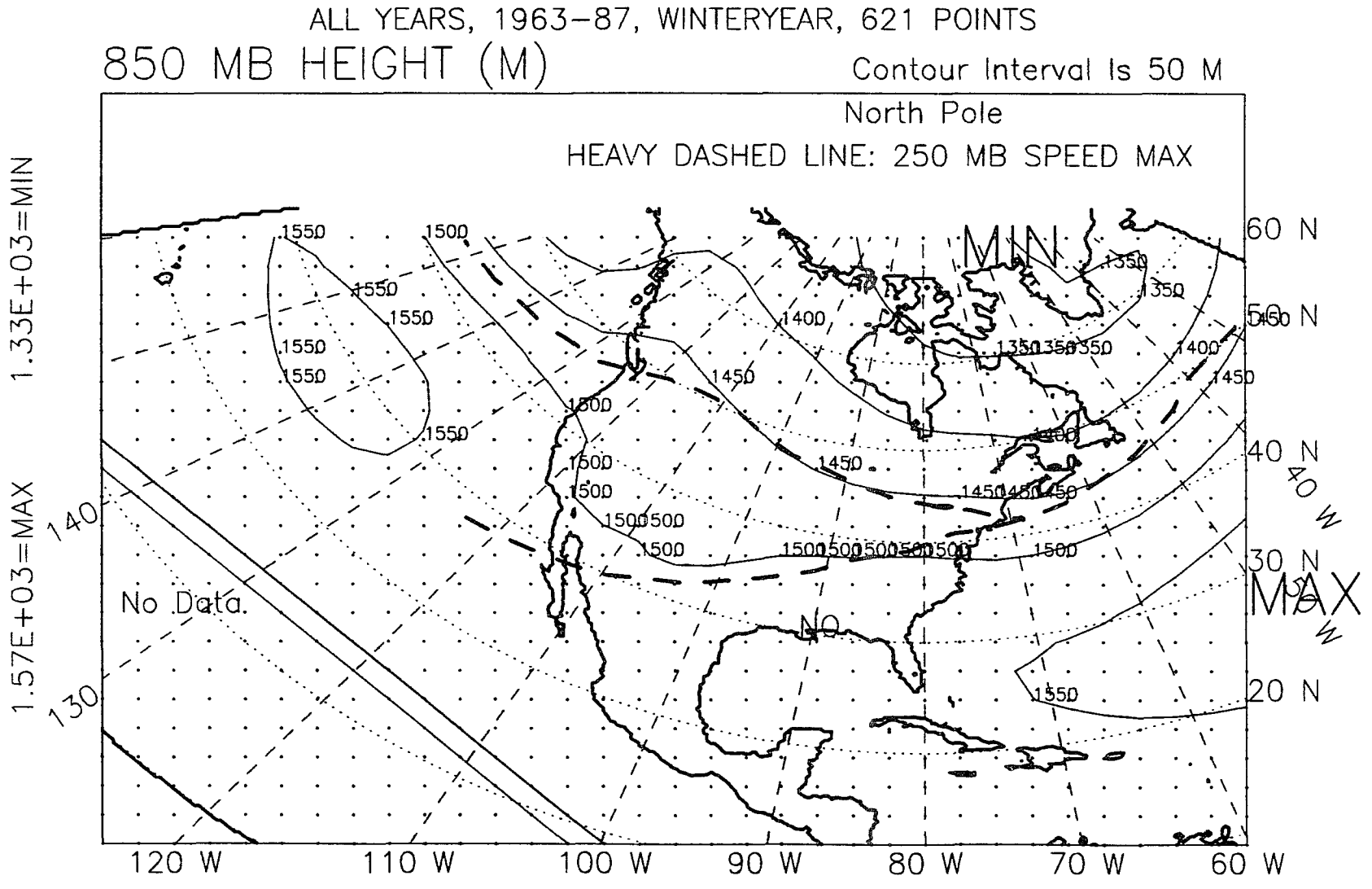

Figure B.18: 850–mb height, winter year, all years, 1963–87.

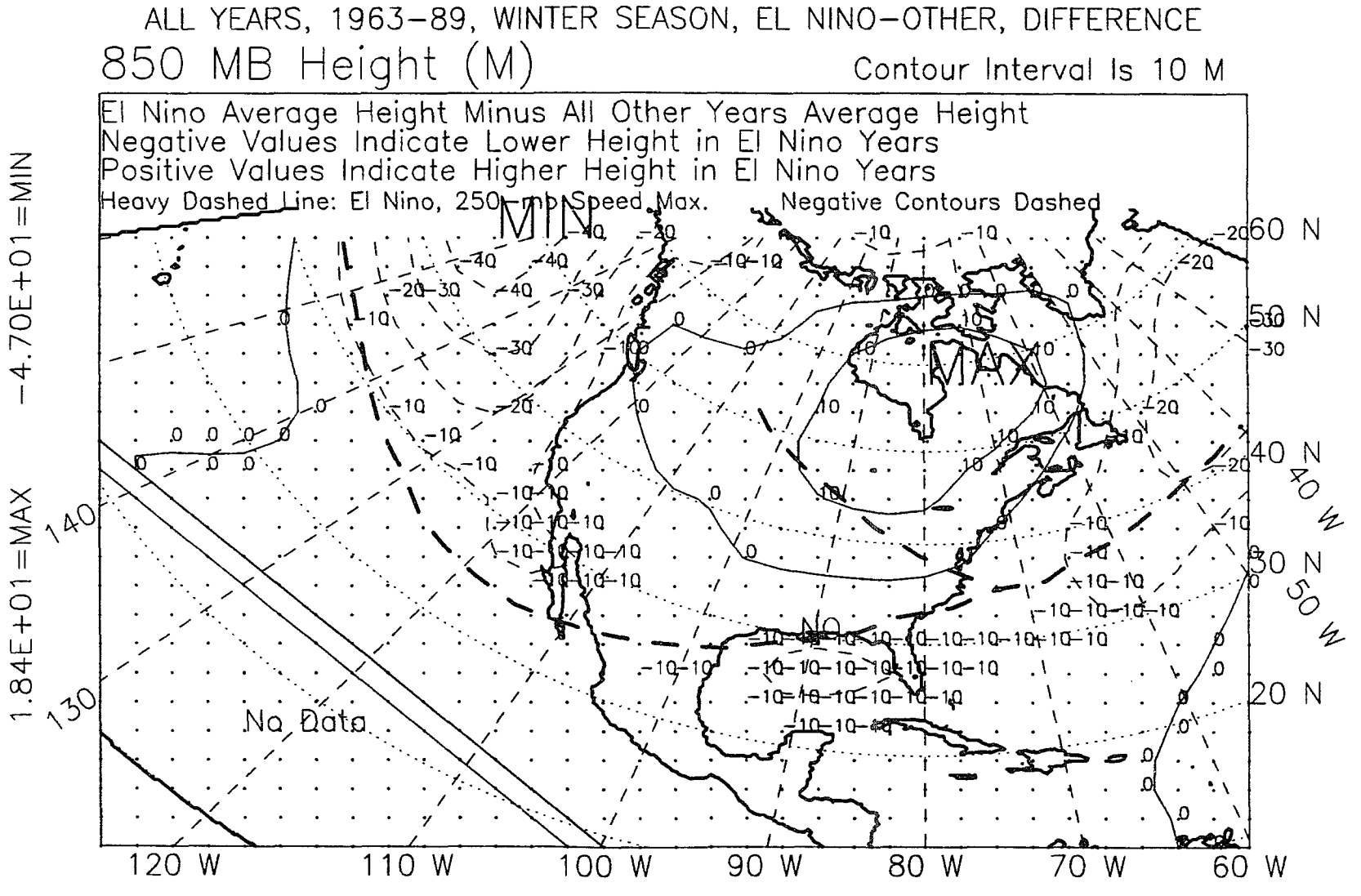

Figure B.19: 850–mb height, winter, 1963–89, difference.

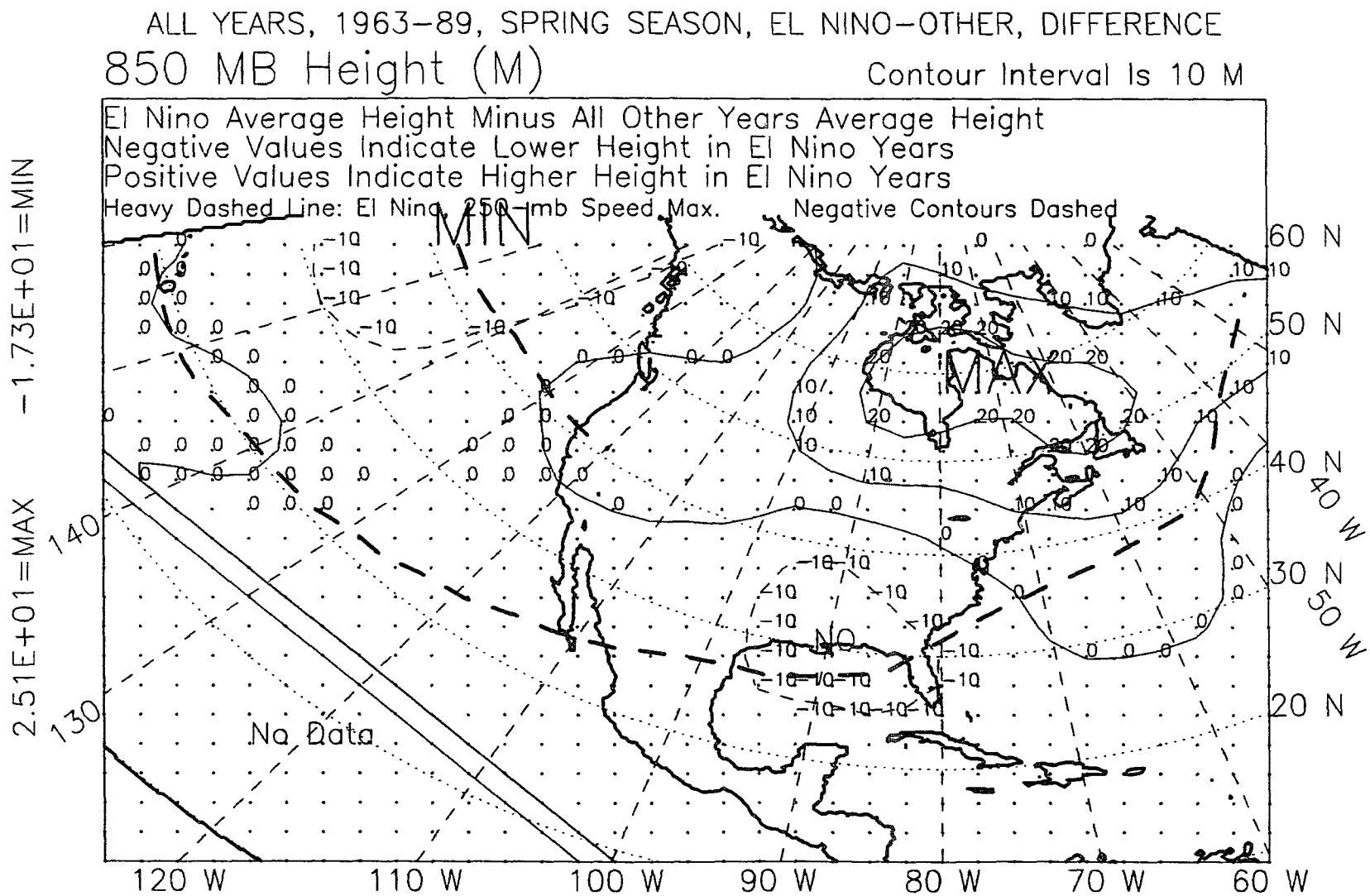

Figure B.20: 850–mb height, spring, 1963–89, difference.

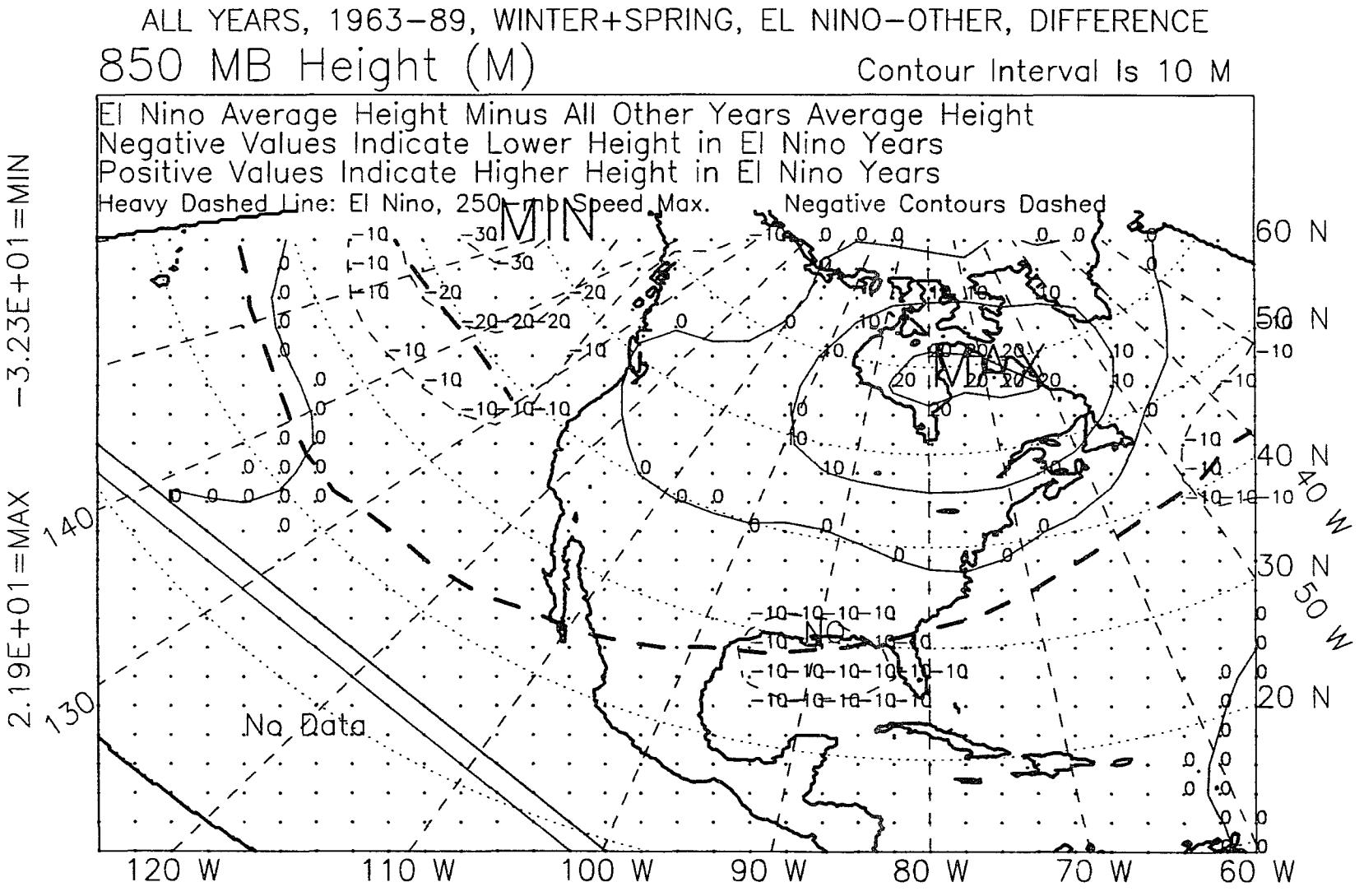

Figure B.21: 850–mb height, winter–plus–spring, 1963–89, difference.

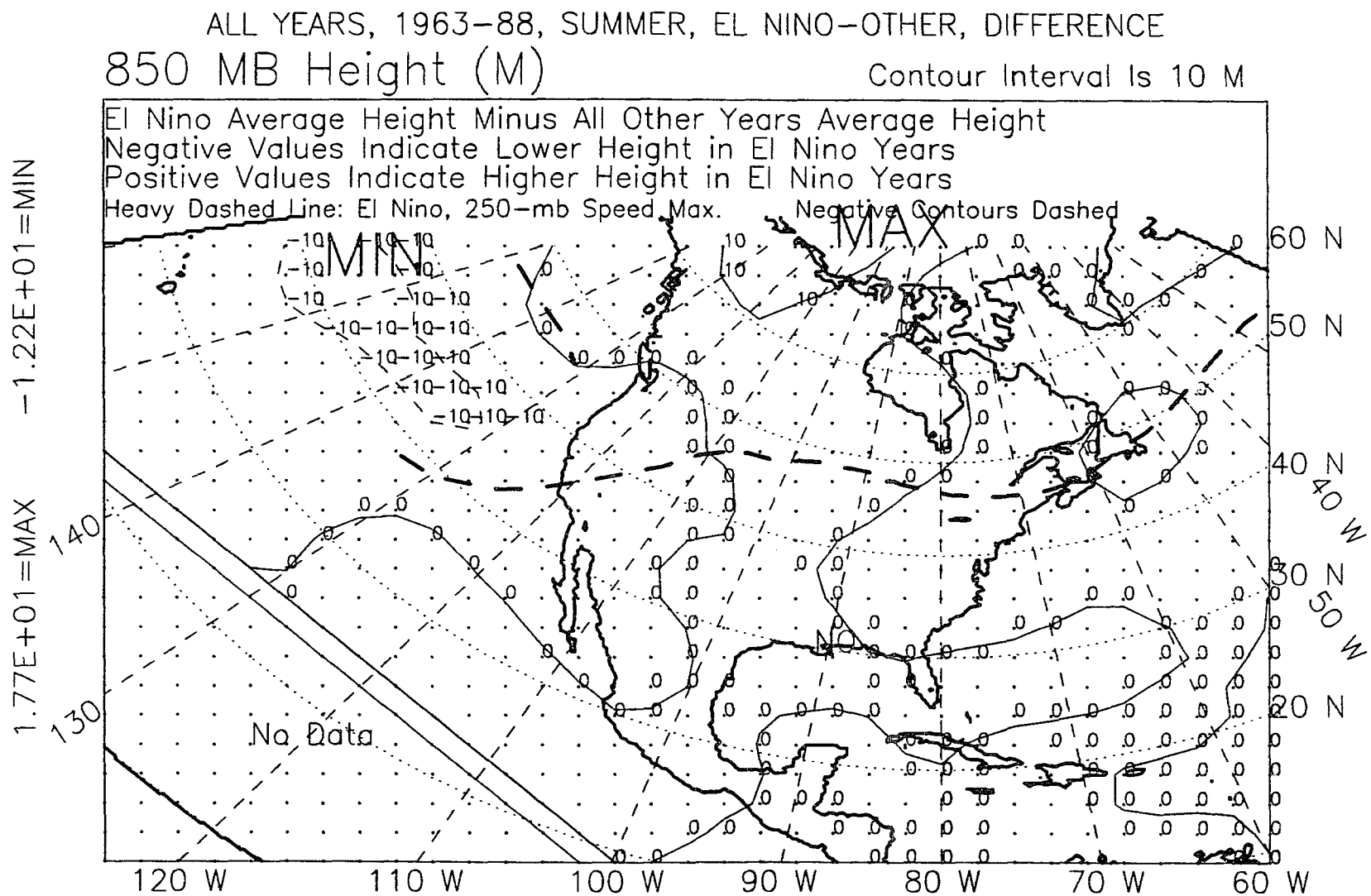

Figure B.22: 850–mb height, summer, 1963–88, difference.

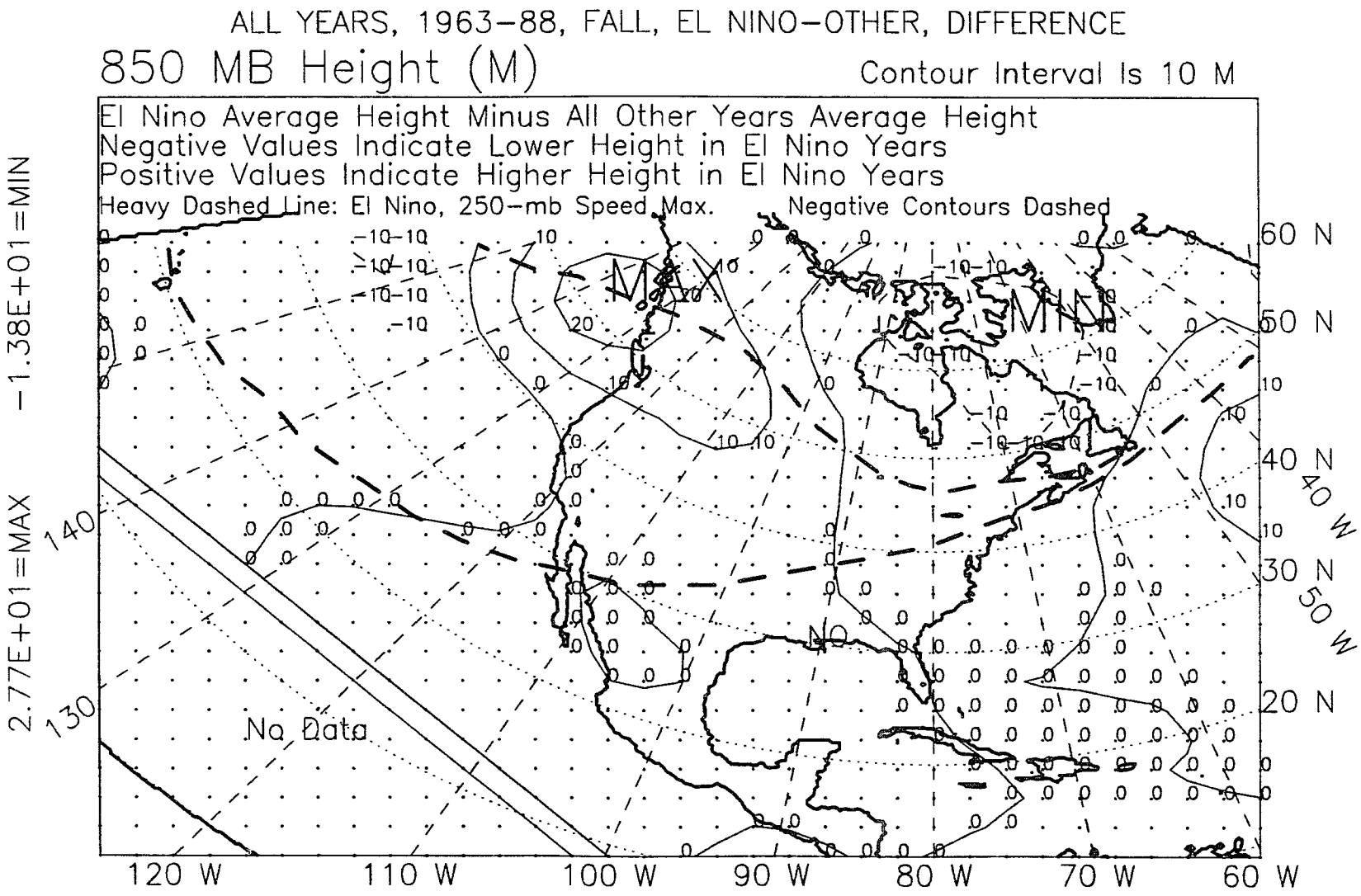

Figure B.23: 850–mb height, fall, 1963–88, difference.

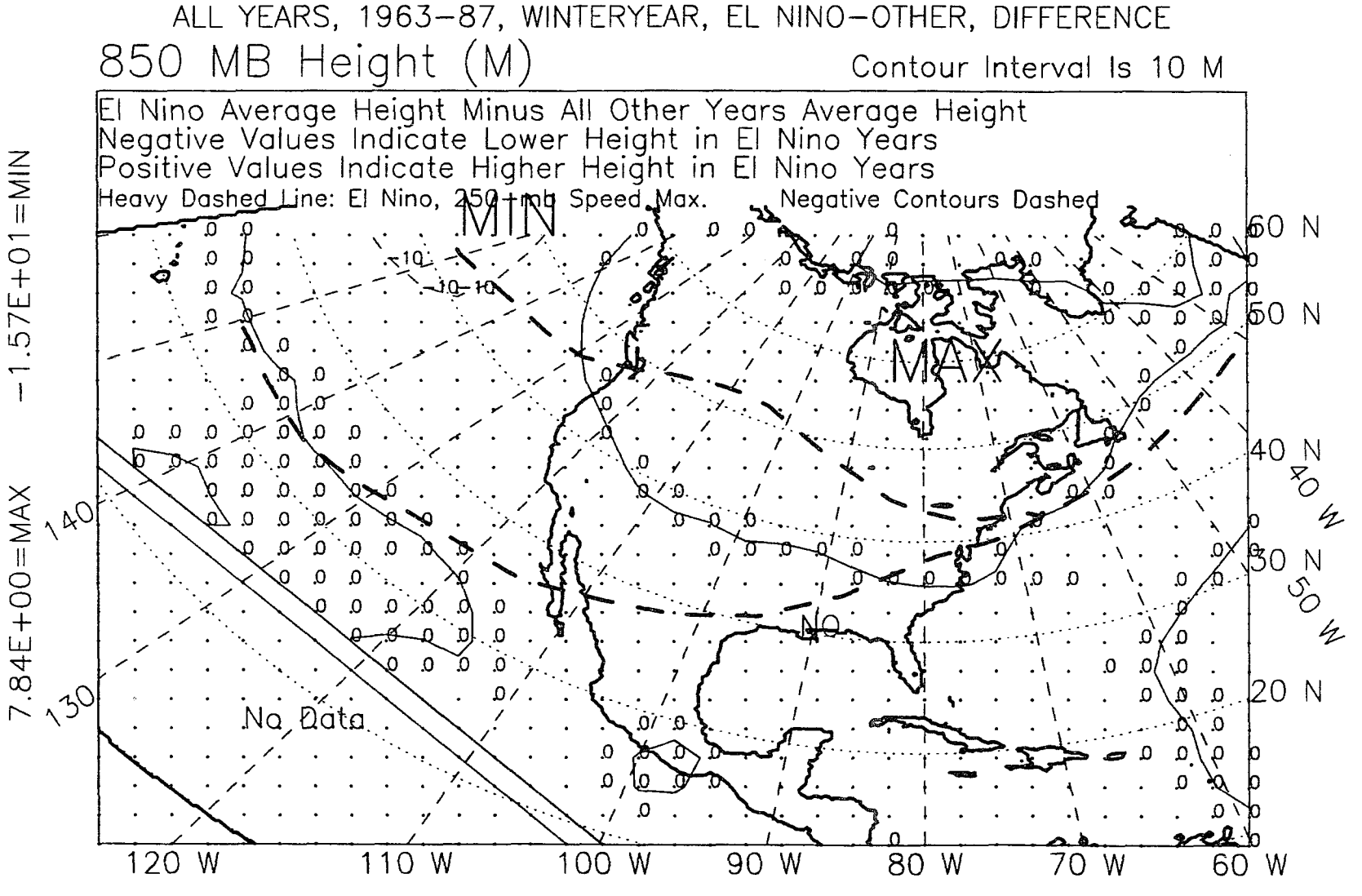

Figure B.24: 850–mb height, winter year, 1963–87, difference.

APPENDIX C
850-MB WIND FIELD

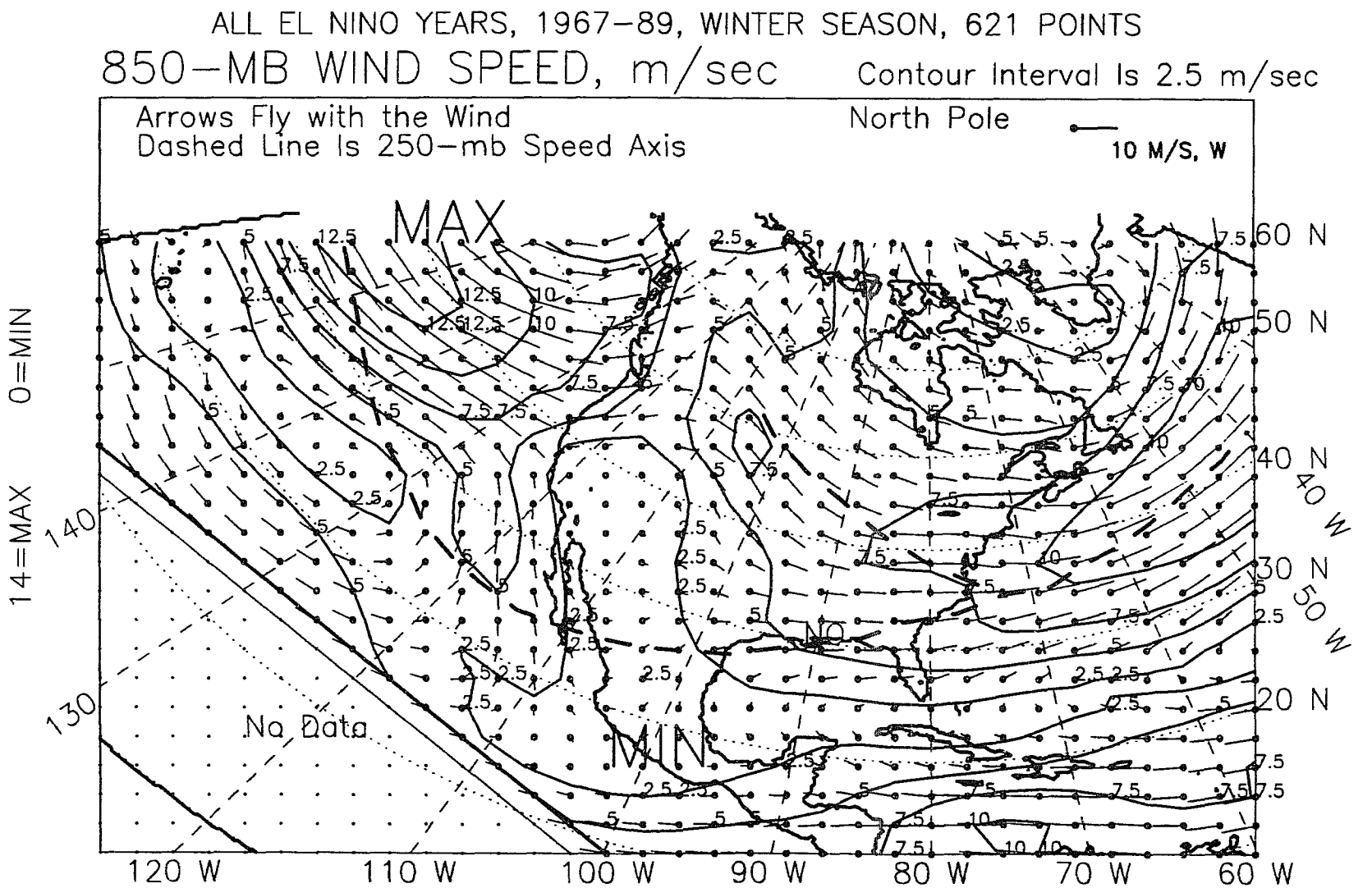

Figure C.1: 850–mb wind vectors, winter, El Niño years, 1967–89.

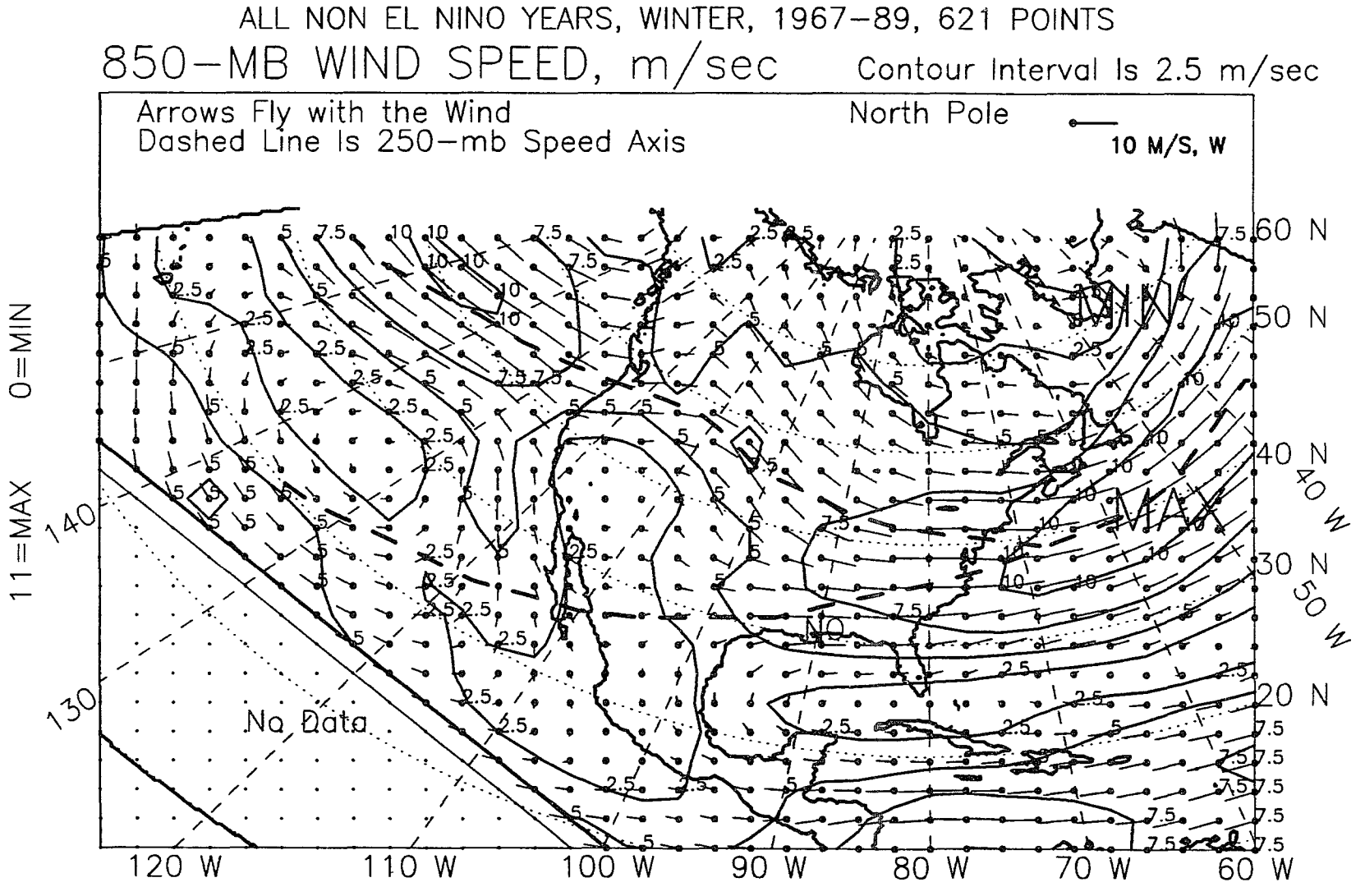

Figure C.2: 850–mb wind vectors, winter, non–El Niño years, 1967–89.

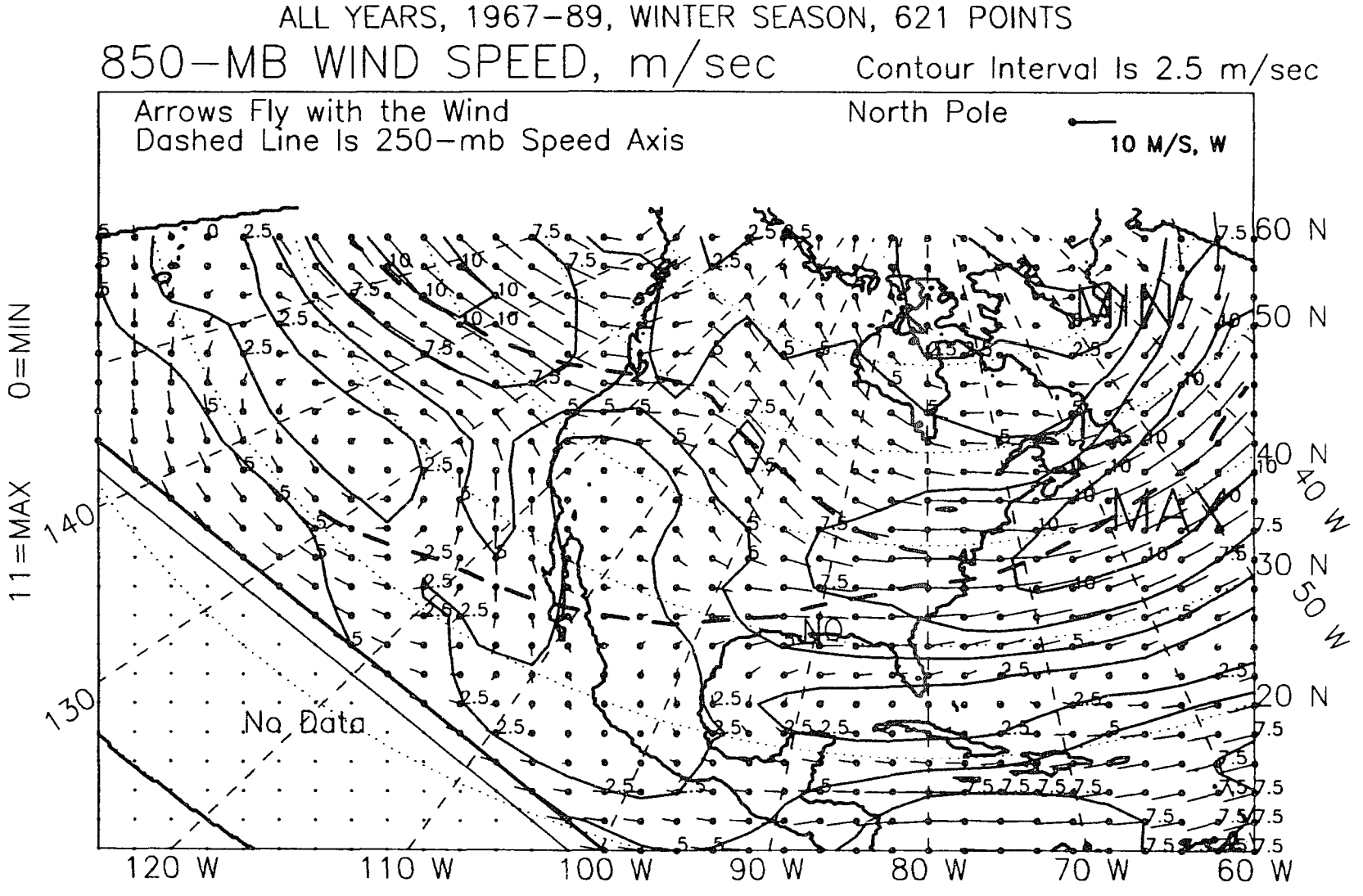

Figure C.3: 850–mb wind vectors, winter, all years, 1967–89.

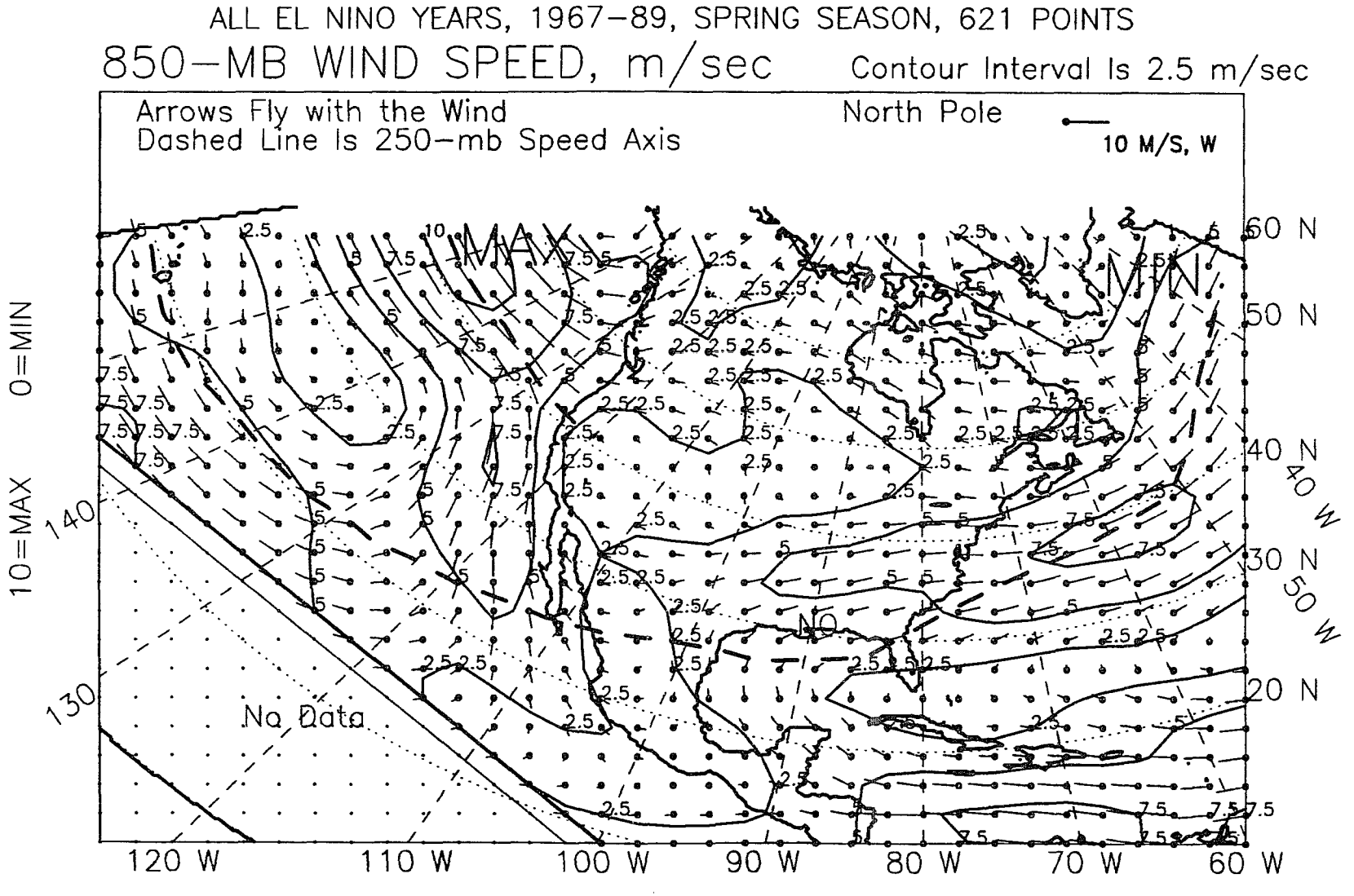

Figure C.4: 850–mb wind vectors, spring, El Niño years, 1967–89.

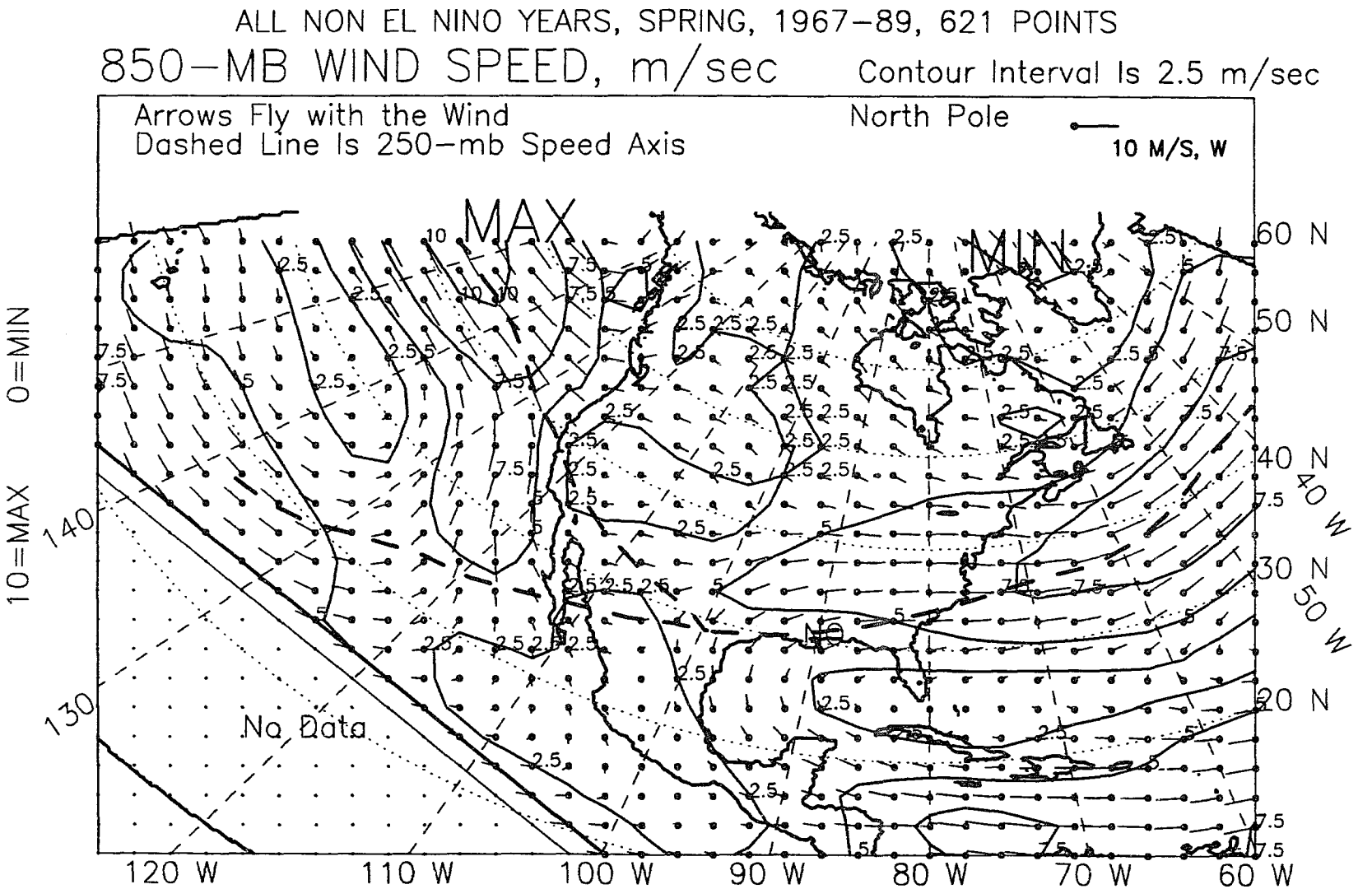

Figure C.5: 850–mb wind vectors, spring, non–El Niño years, 1967–89.

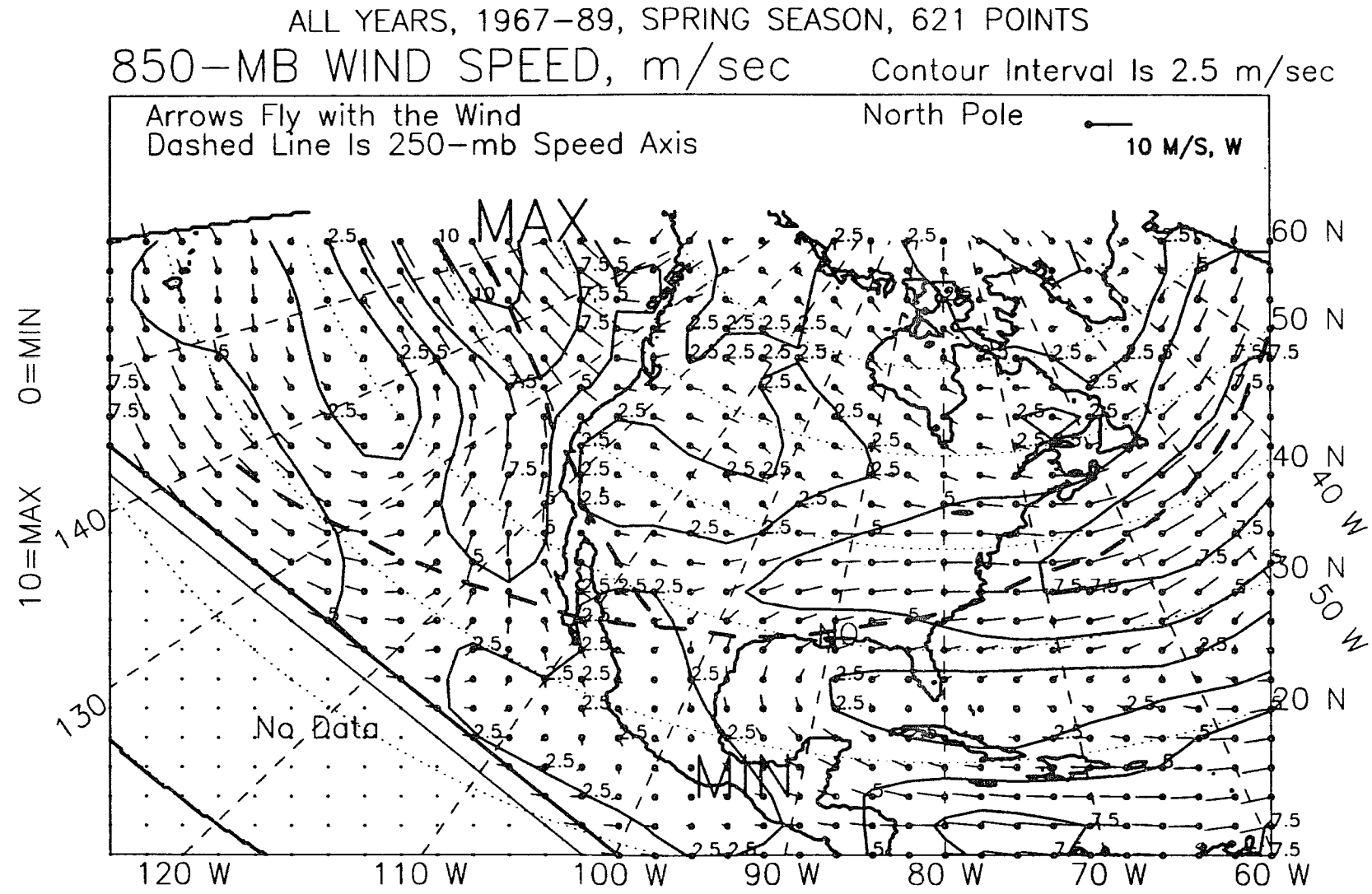

Figure C.6: 850–mb wind vectors, spring all years, 1967–89.

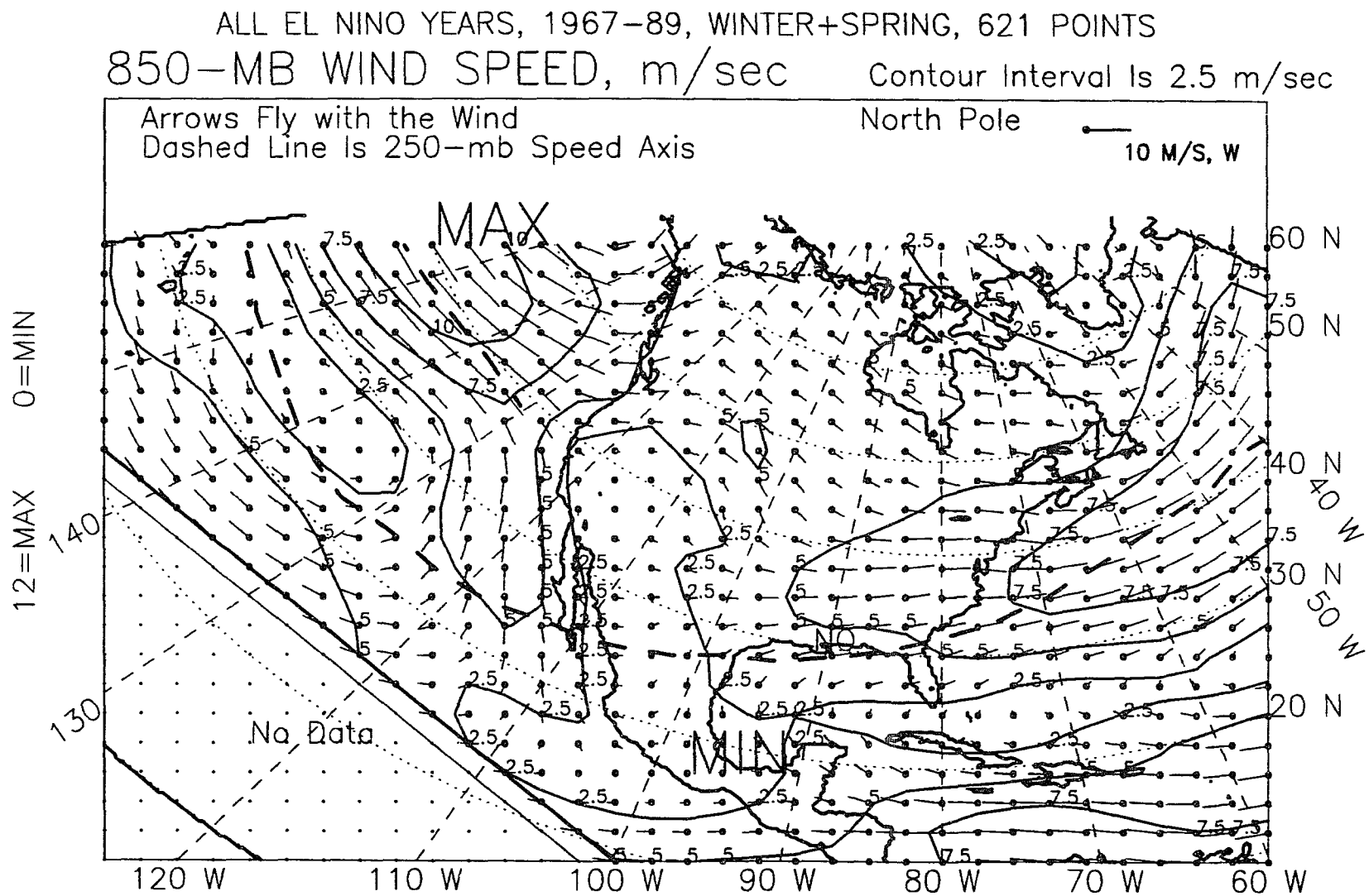

Figure C.7: 850–mb wind vectors, winter–plus–spring, El Niño years, 1967–89.

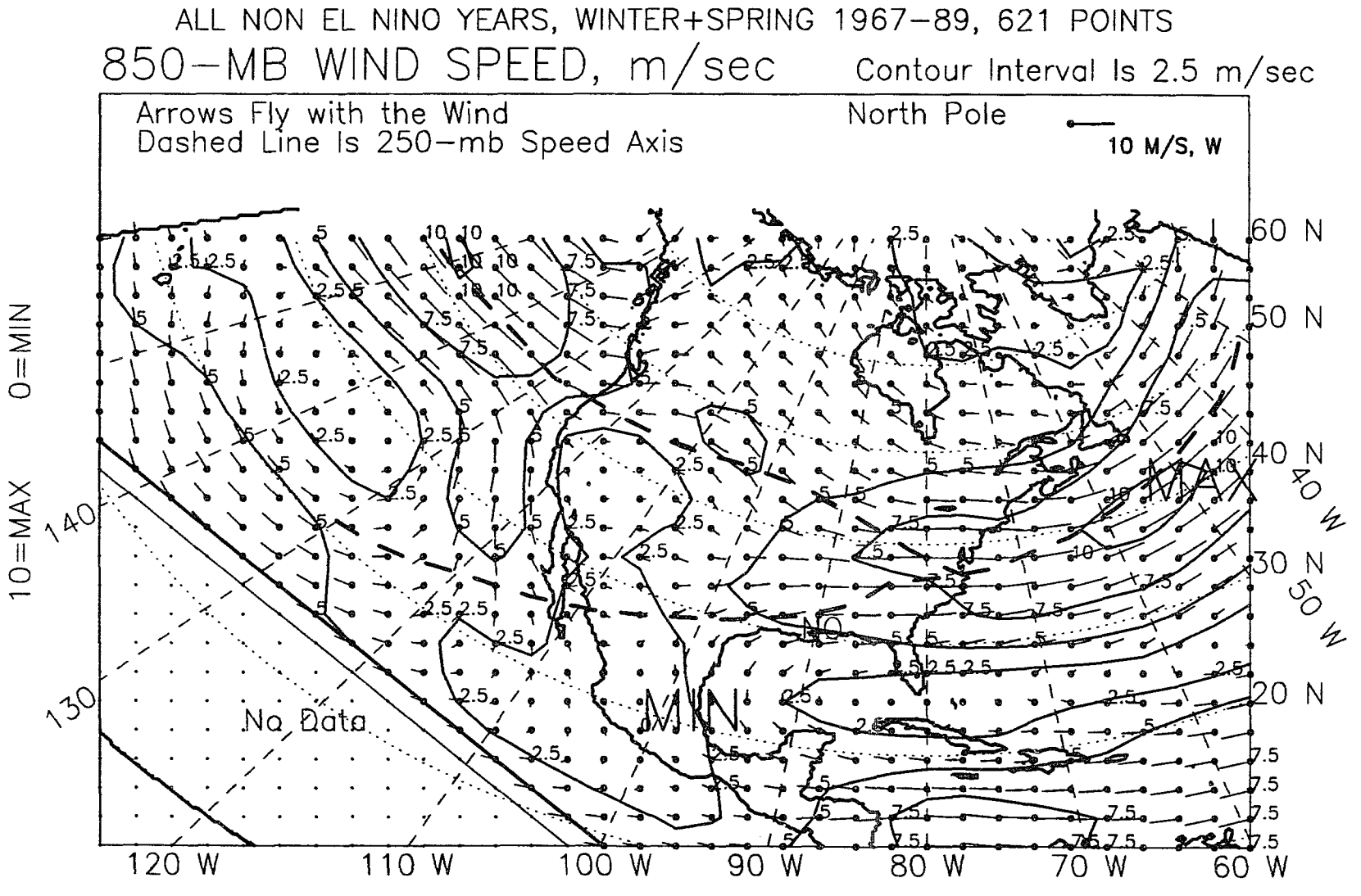

Figure C.8: 850–mb wind vectors, winter–plus–spring, non–El Niño years, 1967–89.

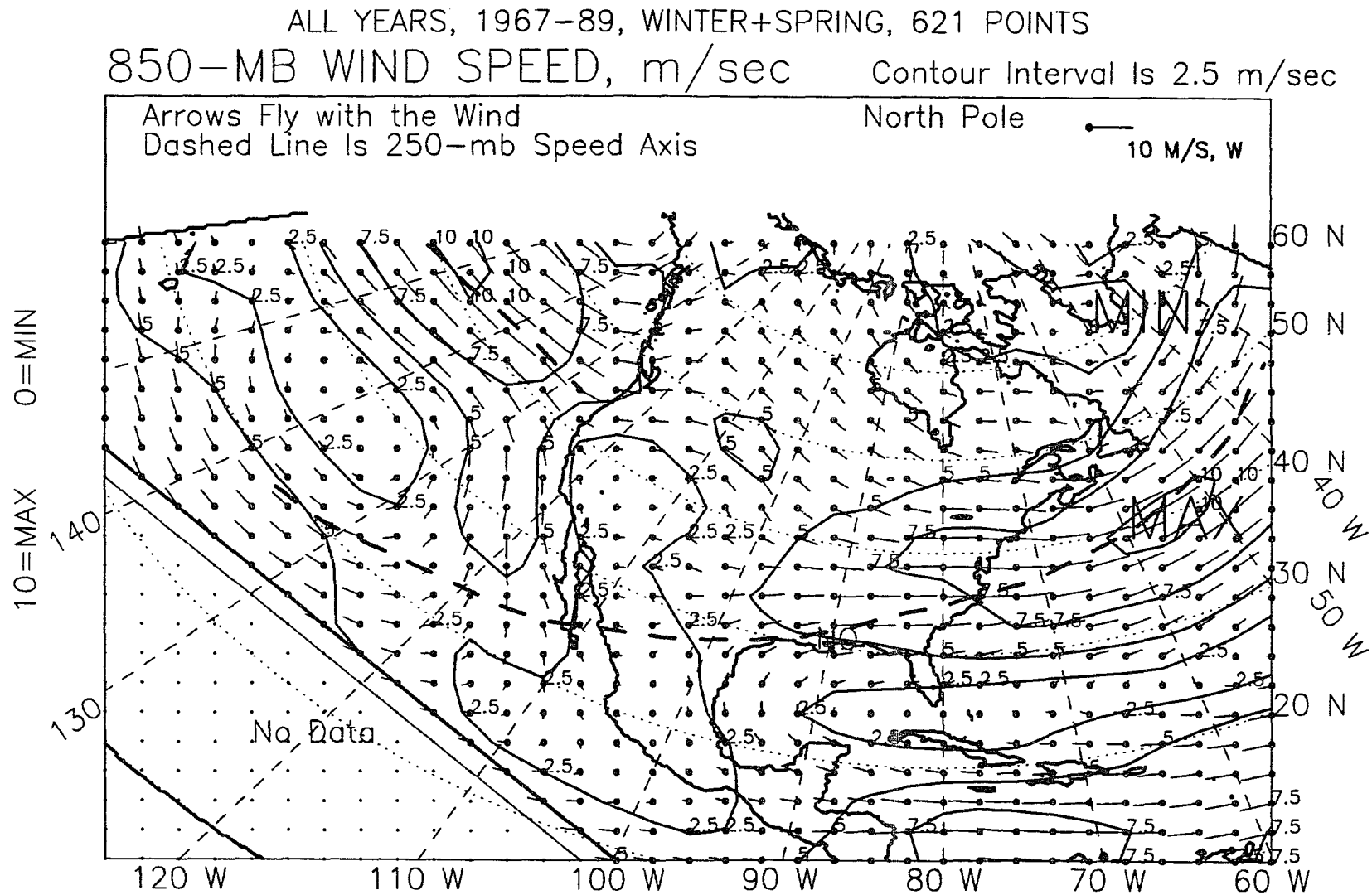

Figure C.9: 850–mb wind vectors, winter–plus–spring, all years, 1967–89.

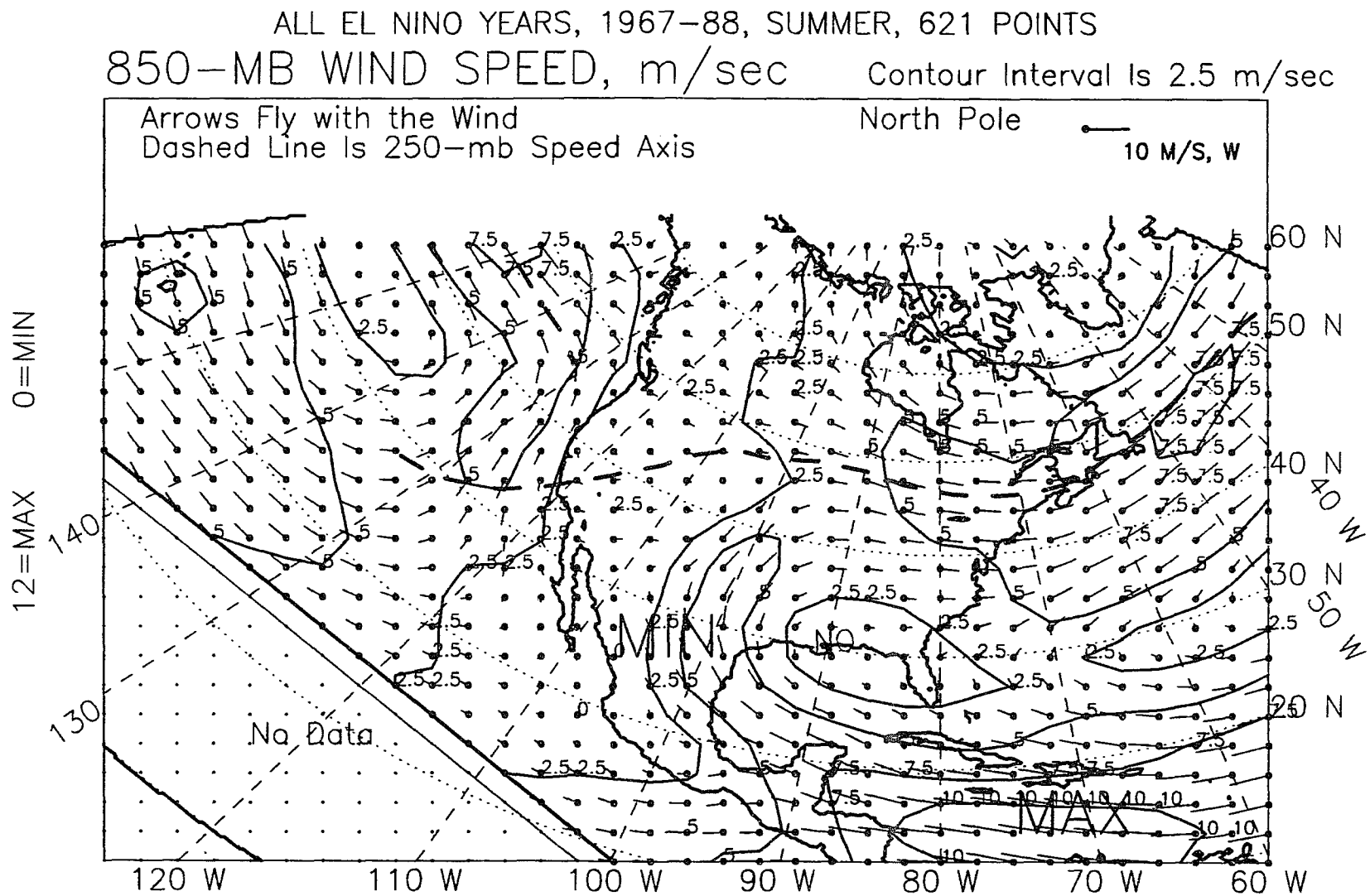

Figure C.10: 850–mb wind vectors, summer, El Niño years, 1967–88.

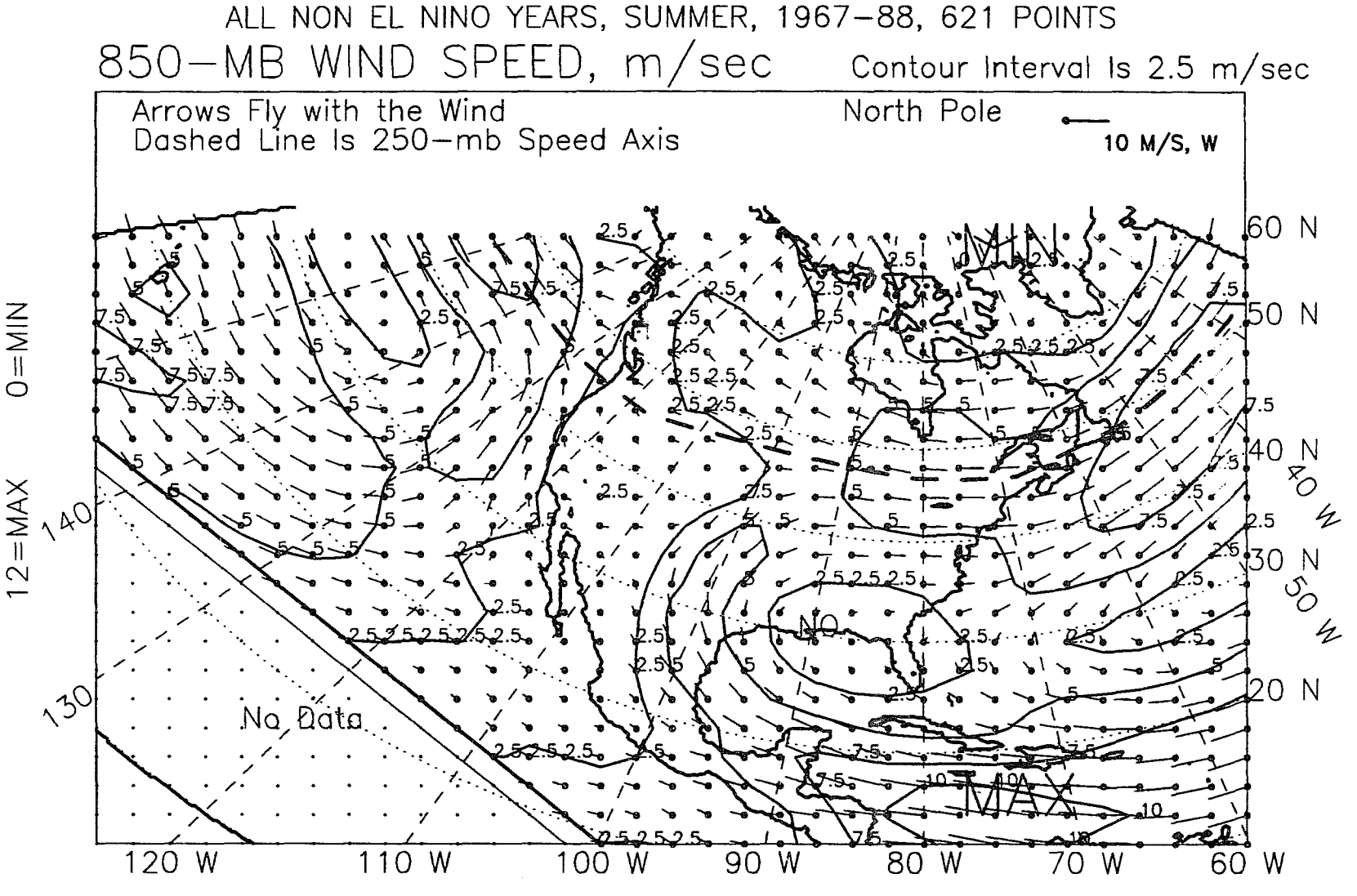

Figure C.11: 850–mb wind vectors, summer, non–El Niño years, 1967–88.

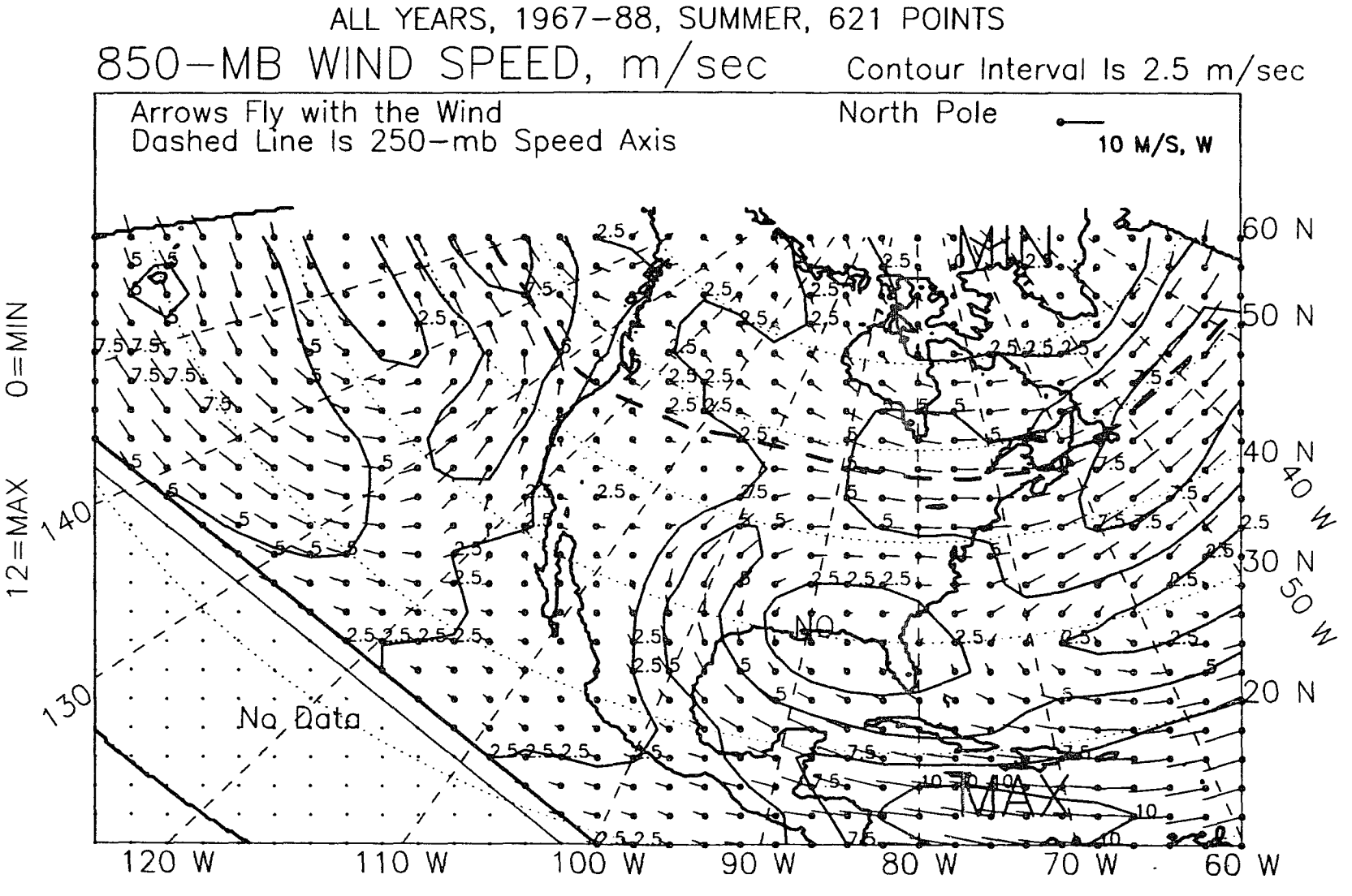

Figure C.12: 850–mb wind vectors, summer, all years, 1967–88.

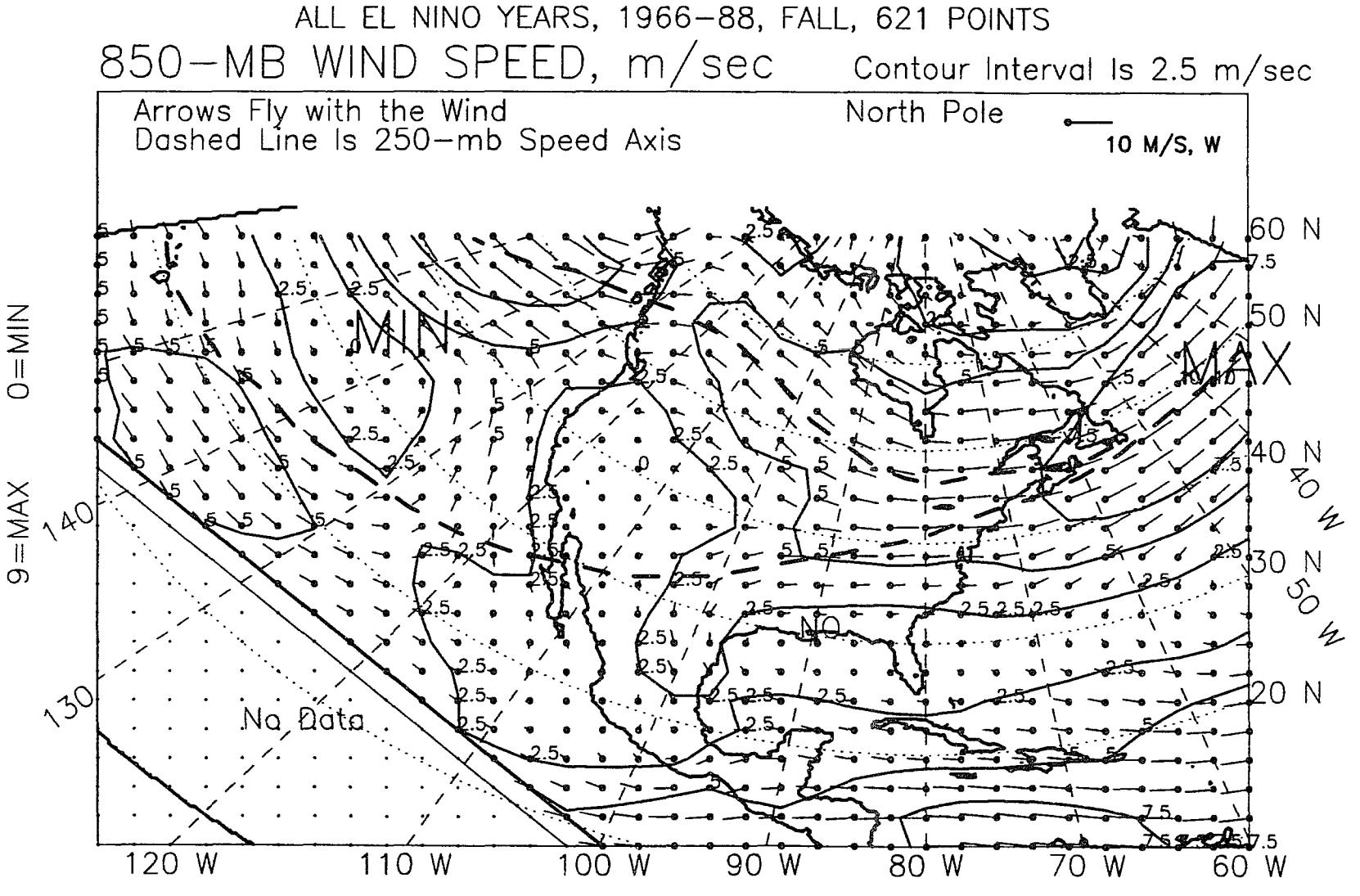

Figure C.13: 850–mb wind vectors, fall, El Niño years, 1966–88.

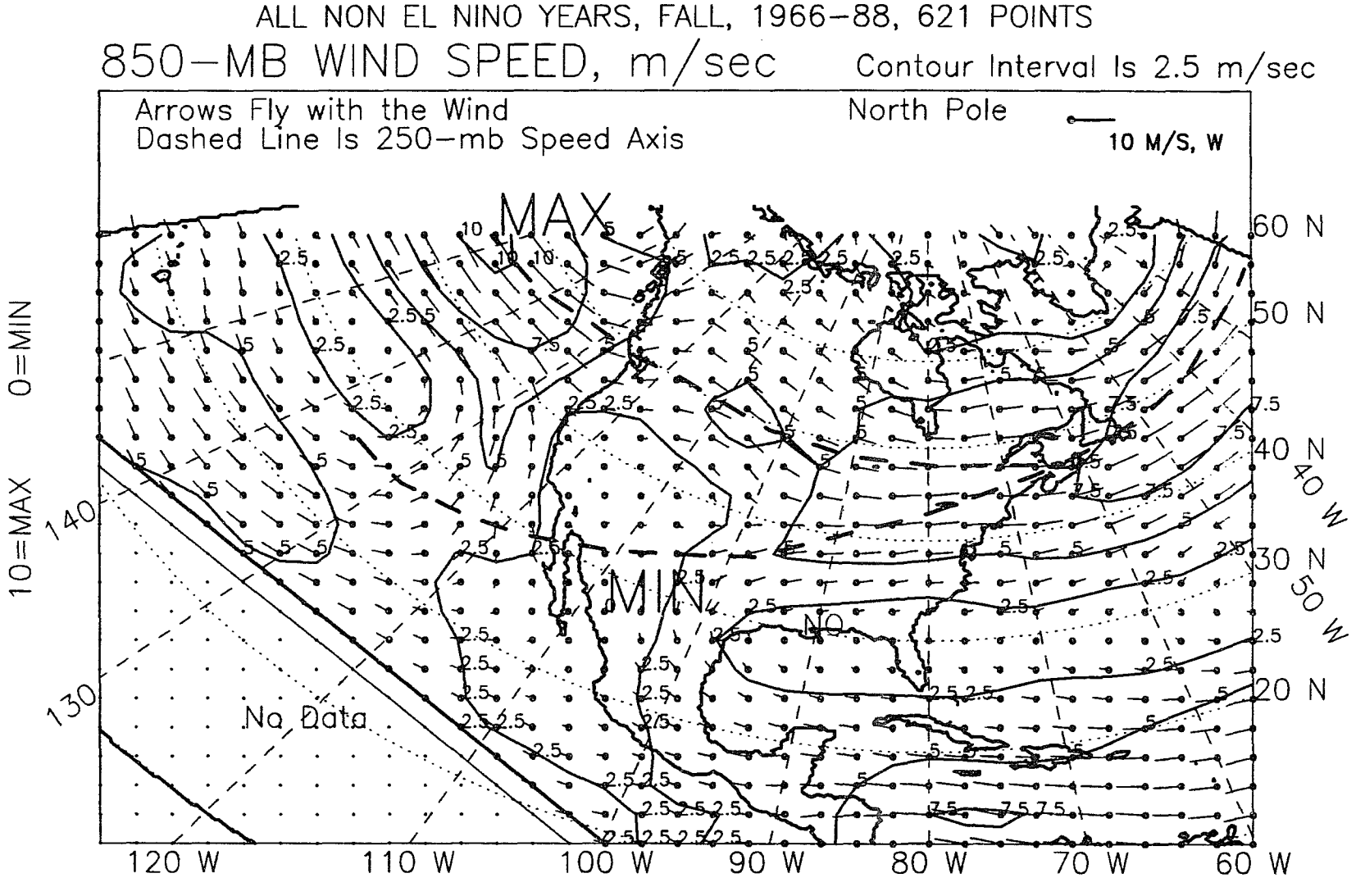

Figure C.14: 850–mb wind vectors, fall, non–El Niño years, 1966–88.

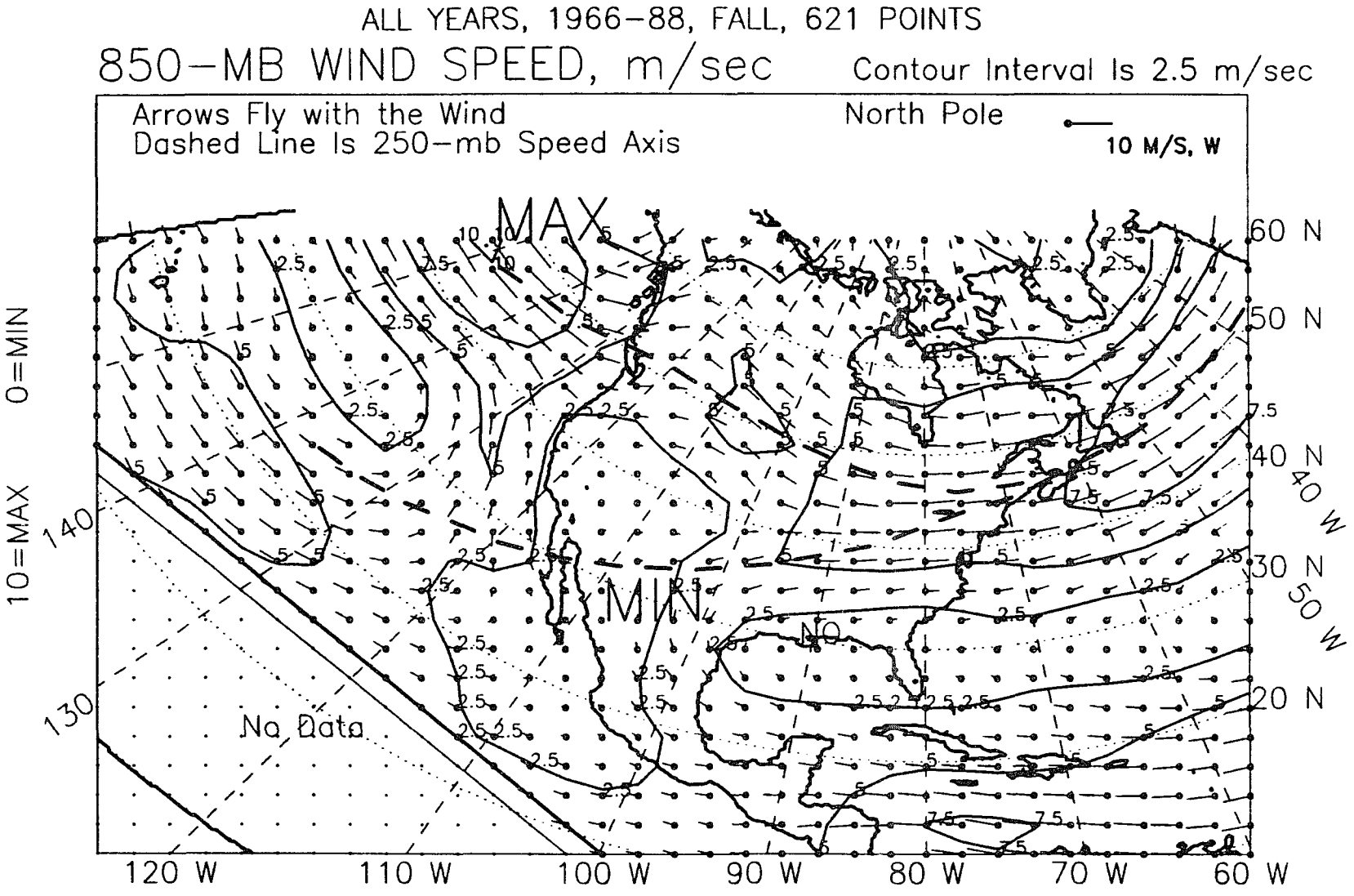

Figure C.15: 850–mb wind vectors, fall, all years, 1966–88.

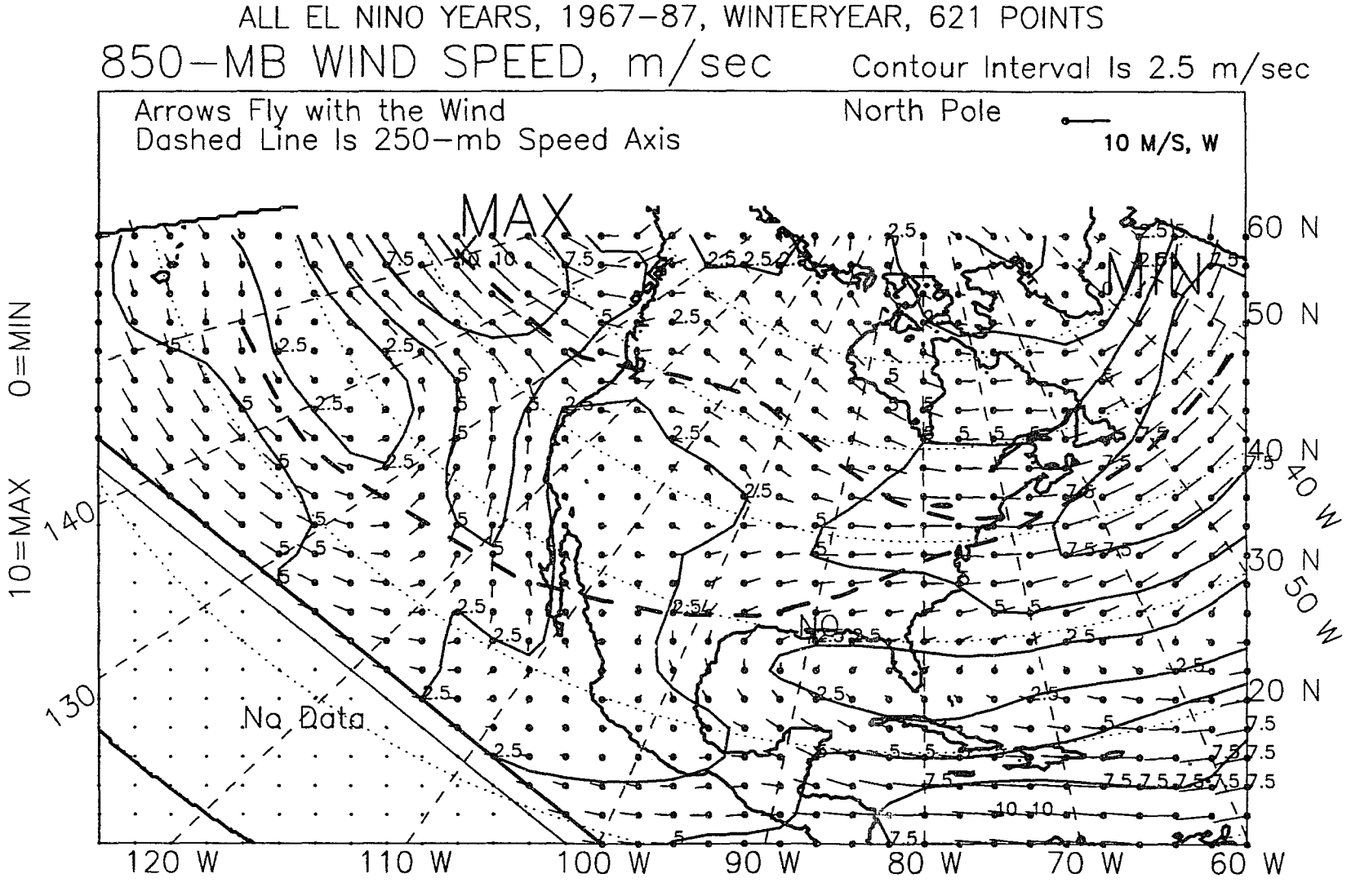

Figure C.16: 850–mb wind vectors, winter year, El Niño years, 1967–87.

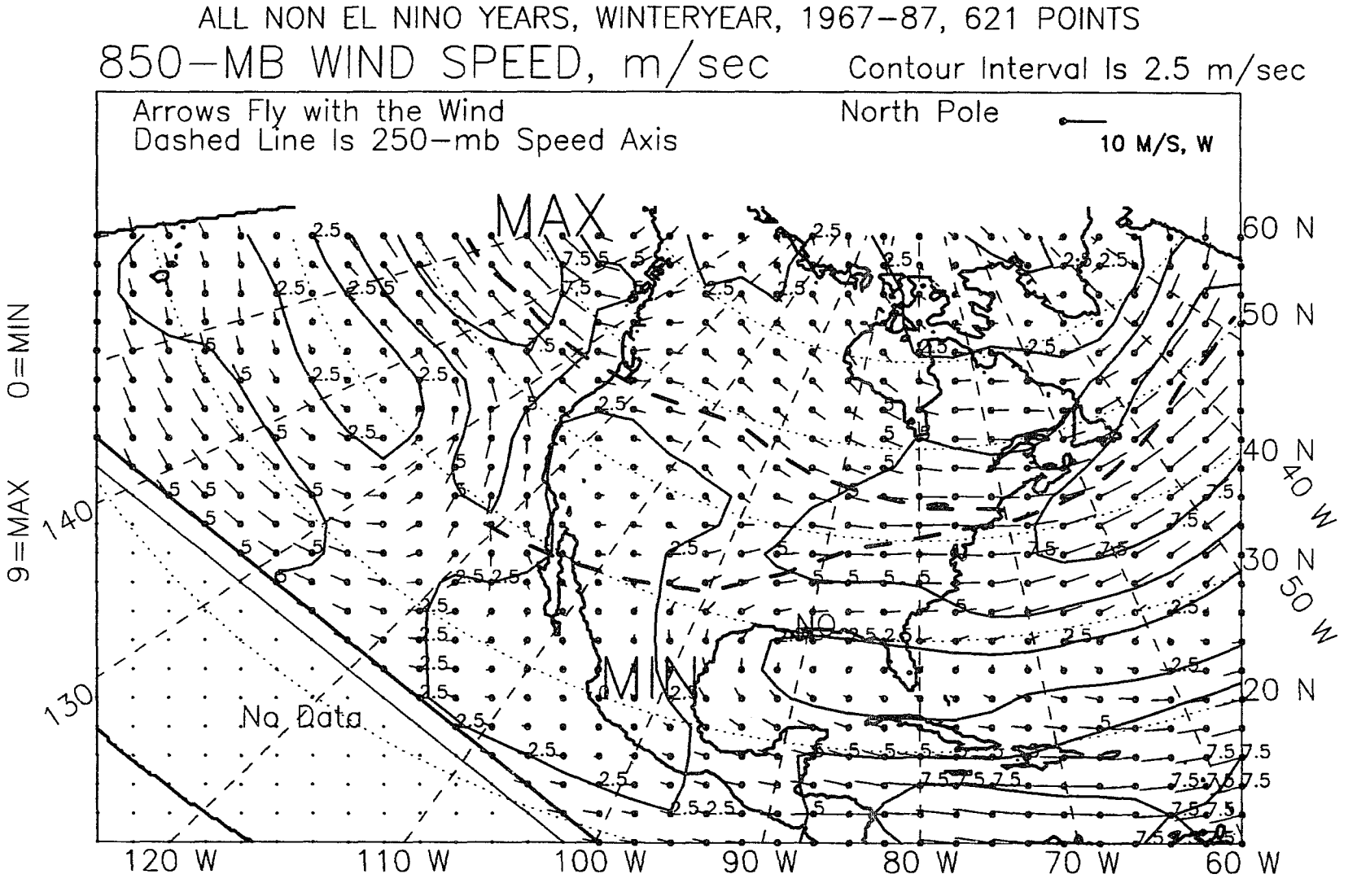

Figure C.17: 850-mb wind vectors, winter year, non-El Niño years, 1967-87.

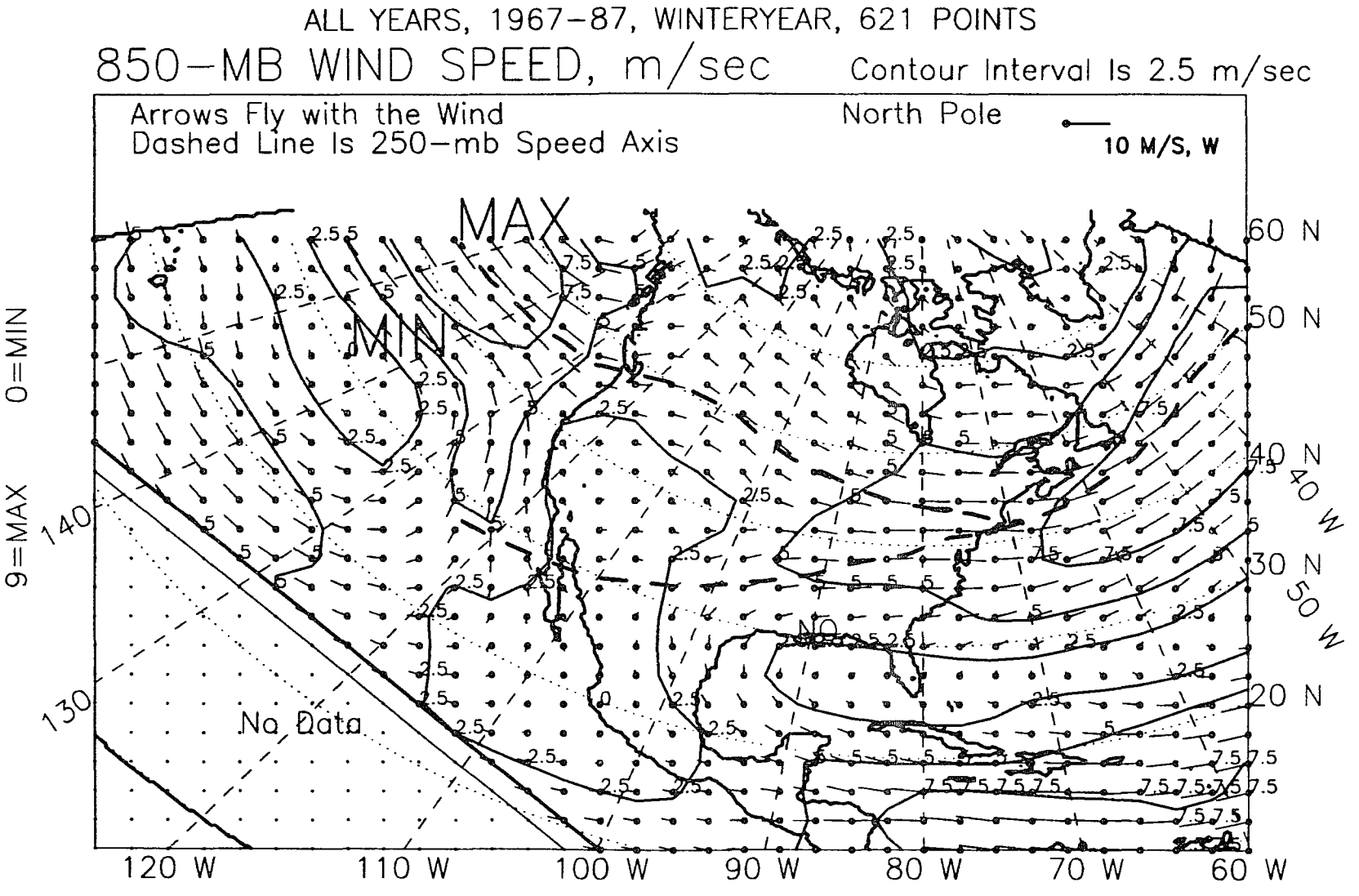

Figure C.18: 850–mb wind vectors, winter year, all years, 1967–87.

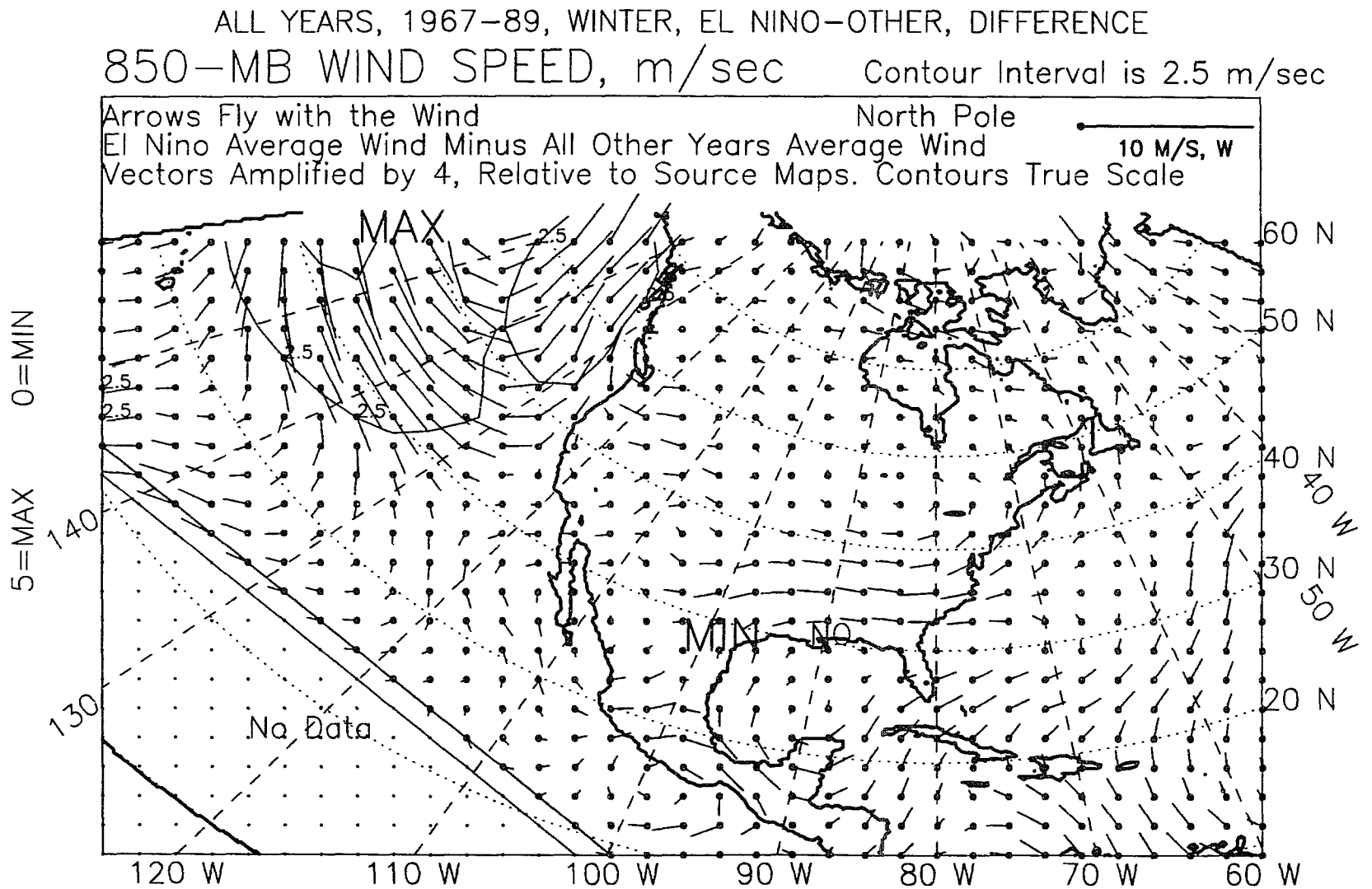

Figure C.19: 850–mb wind vectors, winter, 1967–89, difference.

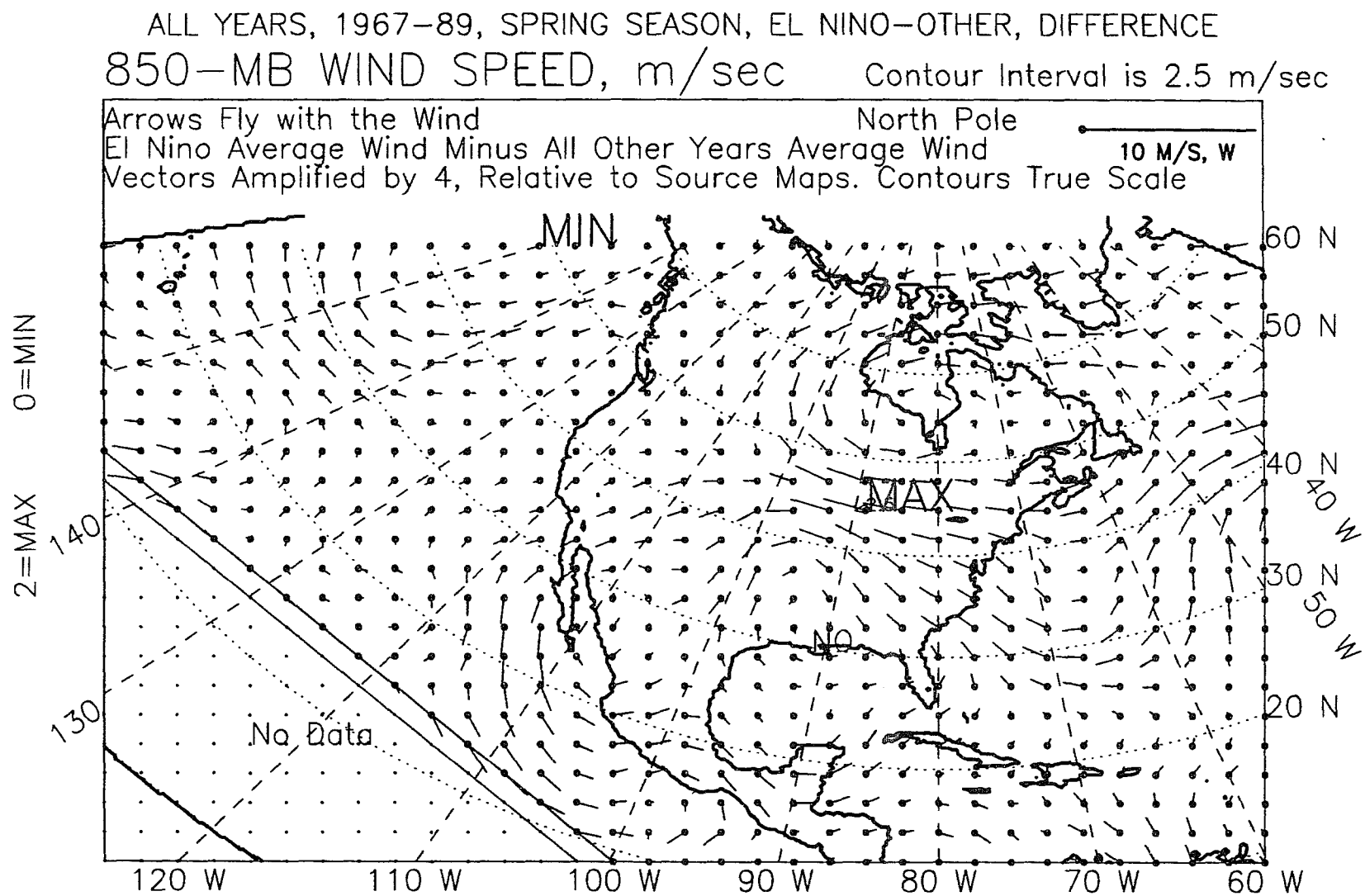

Figure C.20: 850–mb wind vectors, spring, 1967–89, difference.

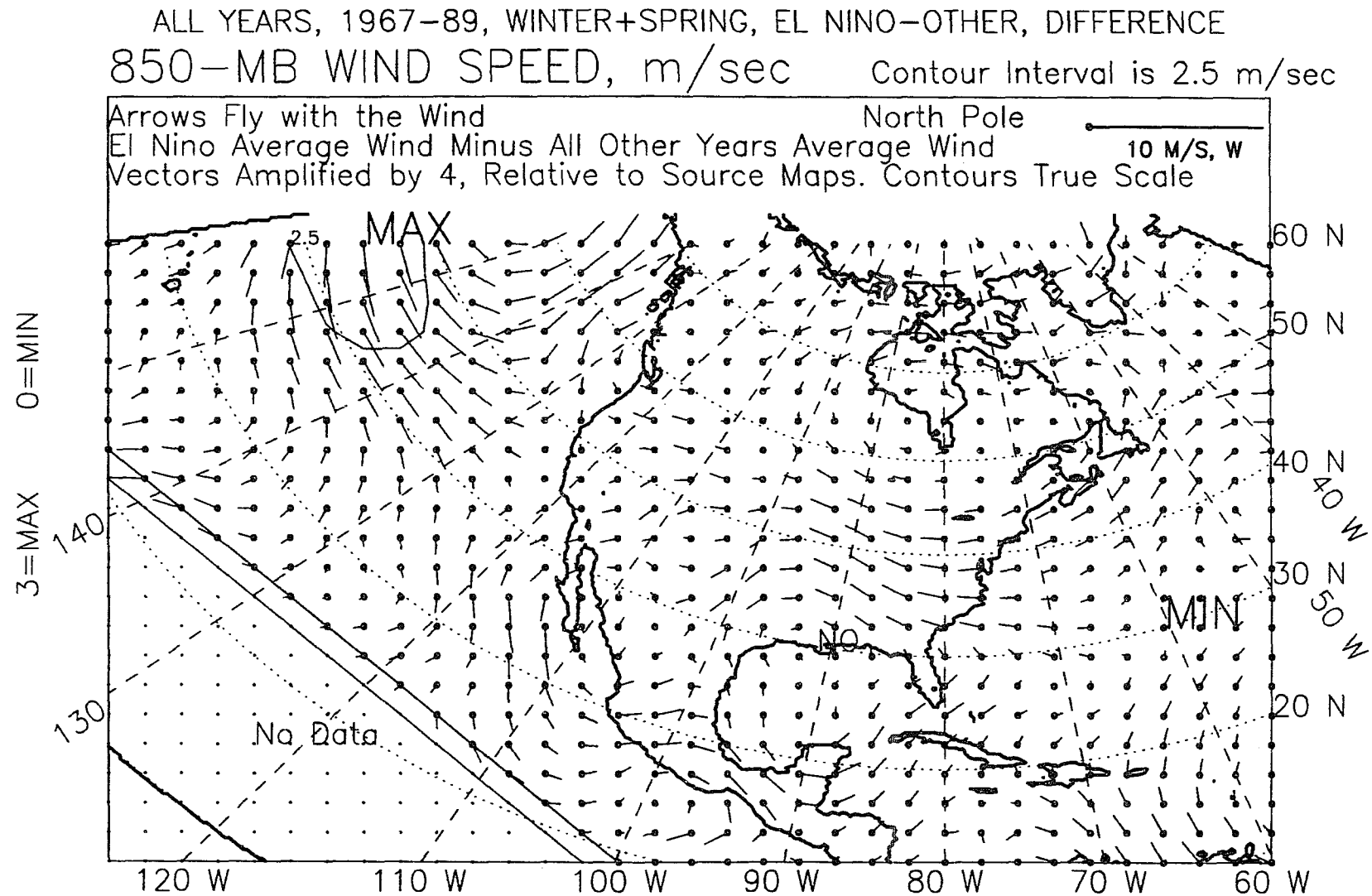

Figure C.21: 850–mb wind vectors, winter–plus–spring, 1967–89, difference.

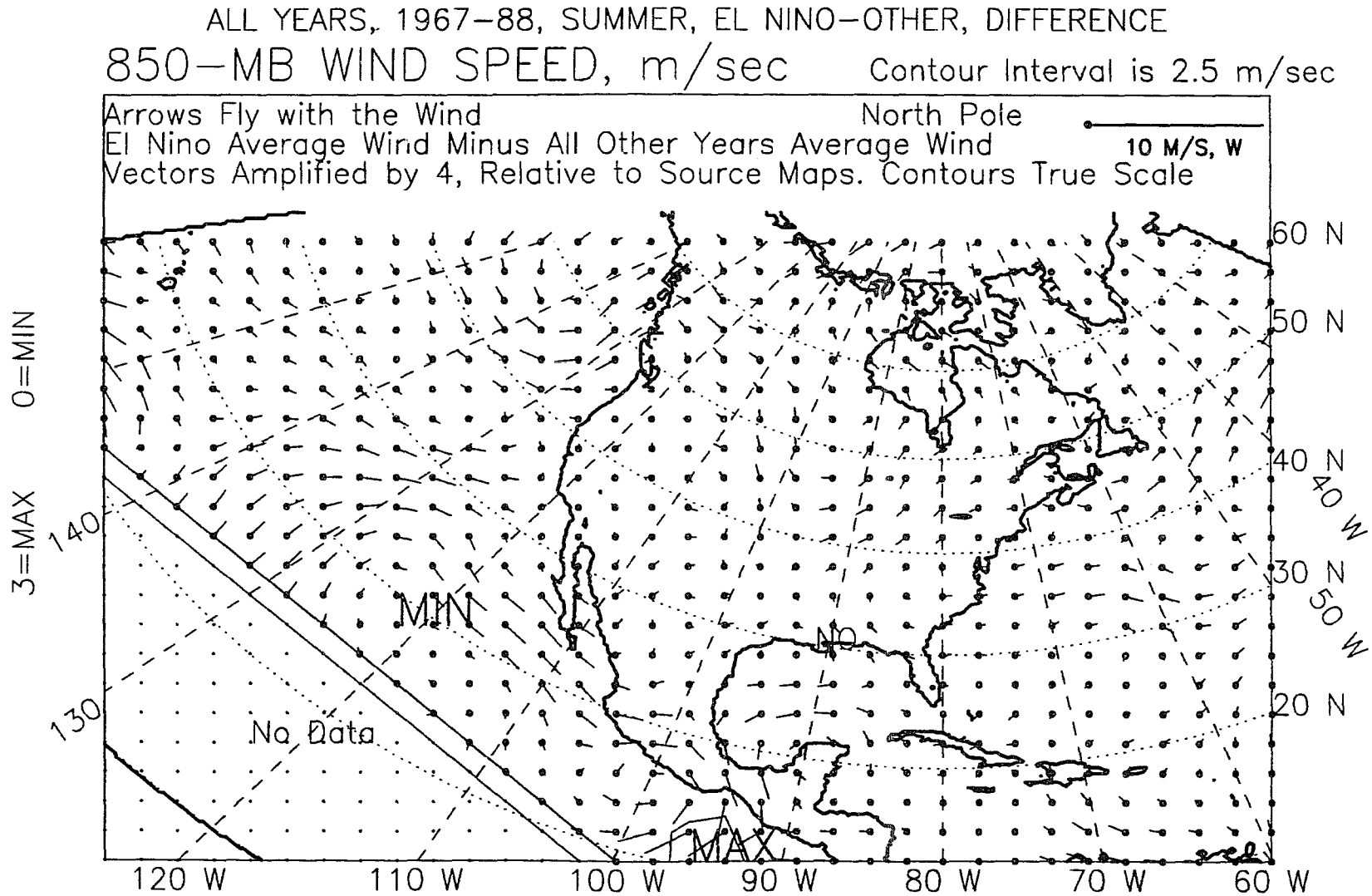

Figure C.22: 850–mb wind vectors, summer, 1967–88, difference.

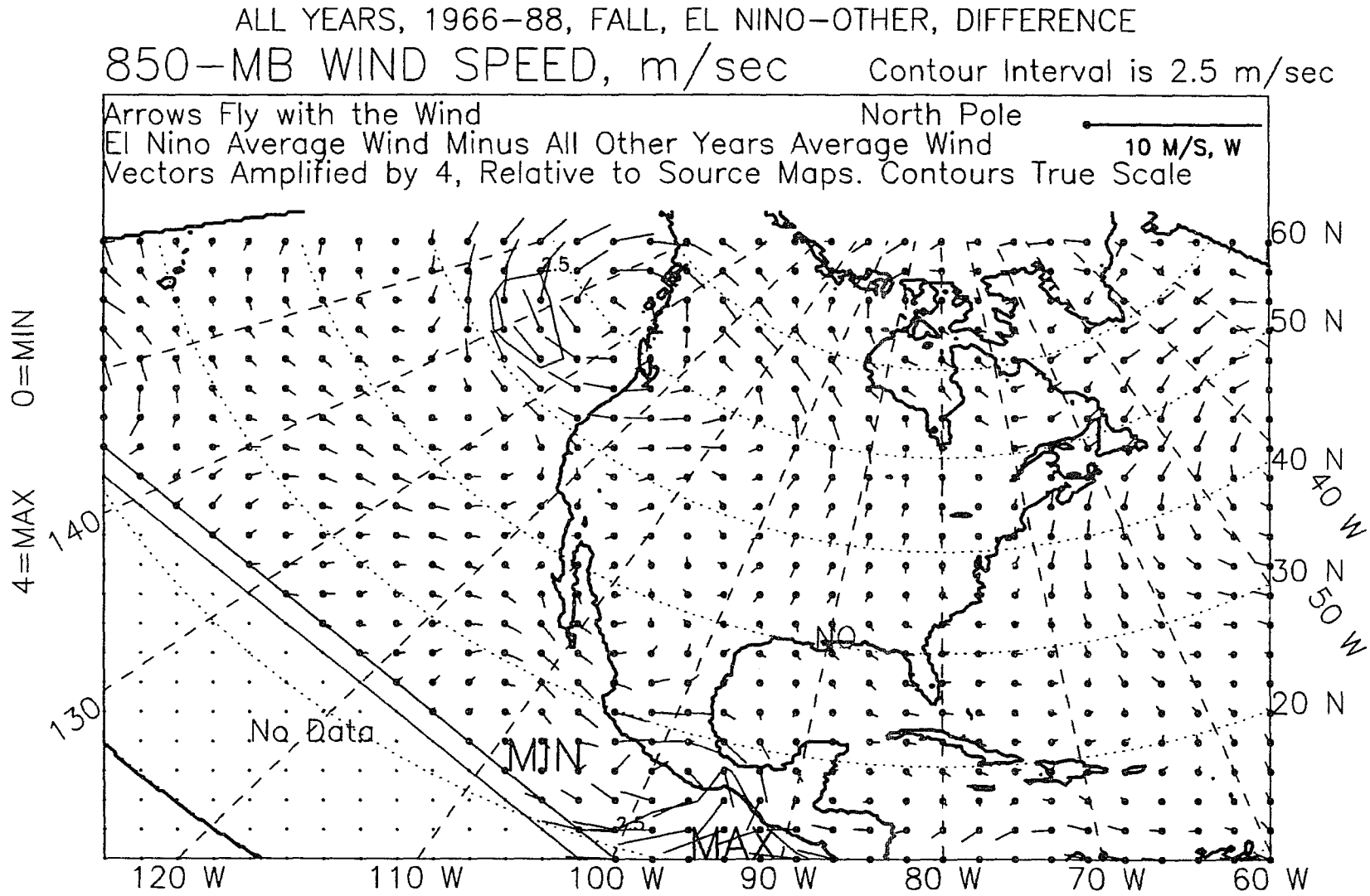

Figure C.23: 850–mb wind vectors, fall, 1966–88, difference.

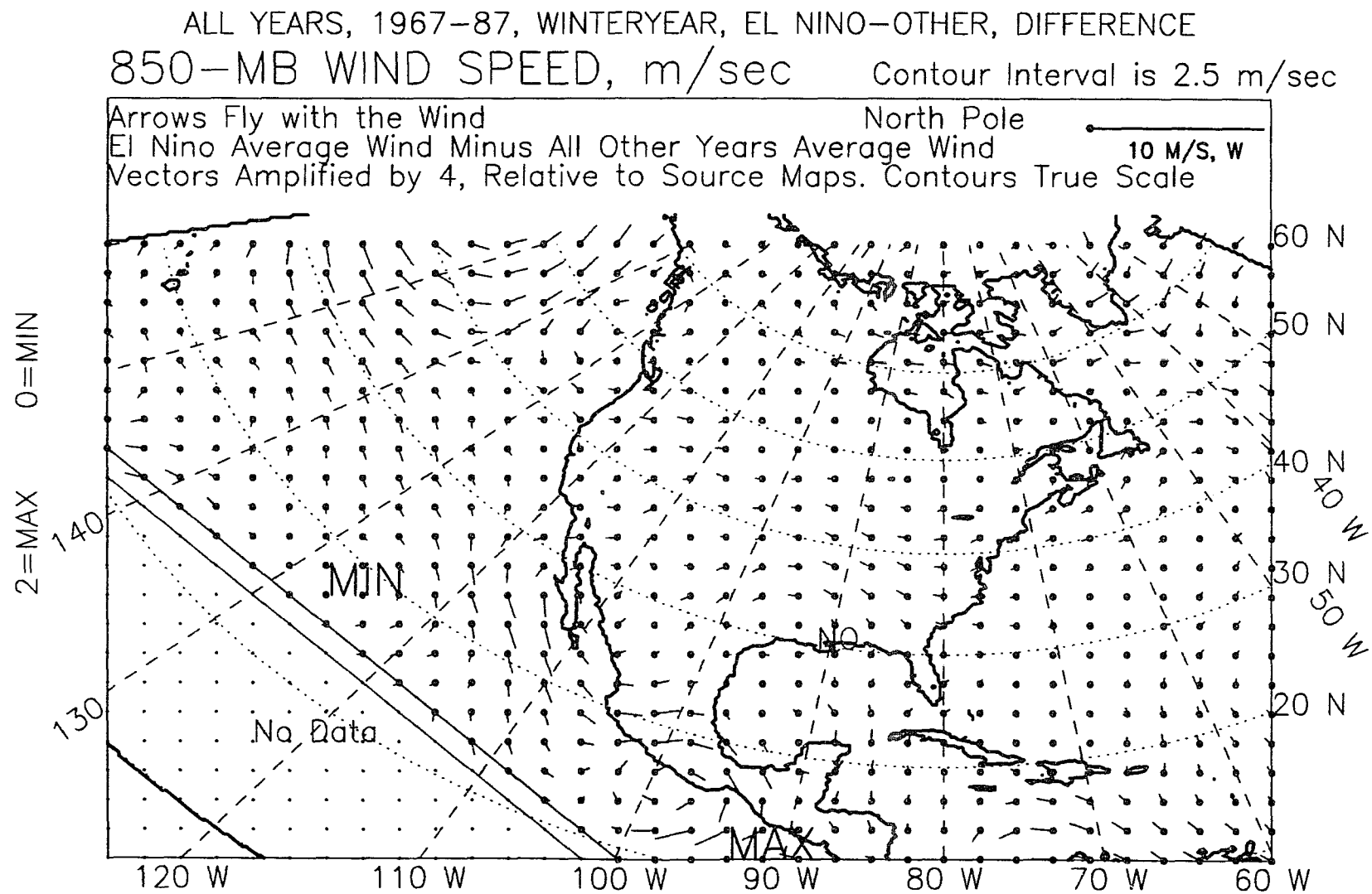

Figure C.24: 850–mb wind vectors, winter year, 1967–87, difference.

APPENDIX D
850-MB TEMPERATURE FIELD

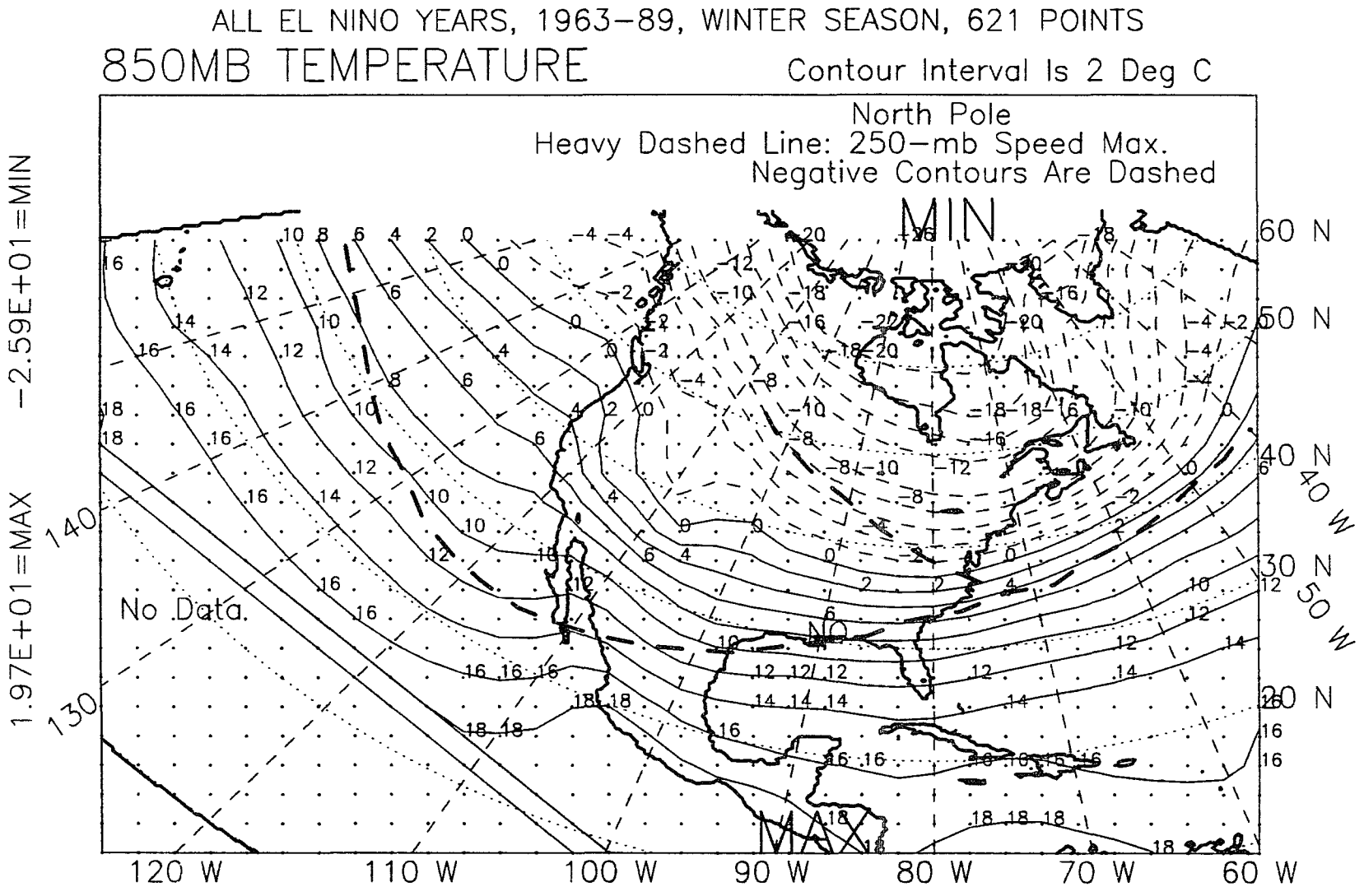

Figure D.1: 850–mb temperature, winter, El Niño years, 1963–89.

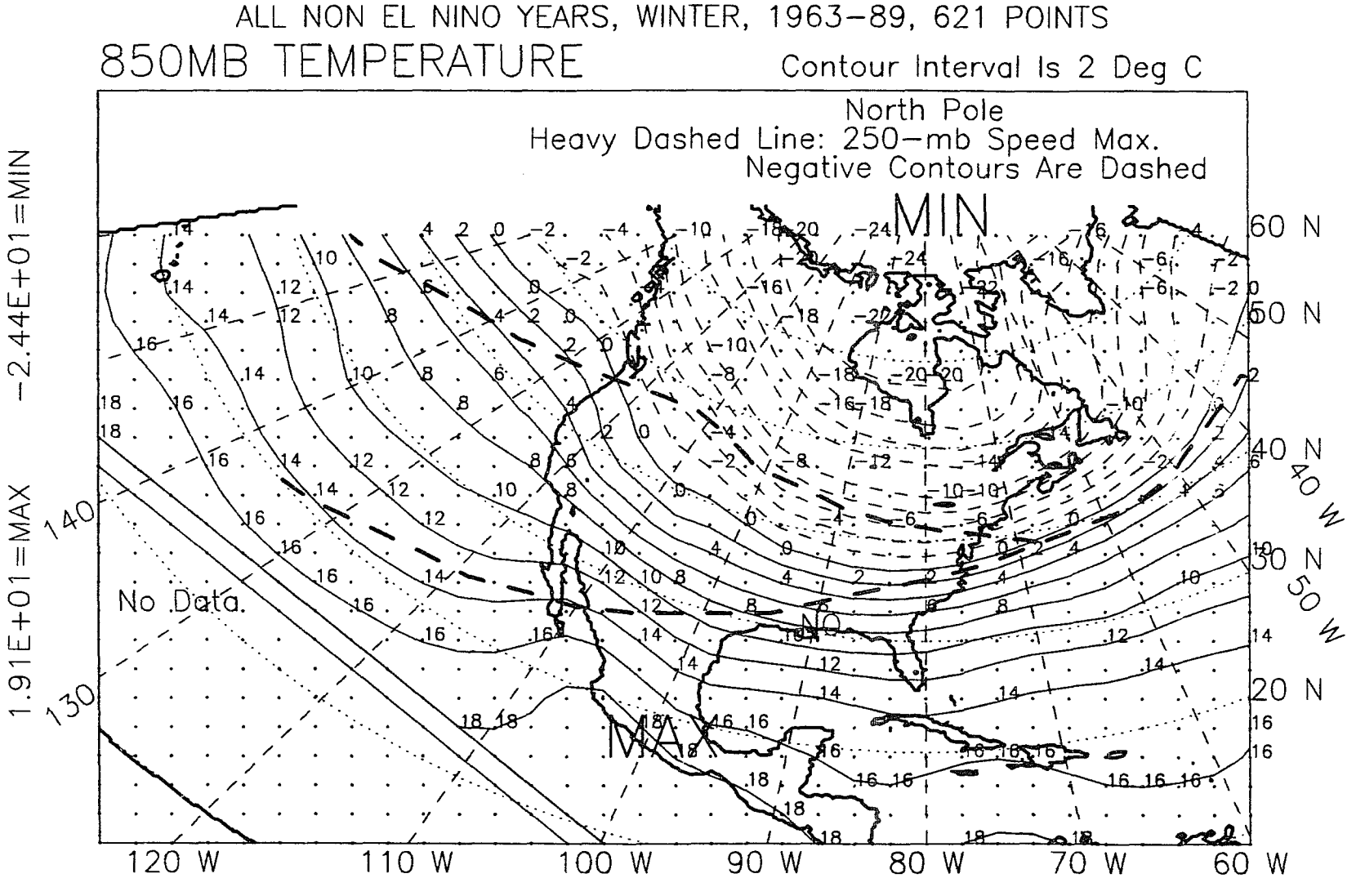

Figure D.2: 850–mb temperature, winter, non–El Niño years, 1963–89.

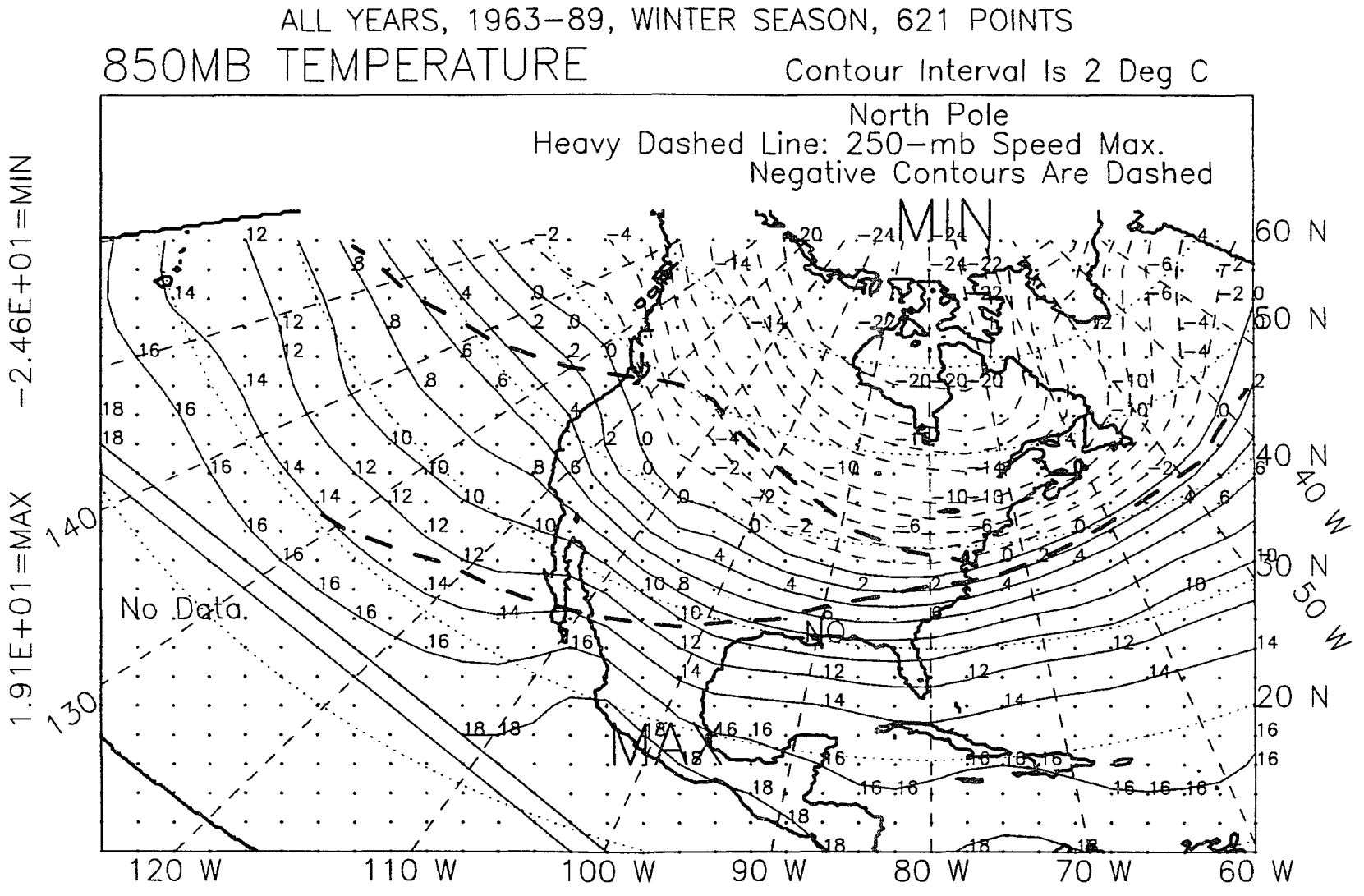

Figure D.3: 850–mb temperature, winter, all years, 1963–89.

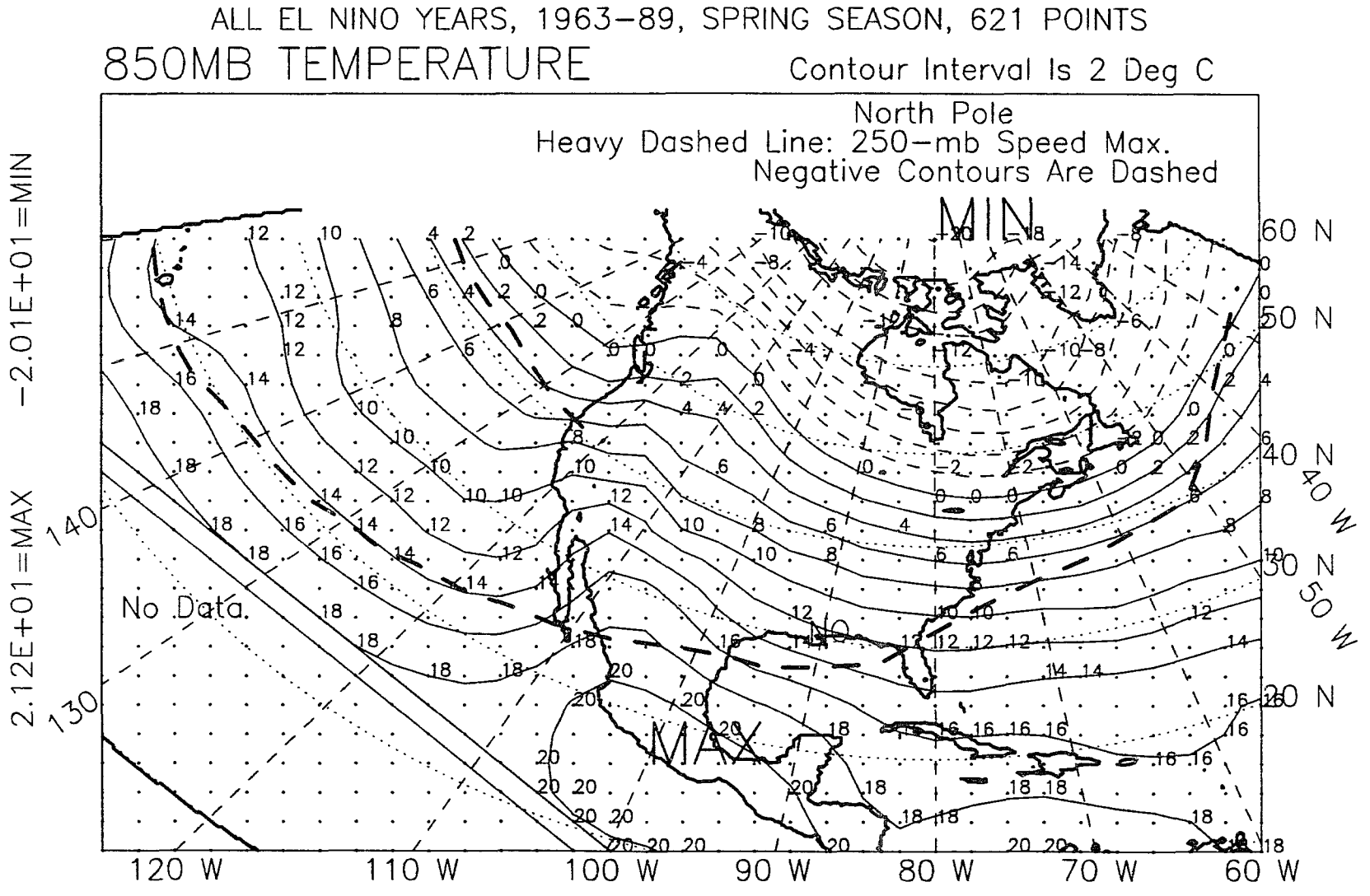

Figure D.4: 850–mb temperature, spring, El Niño years, 1963–89.

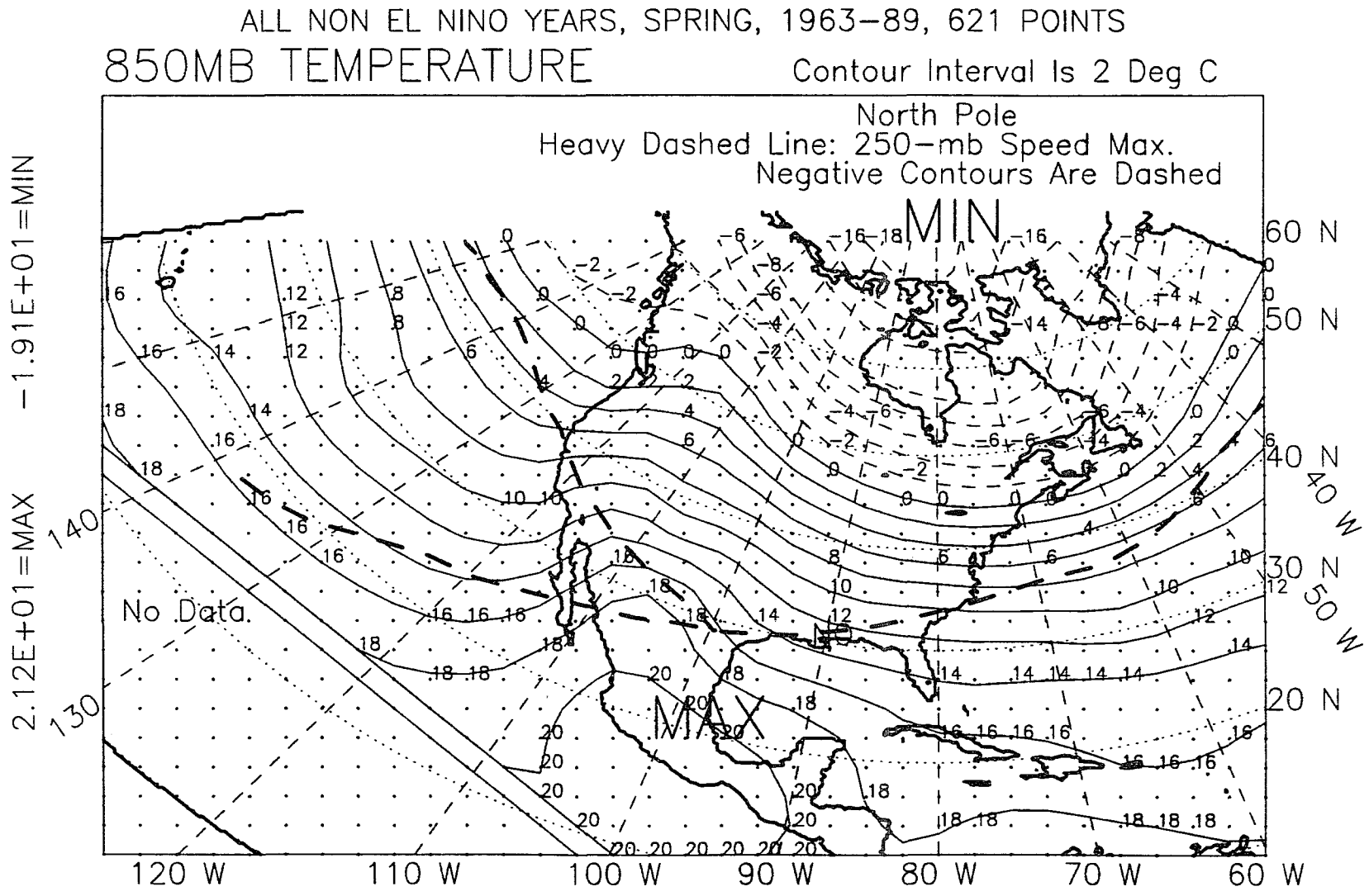

Figure D.5: 850–mb temperature, spring, non–El Niño years, 1963–89.

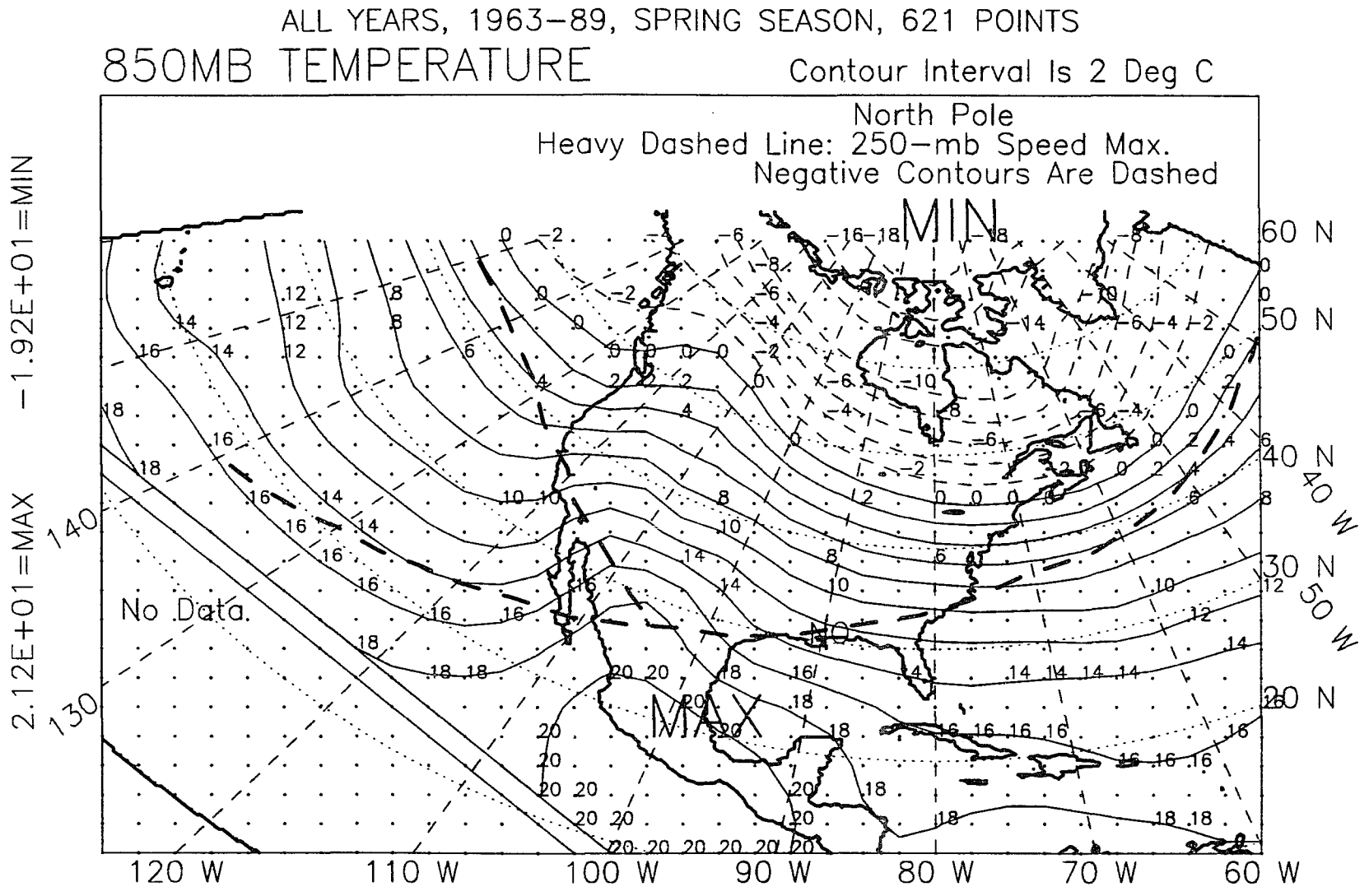

Figure D.6: 850–mb temperature, spring, all years, 1963–89.

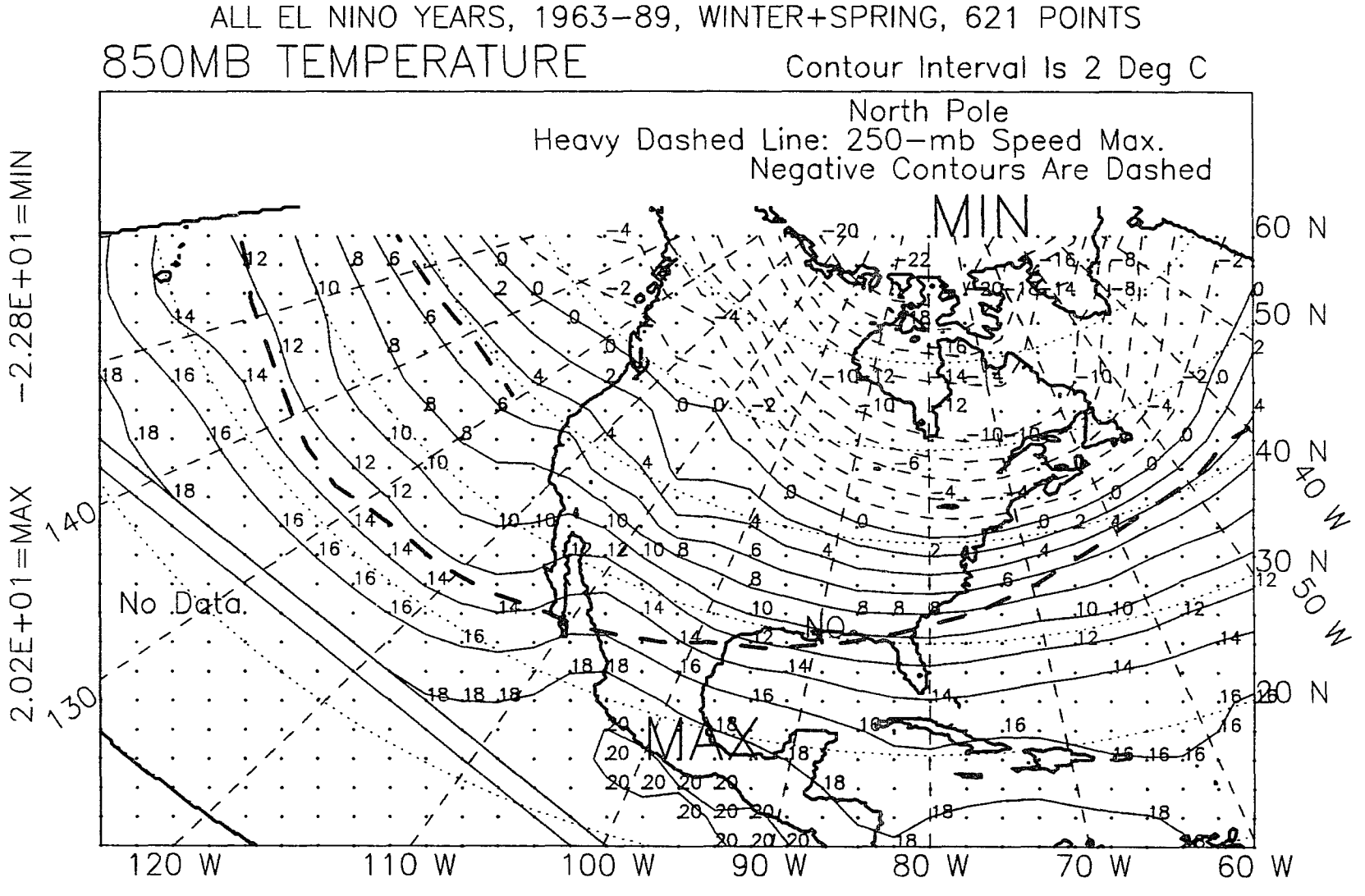

Figure D.7: 850–mb temperature, winter–plus–spring, El Niño years, 1963–89.

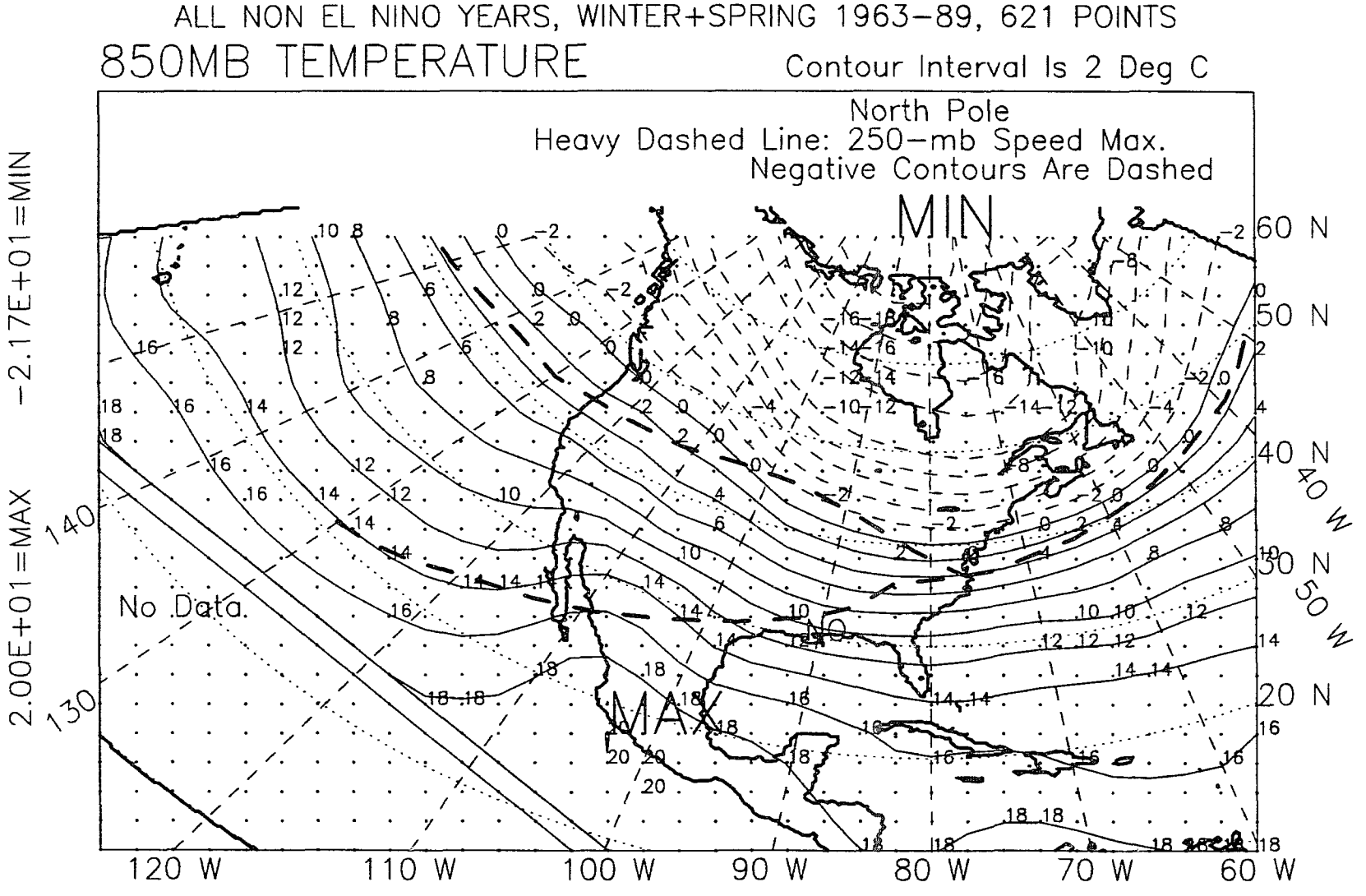

Figure D.8: 850–mb temperature, winter–plus–spring, non–El Niño years, 1963–89.

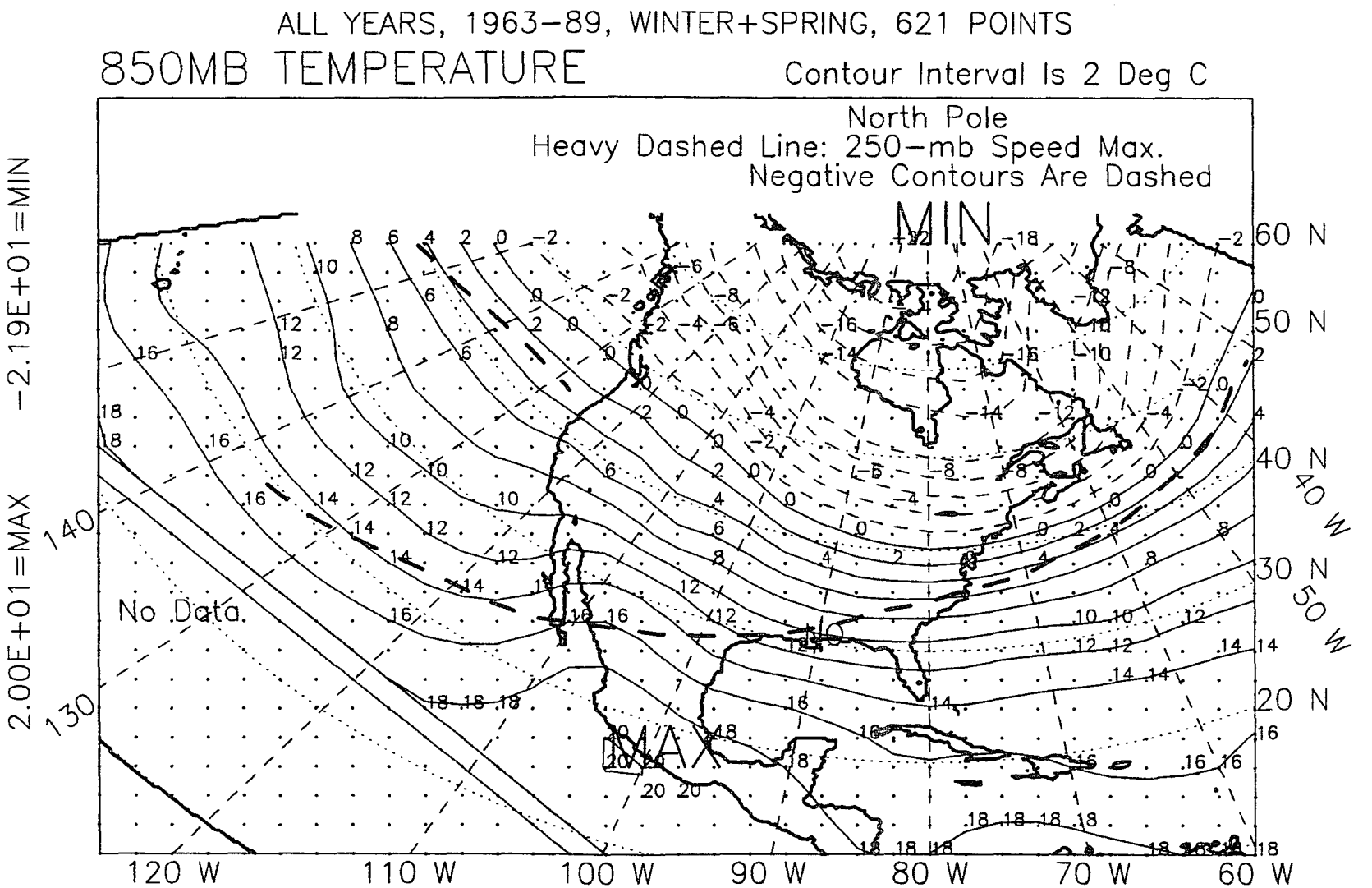

Figure D.9: 850–mb temperature, winter–plus–spring, all years, 1963–89.

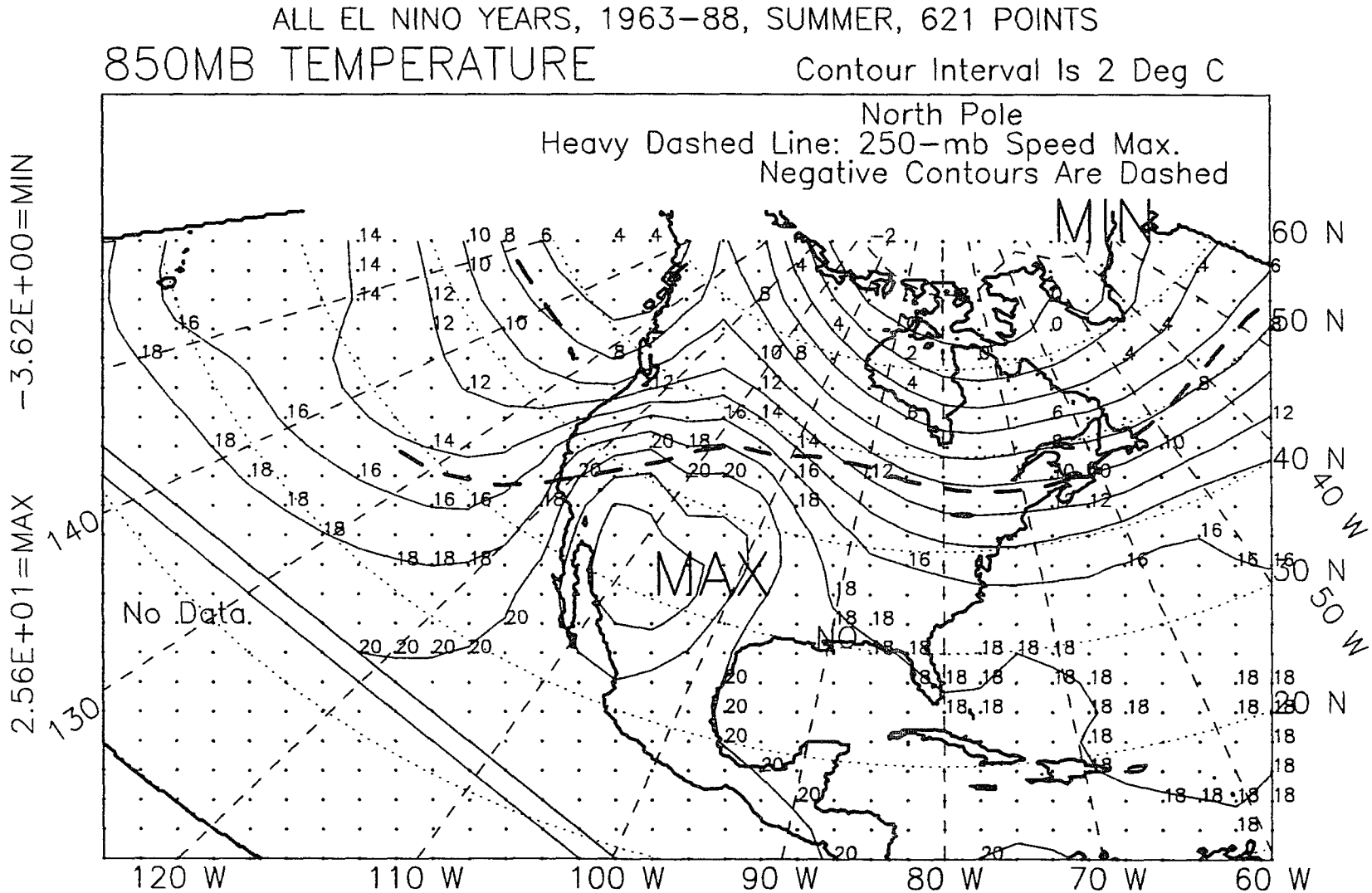

Figure D.10: 850–mb temperature, summer, El Niño years, 1963–88.

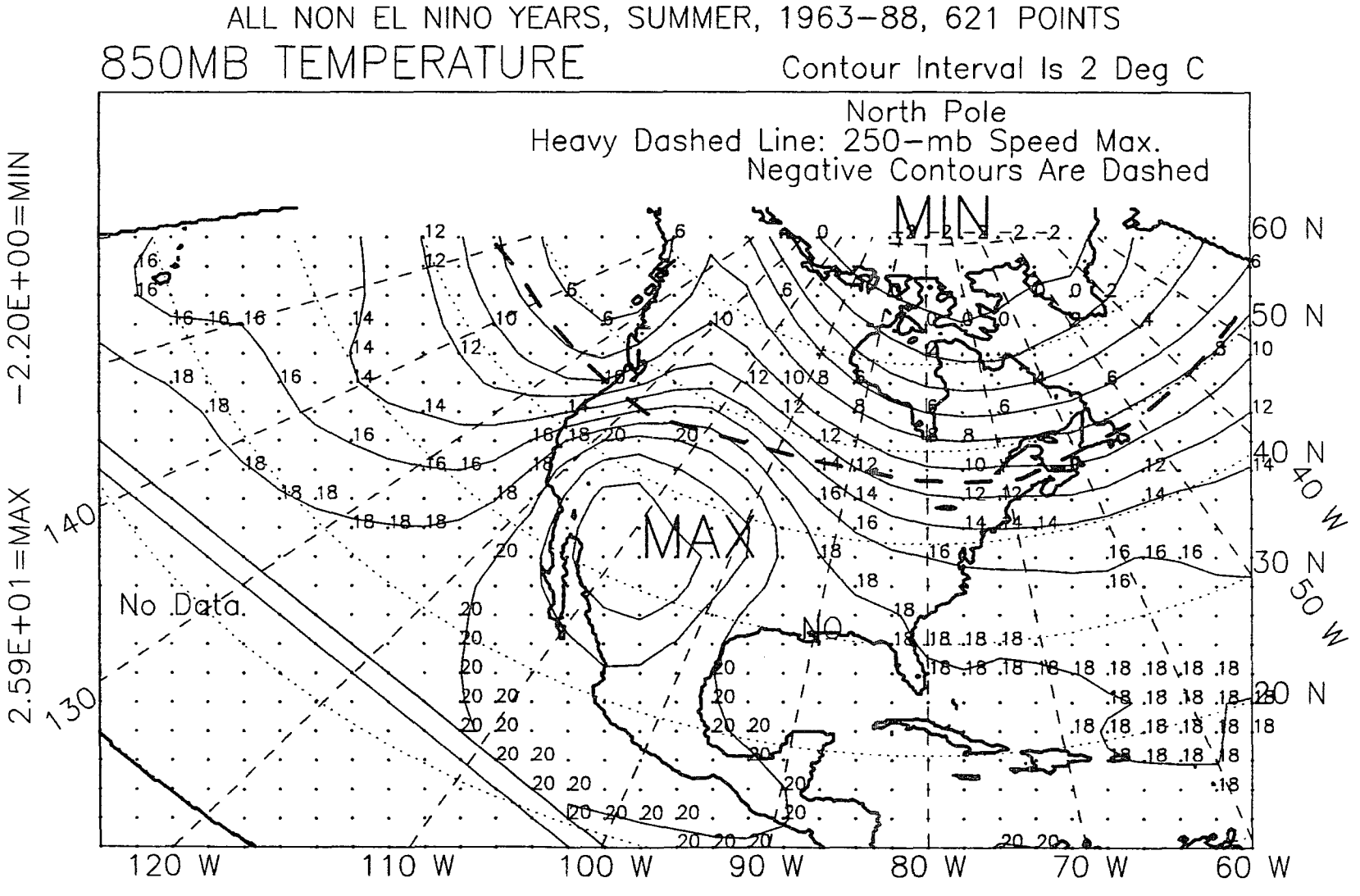

Figure D.11: 850–mb temperature, summer, non–El Niño years, 1963–88.

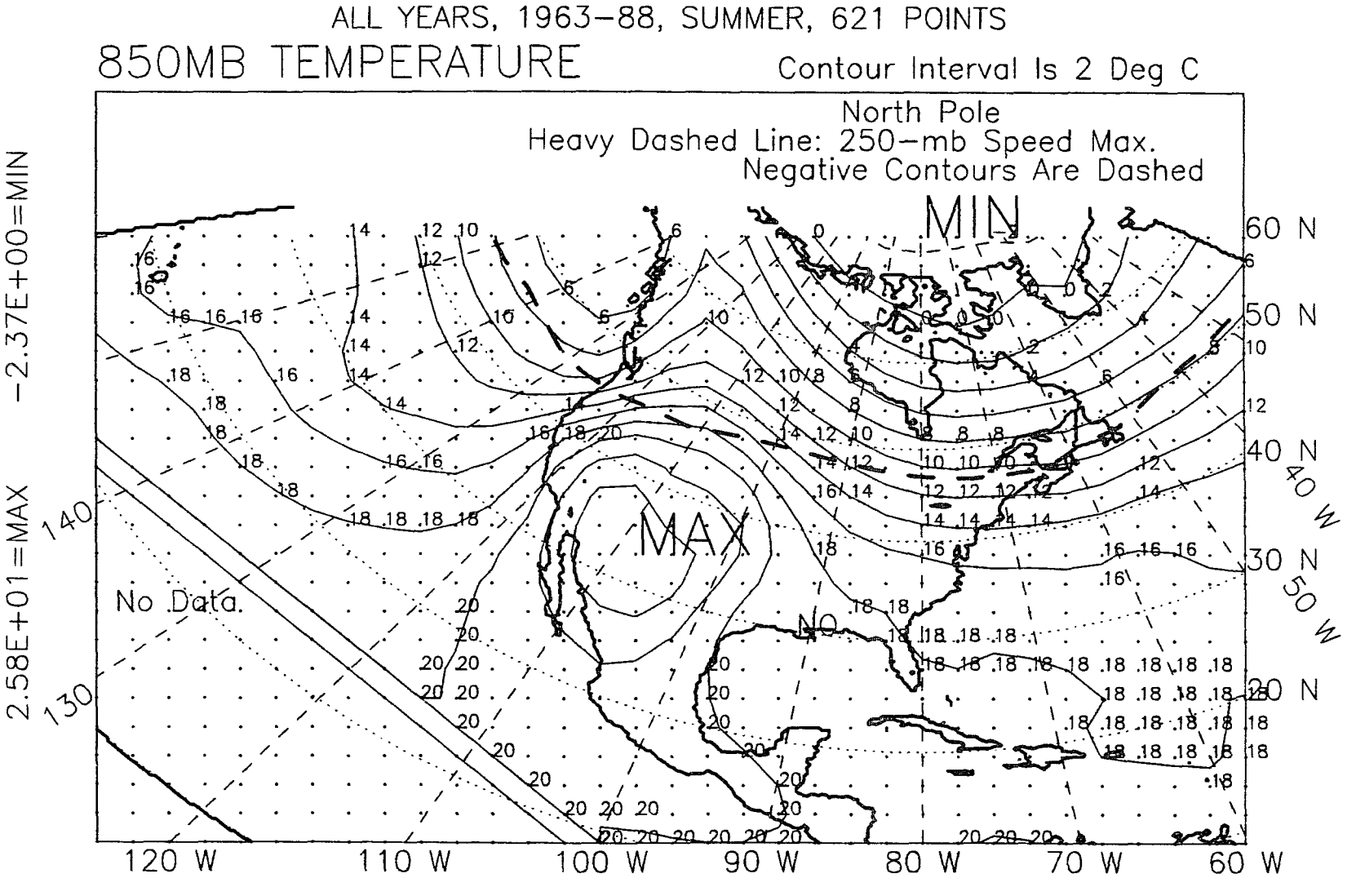

Figure D.12: 850–mb temperature, summer, all years, 1963–88.

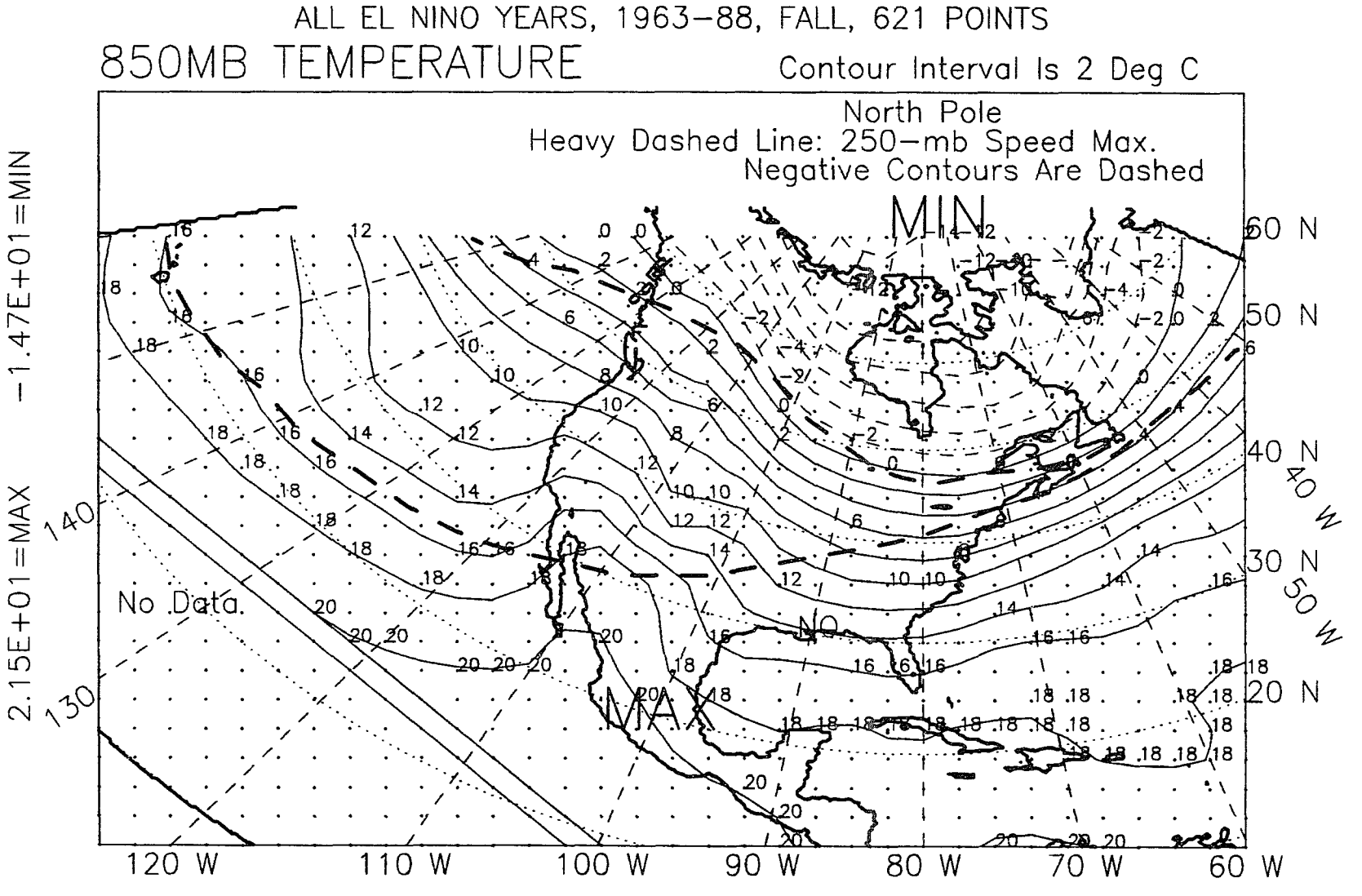

Figure D.13: 850–mb temperature, fall, El Niño years, 1963–88.

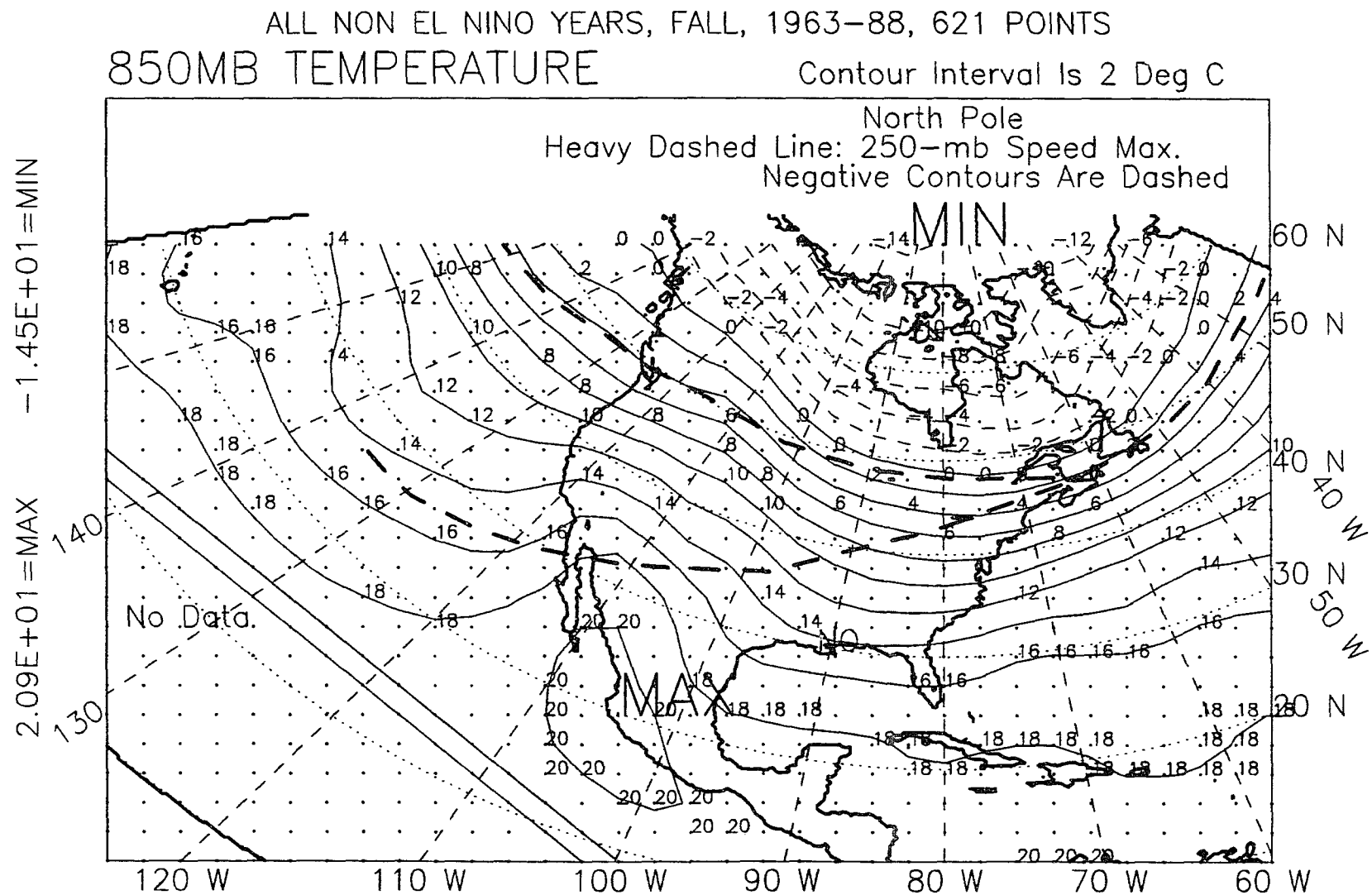

Figure D.14: 850–mb temperature, fall, non–El Niño years, 1963–88.

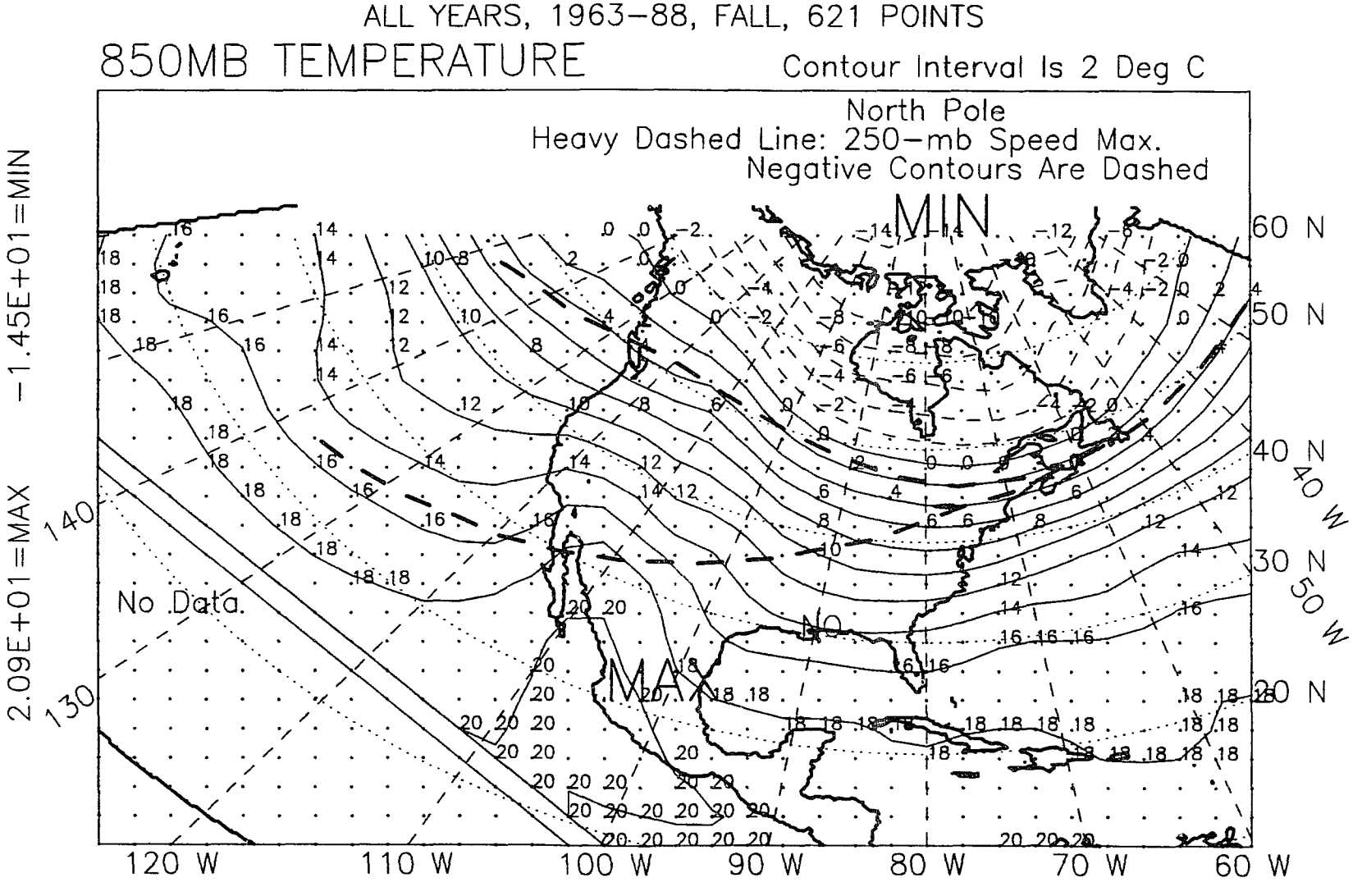

Figure D.15: 850–mb temperature, fall, all years, 1963–88.

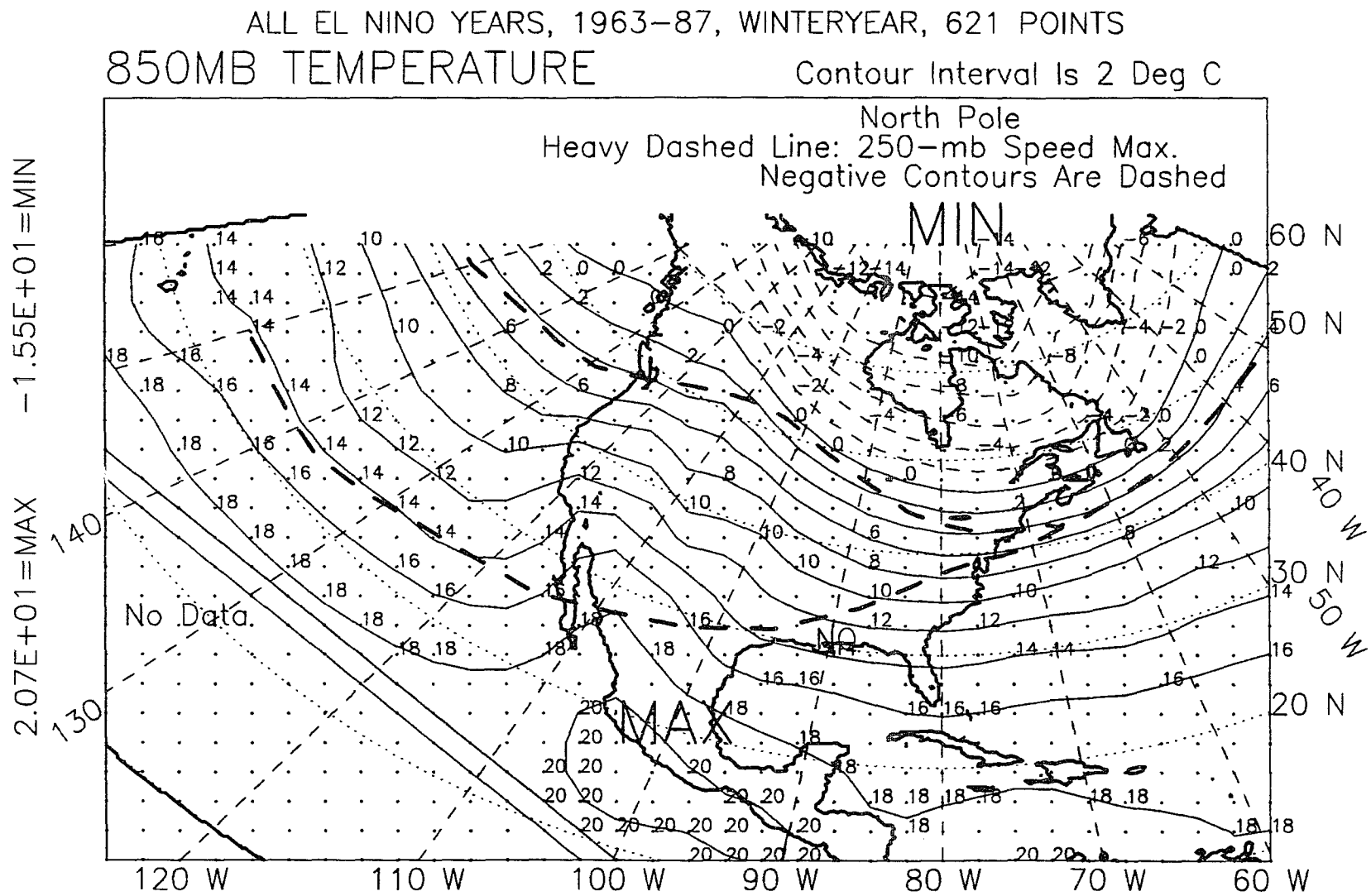

Figure D.16: 850–mb temperature, winter year, El Niño years, 1963–87.

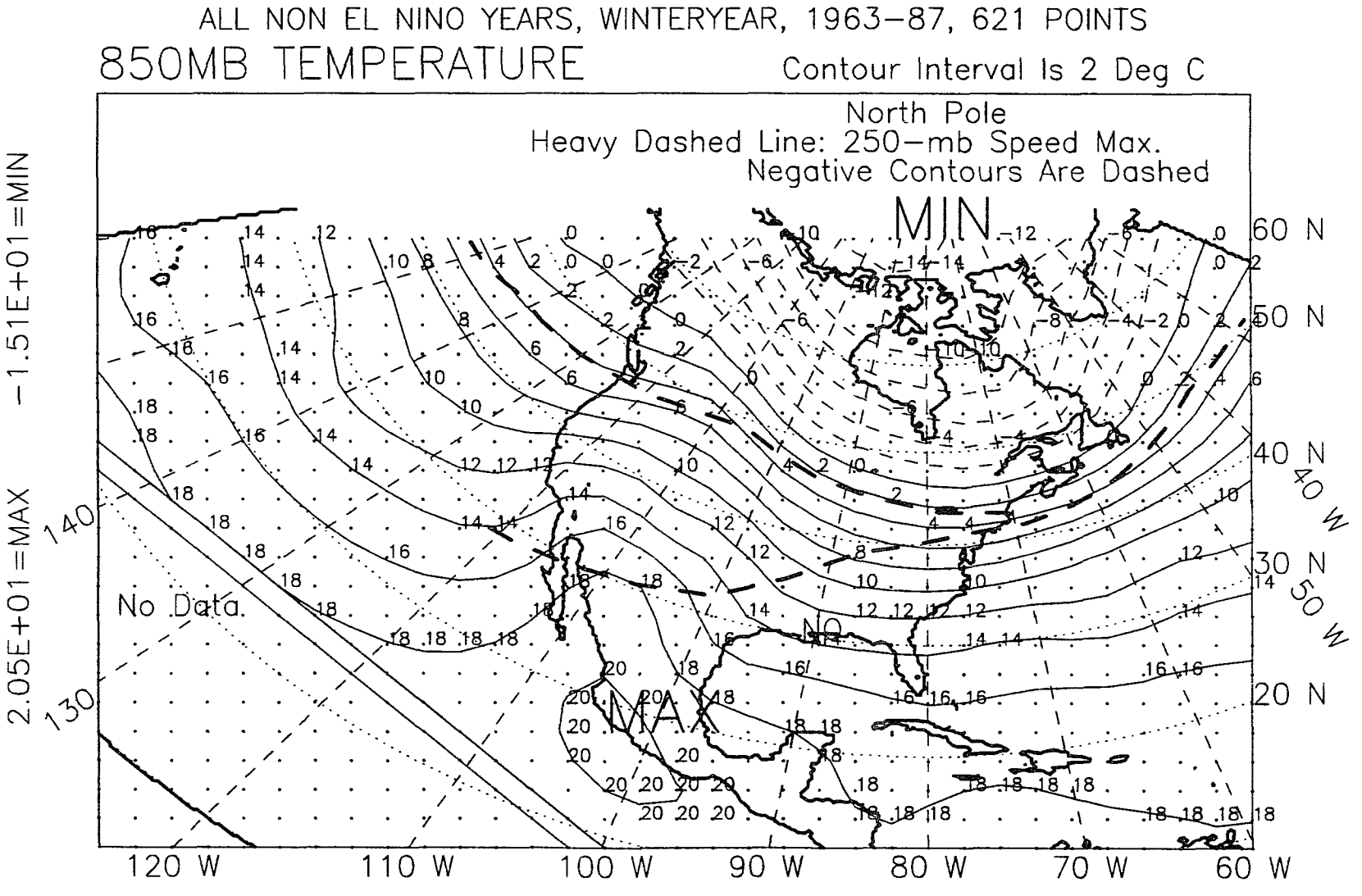

Figure D.17: 850–mb temperature, winter year, non–El Niño years, 1963–87.

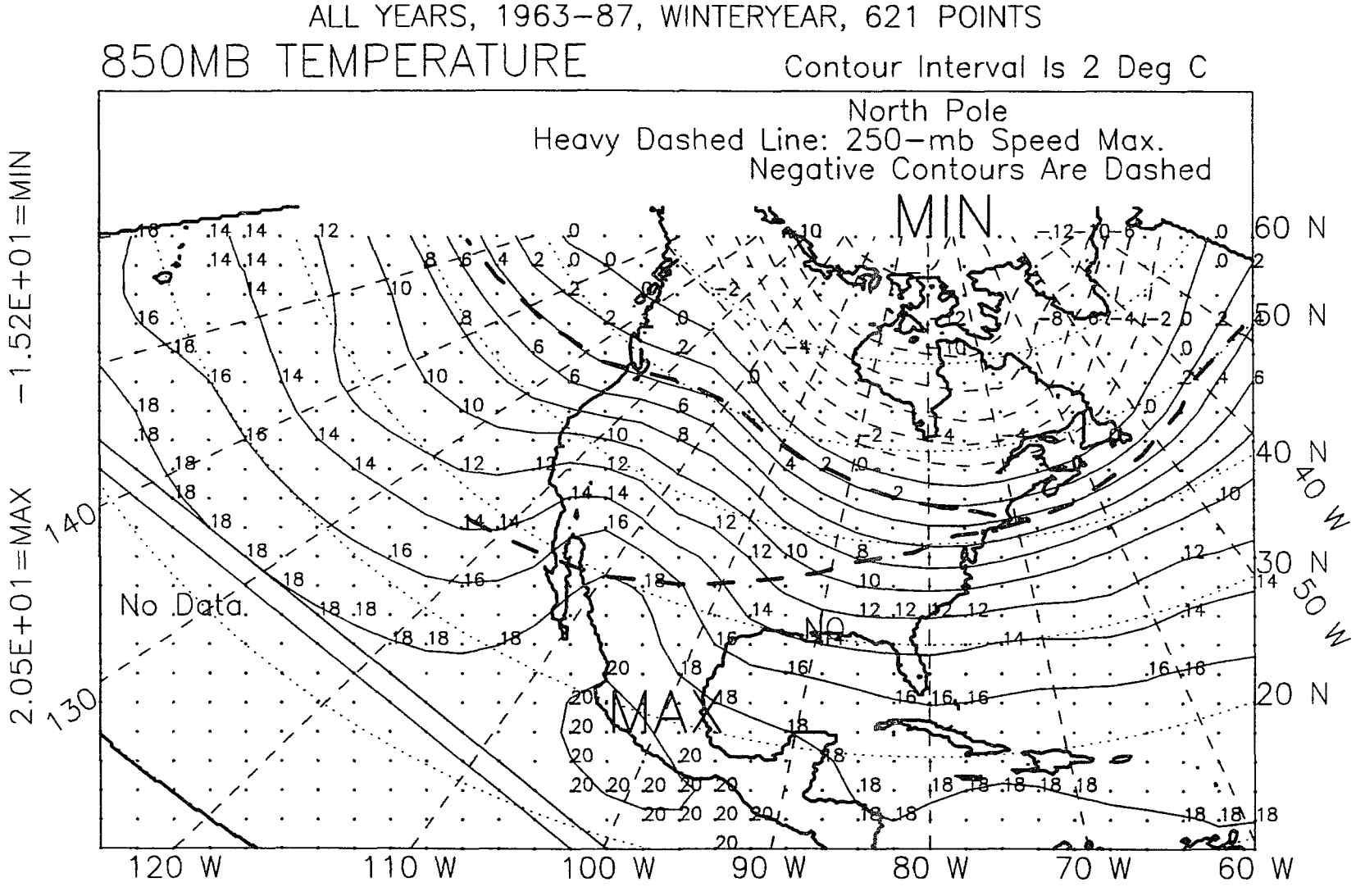

Figure D.18: 850–mb temperature, winter year, all years, 1963–87.

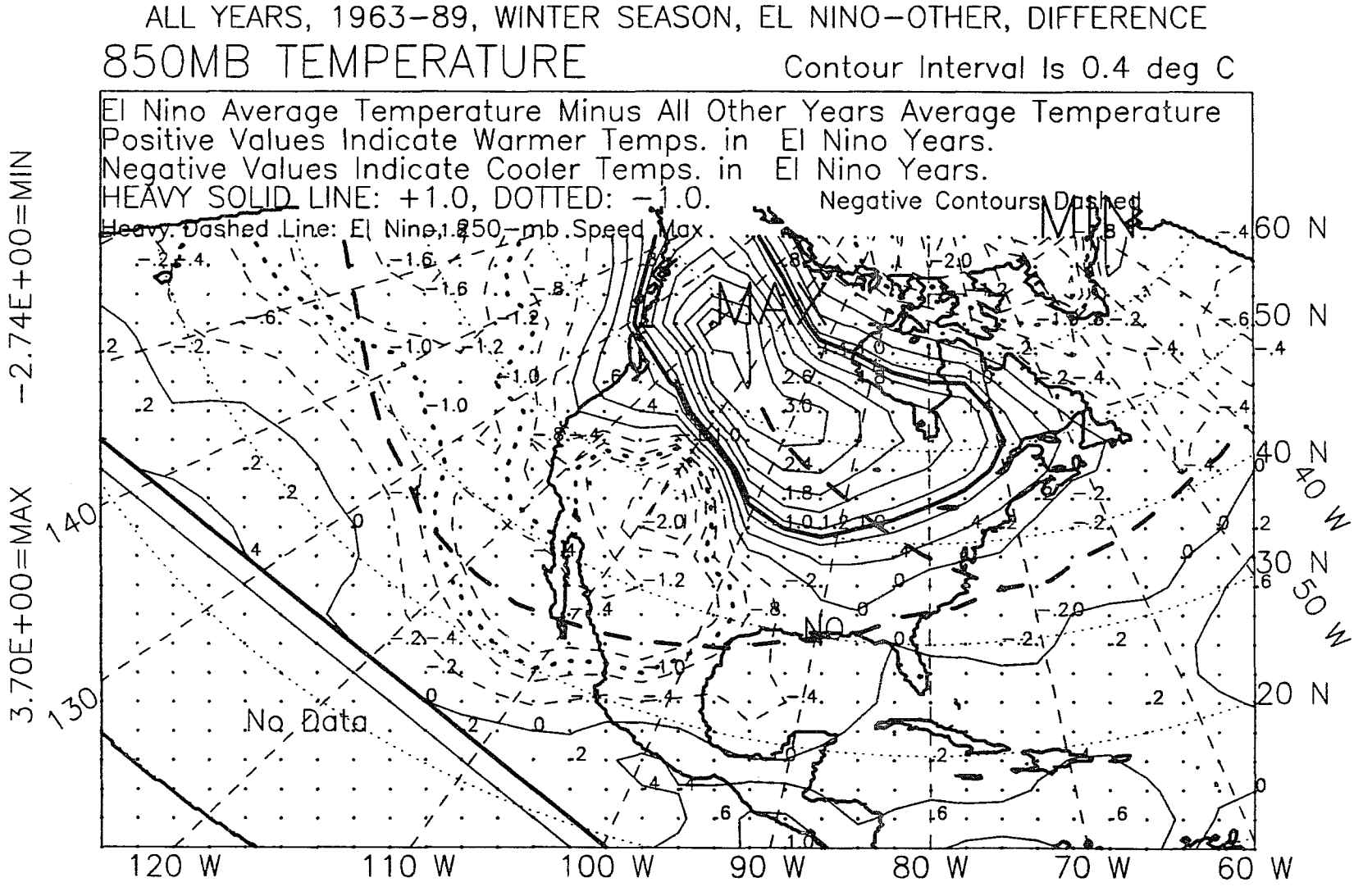

Figure D.19: 850–mb temperature, winter, 1963–89, difference.

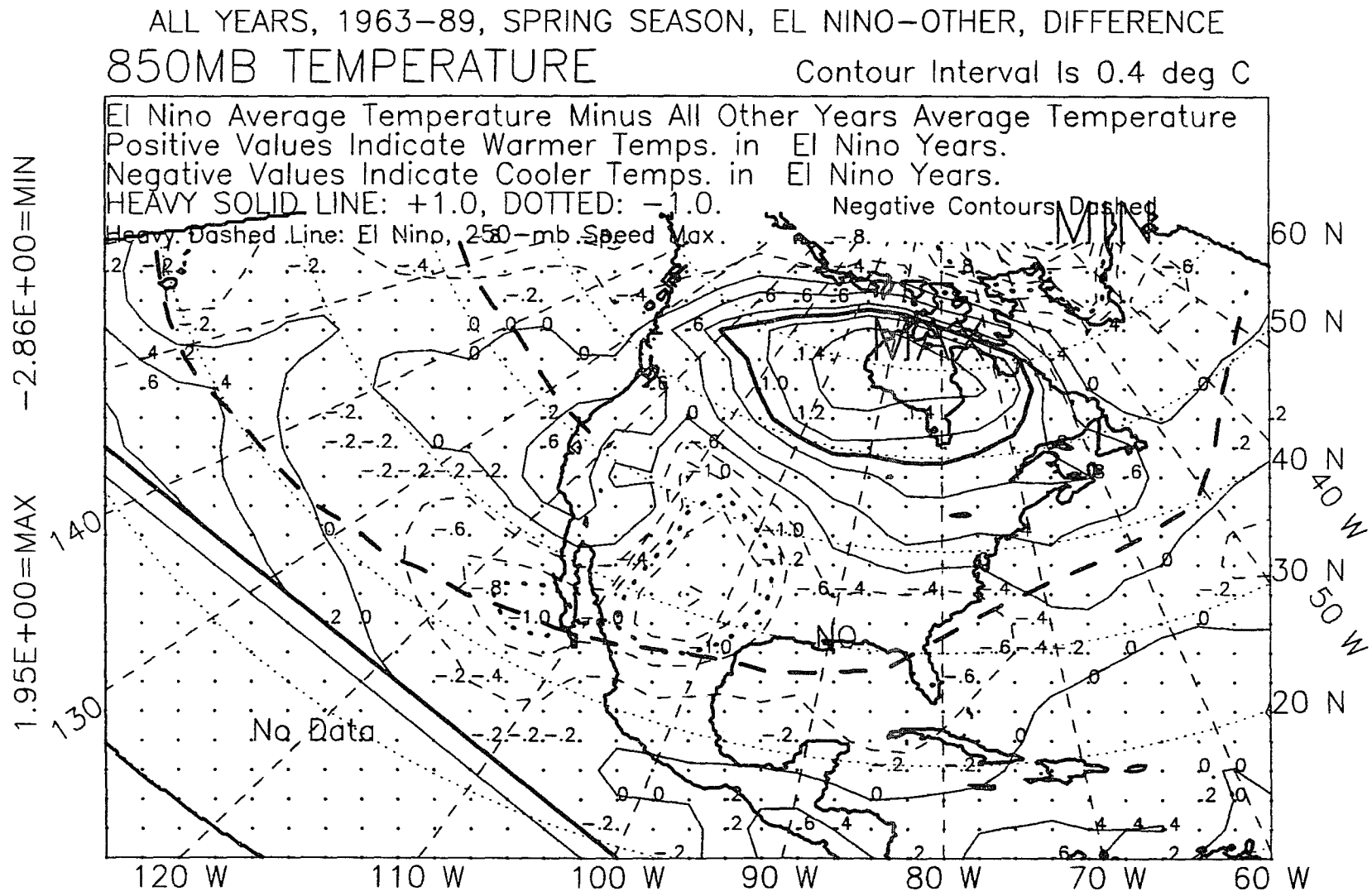

Figure D.20: 850–mb temperature, spring, 1963–89, difference.

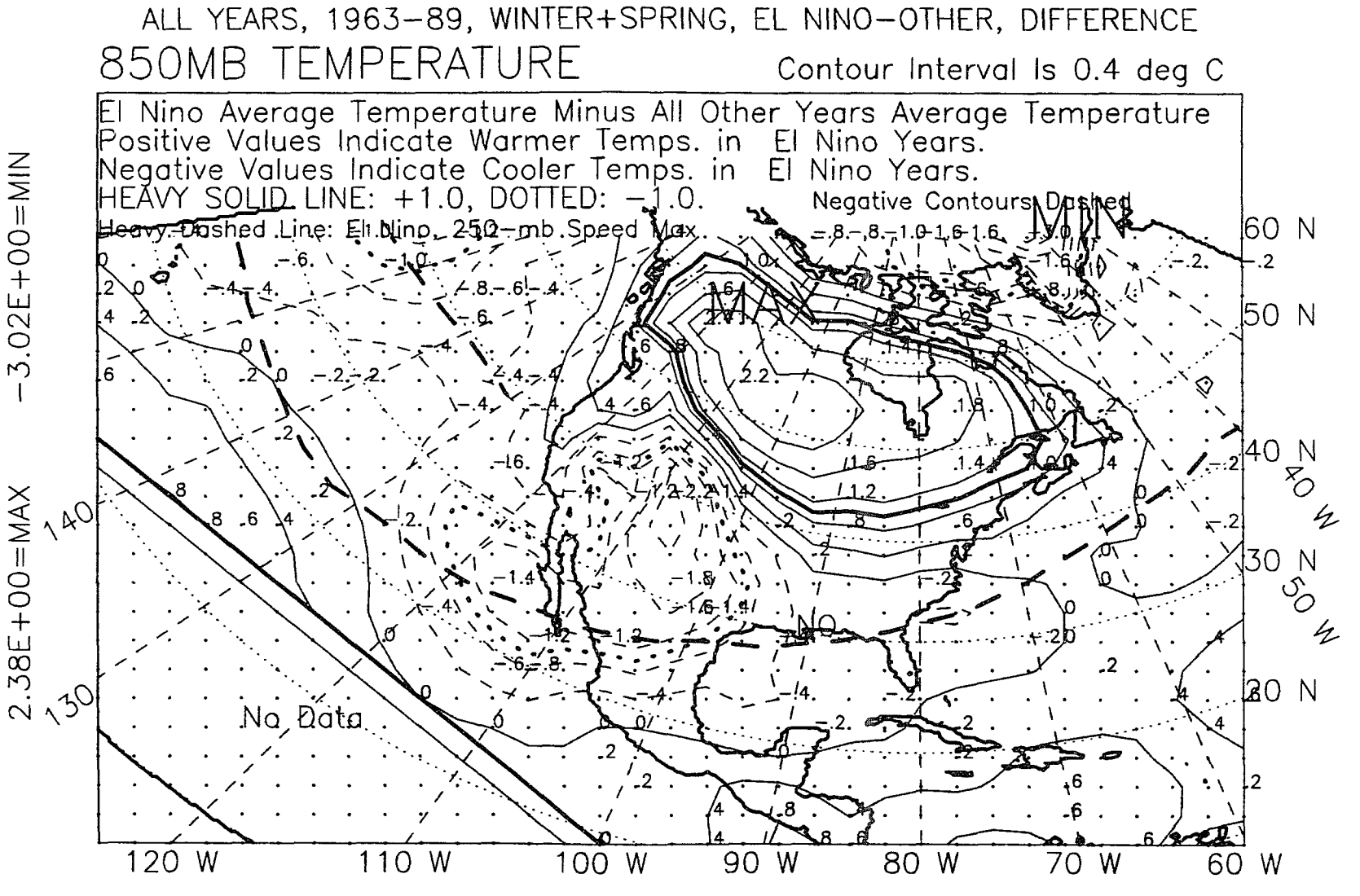

Figure D.21: 850–mb temperature, winter–plus–spring, 1963–89, difference.

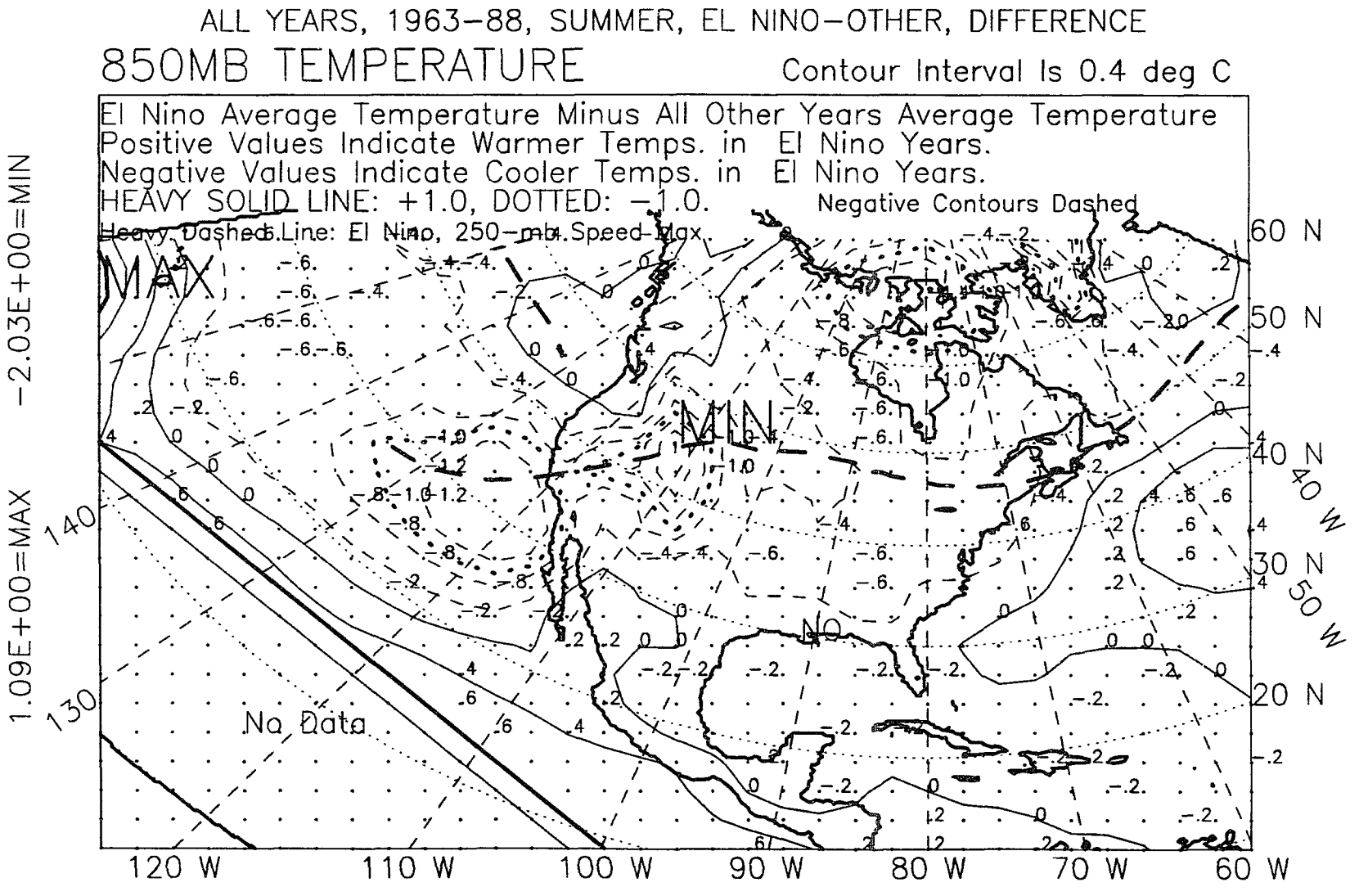

Figure D.22: 850–mb temperature, summer, 1963–88, difference.

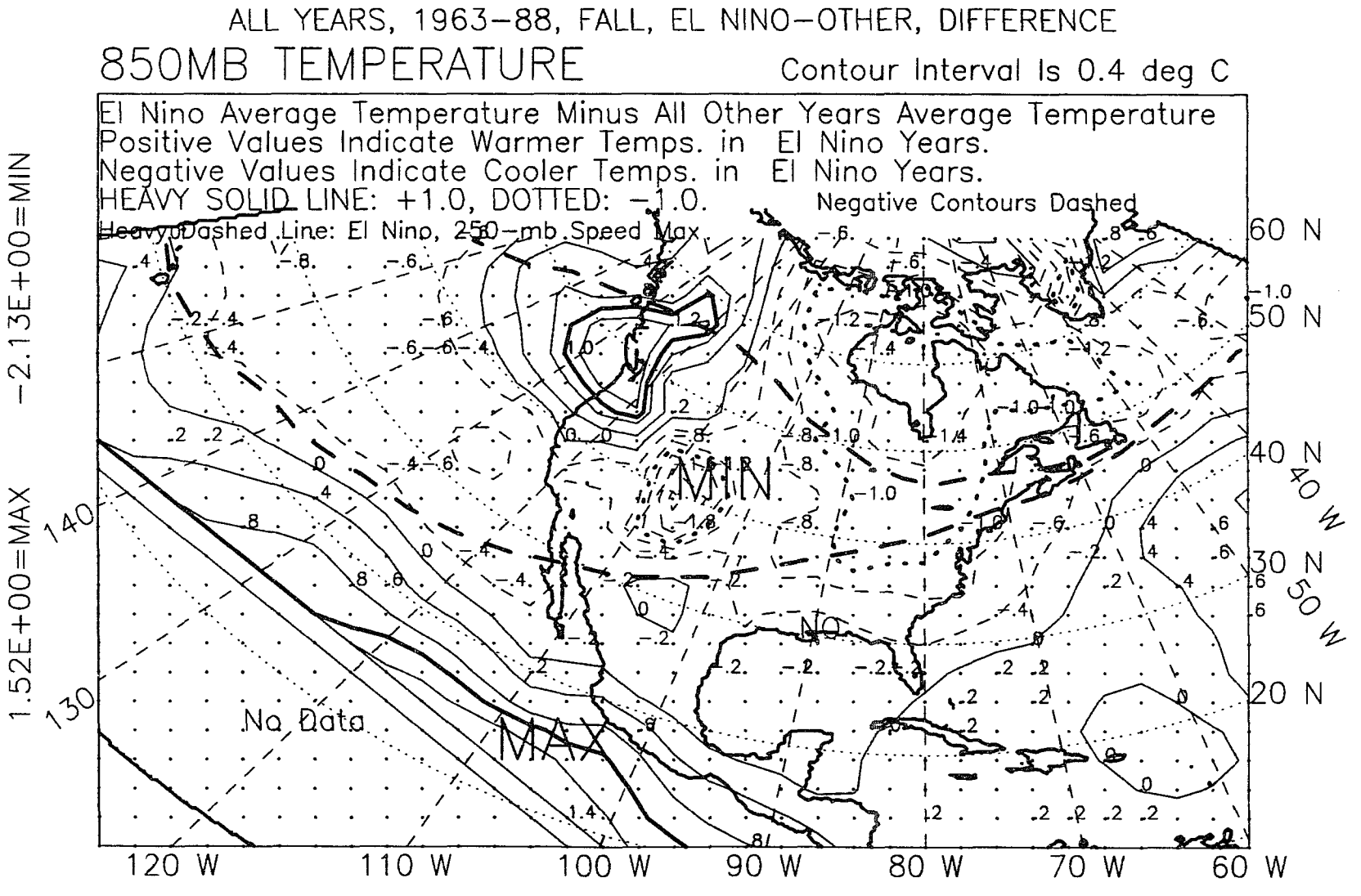

Figure D.23: 850–mb temperature, fall, 1963–88, difference.

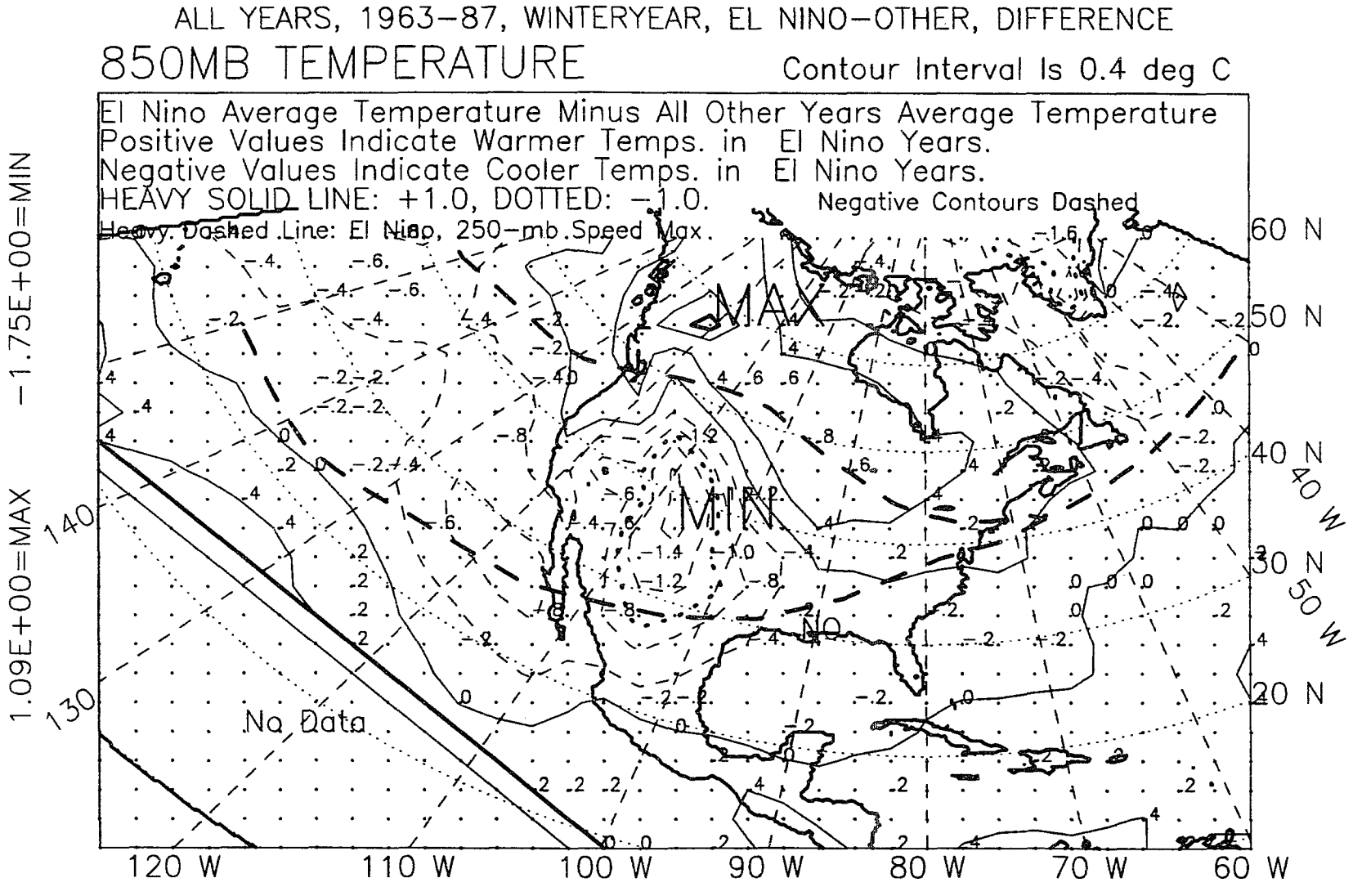

Figure D.24: 850–mb temperature, winter year, 1963–87, difference.

EFFECT OF THE EL NIÑO/SOUTHERN OSCILLATION ON GULF OF MEXICO, WINTER, FRONTAL-WAVE CYCLONES: 1960-89
VOLUME II

A Dissertation

Submitted to the Graduate Faculty of the
Louisiana State University and
Agricultural and Mechanical College
in partial fulfillment of the
requirements for the degree of
Doctor of Philosophy

in

The Department of Geology and Geophysics

by
Rosemary E. Manty
B.S., Wayne State University, 1977
M.S., Louisiana State University, 1981
May 1993

APPENDIX E
850-MB DIVERGENCE FIELD

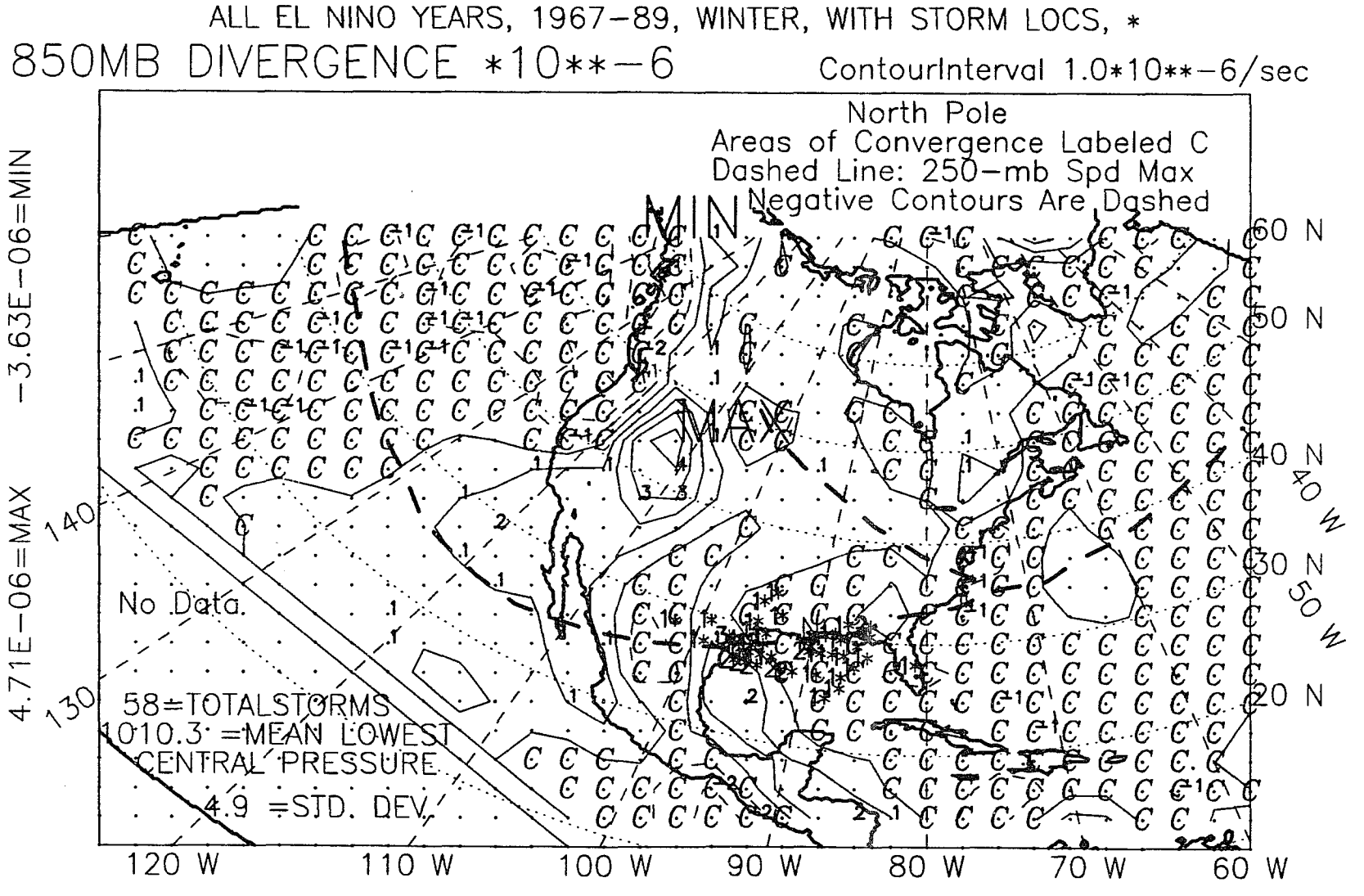

Figure E.1: 850–mb divergence, winter, El Niño years, 1967–89.

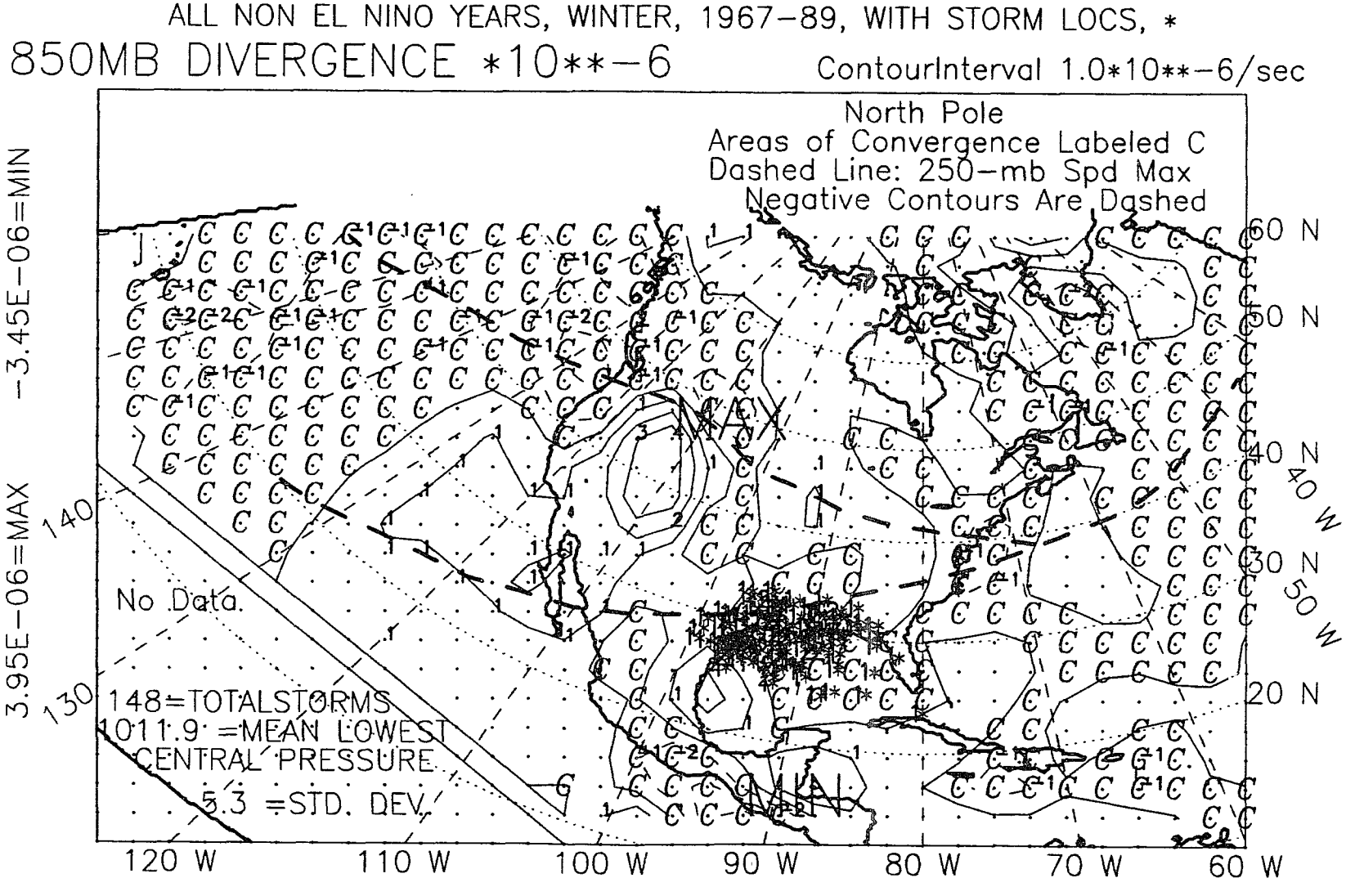

Figure E.2: 850–mb divergence, winter, non–El Niño years, 1967–89.

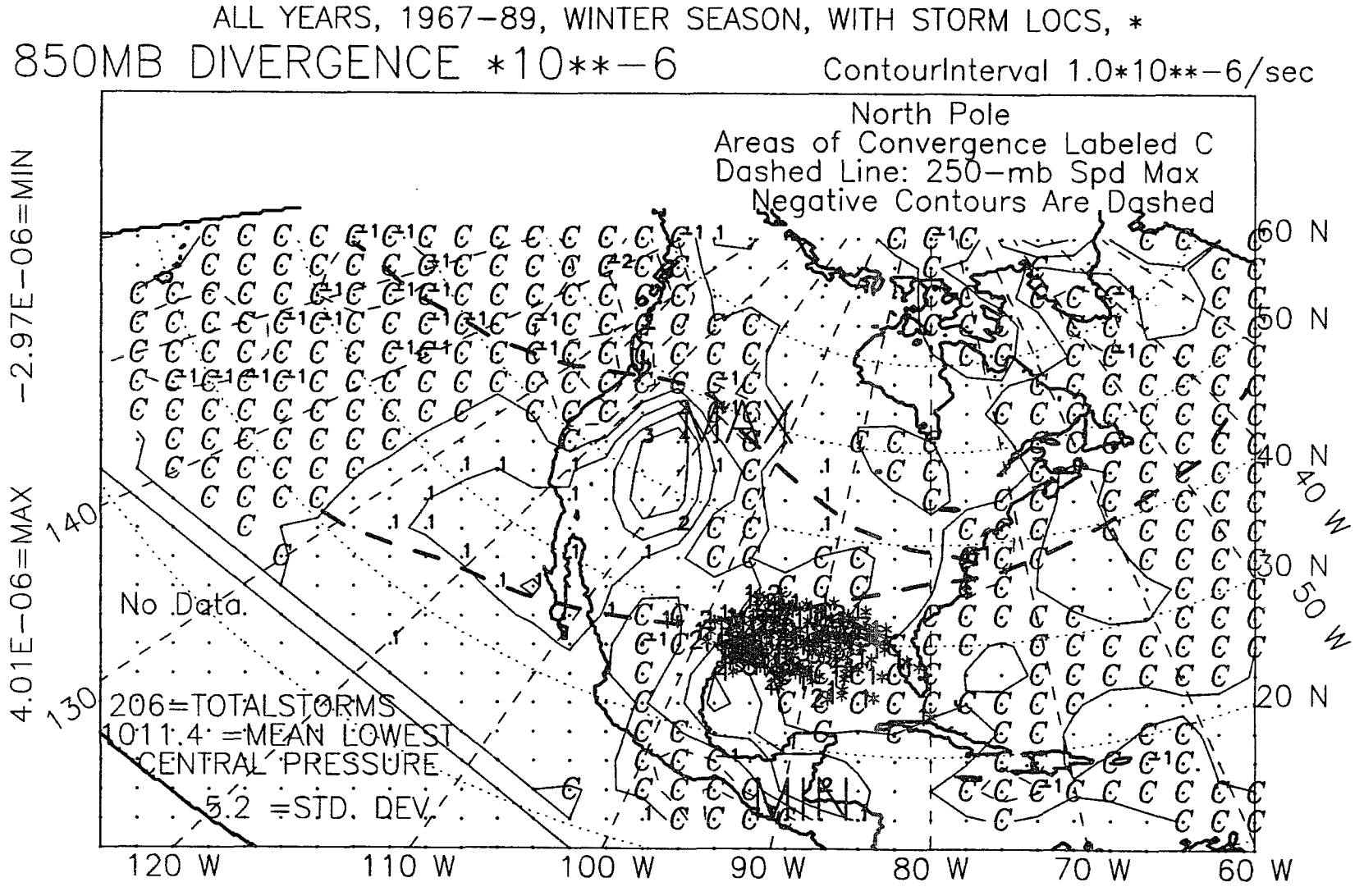

Figure E.3: 850–mb divergence, winter, all years, 1967–89.

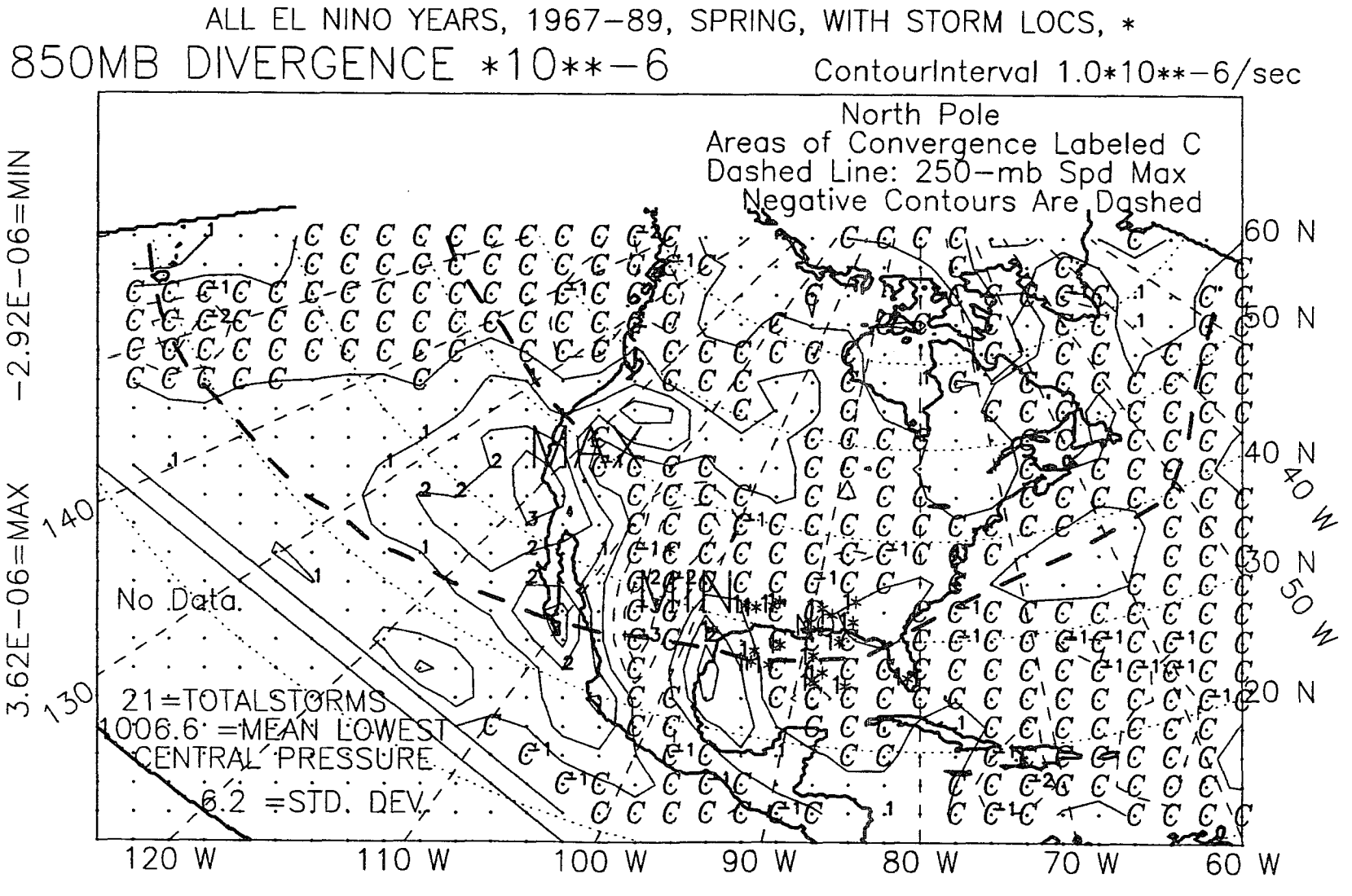

Figure E.4: 850–mb divergence, spring, El Niño years, 1967–89.

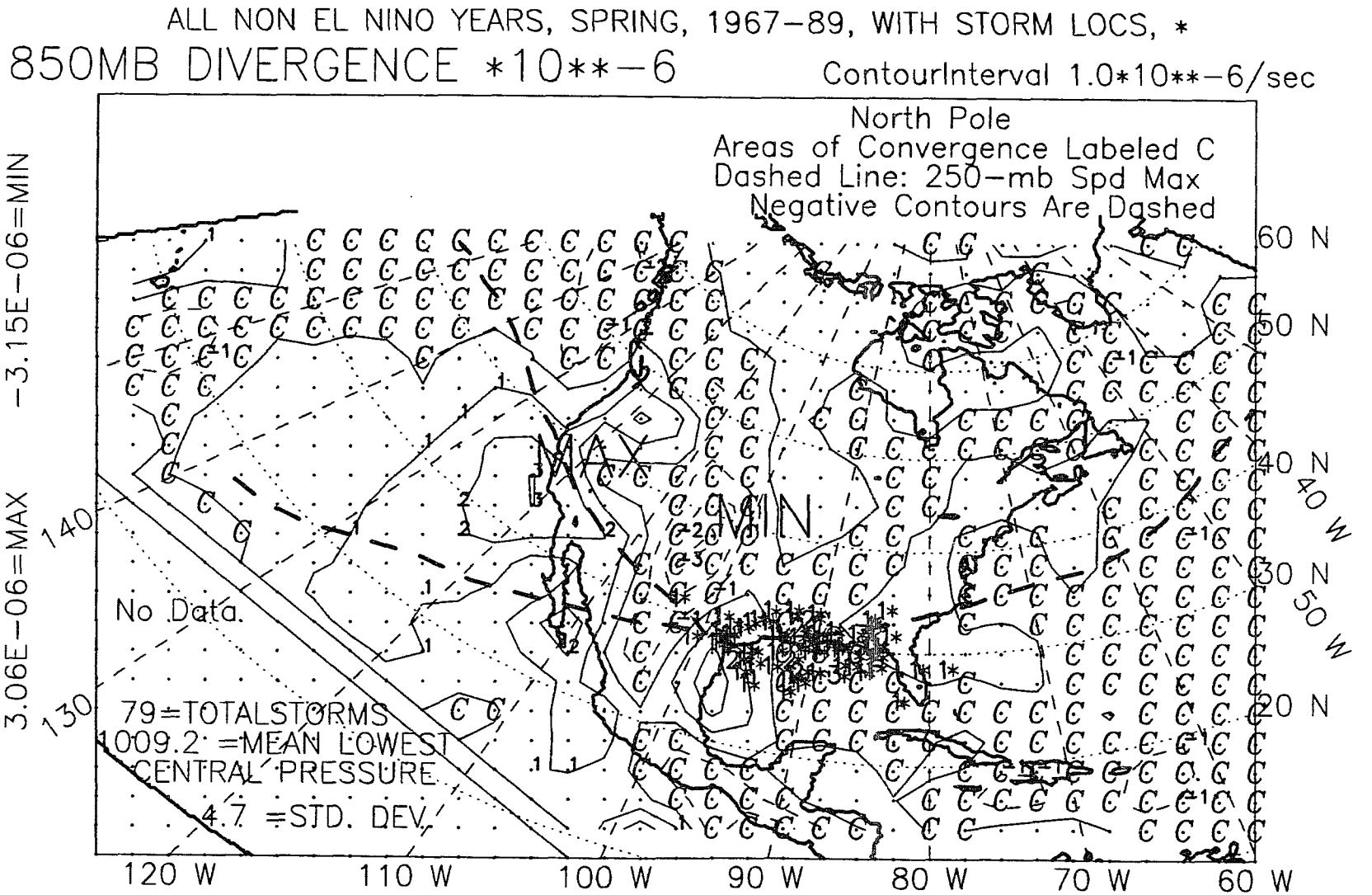

Figure E.5: 850–mb divergence, spring, non–El Niño years, 1967–89.

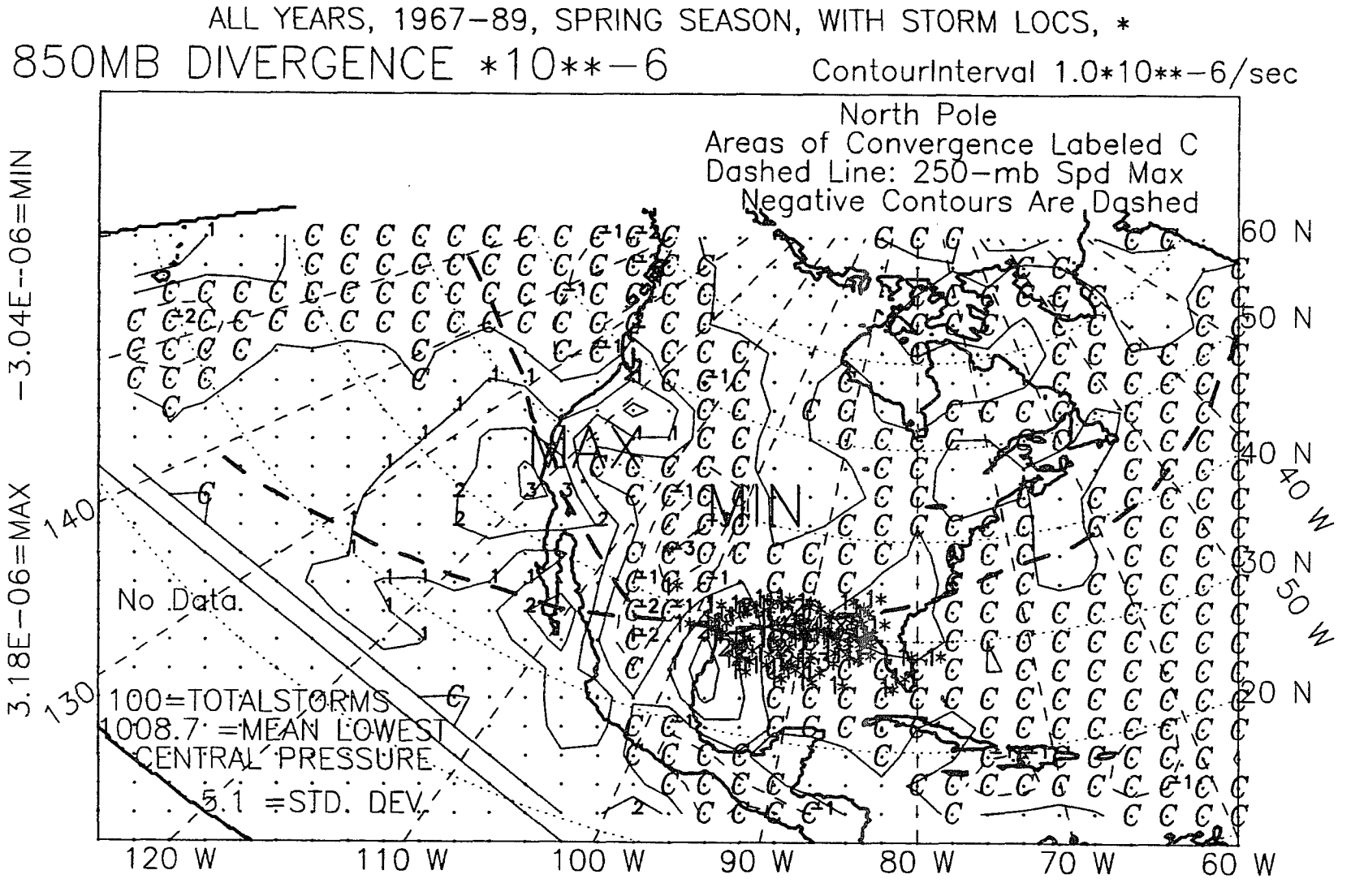

Figure E.6: 850–mb divergence, spring, all years, 1967–89.

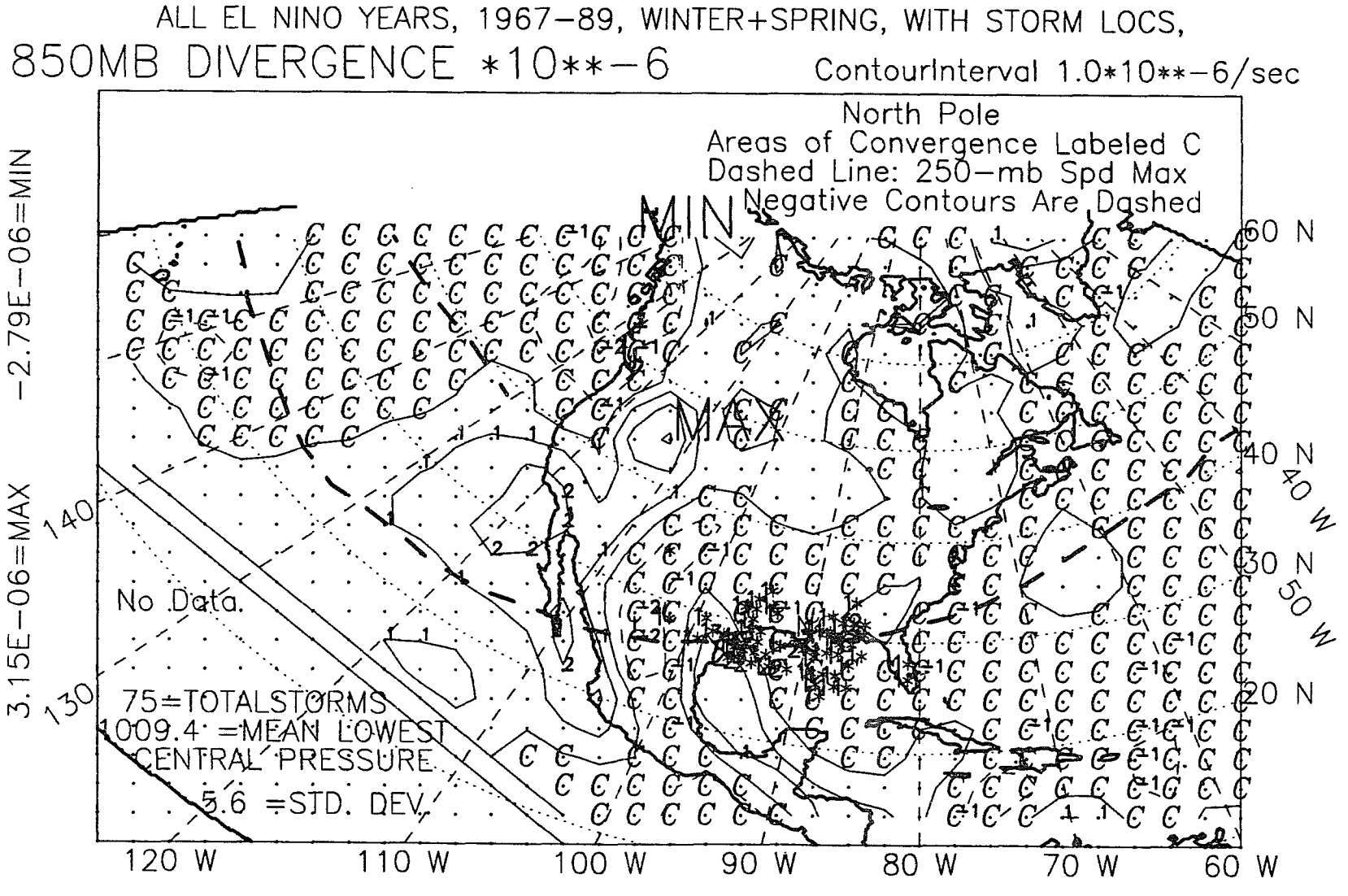

Figure E.7: 850–mb divergence, winter–plus–spring, El Niño years, 1967–89.

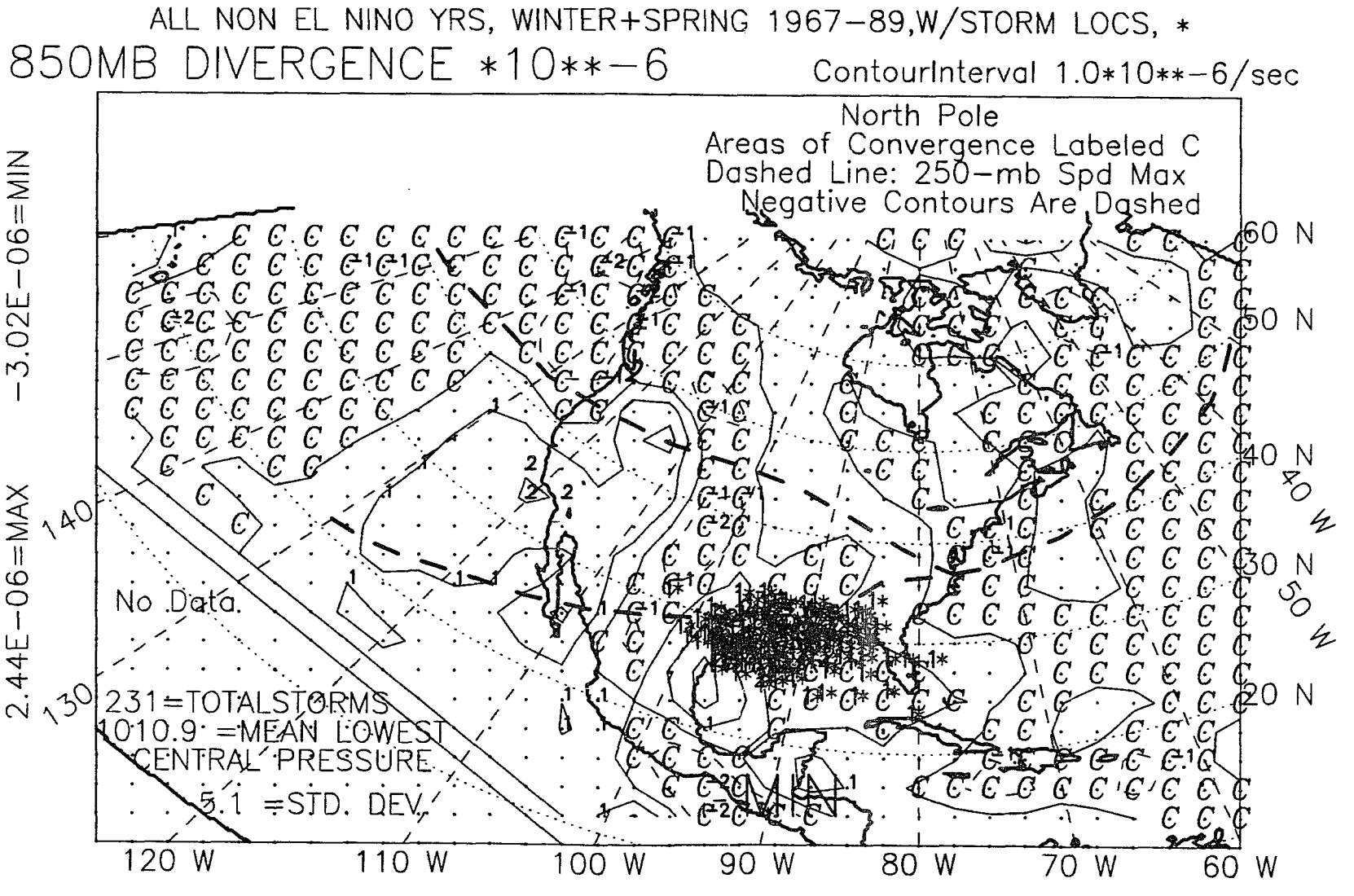

Figure E.8: 850-mb divergence, winter-plus-spring, non-El Niño years, 1967-89.

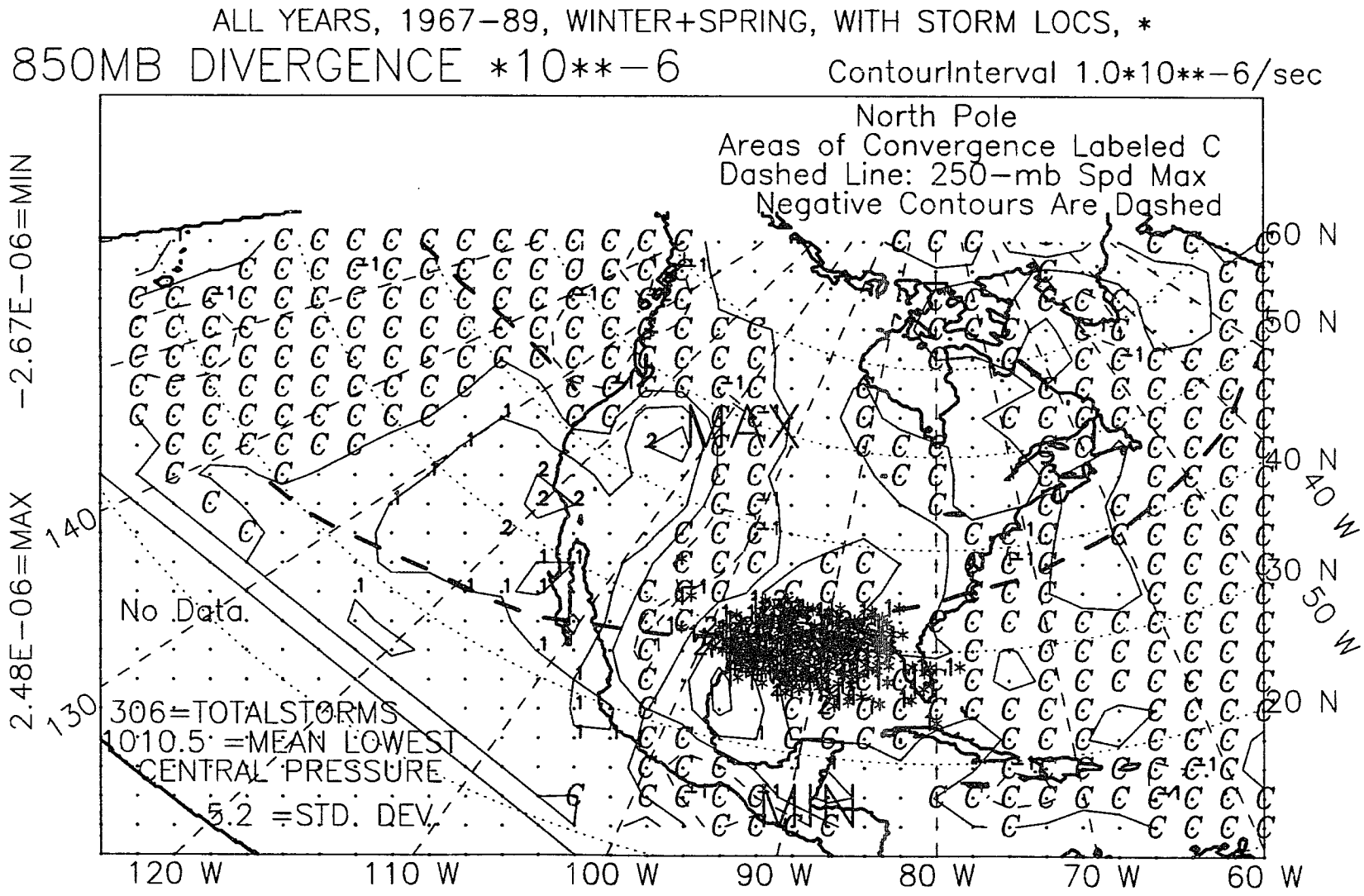

Figure E.9: 850–mb divergence, winter–plus–spring, all years, 1967–89.

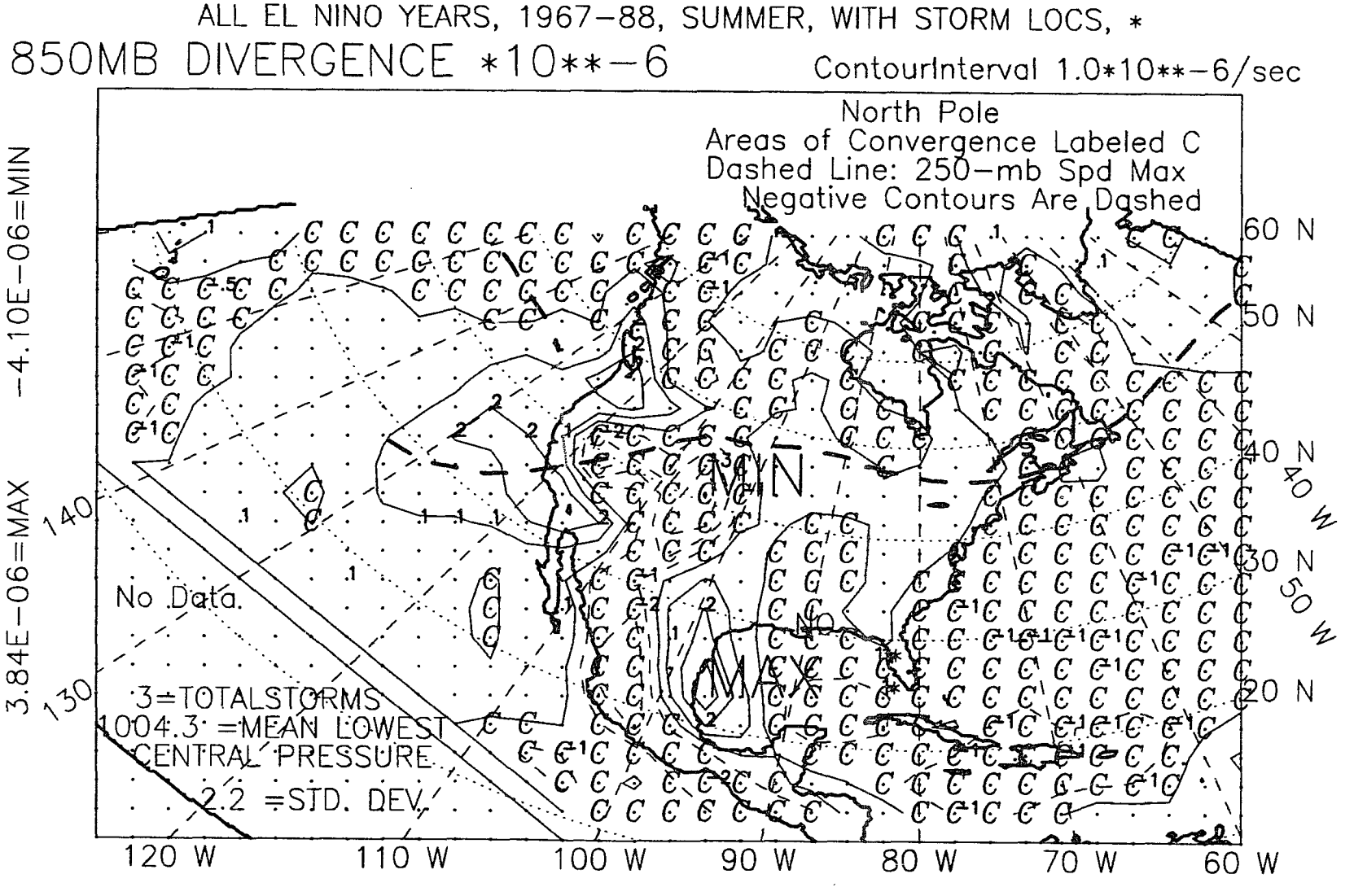

Figure E.10: 850–mb divergence, summer, El Niño years, 1967–88.

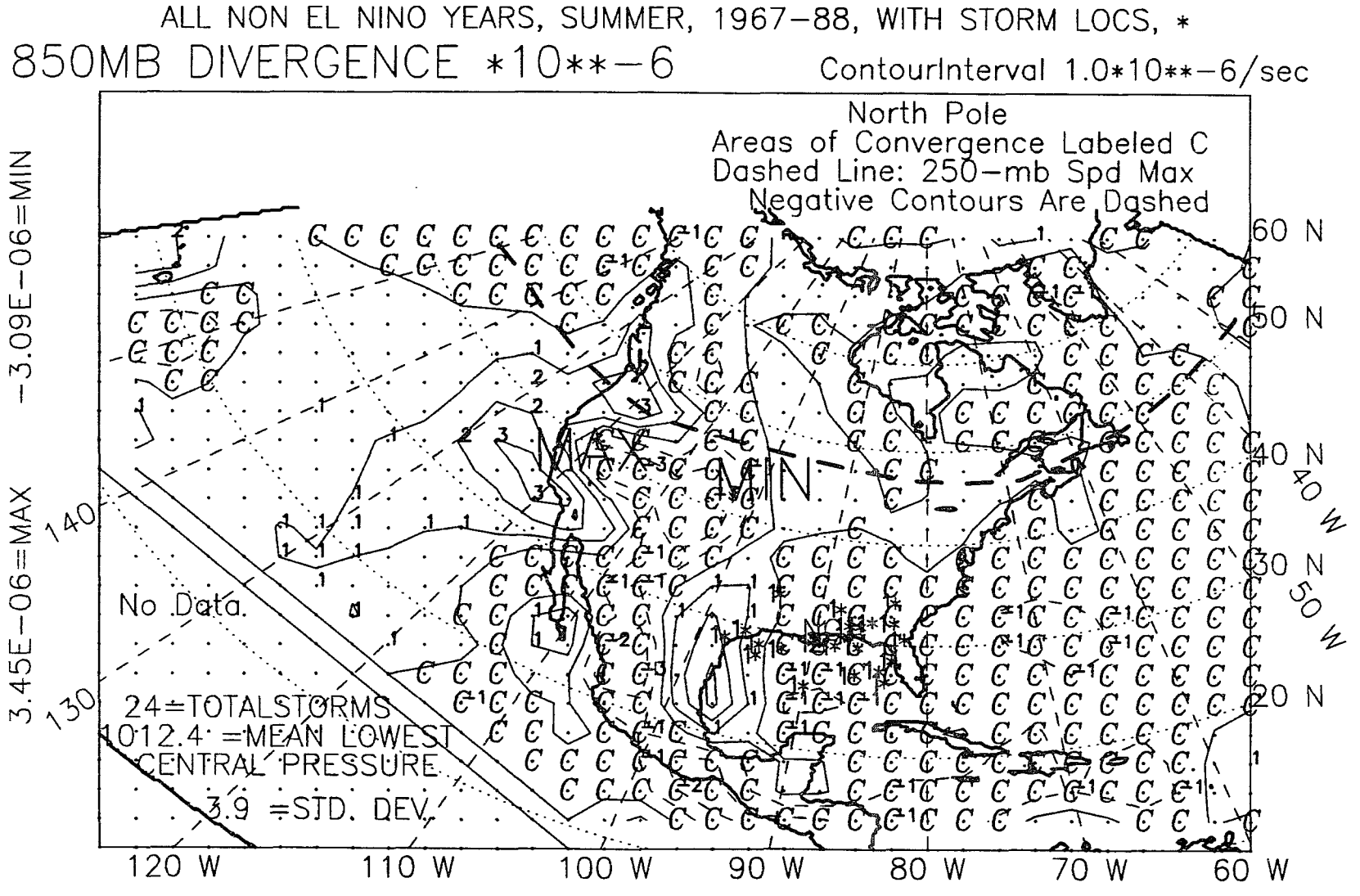

Figure E.11: 850-mb divergence, summer, non-El Niño years, 1967-88.

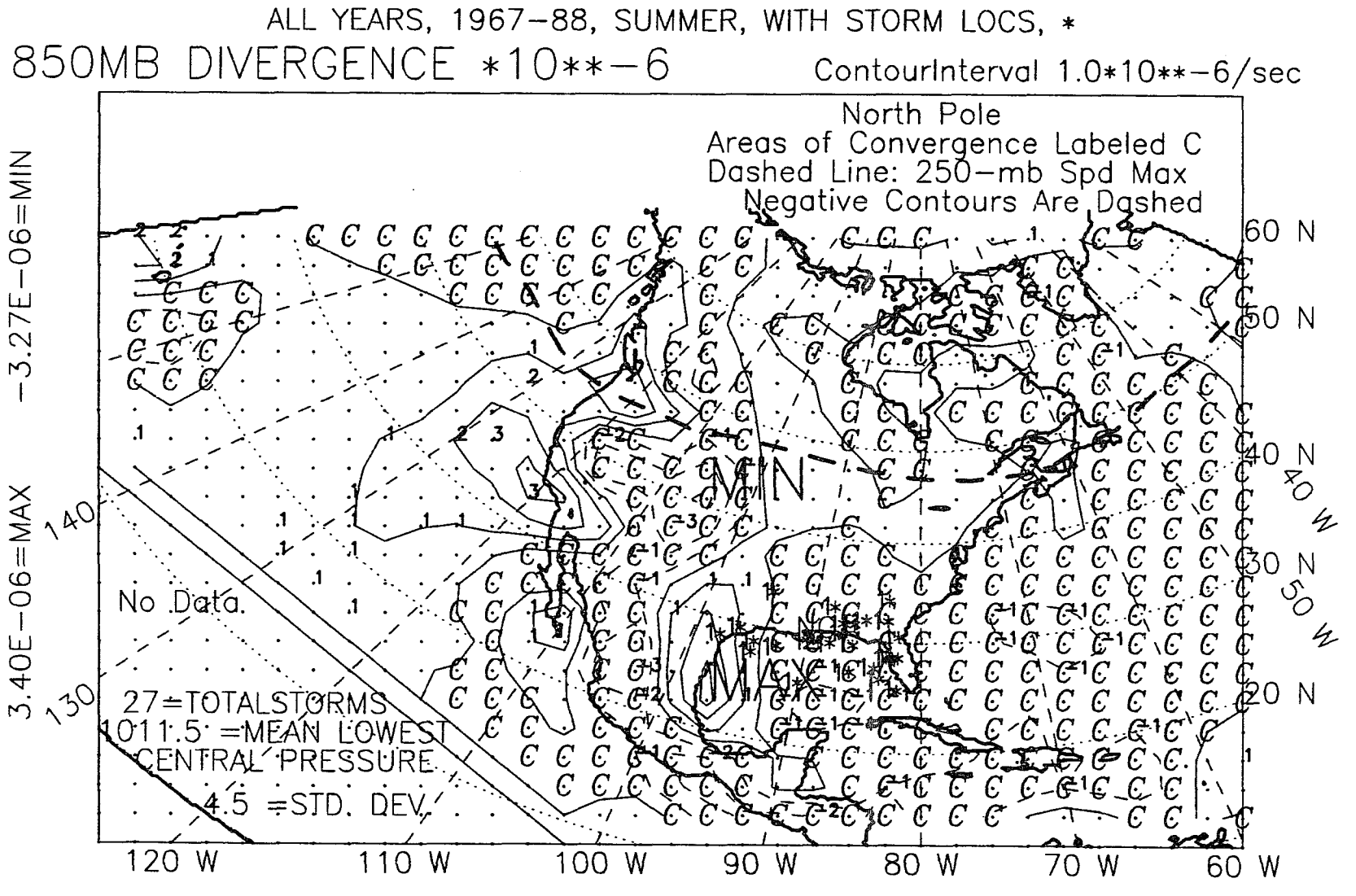

Figure E.12: 850–mb divergence, summer, all years, 1967–88.

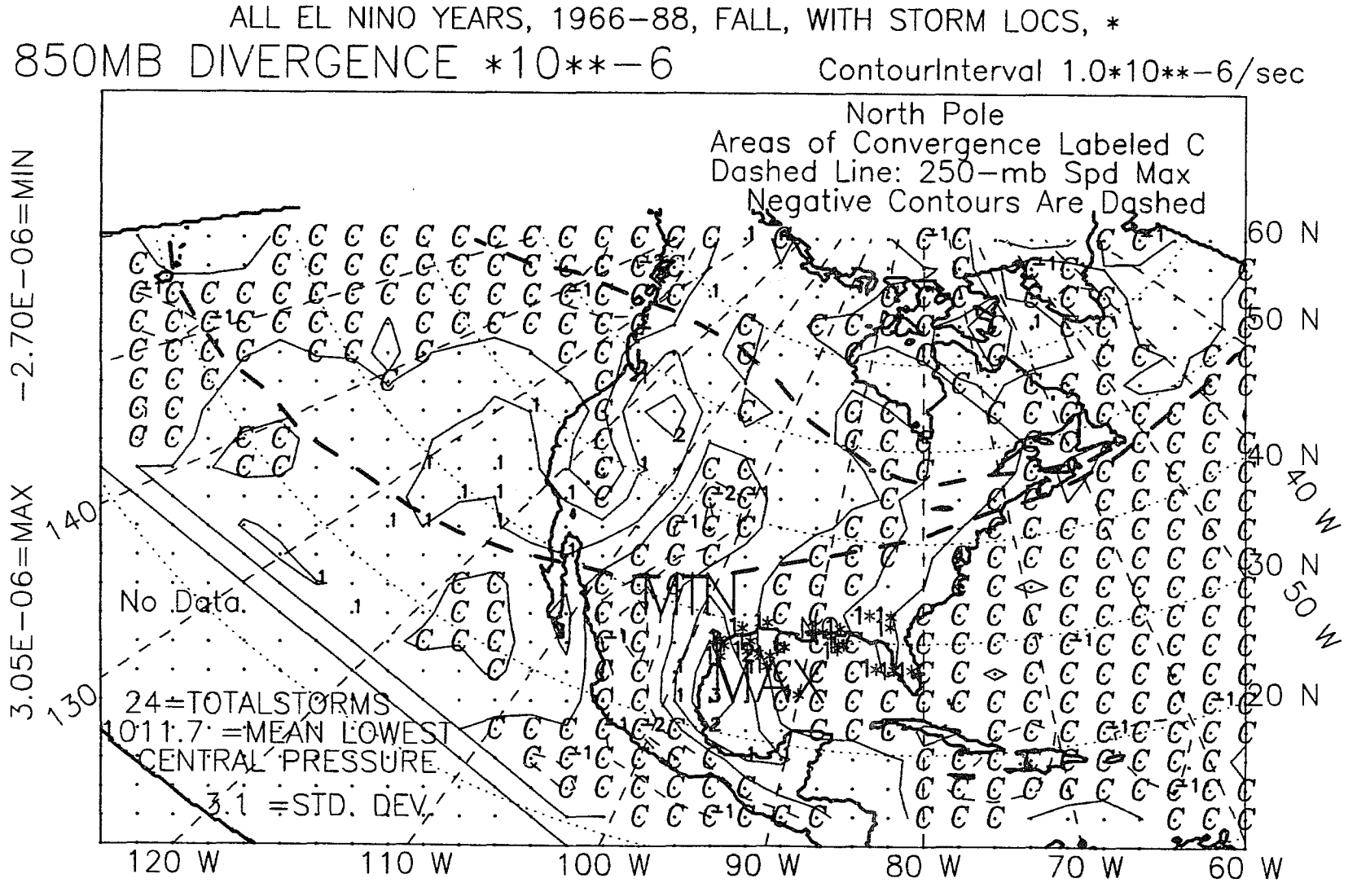

Figure E.13: 850–mb divergence, fall, El Niño years, 1966–88.

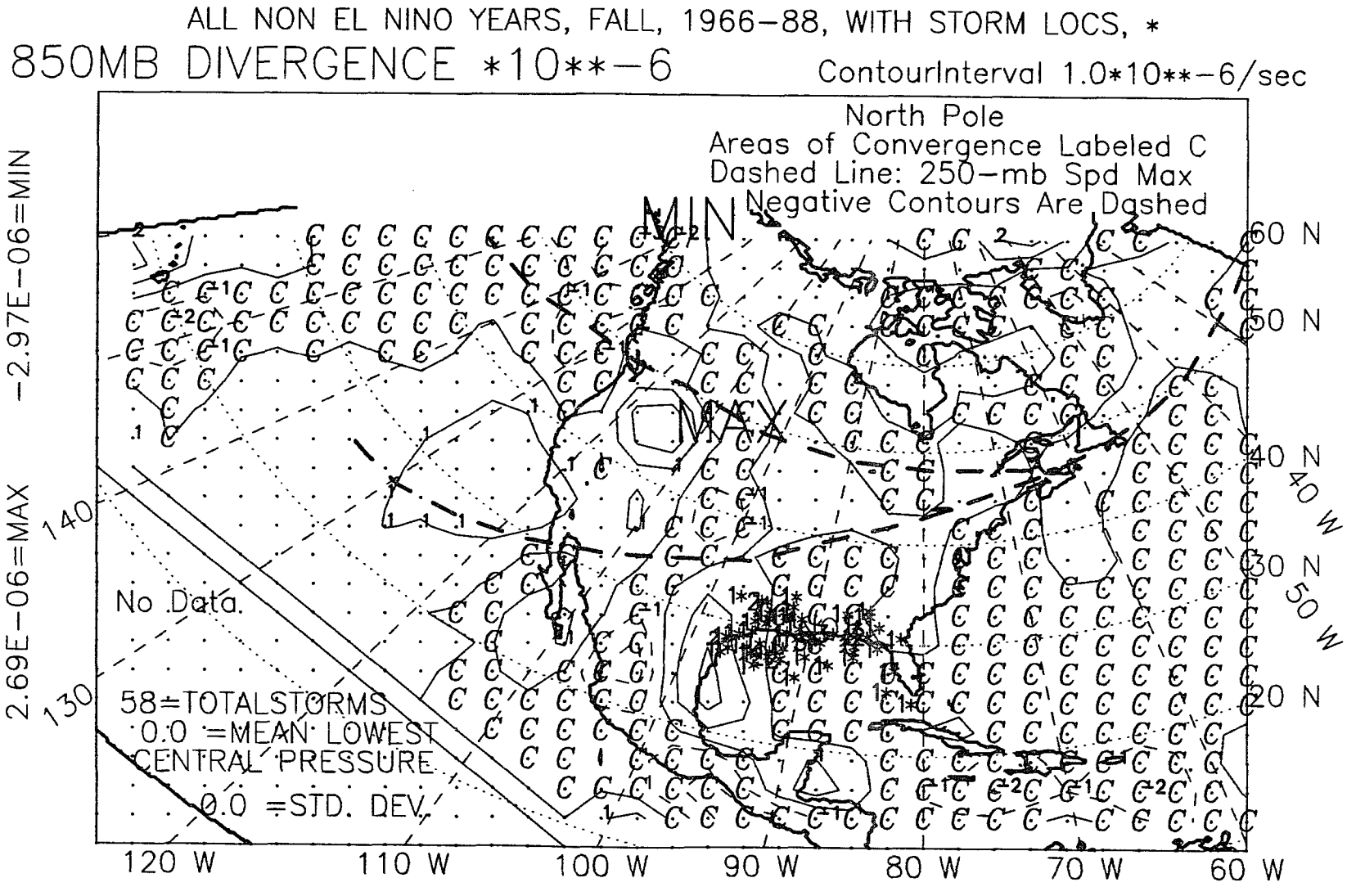

Figure E.14: 850–mb divergence, fall, non–El Niño years, 1966–88.

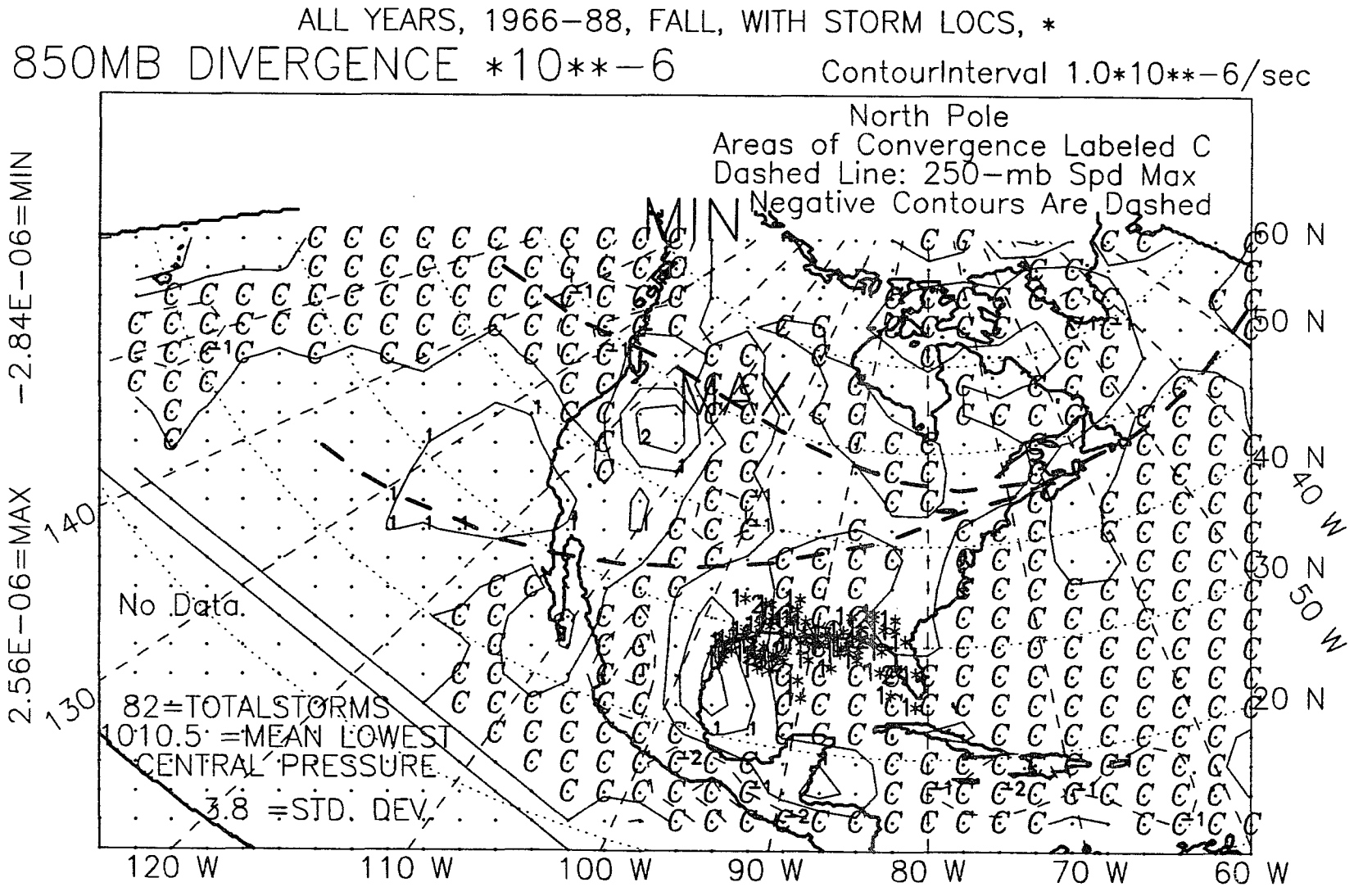

Figure E.15: 850–mb divergence, fall, all years, 1966–88.

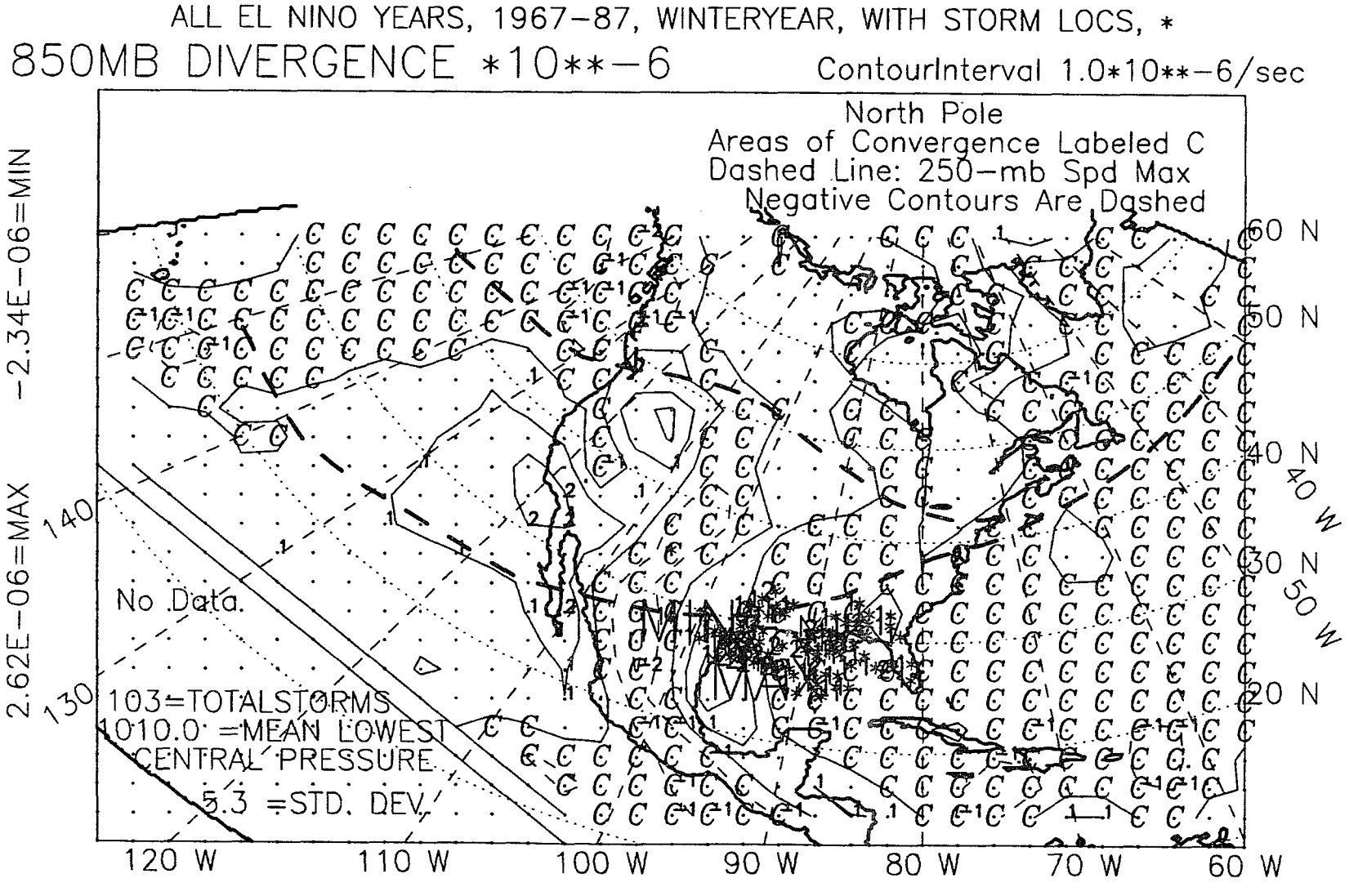

Figure E.16: 850-mb divergence, winter year, El Niño years, 1967-87.

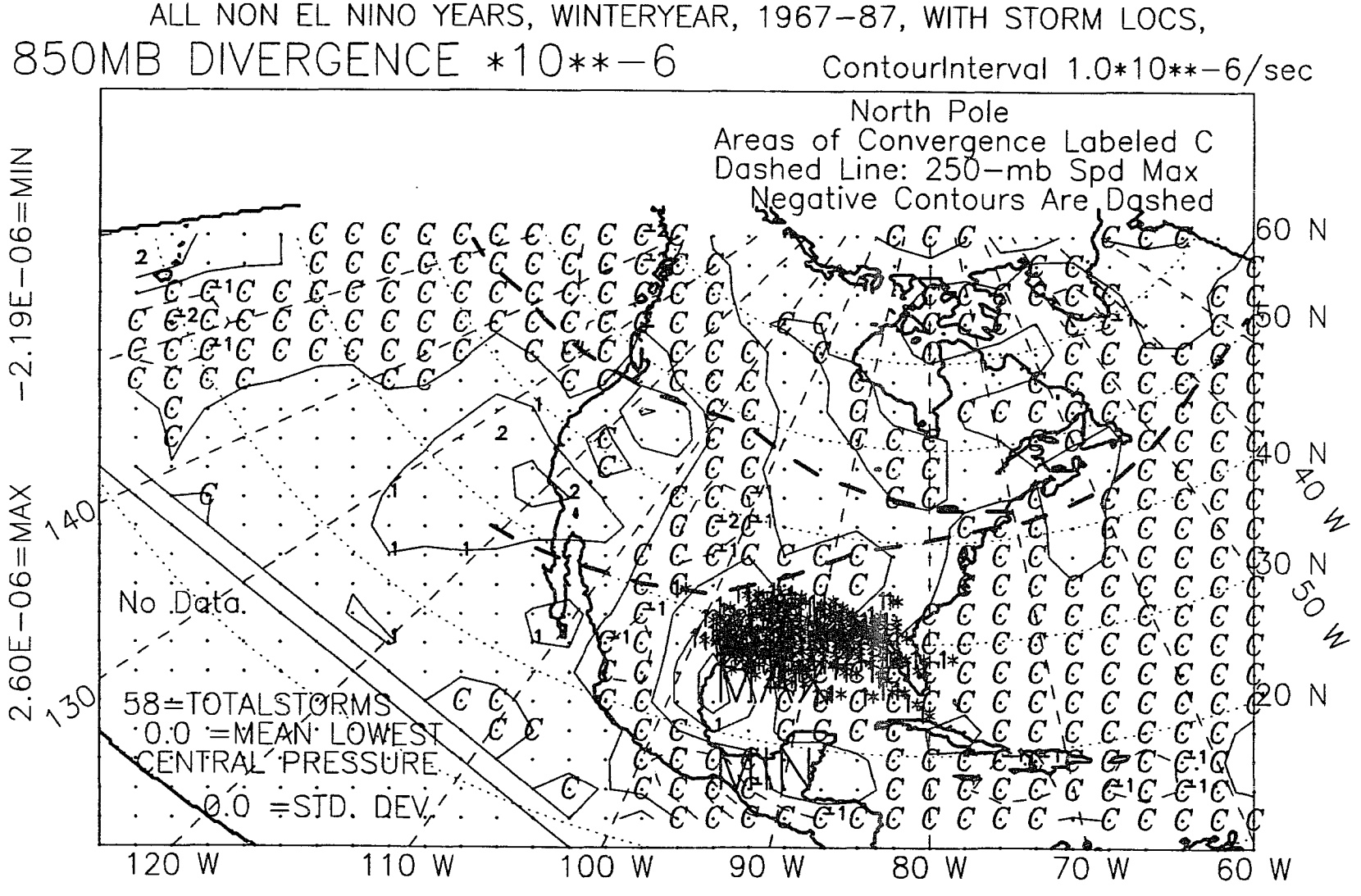

Figure E.17: 850–mb divergence, winter year, non–El Niño years, 1967–87.

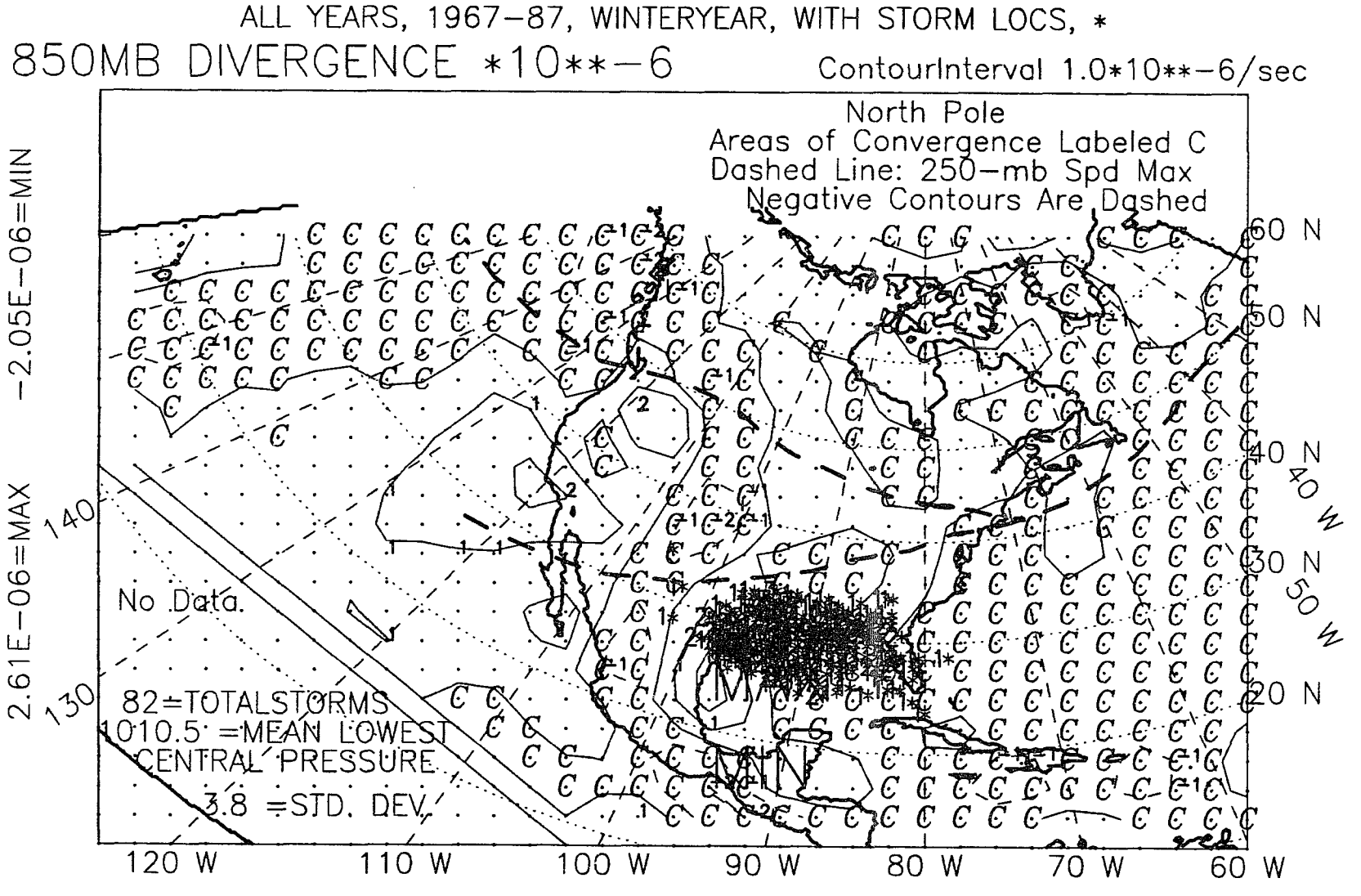

Figure E.18: 850–mb divergence, winter year, all years, 1967–87.

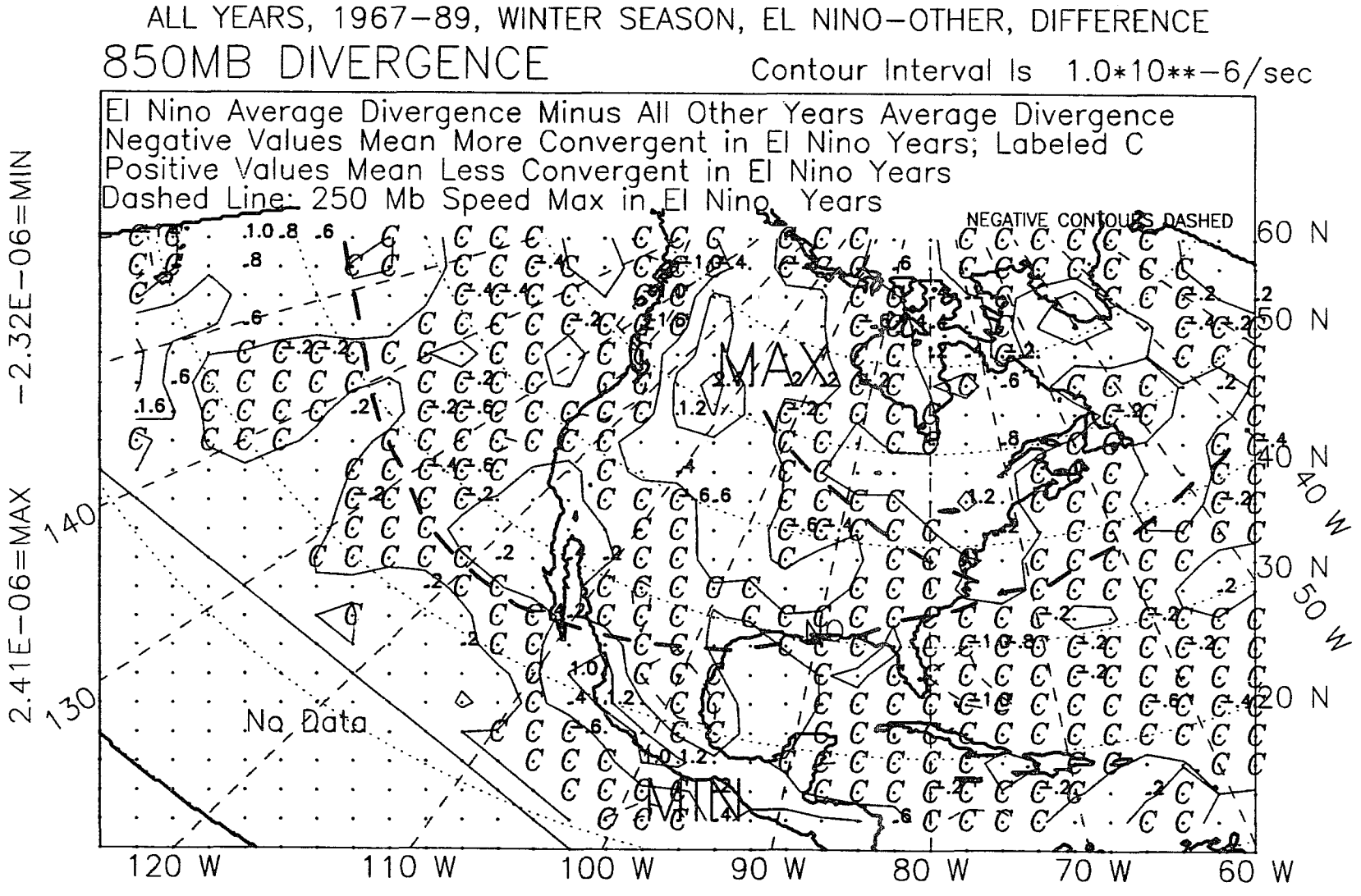

Figure E.19: 850–mb divergence, winter, 1967–89, difference.

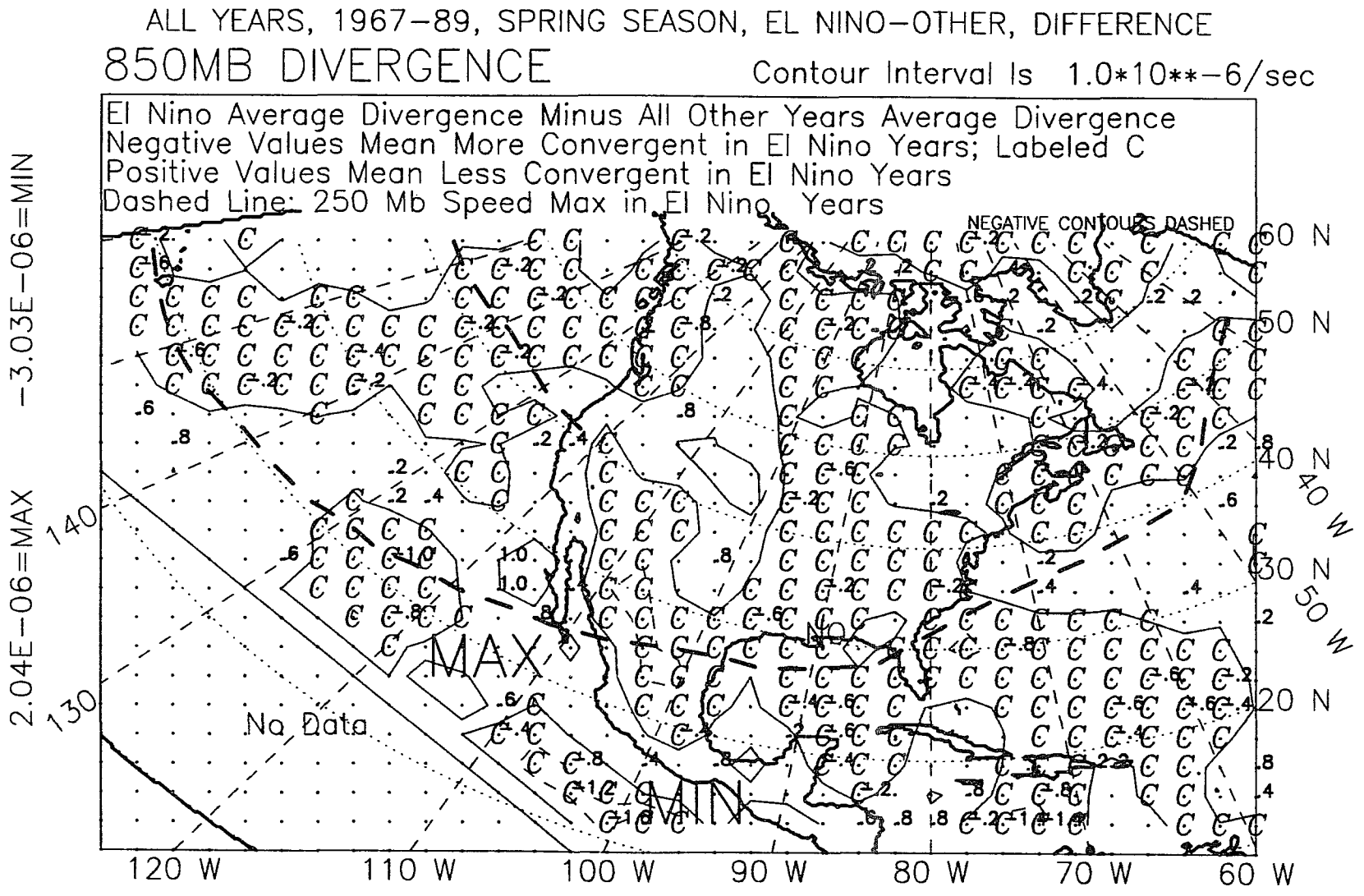

Figure E.20: 850–mb divergence, spring, 1967–89, difference.

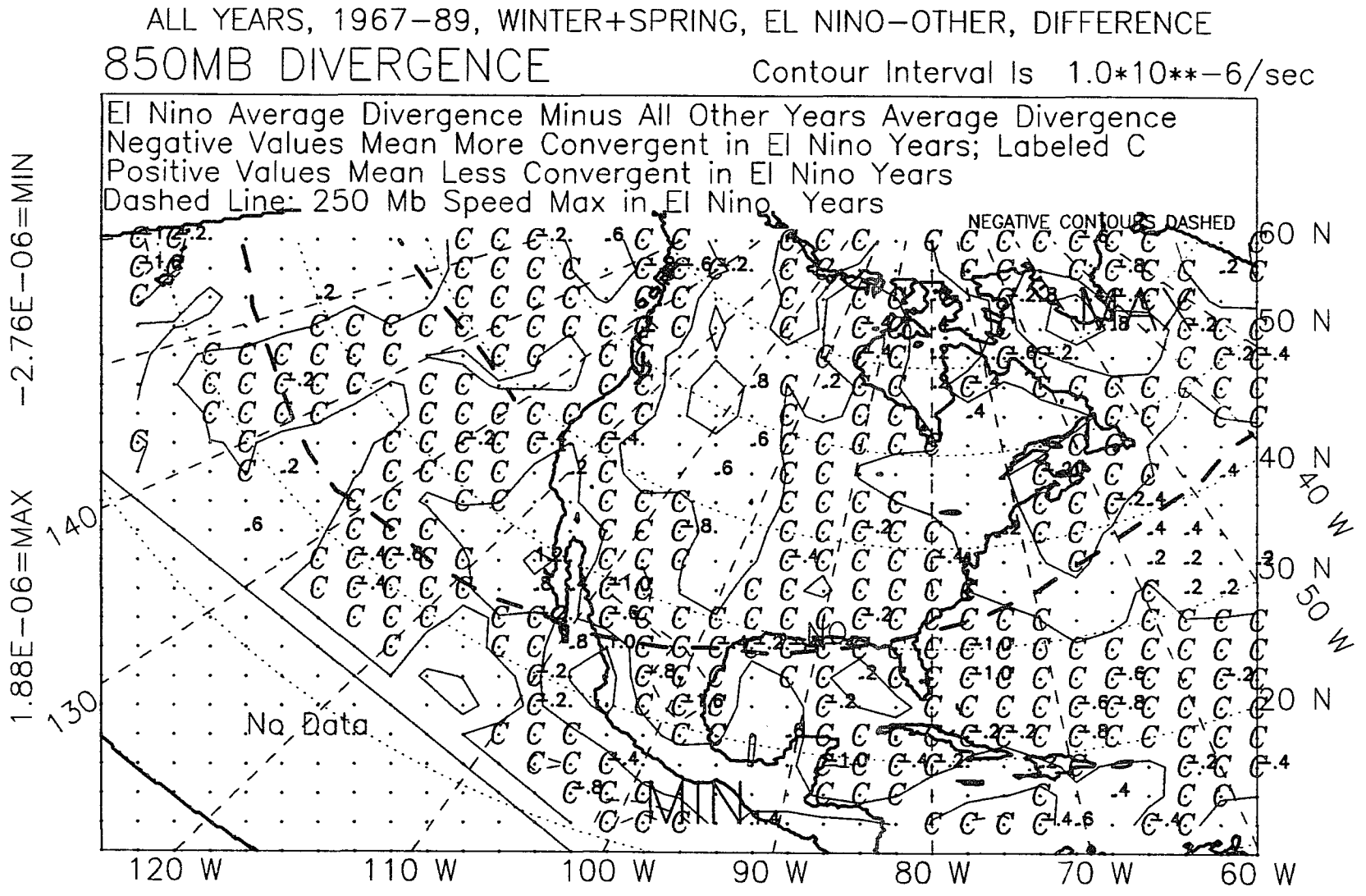

Figure E.21: 850–mb divergence, winter–plus–spring, 1967–89, difference.

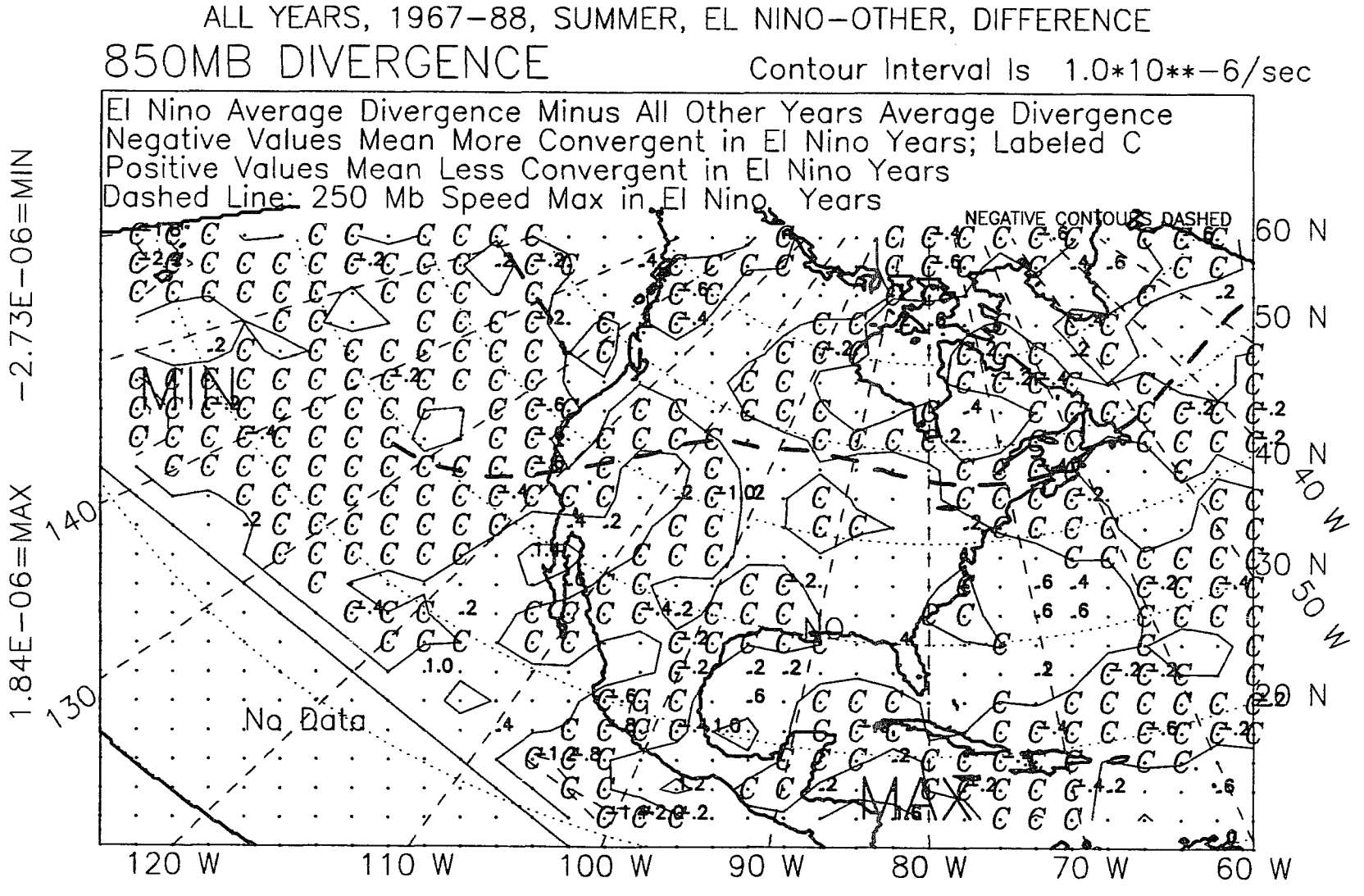

Figure E.22: 850–mb divergence, summer, 1967–88, difference.

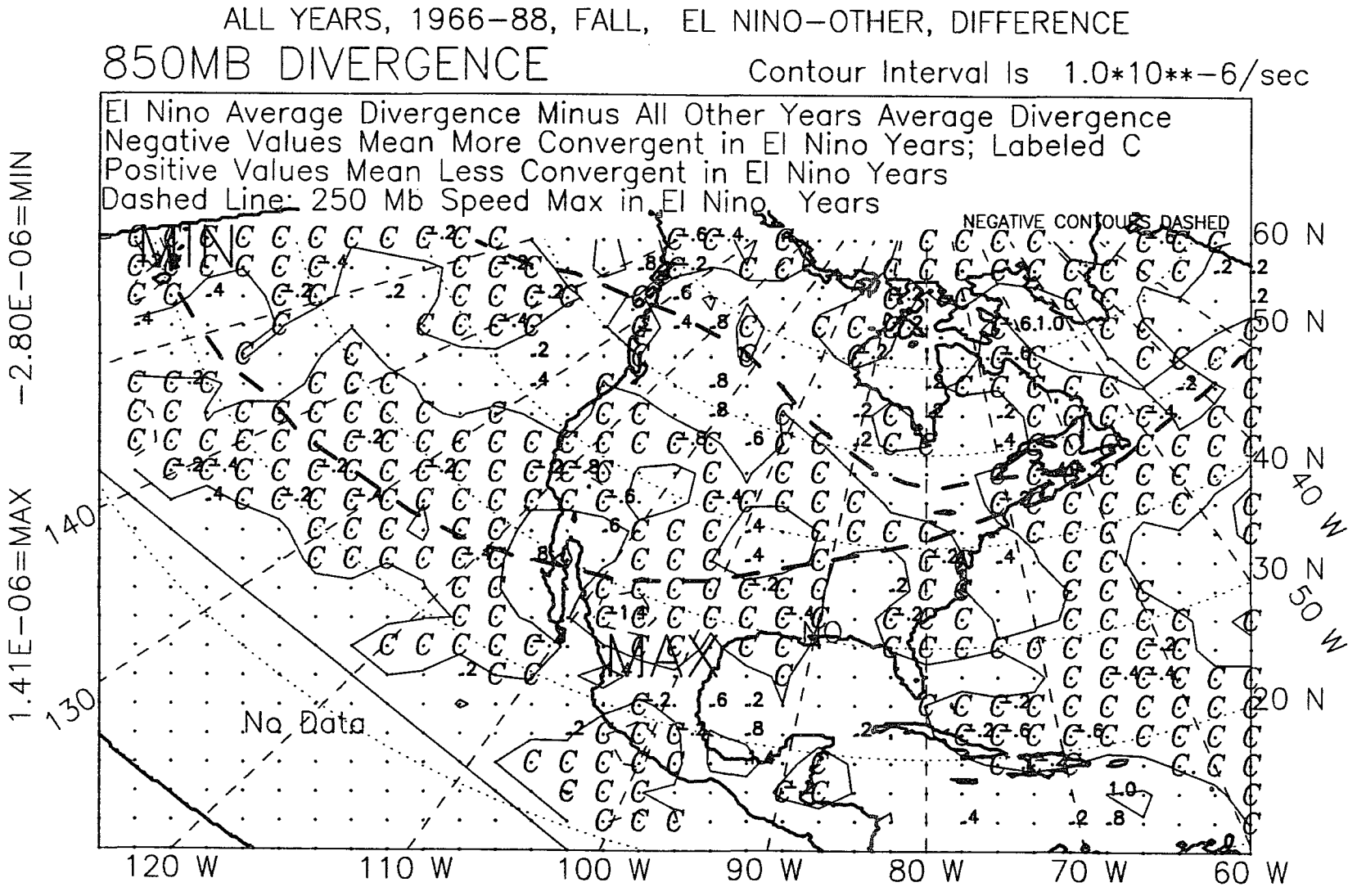

Figure E.23: 850-mb divergence, fall, 1966-88, difference.

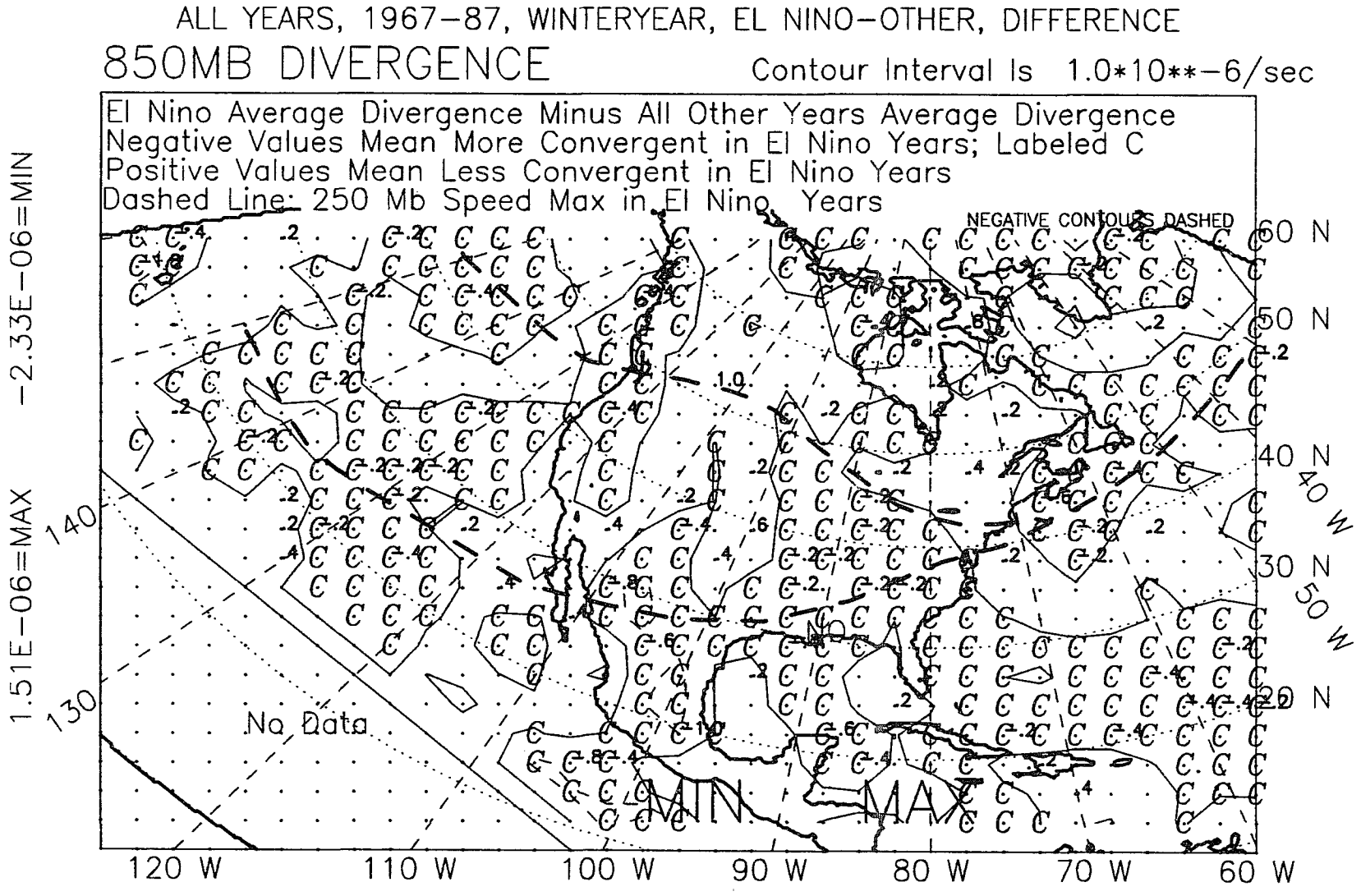

Figure E.24: 850–mb divergence, winter year, 1967–87, difference.

APPENDIX F
850-MB
RELATIVE-VORTICITY FIELD

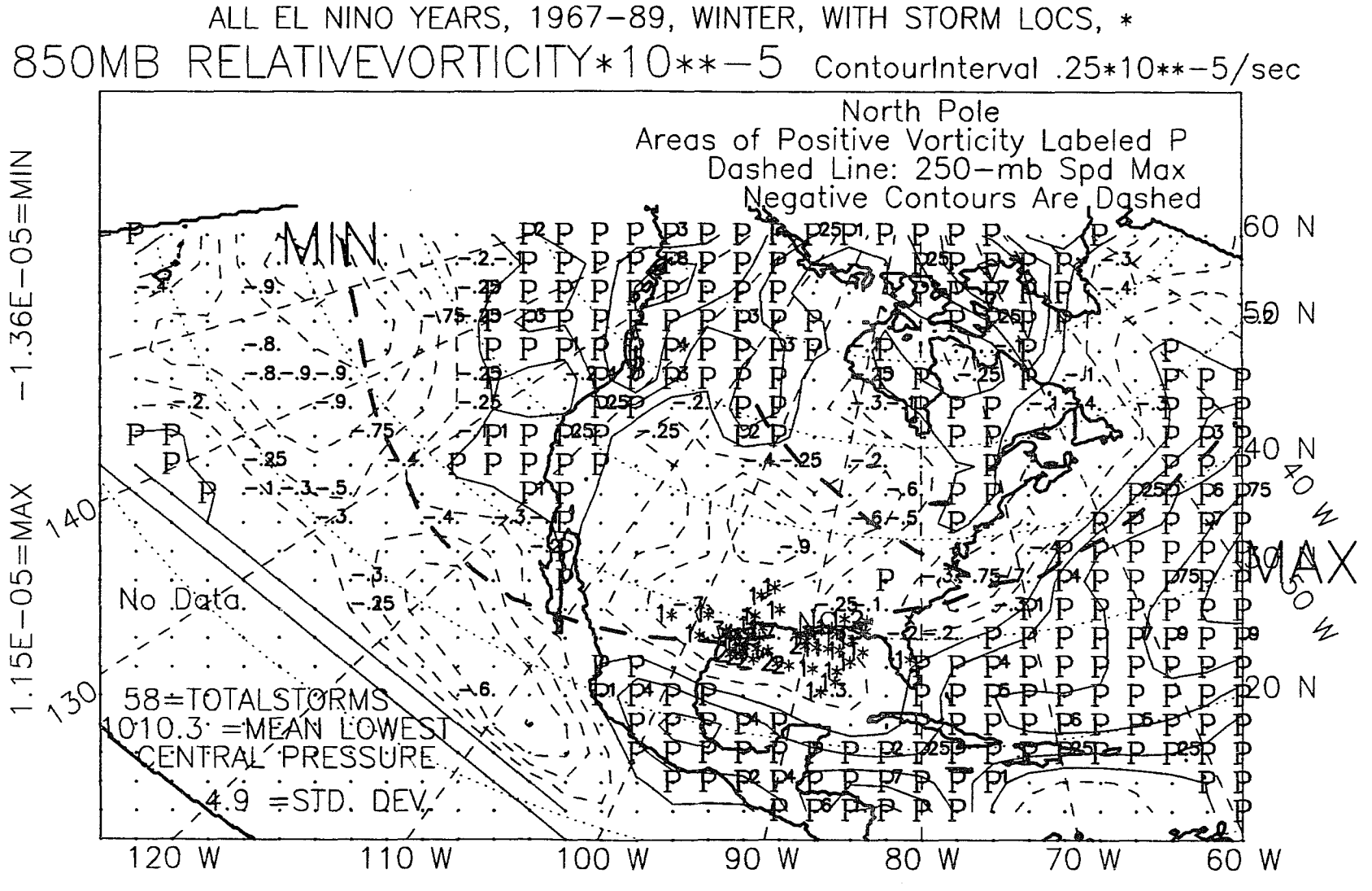

Figure F.1: 850–mb relative vorticity, winter, El Niño years, 1967–89.

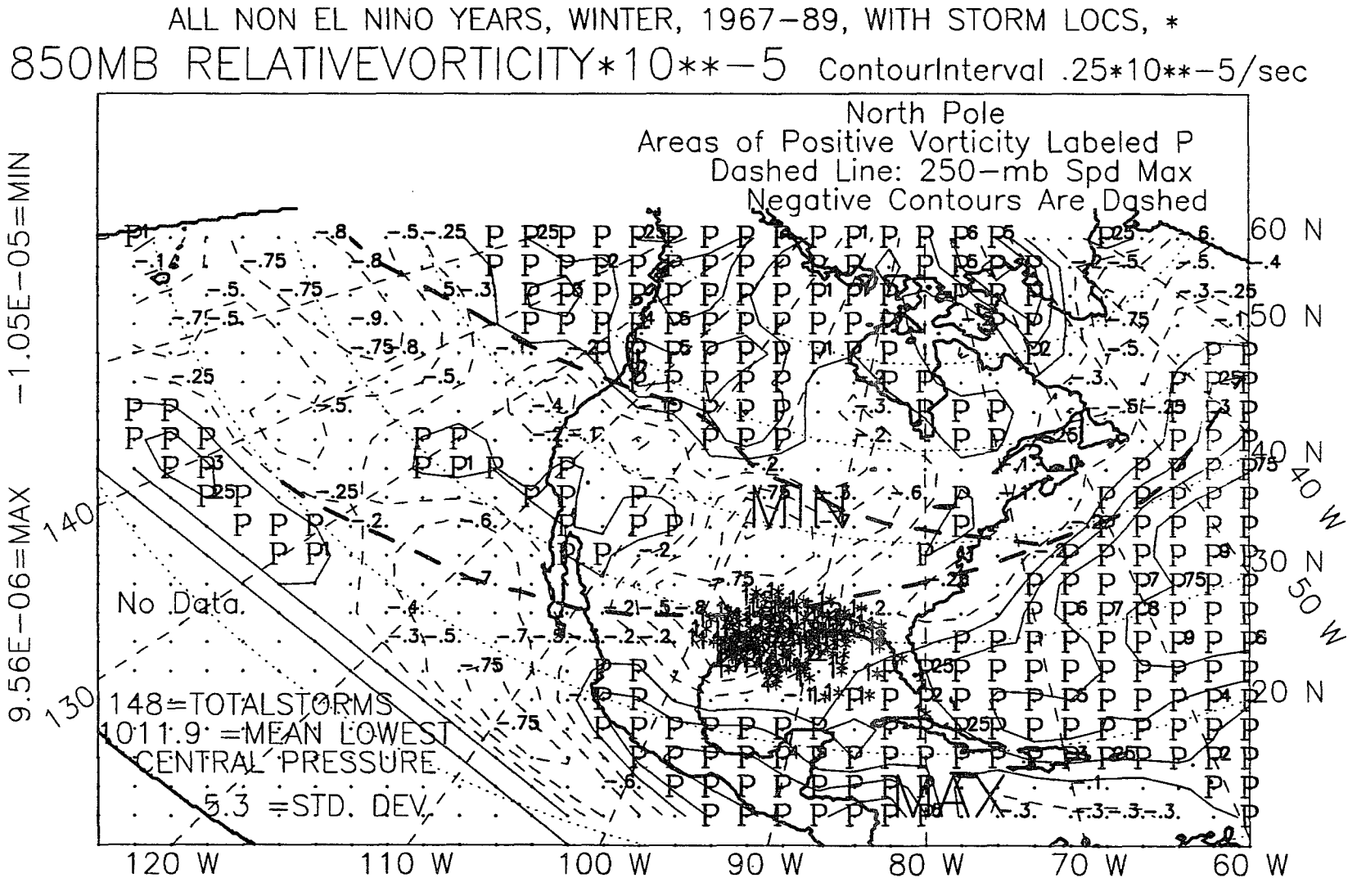

Figure F.2: 850-mb relative vorticity, winter, non-El Niño years, 1967-89.

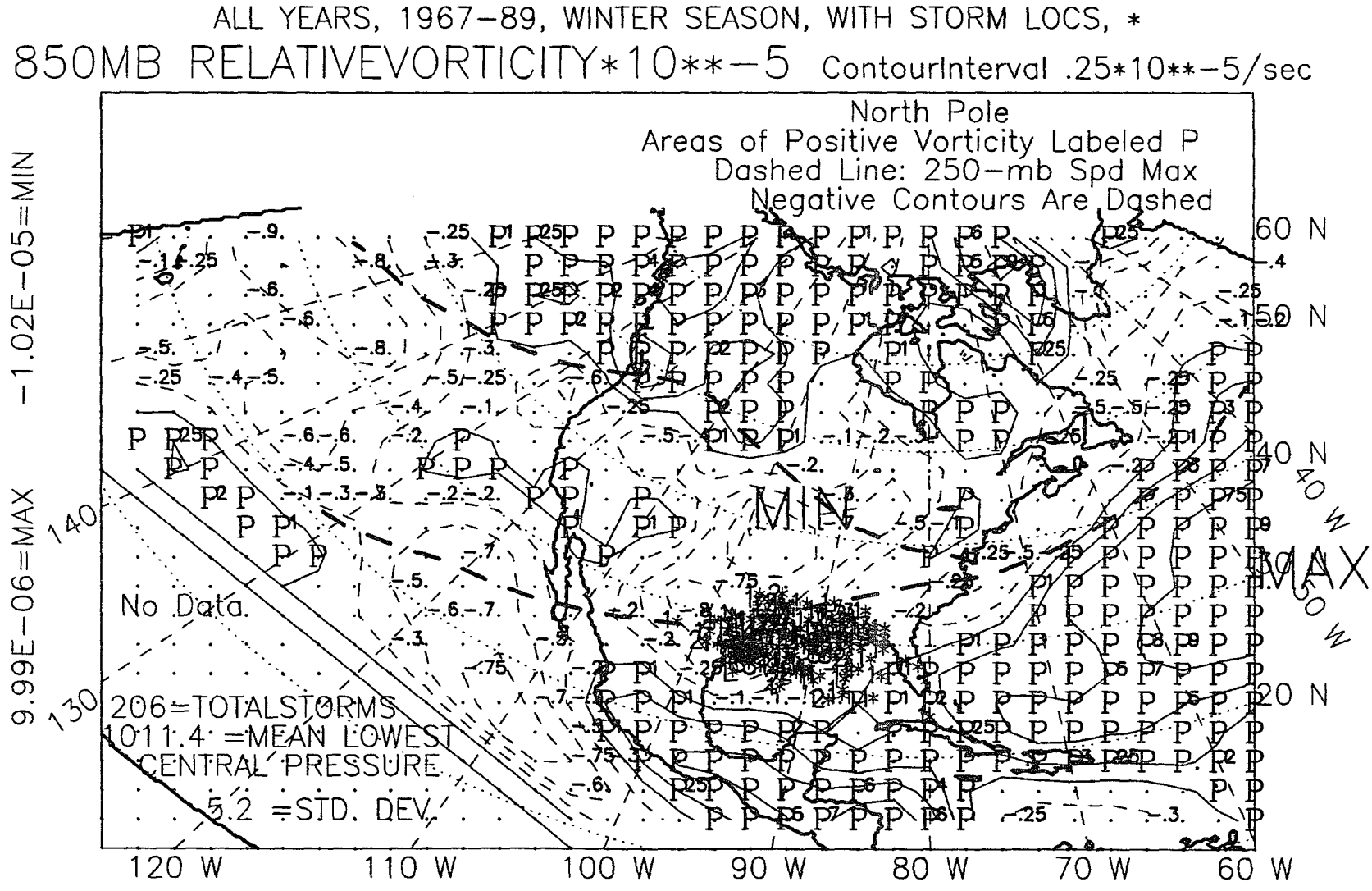

Figure F.3: 850–mb relative vorticity, winter, all years, 1967–89.

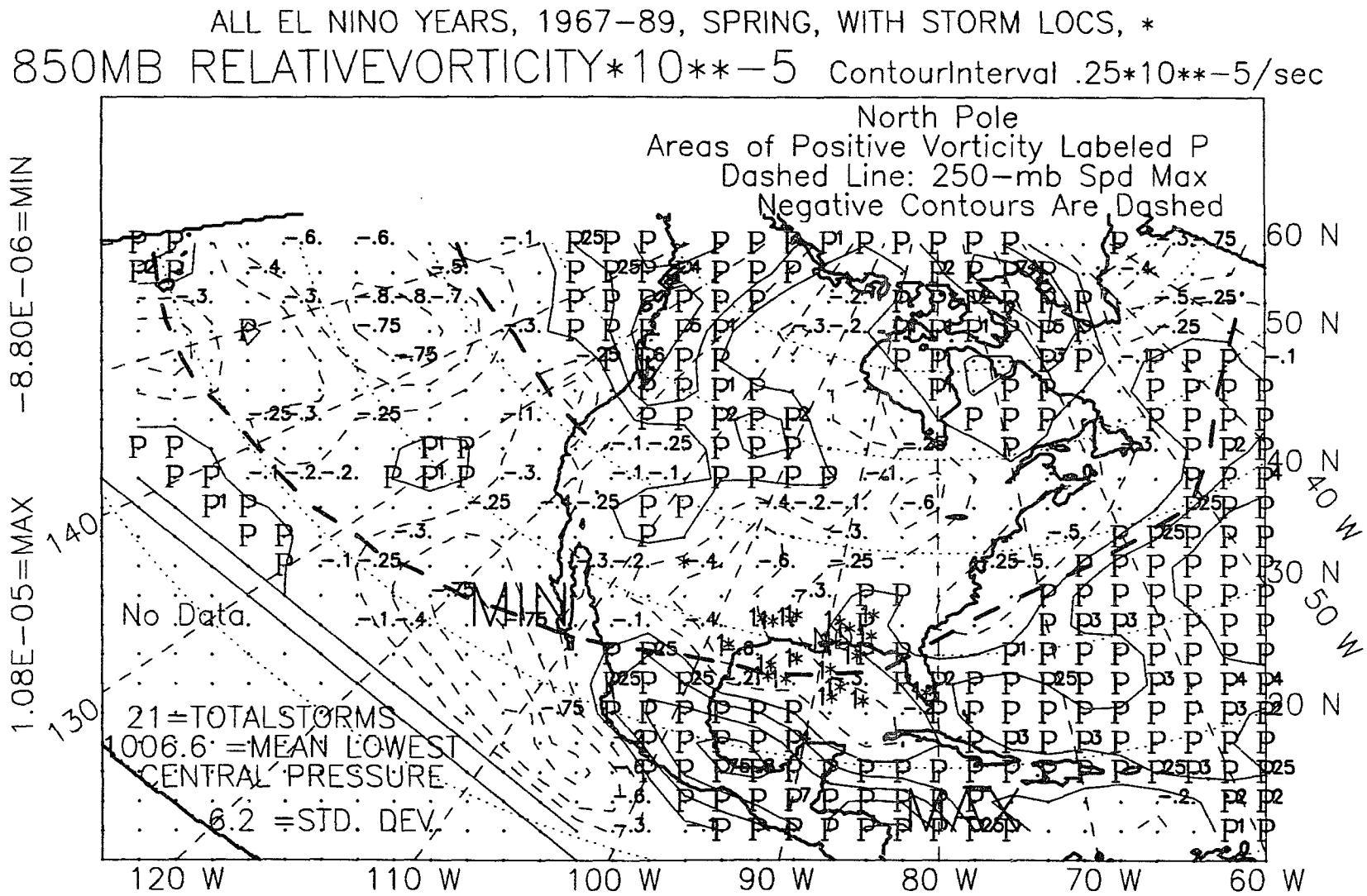

Figure F.4: 850–mb relative vorticity, spring, El Niño years, 1967–89.

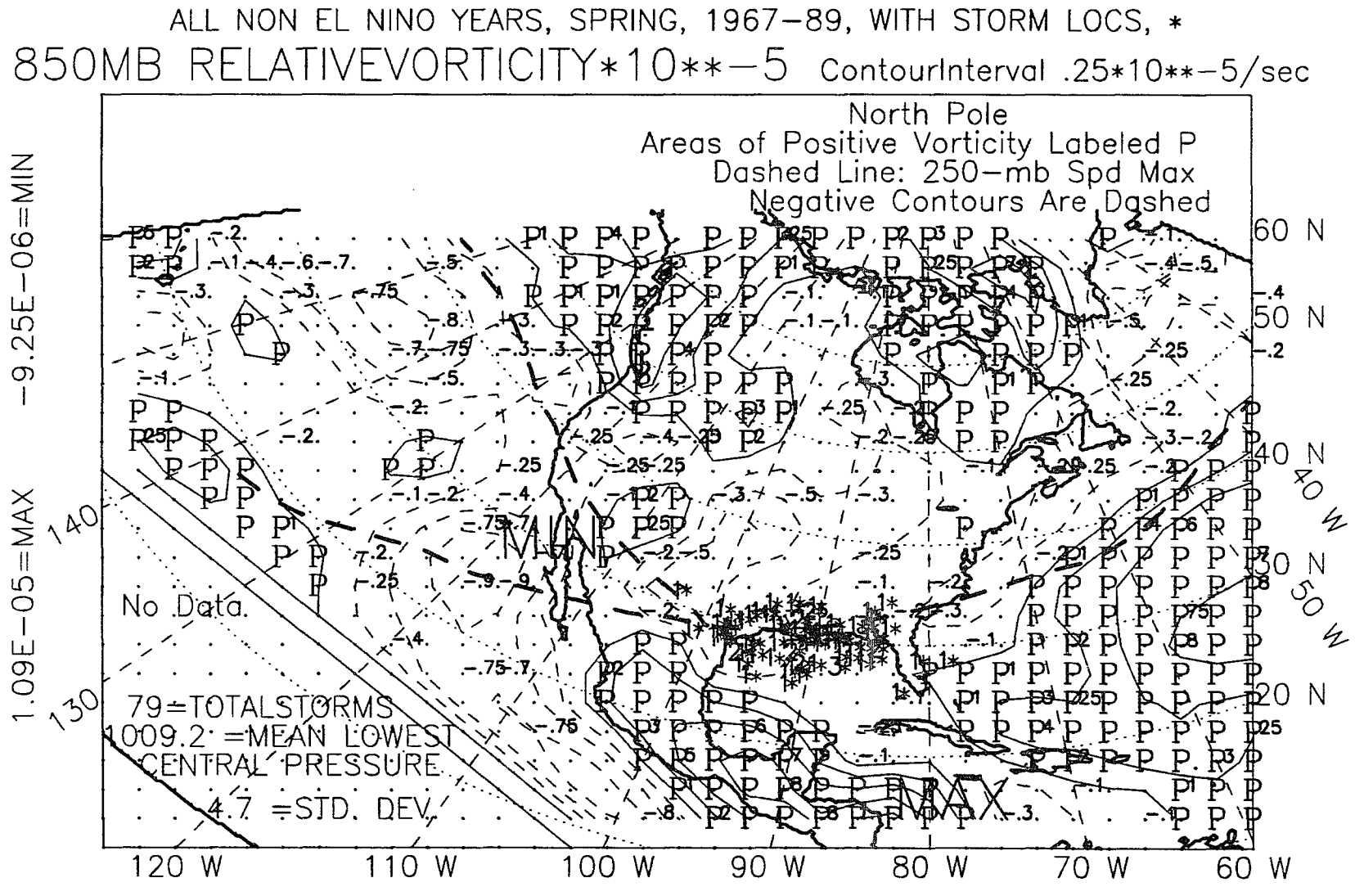

Figure F.5: 850–mb relative vorticity, spring, non–El Niño years, 1967–89.

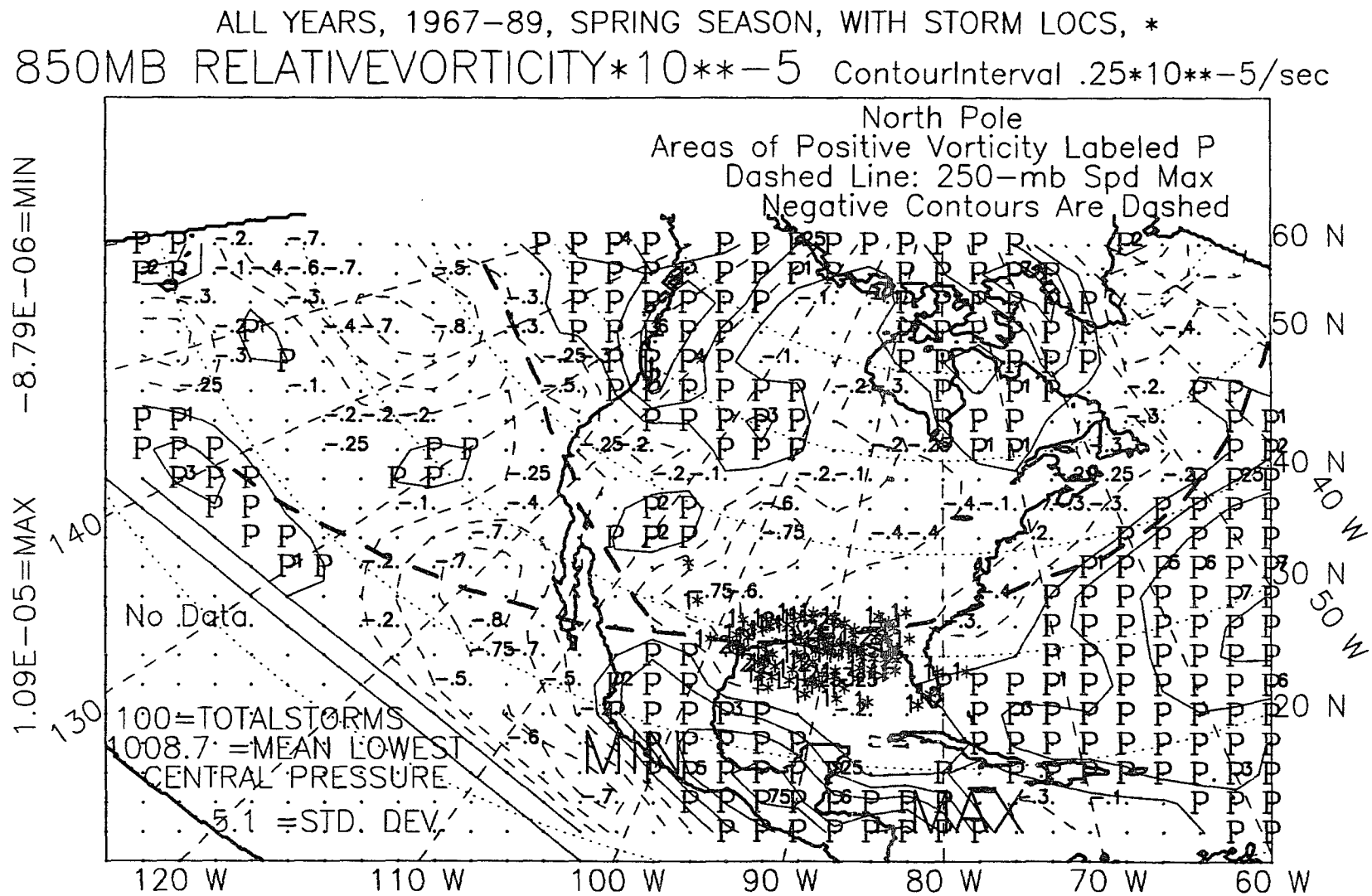

Figure F.6: 850–mb relative vorticity, spring, all years, 1967–89.

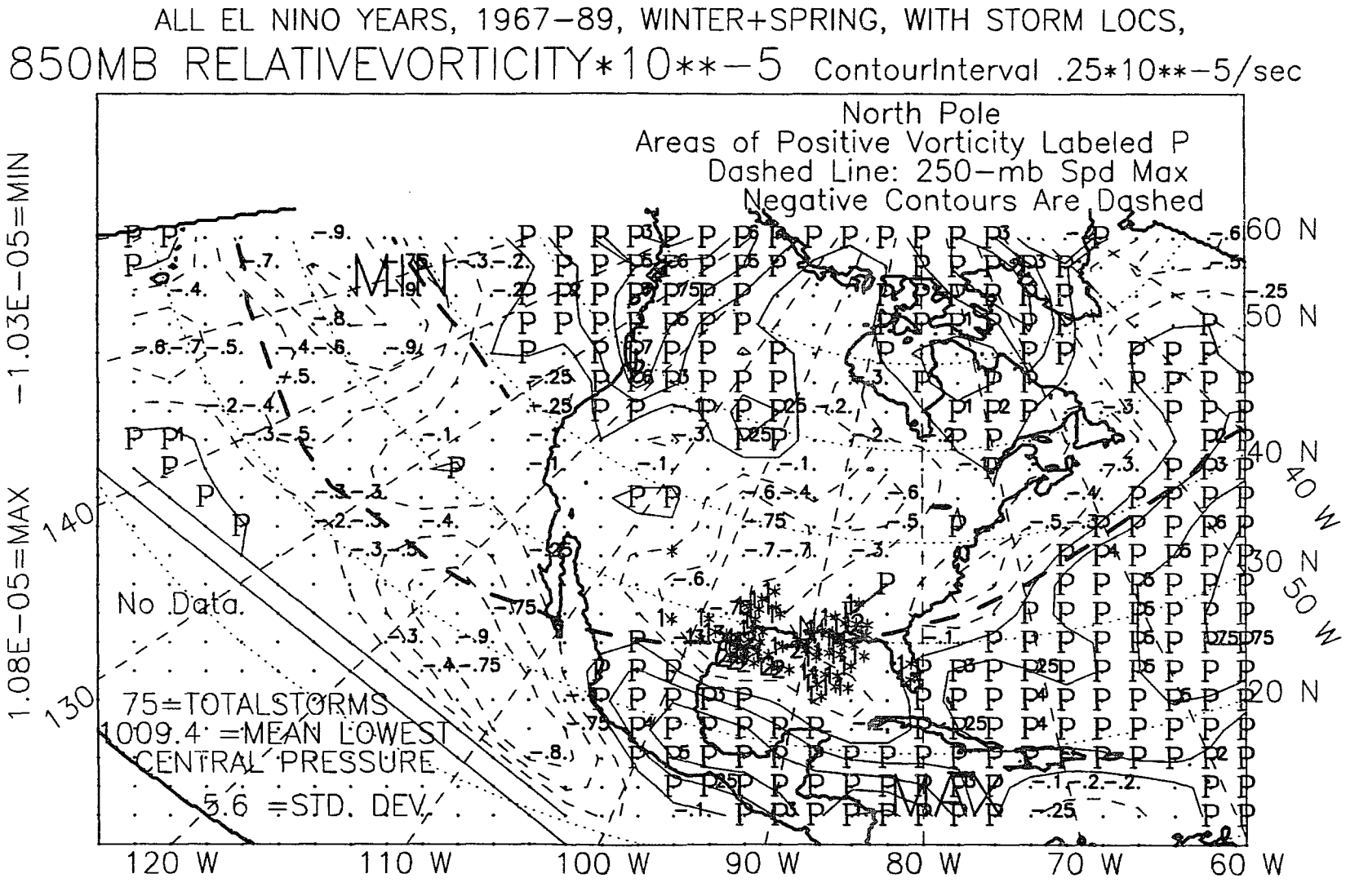

Figure F.7: 850–mb relative vorticity, winter–plus–spring, El Niño years, 1967–89.

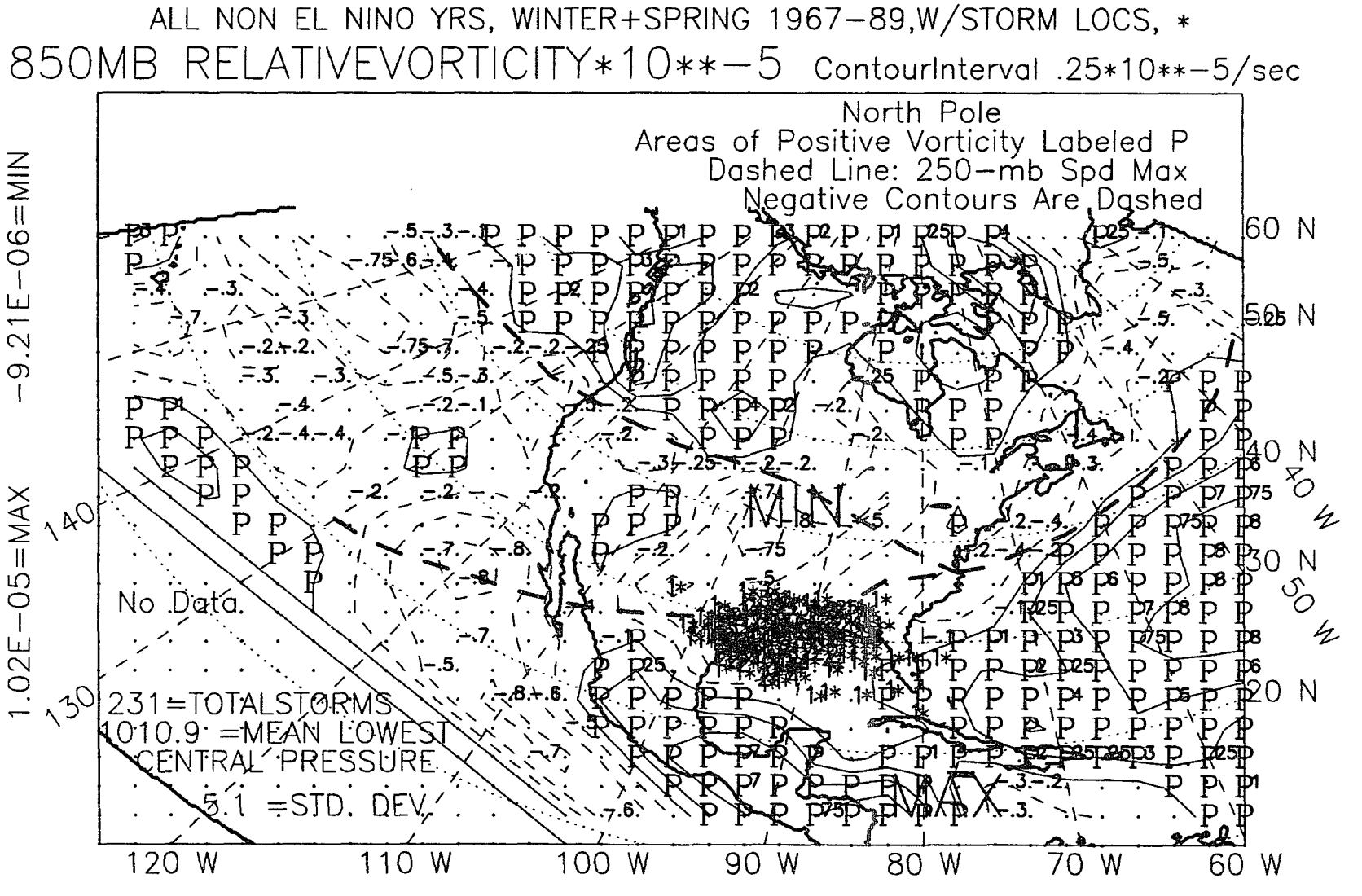

Figure F.8: 850–mb relative vorticity, winter–plus–spring, non–El Niño years, 1967–89.

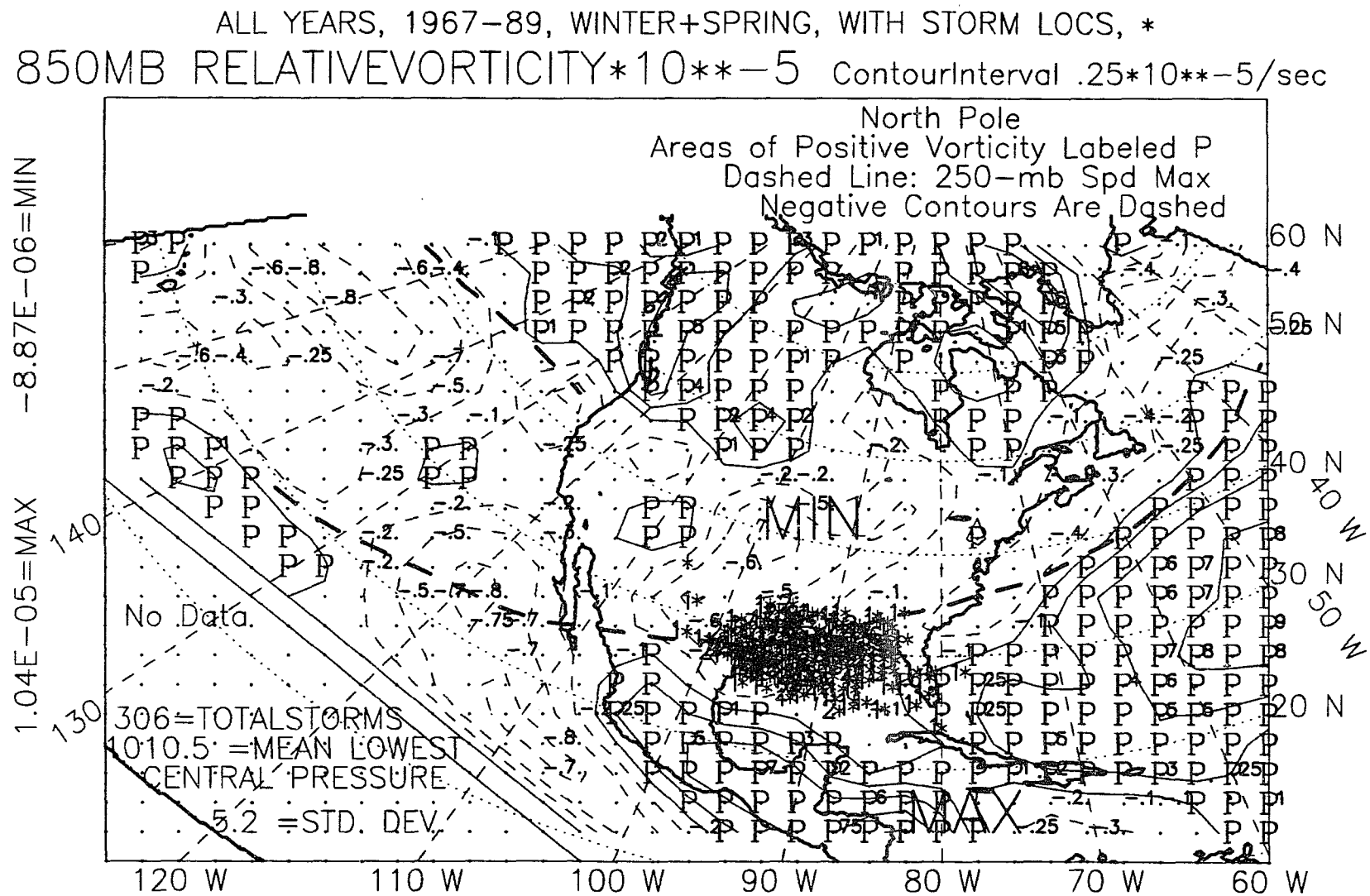

Figure F.9: 850–mb relative vorticity, winter–plus–spring, all years, 1967–89.

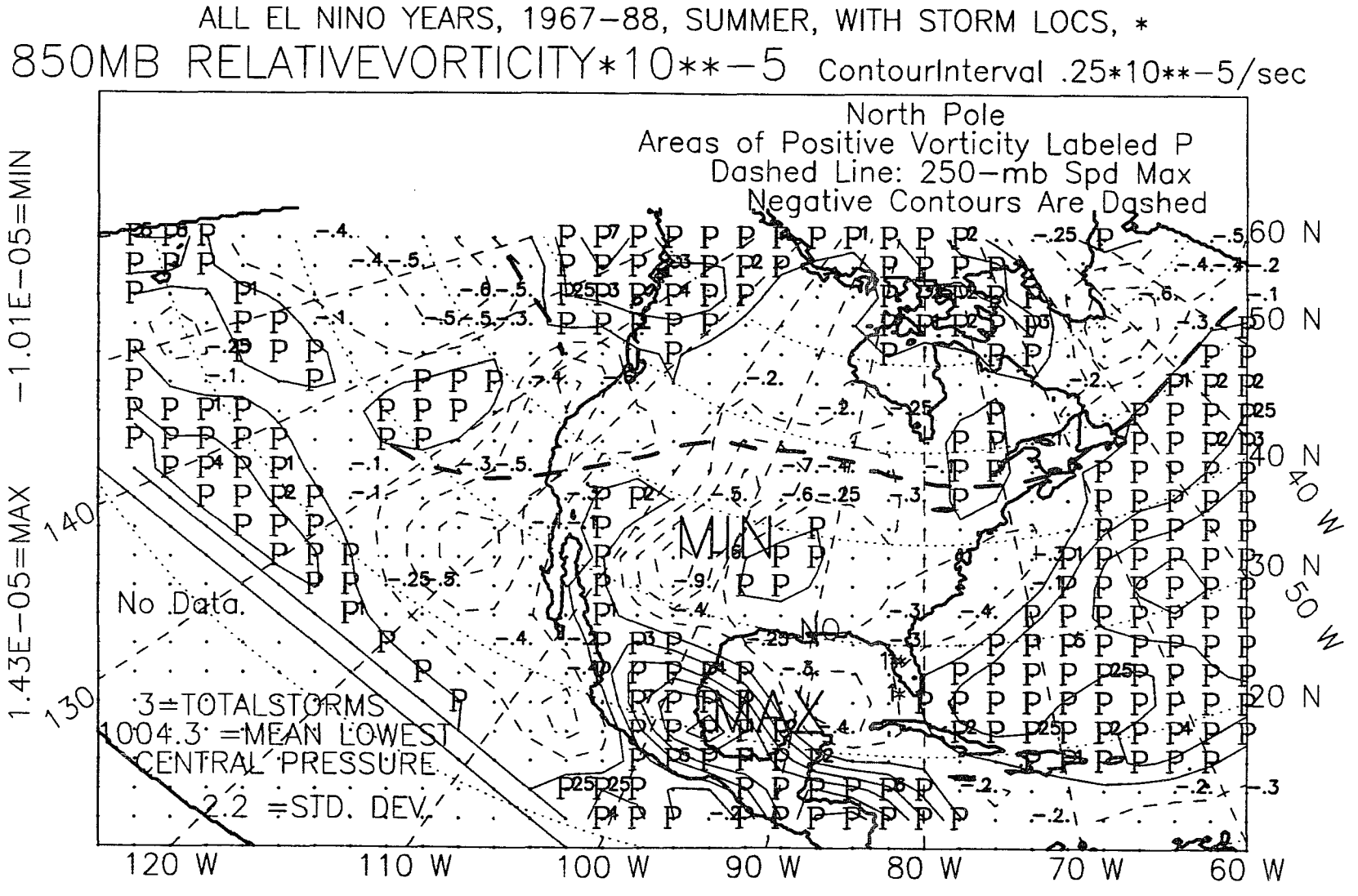

Figure F.10: 850–mb relative vorticity, summer, El Niño years, 1967–88.

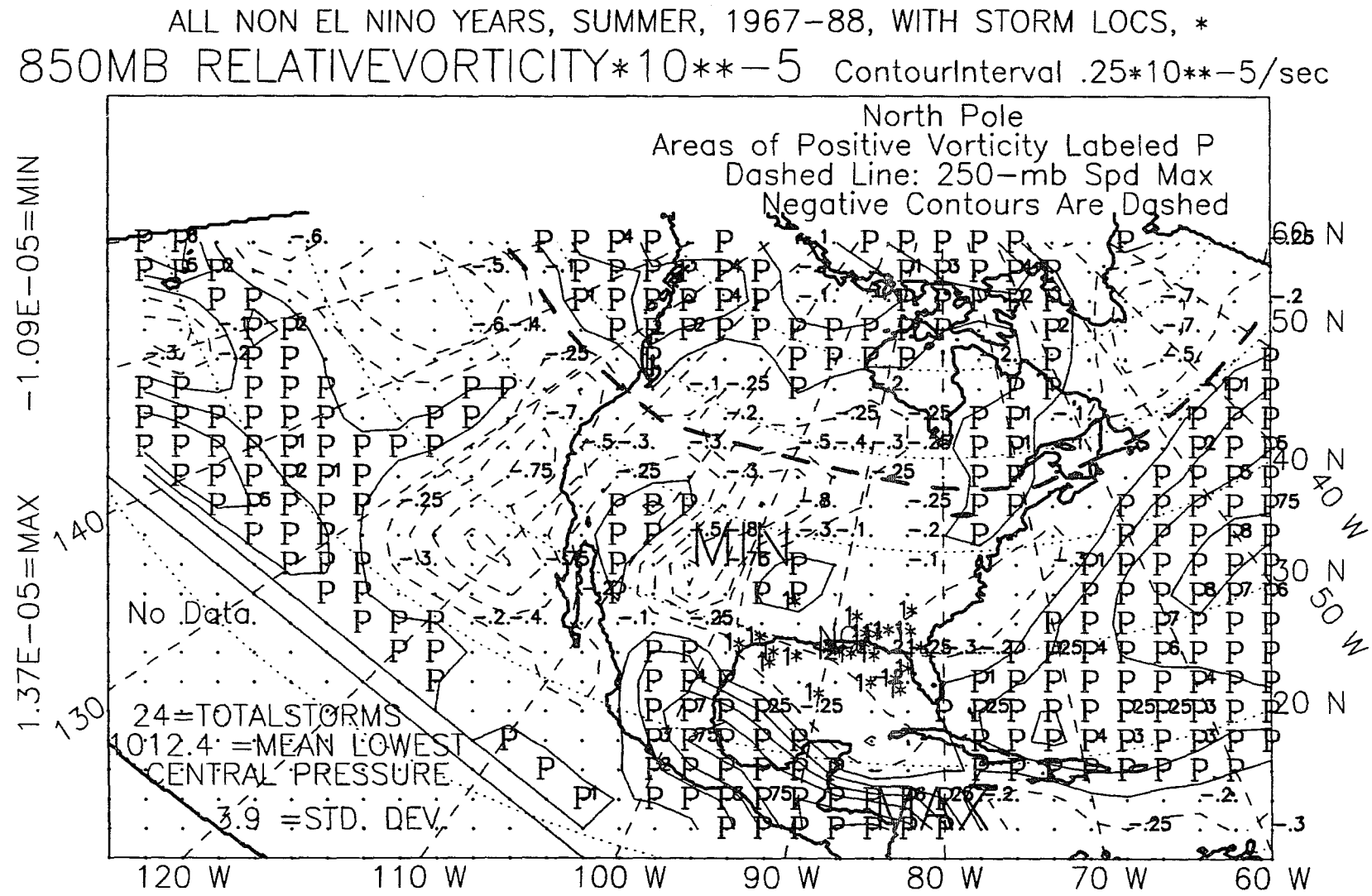

Figure F.11: 850-mb relative vorticity, summer, non-El Niño years, 1967-88.

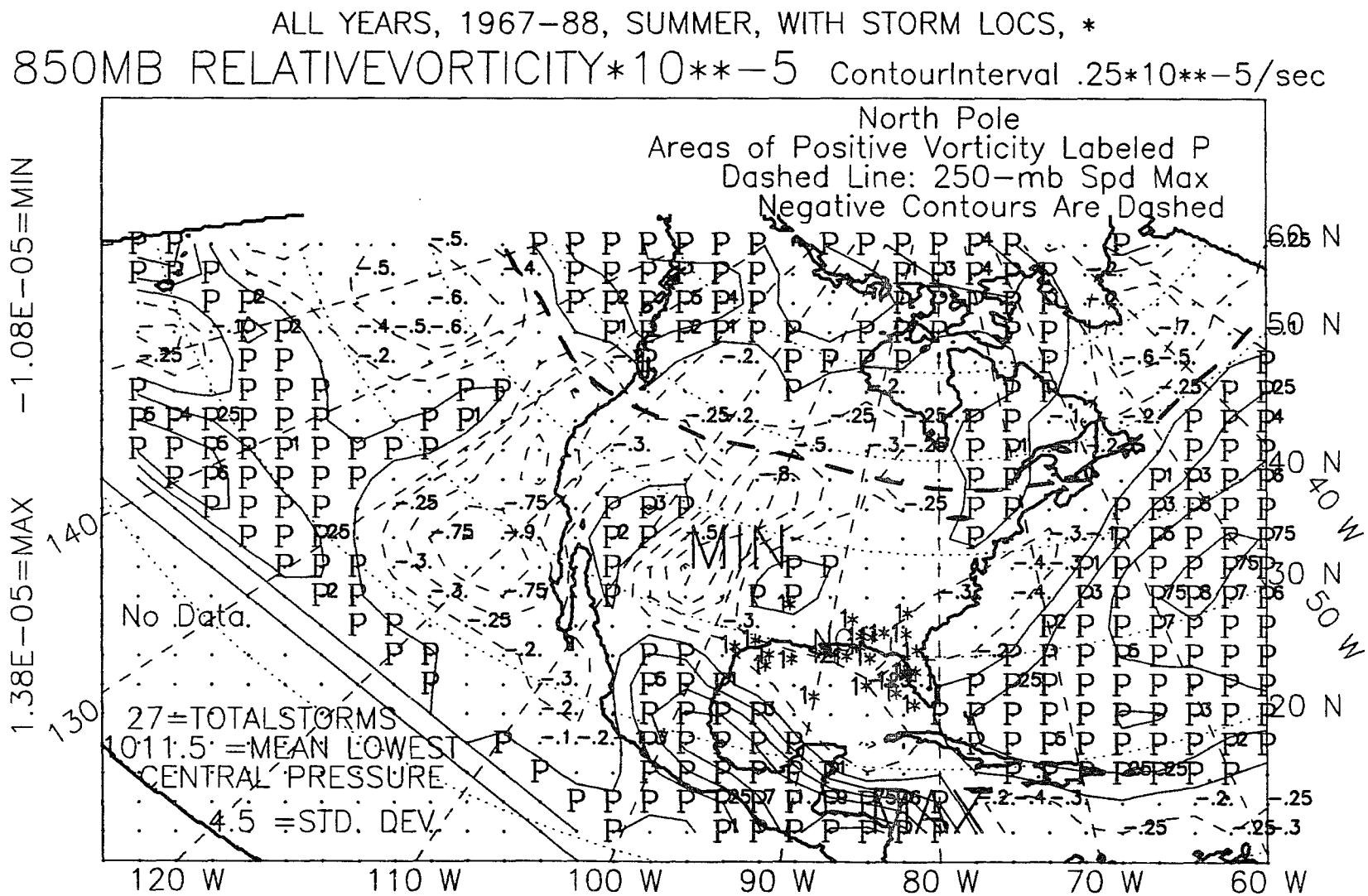

Figure F.12: 850–mb relative vorticity, summer, all years, 1967–88.

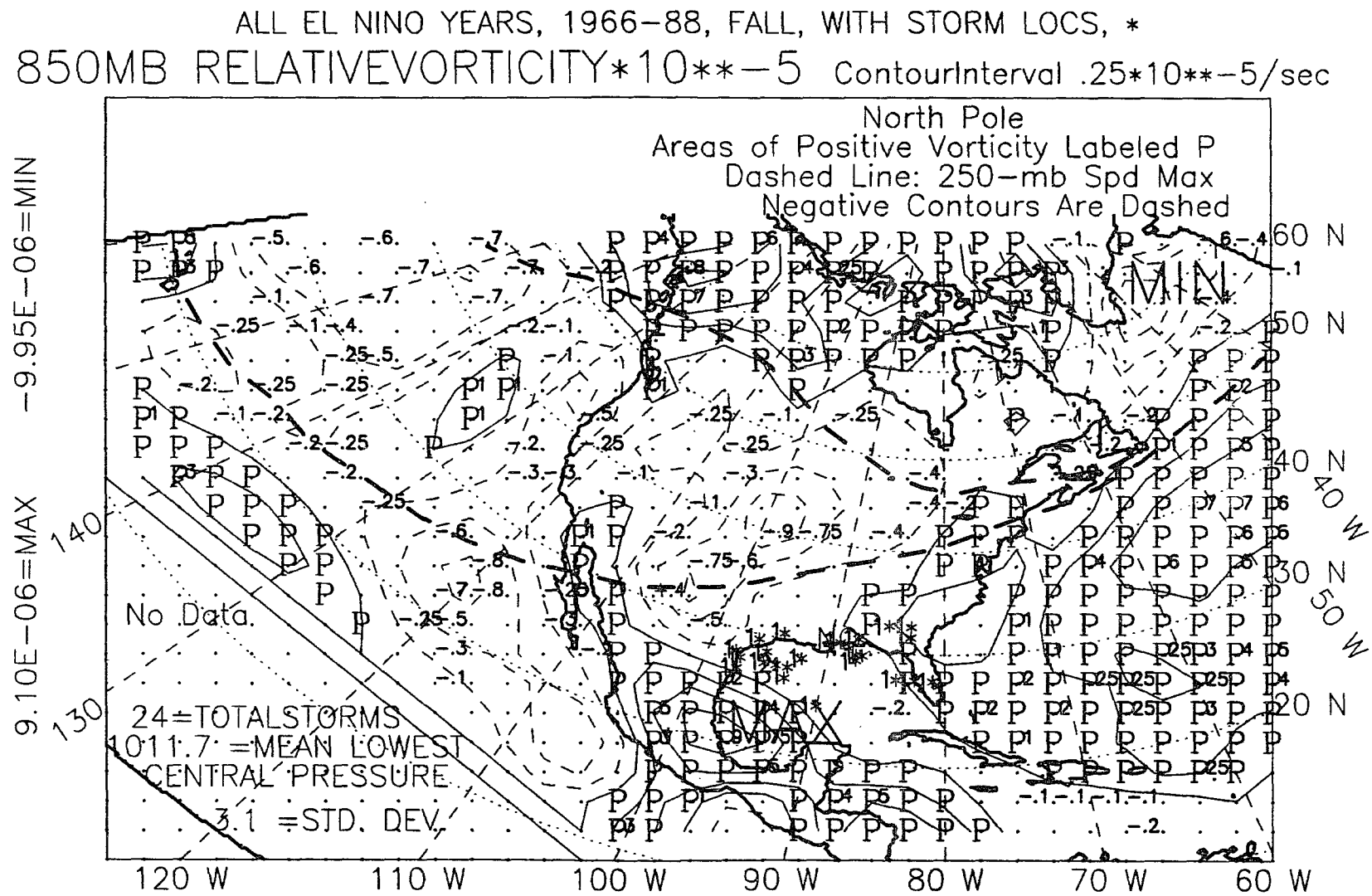

Figure F.13: 850-mb relative vorticity, fall, El Niño years, 1966-88.

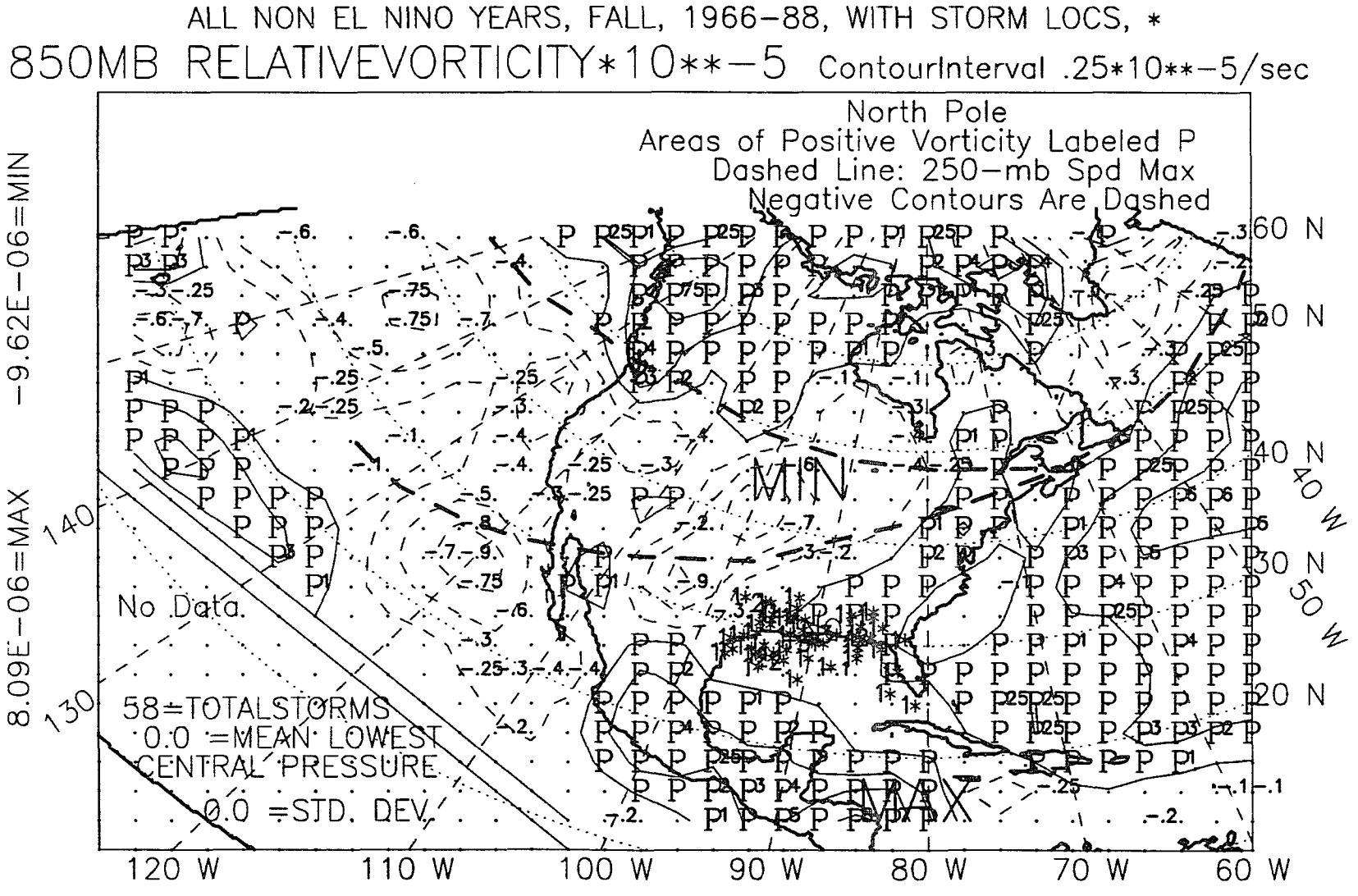

Figure F.14: 850-mb relative vorticity, fall, non-El Niño years, 1966-88.

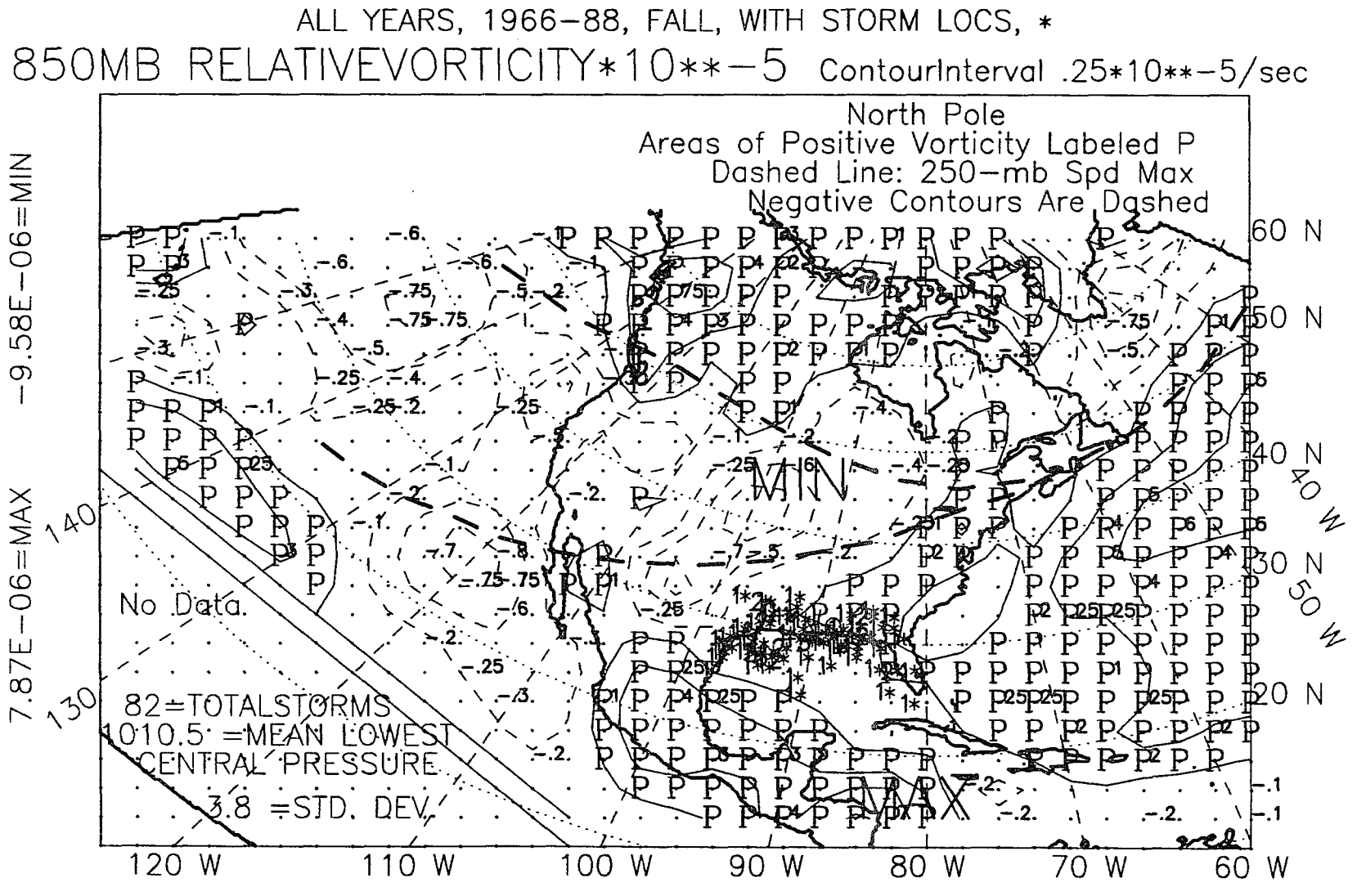

Figure F.15: 850–mb relative vorticity, fall, all years, 1966–88.

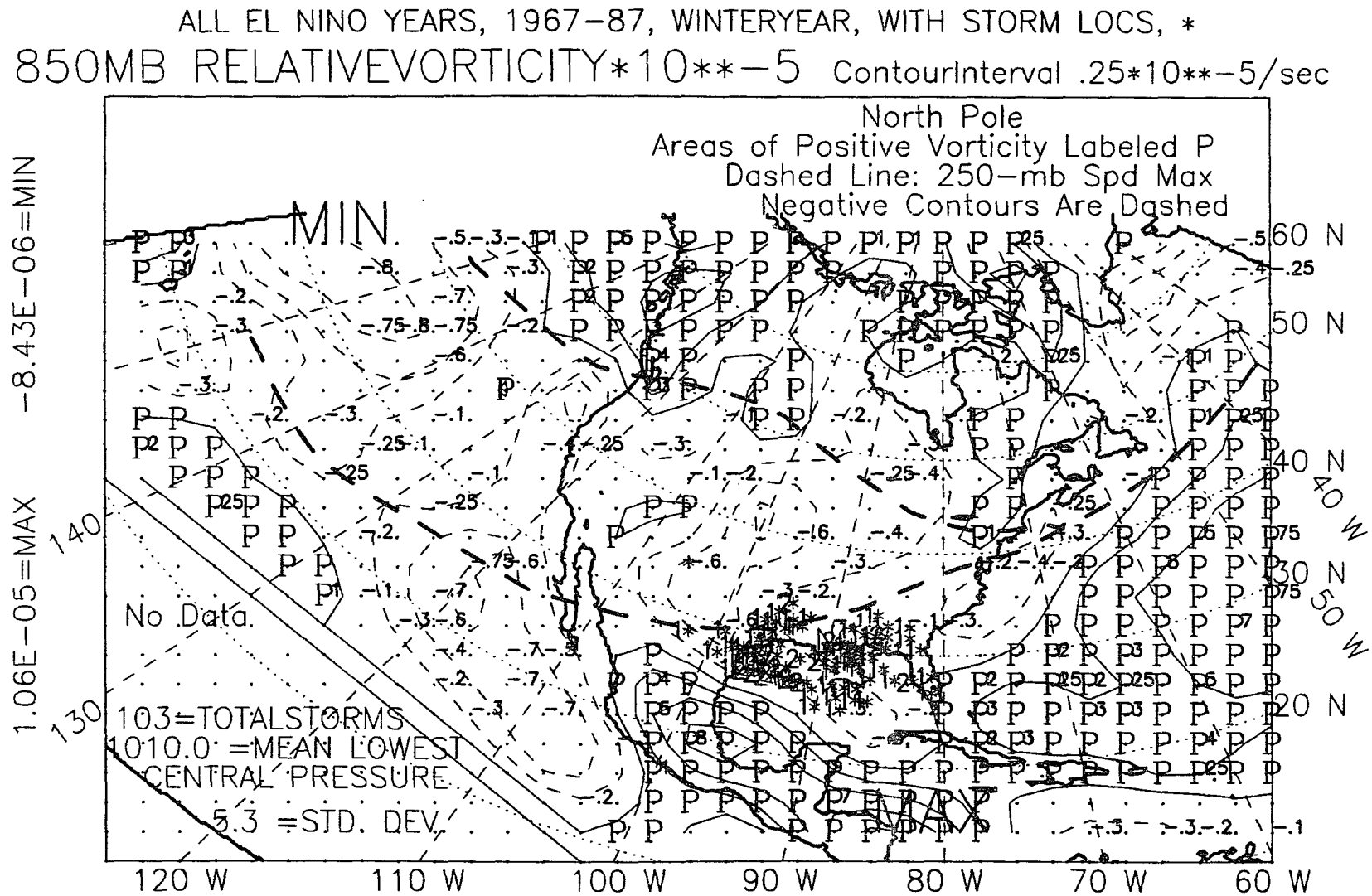

Figure F.16: 850-mb relative vorticity, winter year, El Niño years, 1967-87.

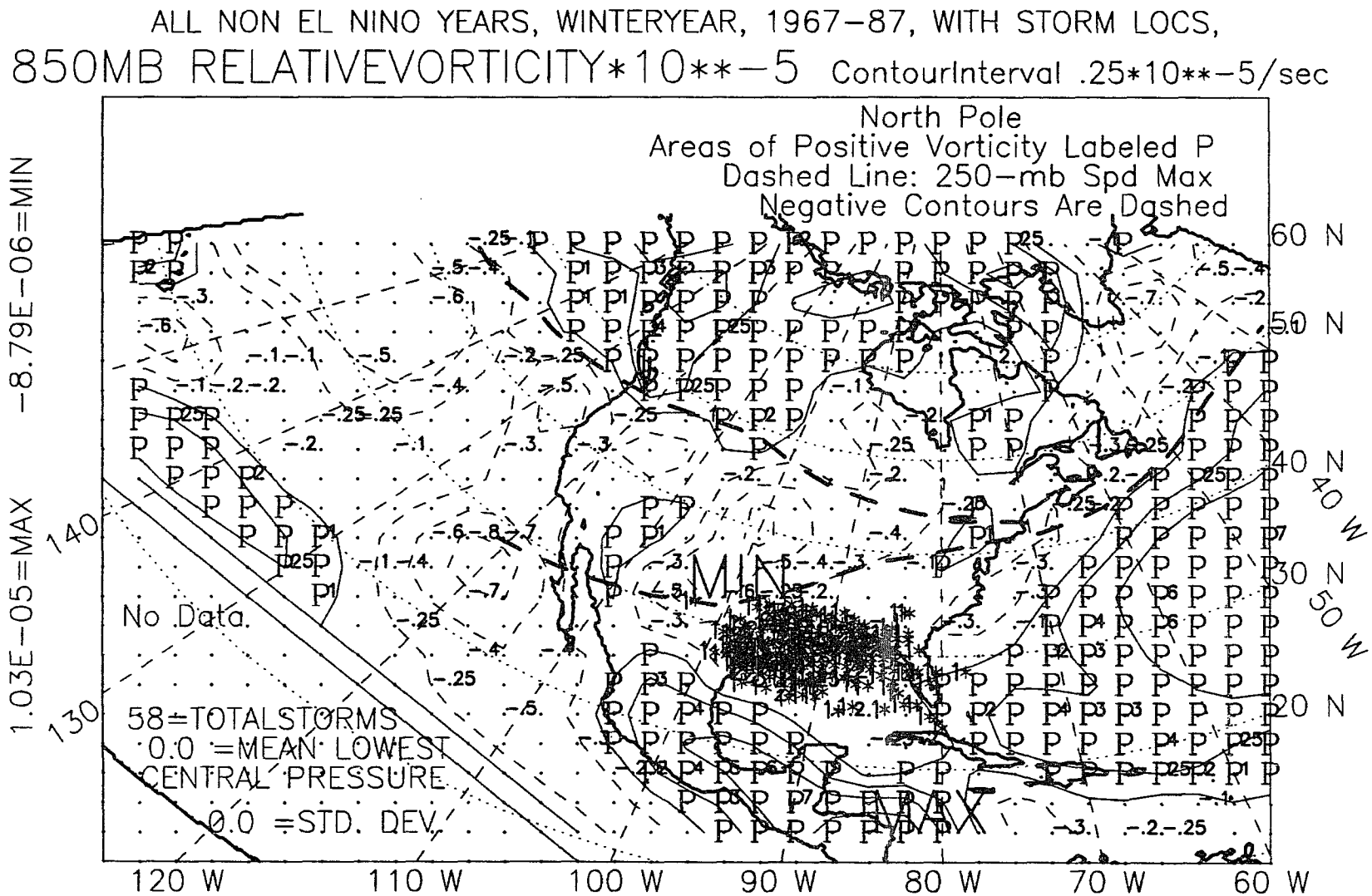

Figure F.17: 850-mb relative vorticity, winter year, non-El Niño years, 1967-87.

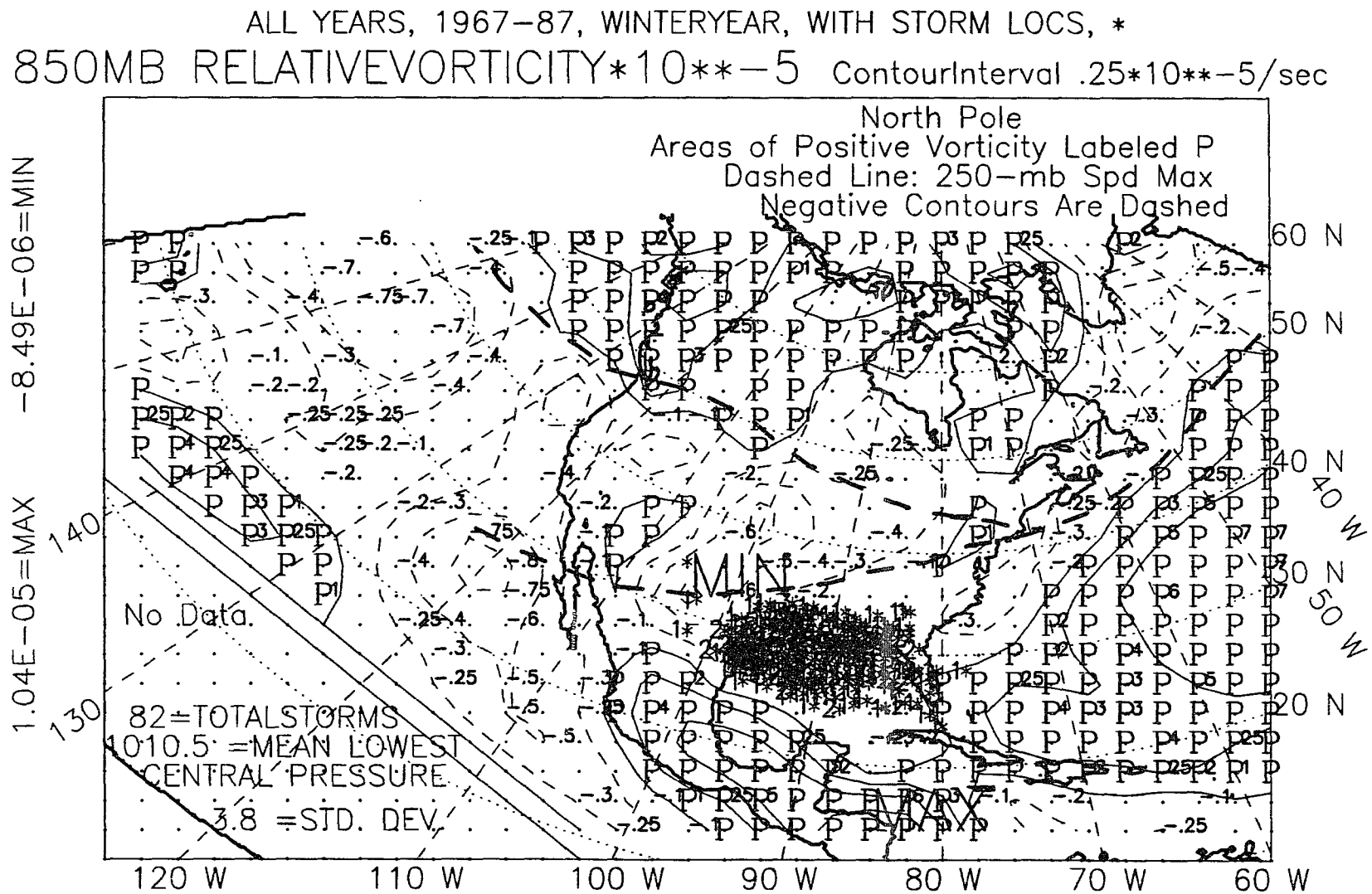

Figure F.18: 850–mb relative vorticity, winter year, all years, 1967–87.

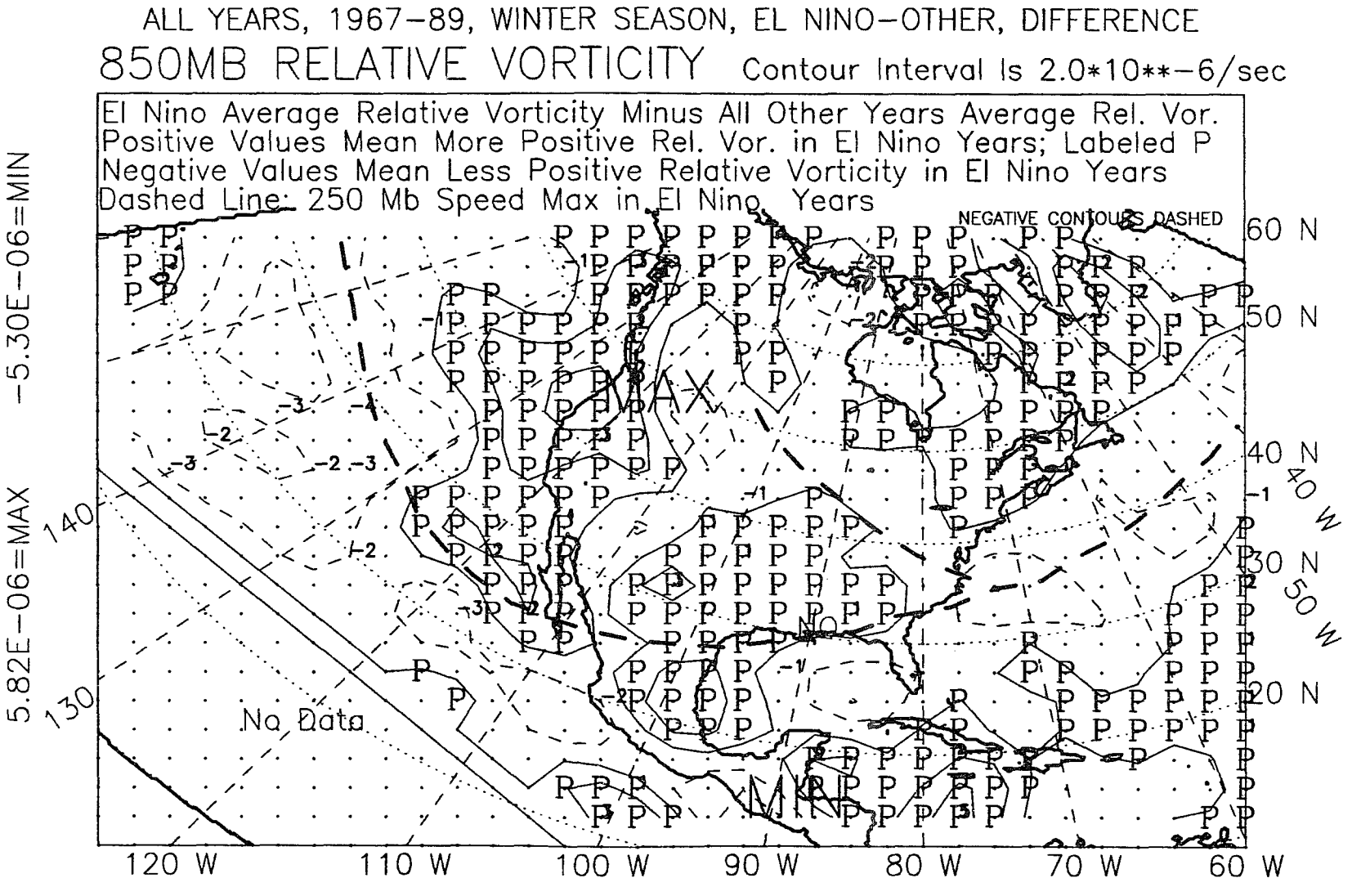

Figure F.19: 850–mb relative vorticity, winter, 1967–89, difference.

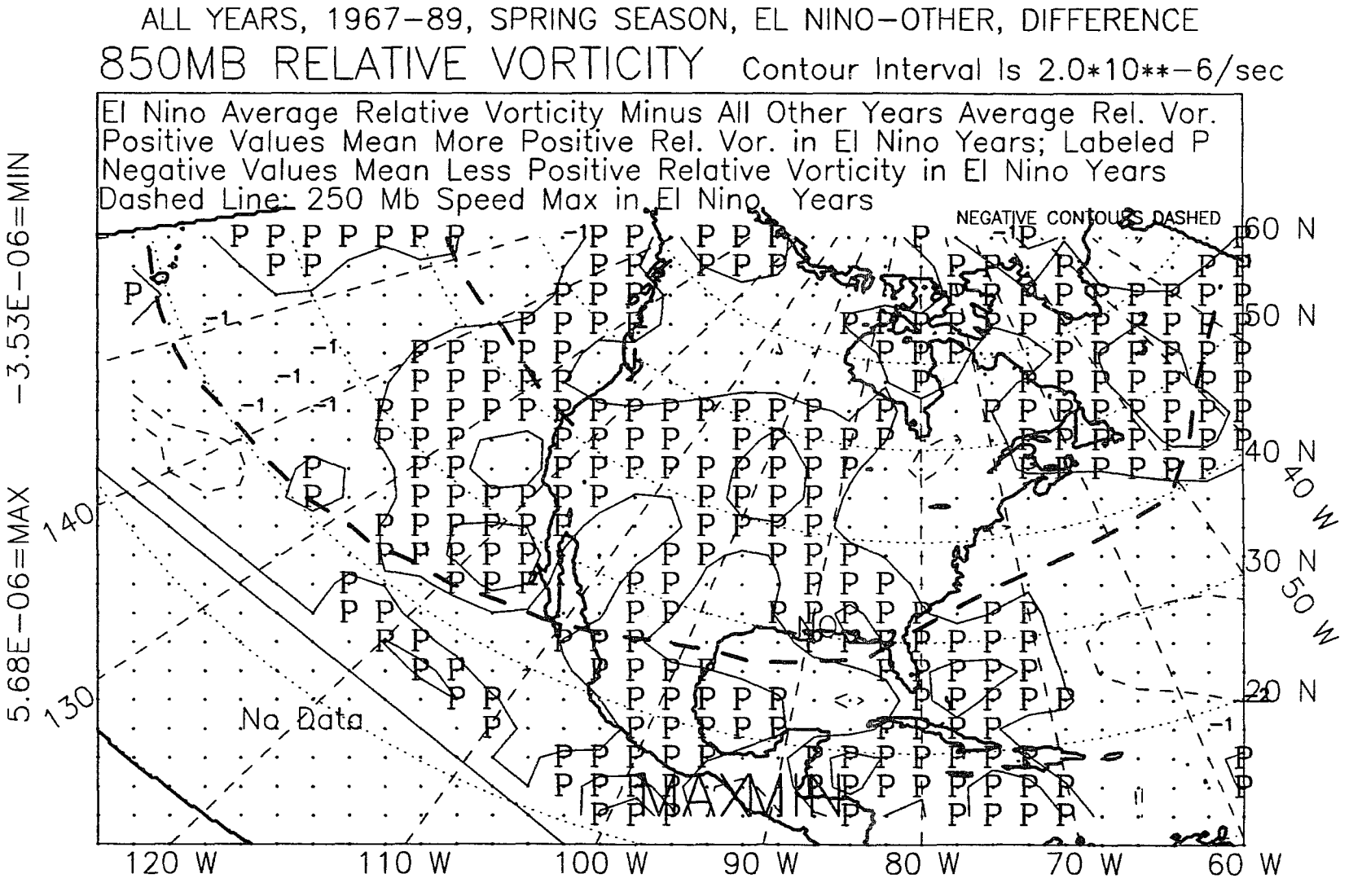

Figure F.20: 850–mb relative vorticity, spring, 1967–89, difference.

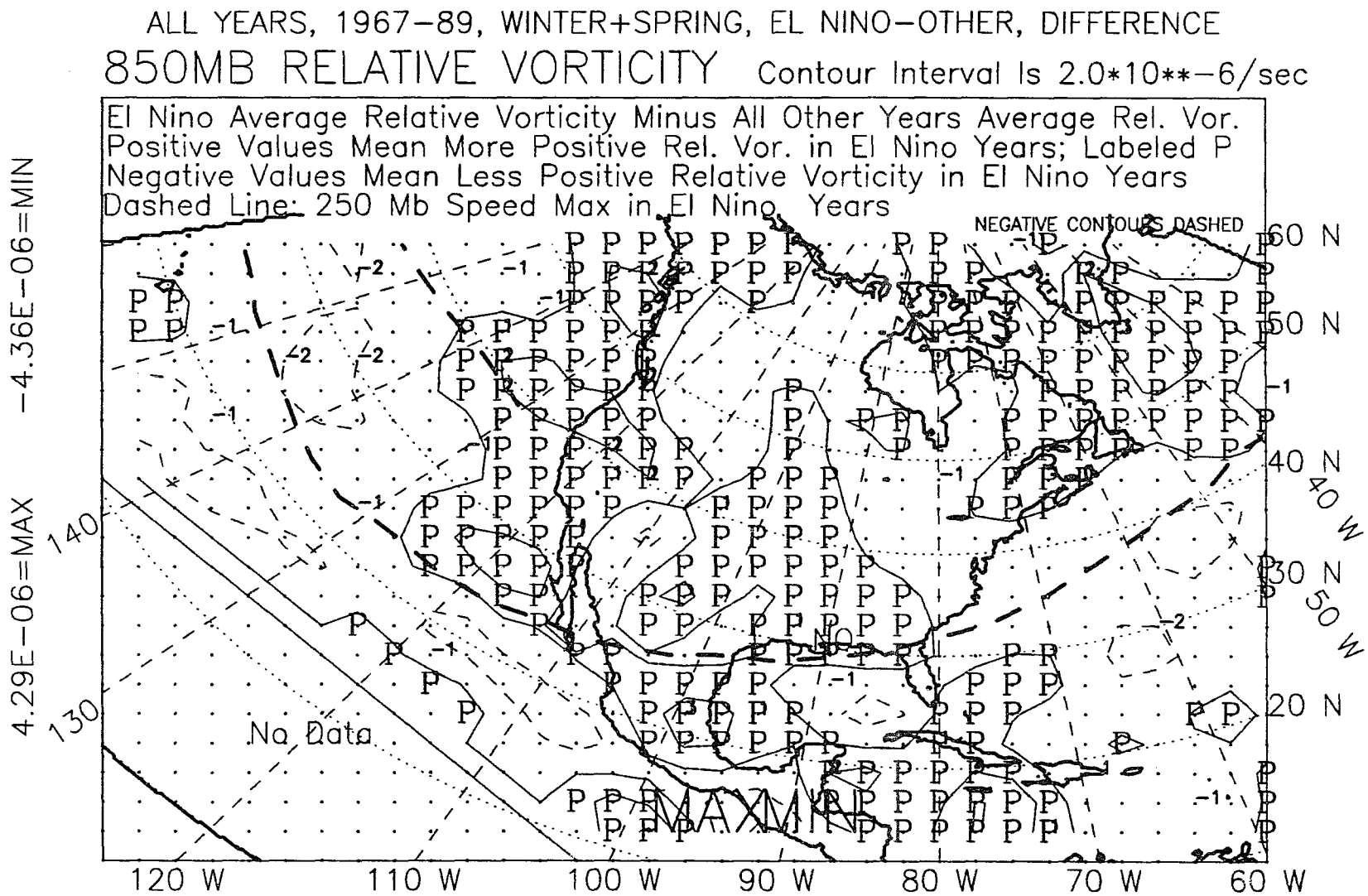

Figure F.21: 850–mb relative vorticity, winter–plus–spring, 1967–89, difference.

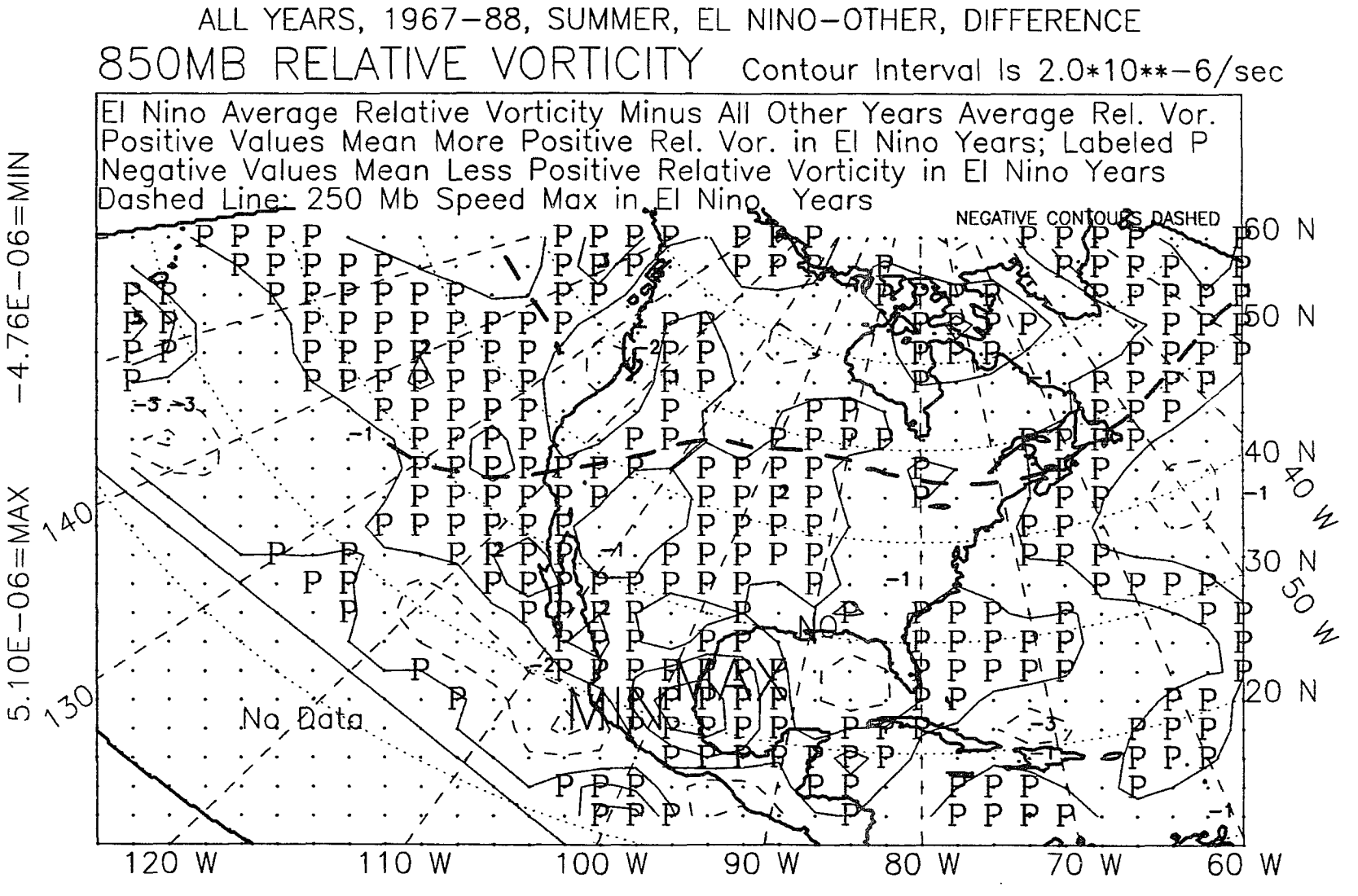

Figure F.22: 850–mb relative vorticity, summer, 1967–88, difference.

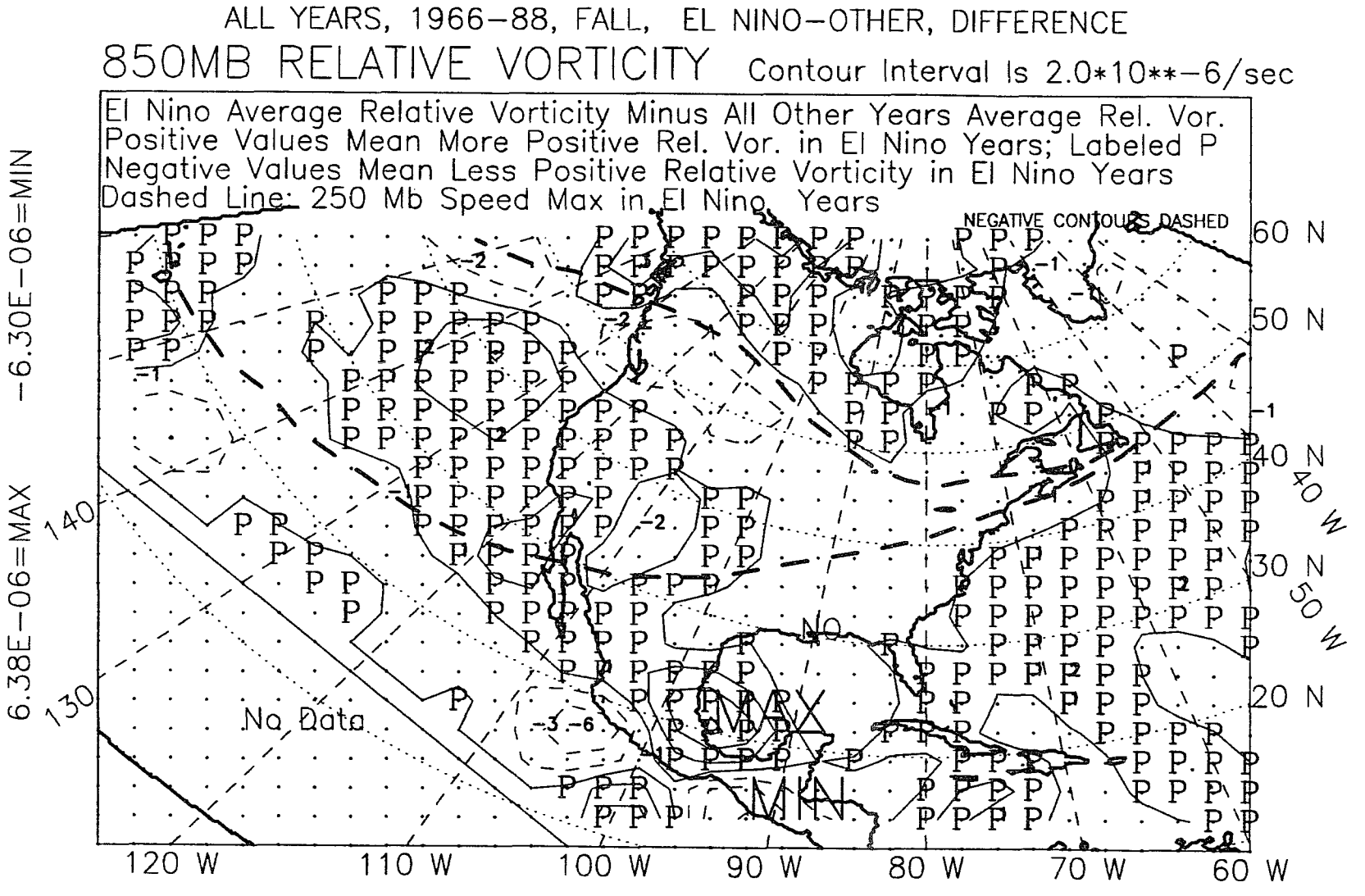

Figure F.23: 850–mb relative vorticity, fall, 1966–88, difference.

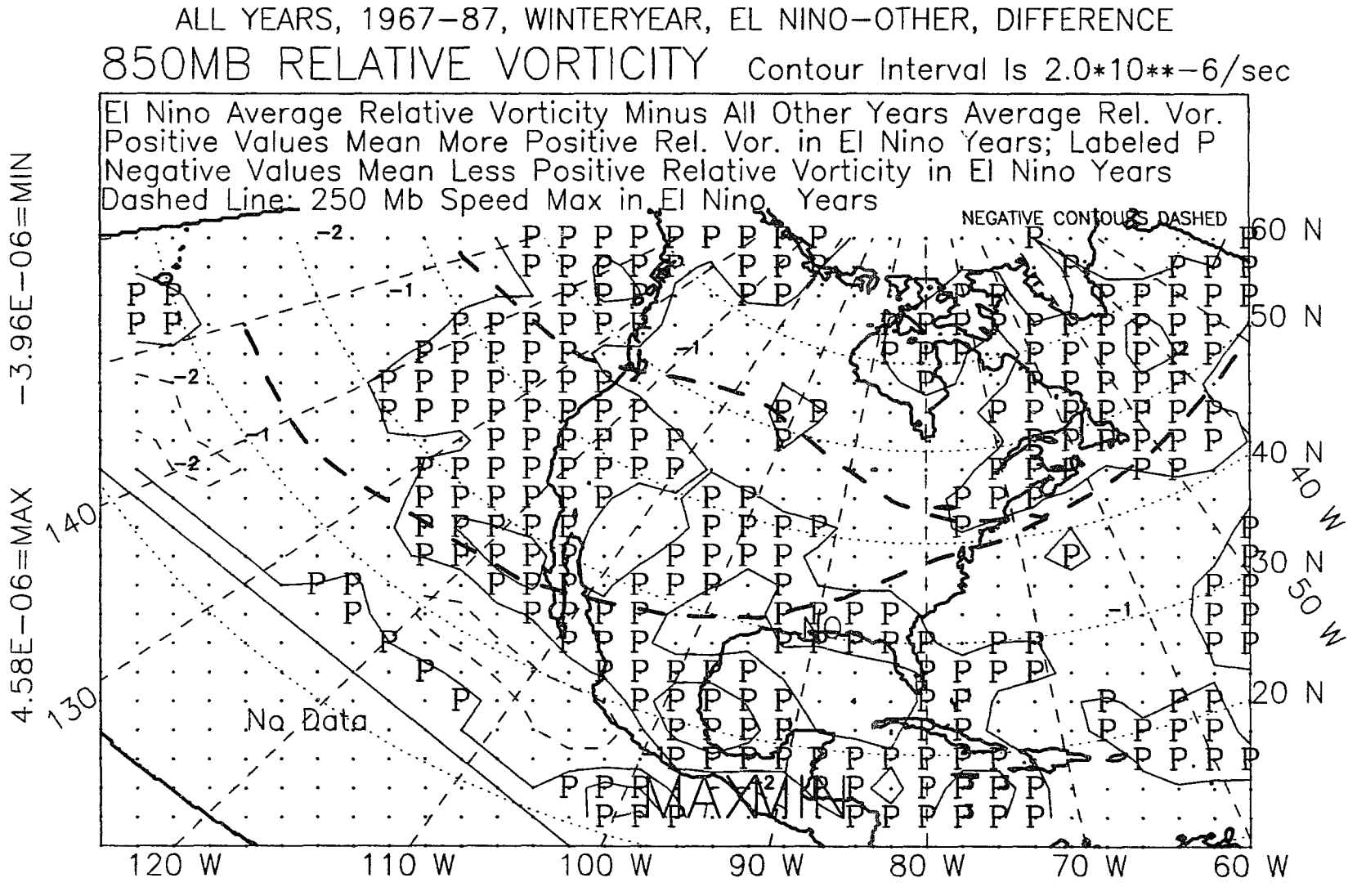

Figure F.24: 850–mb relative vorticity, winter year, 1967–87, difference.

APPENDIX G
700-MB HEIGHT FIELD

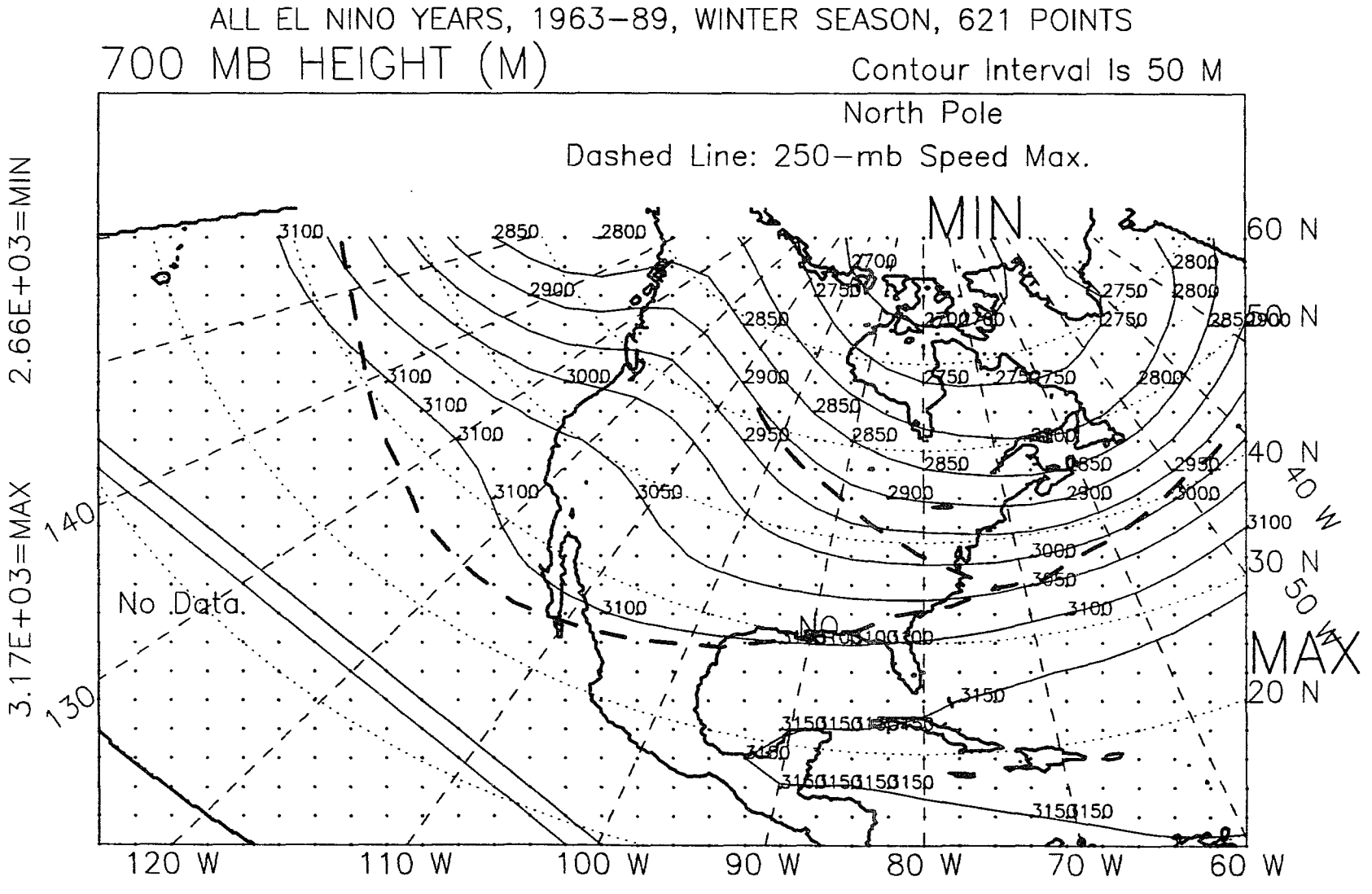

Figure G.1: 700–mb height, winter, El Niño years, 1963–89.

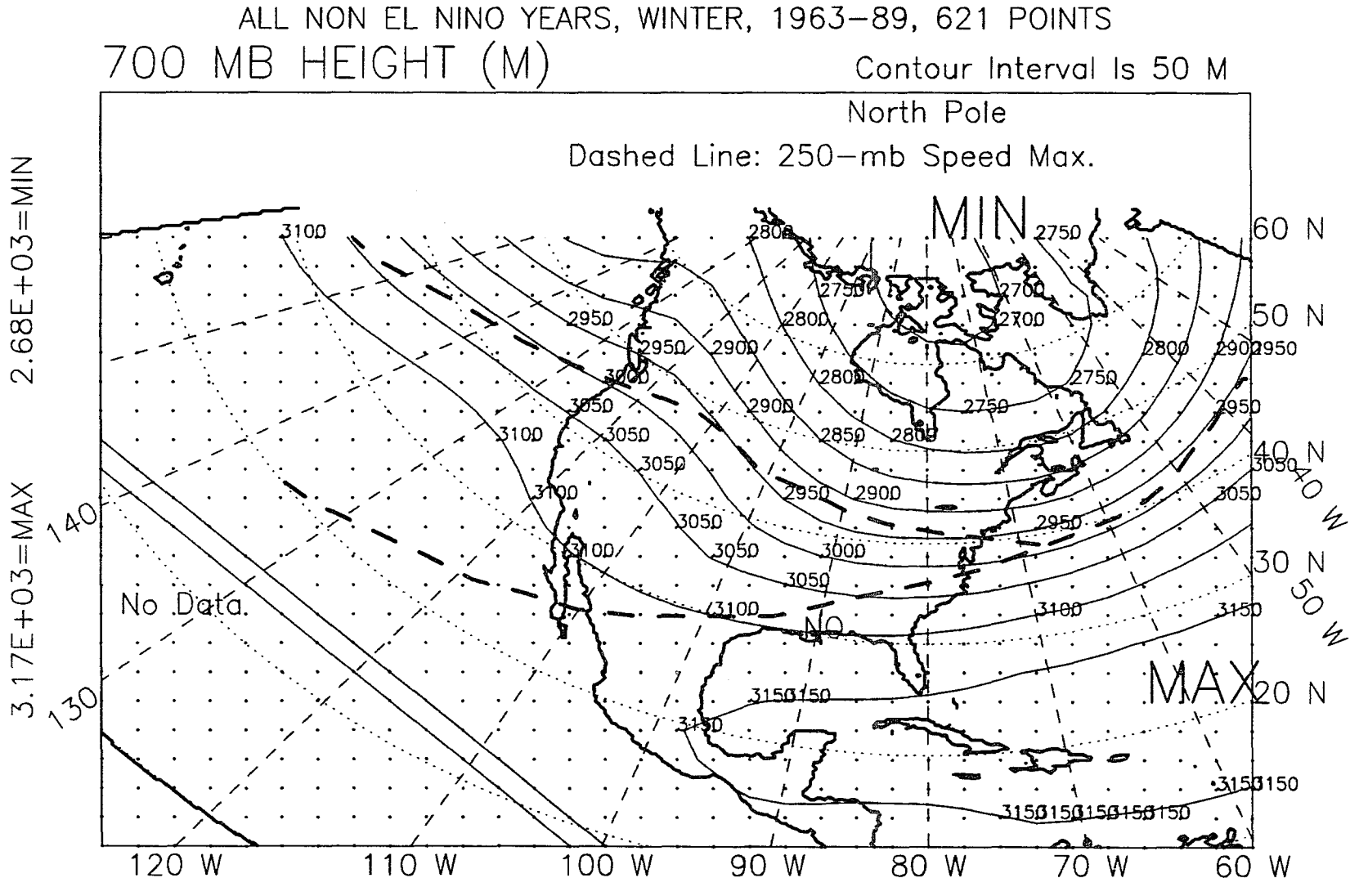

Figure G.2: 700-mb height, winter, non-El Niño years, 1963-89.

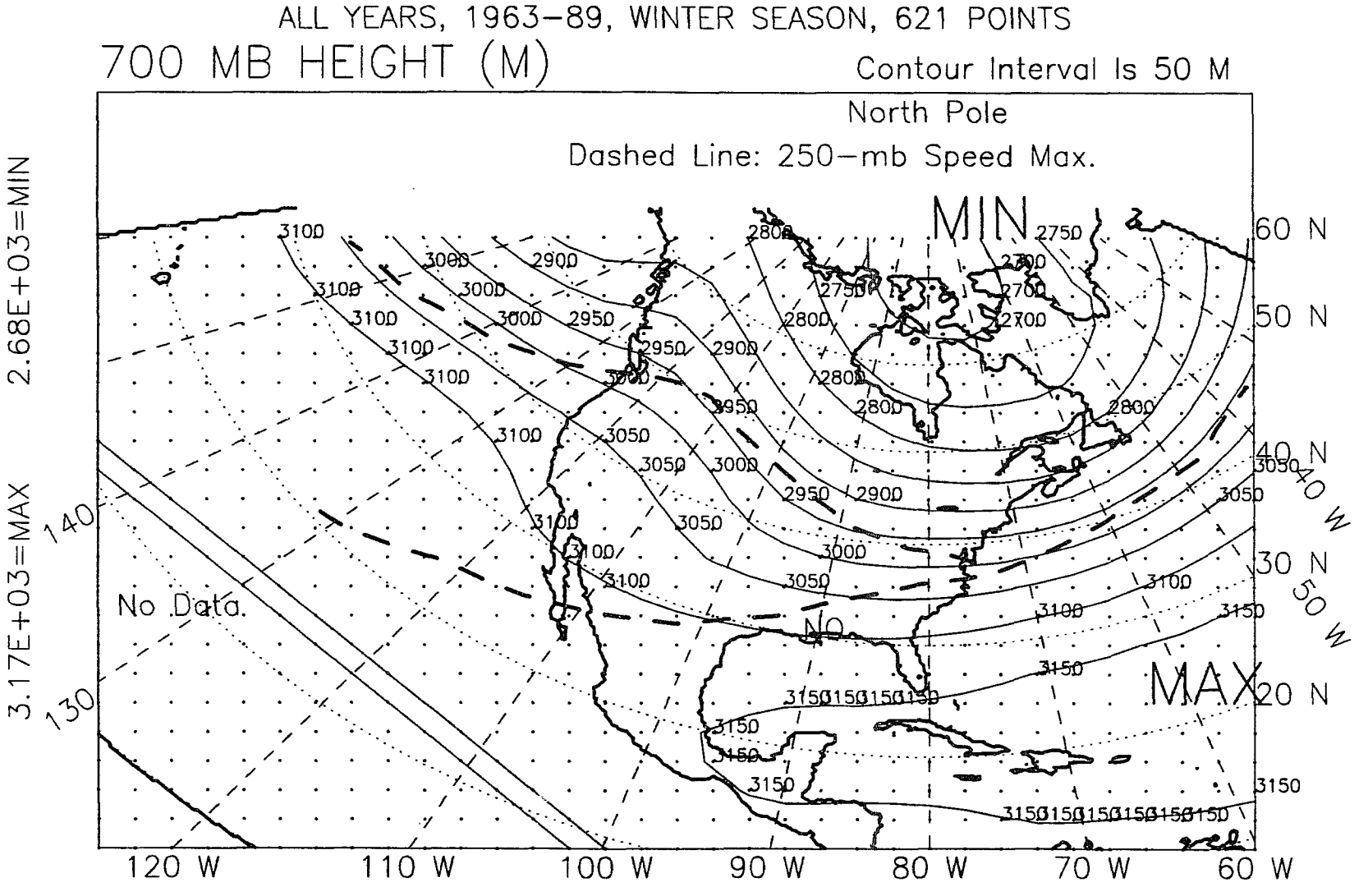

Figure G.3: 700–mb height, winter, all years, 1963–89.

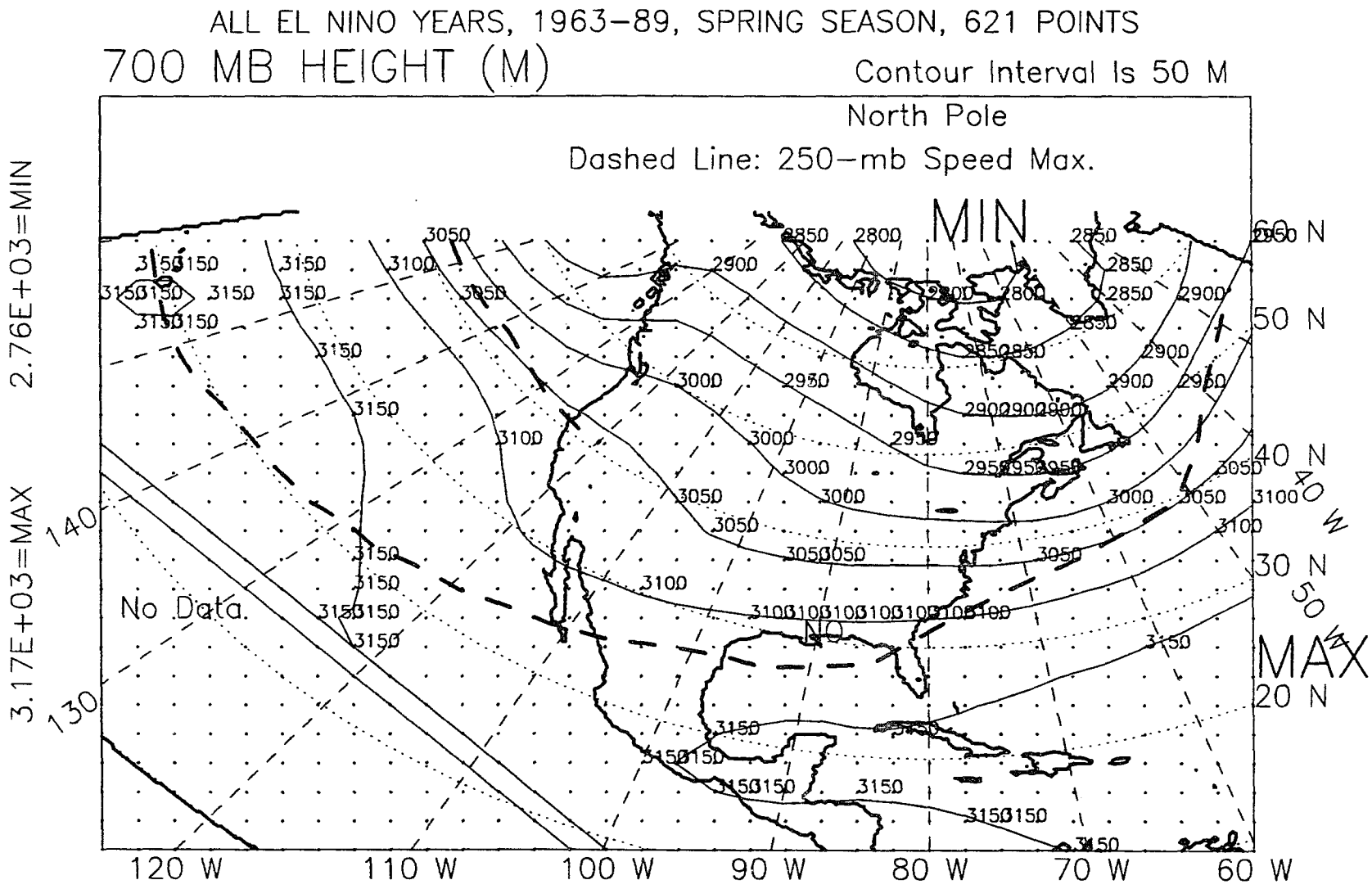

Figure G.4: 700–mb height, spring, El Niño years, 1963–89.

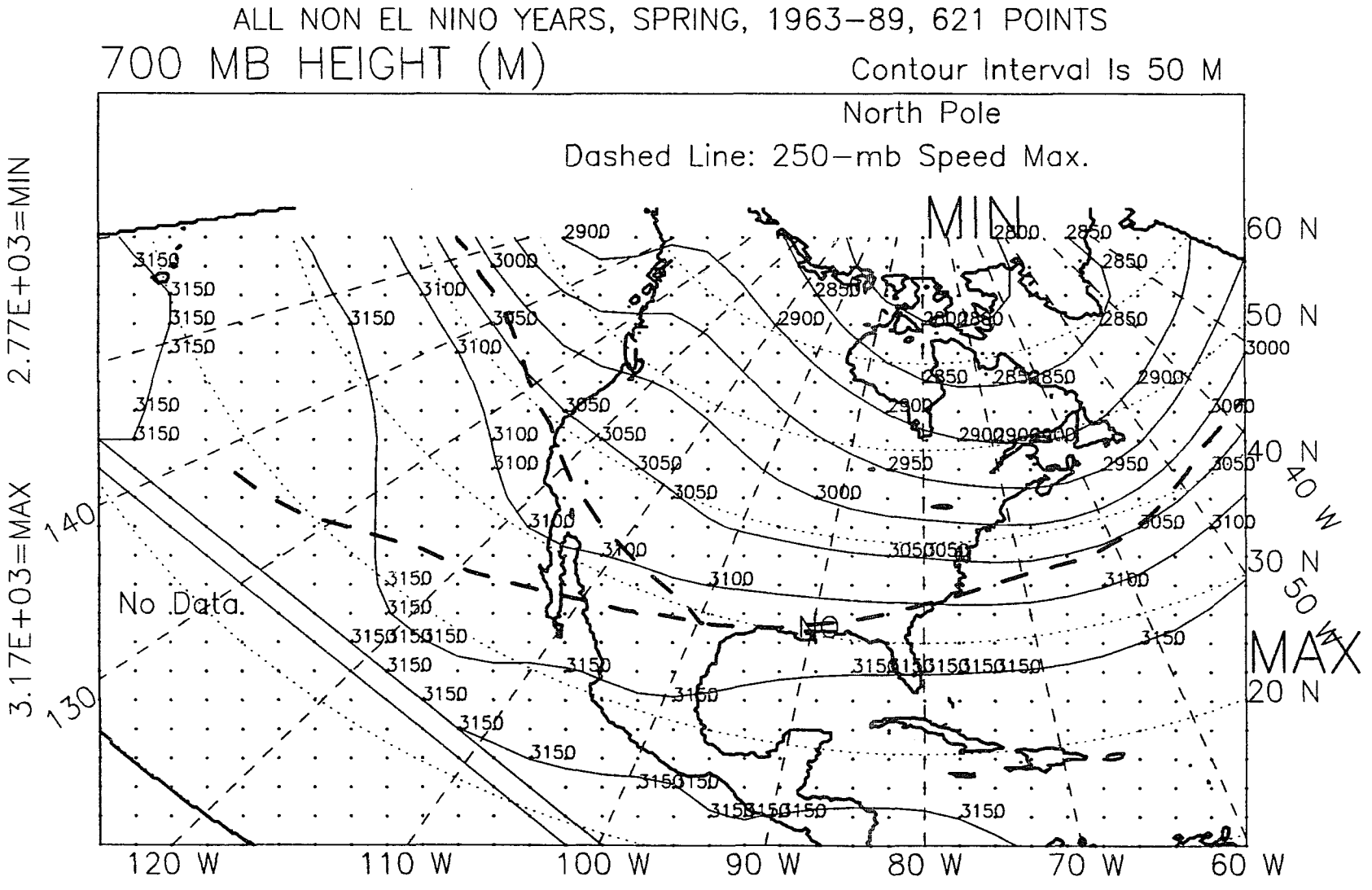

Figure G.5: 700–mb height, spring, non–El Niño years, 1963–89.

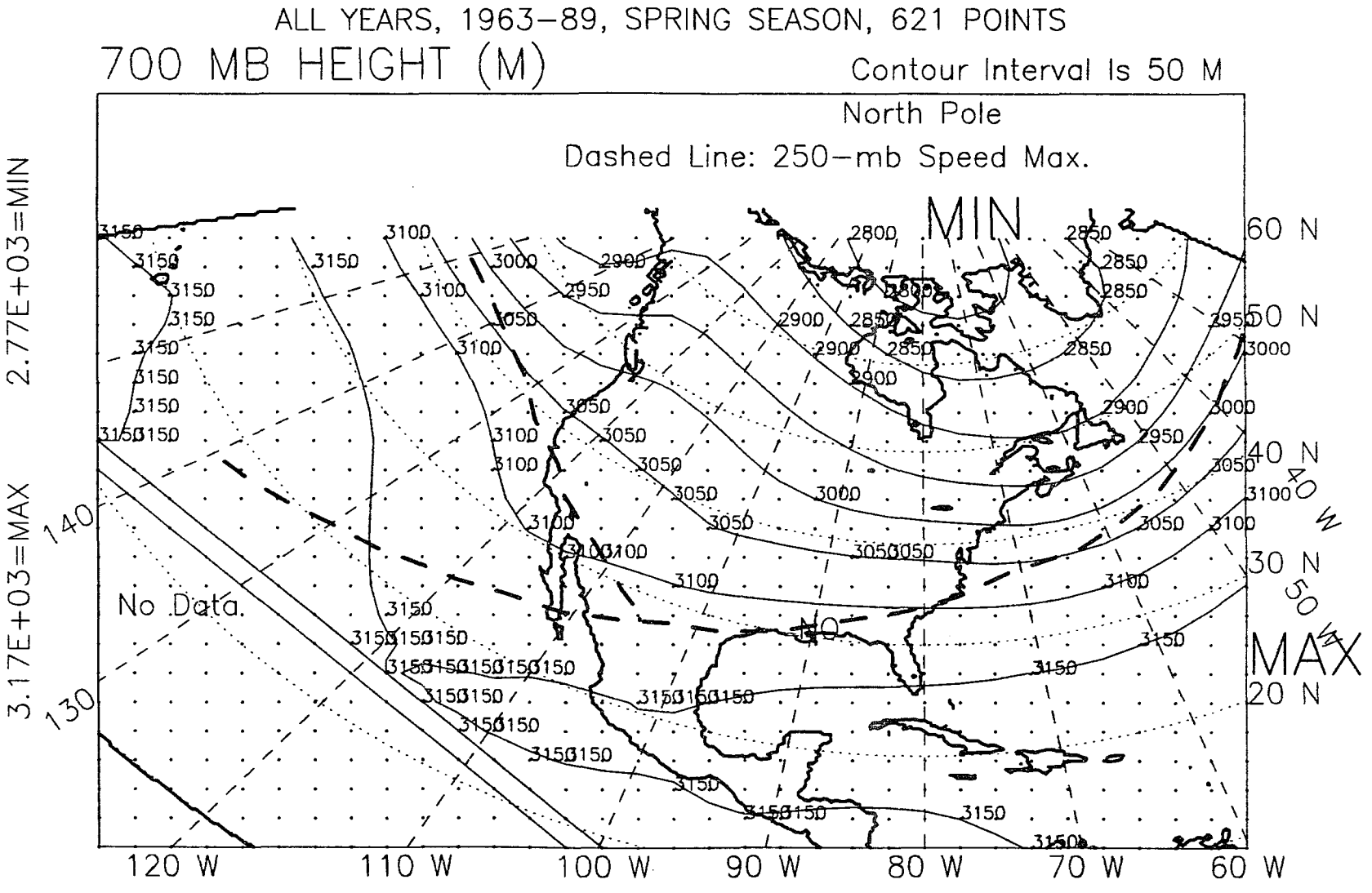

Figure G.6: 700–mb height, spring, all years, 1963–89.

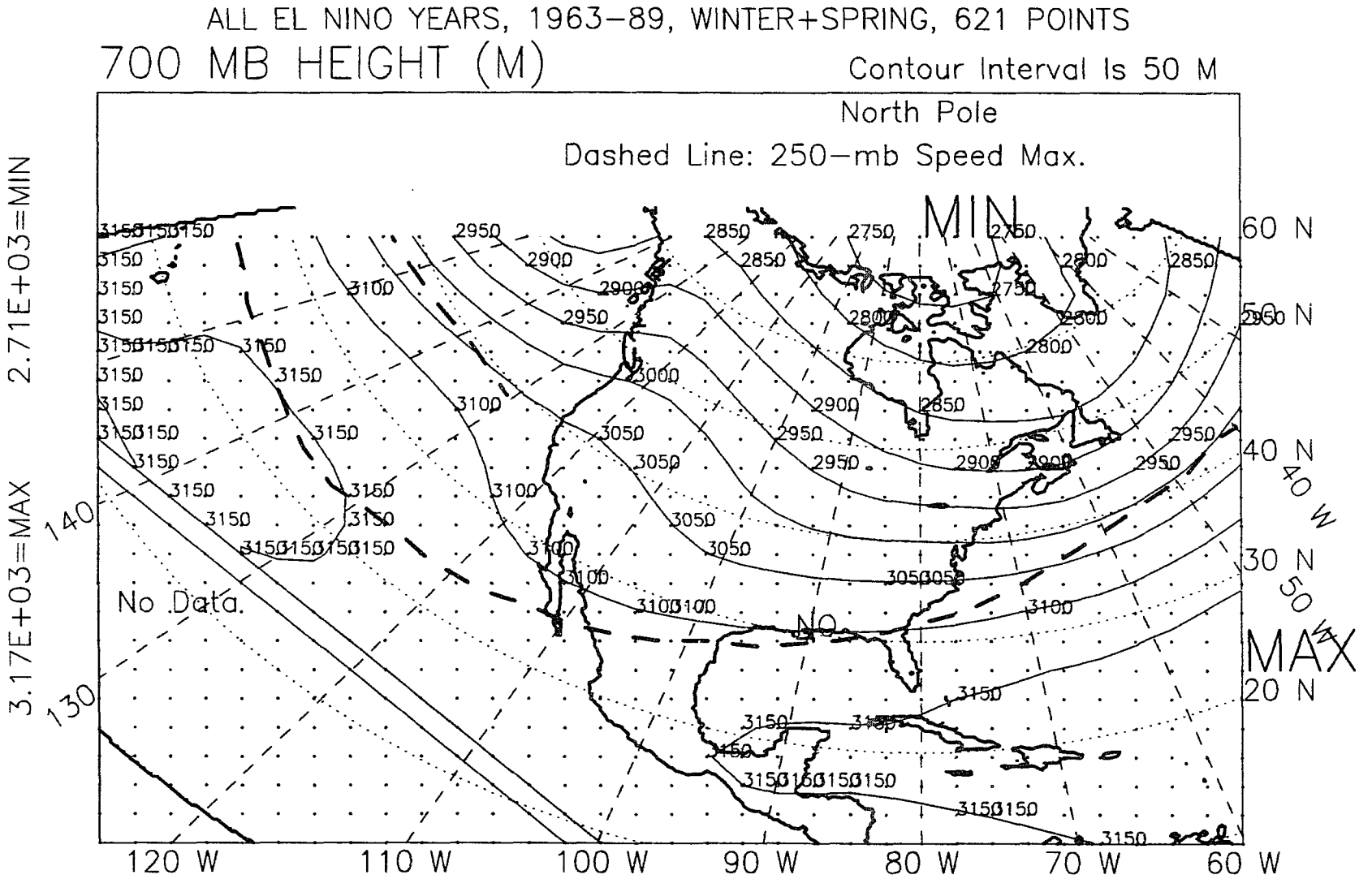

Figure G.7: 700–mb height, winter–plus–spring, El Niño years, 1963–89.

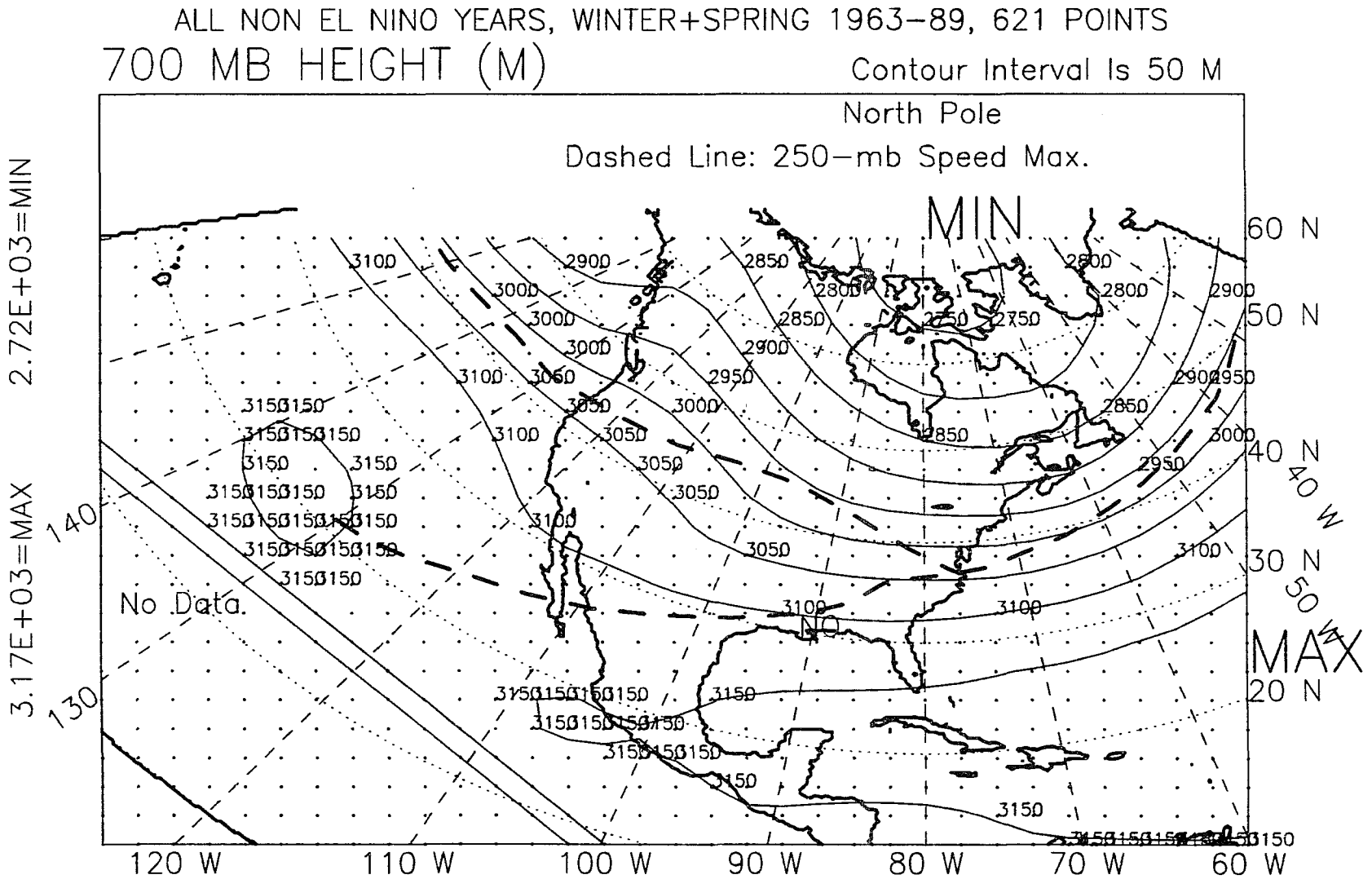

Figure G.8: 700-mb height, winter-plus-spring, non-El Niño years, 1963-89.

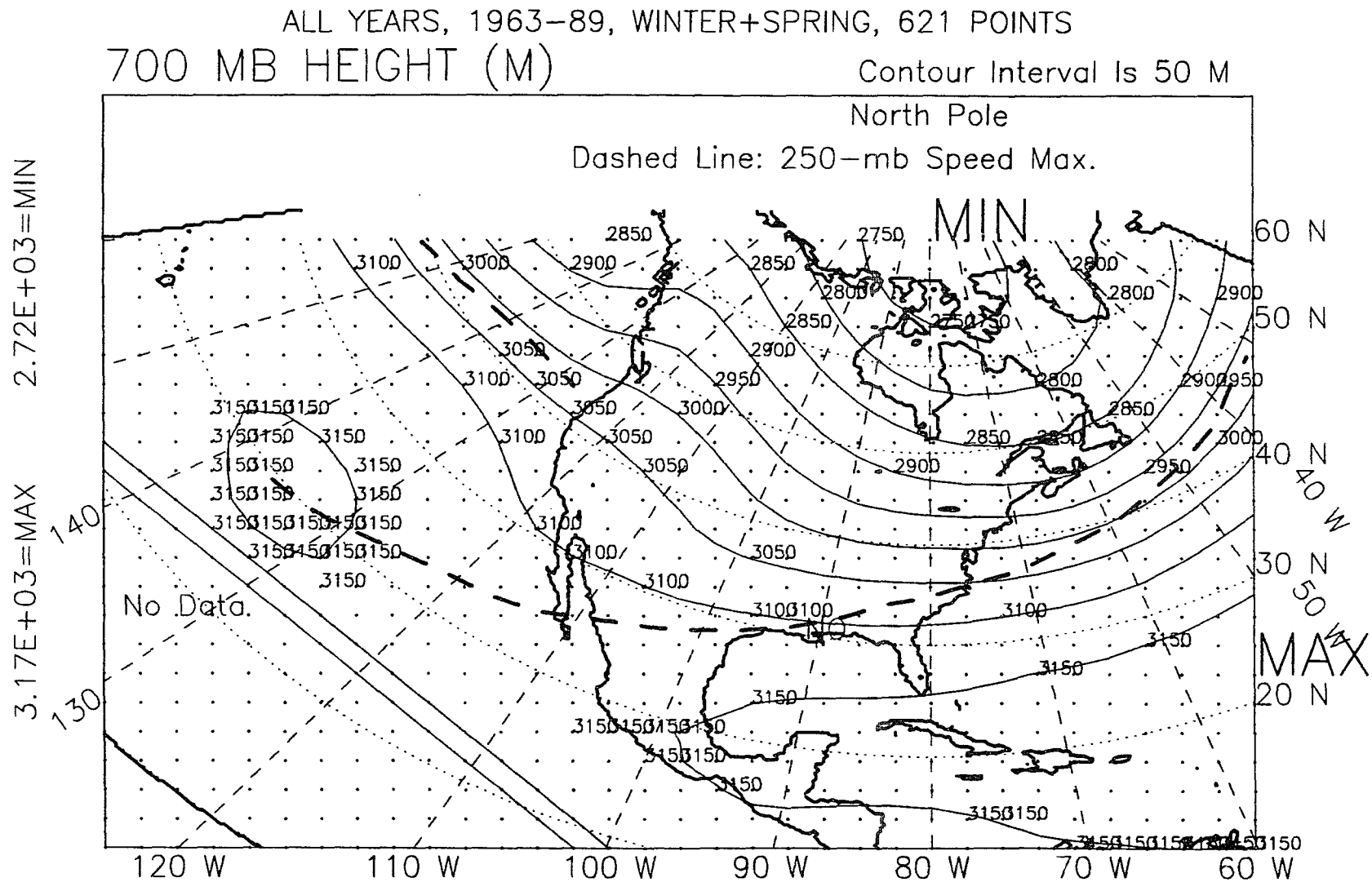

Figure G.9: 700–mb height, winter–plus–spring, all years, 1963–89.

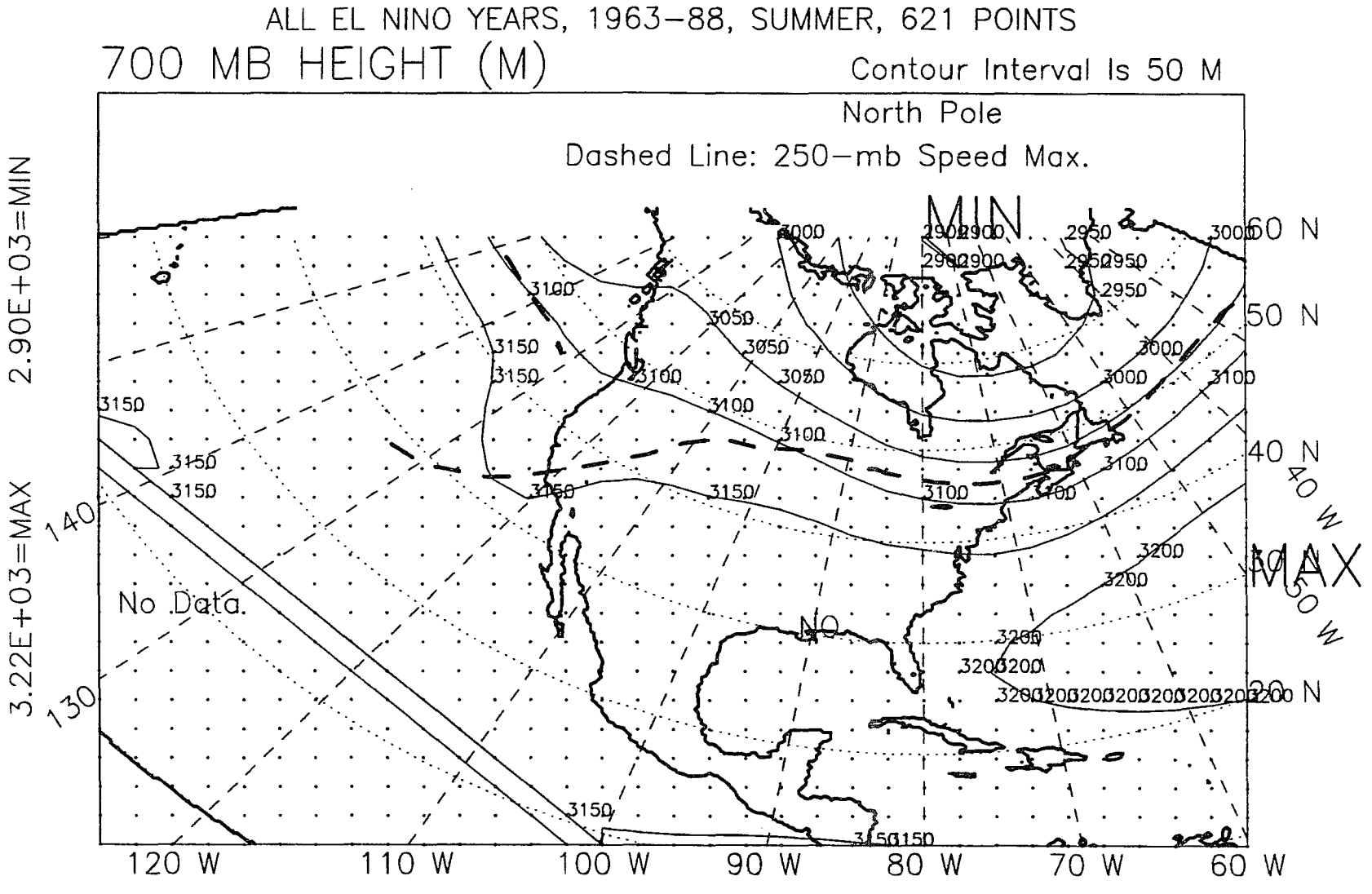

Figure G.10: 700–mb height, summer, El Niño years, 1963–88.

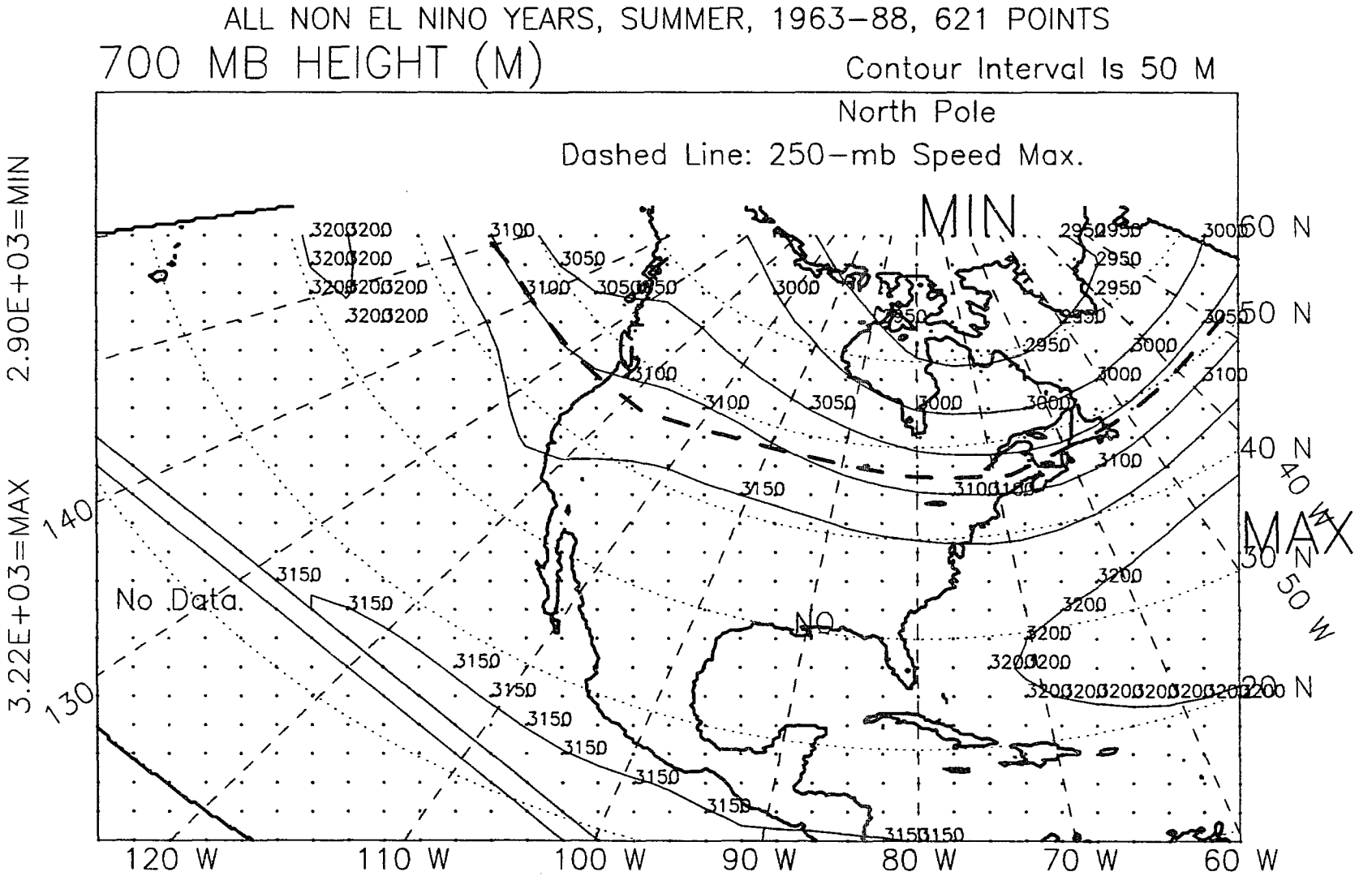

Figure G.11: 700–mb height, summer, non–El Niño years, 1963–88.

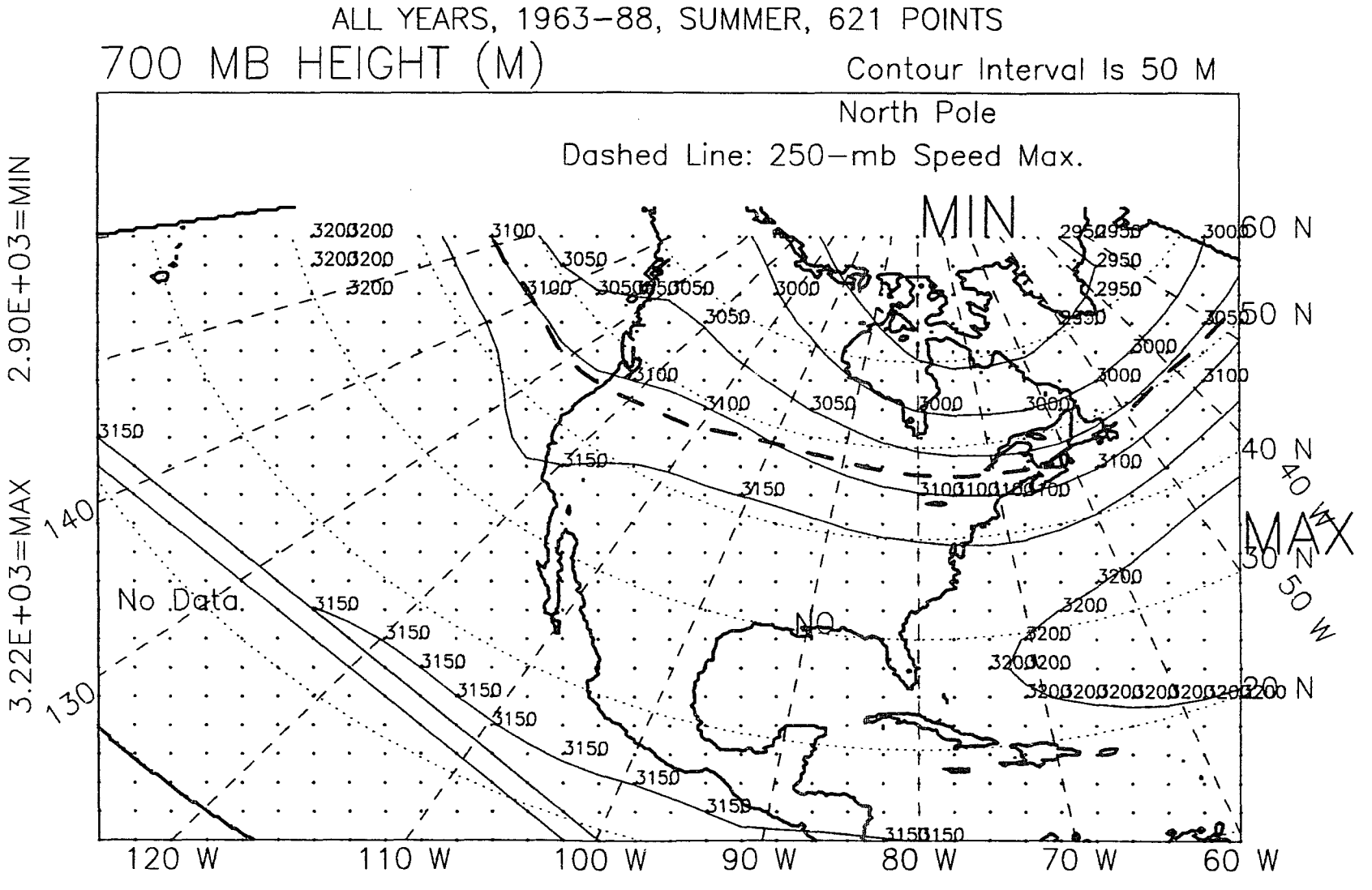

Figure G.12: 700–mb height, summer, all years, 1963–88.

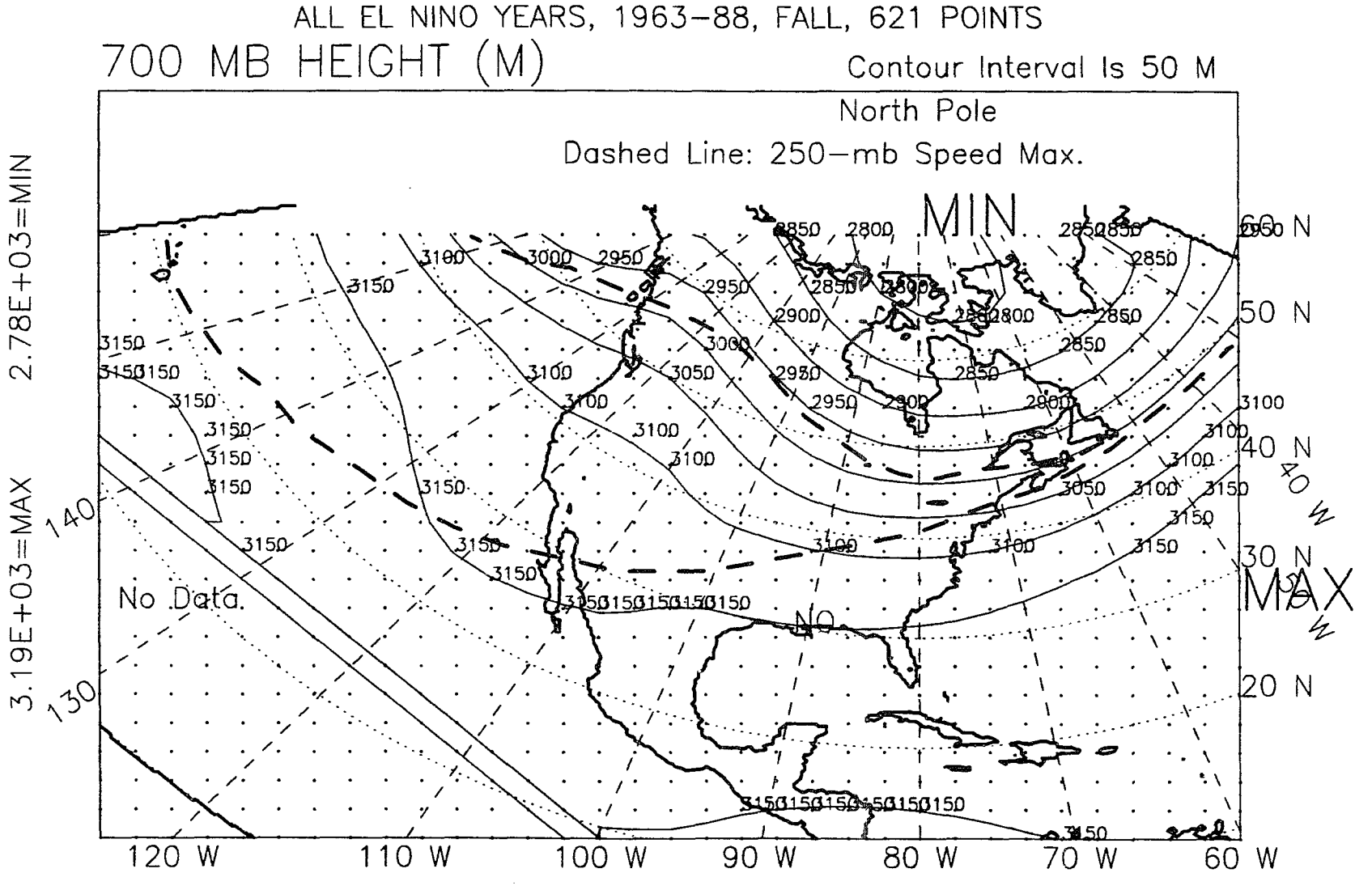

Figure G.13: 700–mb height, fall, El Niño years, 1963–88.

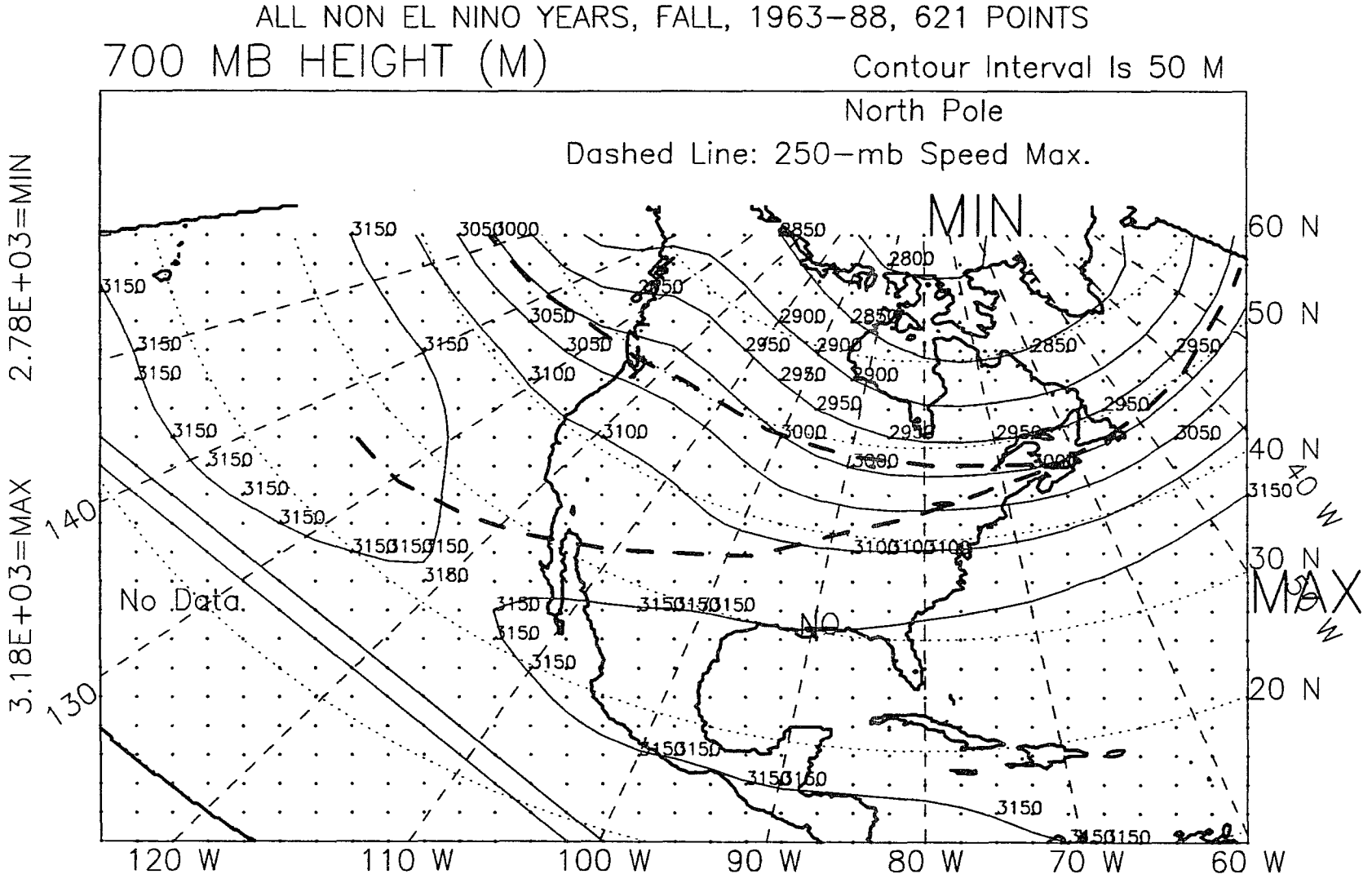

Figure G.14: 700–mb height, fall, non–El Niño years, 1963–88.

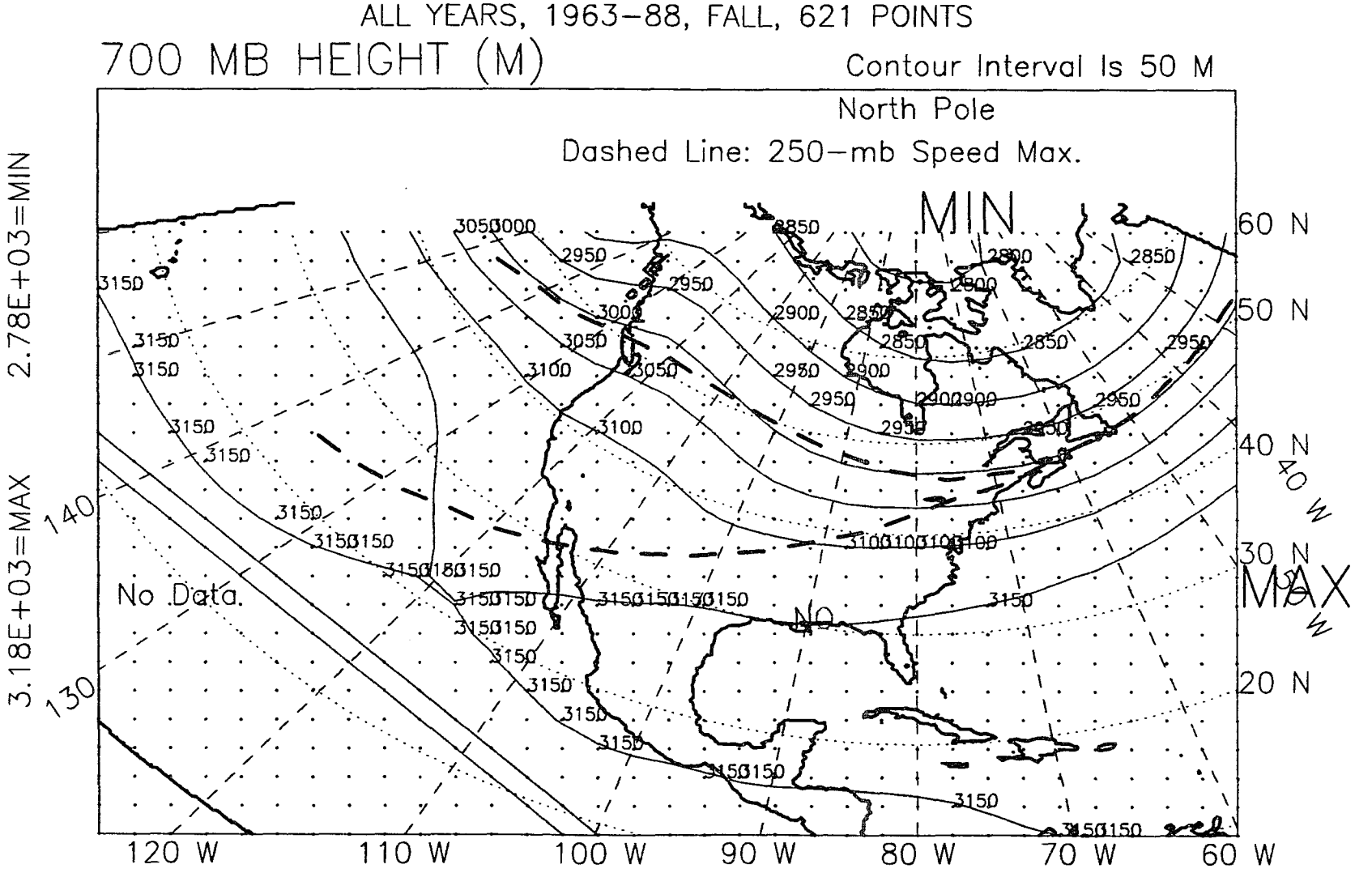

Figure G.15: 700–mb height, fall, all years, 1963–88.

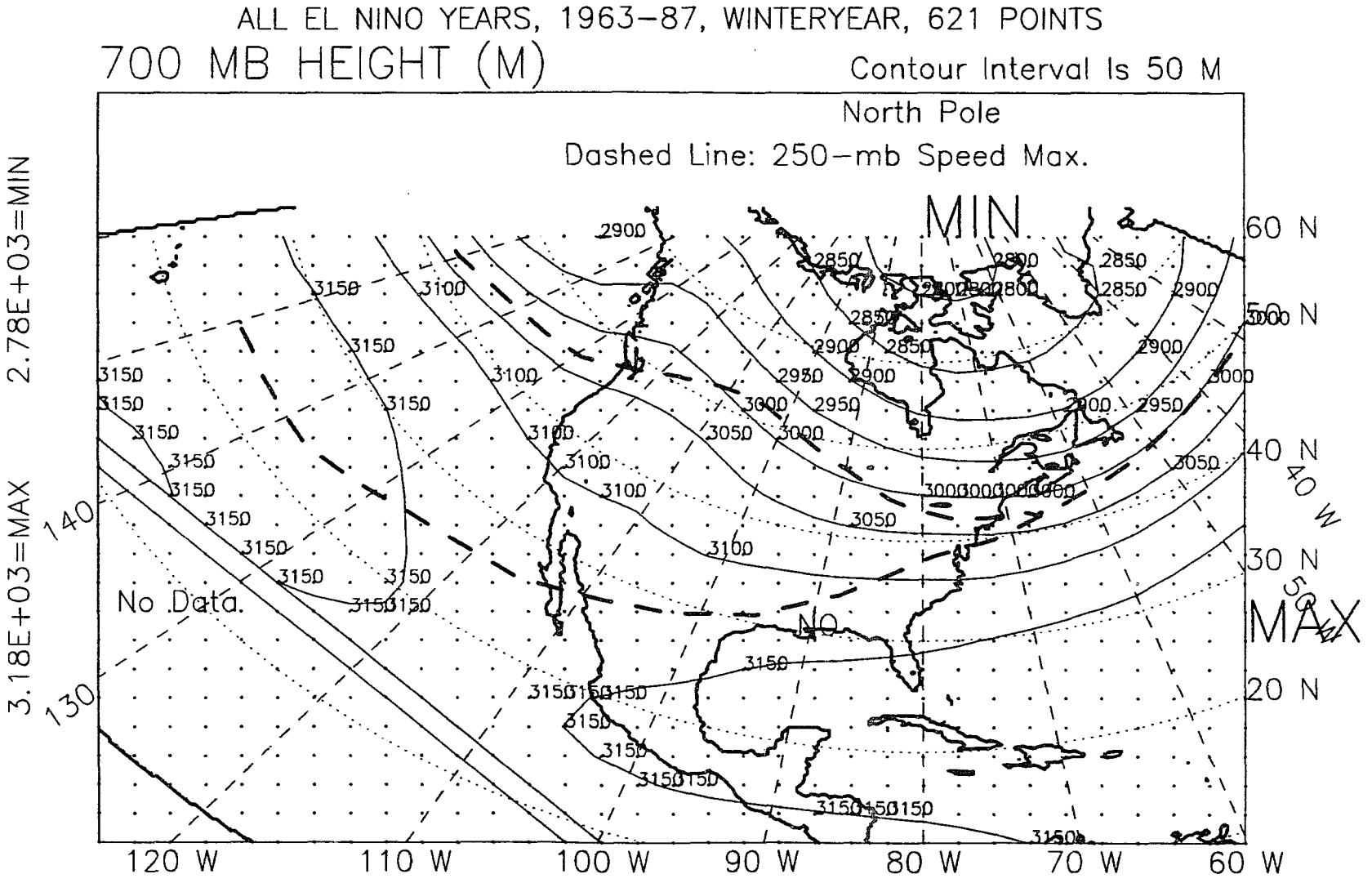

Figure G.16: 700–mb height, winter year, El Niño years, 1963–87.

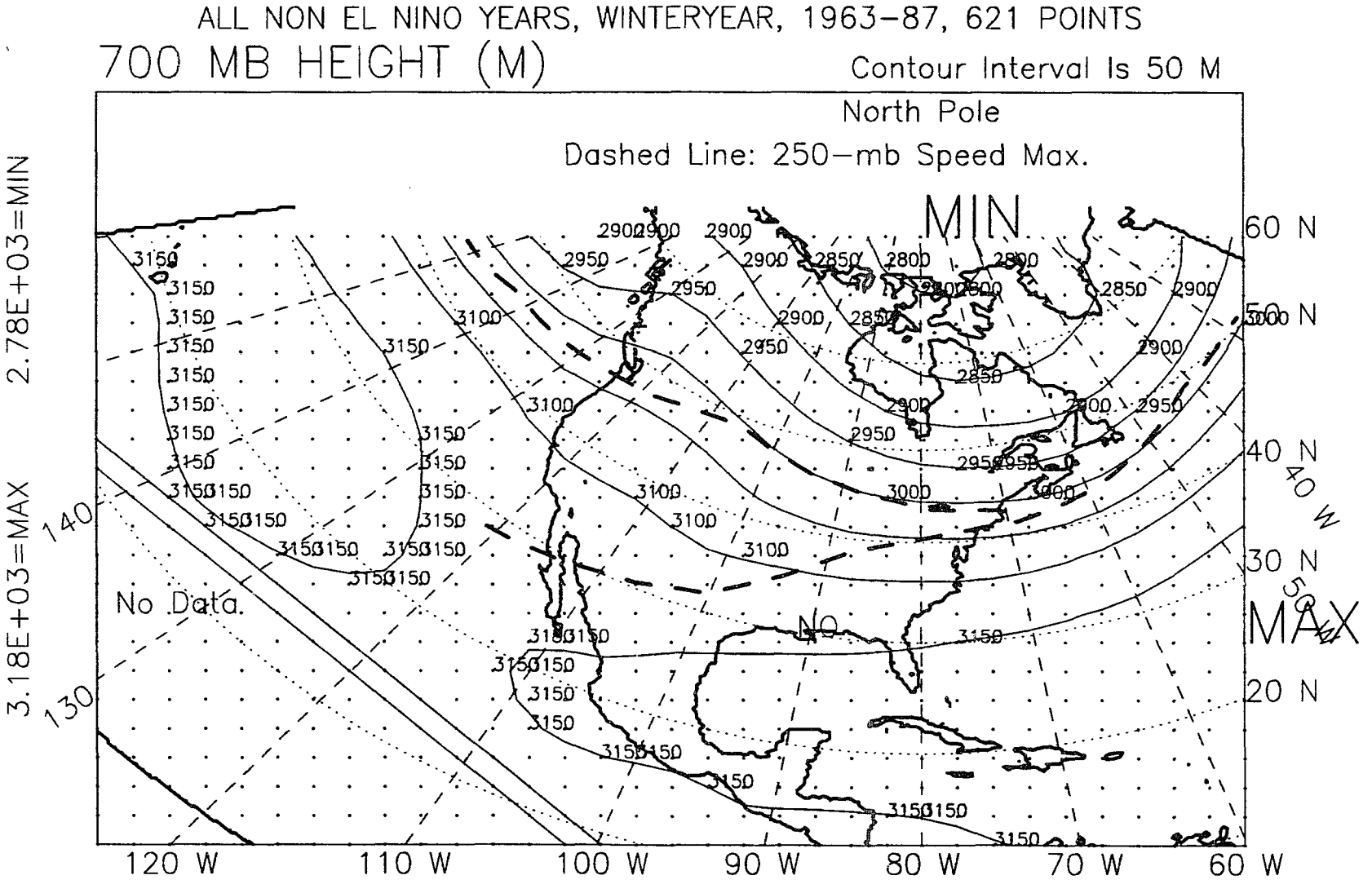

Figure G.17: 700-mb height, winter year, non-El Niño years, 1963-87.

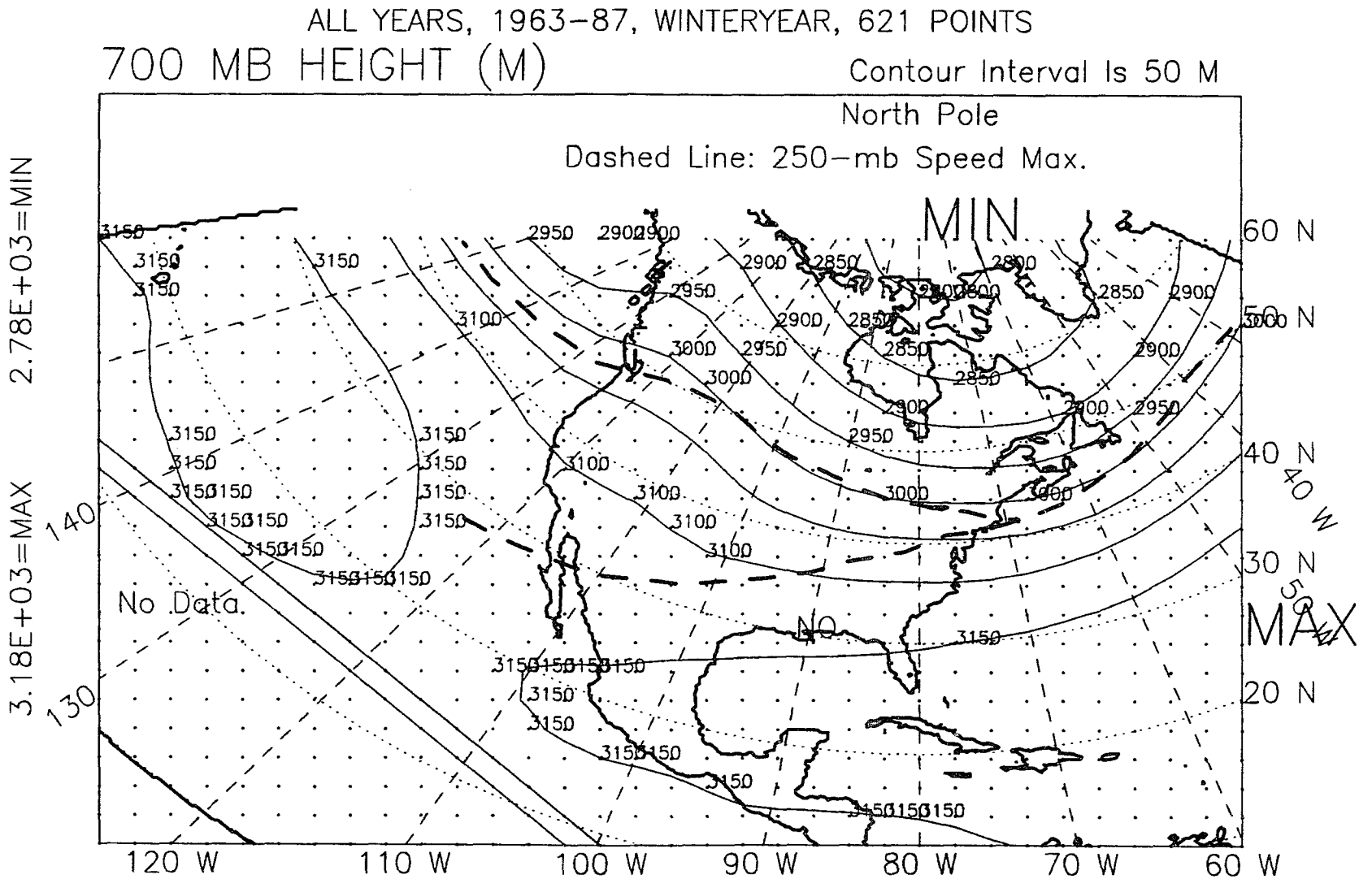

Figure G.18: 700-mb height, winter year, all years, 1963-87.

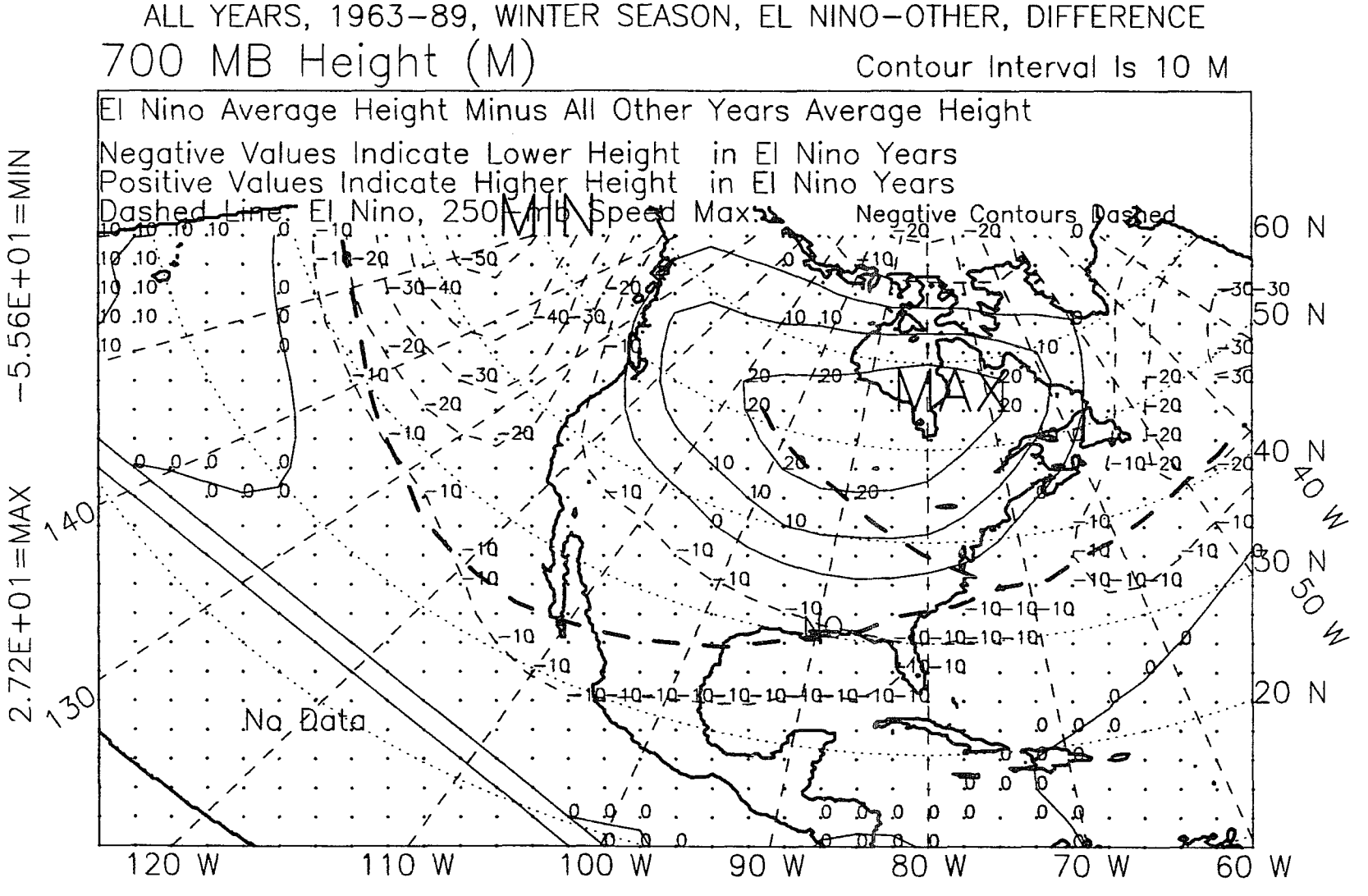

Figure G.19: 700–mb height, winter, 1963–89, difference.

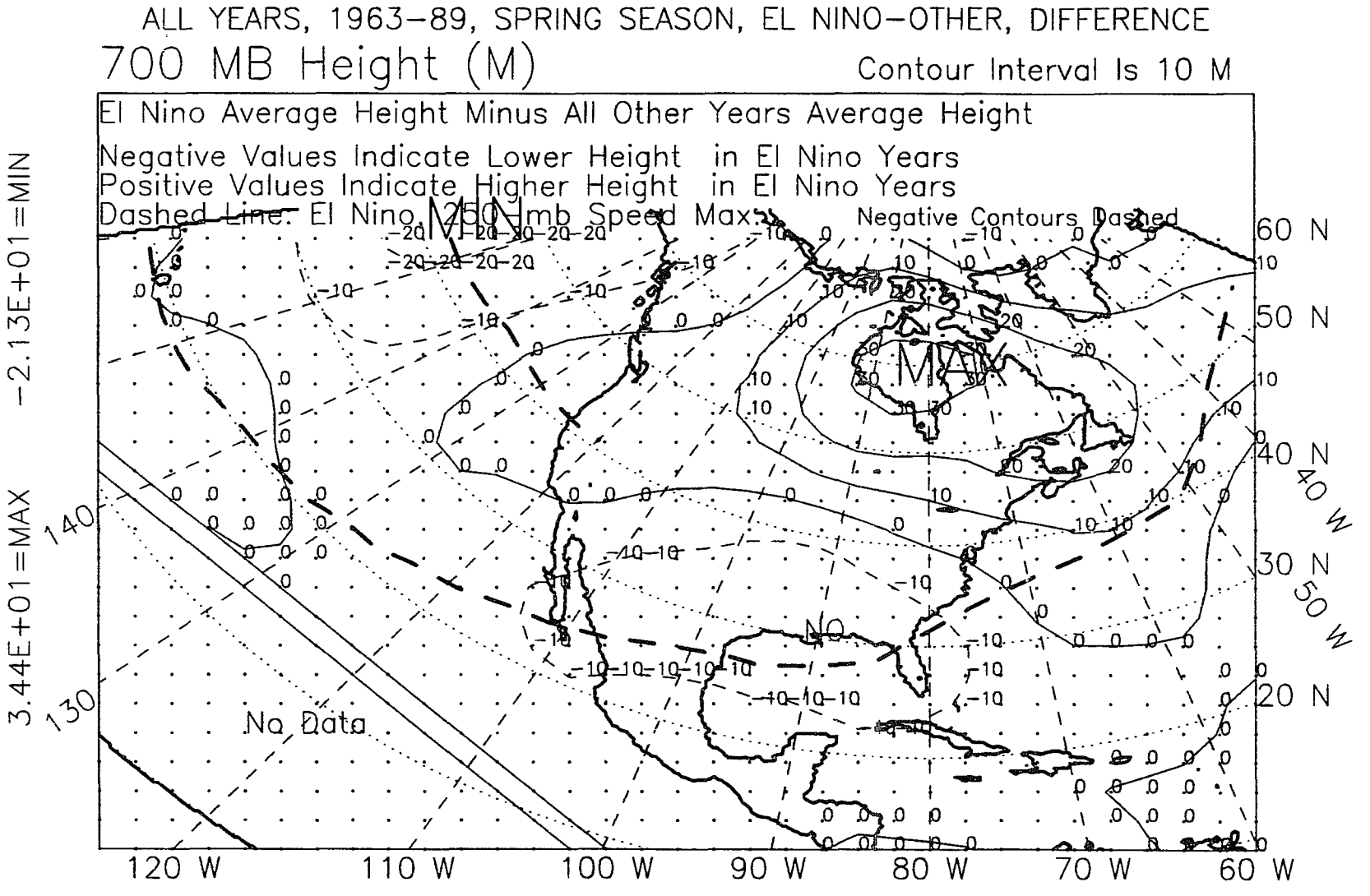

Figure G.20: 700–mb height, spring, 1963–89, difference.

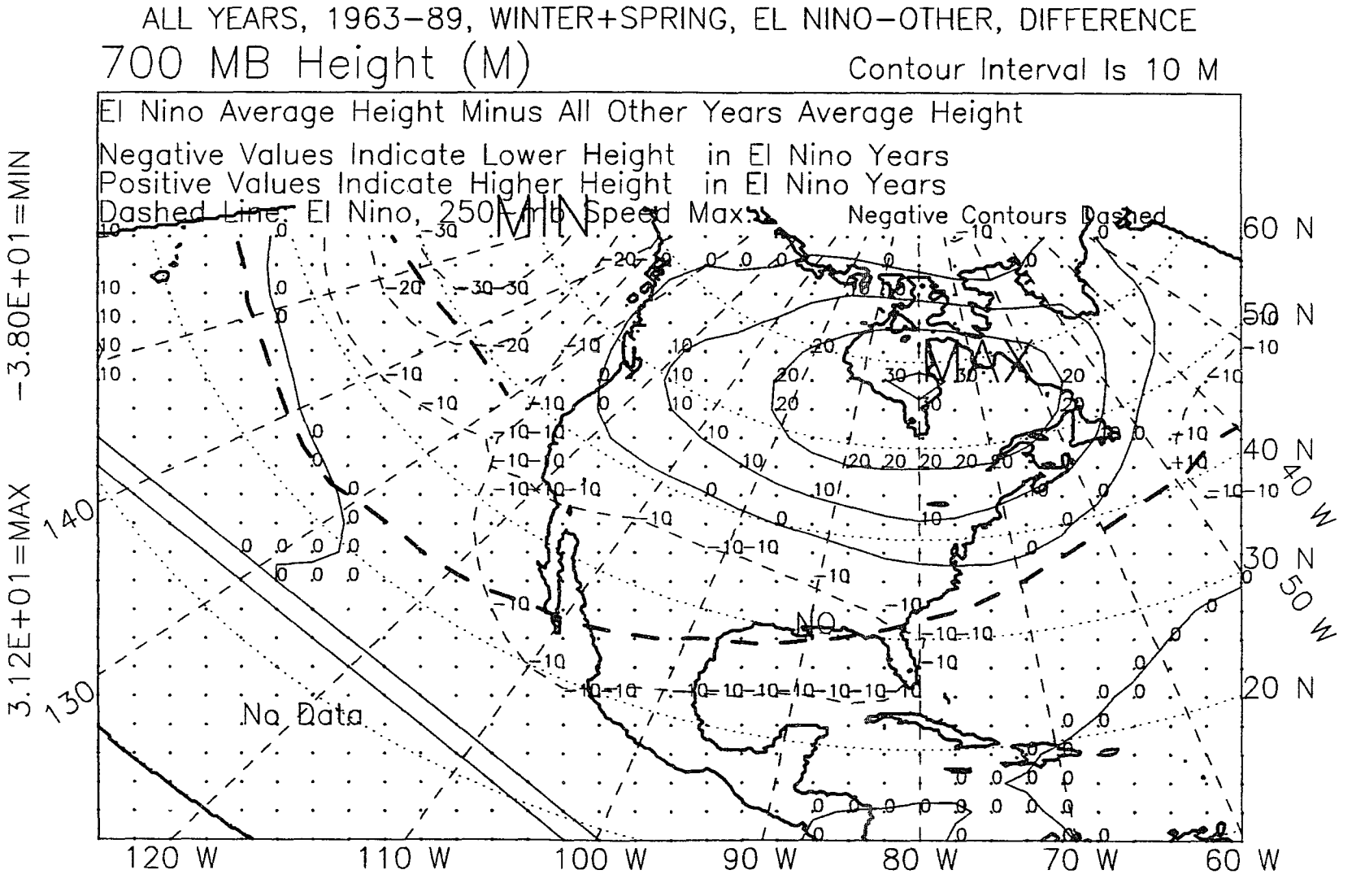

Figure G.21: 700–mb height, winter–plus–spring, 1963–89, difference.

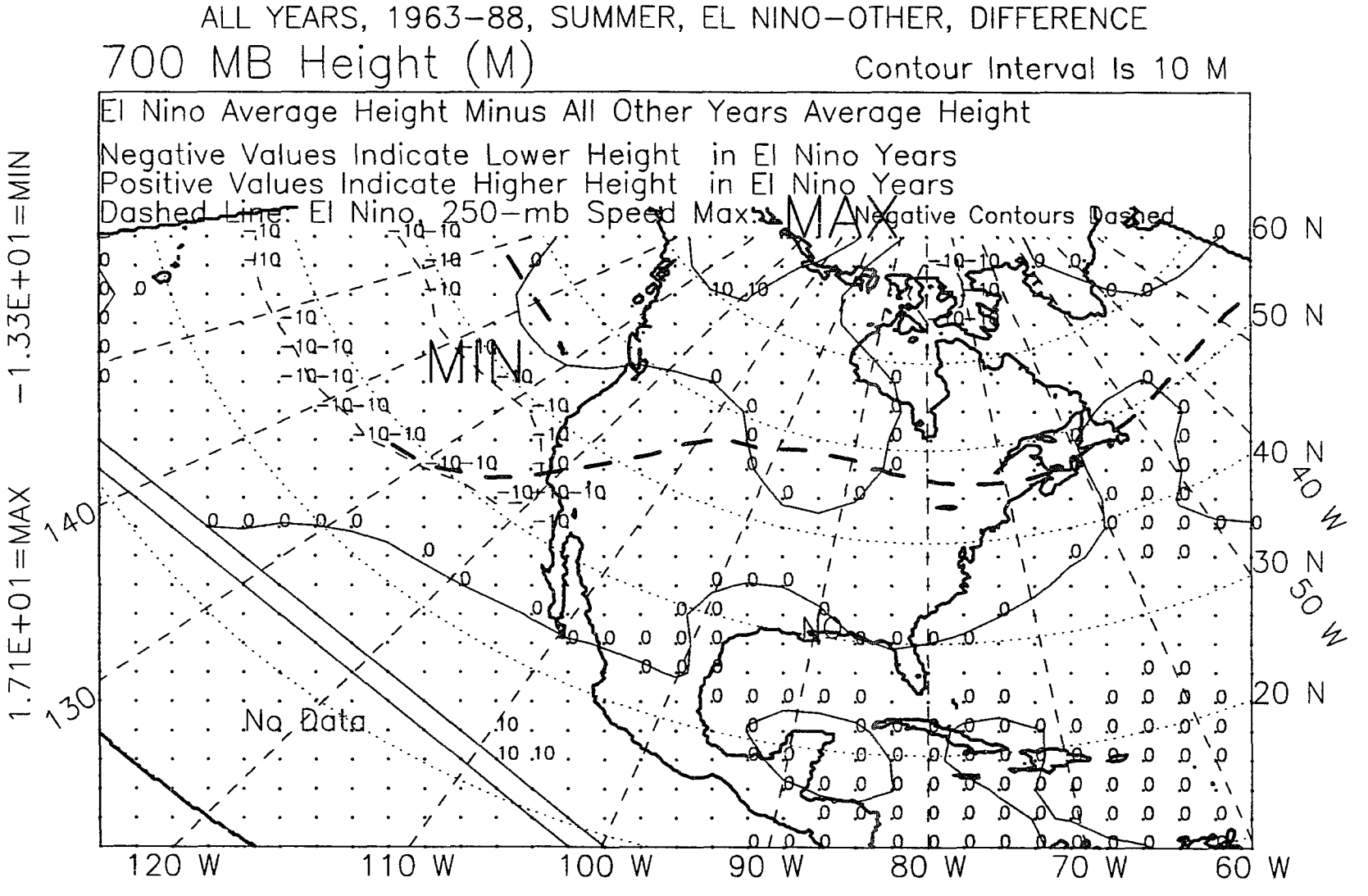

Figure G.22: 700–mb height, summer, 1963–88, difference.

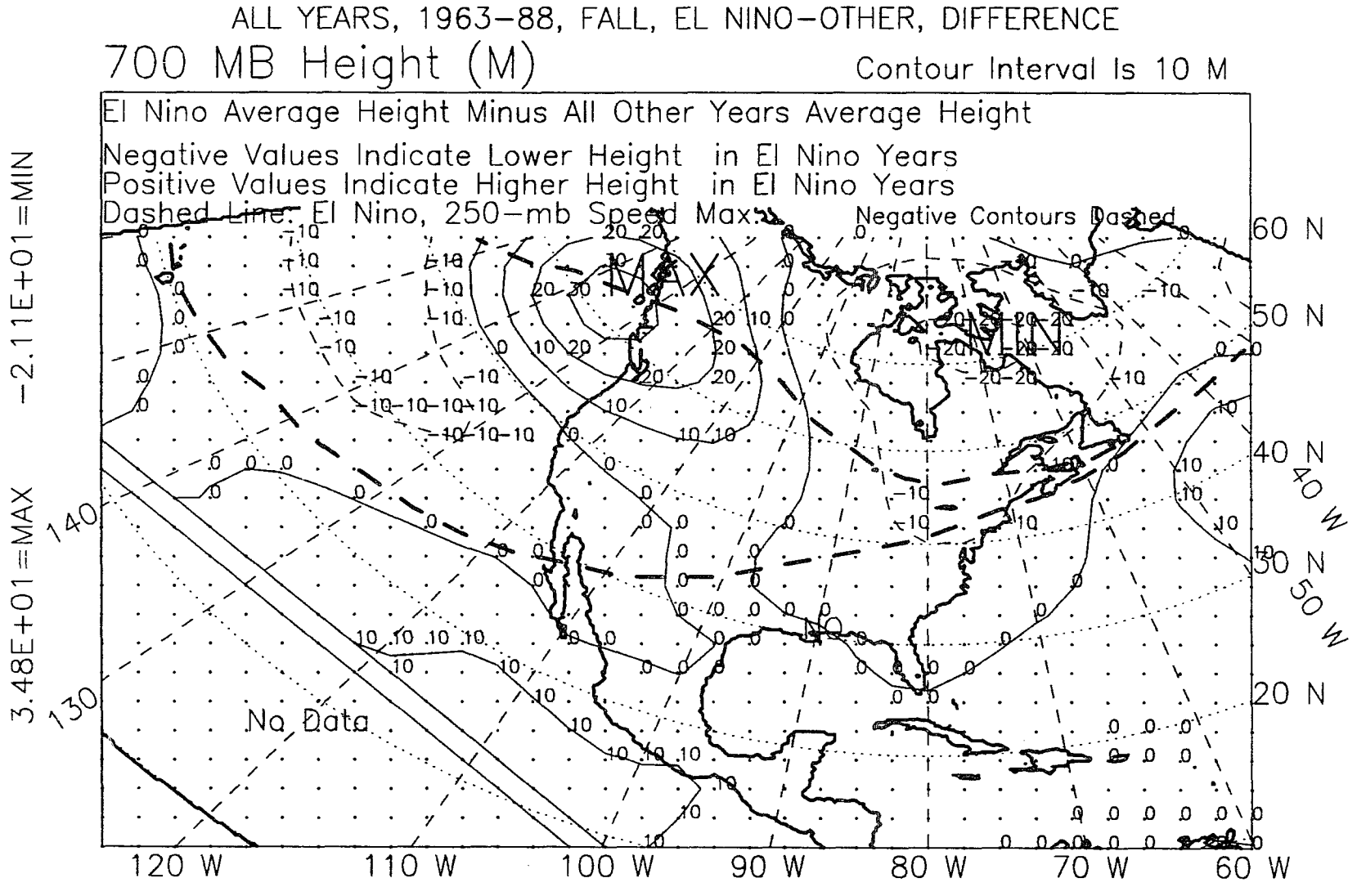

Figure G.23: 700–mb height, fall, 1963–88, difference.

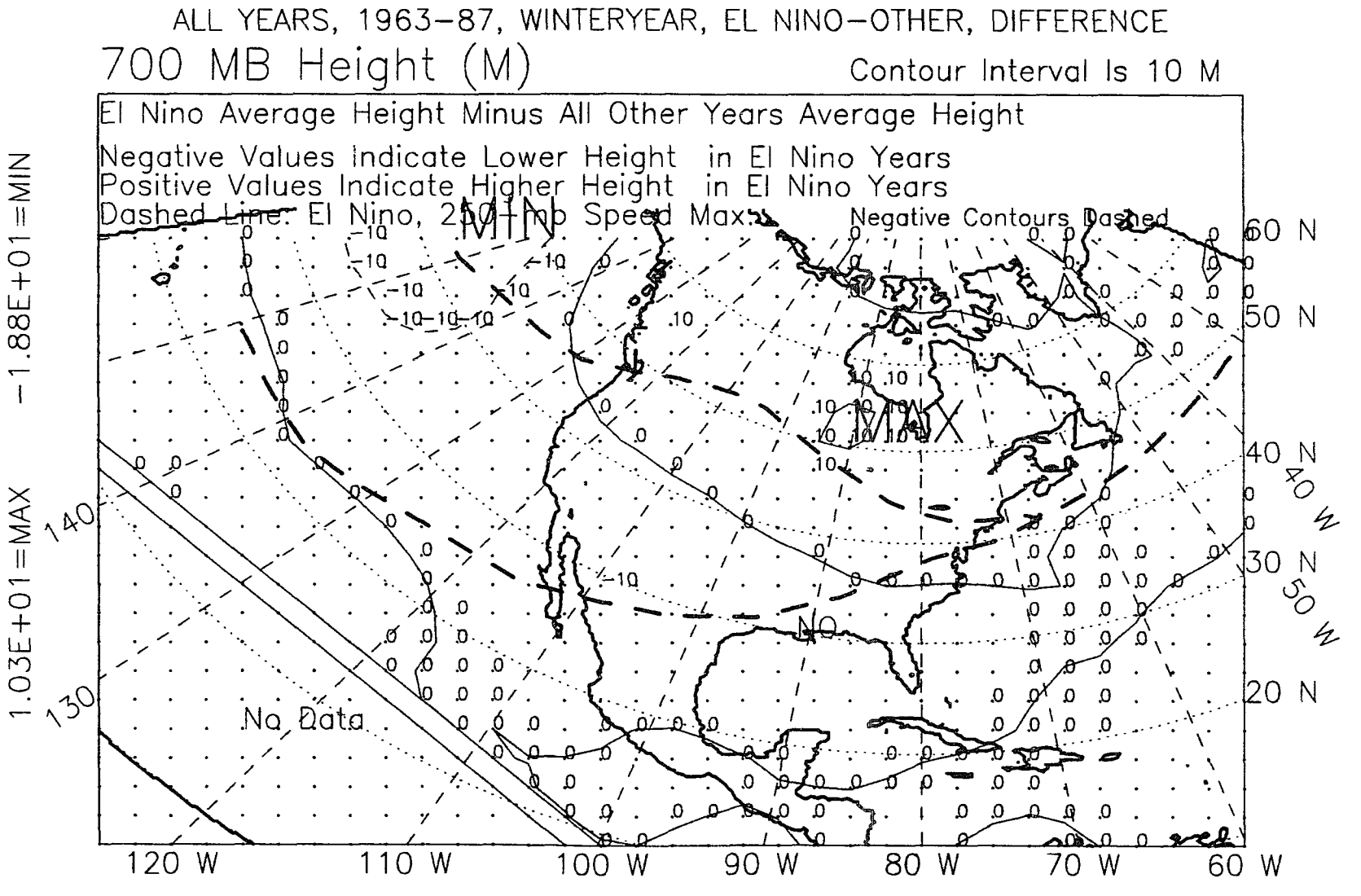

Figure G.24: 700–mb height, winter year, 1963–87, difference.

APPENDIX H
500-MB HEIGHT FIELD

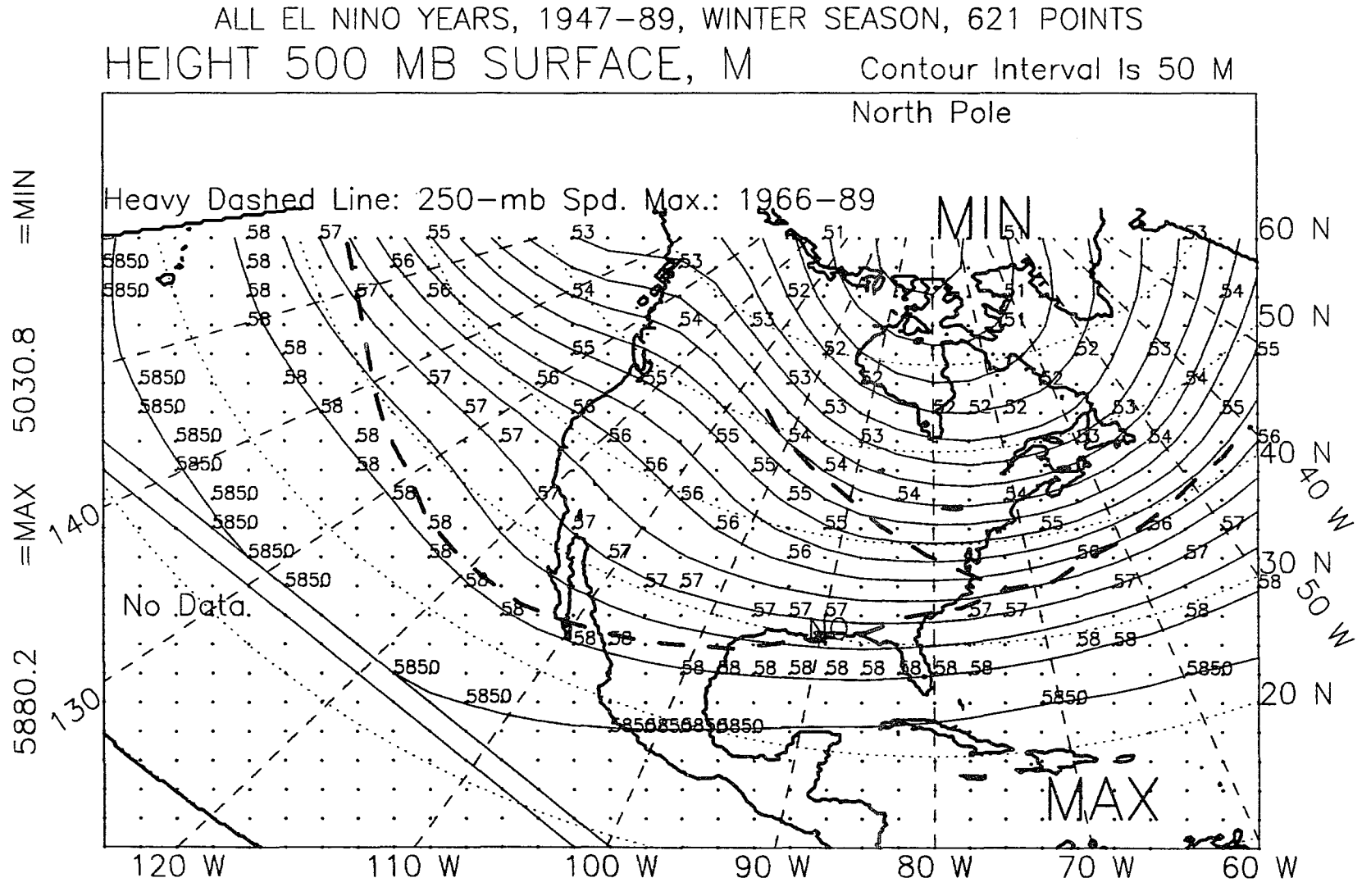

Figure H.1: 500–mb height, winter, El Niño years, 1947–89.

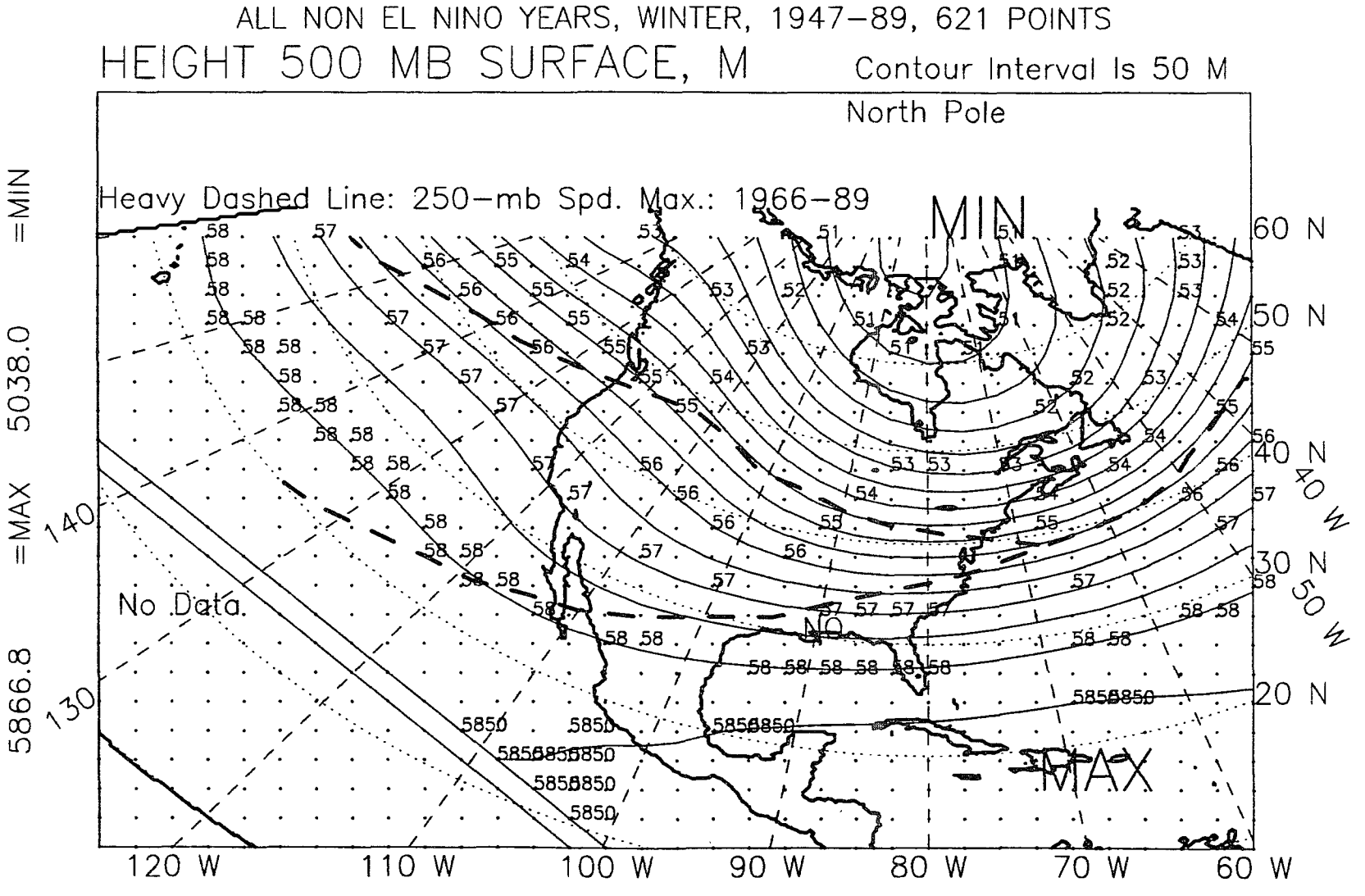

Figure H.2: 500–mb height, winter, non–El Niño years, 1947–89.

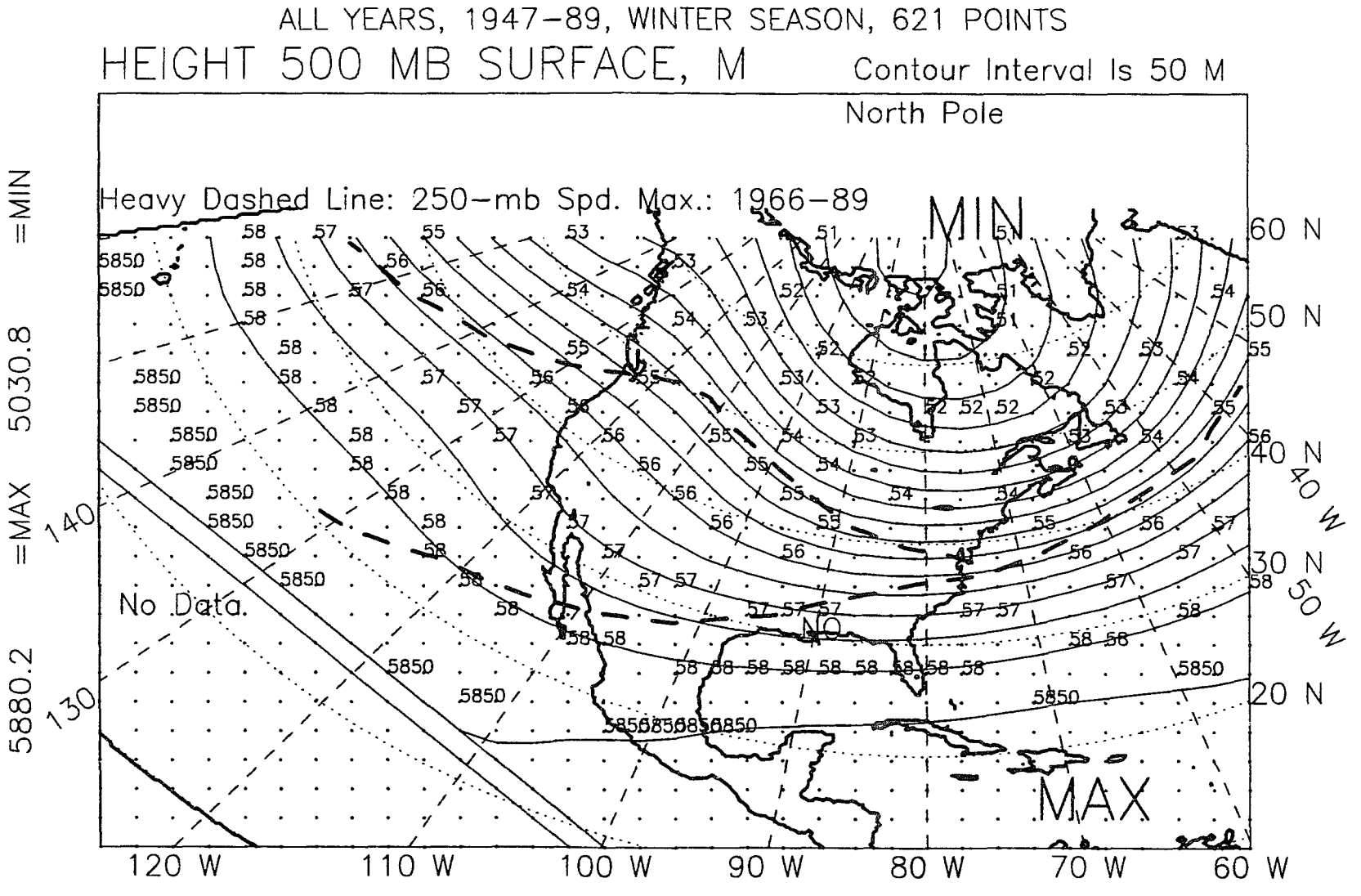

Figure H.3: 500–mb height, winter, all years, 1947–89.

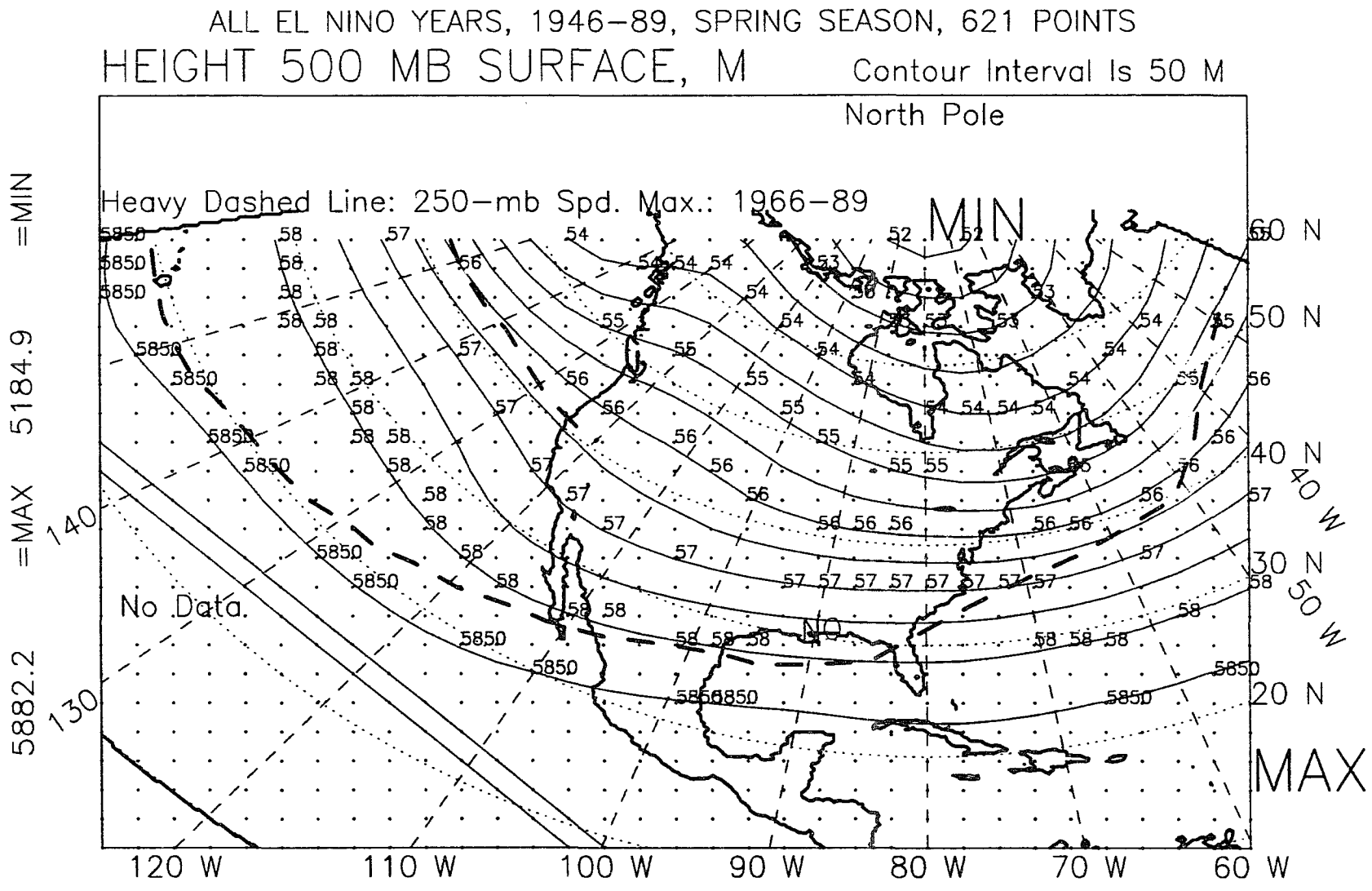

Figure H.4: 500–mb height, spring, El Niño years, 1946–89.

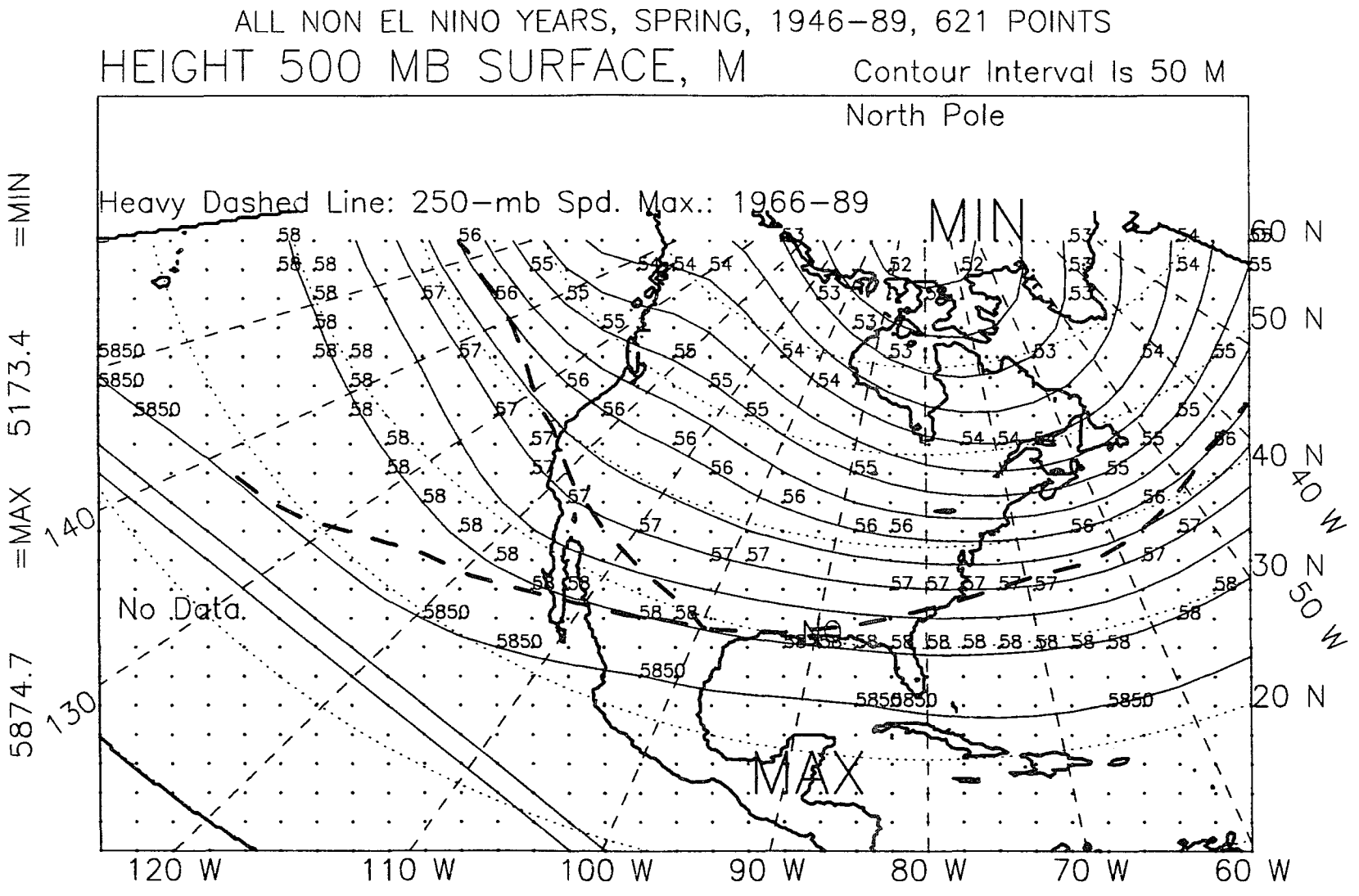

Figure H.5: 500–mb height, spring, non–El Niño years, 1946–89.

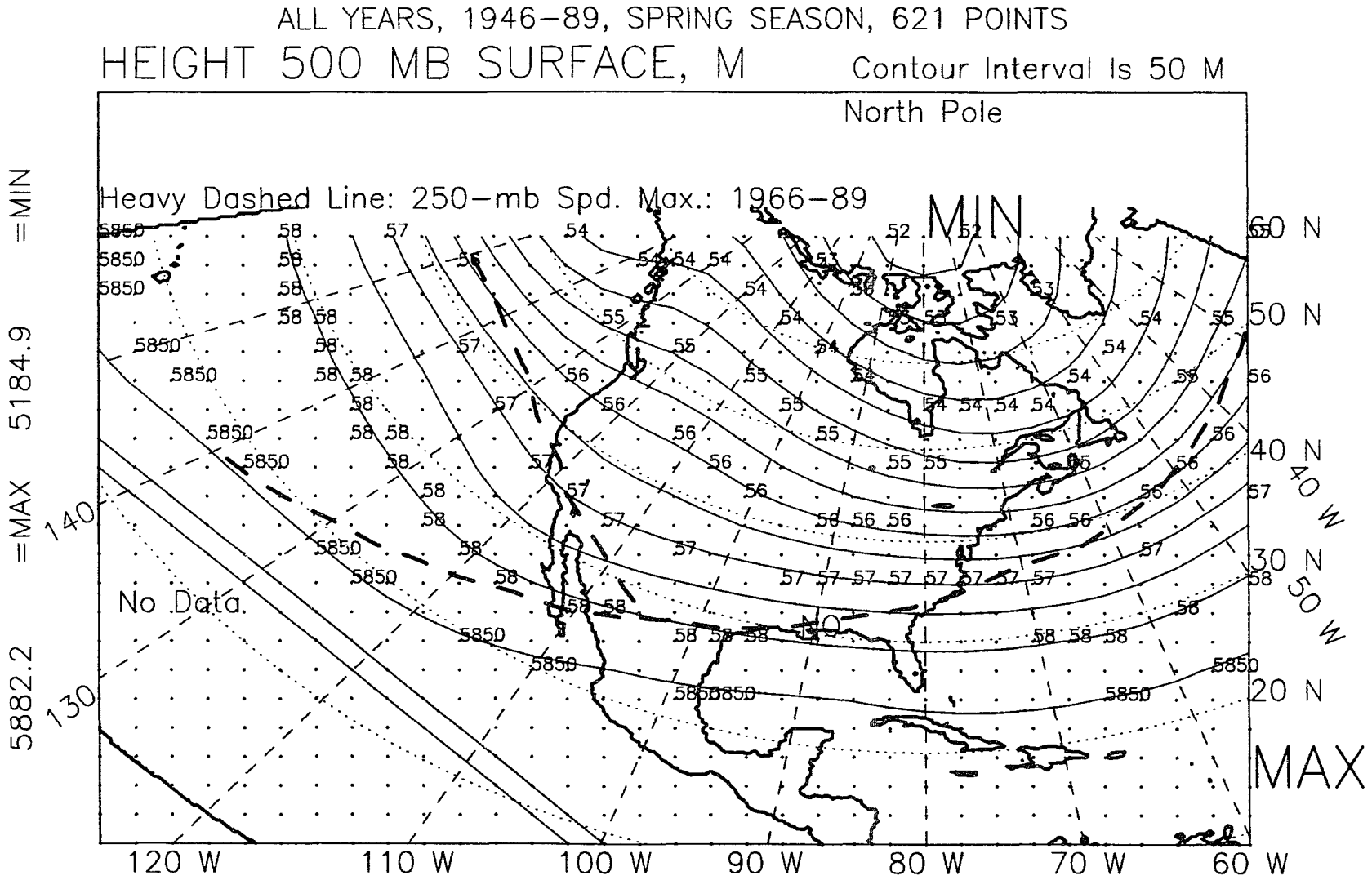

Figure H.6: 500–mb height, spring, all years, 1946–89.

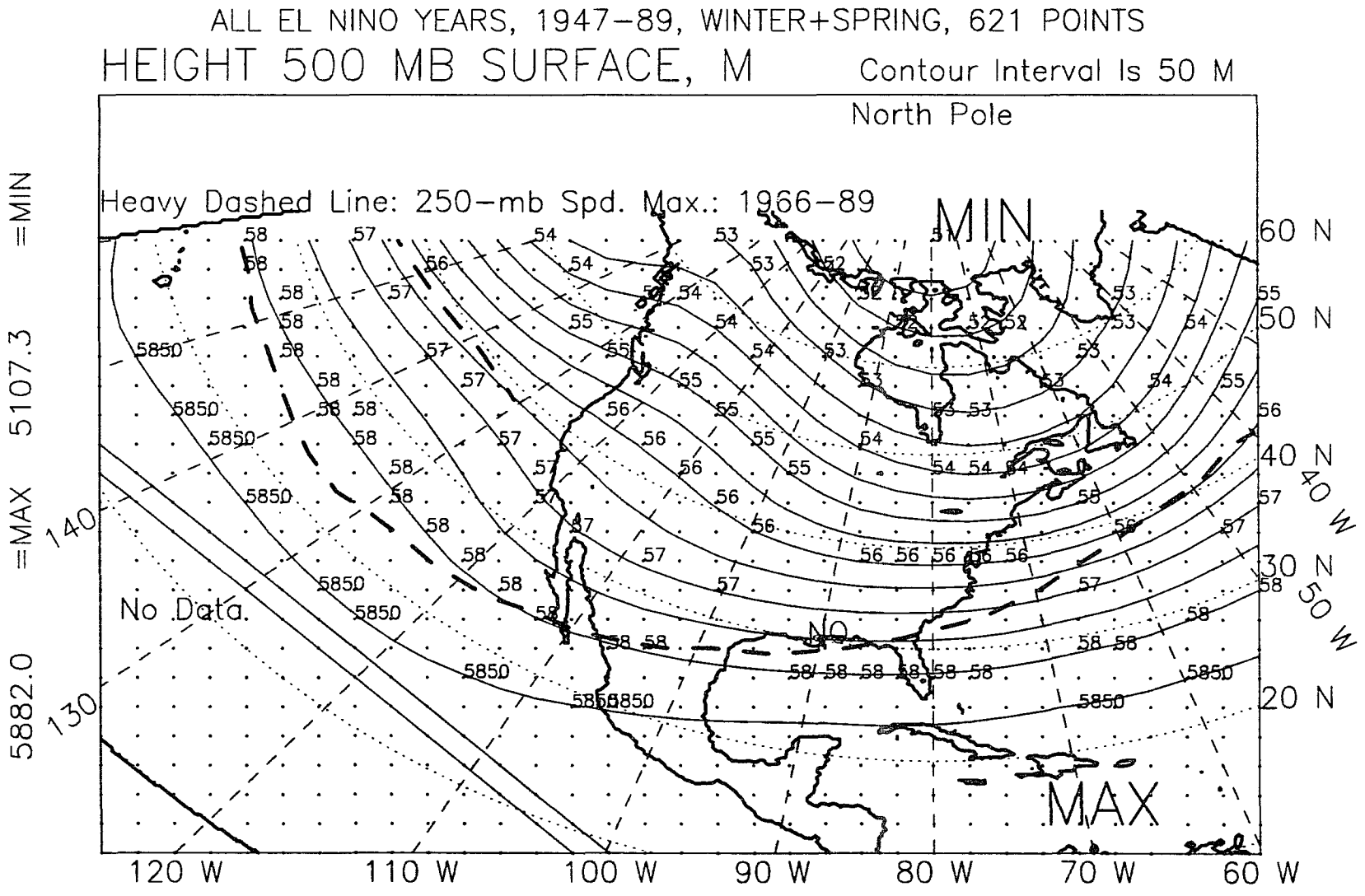

Figure H.7: 500–mb height, winter–plus–spring, El Niño years, 1947–89.

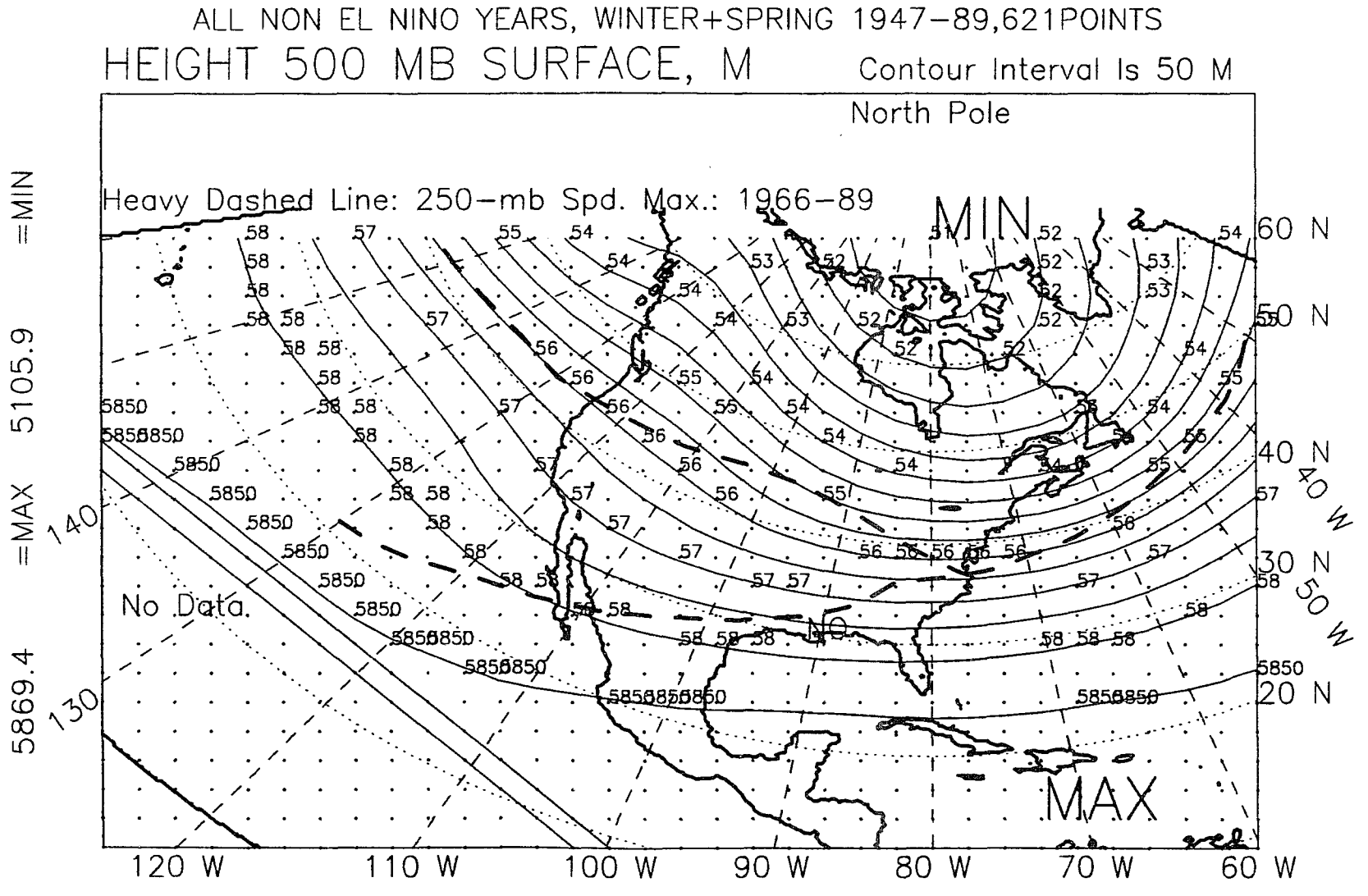

Figure H.8: 500-mb height, winter-plus-spring, non-El Niño years, 1947-89.

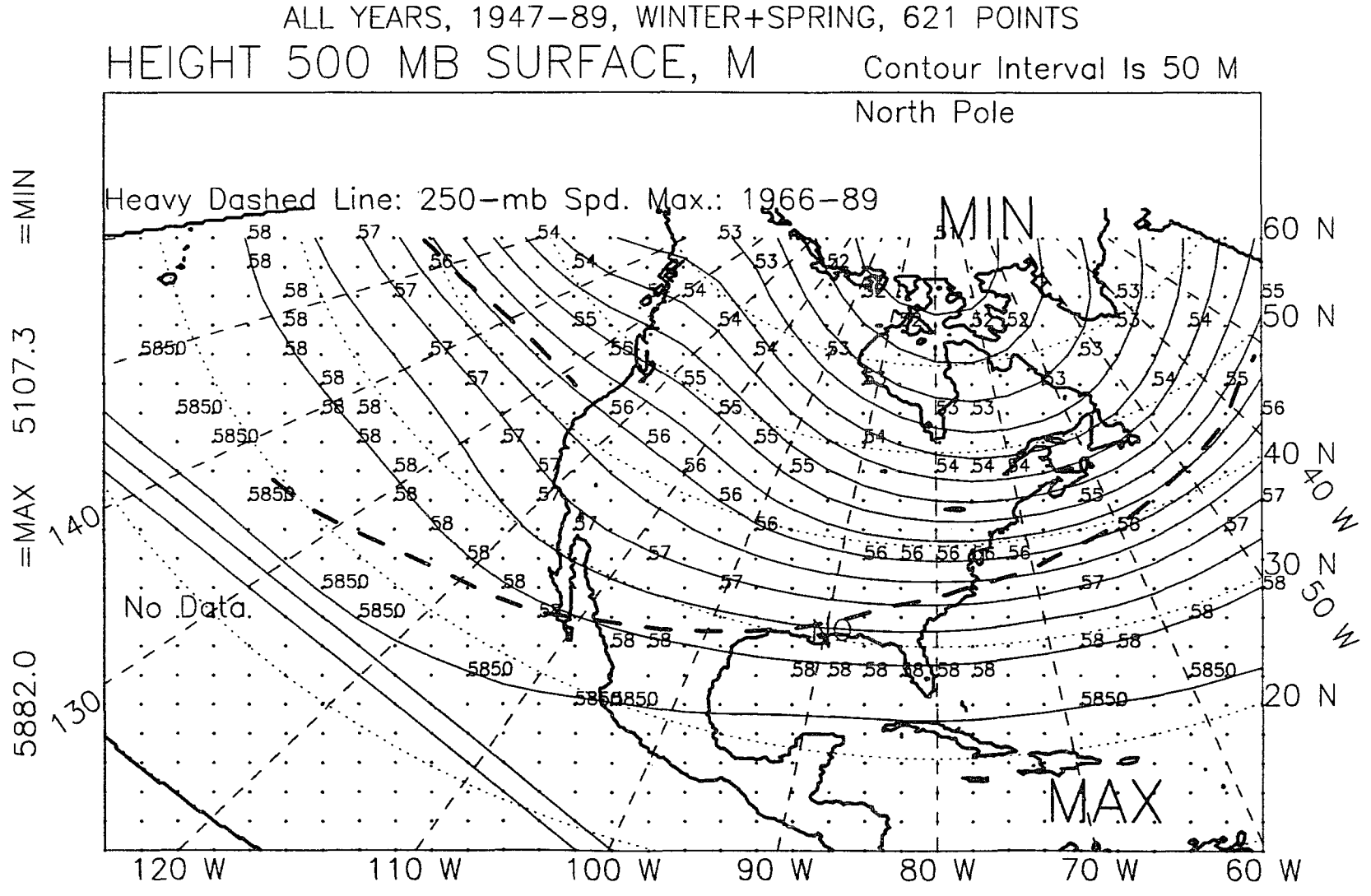

Figure H.9: 500–mb height, winter–plus–spring, all years, 1947–89.

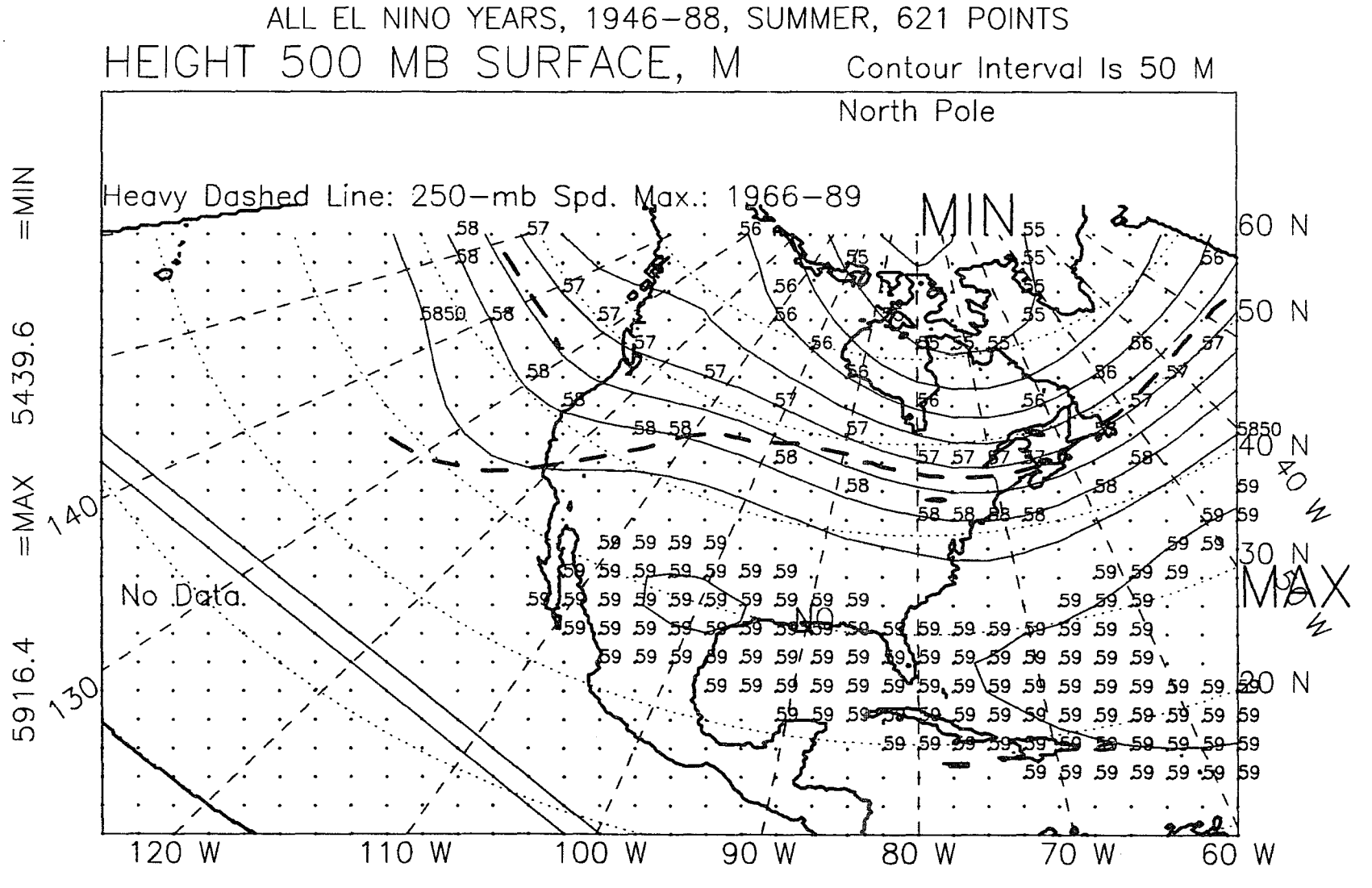

Figure H.10: 500–mb height, summer, El Niño years, 1946–88.

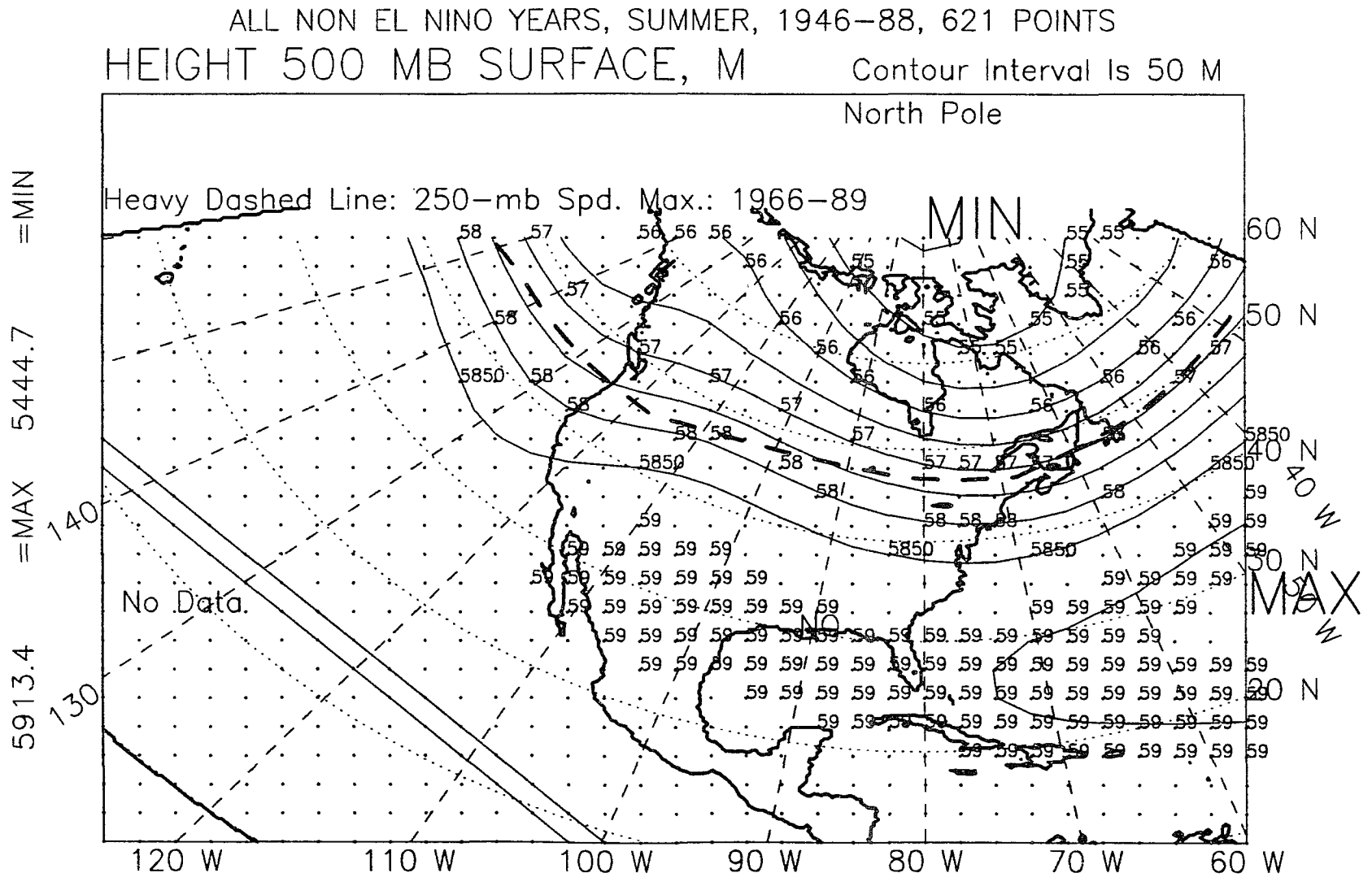

Figure H.11: 500–mb height, summer, non–El Niño years, 1946–88.

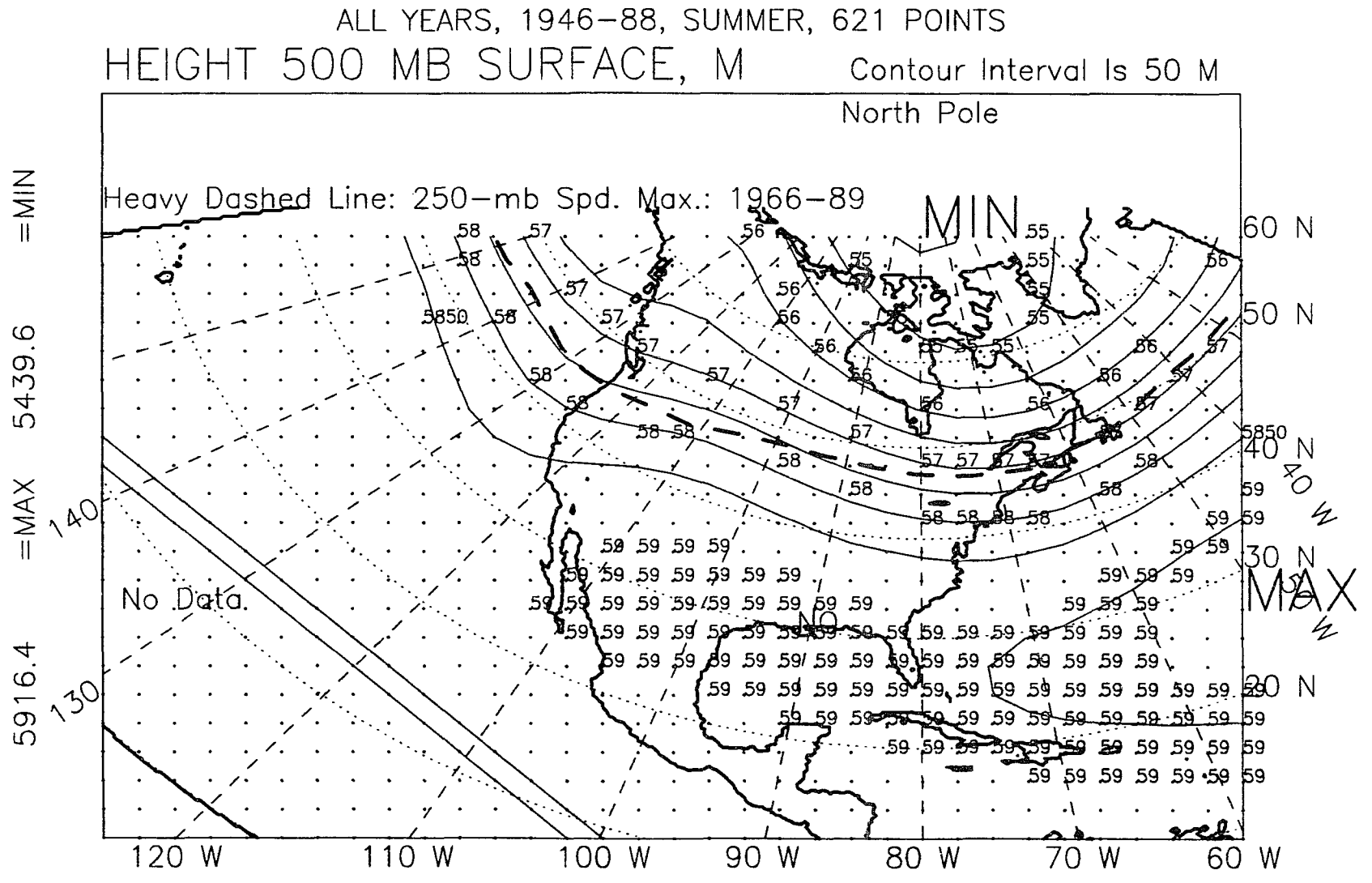

Figure H.12: 500–mb height, summer, all years, 1946–88.

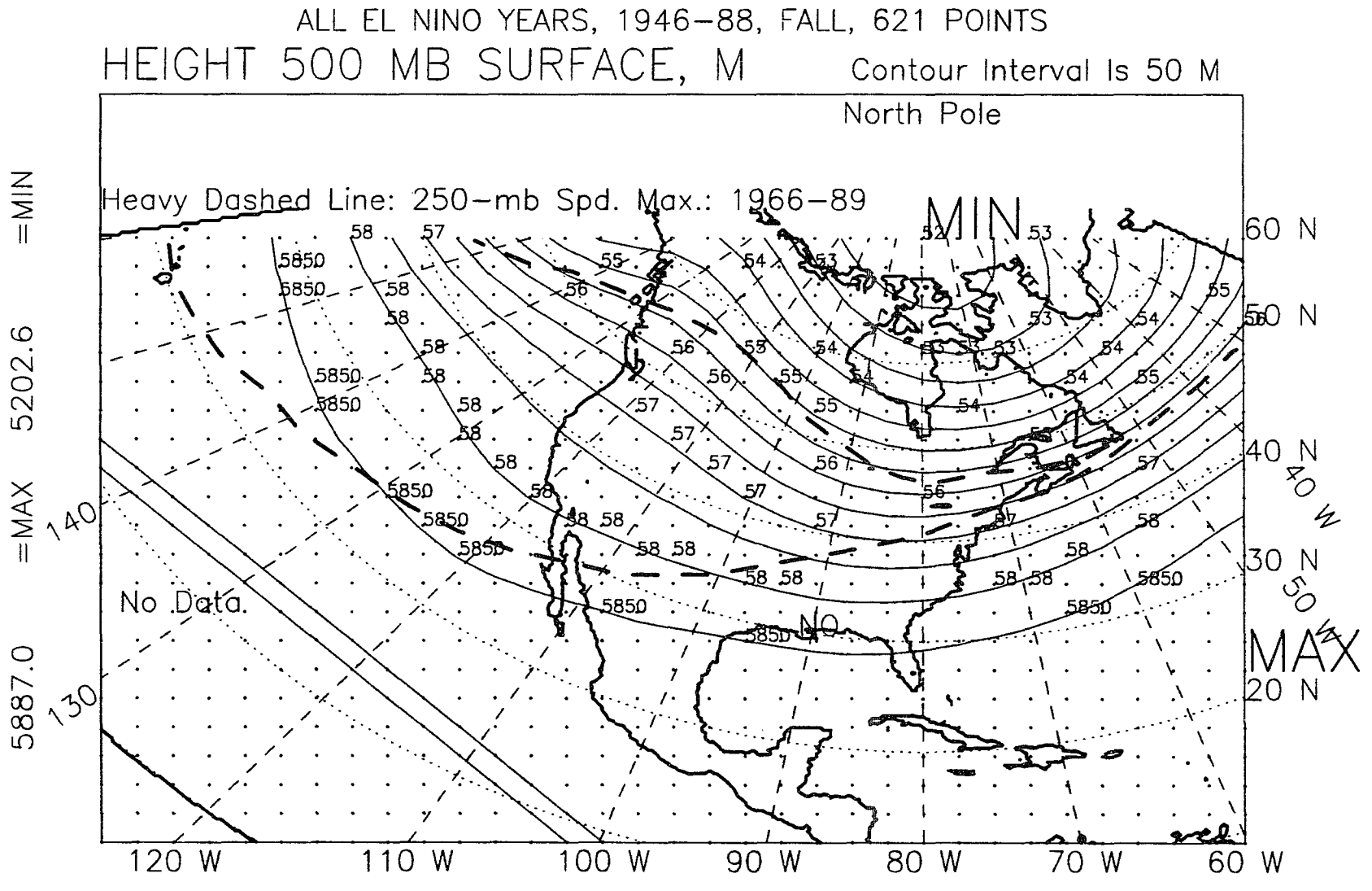

Figure H.13: 500-mb height, fall, El Niño years, 1946-88.

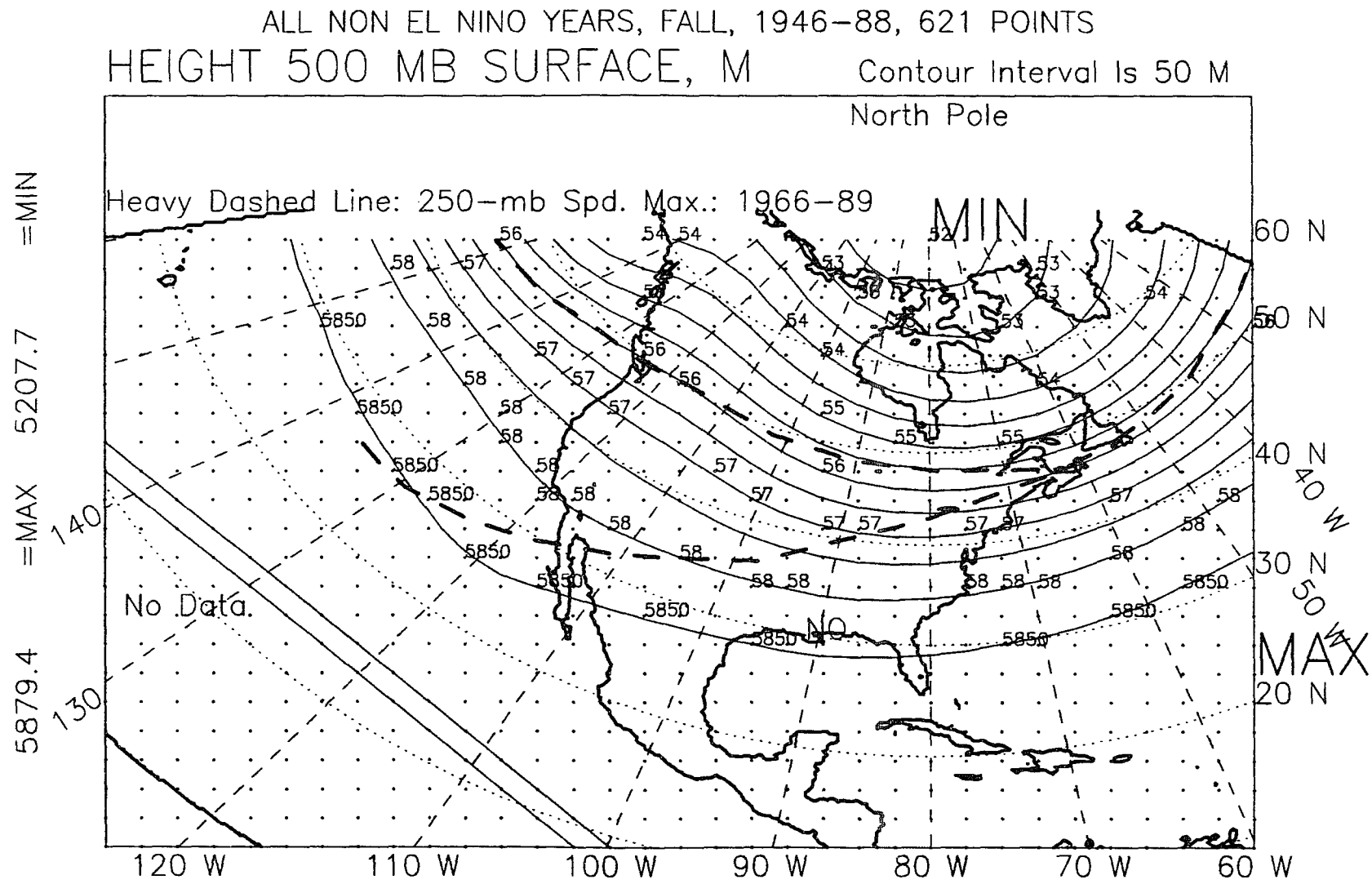

Figure H.14: 500–mb height, fall, non–El Niño years, 1946–88.

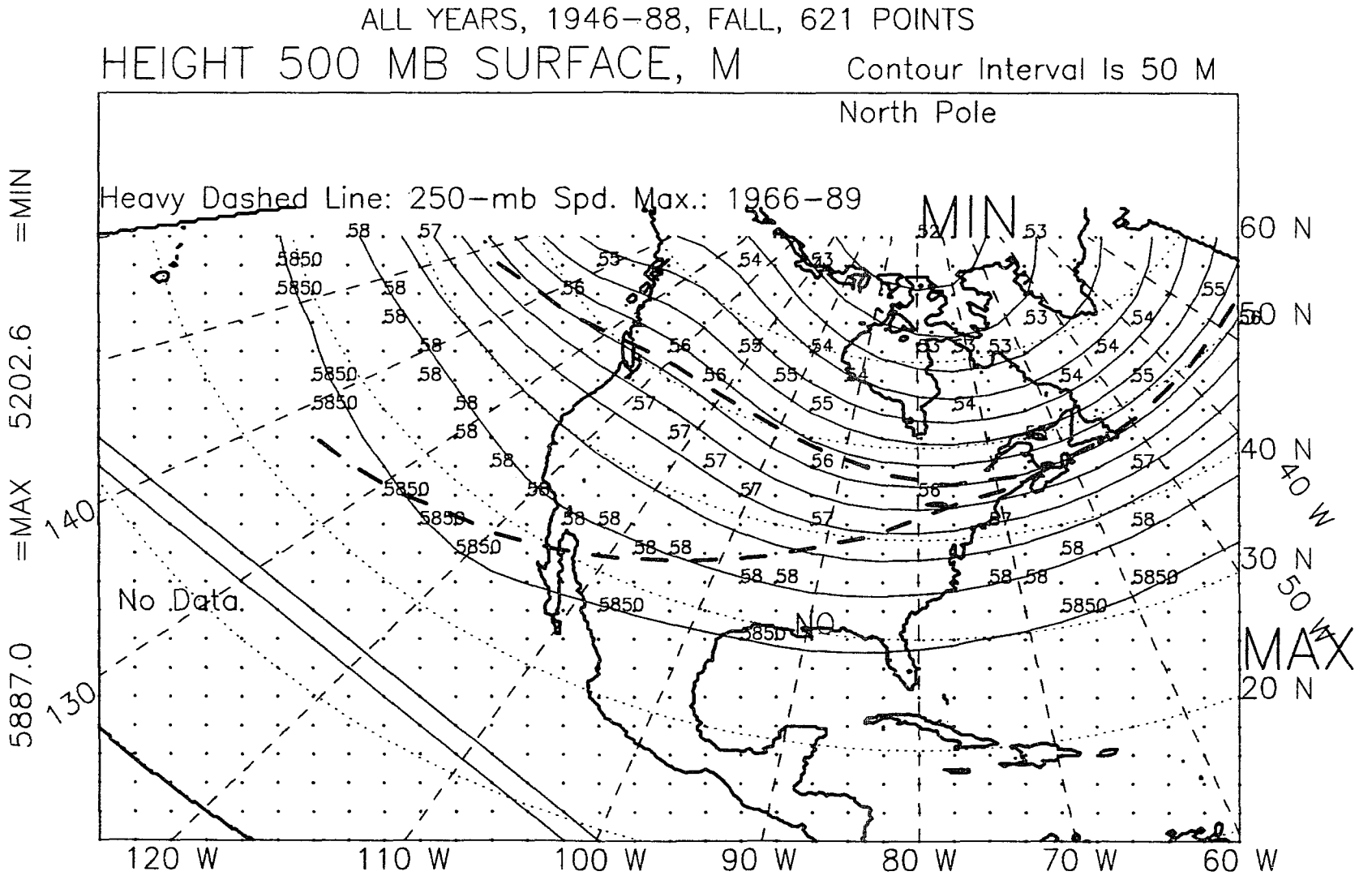

Figure H.15: 500–mb height, fall, all years, 1946–88.

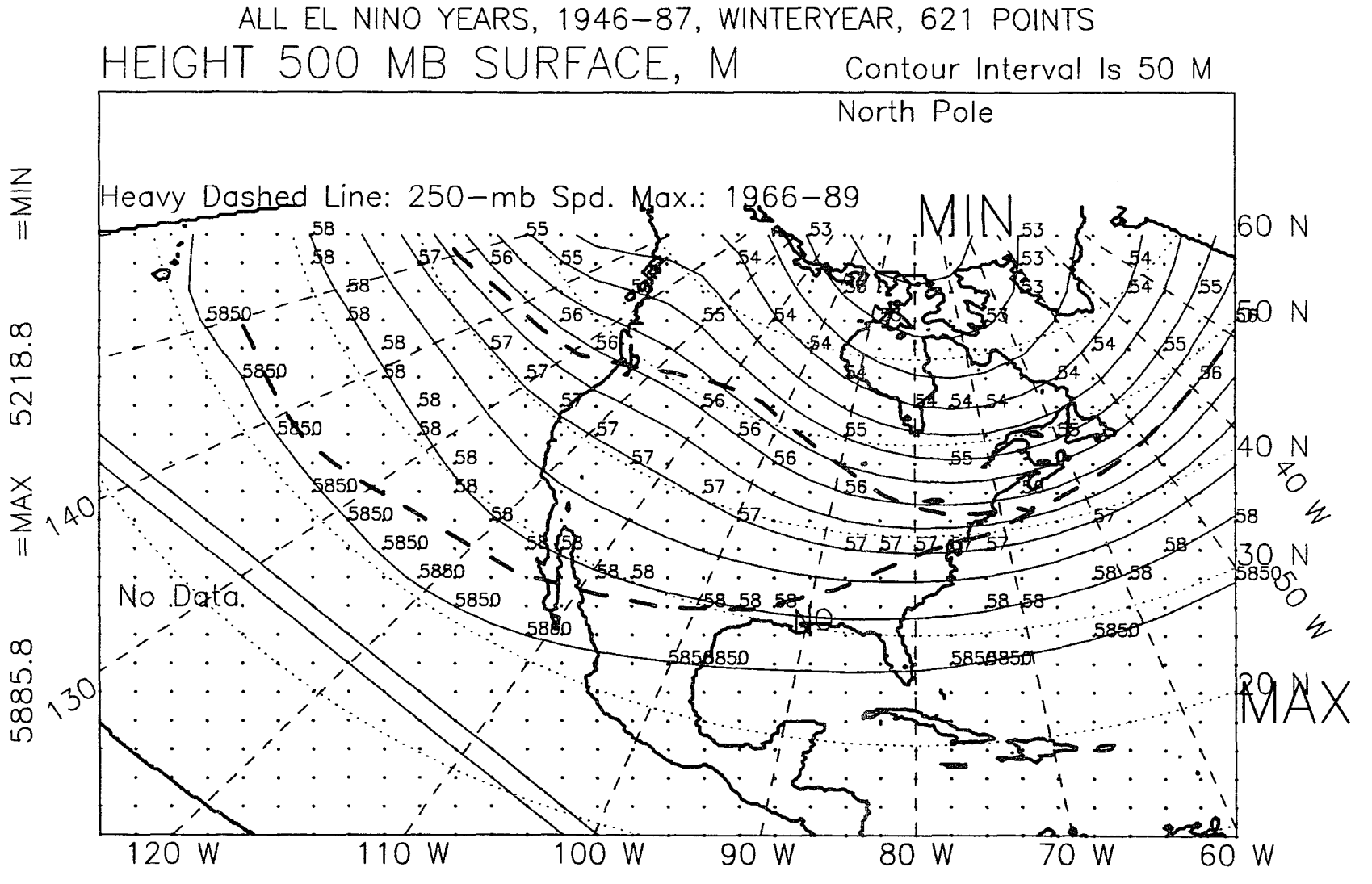

Figure H.16: 500–mb height, winter year, El Niño years, 1946–87.

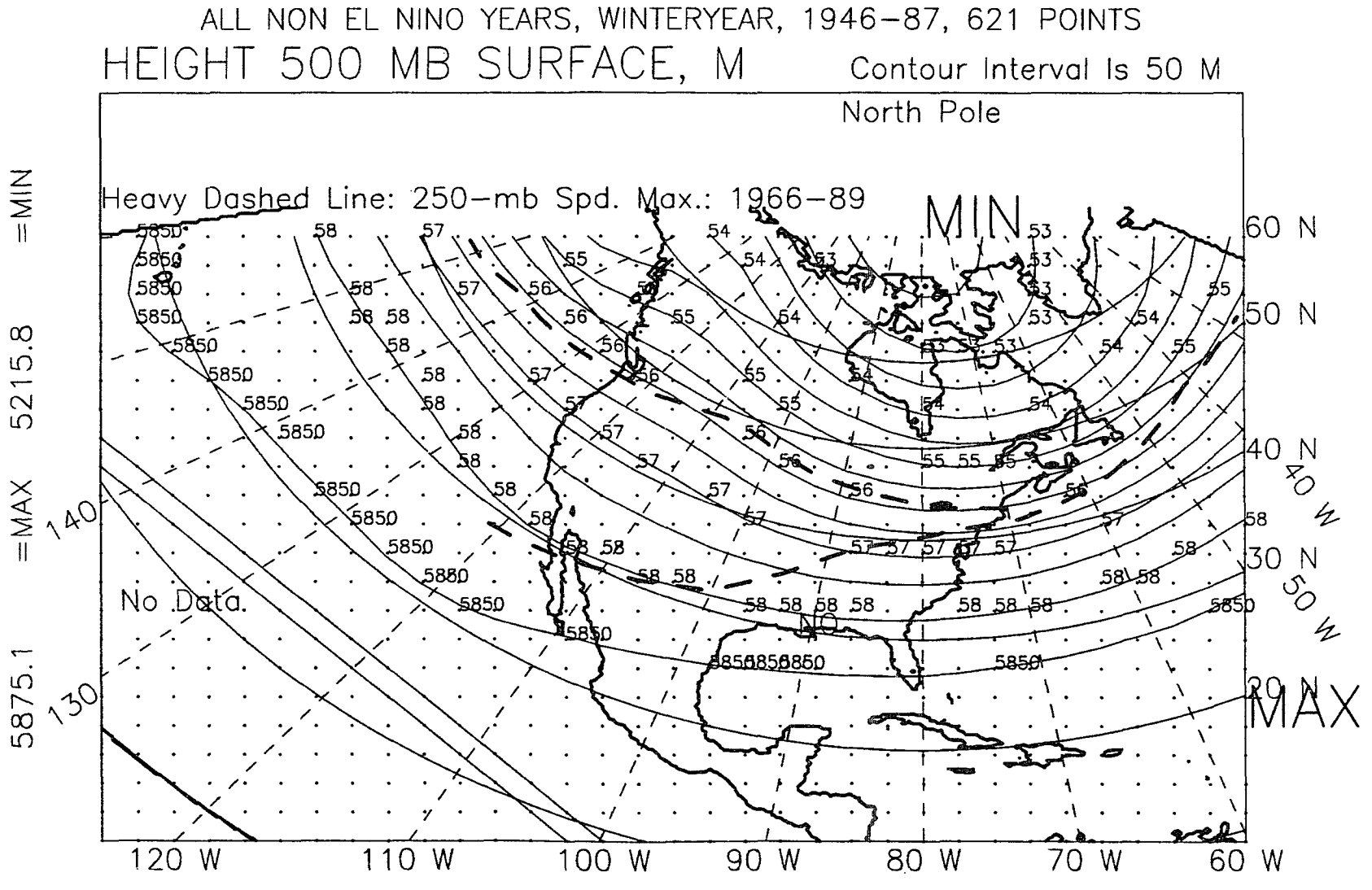

Figure H.17: 500-mb height, winter year, non-El Niño years, 1946-87.

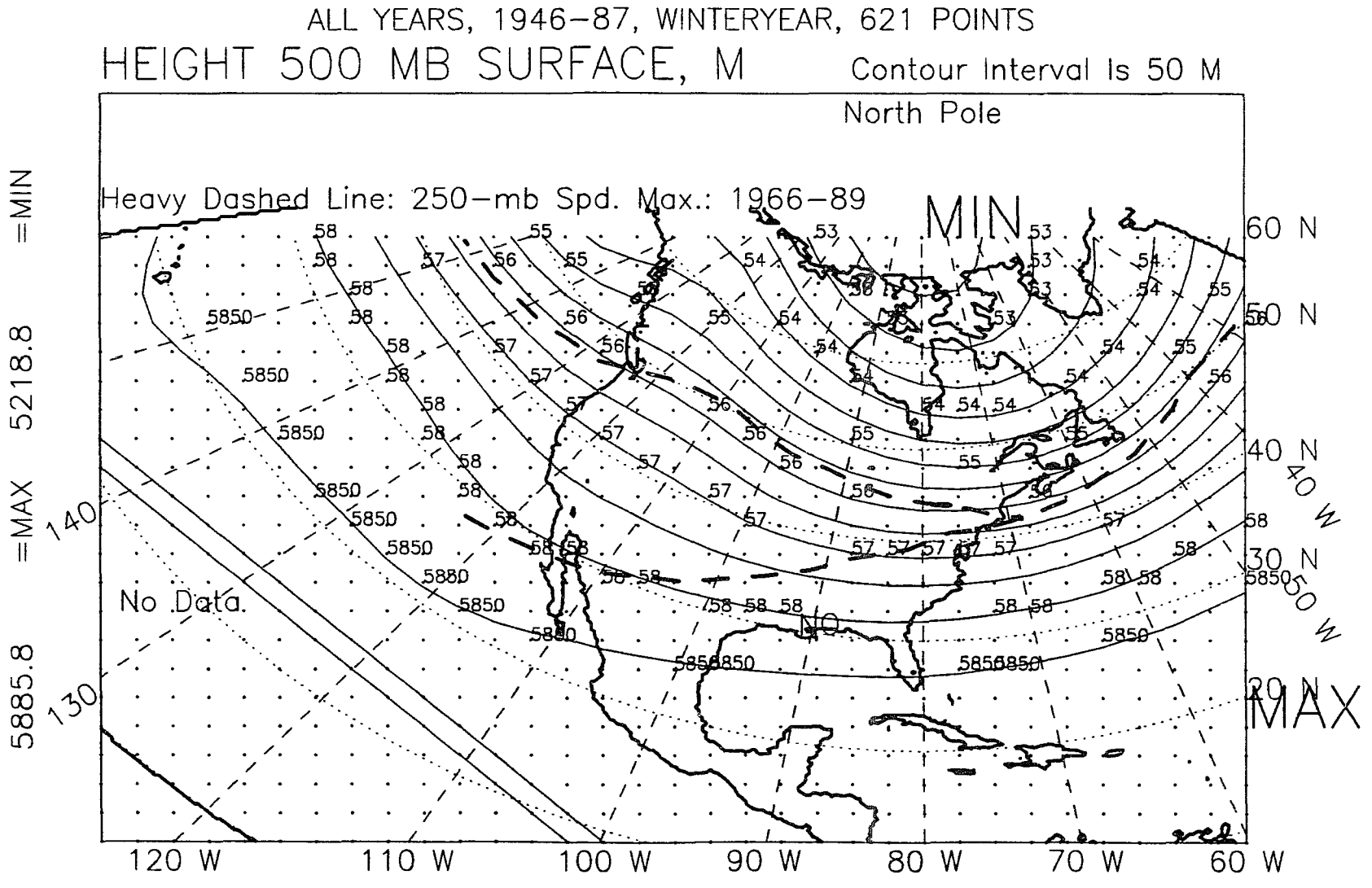

Figure H.18: 500–mb height, winter year, all years, 1946–87.

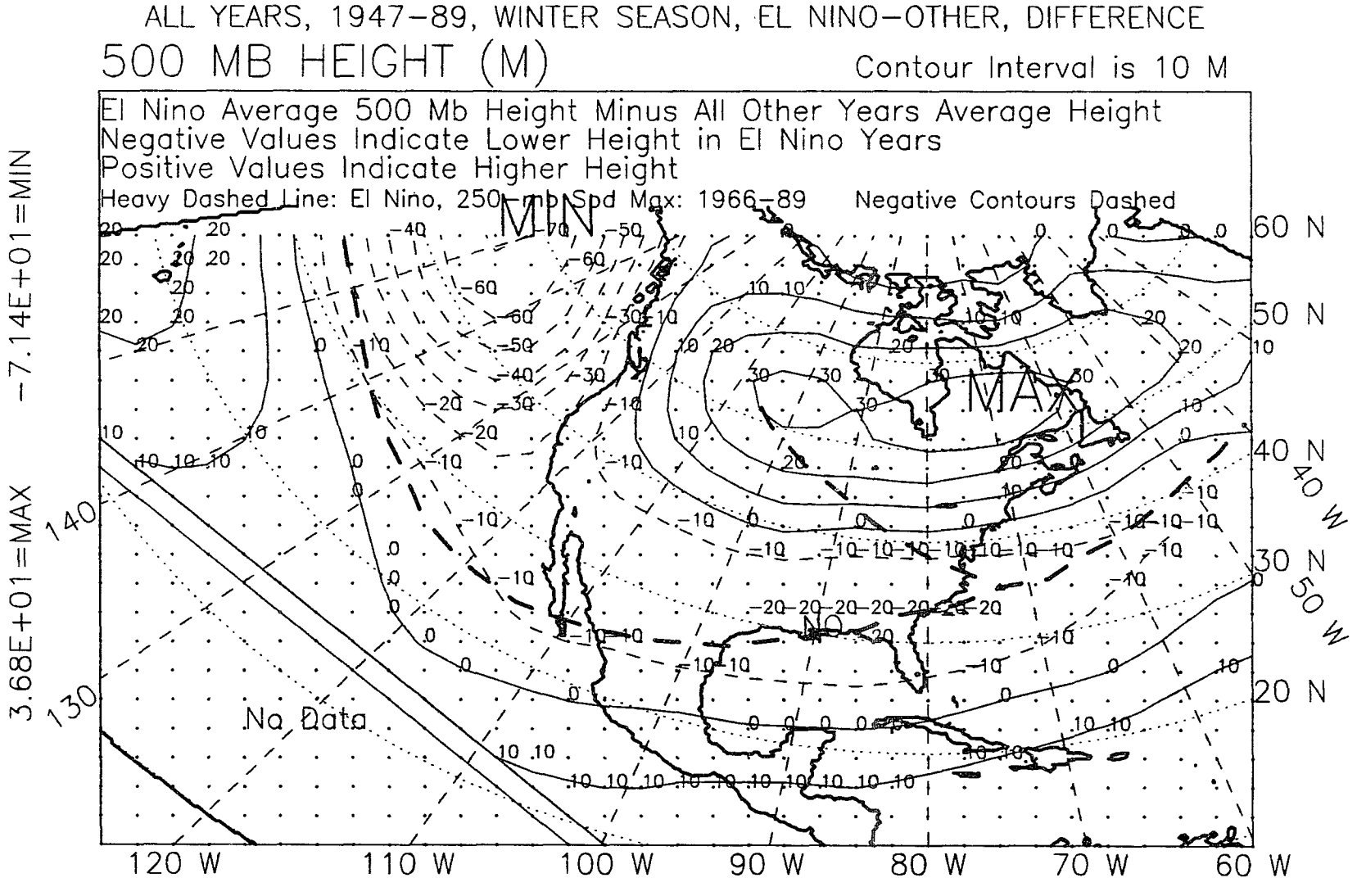

Figure H.19: 500–mb height, winter, 1947–89, difference.

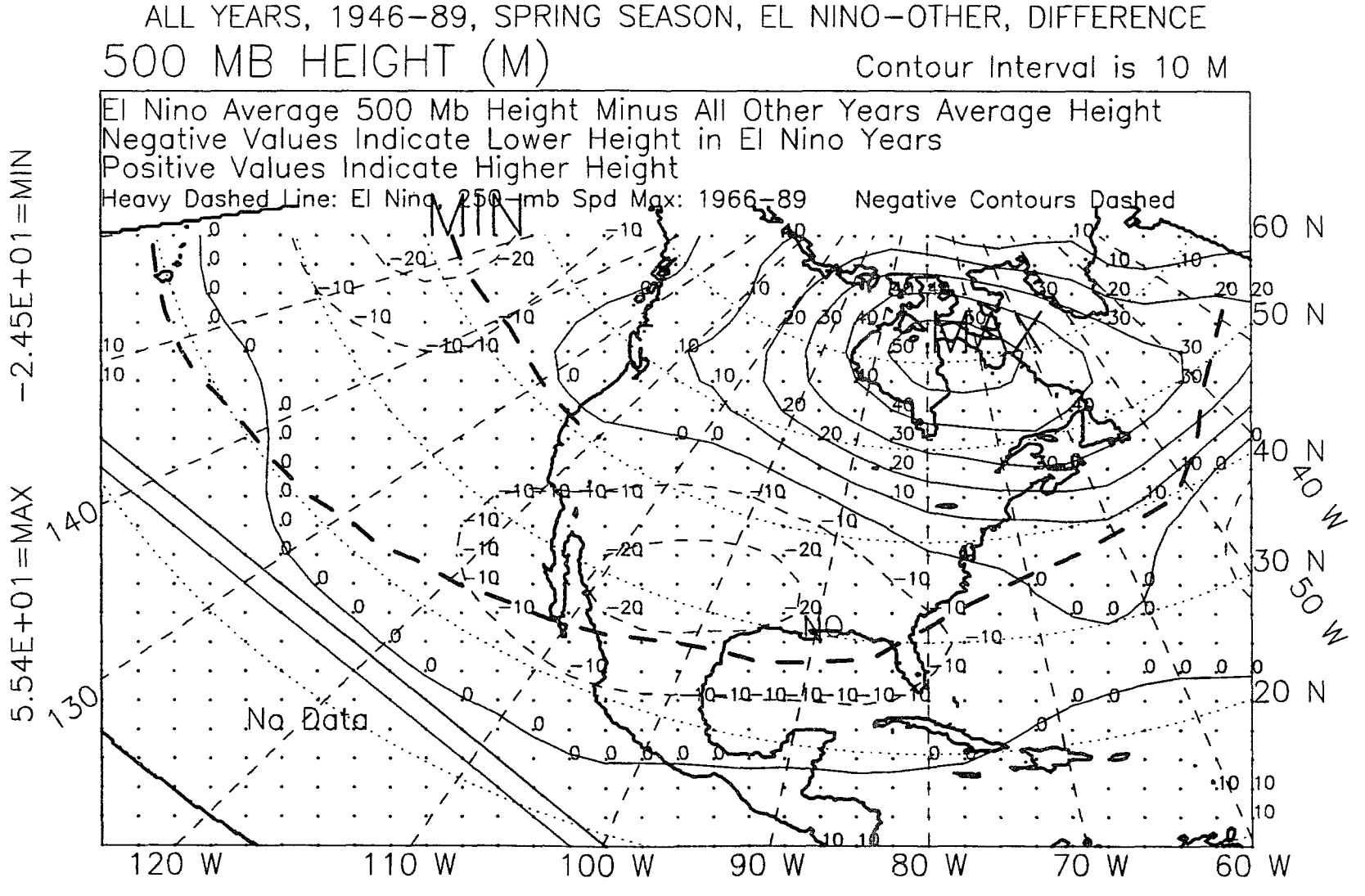

Figure . : 500–mb height, spring, 1946–89, difference.

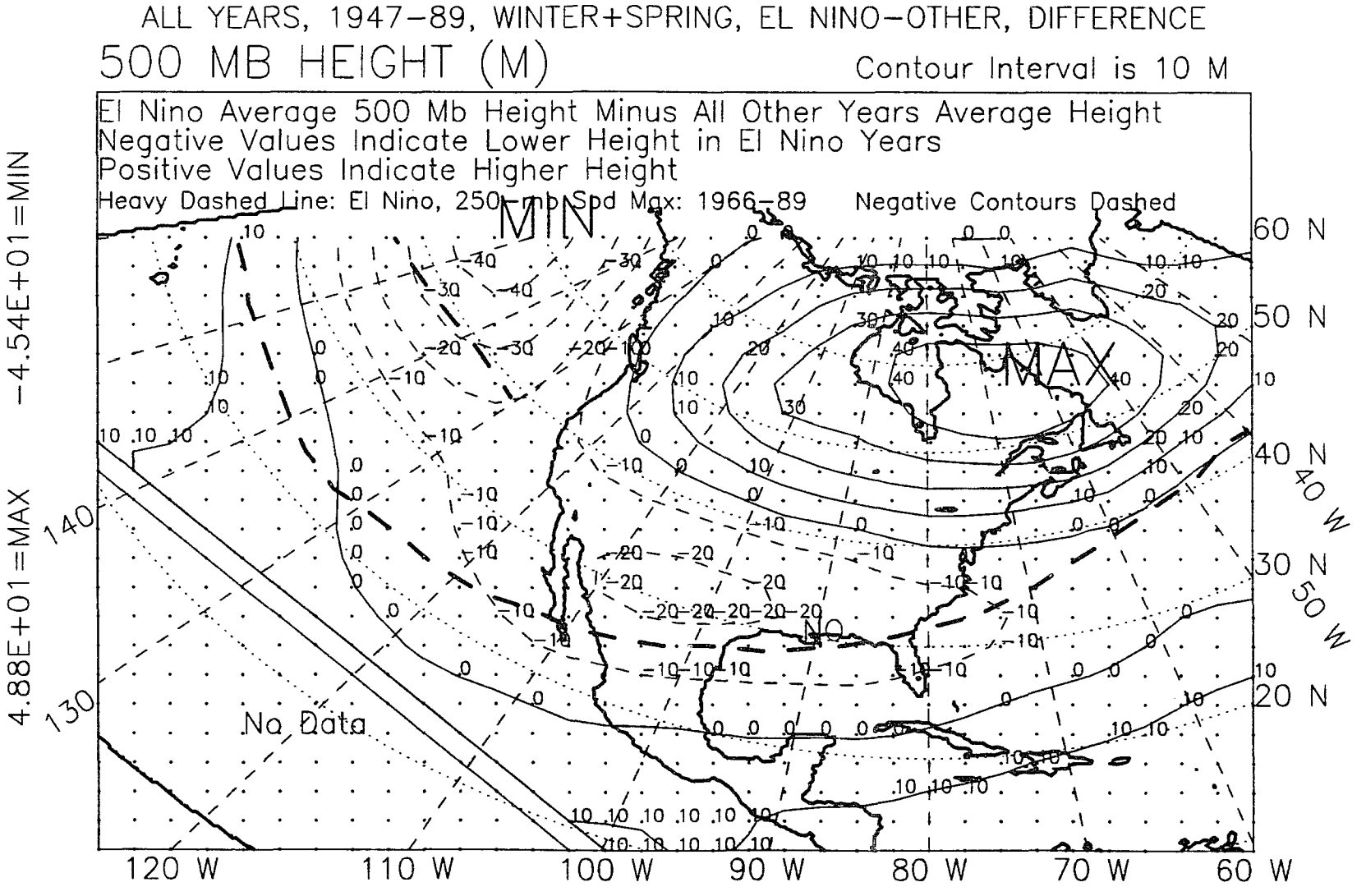

Figure H.21: 500–mb height, winter–plus–spring, 1947–89, difference.

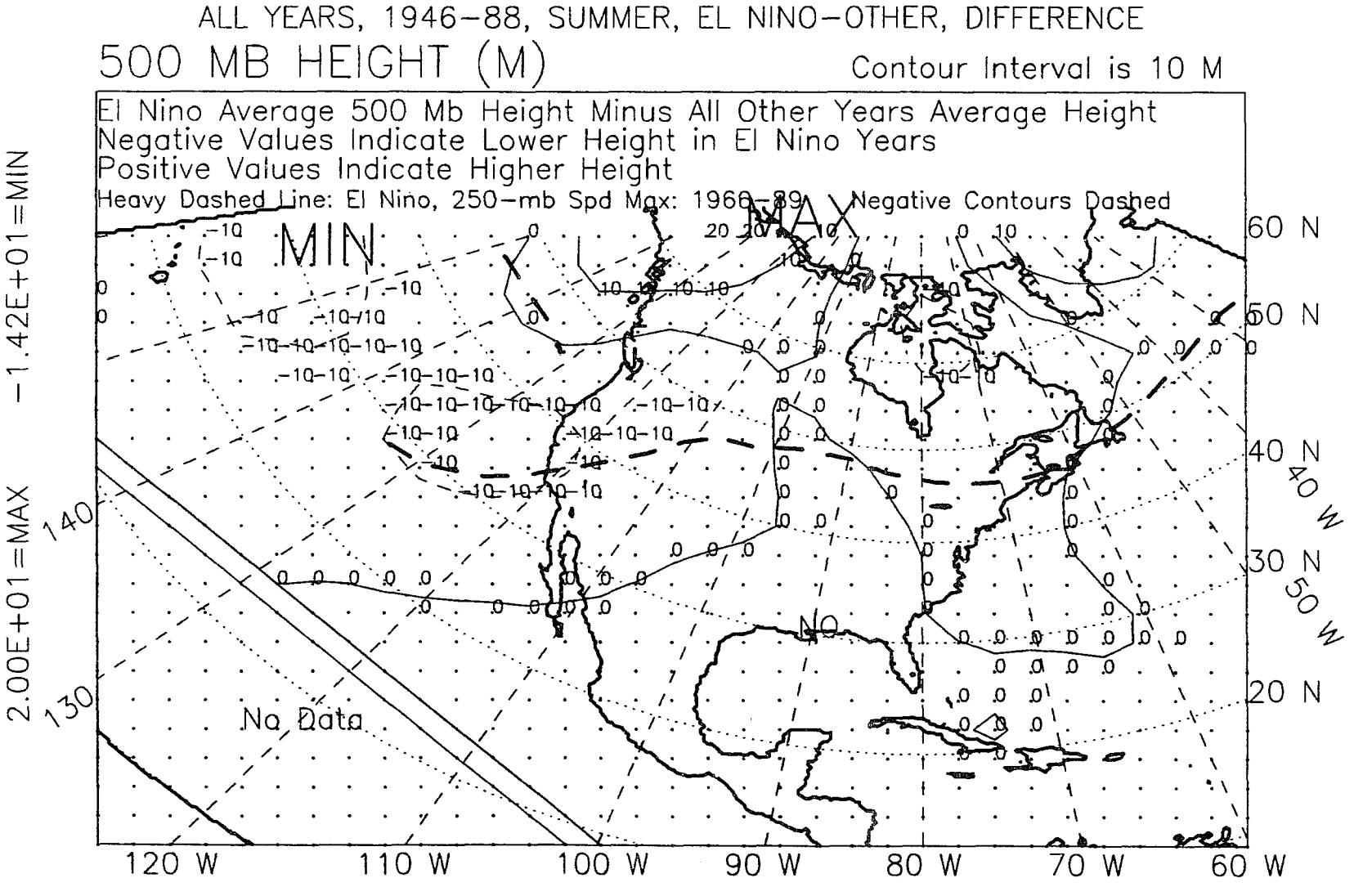

Figure H.22: 500–mb height, summer, 1946–88, difference.

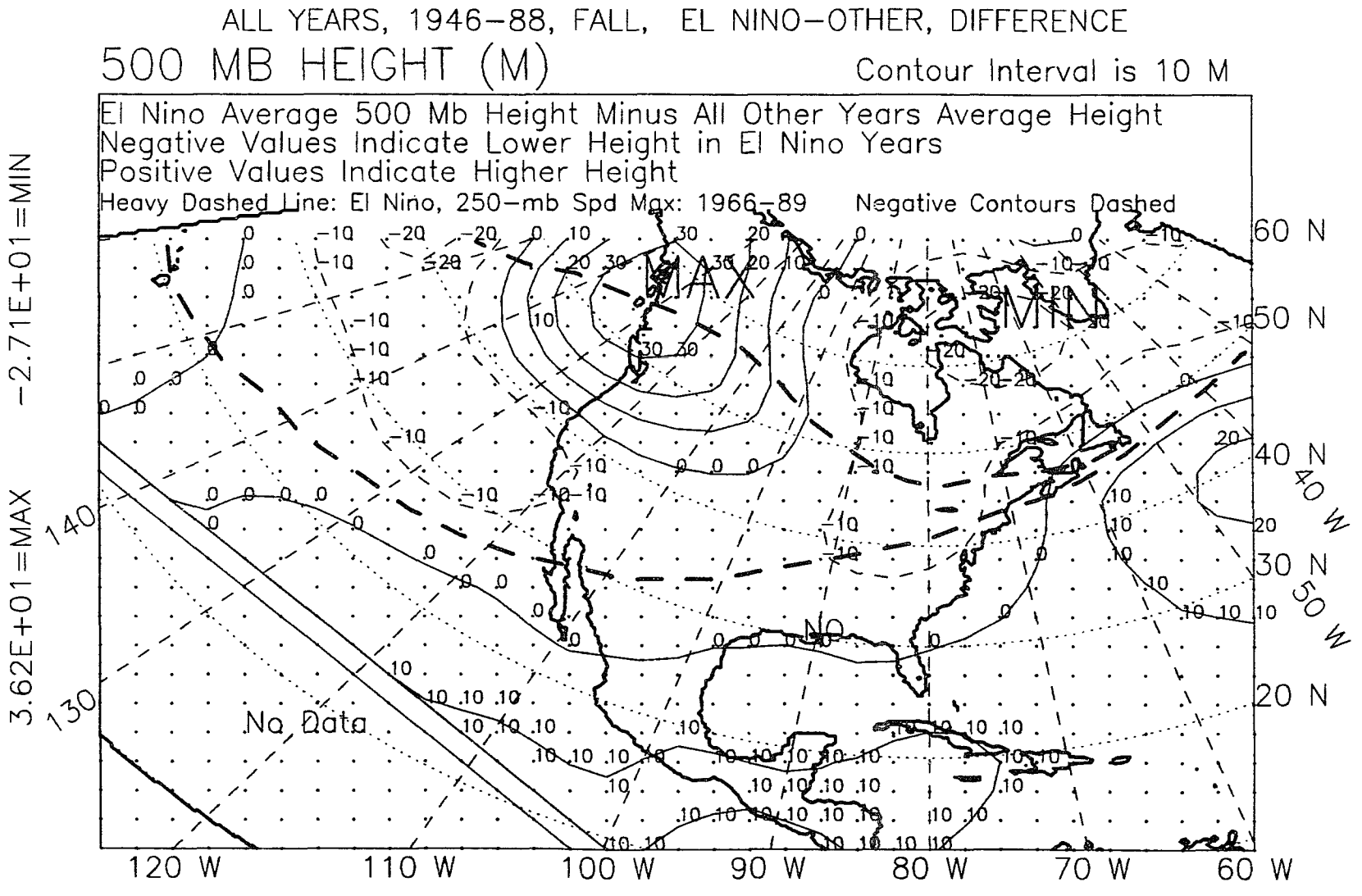

Figure H.23: 500–mb height, fall, 1946–88, difference.

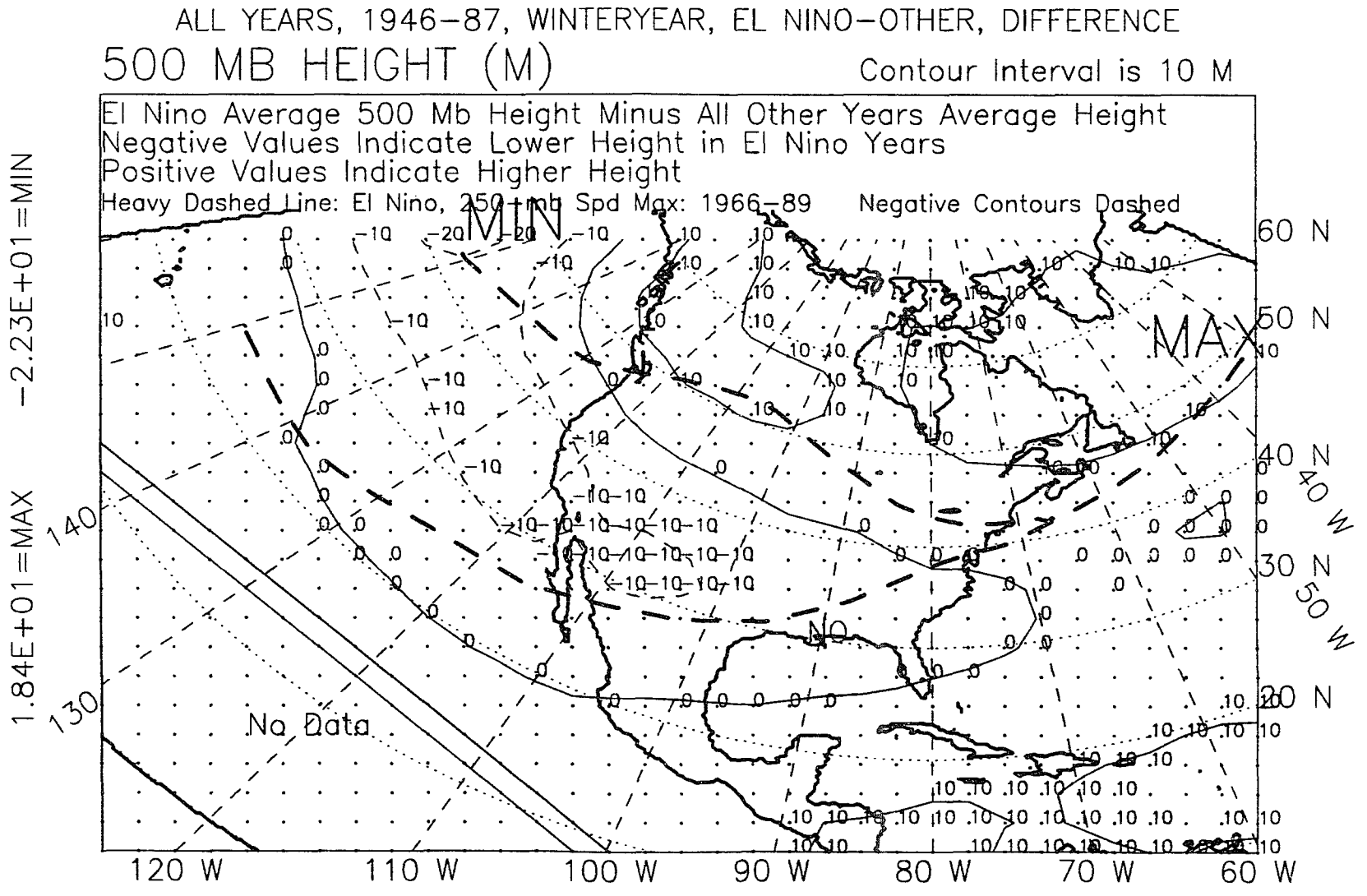

Figure H.24: 500–mb height, winter year, 1946–87, difference.

APPENDIX I
500-MB TEMPERATURE FIELD

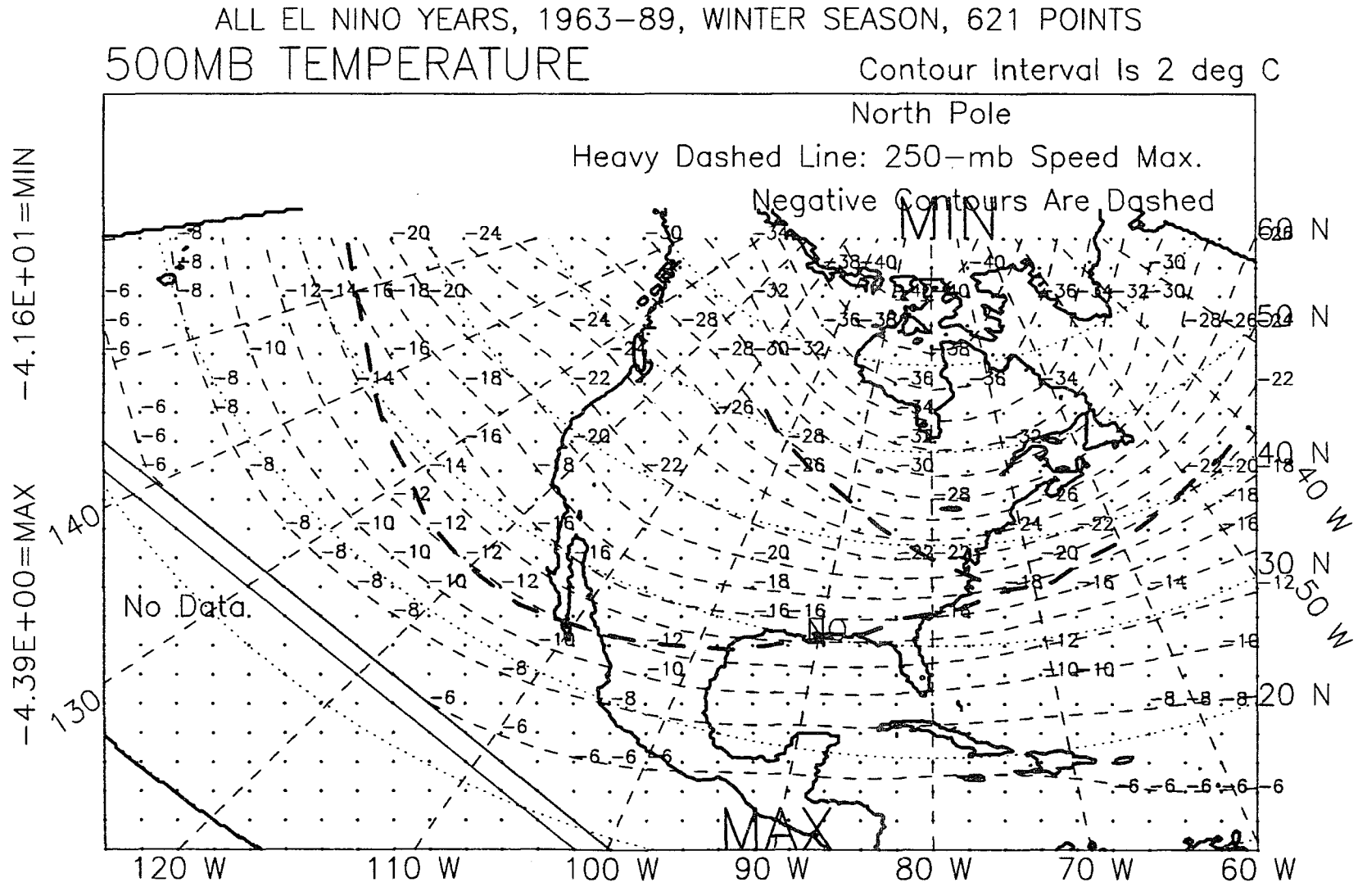

Figure I.1: 500–mb temperature, winter, El Niño years, 1963–89.

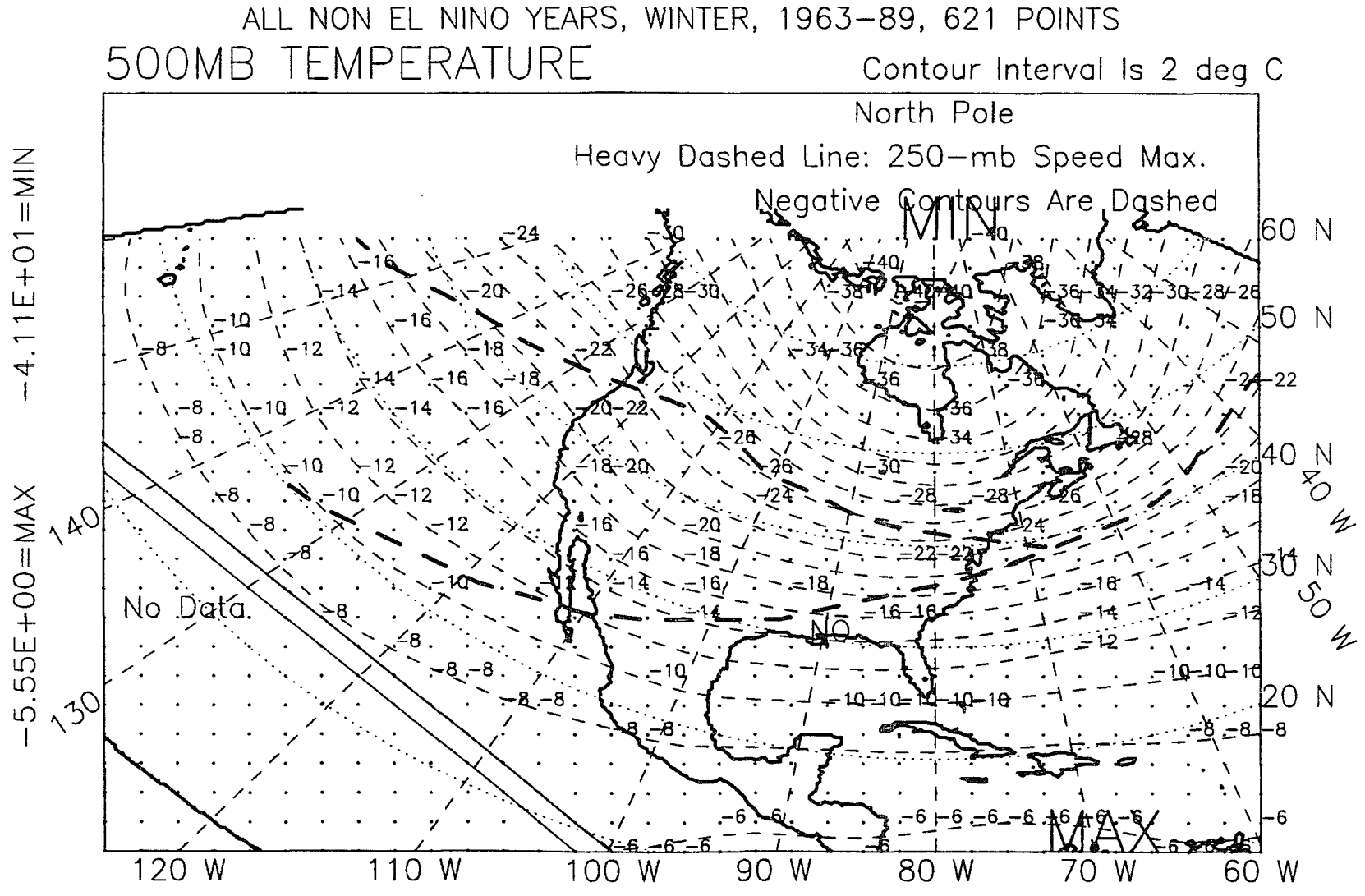

Figure I.2: 500–mb temperature, winter, non–El Niño years, 1963–89.

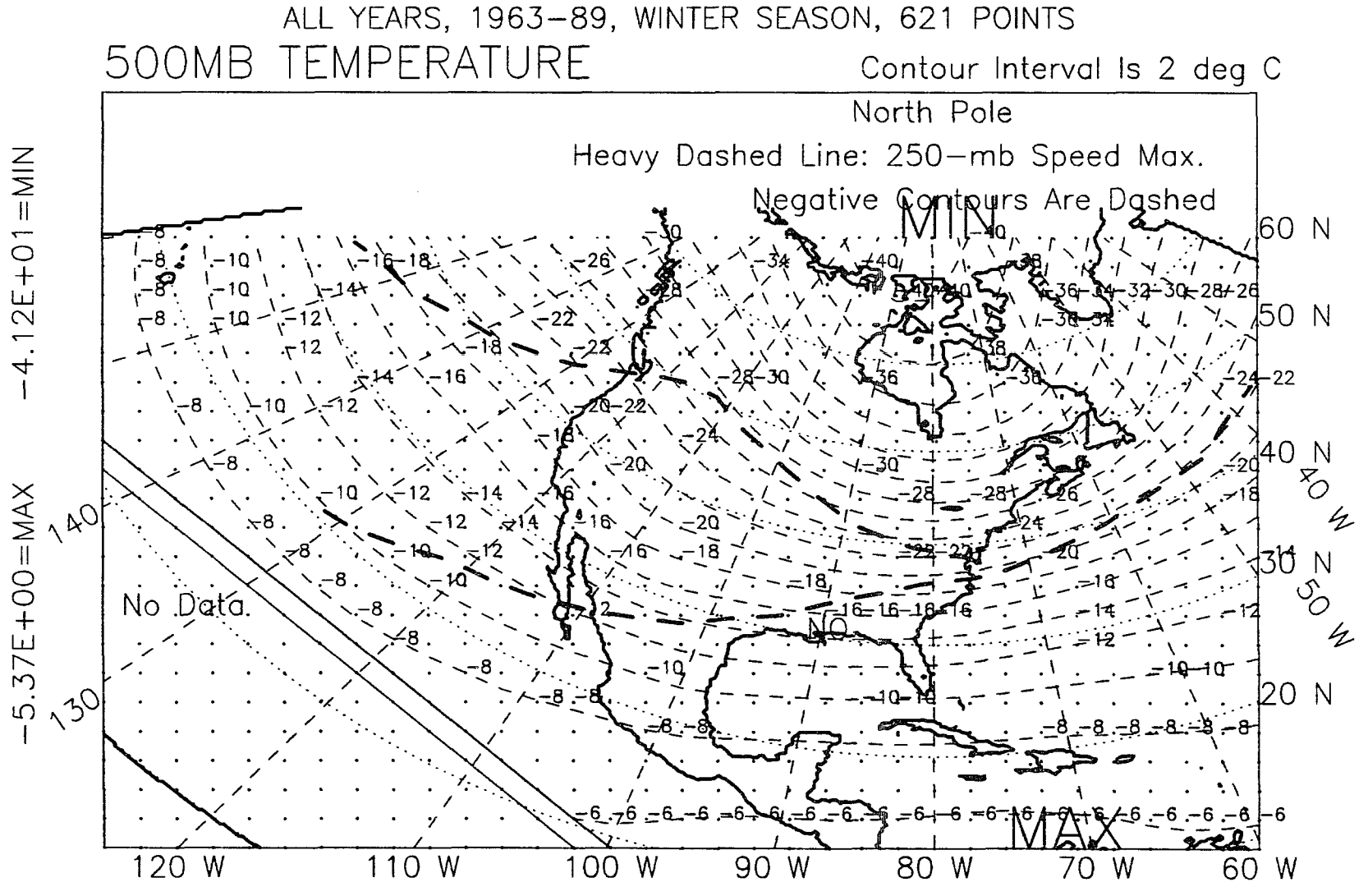

Figure I.3: 500–mb temperature, winter, all years, 1963–89.

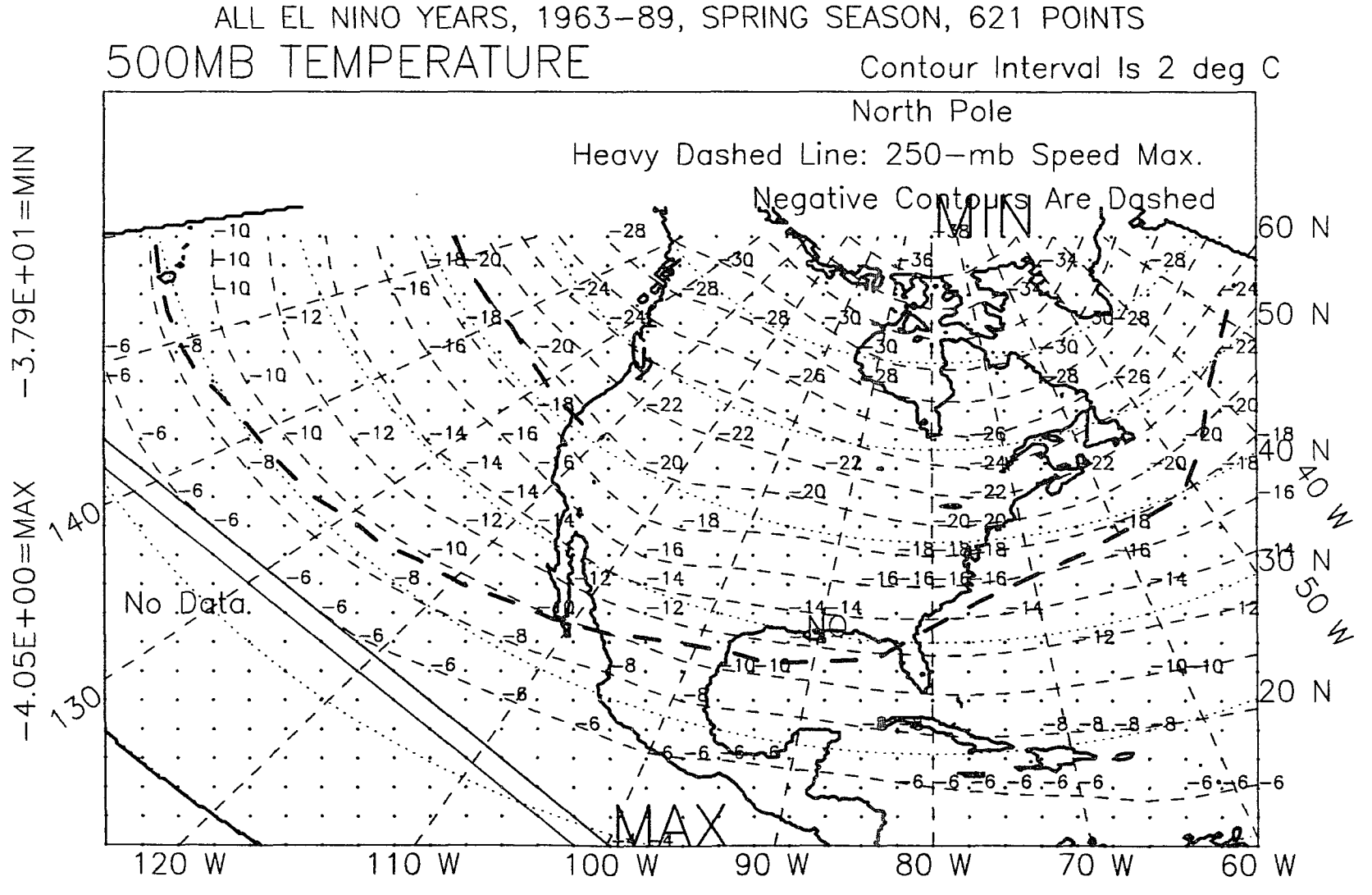

Figure I.4: 500–mb temperature, spring, El Niño years, 1963–89.

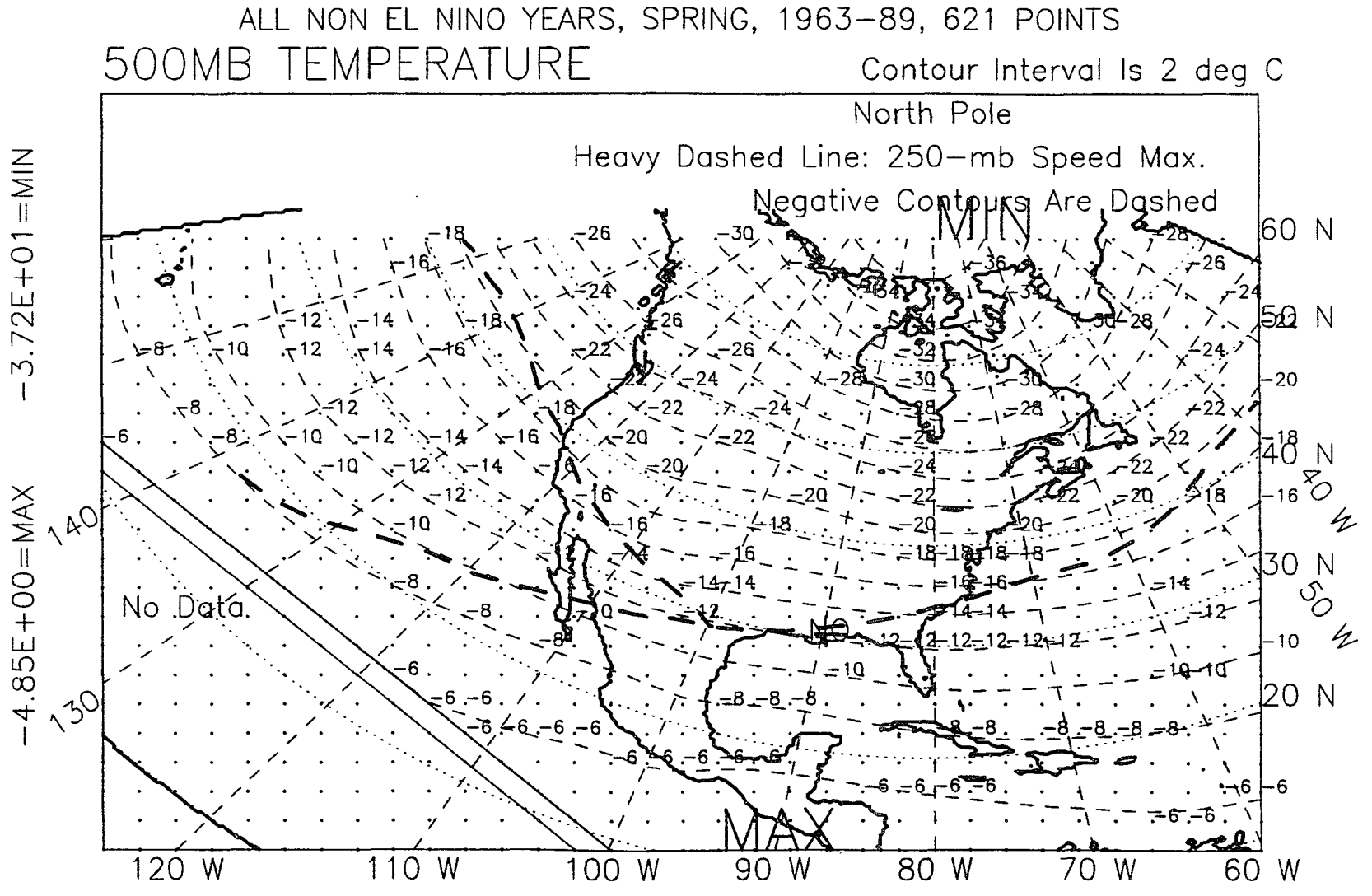

Figure I.5: 500–mb temperature, spring, non–El Niño years, 1963–89.

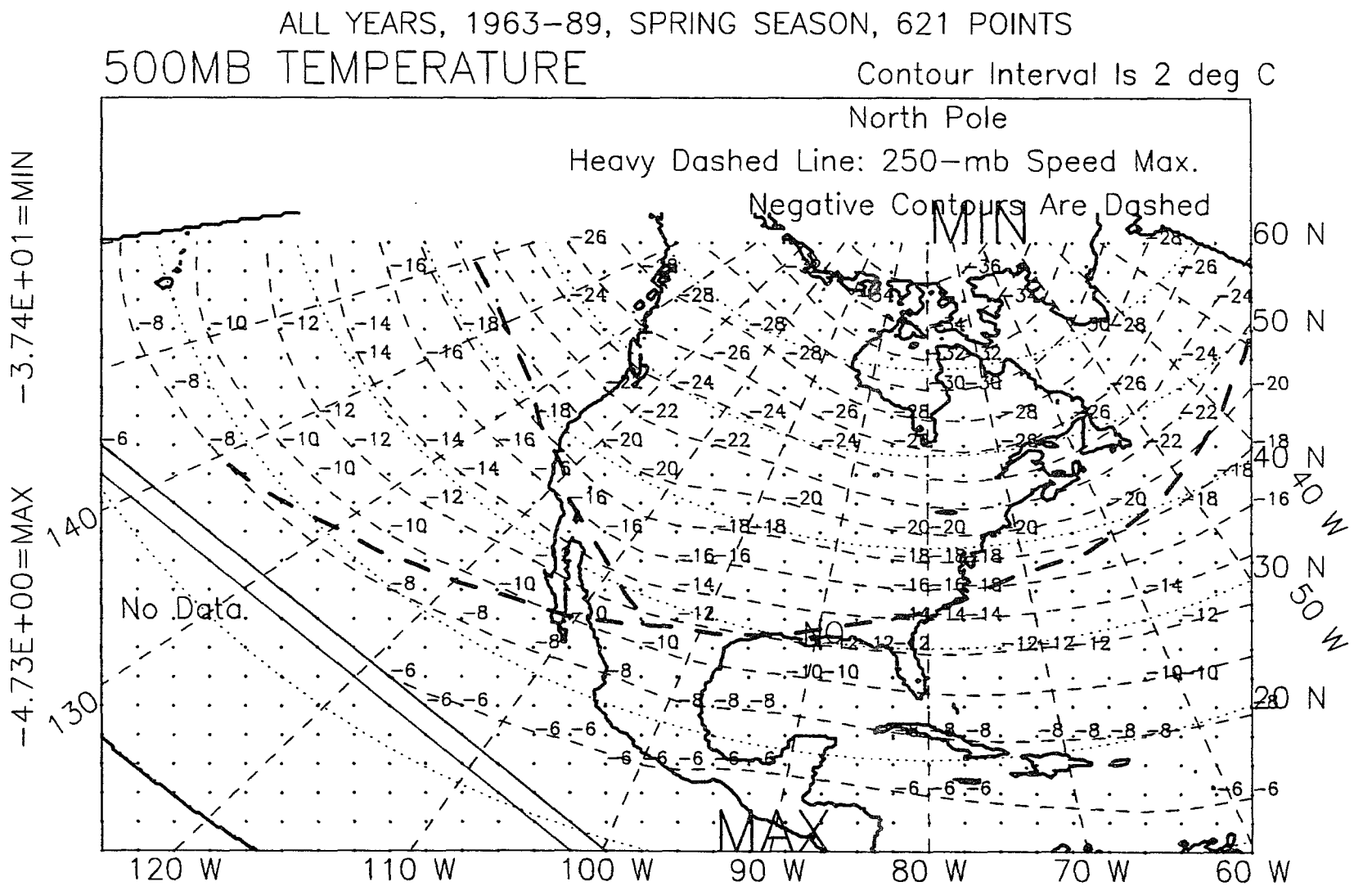

Figure I.6: 500–mb temperature, spring, all years, 1963–89.

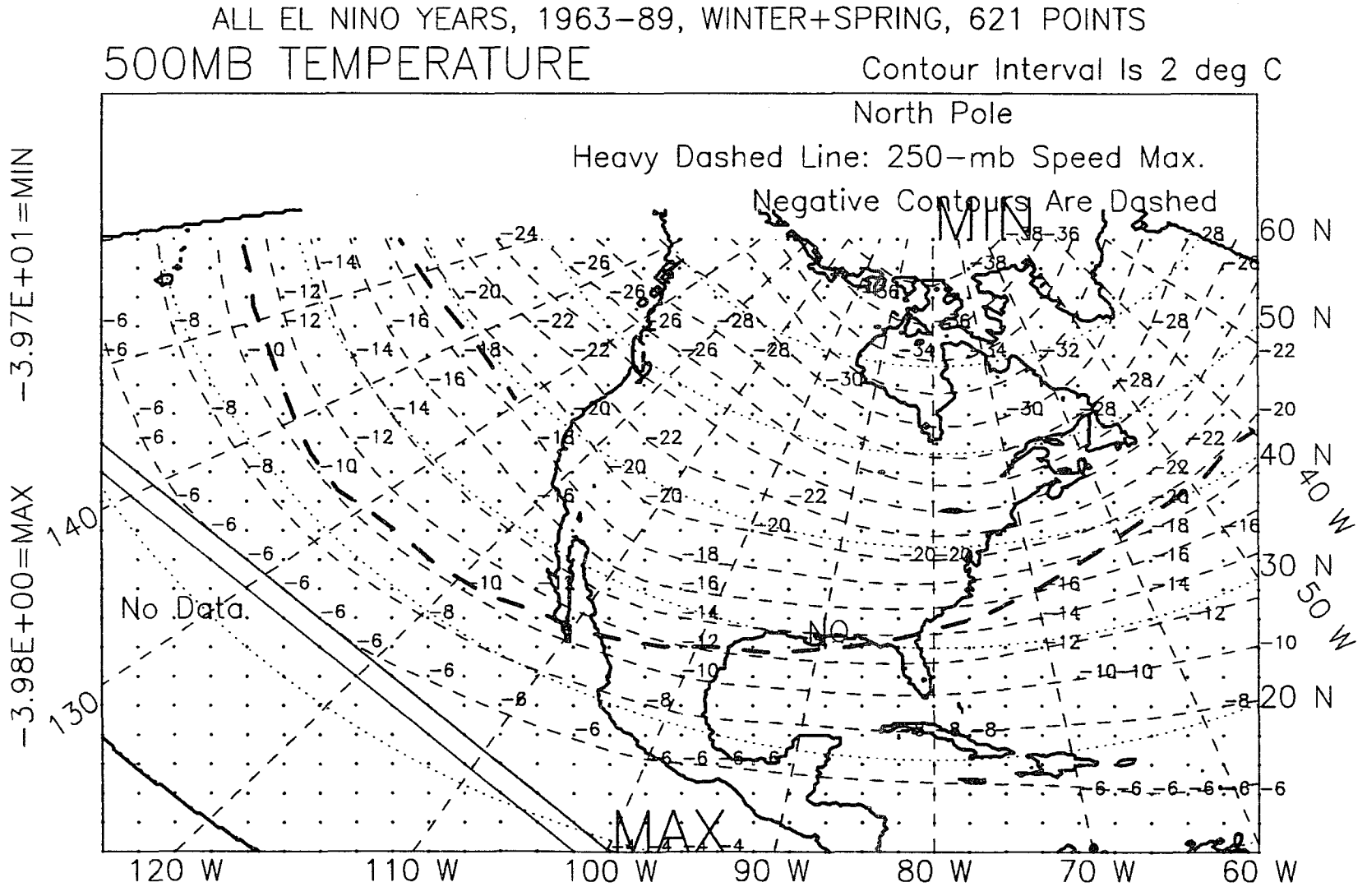

Figure I.7: 500–mb temperature, winter–plus–spring, El Niño years, 1963–89.

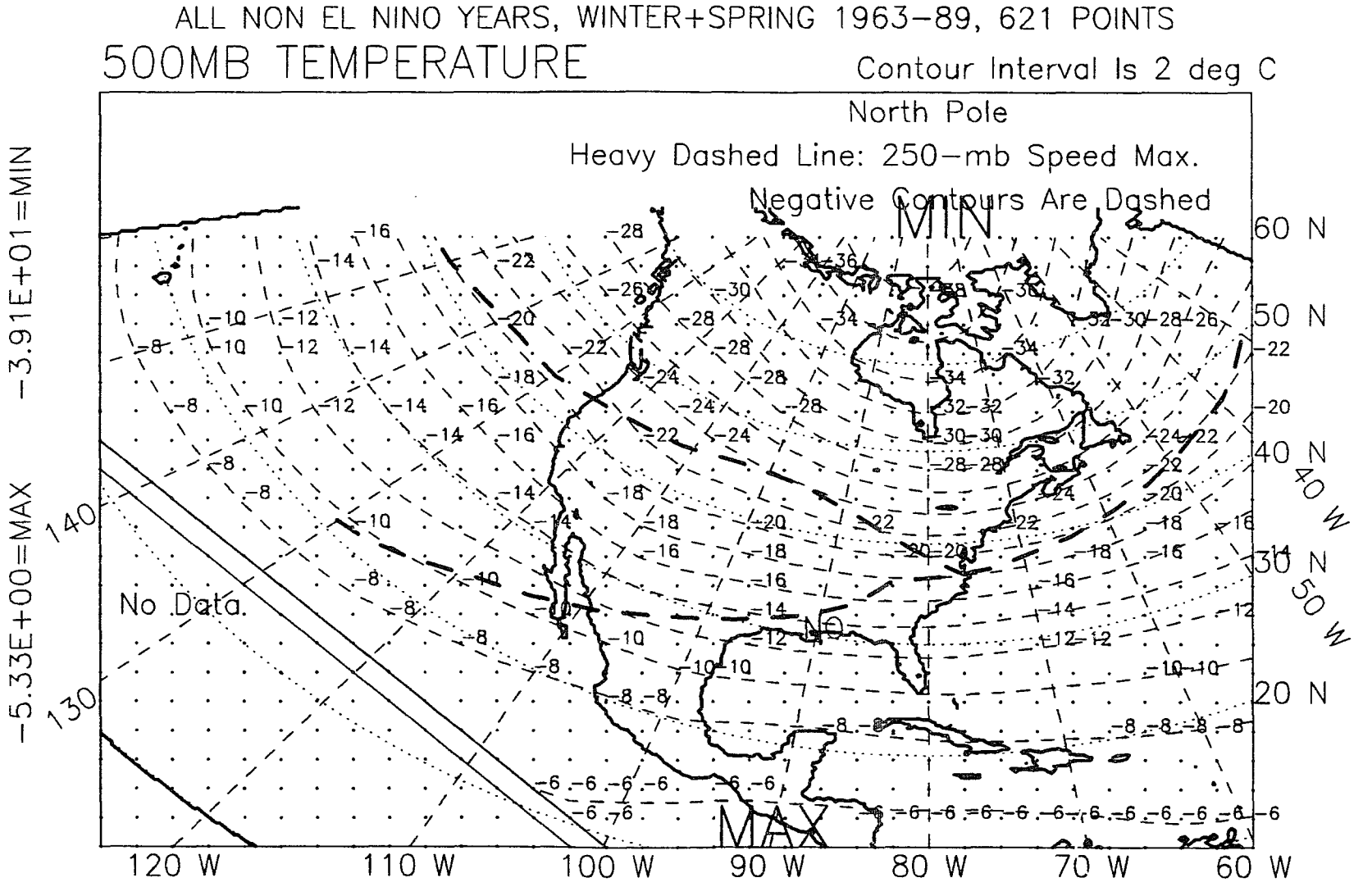

Figure I.8: 500–mb temperature, winter–plus–spring, non–El Niño years, 1963–89.

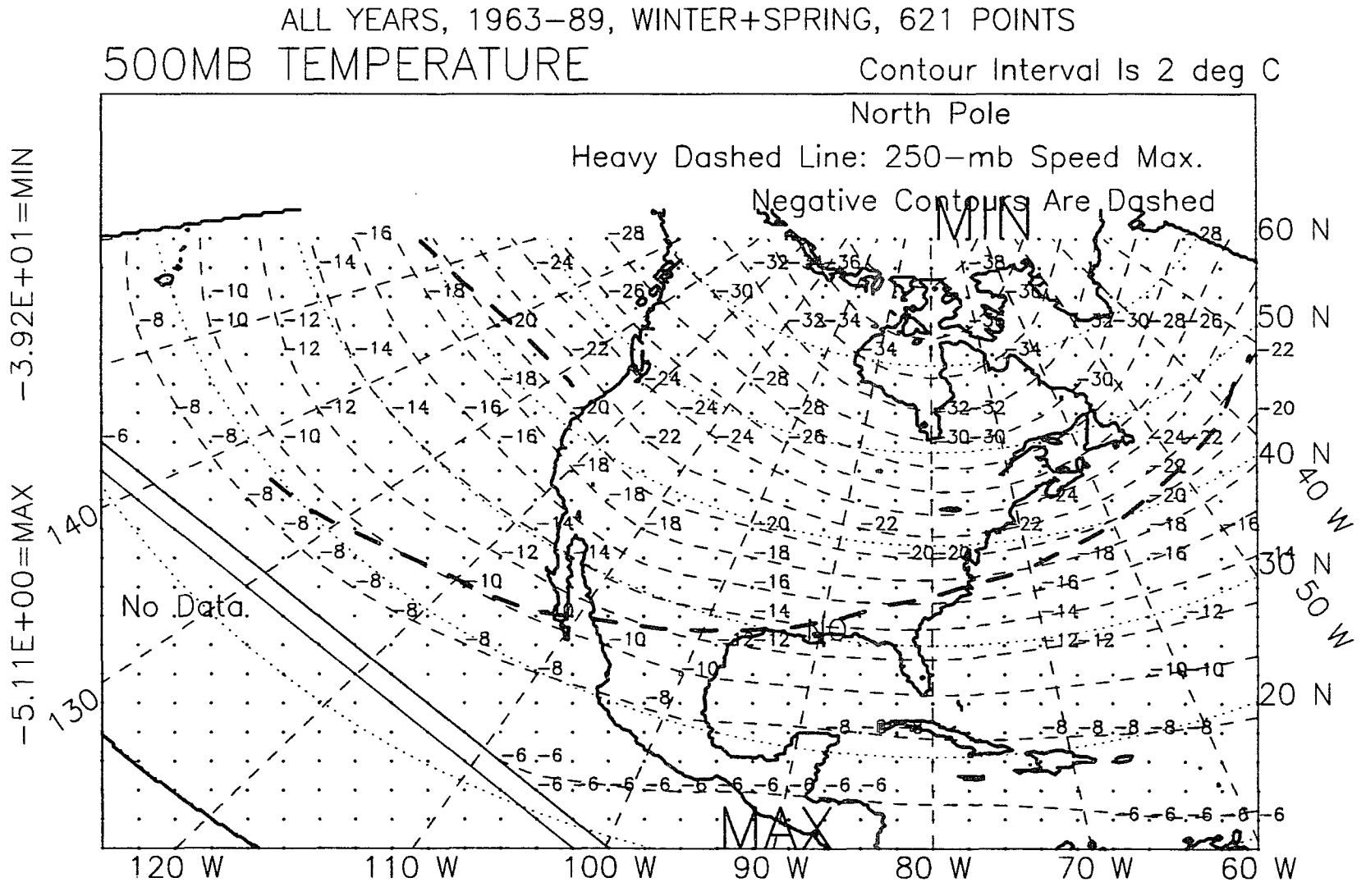

Figure I.9: 500–mb temperature, winter–plus–spring, all years, 1963–89.

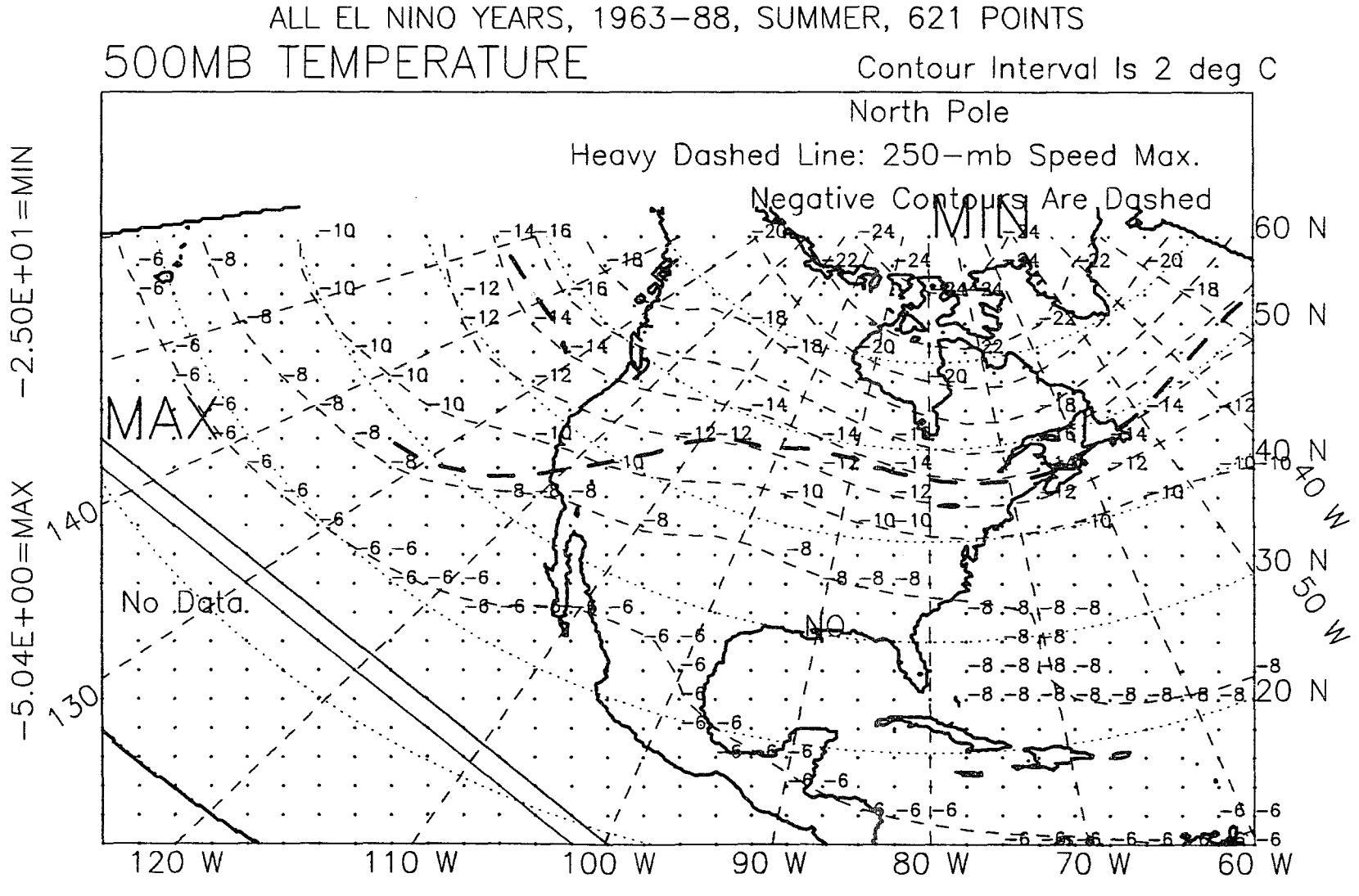

Figure I.10: 500–mb temperature, summer, El Niño years, 1963–88.

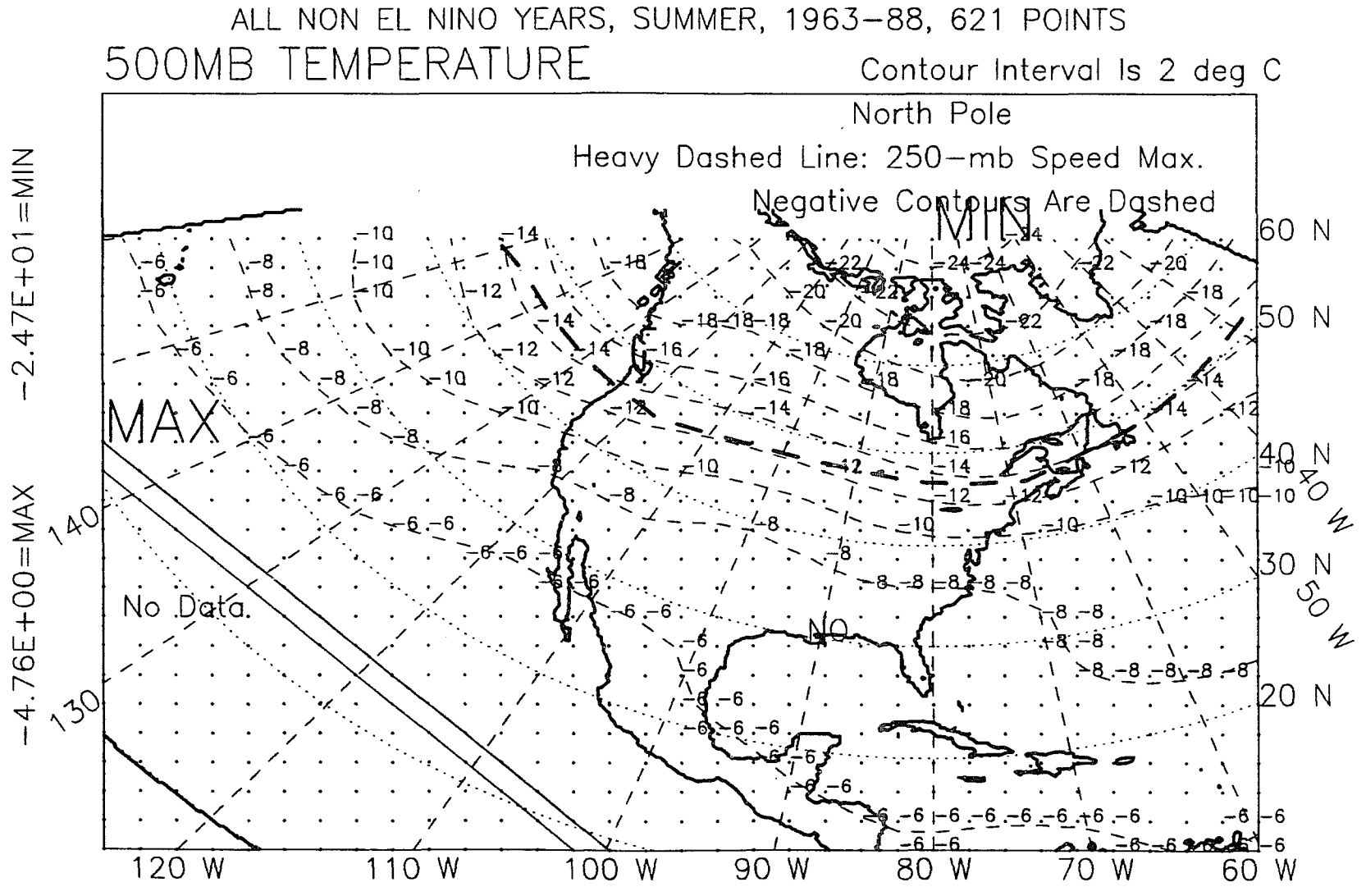

Figure I.11: 500–mb temperature, summer, non–El Niño years, 1963–88.

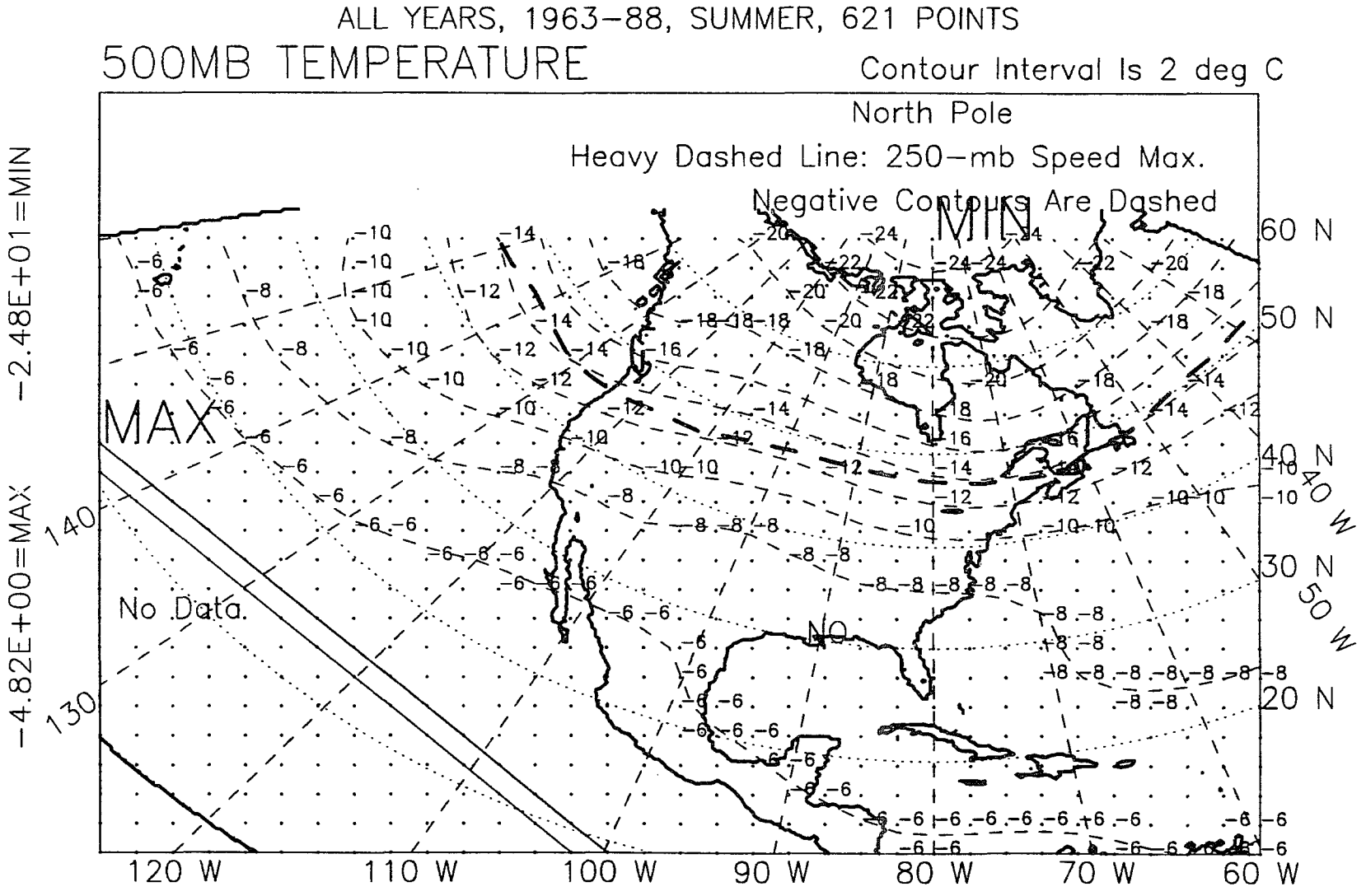

Figure I.12: 500–mb temperature, summer, all years, 1963–88.

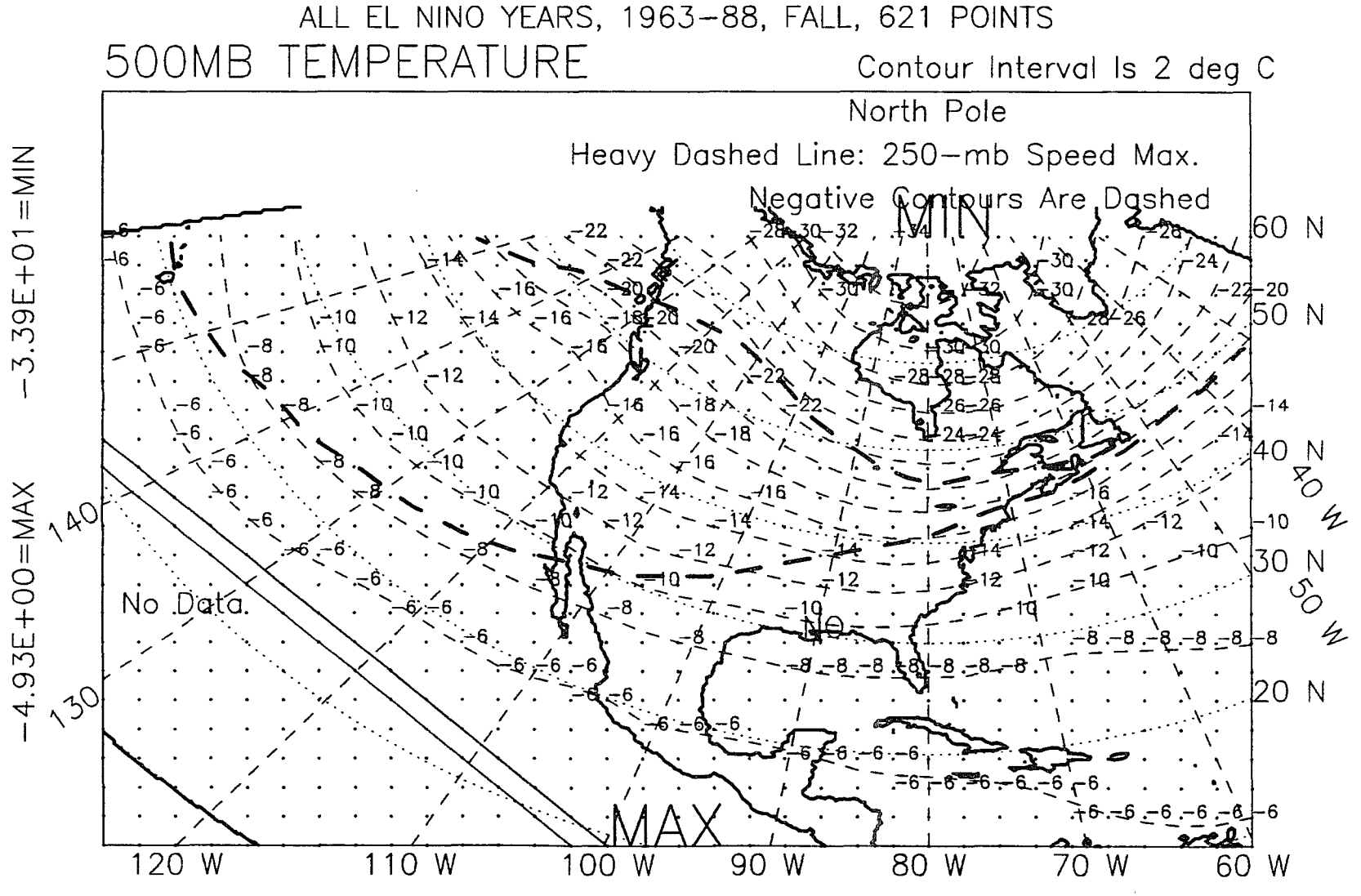

Figure I.13: 500–mb temperature, fall, El Niño years, 1963–88.

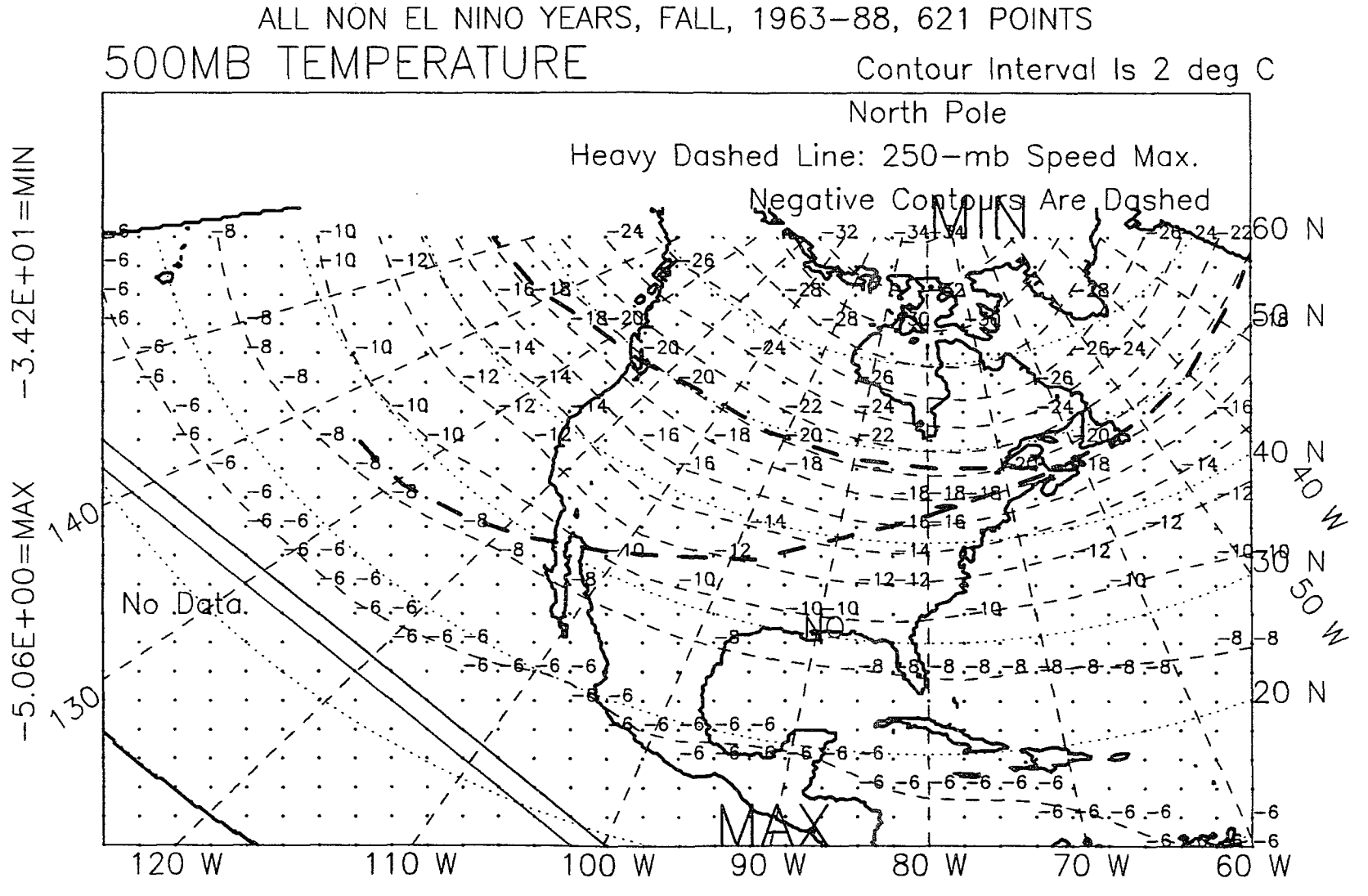

Figure I.14: 500–mb temperature, fall, non–El Niño years, 1963–88.

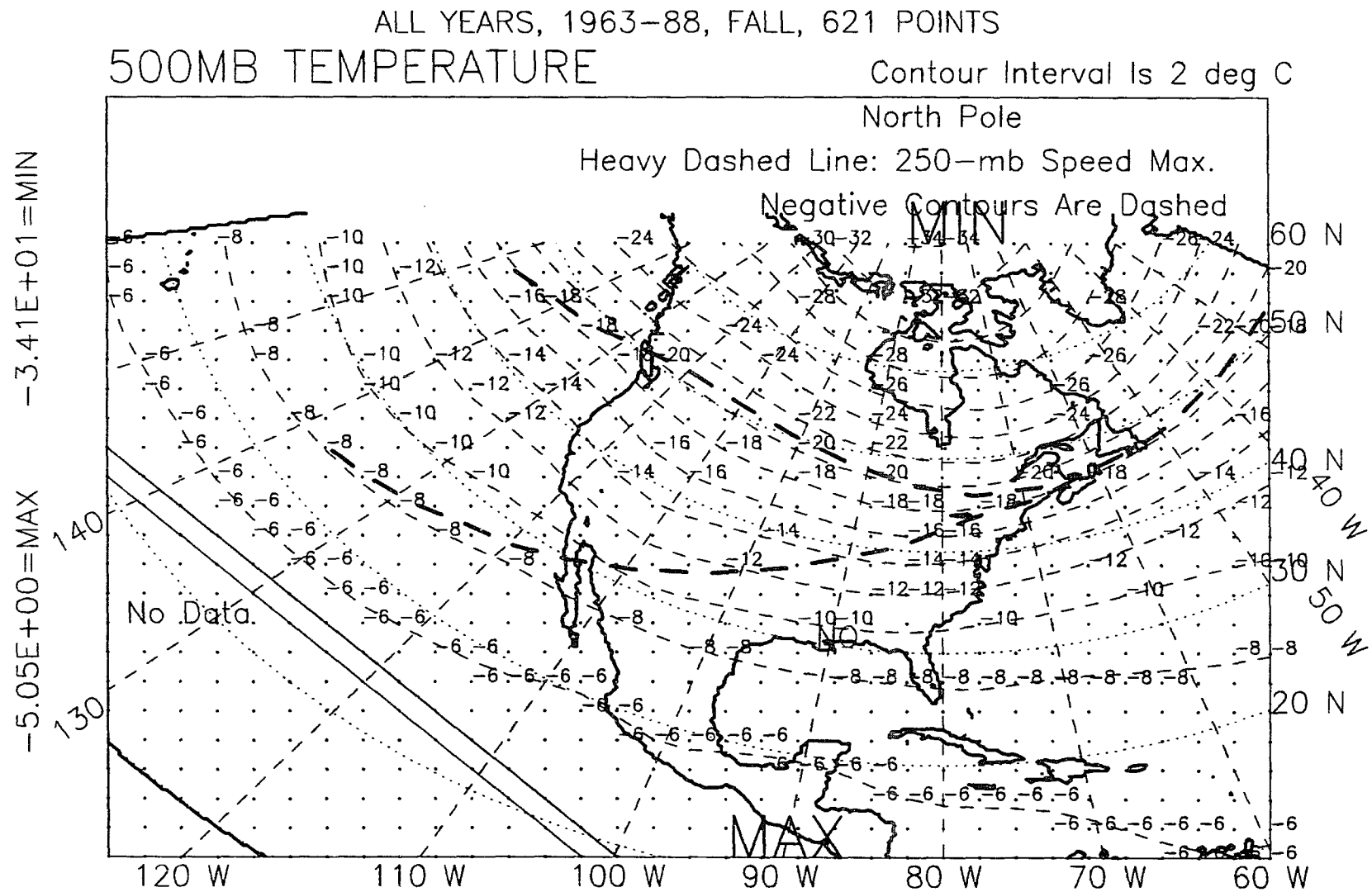

Figure I.15: 500–mb temperature, fall, all years, 1963–88.

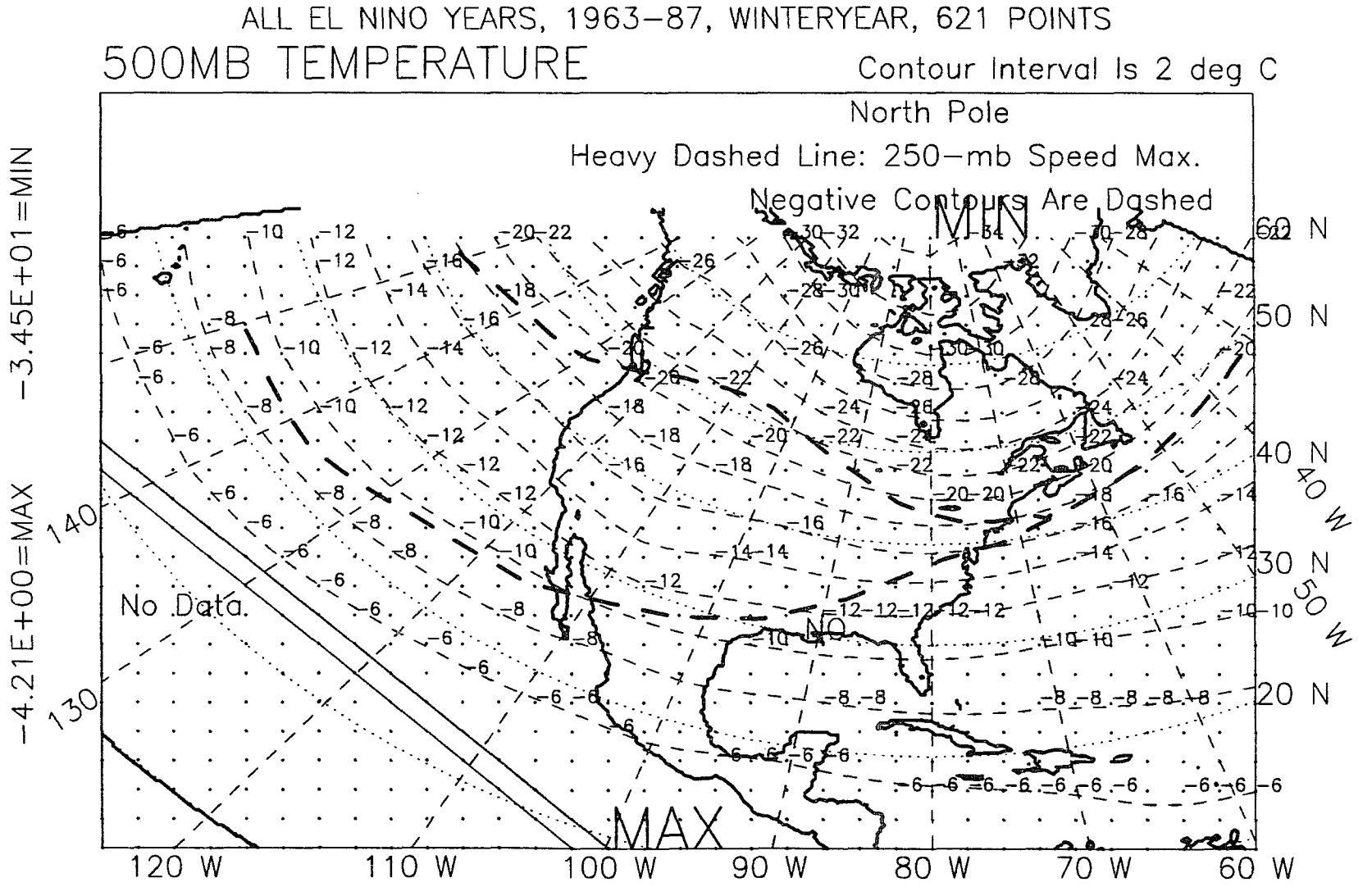

Figure I.16: 500–mb temperature, winter year, El Niño years, 1963–87.

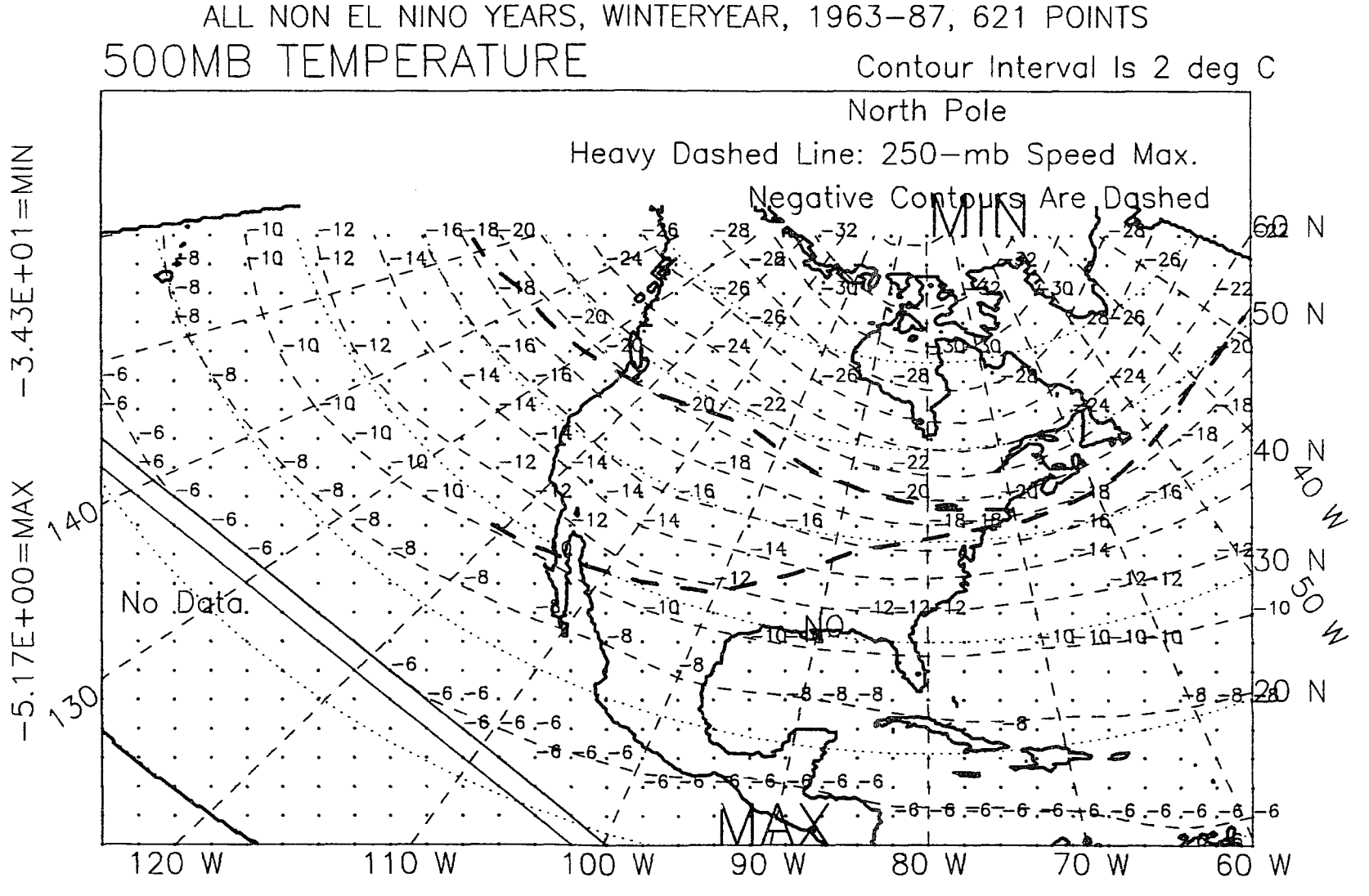

Figure I.17: 500–mb temperature, winter year, non–El Niño years, 1963–87.

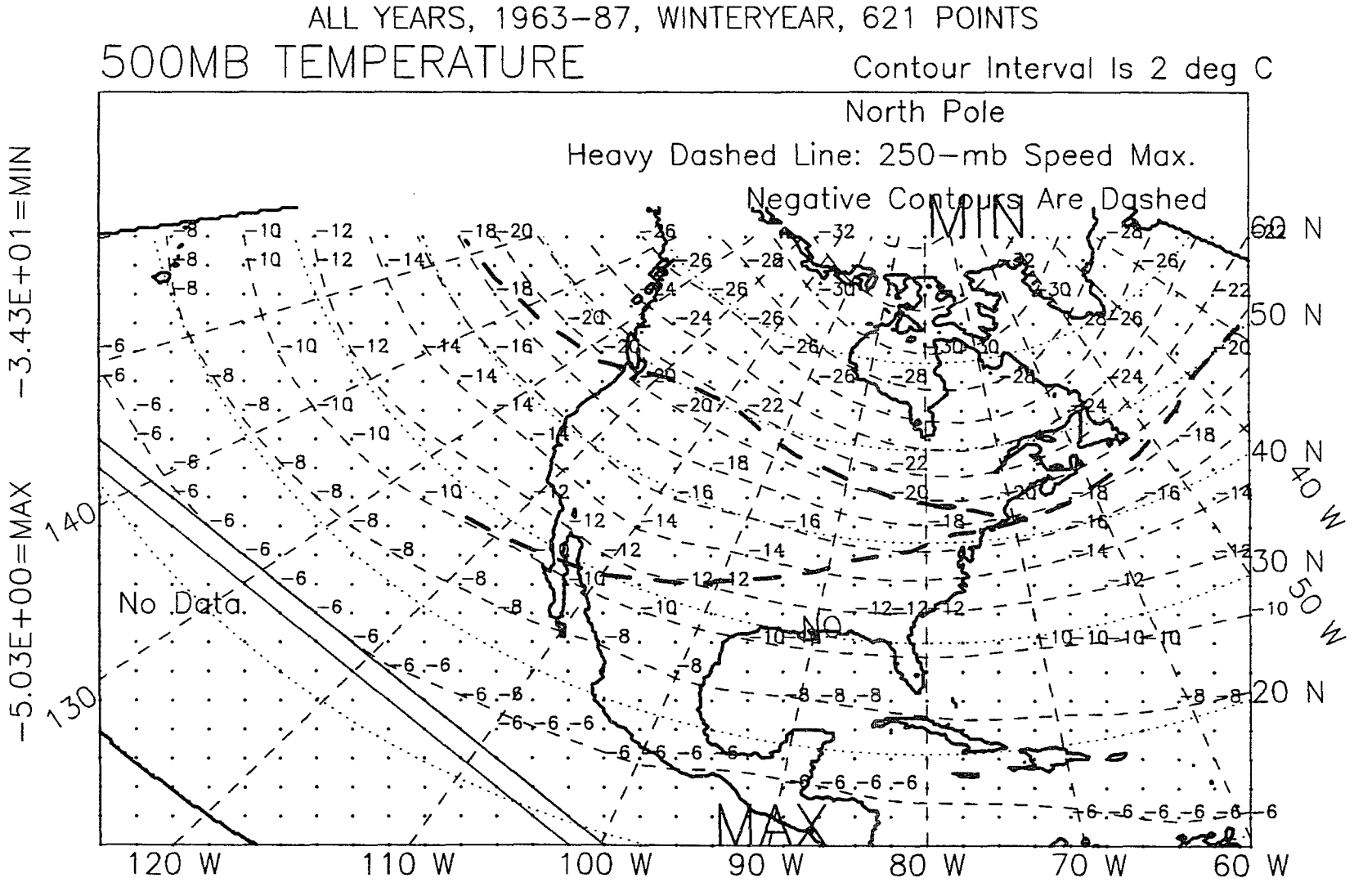

Figure I.18: 500–mb temperature, winter year, all years, 1963–87.

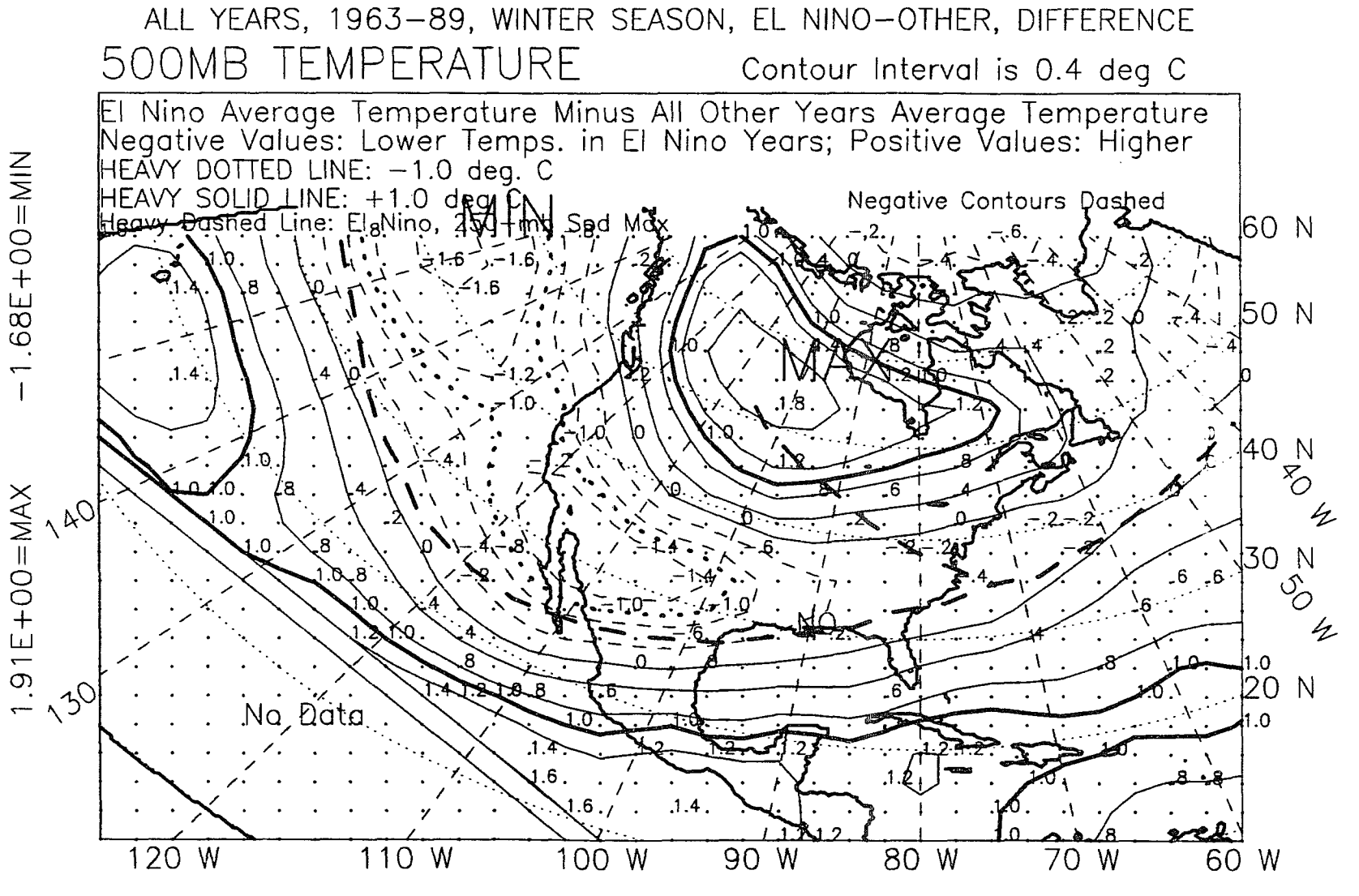

Figure I.19: 500–mb temperature, winter, 1963–89, difference.

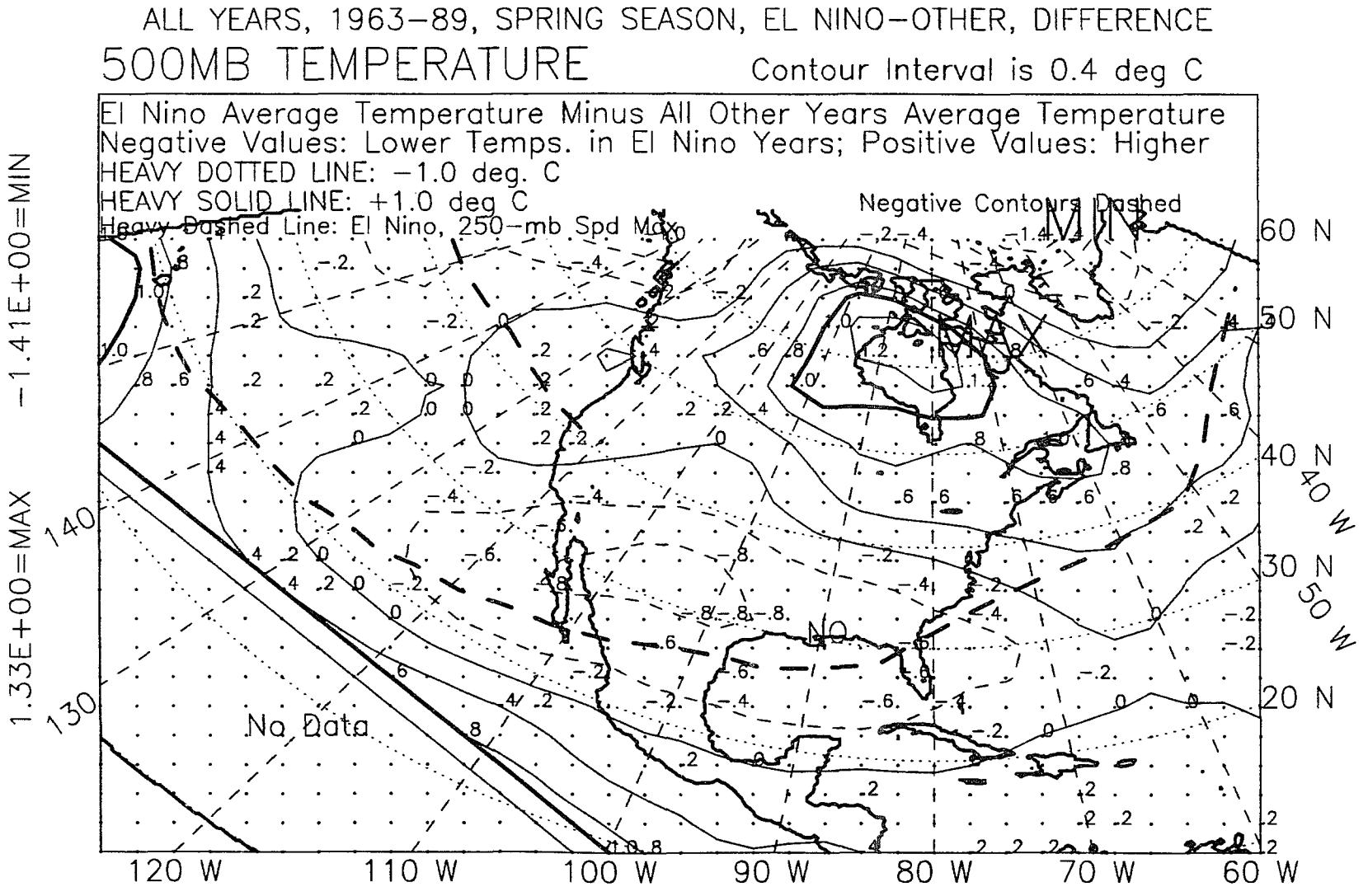

Figure I.20: 500–mb temperature, spring, 1963–89, difference.

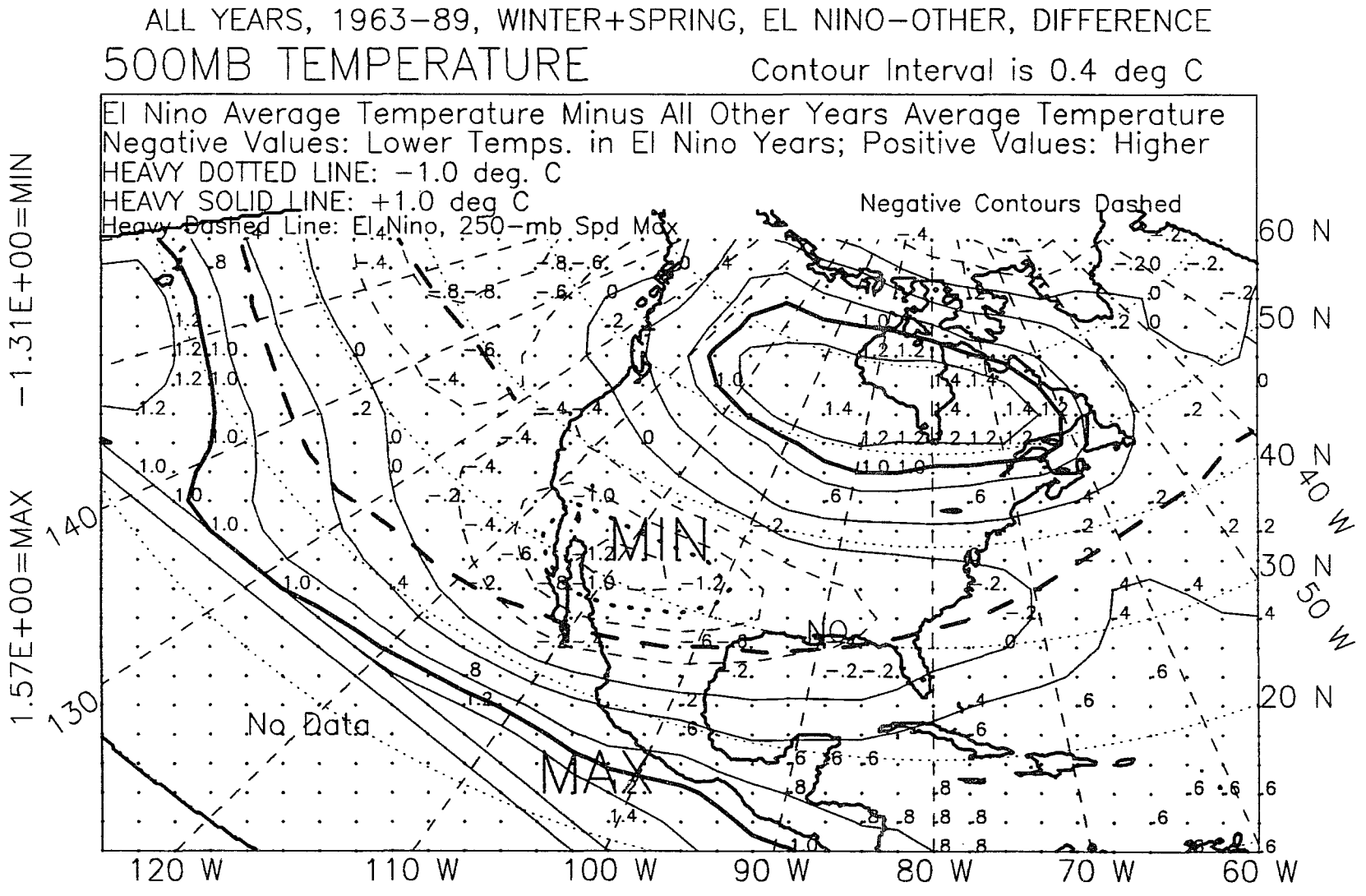

Figure I.21: 500–mb temperature, winter–plus–spring, 1963–89, difference.

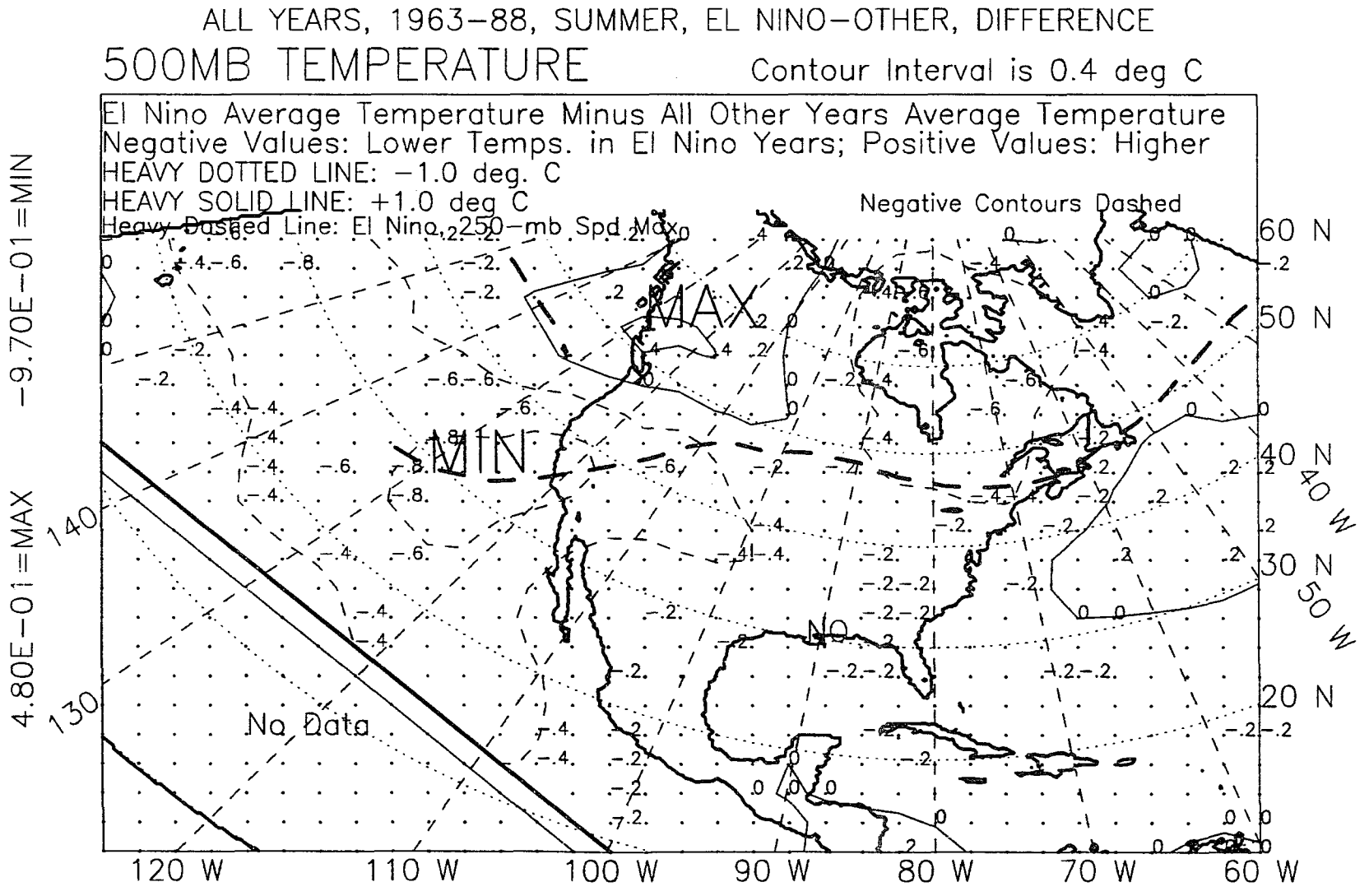

Figure I.22: 500−mb temperature, summer, 1963−88, difference.

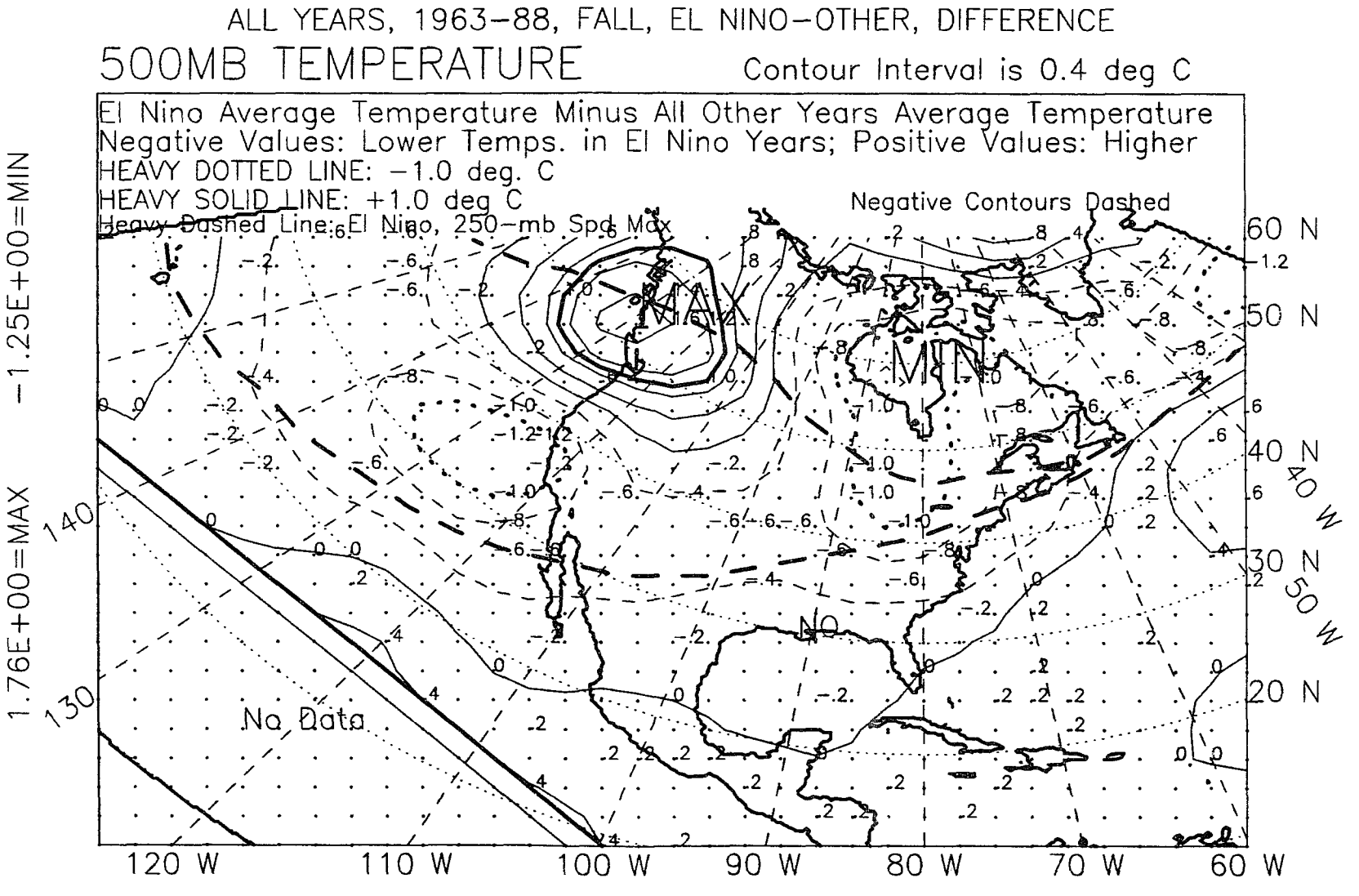

Figure I.23: 500–mb temperature, fall, 1963–88, difference.

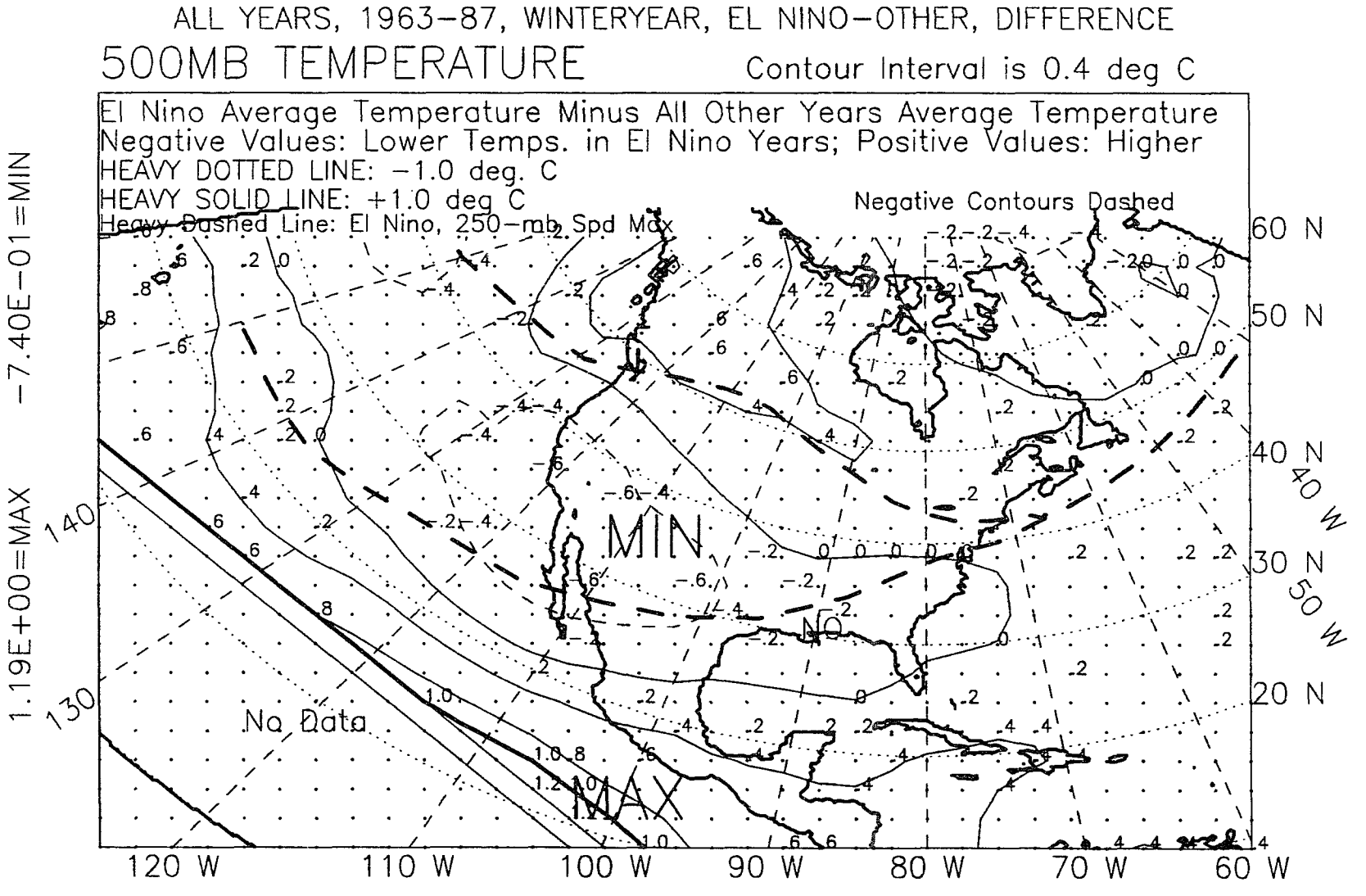

Figure I.24: 500–mb temperature, winter year, 1963–87, difference.

APPENDIX J
250-MB WIND FIELD

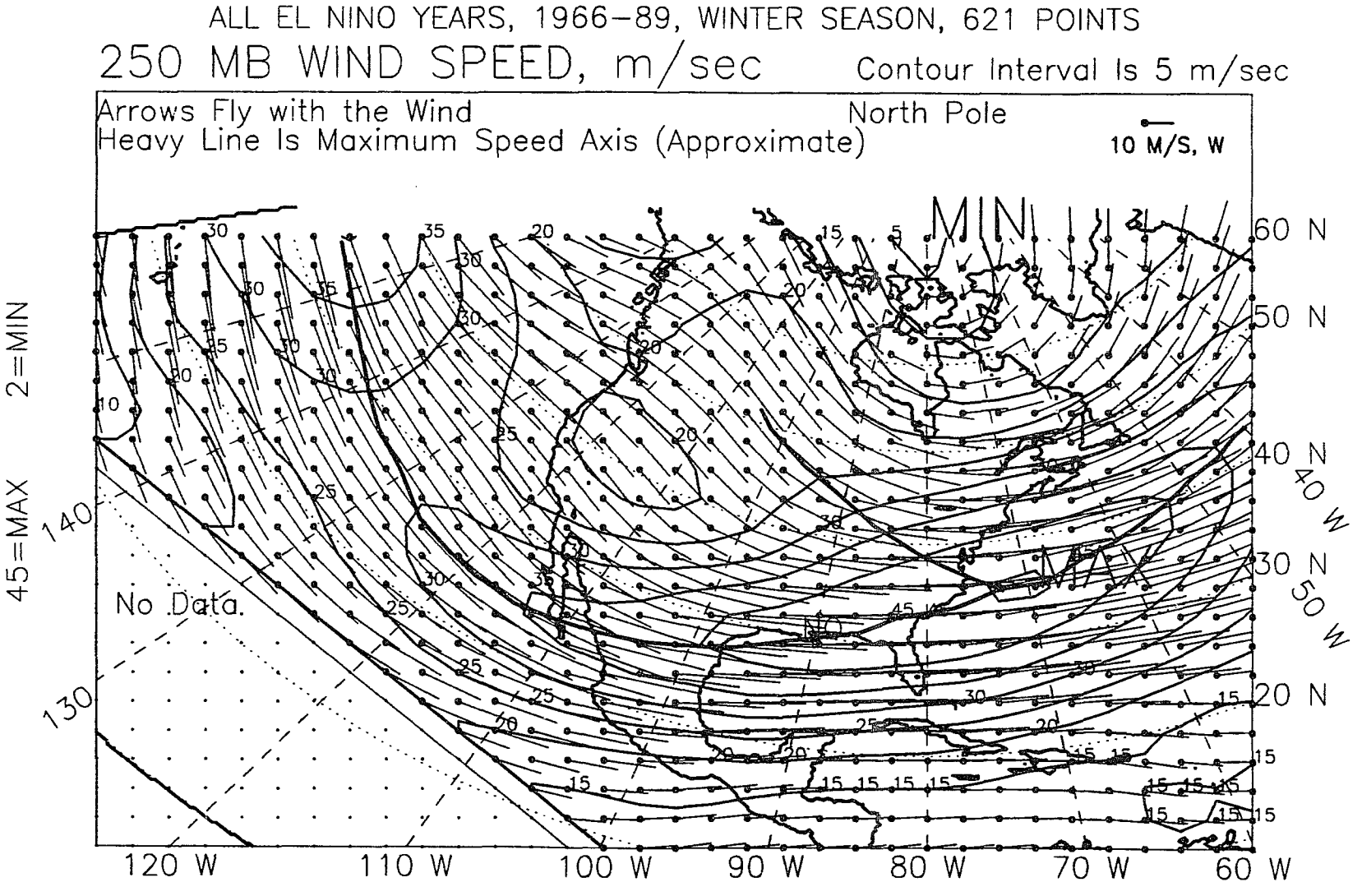

Figure J.1: 250–mb wind vectors, winter, El Niño years, 1966–89.

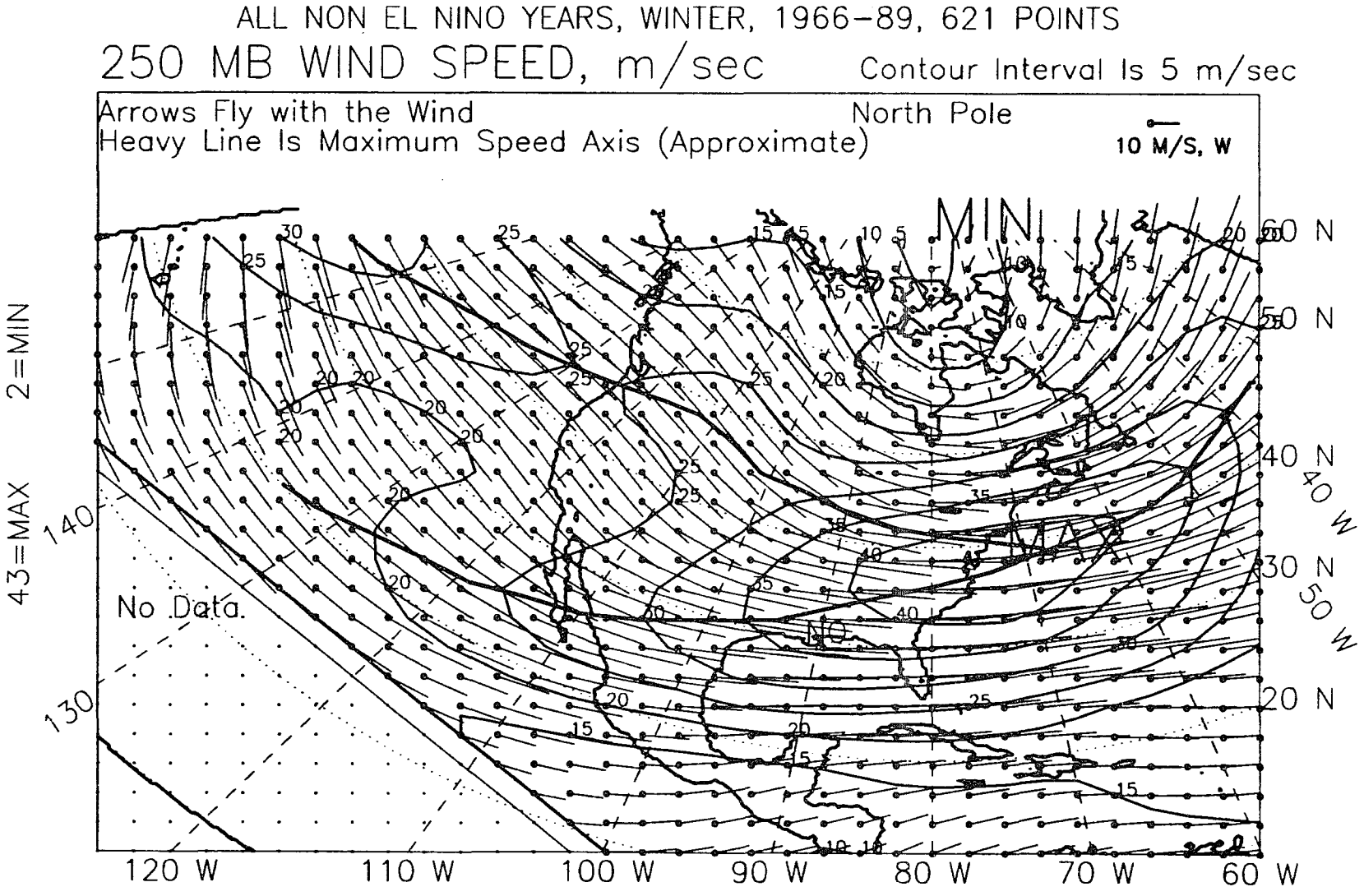

Figure J.2: 250-mb wind vectors, winter, non-El Niño years, 1966-89.

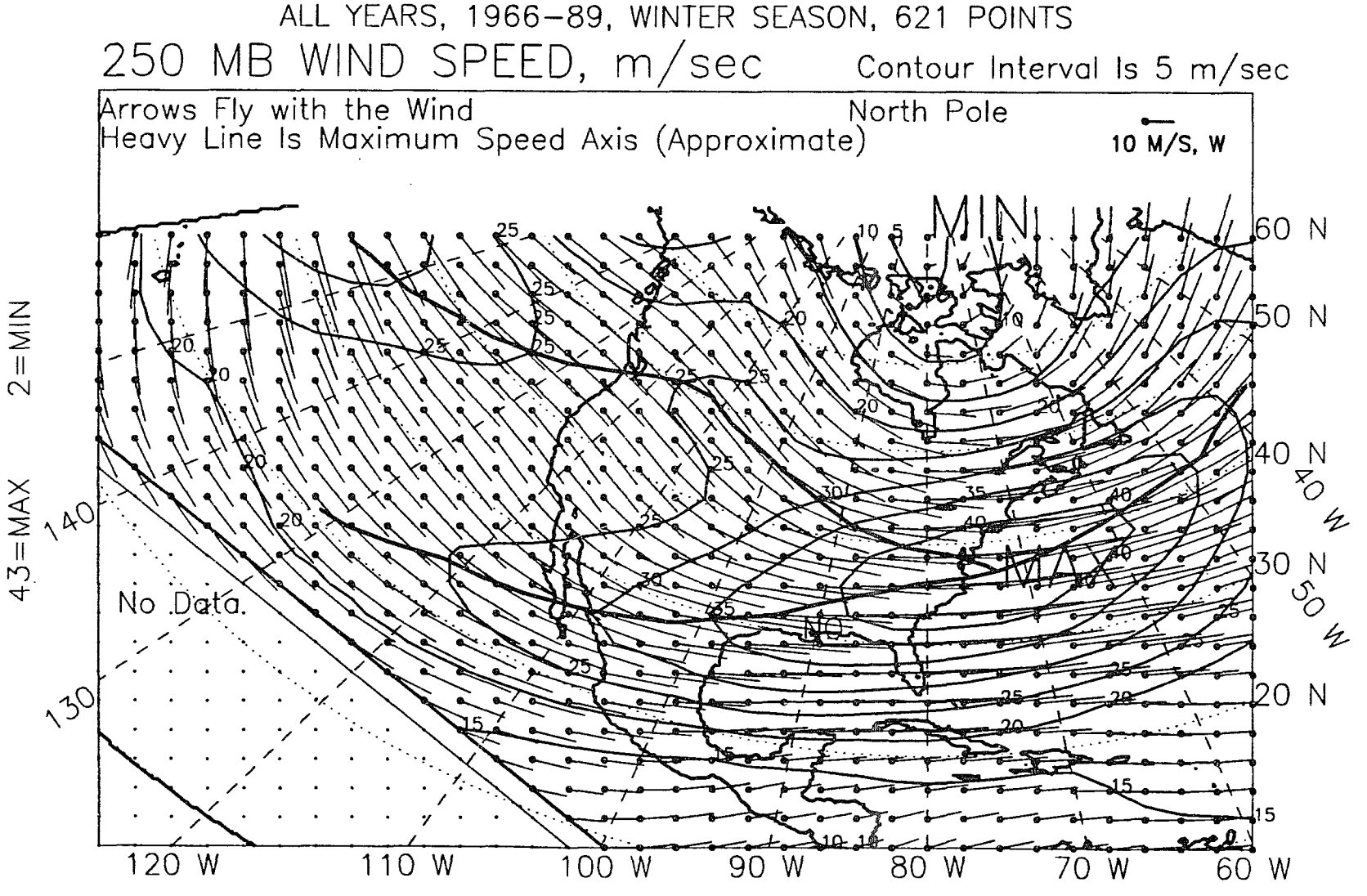

Figure J.3: 250–mb wind vectors, winter, all years, 1966–89.

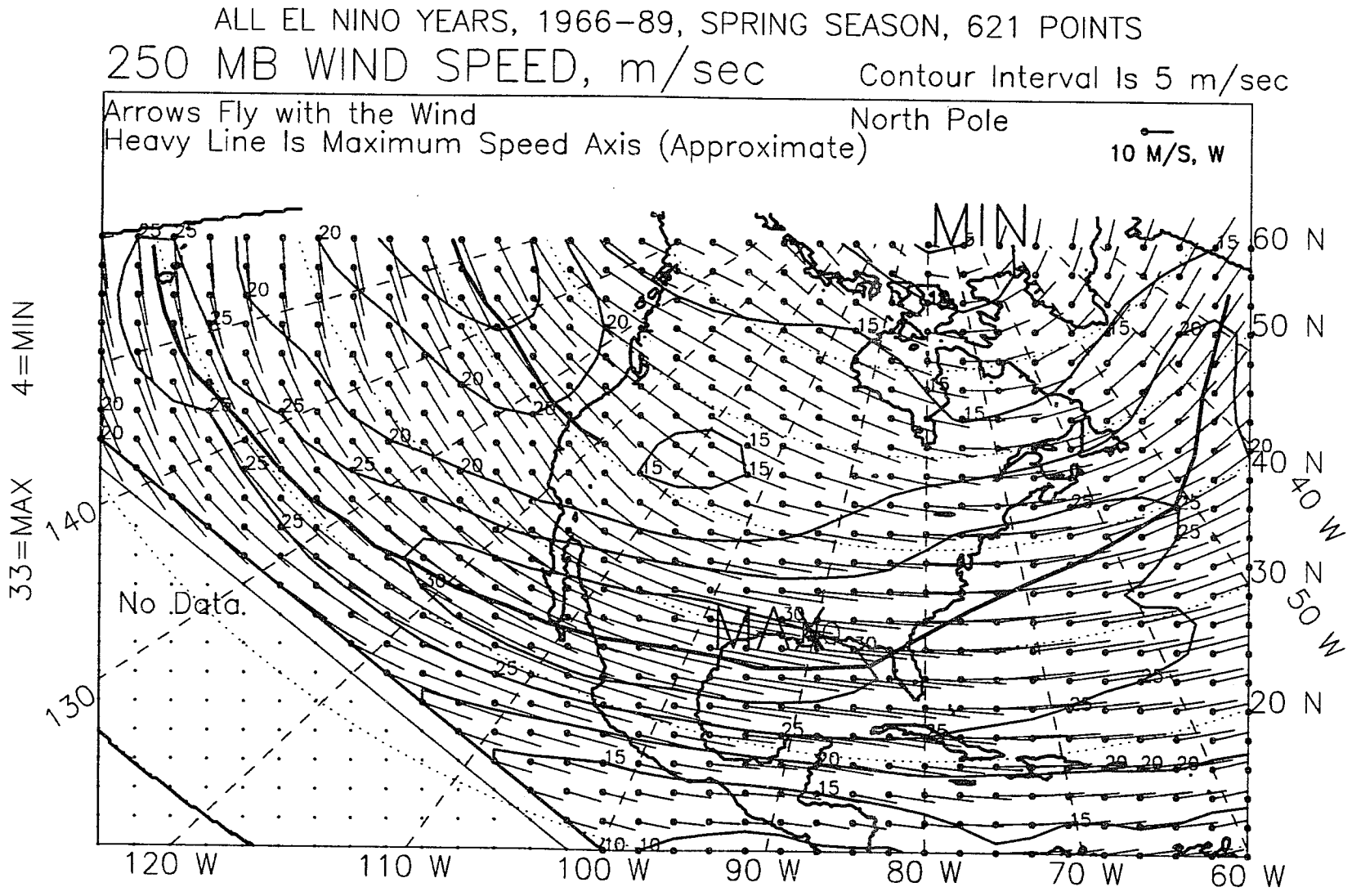

Figure J.4: 250–mb wind vectors, spring, El Niño years, 1966–89.

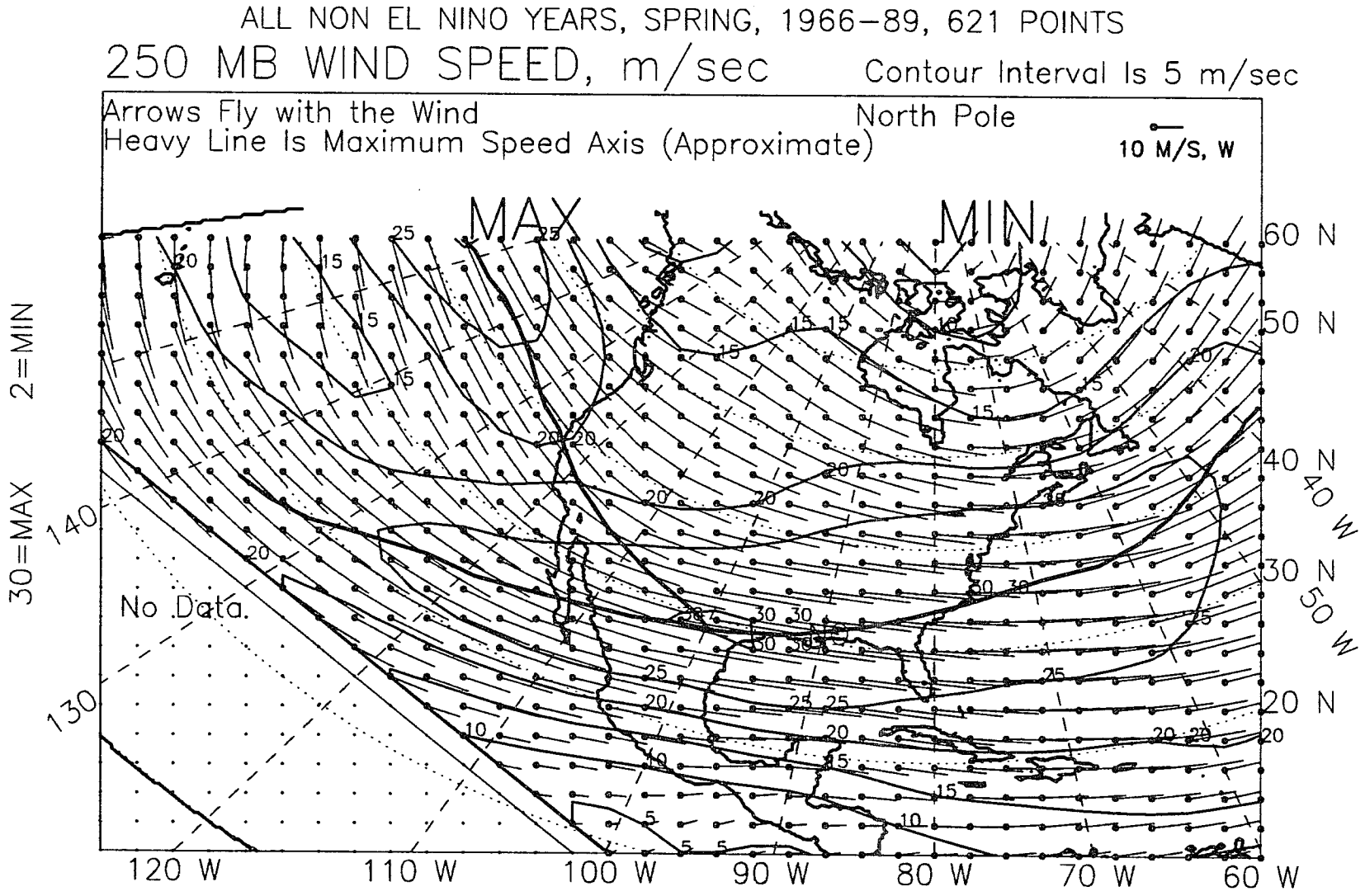

Figure J.5: 250–mb wind vectors, spring, non–El Niño years, 1966–89.

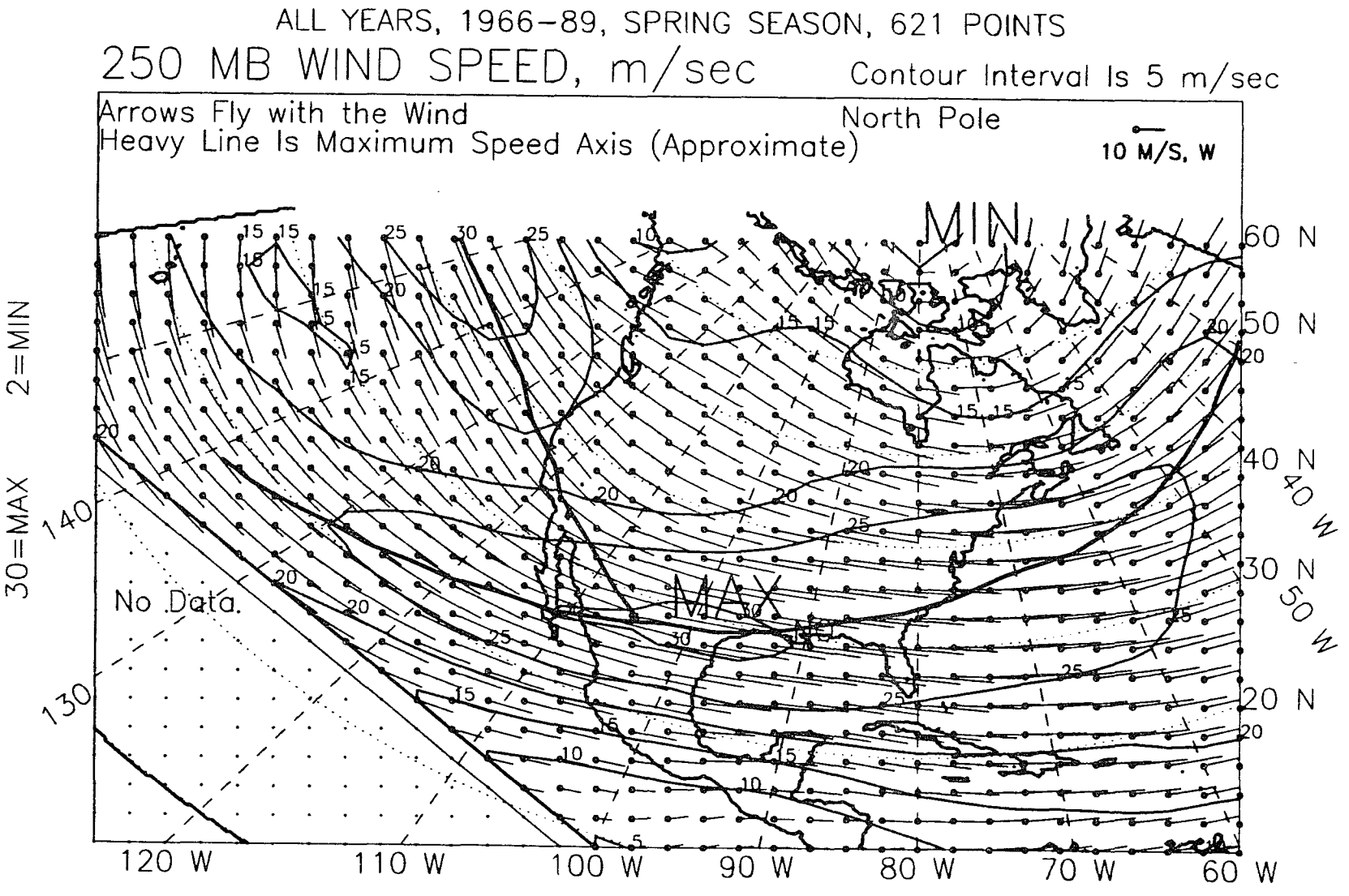

Figure J.6: 250–mb wind vectors, spring, all years, 1966–89.

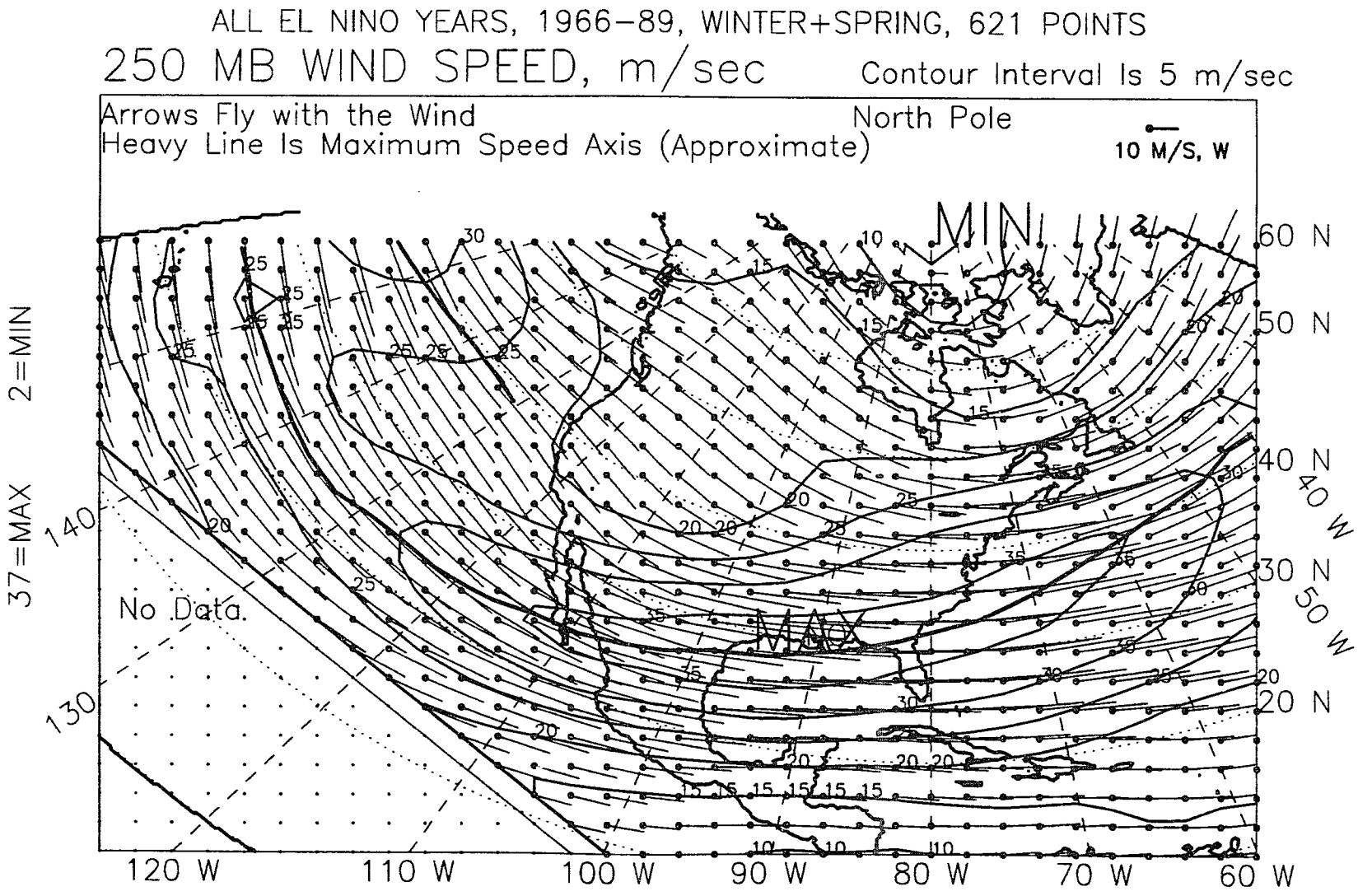

Figure J.7: 250–mb wind vectors, winter–plus–spring, El Niño years, 1966–89.

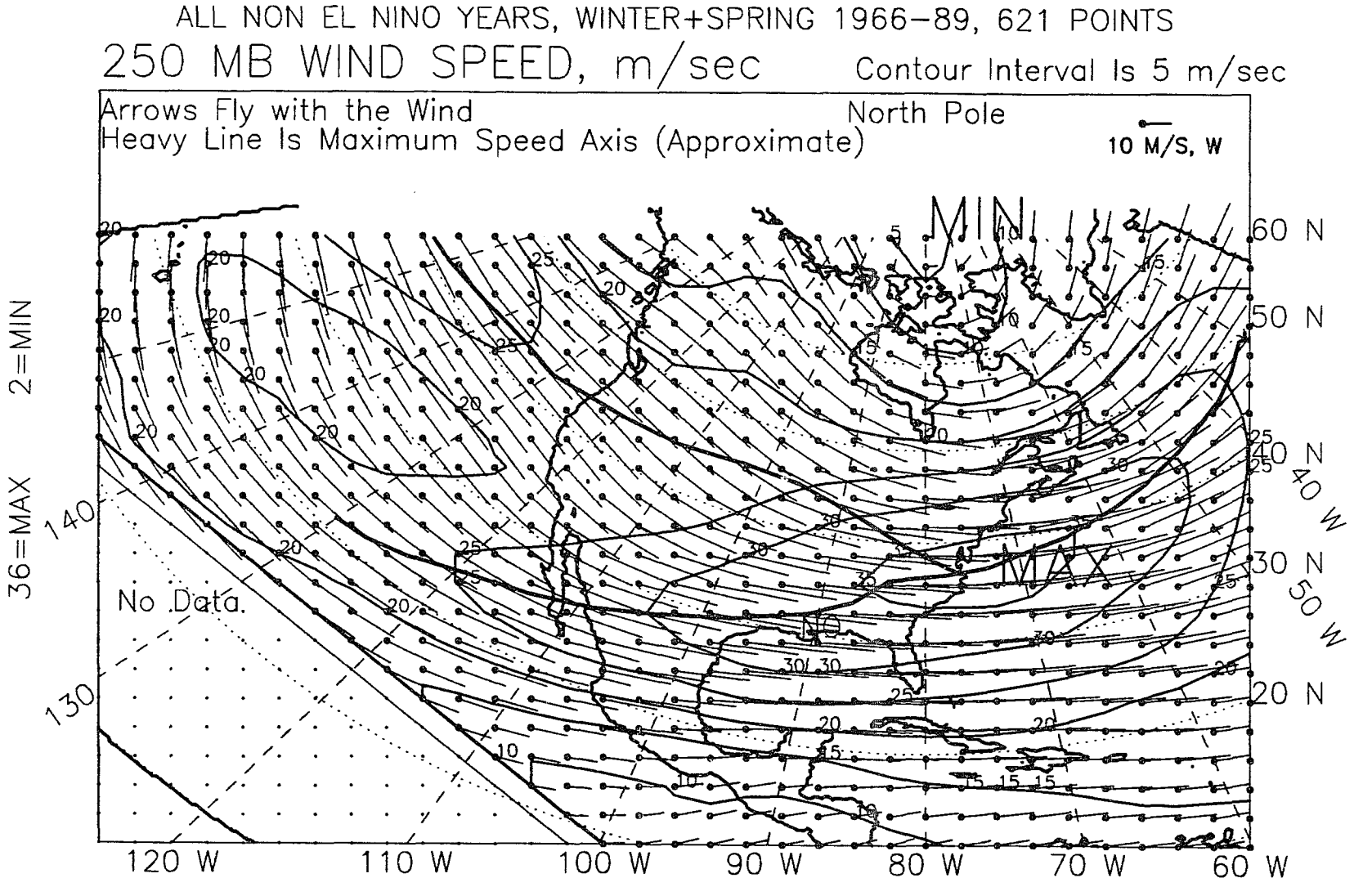

Figure J.8: 250-mb wind vectors, winter-plus-spring, non-El Niño years, 1966-89.

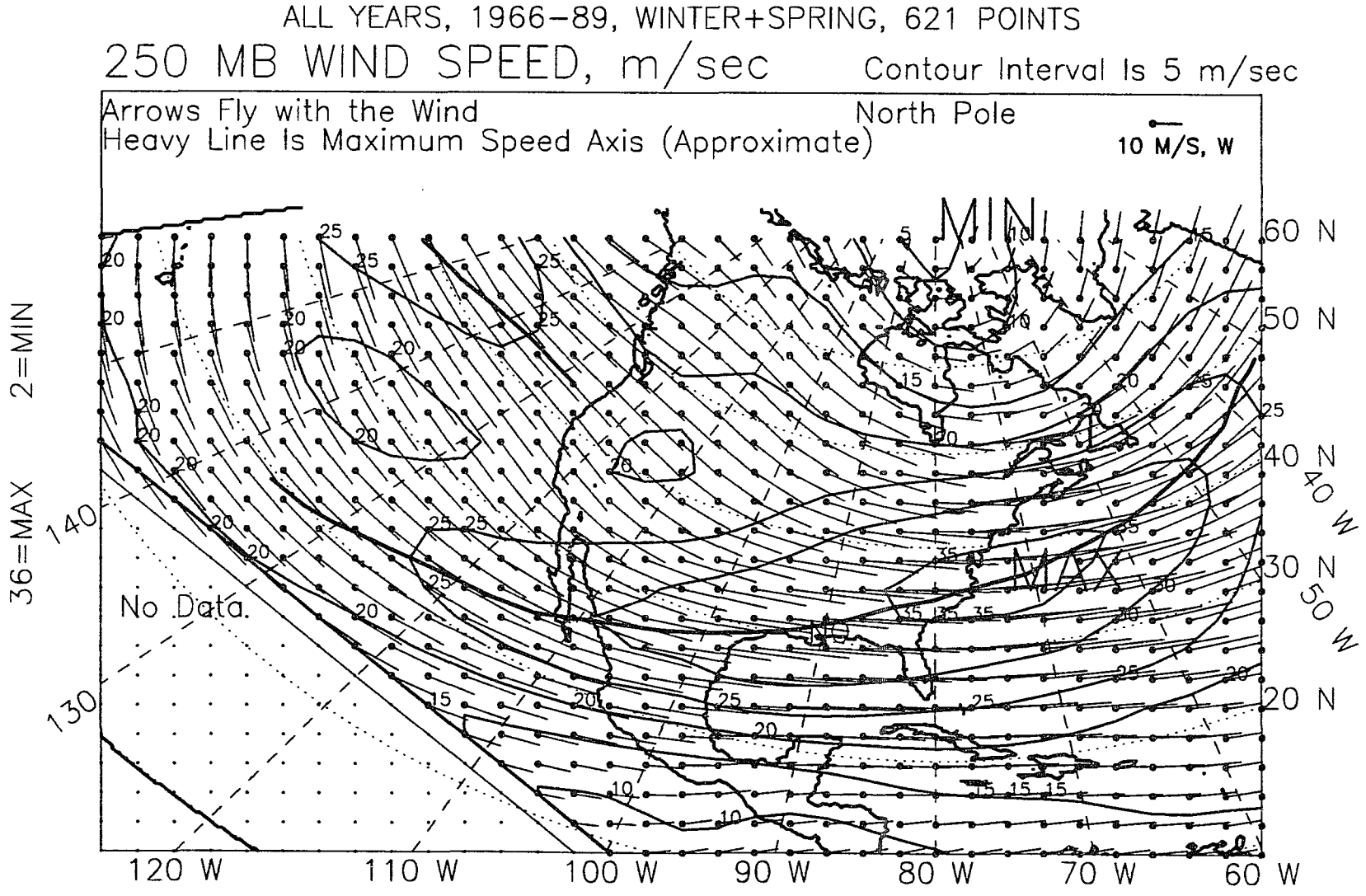

Figure J.9: 250–mb wind vectors, winter–plus–spring, all years, 1966–89.

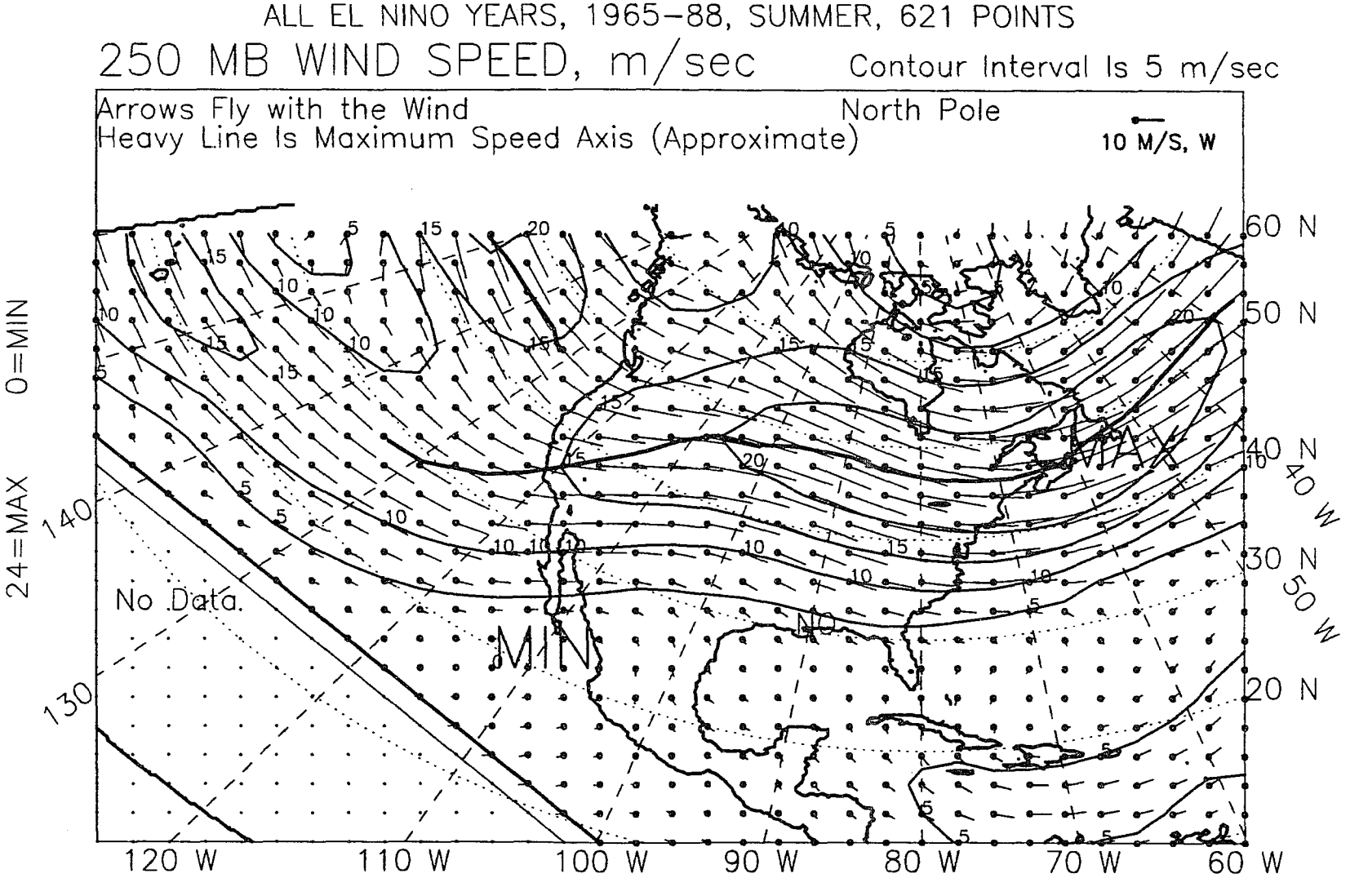

Figure J.10: 250–mb wind vectors, summer, El Niño years, 1965–88.

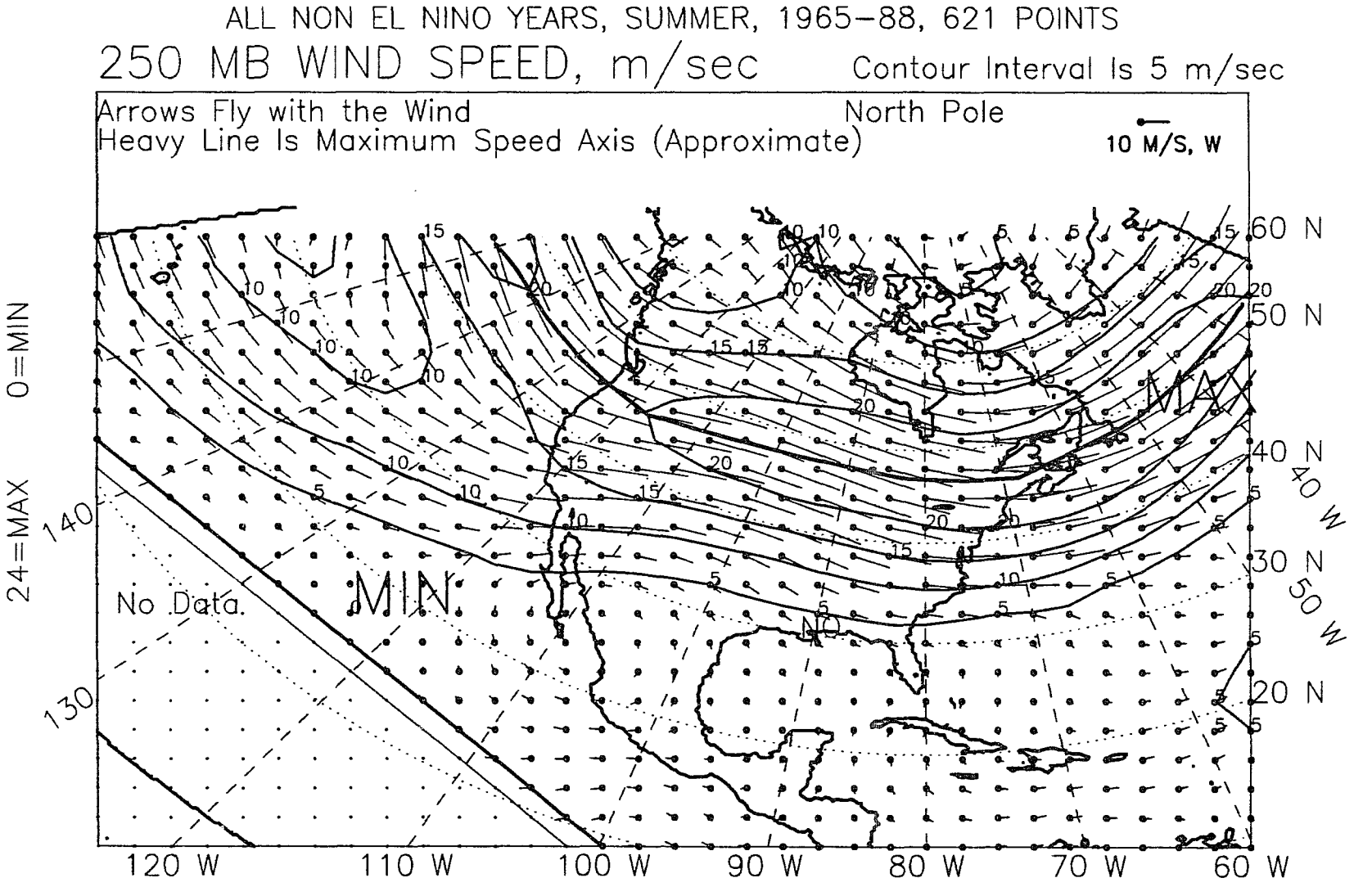

Figure J.11: 250–mb wind vectors, summer, non–El Niño years, 1965–88.

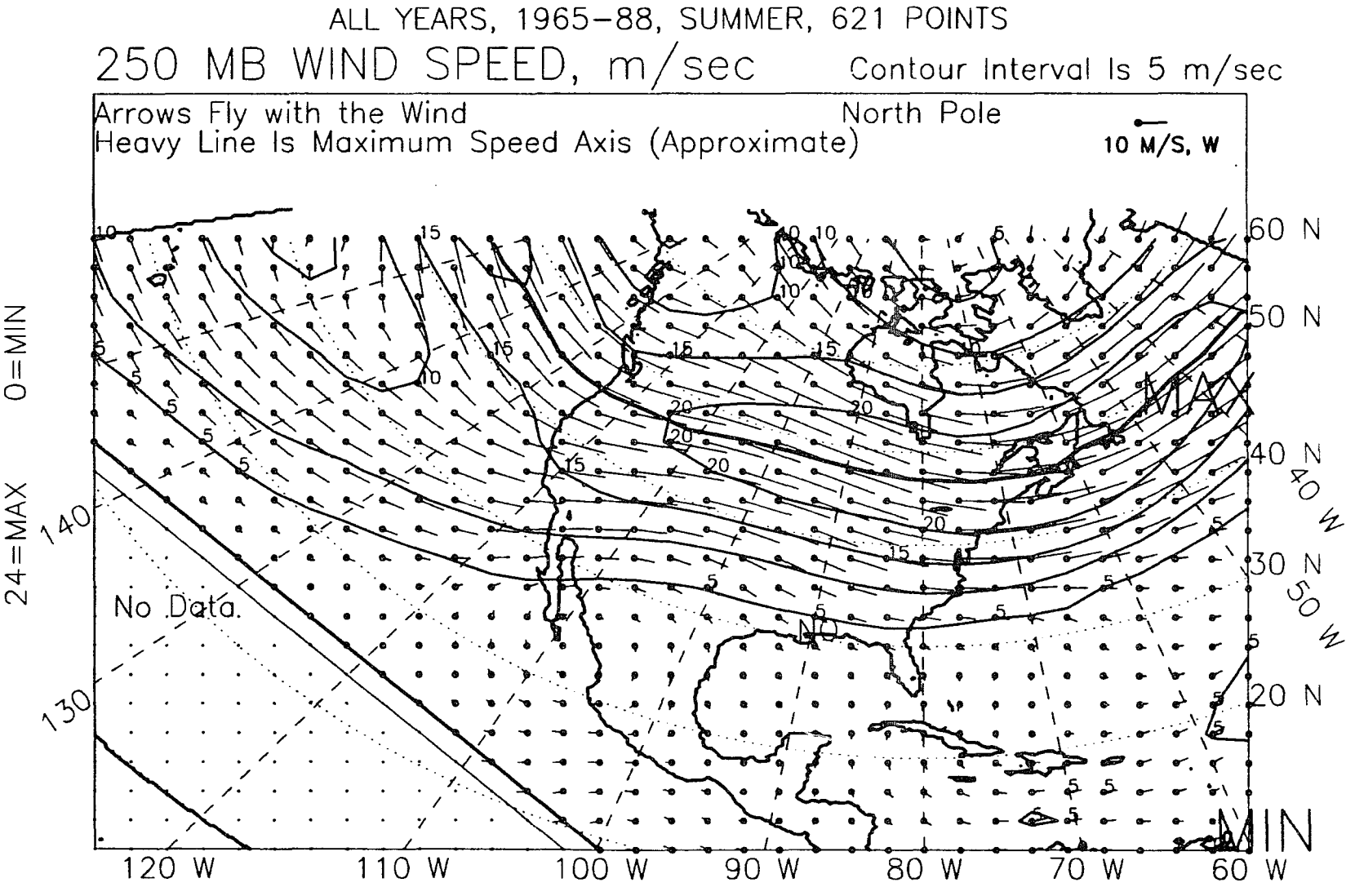

Figure J.12: 250–mb wind vectors, summer, all years, 1965–88.

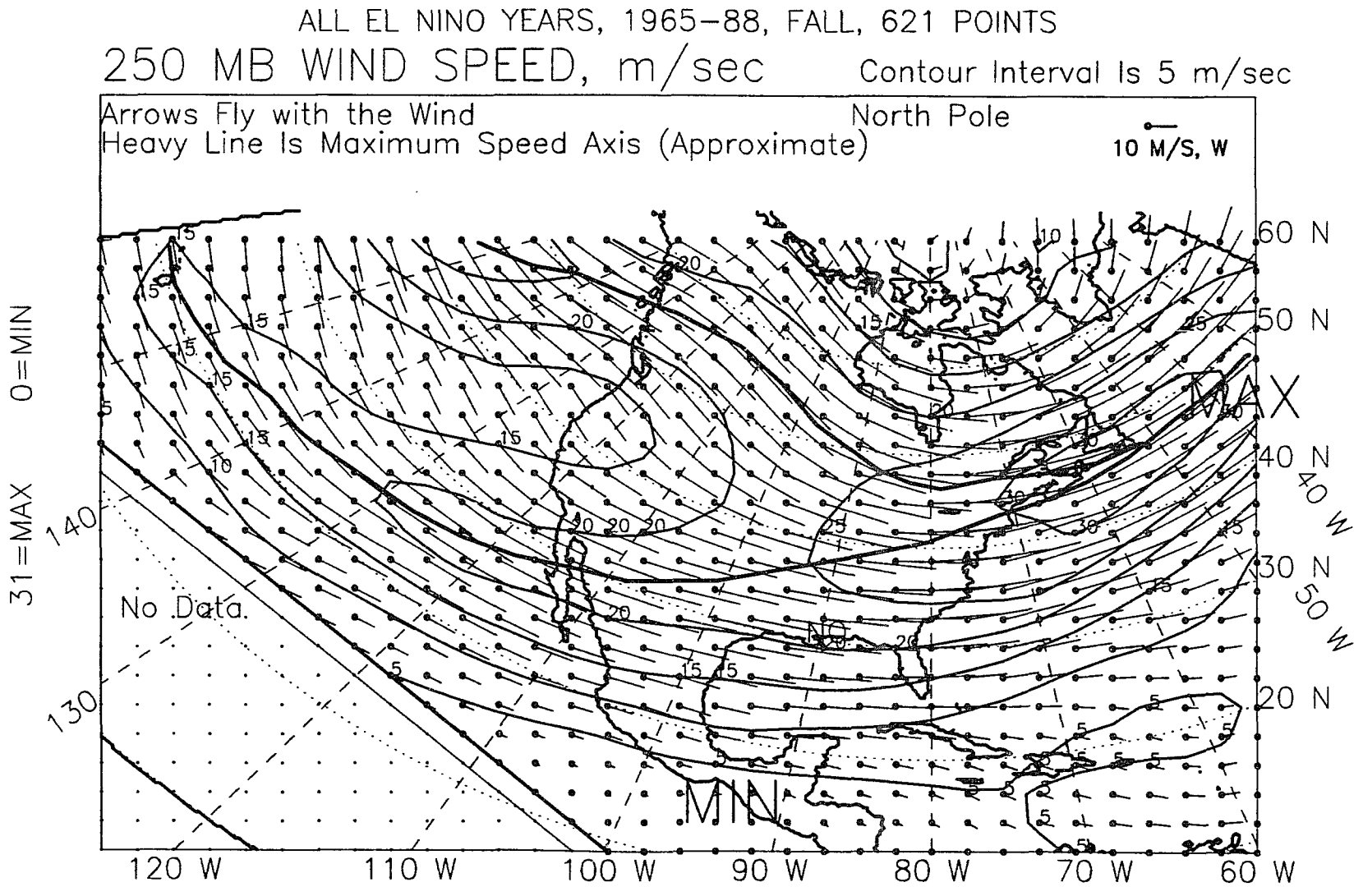

Figure J.13: 250–mb wind vectors, fall, El Niño years, 1965–88.

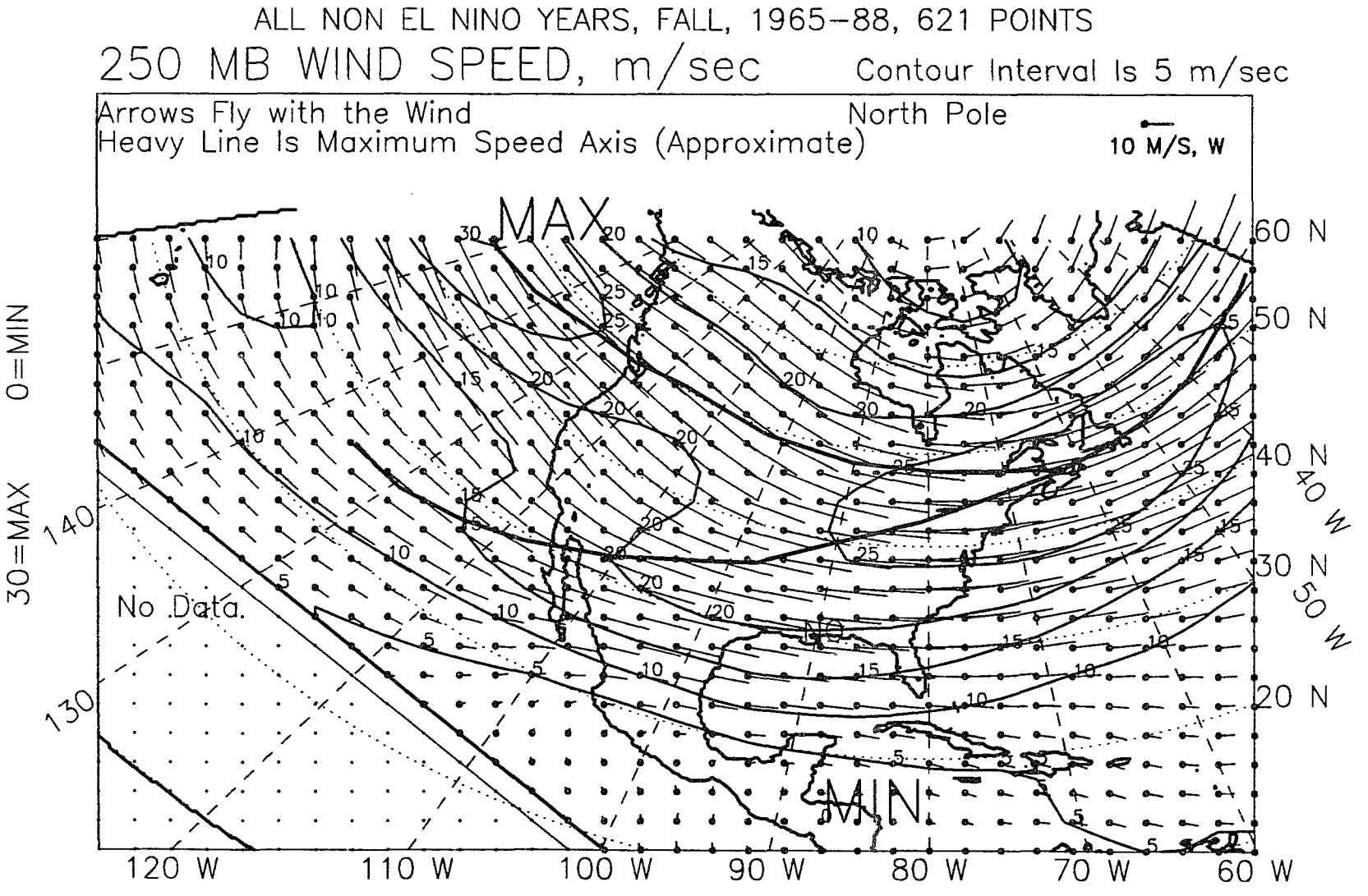

Figure J.14: 250–mb wind vectors, fall, non–El Niño years, 1965–88.

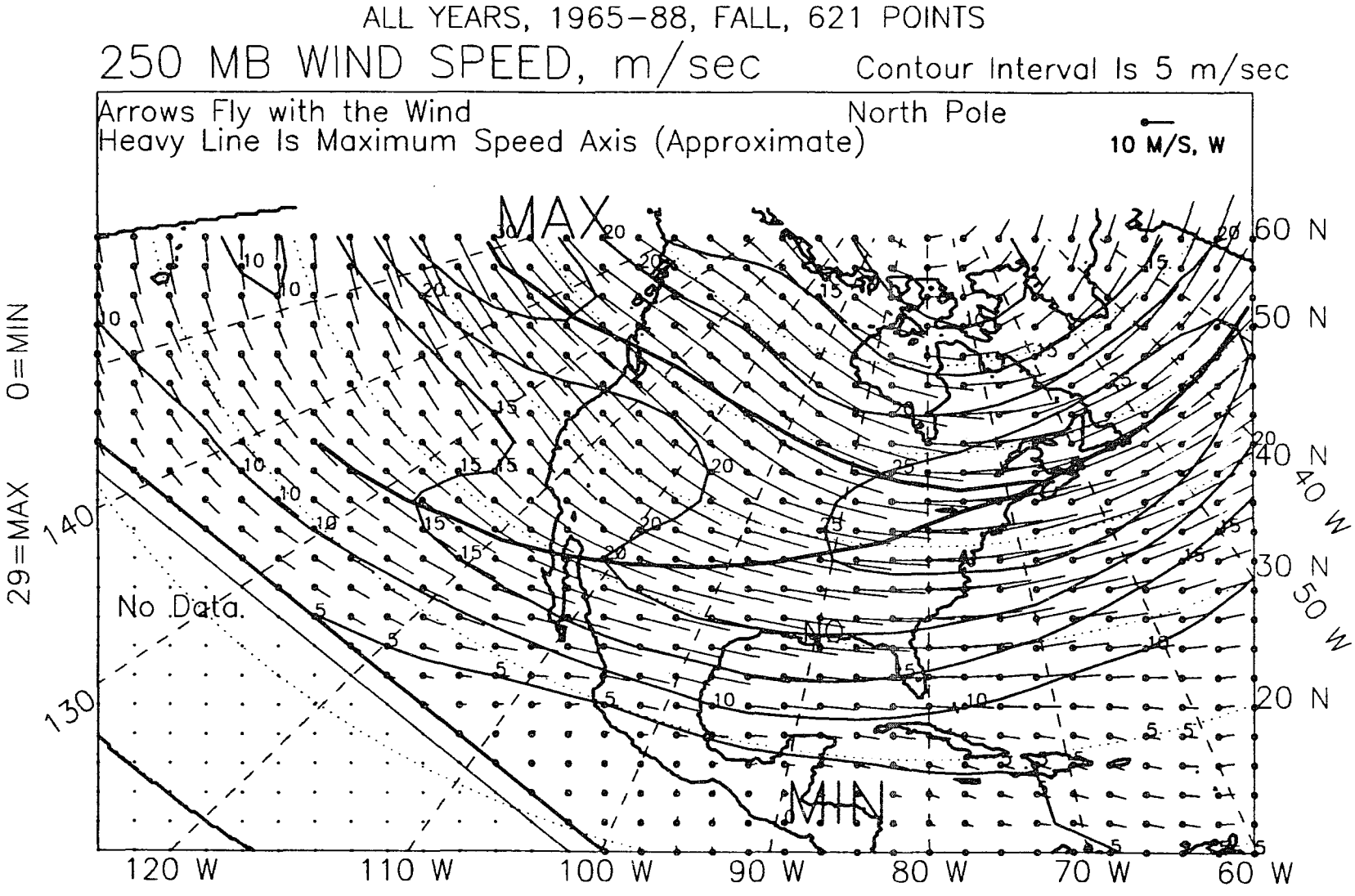

Figure J.15: 250–mb wind vectors, fall, all years, 1965–88.

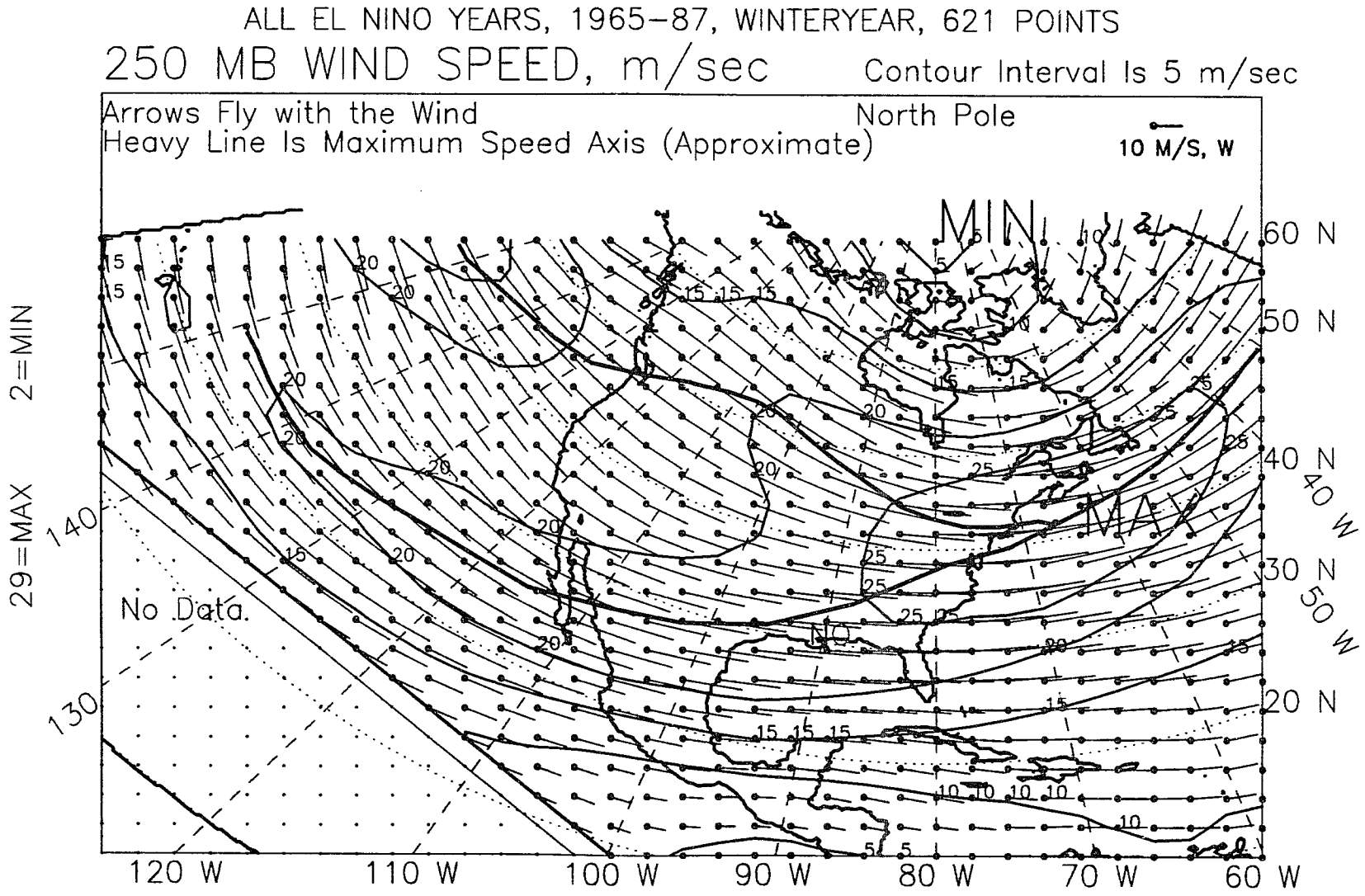

Figure J.16: 250–mb wind vectors, winter year, El Niño years, 1965–87.

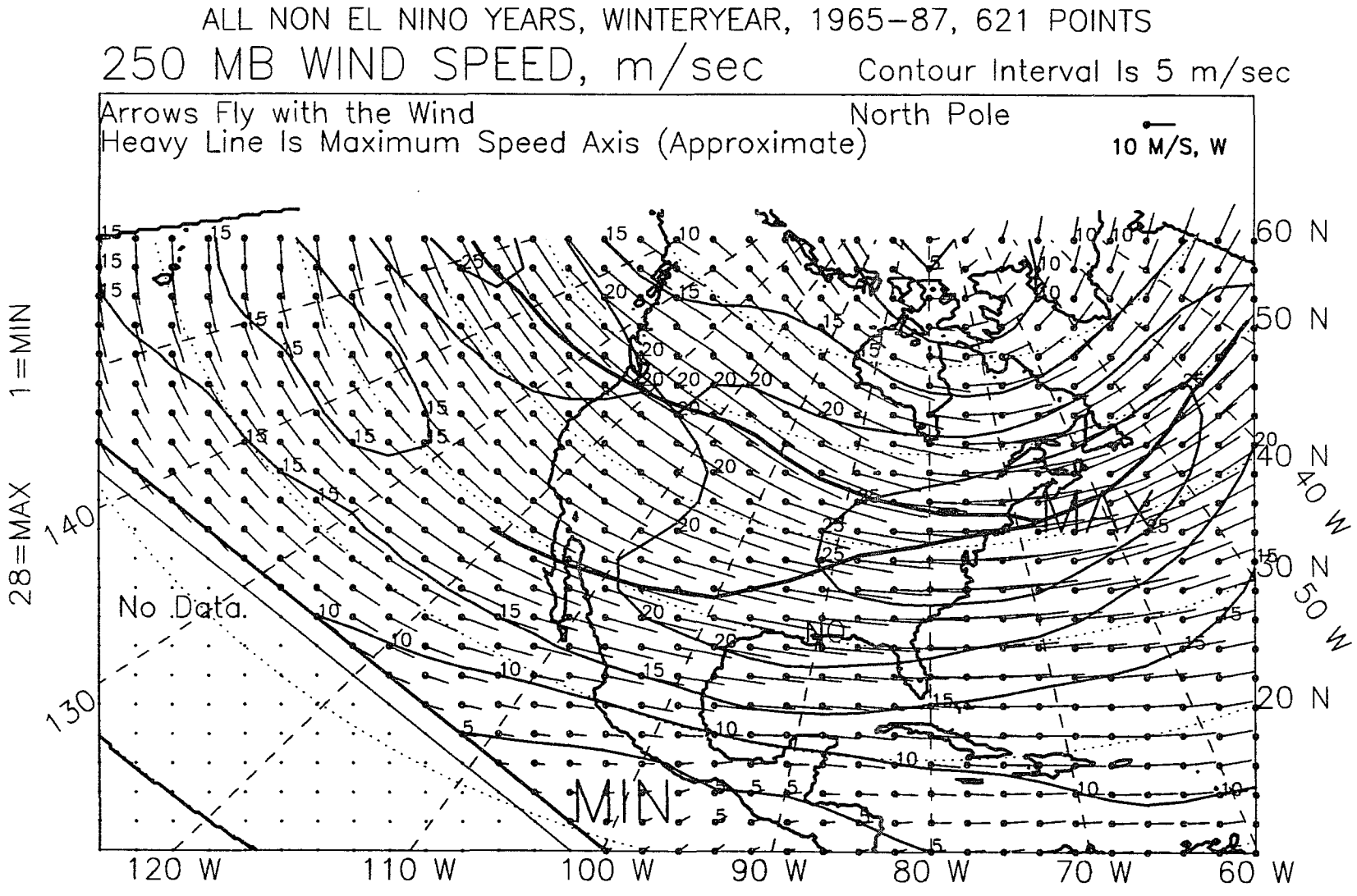

Figure J.17: 250–mb wind vectors, winter year, non–El Niño years, 1965–87.

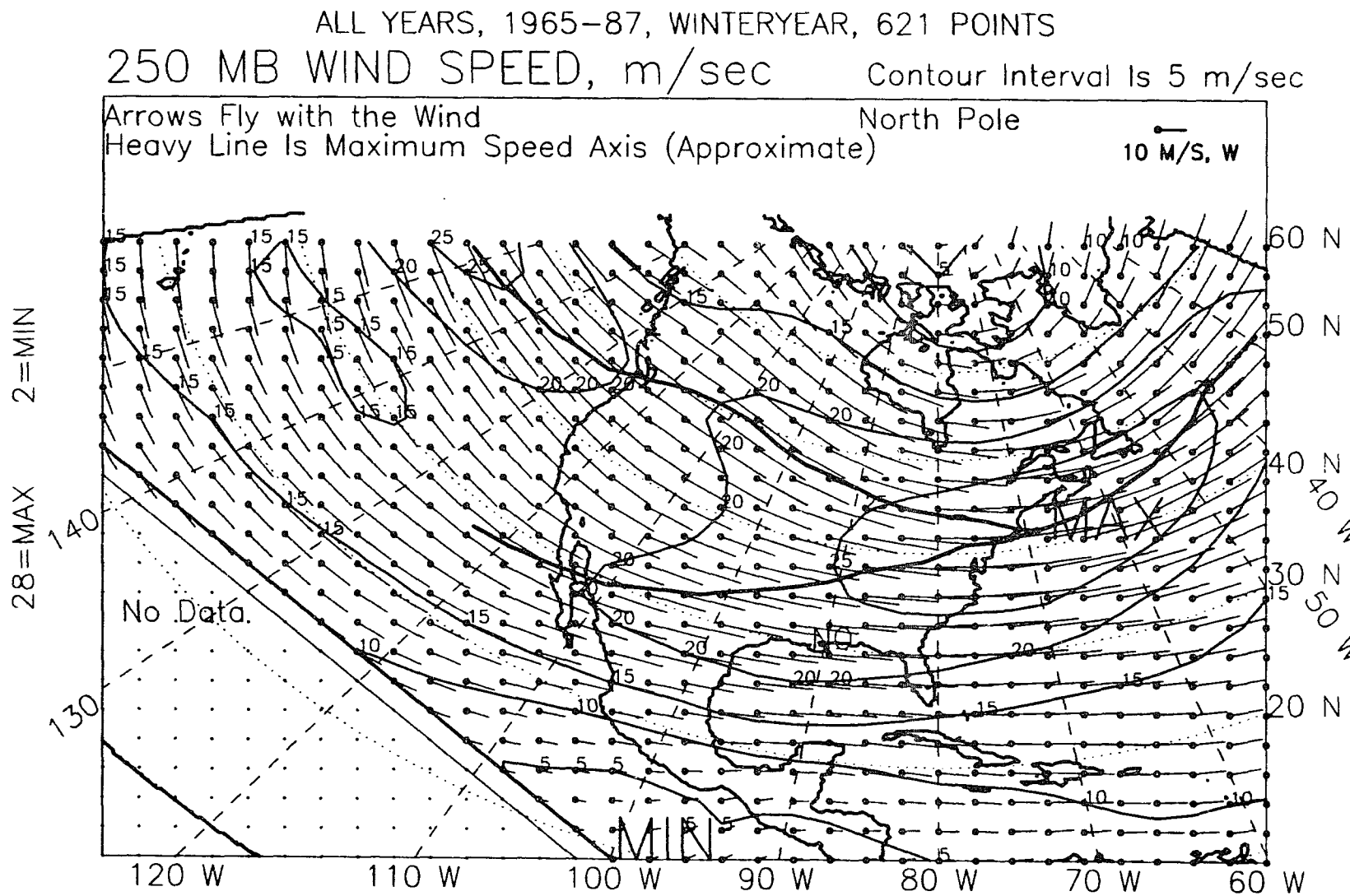

Figure J.18: 250–mb wind vectors, winter year, all years, 1965–87.

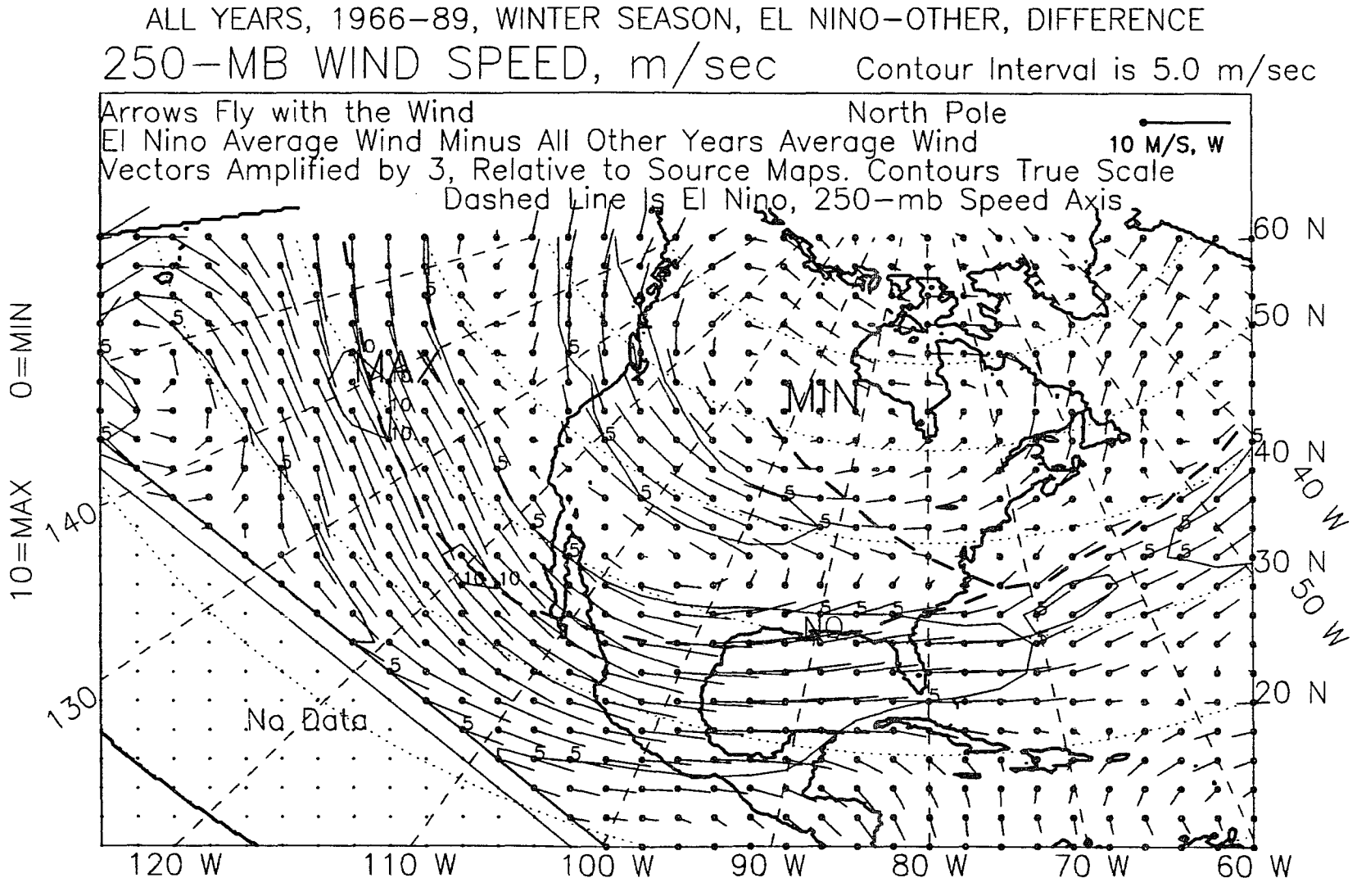

Figure J.19: 250–mb wind vectors, winter, 1966–89, difference.

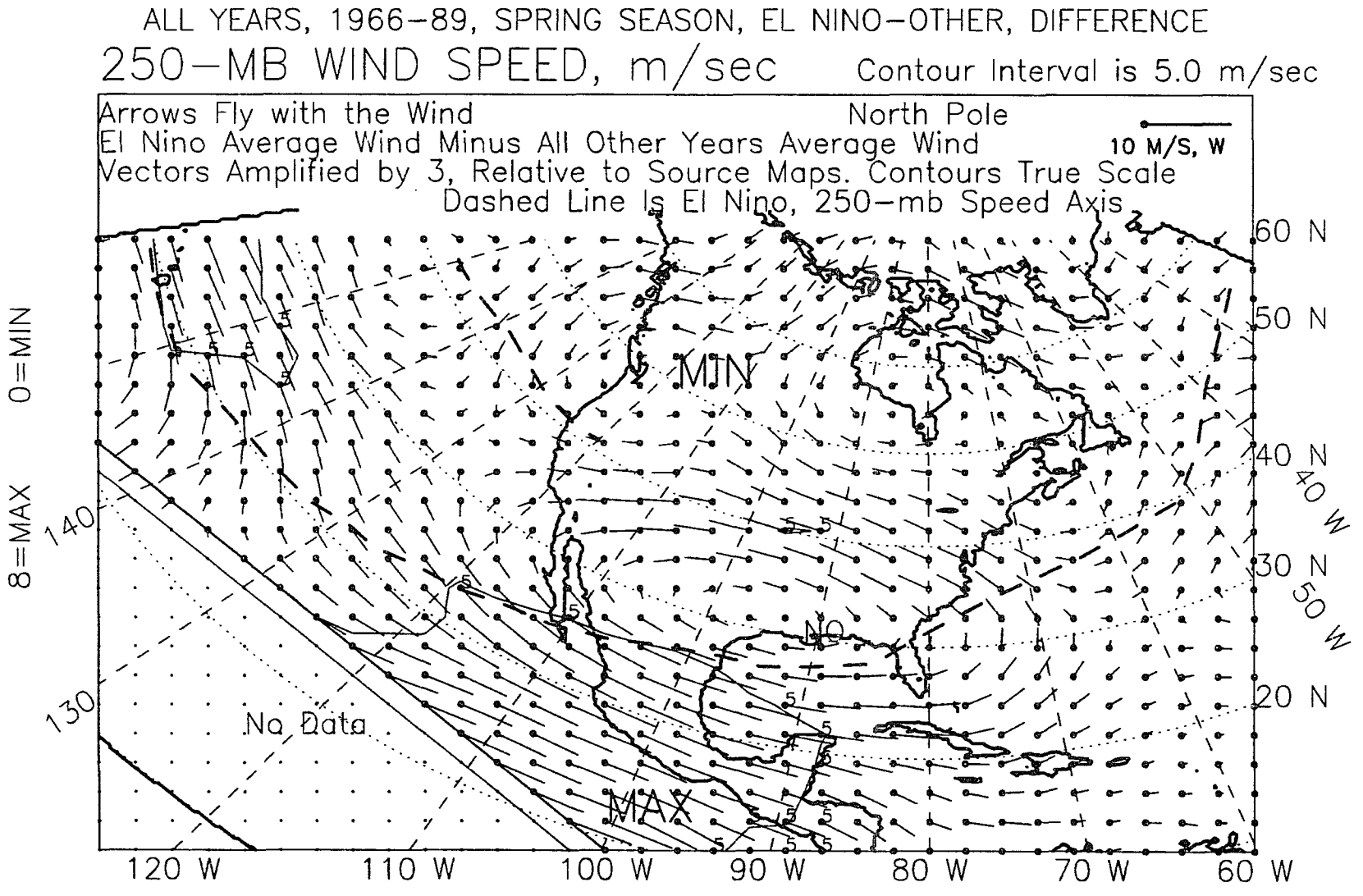

Figure J.20: 250–mb wind vectors, spring, 1966–89, difference.

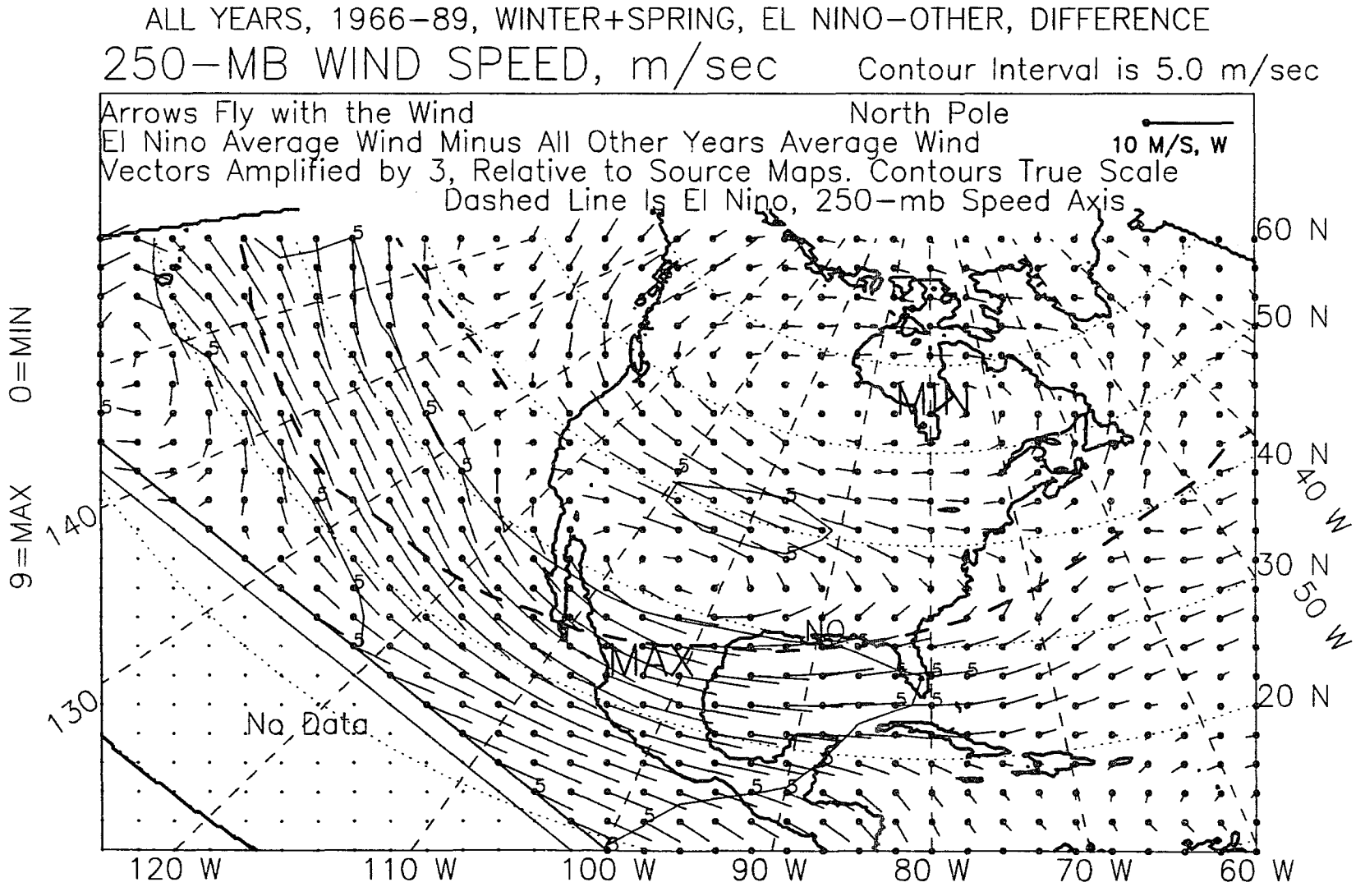

Figure J.21: 250–mb wind vectors, winter–plus–spring, 1966–89, difference.

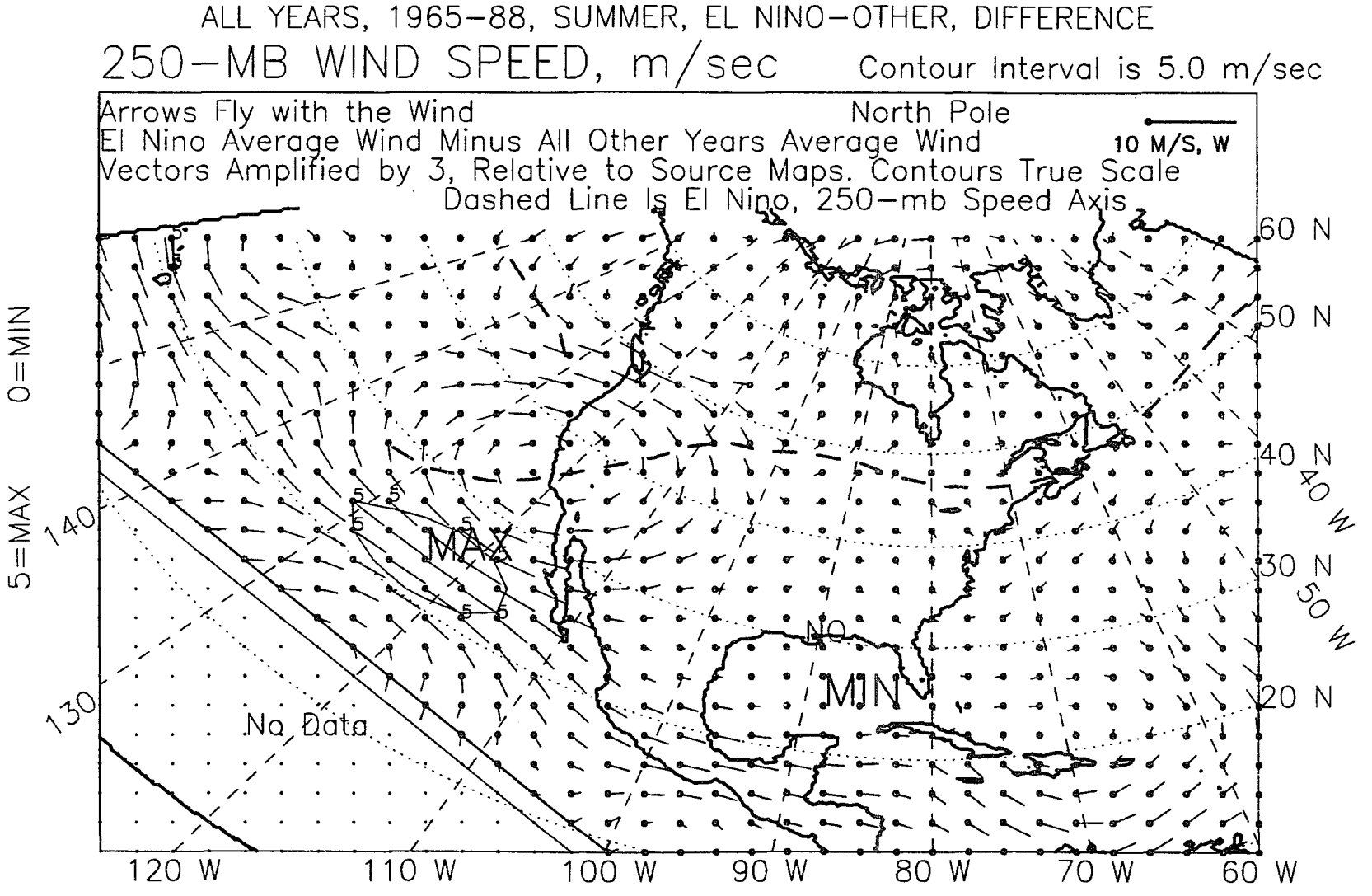

Figure J.22: 250–mb wind vectors, summer, 1965–88, difference.

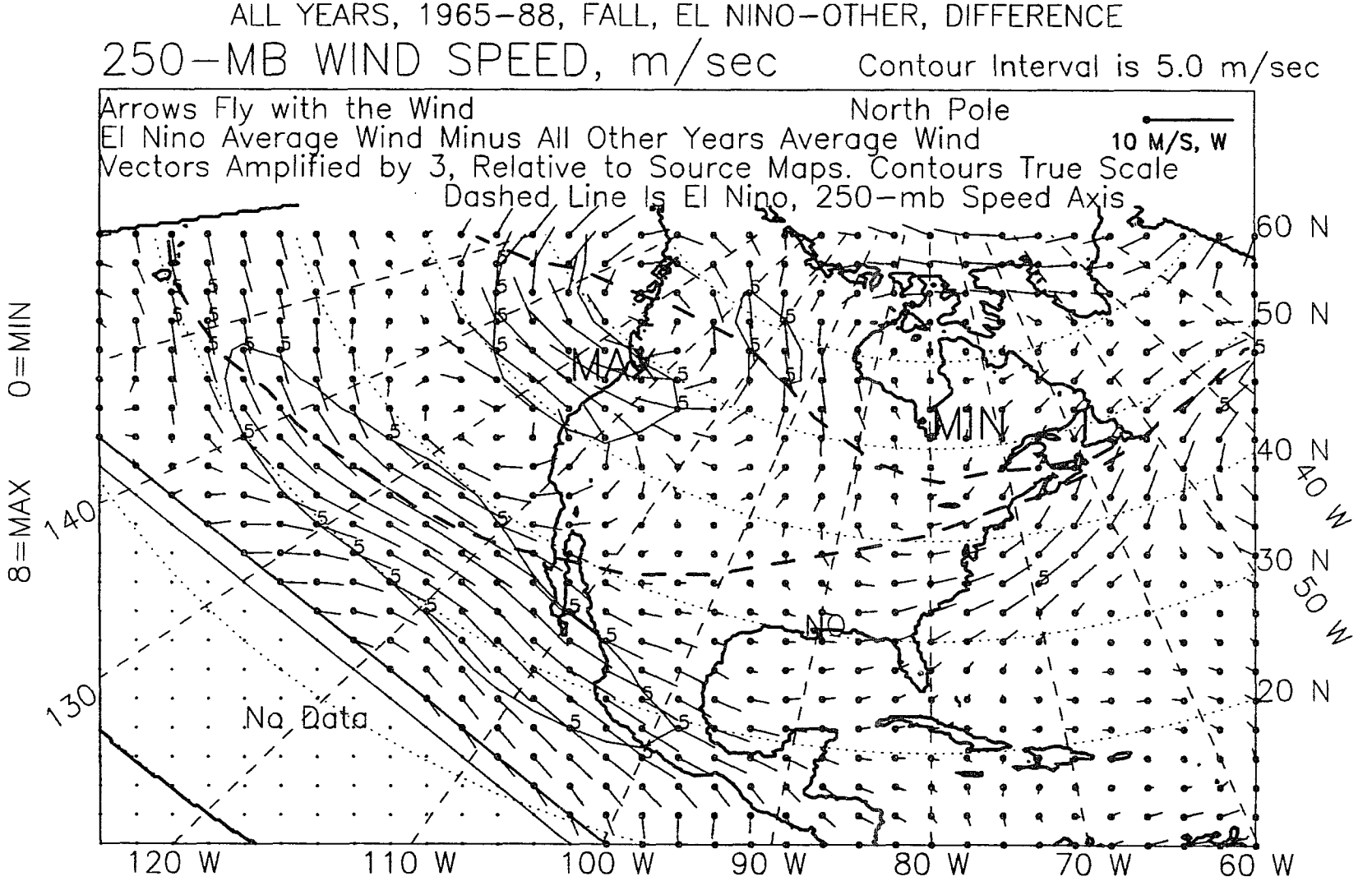

Figure J.23: 250–mb wind vectors, fall, 1965–88, difference.

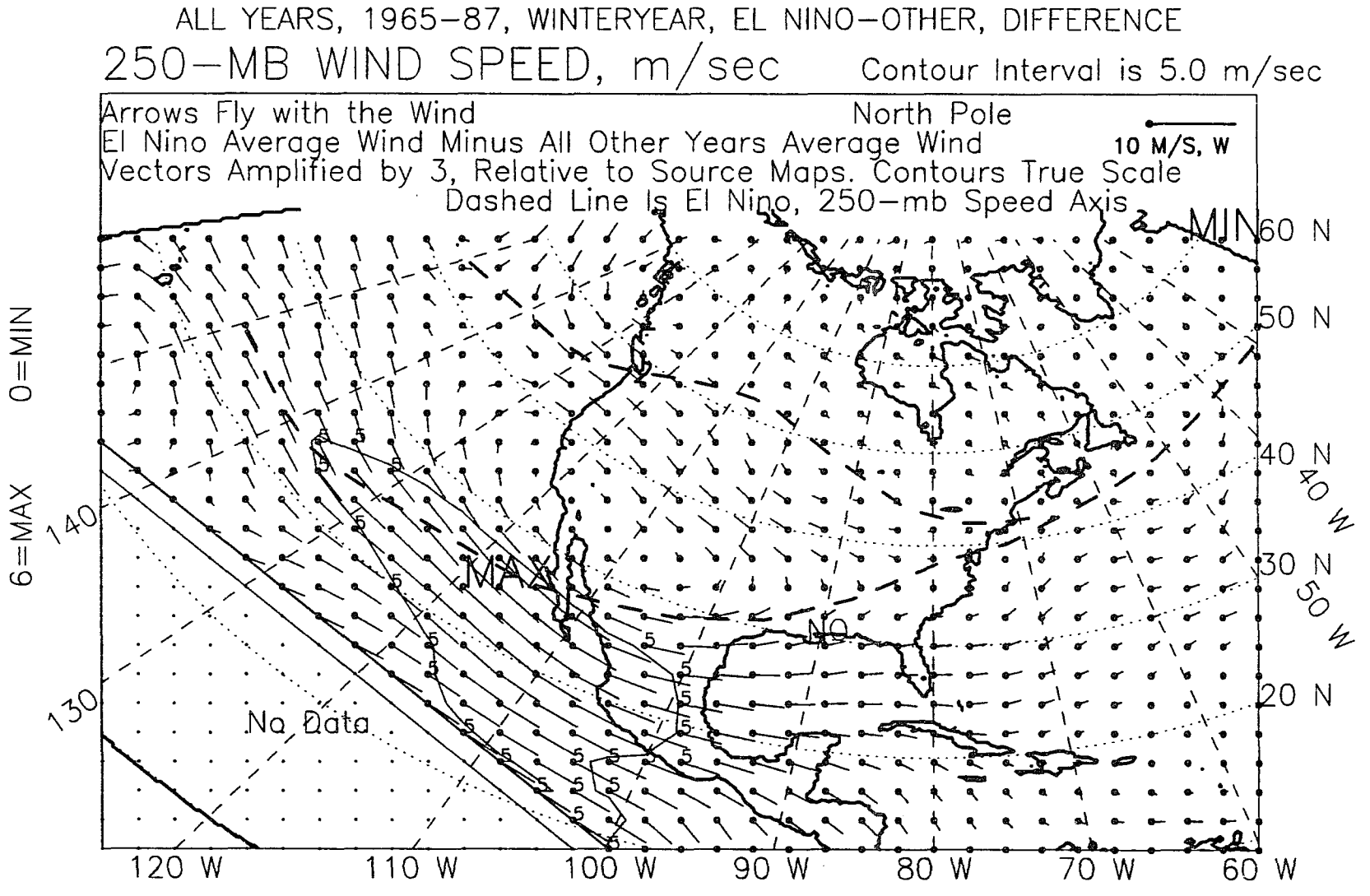

Figure J.24: 250–mb wind vectors, winter year, 1965–87, difference.

APPENDIX K
250-MB JET AXES: SUMMARIES

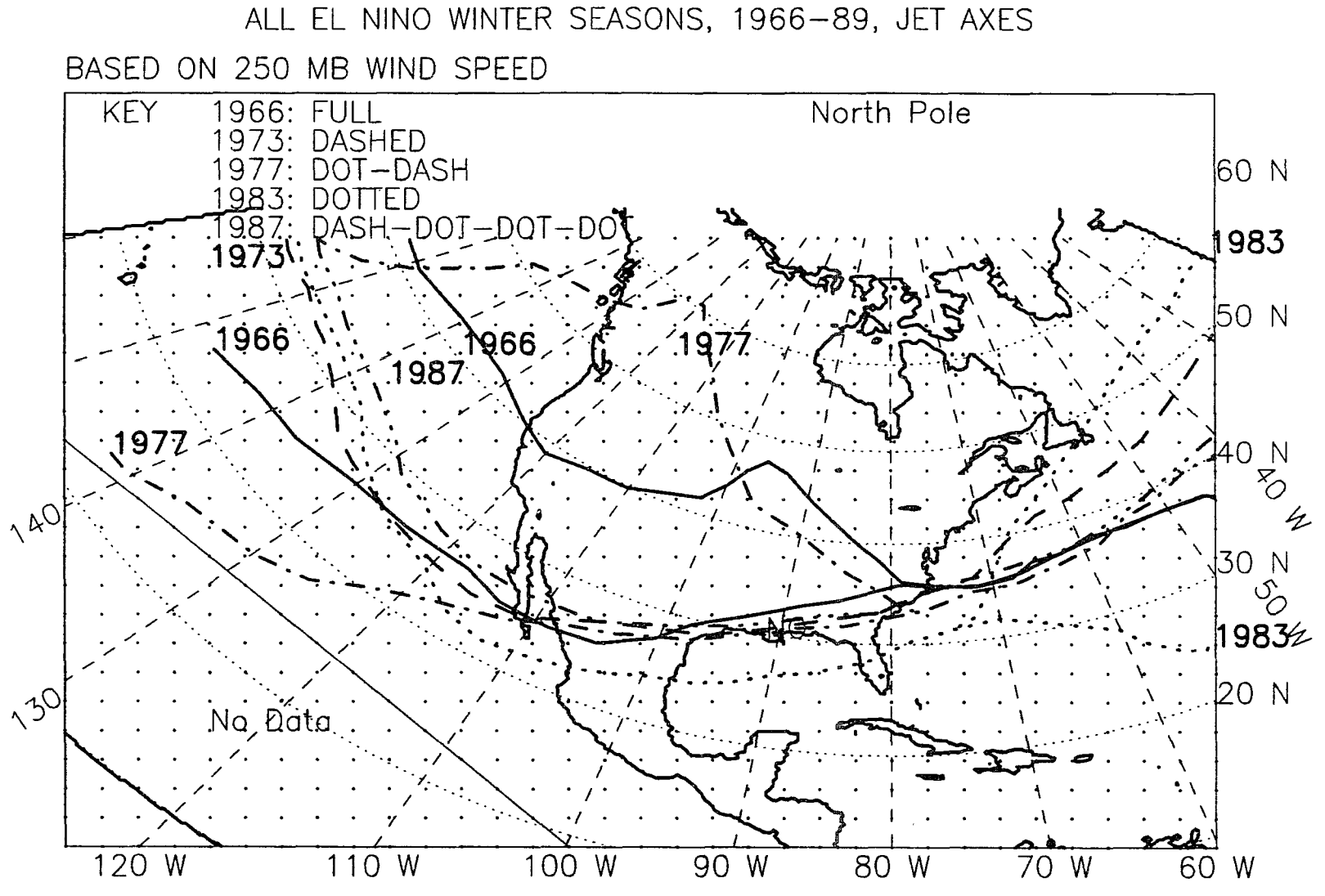

Figure K.1: 250–mb jet axes, five El Niño winters from 1966–89.

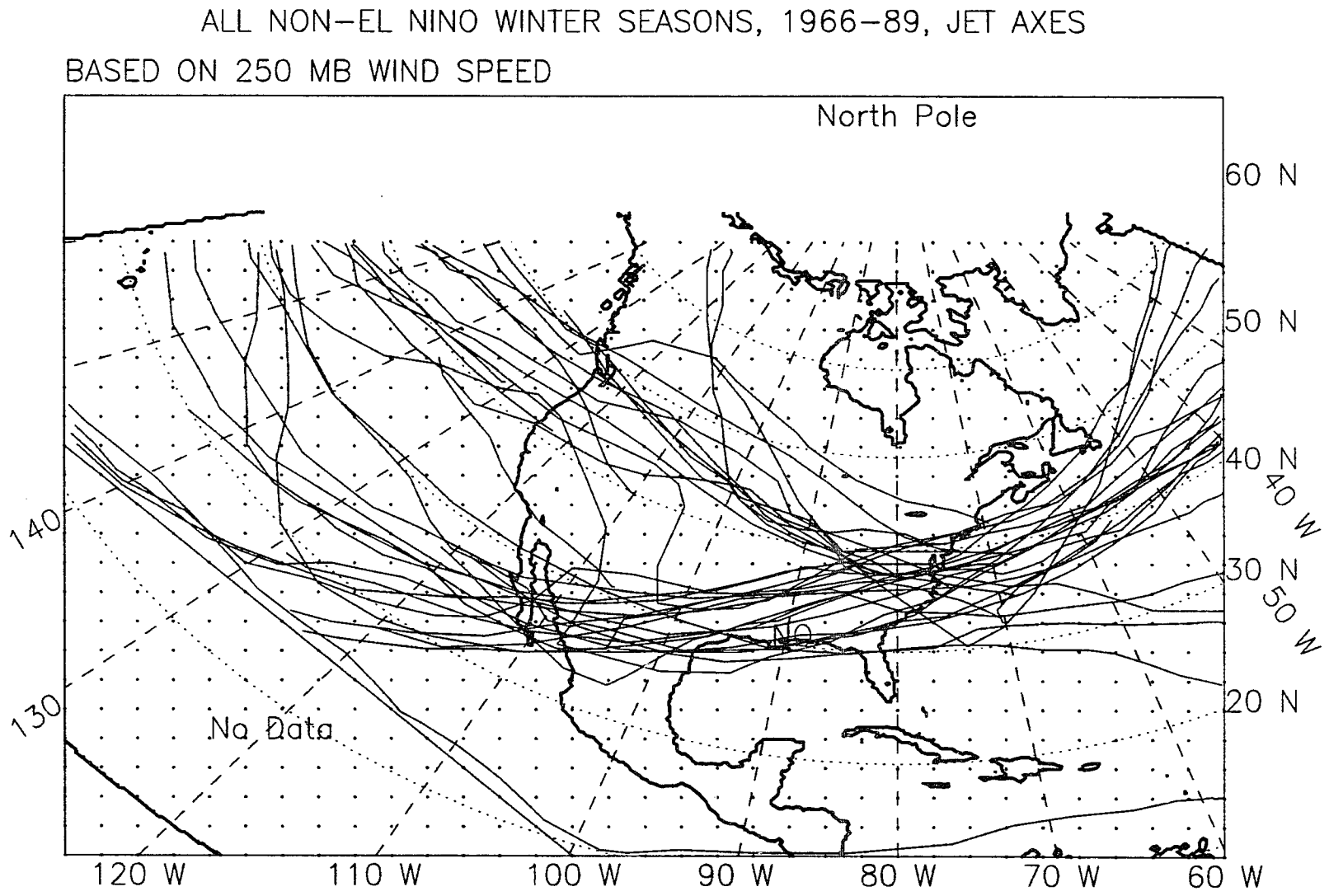

Figure K.2: 250-mb jet axes, 19 non-El Niño winters from 1966-89.

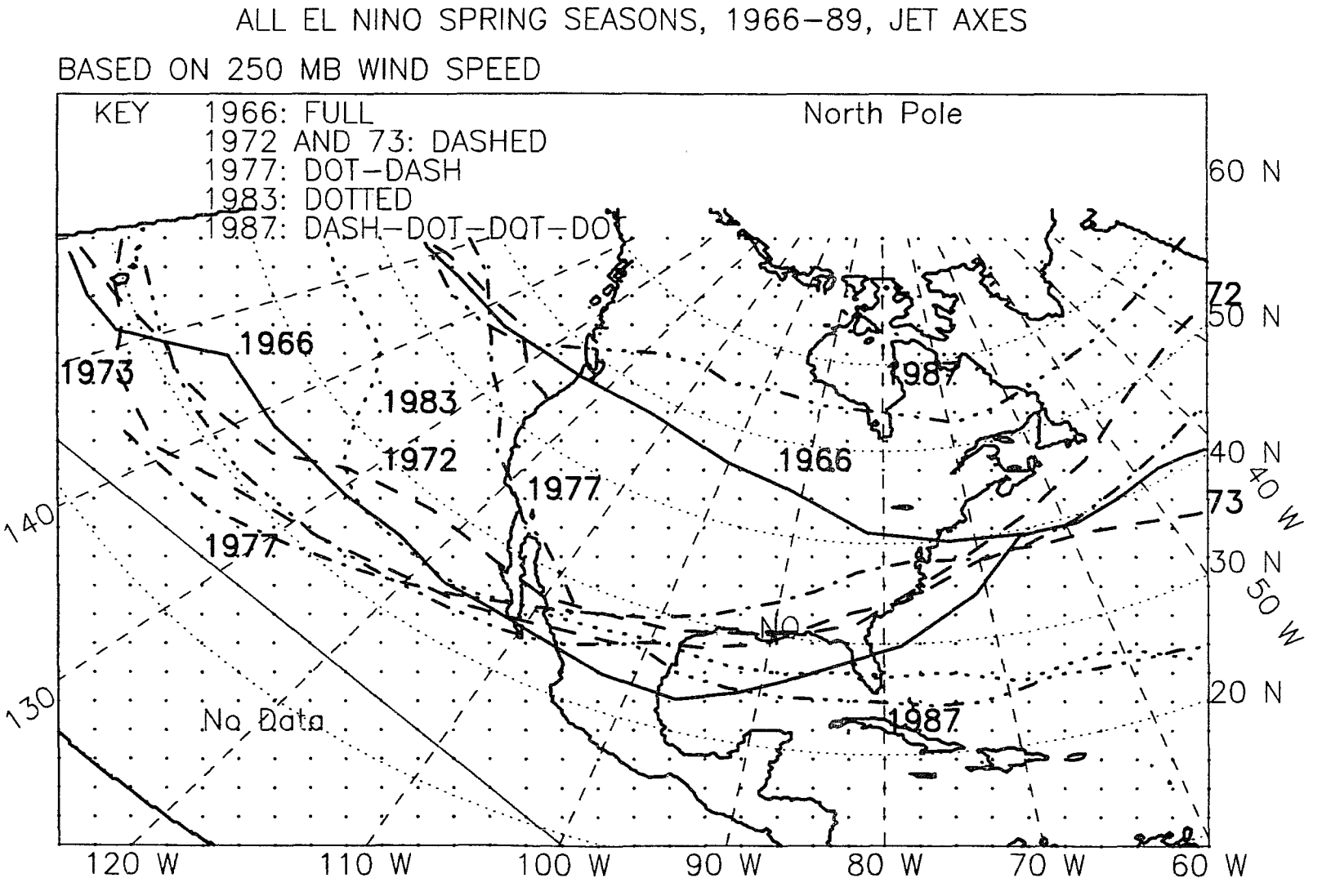

Figure K.3: 250–mb jet axes, six El Niño springs from 1966–89.

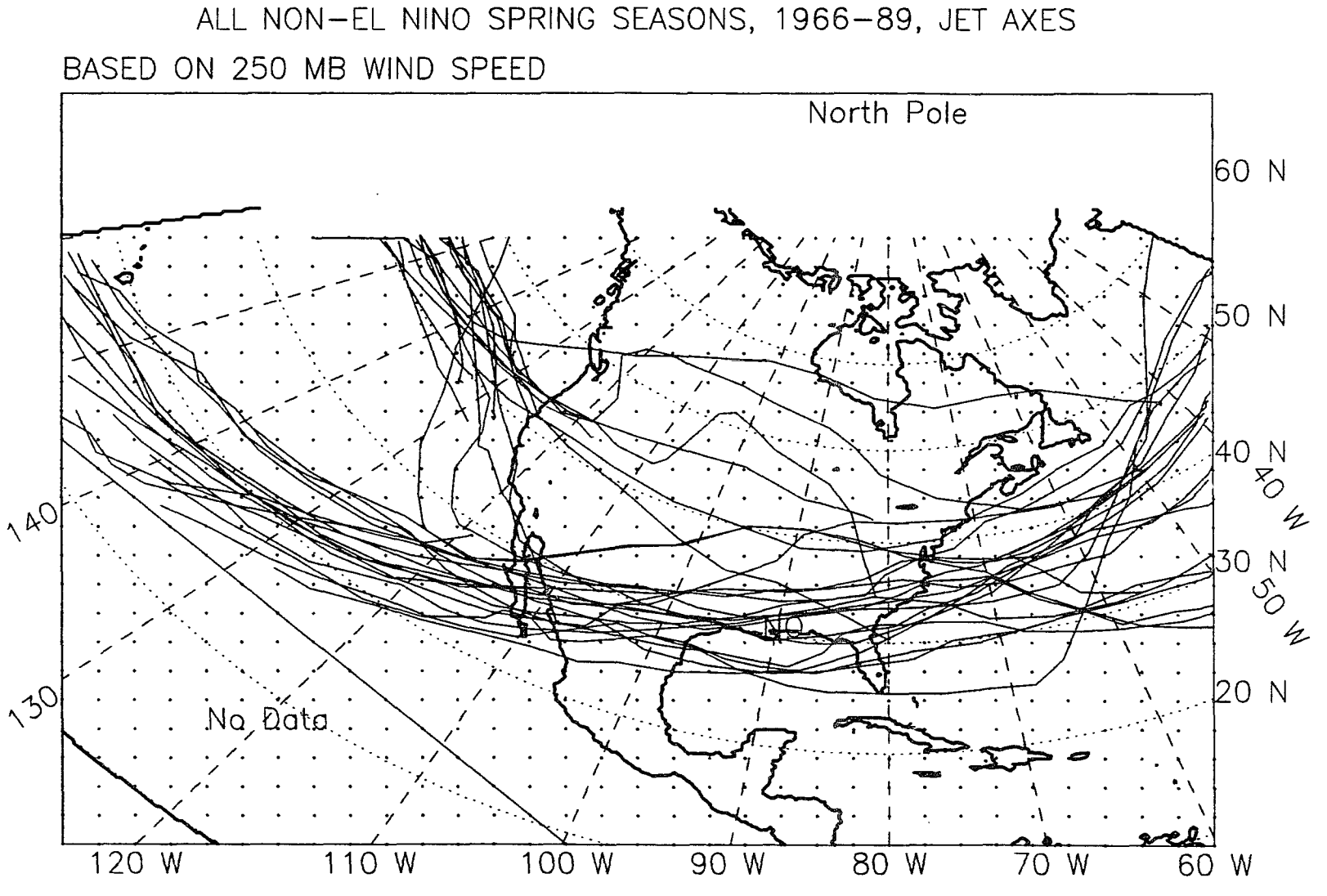

Figure K.4: 250-mb jet axes, 18 non-El Niño springs from 1966-89.

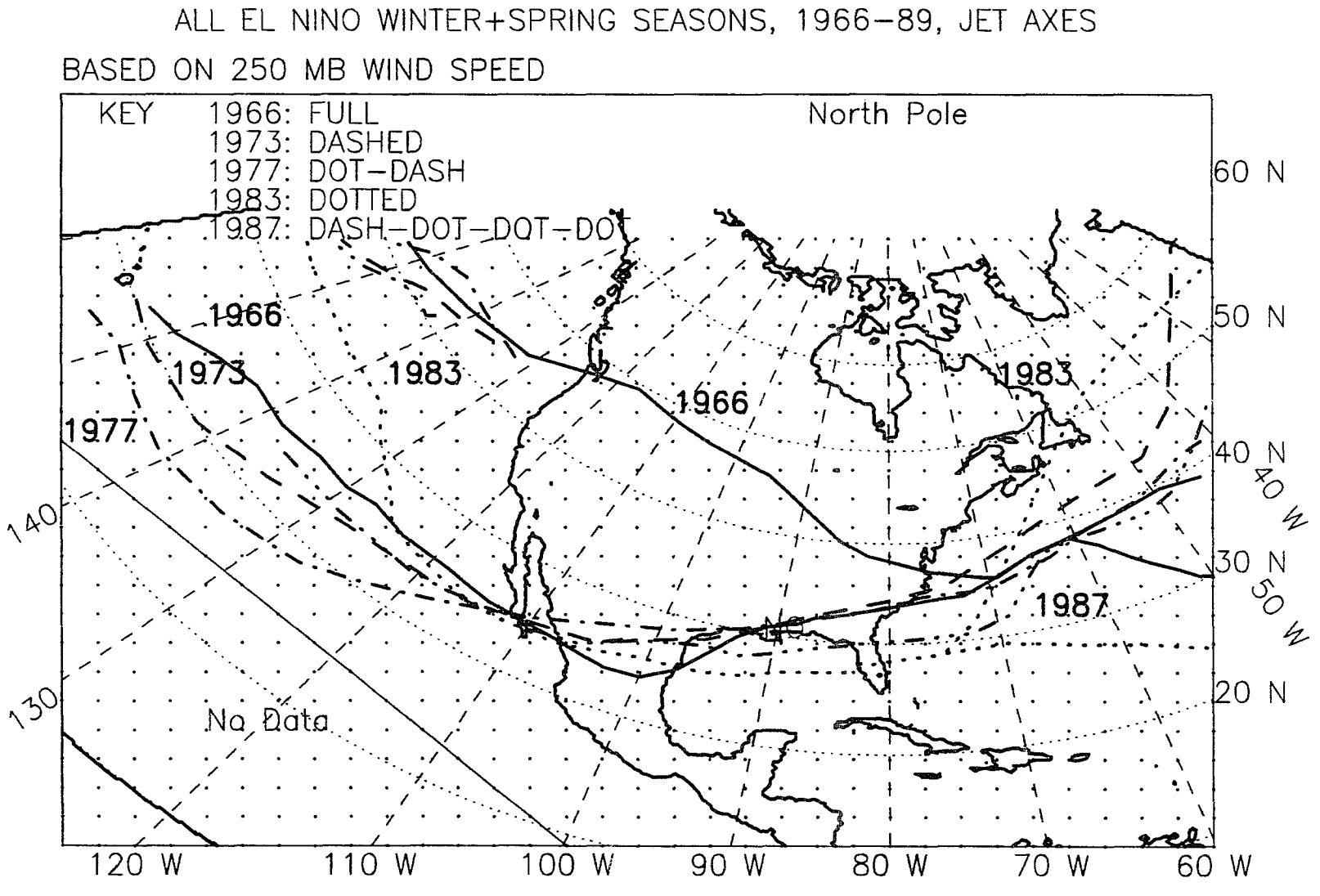

Figure K.5: 250-mb jet axes, five El Niño winter-plus-springs from 1966-89.

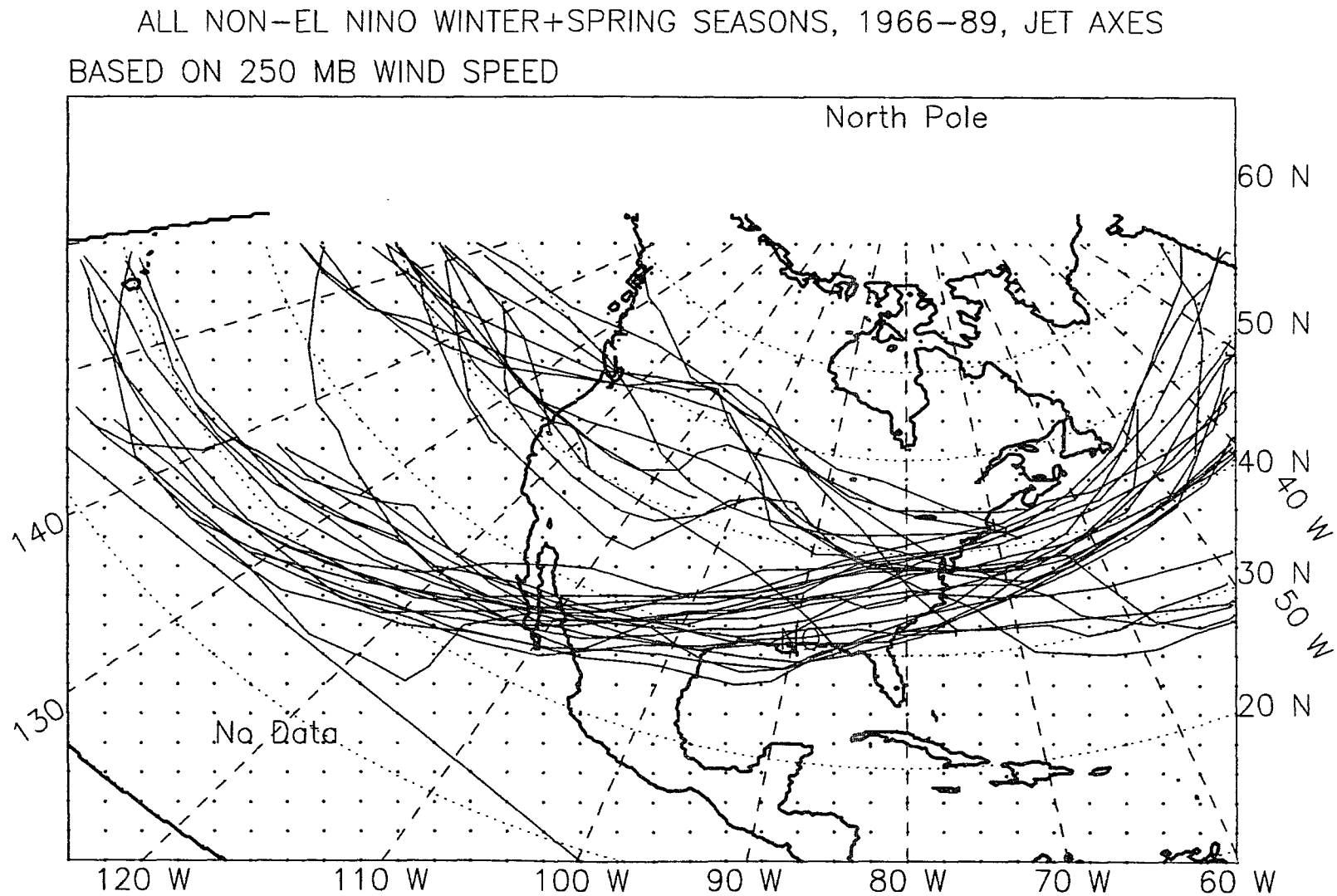

Figure K.6: 250-mb jet axes, 19 non-El Niño winter-plus-springs from 1966-89.

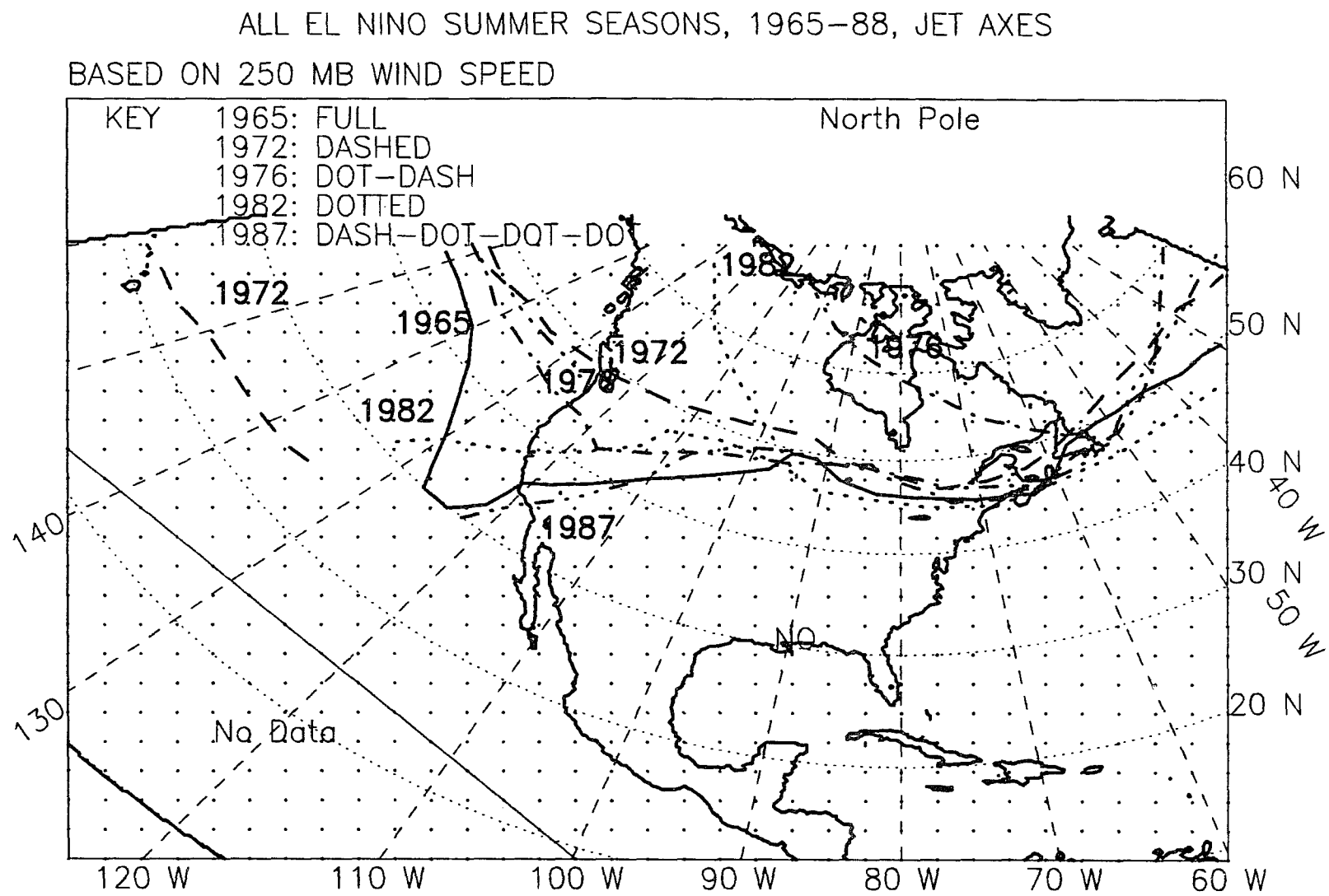

Figure K.7: 250–mb jet axes, five El Niño summers from 1965–88.

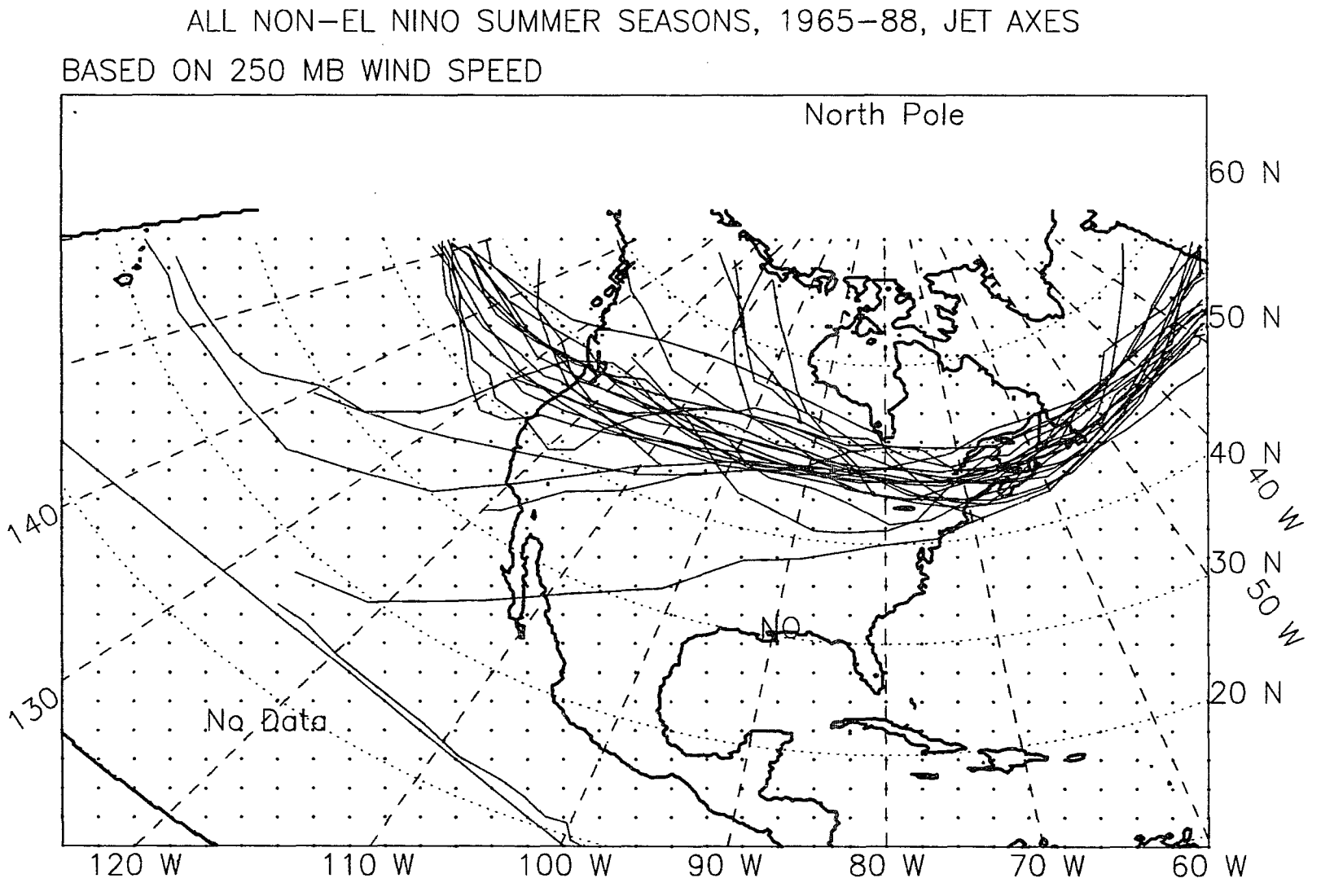

Figure K.8: 250–mb jet axes, 19 non–El Niño summers from 1965–88.

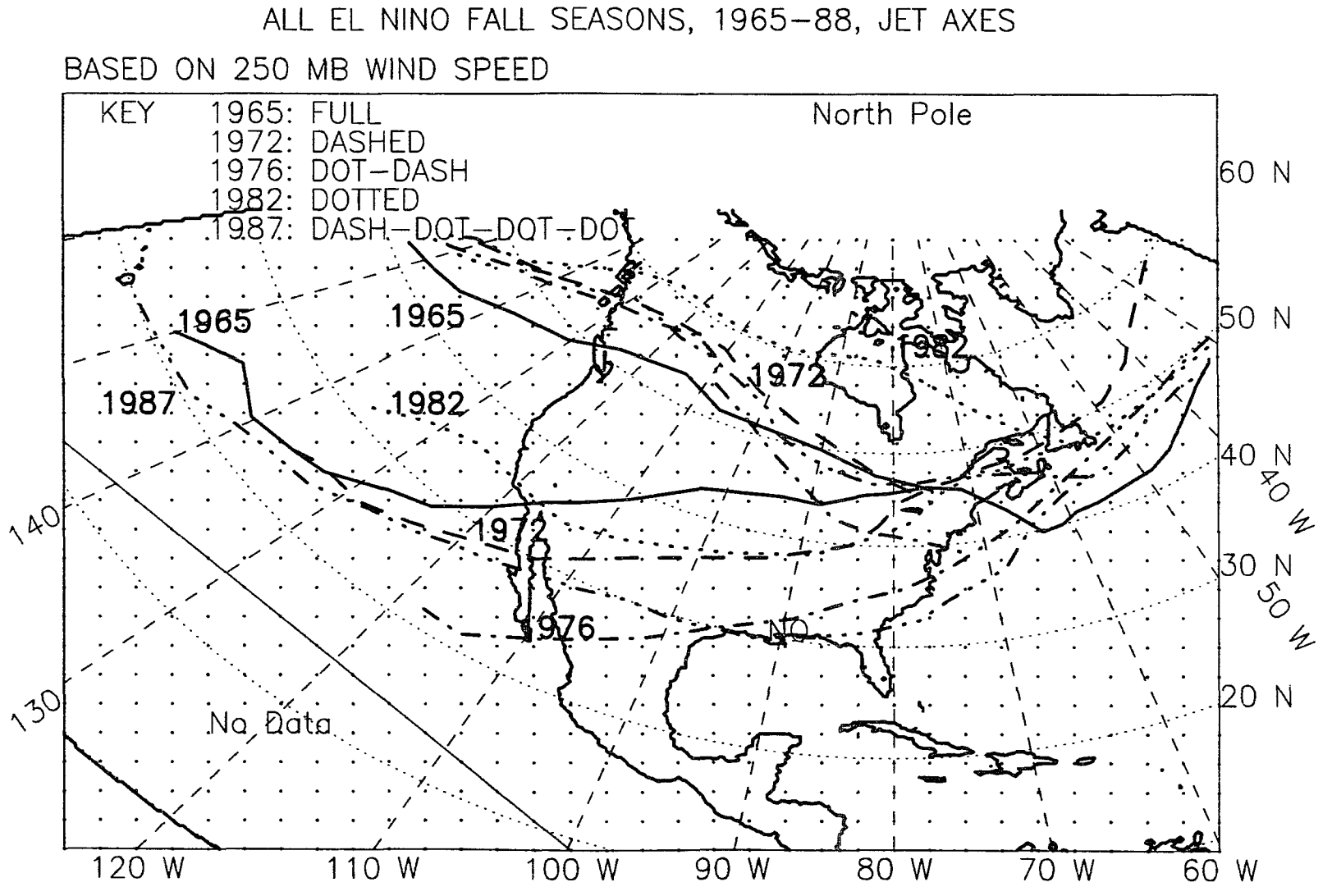

Figure K.9: 250–mb jet axes, five El Niño falls from 1965–88.

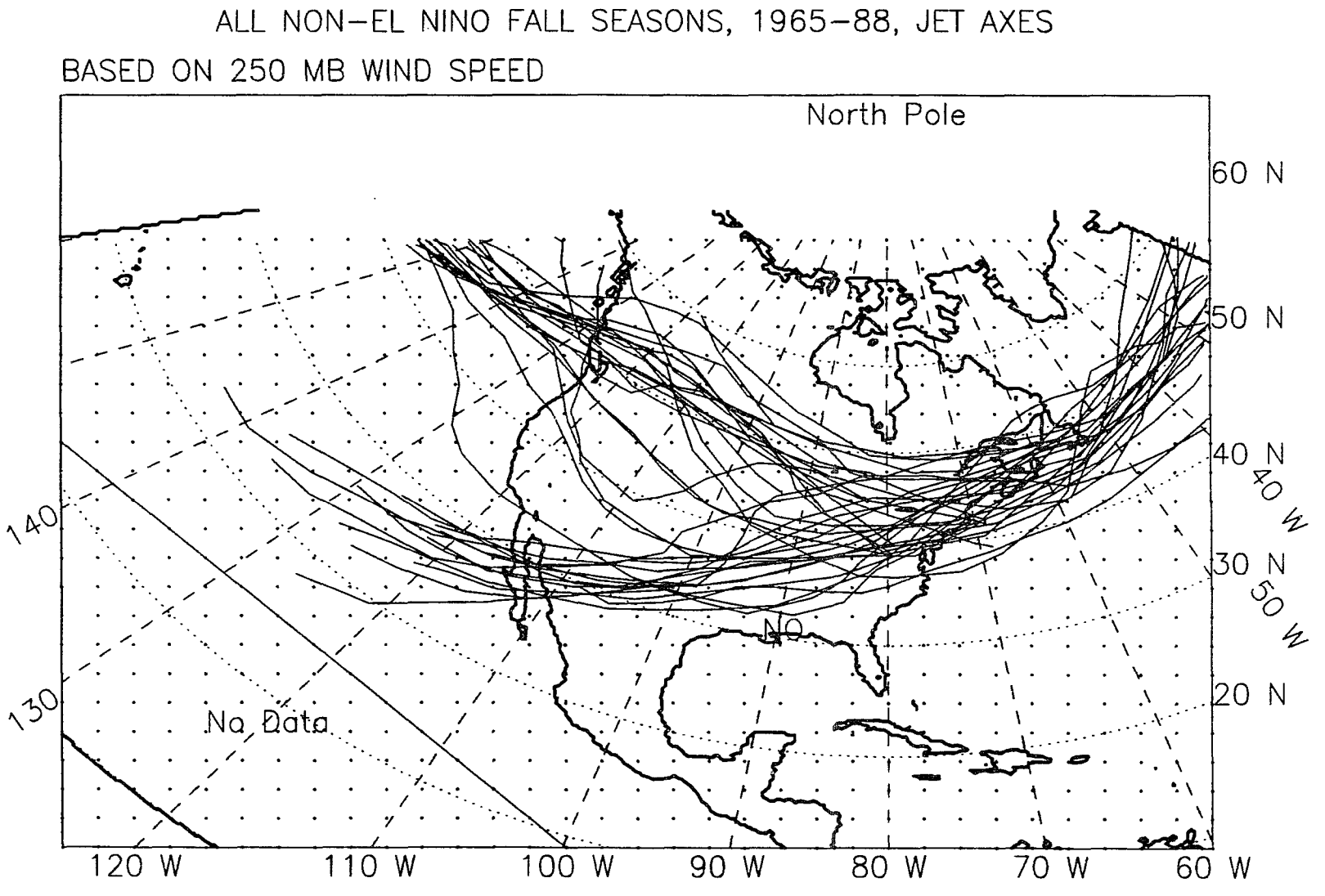

Figure K.10: 250–mb jet axes, 19 non–El Niño falls from 1965–88.

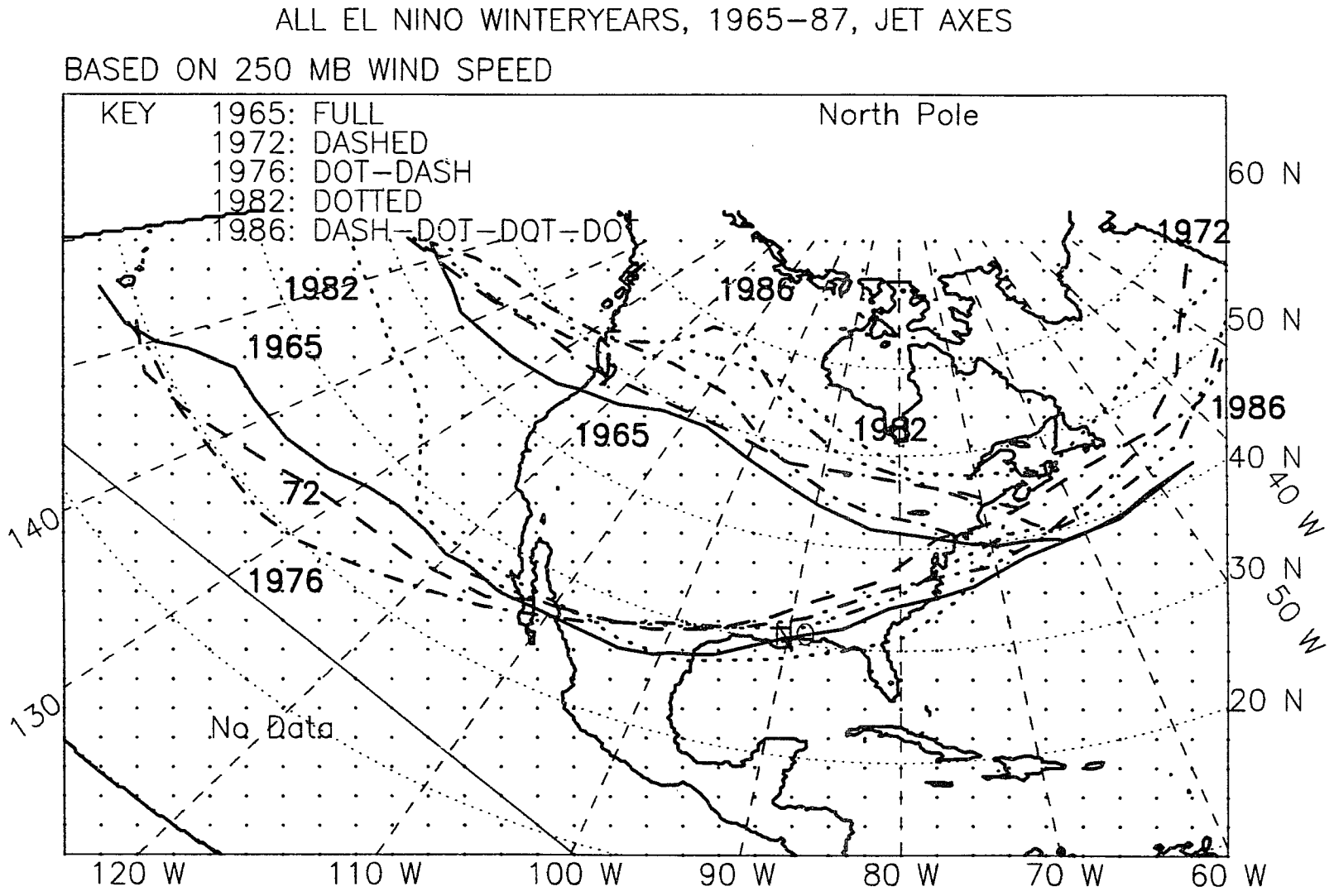

Figure K.11: 250–mb jet axes, five El Niño winter years from 1965–87.

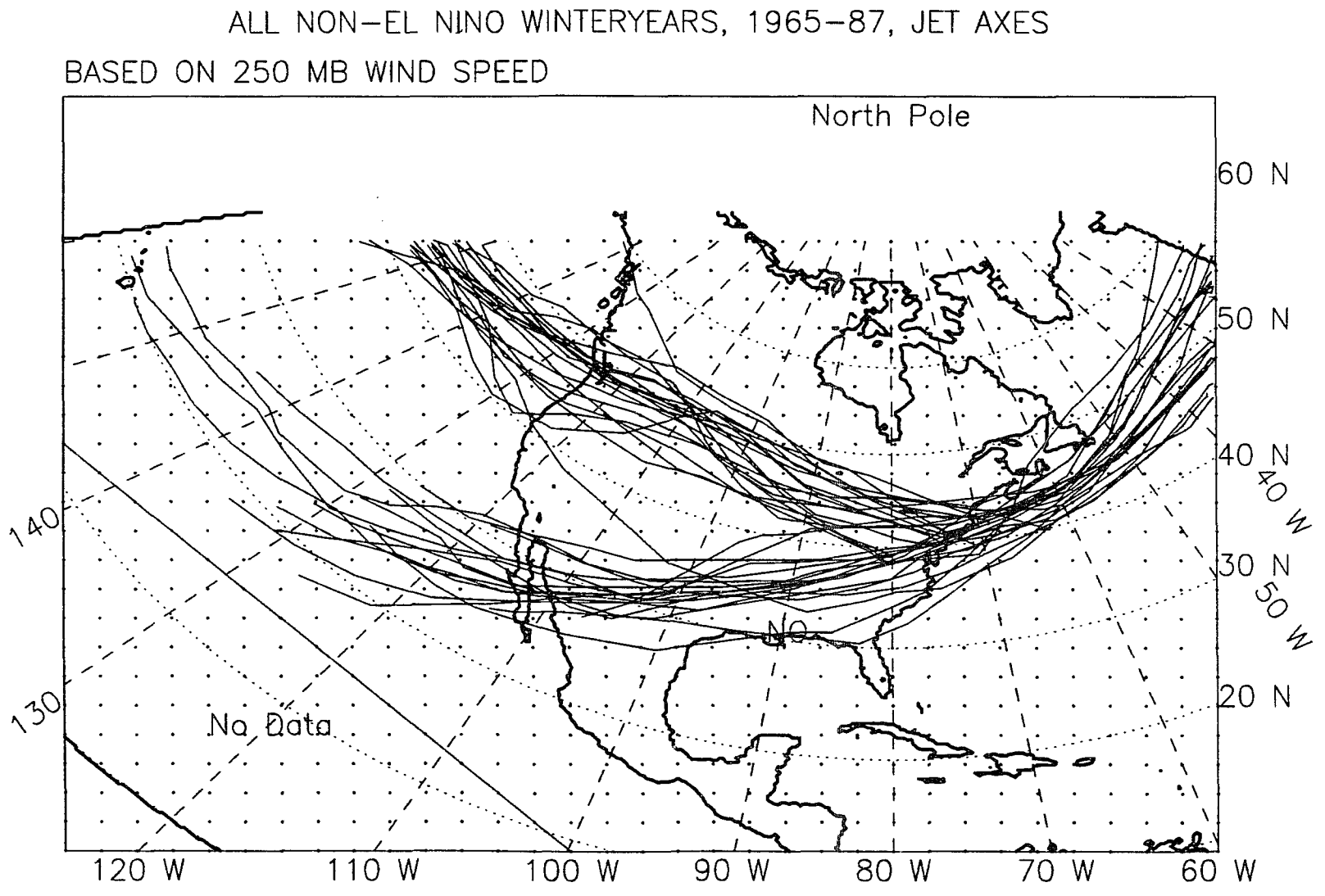

Figure K.12: 250-mb jet axes, 18 non-El Niño winter years from 1965-87.

APPENDIX L
250-MB DIVERGENCE FIELD

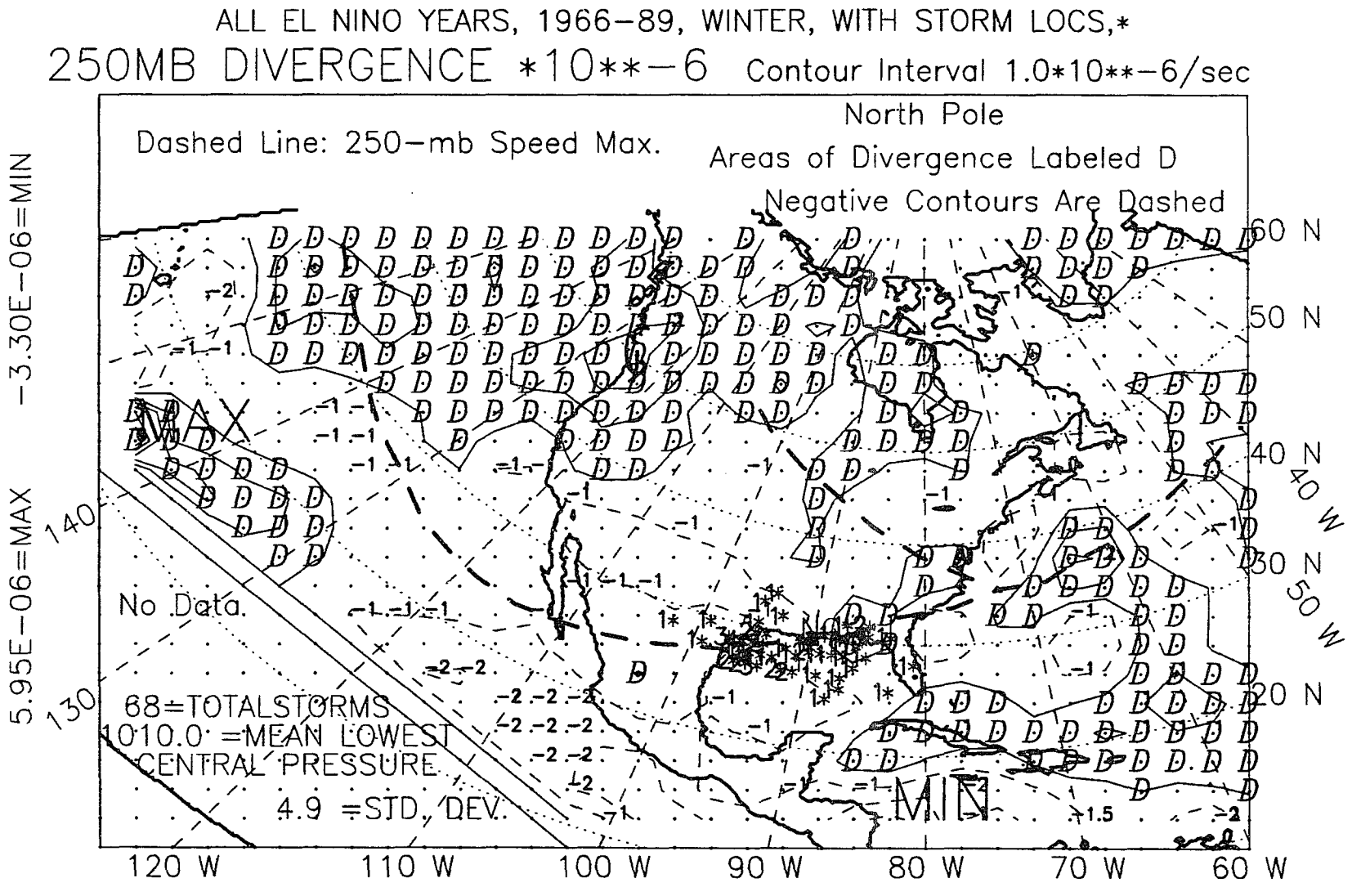

Figure L.1: 250–mb divergence, winter, El Niño years, 1966–89.

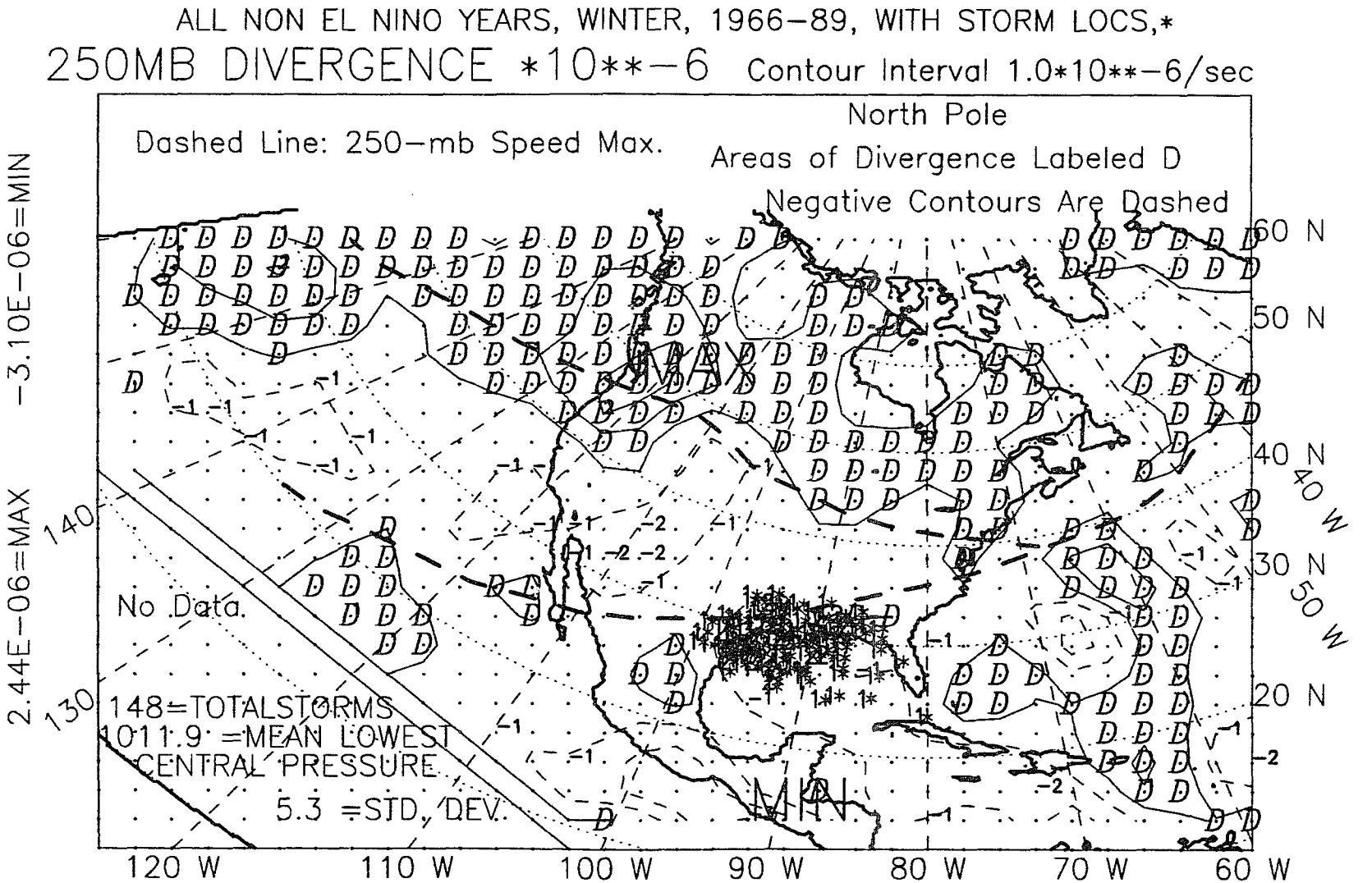

Figure L.2: 250–mb divergence, winter, non–El Niño years, 1966–89.

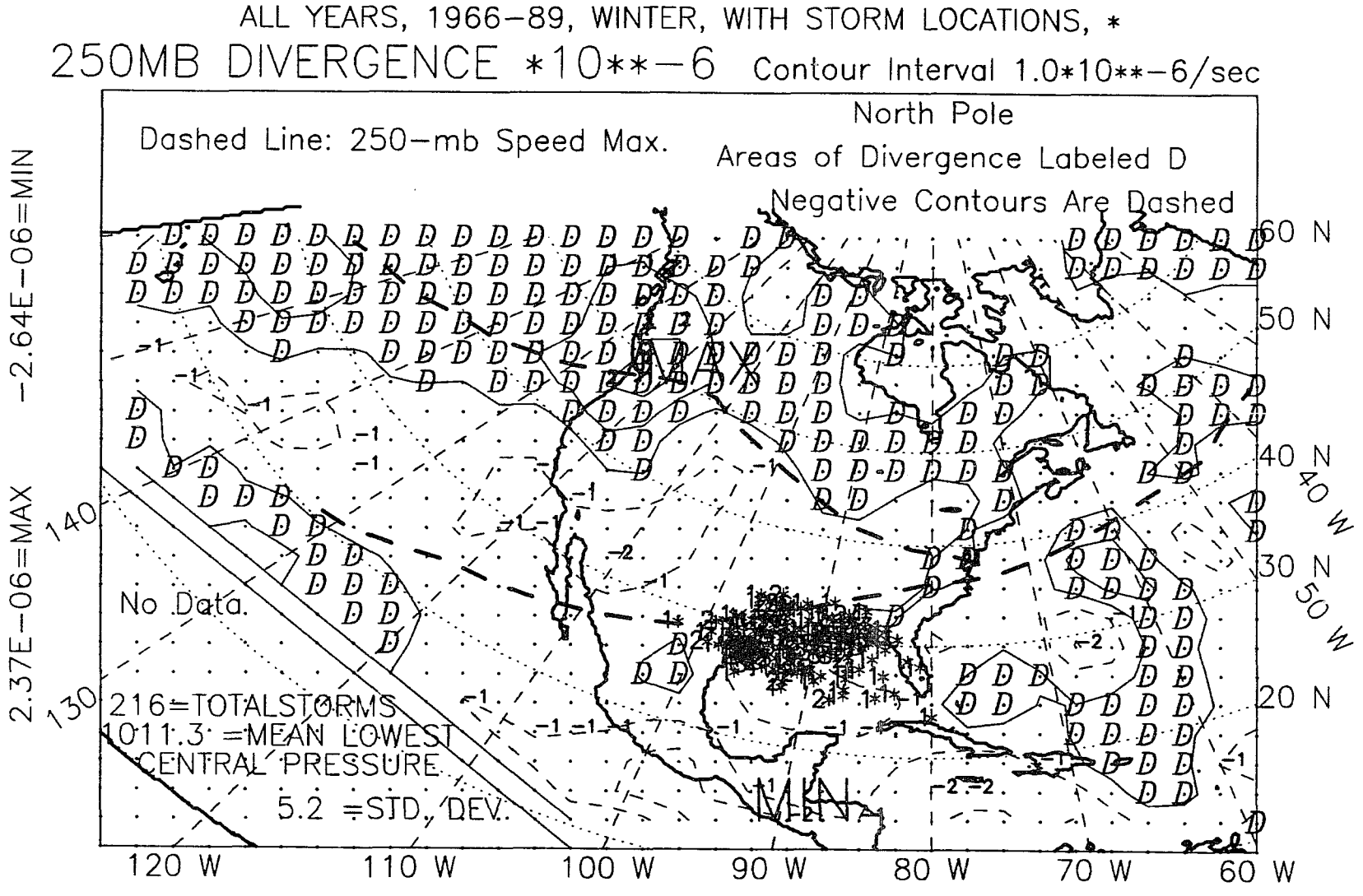

Figure L.3: 250–mb divergence, winter, all years, 1966–89.

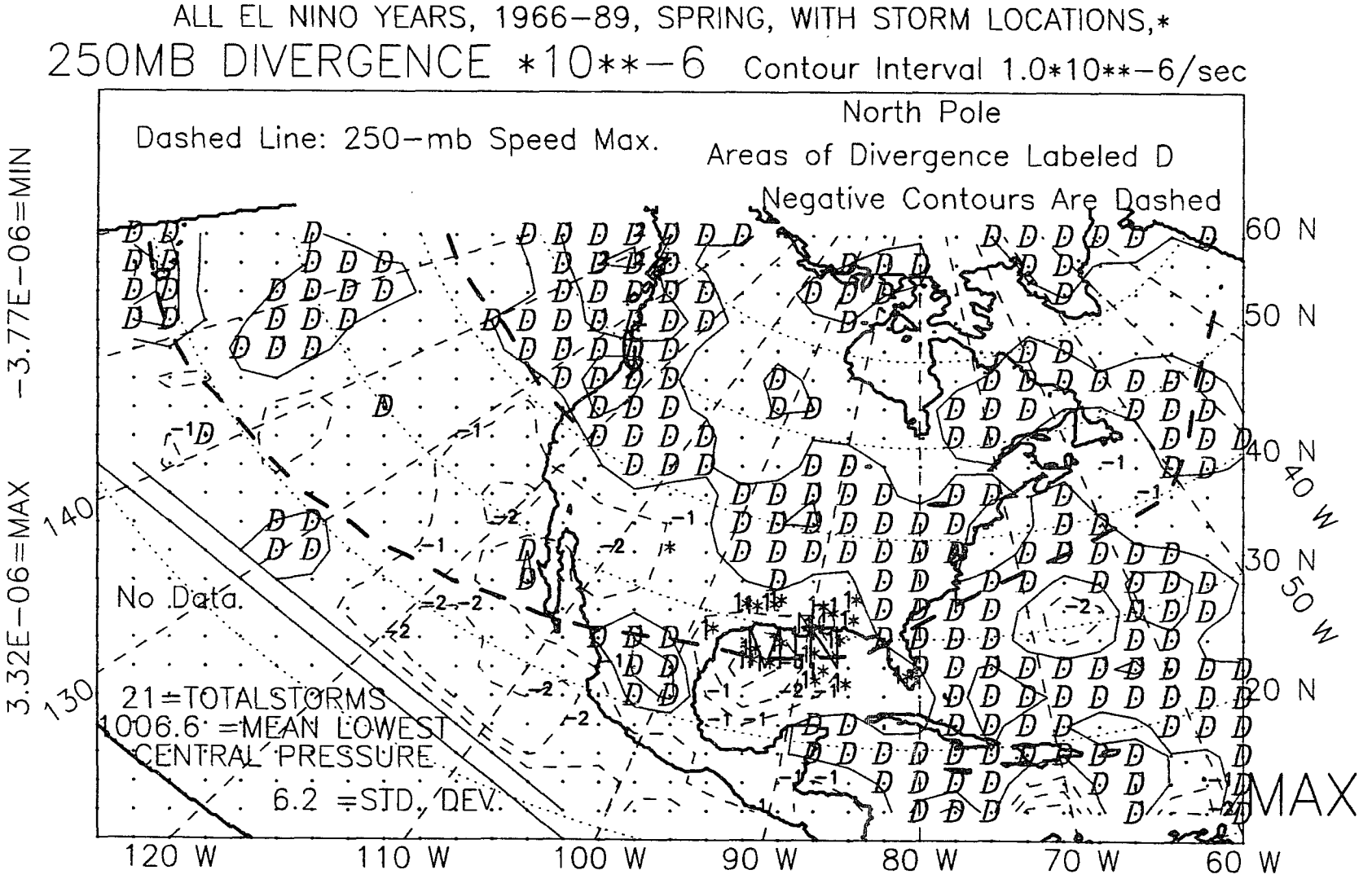

Figure L.4: 250–mb divergence, spring, El Niño years, 1966–89.

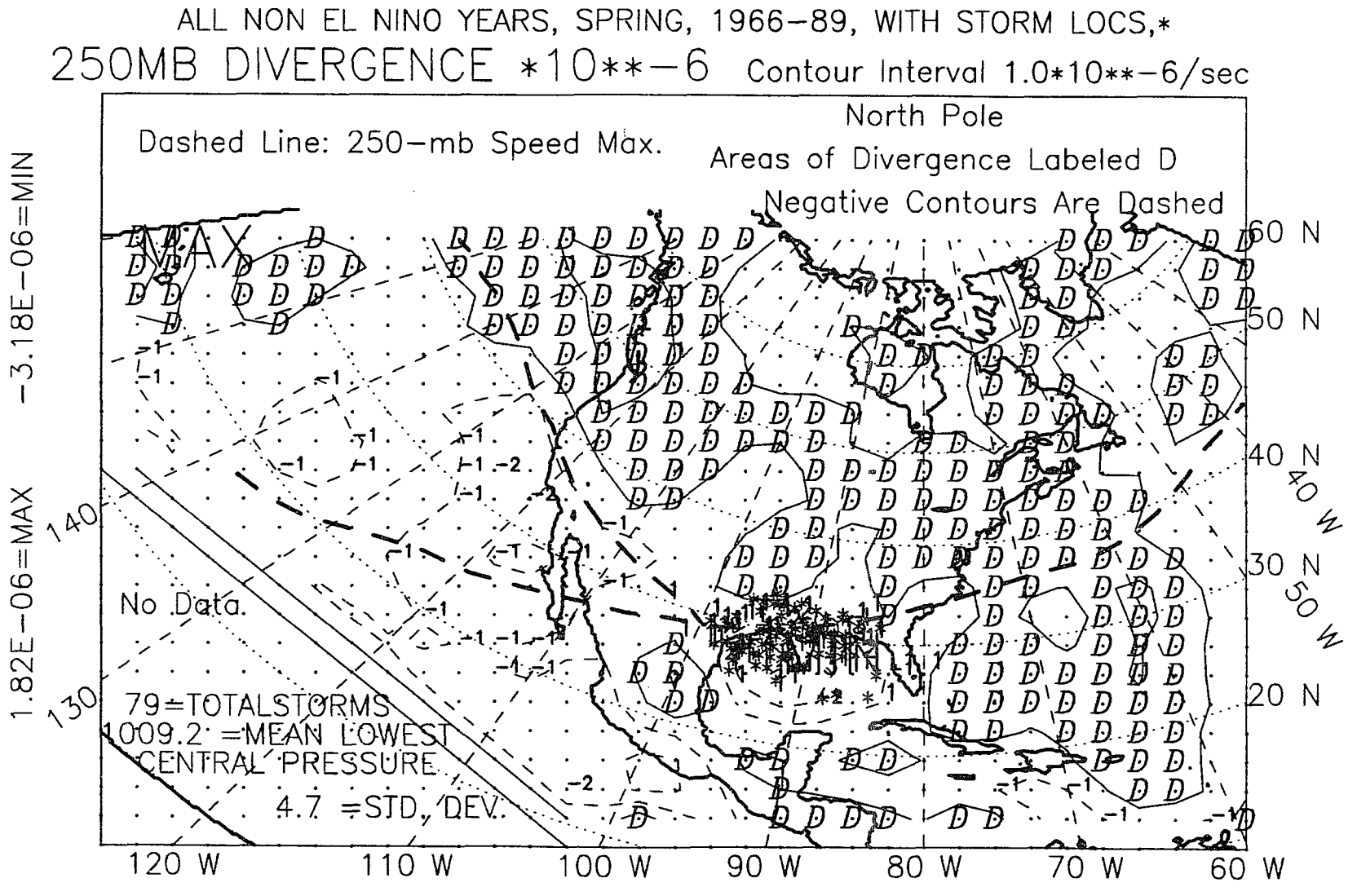

Figure L.5: 250-mb divergence, spring, non-El Niño years, 1966-89.

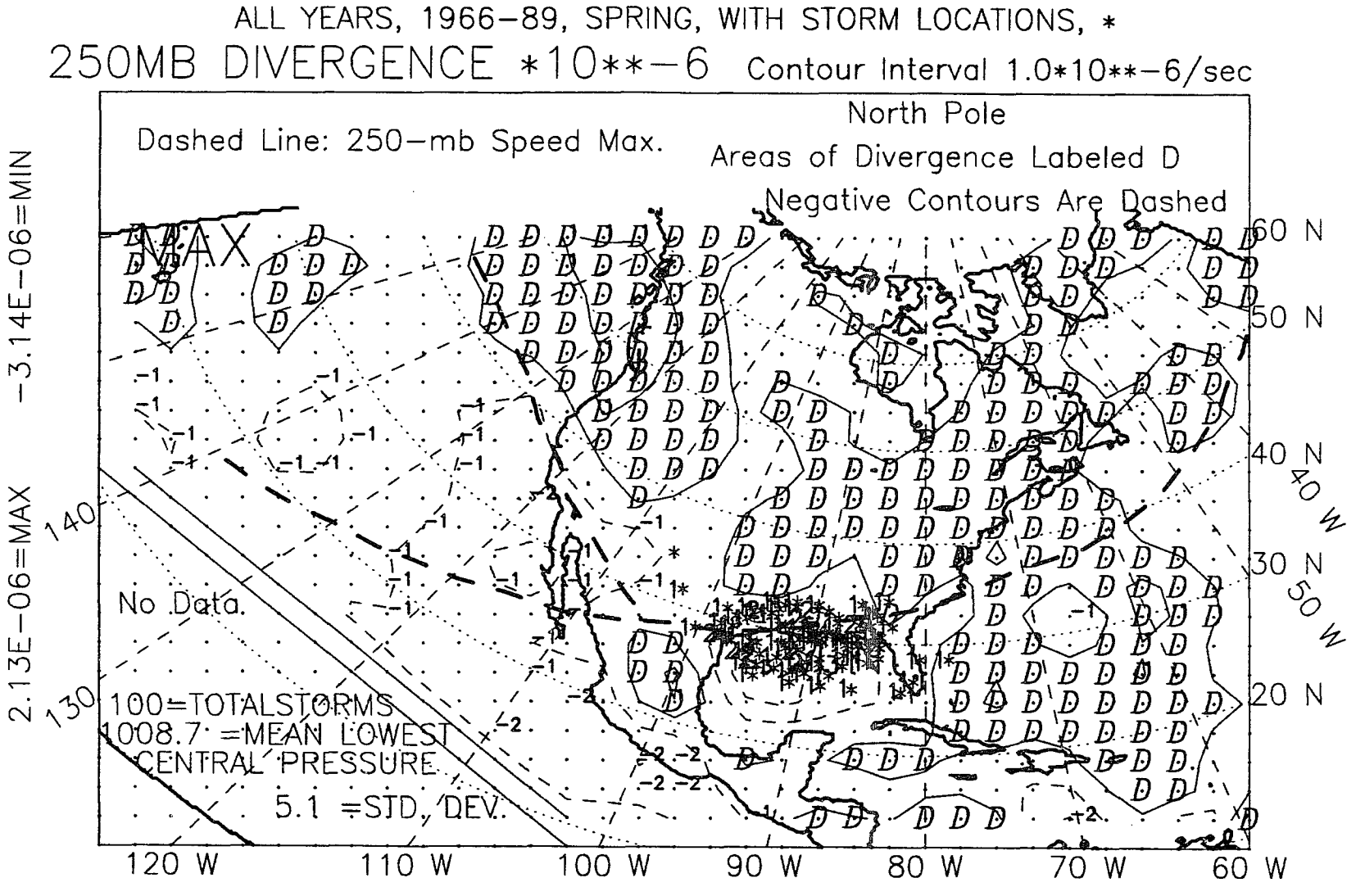

Figure L.6: 250–mb divergence, spring, all years, 1966–89.

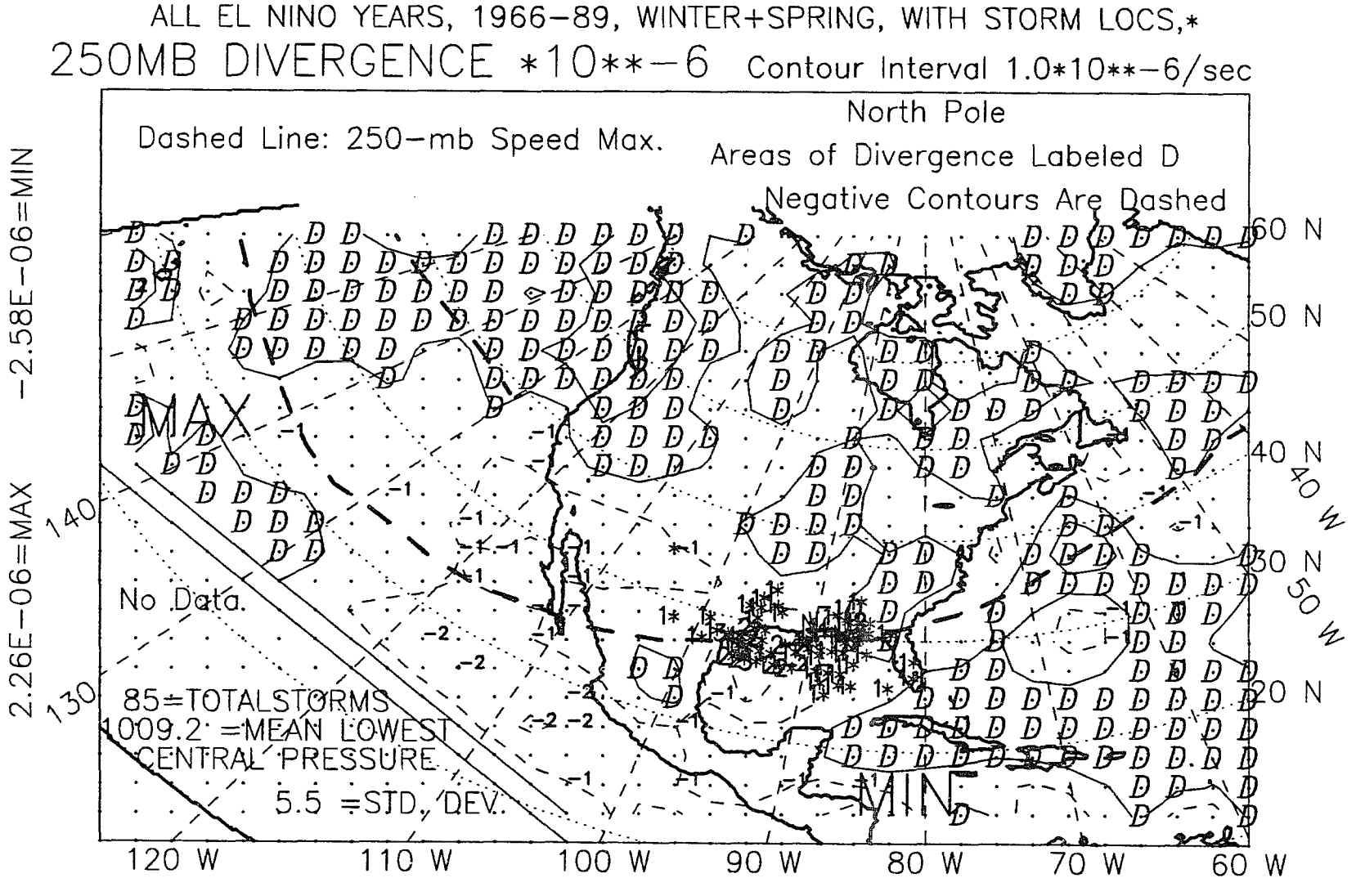

Figure L.7: 250–mb divergence, winter–plus–spring, El Niño years, 1966–89.

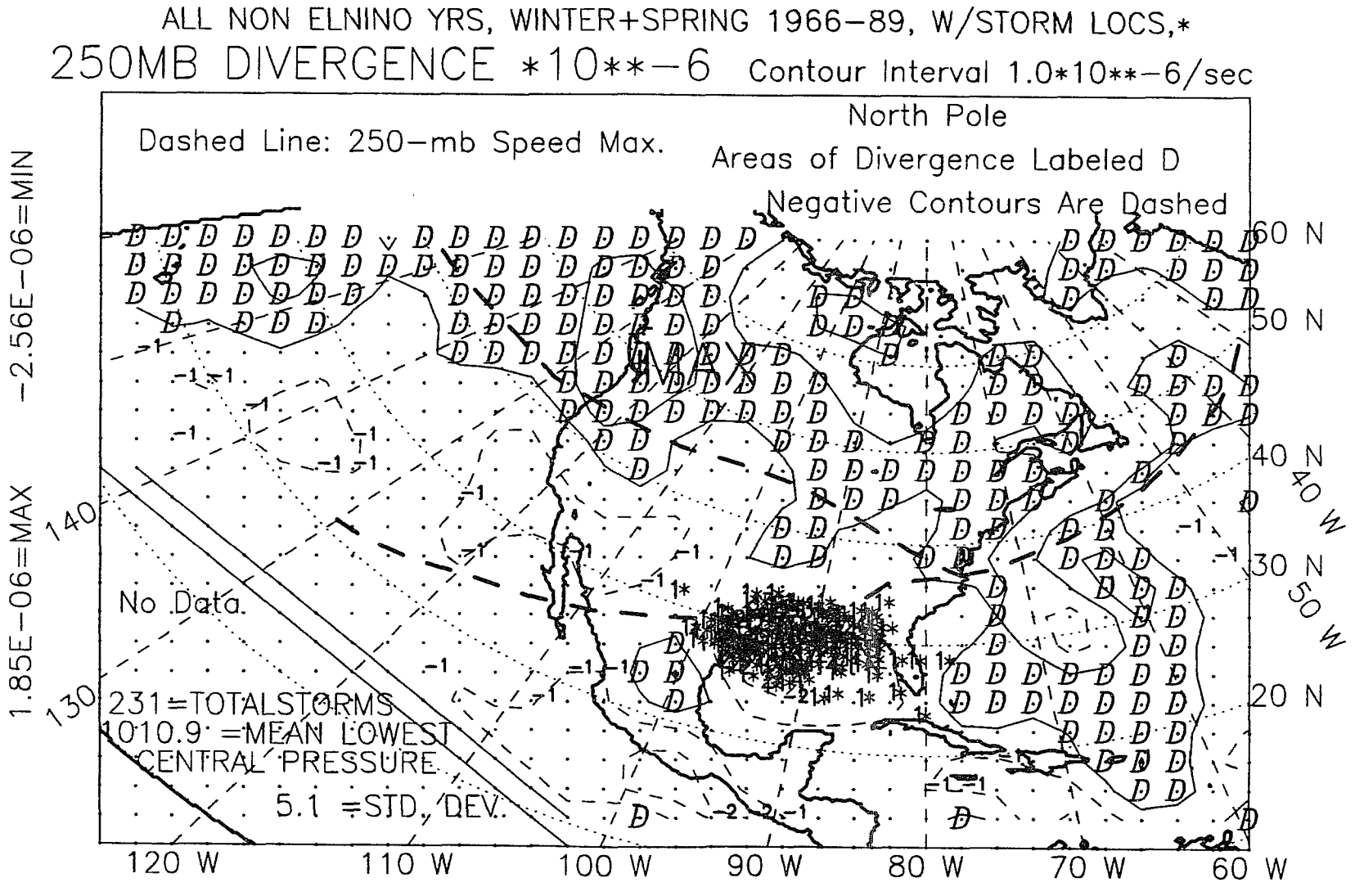

Figure L.8: 250-mb divergence, winter-plus-spring, non-El Niño years, 1966-89.

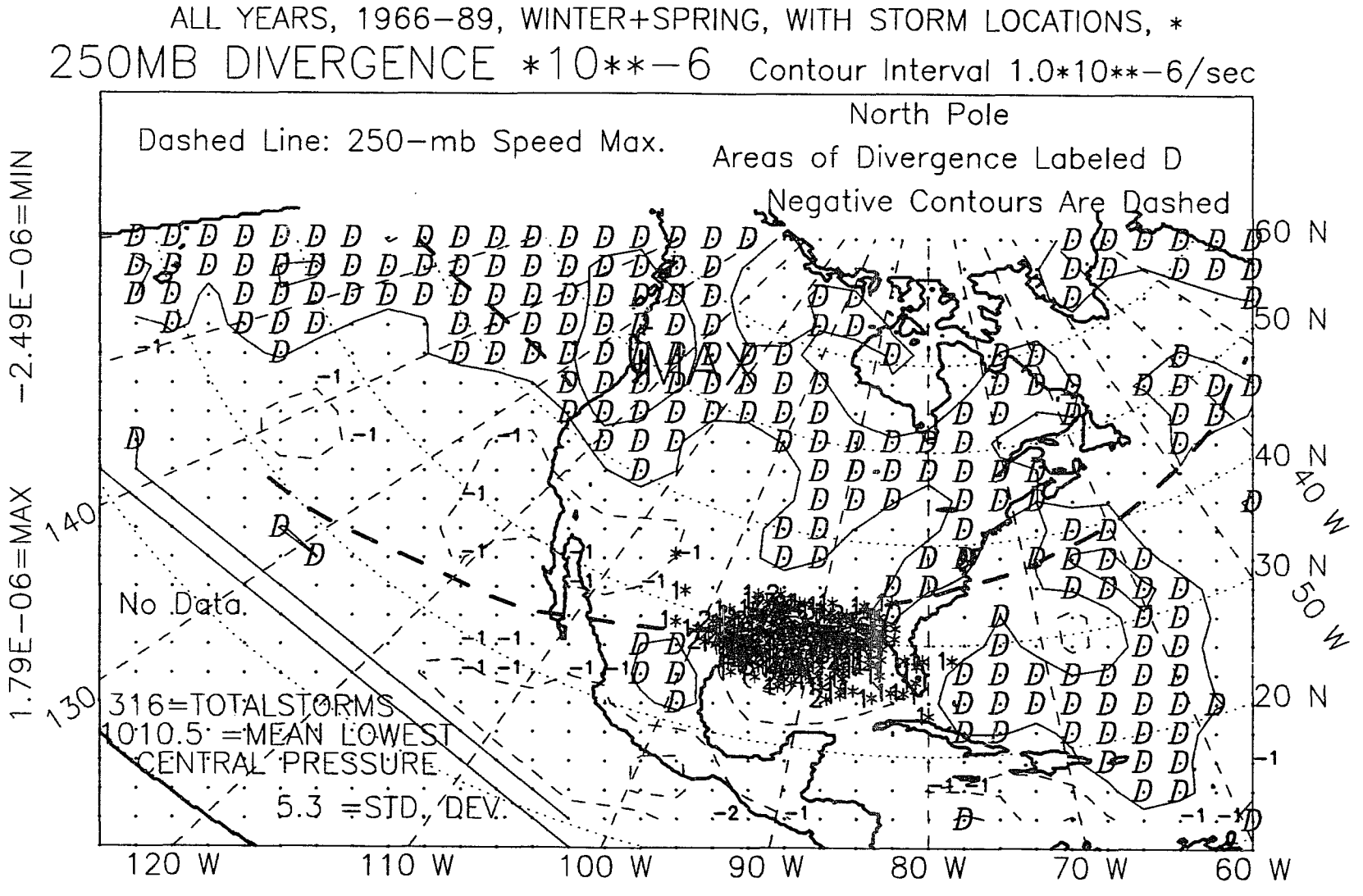

Figure L.9: 250–mb divergence, winter–plus–spring, all years, 1966–89.

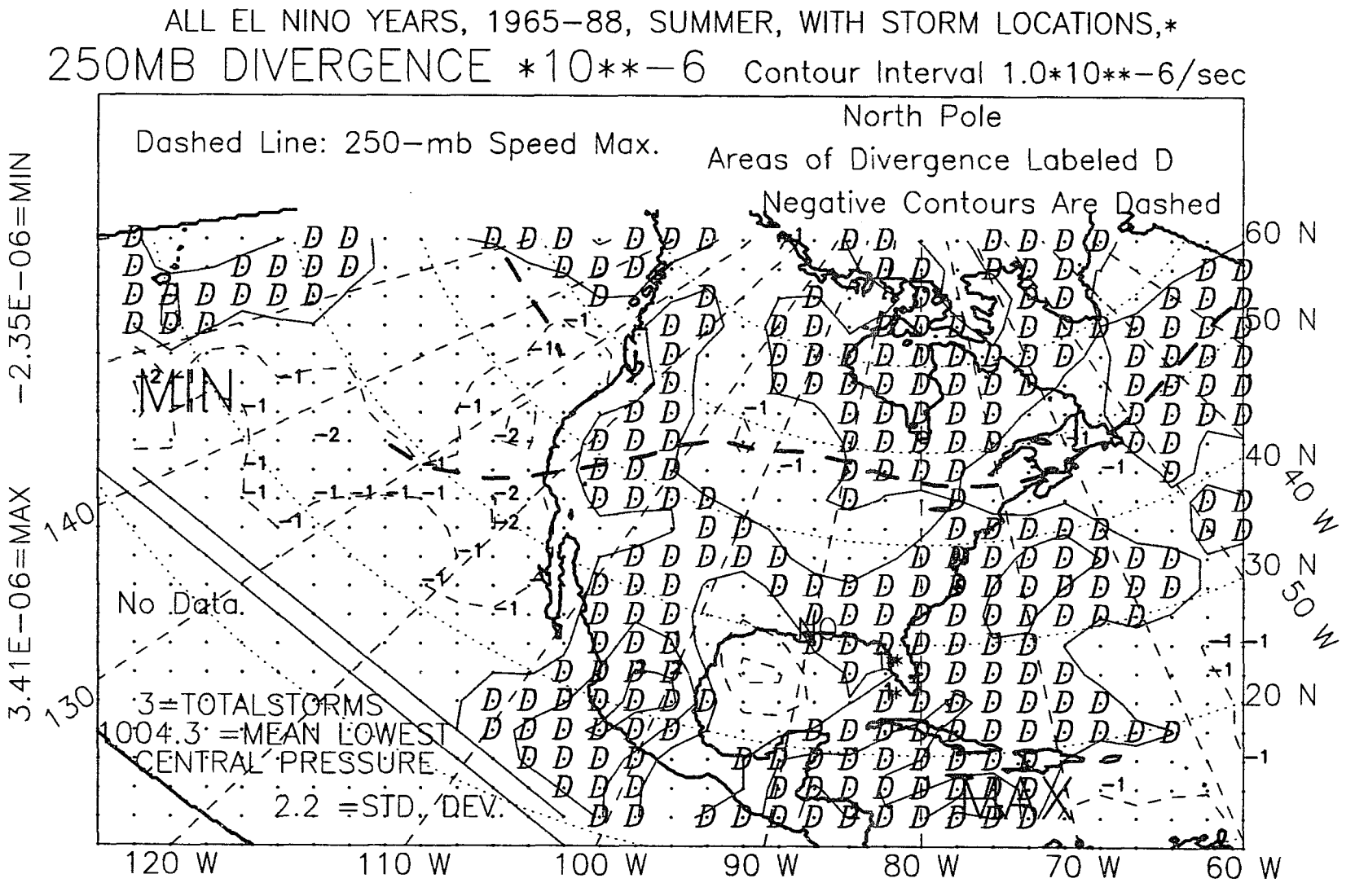

Figure L.10: 250–mb divergence, summer, El Niño years, 1965–88.

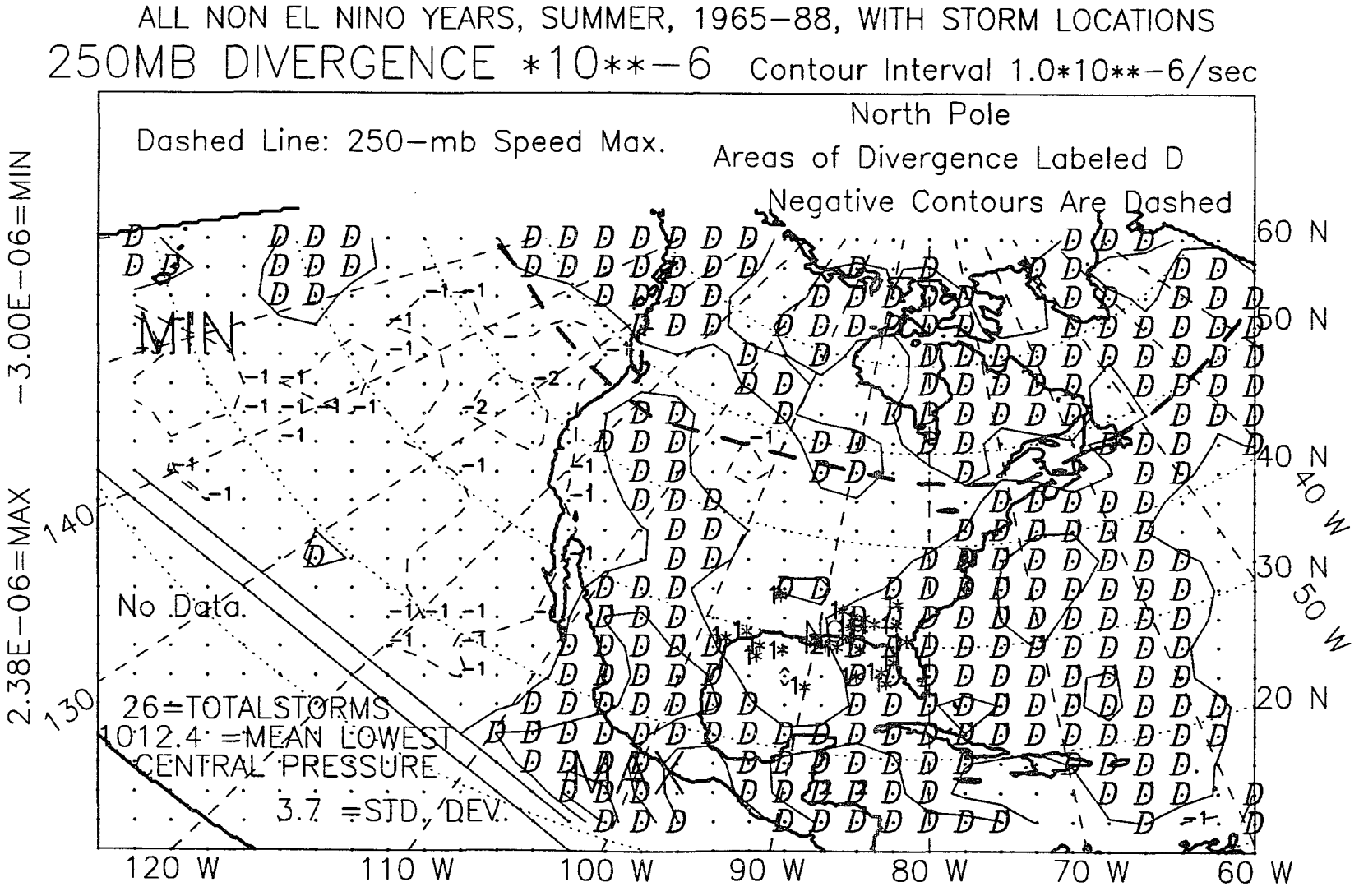

Figure L.11: 250–mb divergence, summer, non–El Niño years, 1965–88.

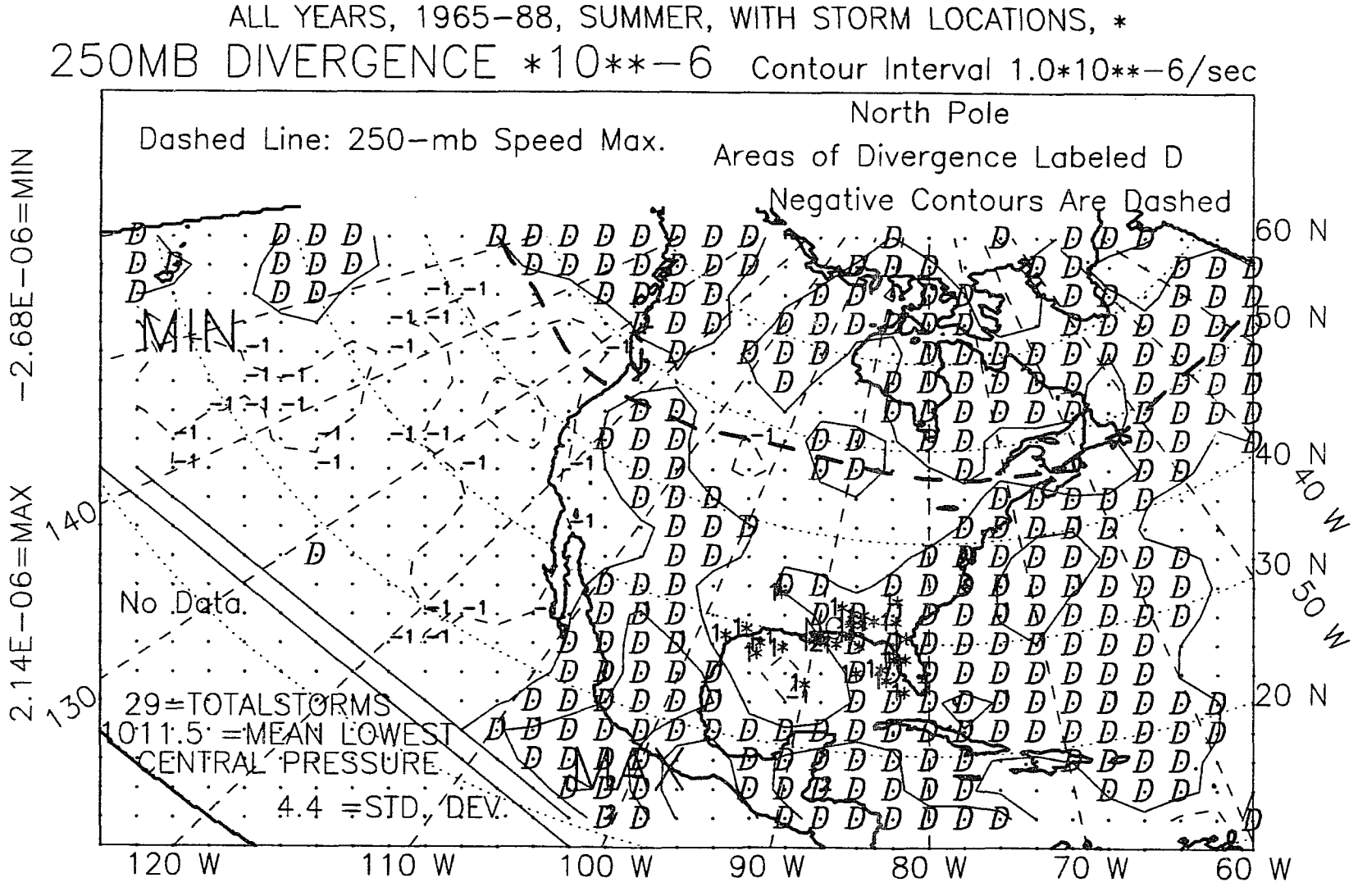

Figure L.12: 250–mb divergence, summer, all years, 1965–88.

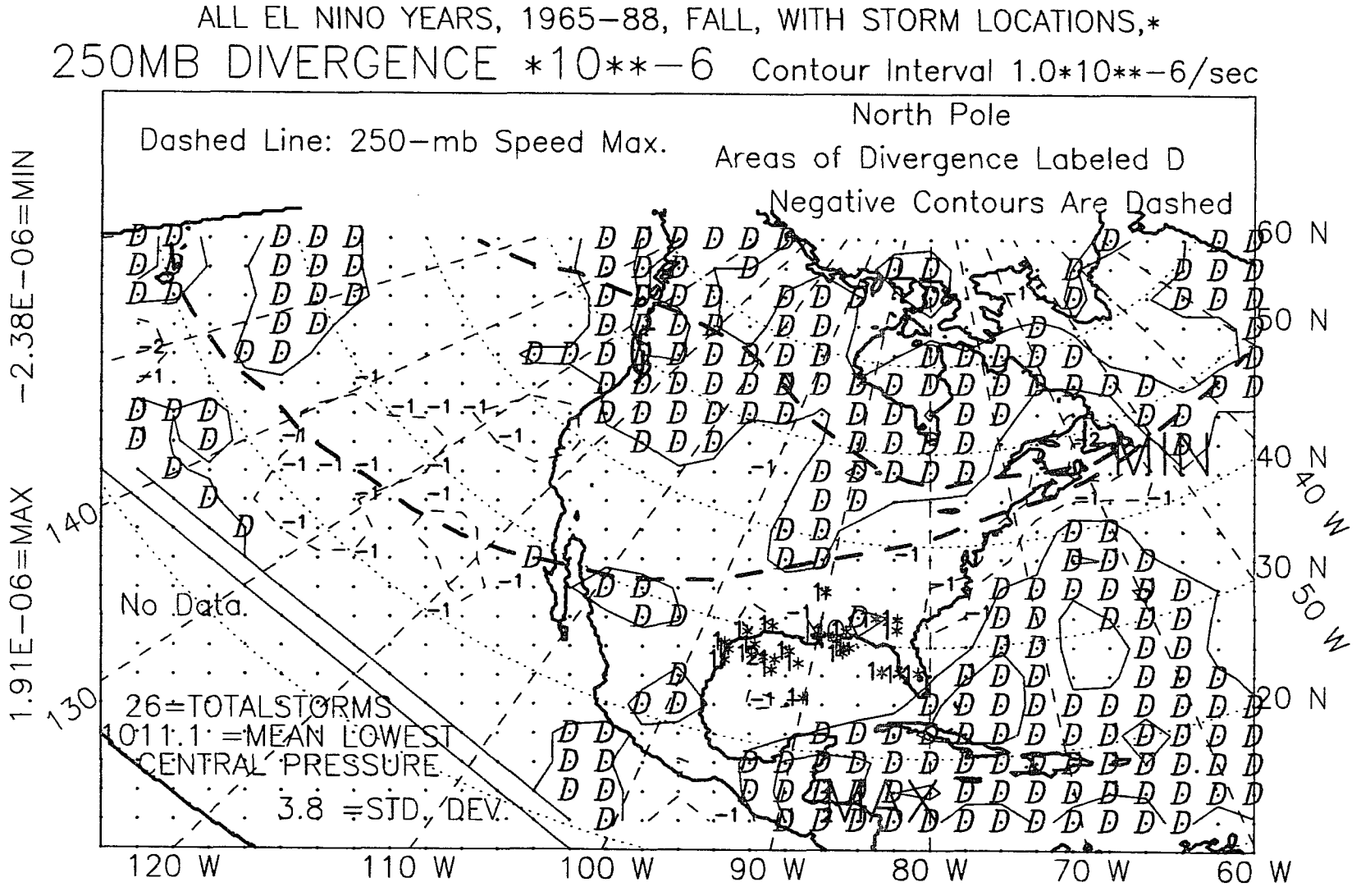

Figure L.13: 250–mb divergence, fall, El Niño years, 1965–88.

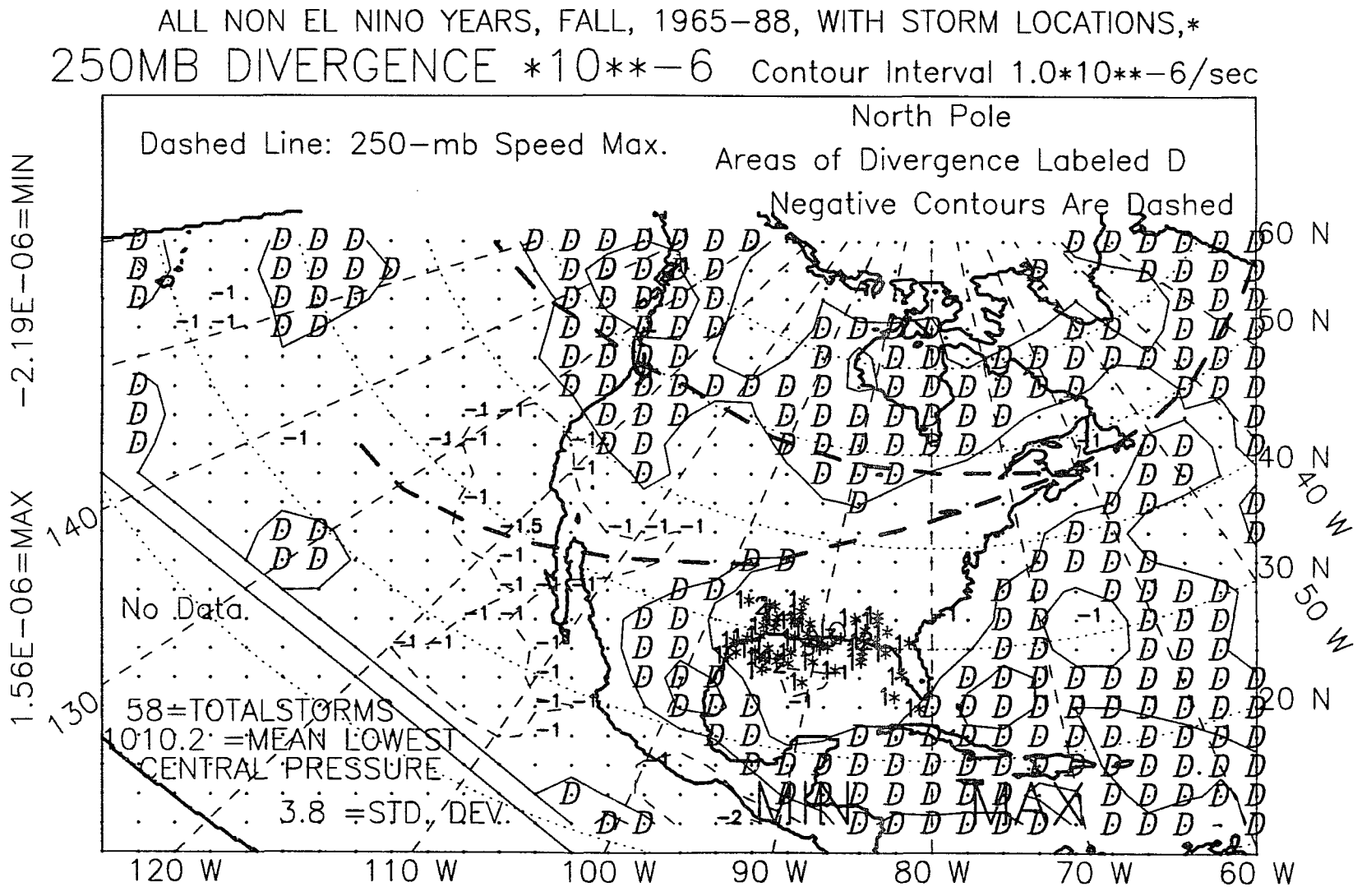

Figure L.14: 250–mb divergence, fall, non–El Niño years, 1965–88.

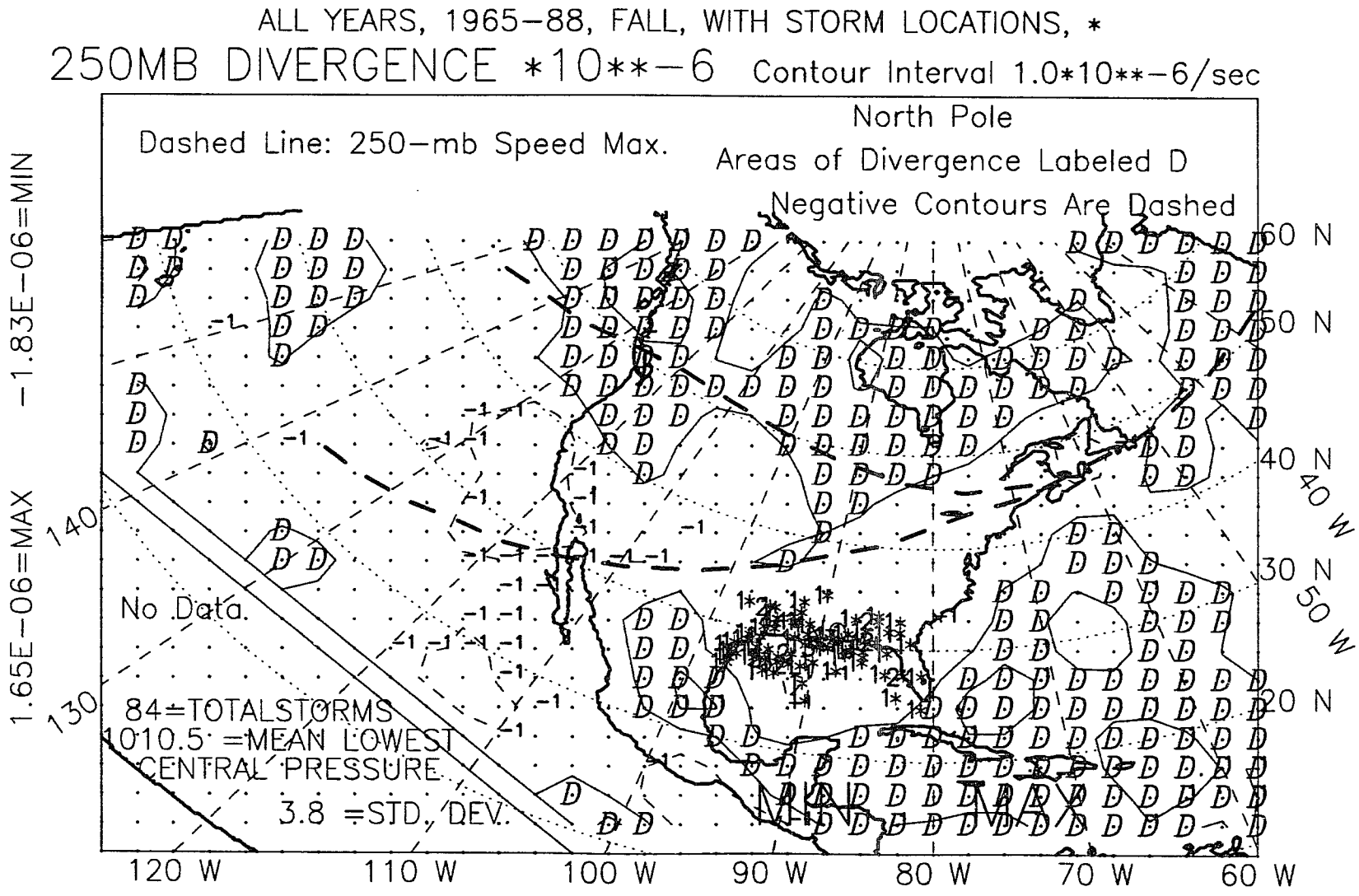

Figure L.15: 250–mb divergence, fall, all years, 1965–88.

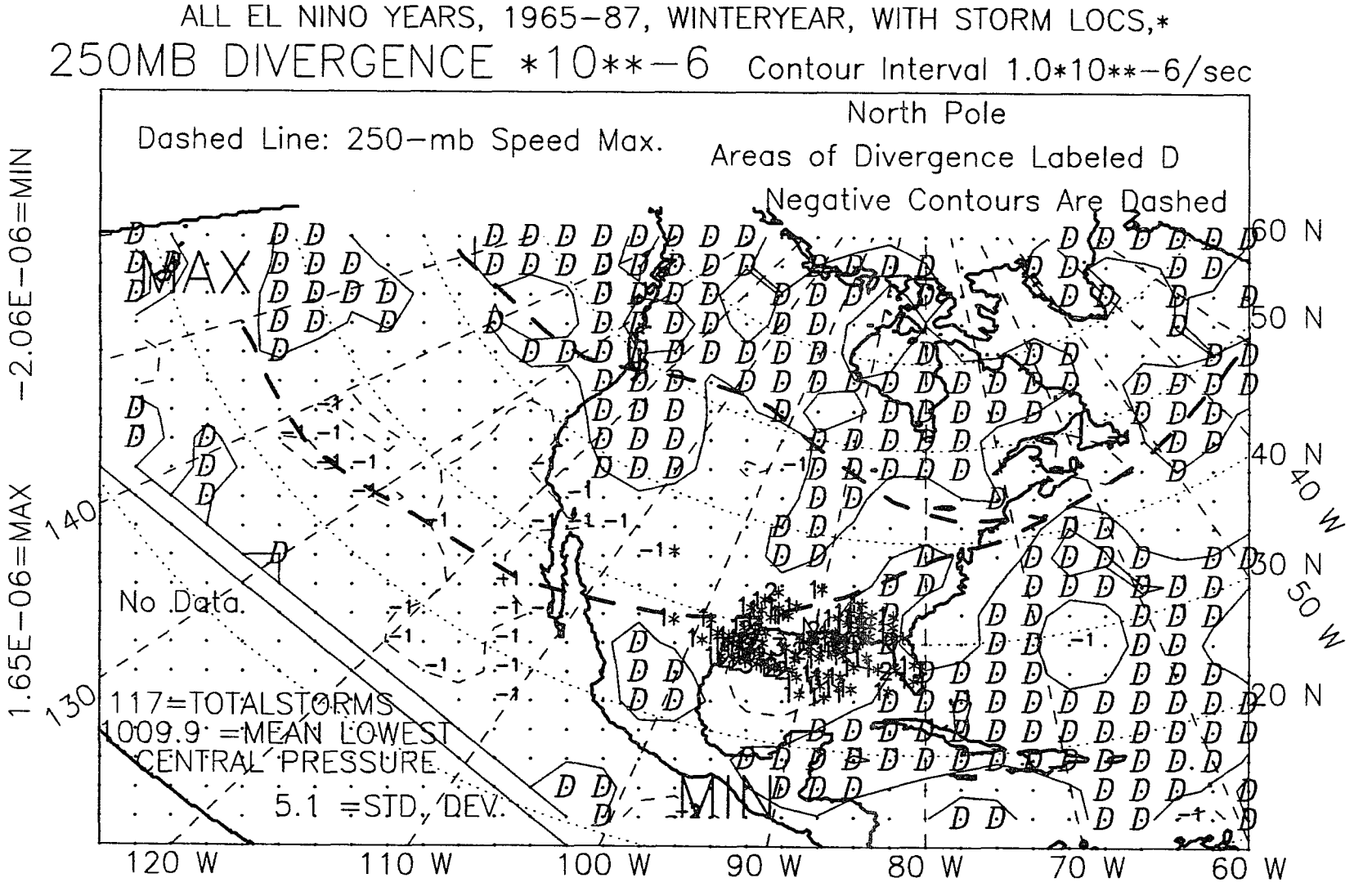

Figure L.16: 250–mb divergence, winter year, El Niño years, 1965–87.

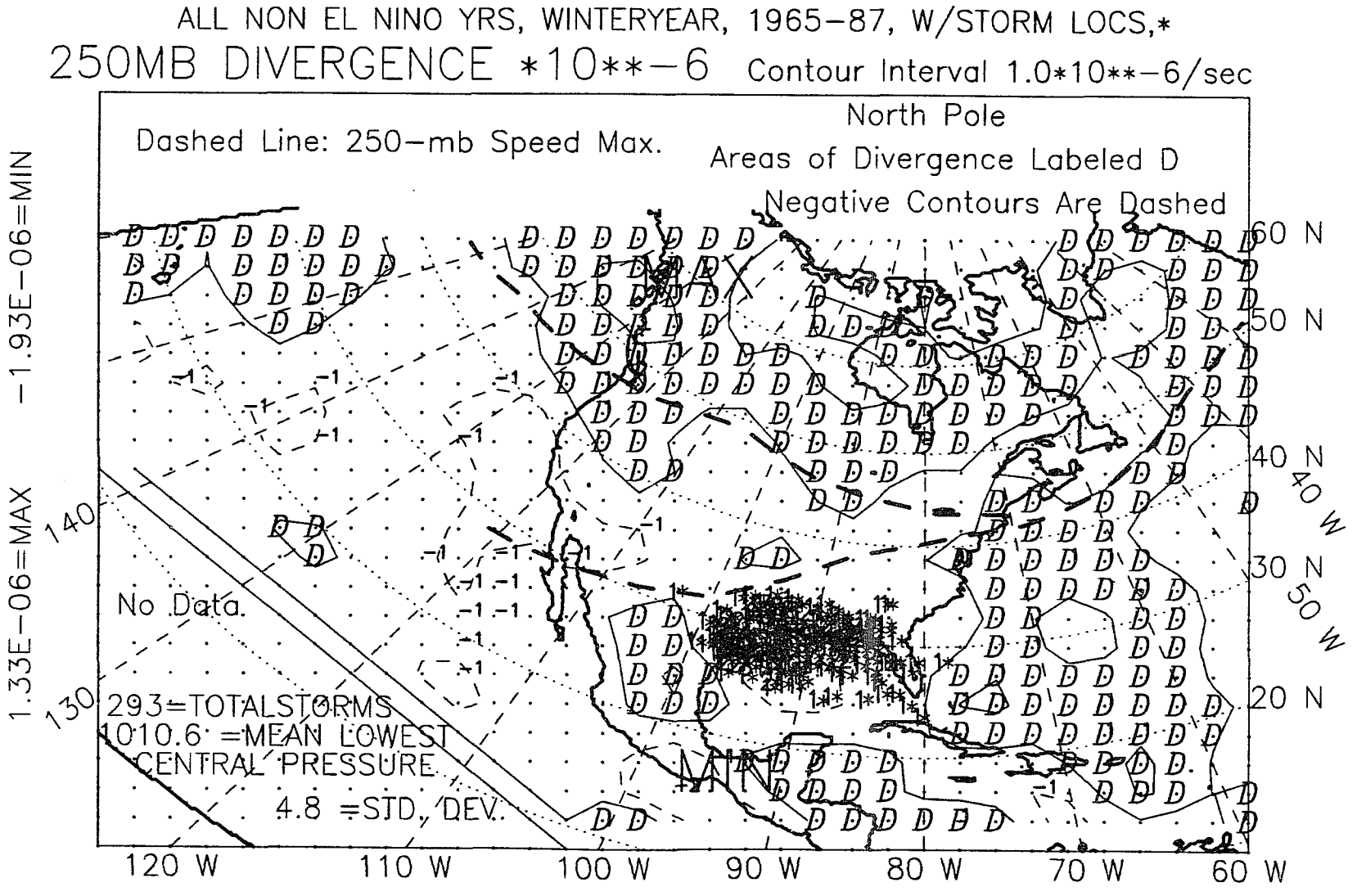

Figure L.17: 250–mb divergence, winter year, non–El Niño years, 1965–87.

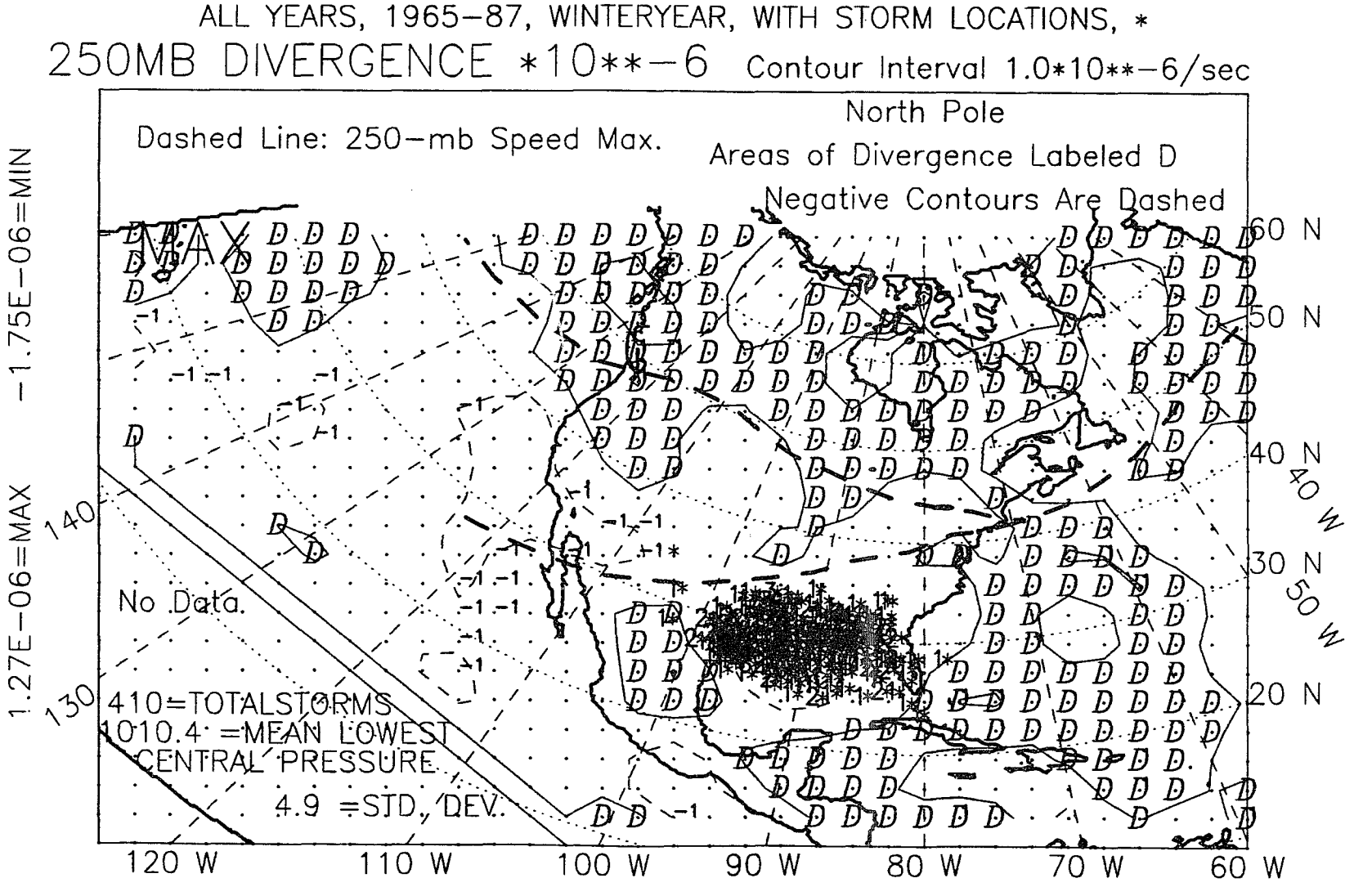

Figure L.18: 250–mb divergence, winter year, all years, 1965–87.

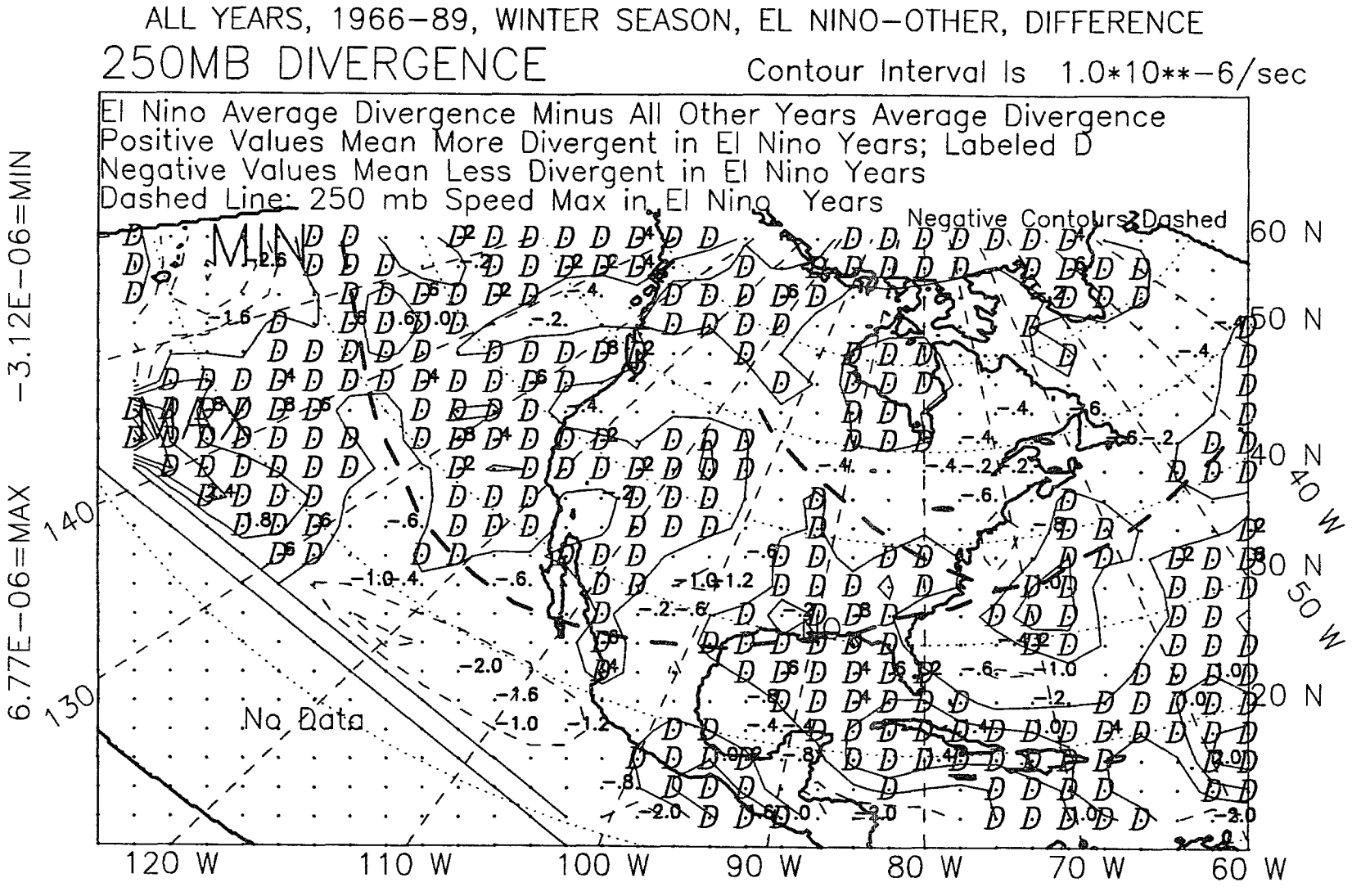

Figure L.19: 250–mb divergence, winter, 1966–89, difference.

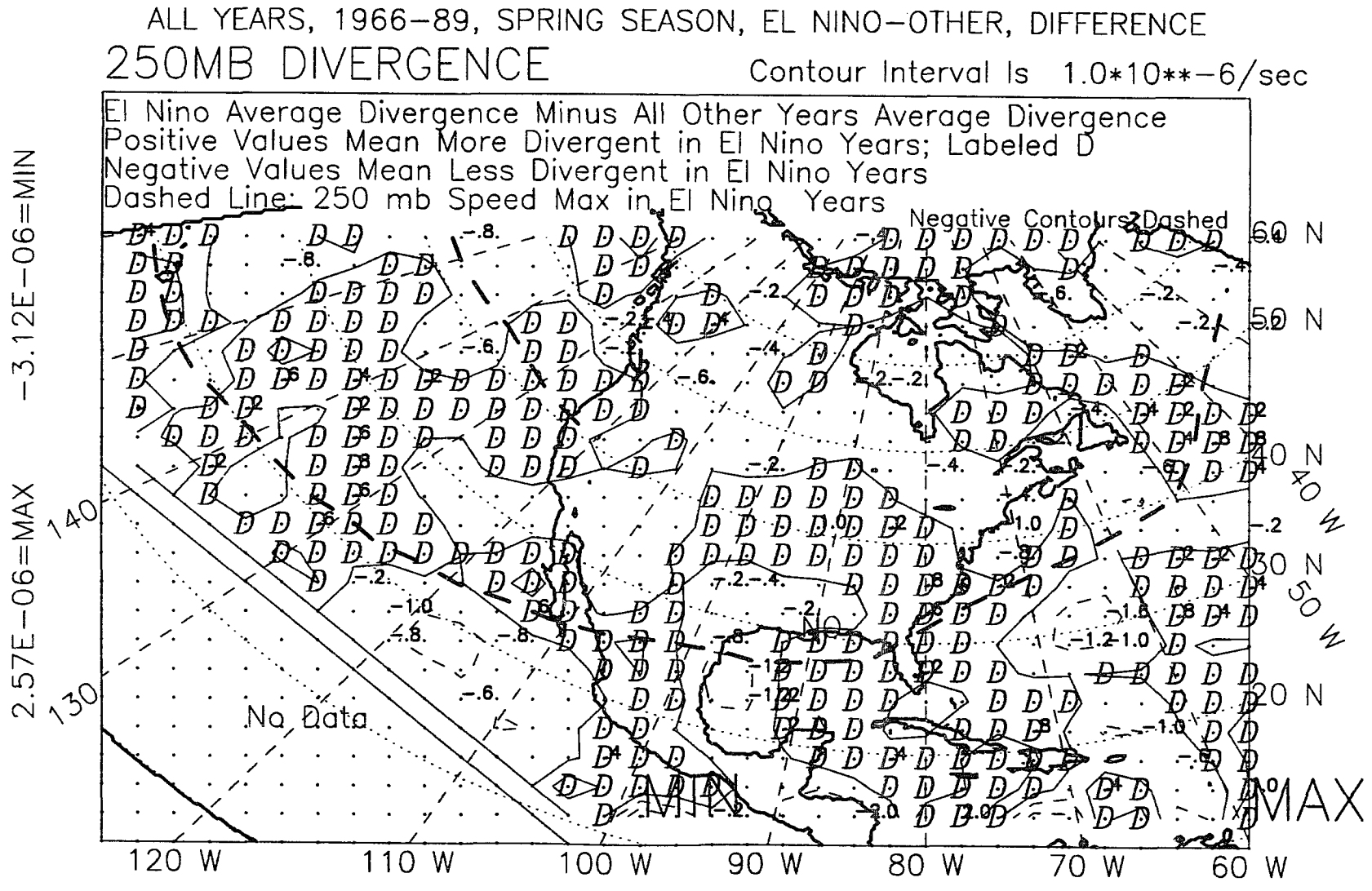

Figure L.20: 250–mb divergence, spring, 1966–89, difference.

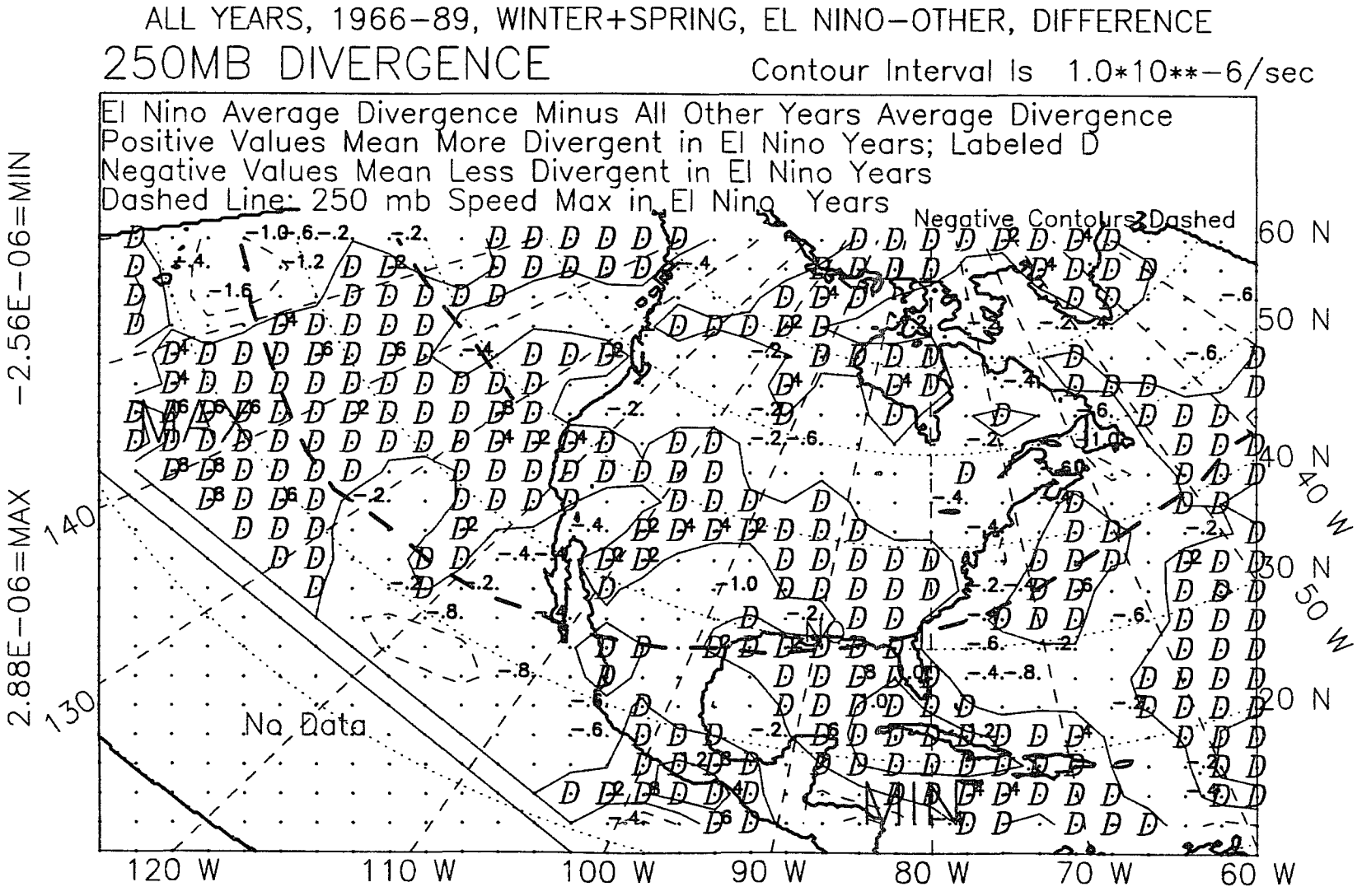

Figure L.21: 250–mb divergence, winter–plus–spring, 1966–89, difference.

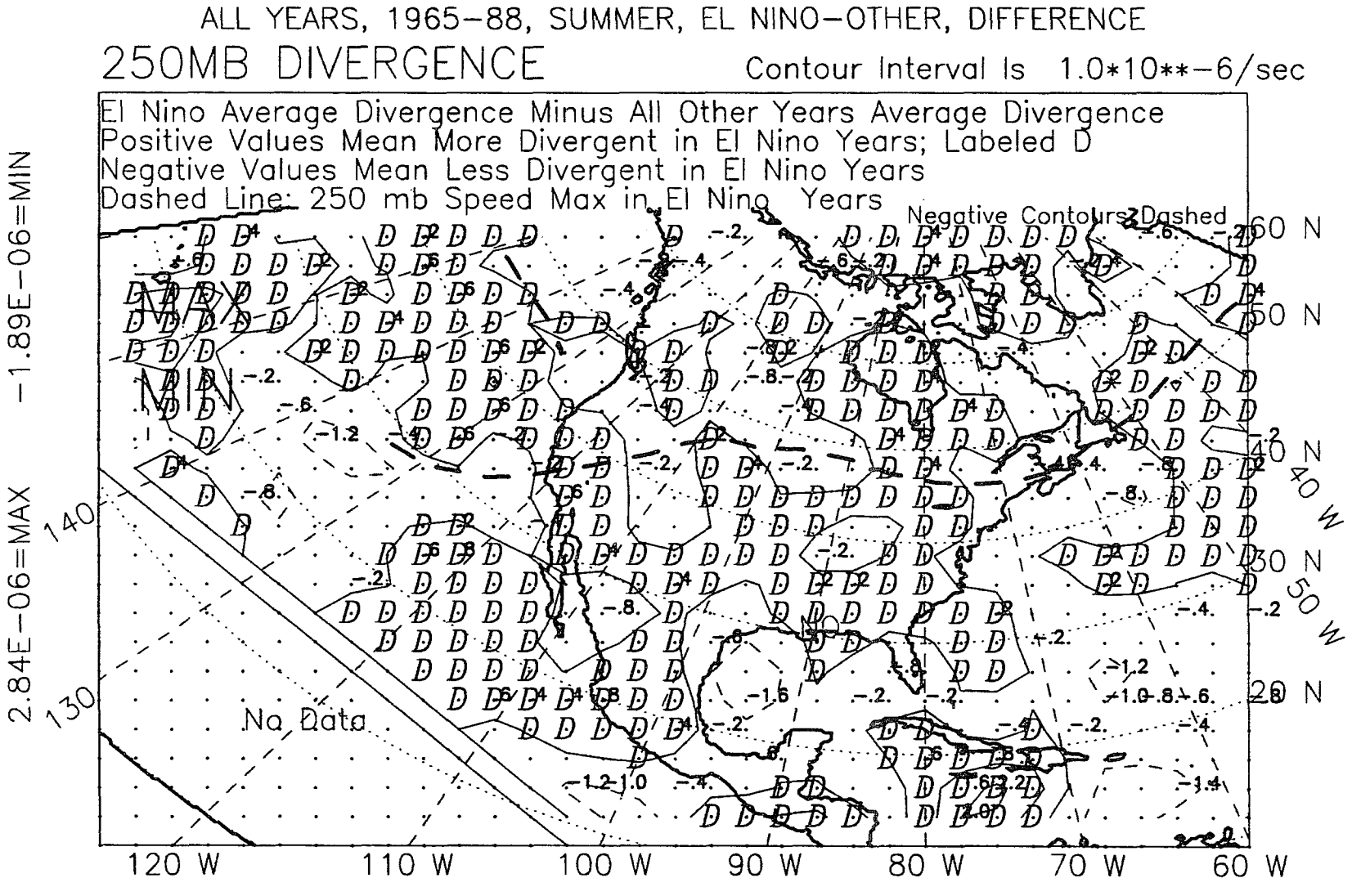

Figure L.22: 250–mb divergence, summer, 1965–88, difference.

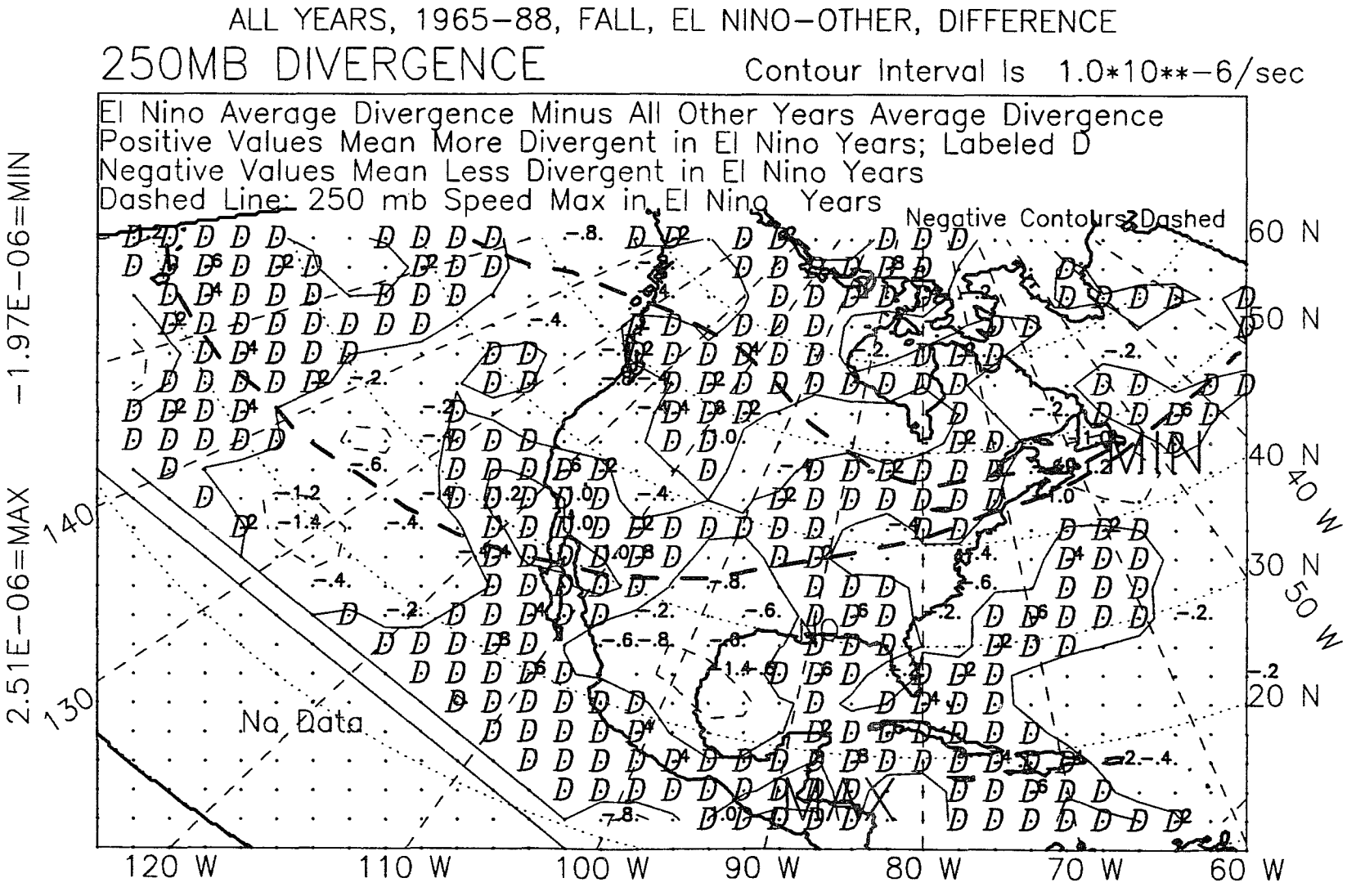

Figure L.23: 250–mb divergence, fall, 1965–88, difference.

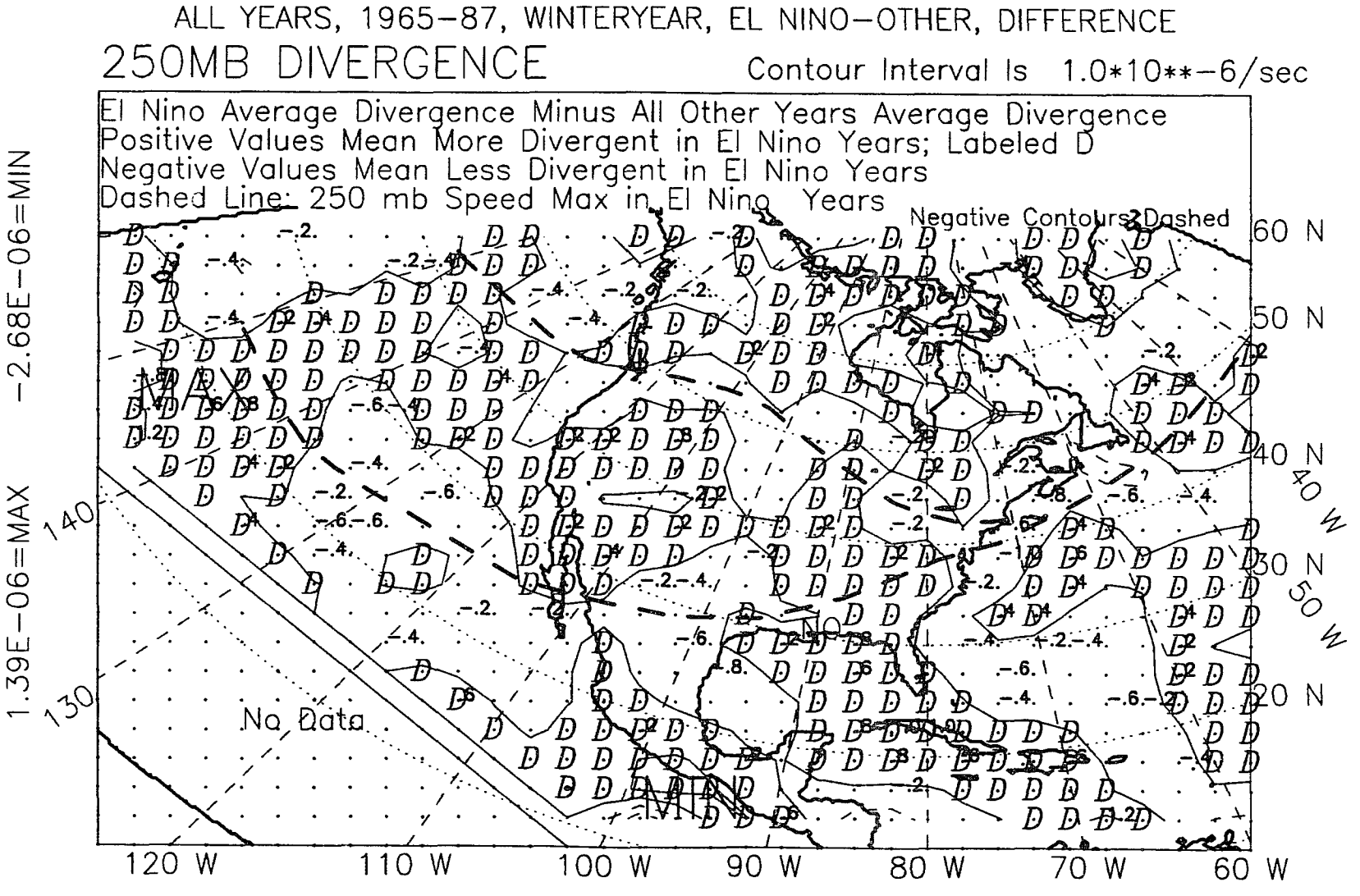

Figure L.24: 250–mb divergence, winter year, 1965–87, difference.

APPENDIX M
250-MB RELATIVE-VORTICITY FIELD

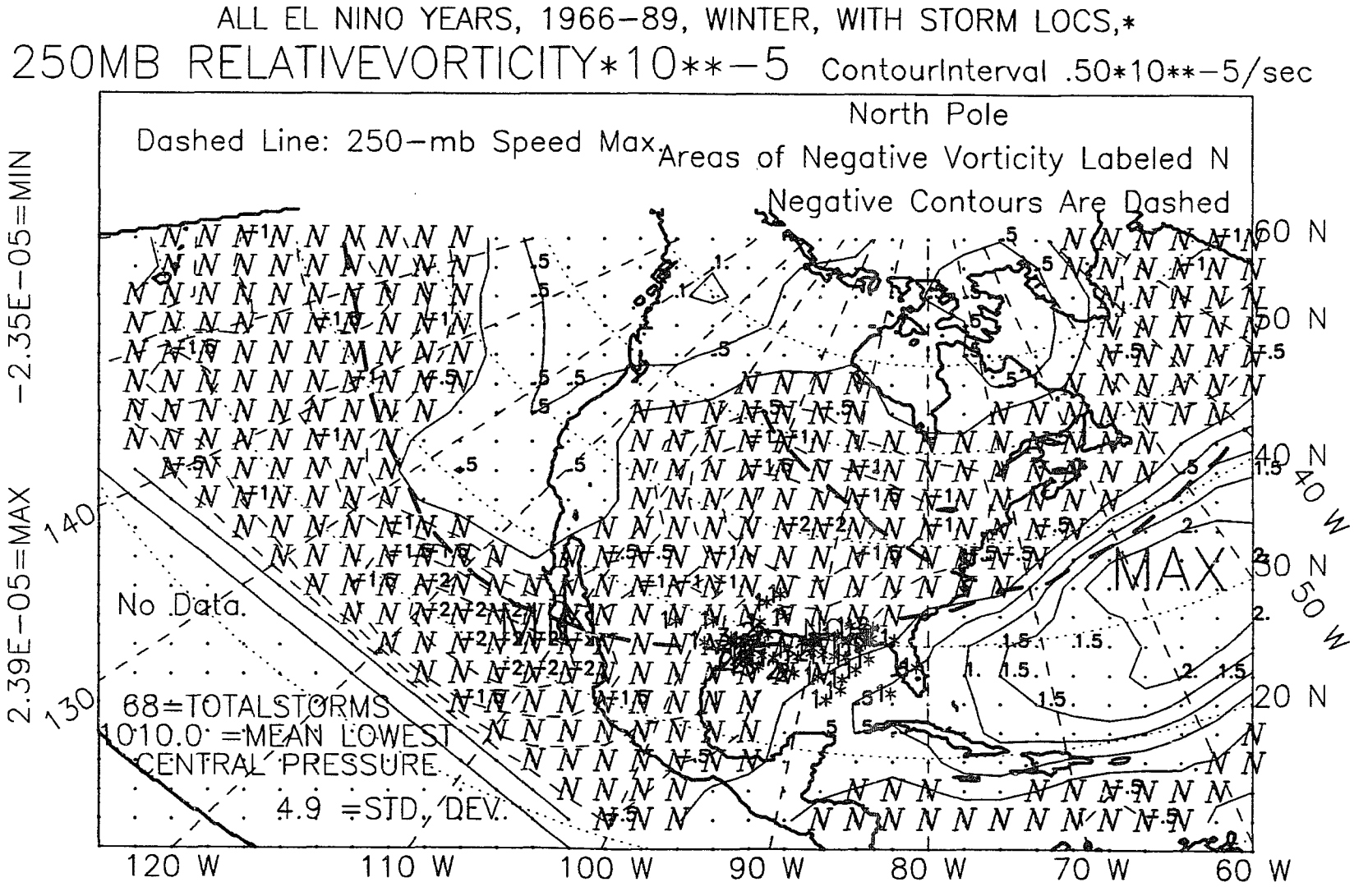

Figure M.1: 250–mb relative vorticity, winter, El Niño years, 1966–89.

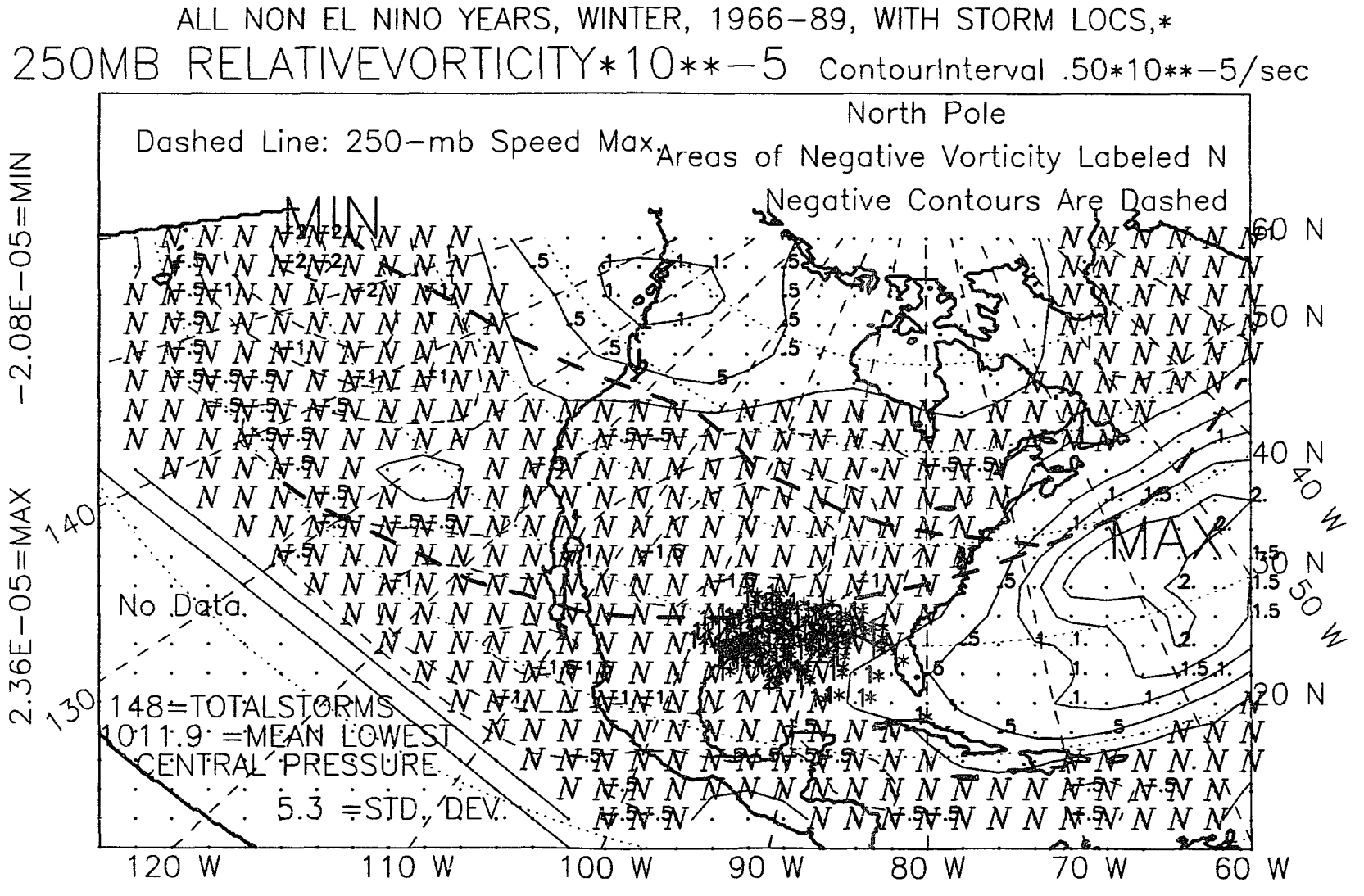

Figure M.2: 250–mb relative vorticity, winter, non–El Niño years, 1966–89.

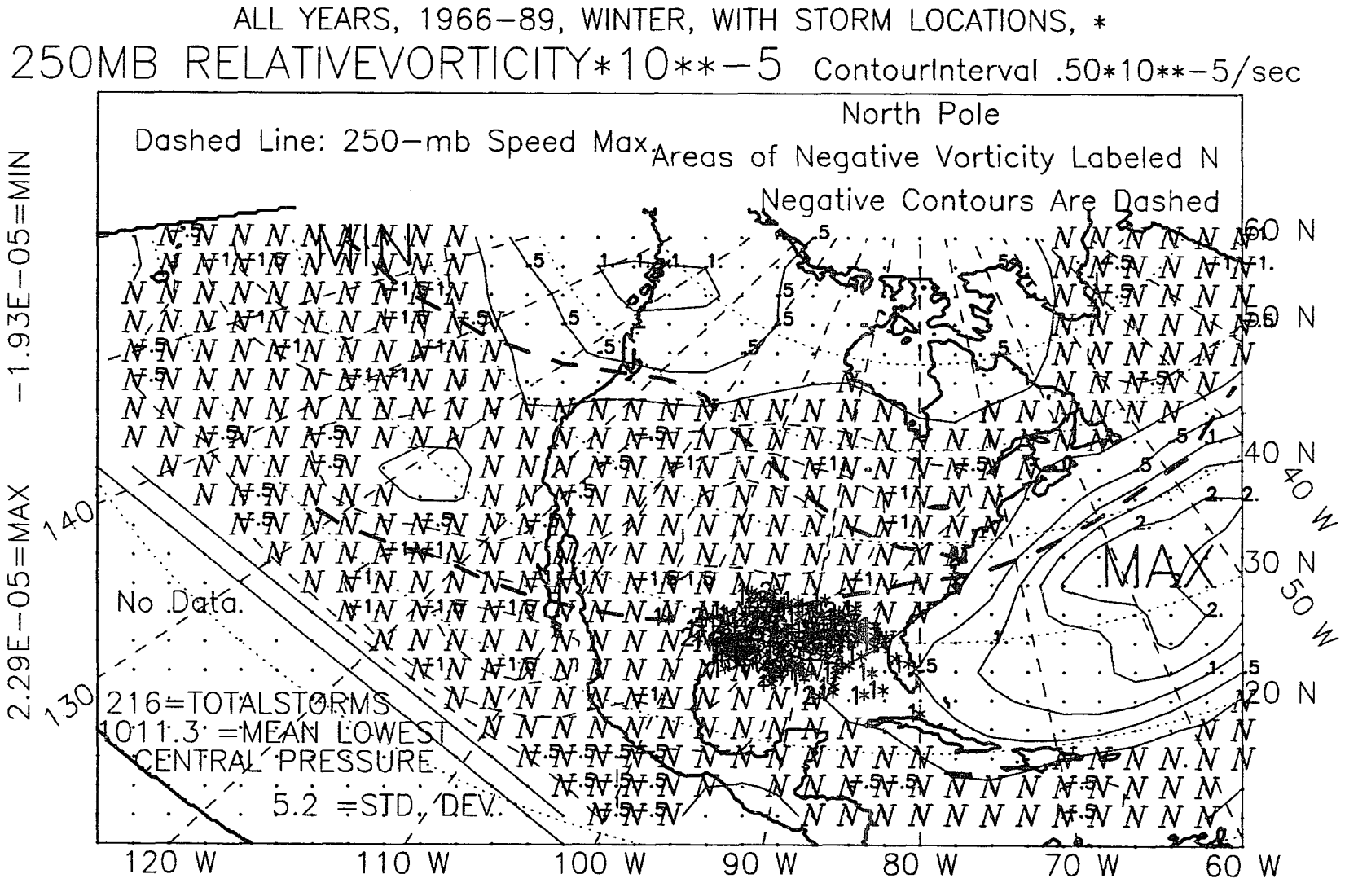

Figure M.3: 250–mb relative vorticity, winter, all years, 1966–89.

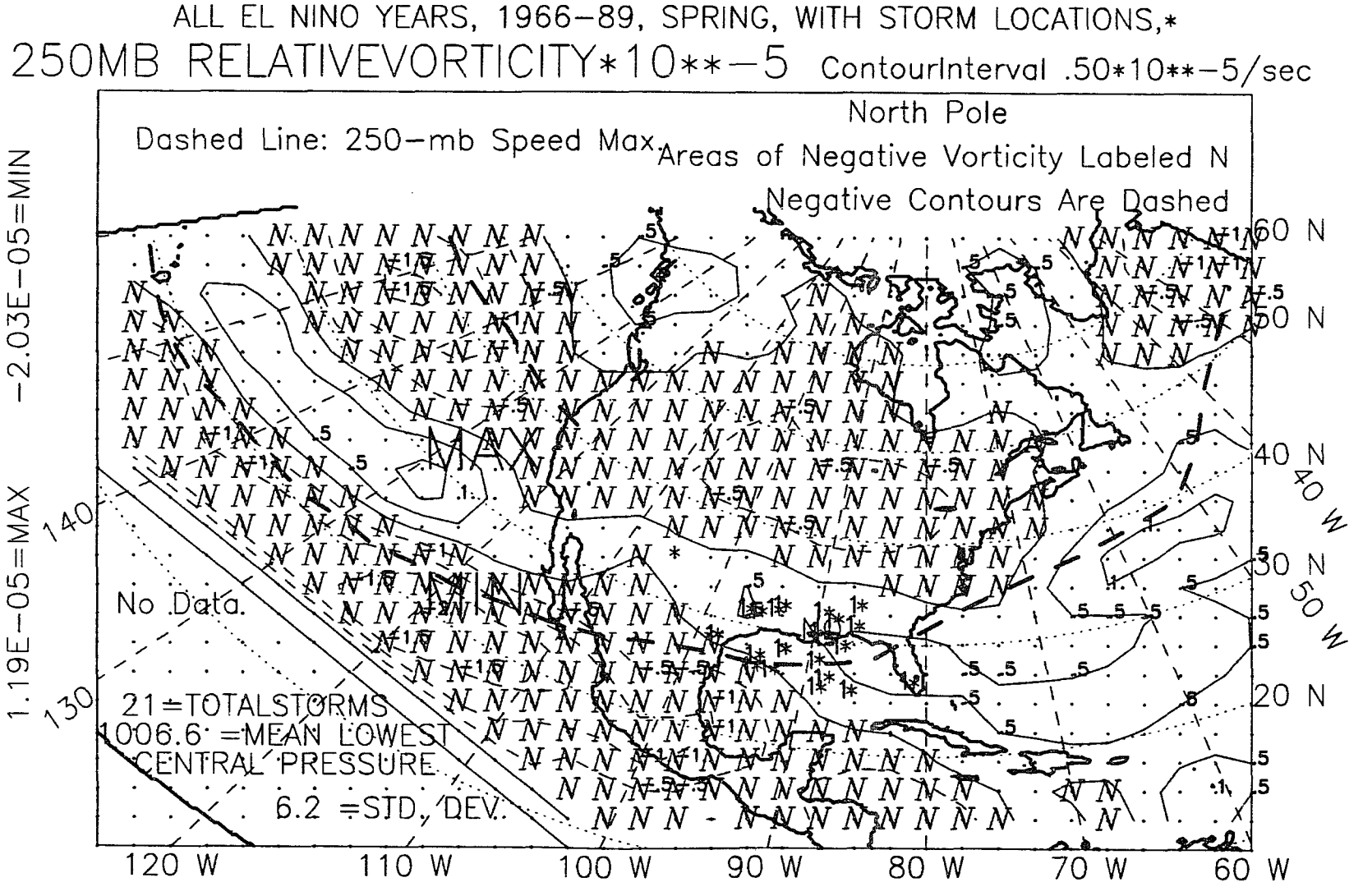

Figure M.4: 250–mb relative vorticity, spring, El Niño years, 1966–89.

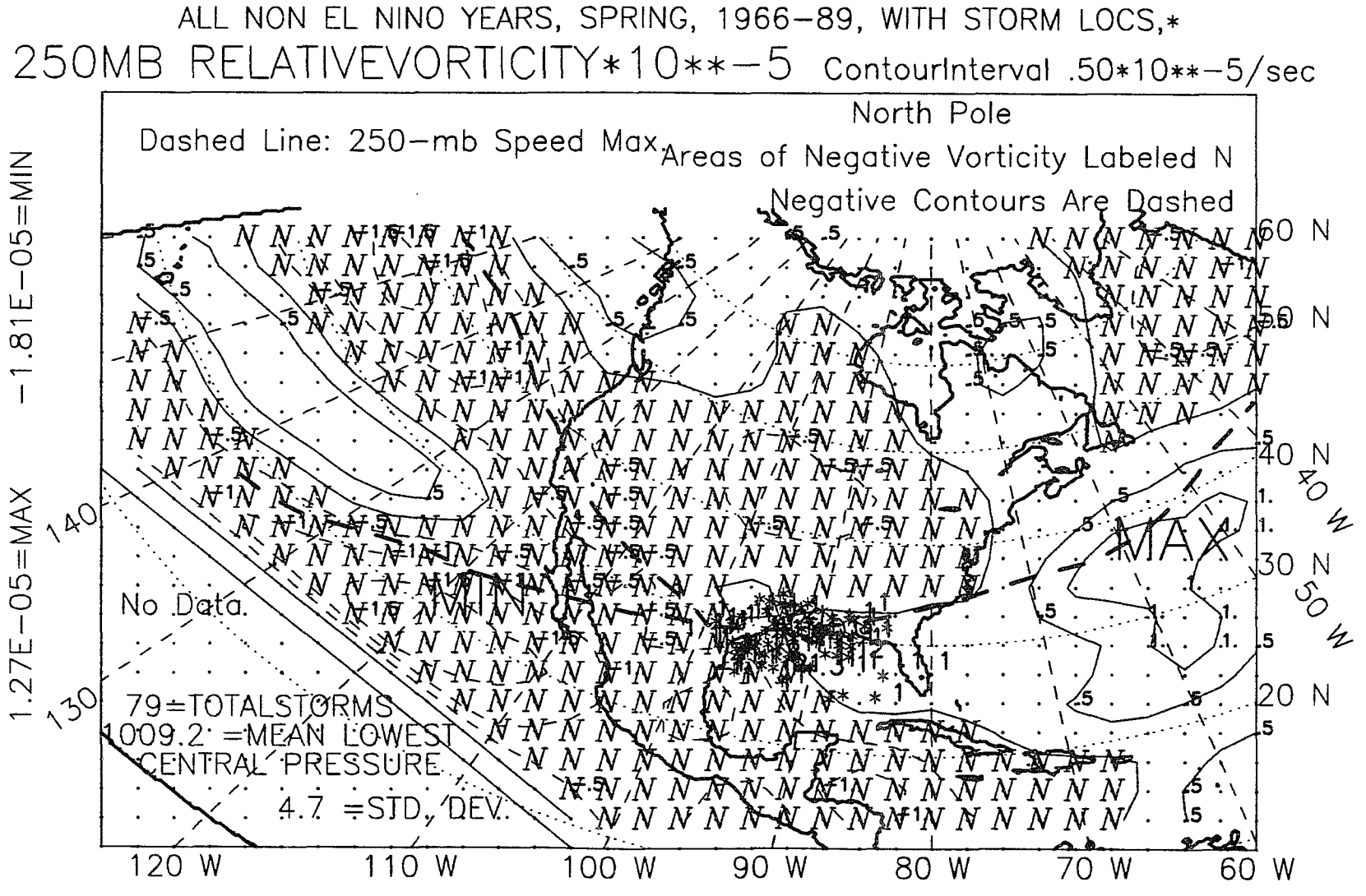

Figure M.5: 250-mb relative vorticity, spring, non-El Niño years, 1966-89.

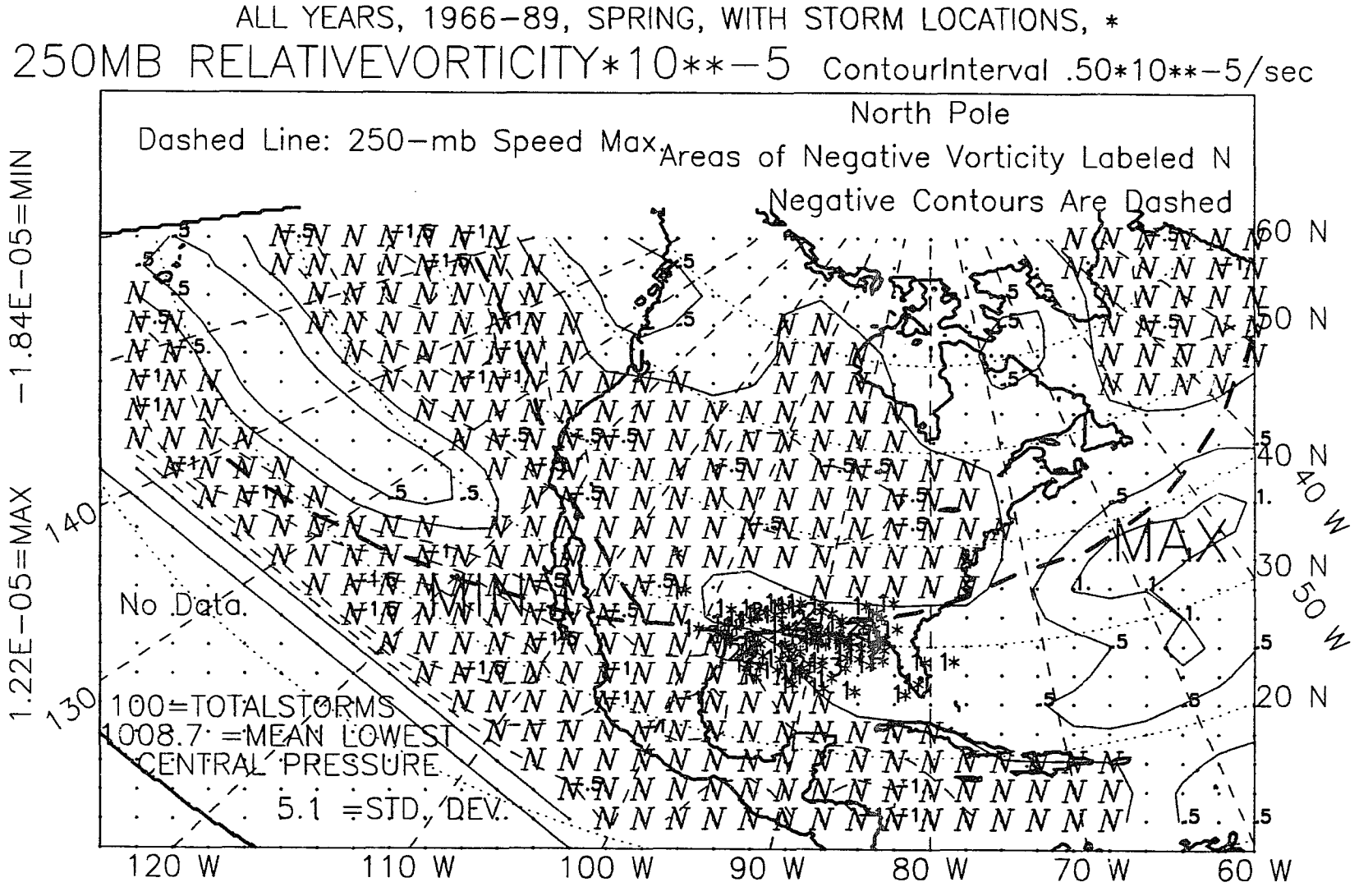

Figure M.6: 250–mb relative vorticity, spring, all years, 1966–89.

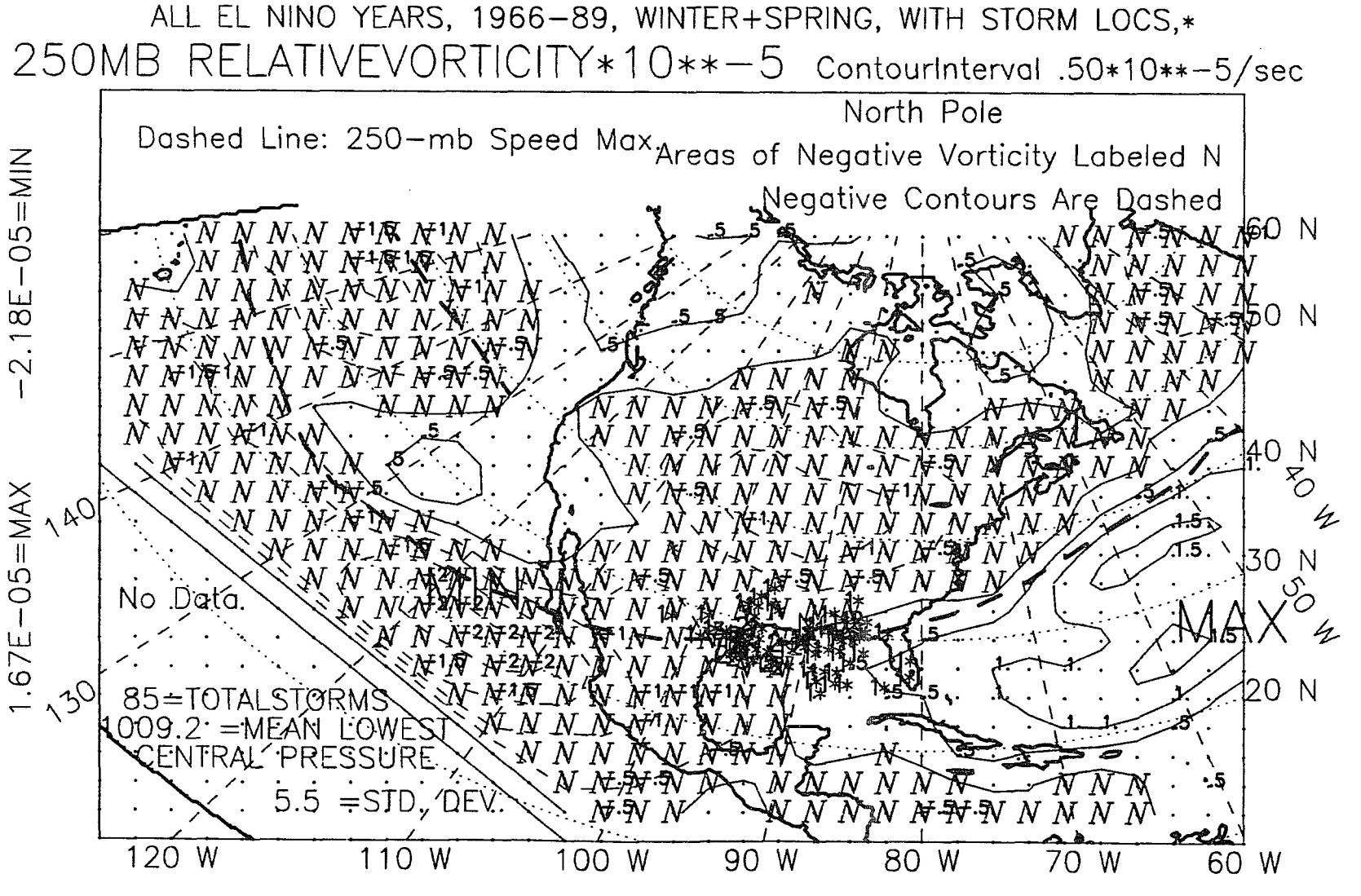

Figure M.7: 250-mb relative vorticity, winter-plus-spring, El Niño years, 1966-89.

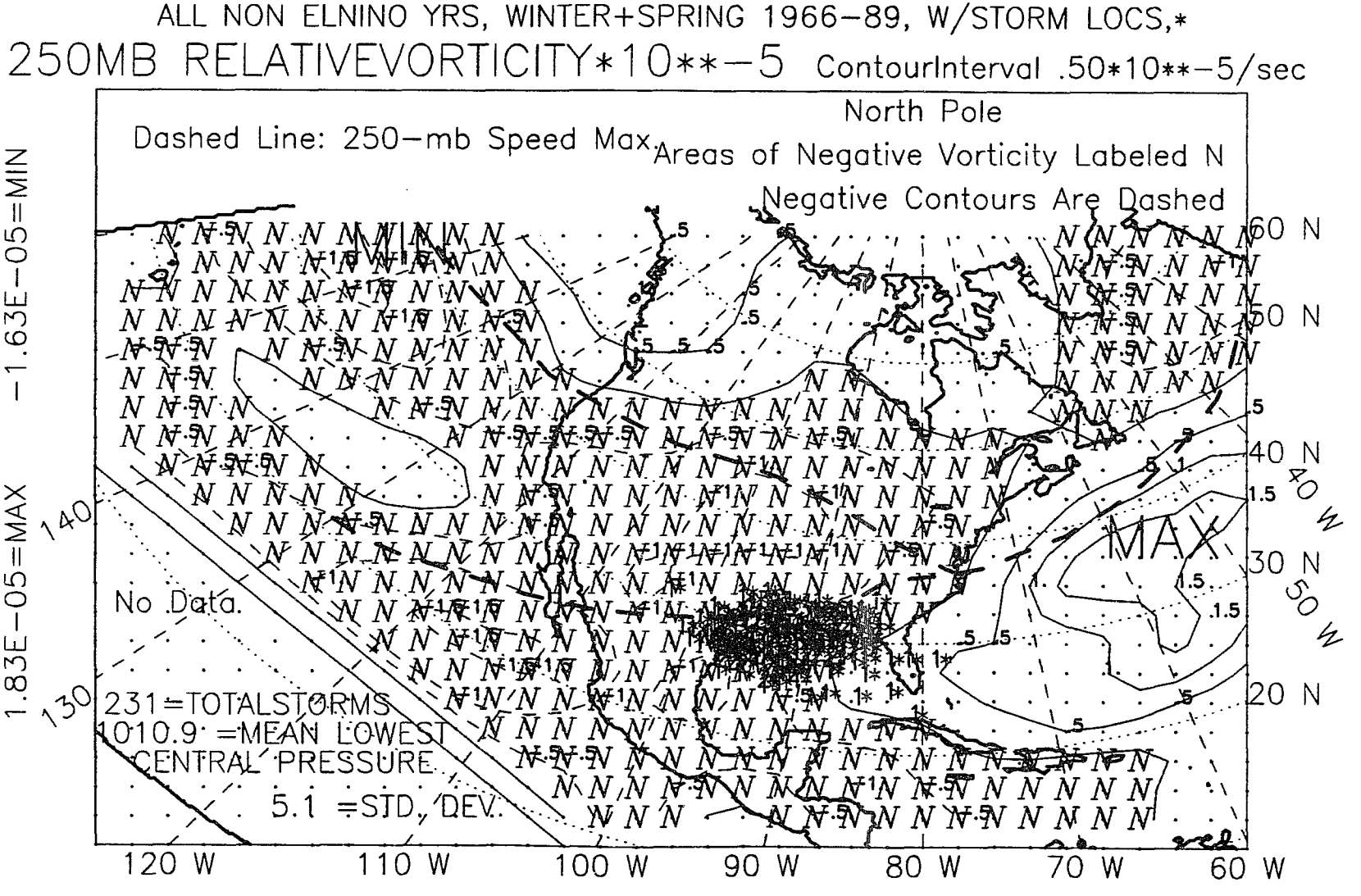

Figure M.8: 250-mb relative vorticity, winter-plus-spring, non-El Niño years, 1966-89.

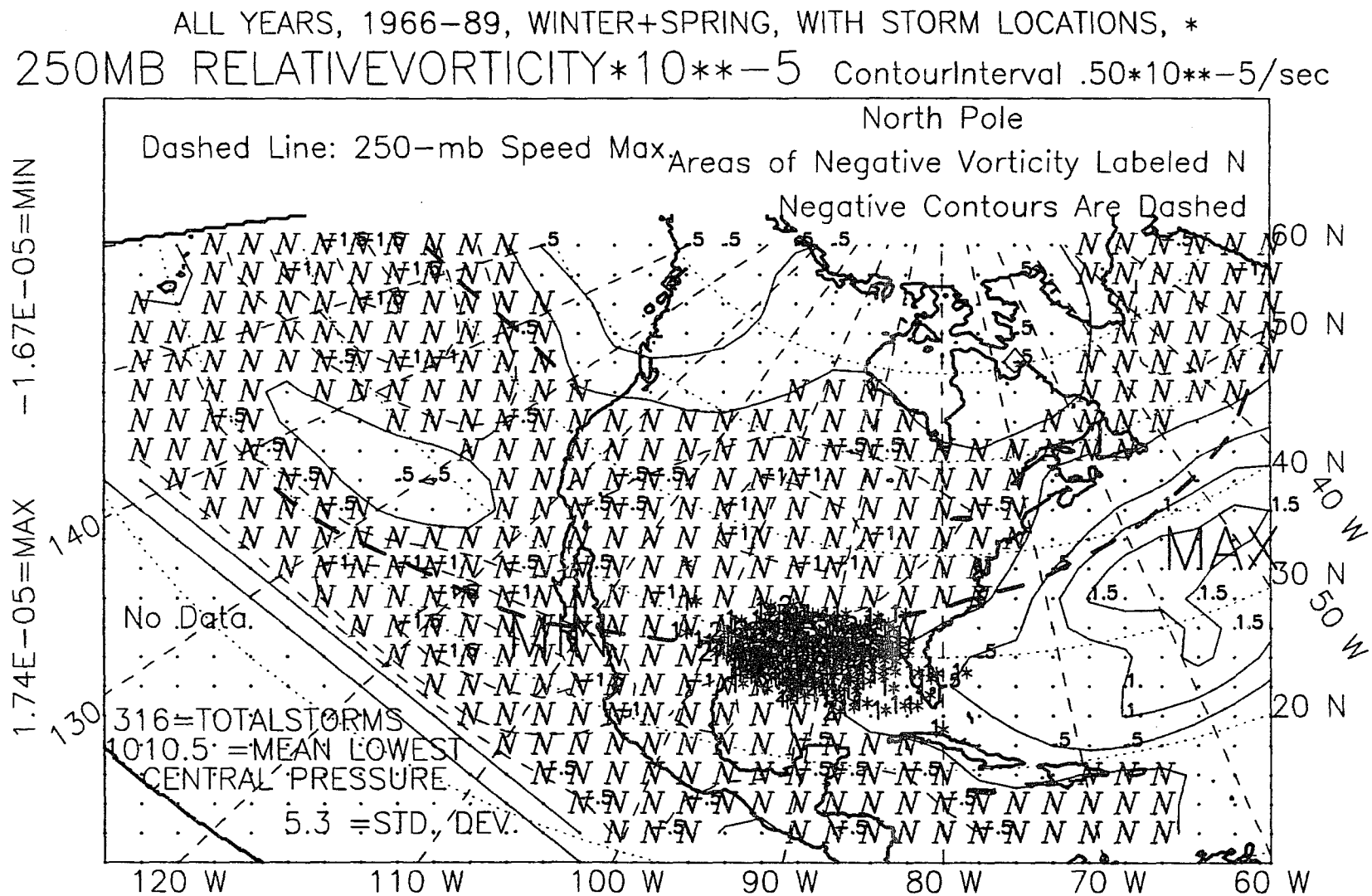

Figure M.9: 250–mb relative vorticity, winter–plus–spring, all years, 1966–89.

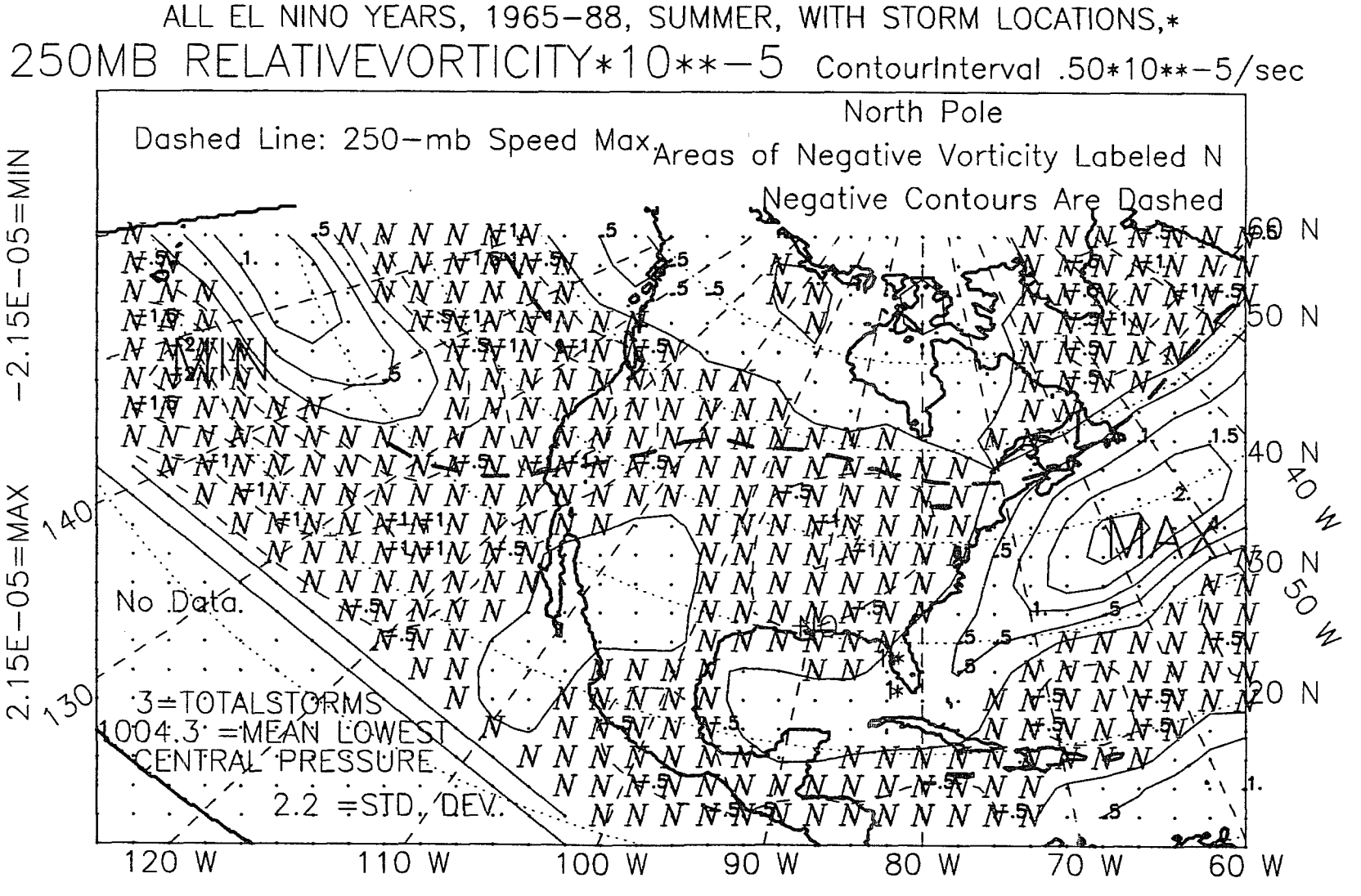

Figure M.10: 250–mb relative vorticity, summer, El Niño years, 1965–88.

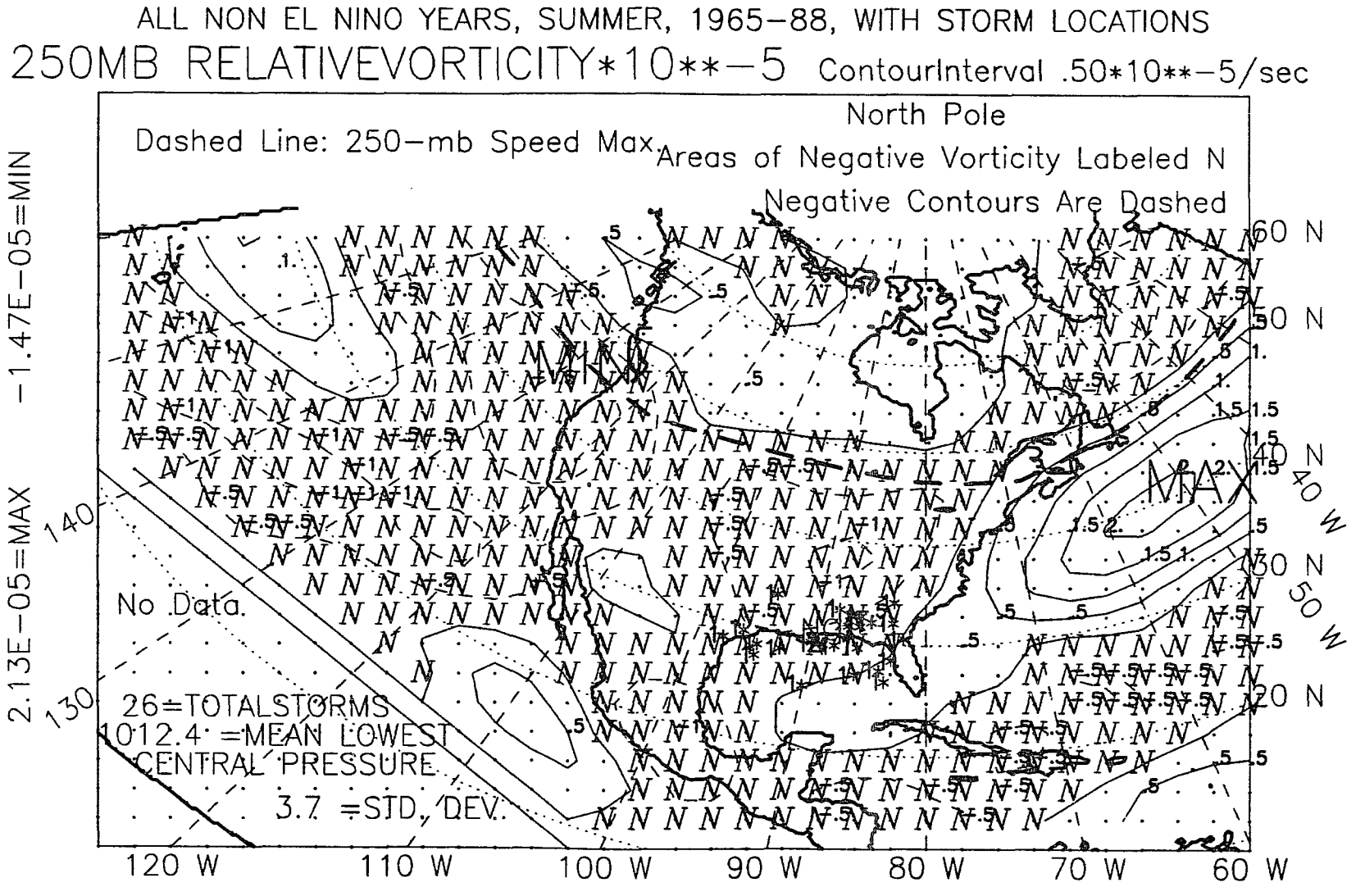

Figure M.11: 250–mb relative vorticity, summer, non–El Niño years, 1965–88.

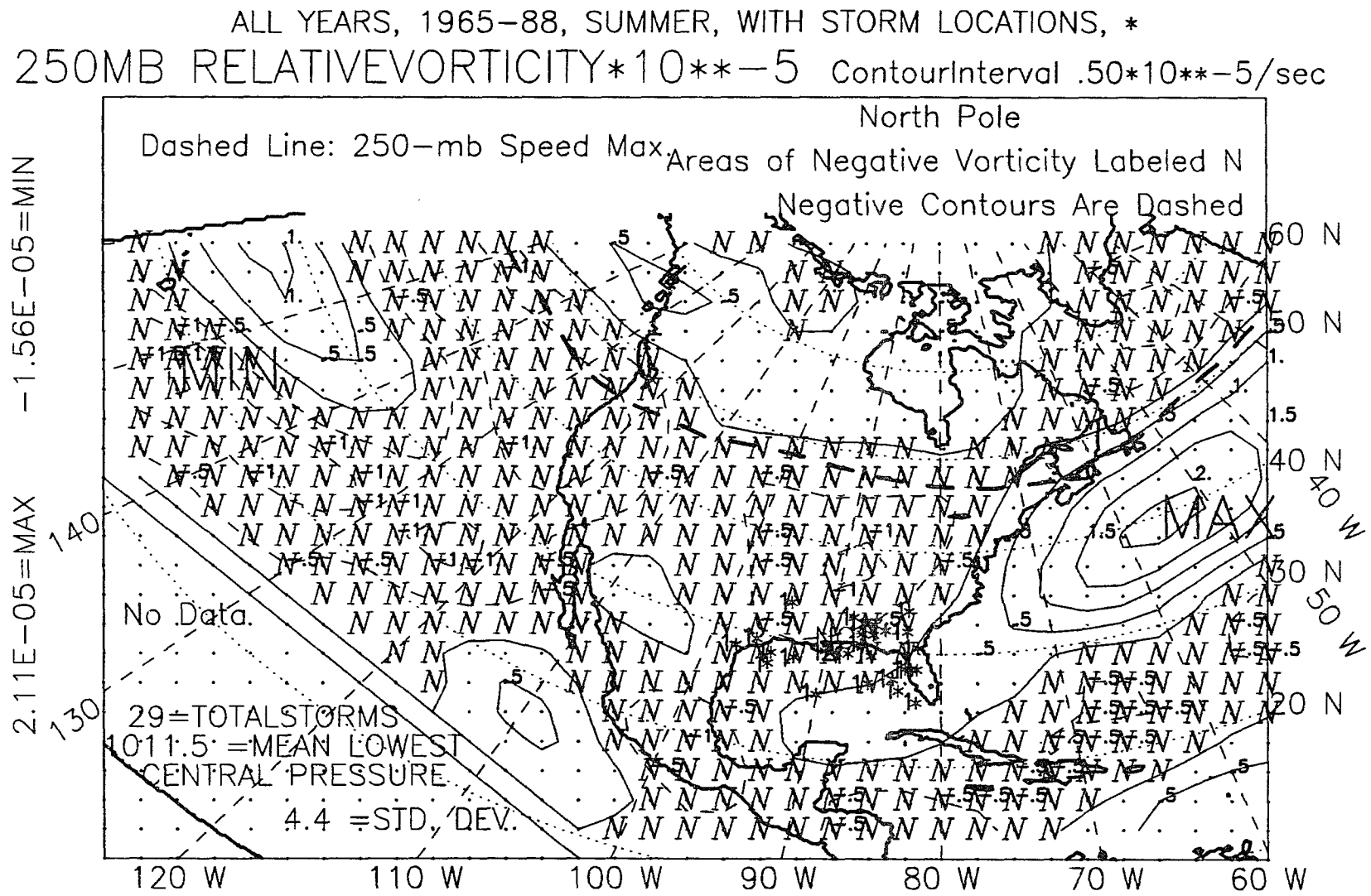

Figure M.12: 250–mb relative vorticity, summer, all years, 1965–88.

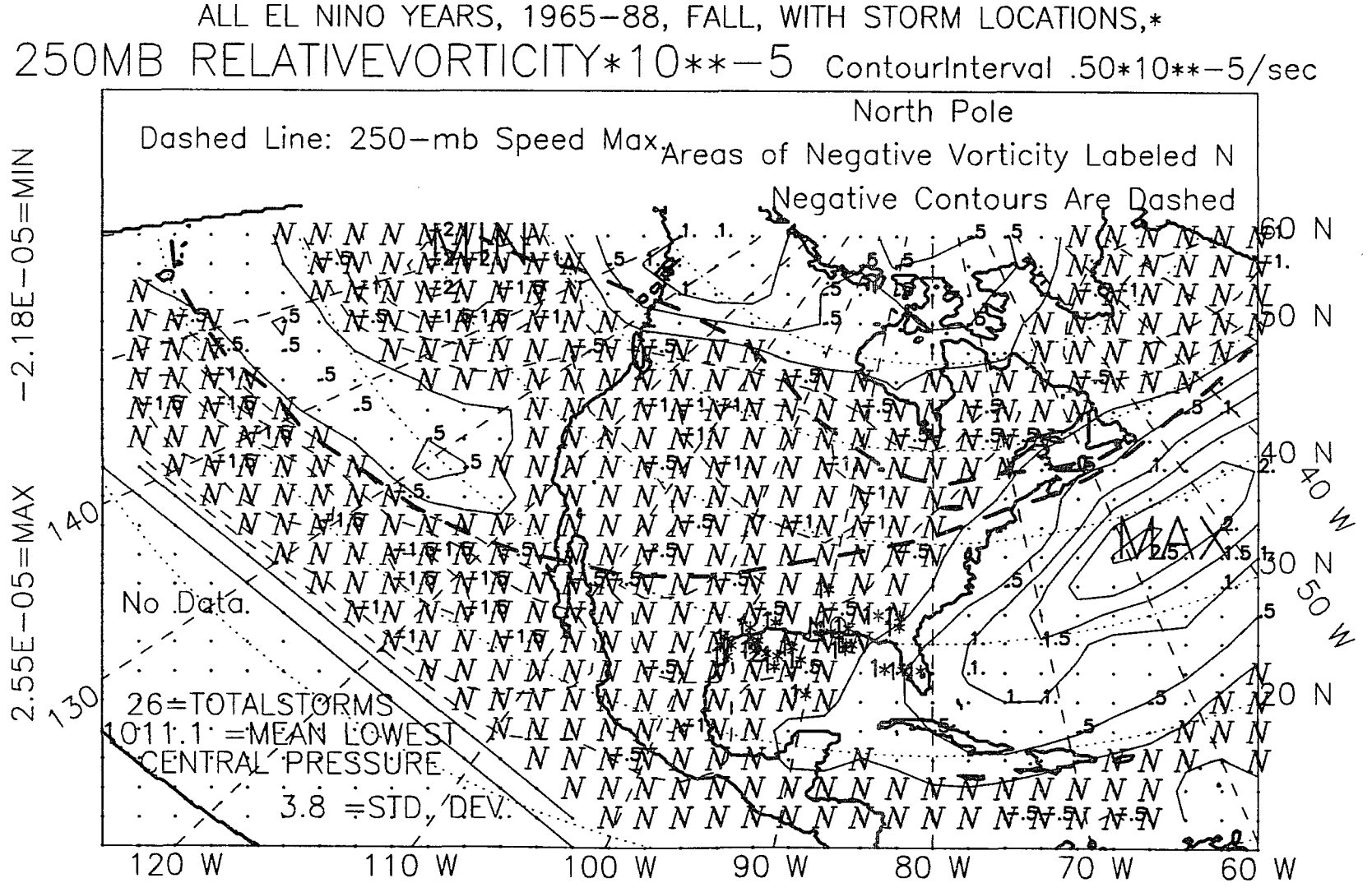

Figure M.13: 250–mb relative vorticity, fall, El Niño years, 1965–88.

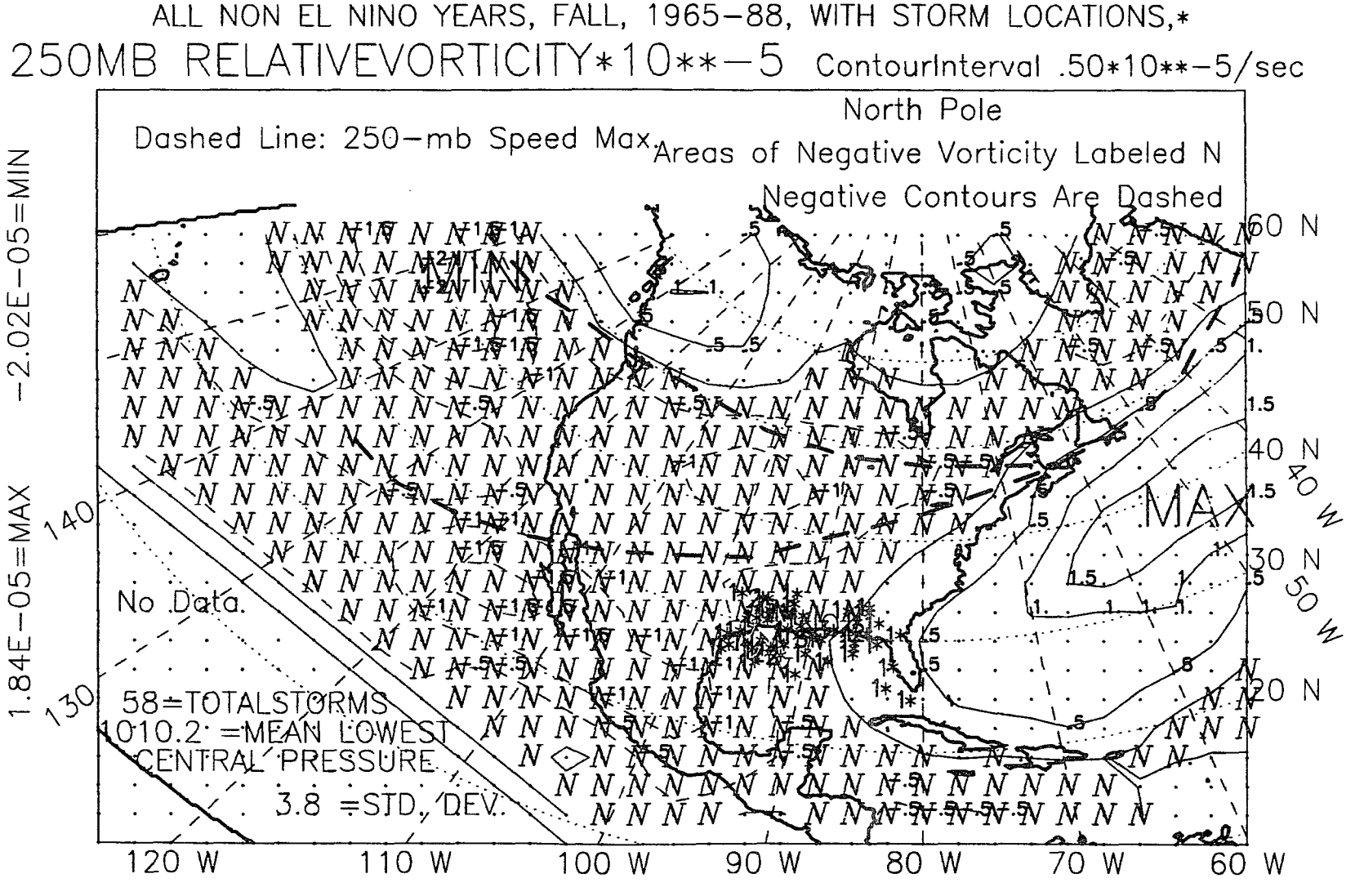

Figure M.14: 250-mb relative vorticity, fall, non-El Niño years, 1965-88.

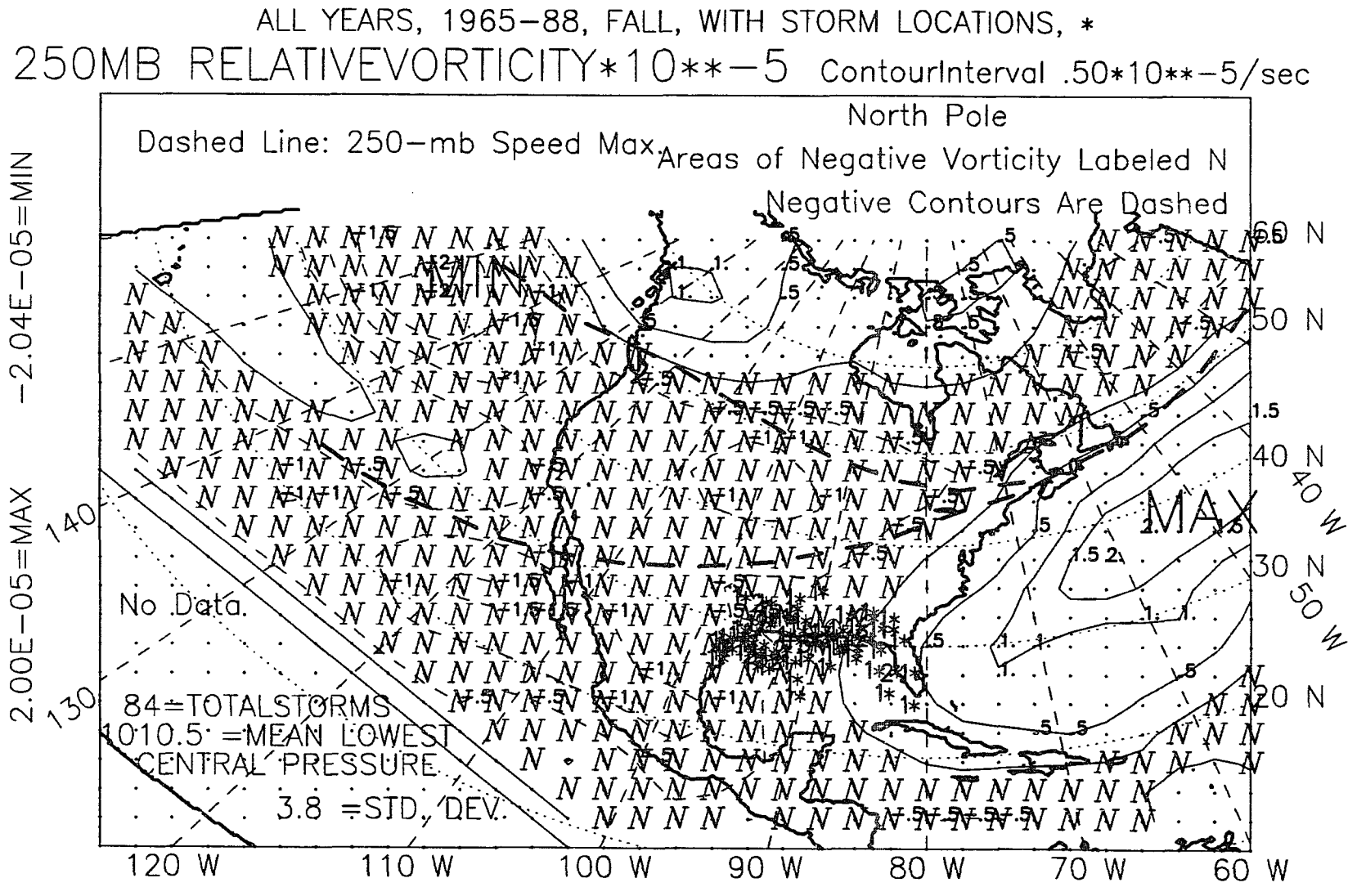

Figure M.15: 250–mb relative vorticity, fall, all years, 1965–88.

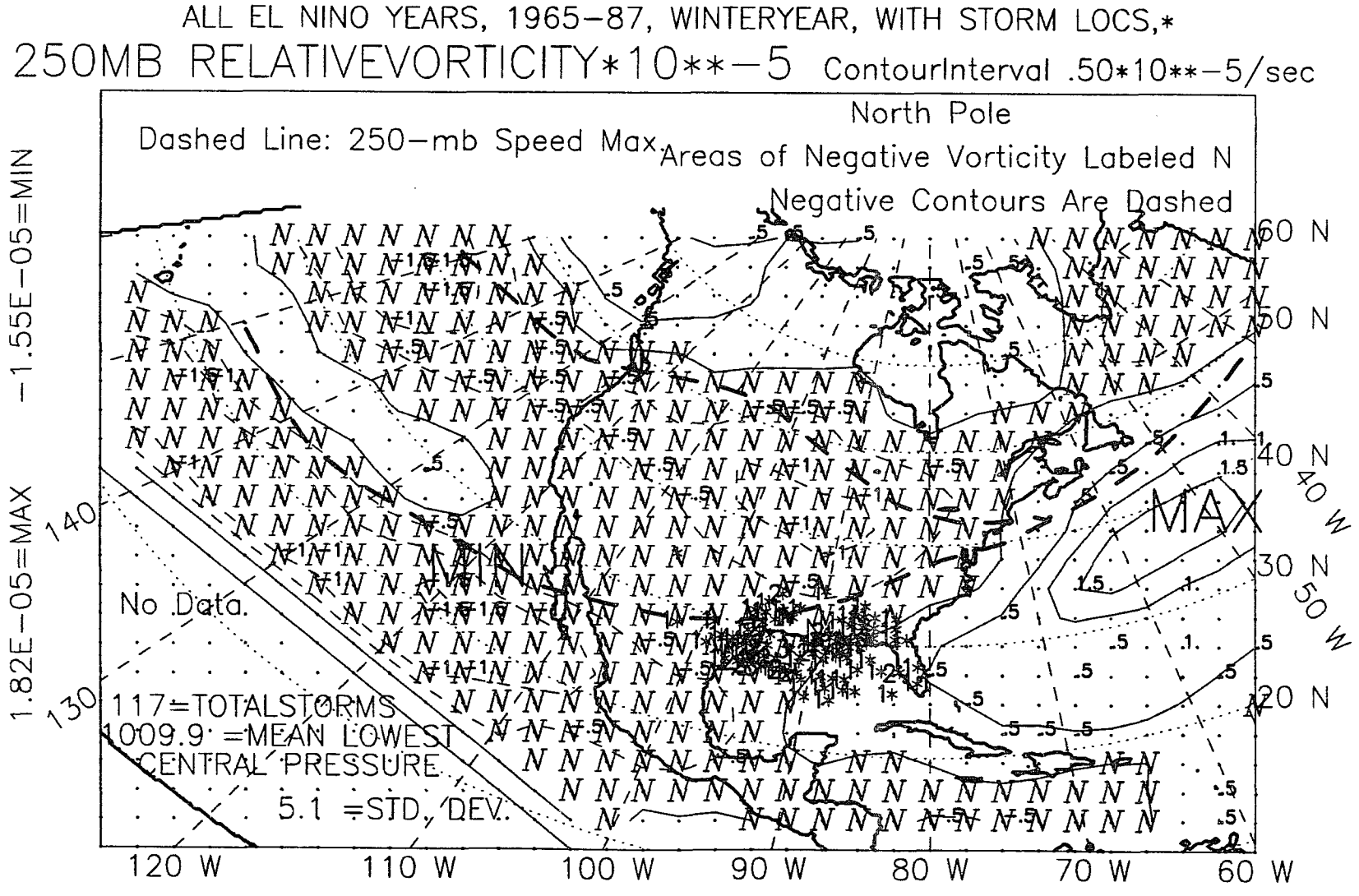

Figure M.16: 250-mb relative vorticity, winter year, El Niño years, 1965-87.

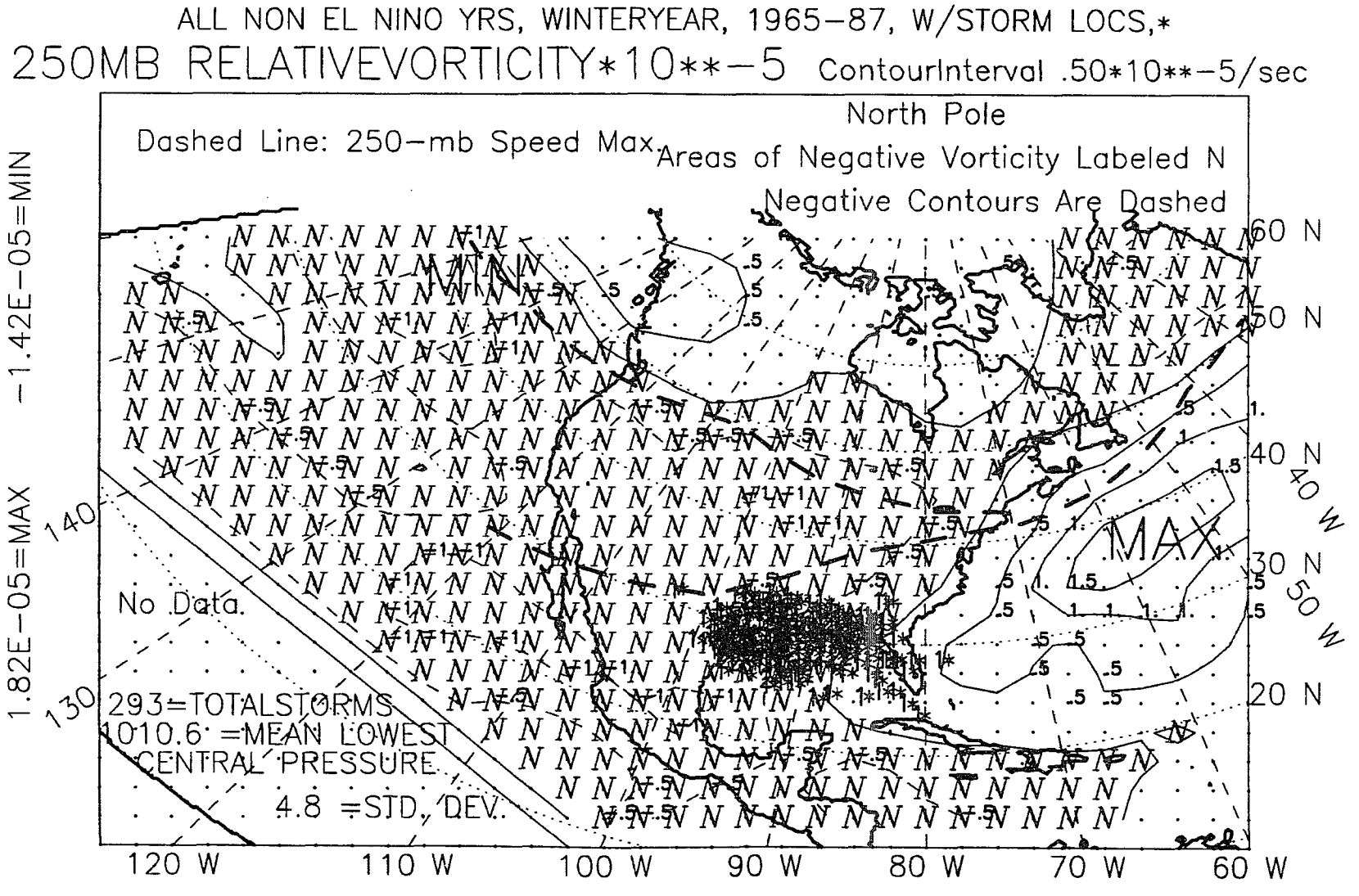

Figure M.17: 250–mb relative vorticity, winter year, non–El Niño years, 1965–87.

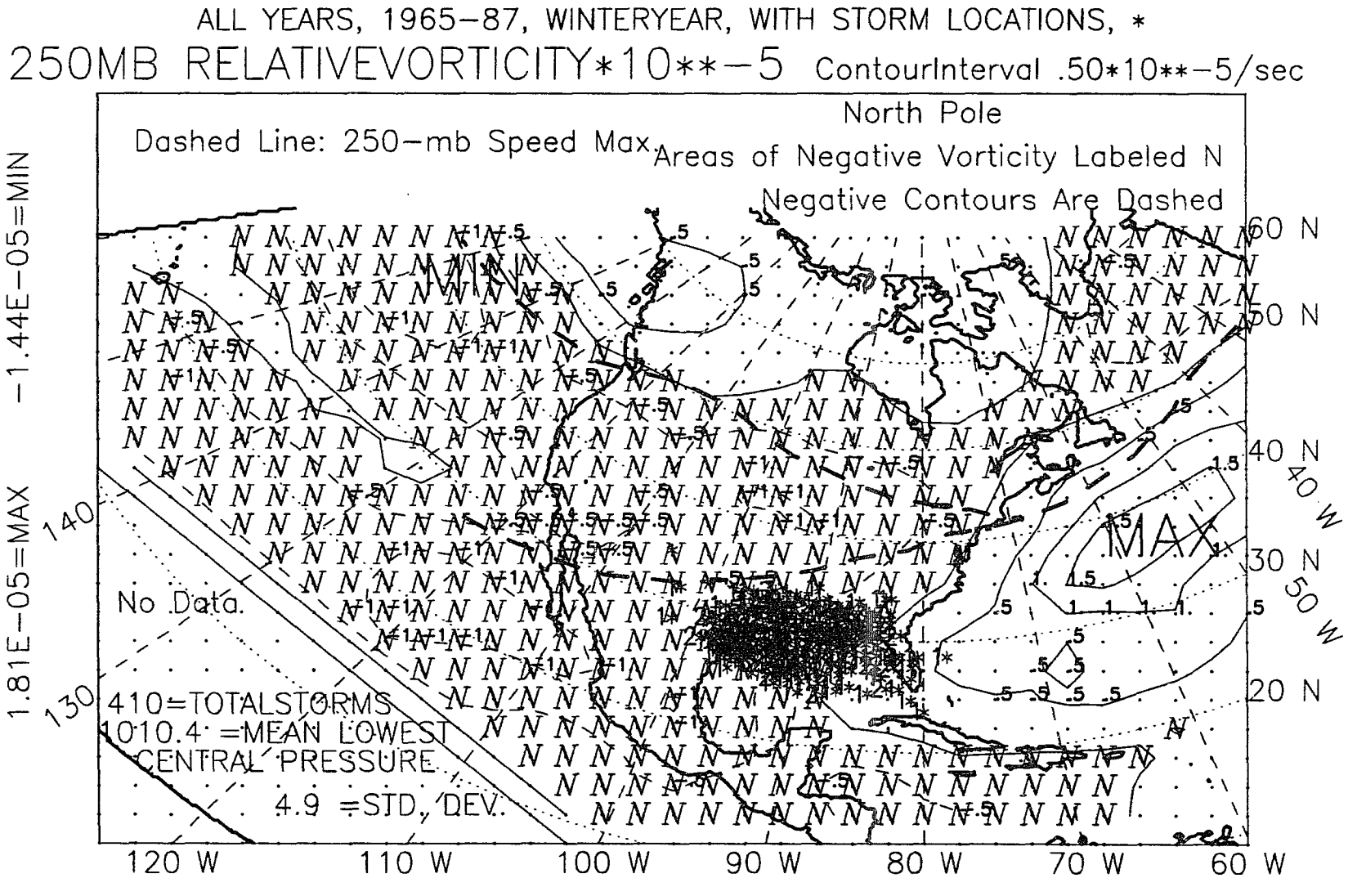

Figure M.18: 250–mb relative vorticity, winter year, all years, 1965–87.

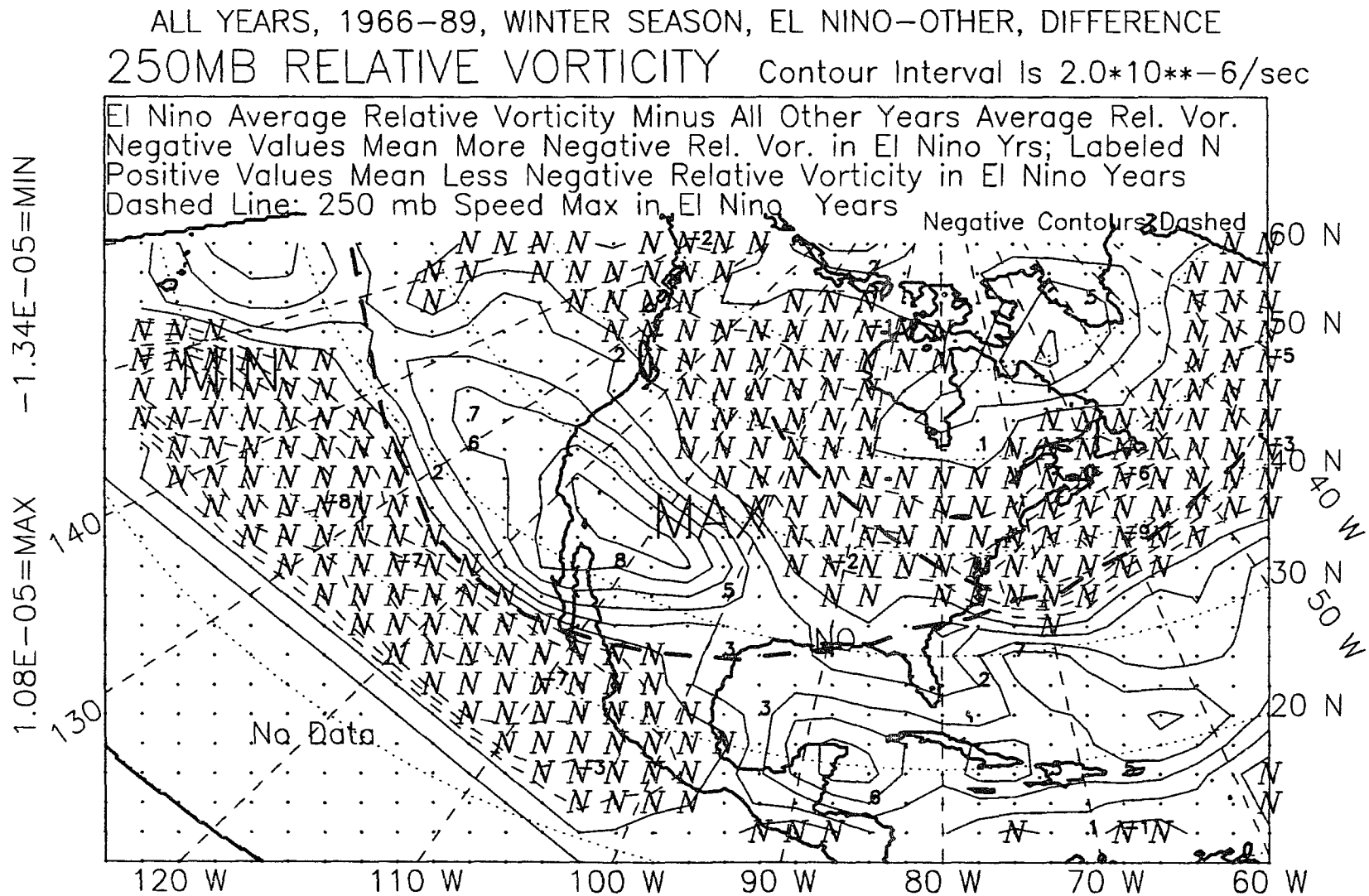

Figure M.19: 250–mb relative vorticity, winter, 1966–89, difference.

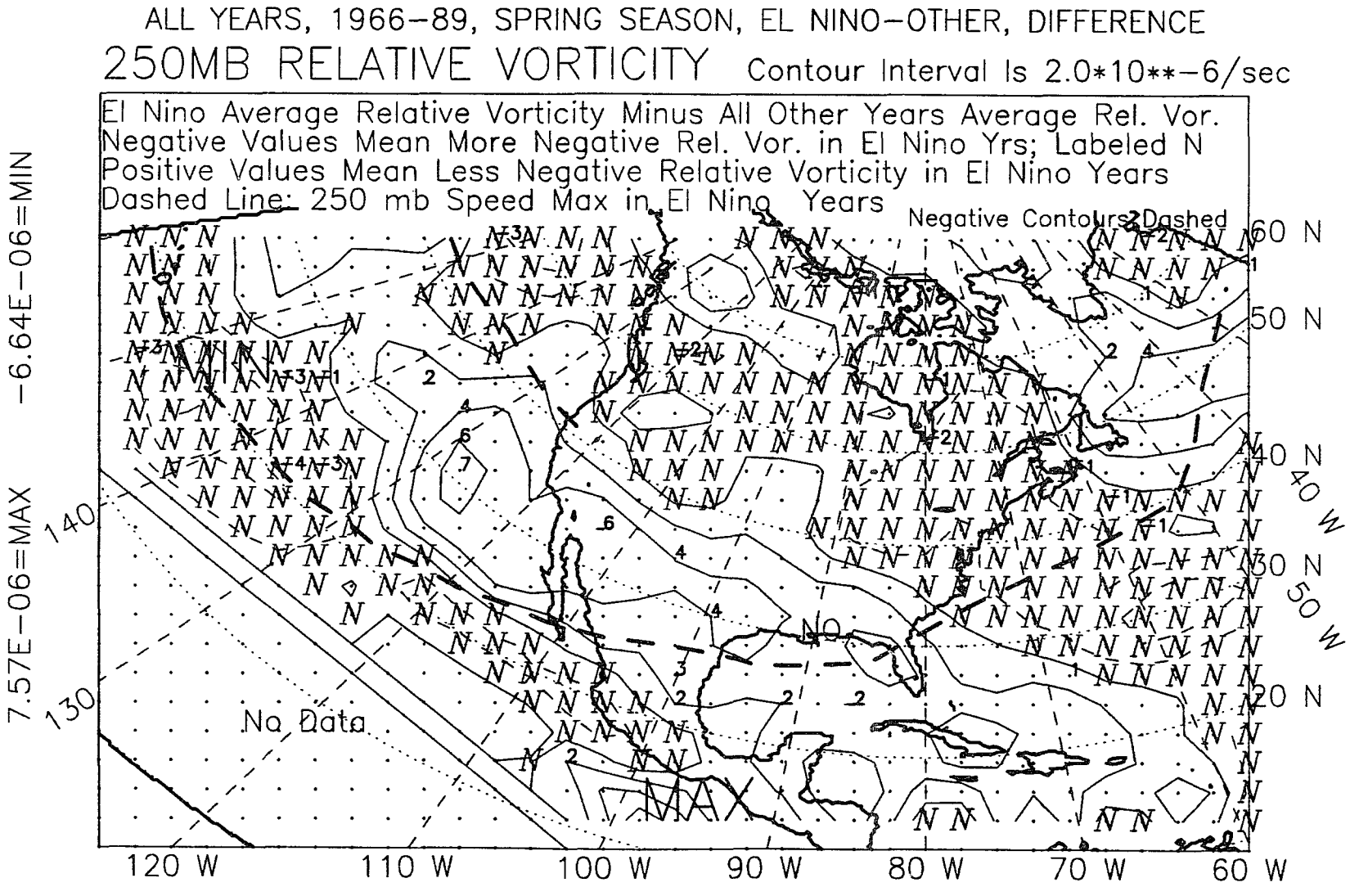

Figure M.20: 250–mb relative vorticity, spring, 1966–89, difference.

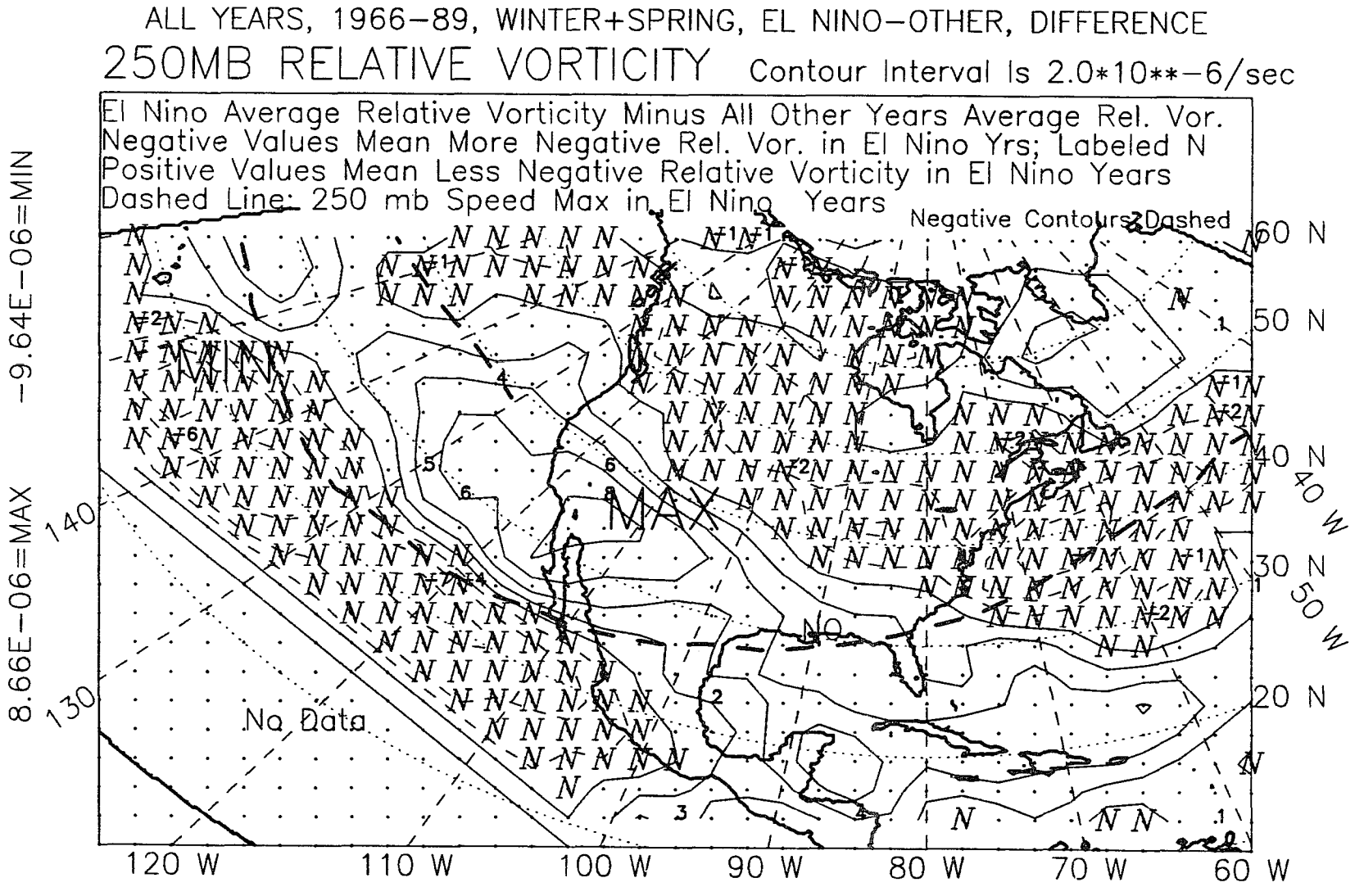

Figure M.21: 250–mb relative vorticity, winter–plus–spring, 1966–89, difference.

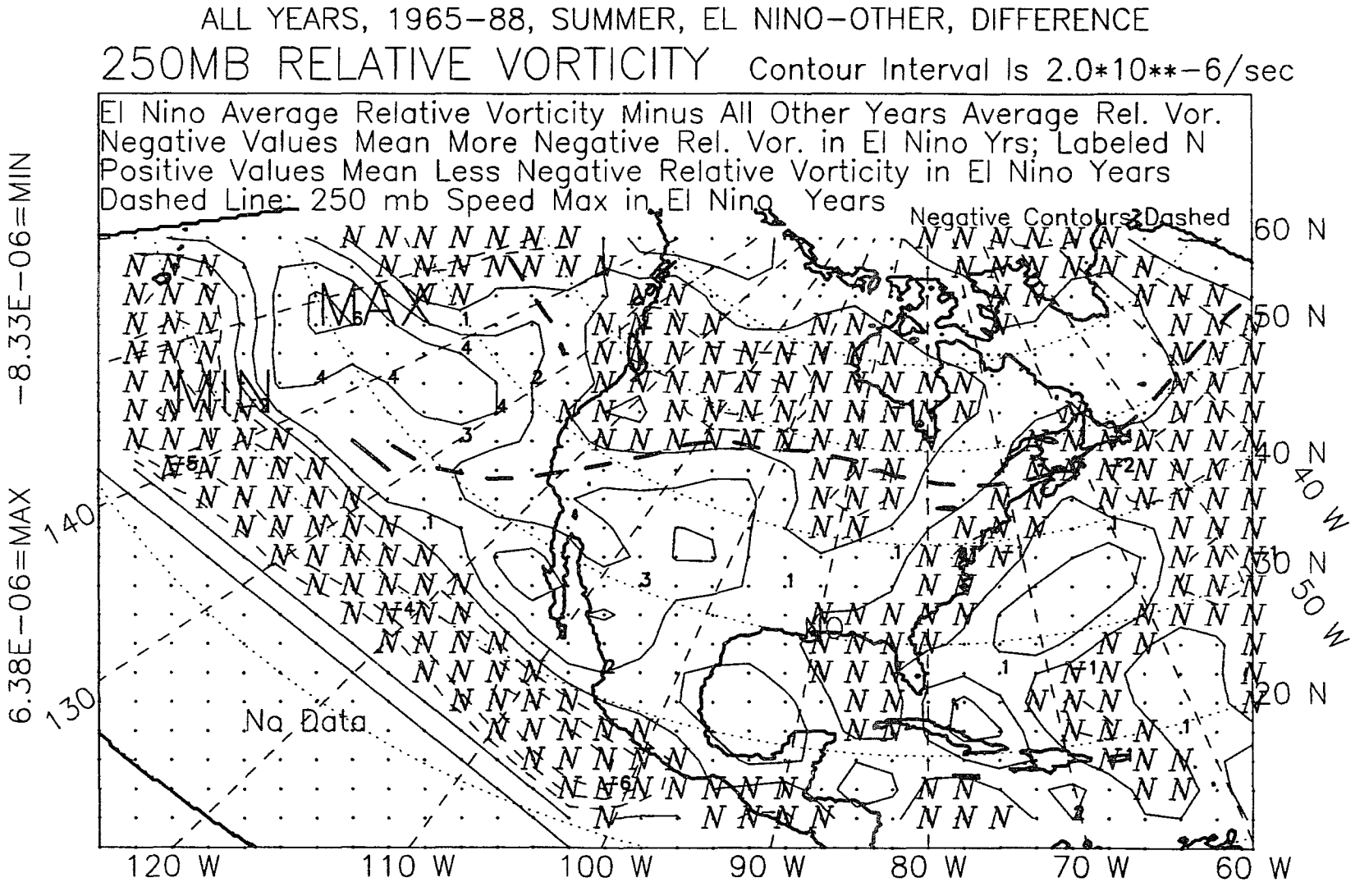

Figure M.22: 250–mb relative vorticity, summer, 1965–88, difference.

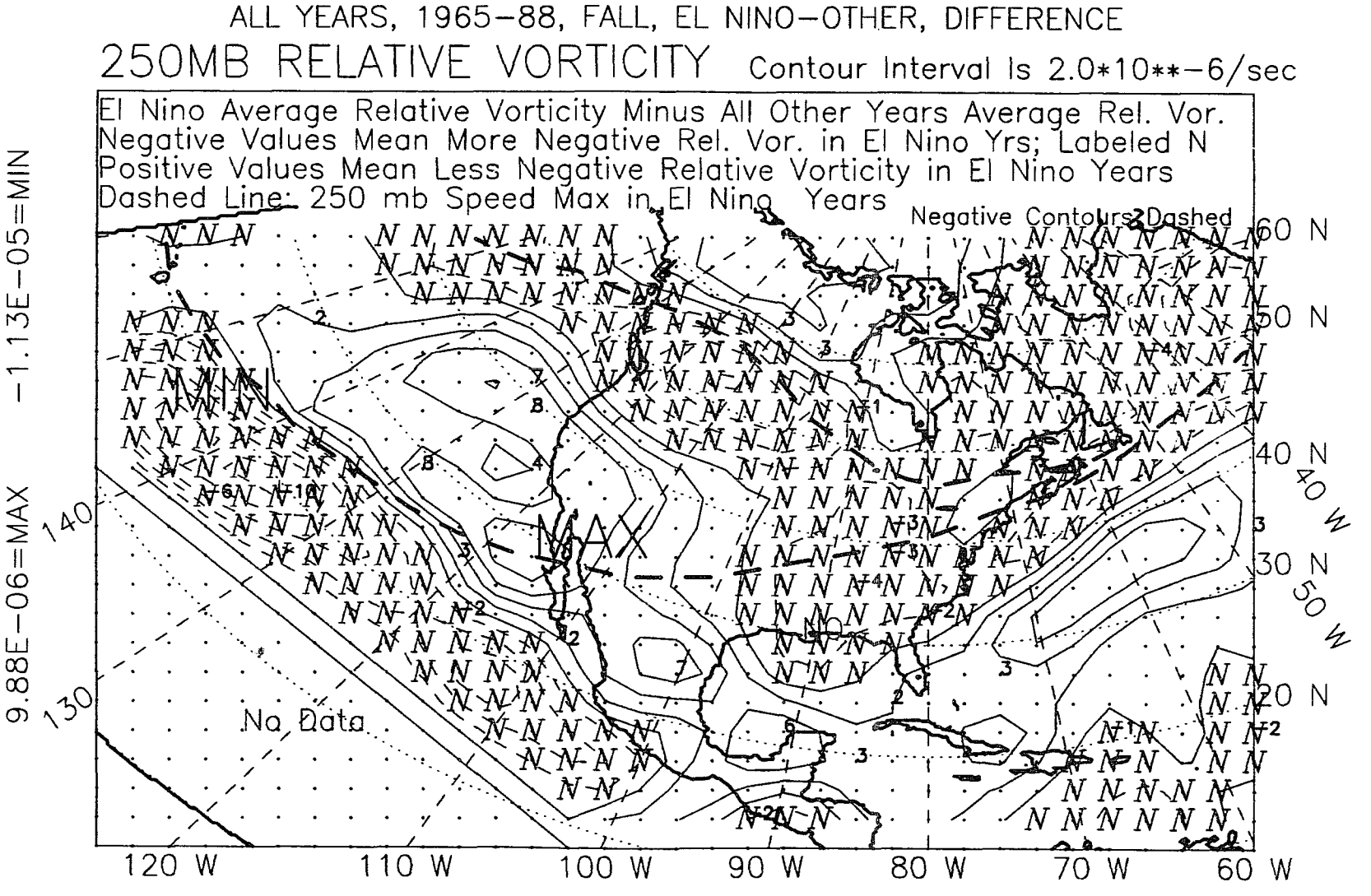

Figure M.23: 250–mb relative vorticity, fall, 1965–88, difference.

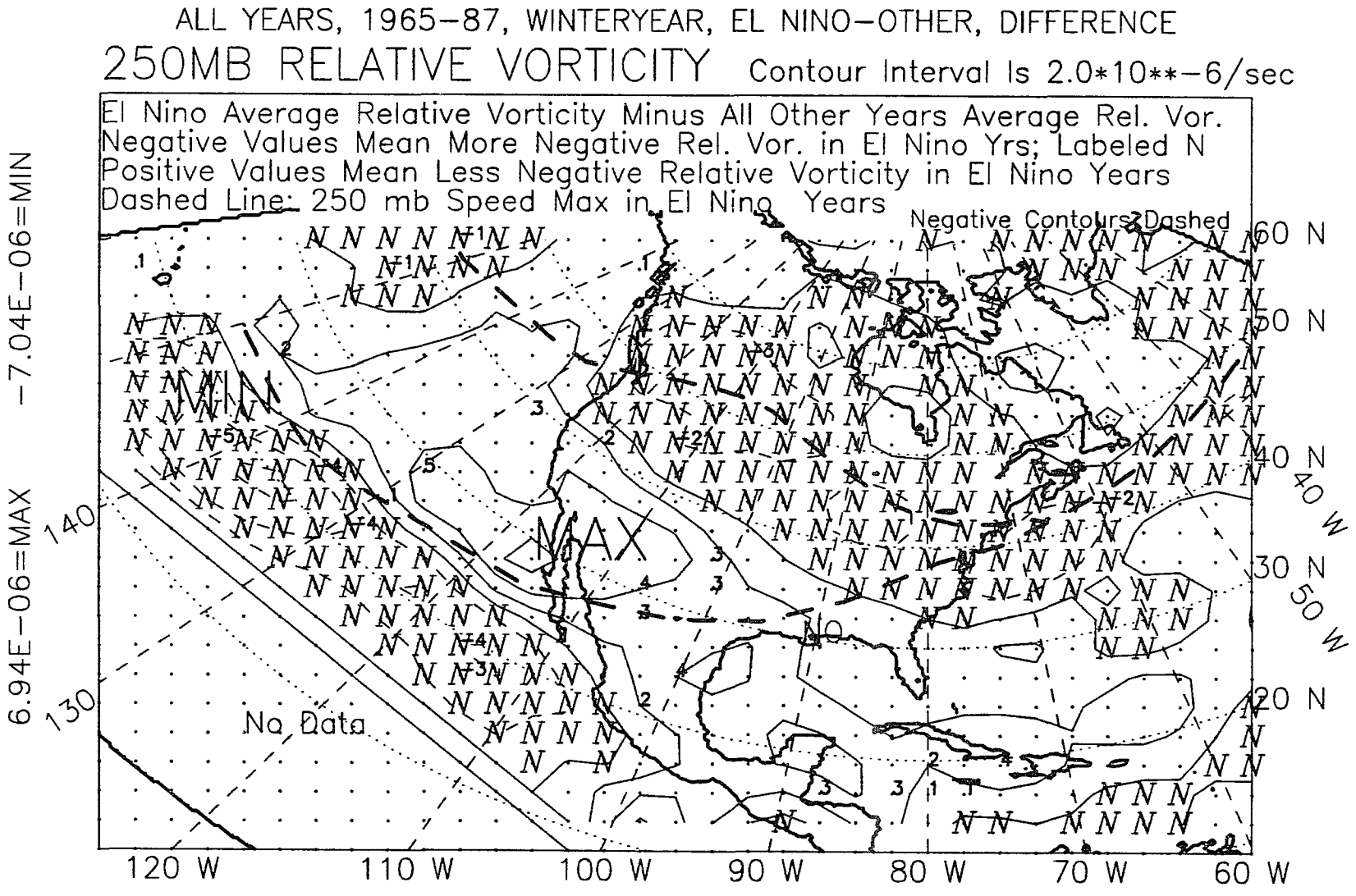

Figure M.24: 250–mb relative vorticity, winter year, 1965–87, difference.

APPENDIX N
200-MB HEIGHT FIELD

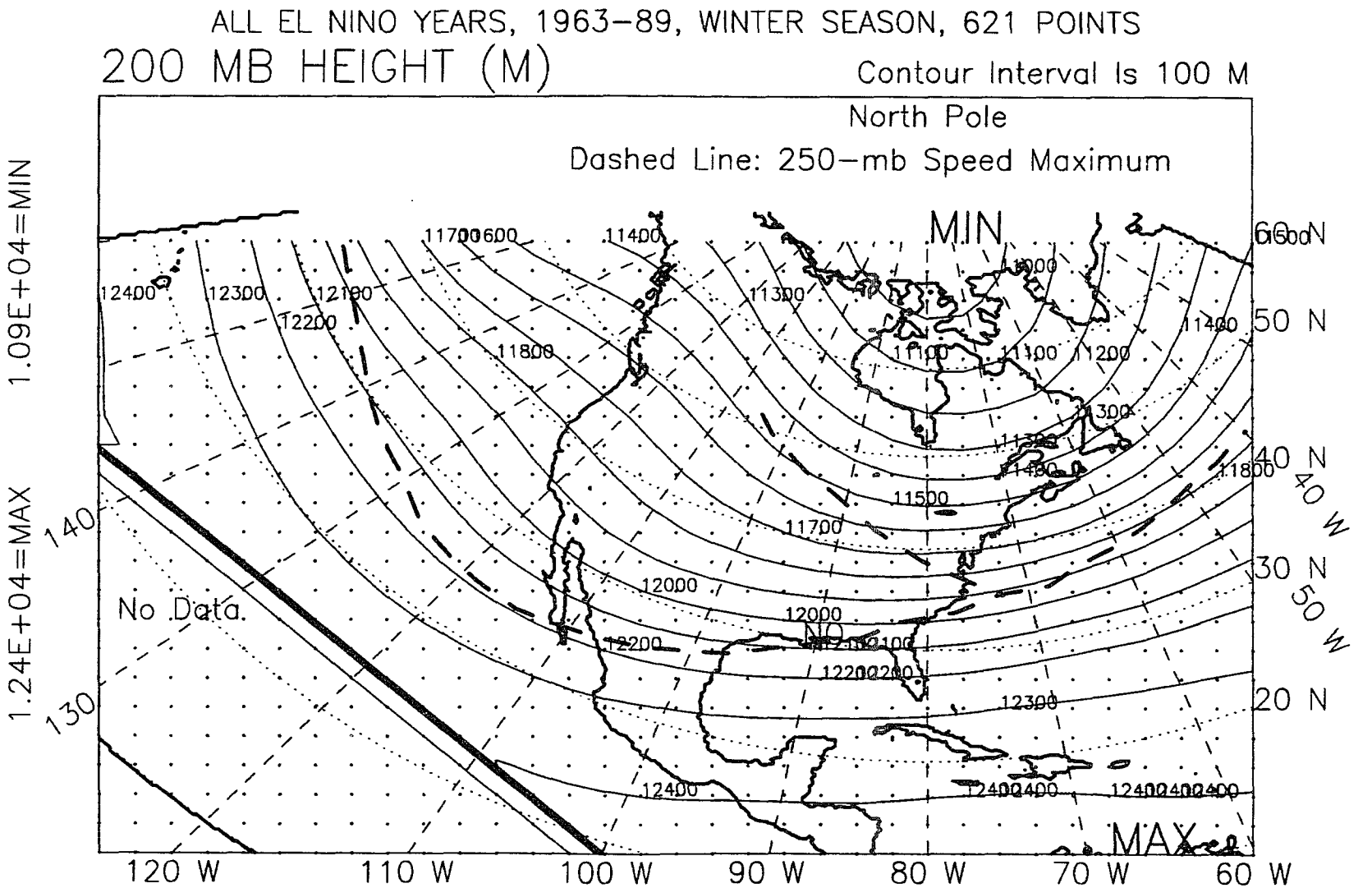

Figure N.1: 200–mb height, winter, El Niño years, 1963–89.

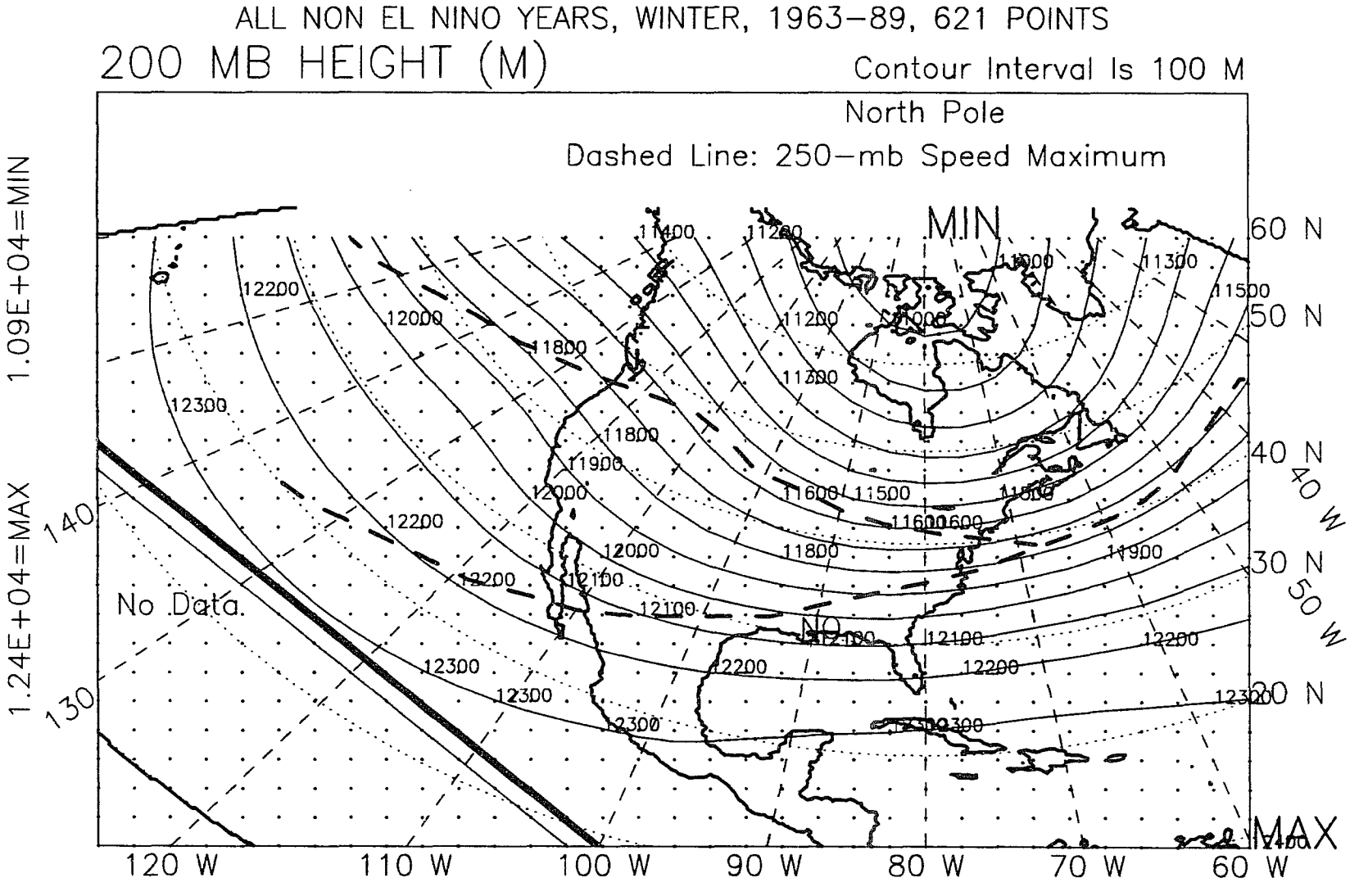

Figure N.2: 200–mb height, winter, non–El Niño years, 1963–89.

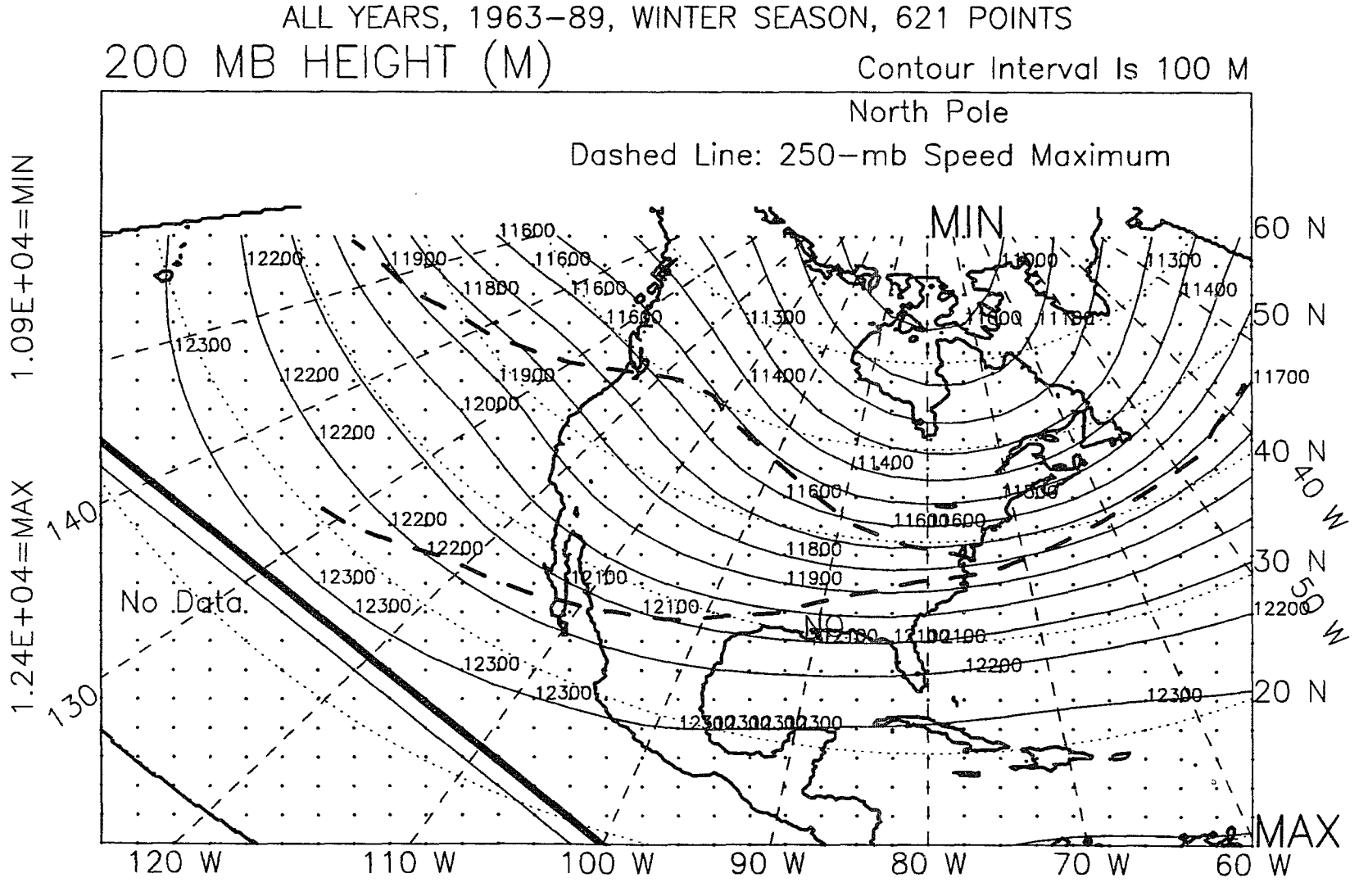

Figure N.3: 200–mb height, winter, all years, 1963–89.

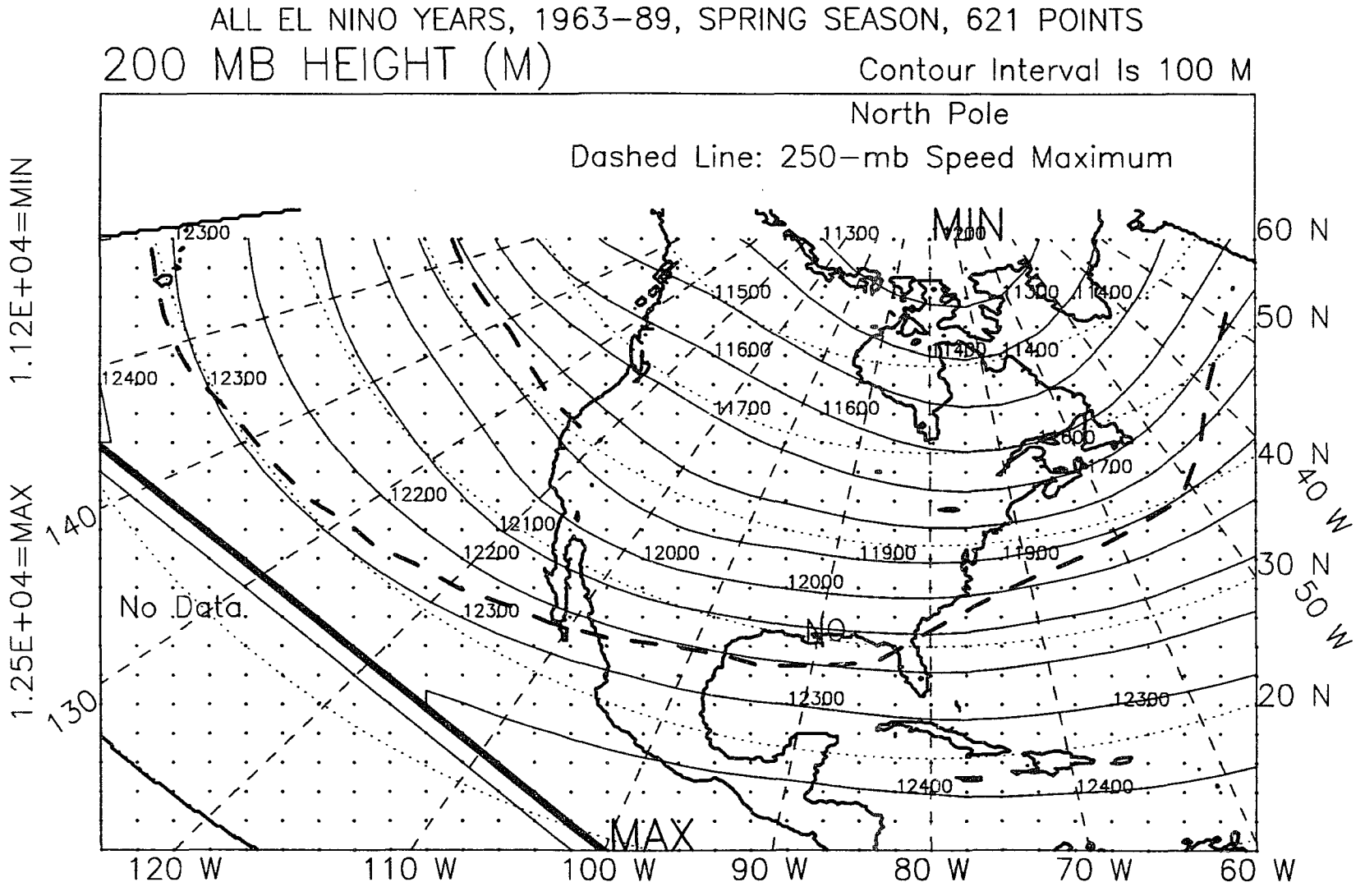

Figure N.4: 200–mb height, spring, El Niño years, 1963–89.

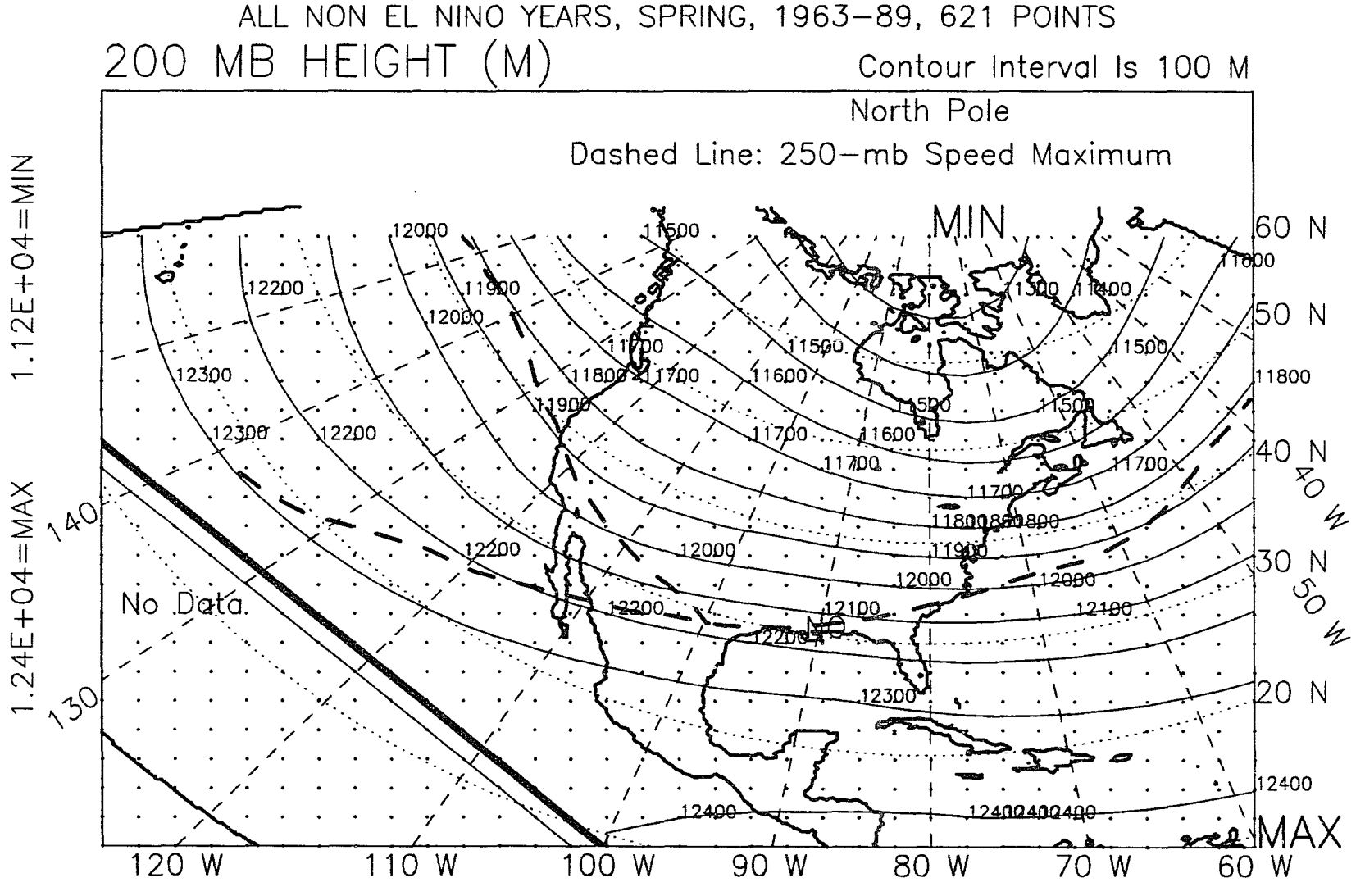

Figure N.5: 200–mb height, spring, non–El Niño years, 1963–89.

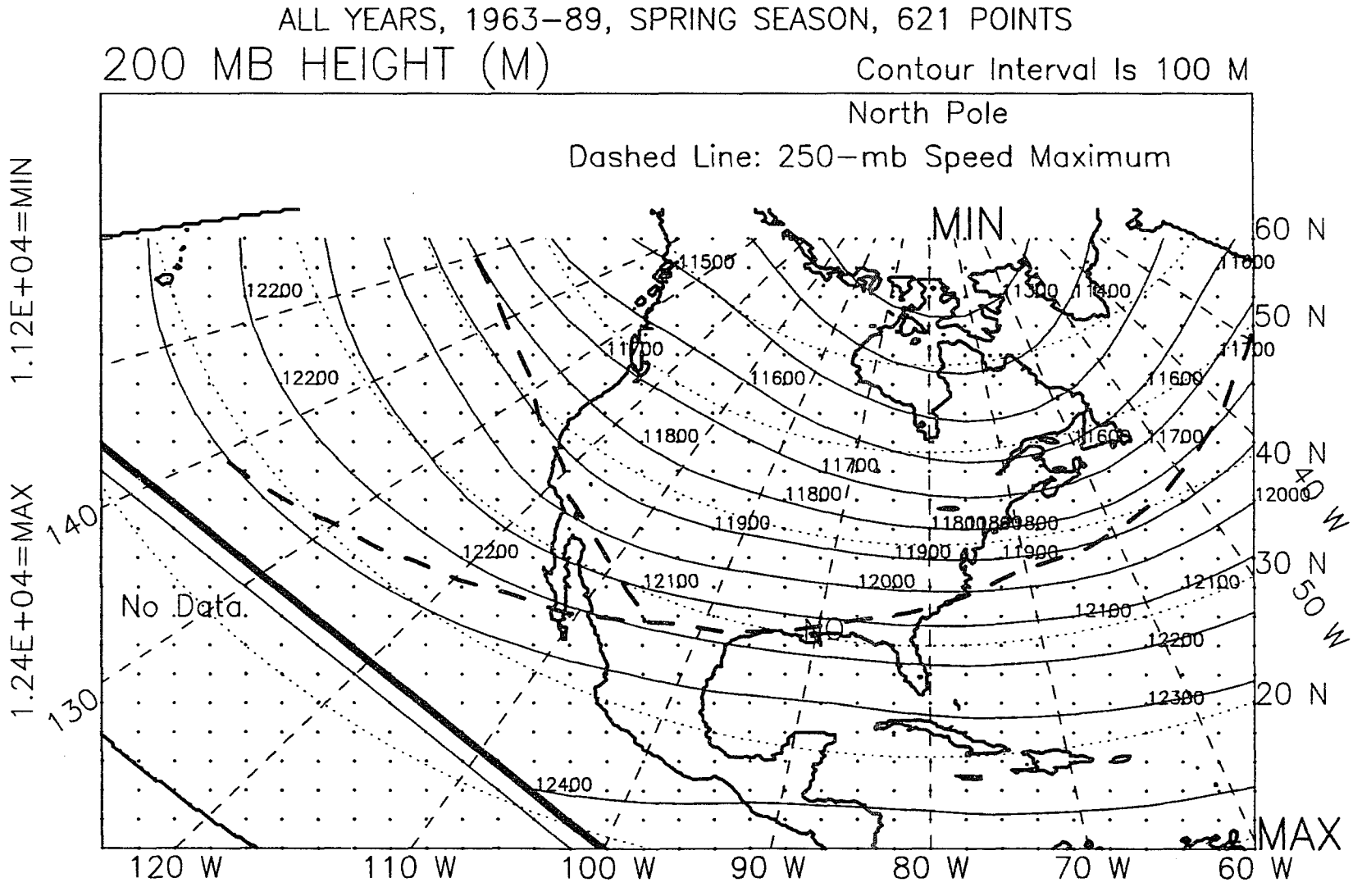

Figure N.6: 200–mb height, spring, all years, 1963–89.

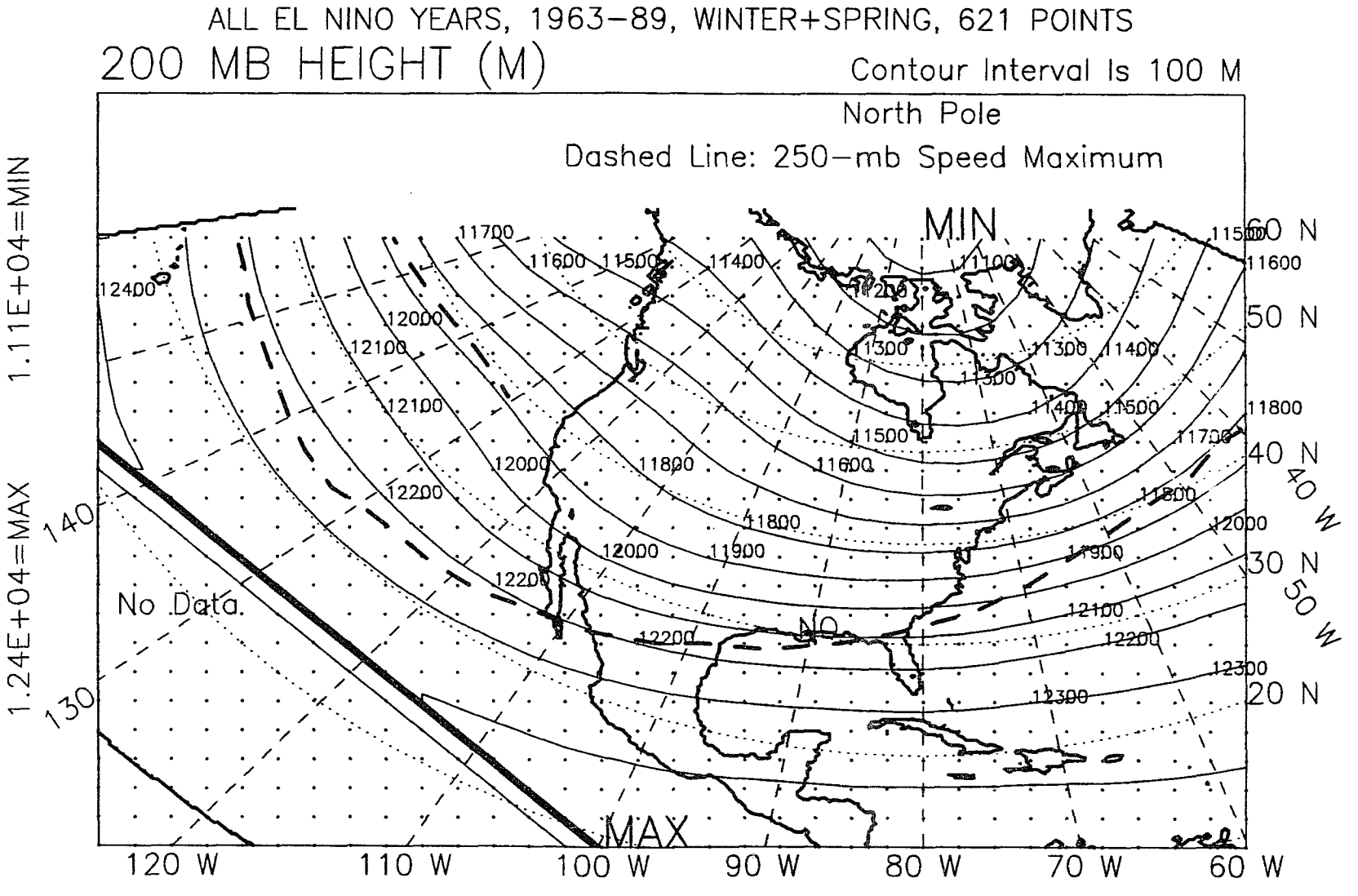

Figure N.7: 200–mb height, winter–plus–spring, El Niño years, 1963–89.

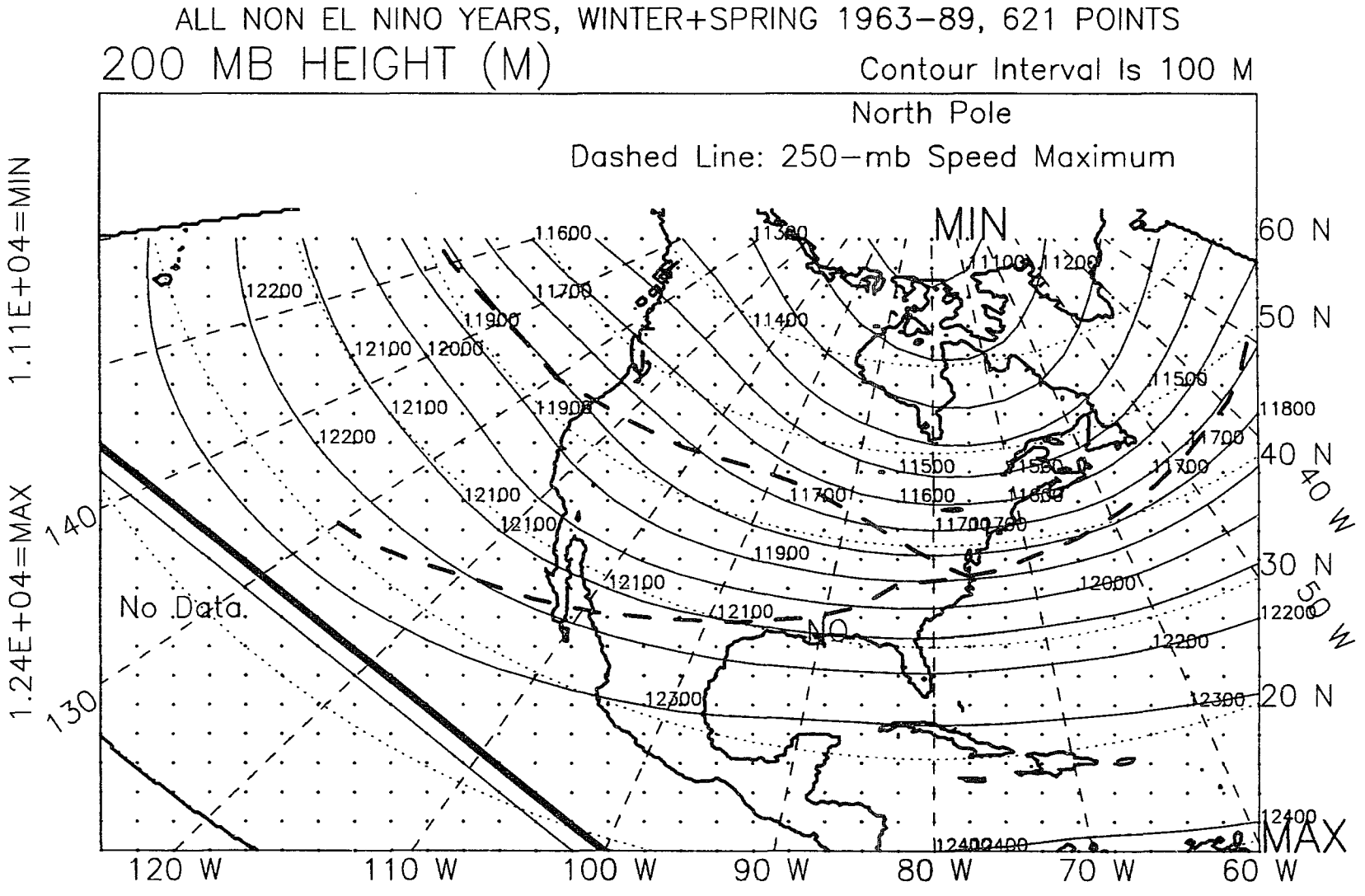

Figure N.8: 200-mb height, winter-plus-spring, non-El Niño years, 1963-89.

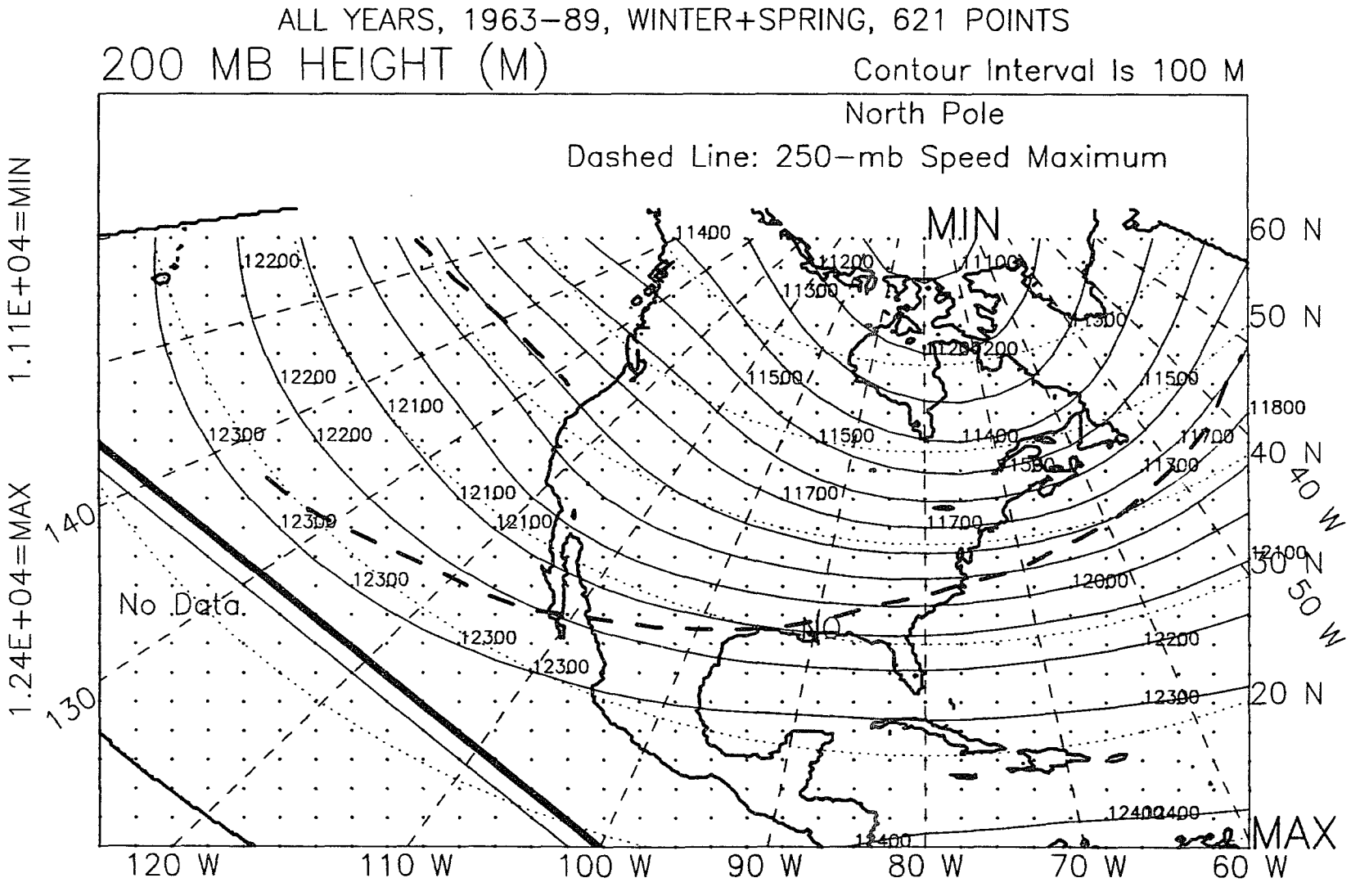

Figure N.9: 200–mb height, winter–plus–spring, all years, 1963–89.

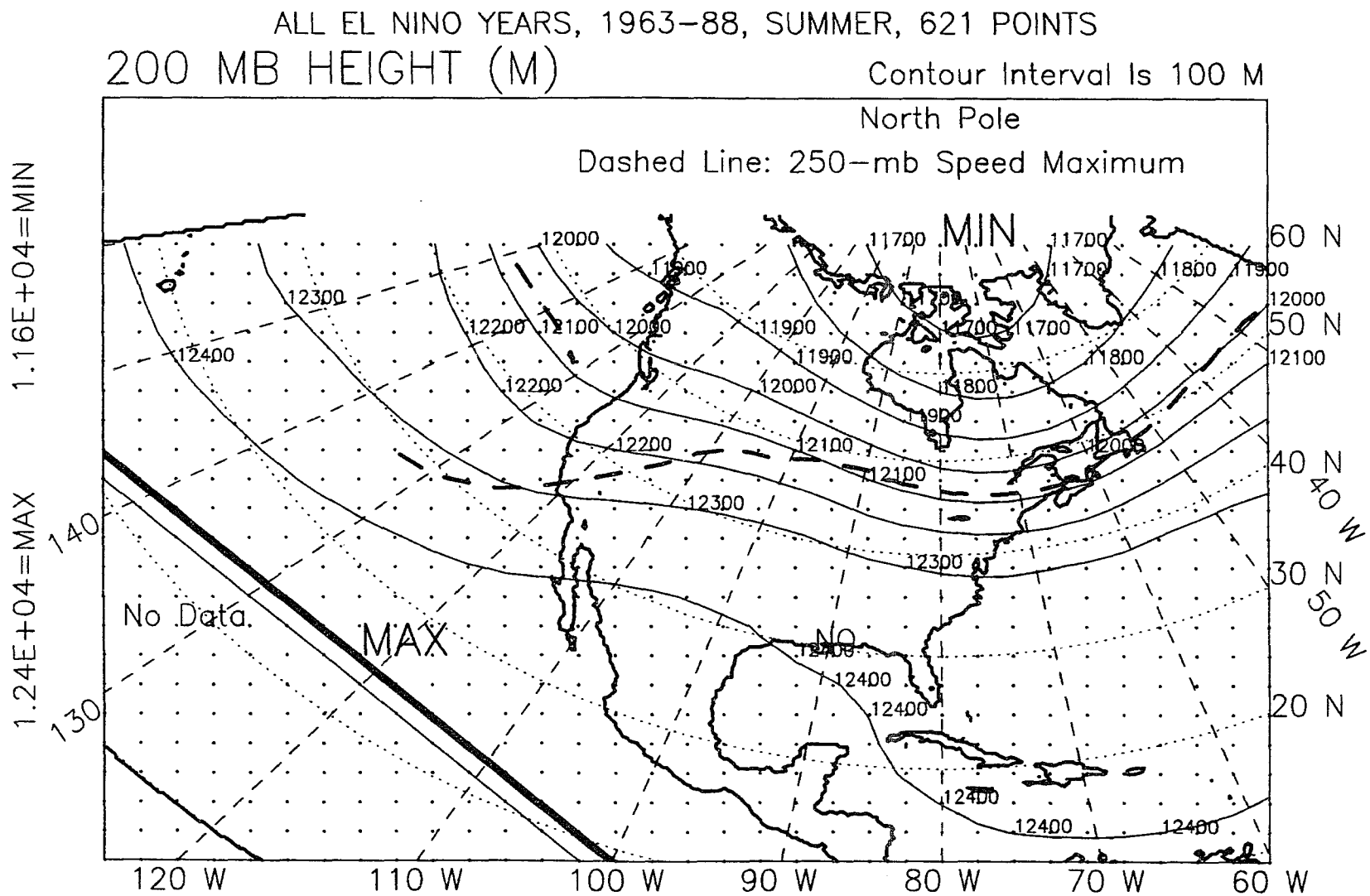

Figure N.10: 200–mb height, summer, El Niño years, 1963–88.

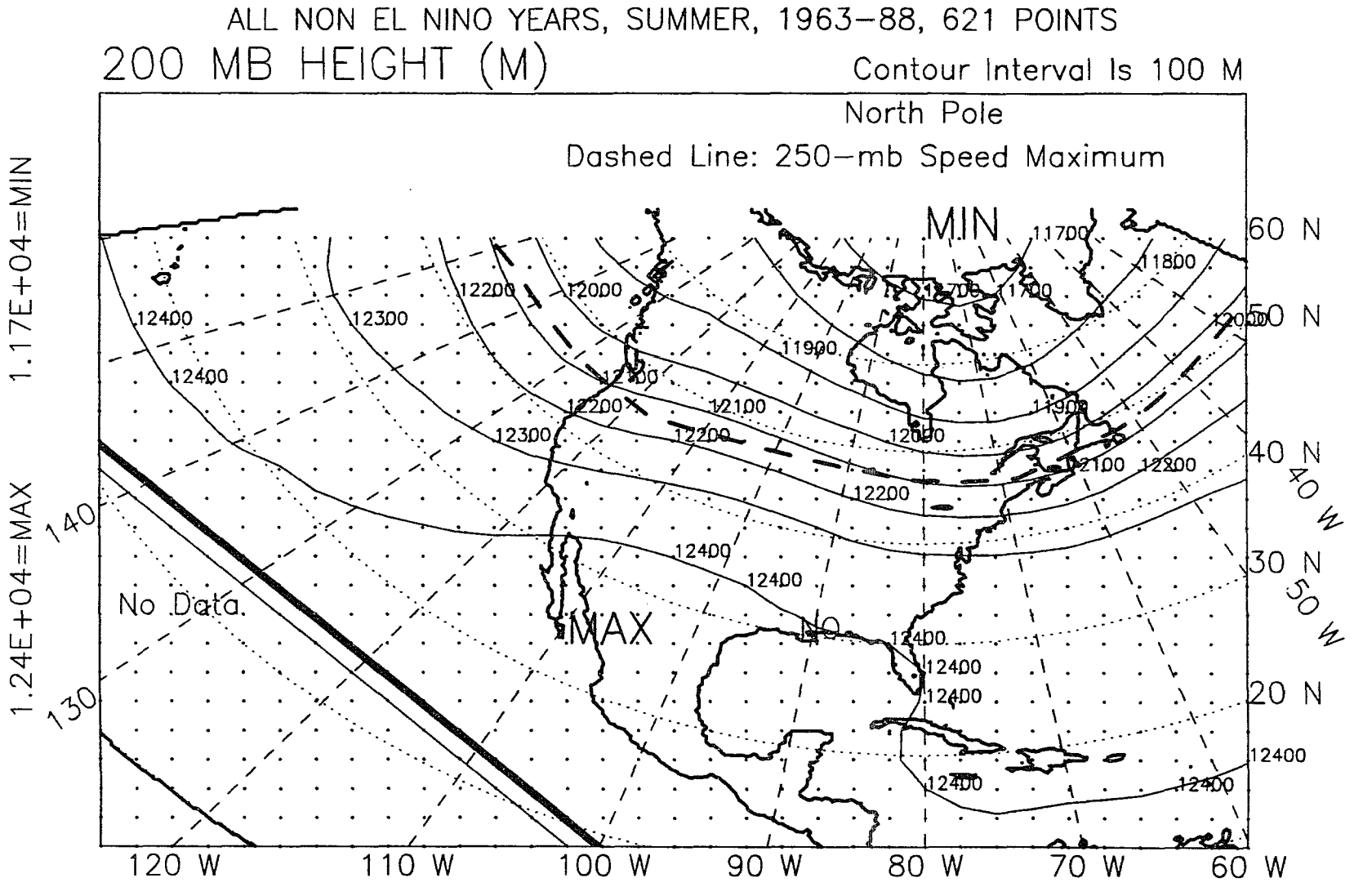

Figure N.11: 200–mb height, summer, non–El Niño years, 1963–88.

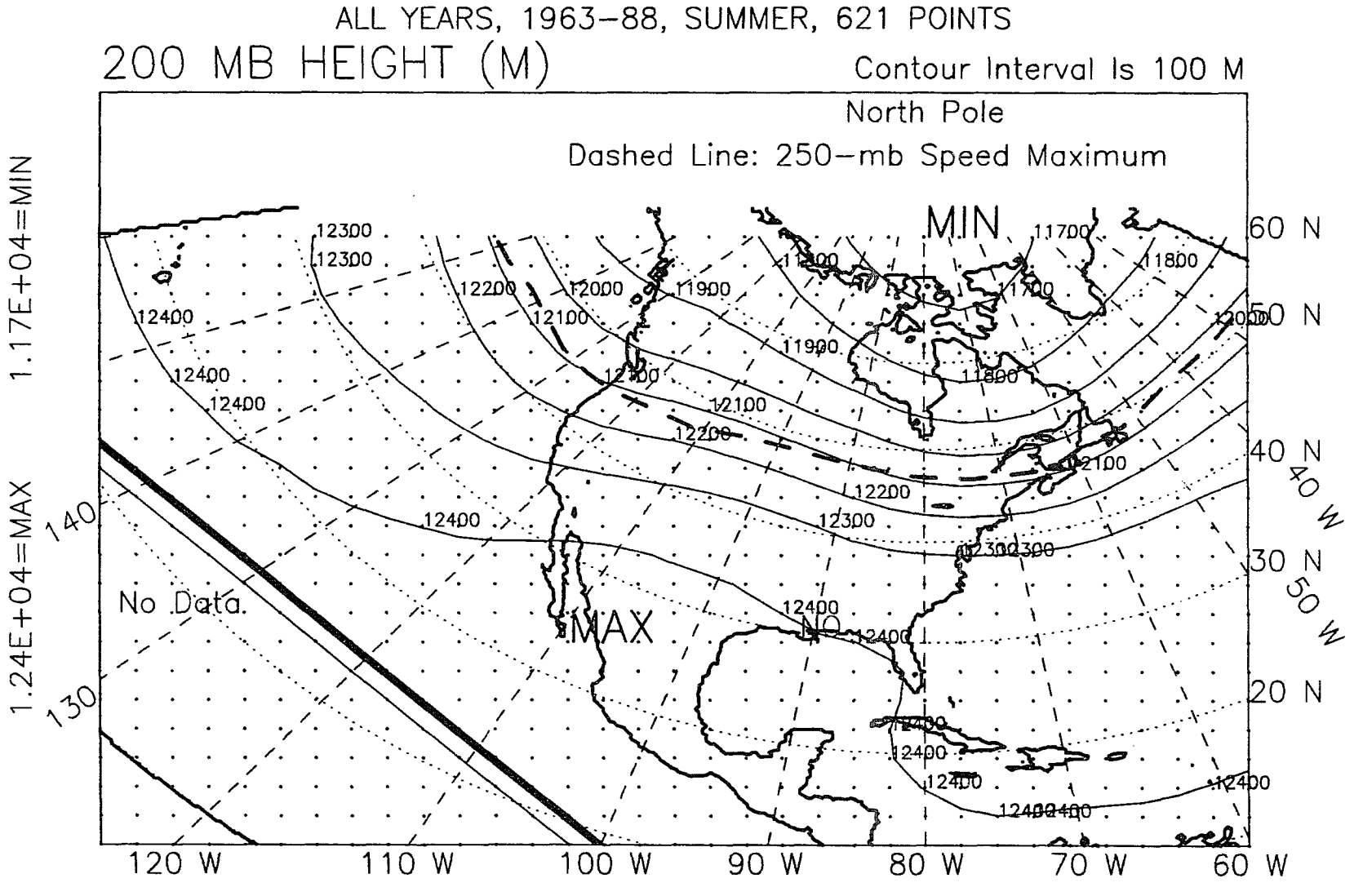

Figure N.12: 200–mb height, summer, all years, 1963–88.

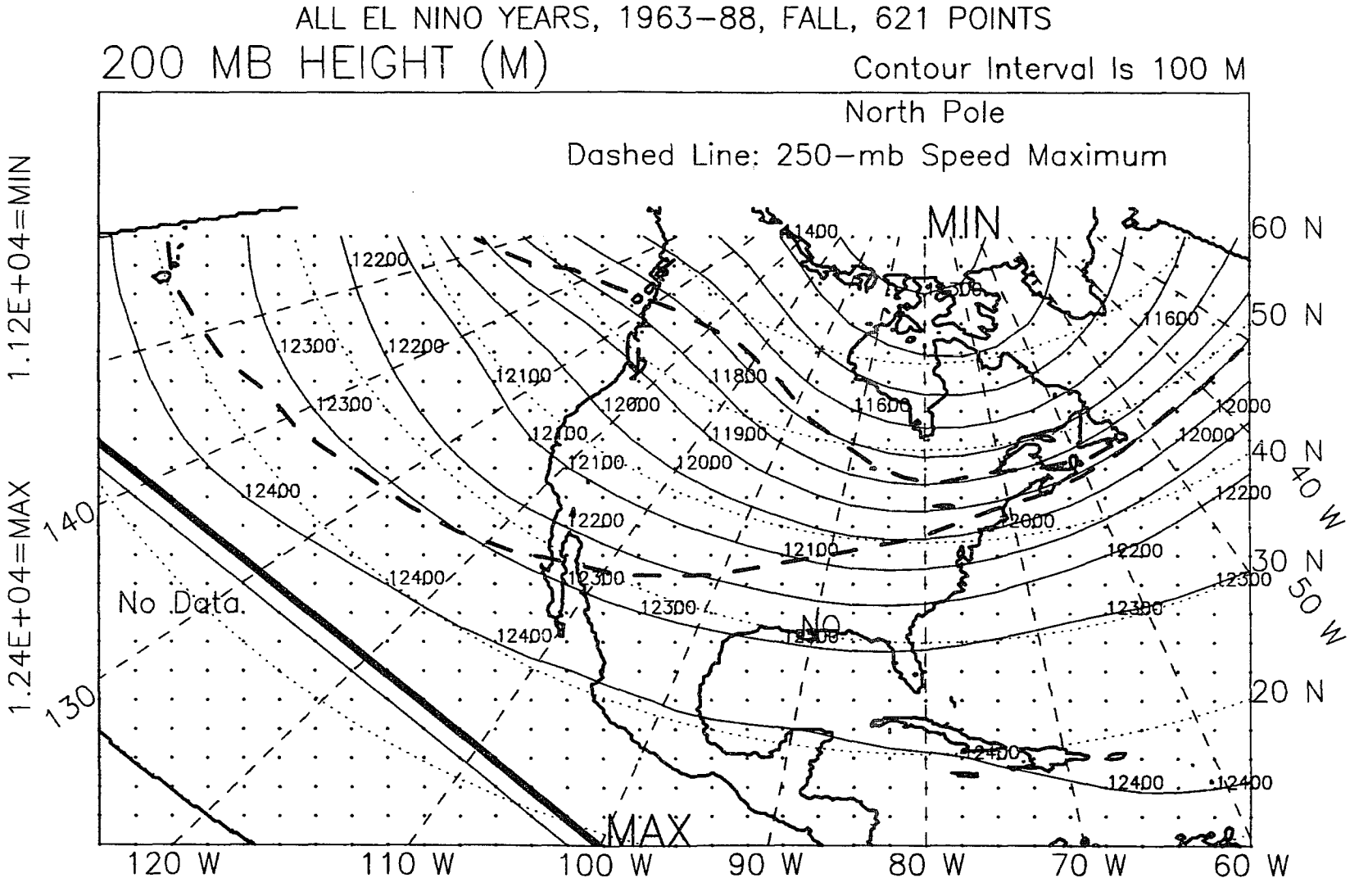

Figure N.13: 200–mb height, fall, El Niño years, 1963–88.

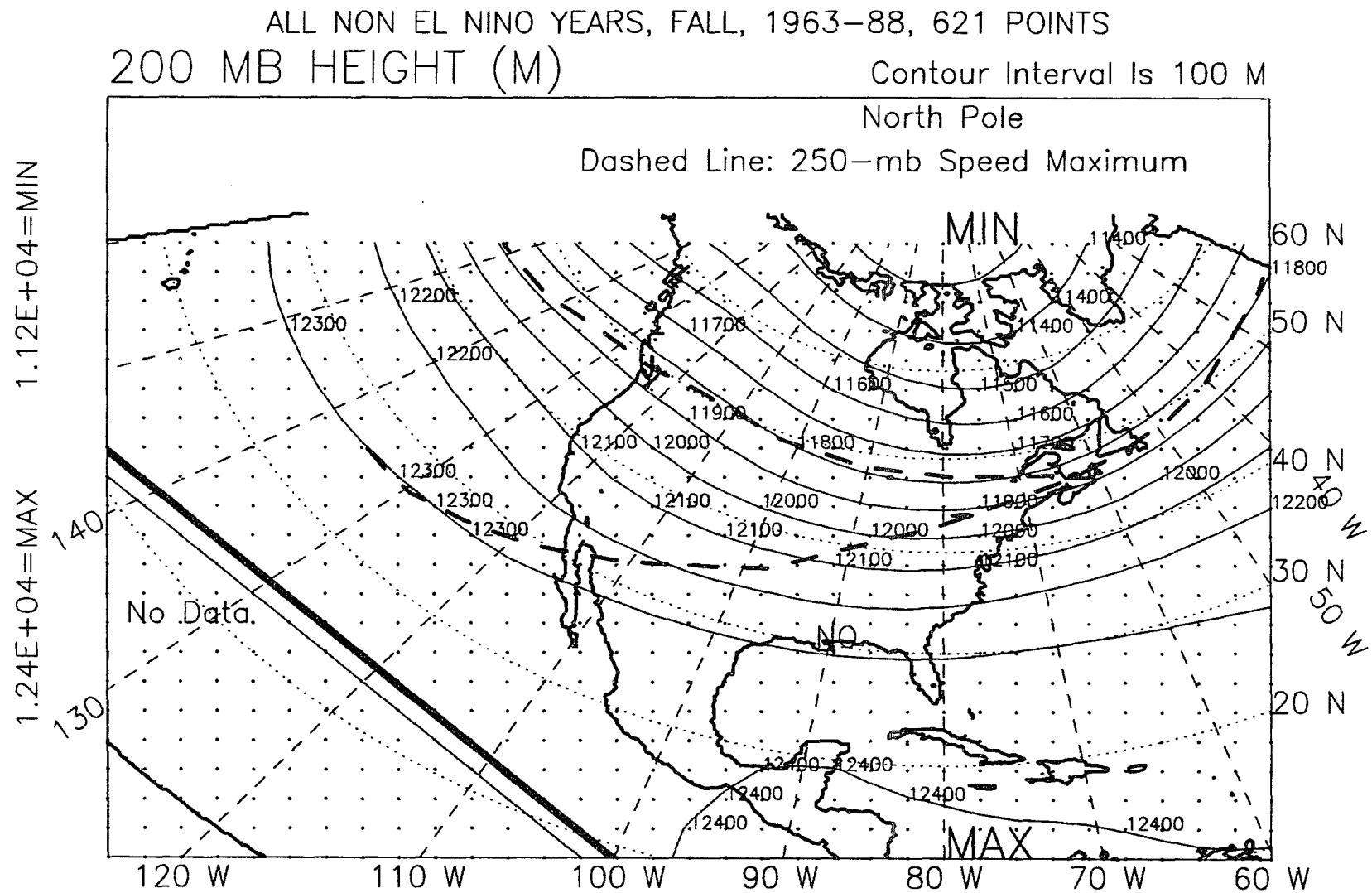

Figure N.14: 200–mb height, fall, non–El Niño years, 1963–88.

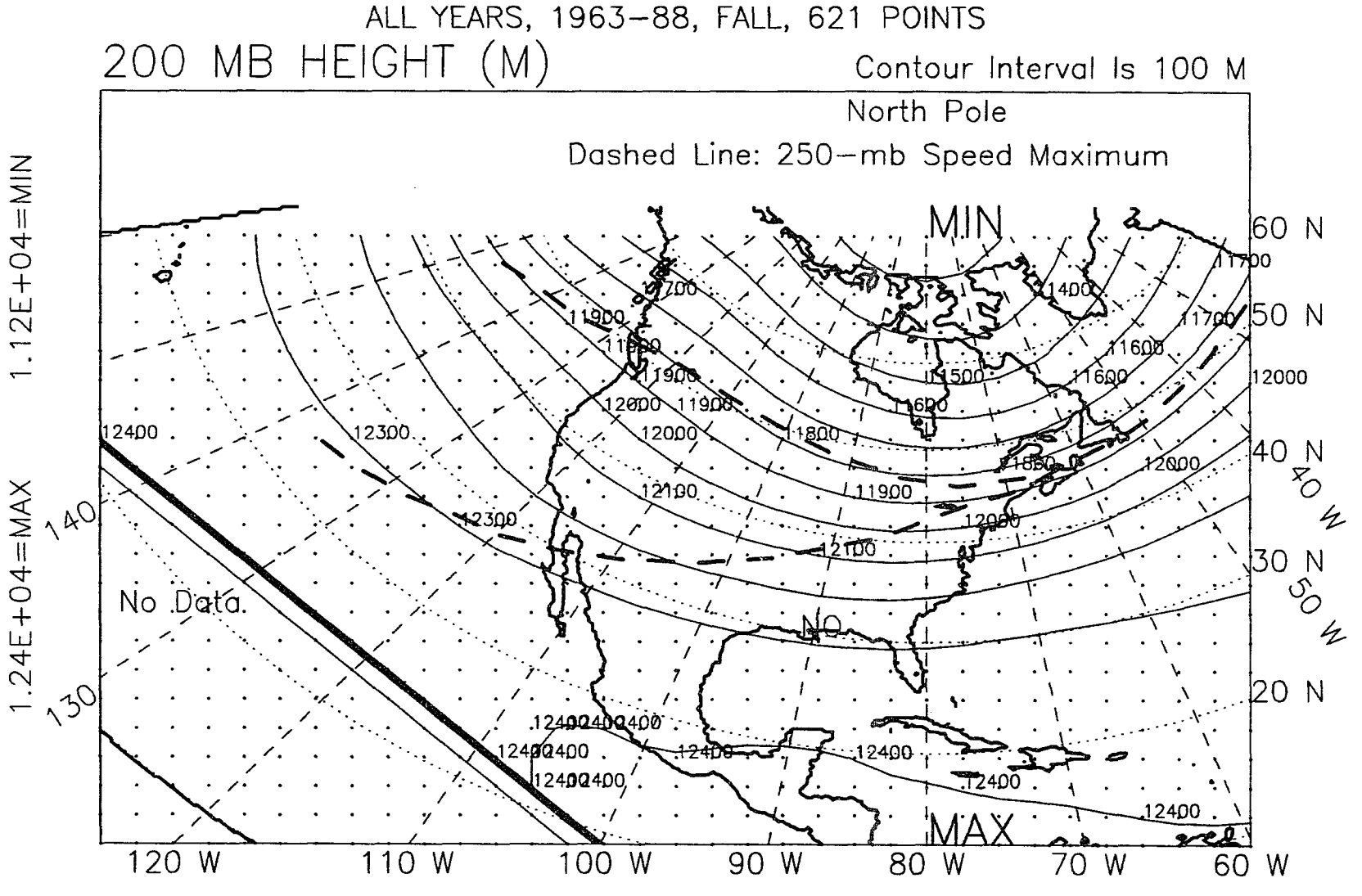

Figure N.15: 200–mb height, fall, all years, 1963–88.

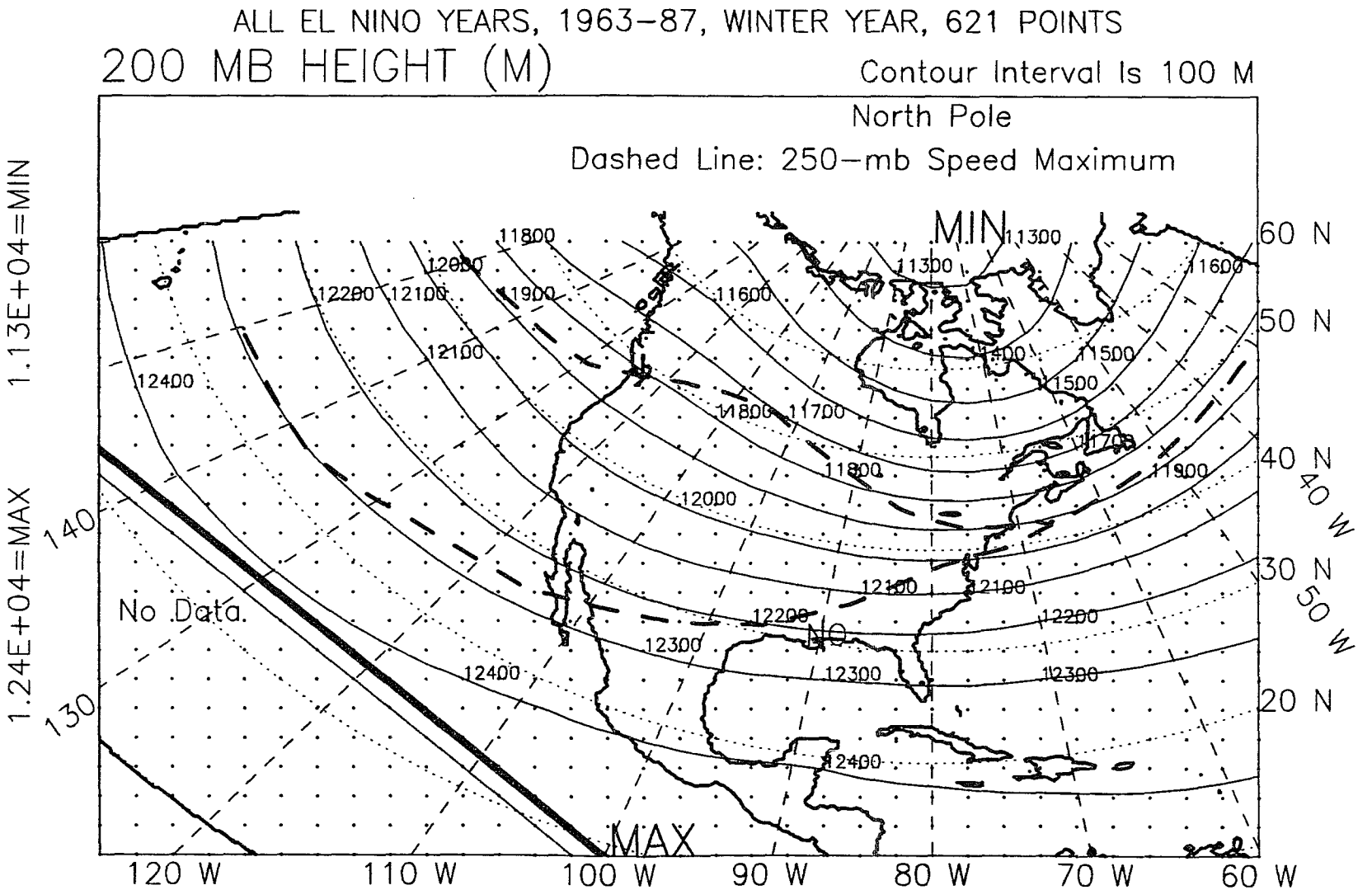

Figure N.16: 200–mb height, winter year, El Niño years, 1963–87.

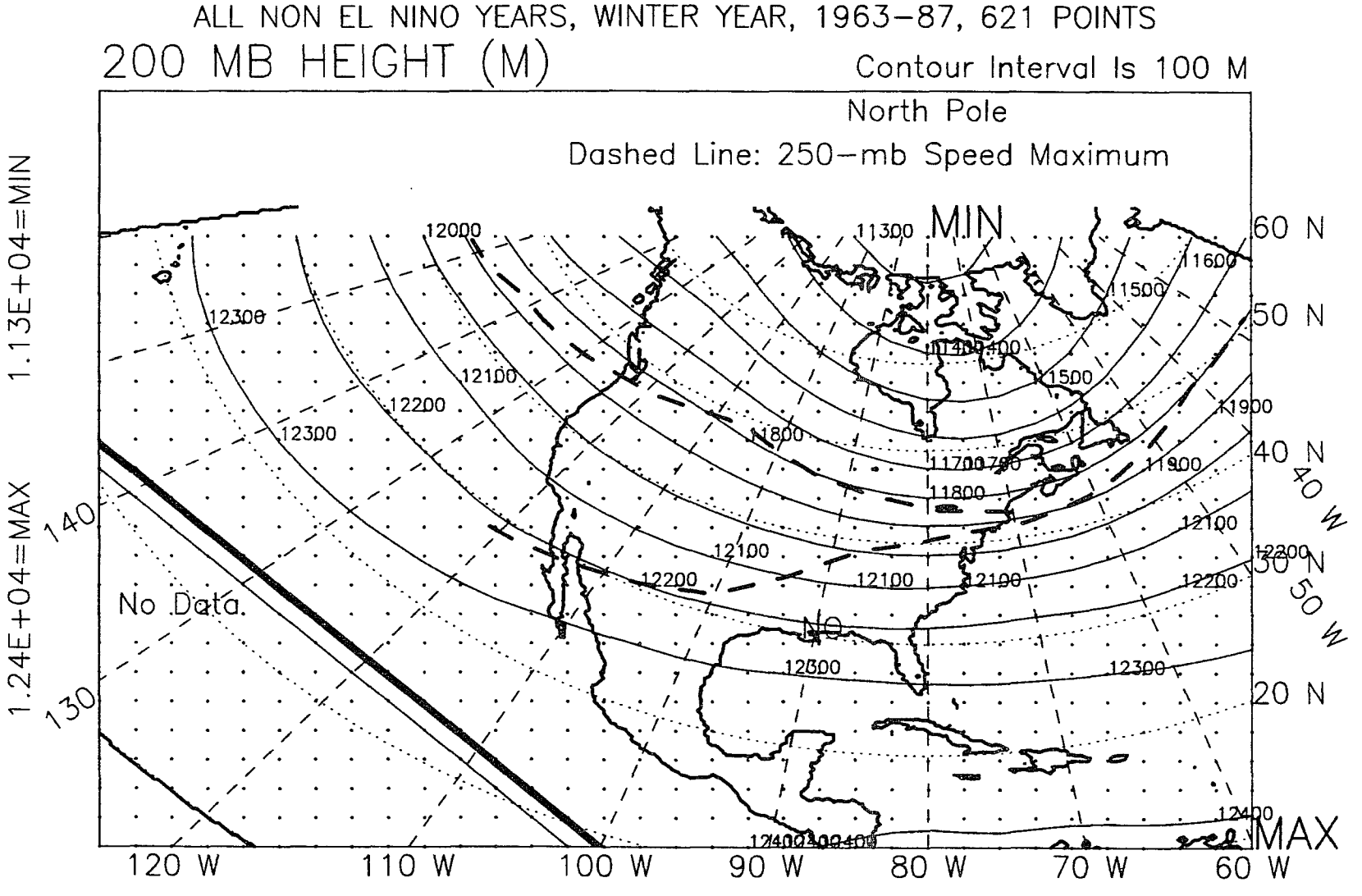

Figure N.17: 200-mb height, winter year, non-El Niño years, 1963-87.

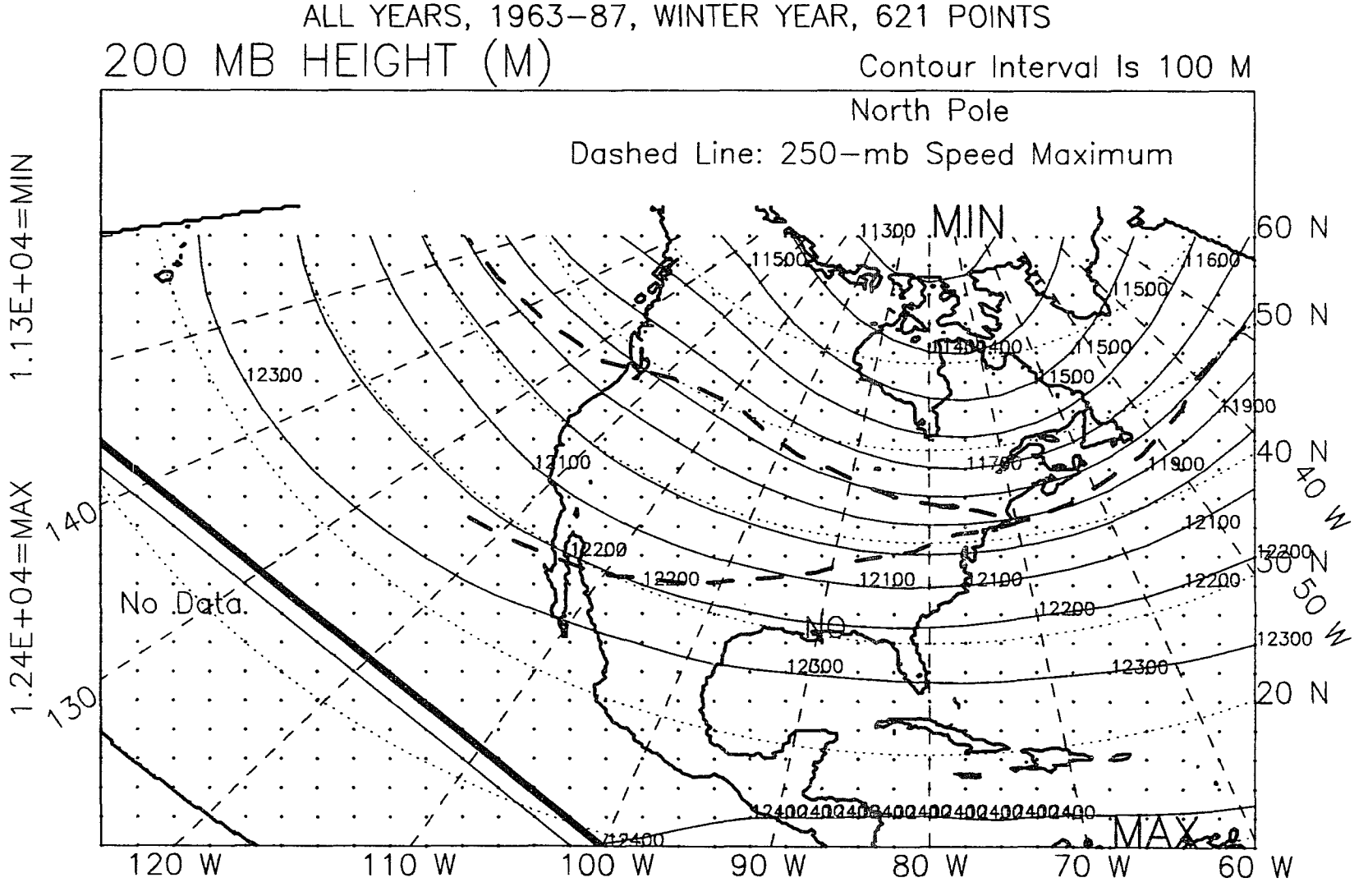

Figure N.18: 200–mb height, winter year, all years, 1963–87.

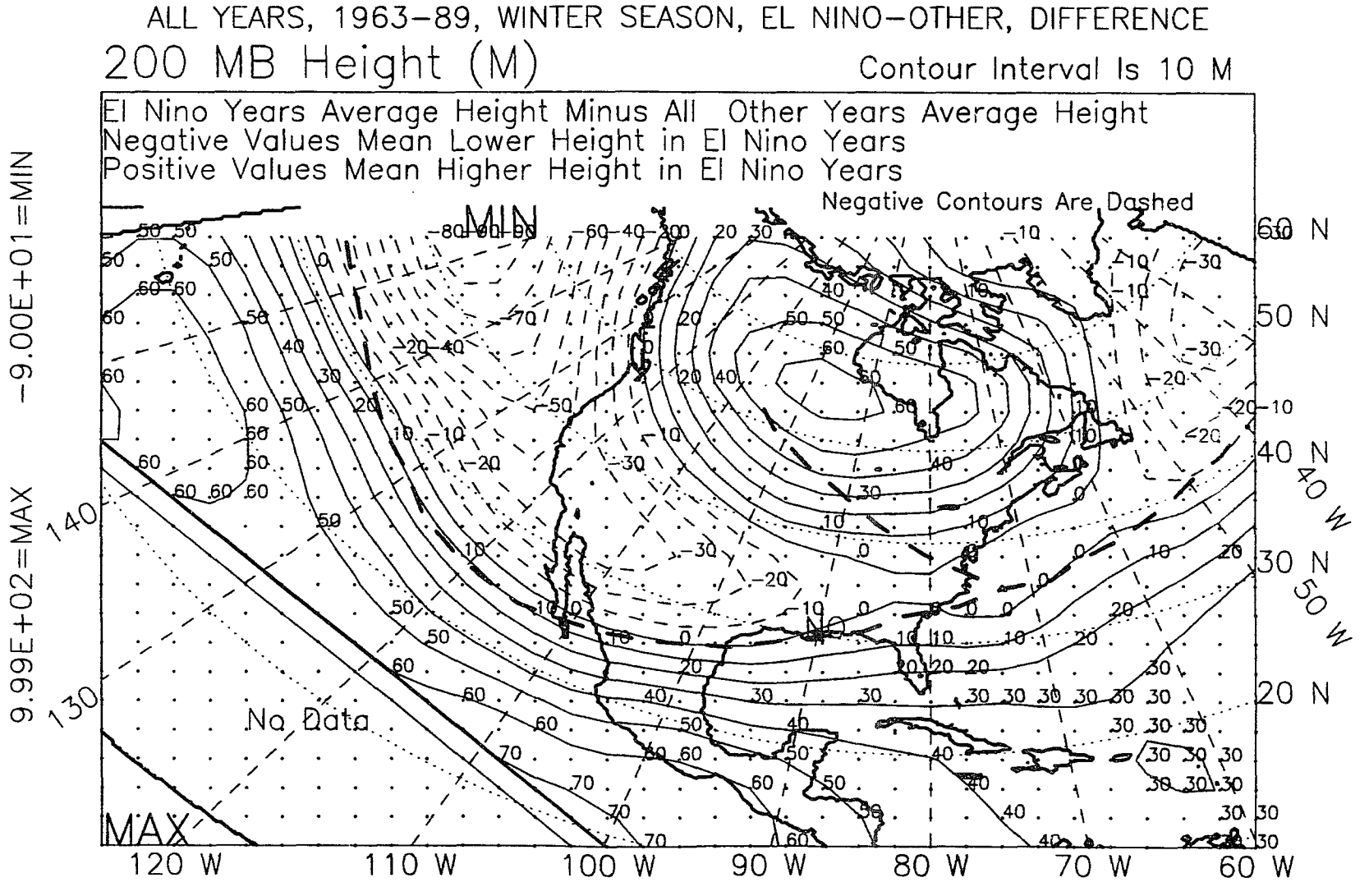

Figure N.19: 200–mb height, winter, 1963–89, difference.

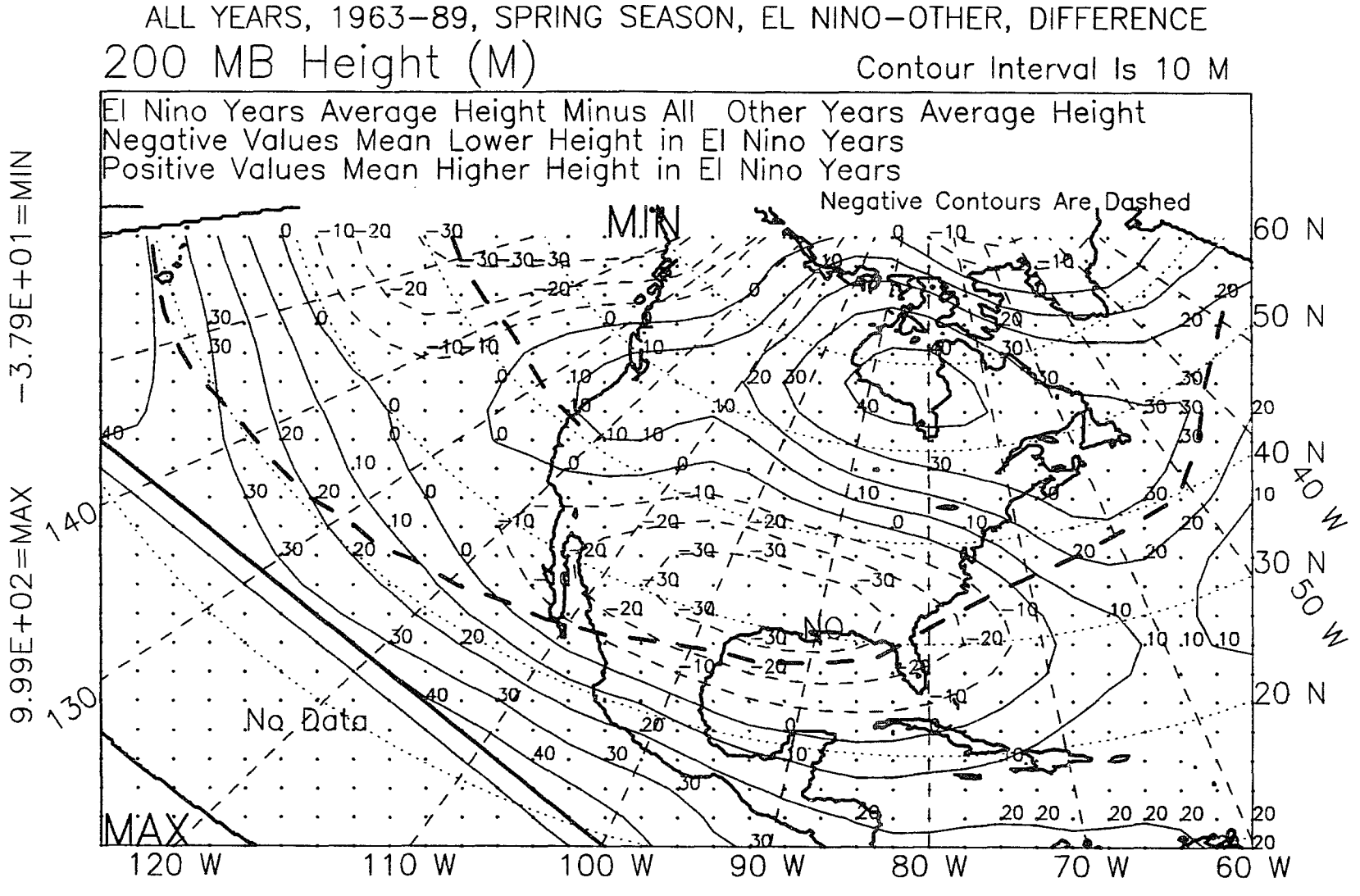

Figure N.20: 200–mb height, spring, 1963–89, difference.

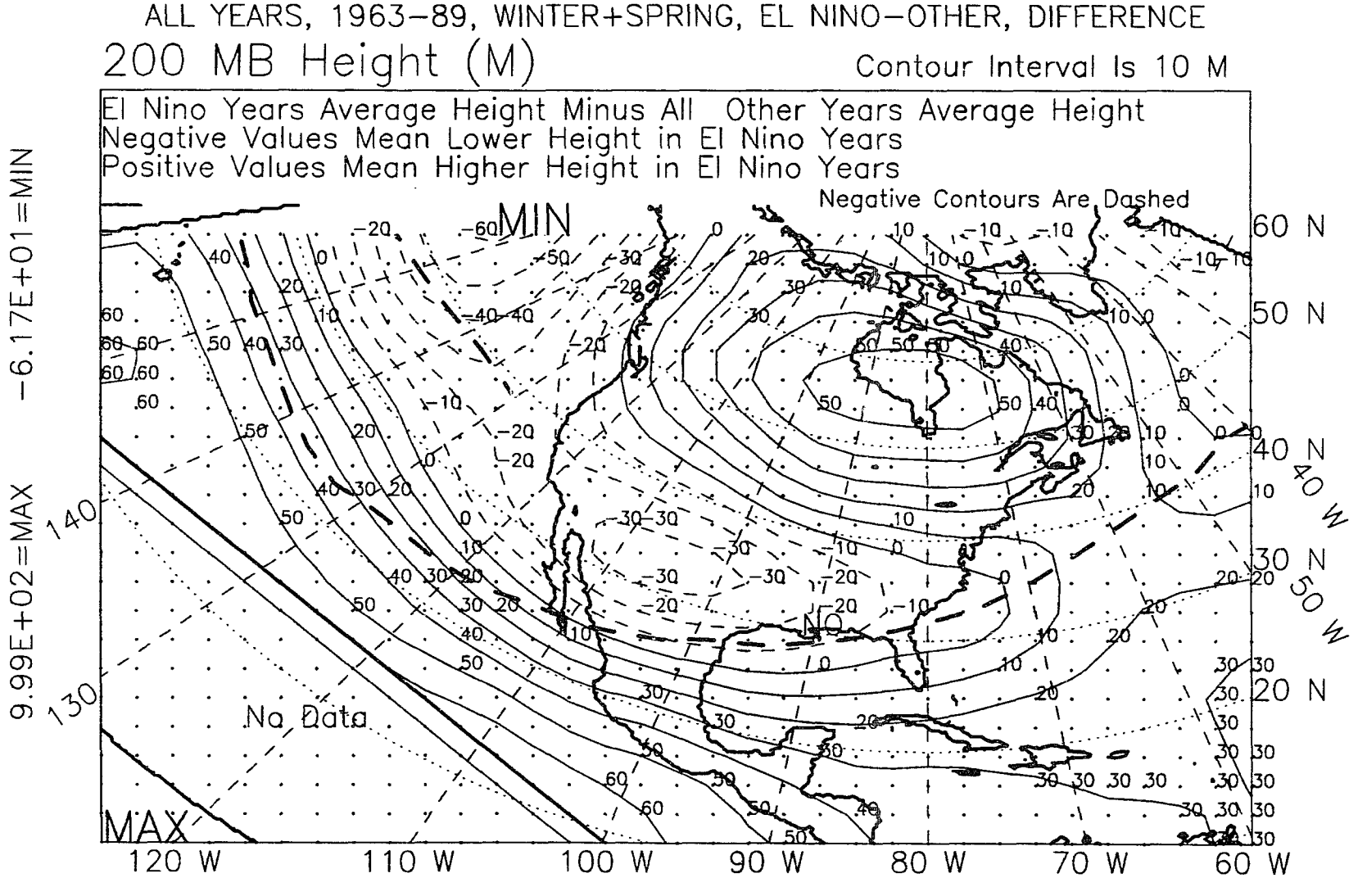

Figure N.21: 200–mb height, winter–plus–spring, 1963–89, difference.

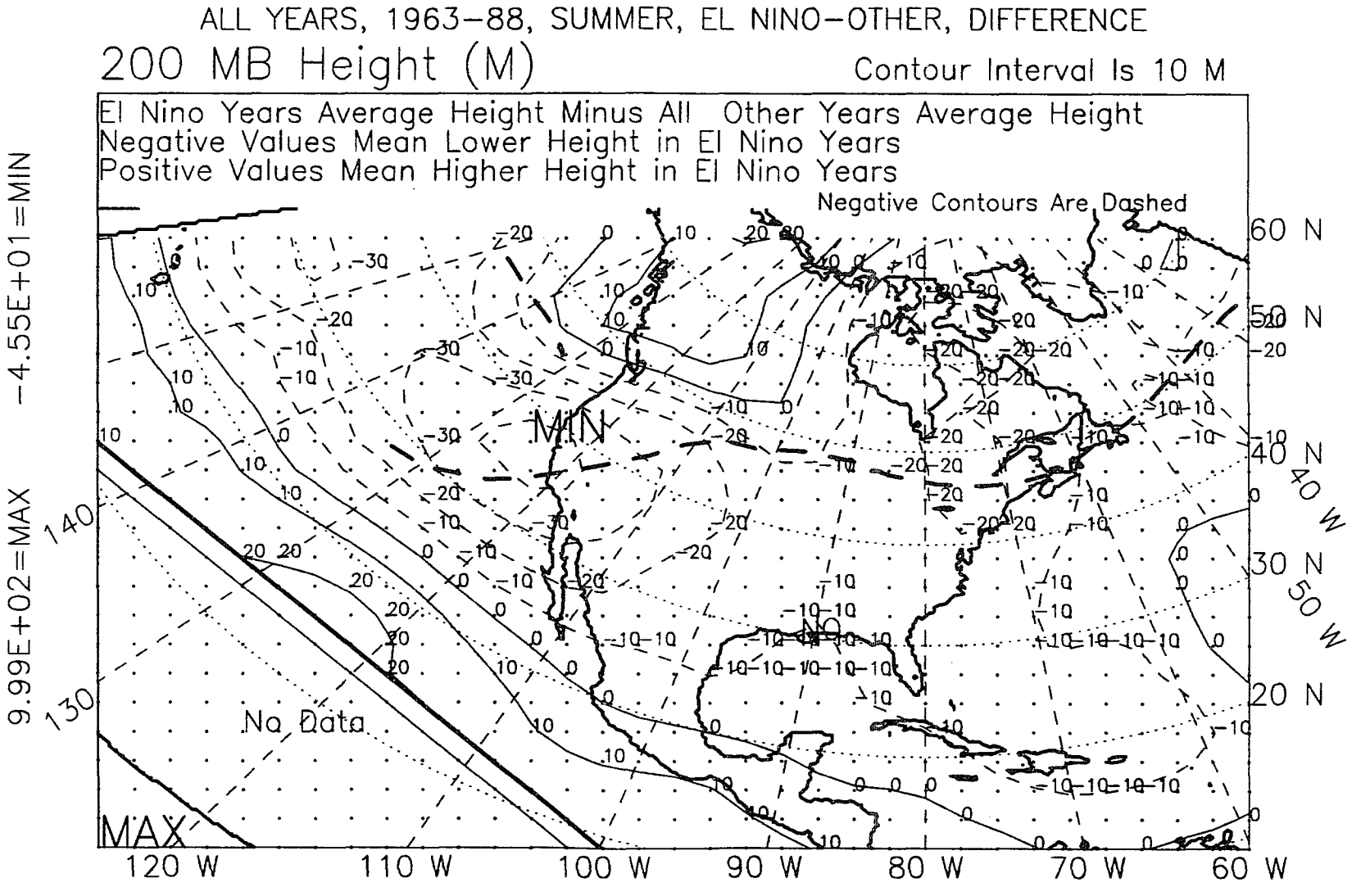

Figure N.22: 200–mb height, summer, 1963–88, difference.

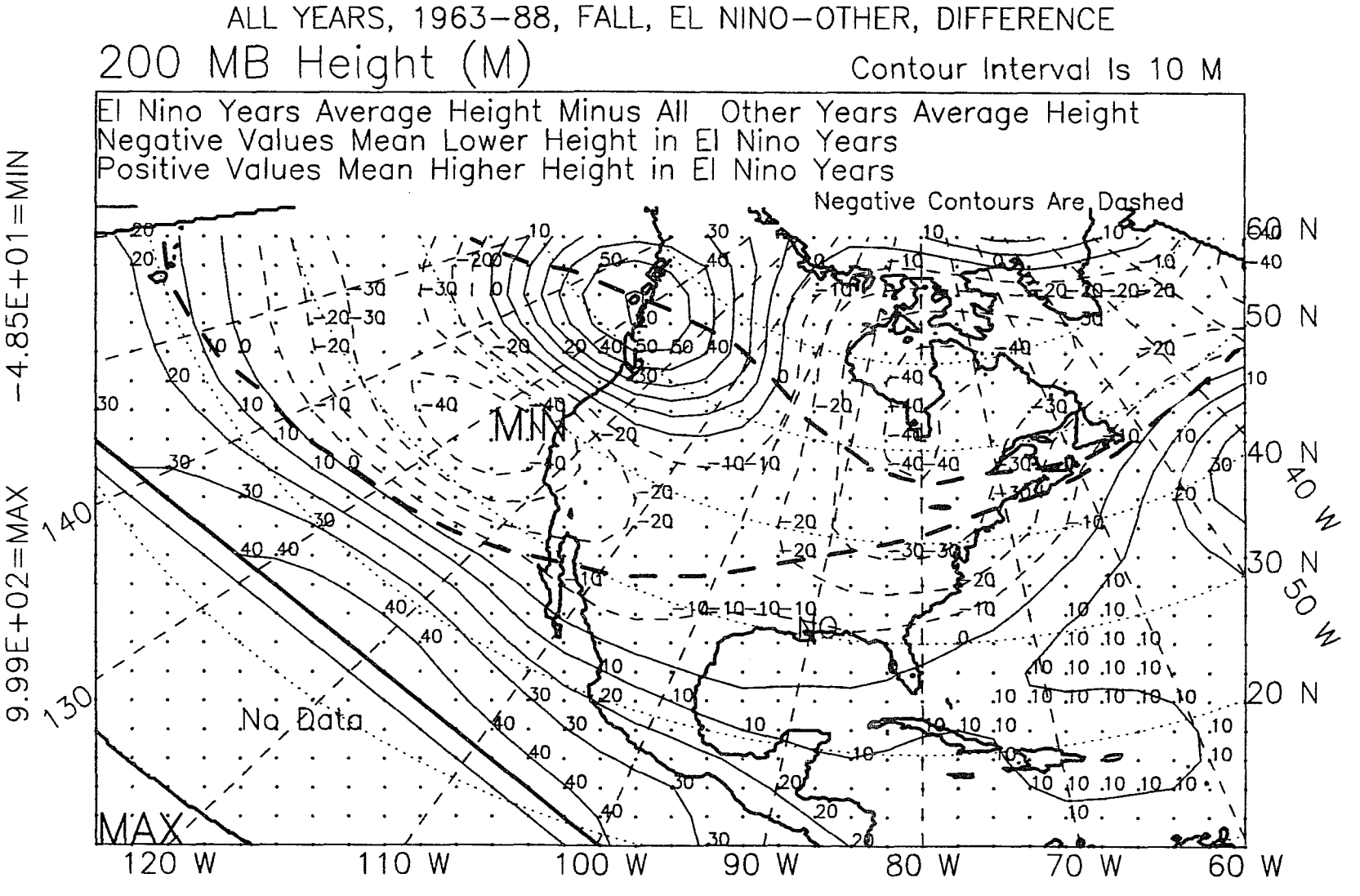

Figure N.23: 200–mb height, fall, 1963–88, difference.

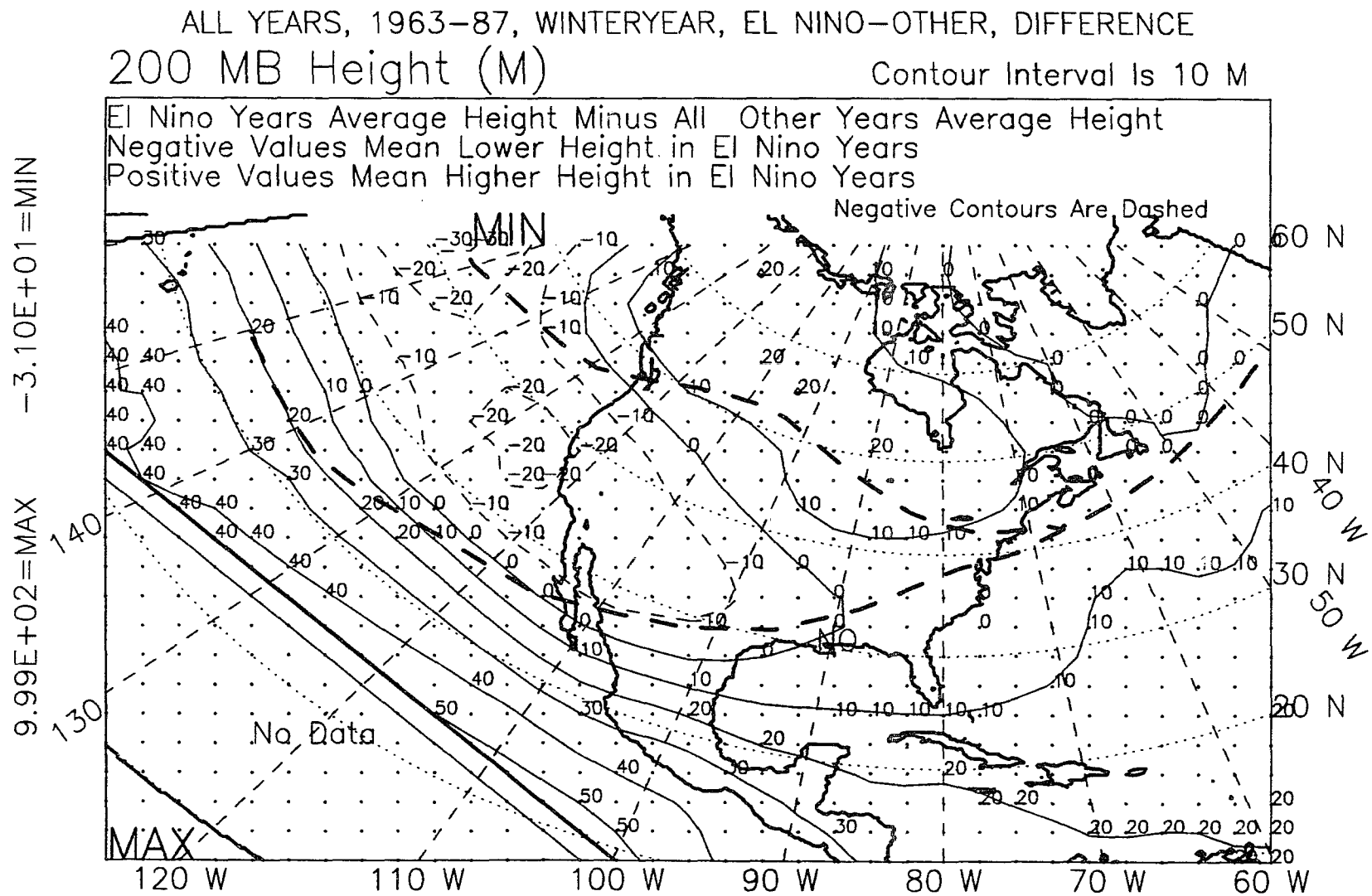

Figure N.24: 200–mb height, winter year, 1963–87, difference.

APPENDIX O
250-MB, WINTER JET STREAM: ANNUALS

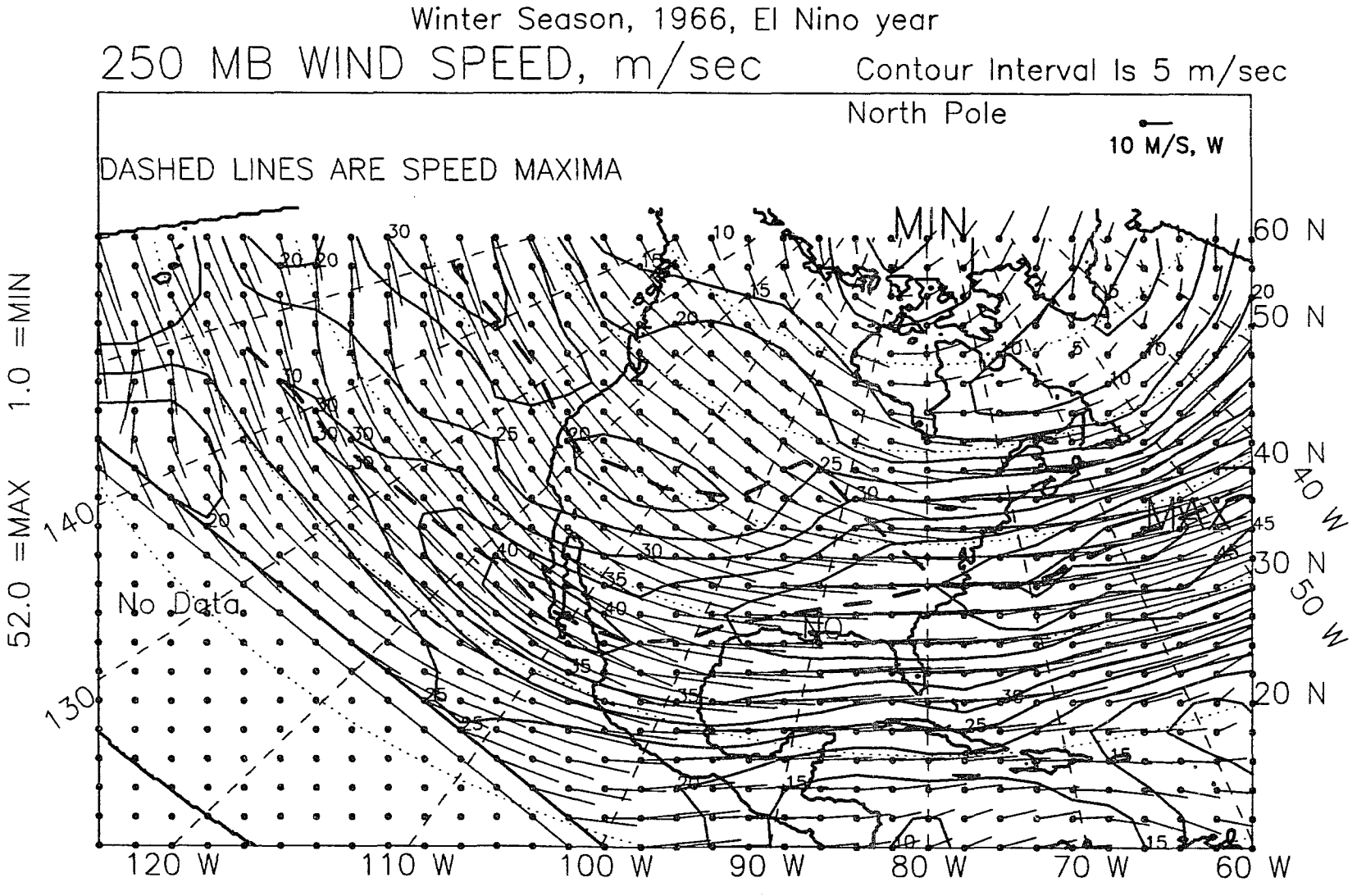

Figure 0.1: 250–mb wind speed, winter, 1966 (D65–F66) El Niño year.

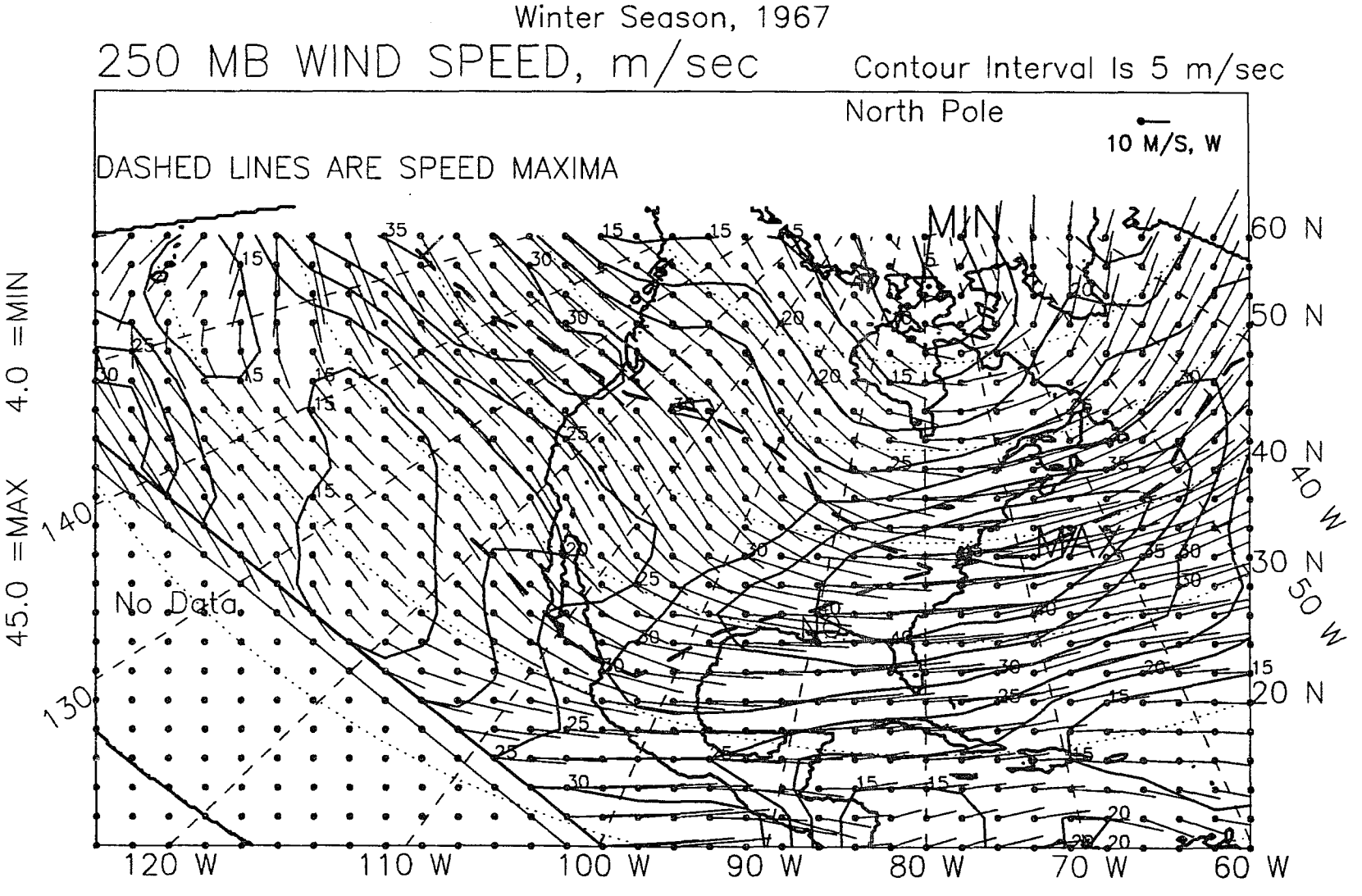

Figure 0.2: 250–mb wind speed, winter, 1967 (D66–F67).

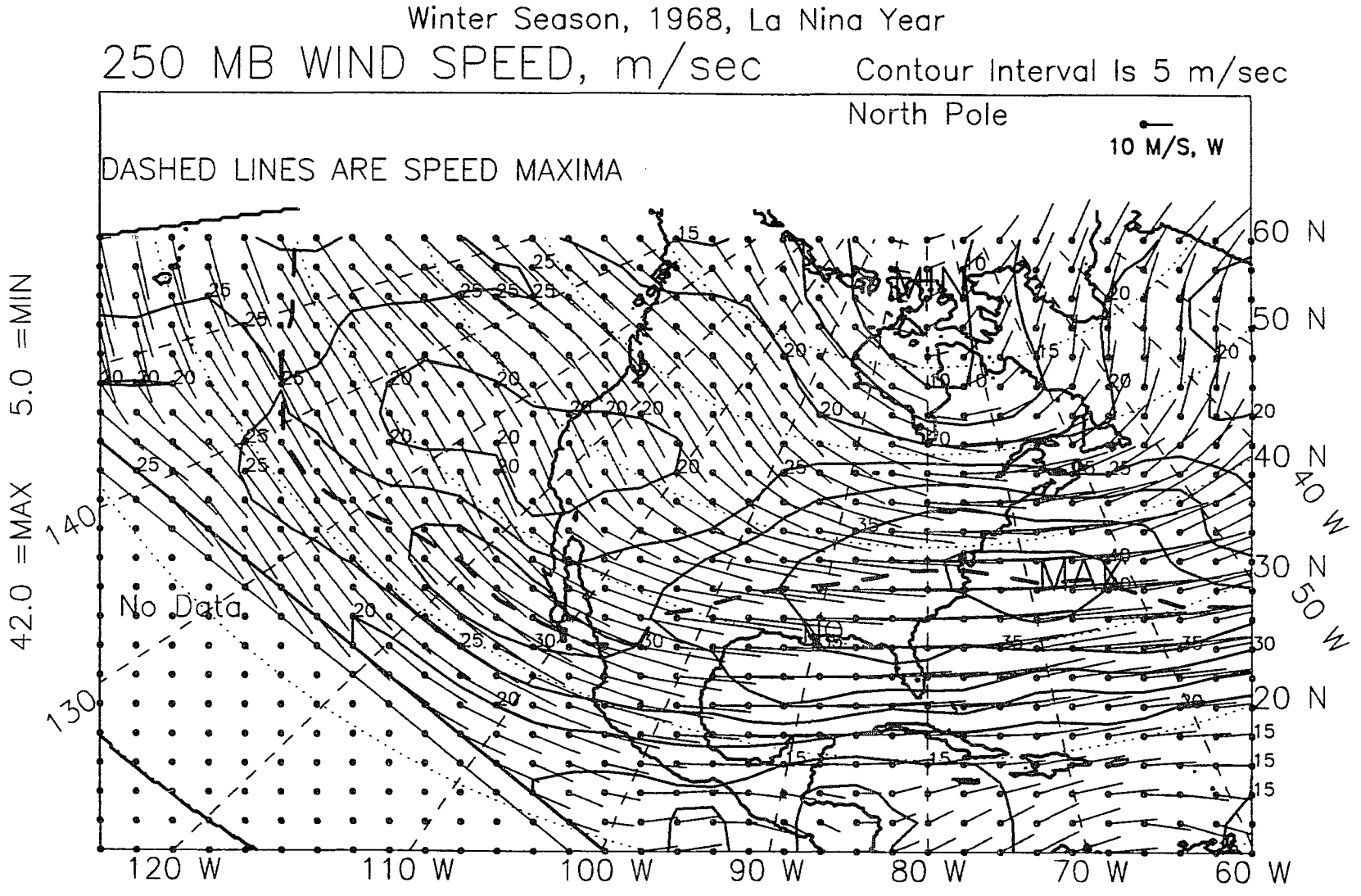

Figure 0.3: 250–mb wind speed, winter, 1968 (D67–F68) La Niña year.

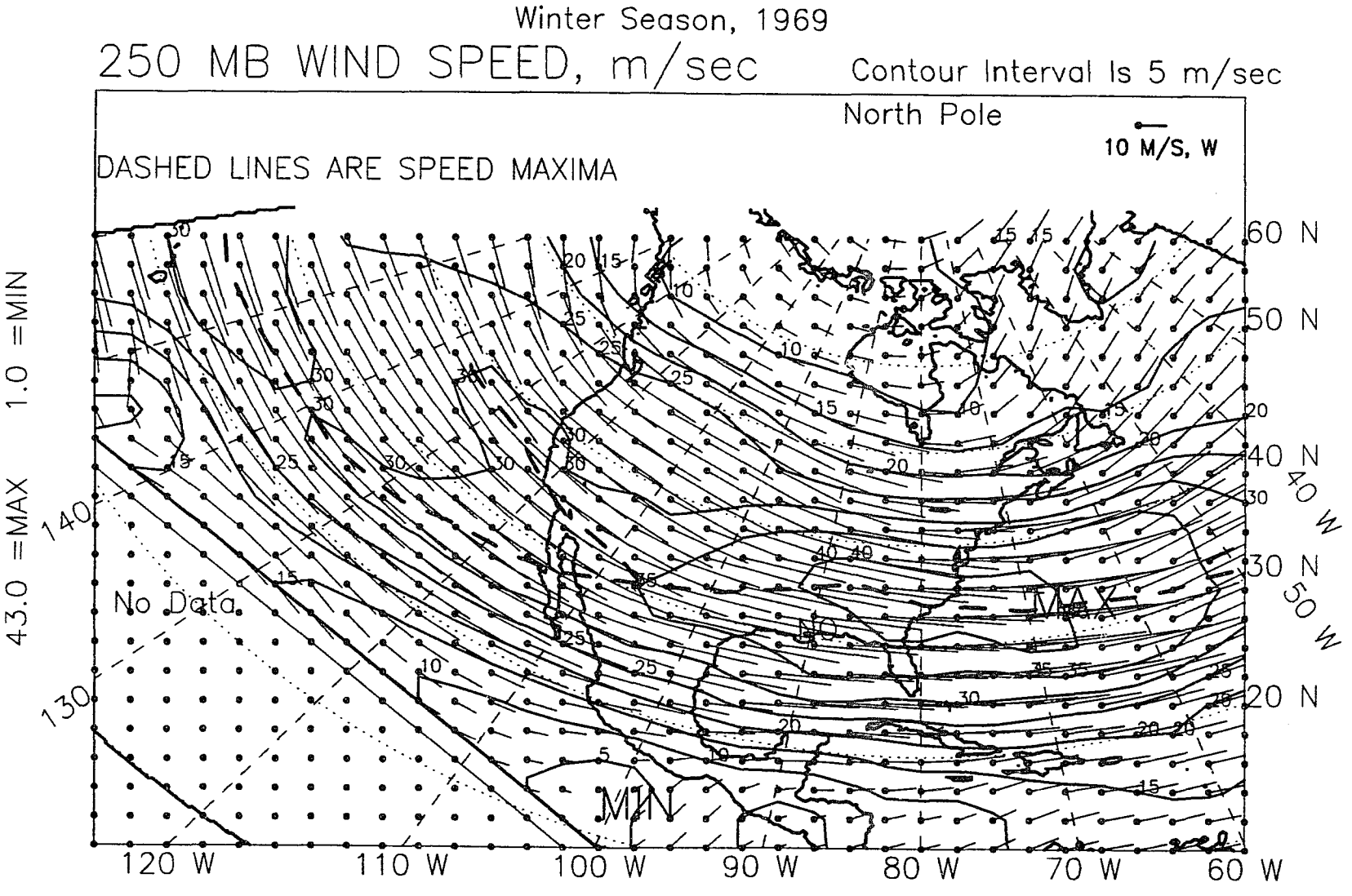

Figure 0.4: 250–mb wind speed, winter, 1969 (D68–F69).

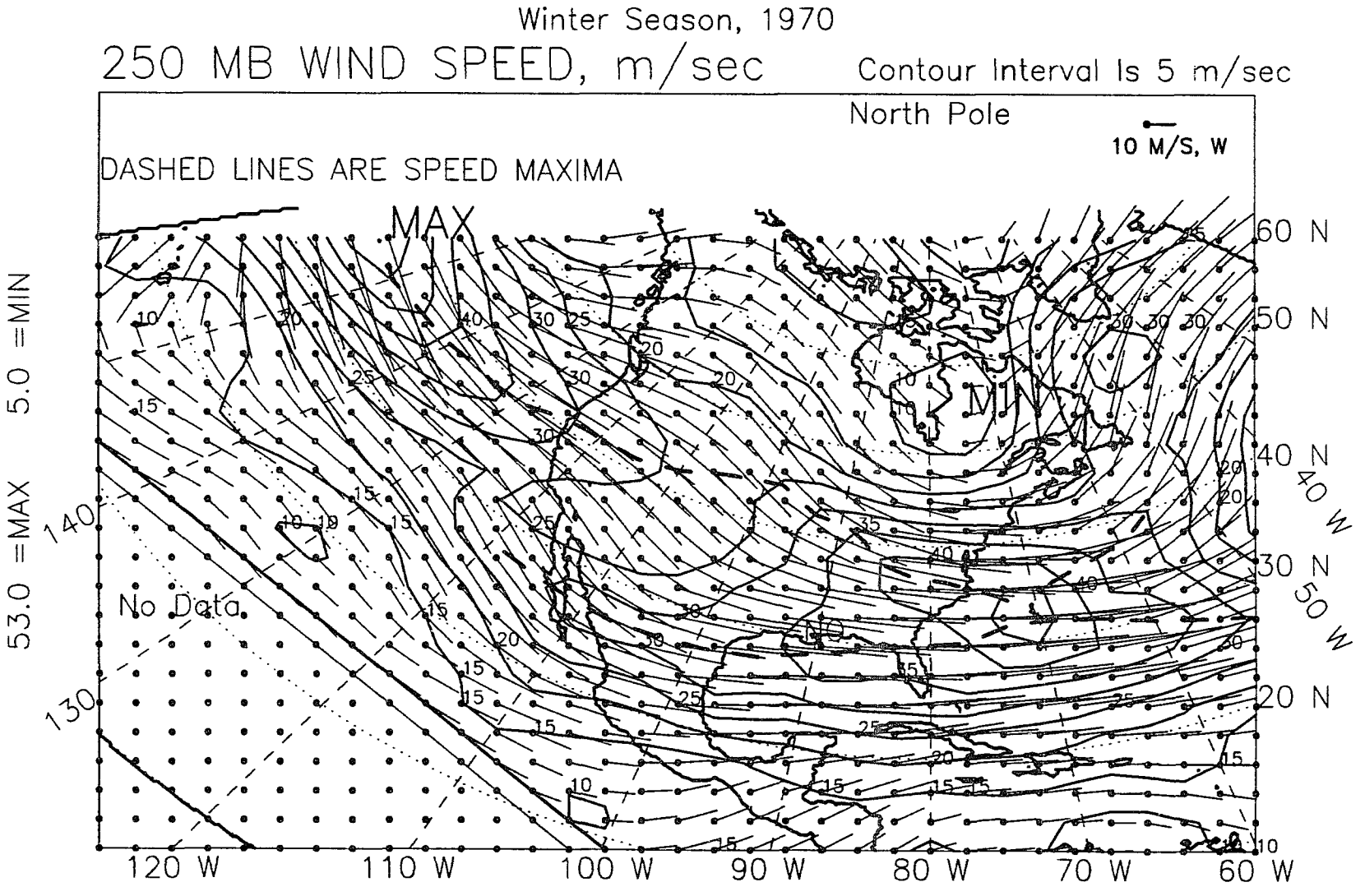

Figure 0.5: 250–mb wind speed, winter, 1970 (D69–F70).

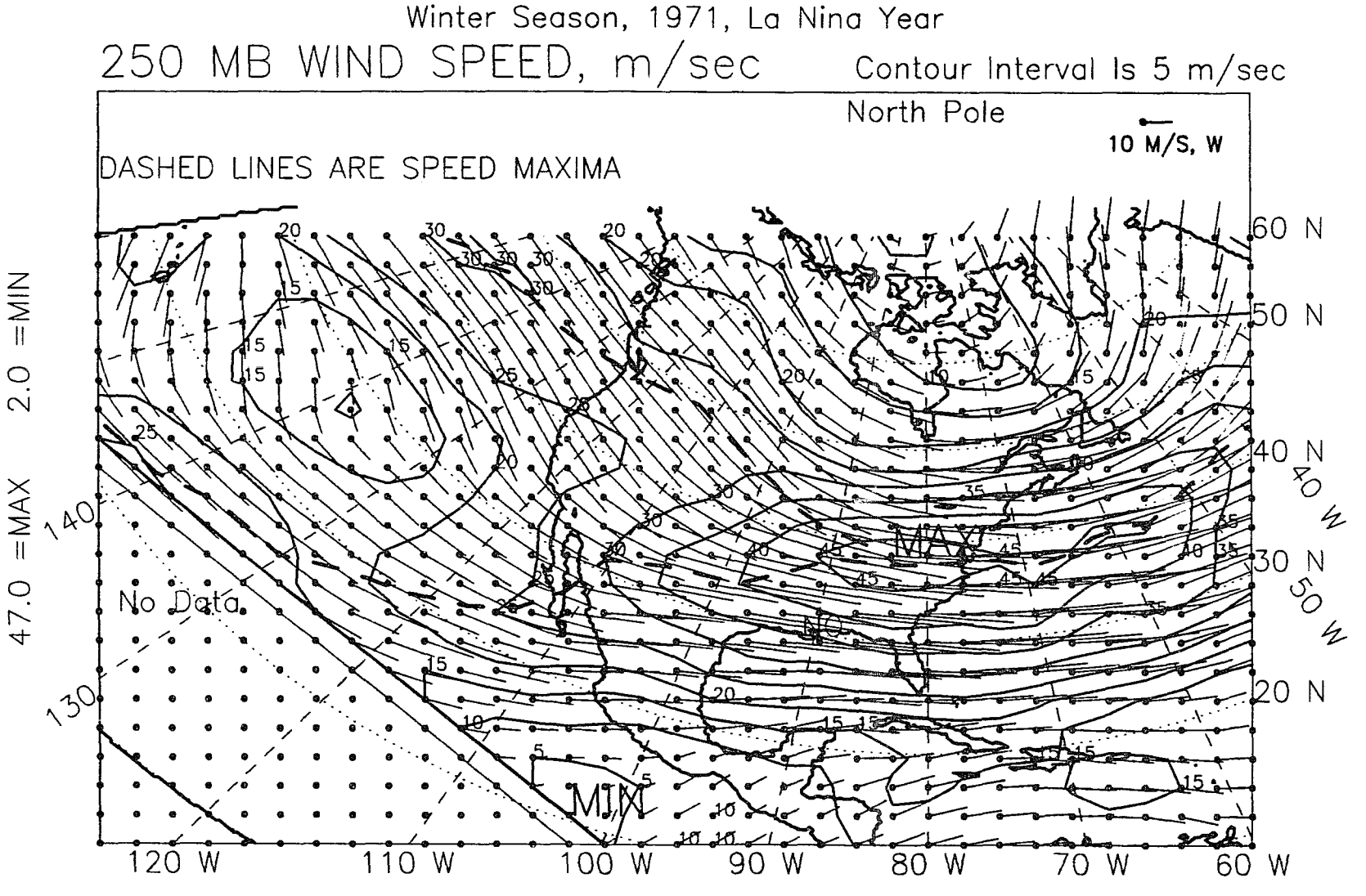

Figure 0.6: 250–mb wind speed, winter, 1971 (D70–F71) La Niña year.

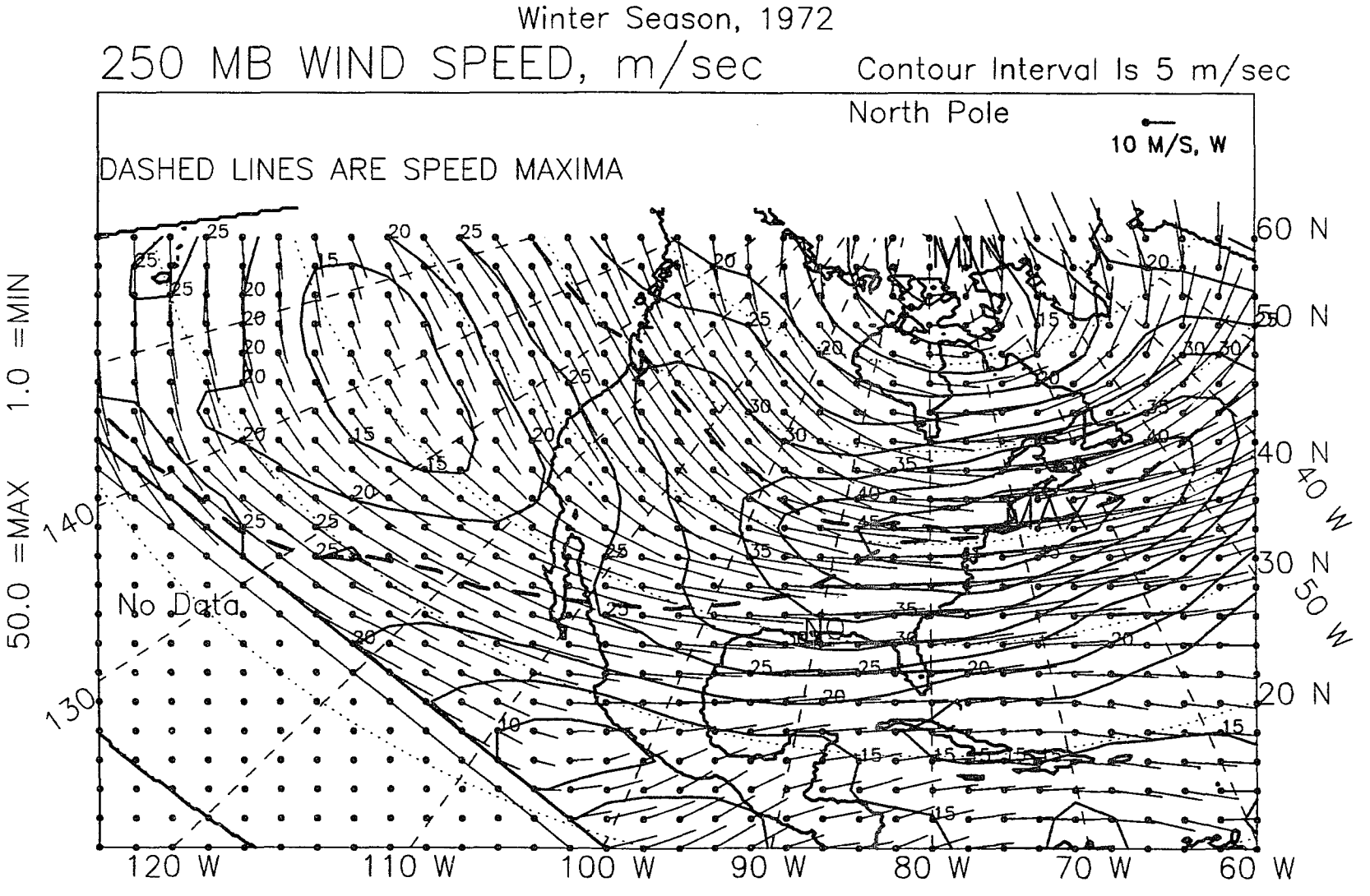

Figure 0.7: 250–mb wind speed, winter, 1972 (D71–F72).

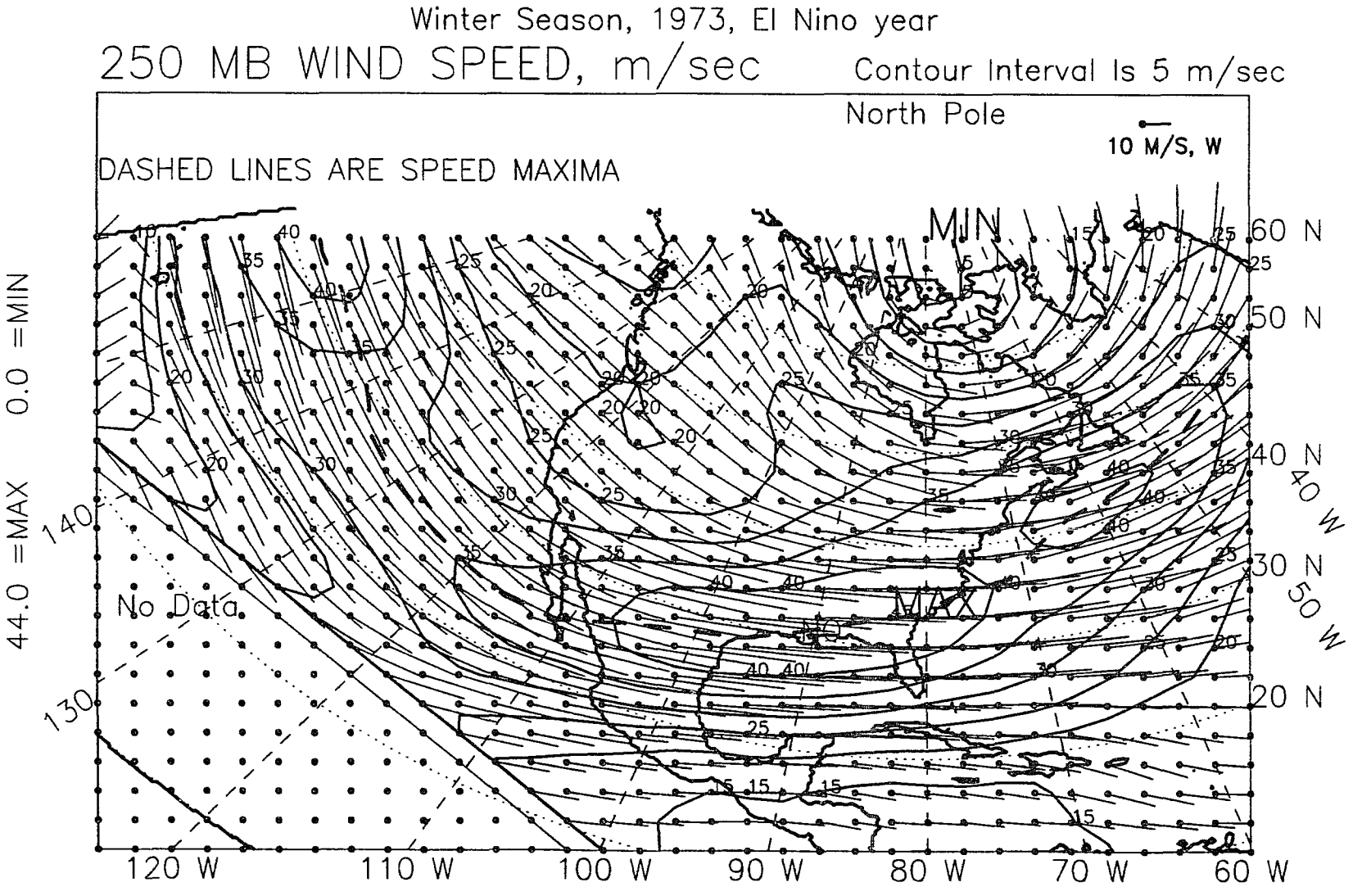

Figure 0.8: 250–mb wind speed, winter, 1973 (D72–F73) El Niño year.

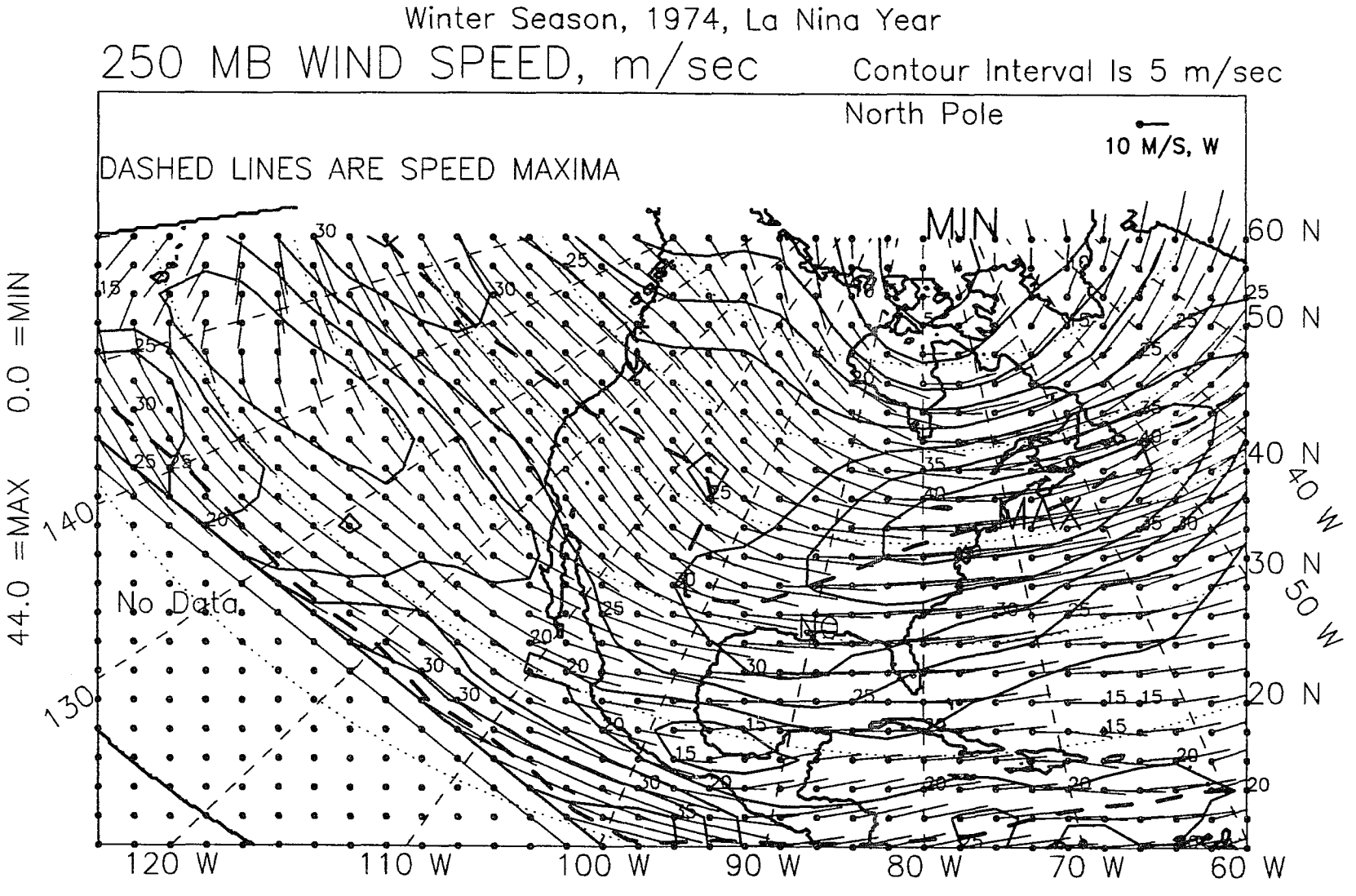

Figure 0.9: 250–mb wind speed, winter, 1974 (D73–F74) La Niña year.

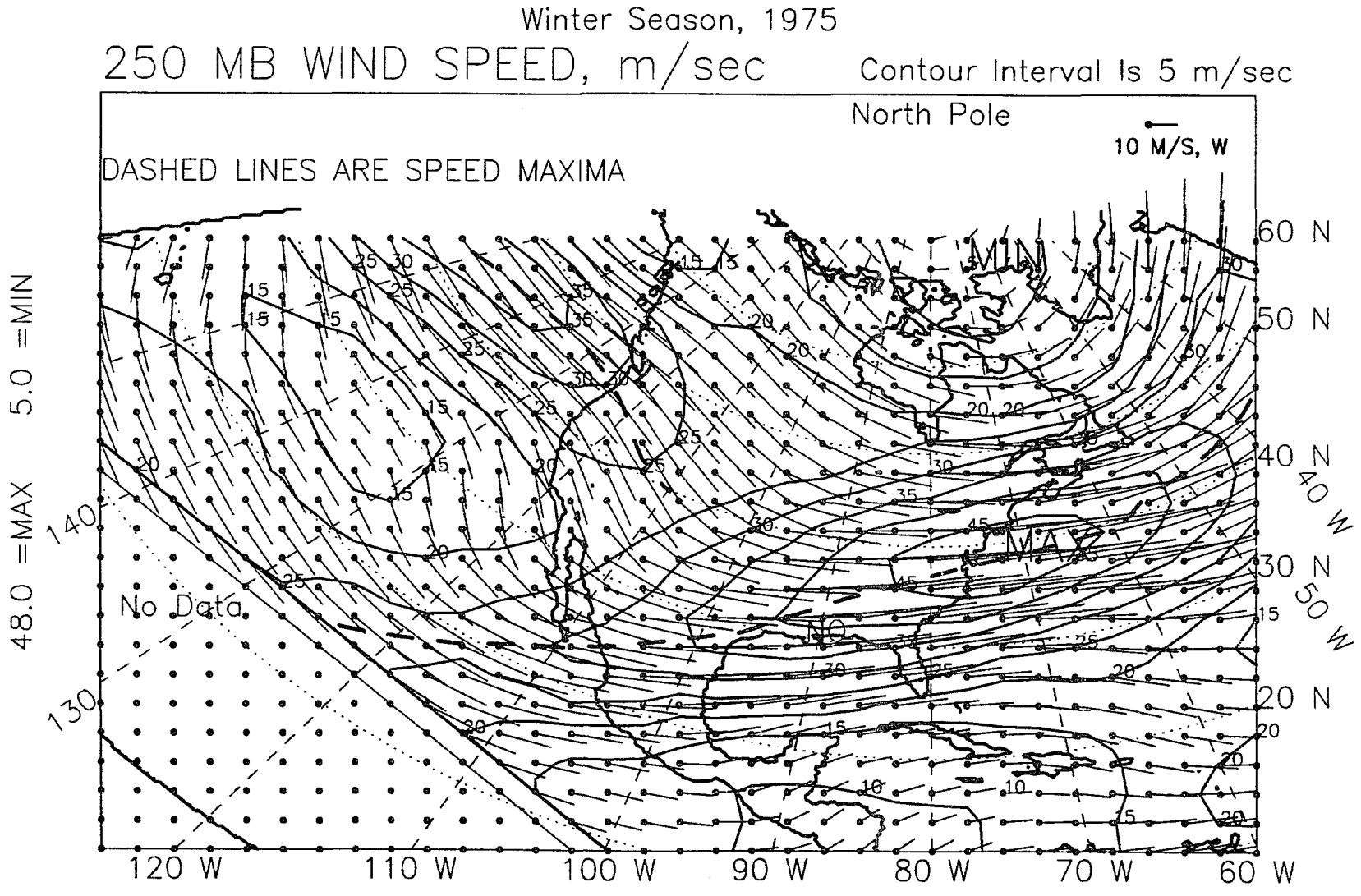

Figure 0.10: 250–mb wind speed, winter, 1975 (D74–F75).

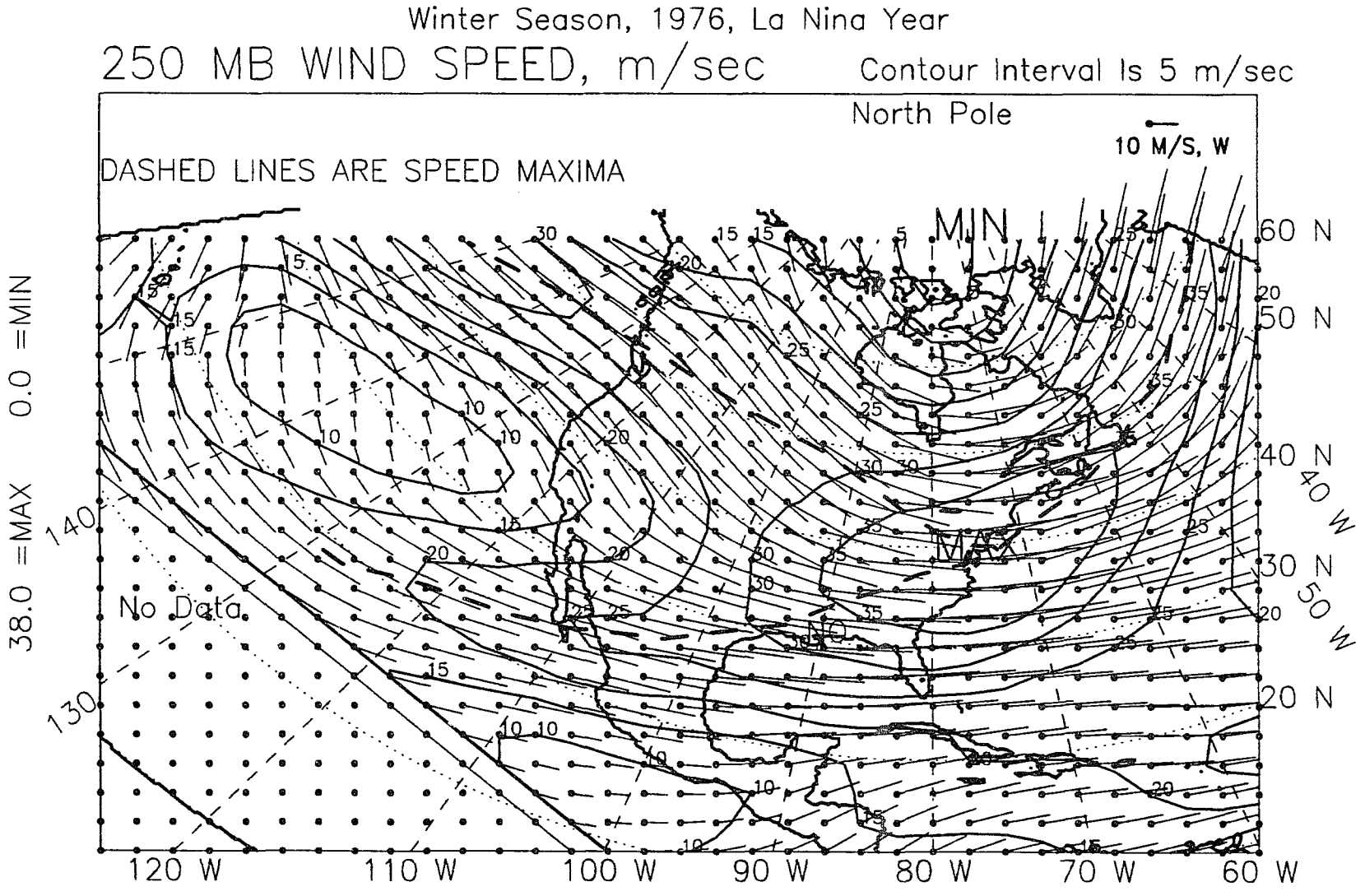

Figure 0.11: 250–mb wind speed, winter, 1976 (D75–F76) La Niña year.

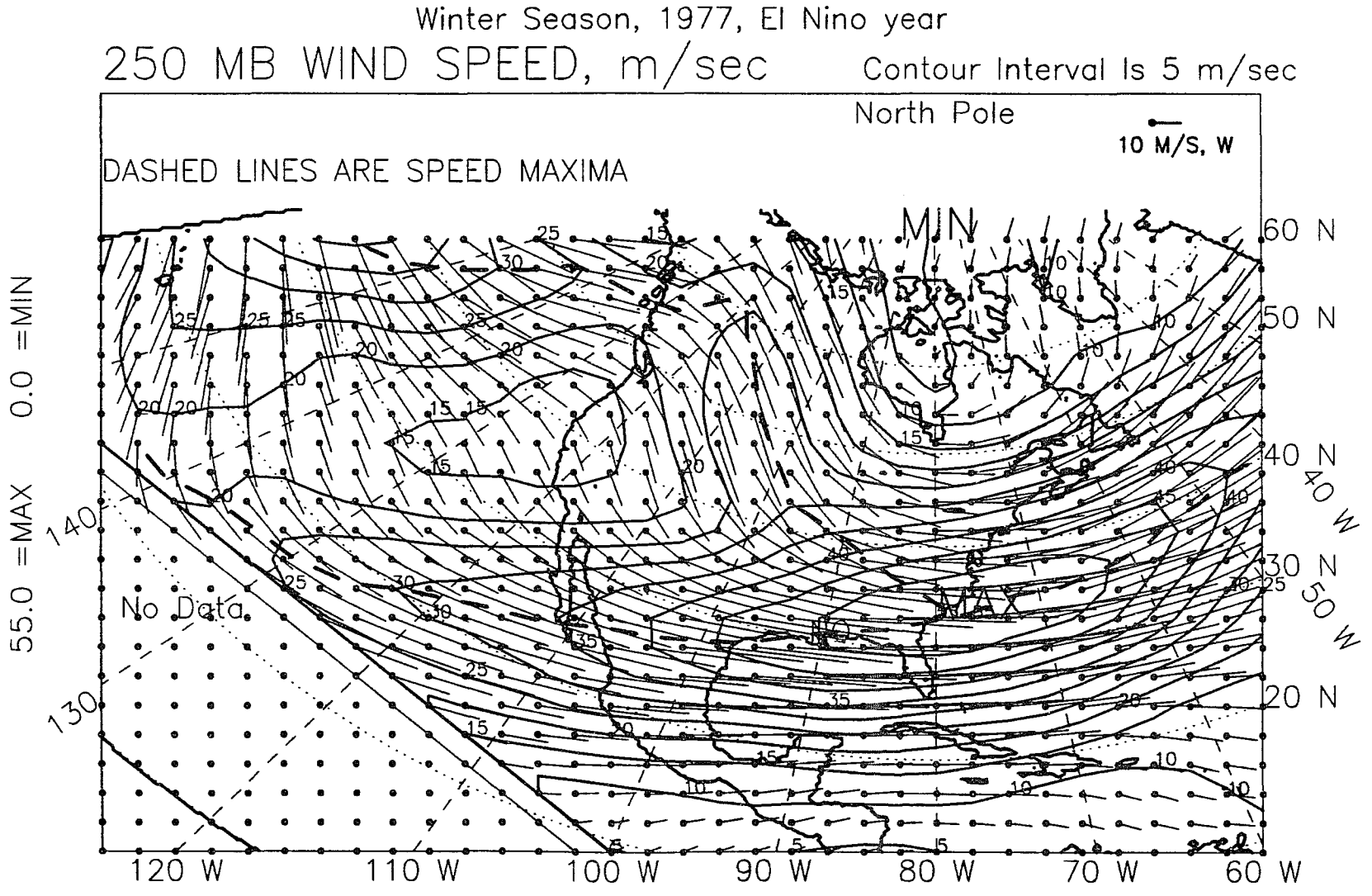

Figure 0.12: 250–mb wind speed, winter, 1977 (D76–F77) El Niño year.

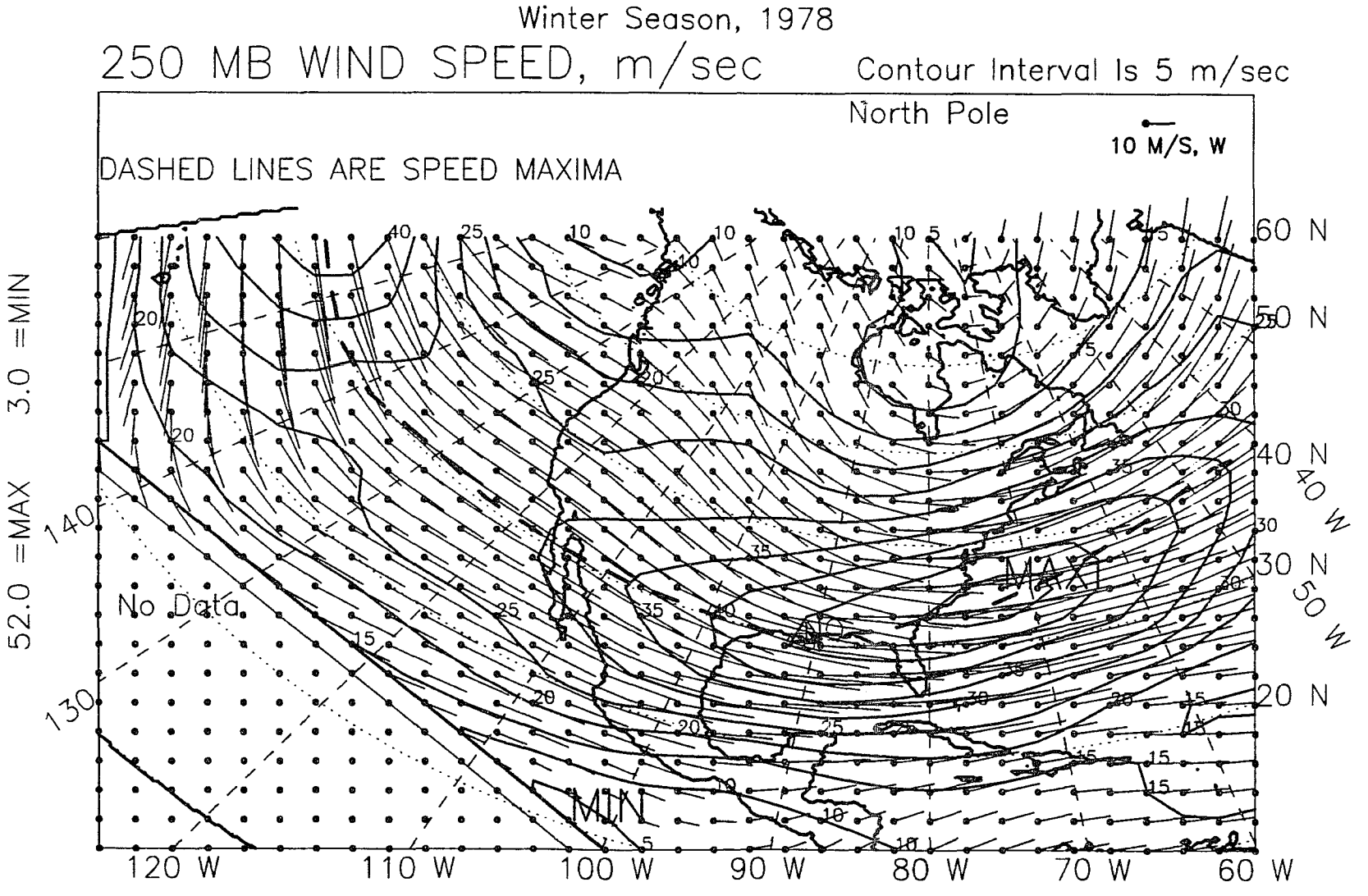

Figure 0.13: 250–mb wind speed, winter, 1978 (D77–F78).

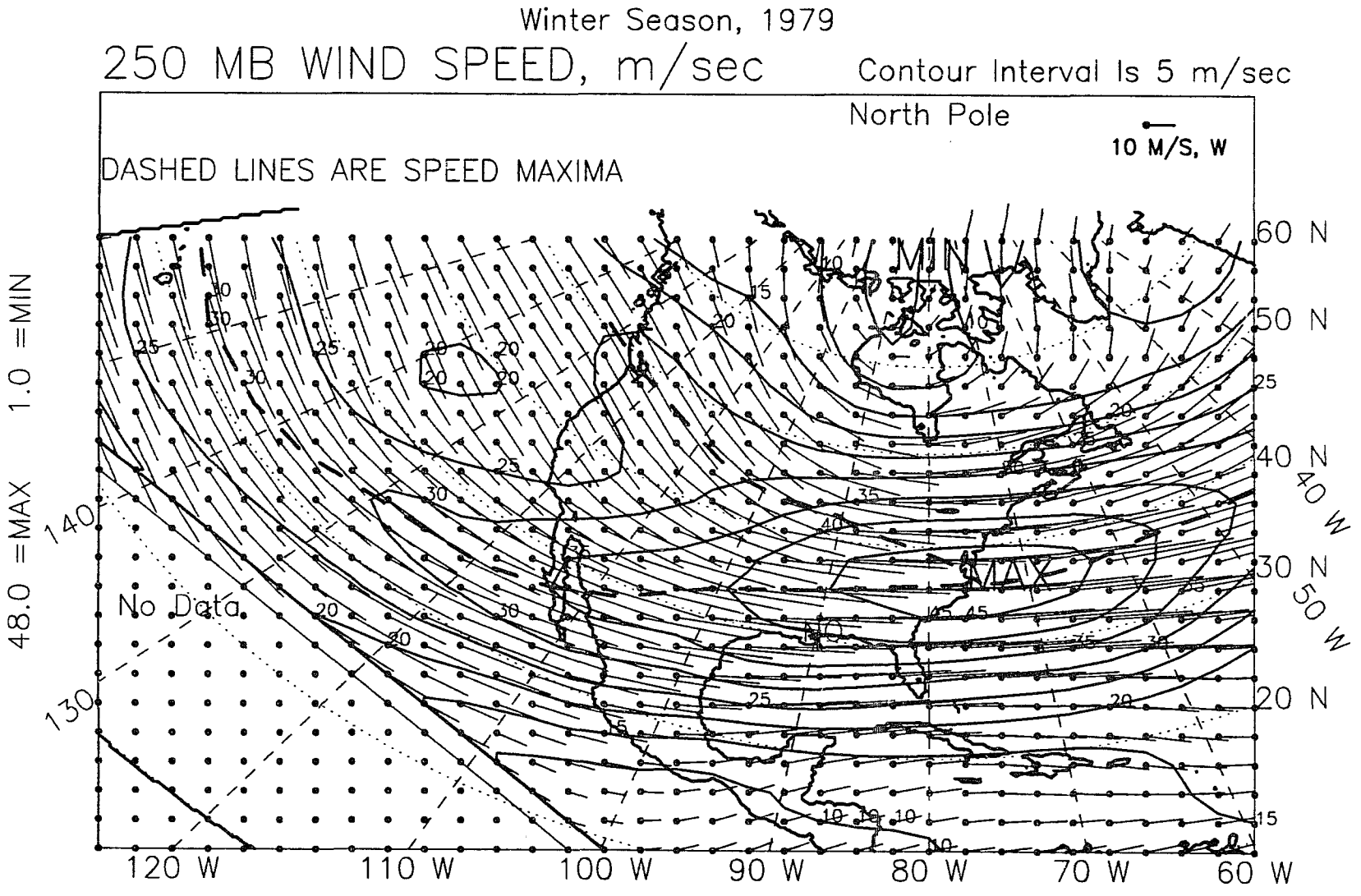

Figure 0.14: 250–mb wind speed, winter, 1979 (D78–F79).

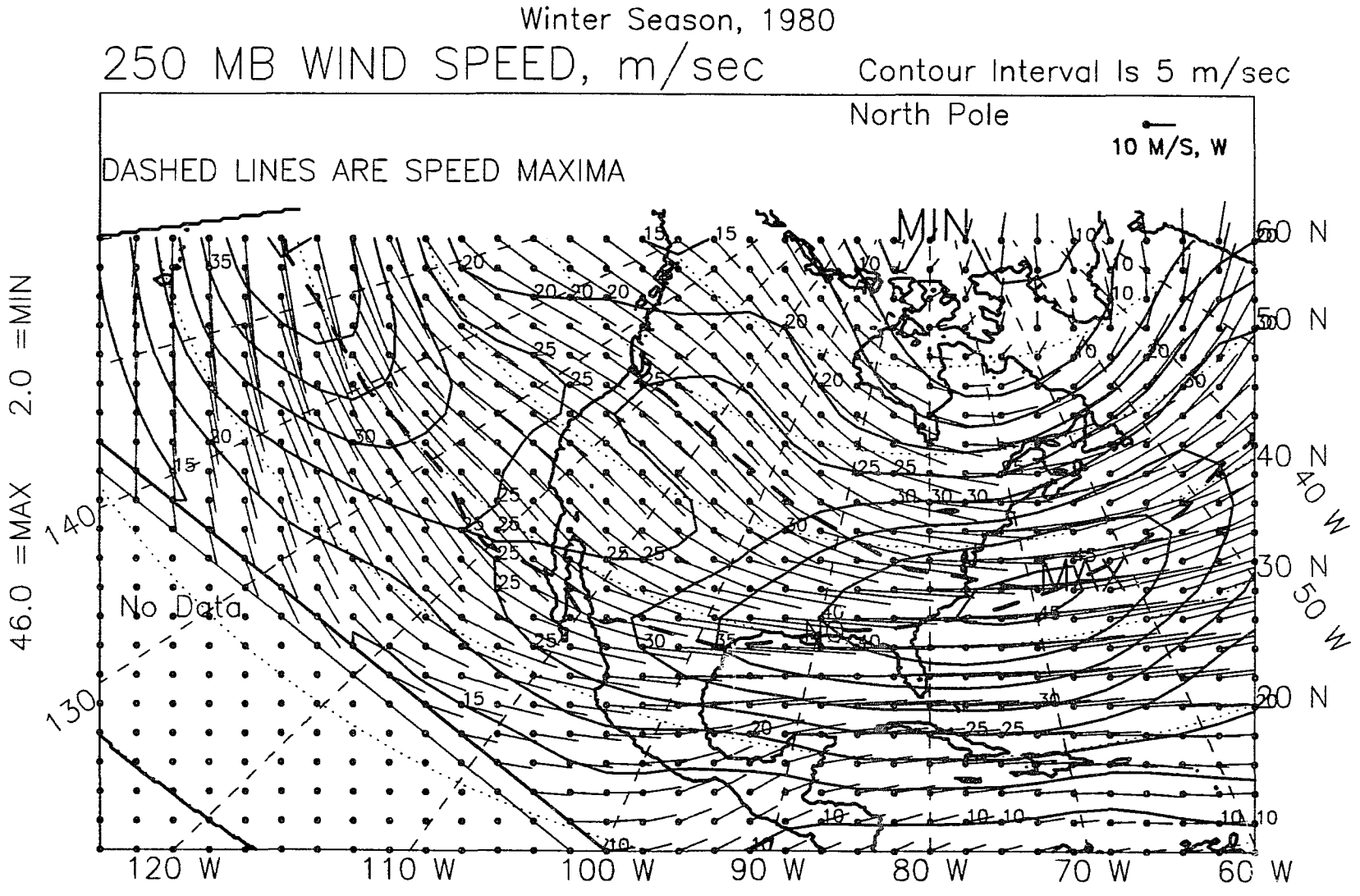

Figure 0.15: 250–mb wind speed, winter, 1980 (D79–F80).

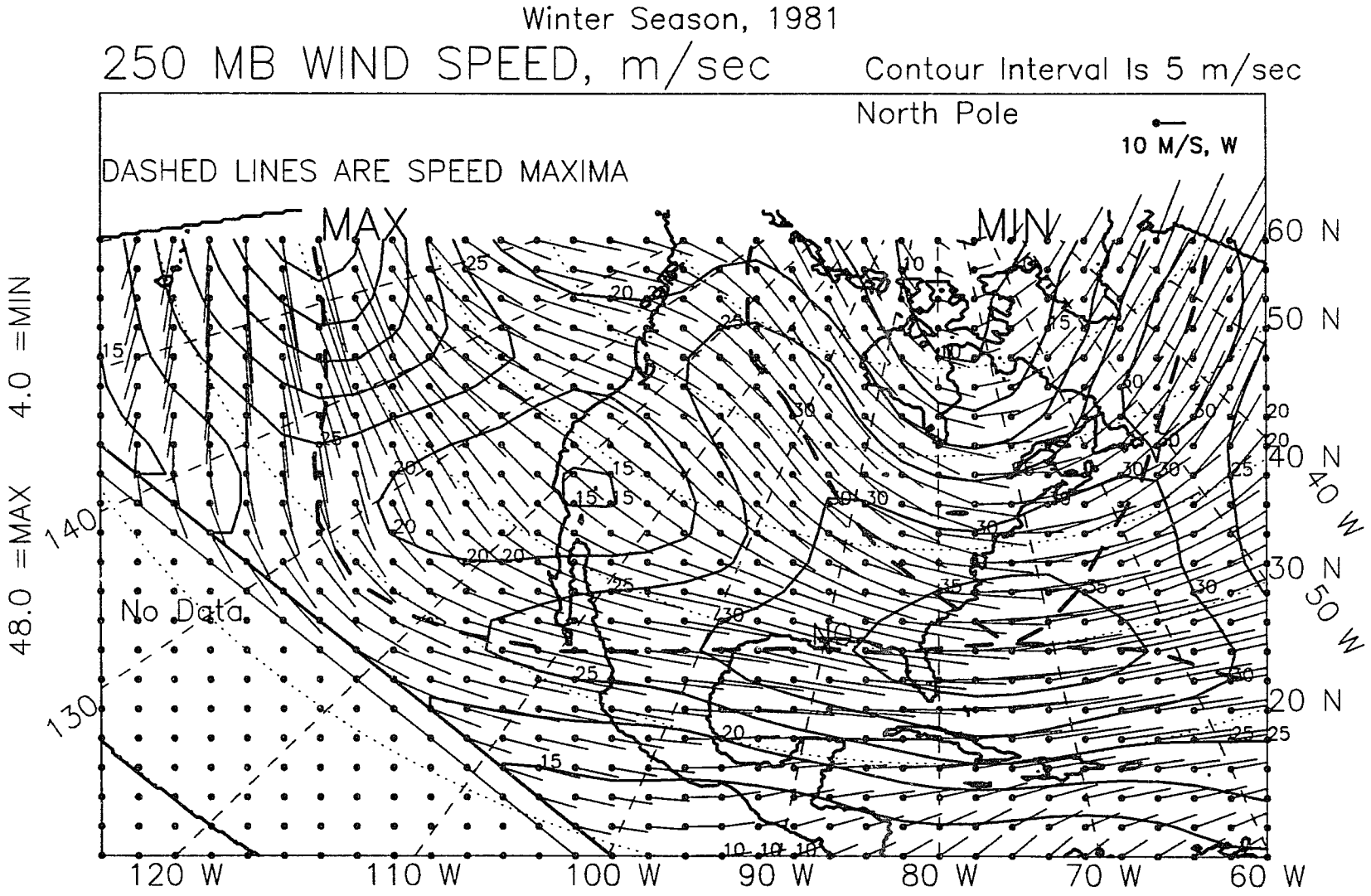

Figure 0.16: 250–mb wind speed, winter, 1981 (D80–F81).

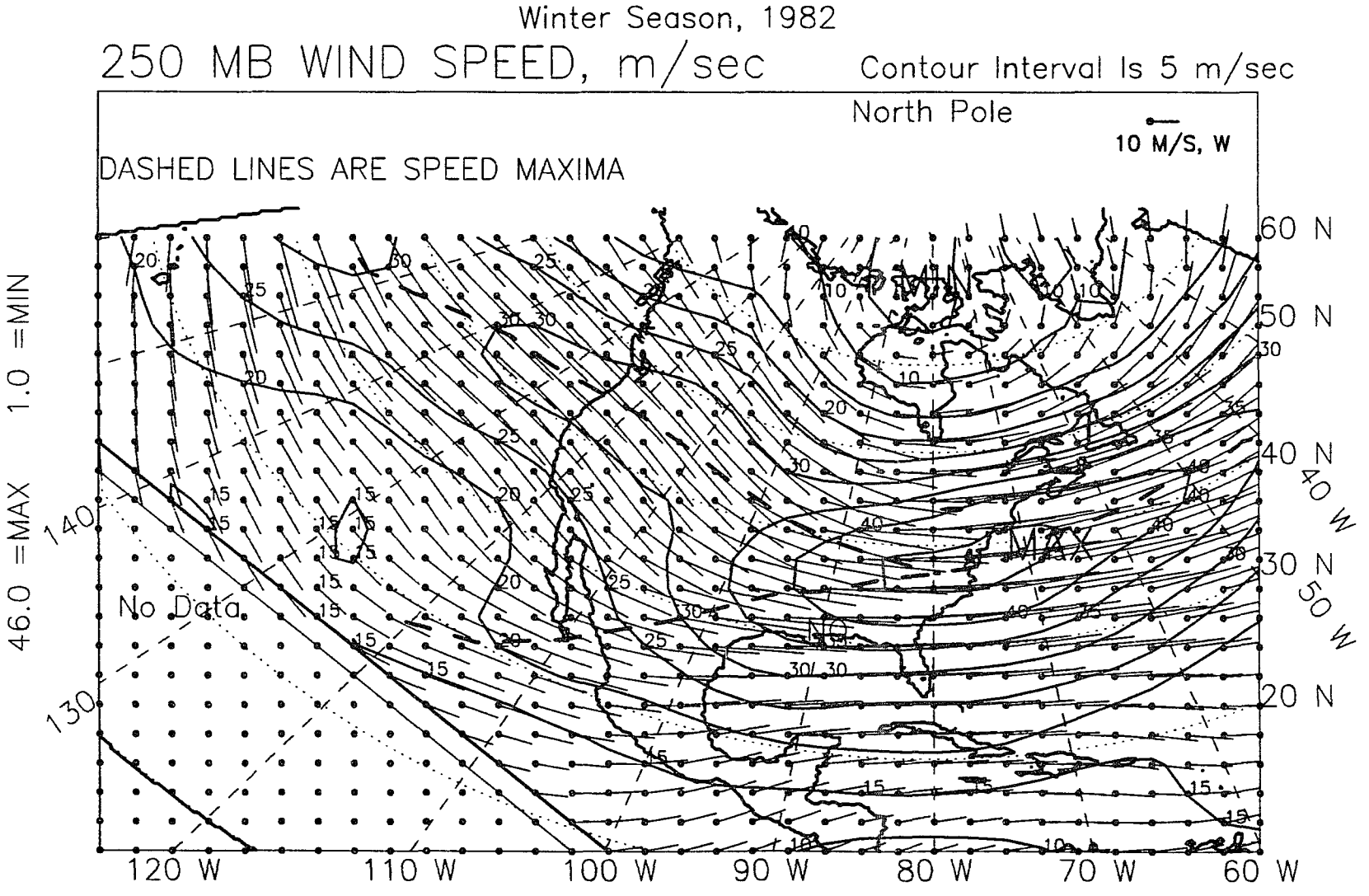

Figure 0.17: 250–mb wind speed, winter, 1982 (D81–F82).

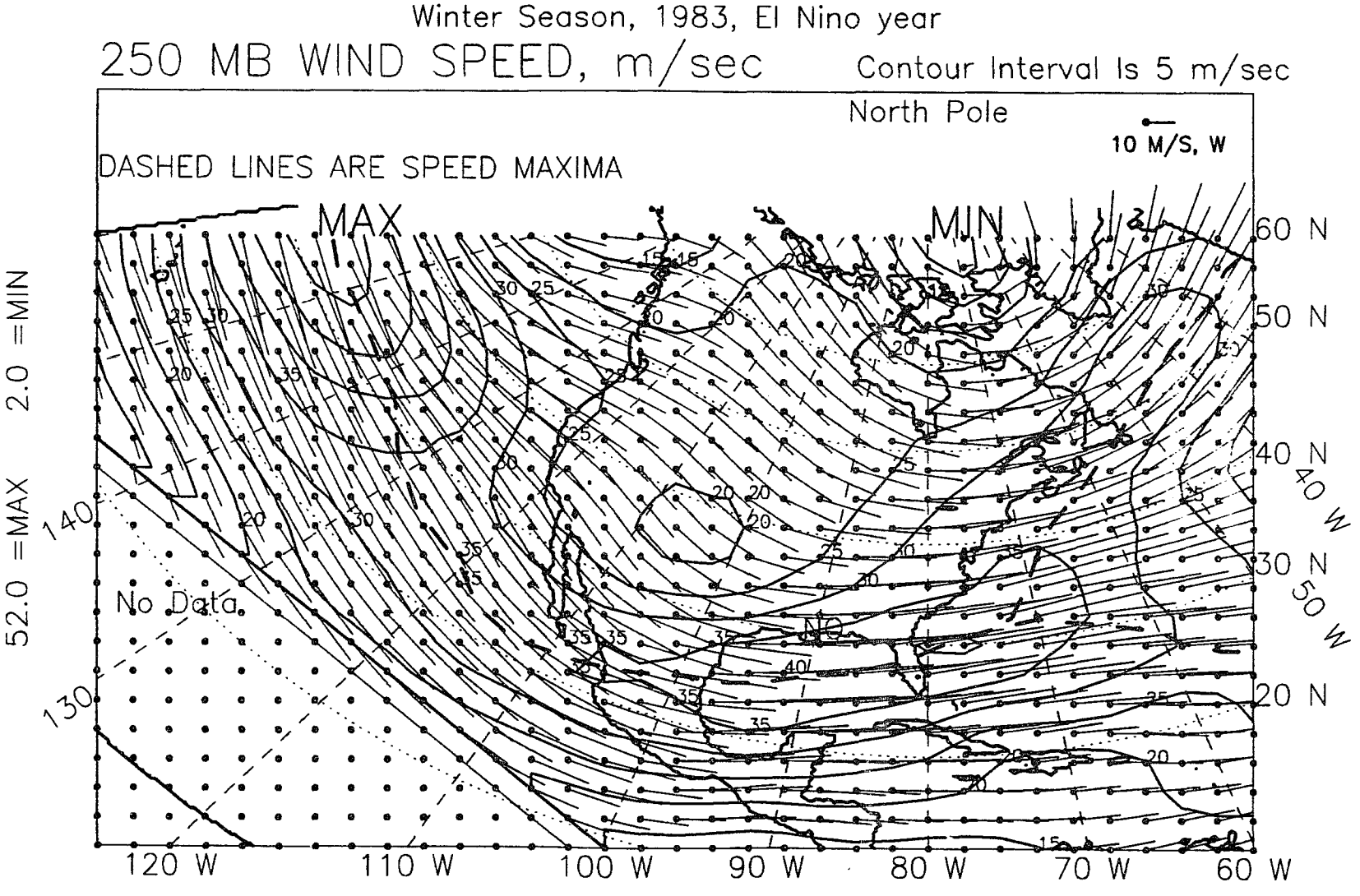

Figure 0.18: 250–mb wind speed, winter, 1983 (D82–F83) El Niño year.

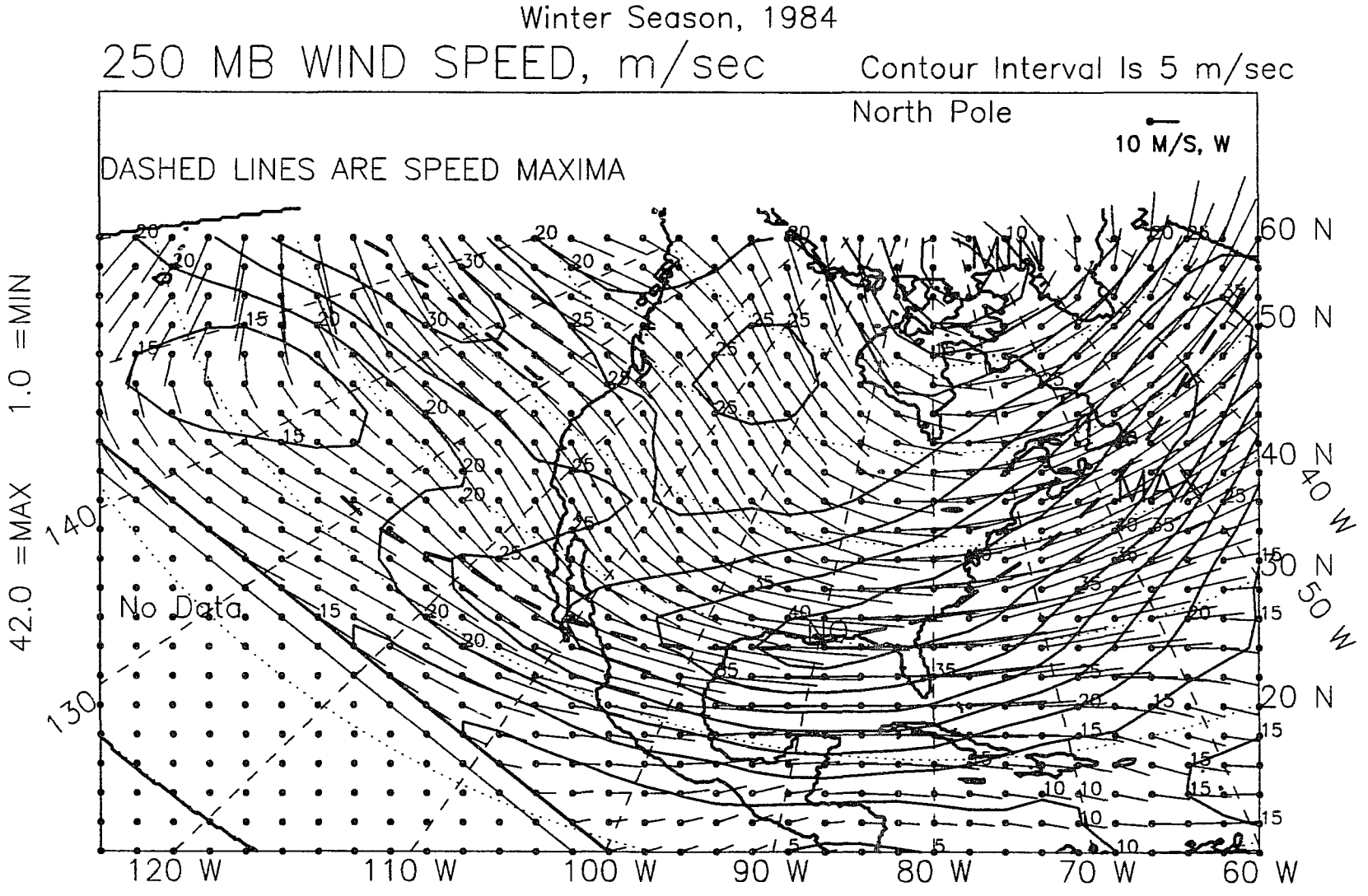

Figure 0.19: 250–mb wind speed, winter, 1984 (D83–F84).

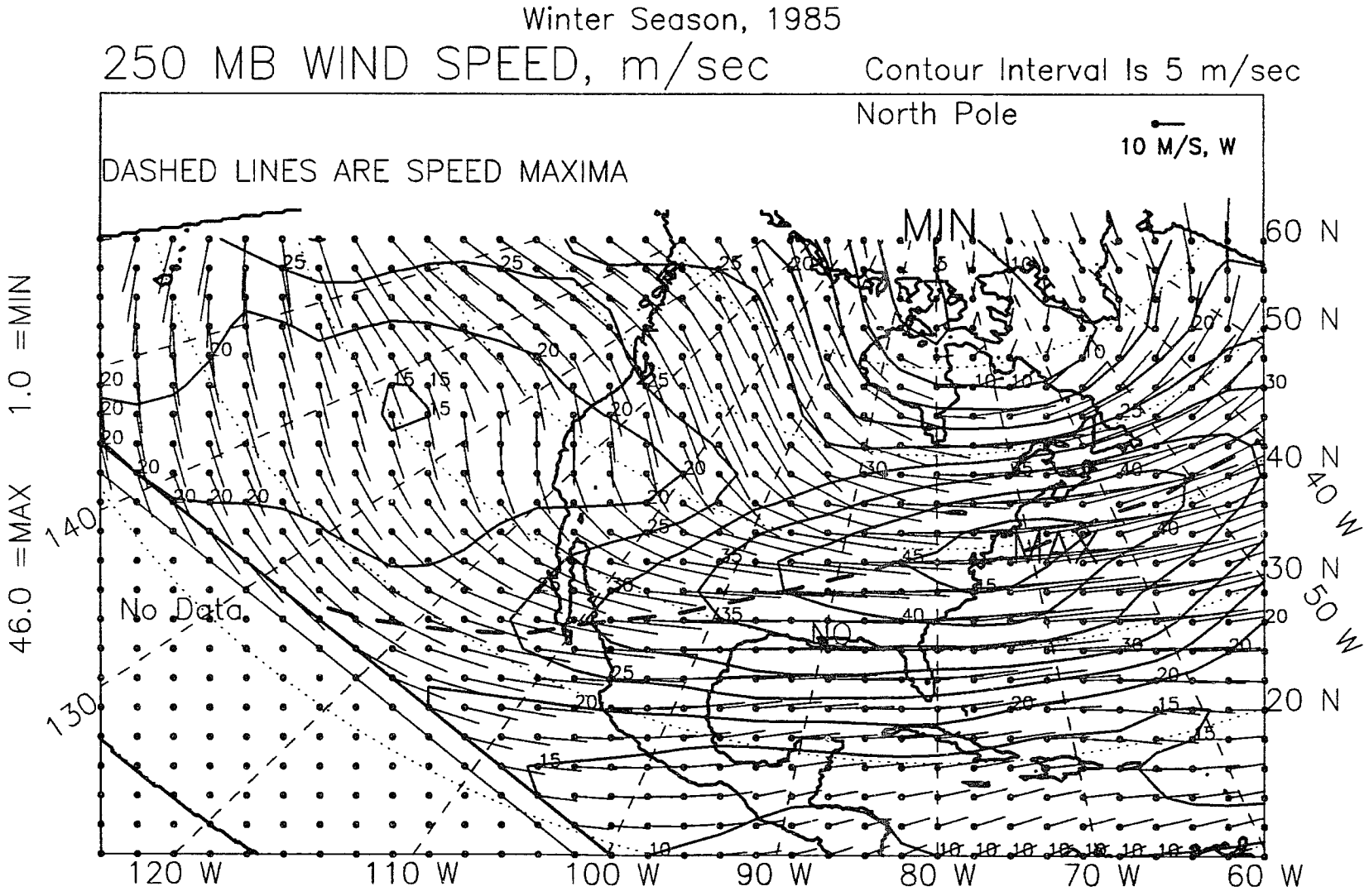

Figure 0.20: 250–mb wind speed, winter, 1985 (D84–F85).

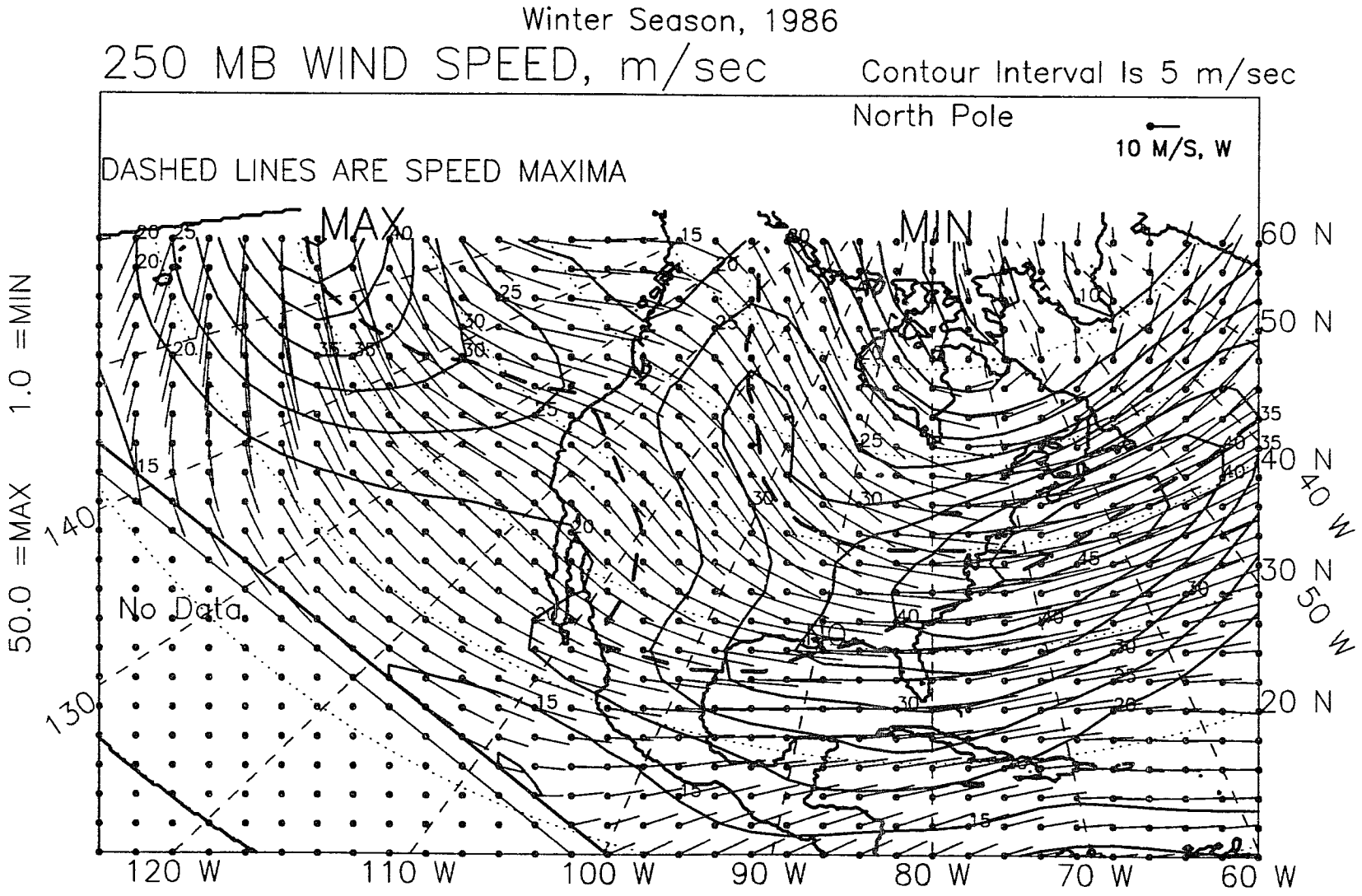

Figure 0.21: 250–mb wind speed, winter, 1986 (D85–F86).

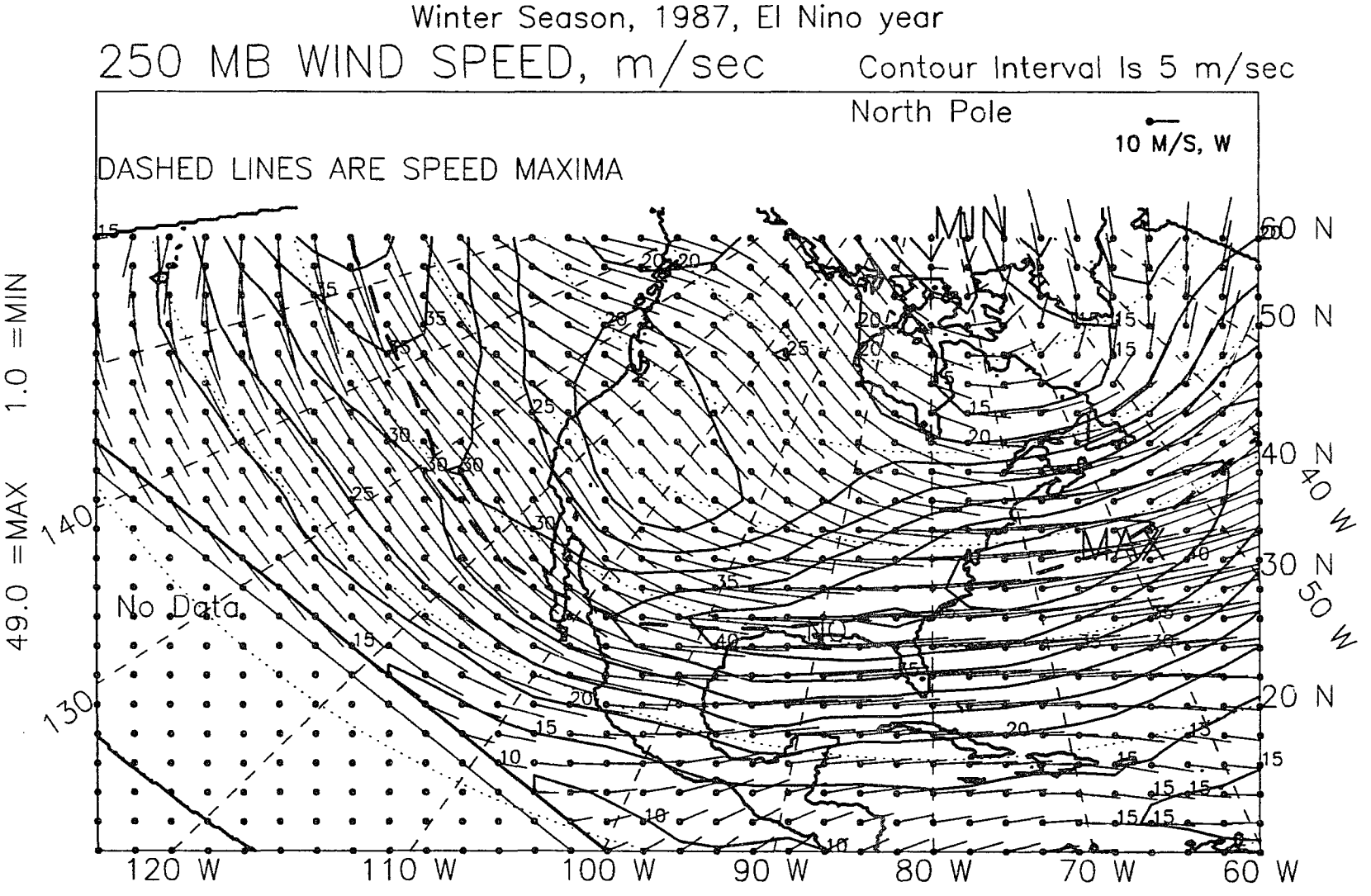

Figure 0.22: 250–mb wind speed, winter, 1987 (D86–F87) El Niño year.

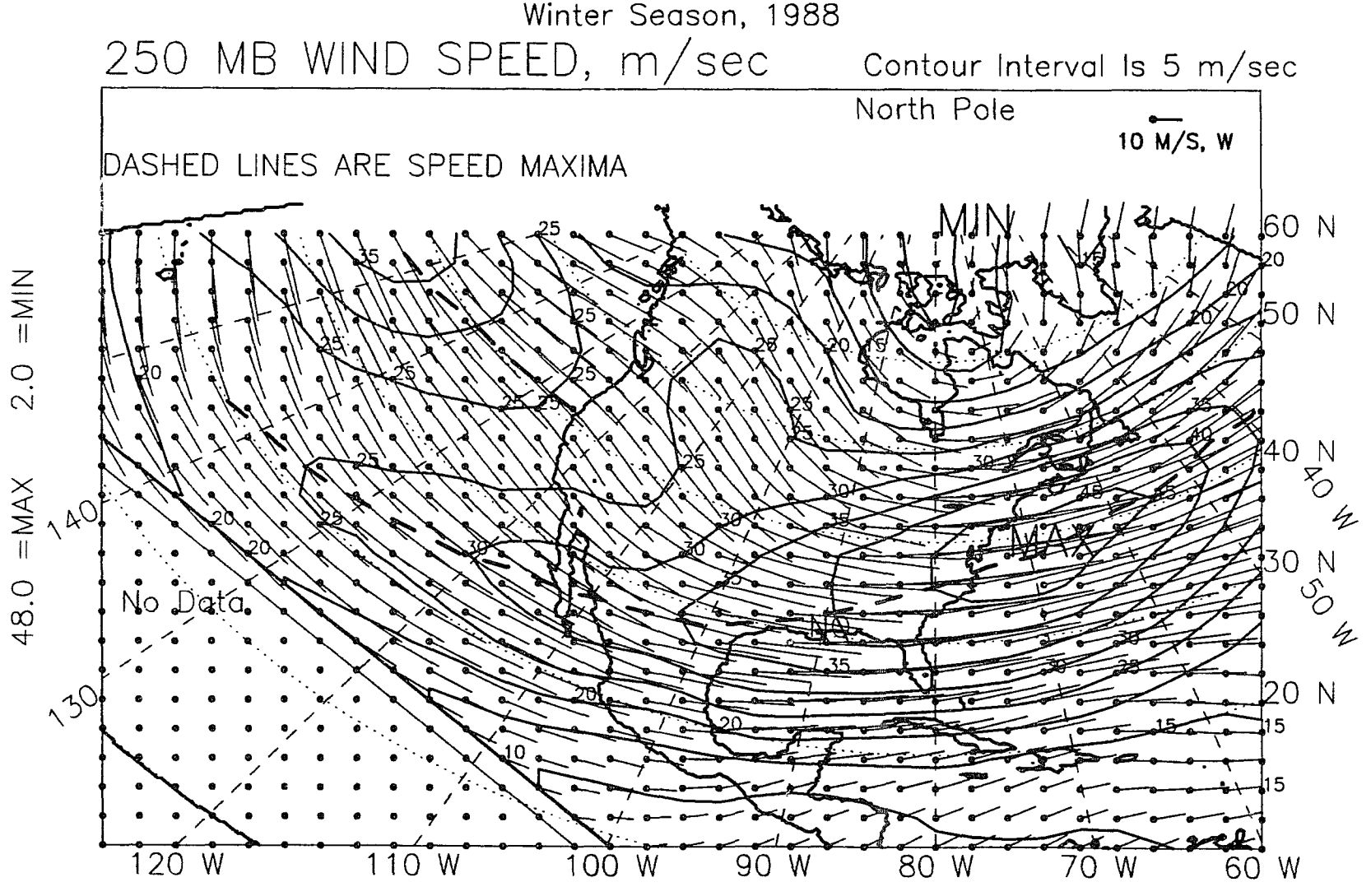

Figure 0.23: 250–mb wind speed, winter, 1988 (D87–F88).

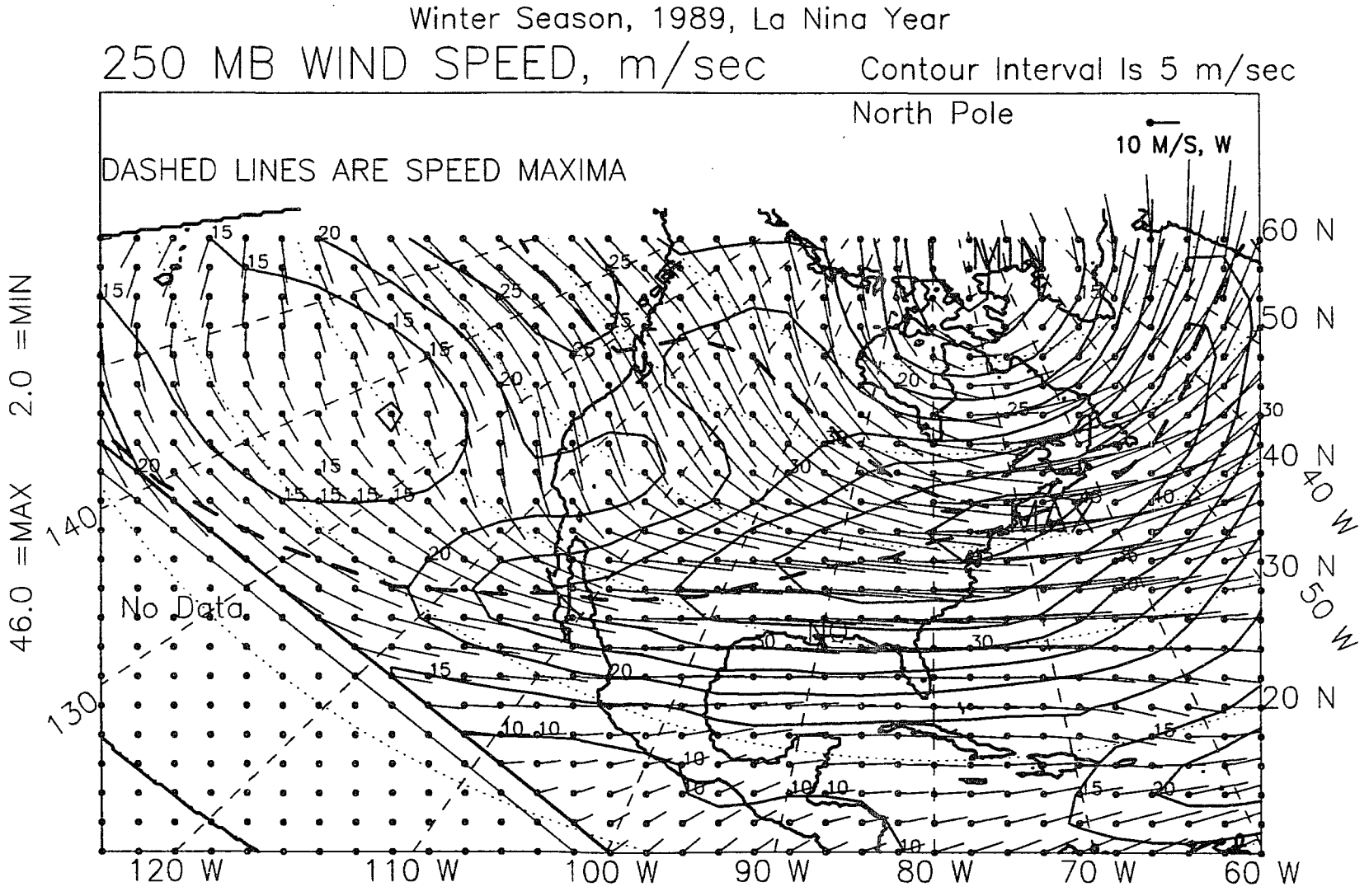

Figure 0.24: 250–mb wind speed, winter, 1989 (D88–F89) La Niña year.

APPENDIX P
STORM LOCATIONS: 1960-89

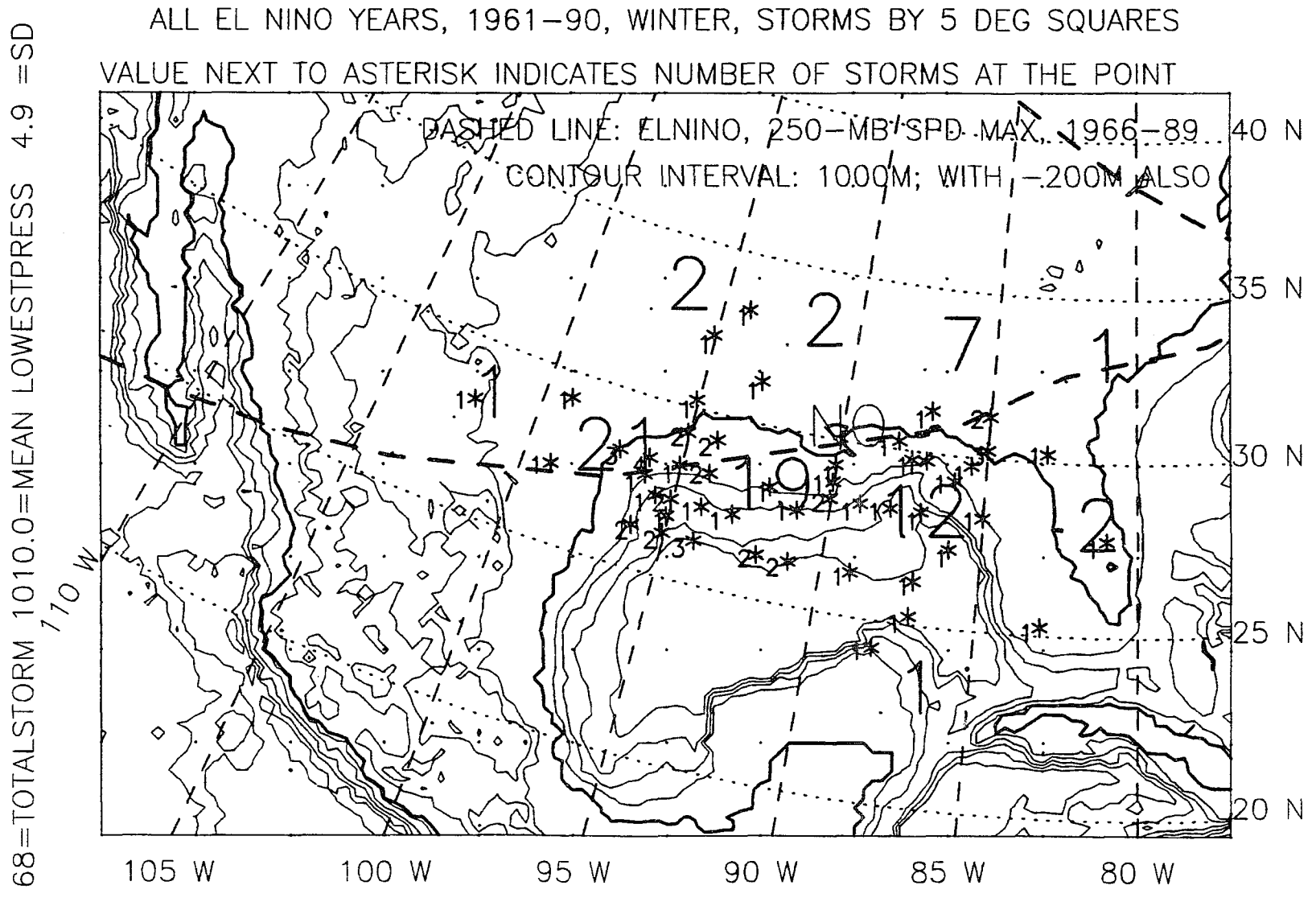

Figure P.1: Storm locations, winter, 5 El Niño years, 1961–90.

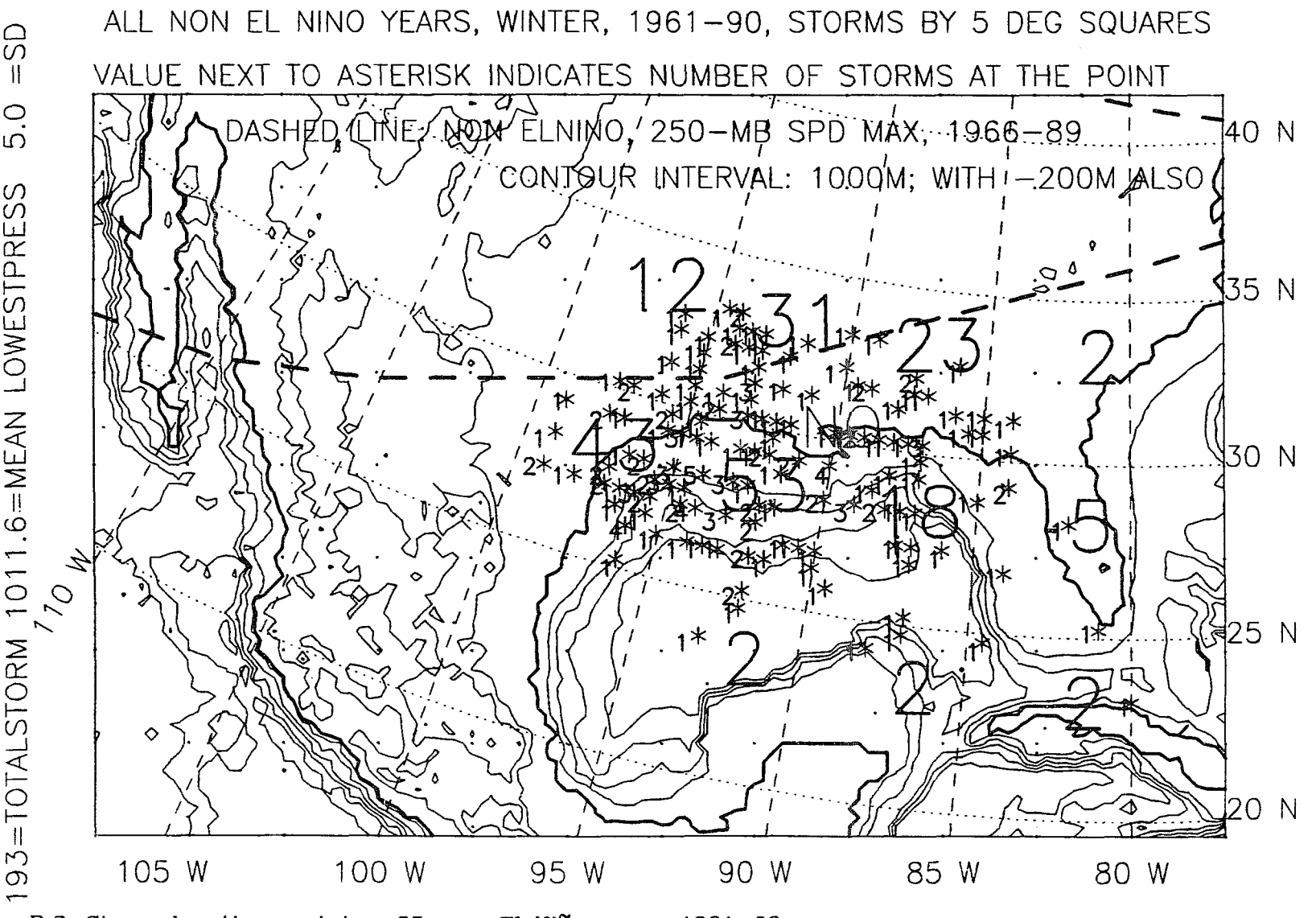

Figure P.2: Storm locations, winter, 25 non-El Niño years, 1961-90.

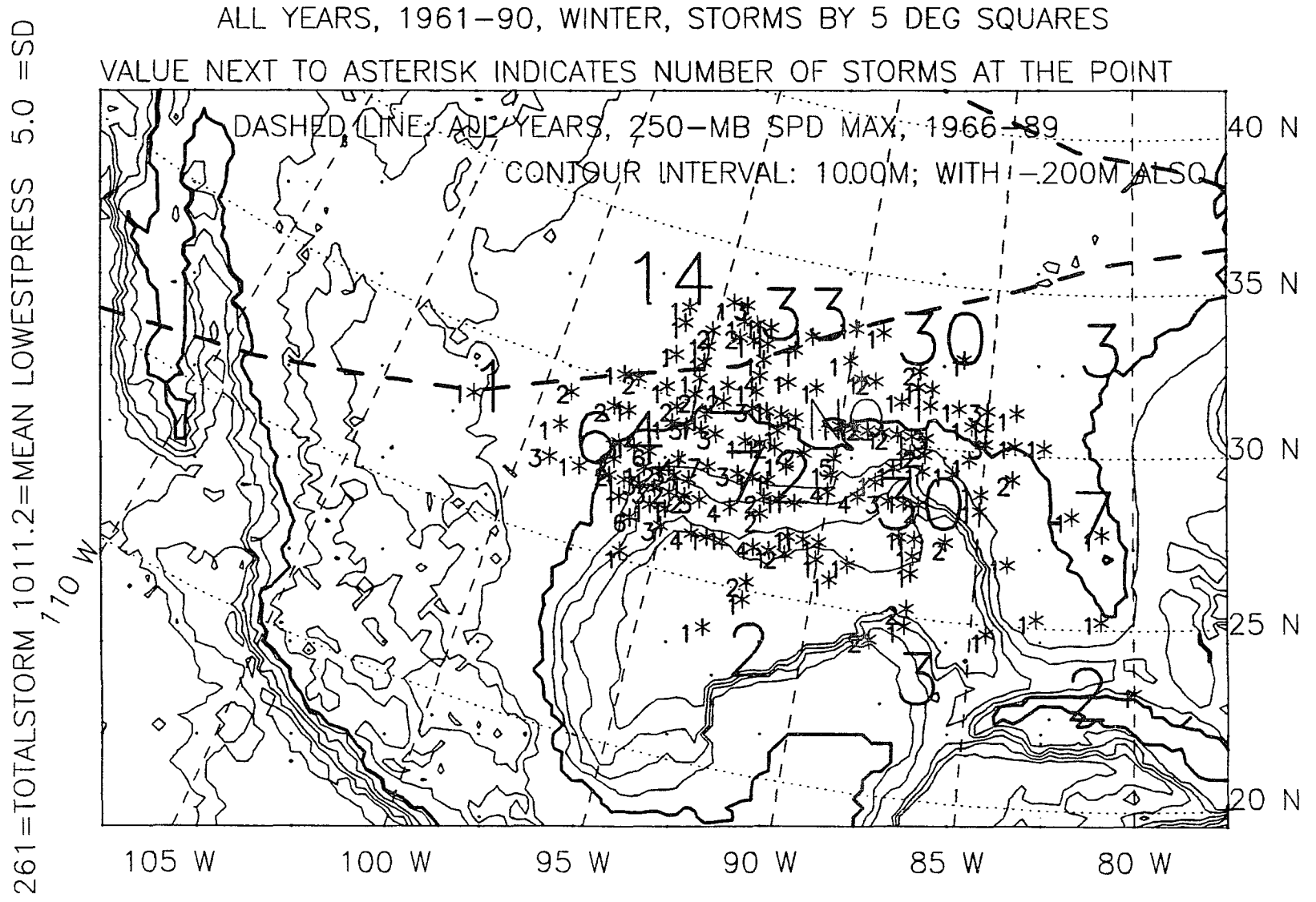

Figure P.3: Storm locations, winter, all 30 years, 1961–90.

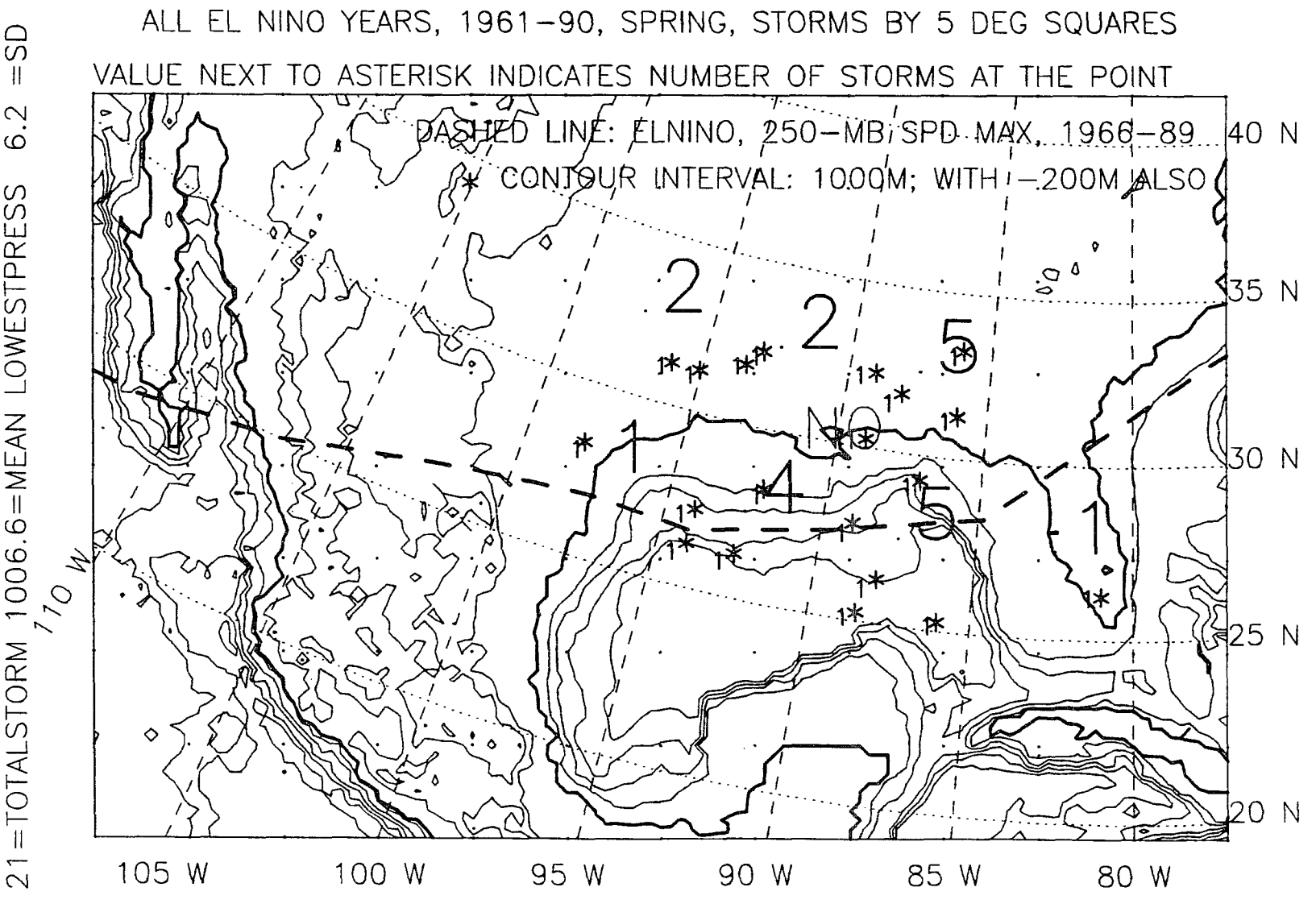

Figure P.4: Storm locations, spring, 6 El Niño springs, 1961–90.

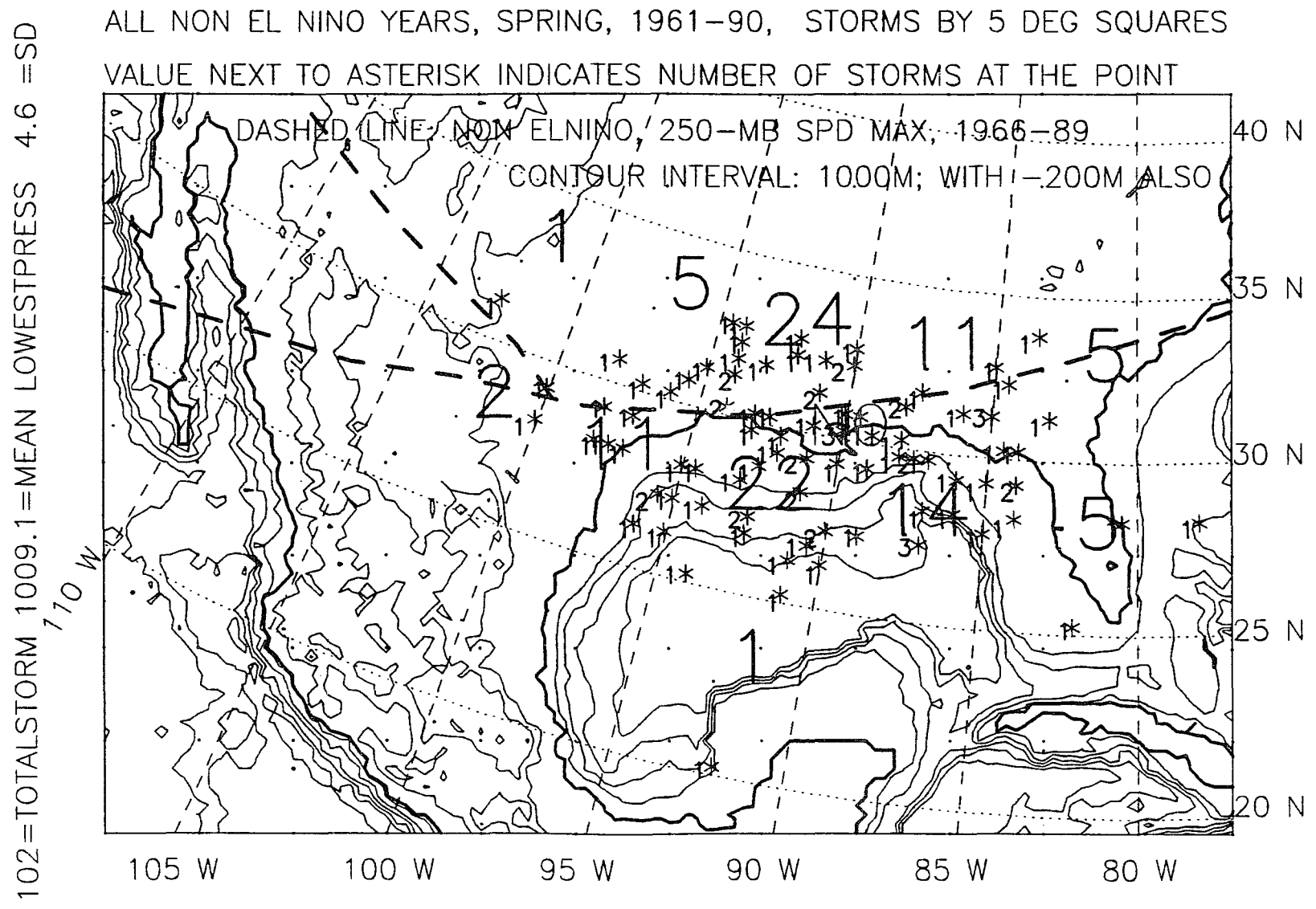

Figure P.5: Storm locations, spring, 24 non-El Niño springs, 1961-90.

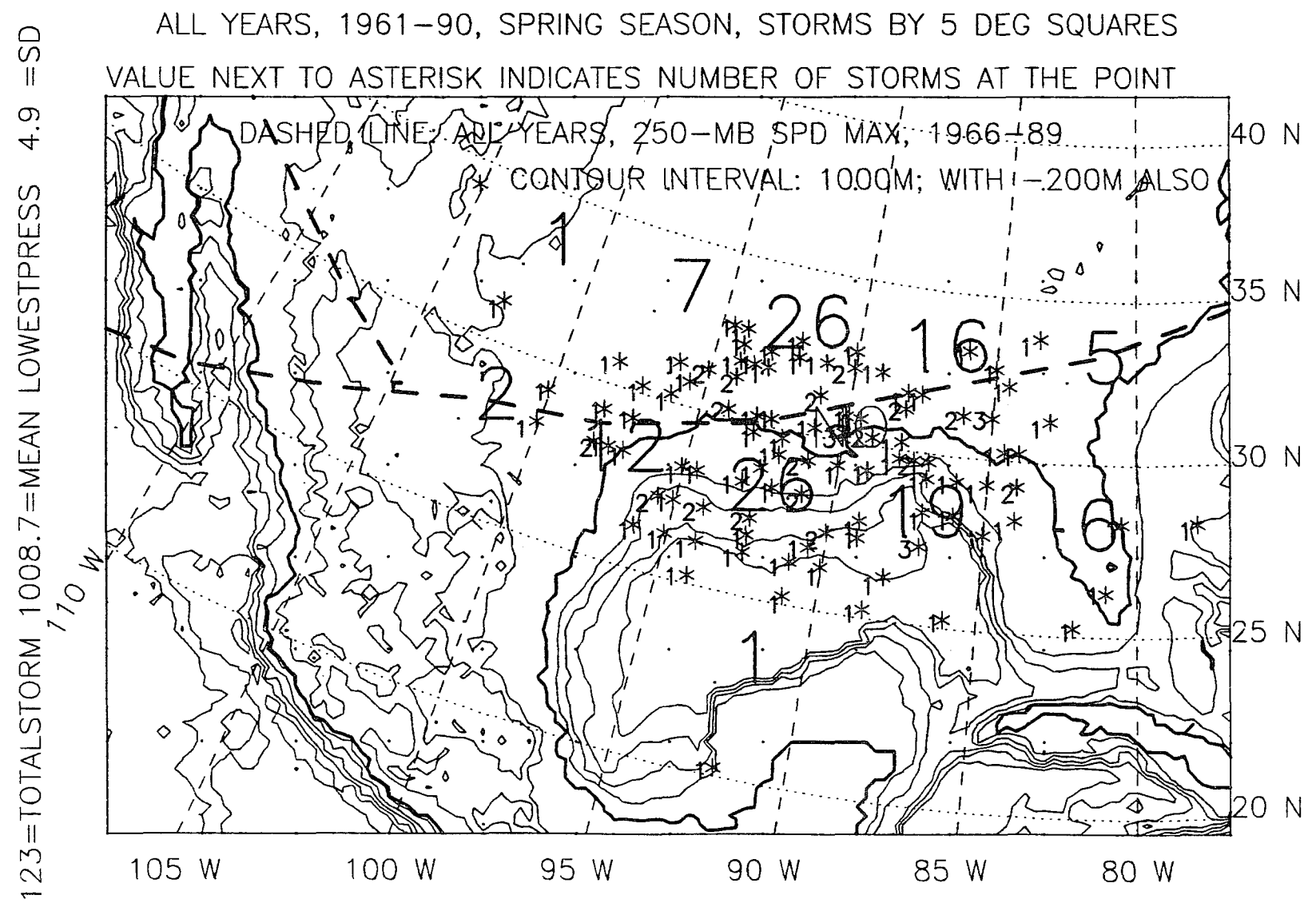

Figure P.6: Storm locations, spring, all 30 springs, 1961–90.

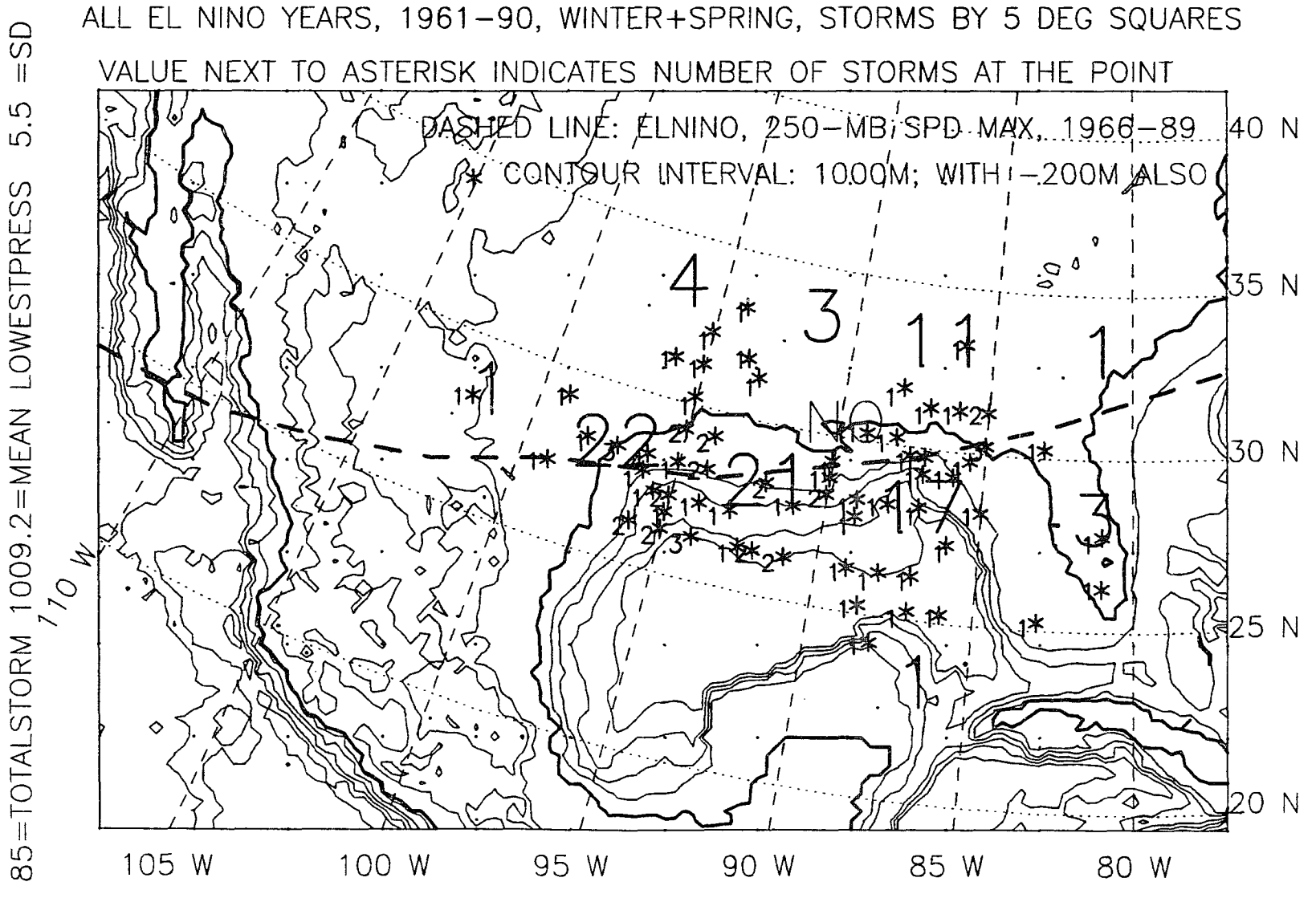

Figure P.7: Storm locations, winter-plus-spring, 5 El Niño years, 1961-90.

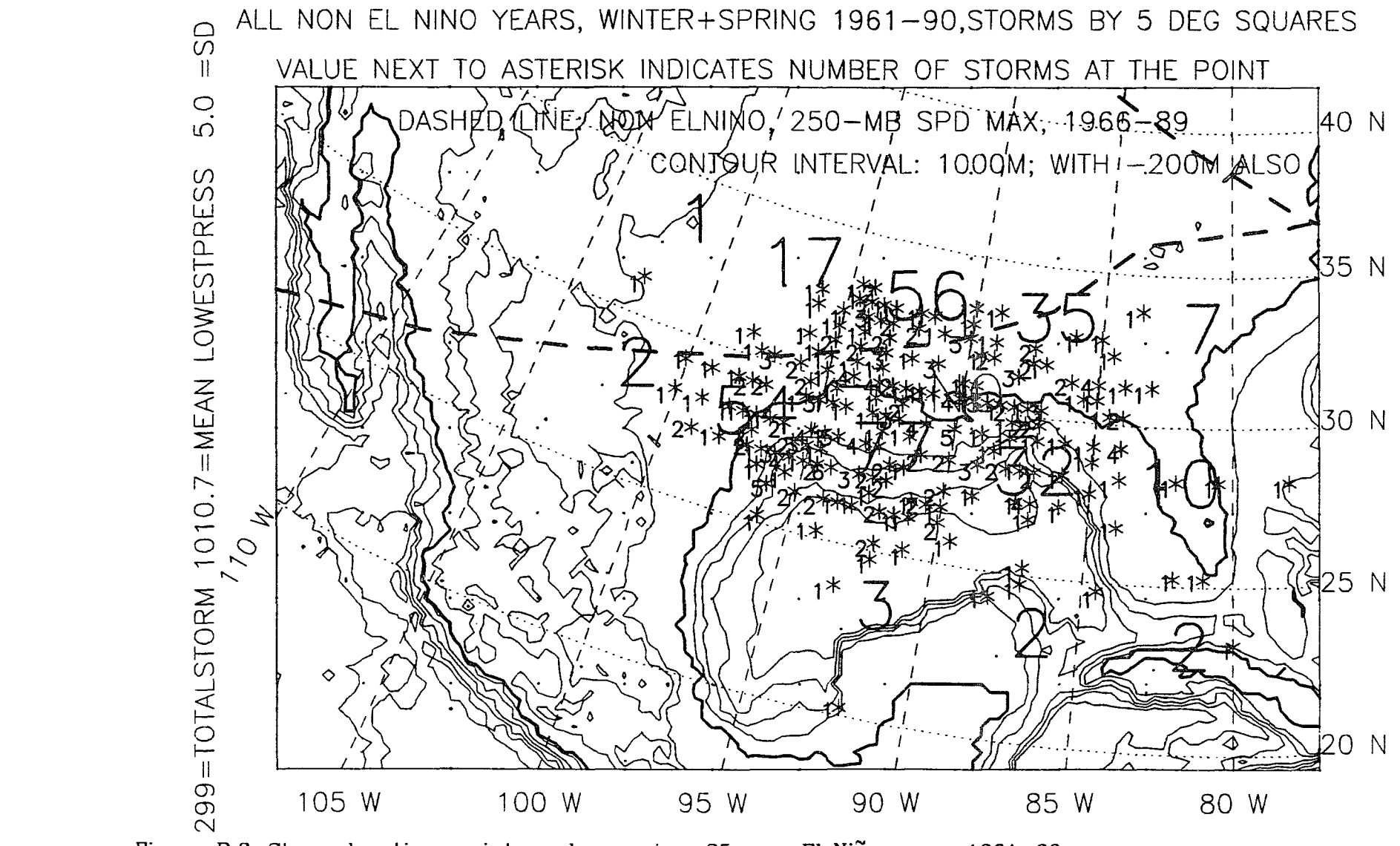

Figure P.8: Storm locations, winter-plus-spring, 25 non-El Niño years, 1961-90.

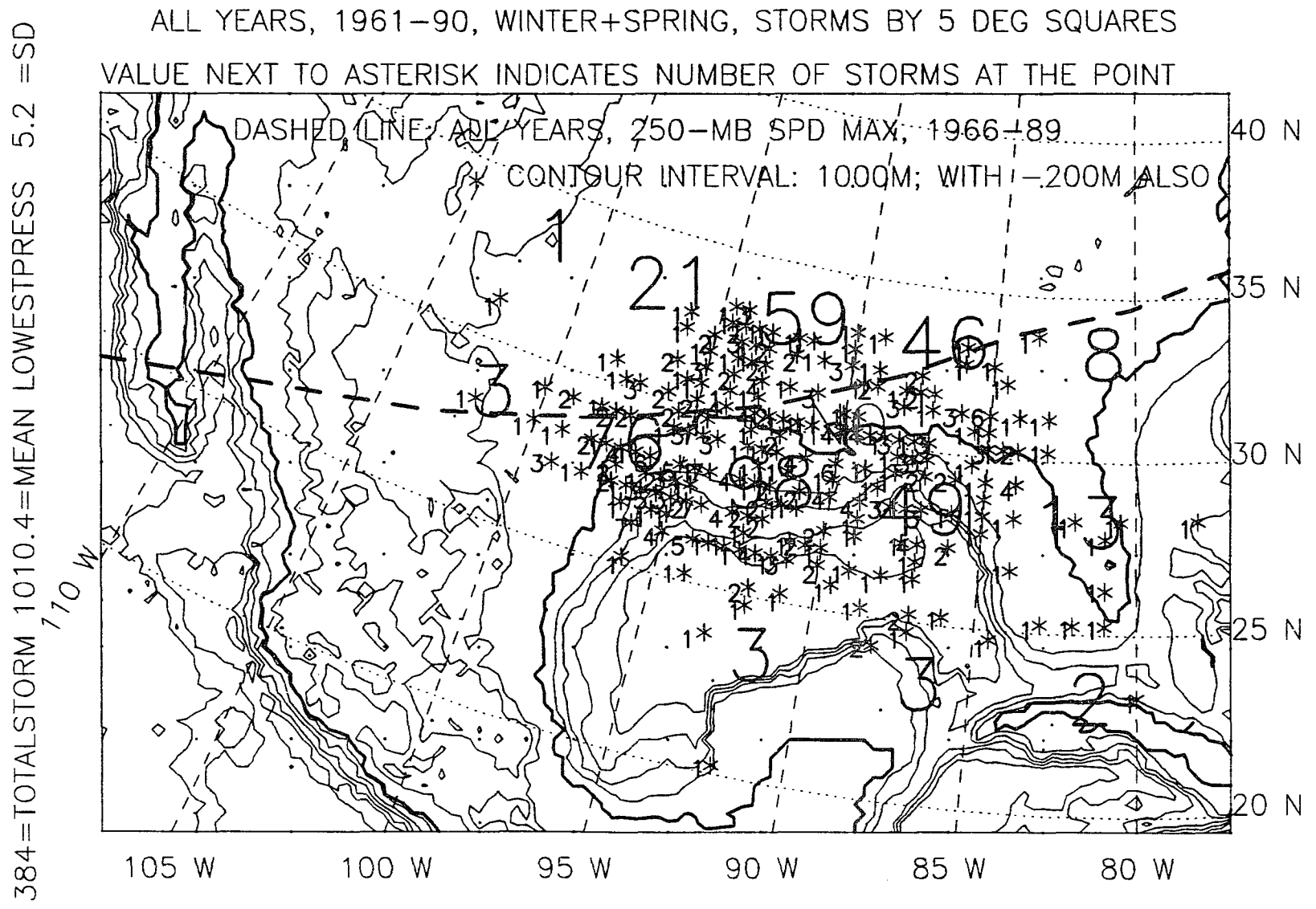

Figure P.9: Storm locations, winter–plus–spring, all 30 years, 1961–90.

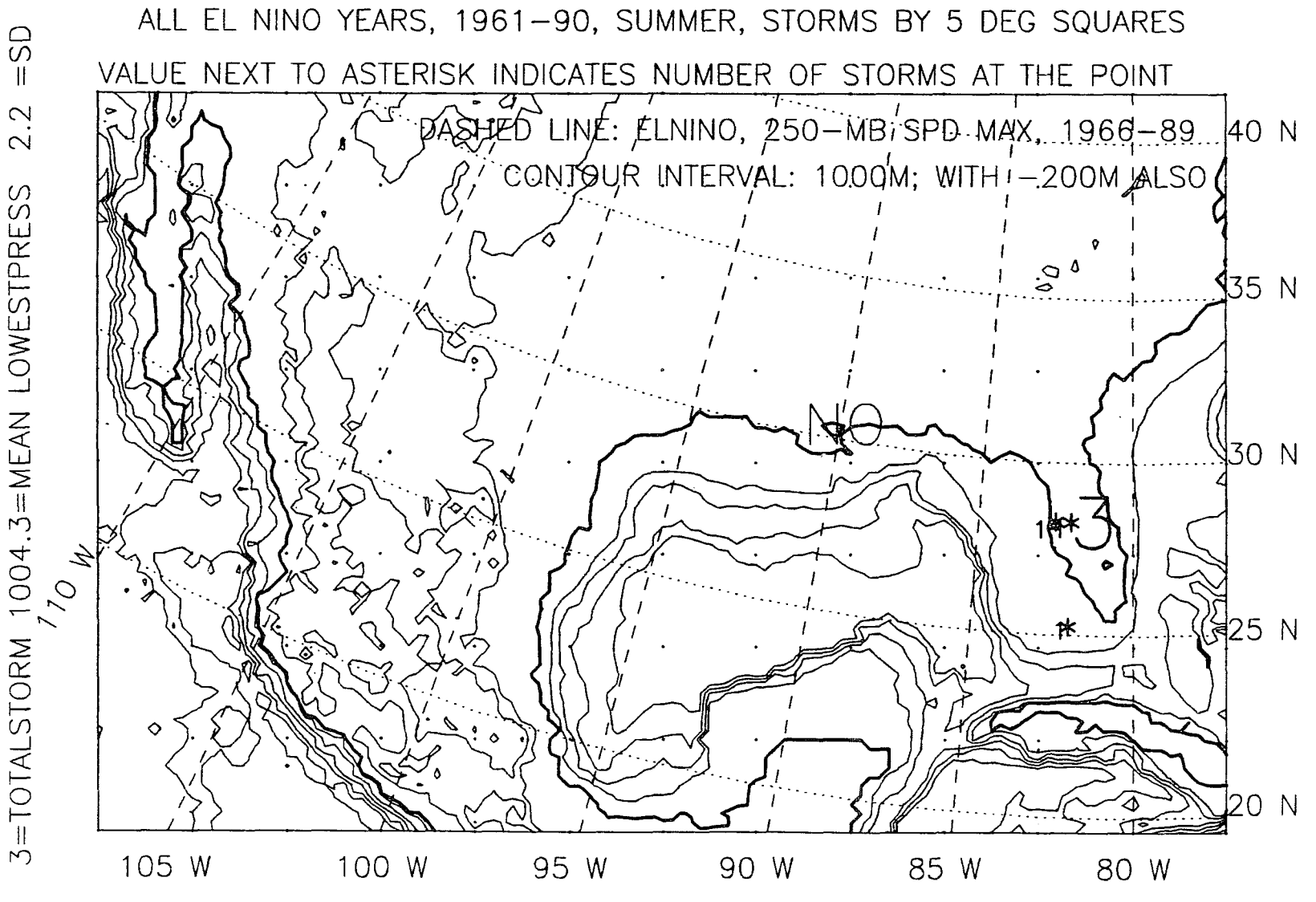

Figure P.10: Storm locations, summer, 5 El Niño years, 1961–90.

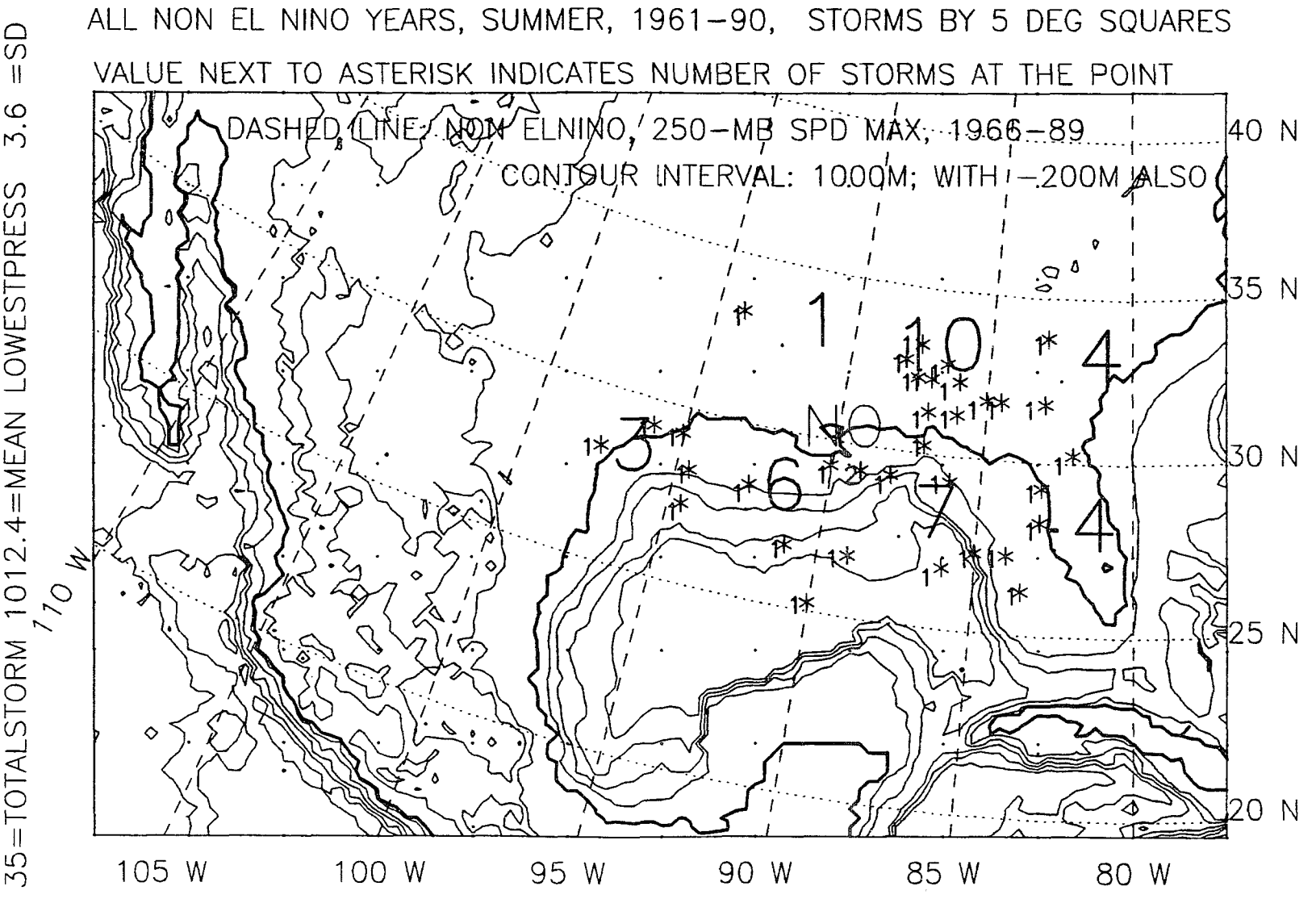

Figure P.11: Storm locations, summer, 25 non–El Niño years, 1961–90.

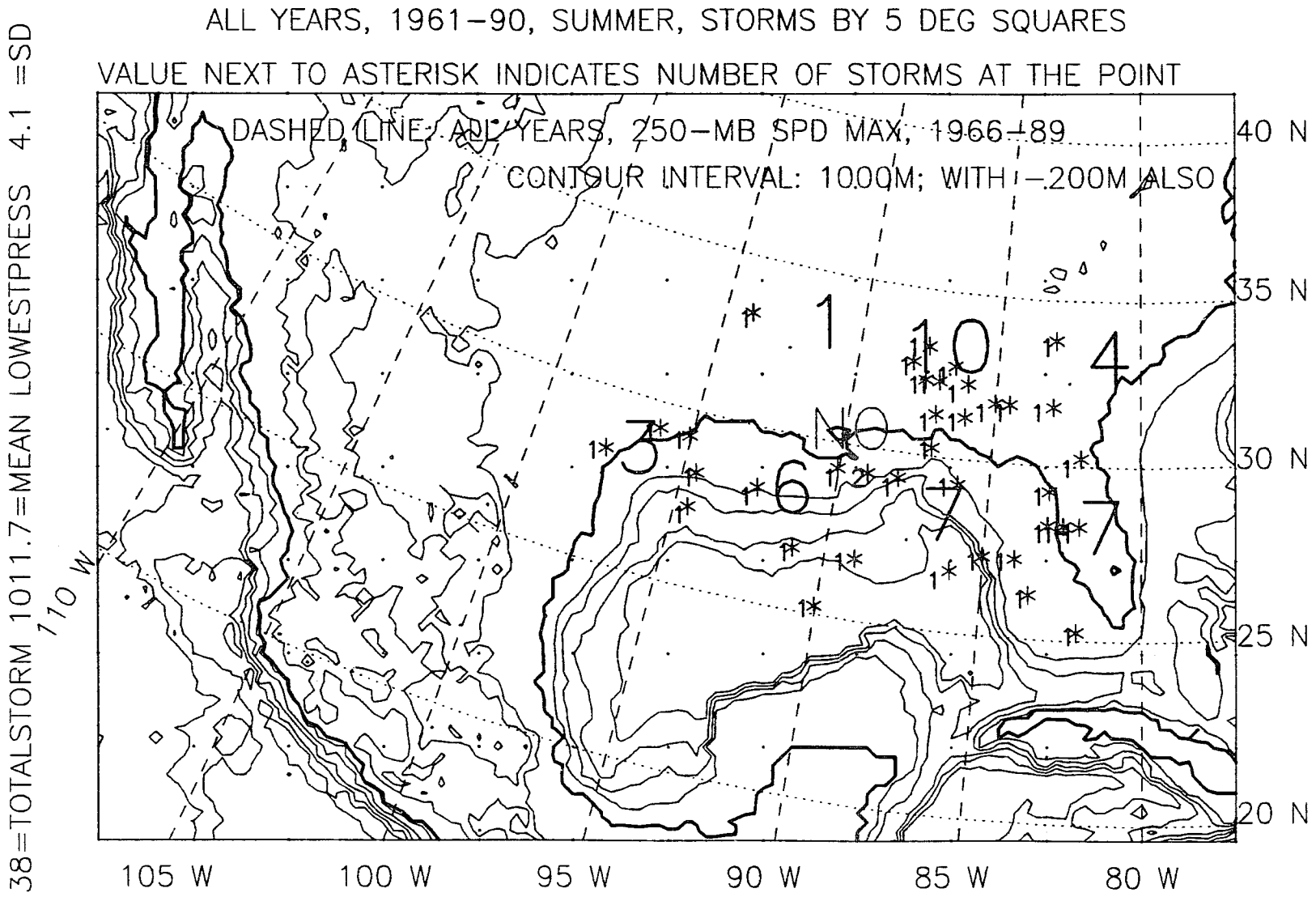

Figure P.12: Storm locations, summer, all 30 years, 1961–90.

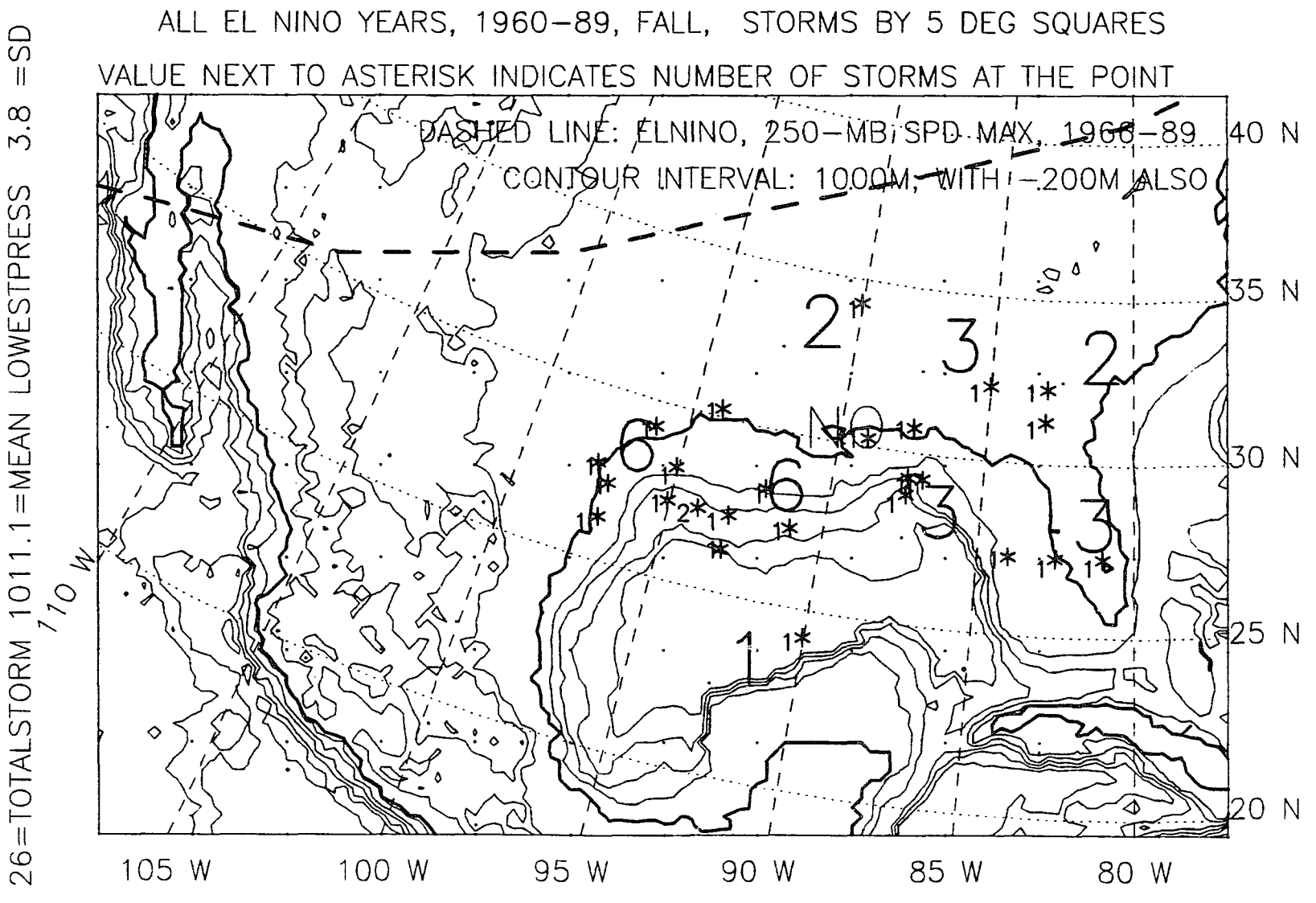

Figure P.13: Storm locations, fall, 5 El Niño years, 1960–89.

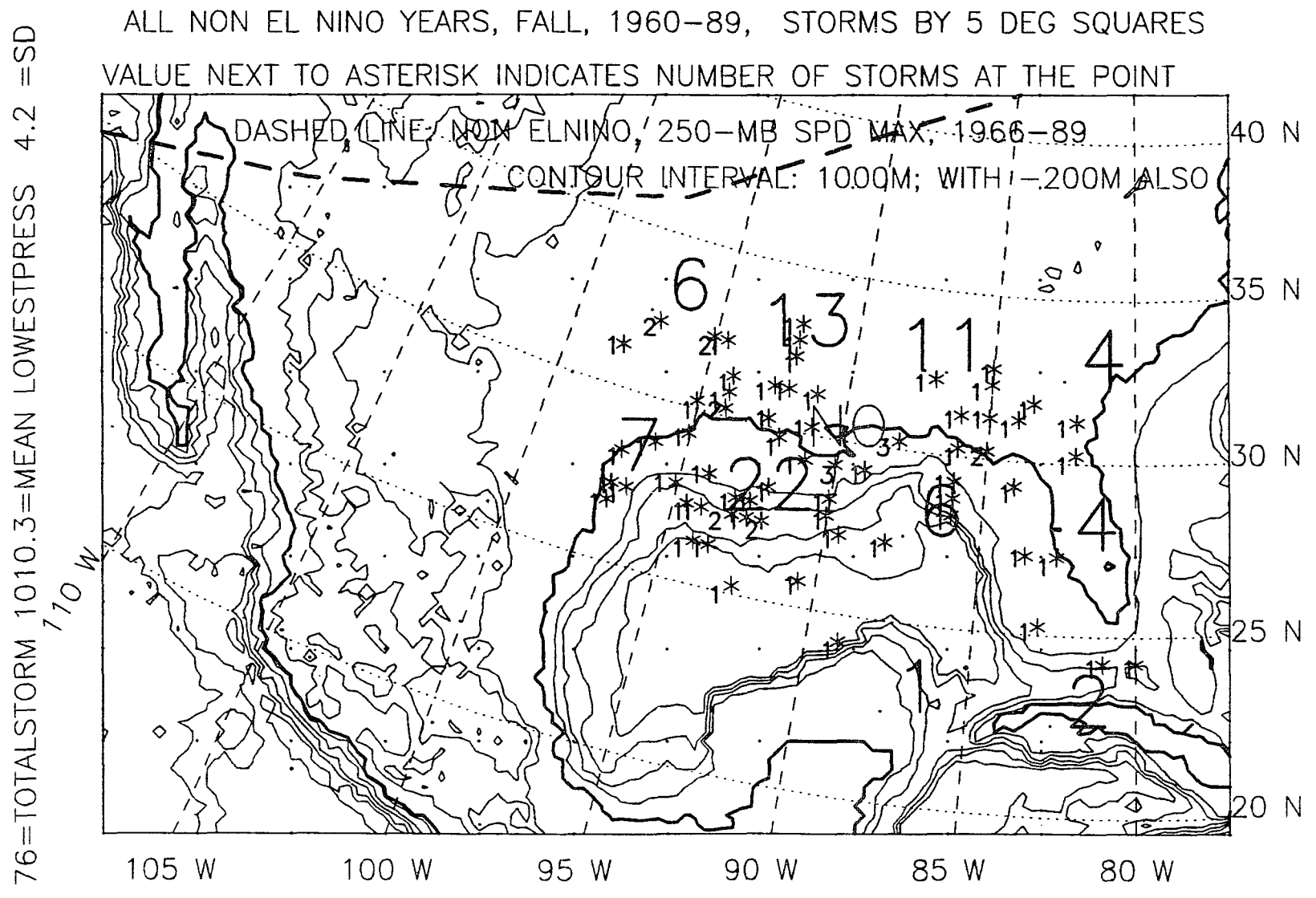

Figure P.14: Storm locations, fall, 25 non–El Niño years, 1960–89.

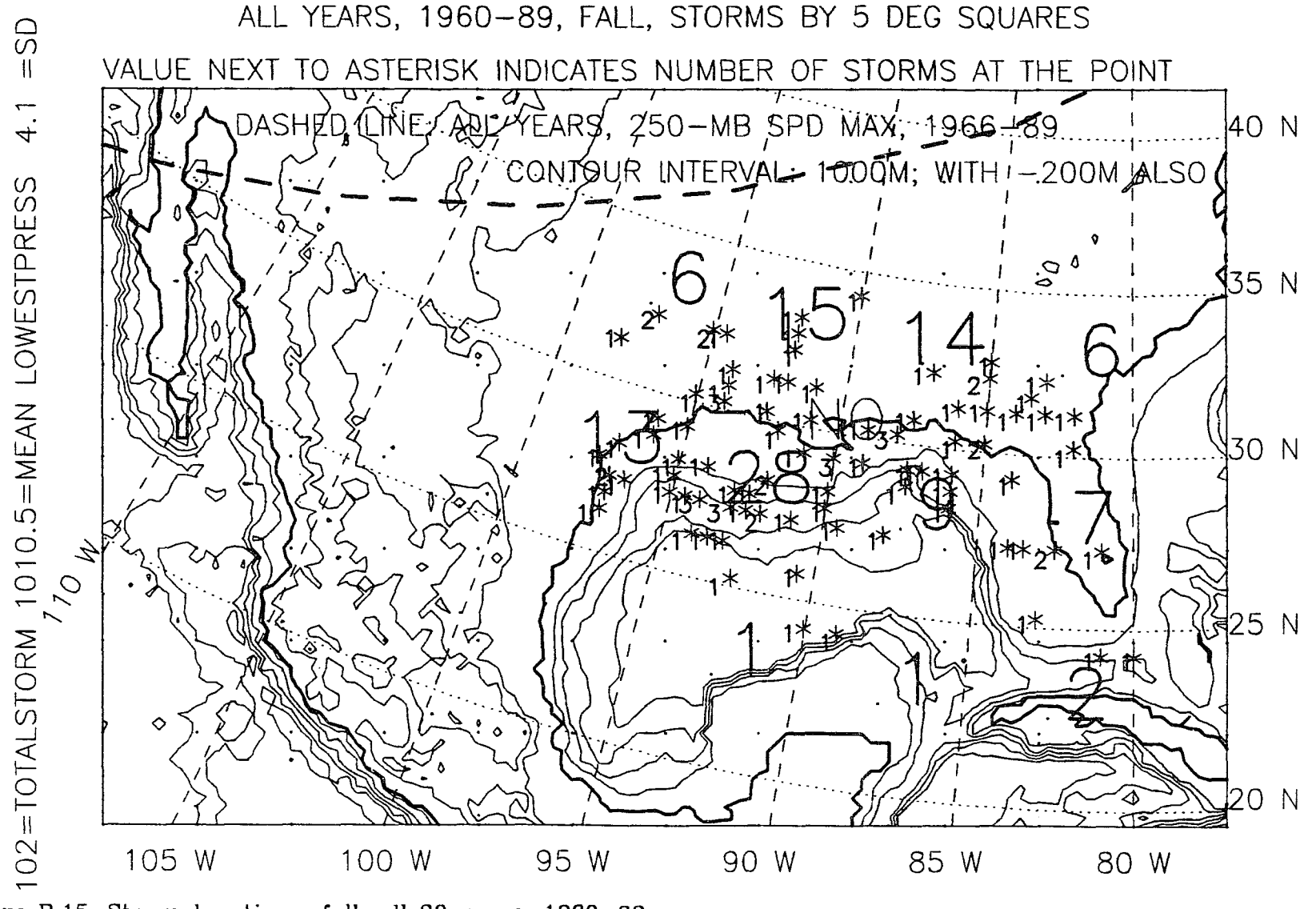

Figure P.15: Storm locations, fall, all 30 years, 1960–89.

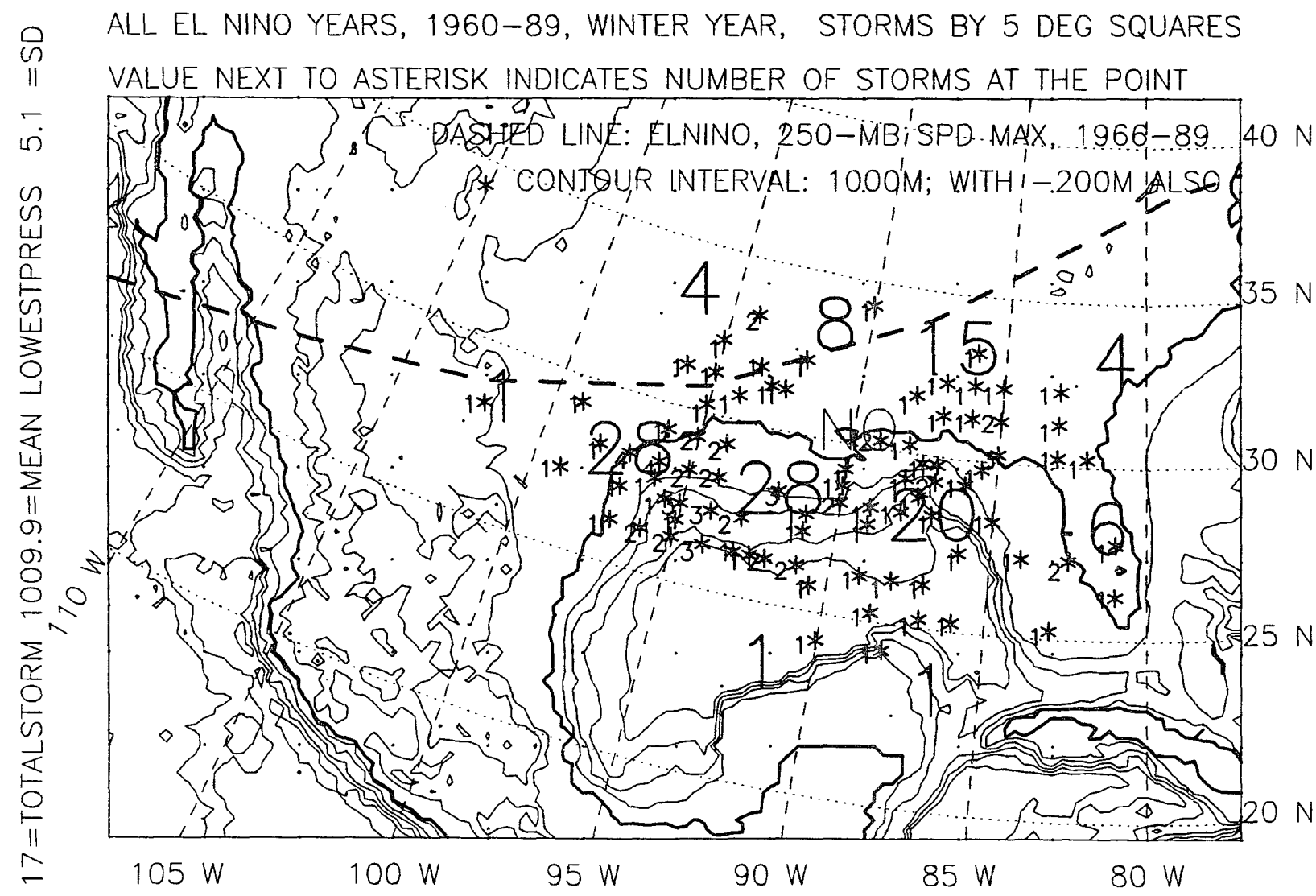

Figure P.16: Storm locations, winter year, 5 El Niño years, 1960–89.

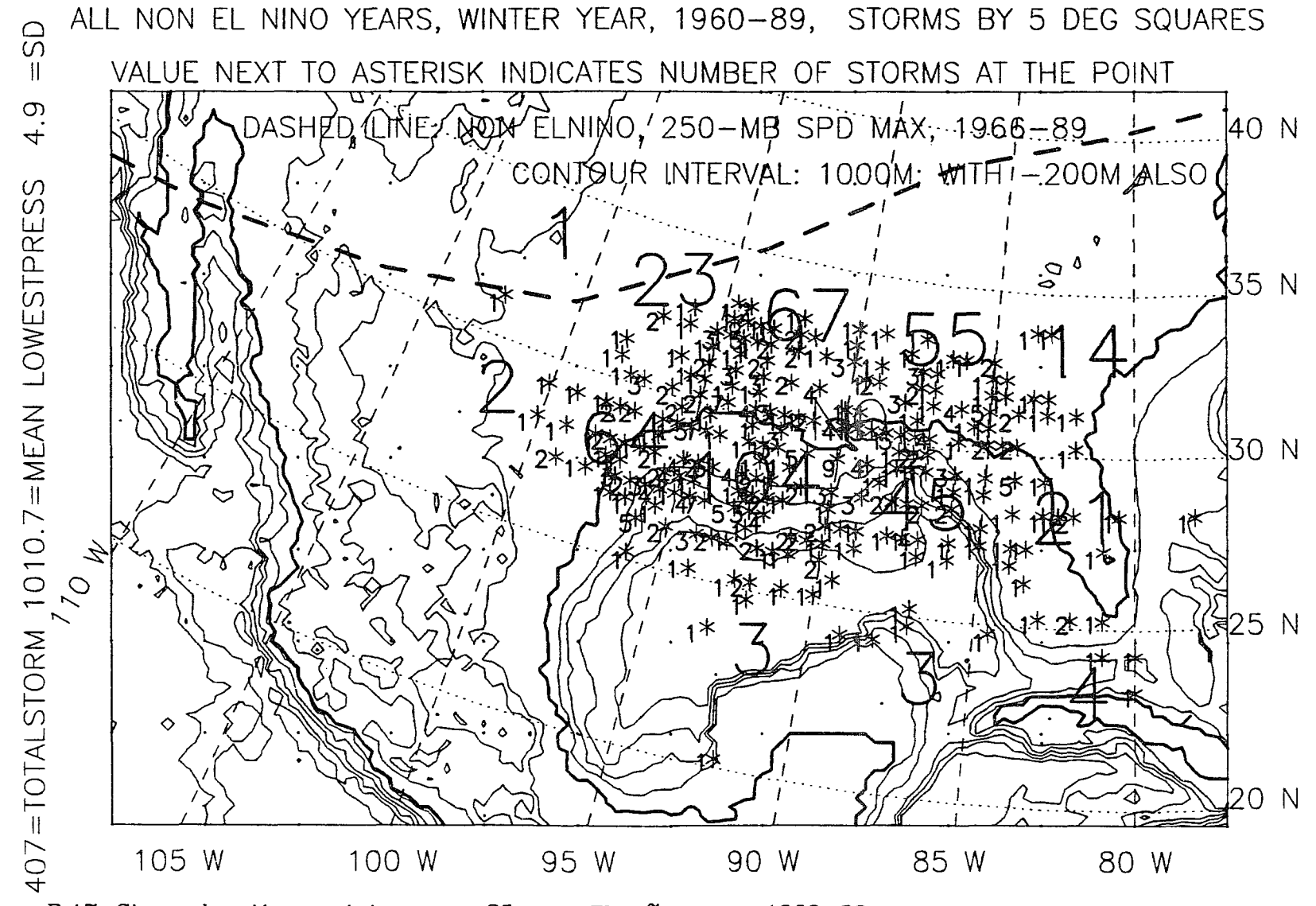

Figure P.17: Storm locations, winter year, 25 non–El Niño years, 1960–89.

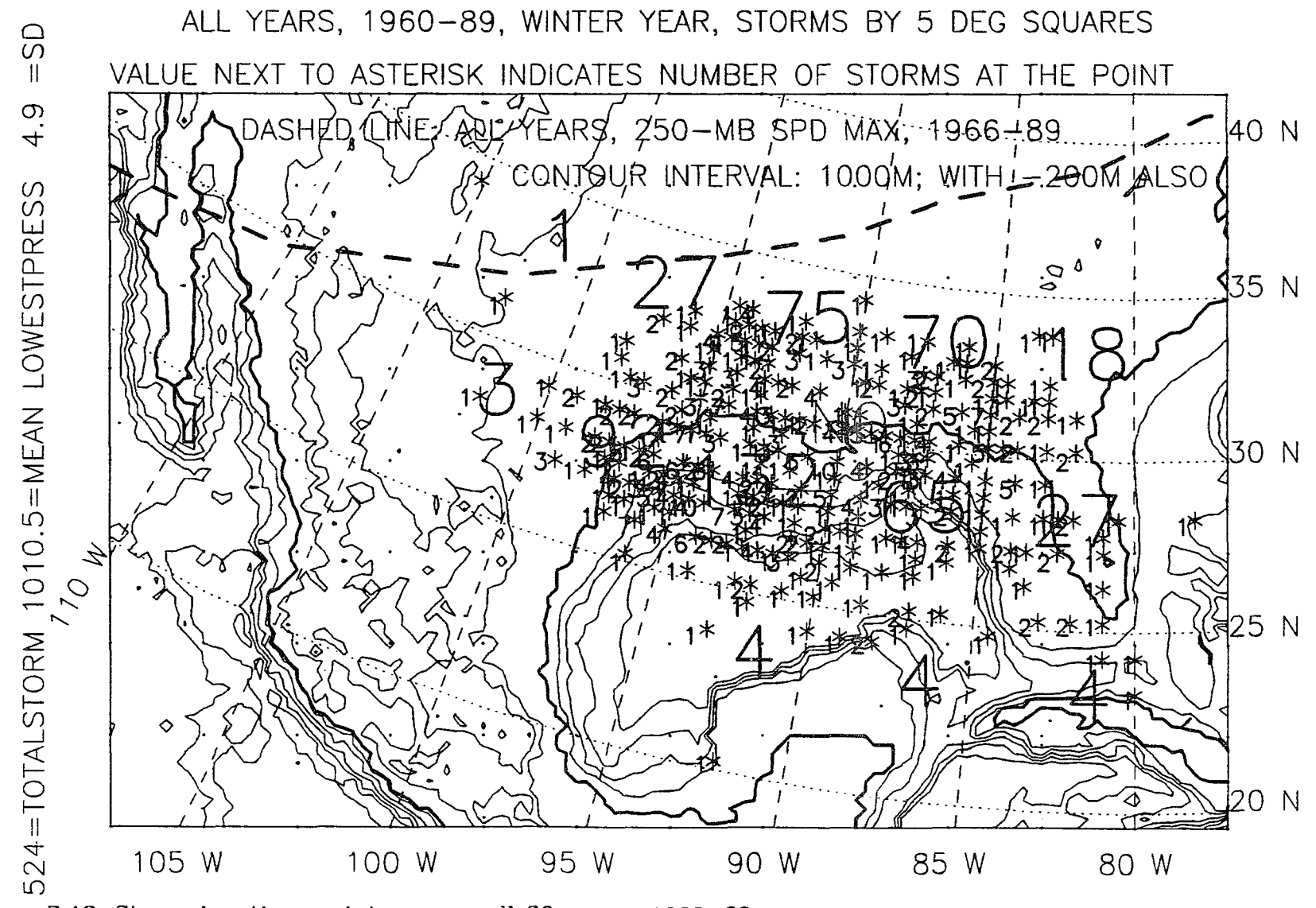

Figure P.18: Storm locations, winter year, all 30 years, 1960–89.

APPENDIX Q
TEMPERATURE AND PRECIPITATION DATA

Table Q.1: Average temperature in 15 Gulf of Mexico-region, single stations in El Niño years; The data is from the Carbon Dioxide Information Analysis Center (Bradley et al. 1985). Results of the rank sum test for differences between El Niño and other years. z-Values are given for test of the hypothesis that temperature varies between El Niño and other years. Two levels of significance are shown: $\alpha = .01$, reject the null hypothesis if $z > 2.575$ or $z < -2.575$; $\alpha = .05$, reject the null hypothesis if $z > 1.960$ or $z < -1.960$. Confidence criteria are not adjusted for multiple use of the test because of varying periods of record.

		Mean Temp $C°$		Number Of Events	
Season	z	El Niño	Other	El Niño	Other
Key West, FL, 1851-1970					
winteryear	-1.303	25.0	25.2	33	81
winter+spring †	-1.999	22.7	23.1	33	81
winter	-1.781	21.0	21.4	33	81
spring †	-2.271	24.4	24.8	36	79
summer	0.235	28.6	28.6	32	84
fall	1.142	26.1	26.0	33	83
Miami, FL, 1895-1980					
winteryear	-0.796	24.0	24.1	21	62
winter+spring	-1.338	21.6	21.9	21	63
winter	-1.861	19.7	20.2	22	63
spring	-1.101	23.5	23.7	25	59
summer	-0.286	27.6	27.6	23	61
fall	-0.163	25.1	25.1	23	62
Tampa, FL, 1851-1980					
winteryear	-1.484	22.2	22.4	24	73
winter+spring	-1.585	18.9	19.3	25	73
winter	-1.679	16.0	16.6	25	73
spring	-0.954	21.9	22.1	29	69
summer	-0.837	27.4	27.5	26	74
fall	-0.975	23.2	23.4	26	74

Table Q.1 continued

Season	z	Mean Temp C^o El Niño	Mean Temp C^o Other	Number of Events El Niño	Number of Events Other
Thomasville, GA, 1892-1980					
winteryear	-1.485	19.6	19.8	19	55
winter+spring †	-2.053	15.4	16.0	21	58
winter †	-2.409	11.2	12.2	22	61
spring	-0.418	19.6	19.7	25	57
summer	1.158	27.0	26.9	21	61
fall	-1.197	20.1	20.4	22	61
Pensacola, FL, 1879-1980					
winteryear ‡	-2.679	19.6	20.0	27	73
winter+spring †	-2.552	15.5	16.1	27	74
winter †	-1.999	11.7	12.4	27	74
spring	-0.858	19.4	19.6	31	70
summer	-0.203	27.1	27.1	27	74
fall	-1.681	20.4	20.9	28	73
Mobile, AL, 1873-1970					
winteryear ‡	-3.216	19.1	19.5	28	68
winter+spring ‡	-2.620	14.9	15.5	28	68
winter †	-2.084	10.9	11.6	28	68
spring	-1.066	19.1	19.3	31	67
summer	0.656	26.9	26.8	27	71
fall	-1.675	19.8	20.1	28	70
New Orleans, LA, 1874-1980					
winteryear ‡	-2.721	20.6	20.9	29	77
winter+spring ‡	-2.718	16.5	17.1	29	77
winter †	-2.434	12.6	13.4	29	77
spring	-0.793	20.6	20.7	34	73
summer	0.203	27.9	27.8	29	78
fall †	-2.033	21.2	21.7	29	78

Table Q.1 continued

Season	z	Mean Temp C^o El Niño	Mean Temp C^o Other	Number of Events El Niño	Number of Events Other
Meridian, MS, 1889-1980					
winteryear	-1.890	17.7	18.0	23	68
winter+spring	-1.954	13.1	13.6	23	68
winter	-1.479	8.6	9.2	23	68
spring	-0.765	17.7	17.9	27	64
summer	0.725	26.6	26.5	24	67
fall	-1.076	18.0	18.4	24	68
Vicksburg, MS, 1871-1980					
winteryear	-1.873	18.5	18.7	30	78
winter+spring	-1.835	14.0	14.3	30	79
winter	-1.282	9.5	10.0	30	79
spring	-0.713	18.5	18.7	34	75
summer	1.896	27.2	26.9	29	80
fall	-1.629	18.9	19.3	31	78
Alexandria, LA, 1894-1980					
winteryear	-1.380	19.2	19.4	20	56
winter+spring	-1.353	14.7	15.1	20	59
winter	-1.562	10.1	10.7	20	59
spring	0.791	19.5	19.4	25	57
summer †	2.099	28.0	27.6	21	61
fall	-1.126	19.5	20.0	21	59
Jennings, LA, 1897-1980					
winteryear ‡	-3.456	19.7	20.3	20	59
winter+spring †	-2.509	15.6	16.3	21	62
winter †	-2.242	11.4	12.4	21	62
spring	-0.328	20.0	20.2	25	58
summer	0.879	27.7	27.6	22	58
fall ‡	-2.662	20.3	21.0	22	61

Table Q.1 continued

Season	z	Mean Temp C^o El Niño	Mean Temp C^o Other	Number of Events El Niño	Number of Events Other
Galveston, TX, 1873-1977					
winteryear ‡	-4.086	20.5	21.0	30	74
winter+spring ‡	-3.229	16.2	16.9	30	74
winter ‡	-2.802	12.4	13.4	30	74
spring	-1.048	20.2	20.4	34	71
summer	0.900	28.0	27.9	29	76
fall ‡	-3.249	21.7	22.4	30	75
Corpus Christi, TX, 1887-1950					
winteryear ‡	-3.295	21.3	21.9	19	44
winter+spring ‡	-3.213	17.3	18.2	19	44
winter †	-2.247	13.8	14.8	19	44
spring †	-2.024	21.0	21.7	21	43
summer	0.257	28.0	27.9	19	45
fall †	-2.499	22.5	23.1	20	44
Merida, Mexico, 1895-1980					
winteryear	-0.212	25.8	25.8	17	51
winter+spring	-1.110	24.9	25.2	17	53
winter †	-2.001	23.0	23.3	17	54
spring	-1.023	26.9	27.0	23	52
summer	-1.138	27.4	27.5	18	59
fall	1.296	25.9	25.7	18	58
Casa Blanca, Cuba, 1871-1980					
winteryear	0.637	25.0	25.0	28	72
winter+spring	-0.417	23.4	23.5	28	73
winter	-1.370	22.1	22.3	28	73
spring	-0.762	24.7	24.7	33	69
summer	1.002	27.5	27.4	29	72
fall	1.232	25.8	25.6	29	72

Notes:

‡ : indicates null hypothesis can be rejected at the .01 level of significance.

† : indicates null hypothesis can be rejected at the .05 level of significance.

Table Q.2: Average temperature in 15 Gulf of Mexico-region, single stations in La Niña years; The data is from the Carbon Dioxide Information Analysis Center (Bradley et al. 1985). Results of the rank sum test for differences between La Niña and other years; z-Values are given for test of the hypothesis that temperature varies between La Niña and other years. Two levels of significance are shown: $\alpha = .01$, reject the null hypothesis if $z > 2.575$ or $z < -2.575$; $\alpha = .05$, reject the null hypothesis if $z > 1.960$ or $z < -1.960$. Confidence criteria are not adjusted for multiple use of the test because of varying periods of record.

		Mean Temp $C°$		Number of Events	
Season	z	La Niña	Other	La Niña	Other
Key West, FL, 1851-1970					
winteryear	0.884	25.2	25.1	18	71
winter+spring	1.554	23.2	22.9	18	72
winter †	2.214	21.8	21.1	18	72
spring	-0.207	24.6	24.6	18	72
summer	0.605	28.6	28.5	18	72
fall	-1.474	25.8	26.0	19	71
Miami, FL, 1895-190					
winteryear	-0.068	24.1	24.1	17	66
winter+spring	0.913	22.0	21.8	17	67
winter	1.346	20.4	20.0	17	68
spring	-0.278	23.6	23.6	17	67
summer	0.239	27.6	27.6	17	67
fall	-1.621	24.9	25.2	17	68
Tampa, FL, 1851-1980					
winteryear	0.015	22.4	22.4	19	72
winter+spring	0.952	19.5	19.2	19	72
winter	1.352	16.9	16.4	19	72
spring	0.220	22.1	22.1	19	72
summer	0.114	27.5	27.5	19	74
fall	-1.453	23.2	23.4	19	74

Table Q.2 continued

Season	z	Mean Temp C^o La Niña	Mean Temp C^o Other	Number of Events La Niña	Number of Events Other
Thomasville, GA, 1892-1980					
winteryear	0.926	19.8	19.7	16	58
winter+spring	1.593	16.1	15.7	17	62
winter †	2.031	12.6	11.8	17	66
spring	0.228	19.6	19.7	16	66
summer	-0.170	26.9	26.9	16	66
fall	0.023	20.3	20.3	17	66
Pensacola, FL, 1879-1980					
winteryear	1.374	20.1	19.9	21	78
winter+spring †	2.382	16.4	15.7	21	79
winter †	2.539	13.0	12.0	21	79
spring	0.622	19.7	19.5	21	79
summer	-0.220	27.0	27.1	21	79
fall	-0.838	20.7	20.8	21	79
Mobile, AL, 1873-1970					
winteryear	1.924	19.6	19.4	17	71
winter+spring †	2.557	15.9	15.2	17	72
winter †	2.427	12.3	11.3	17	72
spring	1.115	19.5	19.2	18	72
summer	-0.843	26.8	26.9	18	72
fall	-1.058	20.0	20.2	19	71
New Orleans, LA, 1874-1980					
winteryear	0.890	20.9	20.8	21	78
winter+spring †	2.154	17.4	16.8	21	79
winter †	2.395	14.0	13.0	21	79
spring	0.135	20.7	20.7	21	79
summer	-1.672	27.7	27.9	21	79
fall	-0.766	21.5	21.7	21	79

Table Q.2 continued

Season	z	Mean Temp C^o La Niña	Mean Temp C^o Other	Number of Events La Niña	Number of Events Other
Meridian, MS, 1889-1980					
winteryear	0.781	18.1	17.9	19	72
winter+spring	1.670	13.9	13.4	19	72
winter †	1.997	9.8	8.9	19	72
spring	1.099	18.0	17.8	19	72
summer	0.010	26.5	26.6	18	73
fall	-1.085	18.1	18.3	19	73
Vicksburg, MS, 1871-1980					
winteryear	1.516	18.9	18.6	20	78
winter+spring ‡	2.670	14.7	14.1	21	79
winter ‡	2.776	10.7	9.6	21	79
spring	1.045	18.8	18.6	21	79
summer	-1.841	26.7	27.0	21	79
fall	-0.841	19.2	19.3	20	79
Alexandria, LA, 1894-1980					
winteryear	0.287	19.4	19.4	16	60
winter+spring	0.720	15.1	14.9	16	63
winter	1.025	10.9	10.5	16	63
spring	0.069	19.5	19.4	17	65
summer	-1.899	27.5	27.8	17	65
fall	0.000	19.9	19.9	17	63
Jennings, LA, 1897-1980					
winteryear	1.055	20.3	20.1	16	63
winter+spring	1.614	16.5	16.0	17	66
winter	1.681	12.8	12.0	17	66
spring	0.875	20.3	20.1	17	66
summer	-1.276	27.5	27.7	16	64
fall	0.333	21.0	20.8	17	66

Table Q.2 continued

Season	z	Mean Temp C° La Niña	Mean Temp C° Other	Number of Events La Niña	Number of Events Other
Galveston, TX, 1873-1977					
winteryear ‡	2.610	21.2	20.8	21	75
winter+spring ‡	3.241	17.3	16.5	21	76
winter ‡	2.882	13.9	12.9	21	76
spring †	2.076	20.6	20.2	21	76
summer	-1.336	27.8	28.0	21	76
fall	0.333	22.4	22.2	21	76
Corpus Christi, TX, 1887-1950					
winteryear	1.286	22.0	21.6	11	52
winter+spring †	2.463	18.7	17.8	11	52
winter †	2.444	15.7	14.2	11	52
spring	1.566	21.9	21.4	11	53
summer	-0.926	27.8	28.0	11	53
fall	-0.080	22.9	22.9	11	53
Merida, Mexico, 1895-1980					
winteryear	-1.416	25.7	25.9	12	56
winter+spring	-1.099	24.9	25.1	12	58
winter	1.390	23.5	23.2	13	58
spring †	-2.184	26.6	27.1	13	62
summer	0.659	27.5	27.5	16	61
fall	-1.166	25.6	25.8	16	60
Casa Blanca, Cuba, 1871-1980					
winteryear	0.151	24.9	24.9	19	72
winter+spring	0.444	23.4	23.4	19	73
winter	1.659	22.4	22.1	19	73
spring	-1.085	24.5	24.6	19	73
summer	0.347	27.4	27.3	19	73
fall	-0.352	25.5	25.6	19	72

Notes:

‡ : indicates null hypothesis can be rejected at the .01 level of significance.

† : indicates null hypothesis can be rejected at the .05 level of significance.

Table Q.3: Total precipitation at 15 Gulf of Mexico-region, single stations in El Niño years; The data is from the Carbon Dioxide Information Analysis Center (Bradley et al. 1985). Results of the rank sum test for differences between El Niño and other years; z-Values are given for test of the hypothesis that precipitation varies between El Niño and other years. Two levels of significance are shown: $\alpha = .01$, reject the null hypothesis if $z > 2.575$ or $z < -2.575$; $\alpha = .05$, reject the null hypothesis if $z > 1.960$ or $z < -1.960$. Confidence criteria are not adjusted for multiple use of the test because of varying periods of record.

		Total Precip (mm)		Number of Events	
Season	z	El Niño	Other	El Niño	Other
Key West, FL, 1851-1970					
winteryear	0.384	1002.4	986.4	31	77
winter+spring †	2.353	337.2	279.3	31	77
winter †	2.007	159.2	130.4	31	77
spring ‡	2.875	184.9	143.1	34	76
summer ‡	-2.609	286.6	347.1	31	80
fall	-1.436	335.3	383.4	32	79
Miami, FL, 1895-1980					
winteryear	0.890	1534.0	1460.5	23	66
winter+spring †	2.267	541.4	440.9	24	68
winter ‡	3.339	207.9	144.8	26	68
spring	1.697	349.9	290.7	29	66
summer	0.270	516.3	515.2	26	68
fall †	-2.058	435.4	528.7	25	69
Tampa, FL, 1851-1980					
winteryear	-0.922	1228.8	1259.8	28	81
winter+spring †	2.161	444.6	372.0	29	82
winter ‡	2.826	232.8	170.9	29	82
spring	1.028	225.1	196.2	34	78
summer	-0.309	580.0	589.3	29	83
fall	0.224	272.3	268.9	31	81

Table Q.3 continued

Season	z	Total Precip (mm) El Niño	Total Precip (mm) Other	Number of Events El Niño	Number of Events Other
Thomasville, GA, 1892-1980					
winteryear	1.403	1382.6	1315.3	27	71
winter+spring	1.831	689.7	612.1	27	72
winter ‡	2.916	375.8	294.9	27	74
spring	0.151	319.1	317.2	32	68
summer	0.345	451.0	442.0	27	74
fall	0.891	277.3	242.7	28	73
Pensacola, FL, 1879-1980					
winteryear	0.905	1567.4	1514.8	27	73
winter+spring	1.435	724.1	662.5	27	74
winter ‡	2.962	388.3	314.4	27	74
spring	0.269	346.7	344.0	31	70
summer	-1.270	472.0	514.1	27	74
fall	1.567	381.9	328.1	28	73
Mobile, AL, 1873-1970					
winteryear	0.996	1638.1	1566.7	30	76
winter+spring	1.095	820.2	765.7	31	76
winter †	2.445	430.2	361.5	31	76
spring	0.448	409.6	394.5	35	74
summer	-0.761	472.4	502.0	31	79
fall	1.672	350.5	297.9	31	78
New Orleans, LA, 1874-1980					
winteryear	0.647	1561.6	1527.3	34	85
winter+spring	1.347	793.8	723.0	34	85
winter ‡	2.894	400.8	342.0	34	85
spring	0.925	406.9	372.0	38	82
summer	-1.237	450.2	477.5	33	88
fall	1.923	351.0	311.2	34	87

Table Q.3 continued

Season	z	Total Precip (mm) El Niño	Total Precip (mm) Other	Number of Events El Niño	Number of Events Other
Meridian, MS, 1889-1980					
winteryear	1.689	1443.6	1338.9	23	68
winter+spring	0.242	797.4	789.6	23	68
winter	0.712	401.8	395.0	23	68
spring	0.343	402.4	391.6	27	64
summer	-1.671	314.0	358.4	24	67
fall	0.609	241.6	223.9	24	68
Vicksburg, MS, 1871-1980					
winteryear	0.463	1325.3	1316.1	31	82
winter+spring	-0.540	779.4	802.1	32	84
winter	-1.229	370.6	407.8	32	84
spring	0.752	420.1	388.4	36	80
summer	-0.186	274.7	279.1	31	84
fall	1.258	271.5	231.5	33	83
Alexandria, LA, 1894-1980					
winteryear ‡	2.408	1545.5	1403.7	24	64
winter+spring	1.313	858.8	794.4	24	65
winter	0.897	440.7	403.5	24	65
spring	0.645	429.0	385.7	28	63
summer	-1.620	305.7	355.1	24	66
fall	1.022	319.0	276.4	25	64
Jennings, LA, 1897-1980					
winteryear ‡	2.661	1652.9	1436.0	21	62
winter+spring †	2.011	827.9	727.5	21	62
winter	0.890	411.9	384.7	21	62
spring	1.867	409.8	334.9	26	58
summer	-0.232	441.9	415.6	22	61
fall †	2.493	378.5	293.1	22	62

Table Q.3 continued

Season	z	Total Precip (mm) El Niño	Total Precip (mm) Other	Number of Events El Niño	Number of Events Other
Galveston, TX, 1873-1977					
winteryear ‡	2.967	1286.9	1065.3	30	76
winter+spring ‡	3.752	583.5	447.9	30	76
winter ‡	3.149	305.4	234.3	30	76
spring †	2.559	275.7	211.1	34	72
summer	-0.583	295.6	313.7	30	77
fall ‡	2.658	407.3	306.5	31	76
Corpus Christi, TX, 1887-1950					
winteryear †	2.528	796.2	610.9	18	44
winter+spring ‡	2.900	361.9	257.3	18	44
winter	1.908	137.3	112.6	18	44
spring †	2.347	211.6	150.0	21	42
summer †	-2.172	121.5	182.5	19	44
fall	1.483	232.1	204.2	19	44
Merida, Mexico, 1895-1980					
winteryear	-0.257	911.6	934.8	14	47
winter+spring	-0.066	214.5	205.4	14	49
winter	-0.116	84.8	86.2	16	52
spring	1.532	143.5	109.1	21	48
summer	-0.171	414.0	429.5	18	58
fall	-0.916	272.8	308.8	18	58
Casa Blanca, Cuba, 1871-1980					
winteryear	0.533	1211.1	1171.8	33	79
winter+spring ‡	2.690	431.6	355.6	33	79
winter ‡	3.448	212.8	151.4	33	80
spring	1.181	219.9	201.4	37	76
summer	-0.603	387.2	412.1	33	81
fall	-1.620	369.6	414.0	33	80

Notes:

‡ : indicates null hypothesis can be rejected at the .01 level of significance.

† : indicates null hypothesis can be rejected at the .05 level of significance.

Table Q.4: Total precipitation in 15 Gulf of Mexico-region, single stations in La Niña years; The data is from the Carbon Dioxide Information Analysis Center (Bradley et al. 1985). Results of the rank sum test for differences between La Niña and other years; z-Values are given for test of the hypothesis that precipitation varies between La Niña and other years. Two levels of significance are shown: $\alpha = .01$, reject the null hypothesis if $z > 2.575$ or $z < -2.575$; $\alpha = .05$, reject the null hypothesis if $z > 1.960$ or $z < -1.960$. Confidence criteria are not adjusted for multiple use of the test because of varying periods of record.

		Total Precip (mm)		Number of Events	
Season	z	La Niña	Other	La Niña	Other
Key West, FL					
winteryear ‡	-2.689	852.0	1019.0	17	67
winter+spring	-0.891	258.2	299.3	17	67
winter	-1.336	100.7	136.5	17	67
spring	-0.994	147.7	164.1	17	68
summer	0.934	333.4	309.6	17	68
fall	-1.501	342.1	390.0	18	67
Miami, FL, 1895-190					
winteryear	-1.629	1351.1	1480.8	17	63
winter+spring	-1.584	401.8	469.6	17	65
winter †	-2.087	116.9	162.5	17	67
spring	-1.501	269.0	315.1	17	66
summer	0.566	525.4	503.9	16	67
fall	-0.812	475.0	504.3	17	66
Tampa, FL, 1851-1980					
winteryear	-0.805	1192.5	1253.5	21	78
winter+spring ‡	-2.890	303.6	411.0	21	79
winter ‡	-2.767	132.3	196.7	21	79
spring	-1.286	174.2	213.6	21	79
summer	0.952	607.2	571.0	21	79
fall	0.334	269.4	272.2	21	79

Table Q.4 continued

Season	z	Total Precip (mm) La Niña	Total Precip (mm) Other	Number of Events La Niña	Number of Events Other
Thomasville, GA, 1892-1980					
winteryear	-1.349	1274.6	1344.5	19	76
winter+spring †	-2.461	565.7	651.6	20	77
winter	-1.194	294.3	323.0	20	79
spring	-1.586	281.1	326.6	19	78
summer	0.044	448.3	441.8	20	78
fall	-0.419	238.7	249.0	20	78
Pensacola, FL, 1879-1980					
winteryear ‡	-3.201	1353.2	1569.5	21	78
winter+spring ‡	-4.210	526.5	721.1	21	79
winter	-0.935	305.6	344.0	21	79
spring ‡	-3.059	259.2	366.9	21	79
summer	0.914	529.2	497.5	21	79
fall	-1.206	294.1	352.5	21	79
Mobile, AL, 1873-1970					
winteryear ‡	-3.641	1374.6	1637.6	17	71
winter+spring ‡	-3.705	627.5	823.2	17	72
winter	-1.372	347.4	390.5	17	72
spring †	-2.088	324.5	421.0	18	72
summer	-0.131	498.9	501.0	18	72
fall	-1.666	250.7	317.0	19	71
New Orleans, LA, 1874-1980					
winteryear ‡	-3.107	1369.5	1591.4	21	78
winter+spring ‡	-4.007	592.0	791.2	21	79
winter †	-2.052	316.6	375.2	21	79
spring †	-2.260	308.9	407.1	21	79
summer	-0.368	469.4	476.9	21	79
fall	-1.354	277.7	331.6	21	79

Table Q.4 continued

Season	z	Total Precip (mm) La Niña	Total Precip (mm) Other	Number of Events La Niña	Number of Events Other
Meridian, MS, 1889-1980					
winteryear ‡	-2.646	1230.1	1401.0	19	72
winter+spring	-1.841	726.4	808.8	19	72
winter	0.474	408.6	393.6	19	72
spring	-1.567	343.5	408.4	19	72
summer	0.389	349.2	346.0	18	73
fall	-1.485	187.3	239.3	19	73
Vicksburg, MS, 1871-1980					
winteryear	-1.036	1272.6	1310.7	21	78
winter+spring	-0.140	780.6	792.5	21	79
winter	0.432	421.4	396.8	21	79
spring	0.021	381.0	389.9	21	79
summer	0.863	289.0	271.9	21	79
fall	-1.477	205.5	242.4	21	79
Alexandria, LA, 1894-1980					
winteryear	-1.831	1323.3	1475.2	19	69
winter+spring	-0.971	764.2	824.6	19	70
winter	1.071	428.1	409.5	19	70
spring	-1.182	357.5	410.0	19	72
summer	1.617	388.6	329.4	19	71
fall	-1.612	239.9	301.5	19	70
Jennings, LA, 1897-1980					
winteryear ‡	-3.171	1298.3	1540.5	17	66
winter+spring ‡	-2.674	633.3	783.7	17	66
winter	-0.372	379.5	394.7	17	66
spring ‡	-2.722	270.0	380.5	17	67
summer †	2.048	471.9	409.9	17	66
fall	-1.564	276.6	325.4	17	67

Table Q.4 continued

Season	z	Total Precip (mm) La Niña	Total Precip (mm) Other	Number of Events La Niña	Number of Events Other
Galveston, TX, 1873-1977					
winteryear	-1.290	1030.6	1127.0	21	75
winter+spring †	-2.531	400.9	502.5	21	76
winter †	-2.277	214.7	263.2	21	76
spring	-0.666	206.9	233.5	21	76
summer	1.182	333.8	295.4	21	76
fall	-1.064	287.6	334.1	21	76
Corpus Christi, TX, 1887-1950					
winteryear	-1.704	534.4	692.8	11	51
winter+spring	-1.115	240.4	297.9	11	51
winter	-1.345	99.3	124.2	11	51
spring	-1.430	131.7	178.7	11	52
summer	0.634	176.8	161.4	11	52
fall ‡	-2.833	134.4	229.2	11	52
Merida, Mexico, 1895-1980					
winteryear	-0.254	928.7	929.7	12	49
winter+spring	0.753	222.4	203.9	12	51
winter	0.936	92.8	84.2	13	55
spring	0.343	120.2	119.4	14	55
summer	-0.484	413.9	429.0	16	60
fall	0.688	326.0	293.4	16	60
Casa Blanca, Cuba, 1871-1980					
winteryear †	-2.109	1047.1	1201.4	19	72
winter+spring	-1.770	315.1	387.1	19	73
winter ‡	-3.318	107.1	179.2	19	73
spring	-0.352	215.0	206.1	19	73
summer	0.757	429.0	387.8	19	73
fall	0.352	398.3	403.4	19	72

Notes:

‡ : indicates null hypothesis can be rejected at the .01 level of significance.

† : indicates null hypothesis can be rejected at the .05 level of significance.

Table Q.5: Average temperature in 8 Gulf of Mexico region, climatic divisions in El Niño years; The data is from the Southern Regional Climate Center (Southern Regional Climate Center). Results of the rank sum test for differences between El Niño and other years. z-Values are given for test of the hypothesis that temperature varies between El Niño and other years. Confidence criteria are adjusted for multiple use of the test. Four levels of significance are shown: $\alpha = .01$, reject the null hypothesis if $z > 3.260$ or $z < -3.260$; $\alpha = .05$, reject the null hypothesis if $z > 2.740$ or $z < -2.740$. Similarly, for the .10 and .20 levels, the criteria are 2.50 and 2.24, respectively.

		Mean Temp C^o		Number of Events	
Season	z	El Niño	Other	El Niño	Other
Key West, FL, 1895-1989					
winteryear	-0.932	25.0	25.1	24	70
winter+spring	-1.413	22.7	23.0	24	70
winter	-1.531	21.0	21.3	24	70
spring	-1.445	24.5	24.8	28	67
summer	-0.173	28.4	28.4	25	70
fall	0.300	26.0	26.0	25	70
St. Petersburg, FL, 1895-1989					
winteryear	-1.010	22.2	22.3	24	70
winter+spring	-1.431	18.9	19.3	24	70
winter	-1.682	16.3	16.7	24	70
spring	-1.331	21.6	21.9	28	67
summer	0.055	27.2	27.2	25	70
fall	-0.334	23.3	23.4	25	70
Tallahassee, FL, 1895-1989					
winteryear	-1.973	19.4	19.6	24	70
winter+spring	-2.020	15.2	15.7	24	70
winter	-1.804	11.3	11.9	24	70
spring	-0.947	19.2	19.4	28	67
summer	0.604	26.9	26.8	25	70
fall	-1.171	20.0	20.3	25	70

Table Q.5 continued

Season	z	Mean Temp C^o El Niño	Mean Temp C^o Other	Number of Events El Niño	Number of Events Other
New Orleans, LA, 1889-1990					
winteryear †	-2.770	20.3	20.7	25	77
winter+spring$^{\cdot 1}$	-2.505	16.3	16.9	25	77
winter	-2.143	12.6	13.3	25	77
spring	-1.394	20.2	20.5	30	73
summer	1.169	27.6	27.5	26	77
fall	-1.655	21.1	21.5	26	77
Lake Charles, LA, 1895-1989					
winteryear †	-2.814	19.5	19.9	24	70
winter+spring$^{\cdot 2}$	-2.289	15.3	15.8	24	70
winter	-1.782	11.2	11.8	24	70
spring	-0.527	19.6	19.8	28	67
summer	2.079	27.5	27.3	25	70
fall$^{\cdot 2}$	-2.299	20.0	20.6	25	70
Houston, TX, 1895-1989					
winteryear †	-2.983	20.4	20.8	24	70
winter+spring †	-2.901	16.2	16.8	24	70
winter	-1.825	12.3	12.9	24	70
spring	-0.988	20.4	20.6	28	67
summer	2.164	28.2	28.0	25	70
fall$^{\cdot 1}$	-2.574	21.1	21.7	25	70
Corpus Christi, TX, 1895-1989					
winteryear ‡	-3.525	20.4	20.9	24	70
winter+spring ‡	-3.473	15.9	16.7	24	70
winter	-1.765	11.8	12.4	24	70
spring	-1.988	20.3	20.8	28	67
summer	1.982	28.8	28.5	25	70
fall$^{\cdot 2}$	-2.265	21.1	21.7	25	70

Table Q.5 continued

Season	z	Mean Temp C^o El Niño	Mean Temp C^o Other	Number of Events El Niño	Number of Events Other
Brownsville, TX, 1895-1989					
winteryear$^{.1}$	-2.580	22.9	23.4	24	70
winter+spring$^{.1}$	-2.692	19.5	20.2	24	70
winter	-1.596	16.0	16.6	24	70
spring	-1.714	23.4	23.8	28	67
summer	1.568	29.2	29.0	25	70
fall	-1.775	23.6	24.0	25	70

Notes:

‡ : indicates null hypothesis can be rejected at the .01 level of significance.

† : indicates null hypothesis can be rejected at the .05 level of significance.

$^{.1}$: indicates null hypothesis can be rejected at the .10 level of significance.

$^{.2}$: indicates null hypothesis can be rejected at the .20 level of significance.

Table Q.6: Average temperature in 8 Gulf of Mexico region, climatic divisions in La Niña years; The data is from the Southern Regional Climate Center (Southern Regional Climate Center). Results of the rank sum test for differences between La Niña and other years; z-Values are given for test of the hypothesis that temperature varies between La Niña and other years. Confidence criteria are adjusted for multiple use of the test. Four levels of significance are shown: $\alpha = .01$, reject the null hypothesis if $z > 3.260$ or $z < -3.260$; $\alpha = .05$, reject the null hypothesis if $z > 2.740$ or $z < -2.740$. Similarly, for the .10 and .20 levels, the criteria are 2.50 and 2.24, respectively.

		Mean Temp C°		Number of Events	
Season	z	La Niña	Other	La Niña	Other
Key West, FL, 1895-1989					
winteryear	0.495	25.1	25.1	18	76
winter+spring	1.293	23.2	22.9	18	76
winter	1.711	21.5	21.1	18	76
spring	-0.186	24.7	24.7	19	76
summer	0.019	28.4	28.4	18	77
fall	-1.249	25.8	26.0	18	77
St. Petersburg, FL, 1895-1989					
winteryear	-0.207	22.2	22.3	18	76
winter+spring	0.961	19.4	19.2	18	76
winter	1.446	16.9	16.5	18	76
spring	-0.074	21.8	21.8	19	76
summer	-0.874	27.2	27.2	18	77
fall	-1.828	23.1	23.4	18	77
Tallahassee, FL, 1895-1989					
winteryear	0.504	19.6	19.5	18	76
winter+spring	1.288	15.8	15.5	18	76
winter	1.677	12.2	11.6	18	76
spring	-0.023	19.3	19.4	19	76
summer	-0.499	26.8	26.8	18	77
fall	-0.964	20.1	20.3	18	77

Table Q.6 continued

Season	z	Mean Temp C^o La Niña	Mean Temp C^o Other	Number of Events La Niña	Number of Events Other
New Orleans, LA, 1889-1990					
winteryear	1.378	20.7	20.6	20	82
winter+spring$^{.2}$	2.373	17.2	16.6	20	82
winter$^{.2}$	2.524	13.9	12.9	20	82
spring	0.147	20.4	20.4	21	82
summer	-1.238	27.4	27.5	20	83
fall	-0.909	21.3	21.4	20	83
Lake Charles, LA, 1895-1989					
winteryear	1.225	19.9	19.8	18	76
winter+spring	1.956	16.0	15.6	18	76
winter	2.181	12.2	11.4	18	76
spring	0.498	19.8	19.7	19	76
summer	-1.904	27.2	27.4	18	77
fall	-0.475	20.5	20.4	18	77
Houston, TX, 1895-1989					
winteryear$^{.2}$	2.282	21.0	20.7	18	76
winter+spring$^{.1}$	2.556	17.1	16.6	18	76
winter$^{.1}$	2.595	13.5	12.6	18	76
spring	1.363	20.8	20.5	19	76
summer	-1.847	27.9	28.1	18	77
fall	0.765	21.7	21.5	18	77
Corpus Christi, TX, 1895-1989					
winteryear$^{.1}$	2.667	21.1	20.7	18	76
winter+spring †	2.974	17.0	16.3	18	76
winter$^{.1}$	2.547	13.0	12.1	18	76
spring$^{.2}$	2.345	21.2	20.6	19	76
summer	-1.173	28.4	28.6	18	77
fall	0.997	21.7	21.5	18	77

Table Q.6 continued

Season	z	Mean Temp C^o La Niña	Mean Temp C^o Other	Number of Events La Niña	Number of Events Other
Brownsville, TX, 1895-1989					
winteryear	1.855	23.5	23.2	18	76
winter+spring$^{\cdot 2}$	2.273	20.5	19.9	18	76
winter$^{\cdot 1}$	2.619	17.2	16.2	18	76
spring	1.484	23.9	23.6	19	76
summer	-1.629	28.8	29.1	18	77
fall	-0.176	23.9	23.9	18	77

Notes:

‡ : indicates null hypothesis can be rejected at the .01 level of significance.

† : indicates null hypothesis can be rejected at the .05 level of significance.

$^{\cdot 1}$: indicates null hypothesis can be rejected at the .10 level of significance.

$^{\cdot 2}$: indicates null hypothesis can be rejected at the .20 level of significance.

Table Q.7: Total precipitation at 8 Gulf of Mexico region, climatic divisions in El Niño years; The data is from the Southern Regional Climate Center (Southern Regional Climate Center). Results of the rank sum test for differences between El Niño and other years; z-Values are given for test of the hypothesis that precipitation varies between El Niño and other years. Confidence criteria are adjusted for multiple use of the test. Four levels of significance are shown: $\alpha = .01$, reject the null hypothesis if $z > 3.260$ or $z < -3.260$; $\alpha = .05$, reject the null hypothesis if $z > 2.740$ or $z < -2.740$. Similarly, for the .10 and .20 levels, the criteria are 2.50 and 2.24, respectively.

		Total Precip (mm)		Number of Events	
Season	z	El Niño	Other	El Niño	Other
Key West, FL, 1895-1989					
winteryear	1.223	1122.1	1061.8	24	70
winter+spring †	2.835	401.6	302.2	24	70
winter ‡	3.694	196.9	123.5	24	70
spring	2.155	207.1	176.3	28	67
summer	-0.220	360.4	366.6	25	70
fall	-0.401	378.8	382.7	25	70
St. Petersburg, FL, 1895-1989					
winteryear	0.143	1309.2	1305.4	24	70
winter+spring †	2.766	475.4	394.2	24	70
winter †	3.009	219.3	163.9	24	70
spring[2]	2.261	267.6	224.4	28	67
summer	0.638	577.6	563.7	25	70
fall	-0.871	314.8	325.2	25	70
Tallahassee, FL, 1895-1989					
winteryear	1.205	1537.8	1463.2	24	70
winter+spring	1.834	726.8	647.6	24	70
winter[1]	2.545	379.1	319.1	24	70
spring	0.763	347.7	328.0	28	67
summer	-1.526	479.3	517.5	25	70
fall	1.361	338.7	296.6	25	70

Table Q.7 continued

Season	z	Total Precip (mm) El Niño	Total Precip (mm) Other	Number of Events El Niño	Number of Events Other
New Orleans, LA, 1889-1990					
winteryear[1]	2.680	1659.2	1506.0	25	77
winter+spring †	3.073	814.1	690.4	25	77
winter †	3.240	424.1	345.2	25	77
spring	2.218	395.4	337.5	30	73
summer	-0.824	473.1	490.2	26	77
fall	1.974	369.7	325.1	26	77
Lake Charles, LA, 1895-1989					
winteryear ‡	4.344	1679.9	1417.2	24	70
winter+spring ‡	3.607	826.3	675.1	24	70
winter[2]	2.328	425.0	361.4	24	70
spring[2]	2.433	393.6	312.0	28	67
summer	-1.192	440.1	443.9	25	70
fall	2.172	370.9	311.9	25	70
Houston, TX, 1895-1989					
winteryear ‡	3.646	1362.5	1134.8	24	70
winter+spring ‡	3.547	631.9	504.7	24	70
winter †	3.139	319.0	253.8	24	70
spring	2.155	308.5	250.2	28	67
summer	-1.445	291.4	340.4	25	70
fall	1.682	360.3	315.2	25	70
Corpus Christi, TX, 1895-1989					
winteryear ‡	3.867	1031.2	818.5	24	70
winter+spring ‡	3.529	490.5	380.1	24	70
winter †	3.165	219.8	160.8	24	70
spring	2.196	269.0	218.4	28	67
summer	-0.989	195.1	219.1	25	70
fall	2.003	282.2	239.6	25	70

Table Q.7 continued

Season	z	Total Precip (mm) El Niño	Total Precip (mm) Other	Number of Events El Niño	Number of Events Other
Brownsville, TX, 1895-1989					
winteryear$^{.1}$	2.714	713.9	621.1	24	70
winter+spring ‡	3.538	303.2	224.3	24	70
winter †	2.861	145.3	93.8	24	70
spring	1.526	157.4	130.4	28	67
summer	-1.133	158.6	179.8	25	70
fall	0.520	217.0	218.4	25	70

Notes:

‡ : indicates null hypothesis can be rejected at the .01 level of significance.

† : indicates null hypothesis can be rejected at the .05 level of significance.

$^{.1}$: indicates null hypothesis can be rejected at the .10 level of significance.

$^{.2}$: indicates null hypothesis can be rejected at the .20 level of significance.

Table Q.8: Total precipitation at 8 Gulf of Mexico region, climatic divisions in La Niña years; The data is from the Southern Regional Climate Center (Southern Regional Climate Center). Results of the rank sum test for differences between La Niña and other years; z-Values are given for test of the hypothesis that precipitation varies between La Niña and other years. Confidence criteria are adjusted for multiple use of the test. Four levels of significance are shown: $\alpha = .01$, reject the null hypothesis if $z > 3.260$ or $z < -3.260$; $\alpha = .05$, reject the null hypothesis if $z > 2.740$ or $z < -2.740$. Similarly, for the .10 and .20 levels, the criteria are 2.50 and 2.24, respectively.

		Total Precip (mm)		Number of Events	
Season	z	La Niña	Other	La Niña	Other
Key West, FL, 1895-1989					
winteryear	-2.200	967.0	1103.3	18	76
winter+spring[2]	-2.455	274.2	340.3	18	76
winter	-1.115	121.5	147.1	18	76
spring	-2.066	157.5	192.3	19	76
summer	-0.204	364.5	365.1	18	77
fall	-1.064	361.4	386.4	18	77
St. Petersburg, FL, 1895-1989					
winteryear	-1.994	1234.8	1323.3	18	76
winter+spring ‡	-3.378	322.4	436.9	18	76
winter †	-2.931	129.0	189.7	18	76
spring[1]	-2.559	196.8	247.2	19	76
summer	-0.945	549.6	571.5	18	77
fall	0.123	324.0	322.1	18	77
Tallahassee, FL, 1895-1989					
winteryear †	-2.988	1331.0	1518.1	18	76
winter+spring ‡	-3.565	546.5	696.6	18	76
winter[2]	-2.383	285.7	346.0	18	76
spring †	-2.796	264.0	351.2	19	76
summer	0.019	512.2	506.3	18	77
fall	-1.757	263.2	318.0	18	77

Table Q.8 continued

Season	z	Total Precip (mm) La Niña	Total Precip (mm) Other	Number of Events La Niña	Number of Events Other
New Orleans, LA, 1889-1990					
winteryear ‡	-4.256	1338.3	1593.6	20	82
winter+spring ‡	-4.353	567.4	758.2	20	82
winter$^{\cdot 2}$	-2.402	309.1	378.2	20	82
spring	-2.132	289.5	380.0	21	82
summer	-0.817	467.6	490.3	20	83
fall	-1.993	280.9	349.7	20	83
Lake Charles, LA, 1895-1989					
winteryear †	-3.027	1326.2	1521.7	18	76
winter+spring$^{\cdot 1}$	-2.719	617.4	736.5	18	76
winter	-0.605	363.2	381.1	18	76
spring	-2.014	274.7	351.4	19	76
summer	1.524	466.5	437.3	18	77
fall$^{\cdot 2}$	-2.312	274.7	339.7	18	77
Houston, TX, 1895-1989					
winteryear$^{\cdot 1}$	-2.719	1052.4	1226.3	18	76
winter+spring$^{\cdot 1}$	-2.532	460.4	555.3	18	76
winter	-1.811	240.6	277.5	18	76
spring	-1.642	229.1	276.9	19	76
summer	1.140	354.8	321.1	18	77
fall$^{\cdot 2}$	-2.312	266.9	341.2	18	77
Corpus Christi, TX, 1895-1989					
winteryear †	-2.931	743.9	903.3	18	76
winter+spring$^{\cdot 2}$	-2.258	344.7	423.3	18	76
winter	-1.903	148.5	182.3	18	76
spring	-2.182	189.9	244.2	19	76
summer	1.415	238.7	206.7	18	77
fall$^{\cdot 2}$	-2.365	210.7	260.2	18	77

Table Q.8 continued

Season	z	Total Precip (mm) La Niña	Total Precip (mm) Other	Number of Events La Niña	Number of Events Other
Brownsville, TX, 1895-1989					
winteryear	.2 -2.470	583.9	650.9	18	76
winter+spring.1	-2.643	200.4	254.9	18	76
winter †	-3.258	71.1	115.4	18	76
spring	-1.321	121.0	142.7	19	76
summer	1.239	198.1	168.6	18	77
fall	-0.223	233.7	214.4	18	77

Notes:

‡ : indicates null hypothesis can be rejected at the .01 level of significance.

† : indicates null hypothesis can be rejected at the .05 level of significance.

.1 : indicates null hypothesis can be rejected at the .10 level of significance.

.2 : indicates null hypothesis can be rejected at the .20 level of significance.

APPENDIX R
ENSO INDICES

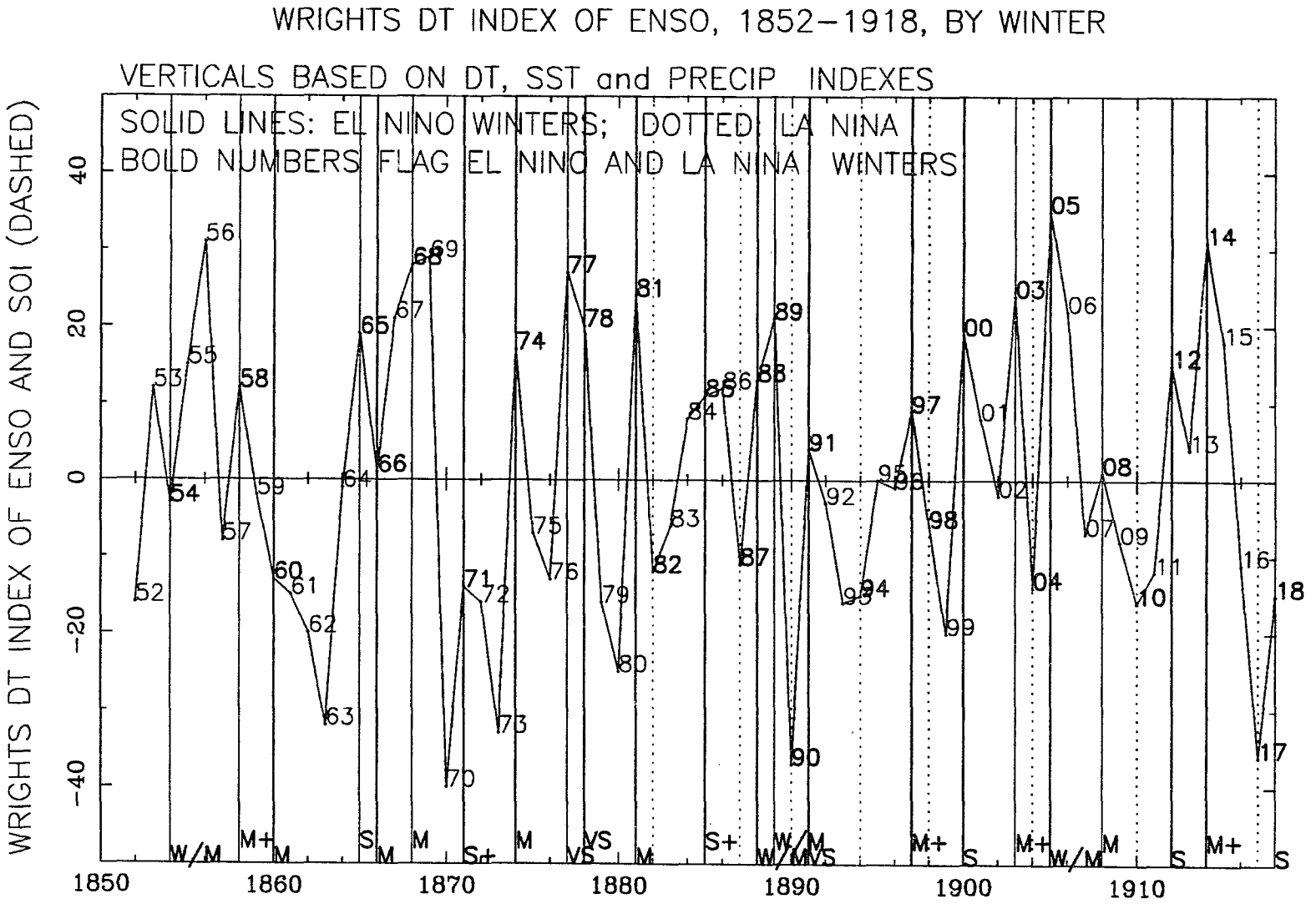

Figure R.1: DT index of ENSO (Wright 1989) by winter, 1852–1918.

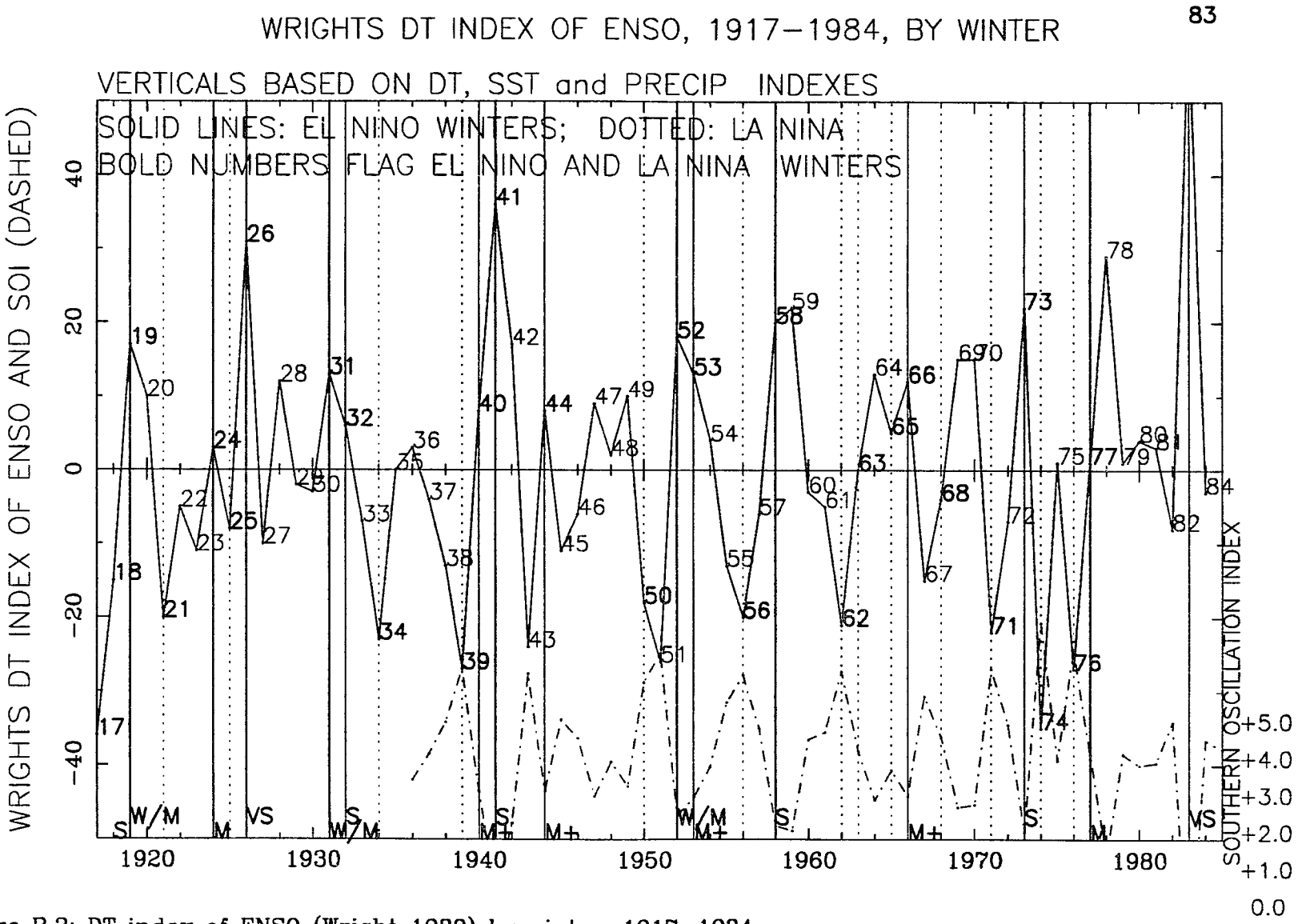

Figure R.2: DT index of ENSO (Wright 1989) by winter, 1917–1984.

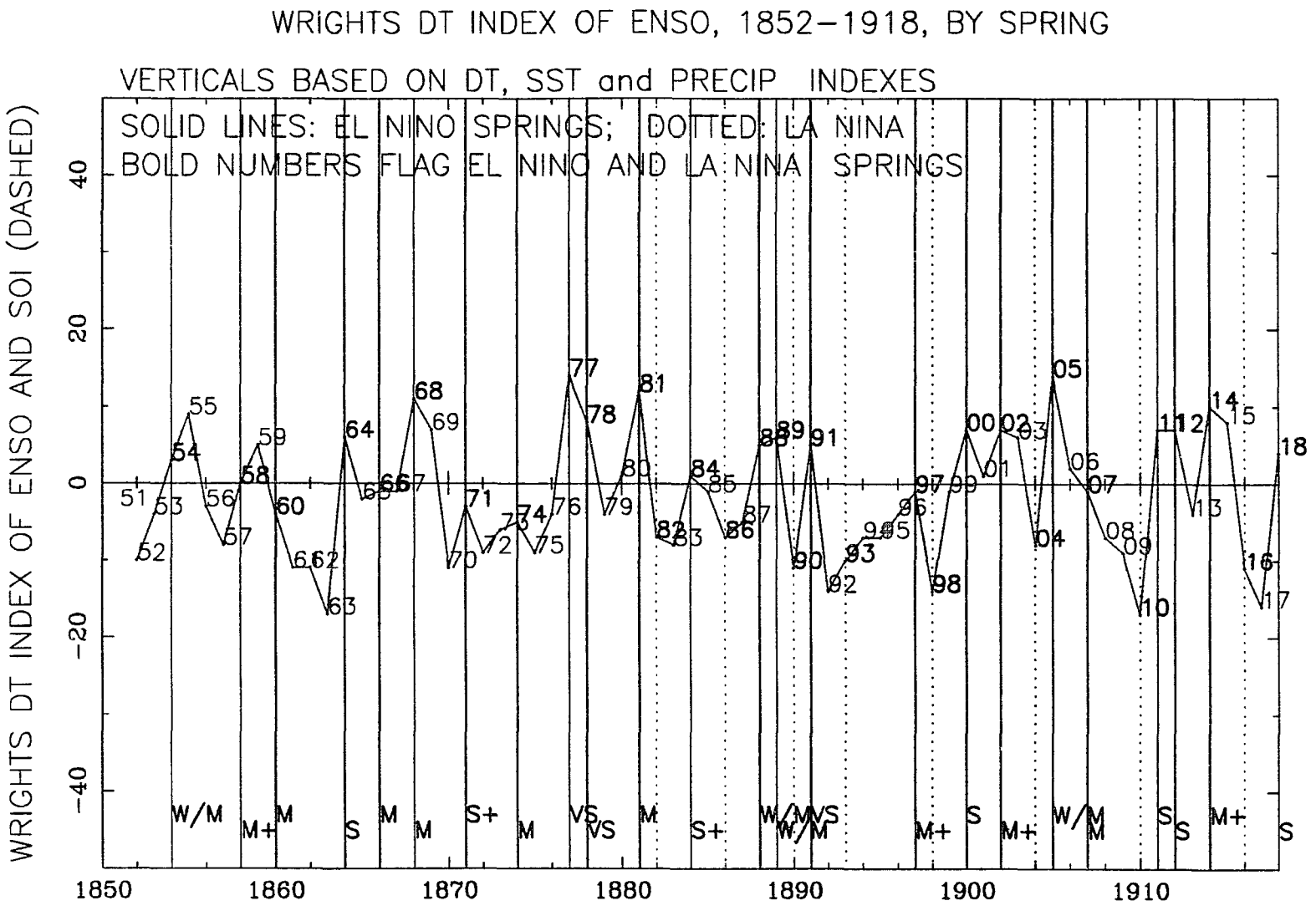

Figure R.3: DT index of ENSO (Wright 1989) by spring, 1852–1918.

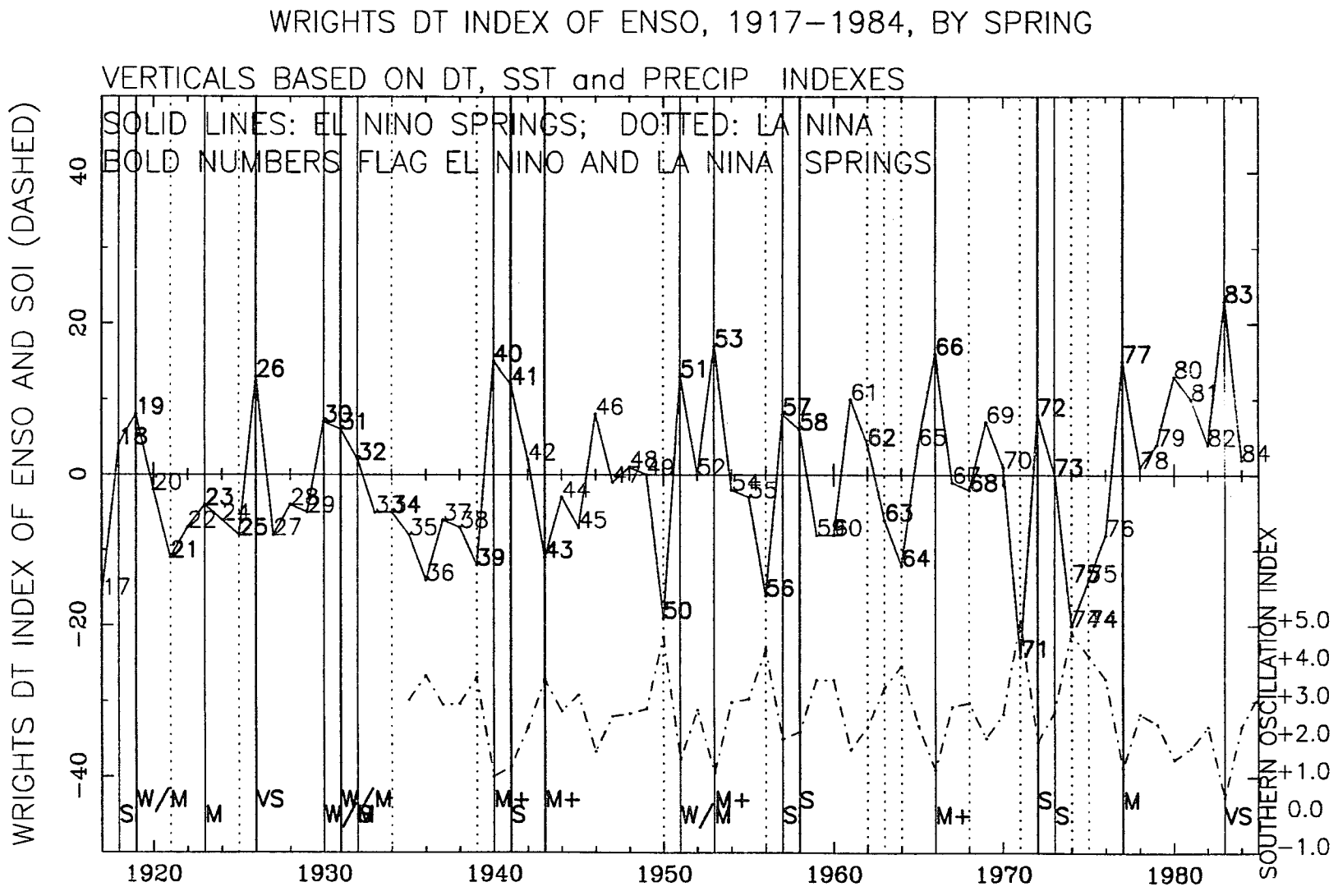

Figure R.4: DT index of ENSO (Wright 1989) by spring, 1917–1984.

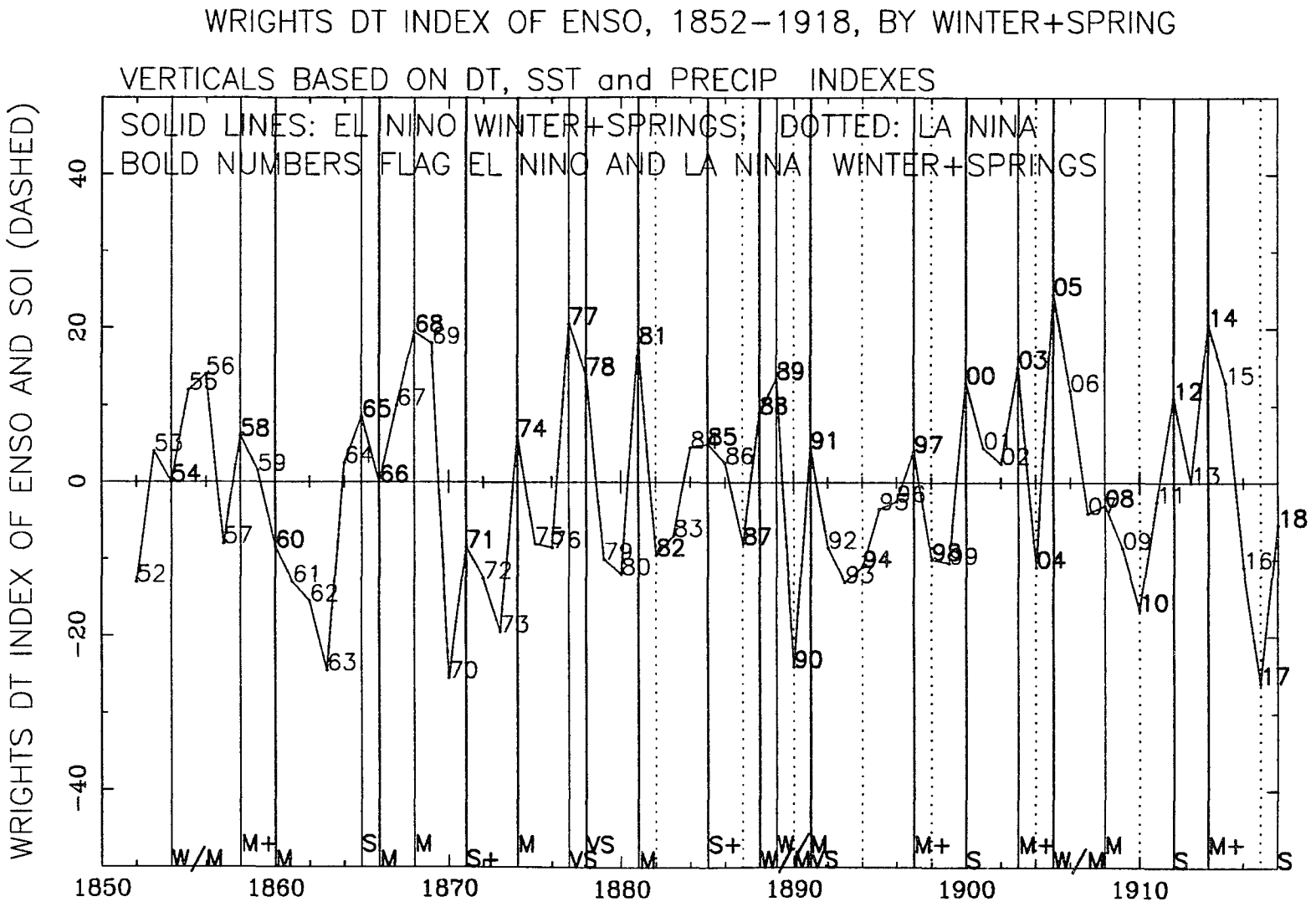

Figure R.5: DT index of ENSO (Wright 1989) by winter–plus–spring, 1852–1918.

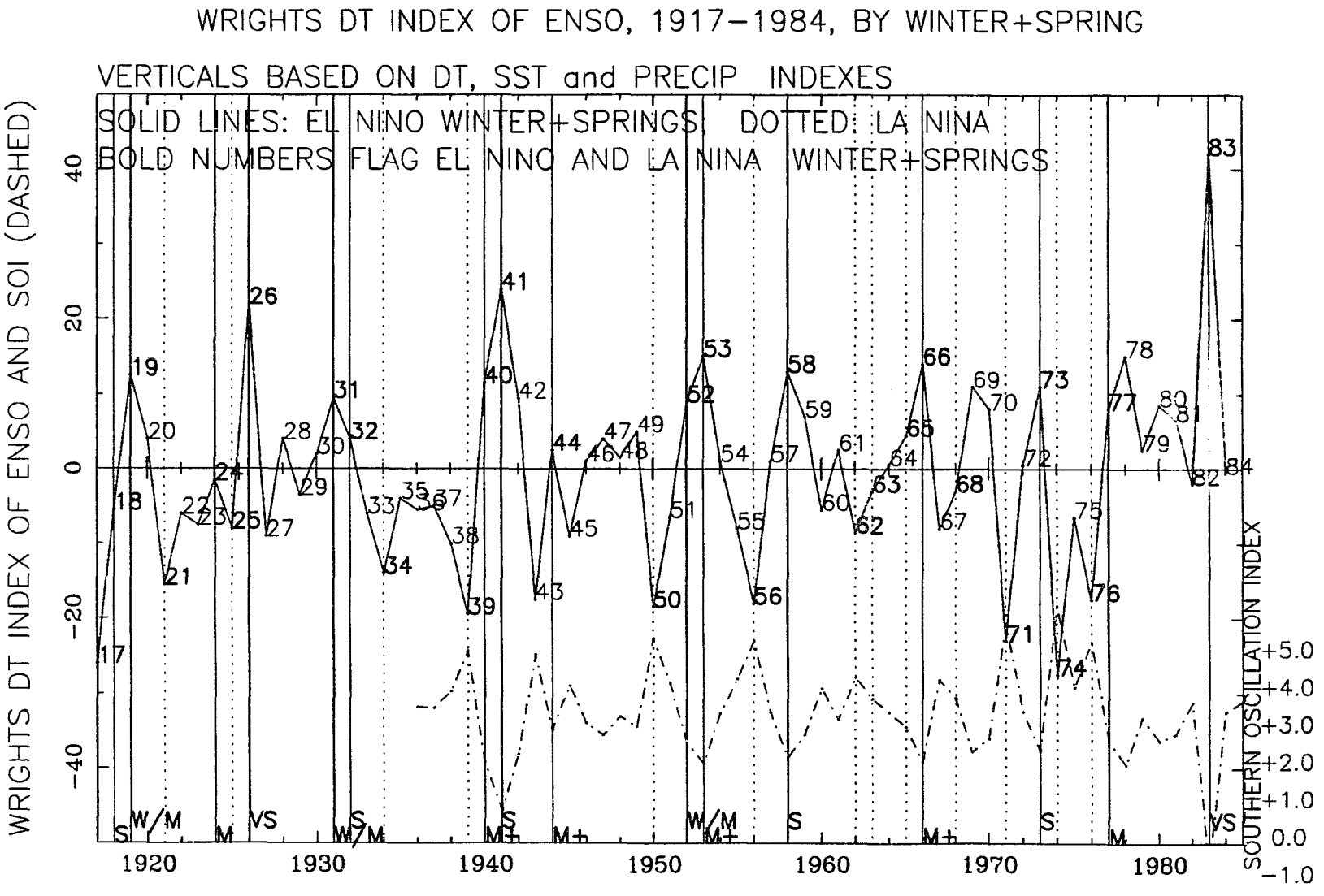

Figure R.6: DT index of ENSO (Wright 1989) by winter–plus–spring, 1917–1984.

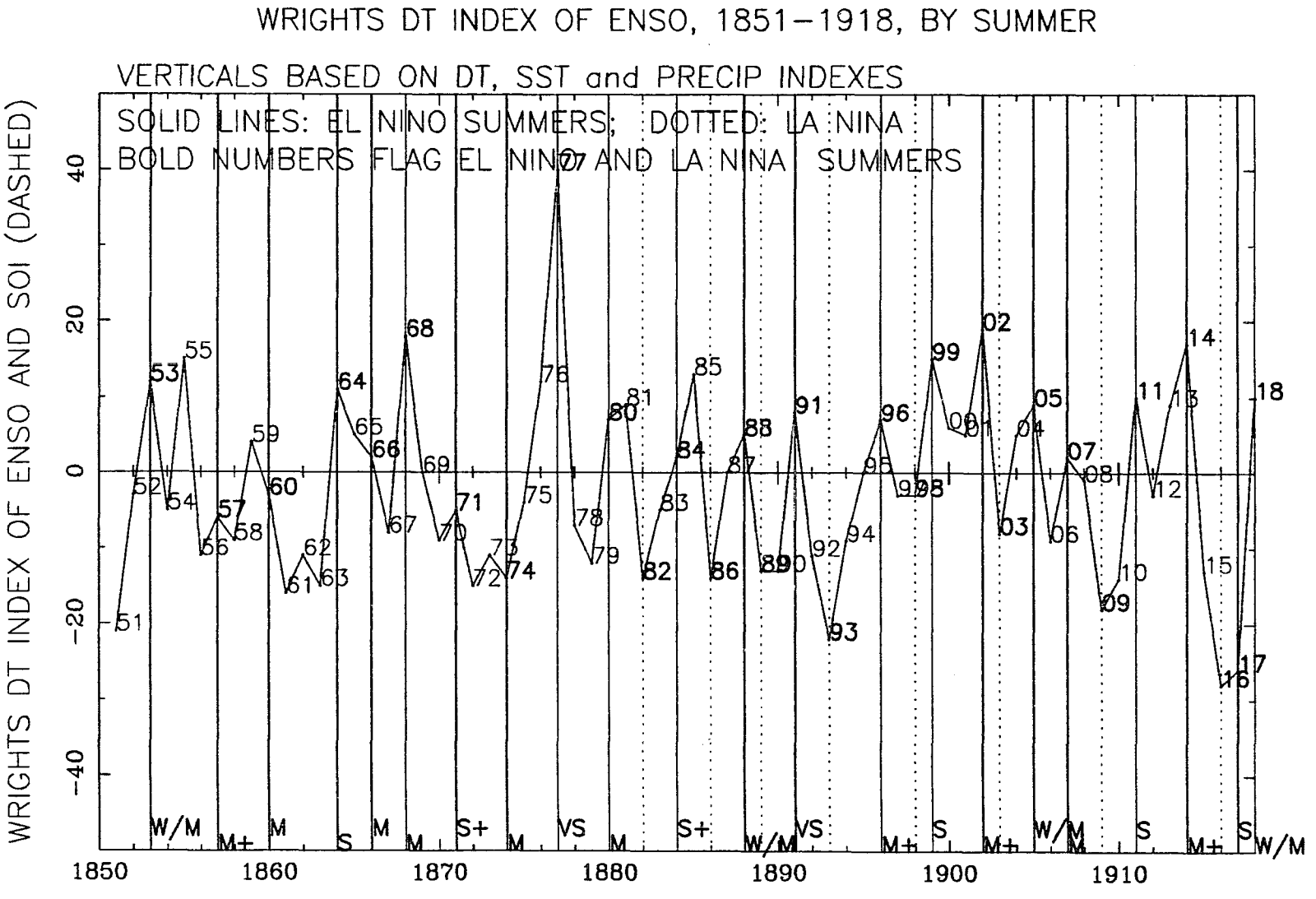

Figure R.7: DT index of ENSO (Wright 1989) by summer, 1851–1918.

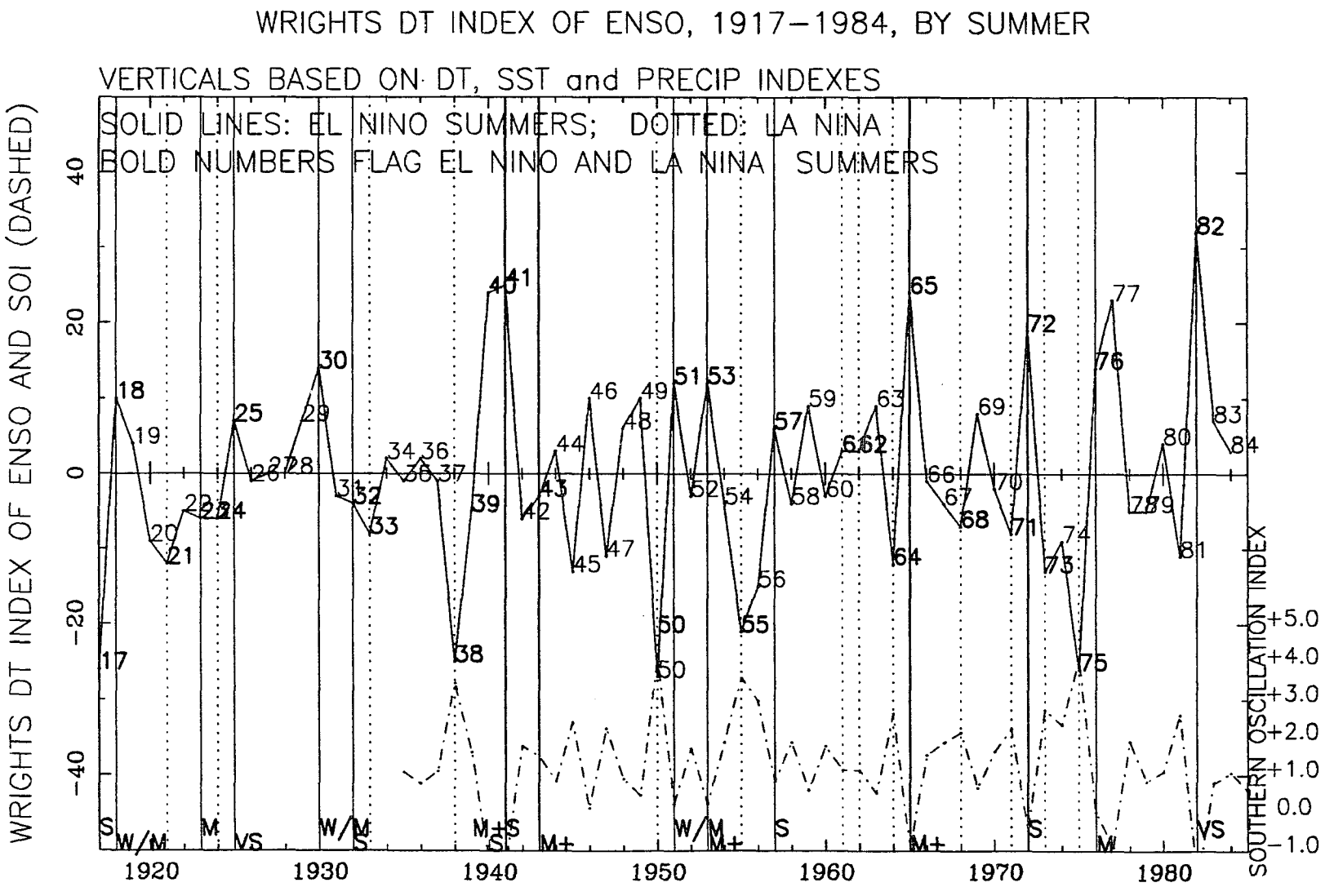

Figure R.8: DT index of ENSO (Wright 1989) by summer, 1917–1984.

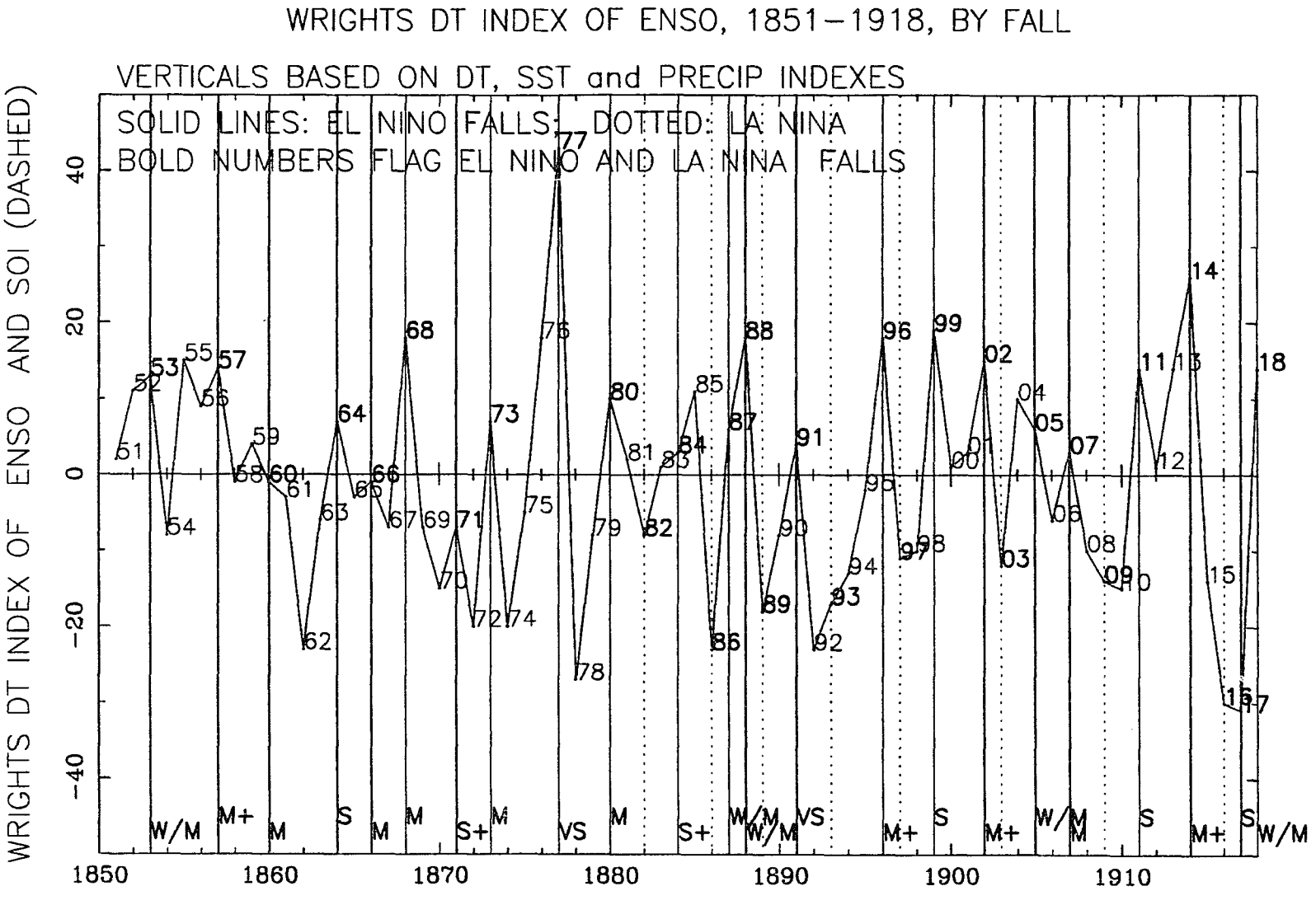

Figure R.9: DT index of ENSO (Wright 1989) by fall, 1851–1918.

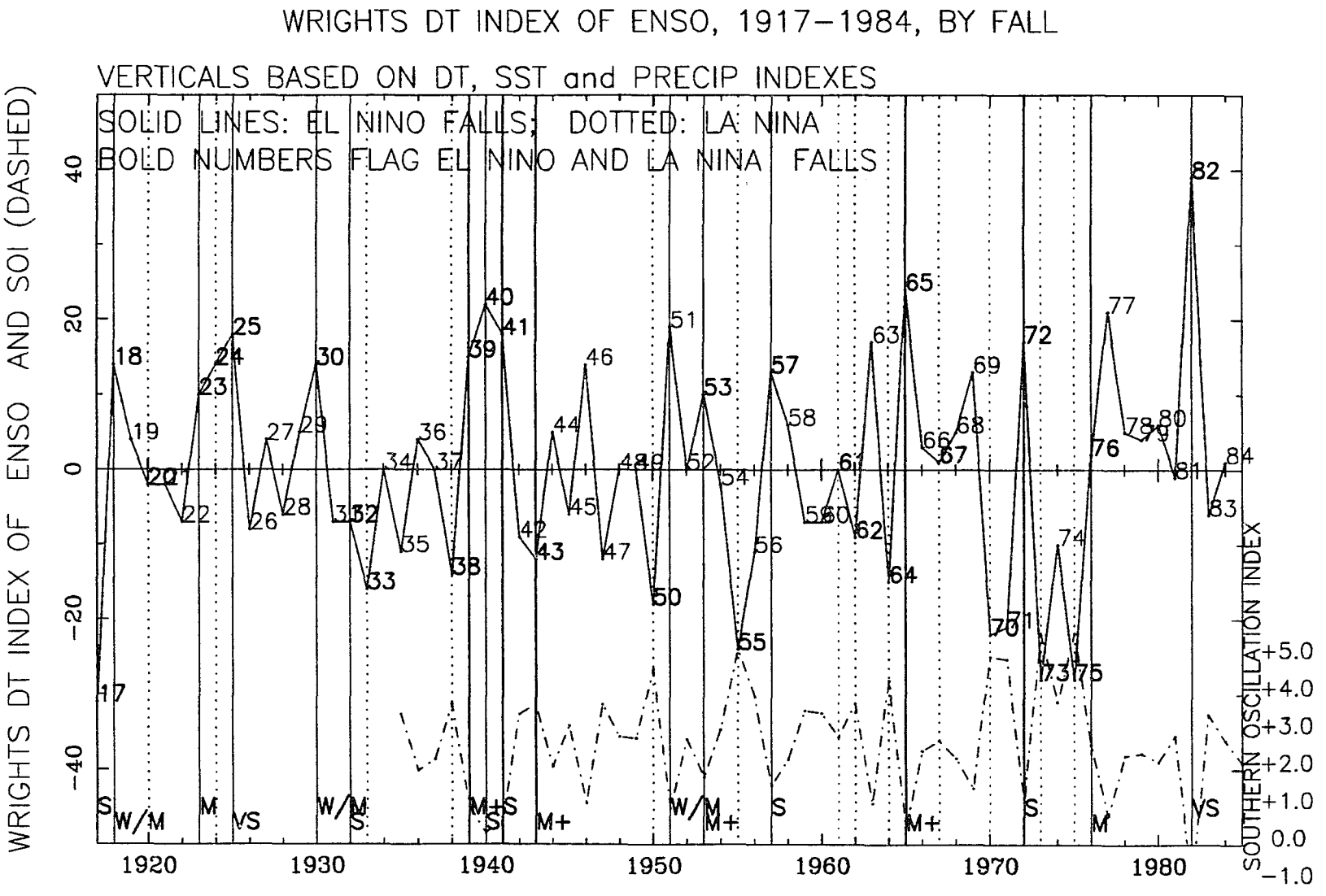

Figure R.10: DT index of ENSO (Wright 1989) by fall, 1917–1984.

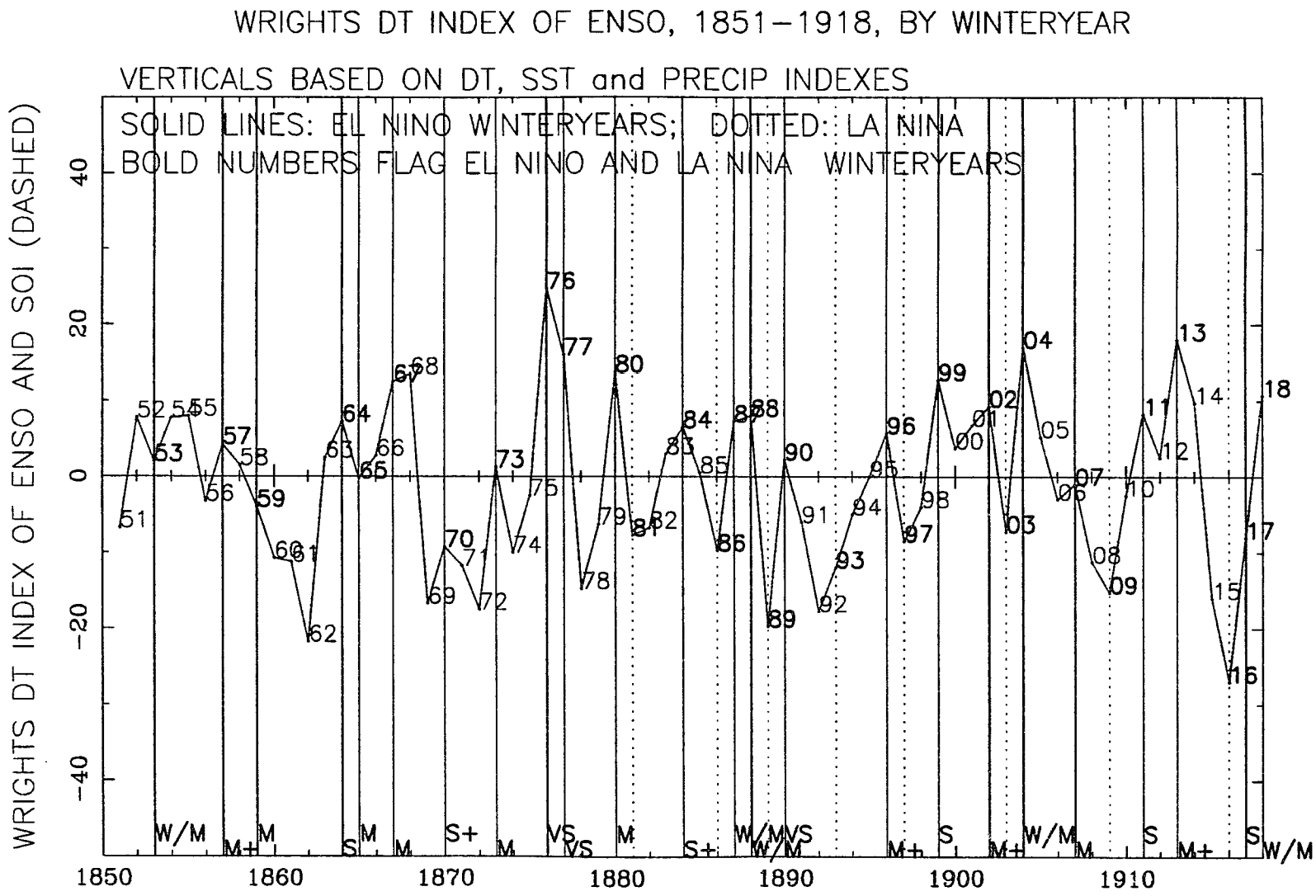

Figure R.11: DT index of ENSO (Wright 1989) by winter year, 1851–1918.

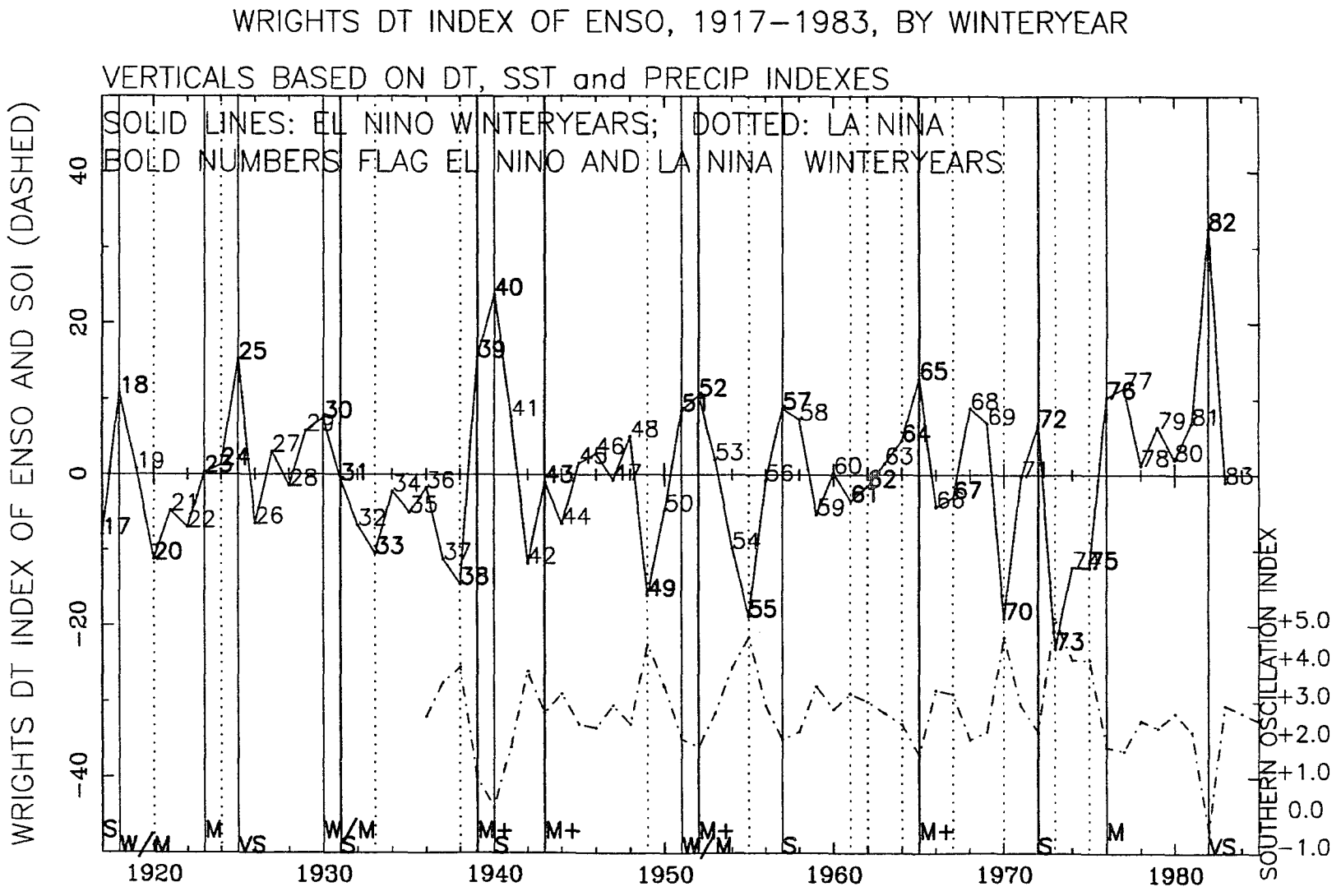

Figure R.12: DT index of ENSO (Wright 1989) by winter year, 1917–1983.

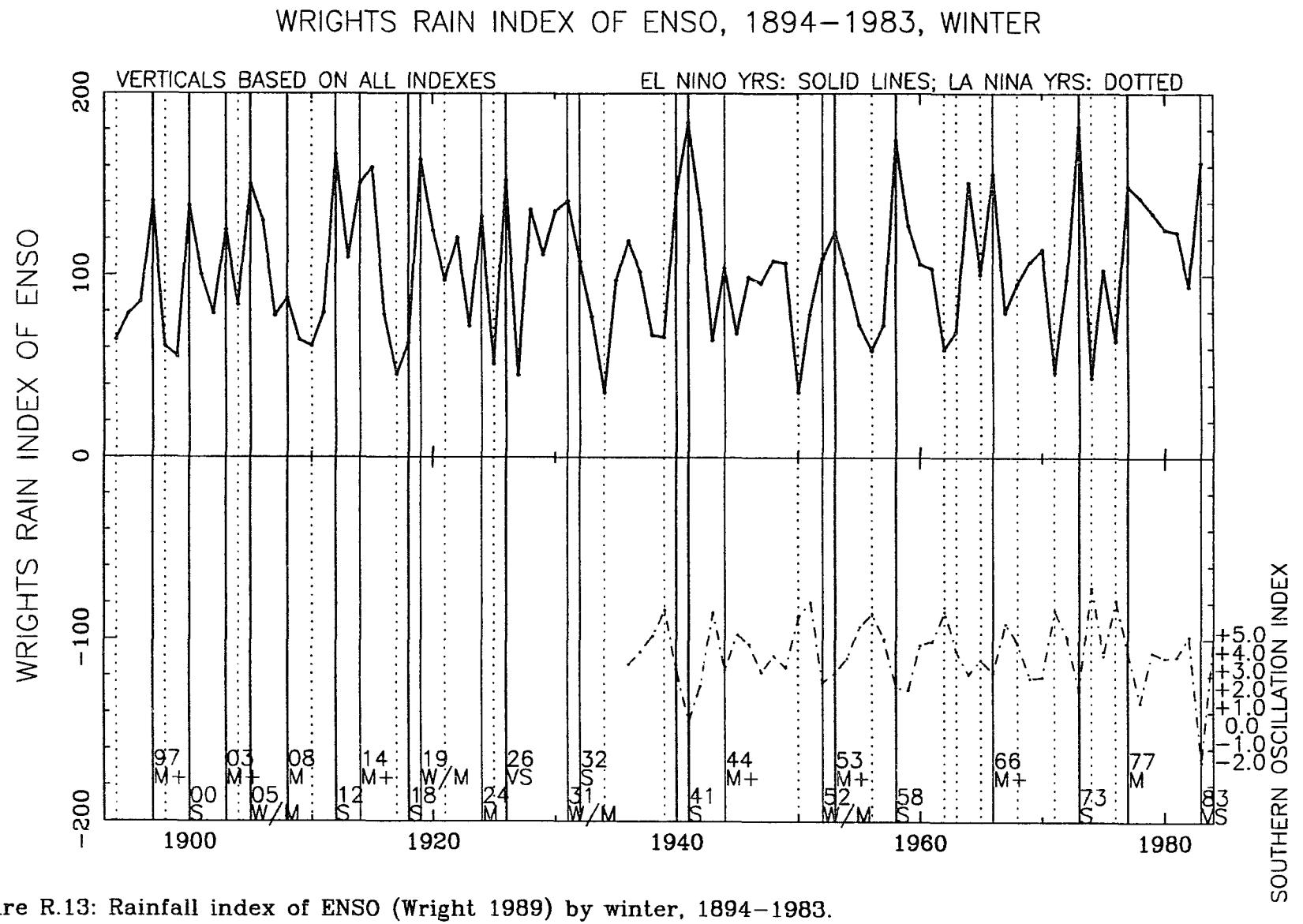

Figure R.13: Rainfall index of ENSO (Wright 1989) by winter, 1894–1983.

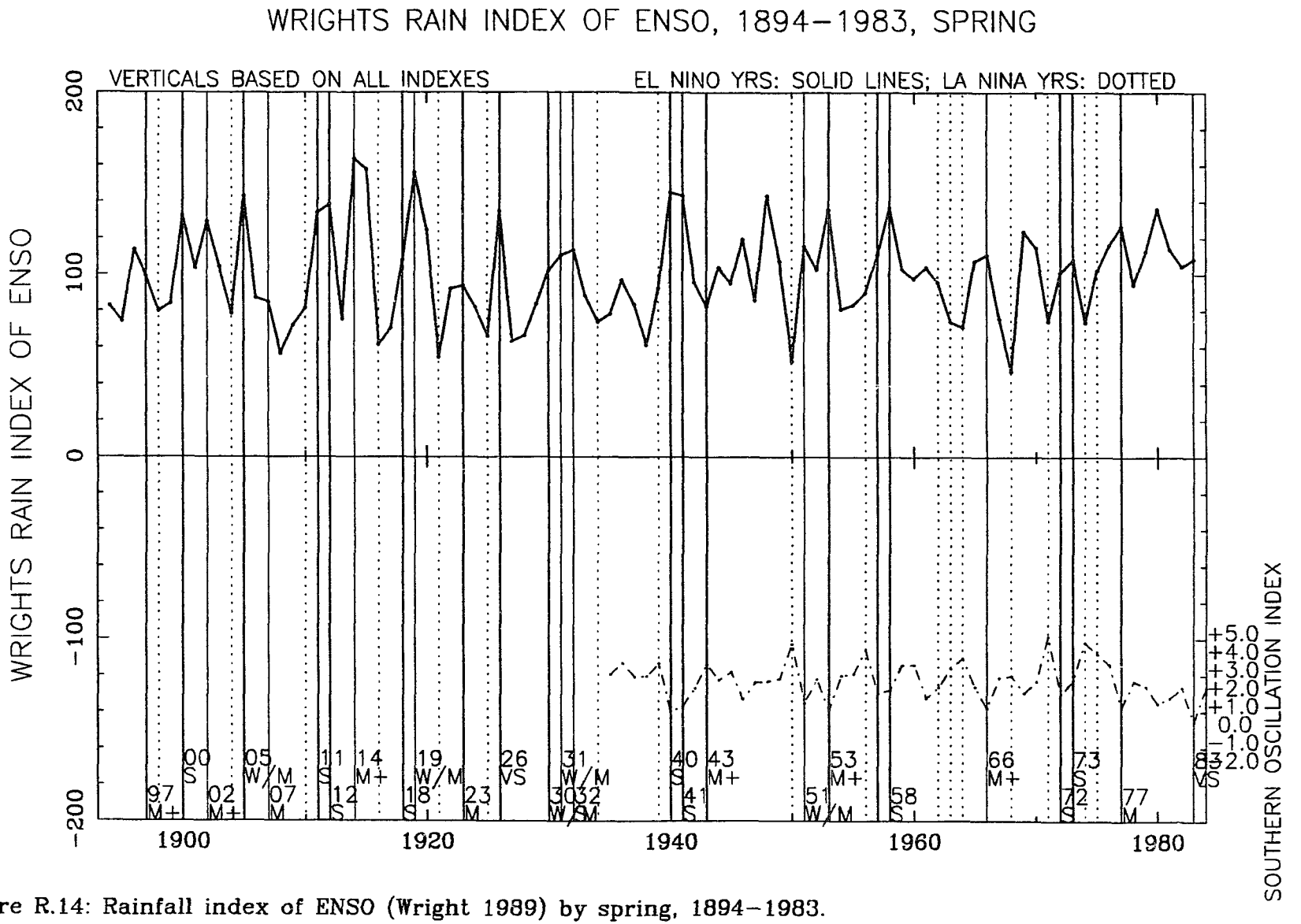

Figure R.14: Rainfall index of ENSO (Wright 1989) by spring, 1894–1983.

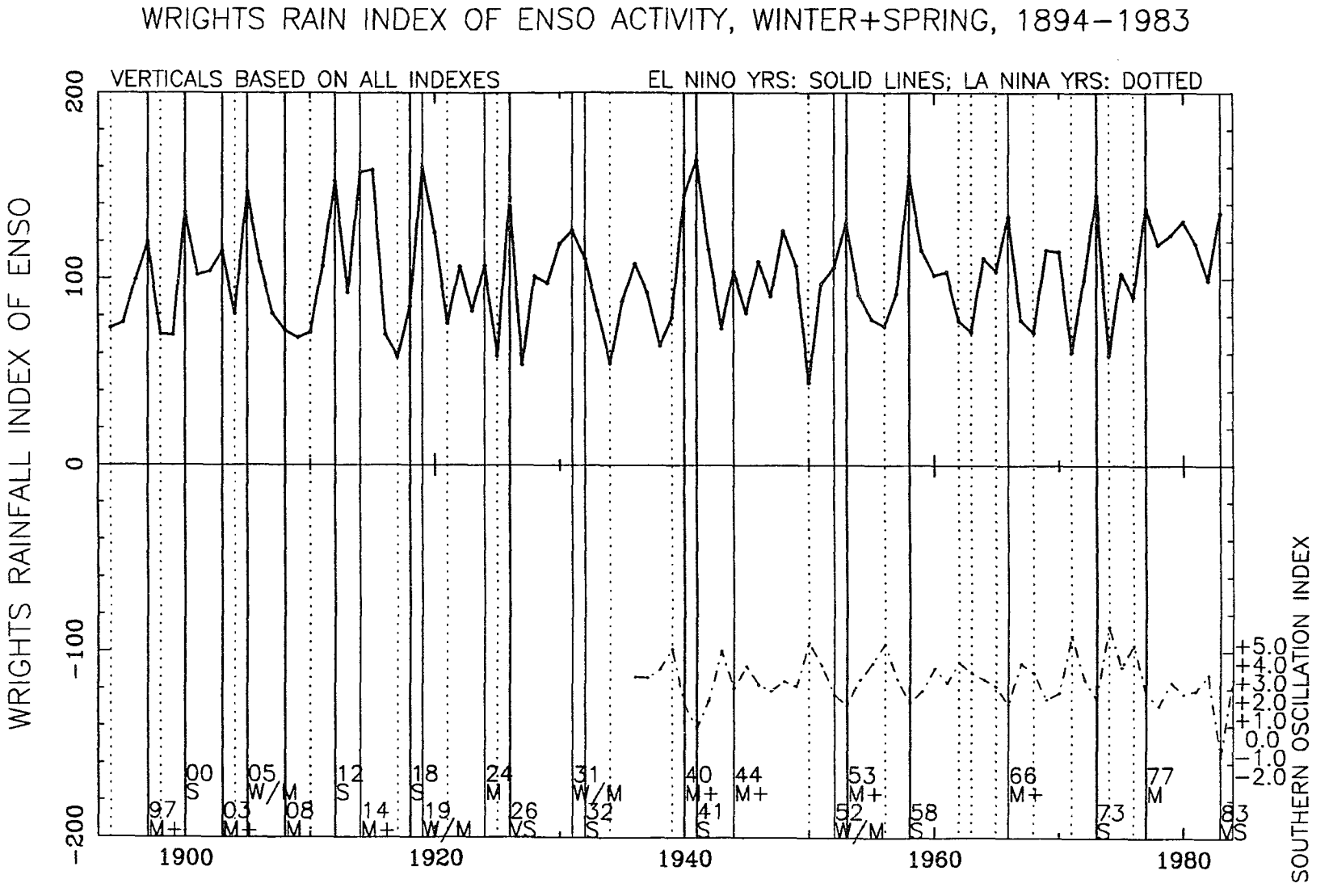

Figure R.15: Rainfall index of ENSO (Wright 1989) by winter–plus–spring, 1894–1983.

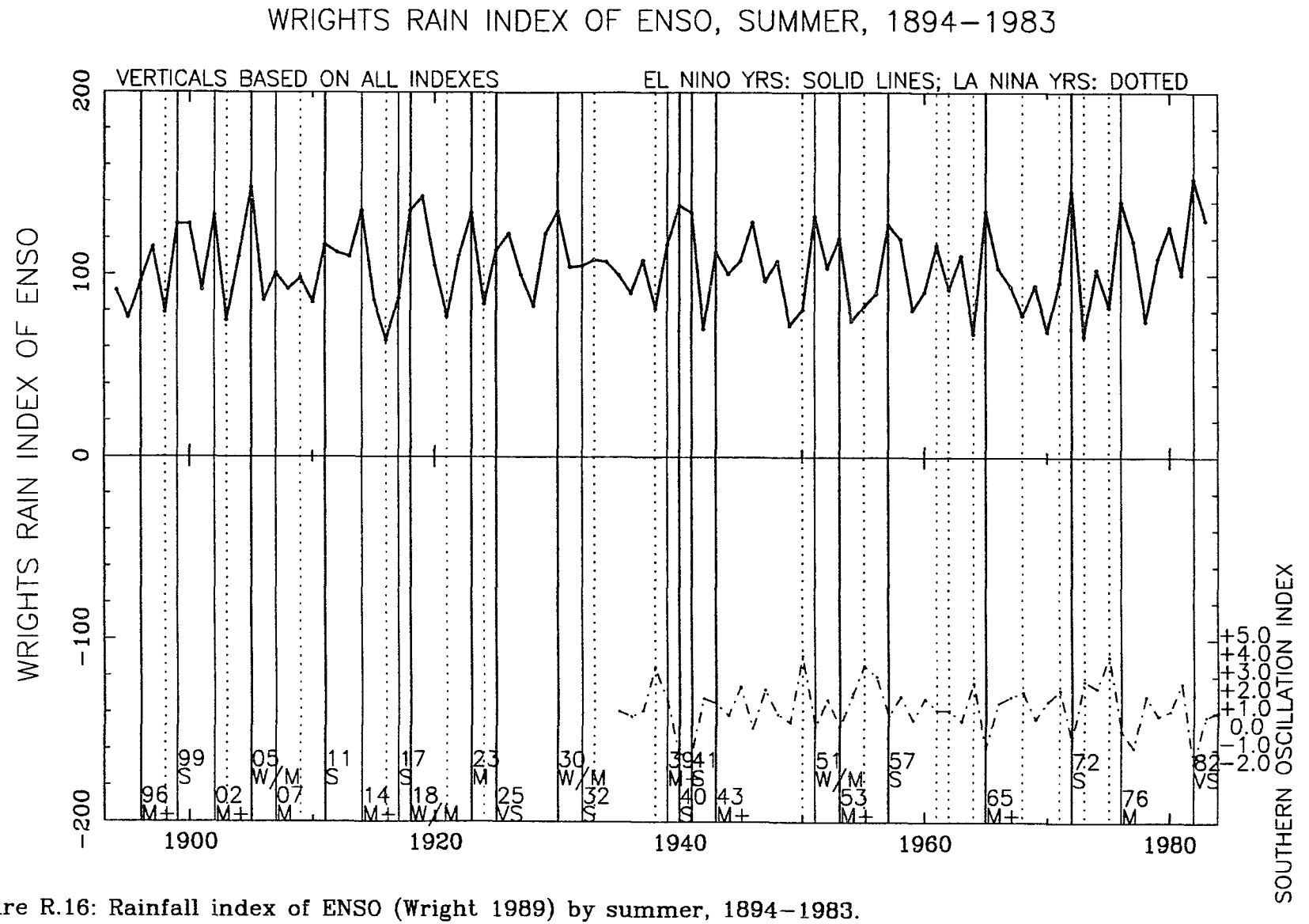

Figure R.16: Rainfall index of ENSO (Wright 1989) by summer, 1894–1983.

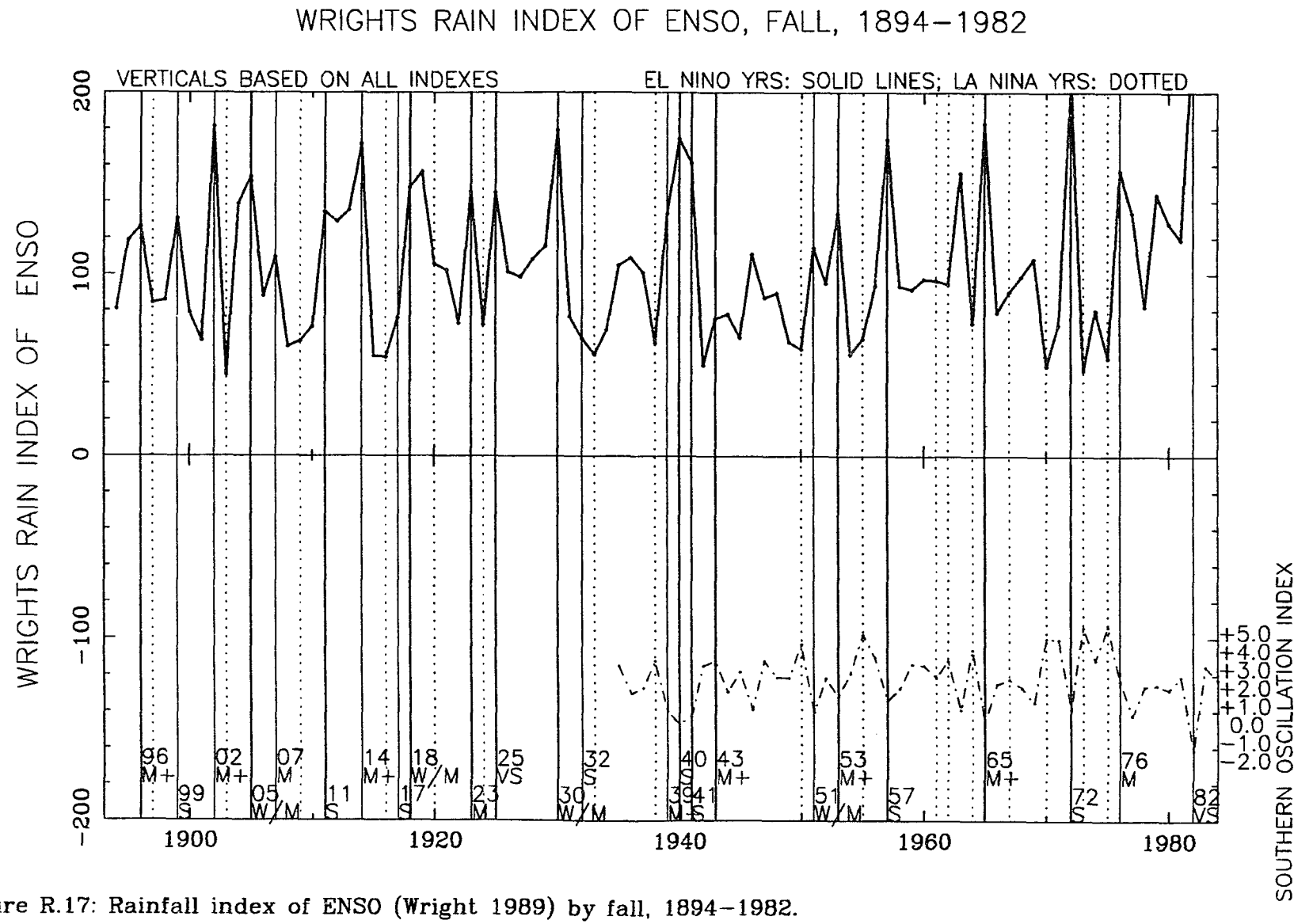

Figure R.17: Rainfall index of ENSO (Wright 1989) by fall, 1894–1982.

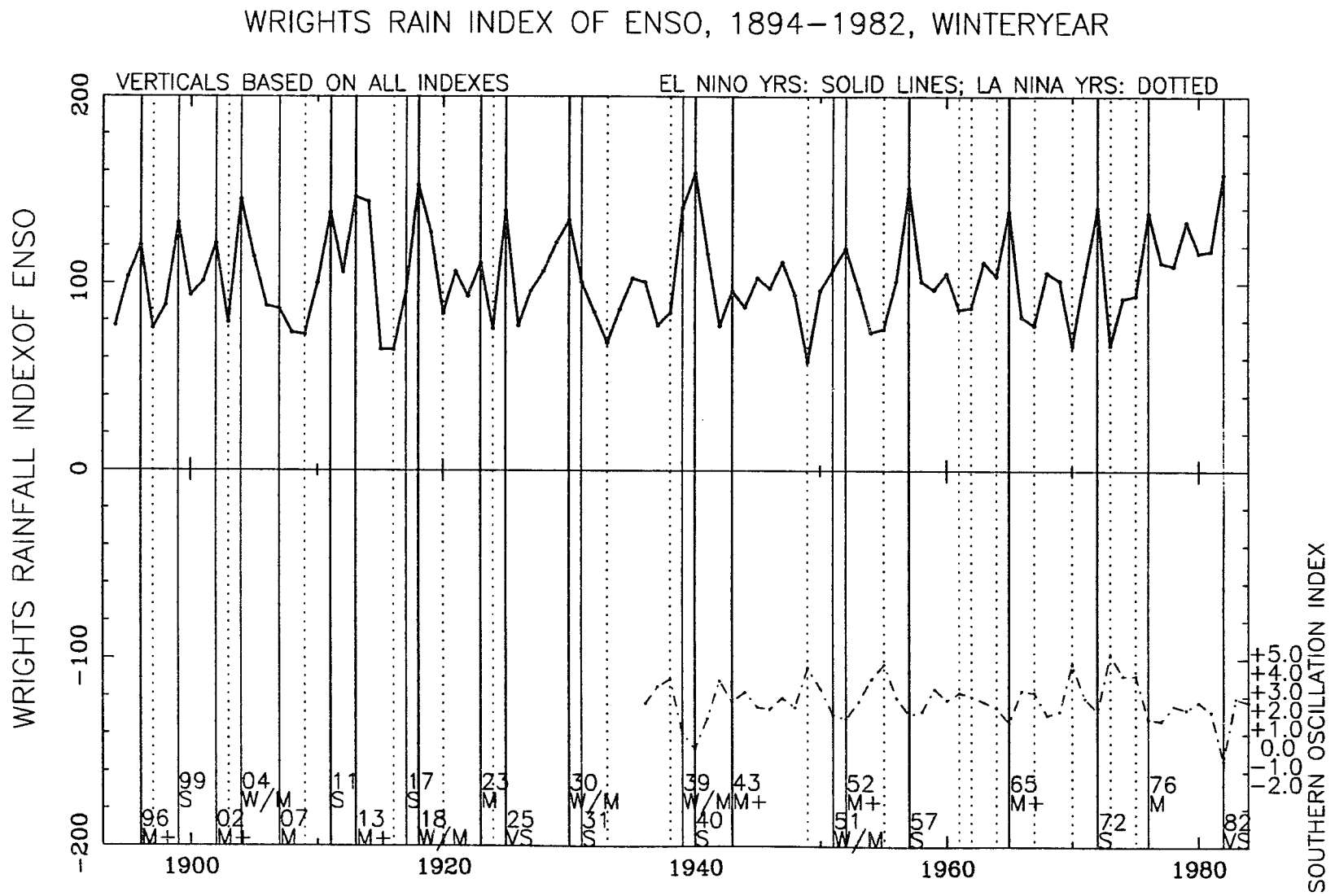

Figure R.18: Rainfall index of ENSO (Wright 1989) by winter year, 1894–1982.

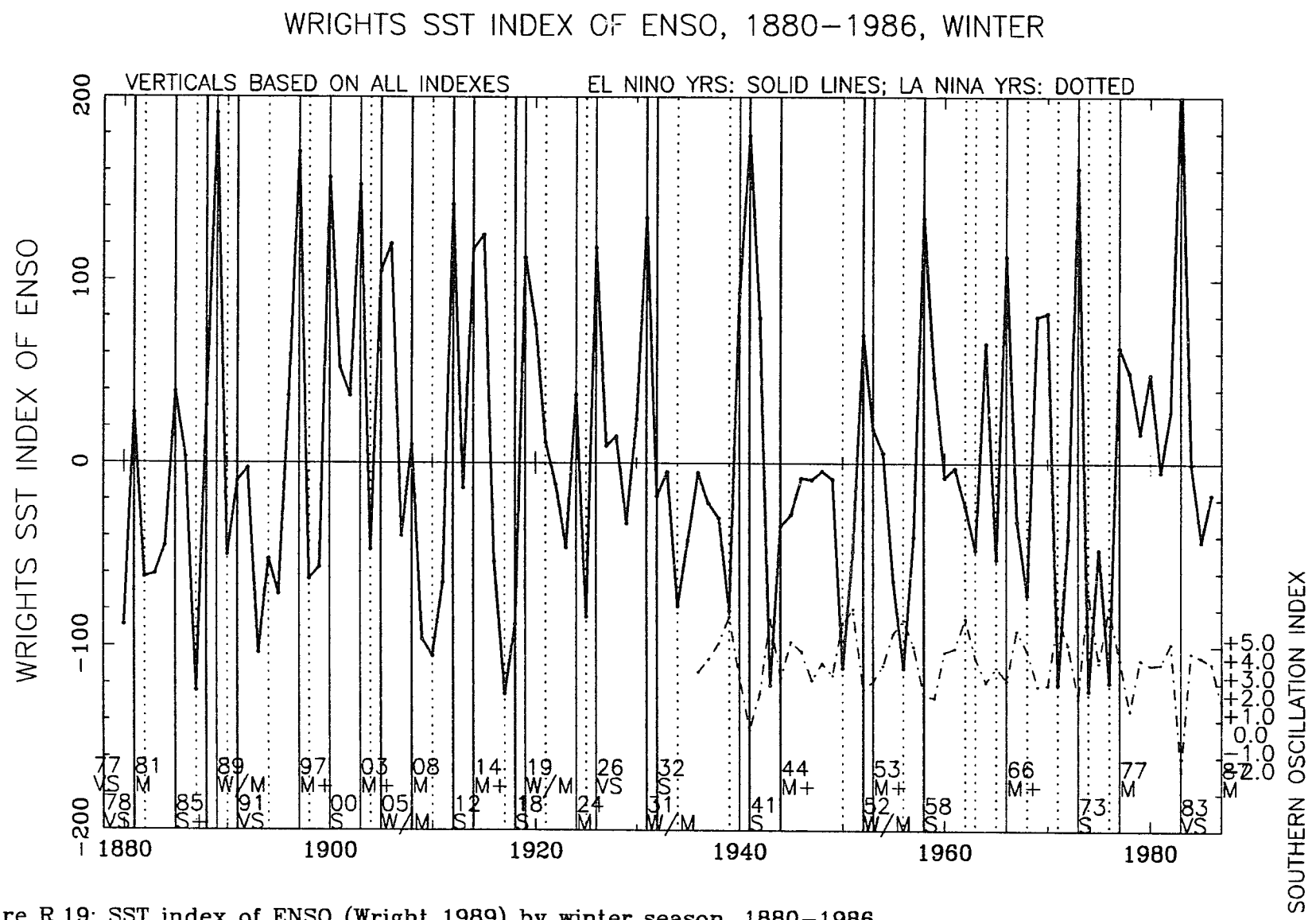

Figure R.19: SST index of ENSO (Wright 1989) by winter season, 1880–1986.

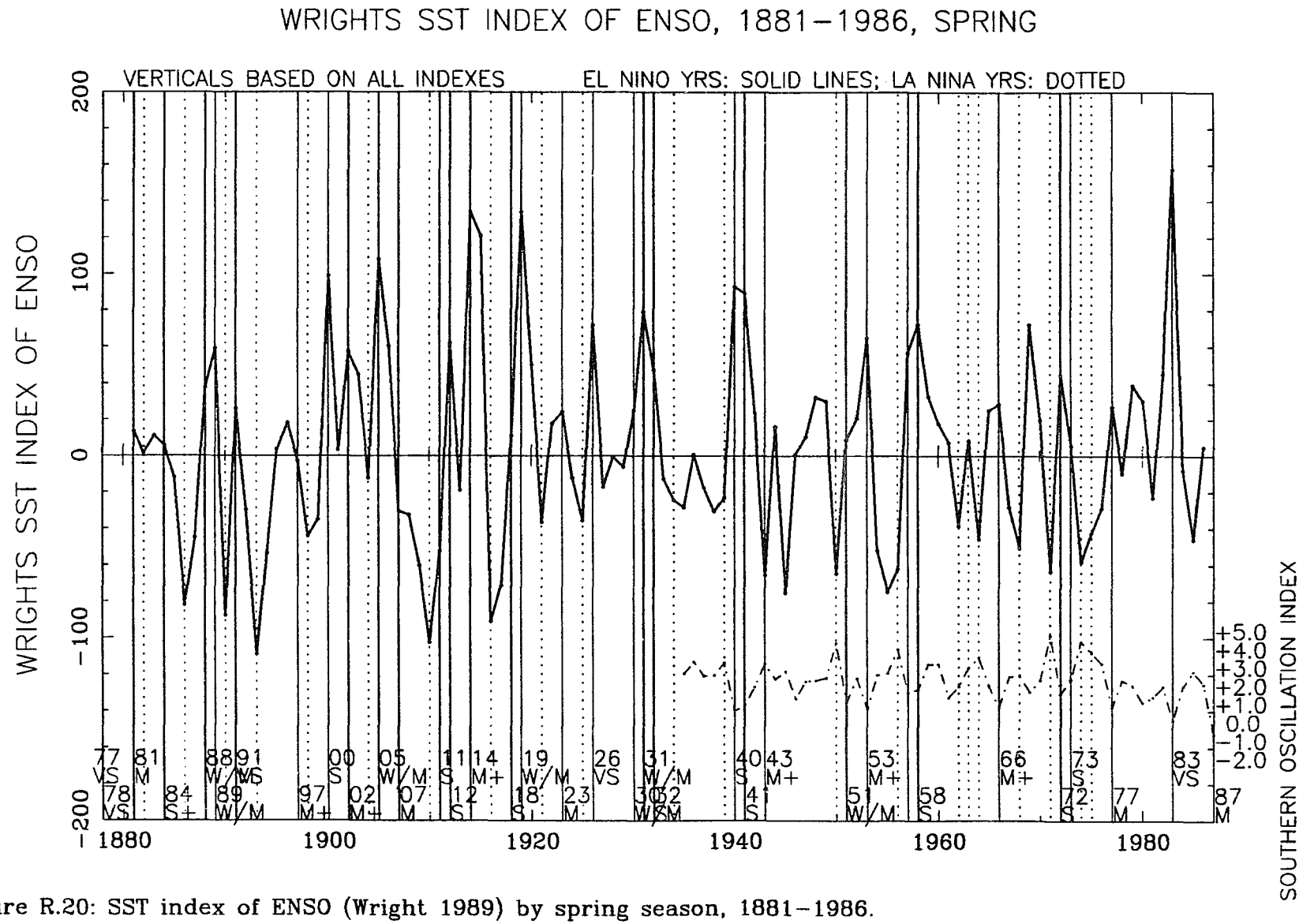

Figure R.20: SST index of ENSO (Wright 1989) by spring season, 1881–1986.

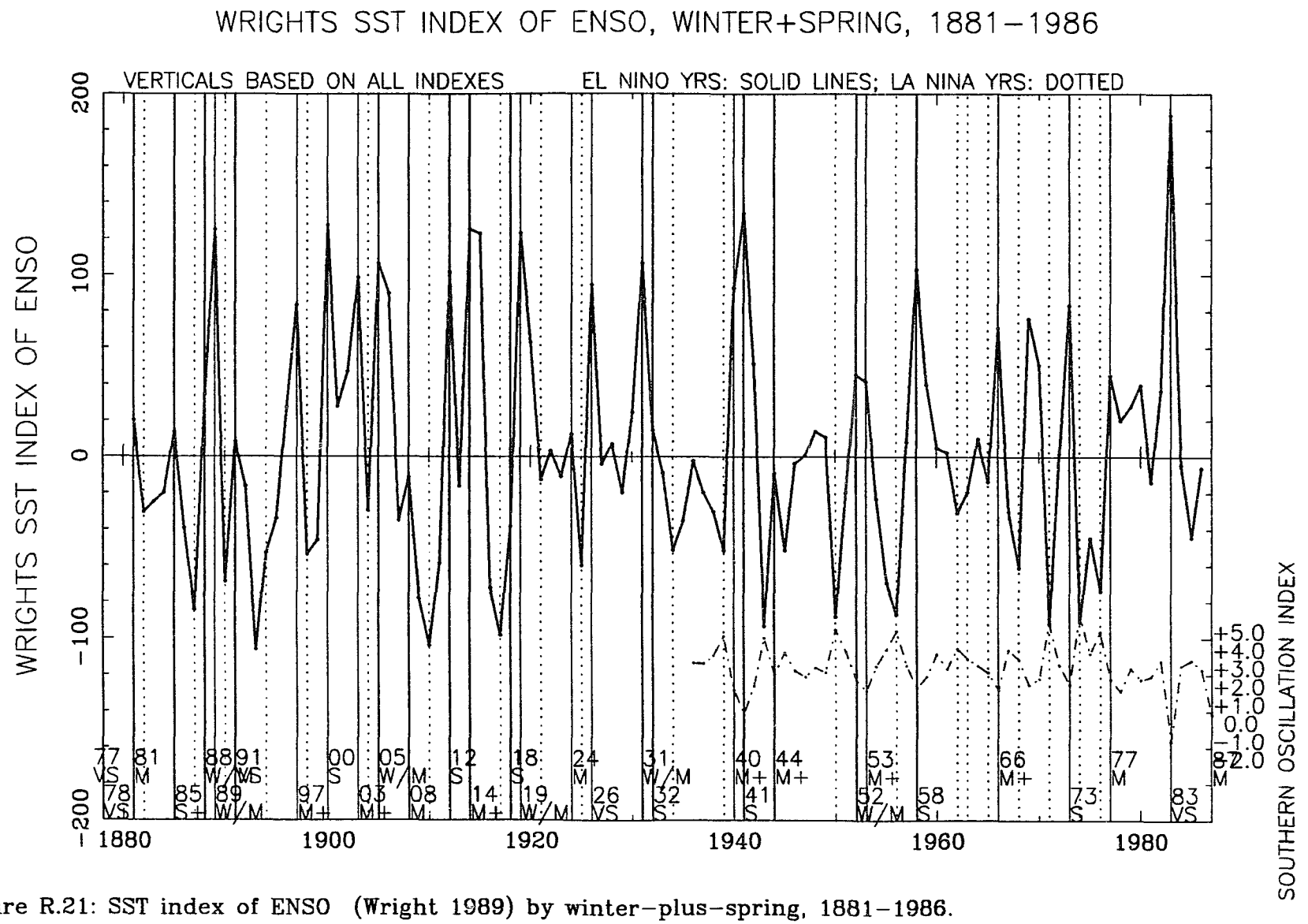

Figure R.21: SST index of ENSO (Wright 1989) by winter–plus–spring, 1881–1986.

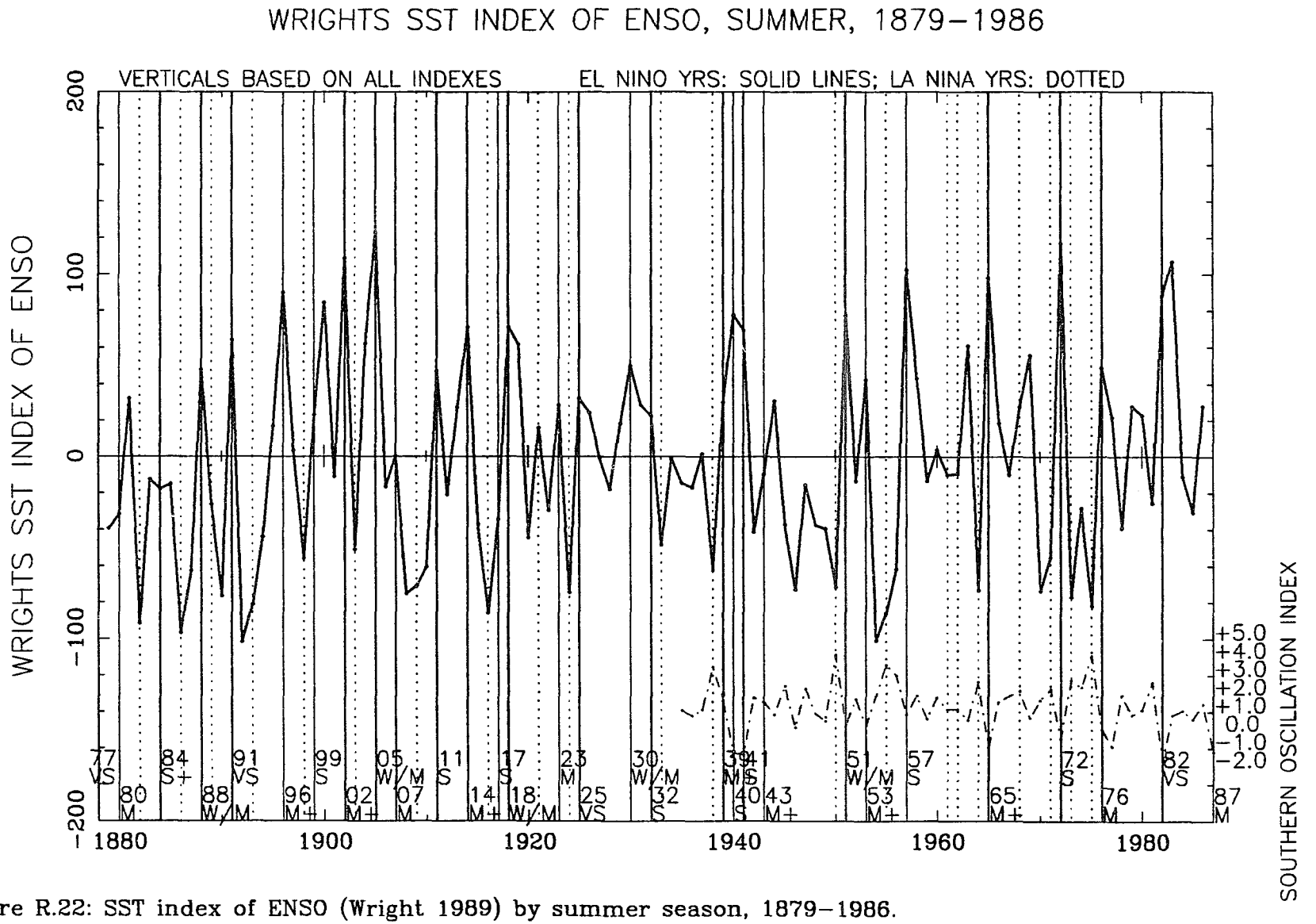

Figure R.22: SST index of ENSO (Wright 1989) by summer season, 1879–1986.

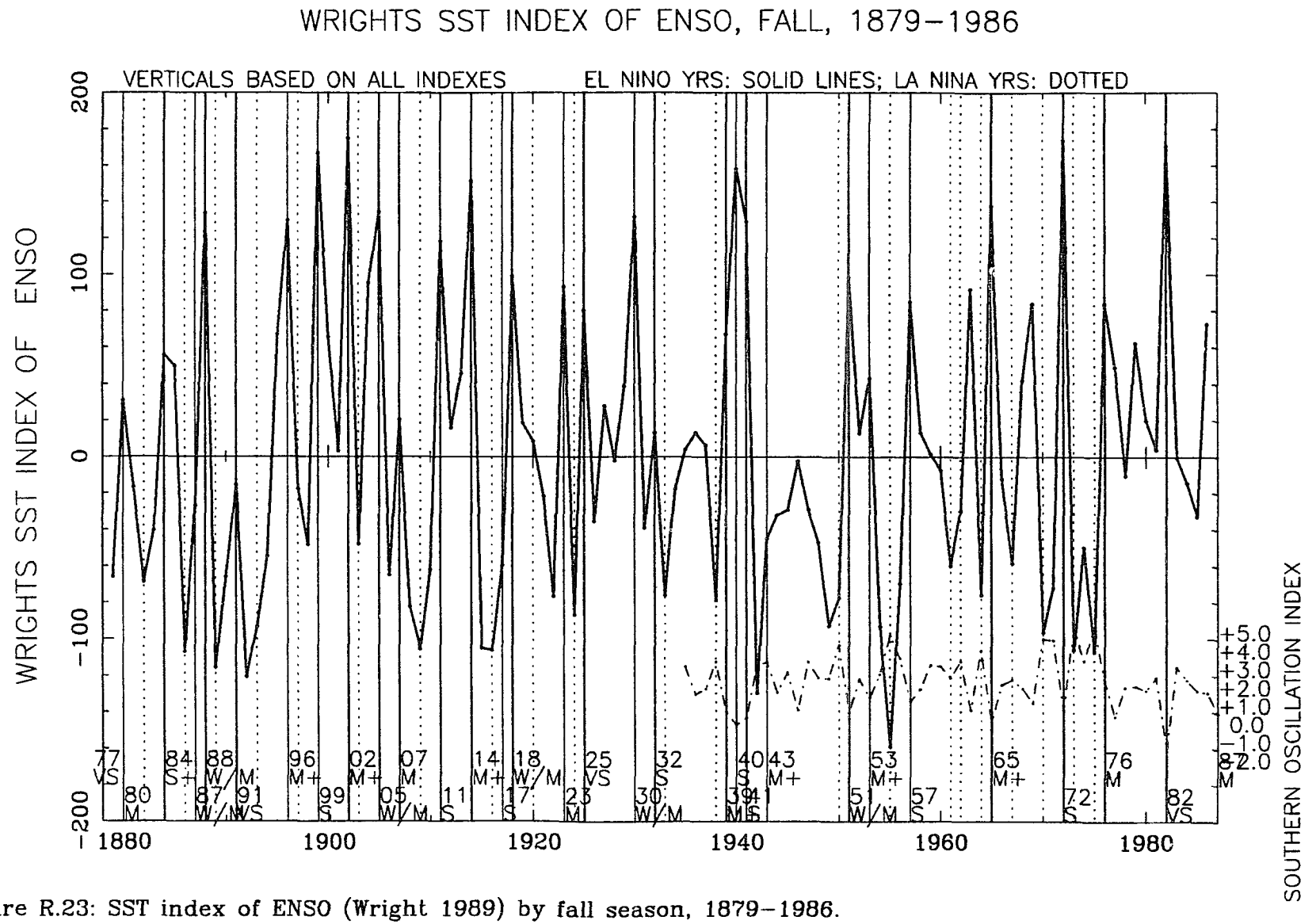

Figure R.23: SST index of ENSO (Wright 1989) by fall season, 1879–1986.

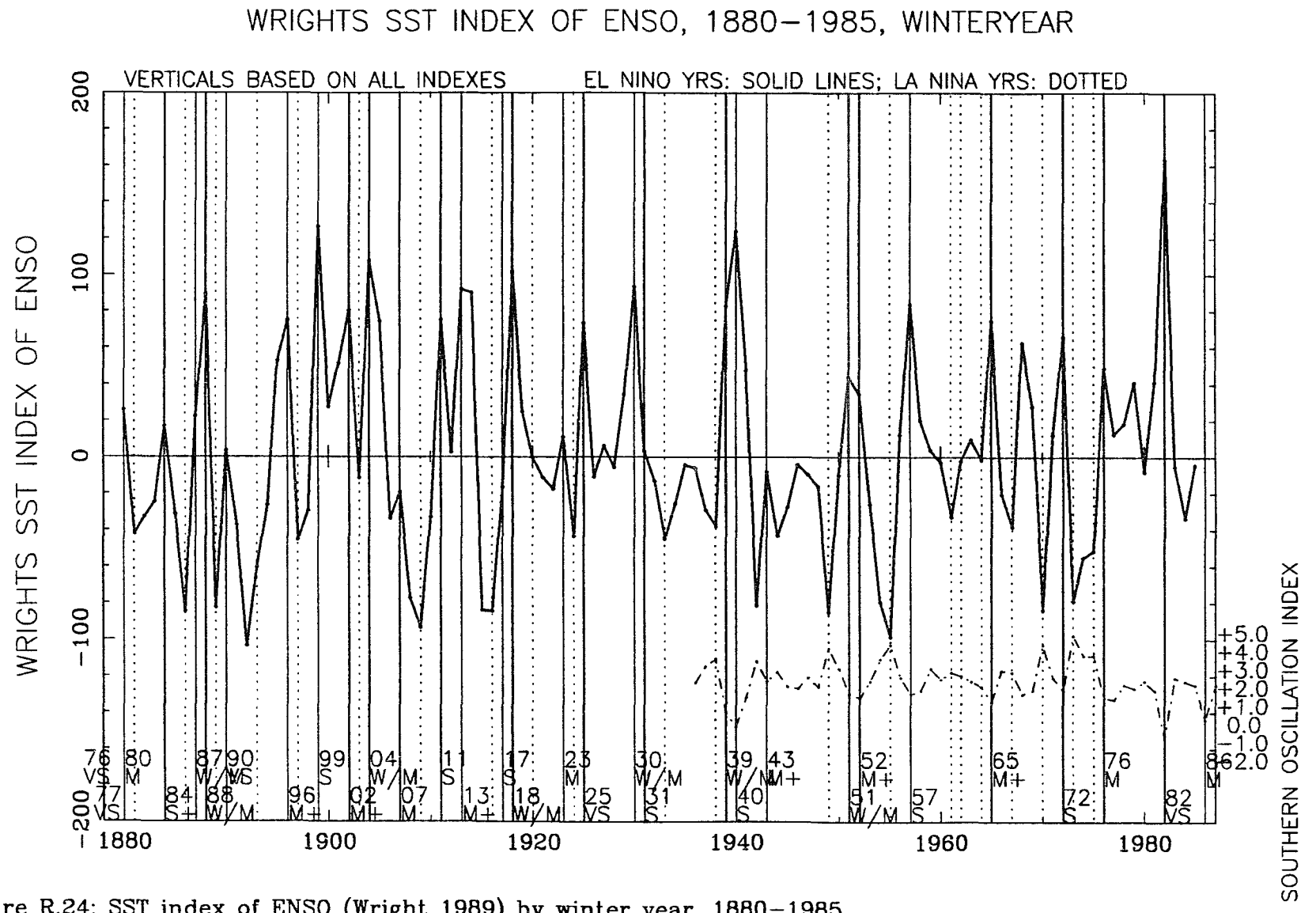

Figure R.24: SST index of ENSO (Wright 1989) by winter year, 1880–1985.

APPENDIX S
STORM LOCATIONS: 1940-89

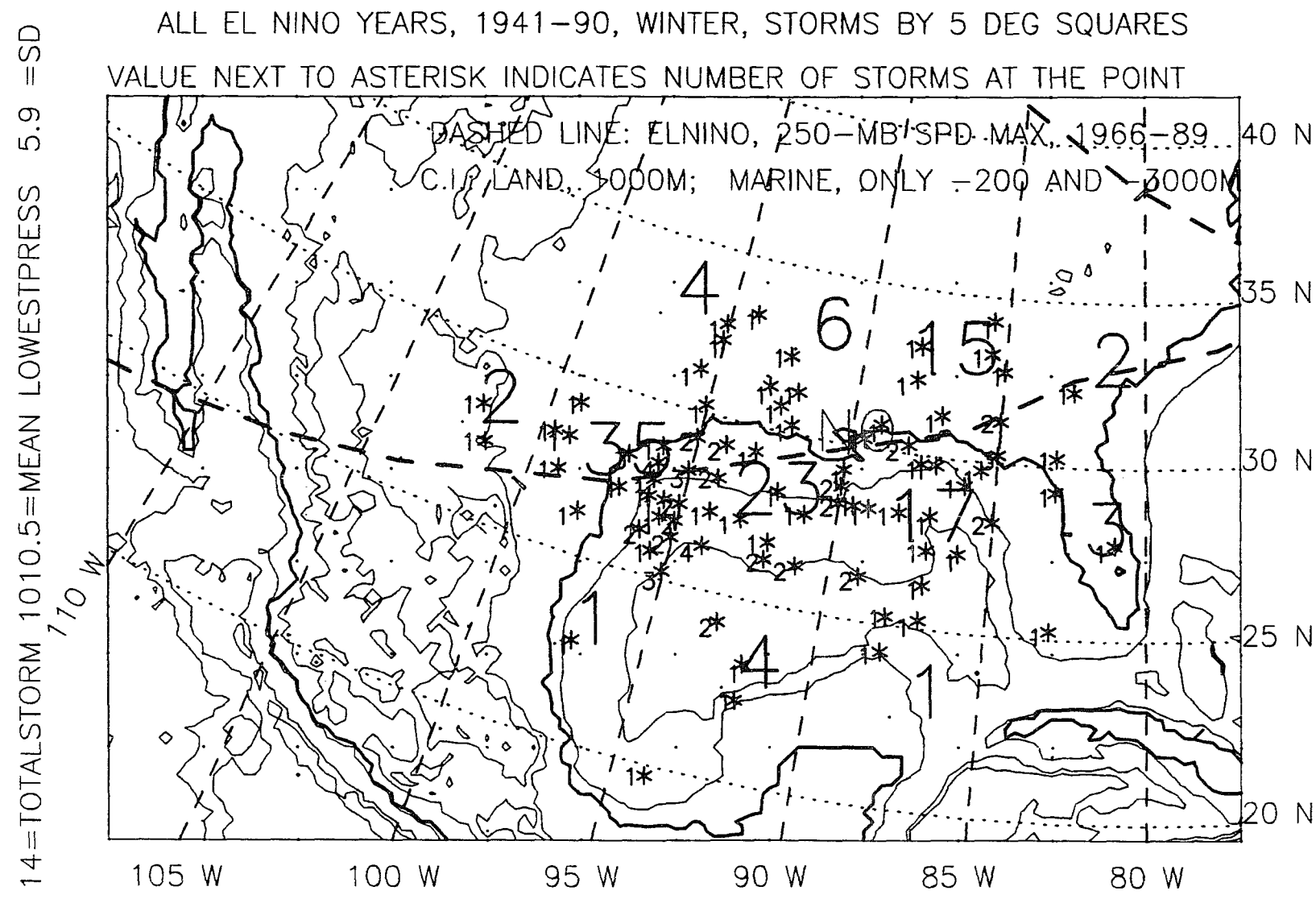

Figure S.1: Storm locations, winter, 10 El Niño years, 1941–90.

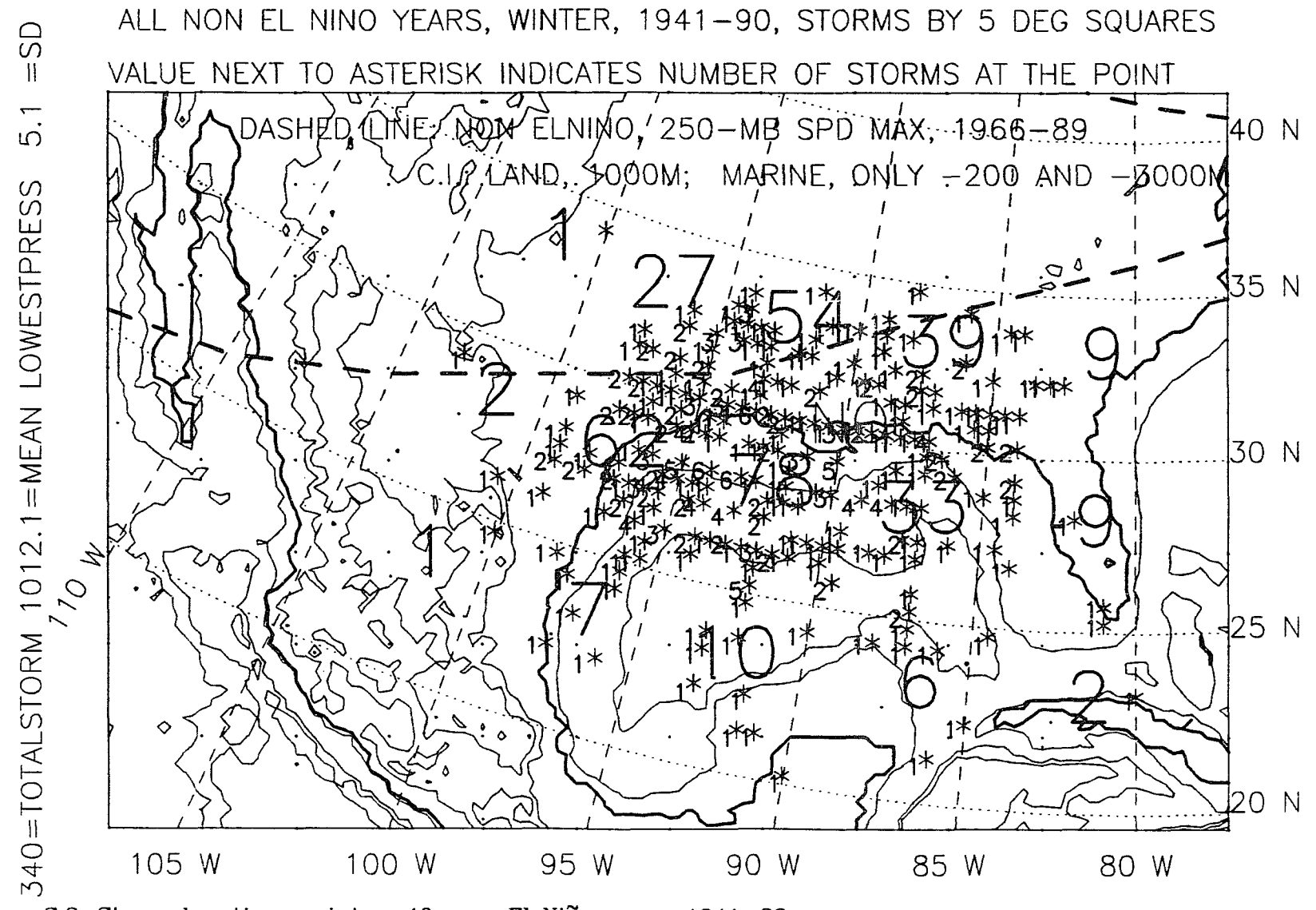

Figure S.2: Storm locations, winter, 40 non-El Niño years, 1941-90.

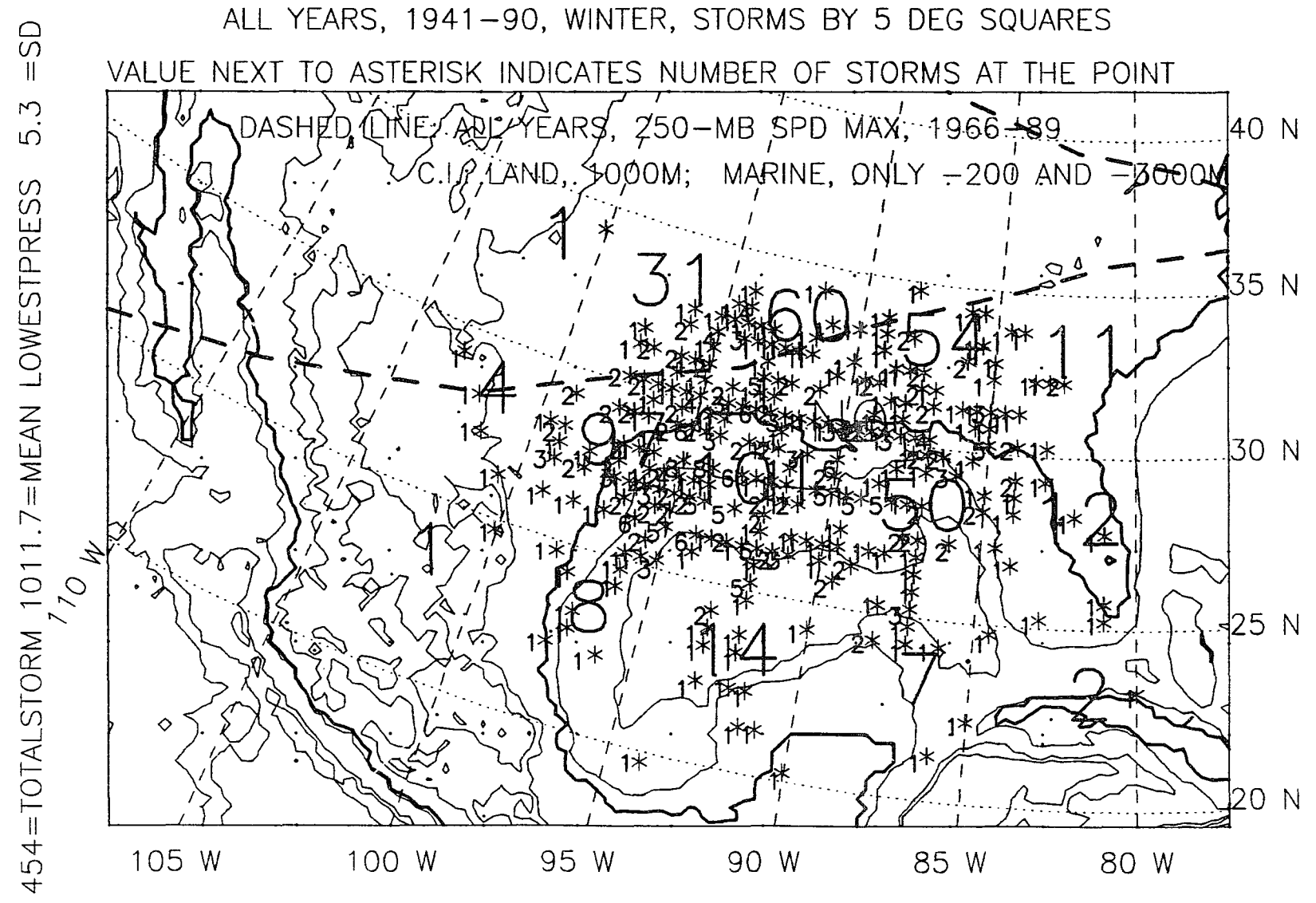

Figure S.3: Storm locations, winter, all 50 years, 1941–90.

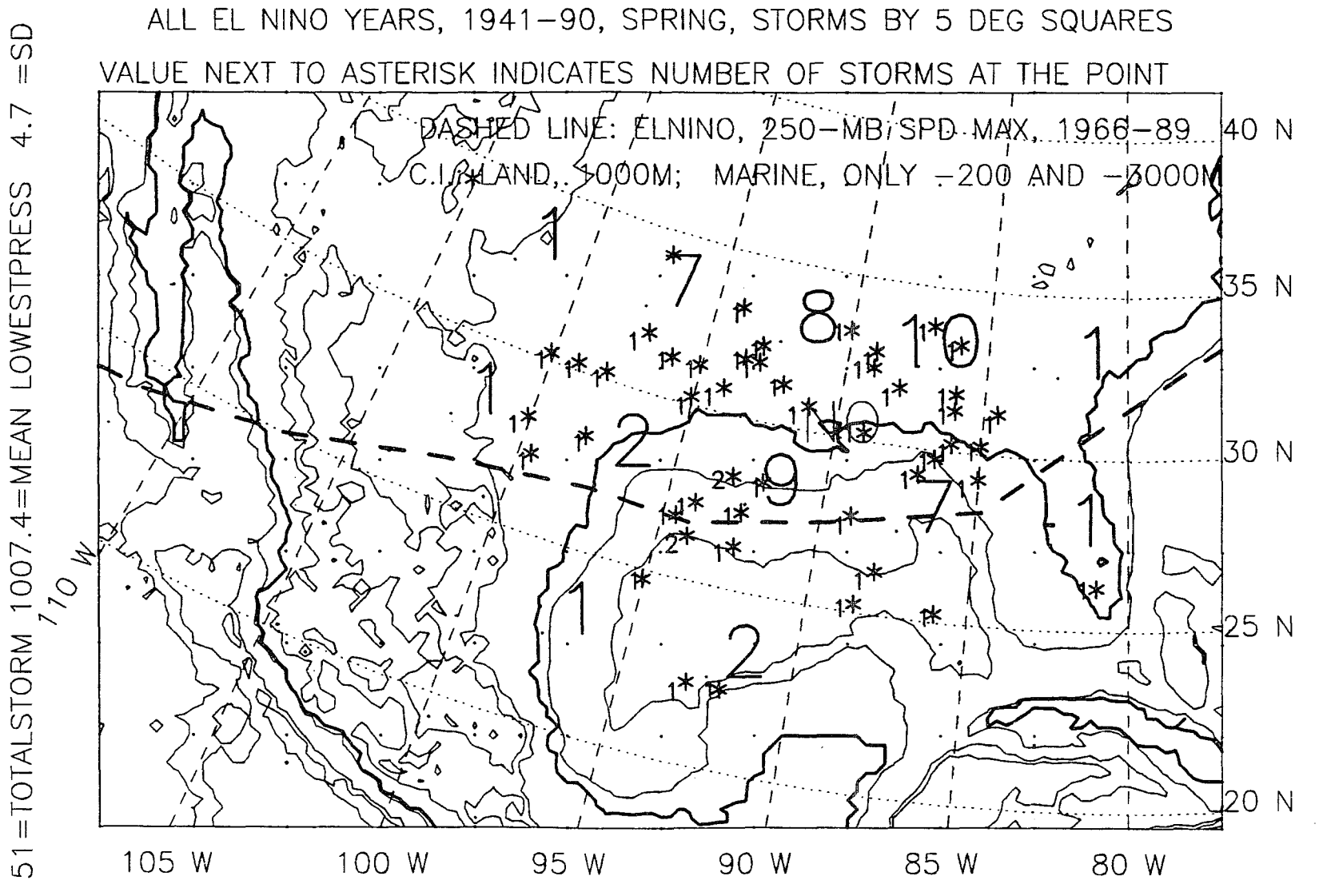

Figure S.4: Storm locations, spring, 12 El Niño springs, 1941–90.

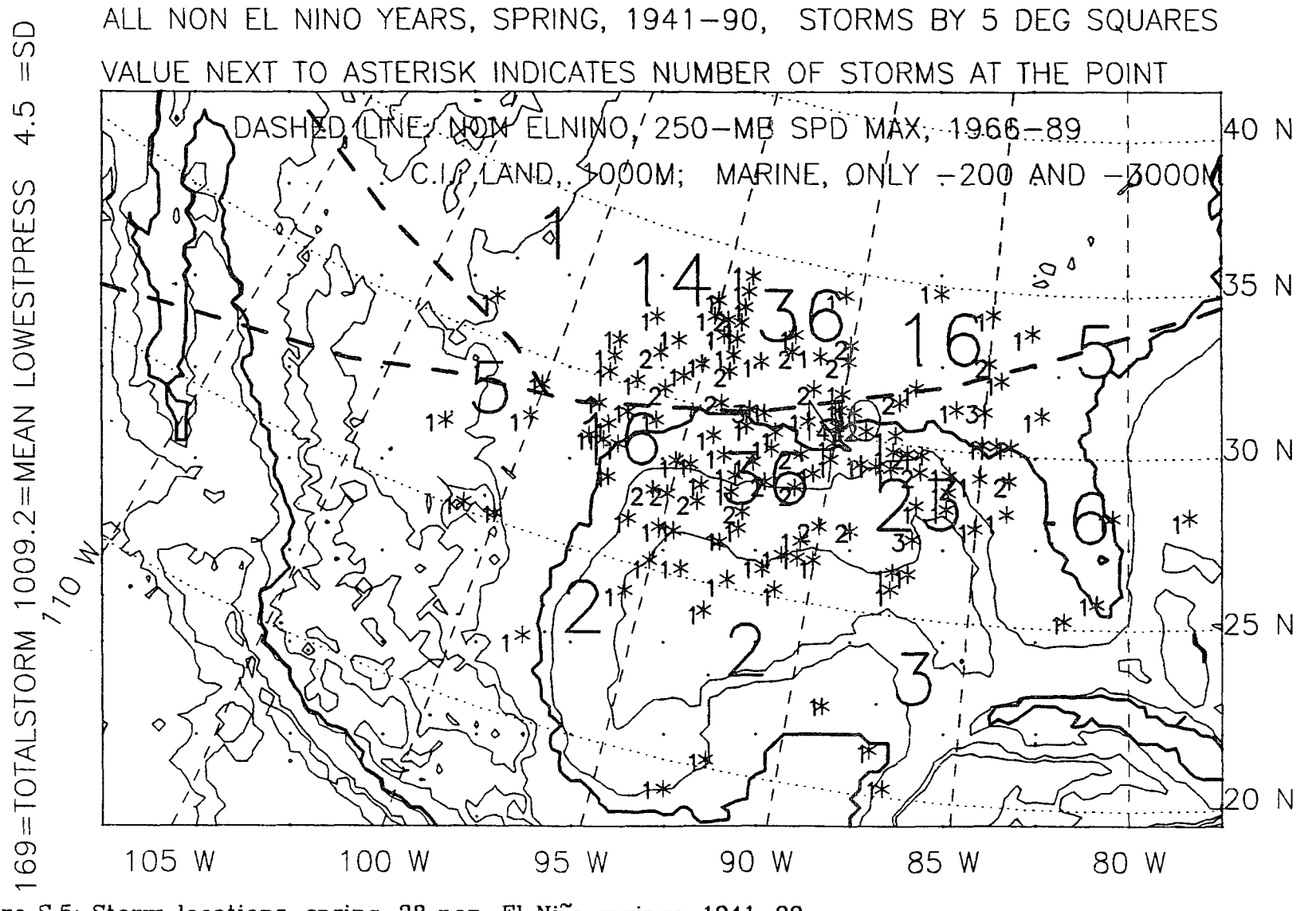

Figure S.5: Storm locations, spring, 38 non–El Niño springs, 1941–90.

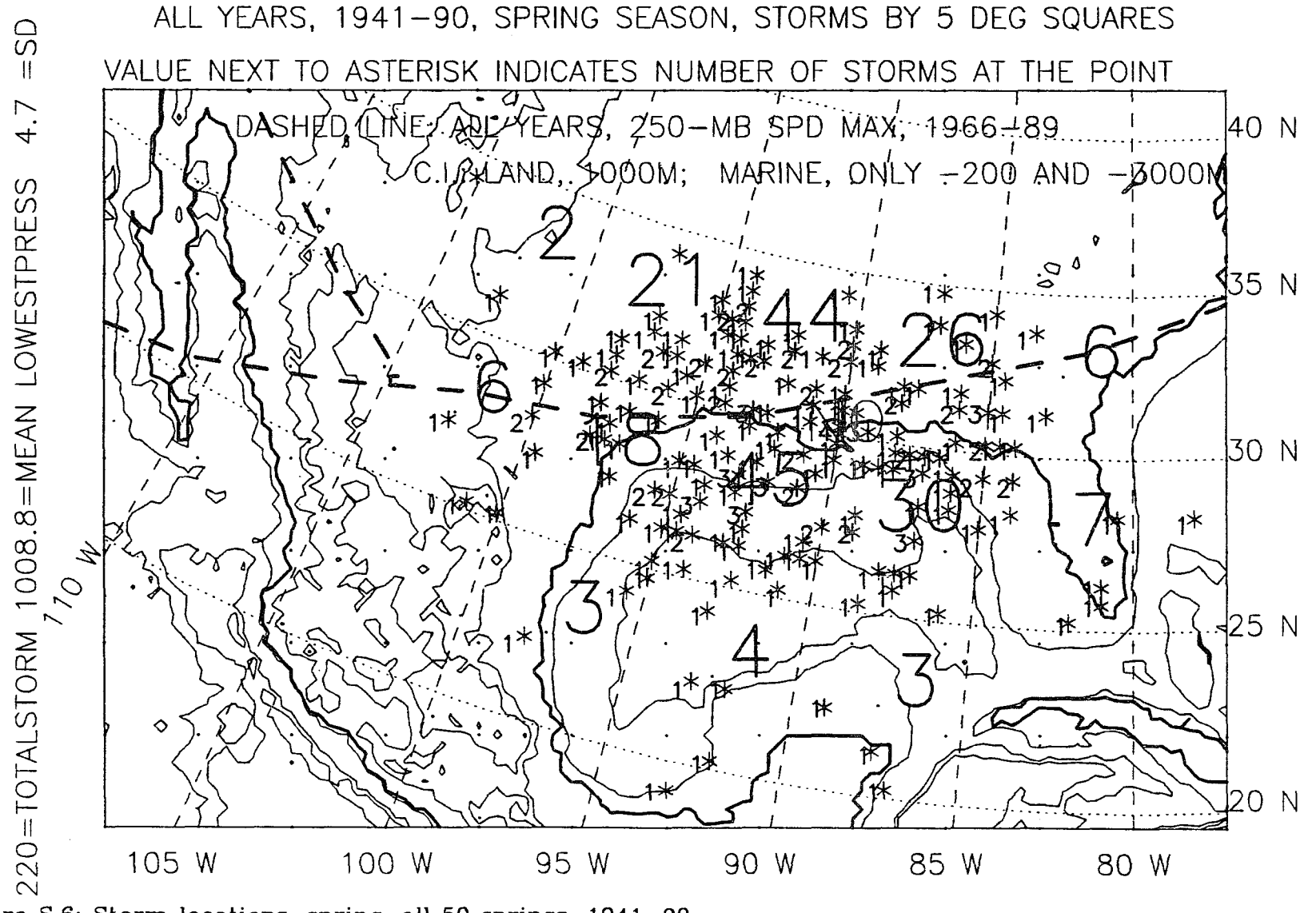

Figure S.6: Storm locations, spring, all 50 springs, 1941–90.

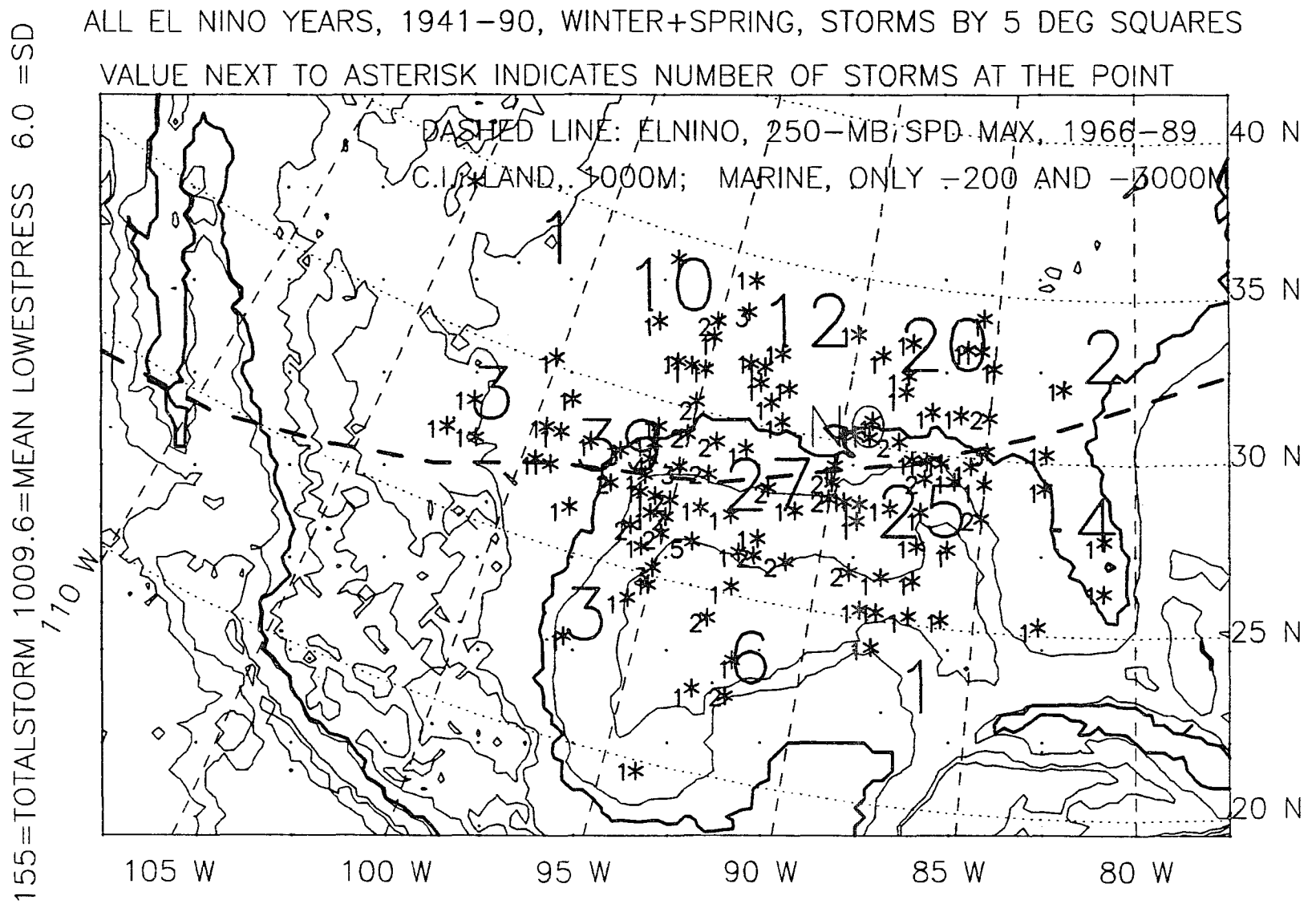

Figure S.7: Storm locations, winter–plus–spring, 10 El Niño years, 1941–90.

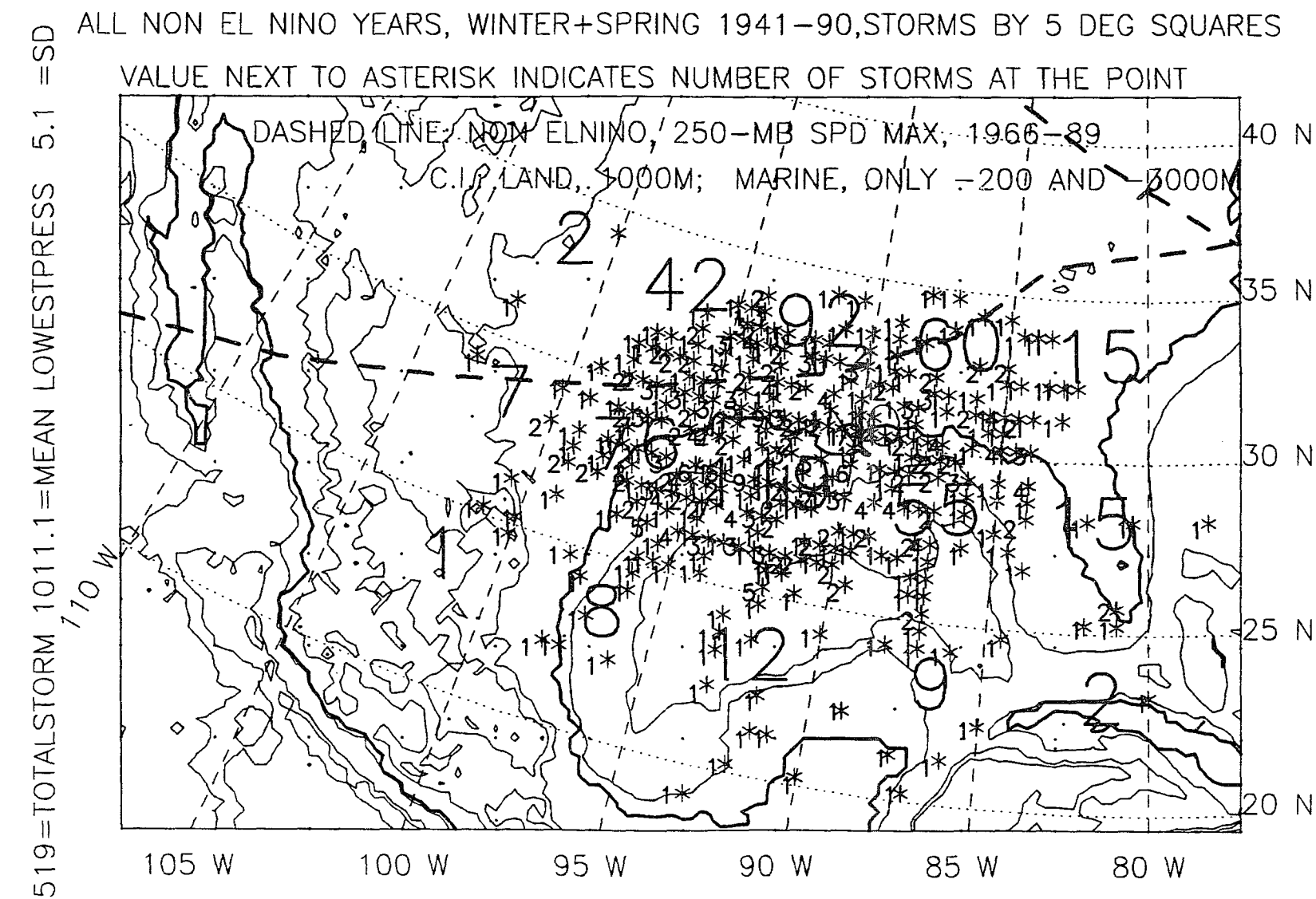

Figure S.8: Storm locations, winter-plus-spring, 40 non-El Niño years, 1941-90.

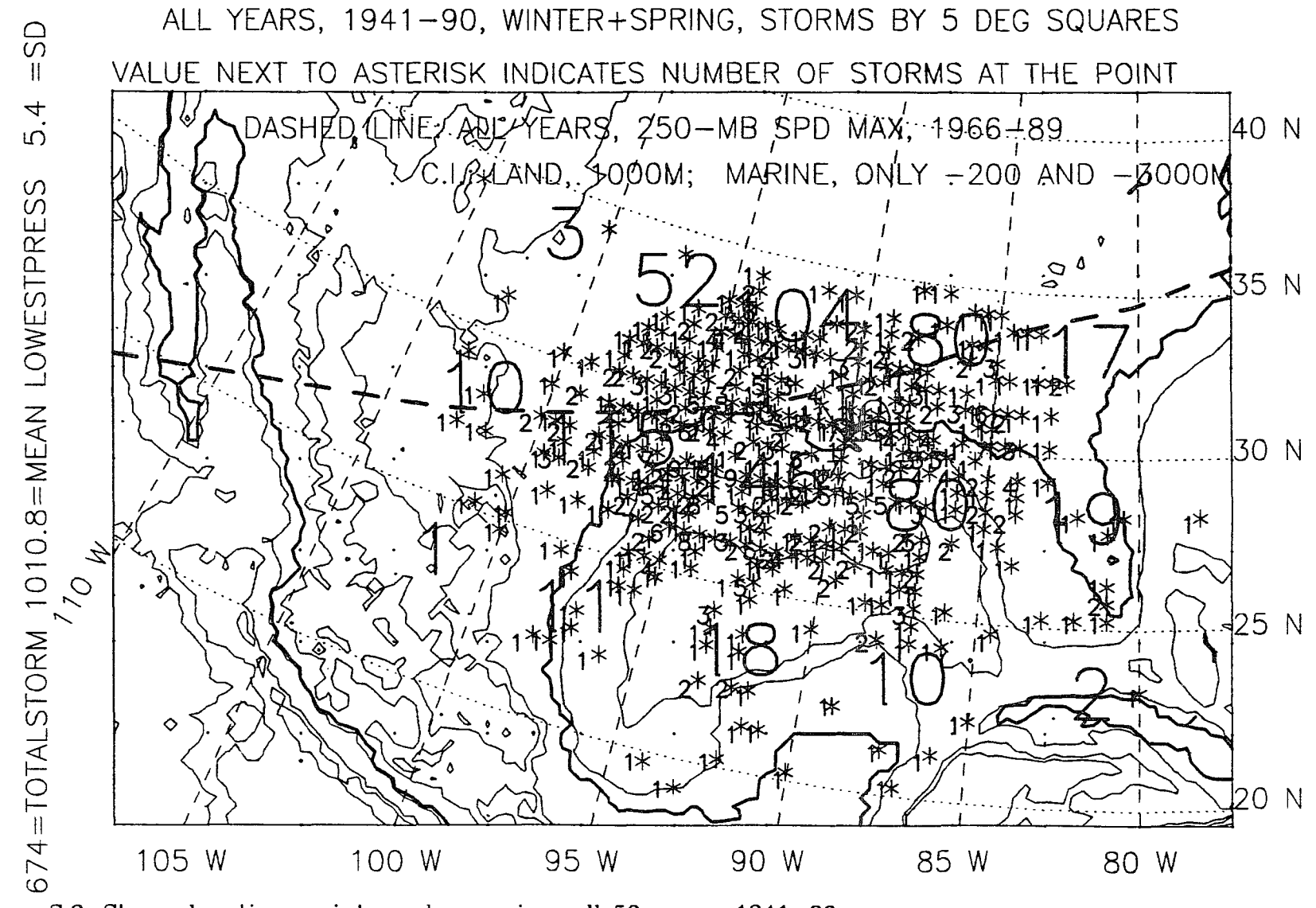

Figure S.9: Storm locations, winter–plus–spring, all 50 years, 1941–90.

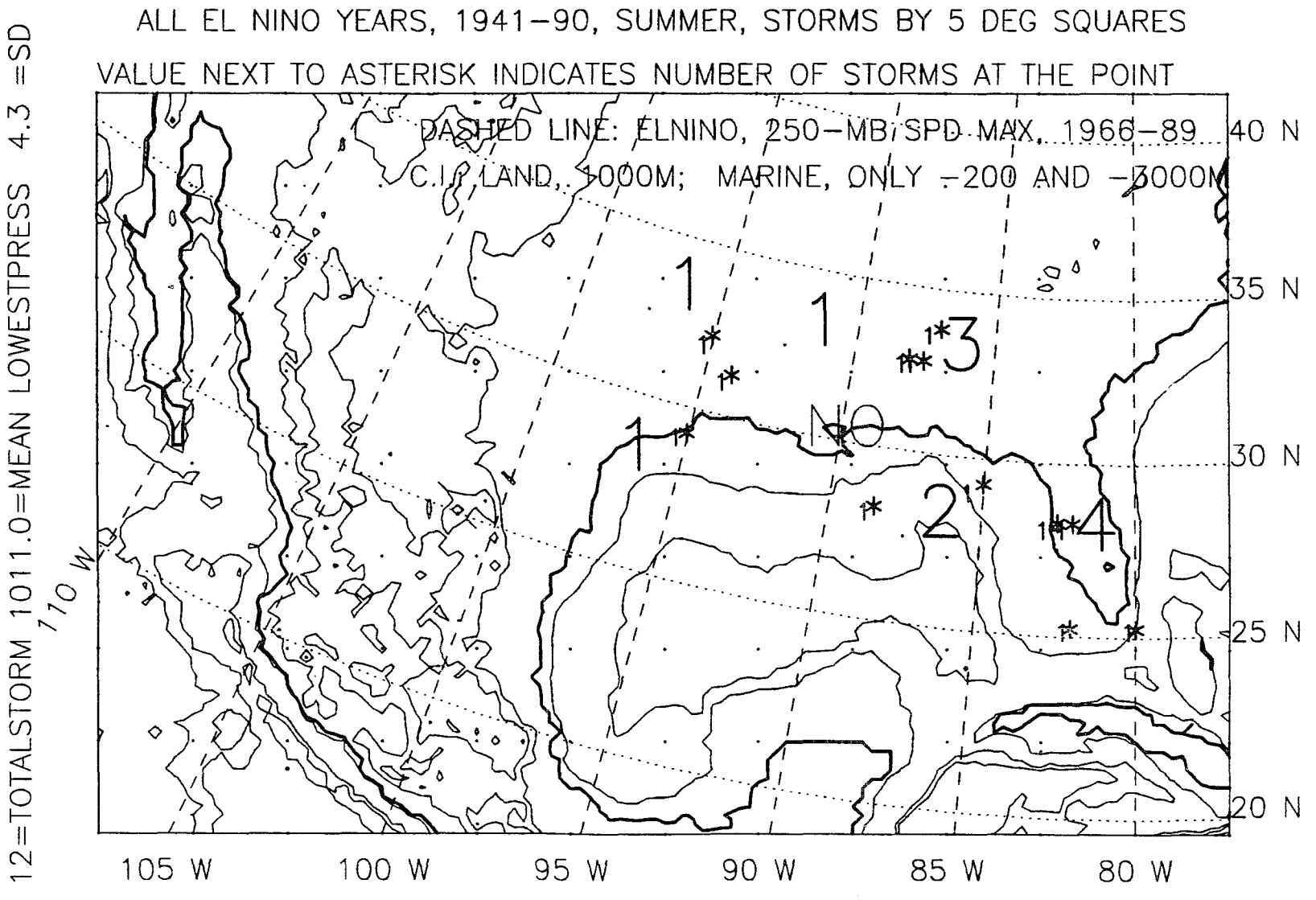

Figure S.10: Storm locations, summer, 10 El Niño years, 1941–90.

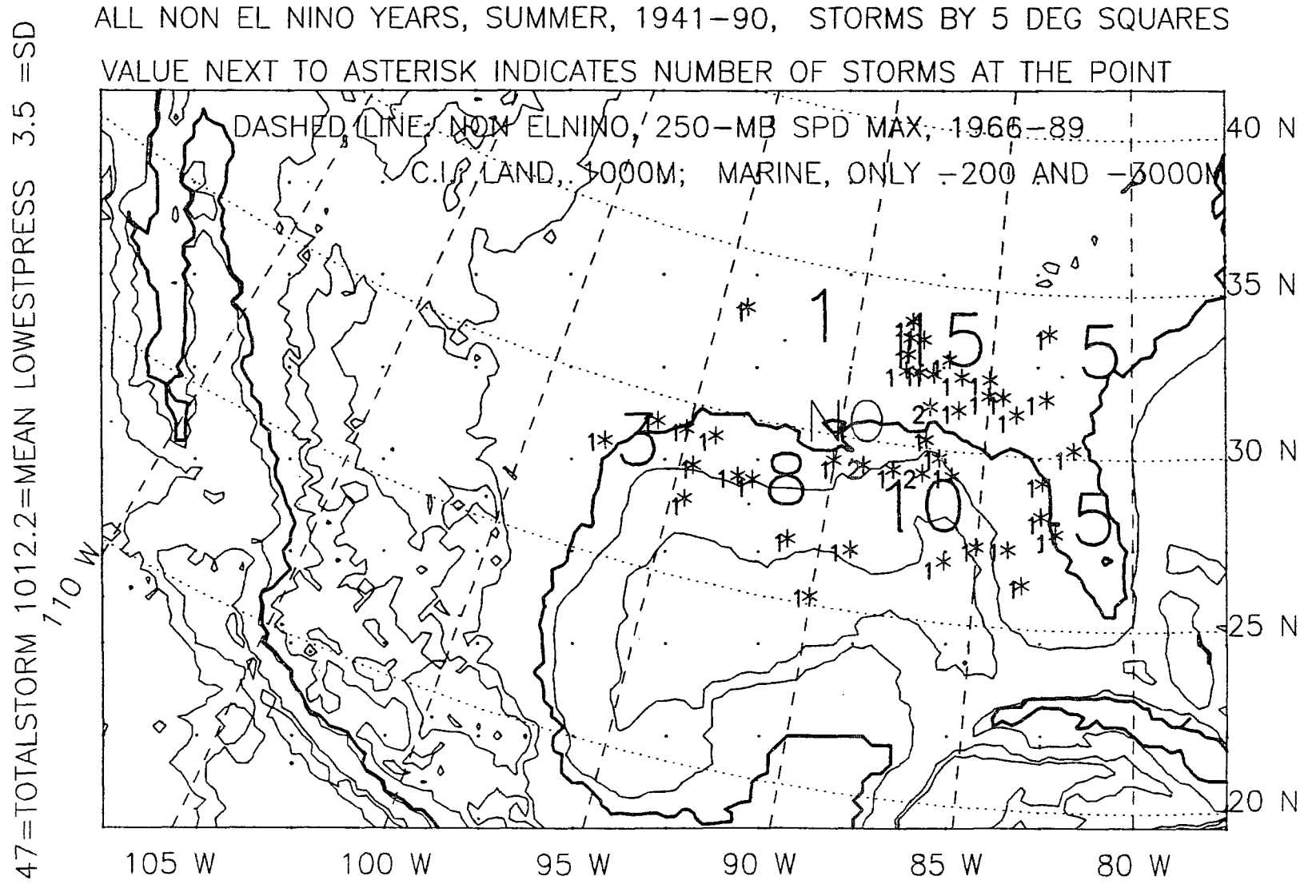

Figure S.11: Storm locations, summer, 40 non–El Niño years, 1941–90.

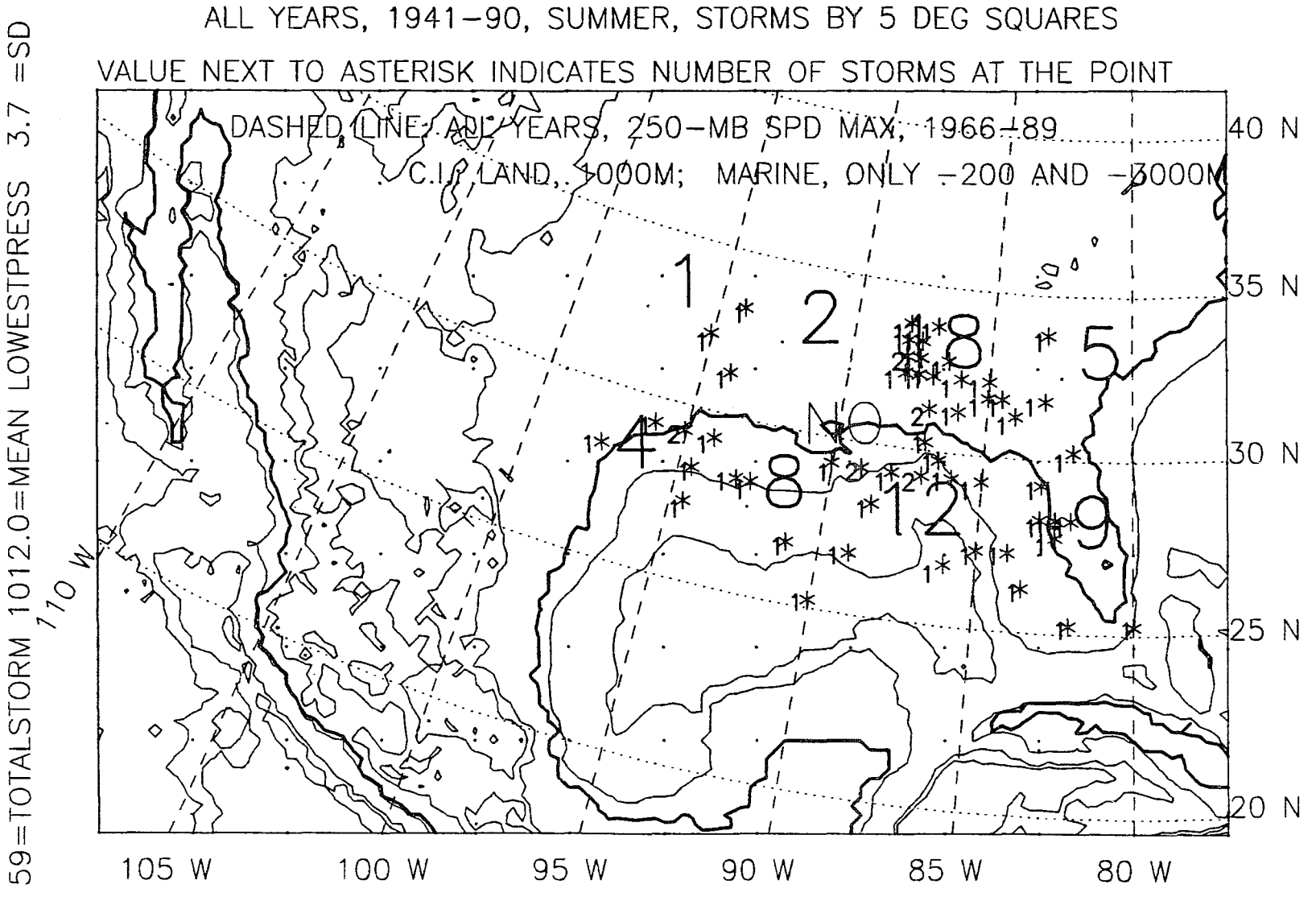

Figure S.12: Storm locations, summer, all 50 years, 1941–90.

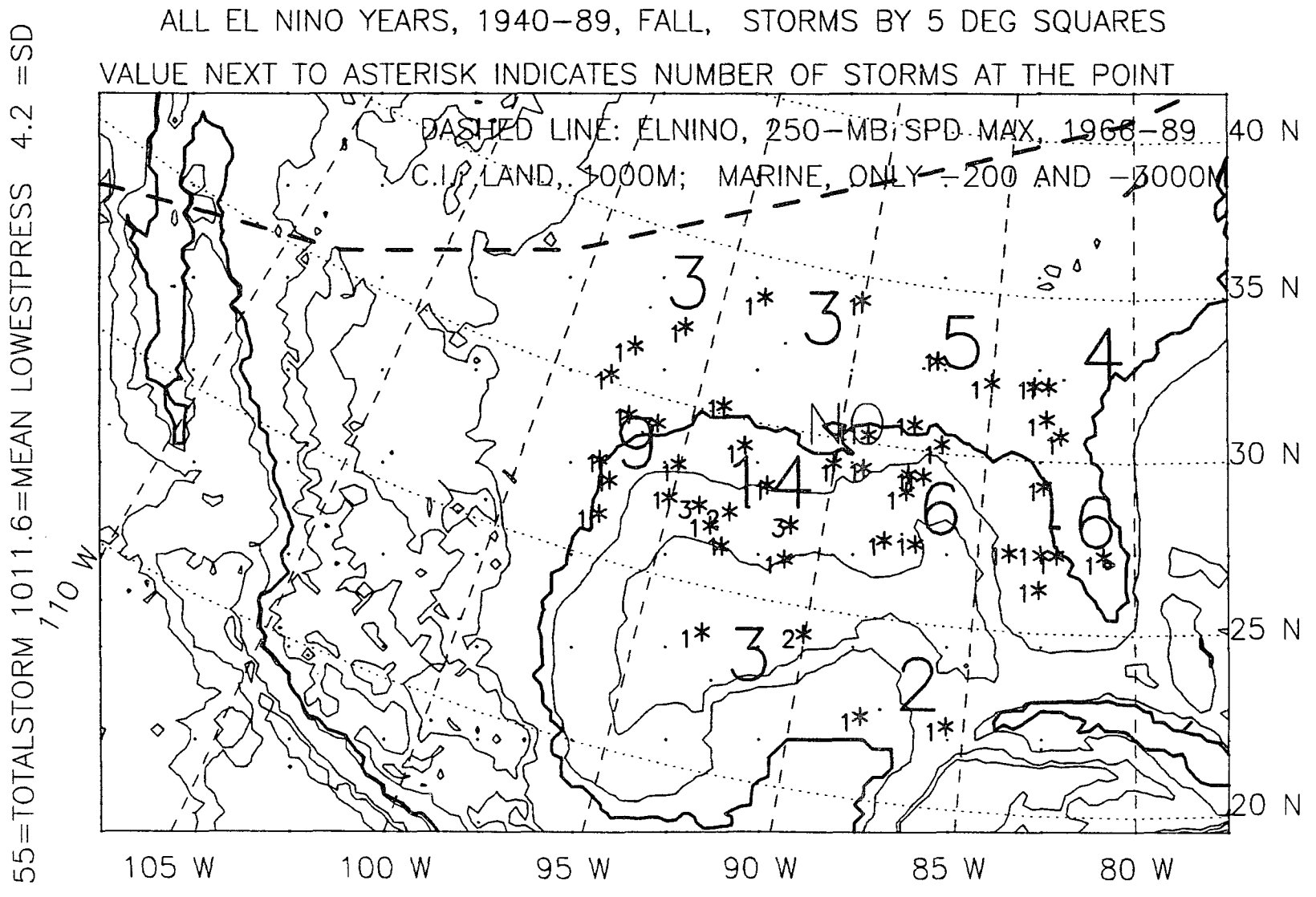

Figure S.13: Storm locations, fall, 11 El Niño years, 1940–89.

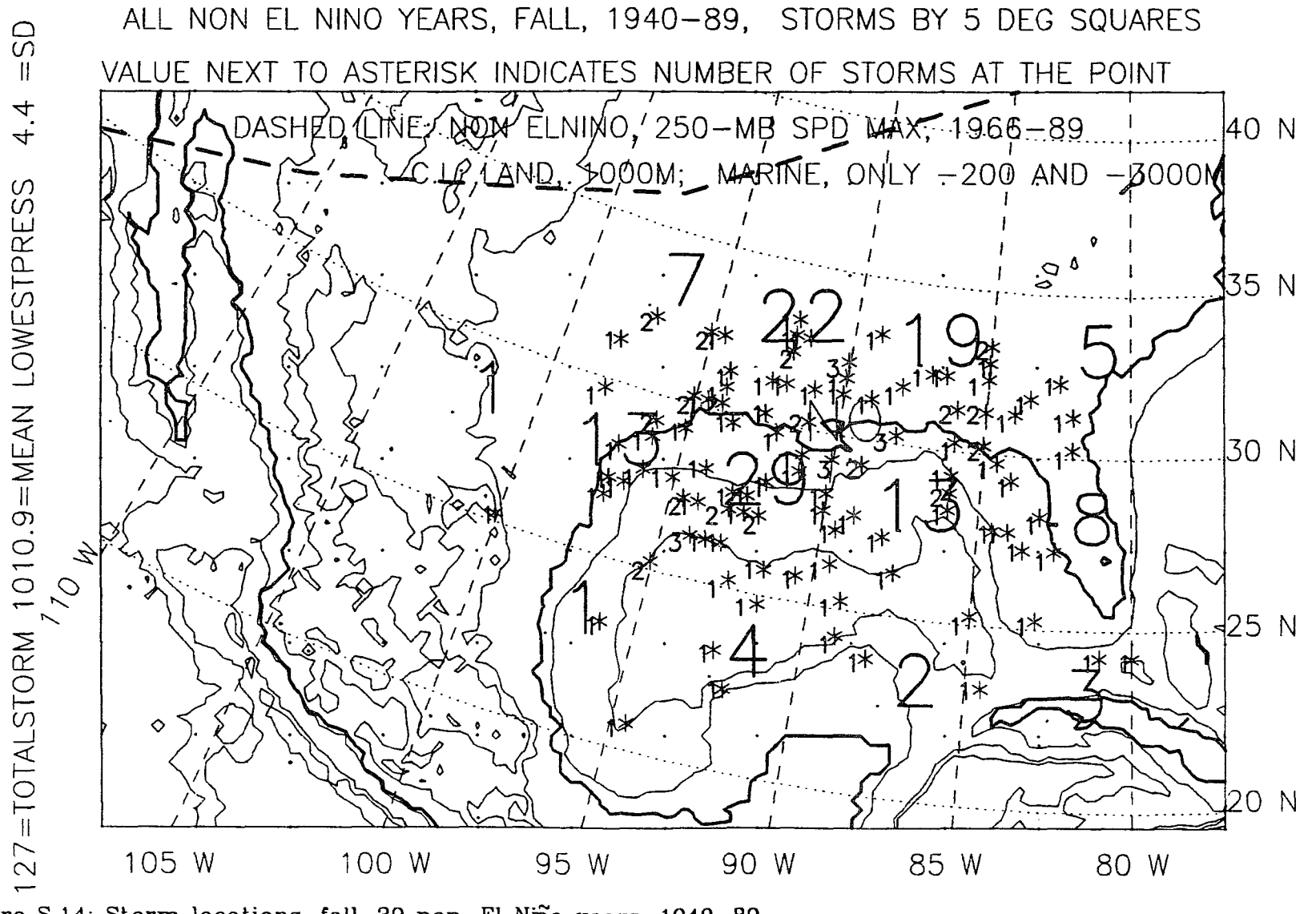

Figure S.14: Storm locations, fall, 39 non–El Niño years, 1940–89.

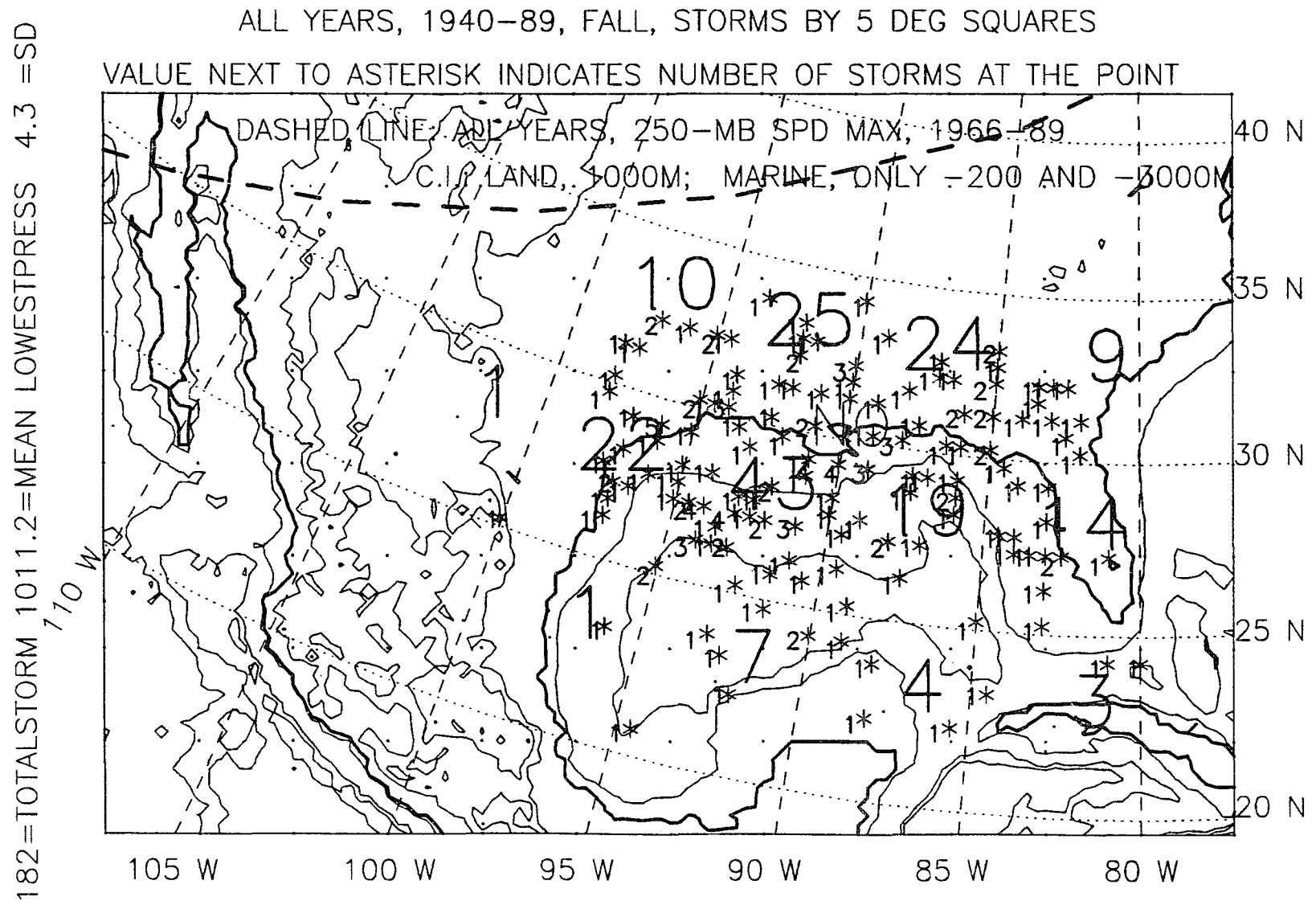

Figure S.15: Storm locations, fall, all 50 years, 1940–89.

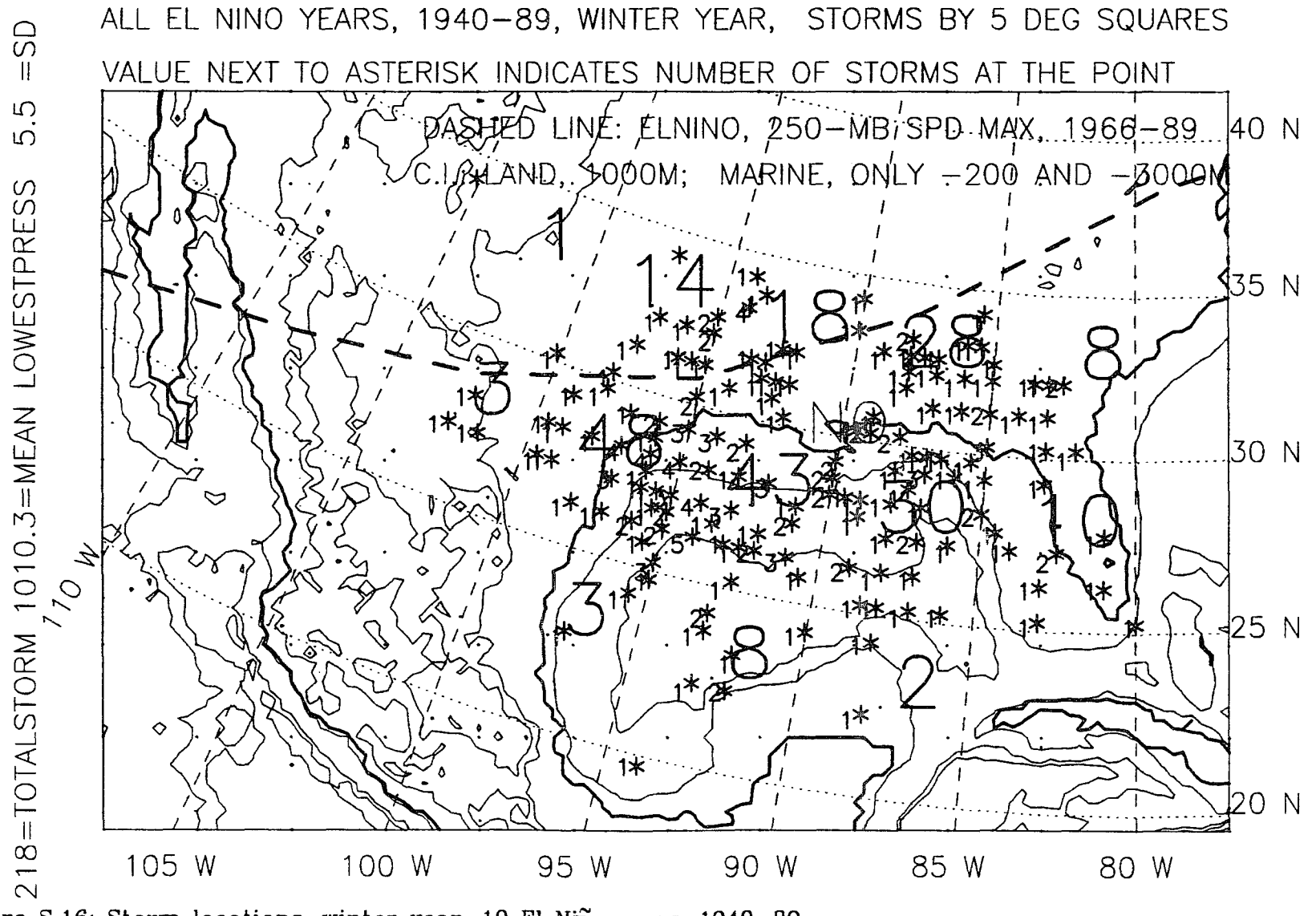

Figure S.16: Storm locations, winter year, 10 El Niño years, 1940–89.

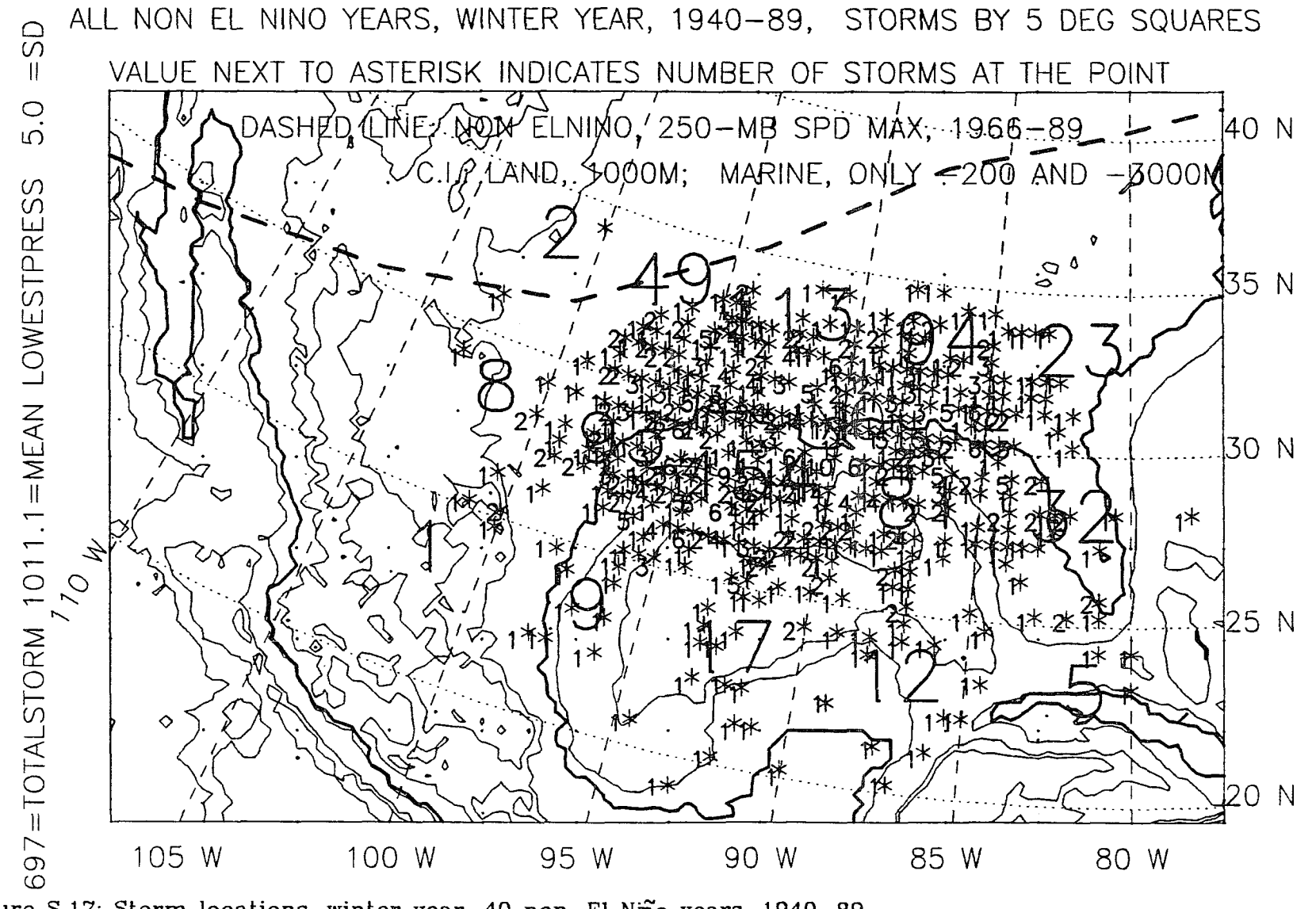

Figure S.17: Storm locations, winter year, 40 non–El Niño years, 1940–89.

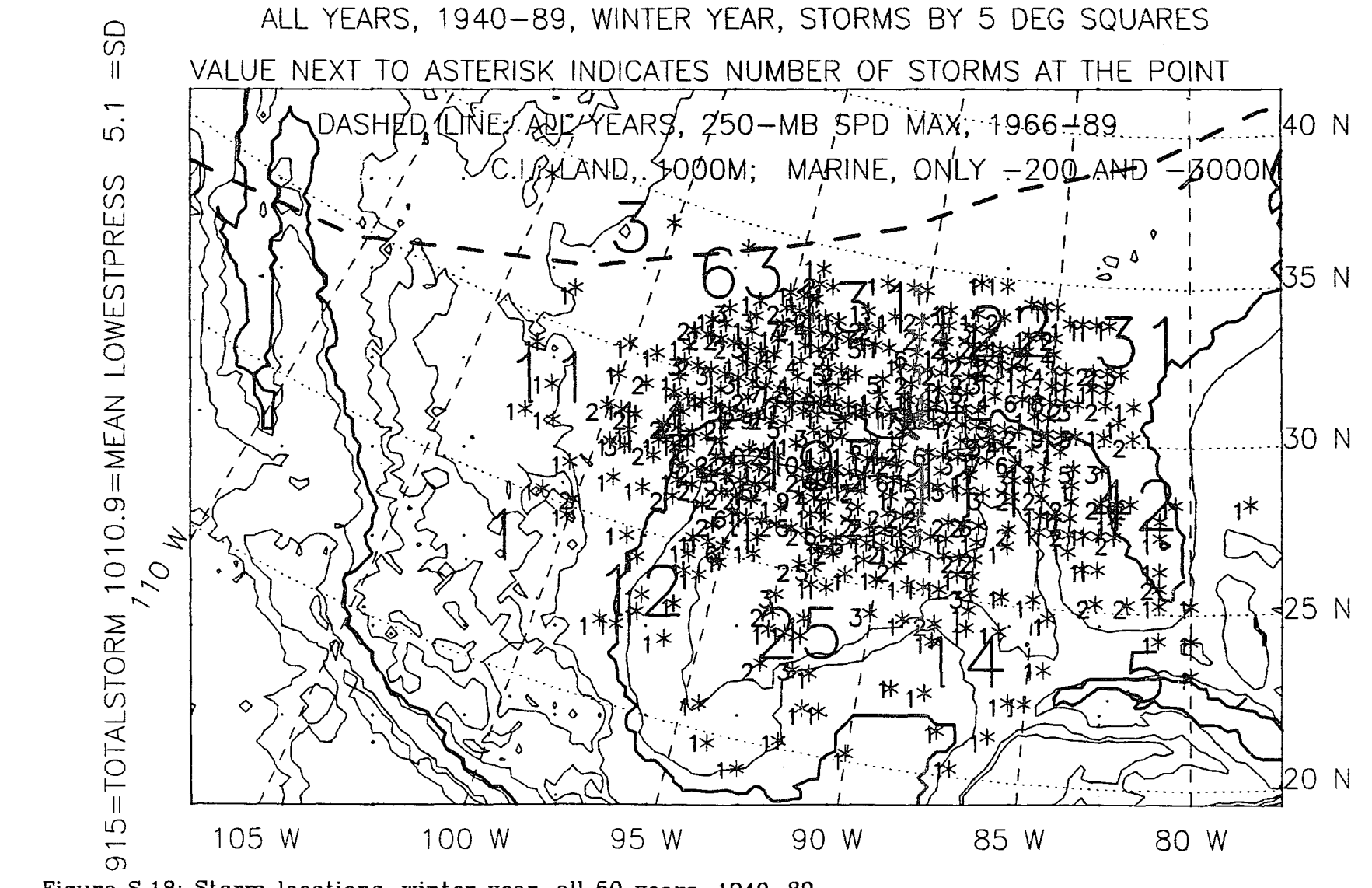

Figure S.18: Storm locations, winter year, all 50 years, 1940–89.

APPENDIX T
1982/83 COLD FRONT AND STORM DATA

Table T.1: Winter year 1982 (1 September 1982 to 31 August 1983) cold front characteristics: temperature, pressure, and precipitation, from daily weather map (United States Department of Commerce 1970 to 1990).

Front No.	Cross Date YMD	ΔTemp −°F	ΔDew −°F	ΔPress +mb	Precip. in.	Crossing Angle* °
1	820902	9	12	2.6	0.03	0
2	820916	6	2	0.1	0.38	25
3	820919	19	23	9.2	0.58	0
4	820925	6	5	5.4	0.00	30
5	821003	0	0	3.4	0.10	0
6	821007	3	2	2.7	0.50	10
7	821010	27	26	7.9	1.20	30
8	821016	1	5	4.3	0.00	0
9	821020	17	24	4.3	0.00	20
10	821029	2	4	1.8	0.96	20
11	821103	29	40	15.7	1.32	30
12	821112	30	33	12.2	0.17	45
13	821114	5	3	8.8	0.00	20
14	821124	24	34	14.1	0.61	35
15	821203	26	29	18.3	2.55	90
16	821209	2	4	2.5	0.02	35
17	821211	25	36	11.5	0.00	25
18	821215	22	27	10.7	0.72	90
19	821219	15	20	4.9	0.01	25
20	821226	38	33	19.8	1.09	65
21	830109	25	35	15.0	0.37	60
22	830115	12	12	1.0	0.00	30
23	830118	13	11	12.1	0.11	0
24	830126	8	8	7.6	0.40	90
25	830129	7	10	3.3	0.05	45
26	830201	26	31	20.6	2.11	70
27	830210	20	19	16.6	0.08	90
28	830221	11	9	3.0	1.02	90
29	830225	7	19	7.1	0.00	0
30	830305	8	11	5.7	0.93	90
31	830307	23	27	16.1	0.02	55
32	830320	21	25	16.3	0.27	60

Table T.1: continued.

Front No.	Cross Date YMD	ΔTemp −°F	ΔDew −°F	ΔPress +mb	Precip. in.	Crossing Angle* °
33	830326	12	18	13.5	1.03	45
34	830402	17	23	8.6	0.09	60
35	830406	27	27	12.7	3.69	66
36	830419	8	12	5.0	0.19	0
37	830423	17	21	13.3	2.50	90
38	830503	24	23	7.6	0.16	35
39	830508	11	14	3.8	0.97	25
40	830515	12	15	4.9	1.18	38
41	830523	19	14	4.9	3.12	20
42	830527	3	0	1.1	0.00	0
43	830531	6	8	7.5	0.21	0
44	830607	11	14	8.0	0.65	40
45	830615	6	4	1.6	0.91	20
46	830706	11	11	2.7	0.04	0
47	830814	1	3	1.5	0.00	0

Notes:

*: Crossing angle is gauged along an east-west, relatively straight segment of the northern gulf coastline, between Houston, Texas and Tallahassee, Florida. It is the acute angle between the front and the coastline. 0° is parallel to coast; 90° is perpendicular to coast; 45° indicates a front trending northeast-southwest. The crossing angle is not a compass direction.

Table T.2: Winter year 1982 (1 September 1982 to 31 August 1983) cold fronts: surface winds after cold front crosses coast, from daily weather map (United States Department of Commerce 1970 to 1990).

Front	Cross	Coastal Winds After			Offshore Winds After		
No.	Date	Speed	Direction	Duration	Speed	Direction	Duration
	YMD	kt.	Compass°	days	kt.	Compass°	days
1	820902	8	45	3	10	135	0
2	820916	5	315	2	5	45	2
3	820919	8	0	4	15	45	1
4	820925	5	315	1	8	45	1
5	821003	4	45	1	10	45	1
6	821007	5	135	0	13	135	0
7	821010	6	45	3	13	45	3
8	821016	8	45	1	8	45	0
9	821020	10	45	5	10	45	3
10	821029	5	0	1	7	135	0
11	821103	13	315	2	23	315	3
12	821112	13	0	2	28	45	1
13	821114	13	0	1	18	315	1
14	821124	15	0	1	13	90	0
15	821203	8	315	3	15	45	4
16	821209	15	45	1	13	135	0
17	821211	15	315	2	25	315	1
18	821215	9	315	1	17	0	2
19	821219	8	315	1	8	45	1
20	821226	17	45	6	17	315	4
21	830109	11	0	2	22	315	3
22	830115	9	315	1	12	45	2
23	830118	8	45	3	11	315	3
24	830126	10	315	1	17	315	1
25	830129	5	45	1	10	45	1
26	830201	10	315	1	20	315	2
27	830210	10	45	3	13	45	2
28	830221	5	315	1	15	315	3
29	830225	15	45	2	15	315	1
30	830305	5	180	0	20	315	1
31	830307	8	315	3	22	315	3
32	830320	11	315	1	12	315	1

Table T.2: continued.

Front No.	Cross Date YMD	Coastal Winds After Speed kt.	Direction Compass°	Duration days	Offshore Winds After Speed kt.	Direction Compass°	Duration days
33	830326	5	315	1	13	315	1
34	830402	13	225	1	18	315	1
35	830406	13	315	2	18	315	2
36	830419	8	45	1	10	45	1
37	830423	10	315	1	17	315	1
38	830503	6	315	1	15	45	1
39	830508	9	45	1	17	135	0
40	830515	8	315	1	10	135	0
41	830523	4	315	1	8	45	2
42	830527	5	0	1	10	135	0
43	830531	6	0	1	10	135	0
44	830607	6	0	1	10	0	1
45	830615	5	45	1	10	90	0
46	830706	5	315	1	10	90	0
47	830814	4	315	1	10	225	0

Table T.3: Winter year 1982 (1 September 1982 to 31 August 1983) cold fronts: 500-mb level parameters after crossing, from daily weather map (United States Department of Commerce 1970 to 1990).

Front No.	Cross Date YMD	[500-mb Level, After Crossing] Height Drop* m	Wind Speed kt	Wind Direction Compass°	[At Lowest 500-mb Height] Height m	Wind Speed kt.	Wind Direction Compass°
1	820902	46	10	0	5869	20	180
2	820916	0	5	45	5915	5	315
3	820919	0	30	315	5838	25	315
4	820925	30	35	315	5732	40	315
5	821003	0	20	225	5854	13	225
6	821007	0	20	225	5884	20	225
7	821010	61	30	225	5823	31	225
8	821016	0	28	270	5762	45	315
9	821020	61	20	315	5793	20	315
10	821029	30	10	315	5793	10	315
11	821103	61	25	270	5701	45	225
12	821112	61	40	315	5823	28	270
13	821114	61	43	270	5762	32	270
14	821124	0	35	225	5793	30	270
15	821203	122	70	180	5701	65	225
16	821209	-31	25	270	5701	65	270
17	821211	122	55	270	5701	65	270
18	821215	0	60	270	5732	50	225
19	821219	31	67	315	5747	50	315
20	821226	30	50	225	5701	50	225
21	830109	61	60	270	5701	50	315
22	830115	92	25	270	5701	25	270
23	830118	76	50	225	5579	77	225
24	830126	-122	25	225	5640	45	225
25	830129	0	40	270	5701	63	270
26	830201	275	70	270	5457	75	270
27	830210	15	35	315	5610	30	225
28	830221	15	25	270	5595	30	225
29	830225	-23	40	315	5587	45	315
30	830305	61	60	225	5640	70	225
31	830307	31	68	315	5518	60	270
32	830320	122	85	270	5549	80	270

Table T.3: continued.

Front No.	Cross Date YMD	[500-mb Level, After Crossing] Height Drop* m	Wind Speed kt	Wind Direction Compass°	[At Lowest 500-mb Height] Height m	Wind Speed kt.	Wind Direction Compass°
33	830326	-7	60	270	5640	72	225
34	830402	46	60	315	5579	80	225
35	830406	92	60	225	5625	75	225
36	830419	-31	50	315	5671	53	45
37	830423	91	55	315	5671	55	315
38	830503	46	40	315	5747	40	315
39	830508	31	40	270	5823	40	270
40	830515	15	50	270	5823	50	270
41	830523	30	40	315	5816	40	315
42	830527	0	20	315	5793	20	315
43	830531	-45	12	270	5732	22	225
44	830607	-15	10	0	5793	35	270
45	830615	23	18	225	5831	18	225
46	830706	0	20	45	5884	20	45
47	830814	0	18	45	5945	10	0

Notes:

*: Height drop = 500-mb height before crossing, minus 500-mb height after crossing; 500-mb heights are usually lower after crossing, so a negative height drop indicates a higher height after crossing.

Table T.4: Winter year 1982 (1 September 1982 to 31 August 1983) cold fronts: 300-mb level parameters on day of crossing, from National Climatic Data Center (National Climatic Data Center 1988).

Front	Cross	[Lake Charles, La.]			[Bootheville, La]		
No.	Date YMD	Height m	Wind Speed kt	Wind Direction Compass°	Height m	Wind Speed kt.	Wind Direction Compass°
11	821103	9450	66	209	9528	41	217
12	821112	9585	92	255	9628	68	265
13	821114	9604	66	257	9606	54	265
14	821124	9514	31	237	9543	16	229
15	821203	9548	47	201	9617	39	185
16	821209	9613	51	274	9613	48	292
17	821211	9487	72	264	9562	64	272
18	821215	9414	66	226	9562	52	224
19	821219	9442	61	317	9442	58	318
20	821226	9591	39	209	9616	48	261
21	830109	9331	58	327	9342	54	238
22	830115	9424	54	276	9429	74	281
23	830118	9388	82	252	9416	88	261
24	830126	9195	78	229	9287	64	230
25	830129	9327	78	284	9409	61	279
26	830201	9240	76	180	9400	21	234
27	830210	9219	58	286	9229	62	255
28	830221	9263	58	163	9275	48	237
29	830225	9275	37	261	9358	70	221
30	830305	9272	64	232	9370	76	248
31	830307	9269	61	245	9334	61	236
32	830320	9237	95	254	9344	103	258
33	830326	9240	109	257	9456	62	254
34	830402	9397	70	255	9256	93	250
35	830406	9441	79	236	9501	66	254
36	830419	9410	101	288	9348	88	289
37	830423	9377	103	266	9452	92	262

Table T.4: continued.

Front No.	Cross Date YMD	[Appalachicola, Fl] Height m	Wind Speed kt	Wind Direction Compass°
11	821103	9529	27	202
12	821112	9645	64	279
13	821114	9610	62	279
14	821124	9543	20	234
15	821203	9648	25	196
16	821209	9576	58	299
17	821211	9519	72	282
18	821215	9550	37	242
19	821219	9449	61	265
20	821226	9622	37	286
21	830109	9361	47	247
22	830115	9357	74	272
23	830118	9394	74	275
24	830126	9325	62	242
25	830129	9393	37	230
26	830201	9433	37	241
27	830210	9295	64	233
28	830221	9394	47	222
29	830225	9279	92	262
30	830305	9455	99	261
31	830307	9459	62	205
32	830320	9381	92	262
33	830326	9484	76	275
34	830402	9327	89	228
35	830406	9509	20	270
36	830419	9274	79	287
37	830423	9277	101	263

Table T.5: Winter year 1982 (1 September 1982 to 31 August 1983) frontal-wave cyclones: surface parameters, from daily weather map (United States Department of Commerce 1970 to 1990).

Storm No.	Front* No.	Origin Date	Length days	Latitude °N	Longitude °W	TravelSpeed miles/day	Path Compass°
1	3	820921	1	28.5	87.5		45
2	4	820926	1	27.0	82.5	600	45
3	7	821012	2	27.0	97.0	450	45
4	11	821103	1	27.0	94.0	300	45
5	13	821116	2	26.0	97.0	200	0
6	14	821126	3	29.0	96.0	250	45
7	15	821202	3	29.0	99.0	325	45
8	16	821210	1	28.0	96.0	500	45
9		821214	2	29.0	95.0	250	45
10	20	821227	1	33.0	94.0	600	45
11	20	821229	1	26.0	89.0	300	45
12	20	821231	2	26.0	96.0	250	45
13	21	830108	2	32.0	95.0	500	45
14	21	830110	1	28.0	90.0	600	45
15	23	830119	2	26.0	96.0	350	45
16	23	830122	1	26.0	87.0	500	45
17	24	830127	1	29.0	86.0	750	45
18	25	830130	1	31.0	85.0		
19	25	830205	2	28.0	102.0	600	45
20	27	830210	2	30.0	88.0	500	45
21	27	830212	1	24.0	88.0	400	45
22		830215	2	23.0	96.0	500	45
23		830216	1	27.0	93.0	500	45
24	28	830220	2	28.0	97.0	263	45
25	29	830226	3	26.0	94.0	300	45
26		830315	3	27.5	89.0	300	45
27	32	830323	1	28.0	98.0	800	45
28	35	830407	2	26.0	92.5	650	45
29	35	830410	1	26.0	81.0	300	45
30	37	830423	1	31.0	86.0	600	45
31		830529	1	26.0	88.0	400	45
32	44	830606	3	33.0	94.0	265	135
33	47	830814	2	29.0	88.0	150	225

*: Blank indicates associated front unable to be determined, or there was none.

Table T.5: continued.

Storm No.	Front* No.	Storm Origin Date	Associated Front Crossing Date	Lowest Central Pressure mb	Maximum Surface Wind(kt)	Precip. (Storm) in
1	3	820921	820919	1015.9	10	0.0
2	4	820926	820925	1008.0	15	2.2
3	7	821012	821010	1010.9	15	1.4
4	11	821103	821103	1007.5	15	1.4
5	13	821116	821114	1015.0	20	0.8
6	14	821126	821124	1007.2	15	2.4
7	15	821202	821203	1004.0	15	2.5
8	16	821210	821209	1011.4	12	1.0
9		821214		1014.0	15	0.7
10	20	821227	821226	1007.6	10	3.2
11	20	821229	821226	1017.1	10	0.6
12	20	821231	821226	1015.3	15	1.7
13	21	830108	830109	1012.4	10	0.2
14	21	830110	830109	1012.0	10	0.0
15	23	830119	830118	1003.3	25	1.8
16	23	830122	830118	1011.1	15	4.0
17	24	830127	830126	1011.5	20	0.4
18	25	830130	830129	1015.5	5	0.0
19	25	830205	830129	1008.1	20	1.7
20	27	830210	830210	1002.4	25	1.2
21	27	830212	830210	1011.5	30	2.1
22		830215		1004.0	30	0.3
23		830216		1003.7	25	0.8
24	28	830220	830221	1005.3	25	1.0
25	29	830226	830225	1004.6	30	1.1
26		830315		988.8	30	1.9
27	32	830323	830320	1002.0	25	1.1
28	35	830407	830406	1005.6	20	1.4
29	35	830410	830406	1015.6	10	0.9
30	37	830423	830423	1001.1	15	0.8
31		830529		1005.9	15	2.7
32	44	830606	830607	1009.1	15	1.9
33	47	830814	830814	1015.5	15	1.1

*: Blank indicates associated front unable to be determined, or there was none.

Table T.6: Winter year 1982 (1 September 1982 to 31 August 1983) frontal-wave cyclones: 500-mb level parameters, from daily weather map (United States Department of Commerce 1970 to 1990).

Storm No.	Front* No.	Origin Date YMD	[On Day of Origin] Height m	Wind kt	Direction Compass°	[At Lowest 500-mb Height] Height m	Wind kt.	Direction Compass°
1	3	820921	5854	35	270	5854	35	270
2	4	820926	5762	50	225	5762	50	225
3	7	821012	5854	25	225	5823	20	225
4	11	821103	5762	38	225	5762	38	225
5	13	821116	5823	45	315	5762	40	270
6	14	821126	5823	40	225	5823	60	225
7	15	821202	5701	65	225	5701	65	225
8	16	821210	5823	35	225	5793	30	225
9		821214	5762	25	225	5701	50	225
10	20	821227	5732	60	225	5732	60	225
11	20	821229	5823	50	225	5823	40	225
12	20	821231	5793	60	225	5762	65	225
13	21	830108	5823	30	270	5640	30	270
14	21	830110	5762	30	225	5762	30	225
15	23	830119	5732	20	225	5518	30	225
16	23	830122	5762	55	225	5762	55	225
17	24	830127	5640	50	225	5640	50	225
18	25	830130	5701	45	305	5701	45	305
19	25	830205	5701	60	225	5701	60	225
20	27	830210	5701	35	270	5579	35	225
21	27	830212	5762	50	225	5762	85	225
22		830215	5579	30	225	5579	28	225
23		830216	5640	40	225	5640	60	225
24	28	830220	5701	20	315	5518	25	0
25	29	830226	5671	10	180	5579	30	135
26		830315	5640	20	135	5518	10	225
27	32	830323	5671	45	225	5579	80	225
28	35	830407	5793	60	225	5701	55	225
29	35	830410	5854	45	225	5854	45	225
30	37	830423	5701	45	225	5701	45	225
31		830529	5823	25	270	5808	40	225
32	44	830606	5777	20	270	5777	20	270
33	47	830814	5884	10	0	5884	10	0

*: Blank indicates associated front unable to be determined, or there was none.

Table T.7: Winter year 1982 (1 September 1982 to 31 August 1983) frontal-wave cyclones: 300-mb level parameters at Lake Charles, Louisiana, from National Climatic Data Center (National Climatic Data Center 1988).

Storm	Front*	Origin	300-mb Level, Lake Charles, La.				
No.	No.	Date	Height	Wind Speed	Direction	u	v
		YMD	m	kt	Compass°	kt	kt
4	11	821103	9450	66	209	31	57
5	13	821116	9454	64	304	53	-35
6	14	821126	9519	70	238	59	37
7	15	821202	9429	101	178	-3	100
8	16	821210	9594	61	245	55	25
9		821214	9414	66	226	47	45
10	20	821227	9477	52	219	32	40
11	20	821229	9377	107	245	96	45
12	20	821231	9421	101	243	89	45
13	21	830108	9331	58	327	31	-48
14	21	830110	9352	84	250	78	28
15	23	830119	9245	27	115	-24	11
16	23	830122	9120	82	236	67	45
17	24	830127	9195	78	229	58	51
18	25	830130	9435	56	270	56	0
19	25	830205	9237	132	248	122	49
20	27	830210	9219	58	286	55	-15
21	27	830212	9194	110	228	81	73
22		830215	9205	41	229	30	26
23		830216	9264	31	273	30	-1
24	28	830220	9263	58	163	-16	55
25	29	830226	9186	37	266	36	2
26		830315	9200	33	219	20	25
27	32	830323	9290	78	248	72	29
28	35	830407	9353	95	226	68	65
29	35	830410	9236	119	236	98	66
30	37	830423	9377	103	266	102	7

*: Blank indicates associated front unable to be determined, or there was none.

Table T.8: Winter year 1982 (1 September 1982 to 31 August 1983) frontal-wave cyclones: 300-mb level parameters at Boothville, Louisiana, from National Climatic Data Center (National Climatic Data Center 1988).

Storm No.	Front No.	Origin Date YMD	300-mb Level, Boothville, La. Height m	Wind Speed kt	Direction Compass°	u kt	v kt
4	11	821103	9528	41	217	24	32
5	13	821116	9455	30	268	29	1
6	14	821126	9605	39	227	28	26
7	15	821202	9617	39	185	3	38
8	16	821210	9605	48	271	47	0
9		821214	9531	43	242	37	20
10	20	821227	9548	39	223	26	28
11	20	821229	9493	74	238	62	39
12	20	821231	9469	86	252	81	26
13	21	830108	9342	54	238	45	28
14	21	830110	9431	64	250	60	21
15	23	830119	9289	51	205	21	46
16	23	830122	9266	99	238	83	52
17	24	830127	9191	82	255	79	21
18	25	830130	9463	58	284	56	-14
19	25	830205	9390	132	254	126	36
20	27	830210	9229	62	255	59	16
21	27	830212	9316	105	226	75	72
22		830215	9237	76	177	-3	75
23		830216	9237	76	177	-3	75
24	28	830220	9275	48	237	40	26
25	29	830226	9252	16	162	-4	15
26		830315	9150	39	41	-25	-29
27	32	830323	9347	78	244	70	34
28	35	830407	9408	107	231	83	67
29	35	830410	9270	92	251	86	29
30	37	830423	9452	92	262	91	12

*: Blank indicates associated front unable to be determined, or there was none.

Table T.9: Winter year 1982 (1 September 1982 to 31 August 1983) frontal-wave cyclones: 300-mb level parameters at Appalachicola, Florida, from National Climatic Data Center (National Climatic Data Center 1988).

No.	Front*	Origin	300-mb Level, Appalachicola, Fl.				
	No.	Date	Height	Wind Speed	Direction	u	v
		YMD	m	kt	Compass°	kt	kt
4	11	821103	9529	27	202	10	25
5	13	821116	9449	33	274	32	-2
6	14	821126	9601	33	256	32	7
7	15	821202	9618	37	193	8	36
8	16	821210	9578	52	290	48	-17
9		821214	9534	61	277	60	-7
10	20	821227	9624	43	231	33	27
11	20	821229	9514	57	248	52	21
12	20	821231	9520	66	251	62	21
13	21	830108	9338	43	253	41	12
14	21	830110	9445	61	254	58	16
15	23	830119	9409	89	256	86	21
16	23	830122	9331	93	238	78	49
17	24	830127	9227	101	239	86	52
18	25	830130	9416	56	298	49	-26
19	25	830205	9416	110	275	109	-9
20	27	830210	9295	64	233	51	38
21	27	830212	9365	113	241	98	54
22		830215	9335	68	210	34	58
23		830216	9335	68	210	34	58
24	28	830220	9376	10	273	9	0
25	29	830226	9288	61	245	55	25
26		830315	9152	30	87	-29	-1
27	32	830323	9387	95	244	85	41
28	35	830407	9553	58	236	48	32
29	35	830410	9359	95	220	61	72
30	37	830423	9277	101	263	100	12

*: Blank indicates associated front unable to be determined, or there was none.

VITA

Rosemary E. Manty received a Bachelor of Science degree in Geology in 1977 from Wayne State University in Detroit, Michigan and a Master of Science degree in Geology in 1981 from Louisiana State University, Baton Rouge, Louisiana. Miss Manty's M. S. thesis is entitled, "Analysis of a Multivariate System: Correlation between Coastal Form and Processes, Long Island, N. Y. to Brownsville, Tx.", and was directed by Dr. D. Nummedal. From 1981 to 1988, Miss Manty was an exploration geologist, working in the Gulf of Mexico, Outer Continental Shelf, Central Leasing Area, employed by Phillips Petroleum Company, Houston Tx. She spent 1988/89 in the Ph. D. Program in Geology at Memorial University of Newfoundland, St. John's, Nfld., in the Recent, marine geology program. From 1989 to 1993, she has been at Louisiana State University, Baton Rouge, La., in the Department of Geology and Geophysics, in the Ph. D. program in marine geology and physical oceanography/marine meteorology.

DOCTORAL EXAMINATION AND DISSERTATION REPORT

Candidate: Rosemary E. Manty

Major Field: Geology

Title of Dissertation: Effect of the El Nino/Southern Oscillation on Gulf of Mexico, Winter, Frontal-Wave Cyclones: 1960-89

Approved:

S. A. Hsu
Major Professor and Chairman

Daniel Fogel
Dean of the Graduate School

EXAMINING COMMITTEE:

Robert A Mullen

James P Scanlon

Date of Examination:

March 16, 1993